ALTERNATIVE THERAPEUTICS AGAINST ANTIMICROBIAL-RESISTANT PATHOGENS

EDITED BY: Rebecca Thombre, Kamlesh Jangid, Ravi Shukla and Noton Kumar Dutta

PUBLISHED IN: Frontiers in Microbiology

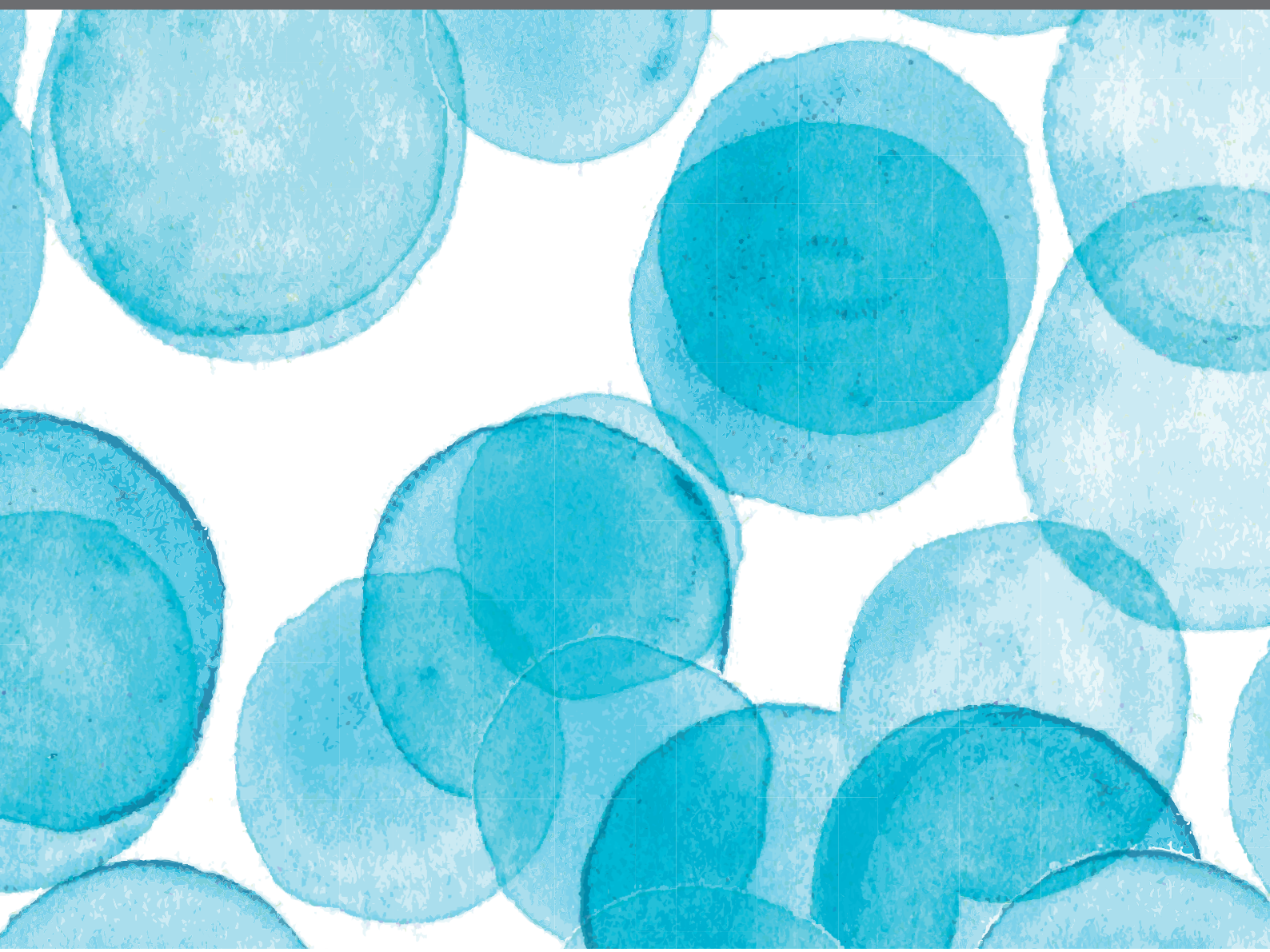

frontiers Research Topics



frontiers

Frontiers eBook Copyright Statement

The copyright in the text of individual articles in this eBook is the property of their respective authors or their respective institutions or funders. The copyright in graphics and images within each article may be subject to copyright of other parties. In both cases this is subject to a license granted to Frontiers.

The compilation of articles constituting this eBook is the property of Frontiers.

Each article within this eBook, and the eBook itself, are published under the most recent version of the Creative Commons CC-BY licence. The version current at the date of publication of this eBook is CC-BY 4.0. If the CC-BY licence is updated, the licence granted by Frontiers is automatically updated to the new version.

When exercising any right under the CC-BY licence, Frontiers must be attributed as the original publisher of the article or eBook, as applicable.

Authors have the responsibility of ensuring that any graphics or other materials which are the property of others may be included in the CC-BY licence, but this should be checked before relying on the CC-BY licence to reproduce those materials. Any copyright notices relating to those materials must be complied with.

Copyright and source acknowledgement notices may not be removed and must be displayed in any copy, derivative work or partial copy which includes the elements in question.

All copyright, and all rights therein, are protected by national and international copyright laws. The above represents a summary only. For further information please read Frontiers' Conditions for Website Use and Copyright Statement, and the applicable CC-BY licence.

ISSN 1664-8714
ISBN 978-2-88963-216-9
DOI 10.3389/978-2-88963-216-9

About Frontiers

Frontiers is more than just an open-access publisher of scholarly articles: it is a pioneering approach to the world of academia, radically improving the way scholarly research is managed. The grand vision of Frontiers is a world where all people have an equal opportunity to seek, share and generate knowledge. Frontiers provides immediate and permanent online open access to all its publications, but this alone is not enough to realize our grand goals.

Frontiers Journal Series

The Frontiers Journal Series is a multi-tier and interdisciplinary set of open-access, online journals, promising a paradigm shift from the current review, selection and dissemination processes in academic publishing. All Frontiers journals are driven by researchers for researchers; therefore, they constitute a service to the scholarly community. At the same time, the Frontiers Journal Series operates on a revolutionary invention, the tiered publishing system, initially addressing specific communities of scholars, and gradually climbing up to broader public understanding, thus serving the interests of the lay society, too.

Dedication to Quality

Each Frontiers article is a landmark of the highest quality, thanks to genuinely collaborative interactions between authors and review editors, who include some of the world's best academicians. Research must be certified by peers before entering a stream of knowledge that may eventually reach the public - and shape society; therefore, Frontiers only applies the most rigorous and unbiased reviews.
Frontiers revolutionizes research publishing by freely delivering the most outstanding research, evaluated with no bias from both the academic and social point of view. By applying the most advanced information technologies, Frontiers is catapulting scholarly publishing into a new generation.

What are Frontiers Research Topics?

Frontiers Research Topics are very popular trademarks of the Frontiers Journals Series: they are collections of at least ten articles, all centered on a particular subject. With their unique mix of varied contributions from Original Research to Review Articles, Frontiers Research Topics unify the most influential researchers, the latest key findings and historical advances in a hot research area! Find out more on how to host your own Frontiers Research Topic or contribute to one as an author by contacting the Frontiers Editorial Office: researchtopics@frontiersin.org

ALTERNATIVE THERAPEUTICS AGAINST ANTIMICROBIAL-RESISTANT PATHOGENS

Topic Editors:
Rebecca Thombre, University of Kent, United Kingdom
Kamlesh Jangid, National Centre for Cell Science Pune, India
Ravi Shukla, RMIT University, Australia
Noton Kumar Dutta, Johns Hopkins University Baltimore, United States

Citation: Thombre, R., Jangid, K., Shukla, R., Dutta, N. K., eds. (2019). Alternative Therapeutics Against Antimicrobial-Resistant Pathogens. Lausanne: Frontiers Media SA. doi: 10.3389/978-2-88963-216-9

Table of Contents

06 ***Editorial: Alternative Therapeutics Against Antimicrobial-Resistant Pathogens***
Rebecca Thombre, Kamlesh Jangid, Ravi Shukla and Noton Kumar Dutta

08 ***Antimicrobial and Antibiofilm Potential of Acyclic Amines and Diamines Against Multi-Drug Resistant* Staphylococcus aureus**
Gurmeet Kaur, P. Balamurugan, Sahana Vasudevan, Saikiran Jadav and S. A. Princy

16 ***Boeravinone B, A Novel Dual Inhibitor of NorA Bacterial Efflux Pump of* Staphylococcus aureus *and Human* P-*Glycoprotein, Reduces the Biofilm Formation and Intracellular Invasion of Bacteria***
Samsher Singh, Nitin P. Kalia, Prashant Joshi, Ajay Kumar, Parduman R. Sharma, Ashok Kumar, Sandip B. Bharate and Inshad A. Khan

28 ***Structure–Function Relationship of Aminopeptidase P From* Pseudomonas aeruginosa**
Cui-Ting Peng, Li Liu, Chang-Cheng Li, Li-Hui He, Tao Li, Ya-Lin Shen, Chao Gao, Ning-Yu Wang, Yong Xia, Yi-Bo Zhu, Ying-Jie Song, Qian Lei, Luo-Ting Yu and Rui Bao

40 ***Repurposing and Revival of the Drugs: A New Approach to Combat the Drug Resistant Tuberculosis***
Divakar Sharma, Yogesh K. Dhuriya, Nirmala Deo and Deepa Bisht

45 ***Harnessing the mTOR Pathway for Tuberculosis Treatment***
Pooja Singh and Selvakumar Subbian

56 ***Defeating Antibiotic- and Phage-Resistant* Enterococcus faecalis *Using a Phage Cocktail* in Vitro *and in a Clot Model***
Leron Khalifa, Daniel Gelman, Mor Shlezinger, Axel Lionel Dessal, Shunit Coppenhagen-Glazer, Nurit Beyth and Ronen Hazan

67 ***Gas Plasma Pre-treatment Increases Antibiotic Sensitivity and Persister Eradication in Methicillin-Resistant* Staphylococcus aureus**
Li Guo, Ruobing Xu, Yiming Zhao, Dingxin Liu, Zhijie Liu, Xiaohua Wang, Hailan Chen and Michael G. Kong

76 ***Liposome Entrapment of Bacteriophages Improves Wound Healing in a Diabetic Mouse MRSA Infection***
Sanjay Chhibber, Jasjeet Kaur and Sandeep Kaur

88 ***Antimicrobial Potential of Epiphytic Bacteria Associated With Seaweeds of Little Andaman, India***
Perumal Karthick and Raju Mohanraju

99 ***Prediction of Cell-Penetrating Potential of Modified Peptides Containing Natural and Chemically Modified Residues***
Vinod Kumar, Piyush Agrawal, Rajesh Kumar, Sherry Bhalla, Salman Sadullah Usmani, Grish C. Varshney and Gajendra P. S. Raghava

109 ***Antibacterial Efficacy of Polysaccharide Capped Silver Nanoparticles is not Compromised by AcrAB-TolC Efflux Pump***
Mitali Mishra, Satish Kumar, Rakesh K. Majhi, Luna Goswami, Chandan Goswami and Harapriya Mohapatra

118 ***Efficacy of Colistin and its Combination With Rifampin* in Vitro *and in Experimental Models of Infection Caused by Carbapenemase-Producing Clinical Isolates of* Klebsiella pneumoniae**
María E. Pachón-Ibáñez, Gema Labrador-Herrera, Tania Cebrero-Cangueiro, Caridad Díaz, Younes Smani, José P. del Palacio, Jesús Rodríguez-Baño, Alvaro Pascual, Jerónimo Pachón and M. Carmen Conejo

127 **Trans-*Cinnamaldehyde and Eugenol Increase* Acinetobacter baumannii *Sensitivity to Beta-Lactam Antibiotics***
Deepti P. Karumathil, Meera Surendran Nair, James Gaffney, Anup Kollanoor-Johny and Kumar Venkitanarayanan

137 ***Advance in Research on* Mycobacterium tuberculosis *FabG4 and its Inhibitor***
Debajyoti Dutta

143 ***Herring Oil and Omega Fatty Acids Inhibit* Staphylococcus aureus *Biofilm Formation and Virulence***
Yong-Guy Kim, Jin-Hyung Lee, Chaitany J. Raorane, Seong T. Oh, Jae G. Park and Jintae Lee

153 ***Nano-Strategies to Fight Multidrug Resistant Bacteria—"A Battle of the Titans"***
Pedro V. Baptista, Matthew P. McCusker, Andreia Carvalho, Daniela A. Ferreira, Niamh M. Mohan, Marta Martins and Alexandra R. Fernandes

179 **In Vitro *Antimicrobial Activity of Green Synthesized Silver Nanoparticles Against Selected Gram-negative Foodborne Pathogens***
Yuet Ying Loo, Yaya Rukayadi, Mahmud-Ab-Rashid Nor-Khaizura, Chee Hao Kuan, Buong Woei Chieng, Mitsuaki Nishibuchi and Son Radu

186 ***Prevention of Dermal Abscess Formation Caused by* Staphylococcus aureus *Using Phage JD007 in Nude Mice***
Bingyu Ding, Qingtian Li, Mingquan Guo, Ke Dong, Yan Zhang, Xiaokui Guo, Qingzhong Liu, Li Li and Zelin Cui

193 ***Non-toxigenic* Clostridioides *(Formerly Clostridium)* difficile *for Prevention of* C. difficile *Infection: From Bench to Bedside Back to Bench and Back to Bedside***
Dale N. Gerding, Susan P. Sambol and Stuart Johnson

206 ***Efficiency of Biosynthesized Silver and Zinc Nanoparticles Against Multi-Drug Resistant Pathogens***
Kapil Punjabi, Sourabh Mehta, Rujuta Chavan, Vidushi Chitalia, Dhanashree Deogharkar and Sunita Deshpande

217 ***Efficient Production of Recombinant Protegrin-1 From* Pichia pastoris*, and its Antimicrobial and* in vitro *Cell Migration Activity***
Evanna Huynh, Nadeem Akhtar and Julang Li

229 ***Bactericidal Property of Oregano Oil Against Multidrug-Resistant Clinical Isolates***
Min Lu, Tianhong Dai, Clinton K. Murray and Mei X. Wu

243 ***Effects of Monolaurin on Oral Microbe–Host Transcriptome and Metabolome***
Viviam de Oliveira Silva, Luciano José Pereira, Silvana Pasetto, Maike Paulino da Silva, Jered Cope Meyers and Ramiro Mendonça Murata

252 ***Purification and Characterization of an Active Principle, Lawsone, Responsible for the Plasmid Curing Activity of* Plumbago zeylanica *Root Extracts***
Rajashree Bhalchandra Patwardhan, Prashant Kamalakar Dhakephalkar, Balu Ananda Chopade, Dilip D. Dhavale and Ramesh R. Bhonde

262 ***Inhibiting Bacterial Drug Efflux Pumps via Phyto-Therapeutics to Combat Threatening Antimicrobial Resistance***
Varsha Shriram, Tushar Khare, Rohit Bhagwat, Ravi Shukla and Vinay Kumar

280 ***Emerging Strategies to Combat ESKAPE Pathogens in the Era of Antimicrobial Resistance: A Review***
Mansura S. Mulani, Ekta E. Kamble, Shital N. Kumkar, Madhumita S. Tawre and Karishma R. Pardesi

frontiers in Microbiology

EDITORIAL
published: 19 September 2019
doi: 10.3389/fmicb.2019.02173

Editorial: Alternative Therapeutics Against Antimicrobial-Resistant Pathogens

Rebecca Thombre[1,2]*, *Kamlesh Jangid*[3], *Ravi Shukla*[4] and *Noton Kumar Dutta*[5]

[1] Department of Biotechnology, Modern College of Arts, Science and Commerce, Pune, India, [2] School of Physical Sciences, University of Kent, Canterbury, United Kingdom, [3] National Centre for Microbial Resource, National Centre for Cell Science, Savitribai Phule Pune University Campus, Pune, India, [4] NanoBiotechnology Research Laboratory, RMIT University, Melbourne, VIC, Australia, [5] Center for Tuberculosis Research, Department of Medicine, Johns Hopkins University School of Medicine, Baltimore, MD, United States

Keywords: antimicrobial resistance (AMR), multidrug-resistance (MDR), nanomaterials, nanoparticles, plant based compounds, antimicrobial agents, alternative therapy, novel compounds

Editorial on the Research Topic

Alternative Therapeutics Against Antimicrobial-Resistant Pathogens

OPEN ACCESS

Edited by:
Henrietta Venter,
University of South Australia, Australia

Reviewed by:
Jianhua Wang,
Feed Research Institute (CAS), China

***Correspondence:**
Rebecca Thombre
rebecca.thombre@gmail.com

Specialty section:
This article was submitted to Antimicrobials, Resistance and Chemotherapy, a section of the journal Frontiers in Microbiology

Received: *26 July 2019*
Accepted: *05 September 2019*
Published: *19 September 2019*

Citation:
Thombre R, Jangid K, Shukla R and Dutta NK (2019) Editorial: Alternative Therapeutics Against Antimicrobial-Resistant Pathogens. Front. Microbiol. 10:2173. doi: 10.3389/fmicb.2019.02173

Antimicrobial resistance (AMR) has emerged as one of the greatest global challenge to public health in the twenty-first century. The use of antibiotics is associated with the serendipitous discovery of Penicillin by Sir Alexander Fleming in 1928 (Fleming, 1929). However, Emmerich and Löw had demonstrated the first application of the antibiotic "Pyocyanase" in hospital in 1899. The golden era of antibiotic was ushered between 1950s and 1970s which was marked by rapid developments in discoveries of many classes and types of antibiotics (Emmerich and Löw, 1899). The increased use and abuse of antibiotics caused the emergence of multidrug resistant bacteria that caused hard-to-treat infections (Aminov, 2010). It is imperative to search alternative therapeutics and strategies to combat AMR and diminish the exacerbated use of antibiotics. In this special issue, we present 26 articles that highlight the use of novel peptides, phage-based therapies, nanomedicine, contemporary and alternative medicines, plant (herbal), and bacteria based antimicrobials as potential alternatives to combat multidrug resistant (MDR) bacteria. The articles are categorized in different groups, including (i) Antimicrobial nanoparticles against drug resistant bacteria, (ii) Bacteriophages: A promising approach to fight MDR, (iii) Anti biofilm agents, (iv) Antimicrobial peptides, (v) Efflux pump inhibitors, and (vi) Host /Pathogen directed therapies.

A variety of repurposing FDA-approved drugs (Sharma et al.) that are employed in the management of pathological conditions of non-infectious etiology have been shown to exhibit broad spectrum antimicrobial activity *in vitro* and *in vivo*. Such compounds including marine eukaryotes like seaweeds (Karthick and Mohanraju), phytochemicals (Kim et al.; Lu et al.), antimicrobial peptides and proteins (Kumar et al.), termed "non-antibiotics" (Dutta et al., 2007; Mazumdar et al., 2009, 2010), possess antibacterial properties, acting through mechanisms different from those of existing drugs, by enhancement of combination-therapy effective (Pachon-Ibanez et al.; Shriram et al.), reversal of drug resistance (Guo et al.; Patwardhan et al.) or re-sensitizing activities (Dutta et al., 2014; Shriram et al.), inhibition of biofilm formation (Guo et al.; Karumathil et al.; Kaur et al.; Khalifa et al.; Kim et al.; Lu et al.; Punjabi et al.), as well as by induction and control of efflux pumps (Dutta et al., 2010; Baptista et al.; Karumathil et al.; Lu et al.; Shriram et al.).

This broad group of antimicrobial agents has two subgroups, each with distinctly different adjunct activities, either pathogen-directed or host directed. The first group is that of the antimicrobial non-antibiotics—drugs that have direct antimicrobial activity and the proposed path for compounds targeting microbial factors. The second group can generally be classified into two categories: those that enhance the antimicrobial activity of the host immune system, and those which dampen the inflammatory response preventing tissue damage (Karumathil et al.; Singh and Subbian). Host-directed therapies are attractive options as they are not prone to the resistance associated with antibiotics (Dutta et al., 2016; Frank et al., 2019). Currently, the following HDT agents are being evaluated in phase 2 clinical trials as adjuncts to rifabutin-modified standard therapy in adults with drug-sensitive, smear-positive pulmonary TB: (1) the mammalian target of rapamycin (mTOR) inhibitor, everolimus (0.5 mg), (2) auranofin (6 mg), (3) vitamin D3, and (4) the phosphodiesterase-4 (PDE4) inhibitor, CC-11050 (ClinicalTrials.gov Identifier: NCT02968927). A randomized clinical trial, Statins as Adjunctive Therapy for TB (StAT-TB), is currently underway to determine if pravastatin adjunctive therapy shortens the median time to sputum-culture negativity and improves lung function outcomes among HIV-infected and uninfected patients with drug-susceptible pulmonary TB (NCT03456102).

In summary, these articles cover a vast expanse of research findings based on emerging trends in combatting antimicrobial resistance using traditional and natural antimicrobials, plant and microbial derivatives and nanomaterials. Currently, AMR is a constantly growing global threat to public health worldwide and has been declared as a thrust area by World Health Organization (WHO). AMR is mediated via various mechanisms such as enzymatic degradation of drugs, alteration of antimicrobial targets, efflux of drugs, alteration of microbial membrane permeability, formation of biofilms, and persister cell states. Most of the AMR resistance genes (ARG) are disseminated via horizontal gene transfer mediated by genetic elements like plasmids, transposons, bacteriophages, and other genetic elements (Thombre et al., 2016). One of the challenges of AMR is annihilating the spread and prevalence of ARGs in the environmental resistome via plasmids. Future strategies and new lines of research need to be undertaken using conjugation inhibitors, plasmid incompatibility systems, and CRISPR/Cas-based approaches to tackle the incredibly profound multidrug resistant bacteria (Buckner et al., 2018).

AUTHOR CONTRIBUTIONS

All authors listed have made a substantial, direct and intellectual contribution to the work, and approved it for publication.

ACKNOWLEDGMENTS

We would like to thank the contributing authors for submission of their papers and reviewers for their valuable time. The Editorial guidance and suggestions of Dr. Rustam Aminov for handling this special issue is highly appreciated. RT thanks the Principal, Modern College, Shivajinagar, Pune, for providing necessary facilities.

REFERENCES

Aminov, R. I. (2010). A brief history of the antibiotic era: lessons learned and challenges for the future. *Front. Microbiol.* 1:134. doi: 10.3389/fmicb.2010.00134

Buckner, M., Ciusa, M. L., and Piddock, L. (2018). Strategies to combat antimicrobial resistance: anti-plasmid and plasmid curing. *FEMS Microbiol. Rev.* 42, 781–804. doi: 10.1093/femsre/fuy031

Dutta, N.K., Pinn, M.L., and Karakousis, P.C. (2014). Reduced emergence of isoniazid resistance with concurrent use of thioridazine against acute murine tuberculosis. *Antimicrob. Agents Chemother.* 58 4048–4053. doi: 10.1128/AAC.02981-14

Dutta, N. K., Annadurai, S., Mazumdar, K., Dastidar, S. G., Kristiansen, J. E., Molnar, J., et al. (2007). Potential management of resistant microbial infections with a novel non-antibiotic: the anti-inflammatory drug diclofenac sodium. *Int. J. Antimicrob. Agents* 30, 242–249. doi: 10.1016/j.ijantimicag.2007.04.018

Dutta, N. K., Bruiners, N., Pinn, M. L., Zimmerman, M. D., Prideaux, B., Dartois, V., et al. (2016). Statin adjunctive therapy shortens the duration of TB treatment in mice. *J. Antimicrob. Chemother.* 71, 1570–1577. doi: 10.1093/jac/dkw014

Dutta, N. K., Mehra, S., and Kaushal, D. (2010). A Mycobacterium tuberculosis sigma factor network responds to cell-envelope damage by the promising anti-mycobacterial thioridazine. *PLoS ONE* 5:e10069. doi: 10.1371/journal.pone.0010069

Emmerich, R., and Löw, O. (1899). Bakteriolytische enzyme als Ursache der erworbenen Immunität und die Heilung von Infectionskrankheiten durch dieselben. *Z. Hyg.* 31, 1–6510. doi: 10.1007/BF02206499

Fleming, A. (1929). On antibacterial action of culture of *Penicillium*, with special reference to their use in isolation of *B. influenzae*. *Br. J. Exp. Pathol.* 10, 226–236.

Frank, D. J., Horne, D. J., Dutta, N. K., Shaku, M. T., Madensein, R., Hawn, T.R., et al. (2019). Remembering the host in tuberculosis drug development. *J. Infect. Dis.* 219, 1518–1524. doi: 10.1093/infdis/jiy712

Mazumdar, K., Asok Kumar, K., and Dutta, N. K. (2010). Potential role of the cardiovascular non-antibiotic (helper compound) amlodipine in the treatment of microbial infections: scope and hope for the future. *Int. J. Antimicrob. Agents* 36, 295–302. doi: 10.1016/j.ijantimicag.2010.05.003

Mazumdar, K., Dastidar, S. G., Park, J. H., and Dutta, N. K. (2009). The anti-inflammatory non-antibiotic helper compound diclofenac: an antibacterial drug target. *Eur. J. Clin. Microbiol. Infect. Dis.* 28, 881–891. doi: 10.1007/s10096-009-0739-z

Thombre, R. S., Shinde, V., Thaiparambil, E., Zende, S., and Mehta, S. (2016) Antimicrobial activity and mechanism of inhibition of silver nanoparticles against extreme halophilic archaea. *Front. Microbiol.* 7:1424. doi: 10.3389/fmicb.2016.01424

Conflict of Interest: The authors declare that the research was conducted in the absence of any commercial or financial relationships that could be construed as a potential conflict of interest.

Copyright © 2019 Thombre, Jangid, Shukla and Dutta. This is an open-access article distributed under the terms of the Creative Commons Attribution License (CC BY). The use, distribution or reproduction in other forums is permitted, provided the original author(s) and the copyright owner(s) are credited and that the original publication in this journal is cited, in accordance with accepted academic practice. No use, distribution or reproduction is permitted which does not comply with these terms.

frontiers in Microbiology

ORIGINAL RESEARCH
published: 15 September 2017
doi: 10.3389/fmicb.2017.01767

Antimicrobial and Antibiofilm Potential of Acyclic Amines and Diamines against Multi-Drug Resistant *Staphylococcus aureus*

*Gurmeet Kaur, P. Balamurugan, Sahana Vasudevan, Saikiran Jadav and S. A. Princy**

Quorum Sensing Laboratory, Centre for Research in Infectious Diseases, School of Chemical and Biotechnology, SASTRA University, Thanjavur, India

Multi-drug resistant *Staphylococcus aureus* (MDRSA) remains a great challenge despite a decade of research on antimicrobial compounds against their infections. In the present study, various acyclic amines and diamines were chemically synthesized and tested for their antimicrobial as well as antibiofilm activity against MDRSA. Among all the synthesized compounds, an acyclic diamine, (2,2′-((butane-1,4-diylbis(azanediyl)bis(methylene))diphenol) designated as ADM 3, showed better antimicrobial activity (minimum inhibitory concentration at 50 μg/mL) and antibiofilm activity ($MBIC_{50}$ at 5 μg/mL). In addition, ADM 3 was capable of reducing the virulence factors expression (anti-virulence). Confocal laser scanning microscope analysis of the *in vitro* tested urinary catheters showed biofilm reduction as well as bacterial killing by ADM 3. On the whole, our data suggest that acyclic diamines, especially ADM 3 can be a potent lead for the further studies in alternative therapeutic approaches.

Keywords: biofilm, *Staphylococcus aureus*, multi-drug resistance, antibiofilm, diamines, antibacterial

OPEN ACCESS

Edited by:
Noton Kumar Dutta, Johns Hopkins University, United States

Reviewed by:
Pankaj Kumar, Johns Hopkins School of Medicine, United States
Divakar Sharma, Interdisciplinary Biotechnology Unit, Aligarh Muslim University, India

****Correspondence:***
S. A. Princy
adlineprinzy@biotech.sastra.edu

Specialty section:
This article was submitted to Antimicrobials, Resistance and Chemotherapy, a section of the journal Frontiers in Microbiology

Received: *12 July 2017*
Accepted: *31 August 2017*
Published: *15 September 2017*

Citation:
Kaur G, Balamurugan P, Vasudevan S, Jadav S and Princy SA (2017) Antimicrobial and Antibiofilm Potential of Acyclic Amines and Diamines against Multi-Drug Resistant Staphylococcus aureus. Front. Microbiol. 8:1767. doi: 10.3389/fmicb.2017.01767

INTRODUCTION

Staphylococcus aureus, a Gram-positive, facultative anaerobic cocci bacterium, is one of the most notorious pathogen, causing infections in humans. Their abilities to evade the host immune defense mechanism and resistance to the first and second generation antibiotics has made the pathogen a subject of interest in the scientific community (Fedtke et al., 2004). *S. aureus* is an opportunistic pathogen related to the various types of infectious diseases such as wound infections, catheter-related bloodstream infections (CRBSI), musculoskeletal infections, toxic shock syndrome and, about 20% of population worldwide found to be the long-term carrier as a part of their normal flora (Kluytmans et al., 1997; Cole et al., 2001). Various factors associated with *S. aureus* such as virulence gene expressions, cell to cell signaling mechanism, inactivation of antibiotics, alteration in target sites, efflux pumps, and biofilm formation have led to the emergence of multi-drug resistant *S. aureus* (MDRSA) (Dinges et al., 2000; Becker et al., 2003; Zhu et al., 2008; Arya et al., 2011; Qayyum et al., 2016).

Planktonic microbes attach to a particular substratum and produce an anchoring polymer called as an extracellular polysaccharide (EPS) which leads to the formation of the multicellular microbial community known as biofilm (Flemming et al., 2007). The altered metabolic activity of the cells that are associated with biofilm formation have high rates of EPS production, activation of specific genes associated with biofilm formation and virulence, reduction in the growth rate than their planktonic

counterparts (Flemming et al., 2007). Biofilm formation accounts for one of the major reasons for the emergence of multi-drug resistance (MDR) in various pathogenic microbes and is common in bacteria. In the biofilm mode of lifestyle, bacterial population acquires adaptation to tolerate and survive a wide range of diverse environmental stress such as scarce nutritional availability, antibiotics exposure, competition for survival in a multi-species environment (Parsek and Singh, 2003). The antibiotics tolerance ability of the biofilm cells complicates the treatment of various infections in humans, such as, cystic fibrosis, endocarditis, which includes biofilm formation on various biological implants such as, urinary catheters, heart catheters, various joint implants, and replacement of heart valves (Singh et al., 2000). Biofilms pose a threat to the human race because of their persistent nature and plays a major role in certain pathogenic infections (Singh et al., 2000; Ravichandiran et al., 2012; Arya and Princy, 2013; Otto, 2013). Several incidences have been reported with MDRSA strain infections such as CRBSI which is primarily due to either bacterial colonization on a device that may be intraluminal, i.e., formation of biofilm inside the lumen and causing persistent infection (Safdar and Maki, 2004). Similarly, musculoskeletal infections, wound infections, and nosocomial infections have also been reported by MDRSA which are very difficult to treat with the existing drugs (Bascones-Martinez et al., 2011; Abad et al., 2014; Vincze et al., 2014). Antibiofilm compounds are one such alternative option in the recent research focus. These small chemical ligands can independently inhibit bacterial biofilm or disrupt the biofilm matrix at the molecular level via, disturbing their metabolic pathways.

Medicinally important chemical compounds play a crucial role in treating various diseases which pose a threat to human survival at times. From our earlier reports, we have understood that acyclic amines could be promising leads against *S. aureus*, as one of our compounds (SarABI-12, 2-[(methylamino)methyl]phenol) was shown to have target specific interaction with the staphylococcal accessory regulator, SarA (Arya and Princy, 2013). In addition, our *in vitro* studies (Balamurugan et al., 2017) have confirmed the antibiofilm and anti-virulence properties against clinical *S. aureus* strains. The data also showed a significant reduction in the expression of SarA regulated virulence genes like *fnbA*, *hla*, and *hld*. It is also interesting to note that several researchers have reported the potential of cyclic amines and diamines to inhibit MDRSA, *Enterococcus* sp., *Clostridium difficile*, *Escherichia coli*, *Aspergillus oryzae*, *Aspergillus niger* (He et al., 2003; Abdel-Rahman et al., 2004; Hensler et al., 2006). The focus on the use of cyclic amines and diamines for antibacterial, antifungal and anti-proliferative activity has also been implicated (He et al., 2003; Juranić, 2014; Kazakova et al., 2014). Previous reports by Chtchigrovsky et al. (2013) shows the anti-proliferative activity of *trans-N*-heterocyclic carbene–amine–Pt(II) complexes. These complexes have the ability to bind to DNA, leading to intrastrand cross-links between two adjacent guanines and minor interstrand cross links, resulting in DNA damage and cell death (Chtchigrovsky et al., 2013). Similarly, Subík et al. (1977) report the antibacterial and antifungal activity of amine oxides due to their ability to disorganize the cellular membranes leading to cidal effects.

It is expected that similar to cyclic amines, acyclic amines can also have medicinally important biological potentials, supported by our previous works (Arya and Princy, 2013; Balamurugan et al., 2017). Hence, we have investigated the antibiofilm and antibacterial properties of acyclic amines which have not yet been explored against pathogenic bacteria.

MATERIALS AND METHODS

Synthesis of Acyclic Amine and Diamine Compounds

The acyclic amines (AAM 1–5) and acyclic diamines (ADM 1–8) compounds were synthesized by a reductive amination process (Ramachandran et al., 2010). The synthesis process of acyclic amine and diamines is shown in the **Figures 1A,B**. For the synthesis of acyclic amines, a solution of the suitable aryl aldehyde (10 mmol) and the suitable acyclic amine (12 mmol) in methanol (5 mL) was stirred at room temperature for 1 h. The reactants

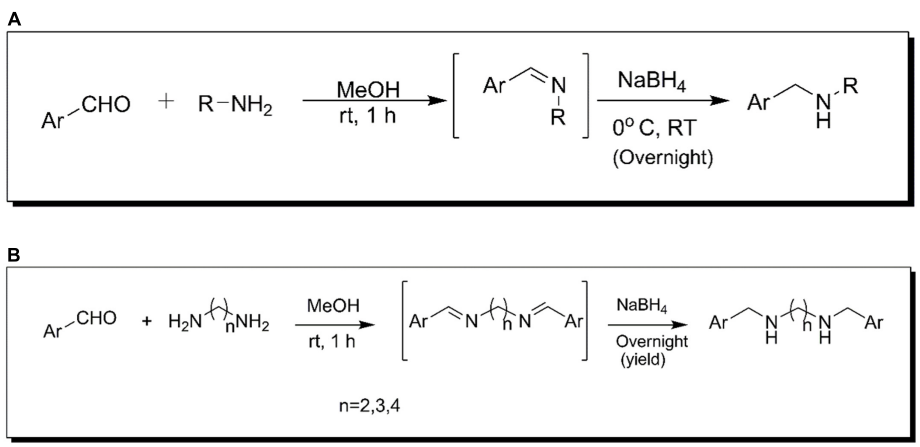

FIGURE 1 | Schematic representation of the reaction scheme for synthesis of **(A)** acyclic amines **(B)** acyclic diamines.

were shown in Supplementary Table S1. The intermediate imines were reduced to the corresponding acyclic amines and diamines by the addition of sodium borohydride (15 mmol) at the ice-cold condition. After stirring, the reaction mixture was incubated at room temperature overnight and further diluted with water and extracted thrice with dichloromethane. The mixed organic phases were dried with anhydrous sodium sulfate, evaporated to dryness under reduced pressure to obtain the acyclic amines and diamines. The structures of the synthesized products were confirmed by ^{1}H-NMR spectroscopy.

Bacterial Strains and Growth Conditions

Clinical isolates of *S. aureus* were received from the rejected urinary catheters, JSS Medical College Mysore with prior approval from the Institutional Ethical Committee (IEC/JSSMC/PG/1050/2015-16). The strains were initially subjected to screening for MDR against the antibiotics: levofloxacin, ampicillin, ciprofloxacin, and methicillin. The *S. aureus* strain (MDRSA - QSL2040) that showed resistance to methicillin as well as other tested antibiotics (**Table 1**) was used as a test strain and the *S. aureus* (ATCC 25923) was used as reference strain (Kumar et al., 2013; Khatkar et al., 2014). These strains were cultured in the cation-adjusted Mueller–Hinton broth (CAMHB) for the minimal drug dose response against the growth and bactericidal actions. For the biofilm assays, the tryptic soy broth (TSB) supplemented with 3% NaCl and 0.5% glucose was used as the biofilm medium.

Evaluation of Acyclic Amine and Diamine Compounds for MIC, MBC, and MBIC

The minimum inhibitory concentration (MIC), the minimum bactericidal concentration (MBC), and the minimum biofilm inhibitory concentrations (MBIC) of the acyclic amines and diamines were determined according to the Clinical and Laboratory Standards Institute (CLSI) with slight modifications. The *S. aureus* clinical isolate (MDRSA - QSL2040) was grown overnight in TSB. The overnight culture was diluted 1:100 in physiological saline and the bacterial suspensions were adjusted to a final inoculum size of 1×10^6 cells (Issam et al., 2015). The adjusted inoculum was added to the wells of a 96-well microtiter plate containing twofold serial dilutions of the compound (varying concentrations from 2 to 400 μg/mL as individual sets keeping different high concentrations) in CAMHB medium. The plates were incubated at 37°C for 24 h. The setup was carried out as independent experiments (in triplicates) to calculate the effective concentration.

The optical density (OD_{600}) was read immediately after inoculation and again after 18 h of incubation at 37°C, in a microtitre plate reader (iMark, Bio-Rad, Japan). The lowest concentration that inhibited growth when compared to the untreated control culture was taken as the MIC. Similarly, MBC was determined by counting the number of colonies (CFU/mL) after 24 h of incubation at 37°C and was defined as the lowest concentration at which the viable cells were reduced to a level by ≥90% in comparison to the untreated control cultures. All independent assays were carried out in triplicates.

For biofilm assay, diluted overnight culture (1:100) was inoculated in TSB and allowed to grow till it reached exponential growth phase (5 h). The culture was tested for 0.5 McFarland unit and followed by inoculation along with varying concentrations of the compounds (2–400 μg/mL) in 96-well microtitre plates. Plates were incubated for 24 h at 37°C without shaking. After incubation, the wells were washed twice with 200 μL of phosphate-buffered saline (PBS) gently to remove the non-adherent cells. Adherent cells in the biofilm were fixed by adding 200 μL of 100% methanol prior to staining with 200 μL of 0.2% (w/v) crystal violet (CV) for 20 min. The excess stain was washed twice with PBS and the plates were air dried. The bound CV in the air dried plates were eluted with 200 μL of 33% acetic acid. The biofilm was quantitatively determined by measuring the absorbance at $OD_{595\ nm}$ in a microtitre plate reader (iMark, Bio-Rad, Japan). The concentration at which the formation of biofilm is inhibited ≥50% when compared to the untreated control culture is defined as $MBIC_{50}$ and ≥90% is $MBIC_{90}$. All the assays were carried out in triplicates.

TABLE 1 | Antibiotic susceptibility profiling of the two strains used in the study.

Antibiotics	Strains used	
	ATCC 25923	QSL2040
Levofloxacin	Sensitive	Resistant
Ampicillin	Sensitive	Resistant
Ciprofloxacin	Sensitive	Resistant
Methicillin	Sensitive	Resistant
Amoxicillin	Sensitive	Resistant
Penicillin	Sensitive	Resistant
Kanamycin	Sensitive	Resistant
Gentamicin	Sensitive	Resistant
Clindamycin	Sensitive	Intermediate
Vancomycin	Sensitive	Resistant
Oxacillin	Sensitive	Intermediate

Sensitivity/resistance pattern was concluded as per the CLSI guidelines.

Anti-virulence Assays

Among the synthesized compounds, ADM 3 was selected as it showed higher antibiofilm activity at minimal concentration. The compound, ADM 3 was tested against the clinical isolate of *S. aureus* with two sub-$MBIC_{50}$ concentrations (i.e., ¼× $MBIC_{50}$, ½× $MBIC_{50}$) and at a higher $MBIC_{50}$ concentration (2× $MBIC_{50}$). *S. aureus* reference strain, untreated with ADM 3 was kept as control. After 24 h, the cultures were centrifuged at 6000 rpm for 10 min at 4°C and filter sterilized in a 0.22 μm filter paper to collect the cell free supernatant. The collected supernatant was stored at 4°C and further used to quantify hemolysin and protease (Pietrow et al., 2013) among the various secreted exotoxins by *S. aureus*.

Hemolytic Assay

Hemolysin in the culture supernatant was quantified according to the procedure described earlier with slight modifications

(Cheung and Otto, 2012). Briefly, 10 mL of sheep blood was centrifuged at 2400 rpm for 5 min and the pellet obtained was washed twice with 10 mL of PBS. Ten microliters of this erythrocyte suspension was incubated with the cell free supernatant for 1 h at 37°C. Finally, the incubated sample was centrifuged at 2400 rpm for 5 min. Erythrocyte suspension treated with 1% Triton X-100 was used as a positive control. The optical density of the supernatant was read at 540 nm. Water along with the erythrocyte suspension was considered as blank. The percentage (%) hemolysis was calculated using the following formula:

$$\%\text{Hemolysis} = \text{absorbance (sample)} - \text{absorbance (blank)} / \text{absorbance (positive control)}$$

Proteolysis Assay

Quantitative estimation of the protease was carried out with azocasein assay. A total of 200 μL of the cell free supernatant was incubated with 800 μL of azocasein for 30 min at 37°C. To this, 1200 μL of 1% trichloroacetic acid was added to arrest the enzymatic reaction. The contents were incubated on ice for 30 min and centrifuged at 12,000 rpm for 5 min. To 1600 μL of the supernatant 400 μL of 1.8 N NaOH was added and the optical density was read at 420 nm against the blank (azocasein + TCA + NaOH). The amount of enzyme required to digest 1 mg of azocasein per minute is known as 1 unit of protein activity (Pietrow et al., 2013). The percentage (%) proteolysis was calculated using the following formula:

$$\%\text{Proteolysis} = \text{absorbance (sample)} - \text{absorbance (blank)} / \text{absorbance (control)}$$

Appraisal of the Therapeutic Challenge of ADM 3 on *S. aureus* Using an *In Vitro* Catheter Model

An *in vitro* catheter model was used to evaluate the effect of ADM 3 on biofilm formation in hydrodynamic conditions (Hancock et al., 2010). Silicone catheter segments of 20 mm length were cut vertically into two halves, sterilized in 0.5% sodium hypochlorite solution followed by washing with sterilized water. The sterilized catheters were placed in a six-well microtitre plate and the surface was coated with human blood plasma by incubation at 37°C for 24 h. Subsequently, the plasma was removed from the wells and the coated catheters were subjected for the establishment of *S. aureus* infection followed by treatment with ADM 3 for 7 days with concentrations of ¼× $MBIC_{50}$, ½× $MBIC_{50}$, $MBIC_{50}$, and 2× $MBIC_{50}$. The plates were incubated at 37°C for 24 h with shaking at 120 rpm. After 24 h of incubation, the medium was changed along with a fresh dosage of the drug each time and this was repeated for 7 days. Also, at every 24 h interval, the catheters from the wells were removed and analyzed for the viability of cells (Weiss et al., 2009). Briefly, the viability of cells from the catheters was processed by immersing the catheters individually into sterile PBS and followed by sonication. The adherent cells recovered in PBS were plated for colony count in TSB agar plates. Microscopy imaging was used to visually analyze the effect of ADM 3 on biofilm removal. The cells were stained with fluorescein isothiocyanate (5 mg/mL) and ethidium bromide (1.25 mg/mL) prepared by mixing 5 μL each of the dyes in 1 mL of cold 0.9% NaCl solution. The samples were incubated for 10 min, and then the excess dye was removed by washing with 0.9% NaCl. All the stained samples were imaged using Olympus FV 1000 confocal microscope with a 10× objective of numerical aperture 0.3. The stained samples were excited at 488 nm using Multi Argon LASER and images were collected from four randomly chosen spots from the sample surface.

Cytotoxicity Analysis of ADM 3 on HEp-2 Cells

Cell viability was assessed by MTT assay. The reduction of MTT is catalyzed by mitochondrial dehydrogenase enzymes and thus considered to be a measure of cell viability. HEp-2 cells were seeded to each well in a 96-well microtiter plate (1×10^5 cells), in 100 μL of DMEM growth medium and the plate was incubated at 37°C for 24 h. After incubation, the fresh growth medium was replaced in the wells. ADM 3 was diluted from an original stock to obtain a concentration of 200 μg/mL. The HEp-2 cells were incubated with ADM 3 and allowed to adhere for a period of 72 h. A total of 10 μL of MTT solution (5 mg/mL in 1× PBS) was added to each well and the plate was incubated in dark for 4 h at 37°C. Further, the content of the each well was removed and the formazan crystals were dissolved in 200 μL of dimethyl sulfoxide (DMSO) solution per well. The absorbance was measured at 590 nm using ELISA plate reader. Only the interior rows of the microtiter plate were used for these experiments to minimize the variations in cell viability due to medium evaporation at the periphery site. The percentage cell viability was calculated with reference to the untreated control cells. The experiment was conducted twice in quadruplicates.

$$\text{Percentage cell viability} = \frac{\text{OD of drug treated sample} - \text{OD of blank}}{\text{OD of control} - \text{OD of blank}} \times 100$$

Statistical Analysis

Graph pad prism software (version 6.01) was used for statistical analysis. One-way ANOVA and multiple comparisons were done. The minimum level of significance was set at $P \leq 0.05$. All the assays were conducted in triplicates and the results were expressed as mean ± SD.

RESULTS

Synthesis of Acyclic Amines and Diamines

The spectral data of all the synthesized compounds were in full agreement with the proposed structures (Supplementary

Table S1). The ^{1}H-NMR data for the synthesized compounds are given below.

AAM 1: *N*-(naphthalene-2-ylmethyl)butan-1-amine

Isolated yield = 78%,^{1}H NMR (300 MHz, $CDCl_3$) δ 8.12 (d, J = 8.3 Hz, 1H), 7.90–7.83 (m, 1H), 7.77 (d, J = 7.9 Hz, 1H), 7.59–7.38 (m, 4H), 4.24 (s, 2H), 2.81–2.71 (m, 2H), 1.61 (s, 1H), 1.52 (dd, J = 8.2, 6.1 Hz, 2H), 1.38 (dq, J = 14.1, 7.1 Hz, 2H), 0.93 (t, J = 7.3 Hz, 3H).

AAM 2: (*N*-benzylbutan-1-amine)

Isolated yield = 55%, ^{1}H NMR (300 MHz, $CDCl_3$) δ 7.38–7.19 (m, 5H), 3.79 (s, 2H), 2.63 (t, J = 7.2 Hz, 2H), 1.76 (s, 1H), 1.50 (dt, J = 14.4, 7.0 Hz, 2H), 1.40–1.24 (m, 2H), 0.91 (t, J = 7.2 Hz, 3H).

AAM 3: (*N*-benzylcyclohexanamine)

Isolated yield = 71%, ^{1}H NMR (300 MHz, $CDCl_3$) δ 7.36–7.22 (m, 5H), 3.81 (s, 2H), 2.53–2.44 (m, 1H), 1.31–1.06 (m, 11H).

AAM 4: 4(*N*-(4-methoxybenzyl)butan-1-amine)

Isolated yield = 65%, ^{1}H NMR (300 MHz, $CDCl_3$) δ 7.28 – 7.22 (m, 2H), 6.91 – 6.81 (m, 2H), 3.79 (s, 3H), 3.74 (s, 2H), 2.66 – 2.58 (m, 2H), 2.49 (s, 1H), 1.52 (ddd, J = 14.4, 8.3, 5.9 Hz, 2H), 1.34 (dd, J = 15.1, 7.4 Hz, 2H), 0.90 (t, J = 7.3 Hz, 3H).

AAM 5: (*N*-(4-chlorobenzyl)butan-1-amine)

Isolated yield = 73%, ^{1}H NMR (300 MHz, $CDCl_3$) δ 7.33–7.21 (m, 4H), 3.75 (s, 2H), 2.64–2.57 (m, 2H), 1.68 (s, 1H), 1.55–1.43 (m, 2H), 1.40–1.27 (m, 2H), 0.91 (t, J = 7.3 Hz, 3H).

ADM 1: 2,2^1-((Ethane-1,2-diylbis(azanediyl)bis(methylene)) diphenol

Yield 72%, ^{1}H-NMR (DMSO-d_6, 300 MHz): δ 2.51 (s, 4H), 3.79 (s, 4H), 6.68–6.73 (m, 4H), 7.03–7.08 (m, 4H).

ADM 2: 2,2′-((Propane-1,3-diylbis(azanediyl)bis(methylene)) diphenol

Yield 79%, ^{1}H-NMR (DMSO-d_6, 300 MHz): δ 1.63 (quin, J = 6.9 Hz, 2H), 2.55 (t, J = 6.9 Hz, 4H), 3.80 (s, 4H), 6.67–6.72 (m, 4H), 7.03–7.08 (m, 4H).

ADM 3: 2,2^1-((Butane-1,4-diylbis(azanediyl)bis(methylene)) diphenol

Yield 69%, ^{1}H-NMR (DMSO-d_6, 300 MHz): δ 1.47 (s, 4H), 2.50 (q, J = 1.8 Hz, 4H), 3.81 (s, 4H), 6.66–6.72 (m, 4H), 7.03–7.09 (m, 4H).

ADM 4: N^1,N^2-dibenzylethane-1,2-diamine

Yield 82%, ^{1}H-NMR (DMSO-d_6, 300 MHz): δ 2.51 (s, 4H), 3.66 (s, 4H), 7.20–7.32 (m, 10H).

ADM 5: N^1,N^2-dibenzylpropane-1, 3-diamine

Yield 73%, ^{1}H-NMR ($CDCl_3$, 300 MHz): δ 1.72 (quin, J = 6.9 Hz, 2H), 2.69 (t, J = 6.9 Hz, 4H), 3.77 (s, 4H), 7.24–7.32 (m, 10H).

ADM 6: N^1,N^2-bis(naphthalene-2-ylmethyl)ethane-1,2-diamine

Yield 76%, ^{1}H-NMR (DMSO-d_6, 300 MHz): δ 2.75 (s, 4H), 4.11 (s, 4H), 7.40–7.52 (m, 8H), 7.80 (d, J = 7.5 Hz, 2H), 7.89–7.92 (m, 2H), 8.13–8.17 (m, 2H).

TABLE 2 | Antimicrobial and antibiofilm values of acyclic amines and diamines.

Compound	MIC (μg/mL)	MBC (μg/mL)	MBIC (μg/mL)	
			50	90
AAM 1	200	200	–	–
AAM 2	200	200	–	–
AAM 3	–	–	–	–
AAM 4	100	200	–	–
AAM 5	–	200	–	–
ADM 1	200	200	–	–
ADM 2	–	50	10	–
ADM 3	50	200	5	–
ADM 4	–	–	25	–
ADM 5	–	200	20	–
ADM 6	–	–	40	–
ADM 7	–	–	40	–
ADM 8	150	–	–	–

ADM 7: N^1,N^3-bis(naphthalene-2-ylmethyl)propane-1,3-diamine

Yield 78%, ^{1}H-NMR ($CDCl_3$, 300 MHz): δ 1.61 (t, J = 6.3 Hz, 4H), 2.76 (t, J = 6.3 Hz, 4H), 4.22 (s, 4H), 7.41–7.55 (m, 8H), 7.76 (d, J = 7.5 Hz, 2H), 7.86 (d, J = 7.5 Hz, 2H), 8.10 (d, J = 7.8 Hz, 2H).

ADM 8: N^1-(naphthalene-2-yl)–N^4-(naphthalene-2-ylmethyl) butane-1,4-diamine

Yield 80%, ^{1}H-NMR (DMSO-d_6, 300 MHz): δ 1.83 (quin, J = 6.9 Hz, 2H), 2.83 (t, J = 6.9 Hz, 4H), 4.21 (s, 4H), 7.37–7.52 (m, 8H), 7.76 (dd, J = 7.5, 1.8 Hz, 2H), 7.85–7.88 (m, 2H), 8.07–8.11 (m, 2H).

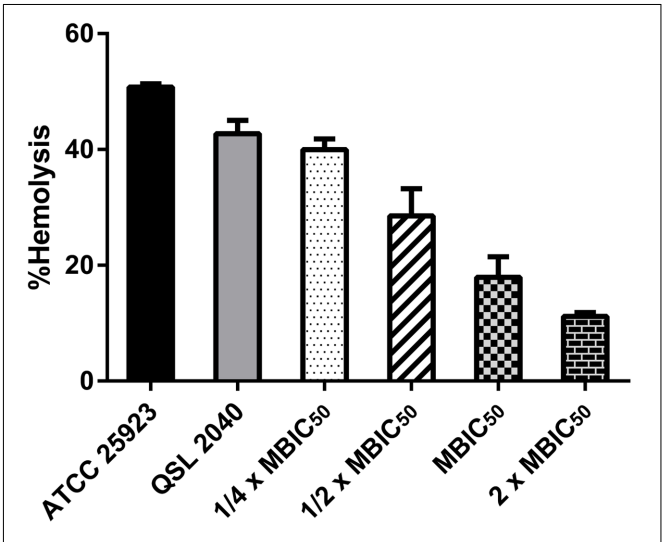

FIGURE 2 | Effect of ADM 3 on hemolysin production in *S. aureus* (ATCC 25923—reference strain; QSL2040—clinical isolate). The concentrations used were ¼× $MBIC_{50}$ (1.25 μg/mL), ½× $MBIC_{50}$ (2.5 μg/mL), $MBIC_{50}$ (5 μg/mL), and 2× $MBIC_{50}$ (10 μg/mL).

Antimicrobial and Antibiofilm Activity of Acyclic Amines and Diamines

The MICs, MBCs, and MBICs of acyclic amines and diamines were shown in **Table 2**. In general, acyclic amines were found to have high MIC and MBC values but no antibiofilm activity. Alternatively, the acyclic diamine compounds, particularly ADM 3 was observed to exhibit good antimicrobial as well as antibiofilm activity. The concentration of antimicrobial and antibiofilm activity of ADM 3 was found to be 50 and 5 μg/mL ($MBIC_{50}$) respectively. The biofilm inhibitory concentration for compound ADM 3 was found to be 10-fold lesser than the MIC. Thus, compound ADM 3 acts as a potential antibacterial as well as antibiofilm agent and was considered for further studies.

Anti-virulence Assays

Percentage hemolysis and proteolysis by ADM 3 on *S. aureus* clinical isolate, MDRSA - QSL2040 are shown in **Figures 2**, **3** respectively. ADM 3 exhibited a similar effect on protease as well as on hemolysin production and a dose-dependent reduction was observed in both the cases. Clinical isolate (MDRSA - QSL2040) treated with ADM 3 showed a significant reduction in proteolytic and hemolytic activity when compared with the untreated control.

In Vitro Catheter Model

Live dead staining of *S. aureus* in the presence and absence of ADM 3 revealed that, ADM 3 treatment induced significant loss of viability and colonization of biofilm on catheters as evidenced by the red fluorescence observed in treated samples at day 7. All the captured images were uniform and a representative image is shown in **Figure 4**. Thus, in consonance with our antibiofilm results in microtitre plate experiments, ADM 3 was effective in inhibition of *S. aureus* biofilm in catheters. The treatment of these catheters showed a decrease in the cell count from day 4 onward compared to untreated control (Supplementary Figure S1).

Cytotoxicity Analysis on HEp-2 Cell Lines

Percentage cell viability of each experimental group was calculated with reference to the untreated control cells and it was observed that cell viability was higher than 85% in all drug doses (**Figure 5**). Statistical analysis was performed using the one way ANOVA and $P \leq 0.001$ was considered significant.

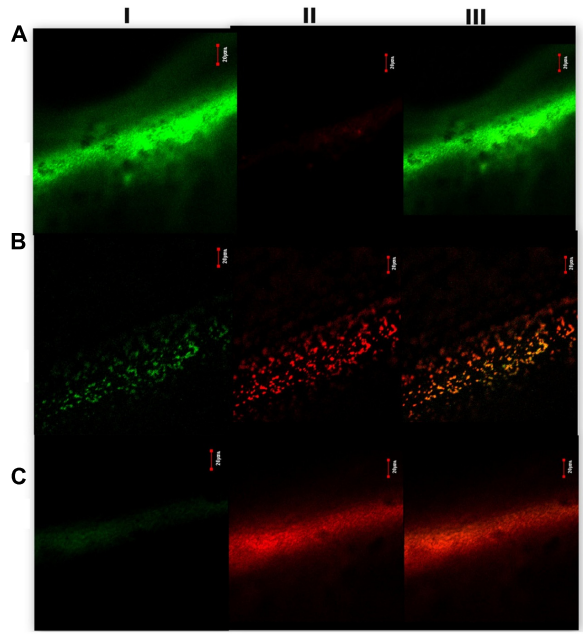

FIGURE 4 | Confocal laser scanning microscope images of biofilm formed on urinary catheters. I—FITC labeled (green/viable cells); II—ethidium bromide labeled (red/non-viable cells); and III—superimposed images of I and II. **(A)** Control, untreated with ADM 3, **(B)** treated with ADM 3 ($MBIC_{50}$ at 5 μg/mL), and **(C)** treated with ADM 3 (2× $MBIC_{50}$ at 10 μg/mL).

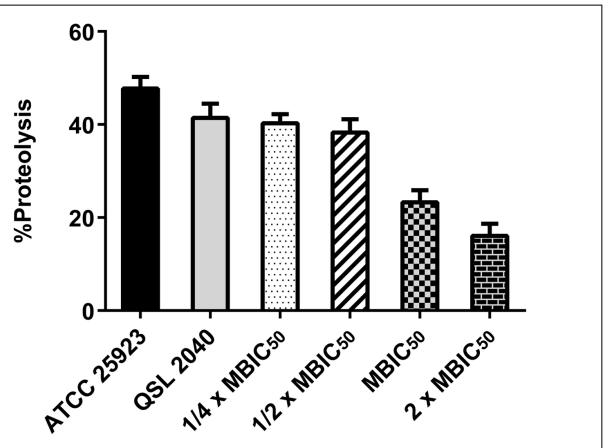

FIGURE 3 | Effect of ADM 3 on protease production in *S. aureus* (ATCC 25923—reference strain; QSL2040—clinical isolate). The concentrations used were ¼× $MBIC_{50}$ (1.25 μg/mL), ½× $MBIC_{50}$ (2.5 μg/mL), $MBIC_{50}$ (5 μg/mL), and 2× $MBIC_{50}$ (10 μg/mL).

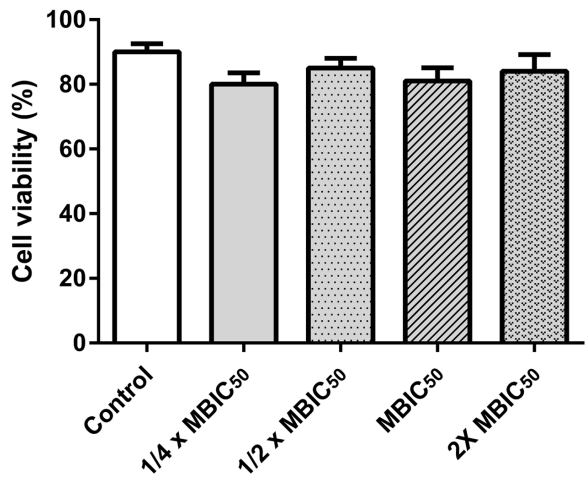

FIGURE 5 | Effect of ADM 3 on HEp-2 cell lines for cell viability by MTT assay. The concentrations used were ¼× $MBIC_{50}$ (1.25 μg/mL), ½× $MBIC_{50}$ (2.5 μg/mL), $MBIC_{50}$ (5 μg/mL), and 2× $MBIC_{50}$ (10 μg/mL).

DISCUSSION

The key consequences of biofilm based infections are resistant to antibiotics as well as many other conventional antimicrobial agents. This eventually leads to the development of MDR pathogens with an extreme capacity for evading the host defense mechanisms. It is well known that bacterial biofilm exhibits antibiotic diffusion barrier (Cloete, 2003). In such cases, a large portion of the cells embedded in biofilms might escape from both antibiotic treatments as well as host's immune system responses. Such bacterial cells lead to the replenishment of biofilm at a new site causing are occurrence of infection with high resistance to antibiotics. Consequently, it becomes difficult to treat the infection using bactericidal drugs via systemic administration and demands the need for the evaluation of novel antibiofilm drugs. As an alternative to conventional antibiotic therapy and to control MDR, we hereby report a series of acyclic amines and diamines as potential drug candidates in the light of our earlier studies (Arya and Princy, 2013; Balamurugan et al., 2017). Among these, ADM 3 (2,2′-((butane-1,4-diylbis(azanediyl)bis(methylene))diphenol) showed a significant reduction in bacterial cell count as well as biofilm inhibition.

Targeting virulence factors in bacteria is an alternative approach to antimicrobial therapy that offers promising insights and opportunities to inhibit bacterial pathogenesis (Kauppi et al., 2003; Åberg and Almqvist, 2007). Certain virulence factors have been shown as potential leads for drug design and therapeutic intervention, whereas new possible insights are crucial for exploring others (Projan, 2002). Among the various virulence factors expressed in *S. aureus*, protease, as well as hemolysin production, plays a crucial role in the interaction of bacteria with the host cell for establishing an infection (Kupferwasser et al., 2003). In the present study, ADM 3 that showed effective $MBIC_{50}$ and MIC was also effective in reducing protease as well as hemolysin production.

In vitro catheter model showed decreased biofilm as well as increased red fluorescence in the confocal laser scanning microscope images at day 7. This suggests that ADM 3 has both antimicrobial and antibiofilm activities. In addition, decreased cell count observed after day 4 till the experimental study period also suggests the potential of ADM 3. This implies that the ADM 3 was proven to show a potent biofilm inhibiting agent as well as an antimicrobial agent. It is already shown through our *in silico* studies that the hydroxyl and amine groups of the compound SarABI-12, interact with the oxygen atoms of E89 and R90 of SarA protein respectively, to form hydrogen bonds (Arya and Princy, 2013). Moreover, our *in vitro* studies also have confirmed the antibiofilm activities by the target specific interaction with SarA, which is a quorum regulator of *S. aureus*. Since ADM 3 is a derivative of SarABI-12, which carries both the hydroxyl and amine groups, it is speculated that the biofilm inhibition activity also could be of the similar mechanism.

Furthermore, a therapeutic molecule should not have cytotoxic effects if it has to be taken for further clinical trials. Generally, a compound is usually considered to have *in vitro* cytotoxicity if the particular concentration of the drug causes a 50% cell killing. Our data suggest that the compound ADM 3 may act as a potential drug which does not cause any cytotoxicity. To the best of our knowledge, our study is the first to report the antimicrobial and antibiofilm activity of acyclic amines and diamines. Our data also provide an insight that these compounds can act as a potential drug candidate to treat MDRSA. It would be interesting to explore the activity of these organic molecules at the molecular level to depict their mode of action involved in antibiofilm and antibacterial activity.

AUTHOR CONTRIBUTIONS

All authors listed have made a substantial, direct and intellectual contribution to the work, and approved it for publication.

ACKNOWLEDGMENTS

We sincerely acknowledge the management and Dr. S. Swaminathan, Dean Sponsored Research of SASTRA University for their support and encouragement throughout this project. The authors are also grateful to the TRR in-house funding scheme of SASTRA University for the purchase of consumables.

SUPPLEMENTARY MATERIAL

The Supplementary Material for this article can be found online at: http://journal.frontiersin.org/article/10.3389/fmicb.2017.01767/full#supplementary-material

REFERENCES

Abad, C. L., Pulia, M. S., Krupp, A., and Safdar, N. (2014). Reducing transmission of methicillin-resistant *Staphylococcus aureus* and vancomycin-resistant *Enterococcus* in the ICU—an update on prevention and infection control practices. *JCOM* 21, 218–232.

Abdel-Rahman, A. H., Keshk, E. M., Hanna, M. A., and El-Bady, S. M. (2004). Synthesis and evaluation of some new spiro indoline-based heterocycles as potentially active antimicrobial agents. *Bioorg. Med. Chem.* 12, 2483–2488. doi: 10.1016/j.bmc.2003.10.063

Åberg, V., and Almqvist, F. (2007). Pilicides—small molecules targeting bacterial virulence. *Org. Biomol. Chem.* 5, 1827–1834. doi: 10.1039/B702397A

Arya, R., Kannan, R. V., Shrivastava, S., and Princy, S. (2011). Studies on the effect of amino acids to curb the pathogenesis of multi drug resistant *Staphylococcus aureus*. *Asian J. Chem.* 23, 4295–4298.

Arya, R., and Princy, S. (2013). Computational approach to design small molecule inhibitors and identify SarA as a potential therapeutic candidate. *Med. Chem. Res.* 22, 1856–1865. doi: 10.1007/s00044-012-0185-9

Balamurugan, P., Praveen Krishna, V., Bharath, D., Lavanya, R., Vairaprakash, P., and Adline Princy, S. (2017). *Staphylococcus aureus* quorum regulator SarA targeted compound, 2-[(Methylamino)methyl]phenol inhibits biofilm and down-regulates virulence genes. *Front. Microbiol.* 8:1290. doi: 10.3389/fmicb.2017.01290

Bascones-Martinez, A., Matesanz-Perez, P., Escribano-Bermejo, M., Gonzalez-Moles, M. A., Bascones-Ilundain, J., and Meurman, J. H. (2011). Periodontal

disease and diabetes-review of the Literature. *Med. Oral Patol. Oral Cir. Bucal* 16, e722–e729. doi: 10.4317/medoral.17032

Becker, K., Friedrich, A. W., Lubritz, G., Weilert, M., Peters, G., and Von Eiff, C. (2003). Prevalence of genes encoding pyrogenic toxin superantigens and exfoliative toxins among strains of *Staphylococcus aureus* isolated from blood and nasal specimens. *J. Clin. Microbiol.* 41, 1434–1439. doi: 10.1128/JCM.41.4.1434-1439.2003

Cheung, G. Y. C., and Otto, M. (2012). The potential use of toxin antibodies as a strategy for controlling acute *Staphylococcus aureus* infections. *Expert Opin. Ther. Targets* 16, 601–612. doi: 10.1517/14728222.2012.682573

Chtchigrovsky, M., Eloy, L., Jullien, H., Saker, L., Ségal-Bendirdjian, E., Poupon, J., et al. (2013). Antitumor trans-N-heterocyclic carbene-amine-Pt(II) complexes: synthesis of dinuclear species and exploratory investigations of DNA binding and cytotoxicity mechanisms. *J. Med. Chem.* 56, 2074–2086. doi: 10.1021/jm301780s

Cloete, T. E. (2003). Resistance mechanisms of bacteria to antimicrobial compounds. *Int. Biodeterior. Biodegradation* 51, 277–282. doi: 10.1016/S0964-8305(03)00042-8

Cole, A. M., Tahk, S., Oren, A., Yoshioka, D., Kim, Y.-H., Park, A., et al. (2001). Determinants of *Staphylococcus aureus* nasal carriage. *Clin. Diagn. Lab. Immunol.* 8, 1064–1069. doi: 10.1128/CDLI.8.6.1064-1069.2001

Dinges, M. M., Orwin, P. M., and Schlievert, P. M. (2000). Exotoxins of *Staphylococcus aureus*. *Clin. Microbiol. Rev.* 13, 16–34. doi: 10.1128/CMR.13.1.16-34.2000

Fedtke, I., Götz, F., and Peschel, A. (2004). Bacterial evasion of innate host defenses–the *Staphylococcus aureus* lesson. *Int. J. Med. Microbiol.* 294, 189–194. doi: 10.1016/j.ijmm.2004.06.016

Flemming, H.-C., Neu, T. R., and Wozniak, D. J. (2007). The EPS matrix: the house of biofilm cells. *J. Bacteriol.* 189, 7945–7947. doi: 10.1128/JB.00858-07

Hancock, V., Dahl, M., and Klemm, P. (2010). Abolition of biofilm formation in urinary tract *Escherichia coli* and *Klebsiella* isolates by metal interference through competition for fur. *Appl. Environ. Microbiol.* 76, 3836–3841. doi: 10.1128/AEM.00241-10

He, Y., Wu, B., Yang, J., Robinson, D., Risen, L., Ranken, R., et al. (2003). 2-Piperidin-4-yl-benzimidazoles with broad spectrum antibacterial activities. *Bioorg. Med. Chem. Lett.* 13, 3253–3256. doi: 10.1016/S0960-894X(03)00661-9

Hensler, M. E., Bernstein, G., Nizet, V., and Nefzi, A. (2006). Pyrrolidine bis-cyclic guanidines with antimicrobial activity against drug-resistant Gram-positive pathogens identified from a mixture-based combinatorial library. *Bioorg. Med. Chem. Lett.* 16, 5073–5079. doi: 10.1016/j.bmcl.2006.07.037

Issam, A.-A., Zimmermann, S., Reichling, J., and Wink, M. (2015). Pharmacological synergism of bee venom and melittin with antibiotics and plant secondary metabolites against multi-drug resistant microbial pathogens. *Phytomedicine* 22, 245–255. doi: 10.1016/j.phymed.2014.11.019

Juranić, I. O., Tošić, A. V., Kolundžija, B., and Drakuliæ, B. J. (2014). Antiproliferative activity of the Michael adducts of aroylacrylic acids and cyclic amines. *Mol. Divers.* 18, 577–592. doi: 10.1007/s11030-014-9528-4

Kauppi, A. M., Nordfelth, R., Uvell, H., Wolf-Watz, H., and Elofsson, M. (2003). Targeting bacterial virulence: inhibitors of type III secretion in *Yersinia*. *Chem. Biol.* 10, 241–249. doi: 10.1016/S1074-5521(03)00046-2

Kazakova, O. B., Giniyatullina, G. V., Medvedeva, N. I., Lopatina, T. V., Baikova, I. P., Tolstikov, G. A., et al. (2014). Synthesis and cytotoxicity of triterpene seven-membered cyclic amines. *Russ. J. Bioorganic Chem.* 40, 198–205. doi: 10.1134/S106816201402006X

Khatkar, A., Nanda, A., Kumar, P., and Narasimhan, B. (2014). Synthesis, antimicrobial evaluation and QSAR studies of p-coumaric acid derivatives. *Arab. J. Chem.* 10, S3804–S3815. doi: 10.1016/j.arabjc.2014.05.018

Kluytmans, J., Van Belkum, A., and Verbrugh, H. (1997). Nasal carriage of *Staphylococcus aureus*: epidemiology, underlying mechanisms, and associated risks. *Clin. Microbiol. Rev.* 10, 505–520.

Kumar, M., Narasimhan, B., Ramasamy, K., Mani, V., Mishra, R. K., and Majeed, A. B. A. (2013). Synthesis, antimicrobial and cytotoxic evaluation of 4-(1-aryl-5-halo-2-oxo-1, 2-dihydro-indol-3-ylideneamino)-N-substituted benzene sulphonamides. *Arab. J. Chem.* 10, S2845–S2852. doi: 10.1016/j.arabjc.2013.11.009

Kupferwasser, L. I., Yeaman, M. R., Nast, C. C., Kupferwasser, D., Xiong, Y.-Q., Palma, M., et al. (2003). Salicylic acid attenuates virulence in endovascular infections by targeting global regulatory pathways in *Staphylococcus aureus*. *J. Clin. Invest.* 112, 222–233. doi: 10.1172/JCI200316876

Otto, M. (2013). Staphylococcal infections: mechanisms of biofilm maturation and detachment as critical determinants of pathogenicity. *Annu. Rev. Med.* 64, 175–188. doi: 10.1146/annurev-med-042711-140023

Parsek, M., and Singh, P. (2003). Bacterial biofilms: an emerging link to disease pathogenesis. *Annu. Rev. Microbiol.* 57, 677–701. doi: 10.1146/annurev.micro.57.030502.090720

Pietrow, O., Panek, A., and Synowiecki, J. (2013). Extracellular proteolytic activity of *Deinococcus geothermalis*. *Afr. J. Biotechnol.* 12, 4020–4027.

Projan, S. J. (2002). New (and not so new) antibacterial targets–from where and when will the novel drugs come? *Curr. Opin. Pharmacol.* 2, 513–522. doi: 10.1016/S1471-4892(02)00197-2

Qayyum, S., Sharma, D., Bisht, D., and Khan, A. U. (2016). Protein translation machinery holds a key for transition of planktonic cells to biofilm state in *Enterococcus faecalis*: a proteomic approach. *Biochem. Biophys. Res. Commun.* 474, 652–659. doi: 10.1016/j.bbrc.2016.04.145

Ramachandran, P., Gagare, P., Sakavuyi, K., and Clark, P. (2010). Reductive amination using ammonia borane. *Tetrahedron Lett.* 51, 3167–3169. doi: 10.1016/j.tetlet.2010.04.014

Ravichandiran, V., Shanmugam, K., Anupama, K., Thomas, S., and Princy, A. (2012). Structure-based virtual screening for plant-derived SdiA-selective ligands as potential antivirulent agents against uropathogenic *Escherichia coli*. *Eur. J. Med. Chem.* 48, 200–205. doi: 10.1016/j.ejmech.2011.12.015

Safdar, N., and Maki, D. G. (2004). The pathogenesis of catheter-related bloodstream infection with noncuffed short-term central venous catheters. *Intensive Care Med.* 30, 62–67. doi: 10.1007/s00134-003-2045-z

Singh, P., Schaefer, A., Parsek, M., and Moninger, T. (2000). Quorum-sensing signals indicate that cystic fibrosis lungs are infected with bacterial biofilms. *Nature* 407, 762–764. doi: 10.1038/35037627

Subík, J., Takácsová, G., Psenák, M., and Devínsky, F. (1977). Antimicrobial activity of amine oxides: mode of action and structure-activity correlation. *Antimicrob. Agents Chemother.* 12, 139–146. doi: 10.1128/AAC.12.2.139

Vincze, S., Stamm, I., Kopp, P. A., Hermes, J., Adlhoch, C., Semmler, T., et al. (2014). Alarming proportions of methicillin-resistant *Staphylococcus aureus* (MRSA) in wound samples from companion animals, Germany 2010–2012. *PLOS ONE* 9:e85656. doi: 10.1371/journal.pone.0085656

Weiss, E. C., Spencer, H. J., Daily, S. J., Weiss, B. D., and Smeltzer, M. S. (2009). Impact of sarA on antibiotic susceptibility of *Staphylococcus aureus* in a catheter-associated in vitro model of biofilm formation. *Antimicrob. Agents Chemother.* 53, 2475–2482. doi: 10.1128/AAC.01432-08

Zhu, J., Lu, C., Standland, M., Lai, E., Moreno, G. N., Umeda, A., et al. (2008). Single mutation on the surface of *Staphylococcus aureus* Sortase A can disrupt its dimerization. *Biochemistry* 47, 1667–1674. doi: 10.1021/bi7014597

Conflict of Interest Statement: The authors declare that the research was conducted in the absence of any commercial or financial relationships that could be construed as a potential conflict of interest.

Copyright © 2017 Kaur, Balamurugan, Vasudevan, Jadav and Princy. This is an open-access article distributed under the terms of the Creative Commons Attribution License (CC BY). The use, distribution or reproduction in other forums is permitted, provided the original author(s) or licensor are credited and that the original publication in this journal is cited, in accordance with accepted academic practice. No use, distribution or reproduction is permitted which does not comply with these terms.

frontiers in Microbiology

ORIGINAL RESEARCH
published: 04 October 2017
doi: 10.3389/fmicb.2017.01868

Boeravinone B, A Novel Dual Inhibitor of NorA Bacterial Efflux Pump of *Staphylococcus aureus* and Human *P*-Glycoprotein, Reduces the Biofilm Formation and Intracellular Invasion of Bacteria

*Samsher Singh[1,2], Nitin P. Kalia[1†], Prashant Joshi[2,3], Ajay Kumar[4], Parduman R. Sharma[2,4], Ashok Kumar[2,4], Sandip B. Bharate[2,3] and Inshad A. Khan[1,2]**

[1] Clinical Microbiology Division, Indian Institute of Integrative Medicine (CSIR), Jammu, India, [2] Academy of Scientific and Innovative Research (AcSIR), Indian Institute of Integrative Medicine (CSIR), Jammu, India, [3] Medicinal Chemistry Division, Indian Institute of Integrative Medicine (CSIR), Jammu, India, [4] Cancer Pharmacology Division, Indian Institute of Integrative Medicine (CSIR), Jammu, India

This study elucidated the role of boeravinone B, a NorA multidrug efflux pump inhibitor, in biofilm inhibition. The effects of boeravinone B plus ciprofloxacin, a NorA substrate, were evaluated in NorA-overexpressing, wild-type, and knocked-out *Staphylococcus aureus* (SA-1199B, SA-1199, and SA-K1758, respectively). The mechanism of action was confirmed using the ethidium bromide accumulation and efflux assay. The role of boeravinone B as a human *P*-glycoprotein (*P*-gp) inhibitor was examined in the LS-180 (colon cancer) cell line. Moreover, its role in the inhibition of biofilm formation and intracellular invasion of *S. aureus* in macrophages was studied. Boeravinone B reduced the minimum inhibitory concentration (MIC) of ciprofloxacin against *S. aureus* and its methicillin-resistant strains; the effect was stronger in SA-1199B. Furthermore, time–kill kinetics revealed that boeravinone B plus ciprofloxacin, at subinhibitory concentration (0.25 × MIC), is as equipotent as that at the MIC level. This combination also had a reduced mutation prevention concentration. Boeravinone B reduced the efflux of ethidium bromide and increased the accumulation, thus strengthening the role as a NorA inhibitor. Biofilm formation was reduced by four–eightfold of the minimal biofilm inhibitory concentration of ciprofloxacin, effectively preventing bacterial entry into macrophages. Boeravinone B effectively inhibited *P*-gp with half maximal inhibitory concentration (IC_{50}) of 64.85 μM. The study concluded that boeravinone B not only inhibits the NorA-mediated efflux of fluoroquinolones but also considerably inhibits the biofilm formation of *S. aureus*. Its *P*-gp inhibition activity demonstrates its potential as a bioavailability and bioefficacy enhancer.

Keywords: NorA, *P*-glycoprotein, biofilm, *Staphylococcus aureus*, efflux inhibition

OPEN ACCESS

Edited by:
Noton Kumar Dutta, Johns Hopkins University, United States

Reviewed by:
Henrietta Venter, University of South Australia, Australia
Xian-Zhi Li, Health Canada, Canada

***Correspondence:**
Inshad A. Khan
inshad@rediffmail.com;
iakhan@iiim.ac.in

†Present address:
Nitin P. Kalia, Lee Kong Chian School of Medicine, Nanyang Technological University, Singapore, Singapore

Specialty section:
This article was submitted to Antimicrobials, Resistance and Chemotherapy, a section of the journal Frontiers in Microbiology

Received: *05 July 2017*
Accepted: *13 September 2017*
Published: *04 October 2017*

Citation:
Singh S, Kalia NP, Joshi P, Kumar A, Sharma PR, Kumar A, Bharate SB and Khan IA (2017) Boeravinone B, A Novel Dual Inhibitor of NorA Bacterial Efflux Pump of Staphylococcus aureus and Human P-Glycoprotein, Reduces the Biofilm Formation and Intracellular Invasion of Bacteria. Front. Microbiol. 8:1868. doi: 10.3389/fmicb.2017.01868

INTRODUCTION

The development of multidrug resistance (MDR) upon chronic exposure to chemotherapeutic agents is considered the major reason for the failure of chemotherapy in cancer and infectious diseases (Poole, 2005; Leitner et al., 2011; Joshi et al., 2014). Efflux pumps are transmembrane proteins, which are the major contributors to multidrug resistance (MDR) in patients with cancer and infectious diseases. *P*-glycoprotein (gp), a multidrug-resistance protein (also called MDR1), accounts for the development of resistance to various drugs as well as for the transport of endogenous and exogenous substrate ligands, such as various toxins, hormones, and drugs (Chen et al., 1986; Joshi et al., 2014). Moreover, *P*-gp alters the pharmacokinetics and pharmacodynamics of its substrates by modulating their absorption, distribution, metabolism, elimination, and toxicity properties (Lin, 2003). Bacterial multidrug efflux pumps are the major contributors to microbial resistance to several classes of antibiotics (Kaatz et al., 2003; Tegos et al., 2011; Kalia et al., 2012).

Presence or augmented expression of efflux pumps is responsible for reduced drug availability to inhibit the specific target. Due to continuous efflux, comparatively lower concentration of antimicrobial agent reaches the target, which may increase the rate of new mutations thus generating newer types resistant mutants exhibiting novel resistance mechanisms (Poole, 2005; Piddock, 2006; Sun et al., 2014). With the continuous emergence of pathogenic resistance to conventional drugs because of efflux through MDR pumps, increasing efforts are directed toward discovering efflux inhibitory molecules. NorA efflux pump is the most widely studied among efflux pumps of *Staphylococcus aureus*. According to a study NorA efflux pump was found to be overexpressed in 43% of resistant strains of *S. aureus* (Patel et al., 2010; Astolfi et al., 2017). NorA, an established multidrug efflux pump model in *S. aureus*, accounts for extruding quinolones, quaternary ammonium salts, acridines, rhodamines, verapamil, and ethidium bromide (Kaatz et al., 2003; Khan et al., 2006; Leitner et al., 2011; Tegos et al., 2011; Holler et al., 2012; Schindler et al., 2013; Fontaine et al., 2015; Tintino et al., 2016). Recently some non-antibiotics derivatives as potent NorA efflux pump inhibitors have been reported utilizing pharmacophore based modeling and drug repurposing utilizing *in silico* approach (Astolfi et al., 2017; Sabatini et al., 2017). In addition, some less toxic benzochromene derivatives and dithiazole thione derivatives have also been reported as NorA efflux inhibitors (Ganesan et al., 2016; Lowrence et al., 2016). A recently published comprehensive review summarized the applications of nanoparticles are also being explored for efflux inhibitory activity in addition to biofilm inhibition (Gupta et al., 2017).

Despite their varying structures, the efflux pumps of bacterial and mammalian systems have sufficient substrate homology. Studies have reported many dual types of natural plant products that act as inhibitors, such as verapamil, reserpine, piperine, and capsaicin (**Figure 1**), as well as osthol and curcumin (Bhardwaj et al., 2002; Khan et al., 2006; Kalia et al., 2012; Joshi et al., 2014). These inhibitors offer advantages, such as enhanced gastrointestinal absorption, improved permeation through the blood–brain barrier, increased drug concentrations in mammalian cells for improved killing of invasive pathogens, and the use of lower concentrations of drugs to eliminate side effects (Khan et al., 2006).

In addition to drug efflux, a critical problem is biofilm formation, which poses a major hindrance in the evolution of novel chemotherapeutic agents (Bjarnsholt et al., 2013). Nearly 80% of human bacterial infections are caused by biofilm formation, and 60% of nosocomial infections are caused by biofilm formation on medical devices and implants (Darouiche, 2004; Hou et al., 2012). Biofilm eradication requires a much higher concentration, namely 10–1000 times the minimum inhibitory concentration (MIC), of antibiotics. Active efflux has been reported to contribute to increased resistance in bacterial biofilms (Lewis, 2001; Kvist et al., 2008; Baugh et al., 2014; Van Acker and Coenye, 2016; Sabatini et al., 2017). Biofilms have slow metabolism and growth, the main reasons for increased resistance, because most antibiotics target metabolic or cell division pathways (Lewis, 2007, 2008). Researchers have reported that the synergistic action of molecules abolishes biofilm formation (Baugh et al., 2012).

Staphylococcus aureus is considered an extracellular pathogen, but there are accumulating evidences to reveal that *S. aureus* causes severe intracellular infections, such as endocarditis and septic shock (Hooper, 2005). This organism, on getting an opportunity to invade, survives and promotes diseases. Hirakata et al. (2009) and Kalia et al. (2012) concluded that efflux pump-overexpressing strains can easily invade cells.

Several natural plant products act as efflux pump inhibitors (Stavri et al., 2007). Boeravinone B, the compound of interest in the present study, was isolated from the roots of *Boerhavia diffusa*, a plant belonging to the Nyctaginaceae family (Patil and Bhalsing, 2016). This plant is also known as Punarnava in the Indian traditional system of medicine, Ayurveda, and is established for its medicinal properties. In ancient times, plants were used to cure various physiological conditions, such as inflammation, jaundice, dyspepsia, nephrotic syndrome, convulsions, spleen enlargement, abdominal pain and stress, nematodal and microbial infections, and asthma (Ahmed-Belkacem et al., 2007; Khan et al., 2013; Bairwa et al., 2014). Boeravinone C and G have been reported to possess *P*-gp

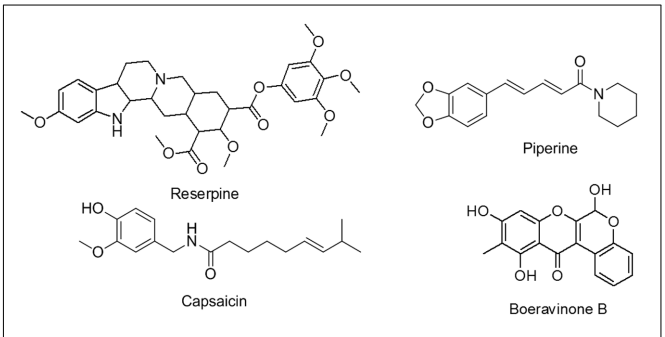

FIGURE 1 | Reserpine, piperine, capsaicin and boeravinone B (molecule used in this study).

TABLE 1 | Characteristics of *Staphylococcus aureus* strains used in this study.

Strain code	Characteristic	Origin
SA-1199	Wild type	Clinical isolate (endocarditis)
SA-1199B	NorA overexpressing	Ciprofloxacin resistant derivative of SA-1199
SA-K1758	NorA knockout	Derivative of NCTC-8325-4
MT23142	NorA overexpressing	Derivative of NCTC-8325
MRSA15187	MRSA	MRSA
ATCC 29213	MSSA	Standard strain; methicillin sensitive

inhibitory activity (Ahmed-Belkacem et al., 2007; Stacy et al., 2013).

In this study, we described the role of boeravinone B in ciprofloxacin potentiating activity against NorA-overexpressing strains of *S. aureus* and *P*-gp inhibition in the colon cancer cell line.

MATERIALS AND METHODS

Chemicals

All fluoroquinolones, ethidium bromide reserpine, piperine, fluorescein isothiocyanate (FITC) and 4′,6-diamidino- 2-phenylindole (DAPI) were purchased from Sigma Chemical Co. (St. Louis, MO, United States). Microbiological media were purchased BD Microbiology Products (Sparks, MD, United States). All other chemicals were of analytical grade.

Bacterial Strains

Staphylococcus aureus ATCC 29213, SA-1199B, SA-1199, SA-K1758, MT23142, and MRSA15187 were cultivated on trypticase soya agar (TSA). Important characteristics are described in **Table 1**.

Boeravinone B Isolation

Authentic samples of *B. diffusa* roots were collected from Jammu region (Voucher Specimen No. 21713), dried and powdered followed by solvent extraction in dichloromethane: methanol mixture (1:1 v/v) using cold maceration method. Crude extract was concentrated and purified by repeated silica gel column chromatography using hexane: ethyl acetate (95: 5 to 75: 25 v/v).

Drug Potentiation by Broth Checkerboard Microdilution

Drug potentiation or synergistic action of compound was assessed by broth checkerboard microdilution technique, which is most known method (Eliopoulos and Wennersten, 2002). Combination of ciprofloxacin and boeravinone B was tested in Mueller Hinton Broth (MHB; pH 7.0) against all bacterial strains using 96 well microtitre plates at a concentration range of 0.06–32 μg/ml and 0.8–50 μM, respectively. Additionally, combination of ethidium bromide and boeravinone B was assessed in similar way using *S. aureus* SA-1199B. Cell suspension of a density of 0.5 McFarland ($\approx 1.5 \times 10^8$ cfu per ml of *Escherichia coli*) was used as inoculum after diluting 1:100, a volume of 0.1 ml (5×10^5) was added to plates. The plates were incubated at 37°C for 18–20 h. Reserpine and piperine (known efflux pump blocker) were used as the control in this study. Minimum effective concentration (MEC) of boeravinone B was determined which is defined as concentration at which there is atleast fourfold reductions in MIC of ciprofloxacin. In a similar way various other fluoroquinolones and ethidium bromide were also assessed for synergistic potential of boeravinone B.

Time Kill Curve

Time-kill study of ciprofloxacin alone and in combination with boeravinone B was performed in 50 ml volume conical flasks containing 25 ml of MHB using the previously described method (Eliopoulos and Moellering, 1996). Ciprofloxacin at 2 μg/ml (0.25 × MIC) was tested alone and in combination with boeravinone B at the MEC concentration (12.5 μM) as determined above. Ciprofloxacin was also tested alone at an MIC of 8 μg/ml. NorA overexpressing *S. aureus* SA-1199B was used as the test bacterium. Ten folds serial dilutions of these aliquots were spotted on TSA plates.

Impact on Frequency of Resistance

Frequency of resistance (FOR) or Mutation prevention concentration (MPC) of ciprofloxacin against *S. aureus* ATCC 29213 was determined by method described elsewhere (Drugeon et al., 1999). MHA plates were supplemented with MIC, 2×, 4×, and 8× MIC of ciprofloxacin's concentrations with or without boeravinone B at MEC. A bacterial suspension of 0.1 mL (10^9 cfu) was plated on to each ciprofloxacin containing plates without and with boeravinone B. MPC was determined as the ratio of colonies appearing on ciprofloxacin or ciprofloxacin with boeravinone B combination to total colonies plated on a drug free plate.

Ethidium Bromide Efflux and Accumulation Studies

Fluorescence based method as described by Brenwald et al. (1998) was used to determine the ethidium bromide efflux inhibitory as well accumulation studies. For this purpose a freshly grown NorA overexpressing *S. aureus* SA-1199B was suspended to an optical density of 0.2 in uptake buffer (110 mM NaCl, 7 mM KCl, 50 mM NH_4Cl, 0.4 mM Na_2HPO_4, 52 mM Tris base and 0.2% glucose, adjusted to pH 7.5 with HCl). Cells were loaded with 10 μg/ml ethidium bromide for 30 min at 37°C. Extracellular ethidium bromide was removed by centrifugation and pellet was resuspended in same volume of uptake buffer with and without boeravinone B (12.5 μM). Reserpine at 25 μg/ml was used as a known efflux pump inhibitor. For accumulation studies bacterial cells loaded with ethidium bromide for 30 min after which EPIs (boeravinone B and reserpine) were added. Loss or gain of fluorescence in presence of compound and known EPI was deduced at 530 and 600 nm for excitation and emission wavelength, respectively, using multimode reader Infinite 200 Pro (Tecan Mannedorf, Switzerland).

Biofilm Inhibition

Effect of boeravinone B on the biofilm inhibitory potential of ciprofloxacin was studied with drug combination on biofilm formation, as previously described (Schillaci et al., 2010). For biofilm formation, cultures (*S. aureus* SA-1199 and SA-1199B) were grown overnight using TSB supplemented with 2% glucose (TSBG) and diluted to an optical density (570 nm) of 0.015 after diluting 1:200 (1×10^9 cells/mL). Microtitre plates for inhibitory studies were prepared as described for synergistic activity with ciprofloxacin by checkerboard microdilution method. After 24 h, wells were washed thrice with PBS followed by fixation with methanol for 15 min and finally air-dried in inverted position at 37°C. The wells of the dried plates were stained with 0.1% (w/v) crystal violet for 10 min and rinsed thoroughly with water until the negative control wells (without biofilms) appeared colorless. To quantify biofilm formation, 0.2 mL of 95% ethanol was added to wells of plate that were stained with crystal violet. Immediately absorbance read at 595 nm using microplate reader. In a separate plate the contents were decanted and washed with PBS to remove the planktonic cells and again filled with fresh TSB. After incubation for 30 min, 15 μl of 0.04% resazurin and 12.5 μl of 20% Tween80 were added in each well of the plate to access the viability of the cells within biofilm. The plates were incubated for 15 min and fluorescence was determined at an excitation at 560 nm and emission at 590 nm (Tecan Infinite M200 microplate reader) as described previously (Bauer et al., 2013). Minimal biofilm inhibitory concentration (MBIC) is defined as the concentration at which absorbance was reduced by ≥90% or was nearly equivalent to media control wells.

Confocal Microscopic Studies for Biofilm Inhibition

The potentiating effect of boeravinone B was further confirmed by staining the biofilms with FITC and DAPI which stains protein (amine reactive) and nucleic acid (DNA), respectively, by modified method as described by Yang (using DAPI in place of Hoechst) followed by visualization by confocal laser scanning microscopy (Yang et al., 2015). The biofilm of *S. aureus* ATCC 29213 was grown in six well poly styrene plate (Nunc) containing sterile 18 mm glass cover slips. Ciprofloxacin was used at 4 μg/ml which is MBIC and at 1 μg/ml which is subMBIC (0.25× MBIC) as determined above. Boeravinone B at 12.5 μM (MBIC) was added to sub-inhibitory concentration of ciprofloxacin (0.25× MBIC). The plates were incubated for 24 h at 37°C. PBS washes were given to eliminate planktonic cells followed by fixation of biofilm with 5% para-formaldehyde for 1 h at 50°C. Fixed biofilm was flooded with 0.001% (w/v) FITC and 1 μg/ml DAPI at kept at room temperature for 1 h. Images were seen and captured on 40× oil immersion lens using CLSM (Olympus flou View 1000).

In Vitro Screening of *P*-Glycoprotein Inhibitory Activity

P-glycoprotein inhibitory activity was assessed by the method described earlier using colorectal cell line LS180 (Jin et al., 2012; Joshi et al., 2014). Cell monolayer was prepared in 96 well plate using Dulbecco's Modified Eagle's medium (DMEM) media. The media was decanted and replaced with Hank's buffer containing 10 mM of Rh123 as a *P*-gp substrate. Twofold serial dilutions of boeravinone B (80–5 μM) were added and plate was incubated at 37°C in CO_2 incubator for 90 min. A known *P*-gp inhibitor elacridar (10 μM) was used as positive control. The contents of the wells were decanted and washed four times with cold PBS followed by cell lysis for 1 h using 200 μl of lysis buffer (0.1% Triton X 100 and 0.2 N NaOH). A total of 100 μl of lysate was used for reading fluorescence of Rh123 at an excitation at 485 nm and emission at 590 nm. All samples were normalized by dividing fluorescence of each sample with total protein present in the lysate. Half minimal inhibitory concentration (IC_{50}) value of boeravinone B was calculated using Graphpad Prism 5 software (GraphPad Software, Inc., La Jolla, CA, United States). Data is expressed as mean ± SD or representative of one of three similar experiments. Comparisons were made between control and treated groups or the entire intra group using one way ANOVA with post Bonferroni test through GraphPad Prism 5.00.288 statistical analysis software. $^*p$-values <0.05 were considered significant.

Molecular Docking Studies against *P*-Glycoprotein and NorA Efflux Pumps

Due to unavailability of crystal structures of human *P*-gp and *S. aureus* NorA, molecular docking studies were carried out using the homology models. The homology models for human *P*-gp (Jin et al., 2012) was prepared from *Caenorhabditis elegans* *P*-gp (PDB ID: 4AZF) and *S. aureus* NorA efflux pump (Aller et al., 2009) was prepared from glycerol 3-phosphate transporter pump from *E. coli* (PDB ID: IPW4) using Glide Induced Fit Docking in default setting. For Nor A docking studies, ciprofloxacin/reserpine binding site was used to construct grid file whereas for *P*-gp docking, verapamil binding site was used (Aller et al., 2009).

Macrophage Invasion Assay

To assess the impact of boeravinone B on invasion of *S. aureus* in macrophage, previously described method was used (Cheung and Bayles, 2007). Murine macrophage cell line J774 maintained on Roswell Park Memorial Institute medium (RPMI) supplemented with 10% (v/v) fetal calf serum was used as host. The macrophages were grown in monolayer to a density to 10^5 cells/well in 24 well plate in physiological conditions, i.e., 37°C and 5% CO_2 for 24 h. 10^6 cfu/well of overnight grown *S. aureus* strains SA-1199B, SA-1199, and SA-K1758 were used to infect macrophages (MOI of 10) in presence and absence of boeravinone B at its MEC (12.5 μM) for 2 h. Extracellular and adherent bacteria washed with PBS (pH 7.4) followed by treatment with 50 μg/ml gentamicin for 30 min. Intracellular bacteria were quantified by host cell lysis by brief treatment of 0.07% SDS which followed neutralization with 6% BSA. Viable bacteria were counted by plating on TSA. In a similar experiment RPMI devoid of FCS was used to assess the role of FCS.

TABLE 2 | Ciprofloxacin potentiation by boeravinone B against various strains of *S. aureus* with different levels of NorA expressions and MRSA.

Compounds	EPI[#] μg/ml (μM)	MIC (μg/ml) of ciprofloxacin					
		SA1199	SA-1199B	SA-K 1758	ATCC 29213	MT-23142	MRSA-15187
Ciprofloxacin	0	0.25	8	0.12	0.25	0.25–0.5	32
Boeravinone B	8 (25)	0.12	1	0.12	0.12	0.03	8
Piperine	50 (88)	0.12	4	0.12	0.06	ND	16
Reserpine	25 (41)	0.06	2	0.12	0.12	ND	ND

[#]*All EPIs tested have no self-antimicrobial activity up to 100 μM.*

TABLE 3 | Activity of boeravinone B on the MICs of ethidium bromide and other fluoroquinolones in susceptible and resistant *S. aureus* strains.

Antibacterial agents	Boeravinone B concentration in μg/ml (μM)	MIC (μg/ml) for given *S. aureus* strain			
		SA-1199B	SA-1199	SA-K1758	MT23142
EtBr	0	32	1	0.5	2
	8 (25)	2	0.25	0.12	0.12
Norfloxacin	0	32	0.25	0.12	32
	8 (25)	4	0.12	0.12	4
Ofloxacin	0	1	1	1	0.5
	8 (25)	0.5	1	0.5	0.5
Moxifloxacin	0	0.25	0.06	0.12	0.06
	8 (25)	0.12	0.06	0.12	0.06
Gatifloxacin	0	1	1	0.12	0.06
	8 (25)	0.25	0.5	0.12	0.06

RESULTS

Isolation and Purity of Boeravinone B

By using the cold maceration method, 6,9,11-trihydroxy-10-methylchromeno[3,4-b]chromen-12(6H)-one (boeravinone B; **Figure 1**) was isolated from the roots of *B. diffusa*. It is a yellow solid compound, with a melting point of 201°C–203°C. The structure was confirmed through high-resolution mass spectroscopy (m/z 313.0708 [M + H^+], as calculated for $C_{17}H_{12}O_6$ + H^+: 313.0707) and comparison of the ^1H and ^{13}C NMR data. Boeravinone B used in this study had 96% purity, as determined through high performance liquid chromatography. Data related to the purity and structure of the isolated boeravinone B was characterized by comparison of spectral data with described reported values (Kadota et al., 1989) (Supplementary Data S1).

Effect of NorA Efflux Pump Inhibition on MIC of Fluoroquinolones and Ethidium Bromide

The resistance reversal activity of boeravinone B was quantified by calculating the fold reduction in the MIC of ciprofloxacin. Boeravinone B lack anti-staphylococcal activity when assessed up to 100 μM against all tested strains. This MIC of ciprofloxacin alone and in combination with boeravinone B was determined (**Table 2**). Boeravinone B reduced the MIC of ciprofloxacin by twofold in *S. aureus* SA-1199 and ATCC 29213, whereas the effect was stronger in the NorA-overexpressing *S. aureus* strains SA-1199B and MT-23142, where the MIC was reduced by eightfold. Conversely, SA-K1758 (NorA knocked out) did not show any reduction in the MIC of ciprofloxacin. Boeravinone B was also active against a methicillin-resistant *S. aureus* (MRSA) strain, which showed a fourfold reduction in the ciprofloxacin MIC.

In addition to ciprofloxacin, spectrum of activity was also assessed using other fluoroquinolones like ofloxacin and norfloxacin which are well known substrates for NorA efflux pump and newer fluoroquinolones like gatifloxacin and moxifloxacin which are poor efflux substrates for NorA. Boeravinone B was used at 4× MEC for ethidium bromide (6.25 μM or 2 μg/ml). Potential of boeravinone B to inhibit the efflux of other fluoroquinolones was investigated using *S. aureus* strains SA-1199B, SA-1199, SA-K1758, and MT23142 (**Table 3**). MIC potentiation using ethidium bromide yielded similar effects of eightfold reduction in the MIC of ethidium bromide (2 μg/mL) compared with that of ethidium bromide alone, which exhibited an MIC of 16 μg/mL against SA-1199B. In NorA overexpressing strains (SA-1199B and MT23142), boeravinone B reduced the MIC of norfloxacin by eightfold while only twofold reduction in MIC of ofloxacin, moxifloxacin, and gatifloxacin was observed. It was observed that ciprofloxacin MIC reduction was relatively less (two–fourfold) in case of wild type *S. aureus* SA-1199 against these fluoroquinolones. There was no synergistic effect against *S. aureus* SA-K1758 due to absence of NorA efflux pump. Significant reduction in MICs against NorA overexpressing strains of *S. aureus* concludes that ciprofloxacin and norfloxacin

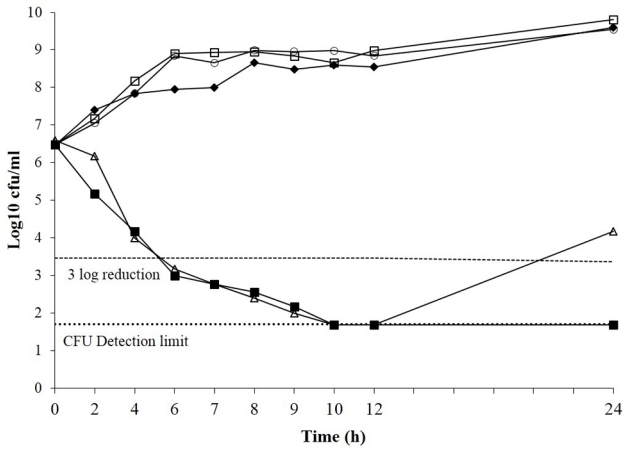

FIGURE 2 | Time kill curve of *Staphylococcus aureus* SA-1199B showing the bactericidal effect of ciprofloxacin alone (open triangle), subMIC alone (closed diamond) and ciprofloxacin at subMIC in combination with boeravinone B at MEC (closed square) including boeravinone B alone (Open circle). Growth control having plain media without ciprofloxacin or EPI served control (Open square). Each time point is mean Log_{10} of three independent readings.

TABLE 4 | Mutation prevention concentration (MPC) of ciprofloxacin with boeravinone B against *S. aureus* ATCC 29213.

Boeravinone	Mutation frequency with ciprofloxacin			
B conc. (μM)	2 × MIC	4 × MIC	8 × MIC	16 × MIC
0	5×10^{-8}	8×10^{-9}	4×10^{-9}	$<10^{-9}$
12.5	2.2×10^{-9}	$<10^{-9}$	$<10^{-9}$	$<10^{-9}$
25.0	$<10^{-9}$	$<10^{-9}$	$<10^{-9}$	$<10^{-9}$

have stronger affinity for NorA and efflux can be inhibited using boeravinone B.

Effect of Boeravinone B on Time–Kill Kinetics of Ciprofloxacin

The effect of boeravinone B on the time–kill kinetics of ciprofloxacin was assessed in *S. aureus* SA-1199B. Ciprofloxacin alone (MIC: 8 μg/mL) showed 3-log reduction in growth, whereas the same was accomplished at a subinhibitory concentration of the ciprofloxacin (0.25 × MIC) in combination with boeravinone B at a minimum effective concentration (MEC; 12.5 μM). The sub MIC of ciprofloxacin alone could not reduce the growth. Ciprofloxacin alone at an MIC effectively reduced the colony-forming units (CFU) in 6 h, but cell growth reoccurred after 24 h. The combination of ciprofloxacin (at subinhibitory concentration) and boeravinone B prevented the growth of resistant colonies (**Figure 2**).

Frequency of Ciprofloxacin Resistance in Presence of Boeravinone B

For effective clinical applications, drugs should be able to suppress mutations and resistance mechanisms. A resistant

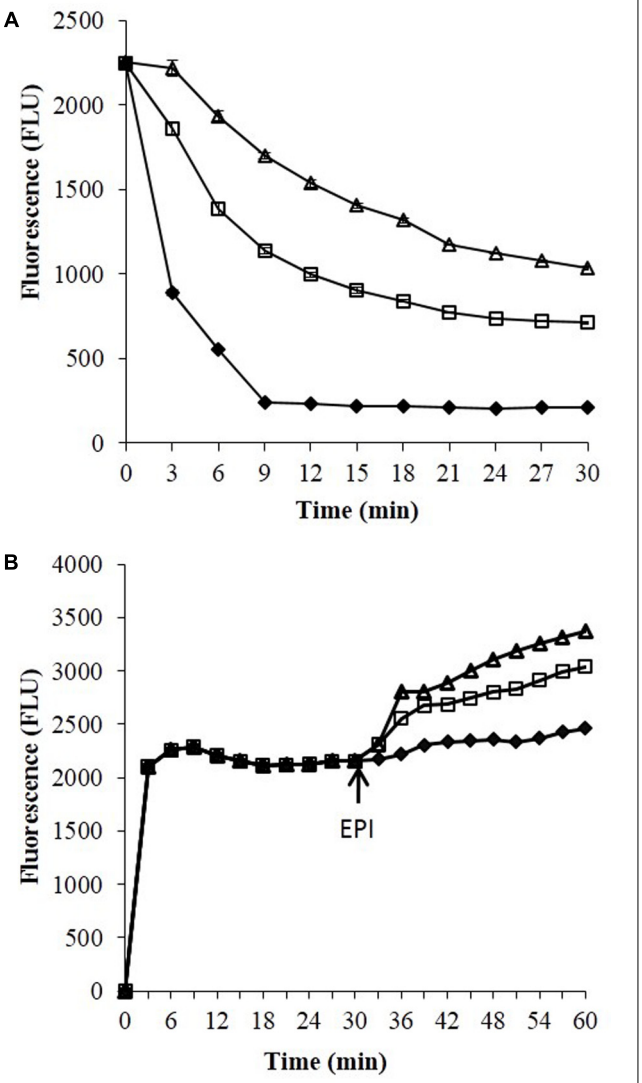

FIGURE 3 | Ethidium bromide studies efflux **(A)** and accumulation **(B)** studies against *S. aureus* SA-1199B. Symbols represents control which have no addition of any EPI (closed diamond), in presence of boeravinone B (open square) and in presence of known EPI, i.e., reserpine (open triangle).

mutant selection study was performed on wild-type *S. aureus* ATCC 29213 because this strain does not have any known mutations in the regulatory region of NorA and drug targets (DNA gyrase and topoisomerase IV). The minimum concentration of a drug at which no resistant mutant is selected is defined as its MPC. Ciprofloxacin alone showed an MPC of 4 μg/ml whereas, in combination with 12.5 and 25 μg/ml of boeravinone B, the MPC of ciprofloxacin reduced to 2 and 1 μg/ml, respectively (**Table 4**). The MPC of this combination was lower than the C_{max} of ciprofloxacin (3–4 μg/ml) in human plasma, indicating the clinical relevance of these combinations in restricting the selection of resistant mutants.

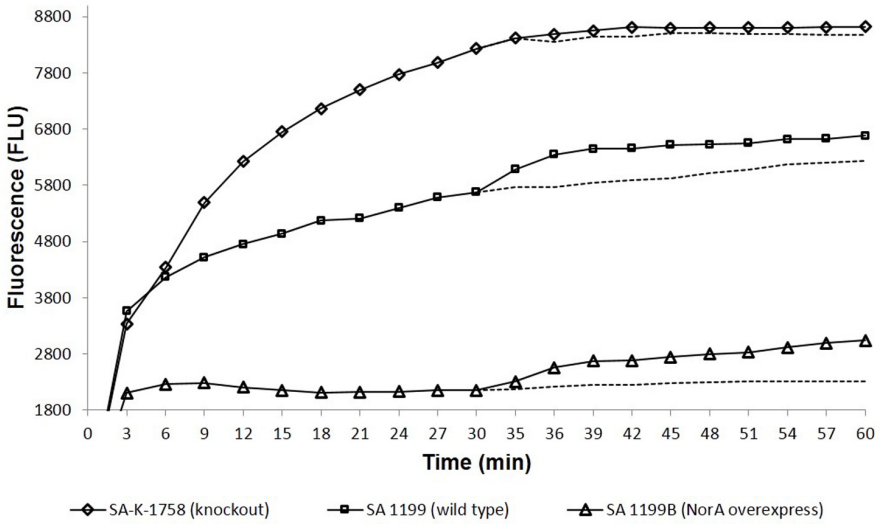

FIGURE 4 | Comparative accumulation of EtBr in presence of Boeravinone B against *S. aureus* SA-1199B (triangle), SA-1199 (square) and SA-K1758 (diamond) having different levels of NorA expressions, i.e., overexpression, wild type and knockout, respectively. Dotted lines after 30 min indicates the respective controls in absence of boeravinone B.

Effect of Boeravinone B on Ethidium Bromide Efflux Inhibition and Accumulation

Ethidium bromide is a well-known substrate for the NorA MDR efflux pump. SA-1199B cells were allowed to be loaded with ethidium bromide with and without boeravinone B and placed in a fluorometer cuvette containing fresh medium. Ethidium bromide fluoresces only when bound to nucleic acids in cells; therefore, a rapid decrease occurred in the fluorescence because of the NorA-mediated efflux of ethidium bromide. As shown in **Figure 3**, only the control cells without boeravinone B maximally extruded ethidium bromide, resulting in significantly decreased fluorescence in the assay period. Conversely, in cells treated with boeravinone B, the efflux of ethidium bromide was prevented, resulting in the prolonged retention of fluorescence. In the accumulation studies, ethidium bromide uptake was allowed in bacterial cells for 30 min. A counterbalance effect occurred because of the simultaneous efflux of ethidium bromide, which effectively increased the fluorescence. The addition of boeravinone B at this stage resulted in a surge in the fluorescence because of the inhibition of efflux pumps, resulting in a higher retention of fluorescence (**Figure 3**). Reserpine, a known efflux pump inhibitor, was used as the positive control in both studies. When compared, ethidium bromide accumulation in SA-1199B, SA-1199, and SA-K1758, accumulation was maximum in knockout followed by wild type and overexpressing which is in correlation with the phenotypes of the tested strains. In presence of boeravinone B, accumulation was significantly increased in NorA overexpressing, while minor effect was seen for wild type. *S. aureus* SA-1199. There was no effect on the accumulation efficiency of SA-K1758 which is devoid of functional *norA* gene (**Figure 4**).

TABLE 5 | Effect on biofilm inhibitory potential of ciprofloxacin when combined with boeravinone B at different concentrations against various strains of *S. aureus*.

Boeravinone B (μM)	MBIC (μg/ml) of ciprofloxacin		
	SA-1199	SA1199B	*S. aureus* ATCC 29213
0	4	16	4
6.25	2	8	2
12.5	1	4	1
25	1	2	1

Biofilm Inhibition

The minimum concentration of a drug for inhibiting a biofilm is defined and expressed as its MBIC. The MBIC of a drug is typically higher than its MIC because of the lesser permeability of the drug within the matrix of a biofilm. In this study, ciprofloxacin showed an MBIC of 4 and 16 μg/mL for *S. aureus* SA-1199 and SA-1199B, respectively. A concentration-dependent decrease occurred in the MBIC of ciprofloxacin against both strains in the presence of boeravinone B (6.25–25 μM; **Table 5**). To ascertain that the biofilm inhibition was caused by the killing of the bacteria embedded in the matrix of biofilm, the resazurin staining of a parallel set of plates was performed. The change in the color of this redox dye from blue to red indicated the viability of the cells in the well. The biofilm inhibition correlated well with the cell viability (Supplementary Figure S1).

Microscopic Studies

Effect of boeravinone B plus ciprofloxacin was evaluated by microscopic studies of the *S. aureus* ATCC 29213-generated biofilm. Fluorescein isothiocyanate stains proteins

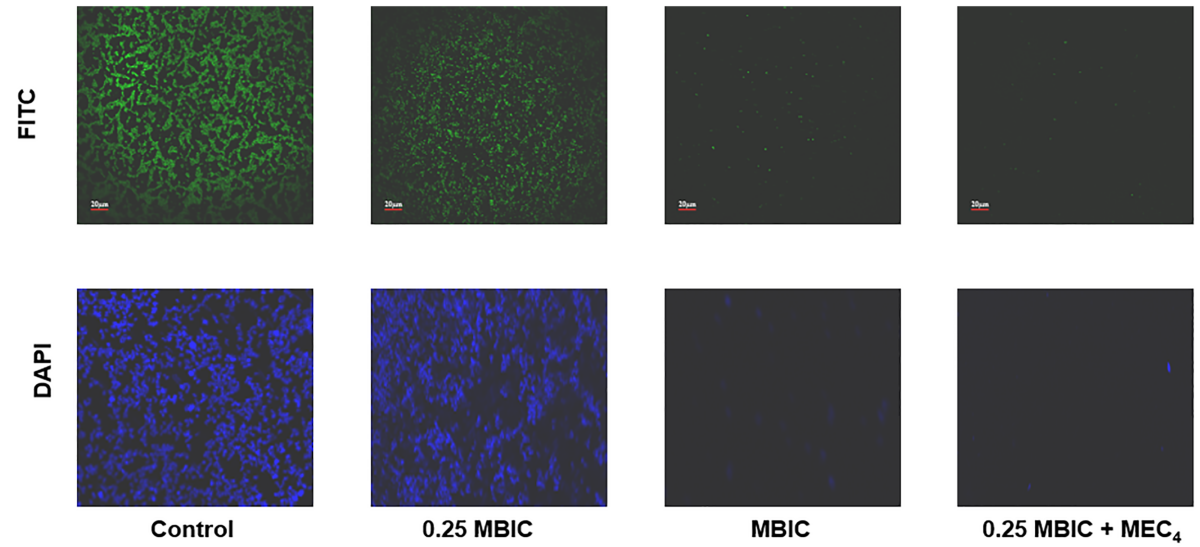

FIGURE 5 | CLSM of biofilm; untreated, treated with ciprofloxacin at subMBIC (0.25 × MBIC) and MBIC alone. Last column shows the presence of boeravinone B combined with subMBIC of ciprofloxacin. Upper line is stained with FITC and lower with DAPI.

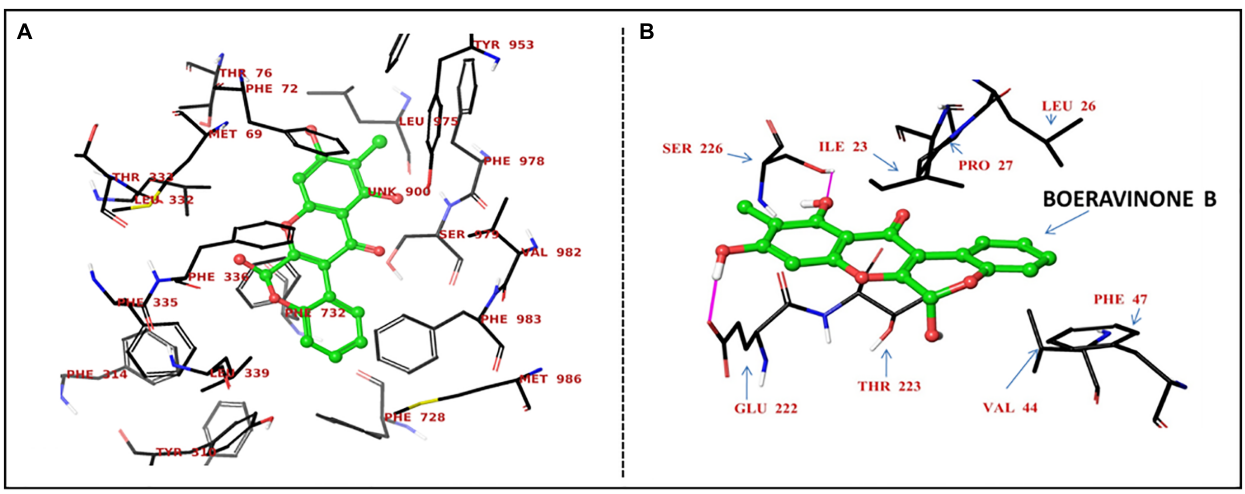

FIGURE 6 | Proposed binding site of boeravinone B with human *P*-gp **(A)** and *S. aureus* NorA efflux pumps **(B)**.

and imparts green fluorescence, whereas 4′,6-diamidino-2-phenylindole binds to nucleic acids and yields blue fluorescence when observed in the whole image field. As shown in **Figure 5**, the untreated biofilms were associated with a large amount of proteins and DNA. The sub MBIC of ciprofloxacin did not inhibit the biofilms; however, in combination with the MEC of boeravinone B, ciprofloxacin inhibited the biofilm, as did the MBIC of ciprofloxacin, as evident by the reduced intensity of green and blue fluorescence.

Molecular Docking on *P*-gp

Boeravinone B was observed to interact with *P*-gp at the verapamil binding site, particularly with the residues Met69, Phe72, Tyr307, Tyr310, Phe314, Leu332, Phe335, Phe336, Leu339, Phe728, Phe759, Phe957, Phe978, and Val982 through hydrophobic π−π interactions (**Figure 6A**). Consequently, it led to an increase in the intracellular accumulation of the substrate Rh123. Similarly, the NorA efflux pump is a transmembrane pump, in which ciprofloxacin or reserpine optimally bind to site 1 through strong hydrogen bonding of carboxyl functionality with the Arg98 cationic guanido group. The hydrophobic and hydrogen interactions of ciprofloxacin were mimicked by boeravinone B. Molecular modeling studies with the bacterial NorA efflux pump homology model revealed that boeravinone B binds to the Ile23 and Glu222 residues of the pump through strong hydrogen bonding formed by phenolic hydroxyl groups and thus block the interaction of substrate quinolones with the efflux binding cavity (**Figure 6B**).

Invasion Inhibition and Role of Fetal Calf Serum

The intracellular invasion of *S. aureus* SA-1199B was nearly 1.5 $\log_{10}$ higher than that of *S. aureus* SA-1199 in the murine macrophage cell line J774. Boeravinone B at its MEC (12.5 μM) was not active when the experiment was performed in the presence of 10% fetal calf serum (FCS). When the experiment was repeated using RPMI media without FCS, the invasiveness of *S. aureus* had reduced, suggesting the binding of boeravinone B to FCS. The invasiveness of SA-1199B showed greater reduction (1.6 $\log_{10}$) than did that of *S. aureus* SA-1199 (0.5 $\log_{10}$). *S. aureus* SA-K1758 exhibited the least penetration into macrophages, and boeravinone B did not affect the invasiveness of this strain (**Figure 7**).

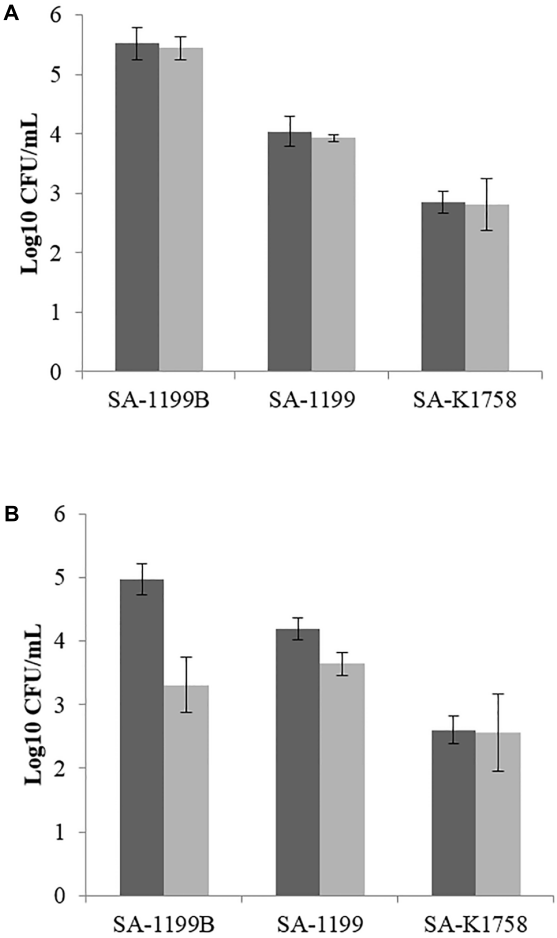

FIGURE 7 | Macrophage invasiveness by various strains of *S. aureus* in presence (gray bars) and absence (black bars) of boeravinone B. Assay was performed using standard RPMI media with **(A)** and without FCS **(B)**.

DISCUSSION

Efflux pumps are membrane-bound proteinaceous transporters known for extruding chemotherapeutic agents or xenobiotics, which are otherwise harmful for bacterial survival. During evolution, microbes were selected and evolved through antibiotic pressure with the overexpression of efflux pumps, which renders the antibiotics inefficient and hence results in the poor efficacy of chemotherapeutic agents. Efflux pumps can export a large pool of structurally unrelated substrates out of cells, which hampers their clinical efficacy. NorA is an MDR efflux pump of the major facilitator superfamily pumps and has 12 transmembrane segments. It is established for expelling various fluoroquinolones. NorA has been well established as a model system for studying efflux pump inhibition in Gram-positive pathogens (Kaatz, 2005; Kumar et al., 2008).

In the present study, boeravinone B obtained from *B. diffusa* was assessed for its NorA inhibitory activity in SA-1199B, which is a model organism for NorA inhibition studies because it mimics the resistance induced by fluoroquinolone pressure. Ethidium bromide MIC potentiation by 16-fold in NorA overexpressing strains in presence of boeravinone B shows inhibition of efflux mediated resistance. Presence of boeravinone B also exhibited two–eightfold reduction in MIC of ciprofloxacin and norfloxacin in these strains. The potentiating effect was less prominent (twofold) in wild type strain *S. aureus* SA-1199. Additionally there was no reduction in MIC of *S. aureus* SA-K1758 which is lacking functional *norA* gene. This concludes that ciprofloxacin and norfloxacin fluoroquinolone are favorable substrate for NorA. Similar observation about the enhanced affinity of NorA for these fluoroquinolones have been reported previously (Gibbons et al., 2003; Mullin et al., 2004). Boeravinone B increased the intrinsic susceptibility of *S. aureus* to ciprofloxacin and significantly reduced the emergence of ciprofloxacin-resistant *S. aureus*. A subinhibitory concentration of ciprofloxacin (2 μg/ml) with the MEC of boeravinone B (12.5 μM) exhibited a bactericidal effect and a 3-$\log_{10}$ reduction in CFU in 6 h, with no emergence of mutants even after 24 h. Conversely, ciprofloxacin alone exhibited the same effect at 8 μg/mL, but resistant mutants were observed after 24 h (**Figure 2**). Ethidium bromide efflux inhibition and accumulation are well-known mechanism-based descriptors for the specificity of NorA inhibition. The fluorescence-based efflux accumulation studies of ethidium bromide-preloaded NorA-overproducing *S. aureus* cells revealed reduced efflux in the presence of boeravinone B, indicating the inhibition of the ethidium bromide efflux mechanism. Furthermore, its effect on the retention of Rh123 in *P*-gp-overexpressing human adenocarcinoma LS-180 cells confirmed its role as a dual inhibitor of *P*-gp and the *S. aureus* efflux pump inhibitor. Studies have reported several similar dual inhibitors, such as osthol, curcumin, piperine, and capsaicin (Khan et al., 2006; Kalia et al., 2012). Docking results with the NorA homologous structure and *P*-gp obtained using Glide clearly elaborated that boeravinone B interacts with both pumps through core hydrophobic π–π interactions and hydrogen bonding.

Both methicillin susceptible *S. aureus* and MRSA are common pathogenic concerns in the hospital environment (Livermore et al., 2015). MRSA remains a major concern in the clinical treatment of *S. aureus*-related infections since half a century. Vancomycin was the only drug of choice for treating the

increased incidence of MRSA, but resistance abolished the drug's mechanism of action. With time, novel candidates were observed to be active against these strains, such as daptomycin, linezolid, and some glycopeptides, but resistance to these drugs was reported (Nannini et al., 2010). Because of frequent reports on resistance to antimicrobials, researchers are now using adjuvant therapy as a treatment strategy (Drugeon et al., 1999).

Active efflux has been reported to be associated with increased resistance in bacterial biofilms (Lewis, 2007; Van Acker and Coenye, 2016). The treatment of biofilm-related infections is a major unmet clinical concern because currently used antibiotics are insufficient to treat these highly persistent infections; some candidate molecules are under early development. Evidently, biofilms have slow metabolism and cell growth, which contribute to increased resistance because most currently used antibiotics have been discovered by targeting metabolic or cell division pathways. The synergistic action of molecules was reported to abolish the formation of biofilms (Baugh et al., 2014). These ideas prompted the assessment of the role of boeravinone B in the prevention and eradication of biofilms, a major clinical problem in the current era of anti-infective drug discovery (Bharate et al., 2015). Current studies have revealed that in combination with boeravinone B, the sub MBIC of ciprofloxacin inhibited the formation of biofilms through enhanced drug accumulation. Therefore, boeravinone B could penetrate the complex matrix of *S. aureus*-generated biofilms to inhibit viable bacteria, as observed in the resazurin assay (Supplementary Figure S1). The involvement of efflux pump inhibitors, such as certain diamines, was reported in reducing the invasiveness of *Pseudomonas aeruginosa* in eukaryotic cells (Hirakata et al., 2009). We obtained the similar results for capsaicin in a previous study (Kalia et al., 2012). This observation shows similar effects of boeravinone B, as expected, after the removal of FCS from the assay media (RPMI).

CONCLUSION

Boeravinone B is a novel dual inhibitor of bacterial NorA efflux pump and human *P*-gp. Such inhibitors play potential role in drug combinations by retaining higher concentrations of drugs in bacterial and host cells.

AUTHOR CONTRIBUTIONS

SS and NK performed microbiological studies. PJ performed isolation of compound and *in silico* studies. AsK and PS performed microscopic studies. SS and IK participated in design and execution of microbiological studies. SB participated in isolation and identification of compound used in this study. PJ and AjK participated in *P*-glycoprotein efflux inhibition studies. IK and SS prepared the manuscript and all authors participated in revising manuscript. All authors approved the study. All authors are accountable for all aspects of work in ensuring that questions related to the accuracy or integrity of the part of work are appropriately investigated and resolved.

FUNDING

SS received a Senior Research Fellowship from the Indian Council of Medical Research, New Delhi, India (80/993/2015-ECD-1). This work was supported by Council of Scientific and Industrial Research (CSIR), New Delhi, India (Grant no. BSC0205).

ACKNOWLEDGMENTS

We are grateful to Professor G. W. Kaatz (Wayne State University School of Medicine, Detroit, MI, United States) for providing *S. aureus* SA-1199, SA-1199B and SA-K1758. MT23142, a NorA over expressing strain was a kind gift from Professor David Hooper (Harvard Medical School, Boston, MA, United States).

SUPPLEMENTARY MATERIAL

The Supplementary Material for this article can be found online at: http://journal.frontiersin.org/article/10.3389/fmicb.2017.01868/full#supplementary-material

REFERENCES

Ahmed-Belkacem, A., Macalou, S., Borrelli, F., Capasso, R., Fattorusso, E., Taglialatela-Scafati, O., et al. (2007). Nonprenylated rotenoids, a new class of potent breast cancer resistance protein inhibitors. *J. Med. Chem.* 50, 1933–1938. doi: 10.1021/jm061450q

Aller, S. G., Yu, J., Ward, A., Weng, Y., Chittaboina, S., Zhuo, R., et al. (2009). Structure of P-glycoprotein reveals a molecular basis for poly-specific drug binding. *Science* 323, 1718–1722. doi: 10.1126/science.1168750

Astolfi, A., Felicetti, T., Iraci, N., Manfroni, G., Massari, S., Pietrella, D., et al. (2017). Pharmacophore-based repositioning of approved drugs as novel *Staphylococcus aureus* NorA efflux pump inhibitors. *J. Med. Chem.* 60, 1598–1604. doi: 10.1021/acs.jmedchem.6b01439

Bairwa, K., Srivastava, A., and Jachak, S. M. (2014). Quantitative analysis of boeravinones in the roots of *Boerhavia diffusa* by UPLC/PDA. *Phytochem. Anal.* 25, 415–420. doi: 10.1002/pca.2509

Bauer, J., Siala, W., Tulkens, P. M., and Van Bambeke, F. (2013). A combined pharmacodynamic quantitative and qualitative model reveals the potent activity of daptomycin and delafloxacin against *Staphylococcus aureus* biofilms. *Antimicrob. Agents Chemother.* 57, 2726–2737. doi: 10.1128/AAC.00181-13

Baugh, S., Ekanayaka, A. S., Piddock, L. J., and Webber, M. A. (2012). Loss of or inhibition of all multidrug resistance efflux pumps of *Salmonella enterica* serovar Typhimurium results in impaired ability to form a biofilm. *J. Antimicrob. Chemother.* 67, 2409–2417. doi: 10.1093/jac/dks228

Baugh, S., Phillips, C. R., Ekanayaka, A. S., Piddock, L. J., and Webber, M. A. (2014). Inhibition of multidrug efflux as a strategy to prevent biofilm formation. *J. Antimicrob. Chemother.* 69, 673–681. doi: 10.1093/jac/dkt420

Bharate, J. B., Singh, S., Wani, A., Sharma, S., Joshi, P., Khan, I. A., et al. (2015). Discovery of 4-acetyl-3-(4-fluorophenyl)-1-(p-tolyl)-5-methylpyrrole as a dual inhibitor of human P-glycoprotein and *Staphylococcus aureus* NorA efflux pump. *Org. Biomol. Chem.* 13, 5424–5431. doi: 10.1039/c5ob00246j

Bhardwaj, R. K., Glaeser, H., Becquemont, L., Klotz, U., Gupta, S. K., and Fromm, M. F. (2002). Piperine, a major constituent of black pepper, inhibits human P-glycoprotein and CYP3A4. *J. Pharmacol. Exp. Ther.* 302, 645–650. doi: 10.1124/jpet.102.034728

Bjarnsholt, T., Ciofu, O., Molin, S., Givskov, M., and Hoiby, N. (2013). Applying insights from biofilm biology to drug development - can a new approach be developed? *Nat. Rev. Drug Discov.* 12, 791–808. doi: 10.1038/nrd4000

Brenwald, N. P., Gill, M. J., and Wise, R. (1998). Prevalence of a putative efflux mechanism among fluoroquinolone-resistant clinical isolates of *Streptococcus pneumoniae*. *Antimicrob. Agents Chemother.* 42, 2032–2035.

Chen, C. J., Chin, J. E., Ueda, K., Clark, D. P., Pastan, I., Gottesman, M. M., et al. (1986). Internal duplication and homology with bacterial transport proteins in the mdr1 (P-glycoprotein) gene from multidrug-resistant human cells. *Cell* 47, 381–389. doi: 10.1016/0092-8674(86)90595-7

Cheung, A. L., and Bayles, K. W. (2007). Tissue culture assays used to analyze invasion by *Staphylococcus aureus*. *Curr. Protoc. Microbiol.* 4, 9C.4.1–9C.4.7. doi: 10.1002/9780471729259.mc09c04s4

Darouiche, R. O. (2004). Treatment of infections associated with surgical implants. *N. Engl. J. Med.* 350, 1422–1429. doi: 10.1056/NEJMra035415

Drugeon, H. B., Juvin, M. E., and Bryskier, A. (1999). Relative potential for selection of fluoroquinolone-resistant *Streptococcus pneumoniae* strains by levofloxacin: comparison with ciprofloxacin, sparfloxacin and ofloxacin. *J. Antimicrob. Chemother.* 43(Suppl. C), 55–59. doi: 10.1093/jac/43.suppl_3.55

Eliopoulos, G. M., and Moellering, R. C. J. (1996). "Antimicrobial combinations," in *Antibiotics in Laboratory Medicine*, 4th Edn, ed. V. Lorian (Baltimore, MD: Williams & Wilkins), 330–336.

Eliopoulos, G. M., and Wennersten, C. B. (2002). Antimicrobial activity of quinupristin-dalfopristin combined with other antibiotics against vancomycin-resistant enterococci. *Antimicrob. Agents Chemother.* 46, 1319–1324. doi: 10.1128/AAC.46.5.1319-1324.2002

Fontaine, F., Hequet, A., Voisin-Chiret, A. S., Bouillon, A., Lesnard, A., Cresteil, T., et al. (2015). Boronic species as promising inhibitors of the *Staphylococcus aureus* NorA efflux pump: study of 6-substituted pyridine-3-boronic acid derivatives. *Eur. J. Med. Chem.* 95, 185–198. doi: 10.1016/j.ejmech.2015.02.056

Ganesan, A., Christena, L. R., Venkata Subbarao, H. M., Venkatasubramanian, U., Thiagarajan, R., Sivaramakrishnan, V., et al. (2016). Identification of benzochromene derivatives as a highly specific NorA efflux pump inhibitor to mitigate the drug resistant strains of *S. aureus*. *RSC Adv.* 6, 30258–30267. doi: 10.1039/C6RA01981A

Gibbons, S., Oluwatuyi, M., and Kaatz, G. W. (2003). A novel inhibitor of multidrug efflux pumps in *Staphylococcus aureus*. *J. Antimicrob. Chemother.* 51, 13–17. doi: 10.1093/jac/dkg044

Gupta, D., Singh, A., and Khan, A. U. (2017). Nanoparticles as efflux pump and biofilm inhibitor to rejuvenate bactericidal effect of conventional antibiotics. *Nanoscale Res. Lett.* 12, 454. doi: 10.1186/s11671-017-2222-6

Hirakata, Y., Kondo, A., Hoshino, K., Yano, H., Arai, K., Hirotani, A., et al. (2009). Efflux pump inhibitors reduce the invasiveness of *Pseudomonas aeruginosa*. *Int. J. Antimicrob. Agents* 34, 343–346. doi: 10.1016/j.ijantimicag.2009.06.007

Holler, J. G., Christensen, S. B., Slotved, H. C., Rasmussen, H. B., Guzman, A., Olsen, C. E., et al. (2012). Novel inhibitory activity of the *Staphylococcus aureus* NorA efflux pump by a kaempferol rhamnoside isolated from *Persea lingue* Nees. *J. Antimicrob. Chemother.* 67, 1138–1144. doi: 10.1093/jac/dks005

Hooper, D. C. (2005). Efflux pumps and nosocomial antibiotic resistance: a primer for hospital epidemiologists. *Clin. Infect. Dis.* 40, 1811–1817. doi: 10.1086/430381

Hou, W., Sun, X., Wang, Z., and Zhang, Y. (2012). Biofilm-forming capacity of *Staphylococcus epidermidis*, *Staphylococcus aureus*, and *Pseudomonas aeruginosa* from ocular infections. *Invest. Ophthalmol. Vis. Sci.* 53, 5624–5631. doi: 10.1167/iovs.11-9114

Jin, M. S., Oldham, M. L., Zhang, Q., and Chen, J. (2012). Crystal structure of the multidrug transporter P-glycoprotein from *Caenorhabditis elegans*. *Nature* 490, 566–569. doi: 10.1038/nature11448

Joshi, P., Singh, S., Wani, A., Sharma, S., Jain, S. K., Singh, B., et al. (2014). Osthol and curcumin as inhibitors of human Pgp and multidrug efflux pumps of *Staphylococcus aureus*: reversing the resistance against frontline antibacterial drugs. *MedChemComm* 5, 1540–1547. doi: 10.1039/C4MD00196F

Kaatz, G. W. (2005). Bacterial efflux pump inhibition. *Curr. Opin. Investig. Drugs* 6, 191–198.

Kaatz, G. W., Moudgal, V. V., Seo, S. M., and Kristiansen, J. E. (2003). Phenothiazines and thioxanthenes inhibit multidrug efflux pump activity in *Staphylococcus aureus*. *Antimicrob. Agents Chemother.* 47, 719–726. doi: 10.1128/AAC.47.2.719-726.2003

Kadota, S., Tezuka, N. Y., and Kikuchi, T. (1989). Constituents of the roots of *Boerhavia diffusa* L.I. examination of sterols and structures of new rotenoids, boeravinones A and B. *Chem. Pharm. Bull.* 37, 3214–3220. doi: 10.1248/cpb.37.3214

Kalia, N. P., Mahajan, P., Mehra, R., Nargotra, A., Sharma, J. P., Koul, S., et al. (2012). Capsaicin, a novel inhibitor of the NorA efflux pump, reduces the intracellular invasion of *Staphylococcus aureus*. *J. Antimicrob. Chemother.* 67, 2401–2408. doi: 10.1093/jac/dks232

Khan, I. A., Mirza, Z. M., Kumar, A., Verma, V., and Qazi, G. N. (2006). Piperine, a phytochemical potentiator of ciprofloxacin against *Staphylococcus aureus*. *Antimicrob. Agents Chemother.* 50, 810–812. doi: 10.1128/AAC.50.2.810-812.2006

Khan, M. S., Ansari, I. A., Ahmad, S., Ahmad, S., Akhter, F., Hashim, A., et al. (2013). Chemotherapeutic potential of *Boerhavia diffusa* Linn: a review. *J. Appl. Pharm. Sci.* 3, 133–139.

Kumar, A., Khan, I. A., Koul, S., Koul, J. L., Taneja, S. C., Ali, I., et al. (2008). Novel structural analogues of piperine as inhibitors of the NorA efflux pump of *Staphylococcus aureus*. *J. Antimicrob. Chemother.* 61, 1270–1276. doi: 10.1093/jac/dkn088

Kvist, M., Hancock, V., and Klemm, P. (2008). Inactivation of efflux pumps abolishes bacterial biofilm formation. *Appl. Environ. Microbiol.* 74, 7376–7382. doi: 10.1128/AEM.01310-08

Leitner, I., Nemeth, J., Feurstein, T., Abrahim, A., Matzneller, P., Lagler, H., et al. (2011). The third-generation P-glycoprotein inhibitor tariquidar may overcome bacterial multidrug resistance by increasing intracellular drug concentration. *J. Antimicrob. Chemother.* 66, 834–839. doi: 10.1093/jac/dkq526

Lewis, K. (2001). Riddle of biofilm resistance. *Antimicrob. Agents Chemother.* 45, 999–1007. doi: 10.1128/AAC.45.4.999-1007.2001

Lewis, K. (2007). Persister cells, dormancy and infectious disease. *Nat. Rev. Microbiol.* 5, 48–56. doi: 10.1038/nrmicro1557

Lewis, K. (2008). Multidrug tolerance of biofilms and persister cells. *Curr. Top. Microbiol. Immunol.* 322, 107–131. doi: 10.1007/978-3-540-75418-3_6

Lin, J. H. (2003). Drug-drug interaction mediated by inhibition and induction of P-glycoprotein. *Adv. Drug Deliv. Rev.* 55, 53–81. doi: 10.1016/S0169-409X(02)00171-0

Livermore, D. M., Mushtaq, S., Warner, M., James, D., Kearns, A., and Woodford, N. (2015). Pathogens of skin and skin-structure infections in the UK and their susceptibility to antibiotics, including ceftaroline. *J. Antimicrob. Chemother.* 70, 2844–2853. doi: 10.1093/jac/dkv179

Lowrence, R. C., Raman, T., Makala, H. V., Ulaganathan, V., Subramaniapillai, S. G., Kuppuswamy, A. A., et al. (2016). Dithiazole thione derivative as competitive NorA efflux pump inhibitor to curtail multi drug resistant clinical isolate of MRSA in a zebrafish infection model. *Appl. Microbiol. Biotechnol.* 100, 9265–9281. doi: 10.1007/s00253-016-7759-2

Mullin, S., Mani, N., and Grossman, T. H. (2004). Inhibition of antibiotic efflux in bacteria by the novel multidrug resistance inhibitors biricodar (VX-710) and timcodar (VX-853). *Antimicrob. Agents Chemother.* 48, 4171–4176. doi: 10.1128/AAC.48.11.4171-4176.2004

Nannini, E., Murray, B. E., and Arias, C. A. (2010). Resistance or decreased susceptibility to glycopeptides, daptomycin, and linezolid in methicillin-resistant *Staphylococcus aureus*. *Curr. Opin. Pharmacol.* 10, 516–521. doi: 10.1016/j.coph.2010.06.006

Patel, D., Kosmidis, C., Seo, S. M., and Kaatz, G. W. (2010). Ethidium bromide MIC screening for enhanced efflux pump gene expression or efflux activity in *Staphylococcus aureus*. *Antimicrob. Agents Chemother.* 54, 5070–5073. doi: 10.1128/AAC.01058-10

Patil, K. S., and Bhalsing, S. R. (2016). Ethnomedicinal uses, phytochemistry and pharmacological properties of the genus *Boerhavia*. *J. Ethnopharmacol.* 182, 200–220. doi: 10.1016/j.jep.2016.01.042

Piddock, L. J. (2006). Clinically relevant chromosomally encoded multidrug resistance efflux pumps in bacteria. *Clin. Microbiol. Rev.* 19, 382–402. doi: 10.1128/CMR.19.2.382-402.2006

Poole, K. (2005). Efflux-mediated antimicrobial resistance. *J. Antimicrob. Chemother.* 56, 20–51. doi: 10.1093/jac/dki171

Sabatini, S., Piccioni, M., Felicetti, T., De Marco, S., Manfroni, G., Pagiotti, R., et al. (2017). Investigation on the effect of known potent *S. aureus* NorA efflux pump inhibitors on the staphylococcal biofilm formation. *RSC Adv.* 7, 37007–37014. doi: 10.1039/C7RA03859C

Schillaci, D., Arizza, V., Parrinello, N., Di Stefano, V., Fanara, S., Muccilli, V., et al. (2010). Antimicrobial and antistaphylococcal biofilm activity from the sea urchin *Paracentrotus lividus*. *J. Appl. Microbiol.* 108, 17–24. doi: 10.1111/j.1365-2672.2009.04394.x

Schindler, B. D., Jacinto, P., and Kaatz, G. W. (2013). Inhibition of drug efflux pumps in *Staphylococcus aureus*: current status of potentiating existing antibiotics. *Future Microbiol.* 8, 491–507. doi: 10.2217/fmb.13.16

Stacy, A. E., Jansson, P. J., and Richardson, D. R. (2013). Molecular pharmacology of ABCG2 and its role in chemoresistance. *Mol. Pharmacol.* 84, 655–669. doi: 10.1124/mol.113.088609

Stavri, M., Piddock, L. J., and Gibbons, S. (2007). Bacterial efflux pump inhibitors from natural sources. *J. Antimicrob. Chemother.* 59, 1247–1260. doi: 10.1093/jac/dkl460

Sun, J., Deng, Z., and Yan, A. (2014). Bacterial multidrug efflux pumps: mechanisms, physiology and pharmacological exploitations. *Biochem. Biophys. Res. Commun.* 453, 254–267. doi: 10.1016/j.bbrc.2014.05.090

Tegos, G. P., Haynes, M., Strouse, J. J., Khan, M. M., Bologa, C. G., Oprea, T. I., et al. (2011). Microbial efflux pump inhibition: tactics and strategies. *Curr. Pharm. Des.* 17, 1291–1302. doi: 10.2174/138161211795703726

Tintino, S. R., Oliveira-Tintino, C. D., Campina, F. F., Silva, R. L., Costa Mdo, S., Menezes, I. R., et al. (2016). Evaluation of the tannic acid inhibitory effect against the NorA efflux pump of *Staphylococcus aureus*. *Microb. Pathog.* 97, 9–13. doi: 10.1016/j.micpath.2016.04.003

Van Acker, H., and Coenye, T. (2016). The role of efflux and physiological adaptation in biofilm tolerance and resistance. *J. Biol. Chem.* 291, 12565–12572. doi: 10.1074/jbc.R115.707257

Yang, H., Wang, M., Yu, J., and Wei, H. (2015). Aspartate inhibits *Staphylococcus aureus* biofilm formation. *FEMS Microbiol. Lett.* 362:fnv025. doi: 10.1093/femsle/fnv025

Conflict of Interest Statement: The authors declare that the research was conducted in the absence of any commercial or financial relationships that could be construed as a potential conflict of interest.

Copyright © 2017 Singh, Kalia, Joshi, Kumar, Sharma, Kumar, Bharate and Khan. This is an open-access article distributed under the terms of the Creative Commons Attribution License (CC BY). The use, distribution or reproduction in other forums is permitted, provided the original author(s) or licensor are credited and that the original publication in this journal is cited, in accordance with accepted academic practice. No use, distribution or reproduction is permitted which does not comply with these terms.

frontiers in Microbiology

ORIGINAL RESEARCH
published: 05 December 2017
doi: 10.3389/fmicb.2017.02385

Structure–Function Relationship of Aminopeptidase P from *Pseudomonas aeruginosa*

Cui-Ting Peng[1,2†], Li Liu[1,2†], Chang-Cheng Li[2], Li-Hui He[2], Tao Li[2], Ya-Lin Shen[2], Chao Gao[2], Ning-Yu Wang[2,3], Yong Xia[2], Yi-Bo Zhu[2], Ying-Jie Song[2], Qian Lei[2], Luo-Ting Yu[1,2] and Rui Bao[2*]*

[1] Pharmaceutical and Biological Engineering Department, School of Chemical Engineering, Sichuan University, Chengdu, China, [2] Center of Infectious Diseases, State Key Laboratory of Biotherapy, West China Hospital, Sichuan University and Collaborative Innovation Center, Chengdu, China, [3] School of Life Sciences and Engineering, Southwest Jiaotong University, Chengdu, China

OPEN ACCESS

Edited by:
Teresa M. Coque,
Instituto Ramón y Cajal de Investigación Sanitaria, Spain

Reviewed by:
Jose L. Martinez,
Consejo Superior de Investigaciones Científicas (CSIC), Spain
Francesco Imperi,
Sapienza Università di Roma, Italy

***Correspondence:**
Rui Bao
baorui@scu.edu.cn
Luo-Ting Yu
yuluot@scu.edu.cn

[†] These authors have contributed equally to this work.

Specialty section:
This article was submitted to Antimicrobials, Resistance and Chemotherapy, a section of the journal Frontiers in Microbiology

Received: 19 July 2017
Accepted: 20 November 2017
Published: 05 December 2017

Citation:
Peng C-T, Liu L, Li C-C, He L-H, Li T, Shen Y-L, Gao C, Wang N-Y, Xia Y, Zhu Y-B, Song Y-J, Lei Q, Yu L-T and Bao R (2017) Structure–Function Relationship of Aminopeptidase P from Pseudomonas aeruginosa. Front. Microbiol. 8:2385. doi: 10.3389/fmicb.2017.02385

PepP is a virulence-associated gene in *Pseudomonas aeruginosa*, making it an attractive target for anti-*P. aeruginosa* drug development. The encoded protein, aminopeptidases P (Pa-PepP), is a type of X-prolyl peptidase that possesses diverse biological functions. The crystal structure verified its canonical pita-bread fold and functional tetrameric assembly, and the functional studies measured the influences of different metal ions on the activity. A trimetal manganese cluster was observed at the active site, elucidating the mechanism of inhibition by metal ions. Additionally, a loop extending from the active site appeared to be important for specific large-substrate binding. Based on the structural comparison and bacterial invasion assays, we showed that this non-conserved surface loop was critical for *P. aeruginosa* virulence. Taken together, these findings can extend our understanding of the catalytic mechanism and virulence-related functions of Pa-PepP and provide a solid foundation for the design of specific inhibitors against pathogenic-bacterial infections.

Keywords: *Pseudomonas aeruginosa*, aminopeptidase P, virulence, tri-nuclear form, X-ray crystallography

INTRODUCTION

Pseudomonas aeruginosa is a common nosocomial pathogen and is notoriously difficult to treat due to its high intrinsic and acquired drug resistance (Hancock, 1998; Stover et al., 2000). To address the challenges of *P. aeruginosa* infections, alternative approaches other than conventional antibiotic therapy were undertaken, with an emphasis on anti-virulence strategies (Hentzer et al., 2003; Luckett et al., 2012; Gi et al., 2014; Hwang et al., 2016; Maura et al., 2016; Johnson and Abramovitch, 2017; Rampioni et al., 2017). The targets for most anti-virulence strategies are those well-studied virulence factors (adhesins, toxins, effector secretion system components) that directly participate in pathogen-host cell interactions (Woods et al., 1982; Hahn, 1997; Hood et al., 2010). However, not all of these virulence factors play significant roles in *P. aeruginosa* infection (Miyata et al., 2003). Instead, there are many genes with unidentified roles in *P. aeruginosa* virulence,

Abbreviations: DMEM, Dulbecco's Modified Eagle's Medium; FBS, fetal bovine serum; IPTG, isopropyl β-D-1-thiogalactopyranoside; LB, Luria–Bertani; MOI, multiplicity of infection; NCPSS, National Center for Protein Sciences Shanghai; OD600, optical cell densities at 600 nm; PBS, phosphate-buffered saline; *P. aeruginosa*, *Pseudomonas aeruginosa;* SDS–PAGE, sodium dodecyl sulfate–polyacrylamide gel electrophoresis; SSRF, Shanghai Synchrotron Radiation Facility.

while the corresponding mutants resulted in obvious virulence attenuation, suggesting potential applications for these genes in anti-virulence therapy discovery.

PepP encodes an enzyme belonging to the aminopeptidases P (APPro) family (E.C.3.4.11.9), a type of metalloprotease that catalyzes the removal of the N-terminal residue from a polypeptide that has proline as the second residue (Taylor, 1993; Gonzales and Robert-Baudouy, 1996; Wilce et al., 1998). It is one of the critical virulence-associated genes identified using a *P. aeruginosa-C. elegans* infection mode (Feinbaum et al., 2012). In this model, transposon mutants of *pepP* in *P. aeruginosa* PA14 have attenuated virulence, leading to reduced *C. elegans* survival. *PepP* is highly conserved in all *P. aeruginosa* genomes sequenced to date and with high similarity to this gene from other *Pseudomonas* species (82.4%–100% identity). In contrast to other metalloaminopeptidases, APPro is a cytoplasmic aminopeptidase and recognizes a restricted scissile Xaa-Pro bond of those polypeptide or protein substrates that may be linked to virulence-associated phenotypes or other biological processes beyond the general protein degradation ability (Lowther and Matthews, 2002). APPro is widely distributed among bacteria, fungi, plants and mammals. It is thought to play a role in many important biological pathways, including hormone regulation in mammals (Simmons and Orawski, 1992) and the terminal degradation of proline-containing peptides and proteins (Wilce et al., 1998), or organophosphate compounds in bacterial (Jao et al., 2004). The gene coding *Escherichia coli* aminopeptidases P (Ec-PepP) was even identified as a factor involved in outer membrane vesicles (OMV) production (McBroom et al., 2006; Vanaja et al., 2016). While structural and biochemical studies on APPro have visualized a general catalytic mechanism and revealed a conserved binding pocket for N-terminal substrates (Wilce et al., 1998; Graham et al., 2005, 2006; Liu et al., 2007; Graham and Guss, 2008; Jeyakanthan et al., 2009; Weaver et al., 2014), further investigations are needed to elucidate the structural basis for APPro's specific substrate recognition and diverse functions. Thus, a better understanding of the structure and function of *P. aeruginosa* APPro (Pa-PepP) would enable us to propose the possible mechanisms involved in bacterial virulence.

In this study, we solved the X-ray crystal structure of Pa-PepP with a resolution of 1.8 Å. A biochemical analysis verified the residues critical for catalysis. The presence of a trinuclear manganese cluster in the reaction center suggests a mechanism for inhibition by excessive metal ion binding. Furthermore, an extended substrate binding site was identified to be responsible for virulence-related protein recognition.

RESULTS

Pa-PepP Adopts a Canonical Pita-Bread Fold and Assembles as a Tetramer in Crystal

Refinement of the Pa-PepP structure resulted in a final model with a free R-factor (Rfree) of 0.2206 at 1.8 Å. Sufficient electron density allowed us to model all residues from 1 to 444. The crystallographic statistics are summarized in **Table 1**. The monomer structure displays a two-domain organization where the N-domain (1–175) is composed of a mainly parallel beta-sheet core (B1–B6) flanked by seven alpha helices (A–G). In contrast, the catalytic C-domain (176–444) adopts a conserved "pita-bread" fold with six beta sheets (B7-B12) in antiparallel configurations (**Figure 1A**). This pita-bread fold is commonly found in N-terminal amido-, imido-, and amidino-scissile bond-cleaving enzymes, and serves as a structural basis for the metal-dependent catalysis (Lowther and Matthews, 2000; Besio et al., 2010).

Although the recombinant Pa-PepP purified from *E. coli* strain BL21 (DE3) exists as a monomer in solution (**Figure 1B**), tetrameric oligomerization was observed in crystal packing (**Figure 1C**). The monomers were arranged as a dimer with an extended loop contributing to the active site of the adjacent subunit and an average interface area of approximately 2050.9 A^2 per subunit. The dimer-of-dimers was generated by crystallographic symmetry operation (x–1/2, –y–1/2, –z), and the major interactions are contributed by the C-domain of each monomer, resulting in an ∼815.6 A^2 buried area per subunit. For most metalloaminopeptidases, the oligomeric state is essential for their biological functions. The loop from the adjacent monomer extends the substrate-binding site and thus enables the enzyme to cleave larger substrates.

TABLE 1 | Data collection and refinement statistics.

	PDB Entry	5WZE
Data collection	Space group	P 21 21 21
	Cell dimension	
	a, b, c (Å)	111.197,123.432,149.485
	α, β, γ (°)	90, 90, 90
	Wavelength	0.97776
	Resolution (Å)	48.01–1.783 (1.847–1.783)
	I/I	19.714 (2.167)
	Completeness (%)	0.99
	R_{merge}	0.099 (0.709)
	Redundancy	8.9 (6.4)
Refinement	Resolution (Å)	48.01–1.783 (1.847–1.783)
	No. of reflections	194404 (18600)
	Rwork/Rfree	0.2105/0.2206
	No. of atoms	
	Protein	1783
	Ligand/ion	90
	Water	1153
	B-factor	
	Protein	27.37
	Ligand/ion	38.94
	Water	30.89
	R.m.s. deviations	
	Bond lengths (Å)	0.011
	Bond angles (°)	1.00
	Ramachandran plot	98/1.5/0

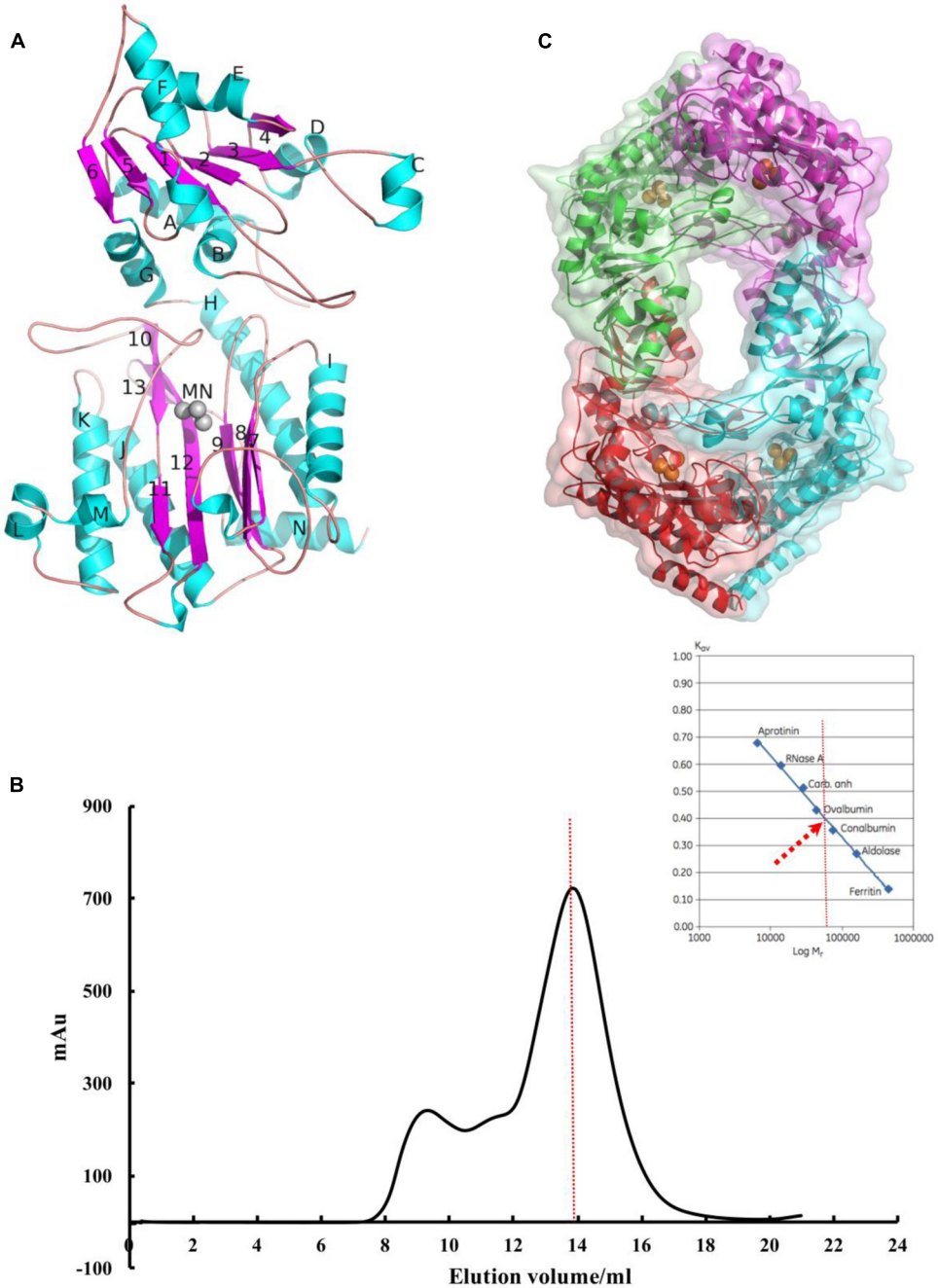

FIGURE 1 | Pa-PepP adopts a canonical pita-bread fold and assembles as a tetramer in crystal. **(A)** The second structure assignments of the Pa-PepP monomer. Beta-sheets are colored blue, alpha-helices are colored green, and the three Mn^{2+} ions are shown as gray spheres. The figure was generated by PyMOL (http://www.pymol.org). **(B)** The gel filtration curve for the purified recombinant Pa-PepP in solution. The AUC results are presented as the ultraviolet absorption in 280 nm. The black solid curve refers to Pa-PepP eluted from GE HiLoad 16/600 Superdex 200 column. The red dash curve refers to the sample elution volume and corresponding molecule mass of the sample when compared with the standard sample proteins. **(C)** 3D structure of Pa-PepP showed a detailed tetramer of four subunits or a homodimer of Pa-PepP. Each subunit is presented as different color with Mn^{2+} ions are shown as orange spheres in the metal binding site.

Thus, the antiparallel dimerization would be the basic active polymerization forms to its biological activity, and the different quaternary arrangement may reflect a possible regulatory mechanism for its activity.

Effect of the Metal Ion in Activity Modulation

Metalloaminopeptidases are well known for their metal-dependent catalysis mechanisms. Proline-specific

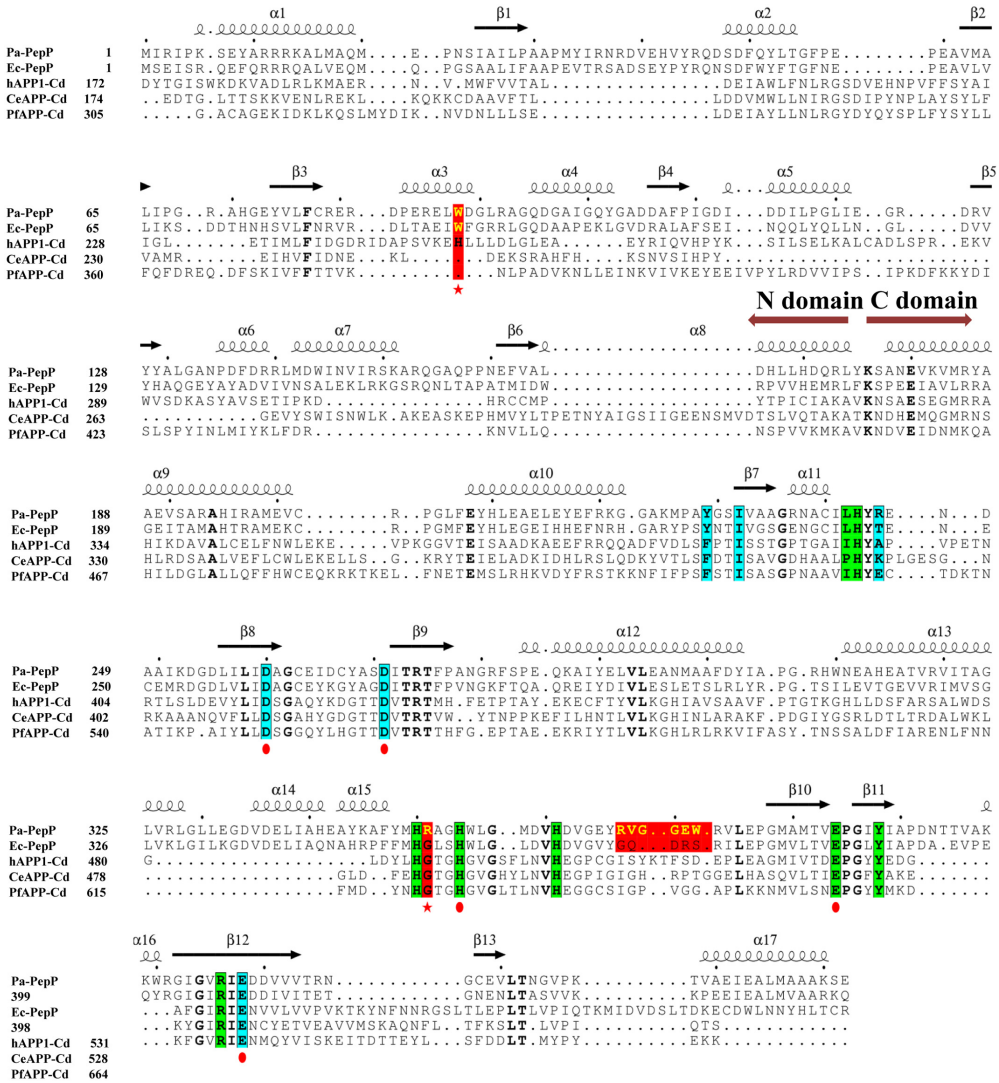

FIGURE 2 | Multiple sequence alignment of the truncated N domain and catalytic C domains from X-prolyl peptidases. From top to bottom, the sequences are aminopeptidases P from *P. aeruginosa* (Pa-PepP), aminopeptidases P from *Escherichia coli* (Ec-PepP), truncated N domain and catalytic C domains from from human XPNPEP1 (hAPP1, 172-618), X-prolyl aminopeptidase from *Caenorhabditis elegans* (CeAPP, 174–616), and aminopeptidase P from *Plasmodium falciparum* (PfAPP, 305–774). Residues for chelating metal ion are highlighted using the red circle under the sequences; Residues contributed to S1 pockets are highlighted with a blue background and residues for S' sites are presented with a green background; The red color displayed residues or short sequences are non-conserved among prokaryotic and eukaryotic APPros, which are also proved to be important to APPros' function. Sequences were aligned using the program ClustalX (Li et al., 2008), and the alignment was presented using the online ESPript 3.0 server (http://espript.ibcp.fr/ESPript/ESPript/).

aminopeptidases such as APPro and prolidase prefer dinuclear Mn(II) cluster as cofactor (Wilce et al., 1998; Graham et al., 2005). The residues coordinating the two Mn atoms (Mn_A and Mn_B) are highly conserved among APPro family members (**Figure 2**), and the non-equivalent roles of the two metal ions in catalysis have been extensively studied (Graham et al., 2005; Hu et al., 2007). To test the role of divalent metal cluster on Pa-PepP, we measured the relative activities of Pa-PepP in the presence of 1 mM Mn^{2+},Ca^{2+},Mg^{2+}, Ni^{2+}, Zn^{2+}, and EDTA (**Figure 3A**). The addition of Mn^{2+} significantly restored the Pa-PepP activity, while the limited enhancement of activity was observed upon addition of Ca^{2+} or Mg^{2+}. The exhibited basal activity may be a result of the partially pre-bound metal ions from the cell, and the limited effects of Ca^{2+} and Mg^{2+} may be due to their weak binding affinity to the active site. Previous studies on metal selection in Ec-PepP revealed that the Zn^{2+} ion has high affinity for APPro and inhibits the hydrolysis reaction by occupying a third metal binding site (Graham et al., 2005; Hu et al., 2007). Although we could not measure the effect of Zn^{2+} ion on Pa-PepP because of the formation of zinc hydroxide precipitates upon adding $ZnCl_2$ to the alkaline enzyme buffer, we observed the complete inhibition of enzyme activity in the presence of both the Ni^{2+} ion and the chelating agent EDTA. These results suggested that the Ni^{2+} may also possess high

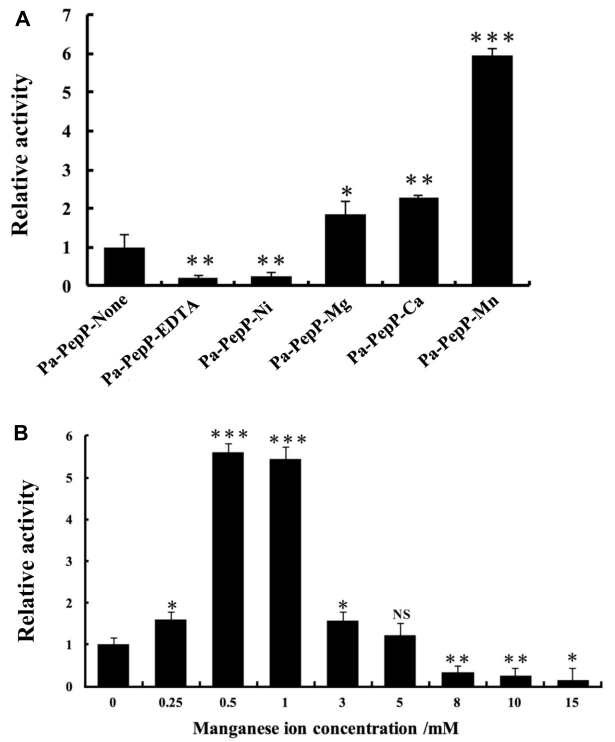

FIGURE 3 | Relative activity assay of Pa-PepP using the quenched fluorescent substrate Lys (Abz)–Pro–Pro–pNA. All assays were performed at 37°C for 5 min in the presence of 50 mM Tris (pH 8.5), 100 mM NaCl, 0–250 μM Lyz(Abz)–Pro–Pro–pNA quenched fluorescent substrate, and 1 $\mu g/mL^{-1}$ Pa-PepP that had been incubated with different metal ions at 37°C for 10 min. Each bar represents the mean of three independent measurements (SEM). **(A)** Relative activity of Pa-PepP in the presence of 1 mM different metal ions or EDTA. **(B)** Relative activity of Pa-PepP in presence of different amount of Mn^{2+}. *P*-values for comparison of each group with Pa-PepP-alone **(A)** or 0 mM Mn^{2+} **(B)** were determined by 2-tailed Student's *t*-test (*$P < 0.05$; **$P < 0.01$; ***$P < 0.001$).

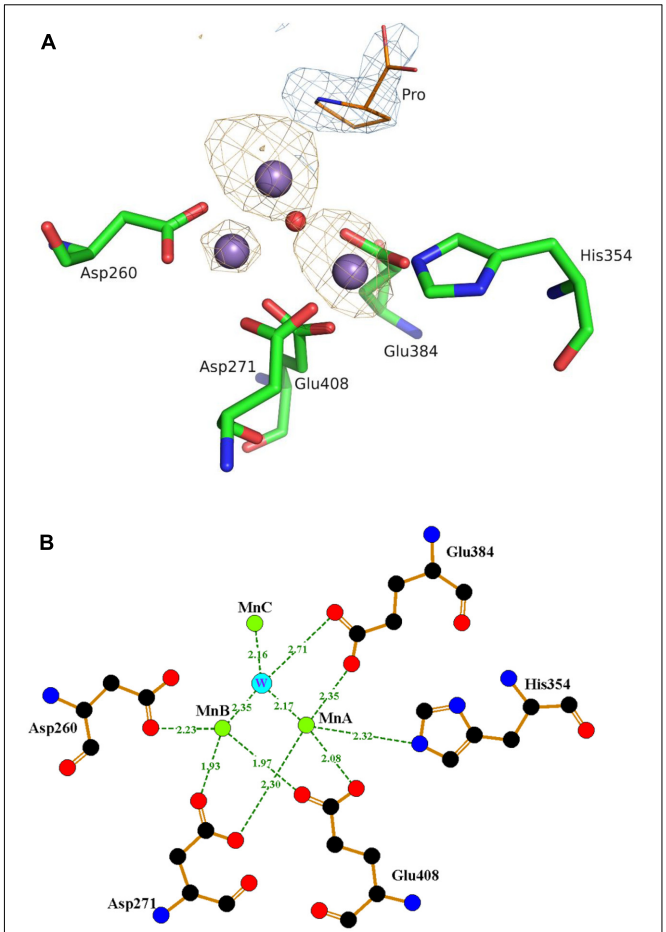

FIGURE 4 | The trimetal Mn cluster center and interactions with the surrounding amino acid residues. **(A)** The anomalous map peaks of the bound Mn in Pa-PepP structure. The three Mn^{2+} ions are shown as dark purple spheres with different anomalous signals and the red sphere refers to the water molecule participated in activity modulation. For clarity, only part of the metal binding residues is shown together with the observed proline with blue electron density near the active site. The figure was generated by PyMOL (http://www.pymol.org). **(B)** Representative interactions around the active sites. Mn_A is liganded by the side chains of His354, Asp271, Glu384, Glu408, and Mn_B interacts with Asp260, Asp271, Glu408. And Mn_C interacts through one solvent molecular (W) to Mn_A and Mn_B with a metal separation distance of 3.1–3.7 Å. Figures were prepared using LIGPLOT (Wallace et al., 1995).

affinity to APPro and tends to bind to those positions equivalent to Zn^{2+} ions in Ec-PepP.

To identify the binding state of Mn^{2+} ions in active site, 10 mM $MnCl_2$ was added during the crystallization experiment, along with 10 mM proline. In the final structure, there are three Mn atoms in each monomer (**Figure 4**). Mn_A is liganded by the side chains of His354, Asp271, Glu384, Glu408, and Mn_B interacts with Asp260, Asp271, Glu408. These interactions are highly conserved among those reported APPro structures that resulted in a distorted trigonal-pyramidal coordination network. The smaller anomalous signals and 0.5 occupancies of the Mn_B site confirmed one of the structural features in metal-dependent aminopeptidase: the metal binding site B has relatively weaker binding affinity comparing to the site A (Hu et al., 2007). Additionally, the third Mn atom (Mn_C) is located in a position previously identified as being occupied by water in Zn-load Ec-PepP structures (Graham et al., 2005). The strong anomalous peak at this position verified its identity as a tightly bound Mn^{2+} ion rather than a water molecule. It is interesting to note that this Mn_C position is different from the third metal binding site found in Ec-PepP, in which the Zn_C is coordinated by His243, His361, and the hydrolysis product Pro residue (Graham et al., 2005). In Pa-PepP, Mn_C interacts through one solvent molecular (W) with Mn_A and Mn_B, with a metal-separation distance of 3.1–3.7 Å. The Pro residue lies immediately above the solvent molecular W but does not participate in the interaction with Mn_C. Remarkably, Mn_C occupies the S1 subsite that ordinarily binds the substrate, providing an explanation for the inhibition effect of excessive metal binding. To verify the inhibitory effect of Mn^{2+} ion, we performed an activity assay in the presence of different amounts of Mn^{2+}. The result is consistent with our structural analysis (**Figure 3B**): there is a Mn^{2+} ion concentration-dependent activity regulation pattern, in which 0.5–1 mM of Mn ion is

the optimal concentration for 20 nM (1 μg/ml) Pa-PepP, and inhibitory effects are observed when Mn^{2+} ion exceeded 5 mM. Inhibition was not observed at ion concentrations up to 20 mM in the assays with Ca^{2+} and Mg^{2+} (**Supplementary Figure S1**).

Conserved Active-Site Motif and Extended Binding Site for Specific Substrate Recognition

Several APPro structures have been reported to date, including APPro from *Escherichia coli* (Ec-PepP, 1M35) (Wilce et al., 1998), *Streptococcus thermophilus* (3IL0), *Bacillus anthracis* (3IG4), *Yersinia pestis* (4PV4), *Thermotoga maritima* (2ZSG), *Streptococcus pyogenes* (3OVK), human (hAPP1, 3CTZ) (Li et al., 2008), *Caenorhabditis elegans* (CeAPP1, 4S2R) (Iyer et al., 2015) and *Plasmodium falciparum* (PfAPP, 5JQK) (Drinkwater et al., 2016). Ec-PepP shares the highest sequence identity with Pa-PepP and both of them are prokaryotic APPro (Gonzales and Robert-Baudouy, 1996). All of these APPros share a common catalytic domain structure that contains a metal center flanked by the S1'-S1 pockets (**Figures 2**, **5A**). Previous structural studies on Ec-PepP in complex with the substrate or inhibitor have revealed those pockets (Graham et al., 2004; Graham and Guss, 2008). We modeled the Val-Pro-Leu bound Pa-PepP complex by superposing Pa-PepP structure with the substrate-bound Ec-PepP structure (PDB code: 2BN7) (**Figure 5A**). The shallow hydrophobic S1' pocket could be defined by the pre-bound Pro residue, Arg406, Tyr388, and His350. S1' sites are conserved in APPro and prolidase but not in other metalloaminopeptidases, which implies that they play critical roles in regulating the activity of proline-specific peptidases. Additionally, in prokaryotic APPros and prolidases, a tryptophan (Trp88' in Pa-PepP) from an adjacent subunit extends the boundary of S1' site and contributes to the P1' Pro binding (Yoshimoto et al., 1994; Jao et al., 2006). At the S1'-S1 junction, His243 and His361 interact with the main-chain carbonyl of P1' Pro and P1 Val, respectively, indicating their specific roles in recognizing and stabilizing the stereospecific scissile X-Pro bond. In the S1 pocket, the side chain of P1 Val faces Tyr229, Ile232, Arg245, while its main chain replaces the Mn_C ion and is involved in the Mn_A and Mn_B ion mediated interactions. In metallomainopeptidases, the dinuclear Mn center is thought to be essential for nucleophilic attack (Graham et al., 2005). To verify the impacts of the critical motifs revealed by structural analysis, we constructed Ala substitutions on those motifs (Trp88 for S1' pocket, His243 for scissile bond stabilizing, Glu384 for metal binding) and verified that the expression level and stability are comparable between the wild type and all the mutants (**Supplementary Figure S2**). The Pa-PepP activity assay shows that all the mutations would eliminate enzymatic activity, which further confirmed that the evolutionary conservation in those regions is strongly associated with the essential functional roles of APPro family (**Figure 5B**).

In contrast to the prolidases that cleave dipeptides only, APPro is capable of modifying protein substrates. The relatively larger substrate binding ability of APPro is partly due to the extension of the substrate binding site beyond the S1'–S1 region (Drinkwater et al., 2016). The modeled tripeptide-bound Pa-PepP structure indicated that Arg153 and Arg351 accommodate the carboxylate group of the P2' Leu, and guide the C-terminus of the substrate toward the tetramer surface (**Figure 5A**). Furthermore, the R351G mutation results in an increase in enzyme activity. The similar Arg153/Arg370 basic patch is also found in Ec-PepP, in which the non-basic residue substitution on either of them leads to an obvious decrease in K_m and an increase in k_{cat}/K_m (Jao et al., 2006). Thus, this basic patch, which is located at the entrance of catalytic cave, can play an important role in specificities of protein substrate recognition and orientation.

Structural Analysis Identified a Surface Loop Participating in *P. aeruginosa* Virulence

The conserved structural properties in active site suggest a common catalytic mechanism for APPro family members, while the differences in the substrate-binding regions indicate the specific functions for each APPro member. Next to the P2' binding site, a surface loop (residue 365–377 in Pa-PepP) between helix α_{15} and sheet β_{10} was identified as a candidate for specific functions due to the diversity in its sequences between APPro members (**Figure 2**). To investigate its impact on enzyme catalytic activity, we mutated residues RVGGEW (Pa-PepP 367-372) to GQDRS (Ec-PepP 368-372). Equivalent activities were observed between the corresponding mutant and the wild-type (**Figure 5B**). Since, in the activity assay, we used a non-specific tripeptide analog instead of the native substrates, these results may not accurately reflect the actual substrate-binding situation.

To further elucidate the impacts of Pa-PepP mutations on the bacterium virulence, three mutants with different effects on enzymatic activity were made in *P. aeruginos* PA14 for use in a Hela-cell invasion assay (**Figure 5C**). The PA14 bacterial growth *in vitro* was not affected by *pepP* deletion or any mutations in *pepP* (data not shown). The results showed that Pa-PepP knockout PA14 (PA14-Δ*pepP*) strain lost half of its ability to enter mammalian cells compared to wild-type PA14, and the cell invasion ability for PA14-Δ*pepP* strain was restored when introducing a complementary plasmid pRK415 for Pa-PepP expression, which confirmed the contribution of Pa-PepP to *P. aeruginos* virulence (Feinbaum et al., 2012). The enzymatic inactive mutant (H243A) exhibited an attenuated invasion ability, suggesting a role for the cleavage activity of Pa-PepP in its biological function. Strikingly, the PA14-R351G mutant also displayed weak cell internalization efficiency comparable to PA14-Δ*pepP*, revealing that the specificity of protein-substrate recognition is indispensable to the virulence-related function. The mutant PA14-Pa-PepP-367-372 also presented an attenuated invasion ability, verifying the critical role of 367-372 loop in the biological function of Pa-PepP, even though it does not have an obvious impact on enzymatic activity.

DISCUSSION

Aminopeptidases hydrolyze the N-terminal residues of peptide/protein substrate and generally have broad specificity.

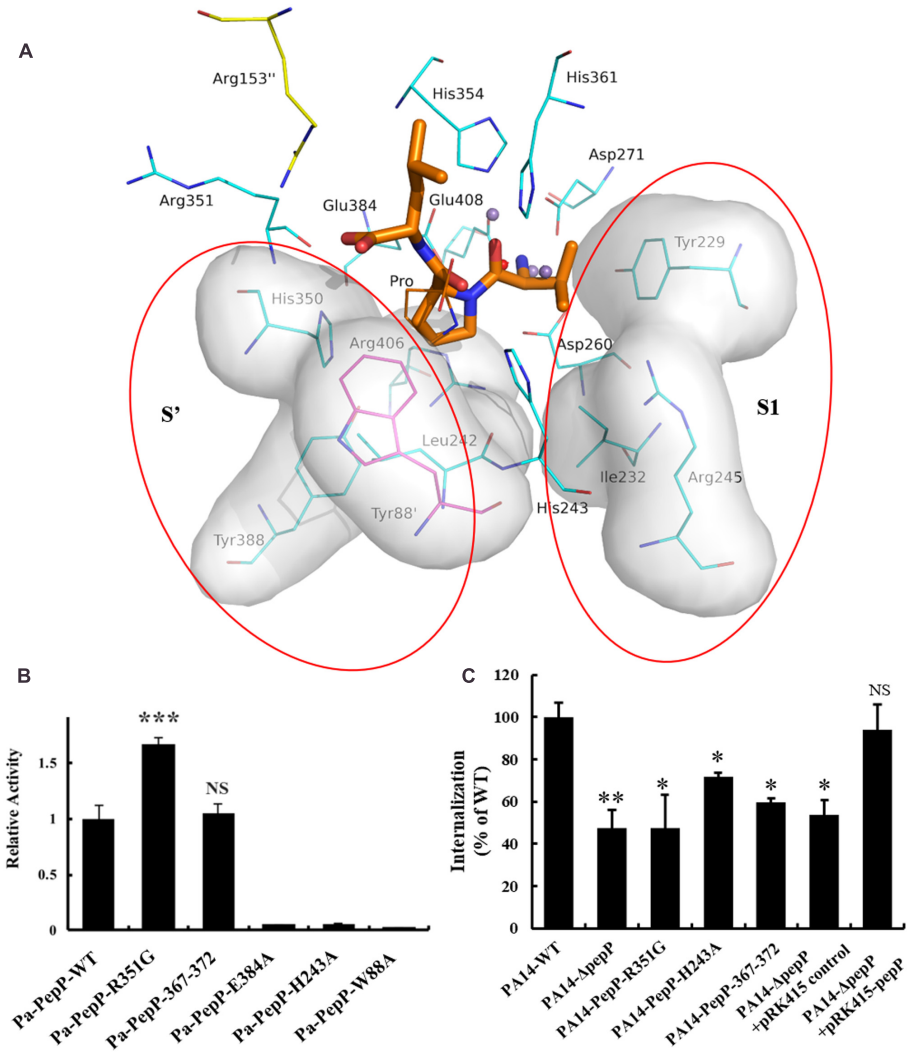

FIGURE 5 | The modeled Val-Pro-Leu bound Pa-PepP complex and the important residues or sequences identified to be important to Pa-PepP enzyme activity and bacterium virulence. **(A)** The modeled Val-Pro-Leu bound Pa-PepP complex by superposing with the substrate bound Ec-PepP structure (PDB code: 2BN7). The left and right shadow highlighted with red circles refers to the predicted substrate binding sites (S' and S1 sites) containing these mainly related residues, with Trp88 from the adjacent subunit colored magenta. Val-Pro-Leu is colored orange for the main carbon chain with thick lines. Other residues for direct interactions to metal ions are colored gray. **(B)** Relative activity of wild-type and mutant Pa-PepP. Activity was measured using the quenched fluorescent substrate Lys(Abz)–Pro–Pro–pNA as mentioned before. Each bar represents the mean of three independent measurements (±SEM). **(C)** Bacterial invasion of HeLa cells upon 1 h of infection at an MOI of 10 with *P. aeruginosa* strains grown at the transition between the exponential and stationary phases in LB broth at 37°C. Each bar represents the mean of three independent measurements (±SEM). *P*-values for comparison of each group with Pa-PepP-WT were determined by 2-tailed Student's *t*-test (*$P < 0.05$; **$P < 0.01$; ***$P < 0.001$).

They are associated with various essential biological functions and have been suggested as suitable therapeutic targets for corresponding diseases (Griffith et al., 1997; Pasqualini et al., 2000; Gardiner et al., 2006; Stack et al., 2007; Trenholme et al., 2010; Skinner-Adams et al., 2010). There are a number of aminopeptidases inhibitors that have already been developed as potent drug candidates (Prechel et al., 1995; Maggiora et al., 1999; Aozuka et al., 2004; Krige et al., 2008). Given the rare occurrence of proline as the second residue in protein, the proline-specific APPro exhibits even narrower substrate specificities, making it an attractive target for specific therapeutic application. In Feinbaum et al.'s (2012) *C. elegans* model, aminopeptidase PepP gene was identified as a virulence related factor and was involved in the highly attenuated *C. elegans* deaths, which suggested that Pa-PepP may be a potential drug target for the treatment of *P. aeruginosa* infections. However, other infection models are still needed to further confirm the role of *pepP* in *P. aeruginosa* virulence, and mechanisms account for Pa-PepP's correlation with bacterium virulence remain unknown. In the *C. elegans* model, the PA14 strain with transposon insertions in gene *pepP* display increased pyocyanin levels, whereas pyocyanin has been demonstrated to play an important role in

P. aeruginosa virulence in many models of infections (Lau et al., 2004; Dietrich et al., 2006). Thus, we predict that there may be other mechanisms linked to the effect of *pepP* on the virulence associated phenotypes. In this work, we analyzed the specific substrate binding site of Pa-PepP based on structural studies, as well as its consensus signatures and mechanisms, which provided clues for better understanding its unique physiologic function.

Like all other metalloaminopeptidase, APPro requires metal ion for its enzyme activity, and the manganese might be the most preferred cation. The dinuclear metal center structure was consistent among all APPro members, with the M_B ion binds more loosely than M_A. Different anomalous map peaks of the bound Mn in Pa-PepP structure verified the inequivalent occupancy of two metal-binding sites. It should be noted that the different binding affinities of the metal sites allow for the sequential addition of multiple types of metal ions in other metalloaminopeptidases, resulting in diverse enzymatic activities (Carpenter and Vahl, 1973; Van Wart and Lin, 1981; Allen et al., 1983; Bayliss and Prescott, 1986; Lin and Van Wart, 1988). Stimulatory or inhibitory effects of various divalent metal ions were also observed in both Ec-PepP and Pa-PepP, suggesting that the metal selectivity contributes to activity-regulating mechanisms in APPro. Furthermore, the additional M_C atom found in Pa-PepP provides a structural basis for the manganese concentration-dependent modulation of activity. In conclusion, the delicate structure of the metal binding sites enables the APPro to precisely sense the type and concentration of metal ions, facilitating its scalability in specific function performances.

The individual domain superposition of the APPros shows a close agreement between the catalytic domain structures (rmsd values of 0.847–1.846) and the nearly identical active sites allow them to maintain the unique catalytic mechanism. However, the extensive sequence diversity between prokaryotic and eukaryotic APPros, especially with respect to the domain assignments, domain motions, and oligomeric assemblies, are the breakthrough points for understanding the particular functions of each member (**Supplementary Figure S3**). For instance, the antiparallel dimerization observed in prokaryotic APPro resulted in an inward extending loop region that reached into the cavity of the neighboring subunits and participated in the P1' residue binding. Instead, in eukaryotic species, this part was replaced by the additional N-domain to ensure the maintenance of the active site pocket (Li et al., 2008). Moreover, those different oligomerization interfaces may affect the substrate selectivity in APPros.

It has been proposed that the tetrameric assembly is indispensable for Ec-PepP's function because the increase of the binding surface area can accommodate larger protein substrates (Yoshimoto et al., 1994). Pa-PepP possesses more positively charged groups on its solvent-accessible area compared to Ec-PepP (**Supplementary Figure S4**), implicating a preference for substrate selection. Notably, the 367:372 loop identified from Pa-PepP is located at the entrance region of the catalytic cave and replacement of this loop by corresponding fragment from Ec-PepP attenuated the cell invasion ability of PA14. These observations revealed that residue variations and charge distribution differences around the substrate binding interfaces can lead to distinct functions for Pa-PepP and Ec-PepP, even though they shared high sequence similarity.

CONCLUSION

APPros exert specific physiologic functions, and many of them are relate to virulence in bacteria. However, due to the insufficiency of information about its biological substrate, the knowledge of its biology functions are limited for now. Here, we discussed the ion modulation mechanism in Pa-PepP and unveiled the differences in the regions surrounding substrate binding site, which extend our understanding about the catalytic mechanism and virulence-related functions of Pa-PepP. Most importantly, the structural analysis provides us a solid foundation for designing specific inhibitors against pathogenic bacterial infection by blocking the particular protein substrate binding site instead of directly interfering the common catalytic center.

MATERIALS AND METHODS

Protein Expression and Purification

Full-length *pepP* was amplified by PCR using gene-specific primers (Supplementary Table S1) from the *P. aeruginosa* PA14 genome DNA on Gene amplification Machine (Gene Touch, BIOER, HangZhou, China). Full-length *pepP* containing six C-terminal histidine residues (LEHHHHHH) was homologous recombined with the linearized pET-22b (+) using a ClonExpressTM II One Step Cloning Kit (Vazyme). All point mutants were generated using the QuickChange (I-5TM2*High Fidelity Master Mix, MCLAB) PCR-based method, on the pET-22b (+) construct. The recombinant plasmid was transformed into *E. coli* strain BL21 (DE3) for protein expression. The bacterial culture was grown in LB medium in the presence of 100 $\mu g\ mL^{-1}$ ampicillin and incubated with shaking at 310 K until the OD600 reached 0.9 (ZhiChu, ShangHai). The culture was cooled to 289 K before protein expression was induced with 0.2 mM IPTG for 20 h (Bao et al., 2013). Following induction, the bacteria were collected and resuspended in a lysis buffer consisting of 25 mM Tris–HCl pH 8.5, 10 mM NaCl, 5 % glycerol and 1 mM phenylmethanesulfonyl fluoride (20 g of cells/100 mL buffer, Sigma–Aldrich) and lysed by sonication. The lysate was cleared by centrifugation at 11000 *g* for 45 min and then the supernatant was loaded onto a 2 mL Ni–NTA affinity resin (Qiagen) for 2 L culture. The Ni–NTA column was washed with ten column volumes of the lysis buffer supplemented with 20 mM imidazole. The target protein was eluted with the same buffer in the presence of 200 mM imidazole. Fractions were pooled and determined by SDS–PAGE, followed by further purification on size-exclusion chromatography Superdex 200 column (GE Healthcare), which was pre-equilibrated with the buffer consisting of 25 mM Tris–HCl pH 8.5, 10 mM NaCl. Fractions containing Pa-PepP were pooled and concentrated to a concentration of approximately

16 mg mL^{-1} using a Centricon filter (10 kDa cutoff; Millipore, Billerica).

Crystallization and Data Collection

Initial crystallization experiments were carried out using four commercial crystallization screens from Hampton Research and Rigaku (Index HT, Crystal Screen HT, WIZARD HT, XTAL QUEST HT). Crystallization screens were conducted as previously described with some modifications (Bao et al., 2009). Briefly, crystallization initially screens were carried out using a Mosquito liquid dispenser by hanging-drop vapor-diffusion method at 291 K in 96-well plates. The 200 nL mixing drop containing protein solution and reservoir buffer by 1:1, with a final protein concentration of 16 mg ml^{-1} in 25 mM Tris–HCl pH 8.5, 10 mM NaCl. The final optimized crystals for the recombinant protein were obtained by mixing 2 μl of the protein sample containing Mn^{2+} and proline with an equal volume of the reservoir solution containing 30% PEG400, 100 mM sodium cacodylate pH 6.5, 200 mM lithium sulfate. Crystals grew in approximately 2–3 days and were transferred to a cryo-protectant solution (reservoir solution with 6% PEG400) prior to flash-cooling in liquid nitrogen. X-ray data were collected with a CCD camera on BL-17U stations of the SSRF, China. The diffraction data were indexed, integrated, and scaled using the HKL2000 program suite (Otwinowski and Minor, 1997).

Structure Determination and Refinement

Data processing and scaling were carried out using the HKL2000 software package. The data were processed to a resolution limit of 1.847–1.783 Å (Rmerge = 0.099) in space group P2, with unit-cell parameters $a = 111.197$, $b = 123.432$, $c = 149.485$ Å. The phase problem was solved by molecular replacement using PHENIX with aminopeptidase P from *E. coli* (PDB entry 1az9; space group P 6422; resolution 1.9 Å) as a template. The process of structure building and refinement was monitored using the COOT (Emsley et al., 2010). Water molecules were automatically added by PHENIX (Adams et al., 2010).

Differential Scanning Calorimetry (DSC) Assays

Differential scanning calorimetry (DSC) is a promising thermoanalytical technique used for evaluating the stability of proteins as well as other biomolecules. The enthalpy value determined by DSC can provide direct information about the energetics of thermally induced processes, and the measured melting temperature(Tm) reflects thermal stability of proteins. The assays were conducted on the MicroCal VP-Capillary DSC System (Malvern). Protein samples were prepared with a final concentration of 1 mg/ml in 400 μl buffer and each sample has another 400 μl blank buffer as reference which were loaded in pairs. Operating parameters (such as pre-scan equilibration time, scan rate, temperature programming) were set and at least three buffer-buffer scans were performed before the sample was scanned. And DSC automated data analysis was conducted after experiments ran out. The DSC curves can read by Origin (Origin Pro 7.5).

Construction of *P. aeruginosa pepP* Gene Mutant

To construct *pepP* mutants of *P. aeruginosa*, a two-step allelic exchange bacterial genome engineering strategy was employed (Hmelo et al., 2015; Sana et al., 2015). Briefly, in the first step of allelic exchange, the suicide vector pEX18Gm was integrated site-specifically into the chromosome of *P. aeruginosa* by homologous recombination, resulting in antibiotic-resistant single-crossover mutants. Then, in the second step of allelic exchange, a double crossover event occurred through a second homologous recombination, and the mutant was isolated using sucrose-mediated counter-selection. The corresponding mutants were finally identified by PCR and DNA sequencing. Specifically, PCRs were performed to amplify the target fragment sequences with upstream (800 bp) and downstream (800 bp) from *P. aeruginosa* chromosomal DNA, while the suicide plasmid pEX18Gm was linearized with gene-specific primers. The two PCR products were recombined with ClonExpress® II One Step Cloning Kit (Vazyme), The resulting plasmid, pEX18-Gm-*pepP*, was then performed Site-directed mutagenesis or deletion. All these primers are listed in Supplementary Table S1. These vectors were then transformed into *E. coli* S17-1 and then mobilized into *P. aeruginosa* strains PA14 by conjugation, in order to transfer suicide plasmids from the *E. coli* donor S17-1 to the *P. aeruginosa* recipient PA14. Colonies were first screened using gentamicin resistance plates to get single-crossover mutants. And then the double-crossover mutants were screened by No-salt LB (NSLB) agar with 15% (wt/vol) sucrose. The *pepP* gene replacement mutant strain was further confirmed by PCR and DNA sequencing.

Construction of Complementation Plasmid pRK415-*pepP*

To construct the complementation plasmid pRK415-*pepP*, PCR-amplified *pepP* was cloned into the EcoRI and HindIII sites of plasmid pRK415, giving rise to the plasmid pRK415- *pepP* (Lin et al., 2017). The recombinant plasmid and plasmid pRK415 were transformed into *E. coli* S17-1, respectively, and then mobilized into *P. aeruginosa* PA14-△*pepP* by conjugation to transfer pRK415-*pepP* from the S17-1 to PA14-△*pepP*. The PA14-△*pepP* strain carried pRK415-*pepP* or pRK415 plasmid were screened by *Pseudomonas* isolation agar (PIA) with 150 μg/ml tetracycline. For expression of PepP in the *P. aeruginosa* strains, the PA14-△*pepP* strain carried pRK415-*pepP* were induced by addition of 1 mM IPTG and then conducted cell invasion assays.

HeLa Cell Invasion Assays

To enumerate bacteria internalized by HeLa cells to verify bacterium virulence, gentamicin survival assays were conducted with slight modifications (Chi et al., 1991). Briefly, mammalian HeLa cells (obtained from ATCC) were grown in DMEM medium, containing 10% (v/v) FBS (Gibco, Auckland, New Zealand) and 1 % antibiotics (penicillin and streptomycin) in 5% CO_2 at 37°C. Suspension cultures of HeLa cells were seeded at 2–5 × 10^5 cells per well in 12-well tissue culture plates for the overnight at 37°C. Cells were washed three times with PBS

(pH 7.2) and changed to antibiotic-free medium immediately before infection. Cells were infected with exponential phase *P. aeruginosa* strains PA14 and mutant strains at a MOI of 10 for 1 h in 5% CO_2 at 37°C. The cells were washed twice with PBS and incubated for an additional 1 h in DMEM medium containing 150 μg/ml of gentamicin in order to kill extracellular bacteria. The monolayers cells were then washed three times with PBS and lysed with 0.5% Triton X-100 for 10–20 min, and appropriate dilutions were plated on LB plates to determine the number of viable intracellular bacteria.

Enzyme Activity Assays

The enzyme activity of wild type Pa-PepP and the mutants were spectrophotometrically determined using the quenched fluorescent substrate Lys (Abz) – Pro–Pro–pNA (synthesized by GL Biochem Shanghai Ltd., China) as the substrate. Prior to the assay, wild type Pa-PepP and the mutant enzyme are dialyzed with EDTA overnight to fully remove the pre-bound metal ions. And all enzyme preparations were freshly diluted with ice-cold 50 mM Tris (pH 8.5) and 100 mM NaCl and treated with $MnCl_2$ for 10 min at 37°C. After addition of substrate, the final reaction conditions were 50 mM Tris (pH 8.5), 100 mM NaCl, 1 mM $MnCl_2$, 0–250 μM substrate, and 20 nM Pa-PepP (final assay volume 100 μL). The assay was allowed to proceed for 5 min at 37°C in the Thermo Scientific Varioskan Flash plate reader. The appearance of fluorescent product ($\lambda ex = 301$ nm, $\lambda em = 410$ nm) was monitored at 10 s intervals. Since the pure fluorescent product was not available to quantitate the changes in fluorescence, the kinetic results are presented as activities in relative fluorescence units. The kinetic parameters Km (Michaelis constant) for all the assays were obtained by fitting experimental data to the Michaelis-Menten equation by non-linear regression using the program OriginPro 7.5 (OriginLab Software). The data were showed in Supplementary Tables S2 and S3.

Statistical Analysis

Statistical analysis was analyzed by 2-tailed Student's *t*-test. In all statistical analysis, *P*-values < 0.05 were considered to be statistically significant.

ACCESSION NUMBERS

Atomic coordinates of the refined structures have been deposited in the Protein Data Bank (www.pdb.org) with the PDB code 5WZE.

AUTHOR CONTRIBUTIONS

C-TP performed the experiments and wrote this manuscript. LL planned experiments and analyzed data. C-CL conducted structural analysis. L-HH made modifications of the manuscript. TL performed the structure determination and refinement. Y-LS performed the HeLa cell invasion assays. CG planned the experiments. N-YW contributed the essential experiment materials. YX guided the experiments. Y-BZ constructed the *P. aeruginosa pepP* gene mutants. Y-JS also performed the HeLa cell invasion assays. QL made modifications of the manuscript and conducted the PCR experiments. L-TY guided the experiments and made modifications of the manuscript. RB wrote part of the paper and performed the drawing.

FUNDING

The work was supported by National Key Research and Development Plan (Grant No. SQ2016YFJC040104), National Natural Science Foundation of China (Grant Nos. 81670008 and 81501787).

ACKNOWLEDGMENTS

We thank Shanghai Synchrotron Radiation Facility (SSRF) beamline BL17U for beamtime allowance (Wang et al., 2015). We thank the staffs of National Center for Protein Sciences Shanghai (NCPSS) beamlines BL18U and BL19U and SSRF, Shanghai, People's Republic of China, for assistance during data collection. We thank Dr. Derek Holman for carefully reading the manuscript.

SUPPLEMENTARY MATERIAL

The Supplementary Material for this article can be found online at: https://www.frontiersin.org/articles/10.3389/fmicb.2017.02385/full#supplementary-material

FIGURE S1 | Relative activity of Pa-PepP in presence of different amount of Ca^{2+} **(A)** and Mg^{2+} **(B)**. All assays were performed at 37°C for 5 min in the presence of 50 mM Tris (pH 8.5), 100 mM NaCl, 50 μM Lyz(Abz)–Pro–Pro–pNA quenched fluorescent substrate, and 1 $\mu g/mL^{-1}$ Pa-PepP that had been incubated with different concentrations of Ca^{2+} **(A)** and Mg^{2+} **(B)** at 37°C for 10 min. Each bar represents the mean of three independent measurements (SEM).

FIGURE S2 | The differential scanning calorimetry (DSC) curves of wide type Pa-PepP and all the mutants. DSC assays were conducted to investigate the thermal stability of wild type Pa-PepP and the mutants. The enthalpy value and the melting temperature(Tm) value determined by DSC were showed in the DSC curves. As it showed in the DSC curves, all these protein samples shared the similar Tm value (66–68°C), with the only exceptional of Pa-PepP-E384A which has a acceptable shift of Tm value of 63°C.

FIGURE S3 | Superposition of the monomer Pa-PepP and other APPros. **(A)** Superposition of the monomer Pa-PepP (red) with Ec-PepP (blue), hAPP1 (light gray), PfAPP (light blue), and CeAPP (light pink). The N domain and C domain of each APPro were circled with black frame and circle, respectively. **(B)** Superposition of the monomer Pa-PepP (red) with Ec-PepP (blue). The black circle refers to the non-conservative surface loop identified as an important motif in Pa-PepP's function. **(C)** Schematic diagrams for the prokaryotic (right) and eukaryotic APPros dimers (left). N and C are labels for their N-terminal and C-terminal domains, respectively. And the plus N-terminal domain is labeled as N'.

FIGURE S4 | Surface charge distribution of Pa-PepP and Ec-PepP. Surface charge distribution of Pa-PepP **(A)** and Ec-PepP **(B)** generated by CCP4mg (McCoy et al., 2007). Pa-PepP possesses more positively charged groups on its solvent-accessible area compared to Ec-PepP. The green circle refers to the predicted substrate entrance of Pa-PepP and Ec-PepP, and the entrance is also indicated by the red arrow near the black colored loop in the ribbon view of tetramer **(C)**.

REFERENCES

Adams, P. D., Afonine, P. V., Bunkóczi, G., Chen, V. B., Davis, I. W., Echols, N., et al. (2010). PHENIX: a comprehensive Python-based system for macromolecular structure solution. *Acta Crystallogr. D Biol. Crystallogr.* 66, 213–221. doi: 10.1107/S0907444909052925

Allen, M. P., Yamada, A. H., and Carpenter, F. H. (1983). Kinetic parameters of metal-substituted leucine aminopeptidase from bovine lens. *Biochemistry* 22, 3778–3783. doi: 10.1021/bi00285a010

Aozuka, Y., Koizumi, K., Saitoh, Y., Ueda, Y., Sakurai, H., and Saiki, I. (2004). Anti-tumor angiogenesis effect of aminopeptidase inhibitor bestatin against B16-BL6 melanoma cells orthotopically implanted into syngeneic mice. *Cancer Lett.* 216, 35–42. doi: 10.1016/j.canlet.2004.06.050

Bao, R., Nair, M. K., Tang, W.-K., Esser, L., Sadhukhan, A., Holland, R. L., et al. (2013). Structural basis for the specific recognition of dual receptors by the homopolymeric pH 6 antigen (Psa) fimbriae of Yersinia pestis. *Proc. Natl. Acad. Sci. U.S.A.* 110, 1065–1070. doi: 10.1073/pnas.1212431110

Bao, R., Zhou, C.-Z., Jiang, C., Lin, S.-X., Chi, C.-W., and Chen, Y. (2009). The ternary structure of the double-headed arrowhead protease inhibitor API-A complexed with two trypsins reveals a novel reactive site conformation. *J. Biol. Chem.* 284, 26676–26684. doi: 10.1074/jbc.M109.022095

Bayliss, M. E., and Prescott, J. M. (1986). Modified activity of *Aeromonas* aminopeptidase: metal ion substitutions and role of substrates. *Biochemistry* 25, 8113–8117. doi: 10.1021/bi00372a047

Besio, R., Alleva, S., Forlino, A., Lupi, A., Meneghini, C., Minicozzi, V., et al. (2010). Identifying the structure of the active sites of human recombinant prolidase. *Eur. Biophys. J.* 39, 935–945. doi: 10.1007/s00249-009-0459-4

Carpenter, F. H., and Vahl, J. M. (1973). Leucine aminopeptidase (Bovine lens) mechanism of activation by Mg2+ and Mn2+ of the zinc metalloenzyme, amino acid composition, and sulfhydryl content. *J. Biol. Chem.* 248, 294–304.

Chi, E., Mehl, T., Nunn, D., and Lory, S. (1991). Interaction of *Pseudomonas aeruginosa* with A549 pneumocyte cells. *Infect. Immun.* 59, 822–828.

Dietrich, L. E., Price-Whelan, A., Petersen, A., Whiteley, M., and Newman, D. K. (2006). The phenazine pyocyanin is a terminal signalling factor in the quorum sensing network of *Pseudomonas aeruginosa*. *Mol. Microbiol.* 61, 1308–1321. doi: 10.1111/j.1365-2958.2006.05306.x

Drinkwater, N., Sivaraman, K. K., Bamert, R. S., Rut, W., Mohamed, K., Vinh, N. B., et al. (2016). Structure and substrate fingerprint of aminopeptidase P from *Plasmodium falciparum*. *Biochem. J.* 473, 3189–3204. doi: 10.1042/BCJ20160550

Emsley, P., Lohkamp, B., Scott, W. G., and Cowtan, K. (2010). Features and development of coot. *Acta Crystallogr. D Biol. Crystallogr.* 66, 486–501. doi: 10.1107/S0907444910007493

Feinbaum, R. L., Urbach, J. M., Liberati, N. T., Djonovic, S., Adonizio, A., Carvunis, A.-R., et al. (2012). Genome-wide identification of *Pseudomonas aeruginosa* virulence-related genes using a *Caenorhabditis elegans* infection model. *PLOS Pathog.* 8:e1002813. doi: 10.1371/journal.ppat.1002813

Gardiner, D. L., Trenholme, K. R., Skinner-Adams, T. S., Stack, C. M., and Dalton, J. P. (2006). Overexpression of leucyl aminopeptidase in *Plasmodium falciparum* parasites TARGET FOR THE ANTIMALARIAL ACTIVITY OF BESTATIN. *J. Biol. Chem.* 281, 1741–1745. doi: 10.1074/jbc.M508955200

Gi, M., Jeong, J., Lee, K., Lee, K.-M., Toyofuku, M., Yong, D. E., et al. (2014). A drug-repositioning screening identifies pentetic acid as a potential therapeutic agent for suppressing the elastase-mediated virulence of *Pseudomonas aeruginosa*. *Antimicrob. Agents Chemother.* 58, 7205–7214. doi: 10.1128/AAC.03063-14

Gonzales, T., and Robert-Baudouy, J. (1996). Bacterial aminopeptidases: properties and functions. *FEMS Microbiol. Rev.* 18, 319–344. doi: 10.1111/j.1574-6976.1996.tb00247.x

Graham, S. C., Bond, C. S., Freeman, H. C., and Guss, J. M. (2005). Structural and functional implications of metal ion selection in aminopeptidase P, a metalloprotease with a dinuclear metal center. *Biochemistry* 44, 13820–13836. doi: 10.1021/bi0512849

Graham, S. C., and Guss, J. M. (2008). Complexes of mutants of *Escherichia coli* aminopeptidase P and the tripeptide substrate ValProLeu. *Arch. Biochem. Biophys.* 469, 200–208. doi: 10.1016/j.abb.2007.10.009

Graham, S. C., Lilley, P. E., Lee, M., Schaeffer, P. M., Kralicek, A. V., Dixon, N. E., et al. (2006). Kinetic and crystallographic analysis of mutant *Escherichia coli* aminopeptidase P: insights into substrate recognition and the mechanism of catalysis. *Biochemistry* 45, 964–975. doi: 10.1021/bi0518904

Graham, S. C., Maher, M. J., Simmons, W. H., Freeman, H. C., and Guss, J. M. (2004). Structure of *Escherichia coli* aminopeptidase P in complex with the inhibitor apstatin. *Acta Crystallogr. D Biol. Crystallogr.* 60, 1770–1779. doi: 10.1107/S0907444904018724

Griffith, E. C., Su, Z., Turk, B. E., Chen, S., Chang, Y.-H., Wu, Z., et al. (1997). Methionine aminopeptidase (type 2) is the common target for angiogenesis inhibitors AGM-1470 and ovalicin. *Chem. Biol.* 4, 461–471. doi: 10.1016/S1074-5521(97)90198-8

Hahn, H. P. (1997). The type-4 pilus is the major virulence-associated adhesin of *Pseudomonas aeruginosa*–a review. *Gene* 192, 99–108. doi: 10.1016/S0378-1119(97)00116-9

Hancock, R. E. (1998). Resistance mechanisms in *Pseudomonas aeruginosa* and other nonfermentative gram-negative bacteria. *Clin. Infect. Dis.* 27(Suppl. 1), S93–S99. doi: 10.1086/514909

Hentzer, M., Wu, H., Andersen, J. B., Riedel, K., Rasmussen, T. B., Bagge, N., et al. (2003). Attenuation of *Pseudomonas aeruginosa* virulence by quorum sensing inhibitors. *EMBO J.* 22, 3803–3815. doi: 10.1093/emboj/cdg366

Hmelo, L. R., Borlee, B. R., Almblad, H., Love, M. E., Randall, T. E., Tseng, B. S., et al. (2015). Precision-engineering the *Pseudomonas aeruginosa* genome with two-step allelic exchange. *Nat. Protoc.* 10, 1820–1841. doi: 10.1038/nprot.2015.115

Hood, R. D., Singh, P., Hsu, F., Güvener, T., Carl, M. A., Trinidad, R. R., et al. (2010). A type VI secretion system of *Pseudomonas aeruginosa* targets a toxin to bacteria. *Cell Host Microbe* 7, 25–37. doi: 10.1016/j.chom.2009.12.007

Hu, X. V., Chen, X., Han, K. C., Mildvan, A. S., and Liu, J. O. (2007). Kinetic and mutational studies of the number of interacting divalent cations required by bacterial and human methionine aminopeptidases. *Biochemistry* 46, 12833–12843. doi: 10.1021/bi701127x

Hwang, S., Kim, C. Y., Ji, S.-G., Go, J., Kim, H., Yang, S., et al. (2016). Network-assisted investigation of virulence and antibiotic-resistance systems in *Pseudomonas aeruginosa*. *Sci. Rep.* 6:26223. doi: 10.1038/srep26223

Iyer, S., La-Borde, P. J., Payne, K. A., Parsons, M. R., Turner, A. J., Isaac, R. E., et al. (2015). Crystal structure of X-prolyl aminopeptidase from *Caenorhabditis elegans*: a cytosolic enzyme with a di-nuclear active site. *FEBS Open Bio* 5, 292–302. doi: 10.1016/j.fob.2015.03.013

Jao, S.-C., Huang, L.-F., Hwang, S.-M., and Li, W.-S. (2006). Tyrosine 387 and arginine 404 are critical in the hydrolytic mechanism of *Escherichia coli* aminopeptidase P. *Biochemistry* 45, 1547–1553. doi: 10.1021/bi051786m

Jao, S.-C., Huang, L.-F., Tao, Y. S., and Li, W.-S. (2004). Hydrolysis of organophosphate triesters by *Escherichia coli* aminopeptidase P. *J. Mol. Catal. B Enzym.* 27, 7–12. doi: 10.1021/bi051786m

Jeyakanthan, J., Takada, K., Sawano, M., Ogasahara, K., Mizutani, H., Kunishima, N., et al. (2009). Crystal structural and functional analysis of the putative dipeptidase from *Pyrococcus horikoshii* OT3. *J. Biophys.* 2009:434038. doi: 10.1155/2009/434038

Johnson, B. K., and Abramovitch, R. B. (2017). Small molecules that sabotage bacterial virulence. *Trends Pharmacol. Sci.* 38, 339–362. doi: 10.1016/j.tips.2017.01.004

Krige, D., Needham, L. A., Bawden, L. J., Flores, N., Farmer, H., Miles, L. E., et al. (2008). CHR-2797: an antiproliferative aminopeptidase inhibitor that leads to amino acid deprivation in human leukemic cells. *Cancer Res.* 68, 6669–6679. doi: 10.1158/0008-5472.CAN-07-6627

Lau, G. W., Hassett, D. J., Ran, H., and Kong, F. (2004). The role of pyocyanin in *Pseudomonas aeruginosa* infection. *Trends Mol. Med.* 10, 599–606. doi: 10.1016/j.molmed.2004.10.002

Li, X., Lou, Z., Li, X., Zhou, W., Ma, M., Cao, Y., et al. (2008). Structure of human cytosolic X-prolyl aminopeptidase: a double Mn (II)-dependent dimeric enzyme with a novel three-domain subunit. *J. Biol. Chem.* 283, 22858–22866. doi: 10.1074/jbc.M710274200

Lin, J., Zhang, W., Cheng, J., Yang, X., Zhu, K., Wang, Y., et al. (2017). A *Pseudomonas* T6SS effector recruits PQS-containing outer membrane vesicles for iron acquisition. *Nat. Commun.* 8:14888. doi: 10.1038/ncomms14888

Lin, W. Y., and Van Wart, H. E. (1988). Hydrolysis of dansyl-peptide substrates by leucine aminopeptidase: origin of dansyl fluorescence changes during hydrolysis. *Biochemistry* 27, 5054–5061. doi: 10.1021/bi00414a016

Liu, J. W., Hadler, K. S., Schenk, G., and Ollis, D. (2007). Using directed evolution to improve the solubility of the C-terminal domain of *Escherichia coli* aminopeptidase P. *FEBS J.* 274, 4742–4751. doi: 10.1111/j.1742-4658.2007.06022.x

Lowther, W. T., and Matthews, B. W. (2000). Structure and function of the methionine aminopeptidases. *Biochim. Biophys. Acta* 1477, 157–167. doi: 10.1016/S0167-4838(99)00271-X

Lowther, W. T., and Matthews, B. W. (2002). Metalloaminopeptidases: common functional themes in disparate structural surroundings. *Chem. Rev.* 102, 4581–4608. doi: 10.1021/cr0101757

Luckett, J. C., Darch, O., Watters, C., AbuOun, M., Wright, V., Paredes-Osses, E., et al. (2012). A novel virulence strategy for *Pseudomonas aeruginosa* mediated by an autotransporter with arginine-specific aminopeptidase activity. *PLOS Pathog.* 8:e1002854. doi: 10.1371/journal.ppat.1002854

Maggiora, L. L., Orawski, A. T., and Simmons, W. H. (1999). Apstatin analogue inhibitors of aminopeptidase P, a bradykinin-degrading enzyme. *J. Med. Chem.* 42, 2394–2402. doi: 10.1021/jm9805642

Maura, D., Ballok, A. E., and Rahme, L. G. (2016). Considerations and caveats in anti-virulence drug development. *Curr. Opin. Microbiol.* 33, 41–46. doi: 10.1016/j.mib.2016.06.001

McBroom, A. J., Johnson, A. P., Vemulapalli, S., and Kuehn, M. J. (2006). Outer membrane vesicle production by *Escherichia coli* is independent of membrane instability. *J. Bacteriol.* 188, 5385–5392. doi: 10.1128/JB.00498-06

McCoy, A. J., Grosse-Kunstleve, R. W., Adams, P. D., Winn, M. D., Storoni, L. C., and Read, R. J. (2007). Phaser crystallographic software. *J. Appl. Crystallogr.* 40, 658–674. doi: 10.1107/S0021889807021206

Miyata, S., Casey, M., Frank, D. W., Ausubel, F. M., and Drenkard, E. (2003). Use of the Galleria mellonella caterpillar as a model host to study the role of the type III secretion system in *Pseudomonas aeruginosa* pathogenesis. *Infect. Immun.* 71, 2404–2413. doi: 10.1128/IAI.71.5.2404-2413.2003

Otwinowski, Z., and Minor, W. (1997). [20] Processing of X-ray diffraction data collected in oscillation mode. *Methods Enzymol.* 276, 307–326. doi: 10.1016/S0076-6879(97)76066-X

Pasqualini, R., Koivunen, E., Kain, R., Lahdenranta, J., Sakamoto, M., Stryhn, A., et al. (2000). Aminopeptidase N is a receptor for tumor-homing peptides and a target for inhibiting angiogenesis. *Cancer Res.* 60, 722–727.

Prechel, M. M., Orawski, A. T., Maggiora, L. L., and Simmons, W. H. (1995). Effect of a new aminopeptidase P inhibitor, apstatin, on bradykinin degradation in the rat lung. *J. Pharmacol. Exp. Ther.* 275, 1136–1142.

Rampioni, G., Visca, P., Leoni, L., and Imperi, F. (2017). Drug repurposing for antivirulence therapy against opportunistic bacterial pathogens. *Emerg. Top. Life Sci.* ETLS20160018. doi: 10.1042/ETLS20160018

Sana, T. G., Baumann, C., Merdes, A., Soscia, C., Rattei, T., Hachani, A., et al. (2015). Internalization of *Pseudomonas aeruginosa* strain PAO1 into epithelial cells is promoted by interaction of a T6SS effector with the microtubule network. *mBio* 6:e00712-15. doi: 10.1128/mBio.0071215

Simmons, W. H., and Orawski, A. T. (1992). Membrane-bound aminopeptidase P from bovine lung. Its purification, properties, and degradation of bradykinin. *J. Biol. Chem.* 267, 4897–4903.

Skinner-Adams, T. S., Stack, C. M., Trenholme, K. R., Brown, C. L., Grembecka, J., Lowther, J., et al. (2010). *Plasmodium falciparum* neutral aminopeptidases: new targets for anti-malarials. *Trends Biochem. Sci.* 35, 53–61. doi: 10.1016/j.tibs.2009.08.004

Stack, C. M., Lowther, J., Cunningham, E., Donnelly, S., Gardiner, D. L., Trenholme, K. R., et al. (2007). Characterization of the *Plasmodium falciparum* M17 leucyl aminopeptidase A protease involved in amino acid regulation with potential for antimalarial drug development. *J. Biol. Chem.* 282, 2069–2080. doi: 10.1074/jbc.M609251200

Stover, C., Pham, X., Erwin, A., Mizoguchi, S., Warrener, P., Hickey, M., et al. (2000). Complete genome sequence of *Pseudomonas aeruginosa* PAO1, an opportunistic pathogen. *Nature* 406, 959–964. doi: 10.1038/35023079

Taylor, A. (1993). Aminopeptidases: structure and function. *FASEB J.* 7, 290–298.

Trenholme, K. R., Brown, C. L., Skinner-Adams, T. S., Stack, C., Lowther, J., To, J., et al. (2010). Aminopeptidases of malaria parasites: new targets for chemotherapy. *Infect. Disord. Drug Targets* 10, 217–225. doi: 10.2174/187152610791163363

Van Wart, H. E., and Lin, S. H. (1981). Metal binding stoichiometry and mechanism of metal ion modulation of the activity of porcine kidney leucine aminopeptidase. *Biochemistry* 20, 5682–5689. doi: 10.1021/bi00523a007

Vanaja, S. K., Russo, A. J., Behl, B., Banerjee, I., Yankova, M., Deshmukh, S. D., et al. (2016). Bacterial outer membrane vesicles mediate cytosolic localization of LPS and caspase-11 activation. *Cell* 165, 1106–1119. doi: 10.1016/j.cell.2016.04.015

Wallace, A. C., Laskowski, R. A., and Thornton, J. M. (1995). LIGPLOT: a program to generate schematic diagrams of protein-ligand interactions. *Protein Eng.* 8, 127–134. doi: 10.1093/protein/8.2.127

Wang, Q.-S., Yu, F., Huang, S., Sun, B., Zhang, K.-H., Liu, K., et al. (2015). The macromolecular crystallography beamline of SSRF. *Nucl. Sci. Tech.* 26, 12–17.

Weaver, J., Watts, T., Li, P., and Rye, H. S. (2014). Structural basis of substrate selectivity of *E. coli* prolidase. *PLOS ONE* 9:e111531. doi: 10.1371/journal.pone.0111531

Wilce, M., Bond, C., Dixon, N., Freeman, H., Guss, J., Lilley, P., et al. (1998). Structure and mechanism of a proline-specific aminopeptidase from *Escherichia coli*. *Proc. Natl. Acad. Sci. U.S.A.* 95, 3472–3477. doi: 10.1073/pnas.95.7.3472

Woods, D. E., Cryz, S. J., Friedman, R. L., and Iglewski, B. (1982). Contribution of toxin A and elastase to virulence of *Pseudomonas aeruginosa* in chronic lung infections of rats. *Infect. Immun.* 36, 1223–1228.

Yoshimoto, T., Orawski, A. T., and Simmons, W. H. (1994). Substrate specificity of aminopeptidase P from *Escherichia coli*: comparison with membrane-bound forms from rat and bovine lung. *Arch. Biochem. Biophys.* 311, 28–34. doi: 10.1006/abbi.1994.1204

Conflict of Interest Statement: The authors declare that the research was conducted in the absence of any commercial or financial relationships that could be construed as a potential conflict of interest.

Copyright © 2017 Peng, Liu, Li, He, Li, Shen, Gao, Wang, Xia, Zhu, Song, Lei, Yu and Bao. This is an open-access article distributed under the terms of the Creative Commons Attribution License (CC BY). The use, distribution or reproduction in other forums is permitted, provided the original author(s) or licensor are credited and that the original publication in this journal is cited, in accordance with accepted academic practice. No use, distribution or reproduction is permitted which does not comply with these terms.

frontiers in Microbiology

PERSPECTIVE
published: 11 December 2017
doi: 10.3389/fmicb.2017.02452

Repurposing and Revival of the Drugs: A New Approach to Combat the Drug Resistant Tuberculosis

Divakar Sharma[1,2], Yogesh K. Dhuriya[3], Nirmala Deo[1] and Deepa Bisht[1]*

[1] Department of Biochemistry, National JALMA Institute for Leprosy and Other Mycobacterial Diseases, Agra, India, [2] Interdisciplinary Biotechnology Unit, Aligarh Muslim University, Aligarh, India, [3] Developmental Toxicology Laboratory, Systems Toxicology and Health Risk Assessment Group, CSIR-Indian Institute of Toxicology Research (CSIR-IITR), Lucknow, India

Emergence of drug resistant tuberculosis like multi drug resistant tuberculosis (MDR-TB), extensively drug-resistant tuberculosis (XDR-TB) and totally drug resistant tuberculosis (TDR-TB) has created a new challenge to fight against these bad bugs of *Mycobacterium tuberculosis*. Repurposing and revival of the drugs are the new trends/options to combat these worsen situations of tuberculosis in the antibiotics resistance era or in the situation of global emergency. Bactericidal and synergistic effect of repurposed/revived drugs along with the latest drugs bedaquiline and delamanid used in the treatment of MDR-TB, XDR-TB, and TDR-TB might be the choice for future promising combinatorial chemotherapy against these bad bugs.

Keywords: drug resistance tuberculosis, repurposing, revival of drugs, synergistic effect, proteomics and bioinformatics

OPEN ACCESS

Edited by:
Noton Kumar Dutta, Johns Hopkins University, United States

Reviewed by:
Sandeep Sharma, University of Pennsylvania, United States
Shashank Gupta, Brown University, United States

****Correspondence:***
Divakar Sharma
divakarsharma88@gmail.com

Specialty section:
This article was submitted to Antimicrobials, Resistance and Chemotherapy, a section of the journal Frontiers in Microbiology

Received: *29 September 2017*
Accepted: *27 November 2017*
Published: *11 December 2017*

Citation:
Sharma D, Dhuriya YK, Deo N and Bisht D (2017) Repurposing and Revival of the Drugs: A New Approach to Combat the Drug Resistant Tuberculosis. Front. Microbiol. 8:2452. doi: 10.3389/fmicb.2017.02452

INTRODUCTION

Current Scenario

Mycobacterium tuberculosis is a deadly infectious pathogen causing tuberculosis (TB) worldwide. According to WHO (2016) 10.4 million new cases with 1.5 million deaths including 0.4 million individuals with HIV-TB co-infection were reported globally (WHO, 2016). Although TB can be cured by chemotherapy, but the emergence of drug resistant tuberculosis [such as multidrug-resistant tuberculosis (MDR-TB), extensively drug-resistant tuberculosis (XDR-TB) and totally drug resistant tuberculosis (TDR-TB)] has created a new challenge to combat the adverse situation of the disease. Since the decade rates of antibiotic resistance to first and second line anti-TB drugs are dramatically increasing (Cambau et al., 2015). Due to various complexities and high burden of HIV-TB co-infection treatments of MDR-TB, XDR-TB, and TDR-TB are problematic. Apart from the genomics studies various proteomics as well as bioinformatics studies regarding to the drug resistance tuberculosis were accumulated in the last decade (Jiang et al., 2007; Zhang and Yew, 2009; Sharma et al., 2010, 2014, 2015a,b, 2016a,b, 2017; Kumar et al., 2013; Lata et al., 2015a,b; Singh et al., 2015; Sharma and Bisht, 2016, 2017a,b,c;) and suggested the novel drug resistance mechanisms/markers/targets for potential therapeutics in near future. Proteomics and bioinformatics play a crucial role in the diagnostics and therapeutics against the emerging bad bug of tuberculosis. Apart from the expression proteomics studies cited above we have reported that Rv0148 (Putative short-chain type dehydrogenase/reductase) and Rv3841 (ferritin protein) have potentially involved in aminoglycosides resistance (Sharma et al., 2015b, 2016a) and could be the potential diagnostics and

therapeutics against the second line of drug resistance. To combat these worsened situations (MDR-TB, XDR-TB, and TDR-TB) new and effective drugs and diagnostics are urgently needed. However, as we know that development of new drugs and diagnostics are enormously expensive and time consuming process.

Repurposing and Revival of Drugs: A Chemotherapeutic Option against Drug Resistant Tuberculosis

Repurposing and revival of the drugs are the new trends/options or one of the pharmaceutical strategies to treat the particular disease that are already FDA approved for other diseases (Tsukamura, 1980; Van Deun et al., 2010) and also for tuberculosis earlier, in this antibiotics resistance era or in the situation of global emergency. Many compounds in TB advanced clinical trials are the molecules that were formerly used to treat other infectious diseases/tuberculosis earlier and now they have been repurposed for treatment of TB (Nayer and Steinbach, 1939; Tsukamura, 1980; Van Deun et al., 2010; Hasse et al., 2014).

Sulfonamides and sulphanilamide were first used in 1930s as an anti-TB drug (Nayer and Steinbach, 1939) but its use was discontinued due to its lesser efficacy as compared to first line drugs (streptomycin and isoniazid). Revival of sulfamethoxazole (SMX) in TB was first pointed out by its efficacy to prevent the TB infection in HIV patients whose receiving trimethoprim/sulfamethoxazole (TMP/SMX) to prevent other infection such as *Pneumocystis jirovecii* (Hasse et al., 2014). In a Nigerian trial study on patients of HIV-MDR-TB coinfetion, efficiency of MDR-TB treatment by TMP/SMX confirmed a significantly shorter time to sputum conversion in these patients (Oladimeji et al., 2014). Sulfadiazine is an anti-leprosy drug which is repurposed in the treatment of MDR-TB and XDR-TB. Brouqui et al. (2013) suggested that sulfadiazine regimen is safe and effective against MDR-TB and TDR-TB treatment (Ameen and Drancourt, 2013; Brouqui et al., 2013).

Clofazimine (CZM) is one of the repurposed molecules, has been initially used as an anti-leprosy drug since half the century. It was recently repurposed for managing the treatment of MDR-TB (Van Deun et al., 2010). CZM is recommended as a second-line anti-TB drug and used in combination with other anti-TB drugs for the treatment of drug-resistant tuberculosis. CZM-containing regimen can cure MDR-TB cases in 9–12 months. In *M. tuberculosis,* CZM appears to act as a prodrug, which is reduced by type 2-NADH dehydrogenase, to release reactive oxygen species (ROS) upon reoxidation by oxygen (O_2) (Yano et al., 2011). CZM, exhibits noticeable anti-mycobacterial and anti-inflammatory activity by inhibition of phospholipase and effects on potassium transporters, respectively (Steele et al., 1999; Cholo et al., 2006). Previous published studies have reported that CZM has good quality efficacy and little toxicity against drug-resistant mycobacterial strains in animal models, which suggested, CZM as a promising anti-TB drug for the management of MDR-TB (Van Deun et al., 2010; Cholo et al., 2012). Recently, numerous observational studies have reported that CZM including regimens provided a useful role in the treatment of patients with MDR-TB (Cholo et al., 2006; Van Deun et al., 2010).

Linezolid, an oxazolidinone antibiotic which is used for treatment of gram-positive bacterial infections (Till et al., 2002; Yanagihara et al., 2002), has now potentially repurposed for the treatment of drug resistant TB (MDR-TB and XDR-TB) (Fortún et al., 2005). Linezolid is an effective anti-TB drug for treating MDR-TB and XDR-TB with various side effects such as neurotoxicity and hematologic toxicity (Tang et al., 2015). Schecter et al. (2010) suggested that linezolid had low rates of discontinuation, well tolerated and good efficacy in the treatment of MDR-TB. Most recently in a case study Jaspard et al. (2017) reported, bedaquiline and linezolid drug combination might be safe for XDR-TB in the late third trimester of pregnancy or pregnant woman. Pregnant woman gave birth to a child without abnormalities follow-up of the fetal showed that no fetal toxicities upto 2 years after the delivery (Jaspard et al., 2017).

Minocycline is also one of the repurposed molecules, has been initially used in the treatment of leprosy since the 1980s (Tsukamura, 1980). In 2008 it was repurposed for managing the treatment of XDR-TB patient in Japan (Kawada et al., 2008). Combinatorial therapy of amoxicillin/clavulanic acid along with other second-line drugs has been used in the treatment of MDR-TB. It's cheaper cost and less toxicity has made the drug of choice in WHO group five drugs (Cassir et al., 2014). Recently, combinatorial treatment by amoxicillin/clavulanic acid and carbapenems has reduced the *M. tuberculosis* load (Diacon et al., 2016). Hugonnet et al. (2009) reported the *in vitro* activity of meropenem combined with clavulanate against XDR strains and paying attention to repurpose these beta-lactams as new anti-TB drugs (Hugonnet et al., 2009). However, carbapenems have been used successfully as part of salvage therapies for XDR patients, they have to be administered intravenously (Tiberi et al., 2016). Recently, an early bactericidal activity-Phase II (EBA Phase II) clinical trial has validated the promising potential of a carbapenem combined with amoxicillin and clavulanic acid for TB treatment (Diacon et al., 2016).

Singhal et al. (2014) reported that the FDA-approved antidiabetic drug metformin (MET) inhibits the intracellular mycobacterial growth by inducing mitochondrial ROS production, restricts disease immunopathology, enhances the efficacy of other anti-TB drugs and could be used as combinatorial therapy against the drug resistant tuberculosis. Gupta et al. (2013) suggested that tuberculosis treatment shortening by verapamil as an adjunctive therapy in mice has opened the direction for future research on verapamil and other efflux pump inhibitors in human tuberculosis. Gupta et al. (2014) also reported that efflux inhibition with verapamil tremendously decreases the MIC of bedaquiline and CZM to *M. tuberculosis* and suggested the synergistic effects of verapamil and bedaquiline in an animal model of TB infection. Recently Dutta et al. (2016) reported that statin a lipid-lowering drug (repurposed for TB treatment) when added to the first-line antitubercular drugs, reduces the lung bacillary burden in chronically infected mice.

Host-directed therapies are important adjunctive therapies for tuberculosis treatment that expanded by host immune effector mechanisms. Recently Gupta et al. (2017) showed that denileukin diftitox potentiates standard TB treatment in the mouse model, which might be due to depletion of T-regulatory and myeloid-derived suppressor cells during TB infection.

Synergistic Effects of Repurposed/Revived Drugs: With Others Anti-TB Drugs Used in Treatments of Tuberculosis Bad Bug

Synergistic effect of repurposed/revived drugs with other anti-TB drugs has been used for the future selection of these drugs in the WHO regimen which could be used in the treatment of MDR-TB, XDR-TB, and TDR-TB. In a study Zhang et al. (2015) suggested that CZM in combination with ethambutol (EMB) and moxifloxacin (MOX) may be a potential drug regimen for the treatment of MDR-TB. Synergistic effect of SMX has been reported *in vitro* with rifampicin (Macingwana et al., 2012). Tasneen et al. (2011) suggested CZM was the best third drug in combination with bedaquiline and pyrazinamide for the treatment of MDR-TB and a good example of drug synergism. Partial synergistic effect was oveserved between linezolid and capreomycin and suggested the efficacy of this combinatorial therapy against *M. tuberculosis* (Zhao et al., 2016). Most recently synergistic effect of bedaquiline and linezolid combinatorial therapy has been reported in XDR-TB of pregnant woman which is a good symbol of synergy for the last line of drugs (Jaspard et al., 2017). In a study synergistic effect carbapenems with rifampicin have been reported against *M. tuberculosis* (Kaushik et al., 2015).

CONCLUSION AND FUTURE PERSPECTIVE

On the basis of the reported literature and studies (regarding to proteomics, bioinformatics, and repurposing/revival of drugs) cited above we suggest that proteomics and bioinformatics play a crucial role in the exploration of diagnostics, therapeutics and mechanism of resistance against drug resistance tuberculosis. Repurposing and revival of the drugs is an alternative strategy to combat from this inadequate situation of drug resistance tuberculosis in this antibiotic resistance era. Synergistic effect of repurposed/revived drugs (sulfamethoxazole, sulfadiazine, clofazimine, linezolid, minocycline, amoxicillin/clavulanic acid, and carbapenems like meropenem) along with the latest drugs (bedaquiline and delamanid) used in the treatment of MDR-TB and XDR-TB might be one of the promising combinatorial chemotherapy for the treatment of MDR-TB, XDR-TB, and TDR-TB. Synergistic effect of these repurposed/revived drugs with bedaquiline and delamanid combinatorial therapy could be added a different perspective over the existed literature.

AUTHOR CONTRIBUTIONS

DS design the concept and wrote the manuscript. DS, YD, ND, and DB finalized the manuscript.

ACKNOWLEDGMENTS

The authors are grateful to Director, NJIL & OMD for the support. DS is ICMR-PDFs (ICMR, New Delhi).

REFERENCES

Ameen, S. M., and Drancourt, M. (2013). *In vitro* susceptibility of *Mycobacterium tuberculosis* to trimethoprim and sulfonamides in France. *Antimicrob. Agents Chemother.* 57, 6370–6371. doi: 10.1128/AAC.01683-13

Brouqui, P., Aubry, C., Million, M., Drancourt, M., and Raoult, D. (2013). Totally resistant tuberculosis: Will antileprosy drugs be helpful? *Int. J. Antimicrob. Agents* 42, 584–585. doi: 10.1016/j.ijantimicag.2013.08.004

Cambau, E., Viveiros, M., Machado, D., Raskine, L., Ritter, C., Tortoli, E., et al. (2015). Revisiting susceptibility testing in MDR-TB by a standardized quantitative phenotypic assessment in a European multicentre study. *J. Antimicrob. Chemother.* 70, 686–696. doi: 10.1093/jac/dku438

Cassir, N., Rolain, J. M., and Brouqui, P. (2014). A new strategy to fight antimicrobial resistance: the revival of old antibiotics. *Front. Microbiol.* 5:551. doi: 10.3389/fmicb.2014.00551

Cholo, M., Boshoff, H. I., Steel, H. C., Cockeran, R., Matlola, N. M., Downing, K. J., et al. (2006). Effects of clofazimine on potassium uptake by a Trk-deletion mutant of *Mycobacterium tuberculosis*. *J. Antimicrob. Chemother.* 57, 79–84. doi: 10.1093/jac/dki409

Cholo, M. C., Steel, H. C., Fourie, P. B., Germishuizen, W. A., and Anderson, R. (2012). Clofazimine: current status and future prospects. *J. Antimicrob. Chemother.* 67, 290–298. doi: 10.1093/jac/dkr444

Diacon, A. H., van der Merwe, L., Barnard, M., von Groote-Bidlingmaier, F., Lange, C., García-Basteiro, A. L., et al. (2016). beta-Lactams against Tuberculosis–new trick for an old dog? *N. Engl. J. Med.* 375, 393–394. doi: 10.1056/NEJMc1513236

Dutta, N. K., Bruiners, N., Pinn, M. L., Zimmerman, M. D., Prideaux, B., Dartois, V., et al. (2016). Statin adjunctive therapy shortens the duration of TB treatment in mice. *J. Antimicrob. Chemother.* 71, 1570–1577. doi: 10.1093/jac/dkw014

Fortún, J., Martín-Dávila, P., Navas, E., Pérez-Elías, M. J., Cobo, J., Tato, M., et al. (2005). Linezolid for the treatment of multidrug-resistant tuberculosis. *J. Antimicrob. Chemother.* 56, 180–185. doi: 10.1093/jac/dki148

Gupta, S., Cheung, L., Pokkali, S., Winglee, K., Guo, H., Murphy, J. R., et al. (2017). Suppressor cell-depleting immunotherapy with denileukin diftitox is an effective host-directed therapy for tuberculosis. *J. Infect. Dis.* 215, 1883–1887. doi: 10.1093/infdis/jix208

Gupta, S., Cohen, K. A., Winglee, K., Maiga, M., Diarra, B., and Bishai, W. R. (2014). Efflux inhibition with verapamil potentiates bedaquiline in *Mycobacterium tuberculosis*. *Antimicrob. Agents Chemother.* 58, 574–576. doi: 10.1128/AAC.01462-13

Gupta, S., Tyagi, S., Almeida, D. V., Maiga, M. C., Ammerman, N. C., and Bishai, W. R. (2013). Acceleration of tuberculosis treatment by adjunctive therapy with verapamil as an efflux inhibitor. *Am. J. Respir. Crit. Care Med.* 188, 600–607. doi: 10.1164/rccm.201304-0650OC

Hasse, B., Walker, A. S., Fehr, J., Furrer, H., Hoffmann, M., Battegay, M., et al. (2014). Cotrimoxazole prophylaxis is associated with reduced risk of incident tuberculosis in participants in the Swiss HIV Cohort Study. *Antimicrob. Agents Chemother.* 58, 2363–2368. doi: 10.1128/AAC.01868-13

Hugonnet, J. E., Tremblay, L. W., Boshoff, H. I., Barry, C. E. III, and Blanchard, J. S. (2009). Meropenem-clavulanate is effective against extensively drug-resistant *Mycobacterium tuberculosis*. *Science* 323, 1215–1218. doi: 10.1126/science.1167498

Jaspard, M., Elefant-Amoura, E., Melonio, I., De Montgolfier, I., Veziris, N., and Caumes, E. (2017). Bedaquiline and linezolid for extensively drug-resistant tuberculosis in pregnant woman. *Emerg. Infect. Dis.* 23, 1731–1732. doi: 10.3201/eid2310.161398

Jiang, X., Zhang, W., Gao, F., Huang, Y., Lv, C., and Wang, H. (2007). Comparison of the proteome of isoniazid-resistant and -susceptible strains of *Mycobacterium tuberculosis*. *Microb. Drug Resist.* 12, 231–238. doi: 10.1089/mdr.2006.12.231

Kaushik, A., Makkar, N., Pandey, P., Parrish, N., Singh, U., and Lamichhane, G. (2015). Carbapenems and rifampin exhibit synergy against *Mycobacterium tuberculosis* and *Mycobacterium abscessus*. *Antimicrob. Agents Chemother.* 59, 6561–6567. doi: 10.1128/AAC.01158-15

Kawada, H., Yamazato, M., Shinozawa, Y., Suzuki, K., Otani, S., Ouchi, M., et al. (2008). Achievement of sputum culture negative conversion by minocycline in a case with extensively drug-resistant pulmonary tuberculosis. *Kekkaku* 83, 725–728.

Kumar, B., Sharma, D., Sharma, P., Katoch, V. M., Venkatesan, K., and Bisht, D. (2013). Proteomic analysis of *Mycobacterium tuberculosis* isolates resistant to kanamycin and amikacin. *J. Proteomics* 94, 68–77. doi: 10.1016/j.jprot.2013.08.025

Lata, M., Sharma, D., Deo, N., Tiwari, P. K., Bisht, D., and Venkatesan, K. (2015a). Proteomic analysis of ofloxacin-mono resistant *Mycobacterium tuberculosis* isolates. *J. Proteomics* 127, 114–121. doi: 10.1016/j.jprot.2015.07.031

Lata, M., Sharma, D., Kumar, B., Deo, N., Tiwari, P. K., Bisht, D., et al. (2015b). Proteome analysis of ofloxacin and moxifloxacin induced *Mycobacterium tuberculosis* isolates by proteomic approach. *Protein Pept. Lett.* 22, 362–371.

Macingwana, L., Baker, B., Ngwane, A. H., Harper, C., Cotton, M. F., Hesseling, A., et al. (2012). Sulfamethoxazole enhances the antimycobacterial activity of rifampicin. *J. Antimicrob. Chemother.* 67, 2908–2911. doi: 10.1093/jac/dks306

Nayer, H., and Steinbach, M. (1939). Sulfanilamide in clinical tuberculosis. *Am. Rev. Tuberc.* 40, 470–472.

Oladimeji, O., Isaakidis, P., Obasanya, O. J., Eltayeb, O., Khogali, M., Van den Bergh, R., et al. (2014). Intensive-phase treatment outcomes among hospitalized multidrug-resistant tuberculosis patients: results from a nationwide cohort in Nigeria. *PLOS ONE* 9:e94393. doi: 10.1371/journal.pone.0094393

Schecter, G. F., Scott, C., True, L., Raftery, A., Flood, J., and Mase, S. (2010). Linezolid in the treatment of multidrug-resistant tuberculosis. *Clin. Infect. Dis.* 50, 49–55. doi: 10.1086/648675

Sharma, D., and Bisht, D. (2016). An efficient and rapid lipophilic proteins extraction from *Mycobacterium tuberculosis* H37Rv for two dimensional gel electrophoresis. *Electrophoresis* 37, 1187–1190. doi: 10.1002/elps.201600025

Sharma, D., and Bisht, D. (2017a). Secretory proteome analysis of streptomycin resistant *Mycobacterium tuberculosis* clinical isolates. *SLAS Discov.* 22, 1229–1238. doi: 10.1177/2472555217698428

Sharma, D., and Bisht, D. (2017b). *M. tuberculosis* hypothetical proteins and proteins of unknown function: Hope for exploring novel resistance mechanisms as well as future target of drug resistance. *Front. Microbiol.* 8:465. doi: 10.3389/fmicb.2017.00465

Sharma, D., and Bisht, D. (2017c). Role of bacterioferritin & ferritin in *M. tuberculosis* pathogenesis and drug resistance: a future perspective by interactomic approach. *Front. Cell. Infect. Microbiol.* 7:240. doi: 10.3389/fcimb.2017.00240

Sharma, D., Deo, N., and Bisht, D. (2017). Proteomics and bioinformatics: a modern way to elucidate the resistome in *Mycobacterium tuberculosis*. *J. Proteomics Bioinform.* 10:e33. doi: 10.4172/jpb.1000e33

Sharma, D., Kumar, B., Lata, M., Joshi, B., Venkatesan, K., Shukla, S., et al. (2015a). Comparative proteomic analysis of aminoglycosides resistant and susceptible *Mycobacterium tuberculosis* clinical isolates for exploring potential drug targets. *PLOS ONE* 10:e0139414. doi: 10.1371/journal.pone.0139414

Sharma, D., Lata, M., Faheem, M., Khan, A. U., Joshi, B., Venkatesan, K., et al. (2015b). Cloning, expression and correlation of Rv0148 to amikacin & kanamycin resistance. *Curr. Proteomics* 12, 96–100. doi: 10.2174/1570164612021509031 13053

Sharma, D., Lata, M., Faheem, M., Khan, A. U., Joshi, B., Venkatesan, K., et al. (2016a). *M. tuberculosis* ferritin (Rv3841): potential involvement in Amikacin (AK) & Kanamycin (KM) resistance. *Biochem. Biophys. Res. Commun.* 478, 908–912. doi: 10.1016/j.bbrc.2016.08.049

Sharma, D., Lata, M., Singh, R., Deo, N., Venkatesan, K., and Bisht, D. (2016b). Cytosolic proteome profiling of aminoglycosides resistant *Mycobacterium tuberculosis* clinical isolates using MALDI-TOF/MS. *Front. Microbiol.* 7:1816. doi: 10.3389/fmicb.2016.01816

Sharma, D., Shankar, H., Lata, M., Joshi, B., Venkatesan, K., and Bisht, D. (2014). Culture filtrate proteome analysis of aminoglycoside resistant clinical isolates of *Mycobacterium tuberculosis*. *BMC Infect. Dis.* 14(Suppl.):60. doi: 10.1186/1471-2334-14-S3-P60

Sharma, P., Kumar, B., Gupta, Y., Singhal, N., Katoch, V. M., Venkatesan, K., et al. (2010). Proteomic analysis of streptomycin resistant and sensitive clinical isolates of *Mycobacterium tuberculosis*. *Proteome Sci.* 8:59. doi: 10.1186/1477-5956-8-59

Singh, A., Gopinath, K., Sharma, P., Bisht, D., Sharma, P., Singh, N., et al. (2015). Comparative proteomic analysis of sequential isolates of *Mycobacterium tuberculosis* from a patient with pulmonary tuberculosis turning from drug sensitive to multidrug resistant. *Indian J. Med. Res.* 141, 27–45. doi: 10.4103/0971-5916.154492

Singhal, A., Jie, L., Kumar, P., Hong, G. S., Leow, M. K., Paleja, B., et al. (2014). Metformin as adjunct antituberculosis therapy. *Sci. Transl. Med.* 6:263ra159. doi: 10.1126/scitranslmed.3009885

Steele, H., Matlola, N. M., and Anderson, R. (1999). Inhibition of potassium transport and growth of mycobacteria exposed to clofazimine and B669 is associated with a calcium-independent increase in microbial phospholipase A2 activity. *J. Antimicrob. Chemother.* 44, 209–216. doi: 10.1093/jac/44.2.209

Tang, S., Yao, L., Hao, X., Zhang, X., Liu, G., Liu, X., et al. (2015). Efficacy, safety and tolerability of linezolid for the treatment of XDR-TB: a study in China. *Eur. Respir. J.* 45, 161–170. doi: 10.1183/09031936.00035114

Tasneen, R., Li, S., Peloquin, C., Taylor, D., Williams, K., Andries, K., et al. (2011). Sterilizing activity of novel TMC207- and PA-824-containing regimens in a murine model of tuberculosis. *Antimicrob. Agents Chemother.* 55, 5485–5492. doi: 10.1128/AAC.05293-11

Tiberi, S., D'Ambrosio, L., De Lorenzo, S., Viggiani, P., Centis, R., Sotgiu, G., et al. (2016). Ertapenem in the treatment of multidrug-resistant tuberculosis: first clinical experience. *Eur. Respir. J.* 47, 333–336. doi: 10.1183/13993003.01278-2015

Till, M., Wixson, R. L., and Pertel, P. E. (2002). Linezolid treatment for osteomyelitis due to vancomycin-resistant *Enterococcus faecium*. *Clin. Infect. Dis.* 34, 1412–1414. doi: 10.1086/340265

Tsukamura, M. (1980). *In-vitro* antimycobacterial activity of minocycline. *Tubercle* 61, 37–38. doi: 10.1016/0041-3879(80)90058-6

Van Deun, A., Maug, A. K., Salim, M. A., Das, P. K., Sarker, M. R., Daru, P., et al. (2010). Short, highly effective, and inexpensive standardized treatment of multidrug-resistant tuberculosis. *Am. J. Respir. Crit. Care Med.* 182, 684–692. doi: 10.1164/rccm.201001-0077OC

WHO (2016). *Global Tuberculosis Control 2016*. Available at: http://www.who.int/tb/publications/global_report/en/

Yanagihara, K., Kaneko, Y., Sawai, T., Miyazaki, Y., Tsukamoto, K., Hirakata, Y., et al. (2002). Efficacy of linezolid against methicillin-resistant or vancomycin-insensitive *Staphylococcus aureus* in a model of hematogenous pulmonary infection. *Antimicrob. Agents Chemother.* 46, 3288–3291. doi: 10.1128/AAC.46.10.3288-3291.2002

Yano, T., Kassovska-Bratinova, S., The, J. S., Winkler, J., Sullivan, K., Isaacs, A., et al. (2011). Reduction of clofazimine by mycobacterial type 2 NADH:quinone oxidoreductase: a pathway for the generation of bactericidal levels of reactive oxygen species. *J. Biol. Chem.* 286, 10276–10287. doi: 10.1074/jbc.M110.200501

Zhang, Y., and Yew, W. W. (2009). Mechanisms of drug resistance in *Mycobacterium tuberculosis*. *Int. J. Tuberc. Lung Dis.* 13, 1320–1330.

Zhang, Z., Li, T., Qu, G., Pang, Y., and Zhao, Y. (2015). In vitro synergistic activity of clofazimine and other antituberculous drugs against multidrug-resistant *Mycobacterium tuberculosis* isolates. *Int. J. Antimicrob. Agents* 45, 71–75. doi: 10.1016/j.ijantimicag.2014.09.012

Zhao, W., Zheng, M., Wang, B., Mu, X., Li, P., Fu, L., et al. (2016). Interactions of linezolid and second-line anti-tuberculosis agents against multidrug-resistant *Mycobacterium tuberculosis* in vitro and in vivo. *Int. J. Infect. Dis.* 52, 23–28. doi: 10.1016/j.ijid.2016.08.027

Conflict of Interest Statement: The authors declare that the research was conducted in the absence of any commercial or financial relationships that could be construed as a potential conflict of interest.

Copyright © 2017 Sharma, Dhuriya, Deo and Bisht. This is an open-access article distributed under the terms of the Creative Commons Attribution License (CC BY). The use, distribution or reproduction in other forums is permitted, provided the original author(s) or licensor are credited and that the original publication in this journal is cited, in accordance with accepted academic practice. No use, distribution or reproduction is permitted which does not comply with these terms.

frontiers in Microbiology

REVIEW
published: 30 January 2018
doi: 10.3389/fmicb.2018.00070

Harnessing the mTOR Pathway for Tuberculosis Treatment

*Pooja Singh and Selvakumar Subbian**

Public Health Research Institute at New Jersey Medical School, Rutgers Biomedical and Health Sciences Rutgers, The State University of New Jersey, Newark, NJ, United States

Tuberculosis (TB) remains as one of the leading killer infectious diseases of humans. At present, the standard therapeutic regimen to treat TB comprised of multiple antibiotics administered for a minimum of six months. Although these drugs are useful in controlling TB burden globally, they have not eliminated the disease. In addition, the lengthy duration of treatment with multiple drugs contributes to patient non-compliance that can result in the development of drug resistant strains (MDR and XDR) of Mycobacterium tuberculosis (Mtb), the causative agent of TB. Therefore, new and improved therapeutic strategies are urgently needed for effective control of TB worldwide. The intracellular survival of Mtb is regarded as a cumulative effect of the host immune response and the bacterial ability to resist or subvert this response. When the host innate defensive system is manipulated by Mtb for its survival and dissemination, the host develops disease conditions that are hard to overcome. The host intrinsic factors also contributes to the poor efficacy of anti-mycobacterial drugs and to the emergence of drug resistance. Hence, strengthening the immune repertoire involved in combating Mtb through host-directed therapeutics (HDT) can be one of the approaches for effective bacterial killing and clearance of infection/disease. Recently, more scientific research has been focused toward HDT strategies that empowers host cells for effective killing of Mtb, reduce the duration of treatment and/or alleviates the development of MDR/XDR, since Mtb cannot develop resistance against a drug that targets the host cell function. Autophagy is a conserved cellular process critical for maintaining cellular integrity and function. Autophagy is regulated by multiple pathways that are either dependent or independent of mTOR (mechanistic target of rapamycin; a.k.a. mammalian target of rapamycin), a master regulatory molecules that impacts several cellular functions. In this review, we summarize the role of autophagy in Mtb pathogenesis, the mTOR pathway and, modulating the mTOR pathway with inhibitors as potential adjunctive HDT, in combination with standard anti-TB antibiotics, to improve the outcome of current TB treatment.

Keywords: mTOR, autophagy, everolimus, host directed therapy, tuberculosis, drug resistance, adjunct therapy, phagocytosis

OPEN ACCESS

Edited by:
Noton Kumar Dutta, Johns Hopkins University, United States

Reviewed by:
Osmar Nascimento Silva, Universidade Católica Dom Bosco, Brazil
Vikram Saini, University of Alabama at Birmingham, United States

****Correspondence:***
Selvakumar Subbian
subbiase@njms.rutgers.edu

Specialty section:
This article was submitted to Antimicrobials, Resistance and Chemotherapy, a section of the journal Frontiers in Microbiology

Received: *23 October 2017*
Accepted: *11 January 2018*
Published: *30 January 2018*

Citation:
Singh P and Subbian S (2018) Harnessing the mTOR Pathway for Tuberculosis Treatment. Front. Microbiol. 9:70. doi: 10.3389/fmicb.2018.00070

INTRODUCTION

Tuberculosis (TB) is one of the leading killer among infectious diseases of humans, accounting for about 10.4 million new cases and 1.8 million deaths in 2015 (World Health Organization, 2016). The global burden of TB has also been exacerbated by other co-morbid conditions, including diabetes and HIV-infection, and TB is a leading cause of mortality among HIV infected

individuals with nearly 400,000 deaths reported in 2015. The standard therapeutic regimen recommended by the WHO for treating drug-sensitive pulmonary TB, known as DOTS (Directly Observed Treatment, Short course), is comprised of four antibiotics: isoniazid (INH), rifampicin (RIF), pyrazinamide (PZA) and ethambutol (ETH) for 2 months (initial phase) followed by INH, and RIF for 4 months (continuation phase). This multi-drug regimen is essential and necessary to ensure successful bacteriological cure in patients with TB. Although these drugs are useful in controlling the overall disease burden at the level of individual patients as well as global TB control measures, they have not eliminated the disease at both these levels (Ryan, 1992). This is in part due to the lengthy duration of treatment with multiple drugs, which promotes the fear of drug dependency and doubts of not getting cured and contributes to drug-induced tissue toxicity issues. Adverse effects, ranging from serious ones, like hepatitis and pneumonia, to minor ones, like vomiting, acne and nausea, have been reported to be associated with DOTs therapy (Michael et al., 2016). Thus, high drop-out rate of TB patients from treatment regimens (a.k.a. patient non-compliance) is a serious issue contributing directly to the development of drug resistance in *Mycobacterium tuberculosis* (Mtb), the causative agent of TB.

Development of drug resistance in a single bacterium has been suggested to be sufficient to create an outbreak of drug resistant bacteria (Borrell and Gagneux, 2009). In 2015, nearly 4.8 million cases of isoniazid- and rifampicin-resistant [a.k.a. multidrug-resistant TB (MDR-TB)] cases were reported. In addition to INH and RIF (the first line drugs), Mtb can develop resistance to PZA and ETH (second line drugs) and other injectable aminoglycosides, leading to extensively drug-resistant TB (XDR-TB) cases. Nearly 9.5 % of all MDR-TB cases in 2015 were estimated to be XDR-TB. A recent study aimed at predicting the future burden of TB suggests an increased prevalence of MDR and XDR cases due mainly to person-to-person transmission of drug-resistant Mtb, rather than the pathogen acquiring drug resistance within the infected host (Sharma et al., 2017). Hence, current treatment strategies demand intense patient monitoring during and after drug treatment, which poses major strategical and economical challenges for the global TB control programs conducted by various health agencies. Therefore, it is imperative that new anti-TB therapies are developed and implemented to shorten the number of antibiotics taken and/or duration of treatment, to lower the drug- induced toxicities, and to improve the drug efficacy among TB patients with co-morbid conditions, such as HIV-infection and/or patients with MDR/XDR-TB.

Development of drug resistance among infecting Mtb is also dependent on host intrinsic factors, such as genetic make-up, health, and well-being, all of which impact the immune response against the bacteria. A key component of the host innate defense system are macrophages, phagocytic cells that engulf and destroy infecting microorganisms. However, Mtb can "invade" macrophages (and other host cells), where it is able to survive, proliferate and cause infection/disease. Invasion of macrophages by Mtb brings changes to the normal phagocytosis events, such as calcium ion homeostasis, membrane protein distribution and phagosome-lysosome fusion. If/when Mtb survives, it continues to multiply intracellularly and induce a pro-inflammatory response, leading to the onset of cell mediated/adaptive immunity and granuloma formation, which is generally thought of as a region of equilibrium between the host and the bacterium. For Mtb, the granuloma serves as an environment where the bacteria can exist in a dormant, semi- and/or non-replicating state. For the host, the granulomas restrict the spread of Mtb to other tissues/organs because the diseased area is cordoned-off by the activated immune cells (Guirado et al., 2013). The host-pathogen interactions in the granuloma are highly complex, where the bacteria may get killed or able to survive and persist (Flynn and Chan, 2003). Taken together, the intracellular survival of Mtb is regarded as a cumulative effect of the host immune response and the bacterial ability to resist or subvert this response. Hence, strengthening the immune repertoire involved in combating Mtb through host-directed therapeutics (HDT) can be one of the approaches for effective bacterial killing and clearance of infection/disease.

Host directed therapy (HDT) aims at manipulating the metabolism and/or immune cell function to optimize the pro-inflammatory response or to modify the tissue physiology (Subbian et al., 2011a,b; Tobin et al., 2012). Recently, research on HDT as potential therapeutic strategy for infectious diseases has gained significant momentum due to the possibility of re-purposing drugs that have been already approved to treat chronic ailments and the advantage that pathogenic bacteria, such as Mtb, cannot develop resistance against a HDT, which targets host cell functions (Zumla et al., 2015). Autophagy is a homeostatic cellular process that removes intracellular debris derived from endo-and exo-genous sources, thus ensuring efficient functioning of cells. It is also a key innate immune response of the host cells to protect against invading pathogens. Therefore, targeting the autophagy machinery using small molecules and drugs to improve the host cell effector functions is an emerging concept in the treatment of several chronic diseases (Rubinsztein et al., 2012). Autophagy is regulated by multiple, complex networks and pathways that are either dependent or independent of mTOR (mechanistic target of rapamycin; a.k.a. mammalian target of rapamycin), a master regulatory molecule that impacts several cellular functions (**Figure 1**). In this review, we focus mainly on the role of autophagy in Mtb pathogenesis and modulating the mTOR pathway as potential adjunctive HDT to improve current, antibiotic-based treatment for pulmonary TB.

MODULATION OF PHAGOCYTE FUNCTION BY *MYCOBACTERIUM TUBERCULOSIS*

Successful intracellular pathogens inhibit host cell antimicrobial processes involved in restricting their survival (Flynn and Chan, 2003; Kim et al., 2012). In that context, Mtb is known to inhibit killing within the phagolysosome of macrophages and other antigen presenting cells (APC) by modulating phagosome maturation and its fusion with the lysosome. In the infected APC, pathogenic Mtb inhibits actin assembly around the phagosome, thereby inhibiting host lipid molecules from interacting with

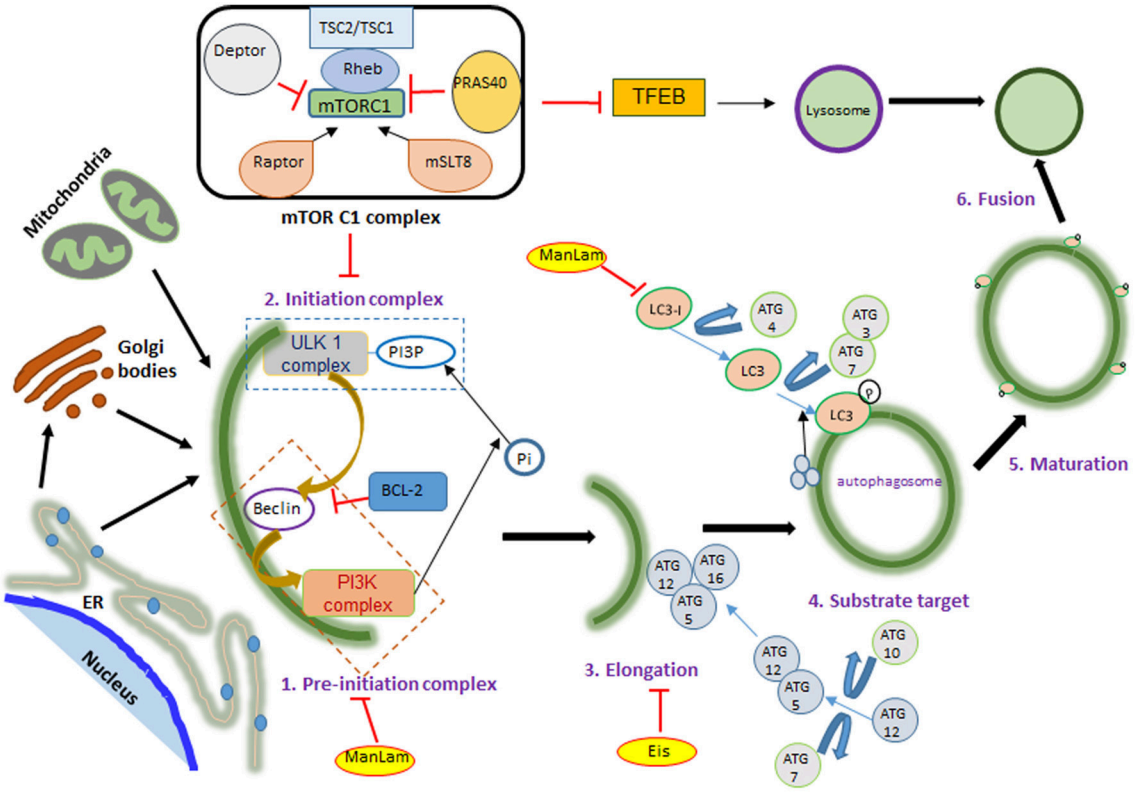

FIGURE 1 | mTOR signaling during autophagy. mTOR has two complexes: mTORC1 and mTORC2, differentiated according to their activator proteins Raptor and Rictor. When activated, mTOR blocks ULK complex formation by phosphorylating it. ULK and PI3K complex formation marks the initiation of autophagy, followed by ATG-5, 12, and 16 binding on the phagophore membrane. This leads to LC3 translocation on the autophagosome membrane, which is required for fusion with lysosome and ultimately bacterial killing. Autophagy activating factors and pathways are denoted in black color and autophagy inhibitors are in red color letters and lines; mTOR activation leads to protein synthesis, nucleotide synthesis, cytoskeletal regulation and ion transport. These are denoted in blue color. Yellow color highlight denotes mycobacterial factors influencing autophagy.

phagosomal proteins necessary for further maturation and fusion with the lysosome (Vergne et al., 2003; Rohde et al., 2007; Ehrt and Schnappinger, 2009; Shui et al., 2011; Seto et al., 2012). When bacteria are phagocytosed by APC, the phagosome acquires early endosomal protein markers, such as EEA1 (early endosomal antigen 1) and Rab5, which are gradually replaced with Rab7 during the maturation of the phagosome (Chandra et al., 2015); ultimately, LAMP1 (lysosome-associated membrane protein 1) and acid hydrolases mark the late phagosome for fusion with lysosome (Huynh et al., 2007). It has been reported that phagosomes containing live Mtb do not acquire Rab5 due to the presence of tryptophan aspartate coat protein (TACO). Phagosomal association with TACO is also reported in macrophages that can engulf other pathogenic mycobacteria, which also result in the inhibition of phagosomal maturation (Pieters and Gatfield, 2002). Proper maturation of phagosomes is the key to its fusion with lysosomes, which can kill the bacteria by delivering toxic molecules. However, due to the absence of proton-ATPase molecules in Mtb-containing phagosomes, the phagosome-lysosome fusion does not take place and the bacteria survive intracellularly (Vergne et al., 2005).

Another mechanism used by Mtb to manipulate APC involves perturbation of intracellular calcium ion (Ca^{2+}) levels (Kusner and Barton, 2001). Several studies have demonstrated fluctuations in intracellular Ca^{2+} levels in Mtb-infected macrophages (Vergne et al., 2003; Jayachandran et al., 2007). During phagocytosis of opsonized or heat-killed Mtb, intracellular Ca^{2+} concentrations increase, while macrophages infected with live pathogenic Mtb have reduced calcium ion level, which in turn significantly reduce the levels of Ca^{2+} associated-calmodulin and the phosphorylated Ca^{2+}/calmodulin-dependent protein kinase II (CaMKII) (Jayachandran et al., 2007). Reduction in CaKMII level also blocks the delivery of lysosomal components to phagosome. Mtb reportedly prevents intracellular Ca^{2+} increase through its cell wall glycolipid, ManLAM (mannose-capped lipoarabinomannan), and by inhibiting host sphingosine kinase (SK). ManLAM also inhibits ionophore-induced increase in Ca^{2+} levels in macrophages. Reduced Ca^{2+}/Calmodulin association impairs PI3K signaling, which inhibits recruitment of EEA1 to phagosomes (Rojas et al., 2000). Inhibition of SK abrogates phosphorylation of sphingosine, which is required

for G-protein coupled receptor (GPCR) signaling that regulates Ca^{2+} homeostasis. Thus, ManLAM triggers a sequence of events leading to Ca^{2+} signaling disruption and phagosomal maturation arrest, which facilitate successful intracellular survival of infecting Mtb (Chan et al., 1991; Rojas et al., 2000).

Apart from its function in maintaining cellular homeostasis, autophagy is also known to sense and destroy intracellular bacteria in innate immune cells, such as macrophages. Although intracellular Mtb can efficiently modulate the bactericidal mechanisms of phagocytes, autophagy has been shown to be effective in killing Mtb (Gutierrez et al., 2004; Maiuri et al., 2007). Xenophagy, a type of autophagy whereby microorganisms can be sequestered and subject to lysosomal degradation, has been proposed to play an important role in elimination of bacteria (Gutierrez et al., 2004; Rubinsztein et al., 2012; Songane et al., 2012). In Mtb-infected host cells, the autophagosome collects ubiquitin while maturing, which then ultimately fuses with lysosome, thereby enhancing the lysosome-mediated bacterial killing. Survival of Mtb in macrophages has been reported to be dependent on the autophagosome delivery to the lysosome. However, *in vivo* and *in vitro* results have shown disparity in Mtb survival following inhibition of autophagy markers (**Table 1**) (Levine and Deretic, 2007; Lerena et al., 2008; Levine et al., 2011). Mutation or knockdown of autophagy associated host genes, such as Unc-51-like kinase 1 (Ulk1), Beclin1, Atg5, Atg7 or p62, has been reported to increase the survival of intracellular bacteria (Kim et al., 2011; Mizushima et al., 2011; Shang et al., 2011; Alers et al., 2012). However, although xenophagy is reported to restrict the survival of Mtb and BCG (bacille Calmette-Guerin) within macrophages, there are studies suggesting that intracellular pathogens such as *Shigella flexneri*, *Listeria monocytogenes*, *Burkholderia pseudomallei*, *Orientia tsutsugamushi*, *Porphyromonas gingivalis*, *Staphylococcus, Brucella abortus,* and *Salmonella typhimurium* are capable of blocking induction of autophagy by downregulating the co-localization of LC3 (microtubule-associated protein 1A/1B-light chain 3), restoring activation of mTOR, and utilizing nutrients for their growth and survival (Thurston et al., 2009; Yoshikawa et al., 2009; Zheng et al., 2009; Choy et al., 2012; Fraunholz and Sinha, 2012; Asrat et al., 2014; Yu et al., 2014).

Pathogenic Mtb also inhibits phagosome function in infected macrophages by releasing vesicle-bound lipids and glycolipids, which accumulate in lysosomes and interfere with the phagosome-lysosome fusion (Beatty et al., 2000). Taken together, pathogenic intracellular Mtb uses multiple strategies to manipulate the host defense machinery of APC for its own survival. Manipulation of APC function by Mtb impacts subsequent downstream events, including autophagy, antigen presentation, apoptosis, and activation of various signaling pathways involved in the production of cytokines, chemokines and other effector molecules that are crucial for controlling bacterial growth and replication (Briken et al., 2004; Cooper, 2009; Guenin et al., 2009; Rajaram et al., 2010).

AUTOPHAGY AND mTOR SIGNALING

Autophagy, a Greek word meaning "eating of self," is a conserved cellular process critical for maintaining cellular integrity and function. This catabolic process is activated in cells due to lack of nutrient availability or cellular damage or stress, and involves degradation of damaged organelles and misfolded or abnormal proteins. During starvation, cytosolic components of cells are sequestered by autophagy to release nutrients for de novo biosynthesis of molecules (Laplante and Sabatini, 2012). Autophagy can also be activated by pathological factors, such as infections and other diseases. In these cases, normal cellular functions are facilitated by the elimination of pathogens through autophagy-dependent mechanisms, such as surface antigen presentation (Rubinsztein et al., 2012; Songane et al., 2012). Moreover, autophagy is one of the macrophage defense mechanisms against Mtb infection.

Autophagy is characterized by phagophore formation, elongation and maturation of the autophagosome, which ultimately fuse with the lysosome for the degradation of its contents. Formation of the autophagosome begins with a double membranous structure derived from the lipid bilayers of the endoplasmic reticulum (ER) or Golgi apparatus and conjugated with autophagy related (ATG) proteins (Maiuri et al., 2007; Alers et al., 2012). The three main components of autophagosome generation are: PI3KC3 (class III phosphoinositide 3-kinase

TABLE 1 | Major differences and similarities between mTOR complexes- mTORC1 and mTORC2.

Similarities	Differences	
	mTOR C1	**mTOR C2**
• Both belong to mTOR signaling cascade. • Member of PI3K related kinase family. • mLST8 is a common positive regulator protein. • Cellular stress, such as low level of growth factors, generation of reactive oxygen species and energy depletion inhibits mTOR signaling.	Five components: mTOR, RAPTOR, mLST8, PRAS40, and DEPTOR.	Six components: mTOR, RICTOR, DEPTOR, mSIN-1, mLST8, and PROCTOR.
	Positive regulators: RAPTOR and mLST8.	Positive regulators: RICTOR and mSIN-1.
	Negative regulators; PRAS40 and DEPTOR.	Negative regulators: DEPTOR.
	Rapamycin sensitive.	Rapamycin insensitive.
	Inhibits autophagy by directly interacting with pre initiation complex (ULK complex).	Inhibits autophagy indirectly by regulating mTORC1.
	Regulates p70-S6K and 4E-BP-1 to influence cellular metabolism.	Regulates AKT to influence cellular growth.
	Activating signaling: Growth factors, energy molecules, amino acids level.	Not known.

complex 3), ULK1 (unc-51-like kinase 1) complex and ATG complex (**Figure 1**). This process is negatively regulated by mTOR kinase, which, when activated, blocks the ULK1 complex (Kim et al., 2011; Shang et al., 2011). Under stress conditions, such as nutrient deprivation or bacterial invasion, mTOR gets inactivated, enabling the ULK1 complex to recruit and activate PI3KC3 (Dibble and Cantley, 2015). This initiation complex, formed on the ER, leads to the nucleation of cell membrane, which is followed by recruitment of an ubiquitin-like molecule, LC3. In the final step, LC3 conjugates with phosphotidylethanolamine, resulting in self-fusion of the double membrane to form the autophagosome, which subsequently fuses with lysosome to degrade the engulfed contents.

Apart from mTOR signaling pathway (Lipinski et al., 2010), autophagy is also regulated by the inositol signaling pathway (Sarkar et al., 2005), Ca^{2+} /Calpain signaling pathway (Gordon et al., 1993) and cAMP (cyclic adenosine monophosphate) (Noda and Ohsumi, 1998). Inhibition of these mTOR-independent pathways for promoting autophagy has been studied under different disease conditions (Floto et al., 2007; Grumati et al., 2010; Hidvegi et al., 2010). Promising outcomes of autophagy induction via mTOR-independent pathway have been observed only with a combination therapy strategy, where the small molecules enhancers (SMERs) or inhibitors (SMIRs) of mTOR-independent pathway are used in combination with an mTOR inhibitor. For example, lithium, an inositol (1,4,5)-triphosphate inhibitor, when administered with rapamycin results in a stronger induction of autophagy (Sarkar et al., 2008). On the other hand, rapamycin alone can induce autophagy even at high intracellular inositol (1,4,5)-triphosphate levels, which has autophagy inhibitory effects. Since targeting ULK complex formation or ATG complex, rather than affecting the upstream pathways, seems to have a specific and stronger impact on autophagy, mTOR has been the target of interest for promoting autophagy upon infection with *Mycobacteria* (Gutierrez et al., 2004).

THE mTOR COMPLEX

In addition to its role in autophagy, mTOR is also a master regulator of cell metabolism, growth, proliferation, translation initiation, and cytoskeletal organization. It belongs to the family of phosphoinoside 3-kinase- (PI3K-) related kinase and is a highly conserved serine/threonine protein kinase, which exists in host cells as part of two protein complexes—mTORC1 and mTORC2 (Laplante and Sabatini, 2012; Singh and Cuervo, 2012) (**Figure 2**). Theses complexes differ in their structure and activity, in part due to the difference in mTOR regulatory proteins such as RAPTOR (regulatory associated protein of mTOR; rapamycin sensitive) in mTORC1 and RICTOR (rapamycin-insensitive companion of mTOR) in mTORC2, as well as other accessory proteins (Laplante and Sabatini, 2009). The proteins that are common to both mTORC1 and C2 complexes are the mammalian lethal with Sec13 protein 8 (mLST8) and DEP domain containing mTOR interacting protein (DEPTOR). While mLST8 acts as a positive regulator, DEPTOR functions as a

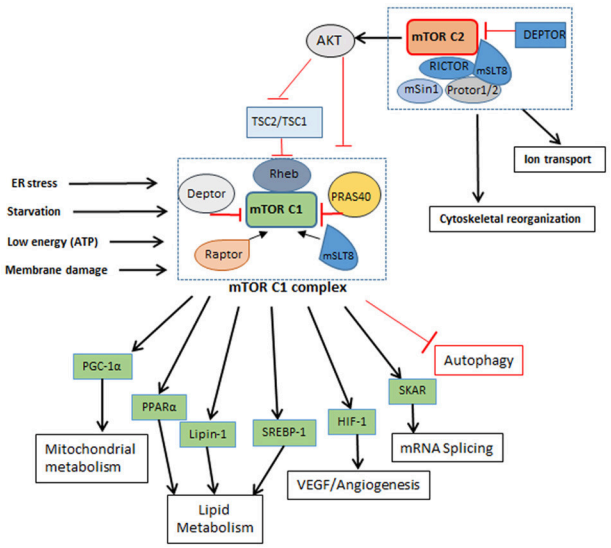

FIGURE 2 | mTORC1 and mTORC2 complexes. mTORC1: Is a five component complex with DEPTOR and PRAS40 as negative regulators and RAPTOR and mSLT8 as positive regulators. It regulates different cellular processes like lipid metabolism and protein metabolism other than autophagy as seen in **Figure 1**. It is influenced by the nutrient and energy level in cell and gets shut down or inhibited when cell encounters reducing nutrient level and decrease in energy. Inhibition of mTORC1 leads to inhibition of cellular metabolic processes. mTORC2; A six component complex has DEPTOR as its negative regulator and RICTOR and mSLT8 as positive regulators. This complex influences activation of mTORC1 by phosphorylation of AKT. How nutrient level influences mTORC2 is not known yet.

negative regulator of mTOR signaling. The mTORC1 is activated by RAPTOR, PRAS40 (proline-rich AKT substrate 40 kDa) and by phosphorylation of tuberous sclerosis protein 2 (TSC2) (Huang et al., 2008). The PI3K/AKT pathway is a positive regulator of mTOR signaling (Kim et al., 2011; Ng et al., 2011; Pan et al., 2012). Apart from PI3K/AKT, arginine, DNA damage, AMPK (AMP-activated protein kinase) and ERK1/2 (extracellular signal-regulated protein kinases 1 and 2) signaling were also reported to regulate mTORC1 activation (Kim et al., 2002; Inoki et al., 2003; Fingar and Blenis, 2004; Laplante and Sabatini, 2009). Importantly, mTORC1 activation inhibits autophagy (Jung et al., 2010). Deactivation of mTORC1 in cells under nutrition depletion or treatment with rapamycin leads to initiation of autophagy. (Seto et al., 2013). Similarly, dephosphorylating ULK1 by inactivation of mTORC1 induces autophagy (Egan et al., 2011; Kim et al., 2011; Shang et al., 2011).

The binding of mTORC2 with RICTOR facilitates the interaction of these proteins with TSC2 and mammalian stress-activated protein kinase interacting protein (mSIN-1); another protein found in association with RICTOR is PROTOR-1, which promotes activation of serum and glucorticoid-induced kinase 1 (SGK1). Interaction of all these proteins ultimately promotes mTORC2 complex formation and phosphorylation of AKT. Therefore, mTORC2 activation also regulates mTORC1 activation via AKT phosphorylation. Similarly, while mTORC1 activation is mediated by PI3K-AKT/PKB pathway in response

to nutrient availability and mitogenic stimulation of the cell, phosphorylation of growth factors by autophosphorylation of their receptor tyrosine kinases activates mTORC2 complex, which also activates class I PI3K-AKT/PKB pathway (Dibble and Cantley, 2015). mTOR complexes also differ in the nature of their stimulant, for example, mTORC1 is activated by low levels of amino acids and growth factors, energy molecules and stress, while mTORC2 remains unaffected by the changing levels of these mTORC1 stimulants. However, role of mTORC2 is important for the regulation of AKT, which in turn governs mTORC1 functions. With use of TSC deficient cells importance of autophagy for cell survival was validated. In conditions like TSC (tuberous sclerosis complex), mTOR inhibition by rapamycin and pro-survival due to autophagy may have beneficial effects (Parkhitko et al., 2011).

In addition to regulating autophagy, activation of mTORC1 also promotes cellular metabolic pathways, such as glucose metabolism, protein and lipid synthesis, all of which contributes to cell growth and proliferation. S6Ks (p70 ribosomal protein S6 kinase 1/2) and 4E-BPs (eukaryotic initiation factor4 binding protein) are the two major proteins interacting with mTORC1 and play a major role in protein synthesis. mTORC1 phosphorylates 4E-BP1 thereby inhibiting its interaction with elF4E, which is then able to promote cap-dependent translation. Similarly, mTORC1 interaction with S6K1 stimulates cap-dependent translation of ribosomal proteins. Phosphorylation of S6K by mTORC1 also activates glucose transporter protein (Glut1) which activates glycolysis, lipogenesis and increases glucose uptake (Zeng et al., 2016). This increased glycolysis due to Glut1 is also reported to elevate T cell function and proliferation (Macintyre et al., 2014). Likewise, lipid synthesis is influenced by positive regulation of SREBP1 (sterol regulatory element binding protein 1) and PPARγ (peroxisome proliferator-activated receptor-γ) (Kim and Chen, 2004), which are regulated by mTORC1. The mTOR inhibitor, rapamycin, reduced phosphatidic acid phosphatase (lipin-1) phosphorylation, which is essential for glycerolipid synthesis; lipin-1 also activates PPARγ and other proteins associated with lipid synthesis (Huffman et al., 2002). Oxidative metabolism is also influenced by mTOR signaling. In a mouse model, inhibition of mTORC1 reduced the muscle mass and oxidative metabolism, leading to early death. It has been shown that PGC1-α is associated with the oxidative metabolism and that mTOR directly interacts with this regulatory protein (Laplante and Sabatini, 2012). Other proteins interacting with mTORC1 are HIF-1α (hypoxia-inducible factor 1-alpha) and STAT3 (signal transducer and activator of transcription 3), which are involved in a plethora of cellular functions, ranging from angiogenesis to inflammation and cytokine response (Laughner et al., 2001).

mTOR INHIBITORS AS POTENTIAL HDT FOR TB

Since mTOR signaling pathway regulates several cellular processes, including autophagy, that are linked to the host immune response to pathogens, it is an attractive target for developing/testing small molecules to modulate host immunity for better protection against infectious agents. Moreover, the peripheral blood mononuclear cells (PBMCs) and $CD^{4+}CD^{25+}FoxP^{3+}$Treg cells isolated from active tuberculosis patients demonstrated mTOR inhibition during infection (Zhang et al., 2017). In contrast, mTOR activation, by deletion of *Tsc1* in hematopoietic stem cells, induces accumulation CDK (cyclin-dependent kinase) inhibitors $p16^{ink4a}$, $p19^{Arf}$, $p21^{Cip1}$ leading to impaired hematopoietic system and decreased lymphopoiesis (Chen et al., 2009). These observations establish that mTOR inhibition improves cell survival and the understanding that mTOR inhibition may be promoting host cell defense mechanisms against invading pathogens (Harrison et al., 2009).

The following are some of the key mTOR inhibitors in use to treat chronic conditions in humans.

Rapamycin

Rapamycin, specifically known for its mTOR inhibitory activity, was first isolated from *Streptomyces hygroscopicus*. Despite of its antifungal and antibacterial properties, Rapamycin is well-known for its immunosuppressant activity, which led to its use in organ transplant cases to reduce graft rejection. Similar to temsirolimus, rapamycin, which is also known as sirolimus, targets FKBP12 (FK506-binding protein 1A, 12 kDa) and inhibits the formation of active mTOR complex. Thus all of the currently known sirolimus derivatives target FKBP12 and inhibit mTOR complex.

In a zebrafish model of *M. marinum* infection, mTOR was shown to be associated with the host resistance to infection. In this model, mTOR mutants were hyper-susceptible to *M. marinum* at higher infection dose; however, when the inoculum size was decreased, the mTOR-deficient zebrafish cleared infection early (Pagan et al., 2016). Inhibition of mTOR in mice by rapamycin treatment at early age did not significantly affect the life expectancy or susceptibility to disease, but administration at an old age improved the survival expectancy (Harrison et al., 2009). In another study, administration of rapamycin to BCG-vaccinated mice has been shown to elicit better vaccination efficacy against Mtb infection, which is associated with induced autophagy, increased antigen presentation on dendritic cells and elevated Th1-type immune response (Gutierrez et al., 2004; Jagannath et al., 2009). Results from a low dose Mtb infection (MOI = 1) of human monocyte-derived-macrophages pre-infected with HIV, showed elevated bacterial load upon administration of rapamycin (1 μM) (Andersson et al., 2016). This study described mTOR inhibition as an advantage for the intracellular survival of Mtb; however, in an already immunocompromised cell (due to HIV infection), it is difficult to assess the impact of mTOR inhibition on Mtb growth. Although rapamycin used to be the popular drug of interest to achieve cellular mTOR inhibition, poor solubility and long intracellular half-life complicates the consideration of this molecule as potential HDT for TB therapy.

Temsirolimus

Temsirolimus, commercially known as CCI-779 or Torisel, is currently approved by the US-FDA for use in renal cell carcinoma

(RCC) treatment. This prodrug can transform to sirolimus when dihydroxymethyl propionic acid ester group at C40 position is removed. Temsirolimus is metabolized by the enzyme CYP3A4 (cytochrome P450 3A4) and has a half-life of 9–27 h (MacKeigan and Krueger, 2015). Intravenous administration of temsirolimus increases its bioavailability and dose intensity (Boni et al., 2009). Mechanistically, temsirolimus targets host FKBP-12 protein. The drug-FKBP-12 interaction inhibits the formation of mTOR-FKBP-12 complex, leading to the inactivation of mTOR complex and inhibition of p70S6k and S6 phosphorylation. These effects cumulatively results in arrested cell growth, proliferation and survival in RCC patients. Nonspecific pneumonitis and gastrointestinal disorders are major side effects in RCC patients treated with this drug. In addition, metabolic diseases such as hyperglycemia, and hypercholesterolemia are associated with temsirolimus administration in these patients (Malizzia and Hsu, 2008). Importantly, temsirolimus treatment has been widely associated with reactivation of latent Mtb infection among RCC patients. Also, progression of tumor was noted in these patients when temsirolimus was administered in combination with rifampicin, a first-line anti-TB drug (Bossé et al., 2016).

Ridaforolimus

Ridaforolimus (AP23573 or MK-8669) is an analog of sirolimus with improved bioavailability, solubility and half-life (30–75 h) (Rivera et al., 2011). It is administered orally or intravenously for the treatment of solid tumors of soft tissues, bone and other hematologic malignancies (Huang et al., 2015). In a phase I clinical trial with 87 ER^+/high-proliferative breast cancer cases, majority of patients treated with ridaforolimus demonstrated reduced tumor activity (Di Cosimo et al., 2015). Similarly, a phase II clinical trial showed promising results for ridaforolimus to treat patients with endometrial, soft tissue and bone cancers (Palavra et al., 2017). The effect of ridaforolimus on cell metabolism and growth is largely dependent on the dose of drug used for treatment. This is due to its varying effect on mTOR inhibition with variation in dosage (Rivera et al., 2011). However, no reactivation of latent Mtb infection has been reported in these studies (Huang et al., 2015; Palavra et al., 2017).

Everolimus

Everolimus (40-O-(2-Hydroxy)-ethyl-rapamycin), commercially known as SDZ-RAD, RAD001, Certican and Afinitor, is a derivative of rapamycin bearing a stable 2-hydroxy ethyl chain substitution at position 40. This agent has a better solubility, oral availability, and decreased mean elimination half-life (∼18–30 h), leading to early removal of drug from the body compared to the parent compound (rapamycin). Because of the better absorption, it has higher bio-availability (30–60%) and a T_{max} of 1–2 h. Everolimus is an immunosuppressive, anti-inflammatory drug that inhibits host cell proliferation by arresting the progression of cell cycle from G1 to S phase; the immune suppressive function is exerted by inhibiting IL-2 and IL-15 mediated lymphocyte proliferation (Kovarik et al., 2002; Lingaraju et al., 2010; Ahya et al., 2011). In addition, everolimus promotes autophagy by inhibiting mTORC1 (Saran et al., 2015).

Inhibition of mTOR pathway by everolimus treatment has been reported to improve cellular immune response in both animal models and human studies. In a study performed with 218 healthy volunteers of >65 years of age, everolimus treatment had beneficial effects over aging-related issues (Mannick et al., 2014). Specifically, these elderly volunteers treated with a low dose of everolimus showed about 20% improvement in their protective response after influenza vaccination. This improvement was associated with reduced expression of programmed death-1 receptor, which is otherwise highly expressed in aging individuals, on CD4 and CD8 T cells, thus increasing T cell antigen processing and expression. This low dose administration (0.5 mg daily or 5 mg weekly) of eveolimus demonstrated minimum number of adverse events, (35 adverse events) compared to a higher dose administration (20 mg weekly), which resulted in 109 adverse events amongst 53 elderly individuals (Mannick et al., 2014). This study clearly highlights the importance of optimizing the dose of mTOR inhibitors, such as everolimus in this case, for better efficacy with minimal adverse effects. In contrast, case studies with organ transplant patients have mentioned a higher risk of Mtb infection and reactivation of LTBI as possible side-effects of everolimus administration (Kovarik et al., 2002; Fijałkowska-Morawska et al., 2011). Although patients in this study were treated with a higher dose of everolimus, than the influenza vaccine study mentioned above, the mechanism underlying the connection between dose of everolimus and reactivation of LTBI is not clearly understood. However, the negative consequences of high dose administration of everolimus can be overcome by co-administration with CYP3A4 enzyme inducers, such as rifampicin, which are used to treat opportunistic TB infections in organ transplant patients (Eisen et al., 2003). Thus, it is important to understand the dose-response of everolimus in the context of host cellular functions and how the drug influences phagocytosis and autophagy-mediated elimination of Mtb during infection.

All the mTOR inhibitors described above are also frequently used in the treatment of various forms of cancer, including breast cancer, renal cell carcinoma and tuberous sclerosis complex, due to their ability to inhibit host cell proliferation and growth (Pohanka, 2006; Koh et al., 2013). However, the idea of using these mTOR inhibitors as potential adjunct HDT for TB therapy needs to be substantiated through experimental evidences related to dosage, pharmacokinetics and pharmacodynamics (PK/PD) parameters and, cost vs. benefit effects on the host immunity. Such evidences need to be reinforced by series of studies on reliable and relevant pre-clinical animal models of Mtb infection. In addition, metabolic dysfunctions, such as hyperglycemia is a common side effect in cancer patients treated with mTOR inhibitors, including everolimus (Porta et al., 2011). Although the impact of such inhibitors in the context of TB treatment remains to be determined, serious side effects of HDT drugs preclude their potential use in any treatment. Moreover, as immune-suppressing agents, the application of mTOR inhibitors as a stand-alone HDT therapy for TB holds a significant risk of reactivation of latent Mtb infection, similar to the situation observed in rheumatoid arthritis patients treated with anti-TNF-α antibody (Kovarik et al., 2002). However, when used

at an immune modulating-, as opposed to immune suppressing-dose, these mTOR inhibitors can be potential candidates to serve as an adjunct therapeutic molecule, along with standard anti-TB drugs, in improving the treatment outcome. Thus, fine-tuning the dose of mTOR inhibitors is an important and necessary step toward application of these HDT compounds for TB treatment. Importantly, since Mtb cannot develop resistance to a drug that targets host signaling pathway, such as mTOR or cellular processes, such as autophagy, HDT drugs has the potential to alleviate the development of MDR- and XDR-Mtb strains and their transmission in the community. Analogous to the trend in cancer treatment that have shifted from chemotherapeutic and radiologic regimens to more-host targeted treatment approaches, Mtb infection and/or disease can benefit from specific HDT drugs that targets, for example, the mTOR pathway and/or autophagy.

SUMMARY AND CONCLUSION

Pathogenic Mtb possess several virulent determinants, such as the unusually lipid-rich cell wall, that serve as permeability barriers and protects the bacteria from the harsh intracellular environment within phagocytes, and from the bactericidal activities of anti-TB drugs. Additionally, these mycobacteria-derived molecules interact with the host immune cells and modulates their function, promoting bacterial survival/persistence, causing disease within the host and enabling the development of bacterial drug resistance. Thus, when the innate defensive mechanisms of phagocytes are manipulated by the pathogen to promote its survival, the host develops active disease, which is hard to overcome. This can be one of the reasons for the inefficiency of current anti-mycobacterial drugs to eliminate TB, and for the emergence of drug-resistant Mtb strains. Perturbing host cell functions through HDT molecules has the potential to enhance the effector functions of these cells, which are the ultimate arsenals in combating bacterial infection. Moreover, these immune modulating drugs do not contribute to the emergence of drug resistance by the infecting bacteria. This criterion is crucial when considering therapy, particularly for patients with MDR, XDR-TB, as well as those patients with co-existing chronic conditions, such as diabetes or HIV infection, in which conventional antibiotics therapy has been shown to be complex, complicated, toxic and insufficient in achieving a bacteriological cure. Host cell autophagy, regulated by mTOR pathway, plays an important role in cellular homeostasis as well as in antibacterial defense mechanism. Therefore, targeting mTOR pathway with small molecules, such as everolimus, has the potential to develop novel and better combination drug therapy, along with standard anti-TB drugs to combat various forms of TB in patients with/without other co-morbid conditions. This approach can also enhance bacterial killing, reduce treatment duration, and/or improve clinical outcome. Clearly, more research and experimental evidence is warranted on these and other HDT molecules, for their efficacy, toxicity and other properties, through extensive pre-clinical studies using appropriate animal models of TB, before they are tried as therapeutic intervention for TB in human clinical trial.

AUTHOR CONTRIBUTIONS

SS: conceived the concept; PS and SS: wrote/edited the manuscript and agreed for submission.

FUNDING

This study was supported by a grant from the Bill and Melinda Gates Foundation (OPP1157210) to SS.

REFERENCES

Ahya, V. N., McShane, P. J., Baz, M. A., Valentine, V. G., Arcasoy, S. M., Love, R. B., et al. (2011). Increased risk of venous thromboembolism with a sirolimus-based immunosuppression regimen in lung transplanta-tion. *J. Heart Lung Transplant.* 30, 175–181. doi: 10.1016/j.healun.2010.08.010

Alers, S., Löffler, A. S., Wesselborg, S., and Stork, B. (2012). Role of AMPK-mTOR-Ulk1/2 in the regulation of autophagy: cross talk, shortcuts, and feedbacks. *Mol. Cell. Biol.* 32, 2–11. doi: 10.1128/MCB.06159-11

Andersson, A. M., Andersson, B., Lorell, C., Raffetseder, J., Larsson, M., and Blomgran, R. (2016). Autophagy induction targeting mTORC1 enhances *Mycobacterium tuberculosis* replication in HIV co-infected human macrophages. *Sci. Rep*. 6:28171. doi: 10.1038/srep28171

Asrat, S., de Jesús, D. A., Hempstead, A. D., Ramabhadran, V., and Isberg, R. R. (2014). Bacterial pathogen manipulation of host membrane trafficking. *Ann. Rev. Cell Dev. Biol*. 30, 79–109. doi: 10.1146/annurev-cellbio-100913-013439

Beatty, W. L., Rhoades, E. R., Ullrich, H. J., Chatterjee, D., Heuser, J. E., and Russell, D. G. (2000). Trafficking and release of mycobacterial lipids from infected macrophages. *Traffic* 1, 235–247. doi: 10.1034/j.1600-0854.2000.010306.x

Boni, J. P., Hug, B., Leister, C., and Sonnichsen, D. (2009). Intravenous temsirolimus in cancer patients: clinical pharmacology and dosing considerations. *Semin. Oncol.* 36(Suppl. 3), S18–S25. doi: 10.1053/j.seminoncol.2009.10.009

Borrell, S., and Gagneux, S. (2009). Infectiousness, reproductive fitness and evolution of drug-resistant *Mycobacterium tuberculosis*. *Int. J. Tuberc. Lung Dis*. 13, 1456–1466.

Bossé, D., Ng, T., Ahmad, C., Alfakeeh, A., Alruzug, I., Biagi, J., et al. (2016). Eastern Canadian gastrointestinal cancer consensus conference 2016. *Curr. Oncol.* 23, e605–e614. doi: 10.3747/co.23.3394

Briken, V., Porcelli, S. A., Besra, G. S., and Kremer, L. (2004). Mycobacterial lipoarabinomannan and related lipoglycans: from biogenesis to modulation of the immune response. *Mol. Microbiol.* 53, 391–403. doi: 10.1111/j.1365-2958.2004.04183.x

Chan, J., Fan, X. D., Hunter, S. W., Brennan., P. J., and Bloom, B. R. (1991). Lipoarabinomannan, a possible virulence factor involved in persistence of *Mycobacterium tuberculosis* within macrophages. *Infect. Immun.* 59, 1755–1761.

Chandra, P., Ghanwat, S., Matta, S. K., Yadav, S. S., et al. (2015). *Mycobacterium tuberculosis* inhibits RAB7 recruitment to selectively modulate autophagy flux in macrophages. *Sci. Rep*. 5:16320. doi: 10.1038/srep16320

Chen, C., Liu, Y., Liu, Y., and Zheng, P. (2009). mTOR regulation and therapeutic rejuvenation of aging hematopoietic stem cells. *Sci. Signal*. 2:ra75. doi: 10.1126/scisignal.2000559

Choy, A., Dancourt, J., Mugo, B., O'Connor, T. J., Isberg, R. R., Melia, T. J., et al. (2012). The Legionella effector RavZ inhibits host autophagy through irreversible Atg8 deconjugation. *Science* 338, 1072–1076. doi: 10.1126/science.1227026

Cooper, A. M. (2009). Cell-mediated immune responses in tuberculosis. *Annu. Rev. Immunol.* 27, 393–422. doi: 10.1146/annurev.immunol.021908.132703

Di Cosimo, S., Sathyanarayanan, S., Bendell, J. C., Cervantes, A., Stein, M. N., Braña, I., et al. (2015). Combination of the mTOR inhibitor ridaforolimus and the anti-IGF1R monoclonal antibody dalotuzumab: preclinical characterization and phase I clinical trial. *Clin. Cancer Res.* 21, 49–59. doi: 10.1158/1078-0432.CCR-14-0940

Dibble, C. C., and Cantley, L. C. (2015). Regulation of mTORC1 by PI3K signaling. *Trends Cell Biol.* 25, 545–555. doi: 10.1016/j.tcb.2015.06.002

Egan, D. F., Shackelford, D. B., Mihaylova, M. M., Gelino, S., Kohnz, R. A., Mair, W., et al. (2011). Phosphorylation of ULK1 (hATG1) by AMP-activated protein kinase connects energy sensing to mitophagy. *Science* 331, 456–461. doi: 10.1126/science.1196371

Ehrt, S., and Schnappinger, D. (2009). Mycobacterial survival strategies in the phagosome: defence against stresses. *Cell. Microbiol.* 11, 1170–1178. doi: 10.1111/j.1462-5822.2009.01335.x

Eisen, H. J., Tuzcu, E. M., Dorent, R., Kobashigawa, J., Mancini, D., Valantine-von Kaeppler, H. A., et al. (2003). Everolimus for the prevention of allograft rejection and vasculopathy in cardiac-transplant recipients. *N. Engl. J. Med.* 349, 847–858. doi: 10.1056/NEJMoa022171

Fijałkowska-Morawska, J. B., Jagodzinska, M., and Nowicki, M. (2011). Pulmonary embolism and reactivation of tuberculosis during everolimus therapy in a kidney transplant recipient. *Ann. Transplant.* 16, 107–110. doi: 10.12659/AOT.882226

Fingar, D. C., and Blenis, J. (2004). Target of rapamycin (TOR): an integrator of nutrient and growth factor signals and coordinator of cell growth and cell cycle progression. *Oncogene* 23, 3151–3171. doi: 10.1038/sj.onc.1207542

Floto, R. A., Sarkar, S., Perlstein, E. O., Kampmann, B., Schreiber, S. L., and Rubinsztein, D. C. (2007). Small molecule enhancers of rapamycin-induced TOR inhibition promote autophagy, reduce toxicity in Huntington's disease models and enhance killing of mycobacteria by macrophages. *Autophagy* 3, 620–622. doi: 10.4161/auto.4898

Flynn, J. L., and Chan, J. (2003). Immune evasion by *Mycobacterium tuberculosis*: living with the enemy. *Curr. Opin. Immunol.* 15, 450–455. doi: 10.1016/S0952-7915(03)00075-X

Fraunholz, M., and Sinha, B. (2012). Intracellular staphylococcus aureus: Live-in and let die. *Front. Cell. Inf. Microbiol.* 2:43. doi: 10.3389/fcimb.2012.00043

Gordon, P. B., Holen, I., Fosse, M., Røtnes, J. S., and Seglen, P. O. (1993). Dependence of hepatocytic autophagy on intracellularly sequestered calcium. *J. Biol. Chem.* 268, 26107–26112.

Grumati, P., Coletto, L., Sabatelli, P., Cescon, M., Angelin, A., Bertaggia, E., et al. (2010). Autophagy is defective in collagen VI muscular dystrophies, and its reactivation rescues myofiber degeneration. *Nat. Med.*. 16, 1313–1320. doi: 10.1038/nm.2247

Guenin-Macé, L., Siméone, R., and Demangel, C. (2009). Lipids of pathogenic Mycobacteria: contributions to virulence and host immune suppression. *Trans. Emerg. Dis.* 56, 255–268. doi: 10.1111/j.1865-1682.2009.01072.x

Guirado, E., Schlesinger, L. S., and Kaplan, G. (2013). Macrophages in tuberculosis: friend or foe. *Semin. Immunopathol.* 35, 563–583. doi: 10.1007/s00281-013-0388-2

Gutierrez, M. G., Master, S. S., Singh, S. B., Taylor, G. A., Colombo, M. I., and Deretic, V. (2004). Autophagy is a defense mechanism inhibiting BCG and *Mycobacterium tuberculosis* survival in infected macrophages. *Cell* 119, 753–766. doi: 10.1016/j.cell.2004.11.038

Harrison, D. E., Strong, R., Sharp, Z. D., et al. (2009). Rapamycin fed late in life extends lifespan in genetically heterogeneous mice. *Nature* 460, 392–395. doi: 10.1038/nature08221

Hidvegi, T., Ewing, M., Hale, P., Dippold, C., Beckett, C., Kemp, C., et al. (2010). An autophagy-enhancing drug promotes degradation of mutant α1-antitrypsin Z and reduces hepatic fibrosis. *Science* 329, 229–232. doi: 10.1126/science.1190354

Huang, J., Dibble, C. C., Matsuzaki, M., and Manning, B. D. (2008). The TSC1-TSC2 complex is required for proper activation of mTOR complex 2. *Mol. Cell. Biol.* 28, 4104–4115. doi: 10.1128/MCB.00289-08

Huang, Z., Wu, Y., Zhou, X., Qian, J., Zhu, W., Shu, Y., et al. (2015). Clinical efficacy of mTOR inhibitors in solid tumors: a systematic review. *Future Oncol.* 11, 1687–1699. doi: 10.2217/fon.15.70

Huffman, T. A., Mothe-Satney, I., and Lawrence, J. C. Jr. (2002). Insulin-stimulated phosphorylation of lipin mediated by the mammalian target of rapamycin. *Proc. Natl. Acad. Sci. U.S.A.* 99, 1047–1052. doi: 10.1073/pnas.022634399

Huynh, K. K., Eskelinen, E.-L., Scott, C. C., Malevanets, A., Saftig, P., and Grinstein, S. (2007). LAMP proteins are required for fusion of lysosomes with phagosomes. *EMBO J.* 26, 313–324. doi: 10.1038/sj.emboj.7601511

Inoki, K., Zhu, T., and Guan, K. L. (2003). TSC2 mediates cellular energy response to control cell growth and survival. *Cell* 115, 577–590. doi: 10.1016/S0092-8674(03)00929-2

Jagannath, C., Lindsey, D. R., Dhandayuthapani, S., Xu, Y., Hunter, R. L. Jr., and Eissa, N. T. (2009). Autophagy enhances the efficacy of BCG vaccine by increasing peptide presentation in mouse dendritic cells. *Nat. Med.* 15, 267–276. doi: 10.1038/nm.1928

Jayachandran, R., Sundaramurthy, V., Combaluzier, B., Mueller, P., Korf, H., Huygen, K., et al. (2007). Survival of mycobacteria in macrophages is mediated by coronin-1 dependent activation of calcineurin. *Cell* 130, 37–50. doi: 10.1016/j.cell.2007.04.043

Jung, C. H., Ro, S. H., Cao, J., Otto, N. M., and Kim, D. H. (2010). mTOR regulation of autophagy. *FEBS Lett.* 584, 1287–1295. doi: 10.1016/j.febslet.2010.01.017

Kim, D. H., Sarbassov, D. D., Ali, S. M., King, J. E., Latek, R. R., Erdjument-Bromage, H., et al. (2002). mTOR interacts with raptor to form a nutrient sensitive complex that signals to the cell growth machinery. *Cell* 110, 163–175. doi: 10.1016/S0092-8674(02)00808-5

Kim, J. E., and Chen, J. (2004). Regulation of peroxisome proliferator-activated receptor-gamma activity by mammalian target of rapamycin and amino acids in adipogenesis. *Diabetes* 53, 2748–2756. doi: 10.2337/diabetes.53.11.2748

Kim, J. J., Lee, H. M., Shin, D. M., Kim, W., Yuk, J. M., Jin, H. S., et al. (2012). Host cell autophagy activated by antibiotics is required for their effective antimycobacterial drug action. *Cell Host Microbe.* 11, 457–468. doi: 10.1016/j.chom.2012.03.008

Kim, J., Kundu, M., Viollet, B., and Guan, K. L. (2011). AMPK and mTOR regulate autophagy through direct phosphorylation of Ulk1. *Nat. Cell Biol.* 13, 132–141. doi: 10.1038/ncb2152

Koh, Y., Lim, H. Y., Ahn, J. M., Lee, J. L., Rha, S. Y., Kim, Y. J., et al. (2013). Phase II trial of everolimus for the treatment of nonclear-cell renal cell carcinoma. *Ann. Oncol.* 24, 1026–1031. doi: 10.1093/annonc/mds582

Kovarik, J. M., Hartmann, S., Figueiredo, J., Rouilly, M., Port, A., and Rordorf, C. (2002). Effect of rifampin on apparent clearance of everolimus. *Ann. Pharmacother.* 36, 981–985. doi: 10.1345/aph.1A384

Kusner, D. J., and Barton, J. A. (2001). ATP stimulates human macrophages to kill intracellular virulent *Mycobacterium tuberculosis* via calcium dependent phagosome-lysosome fusion. *J. Immunol.* 167, 3308–3315. doi: 10.4049/jimmunol.167.6.3308

Laplante, M., and Sabatini, D. M. (2009). mTOR signaling at a glance. *J. Cell. Sci.* 122(Pt 20), 3589–3594. doi: 10.1242/jcs.051011

Laplante, M., and Sabatini, D. M. (2012). mTOR signaling in growth control and disease. *Cell* 149, 274–293. doi: 10.1016/j.cell.2012.03.017

Laughner, E., Taghavi, P., Chiles, K., Mahon, P. C., and Semenza, G. L. (2001). HER2 (neu) signaling increases the rate of hypoxia-inducible factor 1α (HIF-1α) synthesis: novel mechanism for HIF-1-mediated vascular endothelial growth factor expression. *Mol. Cell. Biol.* 21, 3995–4004. doi: 10.1128/MCB.21.12.3995-4004.2001

Lerena, C., Calligaris, S. D., and Colombo, M. I. (2008). Autophagy: for better or for worse, in good times or in bad times. *Curr. Mol. Med.* 8, 92–101. doi: 10.2174/156652408783769634

Levine, B., and Deretic, V. (2007). Unveiling the roles of autophagy in innate and adaptive immunity. *Nat. Rev. Immunol.* 7, 767–777. doi: 10.1038/nri2161

Levine, B., Mizushima, N., and Virgin, H. W. (2011). Autophagy in immunity and inflammation. *Nature* 469, 323–335. doi: 10.1038/nature09782

Lingaraju, R., Blumenthal, N. P., Mendez, J., Hadjiliadis, O., Lee, J. C., Ahya, V. N., et al. (2010). Venous thromboembolic disease after lung transplantation: special focus on sirolimus. *Open. Transplant. J.* 4, 1–4. doi: 10.2174/1874418401004010001

Lipinski, M. M., Hoffman, G., Ng, A., Zhou, W., Py, B. F., Hsu, E., et al. (2010). A genome-wide siRNA screen reveals multiple mTORC1 independent signaling pathways regulating autophagy under normal nutritional conditions. *Dev. Cell* 18, 1041–1052. doi: 10.1016/j.devcel.2010.05.005

Macintyre, A. N., Gerriets, V. A., Nichols, A. G., Michalek, R. D., Rudolph, M. C., Deoliveira, D., et al. (2014). The glucose transporter Glut1 is selectively essential for CD4 T cell activation and effector function. *Cell Metab.* 20, 61–72. doi: 10.1016/j.cmet.2014.05.004

MacKeigan, J. P., and Krueger, D. A. (2015). Differentiating the mTOR inhibitors everolimus and sirolimus in the treatment of tuberous sclerosis complex. *Neuro-Oncology* 17, 1550–1559. doi: 10.1093/neuonc/nov152

Maiuri, M. C., Zalckvar, E., Kimchi, A., and Kroemer, G. (2007). Self-eating and self-killing: crosstalk between autophagy and apoptosis. *Nat. Rev. Mol. Cell Biol.* 8, 741–752. doi: 10.1038/nrm2239

Malizzia, L. J., and Hsu, A. (2008). Temsirolimus, an mTOR inhibitor for treatment of patients with advanced renal cell carcinoma. *Clin. J. Oncol. Nurs.* 12, 639–646. doi: 10.1188/08.CJON.639-646

Mannick, J. B., Del Giudice, D., Lattanzi, M., Valiante, N. M., Praestgaard, J., Huang, B., et al. (2014). mTOR inhibition improves immune function in the elderly. *Sci. Transl. Med.* 6:68ra179. doi: 10.1126/scitranslmed.3009892

Michael, O. S., Sogaolu, O. M., Fehintola, F. A., Ige, O. M., and Falade, C. O. (2016). Adverse events to first line anti-tuberculosis drugs in patients co-infected with HIV and tuberculosis. *Ann. Ib. Postgrad. Med.* 14, 21–29.

Mizushima, N., Yoshimori, T., Ohsumi, Y. (2011). The role of Atg proteins in autopha-gosome formation. *Annu. Rev. Cell Dev. Biol.* 27, 107–132. doi: 10.1146/annurev-cellbio-092910-154005

Ng, S., Wu, Y. T., Chen, B., Zhou, J., and Shen, H. M. (2011). Impaired autophagy due to constitutive mTOR activation sensitizes TSC2-null cells to cell death under stress. *Autophagy* 7, 1173–1186. doi: 10.4161/auto.7.10.16681

Noda, T., and Ohsumi, Y. (1998). Tor, a phosphatidylinositol kinase homologue, controls autophagy in yeast. *J. Biol. Chem.* 273, 3963–3966. doi: 10.1074/jbc.273.7.3963

Pagan, A. J., Levitte, S., Berg, R. D., Hernandez, L., Zimmerman, J., Tobin, D., et al. (2016). mTOR deficiency reveals an immunological trade-off in innate resistance to mycobacterial infection *in vivo*. *J. Immunol.* 196(1 Suppl.) 200.6.

Palavra, F., Robalo, C., and Reis, F. (2017). Recent advances and challenges of mTOR inhibitors use in the treatment of patients with tuberous sclerosis complex. *Oxid. Med. Cell. Longev.* 2017:9820181. doi: 10.1155/2017/9820181

Pan, H., O'Brien, T. F., Zhang, P., and Zhong, X. P. (2012). The role of tuberous sclerosis complex 1 in regulating innate immunity. *J. Immunol.* 188, 3658–3666. doi: 10.4049/jimmunol.1102187

Parkhitko, A., Myachina, F., Morrison, T. A., Hindi, K. M., Auricchio, N., Karbowniczek, M., et al. (2011). Tumorigenesis in tuberous sclerosis complex is autophagy and p62/sequestosome 1 (SQSTM1)-dependent. *Proc. Natl. Acad. Sci. U.S.A.* 108, 12455–12460. doi: 10.1073/pnas.1104361108

Pieters, J., and Gatfield, J. (2002). Hijacking the host: survival of pathogenic mycobacteria inside macrophages. *Trends Microbiol.* 10, 142–146. doi: 10.1016/S0966-842X(02)02305-3

Pohanka, E. (2006). Conversion to everolimus in maintenance patients - current clinical strategies. *Nephrol. Dial. Transplant.* 21(Suppl. 3), iii24–iii29. doi: 10.1093/ndt/gfl301

Porta, C., Osanto, S., Ravaud, A., Climent, M. A., Vaishampayan, U., White, D. A., et al. (2011). Management of adverse events associated with the use of everolimus in patients with advanced renal cell carcinoma. *Eur. J. Cancer* 47, 1287–1298. doi: 10.1016/j.ejca.2011.02.014

Rajaram, M. V., Brooks, M. N., Morris, J. D., Torrelles, J. B., Azad, A. K., and Schlesinger, L. S. (2010). *Mycobacterium tuberculosis* activates human macrophage peroxisome proliferator-activated receptor gamma linking mannose receptor recognition to regulation of immune responses. *J. Immunol.* 185, 929–942. doi: 10.4049/jimmunol.1000866

Rivera, V. M., Miller, S. D., Berk, L., Wardwell, S. D., Ning, Y., Pollock, R., et al. (2011). Ridaforolimus (AP23573; MK-8669), a potent mTOR inhibitor, has broad antitumor activity and can be optimally administered using intermittent dosing regimens. *Mol. Cancer Ther.* 10, 1059–1071. doi: 10.1158/1535-7163.MCT-10-0792

Rohde, K., Yates, R. M., Purdy, G. E., and Russell, D. G. (2007). *Mycobacterium tuberculosis* and the environment within the phagosome. *Immunol. Rev.* 219, 37–54. doi: 10.1111/j.1600-065X.2007.00547.x

Rojas, M., García, L. F., Nigou, J., Puzo, G., and Olivier, M. (2000). Mannosylated lipoarabinomannan antagonizes *Mycobacterium tuberculosis* induced macrophage apoptosis by altering Ca^{2+}-dependent cell signaling. *J. Infect. Dis.* 182, 240–251. doi: 10.1086/315676

Rubinsztein, D. C., Codogno, P., and Levine, B. (2012). Autophagy modulation as a potential therapeutic target for diverse diseases. *Nat. Rev. Drug Discov.* 11, 709–730. doi: 10.1038/nrd3802

Ryan, F. (1992). *The Forgotten Plague: How the Battle against Tuberculosis was Won and Lost*. Boston, MA: Little Brown.

Saran, U., Foti, M., and Dufour, J. F. (2015). Cellular and molecular effects of the mTOR inhibitor everolimus. *Clin. Sci.* 129, 895–914. doi: 10.1042/CS20150149

Sarkar, S., Floto, R. A., Berger, Z., Imarisio, S., Cordenier, A., Pasco, M., et al. (2005). Lithium induces autophagy by inhibiting inositol monophosphatase. *J. Cell Biol.* 170, 1101–1111. doi: 10.1083/jcb.200504035

Sarkar, S., Krishna, G., Imarisio, S., Saiki, S., O'Kane, C. J., and Rubinsztein, D. C. (2008). A rational mechanism for combination treatment of Huntington's disease using lithium and rapamycin. *Hum. Mol. Genet.* 17, 170–178. doi: 10.1093/hmg/ddm294

Seto, S., Tsujimura, K., Horii, T., and Koide, Y. (2013). Autophagy adaptor protein p62/SQSTM1 and autophagy-related gene Atg5 mediate autophagosome formation in response to *Mycobacterium tuberculosis* infection in dendritic cells. *PLoS ONE* 8:e86017. doi: 10.1371/journal.pone.0086017

Seto, S., Tsujimura, K., and Koideet, Y. (2012). Coronin-1a inhibits autophagosome formation around *Mycobacterium tuberculosis*-containing phago-somes and assists mycobacterial survival in macrophages. *Cell. Microbiol.* 14, 710–727. doi: 10.1111/j.1462-5822.2012.01754.x

Shang, L., Chen, S., Du, F., Li, S., Zhao, L., and Wang, X. (2011). Nutrient starvation elicits an acute autophagic response mediated by Ulk1 dephosphorylation and its subsequent dissociation from AMPK. *Proc. Natl. Acad. Sci. U.S.A.* 108, 4788–4793. doi: 10.1073/pnas.1100844108

Sharma, A., Hill, A., Kurbatova, E., van der Walt, M., Kvasnovsky, C., Tupasi, T. E., et al. (2017). Estimating the future burden of multidrug-resistant and extensively drug-resistant tuberculosis in India, the Philippines, Russia, and South Africa: a mathematical modelling study. *Lancet Infect. Dis.* 17, 707–715. doi: 10.1016/S1473-3099(17)30247-5

Shui, W., Petzold, C. J., Redding, A., Liu, J., Pitcher, A., Sheu, L., et al. (2011). Organelle membrane proteomics reveals differential influence of mycobacterial lipoglycans on macro-phage phagosome maturation and autophagosome accumulation. *J. Proteome Res.* 10, 339–348. doi: 10.1021/pr100688h

Singh, R., and Cuervo, A. M. (2012). Lipophagy: connecting autophagy and lipid metabolism. *Int. J. Cell Biol.* 2012:282041. doi: 10.1155/2012/282041

Songane, M., Kleinnijenhuis, J., Nete, M. G., and van Crevel, R. (2012). The role of autophagy in host defense against *Mycobacterium tuberculosis* infection. *Tuberculosis (Edinb.)* 92, 388–396. doi: 10.1016/j.tube.2012.05.004

Subbian, S., Tsenova, L., O'Brien, P., Yang, G., Koo, M. S., Peixoto, B., et al. (2011a). Phosphodiesterase-4 inhibition alters gene expression and improves isoniazid-mediated clearance of *Mycobacterium tuberculosis* in rabbit lungs. *PLoS Pathog.* 7:e1002262. doi: 10.1371/journal.ppat.1002262

Subbian, S., Tsenova, L., O'Brien, P., Yang, G., Koo, M. S., Peixoto, B., et al. (2011b). Phosphodiesterase-4 inhibition combined with isoniazid treatment of rabbits with pulmonary tuberculosis reduces macrophage activation and lung pathology. *Am. J. Pathol.* 179, 289–301. doi: 10.1016/j.ajpath.2011.03.039

Thurston, T. L. M., Ryzhakov, G., Bloor, S., von Muhlinen, N., and Randow, F. (2009). The TBK1 adaptor and autophagy receptor NDP52 restricts the proliferation of ubiquitin-coated bacteria. *Nat. Immunol.* 10, 1215–1221. doi: 10.1038/ni.1800

Tobin, D. M., Roca, F. J., Oh, S. F., McFarland, R., Vickery, T. W., Ray, J. P., et al. (2012). Host genotype-specific therapies can optimize the inflammatory response to mycobacterial infections. *Cell* 148, 434–446. doi: 10.1016/j.cell.2011.12.023

Vergne, I., Chua, J., and Deretic, V. (2003). Tuberculosis toxin blocking phagosome maturation inhibits a novel Ca^{2+}/calmodulin–PI3K hVPS34 cascade. *J. Exp. Med.* 198, 653–659. doi: 10.1084/jem.20030527

Vergne, I., Chua, J., Lee, H. H., Lucas, M., Belisle, J., and Deretic, V. (2005). Mechanism of phagolysosome biogenesis block by viable *Mycobacterium tuberculosis*. *Proc. Natl. Acad. Sci. U.S.A.* 102, 4033–4038. doi: 10.1073/pnas.0409716102

World Health Organization (2016). *Global Tuberculosis Report*. Geneva: World Health Organization.

Yoshikawa, Y., Ogawa, M., Hain, T., Yoshida, M., Fukumatsu, M., Kim, M., et al. (2009). *Listeria monocytogenes* ActA-mediated escape from autophagic recognition. *Nat. Cell Biol.* 11, 1233–1240. doi: 10.1038/ncb1967

Yu, H. B., Croxen, M. A., Marchiando, A. M., Ferreira, R. B., Cadwell, K., Foster, L. J., et al. (2014). Autophagy facilitates Salmonella replication in HeLa cells. *MBio* 5:e00865-14. doi: 10.1128/mBio.00865-14

Zeng, H., Cohen, S., Guy, C., Shrestha, S., Neale, G., Brown, S. A., et al. (2016). mTORC1 and mTORC2 kinase signaling and glucose metabolism drive follicular helper T cell differentiation. *Immunity* 45, 540–554. doi: 10.1016/j.immuni.2016.08.017

Zhang, X. X., Huang, T. Y., Wu, Y., Peng, W. G., Xie, H. B., et al. (2017). Inhibition of the PI3K-Akt-mTOR signaling pathway in T lymphocytes in patients with active tuberculosis. *Int. J. Infect. Dis.* 59, 110–117. doi: 10.1016/j.ijid.2017.04.004

Zheng, Y. T., Shahnazari, S., Brech, A., Lamark, T., Johansen, T., and Brumell, J. H. (2009). The adaptor protein p62/SQSTM1 targets invading bacteria to the autophagy pathway. *J. Immunol.* 183, 5909–5916. doi: 10.4049/jimmunol.0900441

Zumla, A., Maeurer, M., Chakaya, J., Hoelscher, M., Ntoumi, F., Rustomjee, R. et al. (2015). Towards host-directed therapies for tuberculosis. *Nat. Rev. Drug Discov.* 14, 511–512. doi: 10.1038/nrd4696

Conflict of Interest Statement: The authors declare that the research was conducted in the absence of any commercial or financial relationships that could be construed as a potential conflict of interest.

Copyright © 2018 Singh and Subbian. This is an open-access article distributed under the terms of the Creative Commons Attribution License (CC BY). The use, distribution or reproduction in other forums is permitted, provided the original author(s) and the copyright owner are credited and that the original publication in this journal is cited, in accordance with accepted academic practice. No use, distribution or reproduction is permitted which does not comply with these terms.

frontiers in Microbiology

ORIGINAL RESEARCH
published: 28 February 2018
doi: 10.3389/fmicb.2018.00326

Defeating Antibiotic- and Phage-Resistant *Enterococcus faecalis* Using a Phage Cocktail *in Vitro* and in a Clot Model

Leron Khalifa[1], Daniel Gelman[1], Mor Shlezinger[1,2], Axel Lionel Dessal[1], Shunit Coppenhagen-Glazer[1], Nurit Beyth[1,2†] and Ronen Hazan[1†]*

[1] Faculty of Dental Sciences, Hadassah School of Dental Medicine, Hebrew University of Jerusalem, Jerusalem, Israel,
[2] Department of Prosthodontics, Hadassah School of Dental Medicine, Hebrew University of Jerusalem, Jerusalem, Israel

OPEN ACCESS

Edited by:
Rebecca Thombre,
Savitribai Phule Pune University, India

Reviewed by:
Andrei A. Zimin,
Institute of Biochemistry and Physiology of Microorganisms (RAS), Russia
Stephen Tobias Abedon,
The Ohio State University, United States

***Correspondence:**
Ronen Hazan
ronenh@ekmd.huji.ac.il

† These authors have contributed equally to this work.

Specialty section:
This article was submitted to Antimicrobials, Resistance and Chemotherapy, a section of the journal Frontiers in Microbiology

Received: 08 June 2017
Accepted: 12 February 2018
Published: 28 February 2018

Citation:
Khalifa L, Gelman D, Shlezinger M, Dessal AL, Coppenhagen-Glazer S, Beyth N and Hazan R (2018) Defeating Antibiotic- and Phage-Resistant Enterococcus faecalis Using a Phage Cocktail in Vitro and in a Clot Model. Front. Microbiol. 9:326. doi: 10.3389/fmicb.2018.00326

The deteriorating effectiveness of antibiotics is propelling researchers worldwide towards alternative techniques such as phage therapy: curing infectious diseases using viruses of bacteria called bacteriophages. In a previous paper, we isolated phage EFDG1, highly effective against both planktonic and biofilm cultures of one of the most challenging pathogenic species, the vancomycin-resistant *Enterococcus* (VRE). Thus, it is a promising phage to be used in phage therapy. Further experimentation revealed the emergence of a mutant resistant to EFDG1 phage: EFDG1^r. This kind of spontaneous resistance to antibiotics would be disastrous occurrence, however for phage-therapy it is only a minor hindrance. We quickly and successfully isolated a new phage, EFLK1, which proved effective against both the resistant mutant EFDG1^r and its parental VRE, *Enterococcus faecalis* V583. Furthermore, combining both phages in a cocktail produced an additive effect against *E. faecalis* V583 strains regardless of their antibiotic or phage-resistance profile. An analysis of the differences in genome sequence, genes, mutations, and *tRNA* content of both phages is presented. This work is a proof-of-concept of one of the most significant advantages of phage therapy, namely the ability to easily overcome emerging resistant bacteria.

Keywords: bacteriophages, *Enterococcus faecalis*, antibiotic-resistance, phage therapy, phage-resistance, phage cocktail

INTRODUCTION

In 1967, William H. Stewart, the Surgeon General, said in the White House: "It's time to close the books on infectious diseases, declare the war against pestilence won. . .," expressing the general opinion, at the time, that antibiotics succeeded in solving all bacteria-related problems. Ironically, this very success has proved dangerous, as the frequent reliance on antibiotics has resulted in dissemination of resistant variants (Charles and Grayson, 2004; Davies and Davies, 2010).

One of the antibiotic – resistant, most frequently isolated species from hospital-associated infections, is vancomycin-resistant enterococci (VRE) (O'Driscoll and Crank, 2015; Khalifa et al., 2016). While mostly a commensal, when inhabiting the gastro-intestinal tract, Gram-positive *Enterococcus faecalis* bacterium can cause fatal infections (Rice, 2008; Orsi and Ciorba, 2013). In many cases, neither antibiotics (Erlandson et al., 2008; Chong et al., 2010) nor other antibacterial means like endodontic treatments and rinsing with calcium hydroxide, sodium hypochlorite,

and chlorohexidine (Khalifa et al., 2016) have successfully prevented the morbidity or mortality resulting from *Enterococcus* infections especially in cases of biofilm (Donlan, 2001; de la Fuente-Nunez et al., 2013). The hazardous potential of these bacteria is exacerbated by the emergence of antibiotic-resistant strains, primarily VRE (Linden, 2002). So much so, that in 2013 the Center for Disease Control and Prevention (CDC) has declared VRE *enterococci* to be one amongst the top 18 drug-resistant threats to treat today[1].

With the limitations of chemical antibiotics and the emergence of antibiotic-resistant strains, the use of bacteriophages has been regaining interest (Golkar et al., 2014). Their effective potential is magnified as they are highly strain-specific, targeting only their pathogen and tend to only minimally disrupt normal flora (Loc-Carrillo and Abedon, 2011). Moreover, bacteriophages have evolved naturally to be become the most proficient bacterial killers (Srinivasiah et al., 2008) in all forms, including hard-to-eradicate biofilms (Donlan, 2009; Khalifa et al., 2016). Use of bacteriophages has numerous other advantages over antibiotics (Loc-Carrillo and Abedon, 2011; Khalifa et al., 2016), including ease of isolation. Additionally, recent human and animal trials have shown that phages are safe for use (Burrowes et al., 2011).

We recently demonstrated the treatment potential of phages against vancomycin-resistant *E. faecalis* infections. EFDG1, an anti-*E. faecalis* phage, was isolated from sewage and its genome was characterized. This phage proved highly effective against *E. faecalis* V583 in planktonic and biofilm cultures *in vitro* and in an *ex vivo* human root canal model (Khalifa et al., 2015a).

Successful though phage therapy may be, bacterial cells resistant to phages will no doubt emerge, just as in the case of antibiotics (Duerkop et al., 2016), as indeed has occurred in our case too. However, in contrast to the grave challenges facing antibiotics, phage therapy offers several simple approaches to combat phage-resistant bacteria. One strategy would be to isolate new phages and to use them in cocktails. Based on the number of previously isolated phages and phage sequences in microbiomes, it is estimated that a bacterial strain may have as many as several 100 phages capable of combating it Khalifa et al. (2016). A second approach is to improve current phages by random or directed mutagenesis: using UV radiation (Drake, 1966) or gamma rays (Bertram, 1988), by means of chemical mutagens such as methyl methanesulfonate (MMS) (Drake, 1982) or through genetic engineering (Kiro et al., 2014; Pires et al., 2016). In any case, multiple-phage cocktails are preferable to single-phage therapy, as they are better equipped to deal with phage-resistant bacterial mutants and multispecies bacterial cultures (polyphage therapy) (Chan and Abedon, 2012; Gu et al., 2012; Ormala and Jalasvuori, 2013).

In the current article, we demonstrate the first approach: isolating a new phage against phage-resistant bacteria, constructing a phage cocktail and then utilizing it successfully against both naïve and phage-resistant mutant strains in *in vitro* models. The phage EFLK1 was effective against the EFDG1 phage-resistant *E. faecalis* strain (EFDG1^r). Moreover, a cocktail of EFDG1 and EFLK1 phages had an additive effect on planktonic and biofilm cultures.

[1]https://www.cdc.gov/drugresistance/biggest_threats.html

MATERIALS AND METHODS

Emergence and Isolation of Phage-Resistant Bacteria

Following all experiments of EFV583 with phage, survivors were routinely tested for resistance to the phage. The survivors were plated and the resulting single colonies were collected and grown. The bacteria were then tested for susceptibility to the phage, by either spotting phages on them or by cross streak agar assay. For the spotting method, about 100–200 μl of bacterial culture was spread uniformly on a BHI agar plate and once it dried; 10 μl spots of phages were spotted, which was done in duplicates or triplicates. While the cross streak agar assays were performed by horizontally streaking the phage lysate in the middle of the plate and then vertically streaking the bacterial colonies over the phage in unidirectional streaks (Moore, 2011; Tiruvadi Krishnan et al., 2015).

Bacterial colonies that grew in presence of phage were considered to exhibit resistance to the phage. These colonies were then collected and grown at 37°C and checked numerous times for their resistant characteristics against the phage. Once their resistant property was confirmed, these bacteria were frozen with 25% glycerol at −80°C and store for future use.

Bacterial Strains and Materials

Enterococcus faecalis V583 (ATCC 700802) VRE and EFDG1^r, EFDG1 phage-resistant bacterial strain were grown in brain heart infusion (BHI) broth (Difco, Detroit, MI, United States) aerobically in an incubator shaker with shaking at 220 RPM at 37°C. BHI agar (1.5%) was used for isolation streaks and isolations of phage. For top agar, 0.6% of agar (soft agar) was used, with BHI as nutrient supplement.

Isolation and Storage of Phage

In order to combat the phage-resistant mutant strain, a new lytic phage was isolated from the sewage effluents collected from the "Nahal Sorek" decontamination facility located in West Jerusalem, as described previously (Khalifa et al., 2015a). The effluents were centrifuged using a 5430R centrifuge, and a fixed angle rotorFA-45-24-11HS; Eppendorf at 10,000 × *g* for 10 min, to pellet out the debris. The supernatant was filtered twice, initially through 0.45-μm-pore-size filters (Merck Millipore, Ltd., Ireland) to filter out larger particles and then through 0.22-μm-pore-size filters (Merck Millipore) to achieve lysate free from any residues. Different concentrations of the filtrates (between 0.1 and 1 ml) were then added to bacterial broth culture diluted 1:1000 in BHI. Once lysis was obtained, the lysate was centrifuged and filtered using the aforementioned method.

The phage lysate was then applied on bacterial lawn by the method of double layer agar to obtain clear plaques that

symbolize the presence of phages. About 100 µl of bacteria was mixed with 100 µl of phage lysate and incubated for 20 min at 37°C to achieve better adsorption of the phage to the bacteria. The entire mixture was then added to 5 ml of melted 0.6% BHI top agar, poured evenly onto a BHI agar plate and incubated overnight at 37°C. The resultant single plaques were collected and added to 1 ml BHI and incubated at 4°C for diffusion. The liquid was centrifuged at 5000 RPM for 10 min and filtered through 0.22-µm-pore-size filters to obtain a clear phage lysate that was further used to grow large quantities of the phage. The phage was grown in BHI broth with EFV583 bacteria until a titer of 10^9 or higher was achieved. The phage titer of the phage lysate was determined by counting the Plaque forming units per ml (PFU/ml). For this; the phage lysate was serially diluted in BHI broth and 5 µl of these dilutions were spotted onto an overlayer of molten 0.6% agarose with 100 µl of bacteria. This plate was incubated overnight at 37°C and the numbers of plaques were counted to finally calculate the PFU/ml. A large volume of EFLK1 phage lysate with a high titer (10^{10}) was prepared and stored at 4°C.

Characterization of Phage Activity against *E. faecalis* Naïve and Phage-Resistant Form in Planktonic and Biofilm Cultures

To assess the phage effectiveness against planktonic bacteria, the growth kinetics were analyzed using a 96 well plate reader. The phage was added initially to both logarithmic cultures (10^4 to 10^5 CFU/ml) at MOI of 100–1000 (10^8 PFU/ml) and stationary cultures (10^8 to 10^9 CFU/ml) of *E. faecalis* at MOI of 0.1–1 (10^8 PFU/ml). Cell viability was also checked by determining CFU/ml for each well.

The biofilm eradication efficiency of the phage was tested by adding it in a MOI of 0.1 (10^8 PFU/ml) to a 2-week old stationary biofilm of *E. faecalis*. To obtain a 2-week old biofilm, overnight grown bacteria were diluted with BHI to obtain 10^4 to 10^5 CFU/ml of bacteria, which were then plated in a 96-well plate that was incubated for 2 weeks without any change of media or addition of new bacteria. Killing efficacy was validated using viable cell counting by calculating the CFU/ml of the biofilm as described previously (Khalifa et al., 2015a). Briefly, aspirated spent media was removed from the wells followed by washing the wells twice with sterile PBS (100 ul) carefully to not disrupt the biofilm. Sterile PBS (100 ul) was added and the biofilm was scraped and collected. The cells were sonicated in a water-bath for 5–10 min followed by several dilutions (1:10) and plating on BHI plates for CFU count.

One Step Growth

We based our protocol on the one step growth method of Ellis and Delbrück (Ellis and Delbrück, 1939). Briefly, phages were added to stationary-phase bacteria (10^9 CFU/ml) in a final concentration of 1×10^7 PFU/ml followed by incubation in 37°C for 10 min. The samples were diluted at a ratio of $1{:}10^4$ in fresh BHI medium, followed again by incubation at 37°C for 10 more minutes. Starting at 20 min after the introduction of the bacteriophages to the bacterial cultures, the diluted mixtures were enumerated through a double-layered agar plaque assay. To this end, 3 ml of Soft BHI Agar (0.6% Agar) were mixed with 100 µL of the diluted mixture and with 100 µL of stationary-phase bacteria, according to the tested bacterial strain. The plaque assays were conducted in the following time points after the introduction of the bacteriophages: 20, 35, 50, 60, 70, 85, 100, 120 min, in biological duplicates. Latent time and burst size were calculated from this growth curve for each of the bacteriophages described, with each of the bacterial hosts.

Genome Sequencing

To verify that the phage is indeed new, its DNA was isolated using the Norgen Biotek Phage DNA Isolation Kit (Cat. # 46800) and the resulting genome was sequenced and analyzed (Khalifa et al., 2015a,b). Analysis and comparison to other *E. faecalis* phages was performed using the GENIOUS 10.0.6 software and its plugins[2]. Annotation of genes was carried out using PHAST[3].

TEM Visualization

To observe the structure of the isolated phage accurately transmission electron microscopy (TEM) by the classic method of Gill as described in OpenWetWare[4], was conducted following the procedure mention in our previous paper (Khalifa et al., 2015a). Briefly, 1 ml of phage lysate with 10^9 PFU/ml was centrifuged at 19,283 × *g* (centrifuge 5430R, rotor FA-45-24-11HS; Eppendorf) for 2 h at room temperature. The supernatant was discarded, and the pellet was resuspended in 200 µl of 5 mM $MgSO_4$ and incubated overnight at 4°C. 30 µl of 5 mM $MgSO_4$ and 10 µl of the phage sample were mixed gently on a parafilm strip and 30 µl of 2% uranyl acetate was pipetted on it. On these drops of phage samples grids were then placed carefully using forceps, with the carbon side facing down. After about a minute the grids were dried and stored in the desiccator until further use. A TEM (Joel, TEM 1400 plus) with a charge-coupled device camera (Gatan Orius 600) was used to capture images.

Naïve and Resistant Bacterial Mixture

The naïve and resistant *E. faecalis* were mixed in 1:1 ratio (v/v) and the efficacy of phages was checked individually and in cocktail against them. The experiment mirrored the one described above (see section "Characterization of Phage Activity against *E. faecalis* Naïve and Phage-Resistant Form in Planktonic and Biofilm Cultures") for assessing phage activity on planktonic bacteria and on biofilm.

In Vitro Fibrin Clot Model

The *in vitro* fibrin clot model was prepared according to the protocol described by McGrath et al. (1994) and Entenza et al. (2009). Overnight cultures (10^9 CFU/ml) of *E. faecalis* individually or in a mixed cultures of naïve and resistant bacteria were diluted 1:10 with citrated plasma. Clots were formed by triggering coagulation by adding 20 µl bovine thrombin

[2]https://www.geneious.com

[3]http://www.phantome.org

[4]http://openwetware.org/wiki/Gill:Preparing_phage_specimens_for_TEM

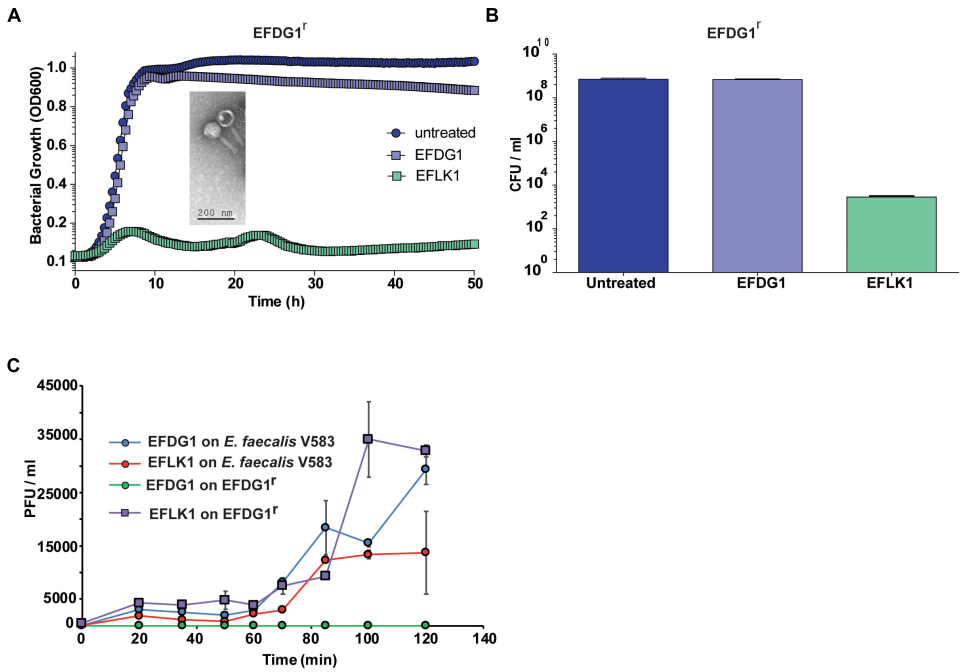

FIGURE 1 | Emergence of phage-resistant bacteria, EFDG1^r. The growth curve and CFU/ml values of EFDG1^r bacteria treated with EFDG1 phage resemble the untreated version of the same. Phage EFLK1 exhibited efficient lysis effect on the bacteria. **(A)** Logarithmic phase EFDG1^r bacteria without phage action (untreated) and with phages EFDG1 and EFLK1. The image inside the graph shows transmission electron microscopy (TEM) visualization image of the phage. **(B)** Colony counts revealing the CFU/ml of untreated and treated EFDG1^r bacteria after phage treatment. **(C)** One step growth curve of phages growing on and bacteria. Phages were added at 10^4 PFU/ml. One-step growth curve of EFDG1 and EFLK1 on *Enterococcus faecalis* V583 and EFDG1^r.

(5000 U/ml) and 20 μl $CaCl_2$ (50 mmol). The resultant clots were then re-suspended in 500 μl of bacteriophage lysate of 10^8 PFU/ml and for the control, 500 μl of BHI were added instead. The tubes were kept in an incubator-shaker for 6 h at 37°C. After incubation, the clots were washed with sterile PBS and lysed with 32 μl of 0.25% of Trypsin EDTA. After a 5-min centrifugation at 14,000 rpm, the cell pellet was re-suspended in 100 μl of PBS and used for calculating CFU/ml.

RESULTS

Emergence of the Phage-Resistant *E. faecalis* Mutant EFDG1^r and Isolation of EFLK1 Phage to Combat It

The lytic phage EFDG1 was isolated against vancomycin-resistant strains of *E. faecalis* V583 planktonic and biofilms cultures (Khalifa et al., 2015a). When strain EFDG1^r (resistant to EFDG1 phage) evolved during the experiments (**Figure 1A**), we screened various sewage effluent samples containing potential anti-*E. faecalis* phages. Within several weeks, a new lytic phage was isolated, EFLK1, from a sample collected from the sewage water of the "Nahal Sorek" decontamination facility. The new phage exhibited clear plaques on double-layered agar lawn of EFDG1^r. It also prevented the growth of EFDG1^r, as observed both in optical density growth curve (**Figure 1A**) and colony forming units (CFUs) count (**Figure 1B**). In agreement, a one-step growth experiment revealed that phage EFLK1 propagated on an EFDG1^r while EFDG1 phage did not (**Figure 1C**).

Phenotypic Differences Between EFDG1 and EFLK1 Phages

Despite the similarity between the two phages (32.187%), the efficiency and kinetics of EFLK1 phage infectivity against the parental strain V583 was distinct from that of EFDG1 phage. The lysis caused by EFDG1 phage during logarithmic growth was observed within 5 h (**Figure 1A**) and it reduced the viable cells number by four logs (**Figure 2A**) and (Khalifa et al., 2015a). In these conditions, EFLK1 phage was markedly slower; its lysis started after 12 h (**Figure 2A**) and it reduced cell viability by three logs (**Figure 2C**). In contrast, EFLK1 phage faired better against stationary cultures of V583 strain: EFLK1 phage lysis was observed after 10 h compared to much less significant lysis by EFDG1 phage (**Figure 2B**). These differences in lysis are reflected in the reduction of cell viability from 10^{11} to $\sim10^5$ by EFLK1 phage and only to $\sim10^8$ by EFDG1 phage (**Figure 2D**).

In Vitro Characterization of Combinatorial Cocktails of EFDG1 and EFLK1 Phages Aimed for Therapy

Since we aim to use EFDG1 and EFLK1 phages as therapeutic agents, we tested various combinations of phage cocktails,

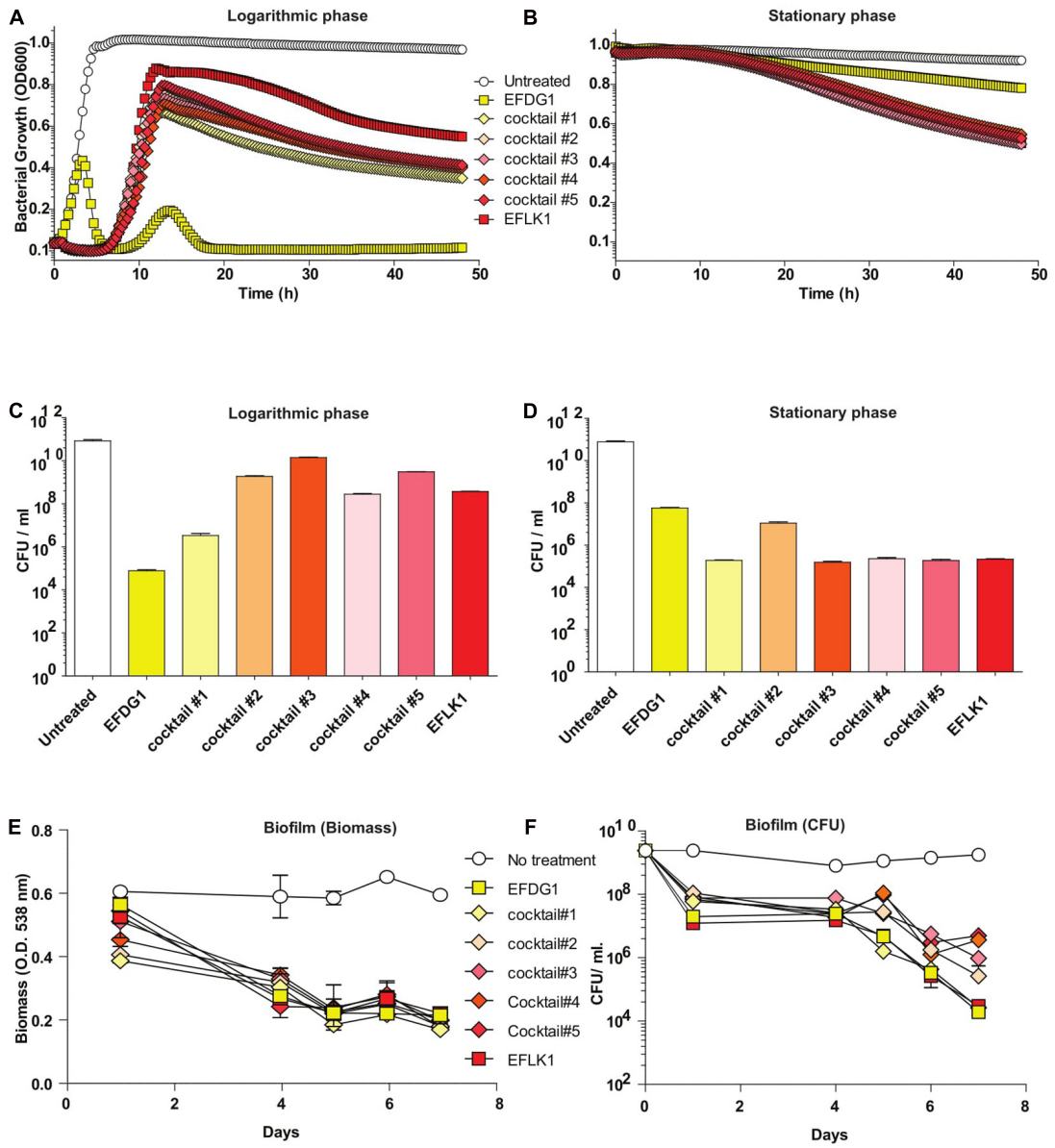

FIGURE 2 | Finding the most effective phage cocktail. **(A)** Logarithmic and **(B)** stationary phase *E. faecalis* V583 treated with EFDG1, EFLK1, and cocktails of these two phages in different ratios. Cocktail#1 (1:1), Cocktail#2 (1:2), Cocktail#3 (2:1), Cocktail#4 (1:3), and Cocktail#5 (3:1). Number of colony forming units per ml (CFU/ml) for logarithmic **(C)** and stationary phase **(D)** bacteria with and without treatment of the phages and their cocktails. **(E)** Biofilm biomass quantified by crystal violet staining of 2-weeks of *E. faecalis* V583 biofilm. **(F)** CFU/ml for phage treated and untreated 2-weeks old *E. faecalis* V583 biofilm.

initially on naïve *E. faecalis* V583. To this end, we combined EFDG1 and EFLK1 phages in various ratios: 1:1 (cocktail#1), 1:2 (cocktail#2), 2:1 (cocktail#3), 1:3 (cocktail#4), and 3:1 (cocktail#5) correspondingly (**Figure 2**). The best cocktail was found to be Cocktail#1 (1:1) as it killed the logarithmic culture of *E. faecalis* V583 as efficiently as EFDG1 phage (**Figures 2A–C**), and the stationary culture like EFLK1 phage (**Figures 2B–D**). Thus, cocktail#1 equaled the better phage in each case and outperformed the other cocktails against the challenging biofilm of *E. faecalis* V583 (**Figure 2E**).

When cocktail#1 was used against EFDG1^r mutants, it was found to be as effective as EFLK1 phage against logarithmic, stationary and biofilm cultures of the resistant mutants (**Figure 3**).

Finally, in order to simulate the evolution of resistant mutants within a culture, we mixed the WT *E. faecalis* V583 with its resistant mutant EFDG1^r and treated them with individual phages and cocktail #1, separately (**Figure 4**). We found that cocktail #1 and EFLK1 phage were effective against the bacterial mixture while EFDG1 phage was not.

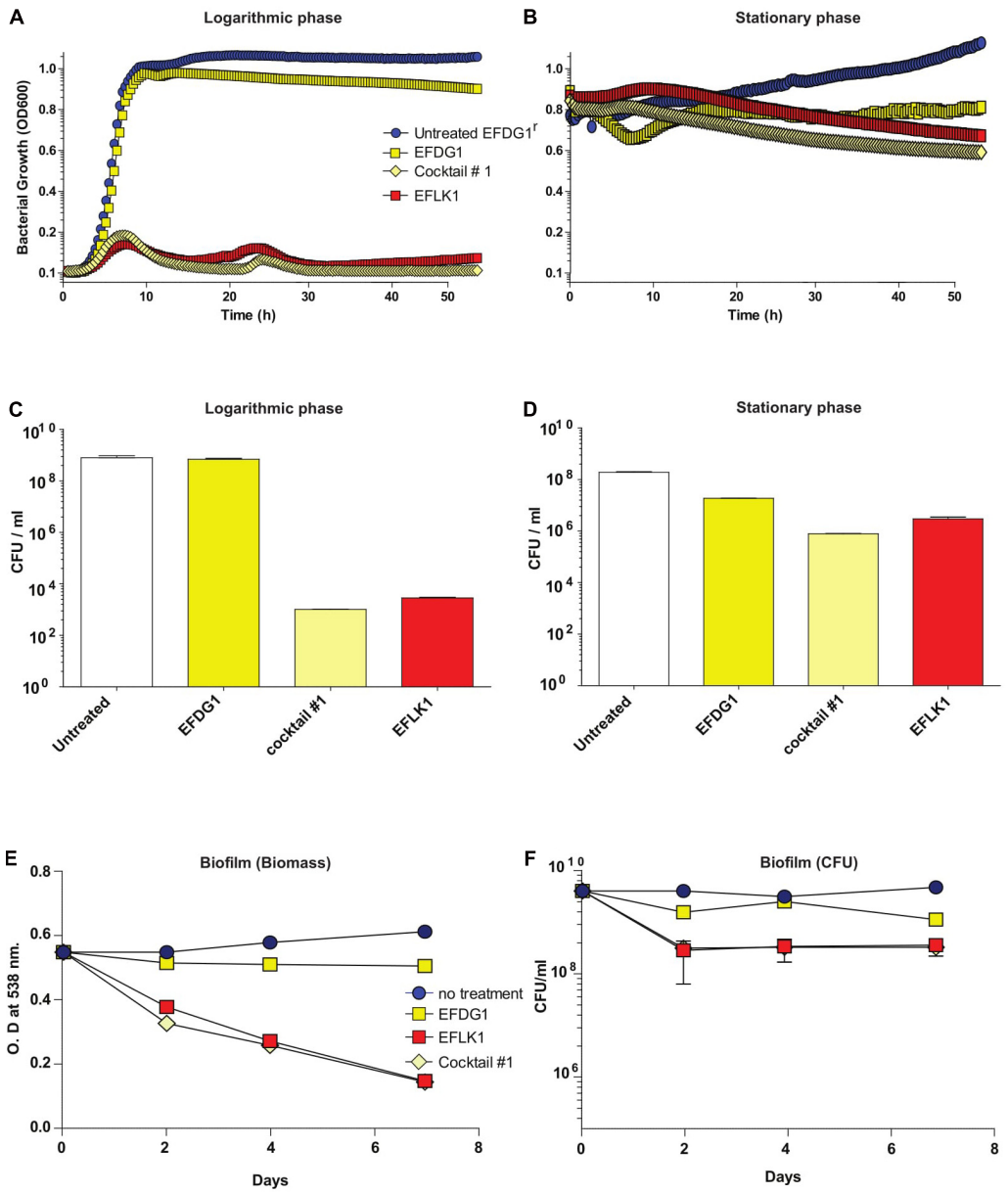

FIGURE 3 | Overcoming phage-resistance. **(A)** Logarithmic growth curve and their **(C)** CFU/ml along with **(B)** stationary growth curve and their **(D)** CFU/ml values depicting the lysis effect of EFLK1 phage and phage cocktail#1 (EFDG1:EFLK1 1:1) on EFDG1^r bacteria, whereas EFDG1 phage has no effect at all. Similarly, reduction is seen in the biofilm biomass **(E)** and the colony count **(F)** of a 2 week old biofilm of EFDG1^r bacteria only when treated with EFLK1 phage or phage cocktail#1.

Demonstrating Phage Efficacy in a Fibrin Clot Model

A recognized tool for the study of bacterial endocarditis (Hershberger et al., 2000), we used the *in vitro* fibrin-clot infection model (McGrath et al., 1994; Entenza et al., 2009) to assess the efficacy of the cocktail and the individual phages EFDG1 and EFLK1 against *E. faecalis* V583 and EFDG1^r (**Figure 5**). CFU/ml results following a 6-h incubation of *E. faecalis* V583 with EFLK1 phage and cocktail#1 showed a CFU reduction of three logs with EFDG1 phage and six logs with EFLK1 phage and cocktail#1. EFLK1 phage and the cocktail also reduced the CFU by five and six logs respectively, against EFDG1^r, while, EFDG1 phage failed as expected.

Genotypic Differences between EFDG1 and EFLK1 Phages

To explain the phenotypic differences between EFLK1 and EFDG1 phages, their genomes were compared (Khalifa et al., 2015a). In addition to EFLK1 phage, three additional *E. faecalis* phages of the Spounavirinae subfamily of the Myoviridae phage

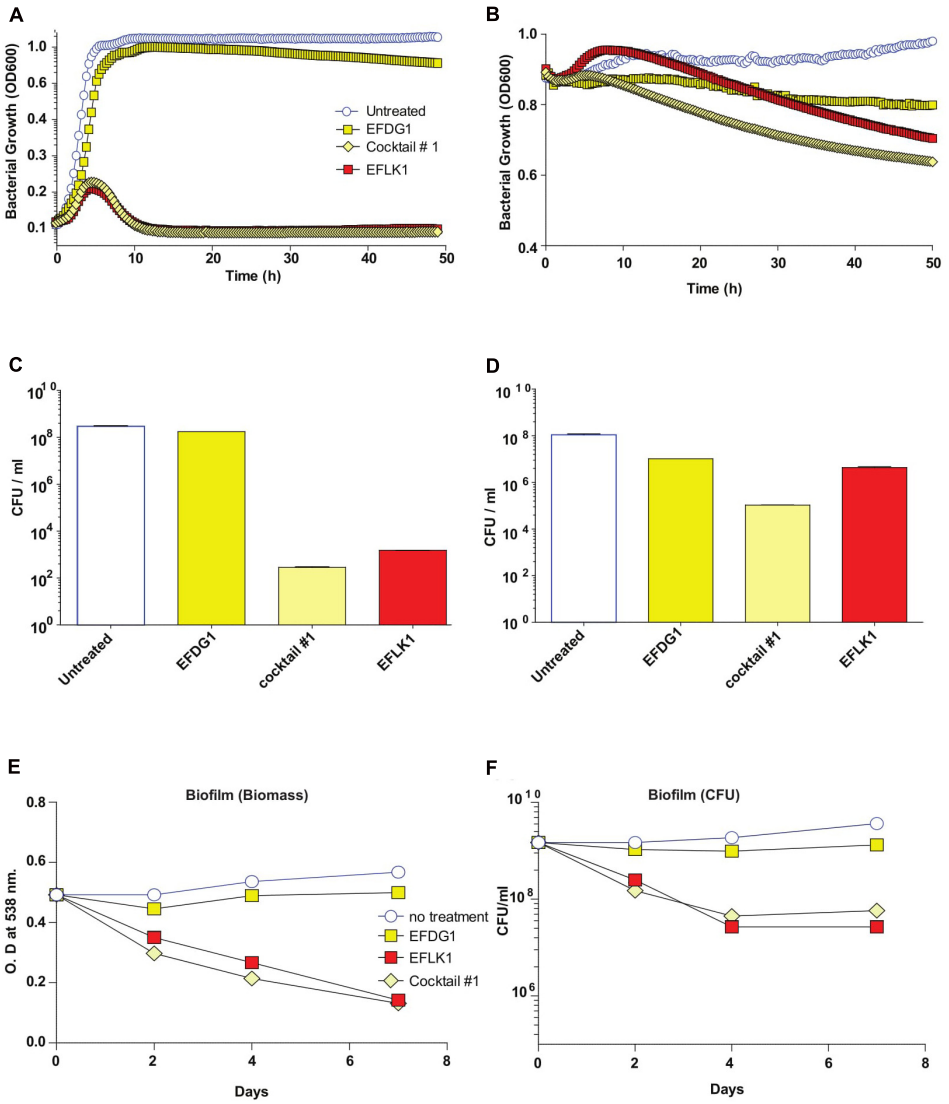

FIGURE 4 | Mixed bacterial population and Phage Cocktails. Similar to EFDG1^r bacteria; when the naïve *E. faecalis* V583 and mutant EFDG1^r are mixed in equal concentrations to get a mixed population; the growth curve **(A)** for logarithmic and **(B)** for stationary phase bacterial mixtures and their CFU/ml count counterparts **(C)** and **(D)** logarithmic and stationary respectively show desirable lysis by EFLK1 phage and its 1:1 phage cocktail. While EFDG1 phage has no significant effect in either case. **(E)** Crystal violet staining reveals a reduction in biofilm biomass and **(F)** CFU/ml also shows reduction in bacterial counts when treated with EFLK1 phage and phage cocktail.

family of lytic phages (Lavigne et al., 2009), were described. The highest resemblance (∼45%) was found with EFDG1 phage, previously isolated by us (Khalifa et al., 2015a), and less with the other two phages phiEF24c and ECP3 (**Figures 6A–C**). All four phages share 60 core genes which are ∼28% of their genes (**Figure 6A**).

The most significant difference between EFDG1 and EFLK1 phages genome sequences found was the number of *tRNA* genes (**Figure 6D**): EFDG1 phage contains 24 of them, EFLK1 phage carries none and the other two phages (phiEF24c and ECP3) contain five each which are all clustered in one region as in EFDG1 phage (**Figure 6D**). An analysis of the distribution of *tRNA* genes among all 2,053 fully sequenced tailed phages (NCBI, Caudovirales, taxid: 28883) revealed that nearly 60% (1,227) lacked *tRNA* genes as well (**Figure 6D**). Of the remainder, the majority carried only 1–5 genes, just like ECP3 and phiEF24c (**Figure 6D**). The highest number of *tRNA* genes (33) was found in the *Streptomyces* phage Jay2Jay (accession: KM652554.1). The cassette of five *tRNA*s in phiEF24c is identical to that in ECP3. EFDG1 phage contains the same five *tRNAs* and 19 more, all in a different order. Blast of these cassettes shows that they are unique and do not correspond to the ones on the *E. faecalis* genome.

One explanation for the presence of *tRNA* genes in phages is variance in codon usage between their own genome and that of the host. Consequently, one would expect EFDG1 phage codon usage to correlate less with that of its *E. faecalis* host than

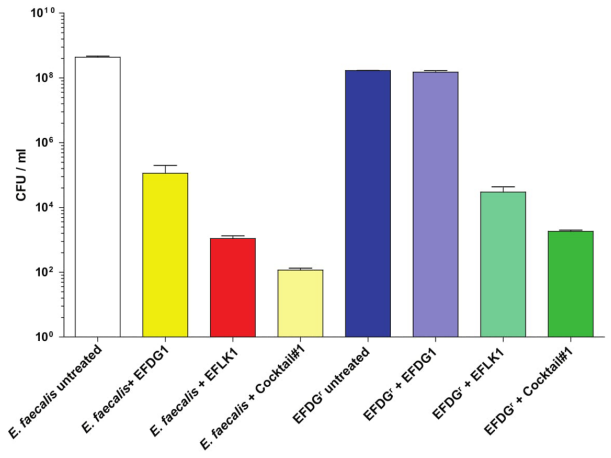

FIGURE 5 | *In vitro* fibrin clot model. The inset picture shows the clot model with phage (right) and without any phage treatment (left). The clot untreated by phage disintegrates due to the presence of *EFV583* bacteria while the treated clot is intact. The number of bacterial colonies in the clot before and after phage treatment were counted and CFU/ml was calculated for each sample after clot degradation.

the codon usage of the other phages and the large amount of *tRNAs* to compensate for that extra bias. However, COR function (R Bioconductor package) analysis disproved this theory, as no significant differences were found between the codon usage of the phages and *E. faecalis*. EFDG1 has 0.921 ECP3; 0.89522, EFLK1; 0.8954, and phiEF24c share 0.8948 correlation with the *E. faecalis* codon usage (**Supplementary Table S1**).

Next, we looked at the specific *tRNA* genes carried by these phages in accordance with their codon usage (**Supplementary Table S1**). The three anti-*E. faecalis* Spounavirinae phages with *tRNA's* (EFDG1, ECP3, and phiEF24c) carry *tRNA* genes corresponding to codons CTA, AGA, GAC, and TGG of leucine, arginine, aspartic acid, and tryptophan respectively. Besides these, EFDG1 phage encodes for two while ECP and phiEF24c phages for single *tRNA* corresponding to the initiation and sole methionine codon AUG. Indeed, in the three phages, the usage of all these codons is higher than their usage in *E. faecalis* (**Supplementary Table S1**), perhaps justifying the corresponding *tRNA* gene's existence. Surprisingly, the codon usage of these five codons is also higher in EFLK1 phage, which does not have any *tRNA* genes (**Supplementary Table S1**). Moreover, the codon usage should lead the four phages to carry the *tRNA* gene corresponding to codon TAC (tyrosine) while EFLK1, ECP3, and phiEF24c phages should carry *tRNA's* for AAG (lysine), AAC (asparagine), ACA (threonine) and GTA (valine) like EFDG1 phage, however this is not the case. On the other hand, EFDG1 phage carries several *tRNA* genes, such as TTA (leucine) which, according to the codon usage, seems to be not required. Thus, the question of the effect of codon usage on the presence of these *tRNA* and its relation to the phenotypic differences remains open.

We also analyzed the P2 mutation described by Uchiyama et al. (2011) in phage phiEF24c. The P2 mutation, located in Orf31, a conserved putative tail fiber, dramatically improves the ability of phiEF24c to adsorb and lyse the cells (Uchiyama et al., 2011). Nevertheless, EFDG1, EFLK1, and ECP3 phages harbor homologs for Orf31 but none of them has the P2 mutant allele (**Figure 6E**).

DISCUSSION

Phage therapy holds the promise of succeeding where antibiotics have failed against resistant bacteria. In some cases, phage resistance actually has led to loss of bacterial virulence (Scott et al., 2007; Zahid et al., 2008; Capparelli et al., 2010). In addition, while production of new antibiotics is slowing down (Silver, 2011; Laxminarayan et al., 2013), the rate of new phages isolation is increasing and new phages are being discovered daily as can be seen in phage databases such as the European Nucleotide Archive (ENA[5]). It is speculated that phages are the most prevalent replicating form on Earth and their number is estimated to be $\sim 10^{31}$, which is about 10 times more than prokaryotes (Diaz-Munoz and Koskella, 2014). Thus, in case of resistance, the likelihood of isolating an appropriate phage is indeed high. Furthermore, the variety of phages supports the construction of an almost unlimited number of combinations of cocktails to combat various strains or multispecies infections.

In this work, we demonstrated the isolation of a new phage when facing phage-resistant mutants and the advantages of a two-phage cocktail against VRE *E. faecalis* and its phage-resistant mutant.

Although similar, phages EFDG1 (Khalifa et al., 2015a) and EFLK1 have interesting phenotypic differences. While EFDG1 phage is more efficient against logarithmic *E. faecalis* V583 cultures, EFLK1 phage is a better killer of stationary (**Figure 2**). Joined in cocktail, they are even better at killing the bacteria than individually. Additionally, where EFDG1 phage failed to kill EFDG1^r, EFLK1 phage and the cocktail were effective against the WT and the phage-resistant mutant alone or in a mixed culture. This simulates the evolution of such mutants. We found the 1:1-ratio phage cocktail to be most effective, but we expect that ratios will vary and should therefore be determined on a case by case basis.

The reason for the phenotypic differences between EFDG1 and EFLK1 phages remains shrouded. One significant feature is the presence of 24 *tRNA* genes in EFDG1 phage, and their absence in EFLK1 phage. Theoretically, phages effective in the logarithmic stage (EFDG1), which benefits from elevated levels of host *tRNA*, should conceivably need to encode a small number of *tRNA* genes while phages effective in the stationary phage (EFLK1) should conceivably need a greater number. However, our findings indicated the opposite. The logarithmic efficient EFDG1 phage has more *tRNA* than the stationary efficient EFLK1 phage. Furthermore, the phages exhibited similar codon usage. In addition, the *tRNA* genes of EFDG1, ECP3, and phiEF24c phages are all encoded in a conserved region which is absent from EFLK1's genome. This suggests that the *tRNA*'s are required for the efficient translation of the proteins encoded in that region.

[5]http://www.ebi.ac.uk/genomes/phage.html

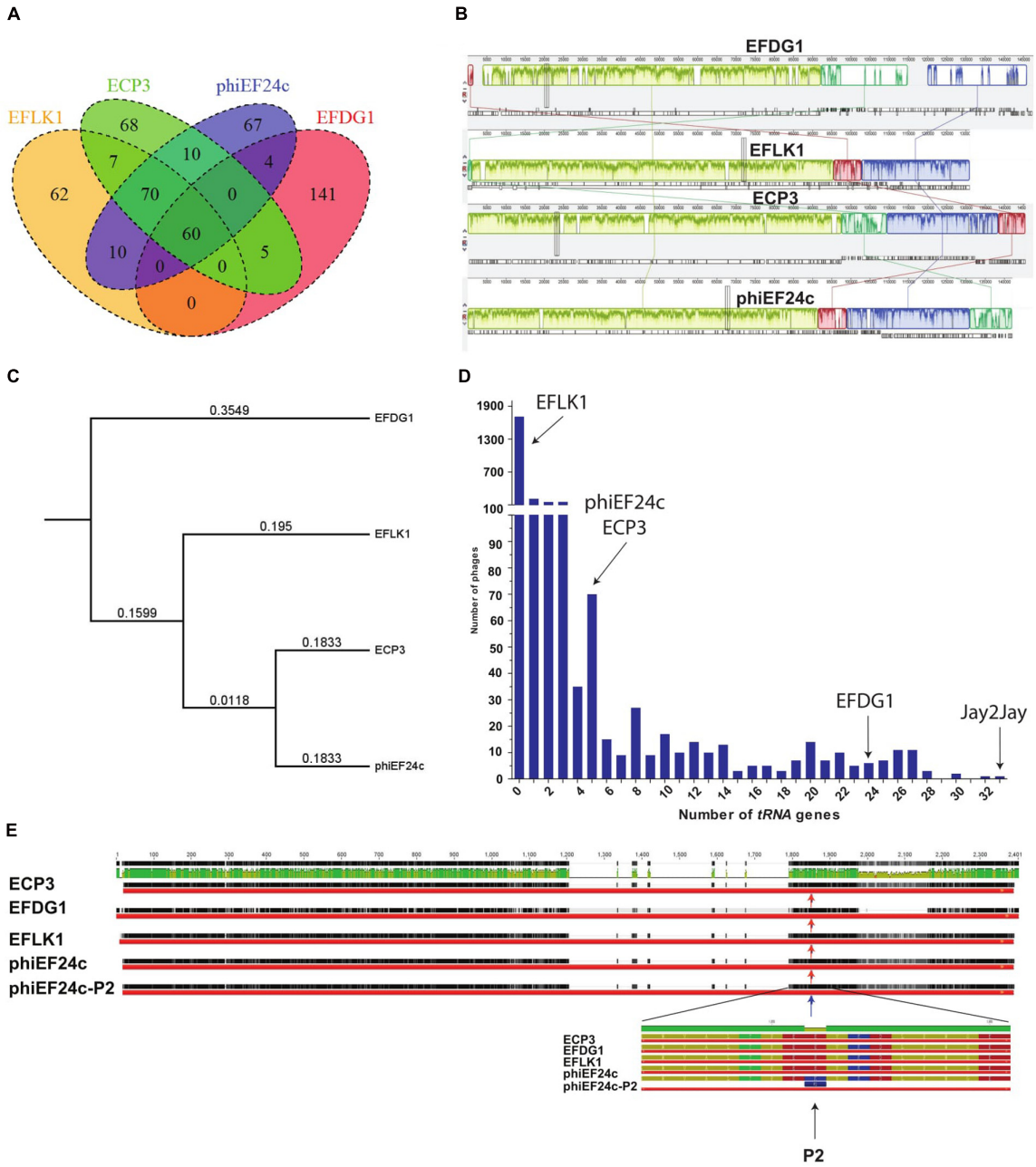

FIGURE 6 | Genomic analysis. **(A)** Venn diagram represents the number of similar *tRNA* between EFLK1, ECP3, phiEF24c, and EFDG1 phages (from left to right). **(B)** Comparative analysis of the genomes of EFDG1, EFLK1, ECP3, and phiEF24c phages (top to bottom). **(C)** Phylogenetic analysis depicting the similarity between the genomes of the four known phages of *E. faecalis*. **(D)** The number of *tRNA* genes present in the genomes of almost all known phages of *E. faecalis* V583 is shown here. With EFLK1 phage **(E)** P2 site mutation is known to be linked to enhanced adsorption as shown by Uchiyama et al., 2011. No differences were found in the P2 mutation site in all the cases.

Though one would expect to find a higher codon usage bias with respect to *E. faecalis* in this region, this is not the case. Despite a correlation between *tRNA* abundancy and virulence against bacteria (Bailly-Bechet et al., 2007) and evidence that deletion of *tRNA* genes reduced burst sizes and protein synthesis rates in the case of phage T4 of *E. coli* (Wilson, 1973), the role of *tRNA* in phages remains enigmatic.

P2 mutation in Orf31 (**Figure 6**), found to enhance adsorption in phiEF24c (Uchiyama et al., 2011), is absent in our phages. Nevertheless, Orf31 of EFDG1 phage appears to be less conserved in general compared to the other three phages of *E. faecalis*. This could mean that EFDG1 phage binds with a different affinity, or binds to another receptor all together. Further research is needed to determine whether the differences in Orf31 are

responsible for the phenotypic differences between EFDG1 and EFLK1 phages. The effectiveness and complementary nature of EFDG1 and EFLK1 phages marks these phages as suitable for *in vivo* experiments toward the development of a high-efficacy anti-*E. faecalis* phage therapy.

AUTHOR CONTRIBUTIONS

RH initiated the research, designed the experiments, analyzed the data, and wrote the paper. LK designed and performed the experiments and wrote the paper. MS performed some of the experiments. AD performed the bioinformatic analysis. SC-G designed the experiments and wrote the paper. DG helped to perform some of the experiments. NB initiated the research, designed the experiments, analyzed the data, and wrote the paper.

FUNDING

We are grateful to the funding committee of the Rosetrees Trust for grant #0364821. Additionally, LK and MS are the recipients of the Ariane de Rothschild fellowship for women.

ACKNOWLEDGMENTS

We would like to thank the following: Hebrew University's interdepartmental core unit at the Ein Kerem Campus for help in deep sequencing, Dr. Violeta Temper of Hadassah Hospital's Infectious Diseases Unit at Ein Kerem for bacterial isolates; Nahal Sorek Sewage Decontamination Institute's Yuri Veinstein for samples for phage isolation, and finally to Dr. Dov Glazer and Elisheva Dorfman for critical editing of this manuscript.

SUPPLEMENTARY MATERIAL

The Supplementary Material for this article can be found online at: https://www.frontiersin.org/articles/10.3389/fmicb.2018.00326/full#supplementary-material

TABLE S1 | *tRNA* codon usage in EFDG1, EFLK1 and the other two *E. faecalis* phages as compared to that in *E. faecalis*. This is depicted by the frequency occurrence of the amino acid codon and the number of *tRNA* encoded by them in each case.

REFERENCES

Bailly-Bechet, M., Vergassola, M., and Rocha, E. (2007). Causes for the intriguing presence of tRNAs in phages. *Genome Res.* 17, 1486–1495. doi: 10.1101/gr.6649807

Bertram, H. (1988). DNA damage and mutagenesis of lambda phage induced by gamma-rays. *Mutagenesis* 3, 29–33. doi: 10.1093/mutage/3.1.29

Burrowes, B., Harper, D. R., Anderson, J., Mcconville, M., and Enright, M. C. (2011). Bacteriophage therapy: potential uses in the control of antibiotic-resistant pathogens. *Expert Rev. Anti. Infect. Ther.* 9, 775–785. doi: 10.1586/eri.11.90

Capparelli, R., Nocerino, N., Iannaccone, M., Ercolini, D., Parlato, M., Chiara, M., et al. (2010). Bacteriophage therapy of *Salmonella enterica*: a fresh appraisal of bacteriophage therapy. *J. Infect. Dis.* 201, 52–61. doi: 10.1086/648478

Chan, B. K., and Abedon, S. T. (2012). Phage therapy pharmacology phage cocktails. *Adv. Appl. Microbiol.* 78, 1–23. doi: 10.1016/B978-0-12-394805-2.00001-4

Charles, P. G., and Grayson, M. L. (2004). The dearth of new antibiotic development: why we should be worried and what we can do about it. *Med. J. Aust.* 181, 549–553.

Chong, Y. P., Lee, S. O., Song, E. H., Lee, E. J., Jang, E. Y., Kim, S. H., et al. (2010). Quinupristin-dalfopristin versus linezolid for the treatment of vancomycin-resistant *Enterococcus faecium* bacteraemia: efficacy and development of resistance. *Scand. J. Infect. Dis.* 42, 491–499. doi: 10.3109/00365541003699623

Davies, J., and Davies, D. (2010). Origins and evolution of antibiotic resistance. *Microbiol. Mol. Biol. Rev.* 74, 417–433. doi: 10.1128/MMBR.00016-10

de la Fuente-Nunez, C., Reffuveille, F., Fernandez, L., and Hancock, R. E. (2013). Bacterial biofilm development as a multicellular adaptation: antibiotic resistance and new therapeutic strategies. *Curr. Opin. Microbiol.* 16, 580–589. doi: 10.1016/j.mib.2013.06.013

Diaz-Munoz, S. L., and Koskella, B. (2014). Bacteria-phage interactions in natural environments. *Adv. Appl. Microbiol.* 89, 135–183. doi: 10.1016/B978-0-12-800259-9.00004-4

Donlan, R. M. (2001). Biofilms and device-associated infections. *Emerg. Infect. Dis.* 7, 277–281. doi: 10.3201/eid0702.010226

Donlan, R. M. (2009). Preventing biofilms of clinically relevant organisms using bacteriophage. *Trends Microbiol.* 17, 66–72. doi: 10.1016/j.tim.2008.11.002

Drake, J. W. (1966). Ultraviolet mutagenesis in bacteriophage T-4. I. Irradiation of extracellular phage particles. *J. Bacteriol.* 91, 1775–1780.

Drake, J. W. (1982). Methyl methanesulfonate mutagenesis in bacteriophage T4. *Genetics* 102, 639–651.

Duerkop, B. A., Huo, W., Bhardwaj, P., Palmer, K. L., and Hooper, L. V. (2016). Molecular basis for lytic bacteriophage resistance in enterococci. *mBio* 7:e01304-16. doi: 10.1128/mBio.01304-16

Entenza, J. M., Haldimann, A., Giddey, M., Lociuro, S., Hawser, S., and Moreillon, P. (2009). Efficacy of iclaprim against wild-type and thymidine kinase-deficient methicillin-resistant *Staphylococcus aureus* isolates in an *in vitro* fibrin clot model. *Antimicrob. Agents Chemother.* 53, 3635–3641. doi: 10.1128/AAC.00325-09

Ellis, E. L., and Delbrück, M. (1939). The growth of bacteriophage. *J. Gen. Physiol.* 22, 365–384. doi: 10.1085/jgp.22.3.365

Erlandson, K. M., Sun, J., Iwen, P. C., and Rupp, M. E. (2008). Impact of the more-potent antibiotics quinupristin-dalfopristin and linezolid on outcome measure of patients with vancomycin-resistant *Enterococcus* bacteremia. *Clin. Infect. Dis.* 46, 30–36. doi: 10.1086/523588

Golkar, Z., Bagasra, O., and Pace, D. G. (2014). Bacteriophage therapy: a potential solution for the antibiotic resistance crisis. *J. Infect. Dev. Ctries.* 8, 129–136. doi: 10.3855/jidc.3573

Gu, J., Liu, X., Li, Y., Han, W., Lei, L., Yang, Y., et al. (2012). A method for generation phage cocktail with great therapeutic potential. *PLoS One* 7:e31698. doi: 10.1371/journal.pone.0031698

Hershberger, E., Coyle, E. A., Kaatz, G. W., Zervos, M. J., and Rybak, M. J. (2000). Comparison of a rabbit model of bacterial endocarditis and an in vitro infection model with simulated endocardial vegetations. *Antimicrob. Agents Chemother.* 44, 1921–1924. doi: 10.1128/AAC.44.7.1921-1924.2000

Khalifa, L., Brosh, Y., Gelman, D., Coppenhagen-Glazer, S., Beyth, S., Poradosu-Cohen, R., et al. (2015a). Targeting *Enterococcus faecalis* biofilms with phage therapy. *Appl. Environ. Microbiol.* 81, 2696–2705. doi: 10.1128/AEM.00096-15

Khalifa, L., Coppenhagen-Glazer, S., Shlezinger, M., Kott-Gutkowski, M., Adini, O., Beyth, N., et al. (2015b). Complete genome sequence of *Enterococcus* bacteriophage EFLK1. *Genome Announc.* 3, e1308-15. doi: 10.1128/genomeA.01308-15

Khalifa, L., Shlezinger, M., Beyth, S., Houri-Haddad, Y., Coppenhagen-Glazer, S., Beyth, N., et al. (2016). Phage therapy against *Enterococcus faecalis* in dental root canals. *J. Oral Microbiol.* 8, 32157. doi: 10.3402/jom.v8.32157

Kiro, R., Shitrit, D., and Qimron, U. (2014). Efficient engineering of a bacteriophage genome using the type I-E CRISPR-Cas system. *RNA Biol.* 11, 42–44. doi: 10.4161/rna.27766

Lavigne, R., Darius, P., Summer, E. J., Seto, D., Mahadevan, P., Nilsson, A. S., et al. (2009). Classification of *Myoviridae* bacteriophages using protein sequence similarity. *BMC Microbiol.* 9:224. doi: 10.1186/1471-2180-9-224

Laxminarayan, R., Duse, A., Wattal, C., Zaidi, A. K., Wertheim, H. F., Sumpradit, N., et al. (2013). Antibiotic resistance-the need for global solutions. *Lancet Infect. Dis.* 13, 1057–1098. doi: 10.1016/S1473-3099(13)70318-9

Linden, P. K. (2002). Treatment options for vancomycin-resistant enterococcal infections. *Drugs* 62, 425–441. doi: 10.2165/00003495-200262030-00002

Loc-Carrillo, C., and Abedon, S. T. (2011). Pros and cons of phage therapy. *Bacteriophage* 1, 111–114. doi: 10.4161/bact.1.2.14590

McGrath, B. J., Kang, S. L., Kaatz, G. W., and Rybak, M. J. (1994). Bactericidal activities of teicoplanin, vancomycin, and gentamicin alone and in combination against *Staphylococcus aureus* in an *in vitro* pharmacodynamic model of endocarditis. *Antimicrob. Agents Chemother.* 38, 2034–2040. doi: 10.1128/AAC.38.9.2034

Moore, S. D. (2011). Assembling new *Escherichia coli* strains by transduction using phage P1. *Methods Mol. Biol.* 765, 155–169. doi: 10.1007/978-1-61779-197-0_10

O'Driscoll, T., and Crank, C. W. (2015). Vancomycin-resistant enterococcal infections: epidemiology, clinical manifestations, and optimal management. *Infect. Drug Resist.* 8, 217–230. doi: 10.2147/IDR.S54125

Ormala, A. M., and Jalasvuori, M. (2013). Phage therapy: should bacterial resistance to phages be a concern, even in the long run? *Bacteriophage* 3:e24219.

Orsi, G. B., and Ciorba, V. (2013). Vancomycin resistant enterococci healthcare associated infections. *Ann. Ig.* 25, 485–492. doi: 10.7416/ai.2013.1948

Pires, D. P., Cleto, S., Sillankorva, S., Azeredo, J., and Lu, T. K. (2016). Genetically engineered phages: a review of advances over the last decade. *Microbiol. Mol. Biol. Rev.* 80, 523–543. doi: 10.1128/MMBR.00069-15

Rice, L. B. (2008). Federal funding for the study of antimicrobial resistance in nosocomial pathogens: no ESKAPE. *J. Infect. Dis.* 197, 1079–1081. doi: 10.1086/533452

Scott, A. E., Timms, A. R., Connerton, P. L., Loc Carrillo, C., Adzfa Radzum, K., and Connerton, I. F. (2007). Genome dynamics of *Campylobacter jejuni* in response to bacteriophage predation. *PLoS Pathog.* 3:e119. doi: 10.1371/journal.ppat.0030119

Silver, L. L. (2011). Challenges of antibacterial discovery. *Clin. Microbiol. Rev.* 24, 71–109. doi: 10.1128/CMR.00030-10

Srinivasiah, S., Bhavsar, J., Thapar, K., Liles, M., Schoenfeld, T., and Wommack, K. E. (2008). Phages across the biosphere: contrasts of viruses in soil and aquatic environments. *Res. Microbiol.* 159, 349–357. doi: 10.1016/j.resmic.2008.04.010

Tiruvadi Krishnan, S., Moolman, M. C., Van Laar, T., Meyer, A. S., and Dekker, N. H. (2015). Essential validation methods for *E. coli* strains created by chromosome engineering. *J. Biol. Eng.* 9:11. doi: 10.1186/s13036-015-0008-x

Uchiyama, J., Takemura, I., Satoh, M., Kato, S., Ujihara, T., Akechi, K., et al. (2011). Improved adsorption of an *Enterococcus faecalis* bacteriophage PhiEF24C with a spontaneous point mutation. *PLoS One* 6:e26648. doi: 10.1371/journal.pone.0026648

Wilson, J. H. (1973). Function of the bacteriophage T4 transfer RNA's. *J. Mol. Biol.* 74, 753–757. doi: 10.1016/0022-2836(73)90065-X

Zahid, M. S., Udden, S. M., Faruque, A. S., Calderwood, S. B., Mekalanos, J. J., and Faruque, S. M. (2008). Effect of phage on the infectivity of *Vibrio cholerae* and emergence of genetic variants. *Infect. Immun.* 76, 5266–5273. doi: 10.1128/IAI.00578-08

Conflict of Interest Statement: The authors declare that the research was conducted in the absence of any commercial or financial relationships that could be construed as a potential conflict of interest.

Copyright © 2018 Khalifa, Gelman, Shlezinger, Dessal, Coppenhagen-Glazer, Beyth and Hazan. This is an open-access article distributed under the terms of the Creative Commons Attribution License (CC BY). The use, distribution or reproduction in other forums is permitted, provided the original author(s) and the copyright owner are credited and that the original publication in this journal is cited, in accordance with accepted academic practice. No use, distribution or reproduction is permitted which does not comply with these terms.

frontiers in Microbiology

TECHNOLOGY REPORT
published: 23 March 2018
doi: 10.3389/fmicb.2018.00537

Gas Plasma Pre-treatment Increases Antibiotic Sensitivity and Persister Eradication in Methicillin-Resistant *Staphylococcus aureus*

Li Guo[1], Ruobing Xu[2], Yiming Zhao[2], Dingxin Liu[1], Zhijie Liu[1], Xiaohua Wang[1], Hailan Chen[3] and Michael G. Kong[1,3,4]**

[1] State Key Laboratory of Electrical Insulation and Power Equipment, Center for Plasma Biomedicine, Xi'an Jiaotong University, Xi'an, China, [2] School of Life Science and Technology, Xi'an Jiaotong University, Xi'an, China, [3] Frank Reidy Center for Bioelectrics, Old Dominion University, Norfolk, VA, United States, [4] Department of Electrical and Computer Engineering, Old Dominion University, Norfolk, VA, United States

Methicillin-resistant *Staphylococcus aureus* (MRSA) is a major cause of serious nosocomial infections, and recurrent MRSA infections primarily result from the survival of persister cells after antibiotic treatment. Gas plasma, a novel source of ROS (reactive oxygen species) and RNS (reactive nitrogen species) generation, not only inactivates pathogenic microbes but also restore the sensitivity of MRSA to antibiotics. This study further found that sublethal treatment of MRSA with both plasma and plasma-activated saline increased the antibiotic sensitivity and promoted the eradication of persister cells by tetracycline, gentamycin, clindamycin, chloramphenicol, ciprofloxacin, rifampicin, and vancomycin. The short-lived ROS and RNS generated by plasma played a primary role in the process and induced the increase of many species of ROS and RNS in MRSA cells. Thus, our data indicated that the plasma treatment could promote the effects of many different classes of antibiotics and act as an antibiotic sensitizer for the treatment of antibiotic-resistant bacteria involved in infectious diseases.

Keywords: cold atmospheric-pressure plasma, antibiotics resistance, methicillin-resistant *Staphylococcus aureus*, reactive oxygen species, reactive nitrogen species

OPEN ACCESS

Edited by:
Noton Kumar Dutta, Johns Hopkins University, United States

Reviewed by:
Airat R. Kayumov, Kazan Federal University, Russia
Xiancai Rao, Army Medical University, China

****Correspondence:***
Li Guo
guoli35@mail.xjtu.edu.cn
Michael G. Kong
mglin5g@gmail.com

Specialty section:
This article was submitted to Antimicrobials, Resistance and Chemotherapy, a section of the journal Frontiers in Microbiology

Received: *14 December 2017*
Accepted: *08 March 2018*
Published: *23 March 2018*

Citation:
Guo L, Xu R, Zhao Y, Liu D, Liu Z, Wang X, Chen H and Kong MG (2018) Gas Plasma Pre-treatment Increases Antibiotic Sensitivity and Persister Eradication in Methicillin-Resistant Staphylococcus aureus. Front. Microbiol. 9:537. doi: 10.3389/fmicb.2018.00537

INTRODUCTION

Antibiotics are the primary treatment for infectious bacterial diseases (Li et al., 2017). Antibiotic resistance typically emerges several years after the development and use of a new antibiotic, usually within an average of 8 years after introduction (Schmieder and Edwards, 2012). Furthermore, infections with multidrug-resistant bacteria are occurring more frequently, and few or no drugs are available to combat them (Boucher et al., 2009; Wright, 2016; Gonzalez-Bello, 2017). One of the major multidrug-resistant bacteria is methicillin-resistant *Staphylococcus aureus* (MRSA), which is recognized as a leading cause of nosocomial infections (Shahsavan et al., 2012; Emaneini et al., 2017). Persisters are a small non-growing population of bacteria which could also escape from different antibiotics (Levin and Rozen, 2006). Persisters extend the duration of antibiotic treatment, cause the recurrence of infectious diseases, and the generation and ascent of antibiotic resistance (Levin and Rozen, 2006). Increased antibiotic resistance and the shortage of new antibiotics threaten global public health (Boucher et al., 2009; Dwyer et al., 2014). Therefore, strategies to

combat antibiotic resistance, such as the development of new antibiotics or prolonging the lifespan of current antibiotics, are in high demand (Melander and Melander, 2017).

One strategy that has been explored recently is developing approaches that induce bacterial killing via the same mechanism as existing antibiotics. Antibiotics with different targets have been proposed to share a common mechanism of bactericidal activity—enhancing intracellular reactive oxygen species (ROS) in bacterial cells (Kohanski et al., 2007, 2010). Although ROS could be developed as antimicrobials to treat infectious diseases, treatment with these highly reactive molecules is problematic because ROS react non-selectively with such a range of critical, macromolecular targets, which could lead to "off-target" effects (Dharmaraja, 2017). Given that oxidative stress is also associated with antibiotic treatment, low levels of ROS could be used as an adjuvant to potentiate the antibacterial activity of commercial antibiotics (Brynildsen et al., 2013; Morones-Ramirez et al., 2013; Shen et al., 2016). A previous study showed that $^{\bullet}OH$ induced in Ag^{+}-treated bacteria potentiated the bactericidal activity of antibiotics against bacterial persisters and biofilms (Morones-Ramirez et al., 2013). Furthermore, fosfomycin, which acts by generating $O_2^{\bullet-}$, was used to successfully treat MRSA infections when combined with many commercial antibiotics (Shen et al., 2016). These strategies relied on the addition of inorganic or organic chemicals, which would bring residues after the treatment.

Cold atmospheric-pressure plasma (referred to as "plasma") generates many reactive oxygen and nitrogen species (ROS and RNS), such as H_2O_2, $^1O_2$, O_3, $^{\bullet}NO$, and $^{\bullet}OH$ as well as electrons, ions, and photons. This form of plasma is atmospheric-pressure and near room temperature, thus it treats cells and tissues without thermal damage, making it attractive for a range of biomedical applications, such as bacteria inactivation (Fridman et al., 2008; Moreau et al., 2008; Kong et al., 2009; Kang et al., 2014). The FDA has authorized the use of at least three gas plasma-based products using "plasma biomedicine" technology, such as blood coagulation. In addition, there have been several phase-II clinical trials for plasma-based therapies, such as chronic wound healing, which is the promising applications of plasma in medicine (Isbary et al., 2010, 2012; Heinlin et al., 2013). In the treatment of wounds, the reactive species of plasma could not only kill the microorganisms in the infectious wounds and burns but also increase proliferation of fibroblasts and other cells (Lloyd et al., 2010). Bayliss et al. (2013) found that treating MRSA with sublethal doses of plasma restored the sensitivity of MRSA to trimethoprim, kanamycin, and oxacillin, but the utility of plasma treatment with other types of antibiotics was not studied.

In the present study, in order to further our understanding of the effect of plasma treatment on antibiotic sensitivity, MRSA was treated with both plasma and plasma-activated saline prior to exposure to multiple antibiotics. Sublethal treatment of MRSA with plasma increased the sensitivity of MRSA to seven antibiotics whilst also reducing the numbers of persisters. These results support the use of plasma as an antibiotic sensitizer for the treatment of antibiotic-resistant bacteria involved in infectious diseases.

MATERIALS AND METHODS

Plasma Device and Plasma Treatments

As shown in **Figure 1A**, the surface discharge structure of the plasma consisted of a high-voltage plane electrode, a liquid-facing grounded mesh electrode of a hexagonal shape and a dielectric layer (made of polytetrafluoroethylene) sandwiched between the two electrodes. The surface plasma was generated when a sinusoidal high voltage was applied and the discharge power density was 0.2 W/cm^2 with good mesh-to-mesh homogeneity (showed in the front view of the plasmas in **Figure 1A**). One milliliter MRSA suspension or saline in a Petri dish (diameter 35 mm) with the depth of 1 mm was placed under the plasma, whereas the air gap between the plasma and the liquid surface was about 8 mm. The gas plasma system was housed in a sealed organic glass box with a gas flow of helium and 1% artificial air (79% N_2 + 21% O_2) at a constant rate of 4 L/min. The artificial air was used as the source of ROS and RNS, while the helium was used to enhance the production efficiency of those species as well as their fluxes on the treated samples via diffusion.

Measurement of ROS and RNS Generated by the Plasma

The concentrations of H_2O_2 and NO_2^-/NO_3^- in 0.9% NaCl were measured using hydrogen peroxide/peroxidase assay kit (Thermo Fisher Scientific) and nitrite/nitrate colorimetric assay kit (Cayman), respectively. $^{\bullet}OH$, $^1O_2$, $^{\bullet}NO$, $O_2^{\bullet-}$, $^{\bullet}NO_2$, and $ONOO^-$ were measured using an electron spin-resonance (ESR) spectroscopy (Bruker) together with relevant spin traps. The latter include: 100 mM DMPO (5,5-Dimethyl-1-pyrroline N-oxide, Dojindo), 5 mM MGD (N-(Dithiocarbamoyl)-N-methyl-D-glucamine, Dojindo), 10 mM TEMP (2,2,6,6-Tetramethylpiperidine, TCI), and 10 mM TEMPONE-H (1-Hydroxy-2,2,6,6-tetramethyl-4-oxo-piperidine, Enzo).

Treatment of *Staphylococcus aureus* With Plasma or Plasma-Activated Saline

A single *S. aureus* ATCC33591 colony was grown in 4 ml of Mueller-Hinton (MH) broth (Oxoid) at 225 r.p.m. at 37°C overnight, and the resulting overnight culture was diluted 1:100 in MH and incubated at 37°C at 225 r.p.m. until an OD_{600} of 0.6 was reached. The bacterial cells were collected by centrifugation, washed once with saline (0.9% NaCl) and resuspended in saline at an OD_{600} of 2.0. *S. aureus* suspensions were treated with plasma directly, or the suspensions were centrifuged and resuspended in plasma-activated saline (saline treated with plasma for the indicated time), saline with 250 μM H_2O_2 + 125 μM NO_2^- + 375 μM NO_3^-, or saline with 500 μM H_2O_2 + 250 μM NO_2^- + 750 μM NO_3^- and then incubated for 30 min at room temperature. Samples were serially diluted with 0.9% NaCl, and 10 μl of each dilution was spotted onto MH agar plates and incubated overnight at 37°C and the numbers of surviving bacteria were determined by counting the resulting CFUs.

Determination of Antibiotic Sensitivity

The *S. aureus* suspensions prepared as described above were either untreated, treated with plasma directly for 30 or 40 s, or

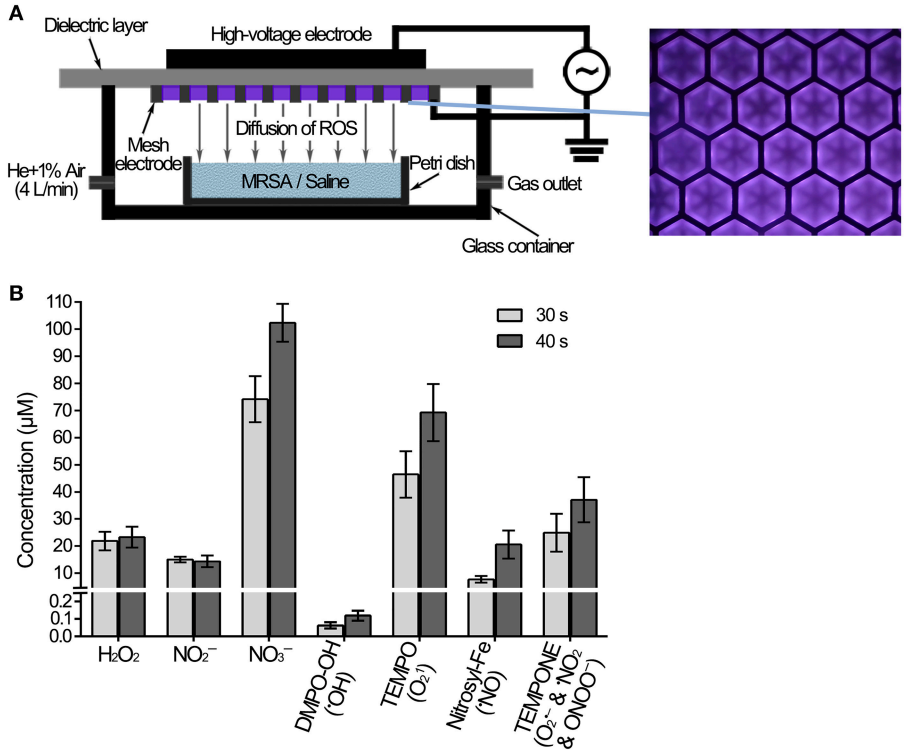

FIGURE 1 | Measurement of the ROS and RNS diffused into the saline treated with plasma. **(A)** Diagram of MRSA suspension or saline treated with plasma. **(B)** The concentrations of ROS, RNS and spin trap adducts diffused into the saline treated with plasma for 30 and 40 s.

centrifuged and resuspended in plasma-activated saline (saline treated by plasma for 30 or 40 s), followed by incubation for 30 min at room temperature. Untreated *S. aureus*, or cells treated with either plasma or plasma-activated saline (100 μl), were plated on MH agar plates. Next, antibiotic susceptibility tests were performed using Etest paper (Biomerieux) for tetracycline (0.016–256 μg/ml), gentamycin (0.016–256 μg/ml), clindamycin (0.016–256 μg/ml), chloramphenicol (0.016–256 μg/ml), ciprofloxacin (0.02–32 μg/ml), rifampicin (0.02–32 μg/ml), and vancomycin (0.016–256 μg/ml) or the Kirby-Bauer method for clindamycin (250, 500, 1,000, and 2,000 μg). Then the plates were cultured overnight at 37°C and bacteriostatic rings were analyzed. The MICs of antibiotics were measured by the microdilution assay using 8–0.016 × MIC of untreated MRSA as described (Lepe et al., 2014).

Quantification of Persister Survival

S. aureus treated with plasma or plasma-activated saline was diluted six times with MH medium containing antibiotics. The final antibiotic concentrations, corresponding to 10× the minimum inhibitory concentration (MIC), were as follows: tetracycline, 500 μg/ml (MP Biomedicals); gentamycin, 200 μg/ml (Sigma); clindamycin, 5,000 μg/ml (TCI); chloramphenicol, 500 μg/ml (MP Biomedicals); ciprofloxacin, 50 μg/ml (Sigma); rifampicin, 4 μg/ml (Sigma); and vancomycin, 50 μg/ml (Sigma). The numbers of surviving bacteria were determined at the time points indicated by harvesting 100 μl of bacterial culture, which was centrifuged at 10,000× g for 1 min. The resulting pellet was resuspended in 100 μl 0.9% NaCl. Samples were serially diluted, and 10 μl of each dilution was spotted onto MH agar plates and incubated overnight at 37°C and the numbers of surviving bacteria were determined by counting the resulting CFUs.

Detection of Reactive Species in MRSA

The probes 3′-(p-aminophenyl) fluorescein (APF, Sigma), 3′-(p-hydroxyphenyl) fluorescein (HPF, Sigma), and MitoSOX™ Red mitochondrial superoxide indicator (ThermoFisher) were incubated with *S. aureus* cultures, at a final concentration of 5 μM, and trans-1-(2′-methoxyvinyl)pyrene (tMVP, J&K Scientific) was used at a final concentration of 10 μM at 37°C for 30 min. Cultures were collected by centrifugation, washed with saline (0.9% NaCl) three times and resuspended in saline at an OD_{600} of 2.0. *S. aureus* suspensions were untreated, treated with plasma directly for 40 s, or the suspensions were centrifuged and resuspended in plasma-activated saline (saline treated with plasma for 40 s). Immediately after the treatments, the fluorescence intensities were detected using a microplate reader (Thermo Scientific Varioskan Flash) at the excitation and emission wavelengths [APF and HPF: 490/515 nm; superoxide indicator: 510/580 nm; trans-1-(2′-methoxyvinyl)pyrene: 405/460 nm] of each probe.

RESULTS

Plasma-Induced Aqueous ROS/RNS

MRSA or saline treated with the plasma device was shown in **Figure 1A**. Gaseous ROS and RNS were generated by the surface discharge, and some of them would diffuse across the air gap and then dissolved into the liquids. The plasma-induced aqueous ROS and RNS dissolved into saline were measured after the plasma treatment for 30 s and 40 s. Long-lived species H_2O_2, NO_2^-, and NO_3^-, as well as the short-lived species $^{\bullet}OH$, $^1O_2$, $^{\bullet}NO$, and $ONOO^-$, were detected in the saline. The concentrations of aqueous H_2O_2, NO_2^-, and NO_3^- after the plasma treatment for 40 s were 23, 14, and 102 μM, respectively (**Figure 1B**). Electron spin resonance (ESR) spectroscopy was used for the measurement of short-lived species, in which the results were the concentrations of spin adducts, only reflecting the relative concentrations of the specific ROS and/or RNS. The concentrations of spin adducts DMPO-OH, TEMPO, Nitrocyl-Fe, and TEMPONE after the plasma treatment for 40 s were 0.1, 69, 21, and 37 μM (**Figure 1B**). The spin adducts concentrations after the plasma treatment for 30 s were lower, such as TEMPO was 30% lower than that after the plasma treatment for 40 s. These results suggested that the concentration of aqueous $^{\bullet}OH$ was very low, and the concentration of aqueous $^1O_2$ should be much larger. The plasma generated many species ROS and RNS, which were thought to play a crucial role in the biological effects.

Sublethal Treatment With Plasma Increased the Sensitivity of MRSA to Antibiotics

The sublethal dose (reduction about 50% viability of MRSA) of plasma and plasma-activated saline were determined by exposing the bacteria to plasma for increasing times or incubating with saline treated with plasma for increasing times and subsequently determining bacterial viability. The treatment of plasma for 40 s or the saline activated by plasma for 40 s lead to about 50% death of MRSA cells (Figure S1). For safety, a lower dose was also employed, so a slightly lower dose (plasma treatment for 30 s) that lead to about 40% death of MRSA cells and the LD_{50} dose (plasma treatment for 40 s) were both used to detect the effects on antibiotic sensitivity.

To study the effect of plasma on the sensitivity of MRSA to the antibiotics, MRSA were sublethally pre-treated with plasma or plasma-activated saline followed by incubation with a range of antibiotics including tetracycline, gentamycin, clindamycin, chloramphenicol, ciprofloxacin, rifampicin, and vancomycin. The minimal inhibitory concentration (MIC) of tetracycline for untreated MRSA measured by Etest paper was ∼32 μg/ml, whilst the MIC of tetracycline for MRSA treated with plasma for 30 or 40 s was 10-fold lower, at ∼3 μg/ml (**Figure 2A**). In the second approach, the MICs were measured by the microdilution assay, and the MIC of tetracycline against MRSA treated with plasma for 40 s was 8-fold lower than that against untreated MRSA (**Table 1**). The effects of plasma pre-treatment on MRSA sensitivity to antibiotics were independent of the particular antibiotic used, and the increase in sensitivity was observed for most of the antibiotics tested. The MICs of gentamycin against untreated MRSA and MRSA treated with plasma for 30 and 40 s measured by Etest paper were ∼1.5, 1.0, and 0.5 μg/ml, respectively, and the MIC of gentamycin against MRSA treated with plasma for 40 s was 16-fold lower than that against untreated MRSA as indicated by the microdilution assay (**Figure 2A**; **Table 1**). The MICs of chloramphenicol, ciprofloxacin, rifampicin, and vancomycin against MRSA treated with plasma also decreased in varying degrees (**Figure 2A**; **Table 1**). Plasma-treated MRSA did not appear to be susceptible to treatment with clindamycin at the tested concentration (**Figure 2A**). Two possible explanations for this were that either the plasma treatment did not change the antibiotic sensitivity of MRSA to clindamycin or the MIC of clindamycin against MRSA was beyond the range of the Etest. Thus, MRSA susceptibility to clindamycin was measured at a higher antibiotic dose using the Kirby-Bauer method. The diameter of the bacteriostatic ring of untreated MRSA to 2,000 μg clindamycin was about 16 mm, and that of the MRSA treated for 30 and 40 s were 23 and 26 mm, respectively (Figures S2A,B). The microdilution assay also demonstrated that the MICs of clindamycin against MRSA treated with plasma for 30 and 40 s was 2- and 4-fold lower, respectively, than that against untreated MRSA (**Table 1**). These data indicated that sublethal plasma treatment to MRSA restored the sensitivity to five different classes of antibiotics.

Next, the effects of plasma-activated saline upon changing the sensitivity of MRSA to these antibiotics were detected. The minimal inhibitory concentration (MIC) of tetracycline against untreated MRSA was ∼32 μg/ml, whilst that for MRSA treated with saline activated by plasma for 30 or 40 s was 10-fold lower, at ∼3 μg/ml (**Figure 2B**). The MIC of tetracycline against MRSA treated with saline activated by plasma for 40 s was also 8-fold lower than that against untreated MRSA as indicated by the microdilution assay (**Table 1**). The MICs of gentamycin, clindamycin, chloramphenicol, ciprofloxacin, rifampicin, and vancomycin against MRSA treated with plasma-activated saline were also lower than those against the untreated MRSA, demonstrating that plasma-activated saline exhibited the same effect in increasing the sensitivity to five different classes of antibiotics (**Figures 2B**, Figures S2C,D; **Table 1**).

Plasma Pre-treatment Promoted Eradication of MRSA Persisters

Given that pre-treatment of MRSA with plasma or plasma-activated saline decreased the MIC of multiple antibiotics, we next asked whether either of these pre-treatment conditions could also promote the killing of persisters. To test this, untreated and sublethal dose plasma-treated MRSA were incubated with different antibiotics, as indicated (**Figure 3A**). Incubation of untreated and double-diluted untreated MRSA with the different antibiotics generally exhibited typical killing curves, with bacterial numbers decreasing from 2×10^8 to 10^4-10^6 CFUs, with a small fraction of persisters detected after 3 days of antibiotic exposure. Of note, the numbers of untreated MRSA and double-diluted untreated MRSA that incubated with rifampicin increased after 1 day. These results indicated that the decrease of the initial MRSA numbers did not greatly influence the killing

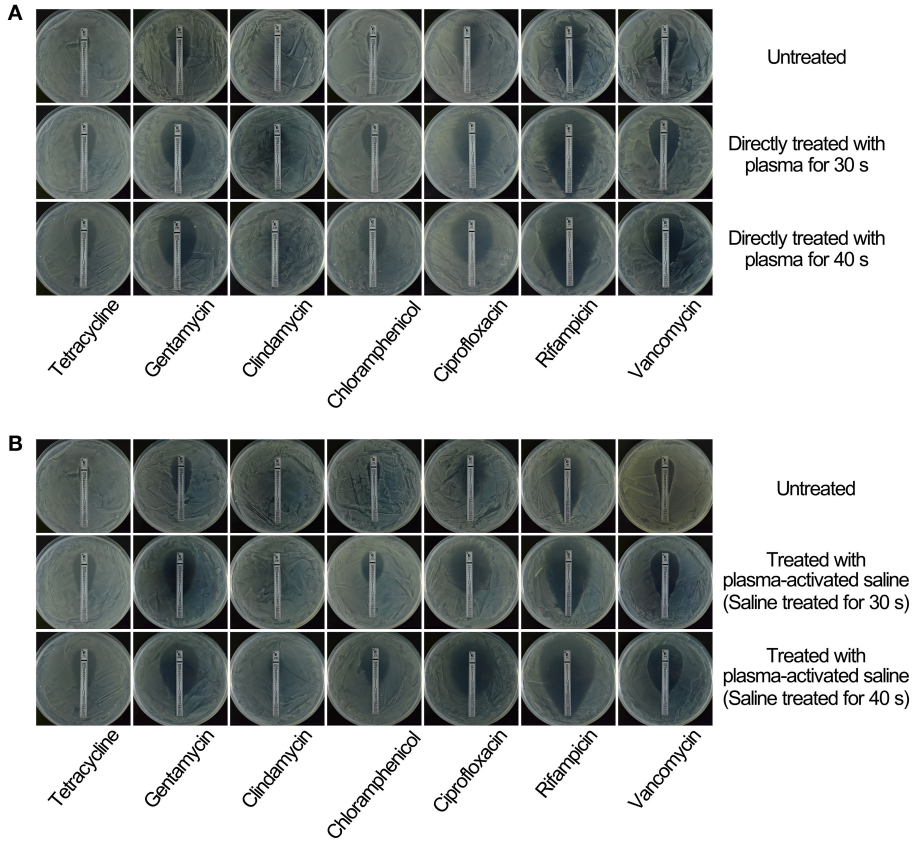

FIGURE 2 | Treatment with sublethal doses of plasma or plasma-activated saline increased the sensitivity of MRSA to antibiotics. **(A)** Direct plasma treatment. **(B)** Plasma-activated saline treatment. Plasma treated, plasma-activated saline treated and untreated MRSA were plated on MH agar with Etest strips and cultured at 37°C overnight.

TABLE 1 | Antibiotic susceptibilities of *Staphylococcus aureus* treated with plasma and plasma-activated saline.

Antibiotics	MIC[a] (mg/liter) of indicated antibiotic				
	Untreated	Directly treated with plasma for 30 s	Directly treated with plasma for 40 s	Treated with plasma-activated saline (Saline treated for 30 s)	Treated with plasma-activated saline (Saline treated for 40 s)
Tetracycline	50	12.5	6.25	12.5	6.25
Gentamycin	20	2.5	1.25	1.25	1.25
Clindamycin	500	250	125	250	250
Chloramphenicol	50	25	12.5	25	25
Ciprofloxacin	5	1.25	0.31	1.25	0.625
Rifampicin	0.4	0.025	0.0125	0.025	0.0125
Vancomycin	5	5	2.5	5	2.5

[a]*MICs were determined by broth microdilution method. The results were read after 24 h of incubation at 37°C.*

curves of antibiotics. In contrast, plasma-treatment reduced the number of MRSA persisters to below the limit of detection when incubated with tetracycline, gentamycin, clindamycin, chloramphenicol, and rifampicin within only 1 day of exposure (**Figure 3A**). A similar decrease was also observed within 2 and 3 days of incubation with ciprofloxacin and chloramphenicol, respectively (**Figure 3A**). For vancomycin, plasma treatment for 30 and 40 s effectively reduced the numbers of remaining MRSA recovered during exposure to this antibiotic to 10^4 and 10^3 CFUs, respectively, though these did not drop below the detection limit (**Figure 3A**). Treatment with plasma-activated saline exhibited the same effect of inactivating persisters as observed by direct plasma treatment (**Figure 3B**). The numbers of plasma-activated saline treated MRSA recovered upon

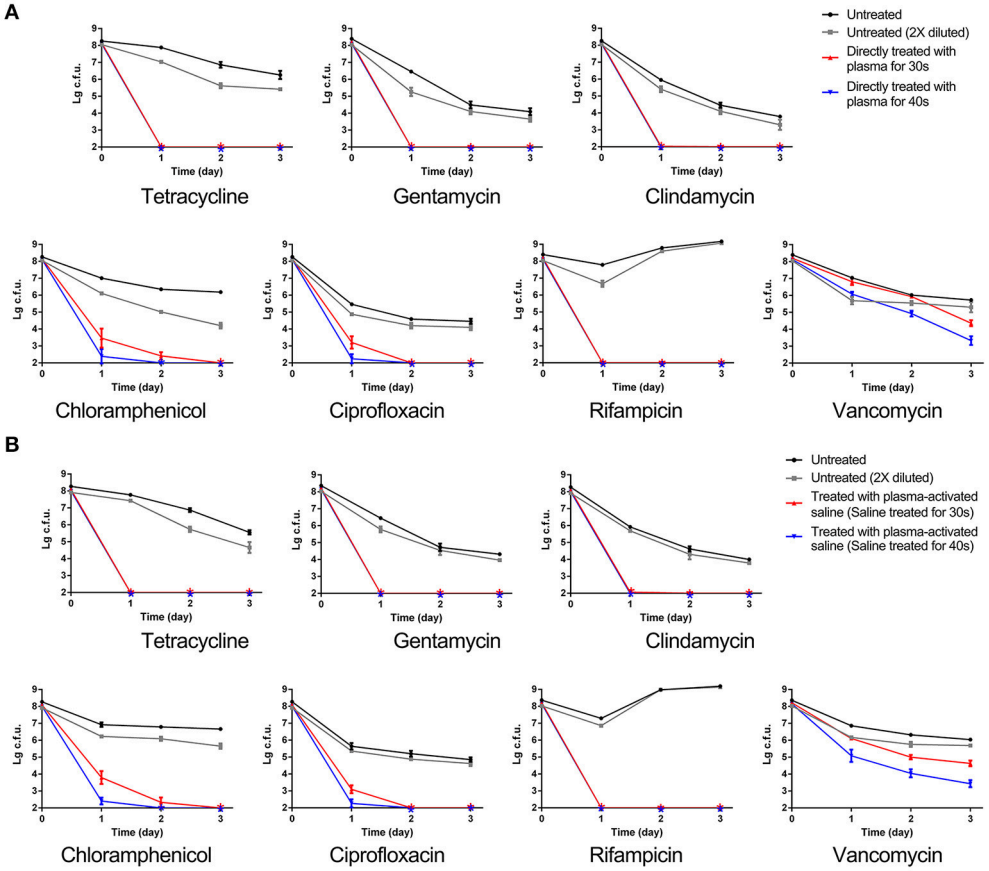

FIGURE 3 | MRSA sublethally treated with plasma or plasma-activated saline increased the eradication of persisters by antibiotics. **(A)** Direct plasma treatment. **(B)** Plasma-activated saline treatment. Plasma treated, plasma-activated saline treated and untreated MRSA were grown in MHB with 10 × MIC of the indicated antibiotics, and aliquots of the cultures were taken at the times indicated, serially diluted and plated. Then the plates were cultured at 37°C overnight and the numbers of bacteria were counted. The asterisks represented eradication to the limit of detection.

exposure to antibiotics tetracycline, gentamycin, clindamycin, and rifampicin dropped to below the detection limit, but plasma-activated saline similarly only decreased the numbers of MRSA to 10^3 CFUs upon exposure to vancomycin (**Figure 3B**). These results indicated that both plasma and plasma-activated saline treatment promoted the eradication of MRSA persisters by antibiotics.

Reactive Species in MRSA

Plasma-treated solutions contain many active species, such as the long-lived species H_2O_2, NO_2^-, and NO_3^- as well as the short-lived species $^{\bullet}OH$, $^1O_2$, $^{\bullet}NO$, $O_2^{\bullet-}$, and $ONOO^-$ (**Figure 1B**). To evaluate the impact of long-lived species, a mixture of H_2O_2 (500 μM), NO_2^- (250 μM), and NO_3^- (750 μM) was used to treat the MRSA. H_2O_2, NO_2^-, and NO_3^- treatment did not change the antibiotic susceptibility of MRSA and the inactivation of persisters by antibiotics, indicating that the three long-lived species are not likely the direct and driving factor (Figure S3). Hence, short-lived species were considered more important, and the ROS and RNS in MRSA cells were measured. MRSA were incubated with 3′-(p-aminophenyl) fluorescein (APF) for $^{\bullet}OH$, ClO^-, and $ONOO^-$, HPF for $^{\bullet}OH$ and $ONOO^-$, MitoSOX™ Red mitochondrial superoxide indicator for $O_2^{\bullet-}$ and trans-1-(2′-methoxyvinyl)pyrene (tMVP) for $^1O_2$, then exposed to plasma or plasma-activated saline for 40 s, and the levels of different ROS/RNS determined by changes in the fluorescence intensities (**Figure 4**). After plasma treatment, the fluorescence intensities of the four probes increased. The fluorescence intensities of MRSA incubated with APF and HPF increased slightly after 30 min of plasma treatment, by 28 and 25%, respectively, which indicates an increase in the levels of $^{\bullet}OH$, ClO^-, and $ONOO^-$ (**Figures 4A,B**). Fluorescence of MRSA incubated with MitoSOX™ Red mitochondrial superoxide indicator increased by 77%, and the trans-1-(2′-methoxyvinyl)pyrene (tMVP) for $^1O_2$ increased by 130% after 30 min of plasma treatment (**Figures 4C,D**). The fluorescence intensities of the probes which incubated with plasma-activated saline-treated MRSA were slightly weaker than those of the direct plasma-treated samples. These data suggested that the plasma and plasma-activated saline treatment induced the increases of many species of ROS and RNS in MRSA cells.

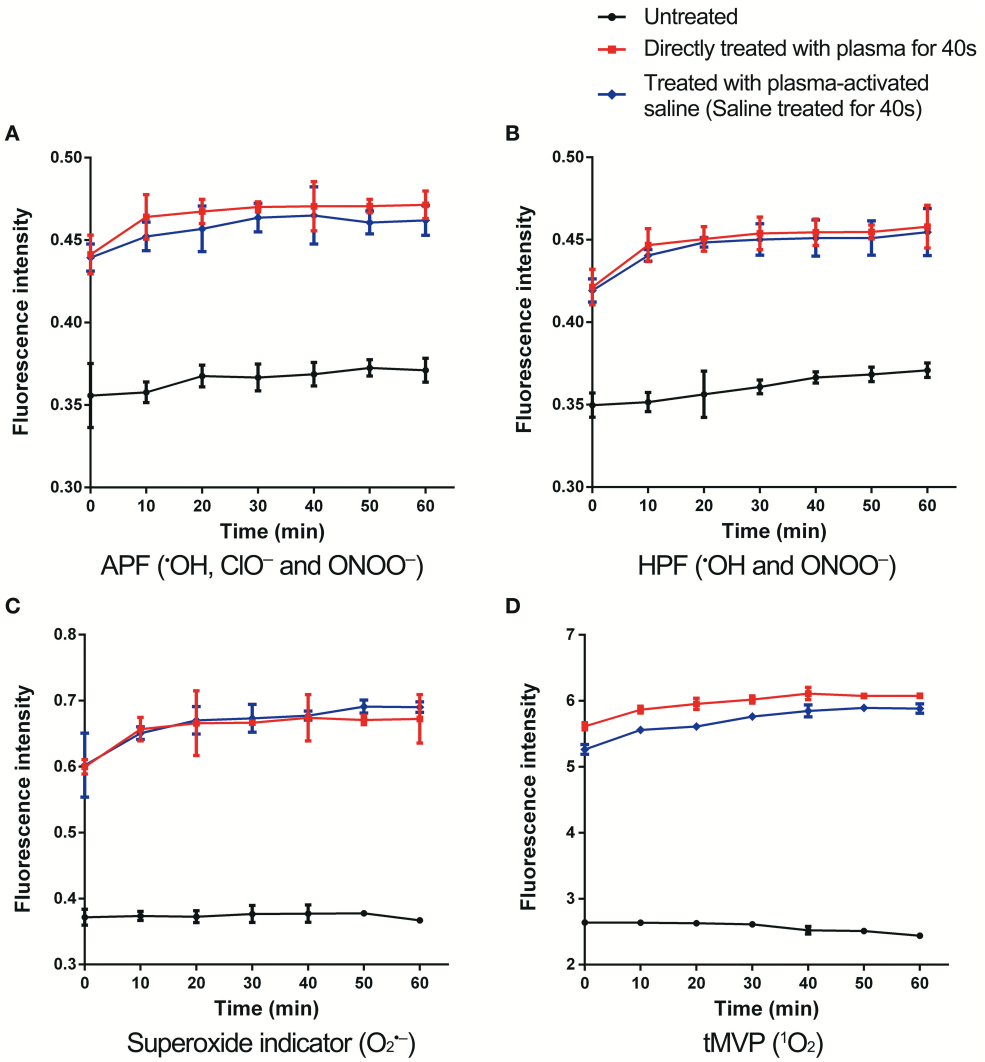

FIGURE 4 | ROS and RNS levels increased in plasma-treated and plasma-activated saline-treated MRSA. MRSA incorporated with APF **(A)**, HPF **(B)**, superoxide indicator **(C),** and tMVP **(D)**, which measured the ROS or RNS as indicated, treated with plasma for 40 s or saline treated with plasma for 40 s. Then the fluorescence intensities of were measured in plasma-treated, plasma-activated saline-treated, and untreated MRSA. Data are representative of three independent experiments. Error bars represent s.d.

DISCUSSION

In this study, we demonstrated that treating MRSA sublethally with plasma-generated ROS and RNS decreased the MICs of several antibiotics and increased persister eradication, along with increases in the levels of ROS and RNS in MRSA cells. Plasma-activated saline had the same effect upon the antibiotic sensitivity of MRSA and persister inactivation as direct plasma treatment, suggesting that the plasma-generated ROS and RNS could be applied in both gaseous or aqueous form depending on the mode of application. The short-lived species in the plasma-activated saline had short half-lives, but they could react and generate long-lived species, which also could generate to short-lived species reversibly, such as $ONOO^-$ generated from NO_3^- (Oehmigen et al., 2011; Liu et al., 2017). Plasma generated various ROS, which are involved in a great many chemical reactions (Oehmigen et al., 2011). The underlying reactions and detailed mechanisms of plasma-activated saline are still not well understand and require further study.

Unlike other treatments that have previously been used as antibiotic adjuvants to enhance ROS production in bacterial cells, plasma induces the production of a wider range of ROS species (Morones-Ramirez et al., 2013; Shen et al., 2016). The ROS and RNS generated by the plasma constitute a complex mix of products, including $^{\bullet}OH$, $^1O_2$, $O_2^{\bullet-}$, $ONOO^-$, and ClO^- (Liu et al., 2016). Subsequently, these many different ROS or RNS species were also detected in plasma-treated bacterial cells. The intracellular ROS and RNS could induce oxidative stresses, such as damaging lipids, proteins and DNA by $^{\bullet}OH$, $^1O_2$, and $O_2^{\bullet-}$, as well as protein damages by

$ONOO^-$ and ClO^- (Davies, 2016). $O_2^{\bullet-}$ could be detoxified by endogenous antioxidants of the oxidative response, but no enzyme can detoxify $^\bullet OH$ or $^1O_2$, and MRSA could not detoxify all the multiple reactive species induced by plasma (Vatansever et al., 2013). It was speculated that the compound damages stimulated multiple response pathways and kept MRSA busy with repairing, which contributed to the effects of antibiotics.

Reactive species generated by plasma could also induce damages in eukaryotic cells, subsequently, the safety and toxicity of this application should be considered. The CC_{50} of the plasma treatment used in this study for human primary dermal fibroblasts was about 40 s treatment, which was close to the LD_{50} on MRSA (Figure S4A). Comparing with bacterial cells, the cultured cells are more easily to be inactivated *in vitro* because of the lack of cell wall. However, the plasma treatment did not increase micronuclei formation in fibroblast cells (Figures S4B,C). Coincidently, a newly published paper found similar results on lymphocyte TK6 cells (Bekeschus et al., 2018). Further, the olive tail moment of plasma-treated cells exhibited little difference with that of untreated cells (Figures S4D,E). So the plasma treatment did not remarkably increase the mutagenicity of fibroblasts as demonstrated by both micronucleus assay and comet assay. Besides, Maisch et al. (2012) showed that gas plasma could efficiently inactivate *S. aureus* and *Escherichia coli* on pig skin without inducing morphological changes or damage-related apoptosis. Clinical trials also demonstrated that 5 min daily treatment with plasma decreased bacteria in chronic wounds of patients without side effects (Isbary et al., 2010). These studies demonstrated the safety of plasma treatment under limited conditions. Many topical biocides are toxic, and the plasma could be developed as alternative, especially the plasma-activated saline could be the save alternative (Wales and Davies, 2015). When used as a sensitizer with antibiotics as was done in this study, the doses of plasma were much lower than that used for bacteria inactivation, which would reduce the risk of toxicity and improve the safety.

In conclusion, sublethal treatment with plasma-generated ROS and RNS decreased the MICs of several antibiotics and increased persister eradication, along with increases in the levels of ROS and RNS in MRSA. Plasma and plasma-activated saline could be explored as a novel antibiotic sensitizer to generate oxidative stress to combat the increasing problem of antibiotic resistance. Further studies are needed to test these methods against other multidrug-resistant bacteria and to elucidate the underlying mechanism.

AUTHOR CONTRIBUTIONS

LG, RX, and YZ designed and executed most of the experiments and analyzed the data. ZL assisted in the execution of some experiments. LG, DL, and MK wrote the manuscript. MK, LG, DL, XW, and HC reviewed and approved the final version of the manuscript.

ACKNOWLEDGMENTS

This work was supported by National Natural Science Foundation of China (51477136 and 51521065), Doctoral Fund of Ministry of Education of China (2017M613106), Doctoral Fund of Ministry of Education of Shaanxi Province, State Key Laboratory of Agricultural Microbiology (AMLKF201705), State Key Laboratory of Electrical Insulation and Power Equipment (EIPE14123), and Fundamental Research Funds for the Central Universities.

SUPPLEMENTARY MATERIAL

The Supplementary Material for this article can be found online at: https://www.frontiersin.org/articles/10.3389/fmicb.2018.00537/full#supplementary-material

REFERENCES

Bayliss, D. L., Shama, G., and Kong, M. G. (2013). Restoration of antibiotic sensitivity in meticillin-resistant *Staphylococcus aureus* following treatment with a non-thermal atmospheric gas plasma. *Int. J. Antimicrob. Agents* 41, 398–399. doi: 10.1016/j.ijantimicag.2012.12.005

Bekeschus, S., Schmidt, A., Kramer, A., Metelmann, H. R., Adler, F., von Woedtke, T., et al. (2018). High throughput image cytometry micronucleus assay to investigate the presence or absence of mutagenic effects of cold physical plasma. *Environ. Mol. Mutagen*. doi: 10.1002/em.22172. [Epub ahead of print].

Boucher, H. W., Talbot, G. H., Bradley, J. S., Edwards, J. E., Gilbert, D., Rice, L. B., et al. (2009). Bad bugs, no drugs: no ESKAPE! An update from the infectious diseases society of America. *Clin. Infect. Dis.* 48, 1–12. doi: 10.1086/595011

Brynildsen, M. P., Winkler, J. A., Spina, C. S., MacDonald, I. C., and Collins, J. J. (2013). Potentiating antibacterial activity by predictably enhancing endogenous microbial ROS production. *Nat. Biotechnol.* 31, 160–165. doi: 10.1038/nbt.2458

Davies, M. J. (2016). Protein oxidation and peroxidation. *Biochem. J.* 473, 805–825. doi: 10.1042/BJ20151227

Dharmaraja, A. T. (2017). Role of Reactive Oxygen Species (ROS) in therapeutics and drug resistance in cancer and bacteria. *J. Med. Chem.* 60, 3221–3240. doi: 10.1021/acs.jmedchem.6b01243

Dwyer, D. J., Belenky, P. A., Yang, J. H., MacDonald, I. C., Martell, J. D., Takahashi, N., et al. (2014). Antibiotics induce redox-related physiological alterations as part of their lethality. *Proc. Natl. Acad. Sci. U.S.A.* 111, E2100–E2109. doi: 10.1073/pnas.1401876111

Emaneini, M., Beigverdi, R., van Leeuwen, W. B., Rahdar, H., Karami-Zarandi, M., Hosseinkhani, F., et al. (2017). Prevalence of methicillin-resistant *Staphylococcus aureus* isolated from burn patients: a systematic review and meta-analysis. *J. Glob. Antimicrob. Resist.* 12, 202–206. doi: 10.1016/j.jgar.2017.10.015

Fridman, G., Friedman, G., Gutsol, A., Shekhter, A. B., Vasilets, V. N., and Fridman, A. (2008). Applied plasma medicine. *Plasma Process. Polym.* 5, 503–533. doi: 10.1002/ppap.200700154

Gonzalez-Bello, C. (2017). Antibiotic adjuvants - a strategy to unlock bacterial resistance to antibiotics. *Bioorg. Med. Chem. Lett.* 27, 4221–4228. doi: 10.1016/j.bmcl.2017.08.027

Heinlin, J., Zimmermann, J. L., Zeman, F., Bunk, W., Isbary, G., Landthaler, M., et al. (2013). Randomized placebo-controlled human pilot study of cold atmospheric argon plasma on skin graft donor sites. *Wound Repair Regen.* 21, 800–807. doi: 10.1111/wrr.12078

Isbary, G., Heinlin, J., Shimizu, T., Zimmermann, J. L., Morfill, G., Schmidt, H. U., et al. (2012). Successful and safe use of 2 min cold atmospheric argon plasma in

chronic wounds: results of a randomized controlled trial. *Br. J. Dermatol.* 167, 404–410. doi: 10.1111/j.1365-2133.2012.10923.x

Isbary, G., Morfill, G., Schmidt, H. U., Georgi, M., Ramrath, K., Heinlin, J., et al. (2010). A first prospective randomized controlled trial to decrease bacterial load using cold atmospheric argon plasma on chronic wounds in patients. *Br. J. Dermatol.* 163, 78–82. doi: 10.1111/j.1365-2133.2010.09744.x

Kang, M. H., Hong, Y. J., Attri, P., Sim, G. B., Lee, G. J., Panngom, K., et al. (2014). Analysis of the antimicrobial effects of nonthermal plasma on fungal spores in ionic solutions. *Free Radic. Biol. Med.* 72, 191–199. doi: 10.1016/j.freeradbiomed.2014.04.023

Kohanski, M. A., Dwyer, D. J., and Collins, J. J. (2010). How antibiotics kill bacteria: from targets to networks. *Nat. Rev. Microbiol.* 8, 423–435. doi: 10.1038/nrmicro2333

Kohanski, M. A., Dwyer, D. J., Hayete, B., Lawrence, C. A., and Collins, J. J. (2007). A common mechanism of cellular death induced by bactericidal antibiotics. *Cell* 130, 797–810. doi: 10.1016/j.cell.2007.06.049

Kong, M. G., Kroesen, G., Morfill, G., Nosenko, T., Shimizu, T., Dijk J. V., et al. (2009). Plasma medicine: an introductory review. *New J. Phys.* 11:115012. doi: 10.1088/1367-2630/11/11/115012

Lepe, J. A., Domínguez-Herrera, J., Pachón, J., and Aznar, J. (2014). Determining accurate vancomycin MIC values for methicillin-resistant *Staphylococcus aureus* by the microdilution method. *J. Antimicrob. Chemother.* 69, 136–138. doi: 10.1093/jac/dkt308

Levin, B. R., and Rozen, D. E. (2006). Non-inherited antibiotic resistance. *Nat. Rev. Microbiol.* 4, 556–562. doi: 10.1038/nrmicro1445

Li, J., Xie, S., Ahmed, S., Wang, F., Gu, Y., Zhang, C., et al. (2017). Antimicrobial activity and resistance: influencing factors. *Front. Pharmacol.* 8:364. doi: 10.3389/fphar.2017.00364

Liu, D. X., Liu, Z. C., Chen, C., Yang, A. J., Li, D., Rong, M. Z., et al. (2016). Aqueous reactive species induced by a surface air discharge: heterogeneous mass transfer and liquid chemistry pathways. *Sci. Rep.* 6:23737. doi: 10.1038/srep 23737

Liu, Z. C., Guo, L., Liu, D. X., Rong, M. Z., Chen, H. L., and Kong, M. G. (2017). Chemical kinetics and reactive species in normal saline activated by a surface air discharge. *Plasma Process. Polym.* 14:1600113. doi: 10.1002/ppap.201600113

Lloyd, G., Friedman, G., Jafri, S., Schultz, G., Fridman, A., and Harding, K. (2010). Gas Plasma: medical uses and developments in wound care. *Plasma Process. Polym.* 7, 194–211. doi: 10.1002/ppap.2009 00097

Maisch, T., Shimizu, T., Li, Y. F., Heinlin, J., Karrer, S., Morfill, G., et al. (2012). Decolonisation of MRSA, *S. aureus* and *E. coli* by cold-atmospheric plasma using a porcine skin model *in vitro*. *PLoS ONE* 7:e34610. doi: 10.1371/journal.pone.0034610

Melander, R. J., and Melander, C. (2017). The challenge of overcoming antibiotic resistance: an adjuvant approach? *ACS Infect. Dis.* 3, 559–563. doi: 10.1021/acsinfecdis.7b00071

Moreau, M., Orange, N., and Feuilloley, M. G. (2008). Non-thermal plasma technologies: new tools for bio-decontamination. *Biotechnol. Adv.* 26, 610–617. doi: 10.1016/j.biotechadv.2008.08.001

Morones-Ramirez, J. R., Winkler, J. A., Spina, C. S., and Collins, J. J. (2013). Silver enhances antibiotic activity against gram-negative bacteria. *Sci. Transl. Med.* 5:190ra181. doi: 10.1126/scitranslmed.3006276

Oehmigen, K., Winter, J., Hähnel, M., Wilke, C., Brandenburg, R., Weltmann, K., et al. (2011). Estimation of possible mechanisms of *Escherichia coli* inactivation by plasma treated sodium chloride solution. *Plasma Process. Polym.* 8, 904–913. doi: 10.1002/ppap.201000099

Schmieder, R., and Edwards, R. (2012). Insights into antibiotic resistance through metagenomic approaches. *Future Microbiol.* 7, 73–89. doi: 10.2217/fmb.11.135

Shahsavan, S., Emaneini, M., Noorazar Khoshgnab, B., Khoramian, B., Asadollahi, P., Aligholi, M., et al. (2012). A high prevalence of mupirocin and macrolide resistance determinant among *Staphylococcus aureus* strains isolated from burnt patients. *Burns* 38, 378–382. doi: 10.1016/j.burns.2011.09.004

Shen, F., Tang, X., Cheng, W., Wang, Y., Wang, C., Shi, X., et al. (2016). Fosfomycin enhances phagocyte-mediated killing of *Staphylococcus aureus* by extracellular traps and reactive oxygen species. *Sci. Rep.* 6:19262. doi: 10.1038/srep19262

Vatansever, F., de Melo, W. C. M. A., Avci, P., Vecchio, D., Sadasivam, M., Gupta, A., et al. (2013). Antimicrobial strategies centered around reactive oxygen species - bactericidal antibiotics, photodynamic therapy, and beyond. *FEMS Microbiol. Rev.* 37, 955–989. doi: 10.1111/1574-6976.12026

Wales, A. D., and Davies, R. H. (2015). Co-Selection of resistance to antibiotics, biocides and heavy metals, and its relevance to foodborne pathogens. *Antibiotics* 4, 567–604. doi: 10.3390/antibiotics4040567

Wright, G. D. (2016). Antibiotic adjuvants: rescuing antibiotics from resistance. *Trends Microbiol.* 24, 862–871. doi: 10.1016/j.tim.2016.06.009

Conflict of Interest Statement: The authors declare that the research was conducted in the absence of any commercial or financial relationships that could be construed as a potential conflict of interest.

Copyright © 2018 Guo, Xu, Zhao, Liu, Liu, Wang, Chen and Kong. This is an open-access article distributed under the terms of the Creative Commons Attribution License (CC BY). The use, distribution or reproduction in other forums is permitted, provided the original author(s) and the copyright owner are credited and that the original publication in this journal is cited, in accordance with accepted academic practice. No use, distribution or reproduction is permitted which does not comply with these terms.

frontiers in Microbiology

ORIGINAL RESEARCH
published: 29 March 2018
doi: 10.3389/fmicb.2018.00561

Liposome Entrapment of Bacteriophages Improves Wound Healing in a Diabetic Mouse MRSA Infection

Sanjay Chhibber, Jasjeet Kaur and Sandeep Kaur*

Department of Microbiology, Panjab University, Chandigarh, India

Diabetic populations are more prone to developing wound infections which results in poor and delayed wound healing. Infection with drug resistant organisms further worsen the situation, driving searches for alternative treatment approaches such as phage therapy. Major drawback of phage therapy, however, is low phage persistence *in situ*, suggesting further refinement of the approach. In the present work we address this issue by employing liposomes as delivery vehicles. A liposome entrapped phage cocktail was evaluated for its ability to resolve a *Staphylococcus aureus*-induced diabetic excission wound infection. Two characterized *S. aureus* specific lytic phages, MR-5 and MR-10 alone, in combination (cocktail), or entrapped in liposomes (versus as free phages) were assesed for their therapeutic efficacy in resolving diabetic wound infection. Mice treated with free phage cocktail showed significant reduction in wound bioburden, greater wound contraction and faster tissue healing than with free monophage therapy. However, to further enhance the availability of viable phages the encapsulation of phage cocktail in the liposomes was done. Results of *in vitro* stability studies and *in vivo* phage titer determination, suggests that liposomal entrapment of phage cocktail can lead to better phage persistence at the wound site. A 2 log increase in phage titre, however, was observed at the wound site with liposome entrapped as compared to the free phage cocktail, and this was associaed with increased rates of infection resolution and wound healing. Entrapment of phage cocktails within liposomes thus could represent an attractive approach for treatment of bacterial infections, not responding to antibiotis as increased phage persistence *in vitro* and *in vivo* at the wound site was observed.

Keywords: bacteriophage, diabetes, phage cocktail, liposome, alloxan

OPEN ACCESS

Edited by:
Stephen Tobias Abedon, The Ohio State University, United States

Reviewed by:
Rodolfo García-Contreras, Universidad Nacional Autónoma de México, Mexico
Xiancai Rao, Army Medical University, China

****Correspondence:***
Sanjay Chhibber
sanjaychhibber8@gmail.com

Specialty section:
This article was submitted to Antimicrobials, Resistance and Chemotherapy, a section of the journal Frontiers in Microbiology

Received: *12 June 2017*
Accepted: *12 March 2018*
Published: *29 March 2018*

Citation:
Chhibber S, Kaur J and Kaur S (2018) Liposome Entrapment of Bacteriophages Improves Wound Healing in a Diabetic Mouse MRSA Infection. Front. Microbiol. 9:561. doi: 10.3389/fmicb.2018.00561

INTRODUCTION

Diabetes is a chronic disease that manifests in the form of a chronic hyperglycemia which is associated with a plethora of complications including visual impairment, blindness, kidney disease, nerve damage, amputation, heart disease, and stroke (Loghmani, 2005). WHO has projected diabetes as the 7th leading contributor to death by 2030 (Mathera and Loncar, 2006). In addition, the total number of people with diabetes is projected to rise from 171 million in 2000 to 366 million in 2030 (Wild et al., 2004). Diabetic patients are five times more susceptible to fungal and bacterial infections (Axelrod, 1985). This is due to several factors that include a high glucose level which

encourages bacterial growth. Secondly, diabetes decreases a body's blood flow, slowing healing of abrasions, open wounds and other injuries, thus making diabetic individuals more prone to infection (King, 2001). Finally, peripheral neuropathy, a primary complication of diabetes, results in loss of sensation (Pendsey, 2010) and has a central role in the development of foot and wound infections (Bader, 2008; Powlson and Coll, 2010). According to the American Diabetes Association (ADA), 25% of people with diabetes suffer from a wound problem during their lifetime, including infections. *Staphylococcus aureus* is one of the most common pathogens isolated from wounds in diabetic patients. Further, with the spread of methicillin resistant strains of *S. aureus* (MRSA), management of such infections in diabetic population has become challenging. Diabetics who contract MRSA are at a greater risk of harboring more serious, slow-healing wounds (Rogers and Bevilacqua, 2009).

With time, the bacteria in diabetic infections tend to evolve greater resistance to antibiotics (Xavier et al., 2014). Consequently, having a comprehensive treatment plan for MRSA is crucial. Phage therapy seems to be a good option for addressing these problems (Barrow and Soothill, 1997; Bull et al., 2002; Wills et al., 2005; Capparelli et al., 2007; Sunagar et al., 2010; Hsieh et al., 2011; Kumari et al., 2011; Chhibber et al., 2013; Chadha et al., 2016). Fish et al. (2016), on the basis of the success obtained with phage therapy of a diabetic foot infected with *S. aureus*, have suggested that in the future controlled clinical trials can be conducted. The ability of phages to rapidly lyse infected bacteria, their specificity and effectiveness against multidrug-resistant pathogenic bacteria, their ability to self-replicate (auto dosing) (Kumari et al., 2009; Chhibber et al., 2013; Kaur et al., 2014), their natural abundance and their proven clinical safety makes this therapy worth considering in immunocompromised individuals such as diabetic patients (Carlton et al., 2005; Hanlon, 2007). Phage therapy in many cases nevertheless can benefit from approaches that can increase phage retention and persistence at the target sites.

Toward improving phage persistence and retention at diabetic wound sites, we propose here the use of liposome entrapment of phages. Liposomes are composed of natural lipids which are biodegradable, non-immunogenic and non-toxic. Along with these advantages, their structural versatility enables us to design a number of liposome-based formulations (Gregoriadis, 1995). Liposomes also mimic biological membranes in terms of their structure and behavior, which enables them to penetrate the epidermal barrier to a greater extent and thus can be used effectively in treating skin infections (Hua, 2015). Use of drug delivery systems (DDSs) such as liposomes also helps to improve the pharmacological properties of conventional ("free") drugs by altering their pharmacokinetics (PK) and bio-distribution (BD) (Zhang et al., 2013; Zylberberg and Matosevic, 2016). Workers in the past have reported the use of liposomes with entrapped antibiotics or other wound healing agent in treating wound infections (Roesken et al., 2000; Kurilko et al., 2009; Fukui et al., 2012). In recent studies, entrapment of phages in liposomes has also been reported (Colom et al., 2015; Nieth et al., 2015; Singla et al., 2015; Chadha et al., 2017). However, none of these workers have studied the use of liposomes to enhance the stability and persistence of phages for the better therapeutic outcome after treatment of diabetic wound infection caused by MRSA. The present study therefore investigated the therapeutic use of liposome entrapped phage cocktail in treating MRSA mediated skin wound infection in diabetic mice.

MATERIALS AND METHODS

Bacterial Strains and Phage Used

Staphylococcus aureus ATCC 43300 (MRSA) from ATCC, Manassas, VA, United States was used in this study. *S. aureus* specific phages, MR-5 and MR-10, both of which have been isolated and characterized in our laboratory as lytic, dsDNA, tailed phages belonging to Myoviridae family, order Caudovirales were used in the present study (Kaur et al., 2012; Chhibber et al., 2013).

Preparation of Purified High Titer Phage Stocks (MR-5 and MR-10)

High-titer MR-5 and MR-10 suspension was prepared according to the method described by Langley et al. (2003). The inoculated broth was centrifuged and supernatant containing phage collected and passed through a 0.22-μm-pore-size filter. The filtrate was concentrated by using Millipore Labscale TFF system (Pellicon) and 10 K (polyethersulfone) membrane until the sample volume was reduced to 25–30 ml. DNase I (0.25 mg/ml) was added and kept for 1 h at 37°C to digest the free DNA. NaCl (final concentration of 1 M) and polyethylene glycol (PEG) 8000 were added to the concentrated lysate and kept at 4°C overnight. The precipitate was collected, dialyzed against phosphate buffered saline (PBS) overnight at 4°C, passed through an0.22-μm-pore-size filter and stored at 4°C till further use. The phage titer was determined in the final product.

Liposomes

Free phage preparations were entrapped within liposomes to increase their persistence and efficacy. For this a series of optimization experiments were carried to select the exact liposomal formulation for *in vivo* use.

Preparation

The method of Bhatia et al. (2004) was used for the preparation of phage cocktail-loaded liposomes. For preparation of cationic liposomal formulation of phage, phosphatidylcholine:cholesterol: tween 80:stearylamine (7:3:1:0.5) was dissolved in chloroform-methanol mixture (2:1 v/v). Thin film was prepared by a rota-evaporator [Heidolph, Hei-VAP Advantage (ML)] using a hydration temperature of 40°C. Phage suspension (10 ml prepared in PBS [pH 7.2]) was added to the thin film at 40°C and rotated for 10 min to detach the film from the glass wall. The suspension was left overnight at room temperature for swelling. The next day the dispersion is sonicated in a water bath sonicator for 30 min.

Characterization

The morphological characteristics of liposomes were monitored viz. shape, uniformity, and structure by using optical microscope

(Olympus CH20i) at suitable magnification (100X). Morphological analysis of liposomes loaded with phage cocktail was then done using TEM following the procedure of Goodridge et al. (2003). Drops of ultra-centrifuged phage samples (1,00,000 *g* for 2 h, 4°C; L-80, Beckman Instrument, Switzerland) were dropped on nitrocellulose coated grids (diameter, 3 mm; 300 meshes), stained with 2% (w/v) potassium phosphotungstate (pH: 6.8–7.2) for 10 s, and examined under a transmission electron microscope (TEM) (Hitachi H 7500, Tokyo, Japan) at Sophisticated Analytic Instrumentation Facility (SAIF), Panjab University, Chandigarh, India. Particle size and polydispersity index of liposomes was measured by dynamic light scattering (DLS) technique on Beckman coulter instrument (Delsa Nano C) at Department of Chemistry, Panjab University, Chandigarh.

The phage entrapment efficiency of liposomes was determined by modified protamine aggregation method (Gulati et al., 1998). Total phage count was determined by adding Triton × (0.02%) in a ratio of 1:1 v/v so as to disrupt liposomes and release entrapped phage particles. The mixture was then centrifuged (10,000 × *g* for 10 min) and total number of phages in the supernatant was determined using plaque assay. Free phages were separated by protamine aggregation method where protamine sulfate was added at a final concentration of 20 mg/ml. The liposomal phage preparation with added protamine sulfate was allowed to stand overnight. Supernatant was collected and the number of free phage particles was determined using plaque assay. Phage entrapment efficiency was then calculated as total number of non-free phages divided by total number of phages, presented as a percentage.

Animal experiments

Animal experimental protocols were approved by the Institutional Animal Ethics Committee (Approval ID: IAEC/411) of Panjab University, Chandigarh, India and performed in accordance with the guidelines of Committee for the Purpose of Control and Supervision of Experiments on Animals (CPCSEA), Government of India, on animal experimentation. All efforts were made to minimize the suffering of animals.

BALB/c female mice, 4–6 weeks old weighing 20–25 g were used in this study. The animals, obtained from Central Animal House, Panjab University, Chandigarh, India, were kept in polycarbonate cages housed in well-aerated rooms with a 12-h light/12-h dark cycle at 25 ± 2°C, and fed with standard rodent diet and water *ad libitum*. Diabetes as per the protocol of Pan and Liu (2008) was induced by giving two intra-peritoneal injections of alloxan monohydrate (150 mg/kg body weight) at 48-h intervals in mice fasted overnight. One week after the second injection, blood glucose levels (both random as well as fasting) were recorded. The blood sample was obtained by tail clipping method of Oladeinde et al. (2007) and glucose levels were checked using pre-calibrated Glucometer (Optium Xceed).

Wound Model

A diabetic excision wound model was developed following the method of Mendes et al. (2012). *S. aureus* 43300 cultivated overnight in brain heart infusion broth was pelleted and washed twice with PBS. Bacterial suspension was adjusted to achieve a cell density corresponding to a range of bacterial inoculums (10^8, 10^9, and 10^{10} CFU/ml). The number of CFU/ml was confirmed by quantitative plate count. Diabetic BALB/c mice were taken and distributed in four different groups of 14 animals (n = 14) each. The mice were anesthetized by giving 0.1 ml of ketamine-xylazine (50–5 mpk) intraperitoneally. Hair was removed by using commercially available hair removing cream followed by disinfection of the dorsal surface with 70% alcohol. A punch biopsy instrument (diameter 5 mm, accu punch) was used to create a full thickness round wound extending through the panniculus carnosus. The wounds created in all the animals were left open and animals were given ibuprofen suspension (20 mg/ml) in drinking water. Each of the three groups received different doses of inoculum. Animals of the fourth group received same volume of PBS injected into their wound. Two mice from each group were sacrificed on days 1, 3, 5, 7, 10, 15, and 20 post-bacterial challenge by cervical dislocation. Complete epithelial and dermal compartments of wound margins, granulation tissue and adjacent muscle and subcutaneous fat tissue was excised from each individual wound and processed. The tissue was homogenized and dilutions of the homogenates were plated to determine the bacterial burden.

Free Phage Efficacy (Study 1)

In vivo work was divided into two studies. In the first study the therapeutic potential of free phages (monophage therapy as well as cocktail of phages) not involving any delivery system was assessed. For further clarity, phage preparations not entrapped within liposomes have been referred as free monophage (FMP) for, e.g., FMP-MR-5 and FMP-MR-10 and free cocktail of phages (FCP).

For the first study, the therapeutic potential of *S. aureus* 43300-specific phages FMP-MR-5, FMP-MR-10 and their cocktail, FCP, was evaluated in diabetic BALB/c mice. The phages were administered locally at a dose of 10^9 PFU/50 μl, at MOI10 as based on a titer of applied phages of 2 × 10^{10} PFU/ml, into the wound on its dorsal surface. Diabetic BALB/c mice were randomly divided into five groups (n = 14 per group; as described immediately below) and seven extra animals were put in the infection control group to check the bacterial load on days 1 and 3. In all cases diabetic mice were first infected with *S. aureus* 43300 (10^8 CFU/50 μl) with treatments following 30-min later.

Group 1 (untreated infection control): No phages or clarithromycin applied.
Group 2: Local administration of phage FMP-MR-5 at MOI10.
Group 3: Local administration of phage FMP-MR-10 at MOI10.
Group 4: Local administration of the phage cocktail, FCP (each phage at MOI10 mixed in an equal ratio).
Group 5: Two I/P doses of clarithromycin (10 mpk) given in 12-h intervals.

All of the animals involved in Study 1 were monitored daily for mortality post-bacterial challenge. In addition to mortality,

wound bioburden, and phage titer was assessed in surviving animals on different days.

Liposome Entrapped Phage Efficacy (Study 2)

In the second study, liposome entrapped phage cocktail was evaluated for its potential in treatment of diabetic wound infection. Phage cocktail (MR-5 + MR-10, 1:1) entrapped within liposomes shall be referred as liposomes entrapped cocktail of phages (LCP). Results were compared with the groups instead treated with FCP and with clarithromycin. Diabetic BALB/c mice with dermal wounds in this study were randomly divided into a total of four groups (n = 14). As above, in all cases diabetic mice were first infected with *S. aureus* 43300 (10^8 CFU/50 μl) with treatments following 30-min later.

Group 1 (untreated infection control): No phages or clarithromycin applied.
Group 2: Local administration of FCP (each phage at MOI10 mixed in an equal ratio).
Group 3: Local administration of LCP (each phage at MOI10 mixed in an equal ratio).
Group 4: Two I/P doses of clarithromycin (10 mpk) given in 12-h intervals.

All animals in Study 2 were monitored daily for mortality post-bacterial challenge. In addition to mortality, wound bioburden, phage titer, wound contraction rate, MPO, Masson's trichrome staining, histopathological examination, and period of epithelization was also assessed in surviving animals on different days.

Wound microbiology and rate of healing

In both Studies 1 and 2, two mice from each group were sacrificed on days 1, 3, 5, 7, 10, and 15 post-infection by cervical dislocation. Bacterial load (wound bioburden) was assessed as per the method of Park et al. (2009). After disinfection, the wound tissue was carefully excised and homogenized in 1 ml of PBS. This tissue homogenate was then serially diluted and plated for CFUs. Phage titer was determined (in terms of PFU/ml) by centrifuging the homogenate (10,000 *g* for 10 min at 4°C). The supernatant was filtered through 0.45 μm pore sized filter and the filtrate so obtained was serially diluted and plated on a lawn of *S. aureus* 43300.

Rate of wound contraction, as a percentage, was calculated by measuring the size of the wound (diameter in mm) on each day of all the animals involved in Study 2 using vernier caliper. This data is presented as percentage decrease in wound size. Thus, $\frac{\text{(initial wound size – wound size on a specific day)}}{} \times 100$. The number of days required for wound healing and eschar to fall off leaving no raw wound behind was taken as period for epithelization.

Myeloperoxidase (MPO) estimation

Two mice from each group (same groups as those described for liposome entrapped phage cocktail protection study, i.e., Study 2 with 14 animals per group) were sacrificed and their wound tissue homogenized. Homogenized samples were processed for MPO determination as per the method of Greenberger et al. (1996). The absorbance was read immediately at 490 nm over a period of 4 min. MPO was calculated as the change in optical density (O.D) × dilution factor (D.F).

Masson's trichrome staining

To assess the wound healing after treatment with LCP, FCP and clarithromycin, collagen formation was checked in each animal group of Study 2. Collagen is used as an essential marker in wound healing studies as it restores the integrity of the skin. Therefore, collagen formation was observed in the skin wound tissue on different days. Samples were fixed on different glass slides, stained as per the protocol[1] and examined under an Olympus microscope (at 100X) to evaluate the amount of collagen formation.

Histopathological examination

Tissue damage and healing following treatment with LCP, FCP, and clarithromycin in Study 2 was assessed on the basis of histopathological examination of infected wound tissue according to the method of Brans et al. (1994). The sections were picked on separate slides, stained with hematoxylin and eosin (Hi-Media, Mumbai) and then examined under a microscope to evaluate the extent of tissue damage and recovery.

Statistical Methods

All the data is expressed as mean ± standard deviation of more than two experimental values for every variable. The statistical significance of difference between groups was determined by Student's t-test (two groups), one-way ANOVA followed by a Tukey test using Sigma Stat, Graph pad prism (GraphPad Software, San Diego, CA, United States). P-value of less than 0.05 was considered statistically significant.

RESULTS

Optimization of Liposomal Formulation and Stability

For phage cocktail entrapment, three different liposomal formulations (7:3:1, 8:2:1, 9:1:1) were made using different ratios of phospholipid phosphatidylcholine (PC), cholesterol (CHOL), and Tween-80. Further, to increase the physical stability of liposomal preparation; positive charge inducer stearylamine (SA) was added in a ratio of 7:3:1:0.5. Liposomal formulation 7:3:1:0.5 showed a minimum liposome size of 230 nm, low PDI of 0.220, uniform liposomes in terms of shape and lamellarity. Both the phages MR-5 and MR-10 (1:1) were entrapped in this liposomal preparation which had an entrapment efficiency of 87% and liposomal size of 212 nm. The photomicrographs (**Figure 1**) obtained after TEM clearly demonstrates presence of phages in the cationic liposomes. LCP was made using 7:3:1:0.5 formulation and tested for stability (drop in phage titer) over a 9 week period. This liposomal preparation had a PDI below 0.3 with minimum size variation and was found to be stable at 4°C in terms of fusion size, aggregation and number of entrapped phages during the entire storage period. Thus, this ratio was selected for further *in vivo* experiments.

[1] http://www.ihcworld.com/_protocols/special_stains/masson_trichrome.htm

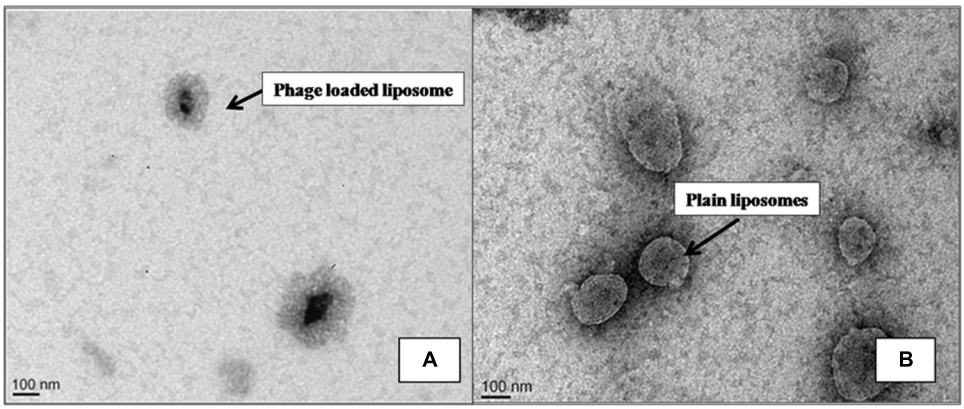

FIGURE 1 | Transmission Electron Micrograph of liposomes. Photomicrograph **(A)** shows phage loaded liposomes. **(B)** Plain liposomes without phage.

Induction of Diabetes in Mice

The average random blood glucose level of normal BALB/c mice was found to be 139 ± 3.8 mg/dl whereas the fasting blood glucose level (after overnight fasting) was 96.2 ± 7.9 mg/dl. Fasting glucose levels were checked daily post-alloxan injection. Mice with fasting blood glucose levels in the range of 150–180 mg/dl, 4–5 days post-injection were termed as moderately diabetic. However, 15 days after alloxan administration, the fasting blood glucose level was found to be 194.6 ± 17.1 mg/dl, whereas the random blood glucose levels were ≥400 mg/dl. Such animals were considered severely diabetic and selected for infection studies.

Excision Wound Infection Model

The excision wound model was developed by inflicting full thickness wound of 5 mm extending through panniculus carnosus with the help of punch biopsy on the dorsal surface of mouse. Since the aim of this study was to assess the efficacy of phages in reducing the mortality and clearing off infection; a high dose of 10^8 CFU/50 μl of *S. aureus* 43300 was chosen as the optimal infectious dose. At this bacterial dose, an acute infection of the inflicted wound was established with 70% of untreated mice exhibiting mortality within 24–48 h post-infection.

Phage Protection Studies

Mortality vs. survival

Animals in all groups were monitored daily for mortality. Untreated mice of Study 1 (group 1) and Study 2 (group 1) exhibited 70% mortality within 24–48 h post-inoculation. However, all treated animals showed no mortality during the experimental period and all infections resolved. This clearly indicated that a single injection of free phages, alone or as cocktail, or liposome-entrapped phages were able to protect the test animals from death.

Wound microbiology

The wound bioburden (bacterial density) and phage titer was also assessed in all the mice groups of Study 1 and Study 2. In Study 1, untreated animals showed an increase in bacterial load that reached ∼9 log CFUs/ml by day 3 (peak day). Mice receiving FMP-MR-5, FMP-MR-10, i.e., groups 2 and 3 respectively, showed bacterial loads which instead were 7 log CFUs/ml on day 1 and day 3 followed by a significant decline ($P < 0.05$) to 3 logs on day 10 and sterile wounds by day 15 (**Table 1**). However, mice treated with cocktail, i.e., FCP showed higher reduction in bacterial burden as compared to infection control as well as monophage treated mice on all days. A significant decrease of 3 log ($P < 0.05$) was observed in cocktail treated group on days 3 and 5 as compared to infection control. Clarithromycin treated mice also showed significant reduction on all days with sterile wounds obtained by day 10.

Phage titer for Study 1 is shown in **Figure 2** was also determined on subsequent days post-treatment. Although an initial titer of 10^9 PFU/50 μl (MOI 10) was administered at the wound site, maximum titer of 10^5 PFU/ml was estimated on day 1, which shows a 4 log reduction from the initial phage titer. This phage count was consistent (approximately 10^5 PFU/ml) in all the groups on days 1 and 3, followed by gradual decline on subsequent days with minimum count of 10^2 PFU/ml present on day 10. However, phage titer was higher on all days in the wound of mice receiving FCP as compared to monophage treated animals. No phage particles were detected in the wound of mice receiving either single or cocktail of phages by day 15.

Results in **Table 2** for Study 2 show that the wounds of mice in the infection control (group 1) also had consistently higher bacterial burden (8–9 log CFU/ml) till day 5 followed by decline from day 7 onwards. In FCP treated mice, a significant decrease of 3 log CFU/ml occurred on day 3 and day 5 itself as compared to untreated mice. However, bacterial load (2.21 log CFU/ml) was detected even by day 10. In case of LCP treated mice maximum reduction in bacterial load equivalent to ∼4 log CFU/ml ($P < 0.05$) was seen on day 3 (peak day of infection). Negligible counts were obtained on day 7 and this correlated well with visible reduction in wound size by day 7 (**Figure 3**). The wound showed complete healing within 9 days unlike 20 days and less than 15 days required for untreated surviving diabetic mice and FCP treated group, respectively. Animals receiving clarithromycin showed higher reduction in bacterial burden on all days as compared to FCP treated mice

TABLE 1 | Bacterial load (in terms of Log CFU/ml) in skin wound of *S. aureus* 43300 (10^8 CFU/50 μl) infected diabetic BALB/c mice following treatment with FMP (MR-5 and MR-10), FCP and clarithromycin (10 mg/kg/ per i.p.).

Treatment groups (n = 14, each group)	Bacterial load (Log CFU/ml) on				
	Day 1	Day 3	Day 5	Day 7	Day 10
Infection control (group 1)	8.37 ± 0.07	9.24 ± 0.26	8.44 ± 0.40	6.84 ± 0.08	NA
FMP-MR-5 (group 2)	7.67 ± 0.8	7.2 ± 0.20	6.29 ± 0.17	5.21 ± 0.38	3.2 ± 0.54
FMP-MR-10 (group 3)	7.69 ± 0.14	7.11 ± 0.20	6.23 ± 0.15	5.14 ± 0.25	3.11 ± 0.31
FCP (group 4)	7.24 ± 0.25	6.83 ± 0.28	5.2 ± 0.40	4.42 ± 0.14	2.10 ± 0.36
Clarithromycin (group 5)	7.16 ± 0.40	6.5 ± 0.36	4.82 ± 0.07	3.18 ± 0.10	(–)

Treatment was given after 30 min of wound inoculation. (–): zero bacterial count; NA: no mice available for determining the wound bio-burden. All values represent mean ± standard error of the mean calculated from three independent values.

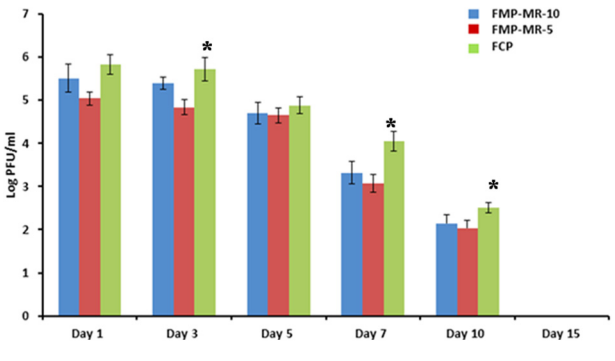

FIGURE 2 | Phage titer (Log PFU/ml) in the wound of *Staphylococcus aureus* 43300 (10^8 CFU/50 μl) infectedmice (n = 14, each group) following treatment with FMP-MR-10, FMP-MR-5, and FCP on different days post-infection. Error bars represent the standard deviation (SD) from three independent values. *$P < 0.05$ indicate statistical significant differences (Student's t-test) between FMP and FCP treated groups.

and reduction in bacterial load was comparable to that seen in LCP treated animals.

Phage titer in Study 2 in terms of log PFU/ml (**Figure 4**) was maximum on day 1 and thereafter a decrease was noticed on subsequent days in both FCP and LCP treated groups. Maximum titer of 7.45 and 7.12 log PFU/ml on day 1 and day 3 was seen in liposome phage entrapped cocktail (LCP) treated mice as compared to 5.80 and 5.68 log PFU/ml present on day 1 and day 3 in FCP treated group. A decline was seen thereafter due to clearance of its host bacteria as no phage particles were obtained on day 15 and after day 10 with FCP and LCP treated groups, respectively. This shows that entrapment of liposomes led to a significant increase in phage titer by 2 log ($P < 0.05$) at the wound site, which explains the faster wound healing process.

Additional Parameters (Study 2)

Wound contraction

Wound area of all the animal groups was measured with the help of vernier caliper (**Figure 5**). In untreated mice (group 1), an initial wound size of 5 mm persisted until day 3 and it was finally resolved by day 20. In FCP treated animals wound contraction was comparatively slower with wound of 3 mm size evident by day 5 and even by day 12 a wound size of 0.5 mm was observed. However, in case of both LCP treated as well as clarithromycin treated animals, significant decrease in wound size was seen by day 3 onwards as compared to both infection control and FCP treated mice. Minimal wound size of less than 1 mm was observed by day 7 with almost complete closure of wound by day 9 in clarithromycin as well as LCP treated mice. Thus wound closure rates were greater given when phages were encapsulated than when they were not.

Myeloperoxidase (MPO) activity

Neutrophils are the first cells to reach the site of infection or inflammation. MPO is then produced by neutrophils into the extracellular space during degranulation. So as to assess the levels of inflammation or bacterial load MPO levels were measured, and results are presented in **Figure 6**. Highest MPO

TABLE 2 | Bacterial load (in terms of Log CFU/ml) in skin wound of *S. aureus* 43300 (10^8 CFU/50 μl) infected diabetic BALB/c mice following treatment with FCP, LCP, and clarithromycin (10 mg/kg/per i.p.).

Treatment groups (n = 14, each group)	Bacterial counts (Log CFU/ml) on				
	Day 1	Day 3	Day 5	Day 7	Day 10
Infection control (group 1)	8.39 ± 0.72	9.08 ± 0.32	8.9.32	6.16 ± 0.27	NA
FCP (group 2)	7.22 ± 0.22	6.78 ± 0.30	5.15.38	4.57 ± 0.44	2.21 ± 0.20
LCP (group 3)	6.22 ± 0.20	5.53 ± 0.41	3.28 ± 0.28	1.84 ± 0.17	(–)
Clarithromycin (group 4)	7.04 ± 0.15	6.28 ± 0.17	4.75 ± 0.45	2.92 ± 0.30	(–)

Treatment was given after 30 min of wound inoculation. (–): zero bacterial count; NA: no mice available for determining the wound bio-burden. All values represent mean ± standard error of the mean calculated from three independent values.



FIGURE 3 | Pictorial representation of wound healing in diabetic BALB/c mice infected with 10^8 CFU/50 μl dose of *S. aureus* 43300 and treated with LCP.

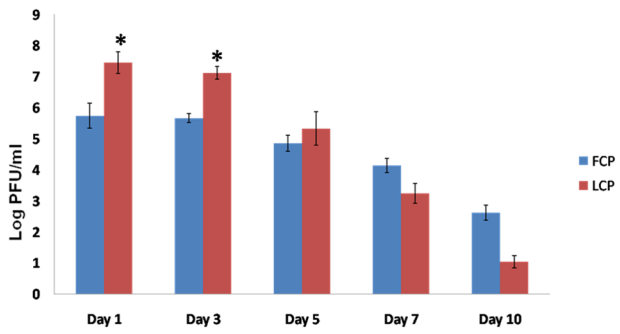

FIGURE 4 | Phage titer (Log PFU/ml) present in the wound of *S. aureus* 43300 (10^8 CFU/50 μl) infected mice (n = 14, each group) following treatment with FCP and LCP on different days post-infection. Error bars represent the standard deviation (SD) from three independent values. *$P < 0.05$ indicate statistical significant differences (Student's t-test) between FCP and LCP treated groups.

levels were present in untreated animals on all days with peak MPO activity of 2.81 units/ml recorded on day 3, that decreased on subsequent days. In case of FCP treated mice, peak MPO activity of 2.41 units/ml was observed on day 1, followed by significant decline thereafter as compared to untreated mice with minimal value of less than 1 unit/ml measured on day 10. However, maximum reduction in MPO levels was seen in mice receiving LCP as it showed peak MPO levels of 1.77 units/ml on day 1 with minimum MPO activity of 0.211 units/ml recorded on day 7 which is significantly less ($P < 0.05$) than activity present in untreated and FCP treated mice Lower levels of MPO activity observed on subsequent days in LCP treated group correlated well with lesser bacterial load seen after treatment. Clarithromycin treated mice also showed significant reduction ($P < 0.05$) in MPO enzyme activity as compared to infection control group and FCP treated group. Thus, these results indicate that neutrophil migration was maximum in untreated animals, while neutrophil migration upon phage and antibiotic treatment decreased due to the decrease in bacterial infection at the site.

Masson's trichrome staining

Wound tissue was taken on day 5 post-infection from all the groups. The tissue of untreated diabetic mice showed little collagen formation as seen in **Figure 7A**. The faint green area seen in the figure depicts early stages of collagen formation. Mostly, growing fibroblast was present in between the majority of blood vessels, capillaries and inflammatory cells, but much less mature collagen fibers were visible with fibroblastic condensation, showing delayed and early stage of wound healing. FCP treated mice (**Figure 7B**) showed growing fibroblasts present between blood vessels and inflammatory cells and thin collagen fibrils, which is an intermediate stage of collagen formation, were common. Mature collagen was also present. The amount of collagen formed was comparatively greater than the untreated mice and less than the cocktail and antibiotic treated groups. LCP treated animals showed maximum formation of mature collagen among all the groups (**Figure 7C**). As is clearly evident that collagen recovered from individual thin fibrils in the dermis into thick bundles or fibers, indicating that mostly mature collagen was present. This correlated well with the less bacterial bioburden on day 5. Together with decreased vascularity and reduced inflammatory cells, the results suggest late stage of wound healing because collagen formation is one of the essential markers of wound healing. Clarithromycin treated animal group also showed presence of mature thick collagen fibers but thin collagen fibrils were comparatively more than LCP treated mice (**Figure 7D**).

Histopathological examination

For histopathological examination, wound tissue was taken on day 5 in order to study tissue damage and extent of wound healing in all the groups. **Figure 8A** depicts wound tissue of untreated animals (group 1). Acute inflammation associated with surface ulceration and breached epidermal layer was seen. A zone of acute inflammatory (AI) reaction with large numbers of infiltrating inflammatory cells and development of vascular granulation tissue (GT) showing large number of capillaries, blood vessels, and inflammatory cells is also visible. But mice receiving FCP (group 2) showed formation of epidermal buds extending toward dermis (**Figure 8B**), growing fibroblasts

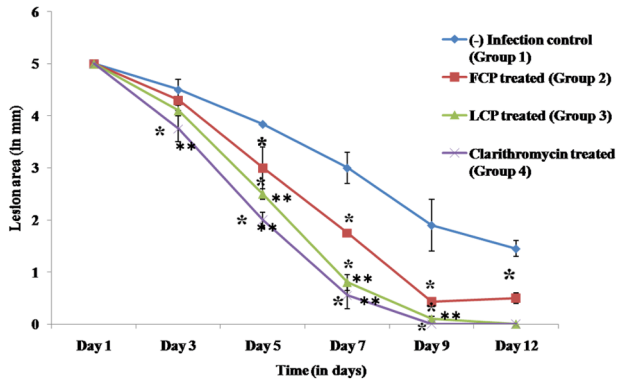

FIGURE 5 | Biometric analysis (mm) of wound area of *S. aureus* 43300 (10^8 CFU/50 μl) infected animals (n = 14, each group) following treatment with FCP, LCP, and clarithromycin. Lesion area was measured on various days post-infection. Error bars represent the standard deviation (SD) from three independent values. *$P < 0.05$ indicate statistical significant differences (Student's t-test) between infected control and treated groups. **$P < 0.05$ indicate statistical significant differences between FCP treated and other treated groups (i.e., LCP and clarithromycin treated).

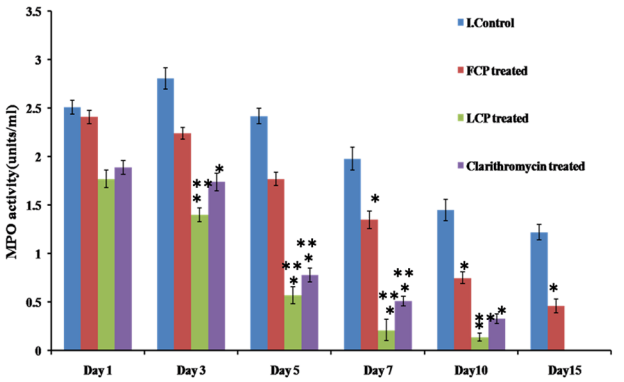

FIGURE 6 | Comparison of MPO levels in the wound tissue of *S. aureus* 43300 (10^8 CFU/50 μl) infected animals (n = 14, each group) following treatment with LCP, FCP, and clarithromycin on different days post-infection. Error bars represent the standard deviation (SD) from three independent values. *$P < 0.05$ indicate statistical significant differences (Student's t-test) between infected control and treated groups. **$P < 0.05$ indicate statistical significant differences between FCP treated and other treated groups (i.e., LCP and clarithromycin treated).

in the granulation tissue and collagen formation, indicating healing along with presence of less inflammatory cells. Hair follicles were also visible indicating regeneration of damaged skin. Similarly, clarithromycin treated mice (group 4) showed progressively reduced inflammation with few neutrophils present in the wound tissue (**Figure 8E**). Presence of granulation tissue with fibroblasts, collagen formation, and epidermal buds indicated rapid and significant wound healing in clarithromycin treated group. However, maximum healing with minimum tissue infiltration and damage was clearly visible in the wound tissue of mice treated with LCP as compared to free phage cocktail treated groups (**Figures 8C,D**). In LCP treated group a thick eschar (Ec) over the surface consisting of necrosed cells in dense eosinophillic coagulated protein background was visible. Epidermal healing was accompanied with hyperplasia of epidermis with buds and streaks extending deep into the dermis. Fewer growing fibroblasts and mostly collagen was seen in the granulation tissue with decreased vascularity and reduced inflammatory cells. Presence of hair follicles was also evident. These results indicate significant wound healing by day 5. This effect might be due to the higher number of phages present at the wound site as compared to phage titre in case of FCP treated animals.

DISCUSSION

Bacteriophage therapy represents an attractive treatment option for the eradication of *S. aureus* induced diabetic wound infections. Sunagar et al. (2010) reported significant protection in diabetic mice (90% survival rate) from lethal bacteremia following single injection of *S. aureus* specific phage (phage GRCS). Similarly, VinodKumar et al. (2011) demonstrated that wounds of diabetic rats which were infected with *S. aureus* were sterilized within 8 days after receiving monophage treatment. Chhibber et al. (2013) focused on the synergistic use of phage and antibiotic in the effective resolution of hindpaw infection in diabetic mice. However, in all of these studies monophage therapy was employed. Monophage based therapies suffer from the drawback of easy emergence of phage resistant bacterial mutants as well as their inability to cover a broad range of possible host targets (Scott et al., 2007; Labrie et al., 2010; Chadha et al., 2016). Thus, use of phage cocktail by incorporating different phages covering the broad host range can provide an effective solution that can be readily delievered without any delay, making it potentialy more effective clinically than monophage therapy (Chan et al., 2013).

In the present study, two already characterized *S. aureus* specific lytic phages, i.e., MR-5 and MR-10 (Kaur et al., 2012; Chhibber et al., 2013) belonging to *Myoviridae* family, were used to study therapeutic efficacy in resolving diabetic wound infection. The main focus of this study was to overcome two major drawbacks of phage therapy. Firstly, therapeutic efficacy of phage cocktail therapy (FCP) was studied and compared with monophage therapy in treatment of MRSA mediated wound infection. The results indicated that when phages were used singly or in cocktail (FCP) there was 100% protection as compared to untreated controls. However, more rapid reduction in bioburden and faster wound healing with FCP treated animals.

Secondly, the problem of potentially low phage retention and persistence *in vivo* was addressed by the use of lipid based carriers, i.e., liposomes. On studying the phage titer post-infection, it was found that phage titer dropped to 10^5 PFU/ml from an initial titer of 10^9 PFU/50 μl within 24 h of phage administration, resulting in presence of low phage number around the wound site. This low titer could be due to phage inactivation by skin's extensive armamentarium of immune-competent cells, that contributed toward delayed phage effect

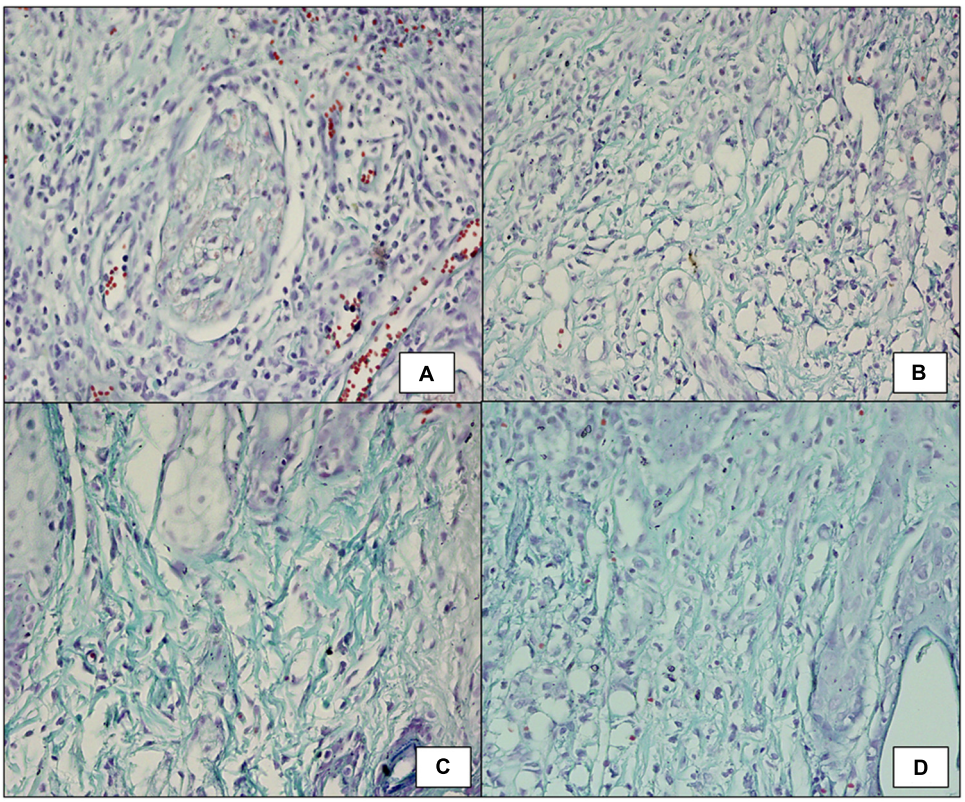

FIGURE 7 | Masson's Trichrome staining (100X) showing collagen formation on day 5 post-infection and treatment in wound tissue of **(A)** infected control mice (diabetic untreated mice) showed fibroblastic condensation along with infiltration of neutrophils. **(B)** Mice treated with FCP showed intermediate stage of collagen formation along with presence of mature collagen fibrils. **(C)** Mice treated with LCP showed thin fibrils of mature collagen present with decreased vascularity and reduced inflammatory cells. **(D)** Mice treated with clarithromycin showed negligible inflamation along with presence of mature collagen fibers, indicating significant wound healing.

(Merril et al., 1996; Keen, 2012; Abedon et al., 2014). The wound bio-burden initially increased as only 10^5 phages were present at the wound site on day 1. The lower number of phage particles probably was unable to tackle the high bacterial load of actively multiplying bacterial population. But as phage growth occurred at the expense of host bacteria, this prevented further increases in bacterial count. This delayed protective response needs to be addressed by preventing rapid phage inactivation and clearance from infection site. Although past workers have made attempts to overcome this problem, however, each approach has its own limitations.

Liposome Entrapment

Our laboratory has for the first time reported successful entrapment of phages within suitable lipid based delivery system, i.e., liposomes that are biocompatible and help to maintain phage titer within *in vivo* system (Singla et al., 2015; Chadha et al., 2017). In another study, encapsulation of *Salmonella* specific phages led to increased stability, prolonged intestinal residence and enhanced therapeutic efficacy (Colom et al., 2015). Liposomes have been regarded as effective DDS due to their GRAS (generally regarded as safe) status, high biocompatibility and high diffusivity in skin as compared to bare drugs (Verma et al., 2003). For drug delivery application liposomes are usually unilamellar and range in diameter from 100 to 300 nm. Large liposomes are rapidly removed from the blood circulation (Barenholz, 1998). Therefore, it is very important to optimize the liposome formulation in terms of size so as to maximize drug loading and minimize leakage and rapid clearance from body. Finally, the cocktail of phages MR-5 and MR-10 (10^9 PFU/50 μl) (1:1) was entrapped within the liposome after optimizing the conditions required for their production and stability. Cocktail entrapped liposomal formulation (LCP) was of unilamellar nature, devoid of any observed aggregation, having a size of 212 nm and exhibited high entrapment efficiency of 87%. Stability studies in terms of size were conducted over a 9 week long period at different temperatures. The liposomal formulation was found to be most stable at 4°C without any physical changes or reduction in number of entrapped phages during storage period. However, at 37°C, an increase in particle size and aggregation was seen in the suspension. Leakage of entrapped drug from the liposomal formulation during storage before administration can lead to poor action of the administered drug (Nallamothu et al., 2006). The results are in consonance with the previous findings of Parmar et al. (2010) who showed that high temperature caused increase in size and aggregation

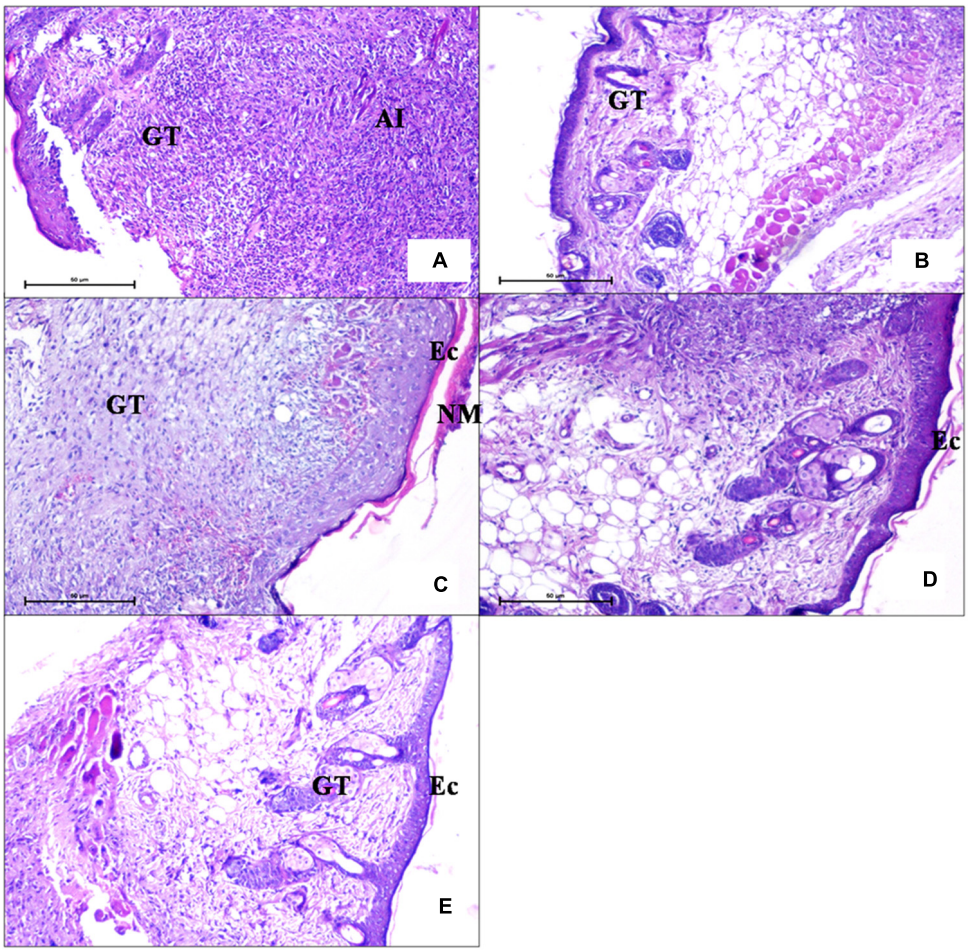

FIGURE 8 | Photomicrographs of wound tissue of **(A)** an infection control mice (diabetic untreated mice) (H and E 100X) showed presence of acute inflammation. **(B)** Mice treated with FCP showed less infiltration of neutrophils and presence of granulation tissue **(C,D)** Mice treated with LCP showed epidermal hyperplasia coupled with reduced inflammation. **(E)** Mice treated with clarithromycin showed nearly normal epidermis with granulation tissue and sweat glands, indicating wound healing (GT, granulation tissue; AI, acute inflammatory; NM, necrotic material; EC, eschar).

as well as leakage of drug from liposomal formulation of budesonide.

The therapeutic efficacy of LCP was evaluated in Study 2. The wound bio-burden correlated well with the visible healing of the wound. No mortality occurred in any of the treatment groups. Maximum reduction was obtained on day 3 in mice treated with liposome entrapped cocktail as compared to infection control group. The entire process of wound healing and re-epithelization was faster and quicker in mice receiving LCP as compared to both untreated diabetic mice as well as animals that received FCP. No phage was present after day 10 in the wound tissue. However, phage titer was higher on all subsequent days in mice treated with liposome entrapped phage cocktail. A significant enhancement of 2 log was observed in LCP mice, clearly indicating that drop in initial titer and phage viability could be prevented by phage entrapment within liposomes. Also, as noted, workers in the past have shown that use of DDS improves the pharmacokinetics and bio-distribution of the associated drug (Allen and Cullis, 2004; Zhang et al., 2013). In addition, efficient uptake of encapsulated bacteriophage by eukaryotic cells has also been reported (Nieth et al., 2015; Singla et al., 2016).

Faster Wound Healing

Wound contraction also demonstrated comparatively rapid healing (measured in terms of wound size) in all the treated groups as compared to infection control mice. Less number of days required for healing and obtaining sterile wounds was due to increased phage titer at wound site in LCP treated mice. Liposomes provided a depot effect and prevented phages from getting cleared off rapidly from the site. This rapid wound healing by day 9 also correlated well with the maximum deposition of mature collagen fiber in wound tissue by day 5 in animals treated with LCP. Mature collagen is an essential marker of wound healing and represents later stages of wound healing (Braiman-Wilksman et al., 2007; Suvik and Effendy, 2012). Histopathological examination of wound tissue of animals also supported these findings, and confirmed that those mice that

received LCP showed minimal tissue damage and inflammation as compared to other groups. Epidermal healing and good amount of granulation tissue indicated significant wound healing by day 5. Besides this, maximum decrease in tissue MPO levels was also seen in group receiving LCP. This could be due to the broad spectrum effect of phage cocktail against MRSA, which efficiently arrested growth of invading bacteria at the site of injury, leading to decrease in neutrophil accumulation that correlated well with tissue healing.

From these observations it is concluded that although FCPs is a better option than monophage therapy, rapid inactivation of phages subsequently affects their ability in clearing the infectious agent. Liposomes are suitable delivery systems that help to increase the therapeutic efficacy of phages by improving their stability and delayed clearance by allowing timely release of phages at the infection site, leading to faster healing. The findings of this study thus provide new insights in the treatment of diabetic wound infection not explored by past workers. The use of liposome entrapped phage preparation is an attractive option.

AUTHOR CONTRIBUTIONS

SC: conceived and designed the experiments/contributed reagents/materials/analysis tools. JK and SK: performed the experiments. SC and SK: analyzed the data. SC, JK, and SK: wrote the paper.

FUNDING

This work was supported by Department of Microbiology, Panjab University, Chandigarh, DST-PURSE and UGC-SAP, New Delhi.

REFERENCES

Abedon, S. T., Kuhl, S. J., Blasdel, B. G., and Kutter, E. M. (2014). Phage treatment of human infections. *Bacteriophage* 1, 66–85. doi: 10.4161/bact.1.2.15845

Allen, T. M., and Cullis, P. R. (2004). Drug delivery systems: entering the mainstream. *Science* 303, 1818–1822. doi: 10.1126/science.1095833

Axelrod, L. (1985). Infections in the diabetic patients. *Clin. Diabetes* 3:98.

Bader, M. S. (2008). Diabetic foot infection. *Am. Fam. Physician* 78, 71–79.

Barenholz, Y. (1998). "Design of liposome-based drug carriers: from basic research to application as approved drugs," in *Medical Applications of Liposomes*, eds D. D. Lasic and D. Papahadjopoulos (New York, NY: Elsevier Science BV), 545–565.

Barrow, P. A., and Soothill, J. S. (1997). Bacteriophage therapy and prophylaxis: rediscovery and renewed assessment of potential. *Trends Microbiol.* 5, 268–271. doi: 10.1016/S0966-842X(97)01054-8

Bhatia, A., Kumar, R., and Katare, O. P. (2004). Tamoxifen in topical liposomes: development, characterization and in-vitro evaluation. *J. Pharm. Pharm. Sci.* 7, 252–259.

Braiman-Wilksman, L., Solomonik, R. S., and Tennenbaum, T. (2007). Novel insights into wound healing sequence of events. *Toxicol. Pathol.* 35, 767–779. doi: 10.1080/01926230701584189

Brans, T. A., Dutrieux, R. P., Hoekstra, M. J., Kreis, R. W., and du Pont, J. S. (1994). Histopathological evaluation of scalds and contact burns in the pig model. *Burns* 20, 48–51. doi: 10.1016/0305-4179(94)90090-6

Bull, J. J., Levin, B. R., DeRouin, T., Walker, N., and Bloch, C. A. (2002). Dynamics of success and failure in phage and antibiotic therapy in experimental infections. *BMC Microbiol.* 2:35. doi: 10.1186/1471-2180-2-35

Capparelli, R., Parlato, M., Borriello, G., Salvatore, P., and Iannelli, D. (2007). Experimental phage therapy against *Staphylococcus aureus* in mice. *Antimicrob. Agents Chemother.* 51, 2765–2773. doi: 10.1128/AAC.01513-06

Carlton, R. M., Noordman, W. H., Biswas, B., de Meester, E. D., and Loessner, M. J. (2005). Bacteriophage P100 for control of *Listeria monocytogenes* in foods: genome sequence, bioinformatic analyses, oral toxicity study, and application. *Regul. Toxicol. Pharmacol.* 43, 301–312. doi: 10.1016/j.yrtph.2005.08.005

Chadha, P., Katare, O. P., and Chhibber, S. (2016). In vivo efficacy of single phage versus phage cocktail in resolving burn wound infection in BALB/c mice. *Microb. Pathog* 99, 68–77. doi: 10.1016/j.micpath.2016.08.001

Chadha, P., Katare, O. P., and Chhibber, S. (2017). Liposome loaded phage cocktail: enhanced therapeutic potential in resolving *Klebsiella pneumoniae* mediated burn wound infections. *Burns* 43, 1532–1543. doi: 10.1016/j.burns.2017.03.029

Chan, B. K., Abedon, S. T., and Loc-Carrillo, C. (2013). Phage cocktails and the future of phage therapy. *Future Microbiol.* 8, 769–783. doi: 10.2217/fmb.13.47

Chhibber, S., Kaur, T., and Kaur, S. (2013). Co-therapy using lytic bacteriophage and linezolid: effective treatment in eliminating methicillin resistant *Staphylococcus aureus* (MRSA) from diabetic foot infections. *PLoS One* 8:e56022. doi: 10.1371/journal.pone.0056022

Colom, J., Cano-Sarabia, M., Otero, J., Cortés, P., Maspoch, D., and Llagostera, M. (2015). Liposome-encapsulated bacteriophages for enhanced oral phage therapy against *Salmonella* spp. *Appl. Environ. Microbiol.* 81, 4841–4849. doi: 10.1128/AEM.00812-15

Fish, R., Kutter, E., Wheat, G., Blasdel, B., Kutateladze, M., and Kuhl, S. (2016). Bacteriophage treatment of intransigent diabetic toe ulcers: a case series. *J. Wound Care* 25, 27–33. doi: 10.12968/jowc.2016.25.Sup7.S27

Fukui, T., Kawaguchi, A. T., Takekoshi, S., Miyasaka, M., and Tanaka, R. (2012). Liposome-encapsulated hemoglobin accelerates skin wound healing in mice. *Artif. Organs* 36, 161–169. doi: 10.1111/j.1525-1594.2011.01371.x

Goodridge, L., Gallacci, A., and Griffiths, M. W. (2003). Morphological, host range and genetic characterization of two coliphages. *Appl. Environ. Microbiol.* 69, 5364–5371. doi: 10.1128/AEM.69.9.5364-5371.2003

Greenberger, M. J., Strieter, R. M., Kunkel, S. L., Danforth, J. M., Laichalk, L. L., McGillicuddy, D. C., et al. (1996). Neutralization of macrophage inflammatory protein-2 attenuates neutrophil recruitment and bacterial clearance in murine *Klebsiella pneumonia*. *J. Infect. Dis.* 173, 159–165. doi: 10.1093/infdis/173.1.159

Gregoriadis, G. (1995). Engineering liposomes for drug delivery: progress and problems. *Trends Biotechnol.* 13, 527–537. doi: 10.1016/S0167-7799(00)89017-4

Gulati, M., Grover, M., Singh, M., and Singh, S. (1998). Study of azathioprine encapsulation into liposomes. *J. Microencapsul.* 15, 485–494. doi: 10.3109/02652049809006875

Hanlon, G. W. (2007). Bacteriophages: an appraisal of their role in the treatment of bacterial infections. *Int. J. Antimicrob. Agents* 30, 118–128. doi: 10.1016/j.ijantimicag.2007.04.006

Hsieh, S. E., Lo, H. H., Chen, S. T., Lee, M. C., and Tseng, Y. H. (2011). Wide host range and strong lytic activity of *Staphylococcus aureus* lytic phage Stau2. *Appl. Environ. Microbiol.* 77, 756–761. doi: 10.1128/AEM.01848-10

Hua, S. (2015). Lipid-based nano-delivery systems for skin delivery of drugs and bioactives. *Front. Pharmacol.* 6:219. doi: 10.3389/fphar.2015.00219

Kaur, S., Harjai, K., and Chhibber, S. (2012). Methicillin-resistant *Staphylococcus aureus* phage plaque size enhancement using sublethal concentrations of antibiotics. *Appl. Environ. Microbiol.* 78, 8227–8233. doi: 10.1128/AEM.02371-12

Kaur, S., Harjai, K., and Chhibber, S. (2014). Bacteriophage mediated killing of *Staphylococcus aureus in vitro* on orthopaedic K wires in presence of linezolid prevents implant colonization. *PLoS One* 9:e90411. doi: 10.1371/journal.pone.0090411

Keen, E. C. (2012). Phage therapy: concept to cure. *Front. Microbiol.* 3:238. doi: 10.3389/fmicb.2012.00238

King, L. (2001). Impaired wound healing in patients with diabetes. *Nurs. Stand.* 15, 39–45. doi: 10.7748/ns2001.06.15.38.39.c3039

Kumari, S., Harjai, K., and Chhibber, S. (2009). Efficacy of bacteriophage treatment in murine burn wound infection induced by *Klebsiella pneumoniae*. *J. Microbiol. Biotechnol.* 19, 622–628.

Kumari, S., Harjai, K., and Chhibber, S. (2011). Bacteriophage versus antimicrobial agents for the treatment of murine burn wound infection caused by *Klebsiella pneumoniae* B5055. *J. Med. Microbiol.* 60, 205–210. doi: 10.1099/jmm.0.018580-0

Kurilko, N. L., Kiiamov, A. K., Ivanova, M. A., Pashkov, E. P., Aleksandrov, M. T., Sorokoumova, G. M., et al. (2009). Impact of liposomes and ceftriaxone-entrapped liposomes on skin wound healing in rats. *Antibiot. Khimioter.* 54, 25–30.

Labrie, S. J., Samson, J. E., and Moineau, S. (2010). Bacteriophage resistance mechanisms. *Nat. Rev. Microbiol.* 8, 317–327. doi: 10.1038/nrmicro2315

Langley, R., Kenna, D. T., Vandamme, P., Ure, R., and Govan, J. R. W. (2003). Lysogeny and bacteriophage host range within the *Burkholderia cepacia* complex. *J. Med. Microbiol.* 52, 483–490. doi: 10.1099/jmm.0.05099-0

Loghmani, E. (2005). Diabetes mellitus: type 1 and type 2. *Diabetelogia* 27, 998–1010.

Mathera, C. D., and Loncar, D. (2006). Projections of global mortality and burden of disease from 2002 to 2030. *PLoS Med.* 3:e442. doi: 10.1371/journal.pmed.0030442

Mendes, J. J., Leandro, C. I., Bonaparte, D. P., and Pinto, A. L. (2012). A rat model of diabetic wound infection for the evaluation of topical antimicrobial therapies. *Comp. Med.* 62, 37–48.

Merril, C. R., Biswas, B., Carlton, R., Jensen, N. C., Creed, G. J., Zullo, S., et al. (1996). Long-circulating bacteriophage as antibacterial agents. *Proc. Natl. Acad. Sci. U.S.A.* 93, 3188–3192. doi: 10.1073/pnas.93.8.3188

Nallamothu, R., Wood, G. C., Kiani, M. F., Moore, B. M., Horton, F. P., and Thoma, L. A. (2006). A targeted liposome delivery system for combretastatin A4: formulation optimization through drug loading and *in vitro* release studies. *PDA. J. Pharm. Sci. Technol.* 60, 144–155.

Nieth, A., Verseux, C., Barnert, S., Süss, R., and Römer, W. (2015). A first step toward liposome-mediated intracellular bacteriophage therapy. *Expert Opin. Drug Deliv.* 12, 1411–1424. doi: 10.1517/17425247.2015.1043125

Oladeinde, F. O., Kinyua, A. M., Laditan, A. A., Michellin, R., Bryant, J. L., Denaro, F., et al. (2007). Effect of *Cnidoscolus aconitifolius* leaf extract on the blood glucose and insulin levels of inbred type 2 diabetic mice. *Cell. Mol. Biol.* 53, 34–41.

Pan, D., and Liu, H. (2008). Preventive effect of ordinary and hyperimmune bovine colostrums on mice diabetes induced by alloxan. *Afr. J. Biotechnol.* 7, 4369–4375.

Park, S., Rich, J., Hanses, F., and Lee, J. C. (2009). Defects in innate immunity predispose C57BL/6J-Leprdb/Leprdb mice to infection by *Staphylococcus aureus*. *Infect. Immun.* 77, 1008–1014. doi: 10.1128/IAI.00976-08

Parmar, J. J., Singh, D. J., Hegde, D. D., Lohade, A. A., Soni, P. S., Samad, A., et al. (2010). Development and evaluation of inhalational liposomal system of budesonide for better management of asthma. *Indian J. Pharm. Sci.* 72, 442–448. doi: 10.4103/0250-474X.73916

Pendsey, S. P. (2010). Understanding diabetic foot. *Int. J. Diabetes Dev. Ctries.* 30, 75–79. doi: 10.4103/0973-3930.62596

Powlson, A. S., and Coll, A. P. (2010). The treatment of diabetic foot infections. *J. Antimicrob. Chemother.* 65, 3–9. doi: 10.1093/jac/dkq299

Roesken, F., Uhl, E., Curri, S. B., Menger, M. D., and Messmer, K. (2000). Acceleration of wound healing by topical drug delivery via liposomes. *Langenbecks Arch. Surg.* 385, 42–49. doi: 10.1007/s004230050010

Rogers, L. C., and Bevilacqua, N. J. (2009). *MRSA in Diabetic Foot. Podiatry Managment*. Available at: http://www.podiatrym.com/cme/Nov09CME1.pdf

Scott, A. E., Timms, A. R., Connerton, P. L., El-Shibiny, A., and Connerton, I. F. (2007). Bacteriophage influence *Campylobacter jejuni* types populating broiler chickens. *Environ. Microbiol.* 9, 2341–2353. doi: 10.1111/j.1462-2920.2007.01351.x

Singla, S., Harjai, K., Katare, O. P., and Chhibber, S. (2015). Bacteriophage-loaded nanostructured lipid carrier: improved pharmacokinetics mediates effective resolution of *Klebsiella pneumoniae*–induced lobar pneumonia. *J. Infect. Dis.* 212, 325–334. doi: 10.1093/infdis/jiv029

Singla, S., Harjai, K., Katare, O. P., and Chhibber, S. (2016). Encapsulation of bacteriophage in liposome accentuates its entry in to macrophage and shields it from neutralizing antibodies. *PLoS One* 11:e0153777. doi: 10.1371/journal.pone.0153777

Sunagar, R., Patil, S. A., and Chandrakanth, R. K. (2010). Bacteriophage therapy for *Staphylococcus aureus* bacteremia in streptozotocin-induced diabetic mice. *Res. Microbiol.* 161, 854–860. doi: 10.1016/j.resmic.2010.09.011

Suvik, A., and Effendy, A. W. (2012). The use of modified masson's trichrome staining in collagen evaluation in wound healing study. *Malays. J. Vet. Res.* 3, 39–47.

Verma, D. D., Verma, S., Blume, G., and Fahr, A. (2003). Particle size of liposomes influences dermal delivery of substances into skin. *Int. J. Pharm.* 258, 141–151. doi: 10.1016/S0378-5173(03)00183-2

VinodKumar, C. S., Srinivasa, H., Basavarajappa, K. G., Patil, U., Bandekar, N., and Patil, R. (2011). Abrogation of *Staphylococcus aureus* wound infection by bacteriophage in diabetic rats. *Int. J. Pharm. Sci. Drug Res.* 3, 202–207.

Wild, S., Roglic, G., Green, A., Sicree, R., and King, H. (2004). Global prevalence of diabetes: estimates for the year 2000 and projections for 2030. *Diabetes Care* 27, 1047–1053. doi: 10.2337/diacare.27.5.1047

Wills, Q., Kerrigan, C., and Soothill, J. (2005). Experimental bacteriophage protection against *Staphylococcus aureus* abscesses in a rabbit model. *Antimicrob. Agents Chemother.* 49, 1220–1221. doi: 10.1128/AAC.49.3.1220-1221.2005

Xavier, W., Sukumaran, M. T., Varma, A. K., Kumar, H., and Chellan, G. (2014). Emergence of multi drug resistant bacteria in diabetic patients with lower limb wounds. *Indian J. Med. Res.* 140, 435–437.

Zhang, Y., Chan, H. F., and Leong, K. W. (2013). Advanced materials and processing for drug delivery: the past and the future. *Adv. Drug Deliv. Rev.* 65, 104–120. doi: 10.1016/j.addr.2012.10.003

Zylberberg, C., and Matosevic, S. (2016). Pharmaceutical liposomal drug delivery: a review of new delivery systems and a look at the regulatory landscape. *Drug Deliv.* 23, 3319–3329. doi: 10.1080/10717544.2016.1177136

Conflict of Interest Statement: The authors declare that the research was conducted in the absence of any commercial or financial relationships that could be construed as a potential conflict of interest.

Copyright © 2018 Chhibber, Kaur and Kaur. This is an open-access article distributed under the terms of the Creative Commons Attribution License (CC BY). The use, distribution or reproduction in other forums is permitted, provided the original author(s) and the copyright owner are credited and that the original publication in this journal is cited, in accordance with accepted academic practice. No use, distribution or reproduction is permitted which does not comply with these terms.

frontiers in Microbiology

ORIGINAL RESEARCH
published: 04 April 2018
doi: 10.3389/fmicb.2018.00611

Antimicrobial Potential of Epiphytic Bacteria Associated With Seaweeds of Little Andaman, India

Perumal Karthick and Raju Mohanraju*

Department of Ocean Studies and Marine Biology, Pondicherry University, Port Blair, India

Seaweeds of the intertidal regions are a rich source of surface associated bacteria and are potential source of antimicrobial molecules. In the present study, 77 epiphytic isolates from eight different algae collected from Little Andaman were enumerated. On testing for their antimicrobial activities against certain pathogens twelve isolates showed positive and six of them showed significant antimicrobial inhibition zone against *Shigella boydii* type 1, *Shigella flexneri* type 2a, *Shigella dysenteriae* type 5, Enterotoxigenic *Escherichia coli* O115, Enteropathogenic *E. coli* serotype O114, *Vibrio cholera*; O1 Ogawa, *Aeromonas hydrophila, Klebsiella pneumoniae, Staphylococcus aureus.* Based on the activity these six isolates (G1C, G2C, G3C, UK, UVAD, and Tor1) were identified by 16S rRNA gene sequence and were found to belong to the phyla Firmicutes and Proteobacteria. Purified antimicrobial compounds obtained from these isolates were identified by GC-MS. Furan derivatives were identified from G2C *Pseudomonas stutzeri* KJ849834, UVAD *Alcanivorax dieselolei* KJ849833, UK *Vibrio* sp. KJ849837, Tor1 *Exiguobacterium profundum* KJ849838. While 2-Pyrrolidinone, Phenol, 2, 4-bis (1, 1-dimethylethyl) were from G3C *Vibrio owensii* KJ849836 and (1-Allylcyclopropyl) methanol from the extracts of G1C *Bacillus* sp. KJ849835. The results of the present study shows that these six potent isolates isolated from the seaweeds are found to be a source of antimicrobial compounds.

Keywords: ***Alcanivorax dieselolei*, Little Andaman, Furan, *Gracilaria corticata*, seaweeds**

OPEN ACCESS

Edited by:
Noton Kumar Dutta,
Johns Hopkins University,
United States

Reviewed by:
Vinay Kumar,
Savitribai Phule Pune University, India
Osmar Nascimento Silva,
Universidade Católica Dom Bosco, Brazil
Pedro Ismael Da Silva Junior,
Instituto Butantan, Brazil

****Correspondence:***
Perumal Karthick
karthickmicrobes@gmail.com

Specialty section:
This article was submitted to Antimicrobials, Resistance and Chemotherapy, a section of the journal Frontiers in Microbiology

Received: *30 June 2017*
Accepted: *16 March 2018*
Published: *04 April 2018*

Citation:
Karthick P and Mohanraju R (2018) Antimicrobial Potential of Epiphytic Bacteria Associated With Seaweeds of Little Andaman, India. Front. Microbiol. 9:611. doi: 10.3389/fmicb.2018.00611

INTRODUCTION

Marine eukaryotes such as seaweeds are one of the primary producers which offers nutrient rich environment for microbial communities (Egan et al., 2008; Wahl, 2008). Biofilm forming bacteria isolated from the surface of seaweeds release certain compounds (Zheng et al., 2005) which serve as nutrient supplement for the algae (Croft et al., 2005), such compounds protect the host plant from the fouling communities (Rao et al., 2007). Surface associated marine organisms such as bacteria, fungi, diatoms, larval forms of marine invertebrate's have been reported to be associated with the thallus of seaweeds (Goecke et al., 2010; Burke et al., 2011; Murthy et al., 2016; Karthick and Mohan, 2017). Such host association particularly epiphytic bacteria are sources of certain natural compounds (Singh et al., 2011; Ali et al., 2012; Martin et al., 2014). Importance of microbial diversity of seaweeds, particularly bacterial genus are highly host specific with novel species, which have emerged from these algal environment (Goecke et al., 2013).

The secondary metabolites produced by these bacteria are highly recognized for their importance in the field of biomedical applications (Armstrong et al., 2001; Kelecom, 2002; Burgess et al., 2003). Antimicrobial activity of the epiphytic bacterial communities from seaweeds have been reported (Kanagasabhapathy et al., 2006, 2008; Vijayalakshmi et al., 2008; Ravisankar et al., 2013; Horta et al., 2014; Martin et al., 2014; Karthick et al., 2015a), similarly anti-diatom activity have also been observed by Kumar et al. (2011). In the Andaman Islands, luxuriant growth of all the three groups of seaweeds are available throughout the year. Some studies on taxonomy of seaweeds have been carried out in this region but information on the epiphytic interaction and its potentiality has not been undertaken. Based on the occurrence of seaweeds in Little Andaman and their bacterial association, the present study has been undertaken to describe the isolation of epiphytic bacterial, screening, optimization, evaluation and identification of potential isolates and their antimicrobial activity against different pathogens as test organisms.

MATERIALS AND METHODS

Isolation of Marine Bacteria

Eight different seaweeds representing all the three groups were handpicked from the intertidal region of Harminder Bay Bridge, Little Andaman, Andaman Islands, India. Among these, six species *Gracilaria corticata, Acanthophora spicifera* (red algae), *Ulva lactuca* (green algae), *Sargassum swartzii, Turbinaria ornata,* and *Padina tetrastromatica* (brown algae) are common and other two species *Mastophora rosea* (red algae) and *Caulerpa microphysa* (green algae) were found to be rare in occurrence in these islands. The collected samples were placed in sterile plastic bags and transported to the laboratory. These were washed thrice with autoclaved seawater to remove loosely bounded epiphytes, sand particles and other attached settlements on the surface of thallus. After rinsing, firmly attached epiphytic bacteria from thallus region were swabbed with sterile cotton buds and these were then swabbed on Zobell marine agar plate (Himedia). Plates were incubated for 5 days at 32°C (Lemos et al., 1985). After incubation, colonies were picked and restreaked for the isolation of individual colonies and the purity of the isolates were checked under the microscope for single morphology. These pure cultures obtained were stored at −20°C in marine broth supplemented with 20% glycerol.

Antimicrobial Assay of Epiphytic Bacteria

The antagonistic activity of epiphytic bacteria obtained were studied on solid media by cross streaking and double-layer method described Lemos et al. (1985) and agar well diffusion method by Karthick et al. (2013b).

Extraction of Antimicrobial Compounds

All the 77 isolates were cultured on 100ml marine broth, Luria broth and minimal media by modifying the methodology slightly by decreasing the incubation time and by increasing the temperature for obtaining better results. The culture broth was centrifuged at 10000 rpm for 30 s to remove the cells and cell free broth was extracted thrice with 100 ml of ethyl acetate. All the solvents were removed under reduced pressure at 40°C (Zheng et al., 2005). Crude extracts obtained were stored at −20°C until usage for the antimicrobial assay against targeted pathogens. Sterile media without culture being adjusted to pH 7 were used as control.

Minimal Medium

All the potential isolates were cultured in inorganic salt medium referred to as minimal medium for the extraction of secondary metabolites (Jafarzade et al., 2013).

Inoculum Preparation

Potential cultures were cultivated in 100 ml minimal medium supplemented with 3% NaCl, 1% glucose and 1% yeast extract as carbon and nitrogen sources in a 250 ml Erlenmeyer flask and incubated at 32°C for 24 h in an incubator shaker. Five milliliter of this culture was used as bacterial (Starter) culture (Jafarzade et al., 2013).

Effect of pH

1 ml of starter cultures were grown with minimal media supplemented with 3% NaCl, 1% glucose, and 1% yeast extract prepared and inoculated with minimal media supplemented with 0.75% of sodium chloride, 1% of glucose and yeast extract for the production of antimicrobial compounds with various pH levels (6–8) at 32°C for 5 days. After incubation, supernatant was extracted three times with ethyl acetate (EtOAc). The sterile media without the culture adjusted to pH was used as control. The extracts were then tested for antimicrobial activity.

Effect of Sodium Chloride Concentration

100 ml of minimal medium was dispensed into 250 ml Erlenmeyer flasks and sterilized. Yeast extract (1%) and glucose (1%) were filter sterilized and added as nitrogen and carbon sources just prior to inoculation. One milliliter of the starter culture was inoculated into the sterilized medium. Effect of salinity in the production of antimicrobial properties at various concentrations of sodium chloride ranging from 1 to 3% with constant pH of 7 at 32°C for 5 days was experimented. After incubation cell free supernatant was extracted three times with ethyl acetate (EtOAc). Sterile media without the inoculum adjusted with various concentration of sodium chloride was used as control (Jafarzade et al., 2013). The extracts were then tested for antimicrobial activity.

Effect of Different Concentrations of Glucose and Yeast Extract

Effect of different concentration (1–3%) of glucose and yeast extract for the production of antimicrobial compound by the epiphytic bacterial isolates was studied using 1 ml of the starter culture inoculated into the minimal medium. Other parameters such as pH 7 and 0.75% sodium chloride were maintained at optimum level during the primary screening at

32°C for 5 days. After incubation supernatant was extracted three times with ethyl acetate (EtOAc). The sterile medium containing glucose, yeast extract and sodium chloride was used as control. The extracts were then tested for antimicrobial activity.

Test Microorganisms

Eighteen bacterial pathogens namely *Escherichia coli* MTCC 443, *Klebsiella pneumoniae* MTCC 109, *Salmonella typhi* MTCC 733, *Staphylococcus aureus* MTCC 96, *Shigella flexneri* MTCC 1457, *Shigella flexneri* type2a 503004, *Shigella boydii* type 1 NK2379, *Shigella sonnei* NK4010, *Shigella dysenteriae* type 5 NK2440, Enterotoxic *E. coli* serotype 0115, Enteropathogenic *E. coli* serotype 0114, Shiga toxin producing *E. coli* serotype O157:H7 VT3, *Vibrio fluvialis* IDH 02036, *Vibrio parahaemolyticus* serovar O3: K6 K5030, *Vibrio cholera* O139, *Vibrio cholera* 01, Ogawa Eltor, *Aeromonas hydrophila* IDH1585, *Salmonella enterica* serovar typhi C6953 and three fungal strains *Aspergillus niger, Aspergillus flavus* and *Rhizopus* sp. were used for studying the antibacterial and antifungal assay.

Determine Minimum Inhibitory Concentration of TLC Purified Metabolites

Minimum inhibitory concentration (MIC) of TLC purified metabolites of potential six isolates (G1C, G2C, G3C, UK, UVAD, and Tor1) was tested against *Klebsiella pneumoniae* and *Staphylococcus aureus* and it was determined by well diffusion assay. 50 mg of TLC purified extracts was dissolved in 1 ml DMSO. 50 and 100 μl/ml concentration of 50 mg/ml concentration of purified extracts was transferred into the well prepared (9 mm) with well cutter. Gentamicin was used as a positive control and Dimethyl sulfoxide (DMSO) was used as a negative control. Growth inhibition zone formed after the incubation was examined with measuring the diameter (mm) and results were recorded. All the assay was performed in triplicates.

Partial Purification and GC-MS Analysis

Concentrated fractions were fractioned by Thin Layer Chromatography (TLC) using Silica gel plates with different solvents in a ratio of 2:2:1 ethyl acetate, chloroform and methanol. Bands was scraped from the plates and screened for antimicrobial assay. Active fraction was collected and analyzed by Gas Chromatography and Mass spectrometry GC-MS QP 2010 Shimadzu Corp (Japan). One μl of purified fractioned extract was loaded into the DB-5 Column with Helium as a carrier gas at a flow rate of 1 ml/min. Split Injection mode of the ratio of 1:20 was adopted. Temperature programming was from 75°C for 2 min further increased to 175°C with 15°C/min and then increased up to 280°C at the rate of 5°C/min. Sample run time was maintained upto 10 min. The peaks representing mass to charge ratio characteristic of the antimicrobial fractions were compared with those in the mass spectrum of NIST library identifying the corresponding organic antimicrobial compounds.

Phenotypic Characterization

Phenotypic characterization of all the seventy seven bacterial isolates were identified following as described in the Bergey's manual of systemic Bacteriology (Brenner et al., 2005).

Molecular Identification by 16S rDNA Sequencing

Genomic DNA was prepared from the bacterial isolates by following the method of Mohandass et al. (2012). PCR amplification of 16S rRNA gene was conducted in a final volume of 25 μl with the bacterial consensus universal forward and reverse 16S rDNA primers 27F and 1492R (Lane, 1991). The reaction mixture contained 1x PCR buffer (Sigma, United States), 2.5 mM $MgCl_2$, 200 μM DNTP's, 1U of Taq DNA polymerase, 25 picomol of each forward and reverse oligonucleotide primers and approximately 20 ng of genomic DNA. The amplification profile consisted of an initial denaturation at 94°C for 3 min, followed by 35 cycles at 94°C for 1 min, 55°C for 1 min and 72°C for 1 min. This was followed by a final extension step of 72°C for 5 min. The samples were held at 4°C until further analysis. The PCR products were sequenced by an automated Sequencer (Applied Biosystems, Foster City, CA, United States) at the National Institute of Oceanography, Goa, India. The sequences were submitted to Gen Bank for which accession numbers were assigned.

BLAST Search and Phylogenetic Analysis

The PINTAIL program (Ashelford et al., 2005) was used to check chimera formations. The partial 16S rRNA gene sequences of the potential isolates were compared with those available in the public databases. Identification upto the species level was determined by a 16S rDNA sequence similarity of more than 99% with that of the prototype sequence in GenBank. Sequence alignment and comparison were performed using the multiple sequence alignment program Clustal X 1.81 (Thompson et al., 1997). Sequences were edited manually to remove the gaps. Neighbor-joining method was employed to construct the Phylogenetic tree using MEGA4 software (Tamura et al., 2007) and the maximum likelihood method was adopted for calculating the evolutionary distance (Tamura et al., 2004).

Bacterial Identification Based on Fatty Acid Methyl Ester (FAME)

Young pure cultures of SG107, 108, 114, 115, 120, and Tor6 were grown on Trypticase Soy Broth Agar (TSBA) for 24 or 48 h at 28°C. The Gas chromatographic analysis of whole cell fatty acid methyl ester (FAME) was performed for further identification and grouping of isolates. FAME extraction were performed using the standard procedures of extraction, purification, and methylation (Sasser, 1990). Fatty acid profiles generated were compared against an inbuilt Sherlock TSBA Library Version 6.0B [S/N 160284] (MIDI Inc., Newark, DE, United States). A similarity index of more than 0.500 was used for clustering of isolates at species level. Cellular fatty acid composition analysis

was done at Regional center of Kochi, National Institute of Oceanography.

RESULTS

Identification of Epiphytic Bacterial Isolates

All the seventy seven cultivable epiphytic bacterial isolates obtained from the thallus of eight different seaweeds were plated on Marine agar. These isolates were purified and based on by phenotypic characterization were assigned to belong to the phylum Firmicutes and Proteobacteria (**Table 1**). Among these isolates, six of them (G1C, G2C, G3C, UK, UVAD, and Tor1) showed wide range of activities against pathogens with an range of 10–30 mm zone of inhibition and were identified by partial 16S rRNA gene sequences (**Table 2**). The isolate G1C showed 99% similarity as *Bacillus* sp., G2C as *Pseudomonas stutzeri,* G3C and UK were identified as *Vibrio owensii* and *Vibrio* sp., respectively. The Isolate UVAD was identified as *Alcanivorax dieselolei* with 99% similarity and Torl strain was identified with 99.7% similarity as *Exiguobacterium profundum* (**Figure 1**).

Six other isolates showed moderate to less activity activities against the pathogens with a range of 5–10 mm zone of inhibition and were identified by FAME analysis. Among them three isolates SG107 as *Bacillus* sp., SG108 *Paenibacillus lentimorbus* and SG115 as *Bacillus sphaericus* belonged to phylum Firmicutes. The other three isolates *Pantoea agglomerans,* SG 120 was *Vibrio aestuarianus* and TR was identified as *Klebsiella pneumoniae ozaena* and were assigned to phylum Proteobacteria, SG114 (**Table 3**).

TABLE 1 | List of bacterial isolates obtained from different seaweeds.

S. no	Name of seaweeds	Number of isolates obtained
	Red algae	
1	*Gracilaria corticata* (J. Agardh) Agardh 1852	9
2	*Acanthophora spicifera* (M.Vahl) Borgesen 1910	11
3	*Mastophora rosea* (C.Agardh) Setchell 1943	6
	Green algae	
4	*Ulva lactuca* Linn 1753	14
5	*Caulerpa microphysa* (Weber van Bosse) J. Feldman	6
	Brown algae	
6	*Sargassum swartzii* (Turner) C. Agardh 1820	14
7	*Turbinaria ornata* (Turner) J. Agardh 1848	7
8	*Padina tetrastromatica* Hauck 1887	10

Antimicrobial Activity of Epiphytic Bacteria

Antimicrobial activity for all the 77 bacterial isolates were tested by adopting three different methods (Agar overlay, cross streaking and agar well diffusion technique) against 21 pathogens. Among these larger zones of inhibition were observed in agar well diffusion assay and this assay was chosen for further antimicrobial activity test. All the isolates were cultured in three different media (marine broth, luria broth and minimal medium) among the medium used minimal media showed broad range of antimicrobial activity (**Table 4**). Based on the preliminary activity only six potential isolates (G1C, G2C, G3C, UK, UVAD, and Tor1) were optimized in minimal medium for the production of antimicrobial compounds.

Zone of Inhibitory Activity With Optimized Bacterial Isolates

Isolate G1C showed strong inhibitory activity against *Shigella boydii* (31 mm), Enterotoxigenic *E. coli* (28 mm), Enteropathogenic *E. coli* and *Aeromonas hydrophila* (23 mm) and this higher inhibition zones were obtained with minimal media supplemented with 1 and 2% Sodium chloride, 1% of glucose and yeast extract with pH in the range of 7–8. Isolate G2C was more effective against Shigatoxin *E. coli* (26 mm), *Aeromonas hydrophila* and *Salmonella typhi* (24 mm) observed from minimal medium containing only 1% of sodium chloride, glucose and yeast extract with pH in the range of 6–7. Isolate G3C was effective against *Salmonella enterica* serovar *typhimurium* (26 mm), *Vibrio cholerae* Eltor and *Shigella dysenteriae* (24 mm) and antimicrobial activity was observed with minimal media with 1 and 2% of sodium chloride, glucose and 1% of yeast extract with pH in the range of 6–7. Isolate TOR1 exhibited broad range of antibacterial activity against *Klebsiella pneumoniae, Shigella dysenteriae* (31 mm), *Shigella sonnei* (25 mm). UVAD isolate showed maximum zone of inhibitory activity against *Staphylococcus aureus* (30 mm), *Salmonella enterica* serovar *typhimurium* (29 mm) and *Shigella dysenteriae* (27 mm) and isolate UK displayed maximum zone of inhibition against *Aeromonas hydrophila* (29 mm), *Shigella flexneri* 2A and *Shigella flexneri* (24 mm), respectively. All these six bacterial isolates showed maximum inhibitory activity against most of the tested pathogens (**Table 4**).

TABLE 2 | 16S rRNA gene sequence identity of six potential bacterial isolates obtained from different seaweeds.

Isolate	Seaweed	Accession number	Identified bacteria	% identity	Phylum
G1C	*Gracilaria corticata*	KJ849835	*Bacillus* sp.	99	Firmicutes
G2C	*Gracilaria corticata*	KJ849834	*Pseudomonas stutzeri*	99	Proteobacteria
G3C	*Gracilaria corticata*	KJ849836	*Vibrio owensii*	100	Proteobacteria
UK	*Mastophora rosea*	KJ849837	*Vibrio* sp.	99	Proteobacteria
UVAd	*Ulva lactuca*	KJ849833	*Alcanivorax dieselolei*	100	Proteobacteria
Tor1	*Turbinaria ornata*	KJ849838	*Exiguobacterium profundum*	100	Firmicutes

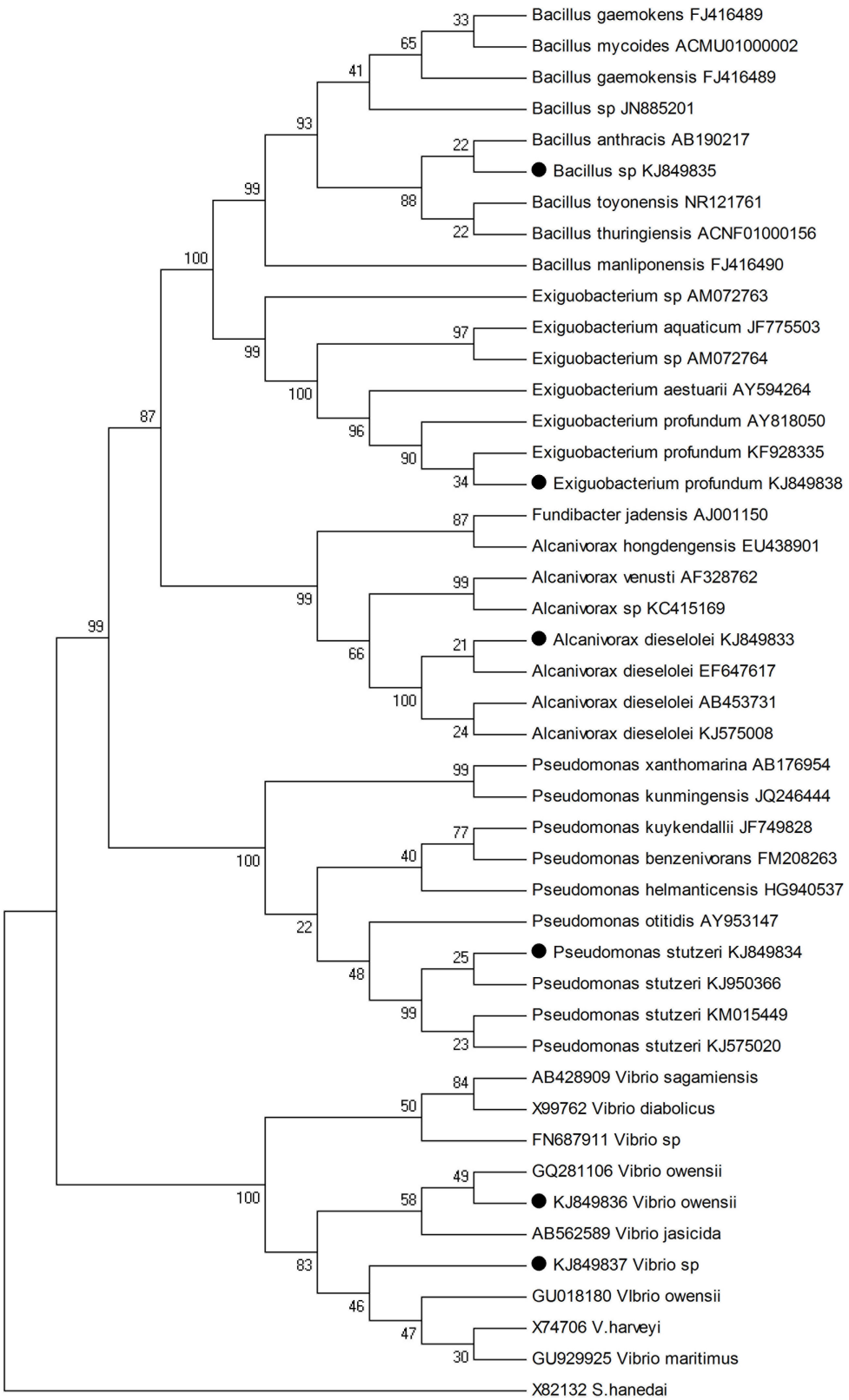

FIGURE 1 | Neighbor-joining phylogenetic tree based on 16S rRNA gene sequences showing the relationship of six potential strains with its closest neighbors. Bootstrap values (50%) are shown at branch points in value and *S. hanedai* X82132 were used as outgroup.

TABLE 3 | Comparison of cellular fatty acid composition of 6 moderate activity identified from brown algae (1) SG107 *Bacillus* sp, (2) SG108 *Paenibacillus lentimorbus*, (3) SG114 *Pantoea agglomerans,* (4) SG115 *Bacillus sphaericus,* (5) SG120 *Vibrio aestuarianus,* (6) Tor6 *Klebsiella pneumoniae ozaenae*.

Fatty acid	SG107	SG108	SG114	SG115	SG120	Tor6
Straight-chain saturated						
14:00	1.99	3.03	0.81	0.75	5.10	9.31
15:00	–	–	–	–	–	–
16:00	8.01	16.57	35.53	1.62	18.34	31.44
17.00	–	–	0.27	–	0.44	–
18:00	1.08	2.48	1.40	0.29	1.33	0.78
Terminally branched saturated						
13:0 iso	0.28	0.43	–	0.11	0.07	–
14:0 iso	8.56	4.58	–	5.67	–	–
15:0 iso	27.43	22.96	–	52.57	0.08	–
16:0 iso	6.11	2.93	–	10.20	0.19	–
17:0 iso	4.50	5.57	0.13	3.75	–	–
18:0 iso	0.28	0.28	–	–	–	–
19:0 iso	–	–	0.51	–	–	0.50
15:0 anteiso	26.59	24.25	–	9.39	–	–
17:0 anteiso	5.57	4.65	–	2.98	–	–
Mono-unsaturated						
16:1w7c alcohol	2.11	0.69	–	6.43	–	–
16:1w11c	4.55	6.41	–	1.71	–	–
Sum of 18:2 w6,9c/18:0 ante	–	0.3	–	–	–	–
Sum of 18:1 w7c	–	0.1	–	–	0.08	–
Sum of 18:1w9c	–	0.20	–	0.16	0.31	–

TABLE 4 | Antimicrobial activity of six potential epiphytic bacterial isolates.

Clinical pathogens	G1C	G2C	G3C	UK	UVAD	Tor1
Shigella boydii type 1	+	++	++	+++	+++	++
Shigella sonnei	+	++	++	–	+++	++
Shigella flexneri	++	–	–	+++	++	++
Shigella flexneri type 2a	++	++	++	+++	++	++
Shigella dysenteriae type 5	–	++	++	+++	+++	+++
Salmonella typhi	+	+	–	+	++	++
Salmonella enterica serovar typhi	+	++	+++	+	++	+
Escherichia coli	++	+	+	++	–	–
Enterotoxigenic *Escherichia coli* O115	++	++	++	+++	++	+
Enteropathogenic *Escherichia coli* serotype O114	++	++	++	+++	++	+
Shiga toxin *Escherichia coli*O157:H7	+	++	++	–	++	+
Aeromonas hydrophila	+	++	++	+++	++	+
Vibrio cholera; O1 Ogawa	++	++	++	–	++	++
Vibrio cholera O139	–	–	–	–	–	–
Vibrio fluvialis	–	–	–	++	+	–
Vibrio parahaemolyticus serovar O3: K6	–	–	–	++	–	–
Klebsiella pneumoniae	+	+	++		+++	+++
Staphylococcus aureus	+	+	++	+++	+++	++

(+) >10 mm, (++) 10–20 mm, (+++), 20–30 mm, (–) No inhibition zone observed.

Identification of Compounds From Purified Extract

Cell free supernatant of the six potential isolates (G1C, G2C, G3C, UK, UVAD, and Tor1) that showed antimicrobial activity were purified by TLC. Results of minimum inhibitory concentration of TLC purified metabolites of all the six potential isolates at 50 mg/mL concentration diluted in 50 and 100 μl/ml concentration showed the positive results against *K. pneumoniae* and *S. aureus*. 50 μl/ml concentration of potential extracts exhibited inhibitory activity against the tested pathogens. Maximum zone of inhibition 10 mm was measured against *K. pneumoniae* by UK, UVAD, Tor1, G1C, and G3C extract at

100 µl concentration. 9 mm zone of inhibition was measured against *S. aureus* by 100 µl concentration of G2C, G3C, UK, and Tor1. Based on the inhibitory growth of bacteria at 50 µl concentration of purified metabolites, it can be concluded that minimum inhibitory concentration was observed at 2.5 mg/mL. Based on the activity purified compounds obtained from these six isolates were characterized and identified. Furan derivatives were found to be present in four of the isolates namely G2C *Pseudomonas stutzeri,* Tor1 *Exiguobacterium profundum*. UVAD *Alcanivorax dieselolei* and UK *Vibrio* sp. While 2-Pyrrolidinone, Phenol, 2, 4-bis (1, 1-dimethylethyl) were identified from the isolate G3C *Vibrio owensii* and (1-Allylcyclopropyl) methanol from G1C *Bacillus* sp.

DISCUSSION

Seaweed biomass were found in large quantities in both intertidal and subtidal regions of all the regions of Andaman Island and in Little Andaman's (Karthick et al., 2013a,b). Good hemolytic activity in certain seaweeds of these Island has been reported recently (Punnam Chander et al., 2014). Besides these studies Karthick et al. (2015b) had reported on antimicrobial activity of certain seaweeds against pathogenic bacterial and fungal stains. Several authors suggested that macro algal associated bacteria were found to be an efficient producer of antimicrobial compounds (Burgess et al., 1999; Lee et al., 2006; Kanagasabhapathy et al., 2008; Karthick et al., 2015a; Ismail et al., 2016). On the other hand, certain brown algae also produced biologically active compounds which inhibited the settlement of bacterial colonies on the thallus (Nagayama et al., 2002).

In the present study it was observed that higher number of epiphytic bacteria were isolated from brown and red algae, certainly the proportion of higher isolates were from brown rather than green and red algae. On surface colonization non-pigmented bacterial isolates were found dominant in most of the seaweeds used in this study. Epiphytic bacteria from marine macro algae have been well studied in reference to their ecological importance with host organisms (Croft et al., 2005) with a dominance of Gram-negative bacteria. Similarly in the present study 46 Gram-negative bacterial isolates were isolated in comparison to 31 being Gram-positive. Bacteria belonging to genus the *Bacillus* were dominant with 20 isolates followed by other genus such as *Vibrio*, *Aeromonas,* and *Pseudomonas*.

Ravisankar et al. (2013) observed that the surface of the brown algae *Hypnea valentiae* and *Padina tetrastromatica* contained more number of non-pigmented bacterial colonies which are similar to our studies wherein 10 isolates were obtained from Padina *tetrastromatica*. Similar observations were observed in Tunisian waters, where 17 isolates were obtained from the thallus of *Ulva intestinalis* (Ali et al., 2010) and 10 isolates were reported from *Ulva lactuca* in Fiji waters, of which majority of the isolates were efficient antimicrobial producers (Kumar et al., 2011).

In the present study twelve isolates (15.7%) of the total 77 isolated exhibited antimicrobial activity and six isolates showed broad spectrum of activity against both bacterial and fungal pathogens. Similarly (Jayanth et al., 2002) isolated 14.52% of associated bacteria from the red algae *Gracilaria* with antagonistic properties against certain human pathogens. On the other hand 11% of associated bacteria isolated from seaweeds were reported to have antagonistic nature against *Bacillus subtilis, E. coli, S. aureus, Agrobacterium tumefaciens,* and *Saccharomyces cerevisiae* (Zheng et al., 2005).

The 16S rRNA sequences of bacterial isolates obtained from the surface of green algae *Ulva australis* and *Delisea pulchra,* belonged to the representative's classes of *Alpha* and *Gammaproteobacteria* and interestingly *Actinobacteria, Firmicutes,* and *Bacteroidetes* were observed as antimicrobial producers (Penesyan et al., 2009). Ali et al. (2012) on 16S rRNA sequence of the isolates obtained from the surface of coralline red algae *Jania rubens* found them belong to the group Proteobacteria. Similar observation made by Singh et al. (2015) also highlighted that bacterial isolates belonged to the order *Bacillales, Pseudomonadales, Alteromonadales,* and *Vibrionales* were dominant in green algae *Ulva lactuca, U. fasciata*, and red algae *Gracilaria corticata* and *G. dura*. In this study also it's evident that all the 77 bacterial isolates were closely related to the phylum Proteobacteria and Firmicutes. These findings substantiate that these groups are more specific to the macro algal surface. Similarly species belonging to the genera *Bacillus* and *Vibrio* were found to be strong antimicrobial producers colonizing more on the surface of seaweeds.

Genus *Bacillus* predominantly colonizes on the surface of marine niche and several studies have been reported *Bacillus* from different marine sources particularly associated with brown algae (Thakur and Anil, 2000) and from the thallus surface of different red algae (Kanagasabhapathy et al., 2008). Apart from their association with seaweeds *Bacillus* were previously isolated from sediments and seaweeds with antimicrobial properties (Prieto et al., 2012). So far, more than 800 metabolites have been reported with various biological activities from the *Bacillus* genera. Recently, cell free supernatant extracted from *Bacillus* associated with a nematode were found to be very effective against multidrug resistant *Staphylococcus aureus* (Susilowati et al., 2015). As observed in the present study one potential isolate G1C identified as *Bacillus* sp. showed remarkable activity against most of the tested pathogens, in particular against toxin producing pathogens like *Shigella boydii*, Enterotoxigenic *E. coli*, Shigatoxin *E. coli* Enteropathogenic *E. coli,* and *Aeromonas hydrophila* etc. Similarly SG107 *Bacillus* sp. and SG115 *Bacillus sphaericus* obtained from the brown algae *Sargassum swartzii* also showed moderate to less activity against few pathogens.

Vibrios being truly marine and they are widespread in various marine niches and are known to produce secondary metabolites for their survival. Earlier genus *Vibrio* sp., *Pseudomonas* sp., and *Bacillus pumilus* were reported to be a probiotic bacteria used in aquaculture (Hill et al., 2009). Kanagasabhapathy et al. (2008) reported that Vibrio strain isolated from red algae showed certain biological activities. In the present study, two potential *Vibrio* isolates GC3 *Vibrio owensii* and UK *Vibrio* sp. were obtained from the surface of red algae *Gracilaria corticata* and *Mastophora rosea,* respectively, and these isolates exhibited wider range of antimicrobial activity against most of the tested pathogens like *Salmonella typhi, Shigella dysenteriae, Vibrio cholerae,* and

Staphylococcus aureus. Similarly, Pawar et al. (2015) extracted antibacterial compounds from marine *Vibrio* sp. which were found to be active against numerous pathogens.

In our study of 14 bacterial isolates were obtained green algae *Ulva lactuca* among these one isolate UVAD *Alcanivorax dieselolei* was found to possess higher range of antimicrobial activity. Previously this species *Alcanivorax dieselolei* has been reported to be isolated from the deep sea sediment involved in degrading alcanes (Liu and Shao, 2005), and petroleum products (Brito et al., 2006). Ali et al. (2010) reported that two epiphytic bacteria obtained from green alga *U. intestinalis* showed potent antimicrobial activity. These studies suggest that green algae *Ulva* species attracts novel bacterial colonization on their surface with potential microbial communities and these isolates produce various compounds to protect the host from the predators and other micro and macro fouling colonization.

Pseudomonas stutzeri has been reported to have wide range of biological activity by the production of secondary metabolites. Previously *Pseudomonas stutzeri* isolated from fish gut exhibited antimicrobial activity (Uzair et al., 2008), hydrocarbon degradation (Vazquez et al., 2009), and reported as uncommon opportunistic pathogen (Park et al., 2013), controlling biofilm formation (Wu et al., 2016). In this study *Pseudomonas stutzeri* isolated from the red algae *Gracilaria corticata* produced antimicrobial compounds which showing potent activity against numerous toxin producing pathogens *S. aureus, Shigella boydii, S. flexneri 2A, S. dysenteriae, K. pneumoniae, Et. E. coli, St. E. coli, V. cholerae* Eltor, *A. hydrophila*.

Earlier *Exiguobacterium* sp. showed antimicrobial properties (Shatila et al., 2013) and this bacterium also known to produce antifouling compound and thus protected the host organisms from fouling communities (Jain et al., 2013). In the present study Tor1 *Exiguobacterium profundum* isolate obtained from *Turbinaria ornata,* showed antibacterial activity against clinical pathogens *S. aureus, Shigella boydii, S. flexneri, S. flexneri 2A, S. dysenteriae, K. pneumoniae, Et. E. coli,* and *St. E. coli*. The same genus was identified in earlier studies from different seaweeds occurring in different geographical locations showing various biological activities. In the present study 6 potential isolates obtained from seaweeds were found to be good antimicrobial producers. The same genus was identified in earlier studies from

TABLE 5 | Biological activities of associated bacteria isolated from seaweeds.

Seaweeds	Associated bacteria	Biological activity	Reference
Jania rubens	*Bacillus firmicutes*	Antimicrobial	Ali et al., 2012
Plocamium telfairiae	*Bacillus anthracis*	Antimicrobial	Kanagasabhapathy et al., 2008
Gelidium amansii	*Bacillus cereus*	Antimicrobial	Kanagasabhapathy et al., 2008
Grateloupia filicina	*Bacillus cereus*	Antimicrobial	Kanagasabhapathy et al., 2008
Porphyra yezoensis	*Bacillus pumilus*	Antimicrobial	Kanagasabhapathy et al., 2008
Lomentaria catenata	*Bacillus clausii*	Antimicrobial	Kanagasabhapathy et al., 2008
Chondrus ocellatus	*Bacillus pumilus*	Antimicrobial	Kanagasabhapathy et al., 2008
Laminaria saccharina	*Bacillus* sp.	Antibacterial	Wiese et al., 2009
Sargassum thunbergii	*Bacillus* sp.	Antimicrobial	Zheng et al., 2005
Ulva lactuca	*Bacillus* sp.	Antidiatom	Kumar et al., 2011
Padina pavonica	*Bacillus pumilus*	Antimicrobial	Ismail et al., 2016
Sargassum sp.	*Bacillus pumilus*	Antibacterial	Susilowati et al., 2015
Gracilaria corticata	*Bacillus* sp.	Antimicrobial	In this study*
Plocamium telfairiae	*Vibrio* sp.	Antimicrobial	Kanagasabhapathy et al., 2008
Ulva lactuca	*Vibrio*	Antidiatom	Kumar et al., 2011
Stoechospermum polypodioides	*Vibrio* sp.	Antifouling	Jain et al., 2013
Laminaria saccharina	*Vibrio* sp.	Antibacterial	Wiese et al., 2009
Stoechospermum polypodioides	*Vibrio* sp.	Antifouling	Jain et al., 2013
Ulva reticulata	*Vibrio* sp.	Antifouling	Harder et al., 2004
Gracilaria corticata	*Vibrio owensii*	Antimicrobial	In this study*
Mastophora rosea	*Vibrio* sp.	Antimicrobial	In this study*
Laminaria saccharina	*Pseudomonas* sp.	Antibacterial	Wiese et al., 2009
Padina pavonica	*Pseudomonas* sp.	Antimicrobial	Ismail et al., 2016
Sargassum sp	*Pseudomonas koreensis*	Antioxidant	Pawar et al., 2015
Chaetomorpha media	*Pseudomonas argentinensis*	Antioxidant	Pawar et al., 2015
Ulva reticulata	*Pseudomonas stutzeri*	Antimicrobial	Dhanya et al., 2016
Gracilaria corticata	*Pseudomonas stutzeri*	Antimicrobial	In this study*
Stoechospermum polypodioides	*Exiguobacterium* sp.	Antifouling	Jain et al., 2013
Turbinaria ornata	*E. profundum*	Antimicrobial	In this study*
Ulva lactuca	*Alcanivorax dieselolei*	Antimicrobial	In this study*

**Indicates the species identified in this study.*

different seaweeds occurring in different geographical locations showing various biological activities (**Table 5**).

In earlier studies Furan derivatives were reported to have antimicrobial properties (Kirilmis et al., 2009; Joshi et al., 2010; Ramasamy and Balasubramanian, 2012), cytotoxic agent (Wang et al., 2008) and were observed to have a wide range of biological activities like antiproliferative, antiviral, antifungal, immunosuppressive, anti-platelet, anti-oxidative, insecticidal, anti-inflammatory, anti-feedant, and cancer preventative activity (Venkateshwarlu et al., 2013). In our present study we have identified Furan compounds from four potential isolates (G2C, UVAD, Tor1, and UK). Apart from antimicrobial properties, these compounds are being used for other pharmacological properties (Bober et al., 2012). In this study G3C *Vibrio owensii* produced antimicrobial compounds such as 2-Pyrrolidinone, Phenol, 2, 4-bisdimetyl ethyl)-ester and Pyrrolo [1,2-a] pyrazine-1,4-dione. Earlier, these compounds were reported to have antimicrobial properties (Sutariya et al., 2012; Khatiwora et al., 2013; Padmavati et al., 2014; Dhanya et al., 2016). Marine *Vibrio* sp. is highly capable of producing Phenol, pyrrolo [1,2-a]pyrazine-1,4-dione, Pyrrolidinone derivative compounds containing pharmacological properties (Pawar et al., 2015). Based on earlier findings and as observed in the present study Vibrios are efficient producer of Phenol and Pyrrolidinone derivatives. In conclusion based on the findings of the present study, the compounds produced from six potential isolates (G1C, G2C, G3C, UK, UVAD, and Tor1) having effective antimicrobial properties, could be further studied for other activities. These isolates could prove to be potential candidates for the production of novel antimicrobial compounds in order to control the pathogens.

AUTHOR CONTRIBUTIONS

PK designed the work, performed all the experiments, analyzed and wrote the manuscript. RM contributed the designation of research work and evaluated the manuscript.

ACKNOWLEDGMENTS

The authors are greatful to Dr. C. Mohandass, Chief Scientist, National Institute of Oceanography (NIO), Goa for sequencing studies, Dr. Anas Abdulaziz, Scientist, Marine Microbial Reference Facility (NIO) RC, Kochi, Dr. R. Babu Rajendran, Professor, Department of Environmental Biotechnology, Bharathidasan University for GC-MS facilities. The authors also thank personally to their colleagues Dr. K. N. Murthy, Dr. C. H. Ramesh, Dr. Sumantha Narayana for their support during field collection and Pondicherry University authorities for providing the facilities.

REFERENCES

Ali, A. I., Bour, M. E., Ktari, L., Bolhuis, H., Ahmed, A., Boudabbous, A., et al. (2012). *Jania rubens*-associated bacteria: molecular identification and antimicrobial activity. *J. Appl. Phycol.* 24, 525–534. doi: 10.1007/s10811-011-9758-0

Ali, I. B., Ktari, L., Bolhuis, H., Boudabbous, A., Stal, L. J., and Bour, M. E. L. (2010). *Ulva intestinalis* associated bacteria: molecular identification and antimicrobial potential. *Rap. Comm. Int. Mer. Medit.* 39:372.

Armstrong, E., Yan, L., Boyd, K. G., Wright, P. C., and Burgess, J. G. (2001). The symbiotic role of marine microbes on living surfaces. *Hydrobiologia* 461, 37–40. doi: 10.1023/A:1012756913566

Ashelford, K. E., Chuzhanova, N. A., Fry, J. C., Jones, A. J., and Weightman, A. J. (2005). At least 1 in 20 16S rRNA sequence records currently held in public repositories is estimated to contain substantial anomalies. *Appl. Environ. Microbiol.* 71, 7724–7736. doi: 10.1128/AEM.71.12.7724-7736.2005

Bober, L., Kawczak, P., and Baczek, T. (2012). Pharmacological classification and activity evaluation of furan and thiophene amide derivatives applying semi-empirical ab initio molecular modeling methods. *Int. J. Mol. Sci.* 13, 6665–6678. doi: 10.3390/ijms13066665

Brenner, D. J., Krieg, N. R., and Staley, J. T. (eds). (2005). *Bergeys Manual of Systematic Bacteriology*. New York, NY: Springer.

Brito, E. M., Guyoneaud, R., Urizza, M., Ranchou-Peyruse, A., Verbaere, A., Crapez, M. C., et al. (2006). Characterization of hydrocarbonoclastic bacterial communities from mangrove sediments in Guanabara Bay, Brazil. *Res. Microbiol.* 157, 752–762. doi: 10.1016/j.resmic.2006.03.005

Burgess, J. G., Boyd, K. G., Armstrong, E., Jiang, Z., Yan, L., Berggren, M., et al. (2003). The development of a marine natural product-based antifouling paint. *Biofouling* 19, 197–205. doi: 10.1080/0892701031000061778

Burgess, J. G., Mearns-Spragg, A., Jordan, E. M., Bregu, M., and Boyd, K. G. (1999). Microbial antagonism: a neglected avenue of natural products research. *J. Biotechnol.* 70, 27–32. doi: 10.1016/S0168-1656(99)00054-1

Burke, C., Thomas, T., Lewis, M., Steinberg, P., and Kjelleberg, S. (2011). Composition, uniqueness and variability of the epiphytic bacterial community of the green alga *Ulva australis*. *ISME J.* 5, 590–600. doi: 10.1038/ismej.2010.164

Croft, M. T., Lawrence, A. D., Raux-Deery, E., Warren, M. J., and Smith, A. G. (2005). Algae acquire vitamin B12 through a symbiotic relationship with bacteria. *Nature* 438, 90–93. doi: 10.1038/nature04056

Dhanya, K. I., Swati, V. I., Vanka, K. S., and Osborne, W. J. (2016). Antimicrobial activity of *Ulva reticulata* and its endophytes. *J. Ocean Univ. China* 15, 363–369.

Egan, S., Thomas, T., and Kjelleberg, S. (2008). Unlocking the diversity and biotechnological potential of marine surface associated microbial communities. *Curr. Opin. Microbiol.* 11, 219–225. doi: 10.1016/j.mib.2008.04.001

Goecke, F., Labes, A., Wiese, J., and Imhoff, J. F. (2010). Chemical interactions between marine macroalgae and bacteria. *Mar. Ecol. Prog. Ser.* 409, 267–299. doi: 10.3354/meps08607

Goecke, F., Thiel, V., Wiese, J., Labes, A., and Imhoff, J. (2013). Algae as an important environment for bacteria – phylogenetic relationships among new bacterial species isolated from algae. *Phycologia* 52, 14–24. doi: 10.2216/12-24.1

Harder, T., Dobretsov, S., and Qian, P.-Y. (2004). Waterborne polar macromolecules act as algal antifoulants in the seaweed *Ulva reticulata*. *Mar. Ecol. Prog. Ser.* 274, 131–141. doi: 10.3354/meps274133

Hill, J. E., Baiano, J. C. F., and Barnes, A. C. (2009). Isolation of a novel strain of *Bacillus pumilus* from penaeid shrimp that is inhibitory against marine pathogens. *J. Fish Dis.* 32, 1007–1016. doi: 10.1111/j.1365-2761.2009.01084.x

Horta, A., Pinteus, S., Alves, C., Fino, N., Silva, J., Fernandez, S., et al. (2014). Antioxidant and antimicrobial potential of the *Bifurcaria bifurcata* epiphytic bacteria. *Mar. Drugs* 12, 1676–1689. doi: 10.3390/md12031676

Ismail, A., Ktari, L., Ahmed, M., Bolhuis, H., Boudabbous, A., Stal, L. J., et al. (2016). Antimicrobial activities of bacteria associated with the brown alga *Padina pavonica*. *Front. Microbiol.* 7:1072. doi: 10.3389/fmicb.2016.01072

Jafarzade, M., Shayesteh, F., Usup, G., and Ahmad, A. (2013). Influence of culture conditions and medium composition on the production of antibacterial compounds by marine *Serratia* sp. WPRA3. *J. Microbiol.* 51, 373–379. doi: 10.1007/s12275-013-2440-2

Jain, S. C., Sivakumar, A. J., and Pandian, P. M. (2013). Surface associated bacteria of marine algae in Kovalam beach, Chennai, had screened for its antifouling activity. *Indian J. Geomarine Sci.* 42, 498–502.

Jayanth, K., Jeyasekaran, G., and Shakila, R. J. (2002). Isolation of marine bacteria, antagonistic to human pathogens. *Ind. J. Mar. Sci.* 31, 39–44.

Joshi, S. D., Ashwini, J., and Gadaginamath, G. S. (2010). Synthesis and antimicrobial evaluation of some new pyrrolylnaphtho [2, 1-b] furan derivatives. *Ind. J. Pharm. Educ. Res.* 44, 148–155.

Kanagasabhapathy, M., Sasaki, H., Haldar, S., Yamasaki, S., and Nagata, S. (2006). Antibacterial activities of marine epibiotic bacteria isolated from brown algae of Japan. *Ann. Microbiol.* 56, 167–173. doi: 10.1007/BF03175000

Kanagasabhapathy, M., Sasaki, H., and Nagata, S. (2008). Phylogenetic identification of epibiotic bacteria possessing antimicrobial activities isolated from red algal species of Japan. *World J. Microbiol. Biotechnol.* 24, 2315–2321. doi: 10.1007/s11274-008-9746-y

Karthick, P., and Mohan, P. M. (2017). Associated epiphytic faunal distribution on brown algae *Sargassum wightii* Greville ex J.Agardh, in the environments, off South Andaman. *J. Terr. Mar. Res.* 1, 41–44.

Karthick, P., Mohanraju, R., Murthy, K. N., and Ramesh, C. H. (2013a). Seaweed potential of Little Andaman, India. *Seaweed Res. Utilin.* 35, 17–21.

Karthick, P., Mohanraju, R., Ramesh, C. H., Murthy, K. N., and Narayana, S. (2013b). Distribution and diversity of seaweeds in North and South Andaman Island. *Seaweed Res. Utilin.* 35, 8–16.

Karthick, P., Mohanraju, R., Mohandass, C., and Rajasabapathy, R. (2015a). Antimicrobial activity of Serratia sp isolated from the coralline red algae *Amphiroa anceps*. *Indian J. Geomarine Sci.* 44, 1857–1866.

Karthick, P., Mohanraju, R., Murthy, K. N., and Ramesh, C. H. (2015b). Antibacterial activity of seaweeds collected from South Andaman, India. *J. Algal Biomass Util.* 6, 33–36.

Kelecom, A. (2002). Secondary metabolites from marine microorganisms. *An. Acad. Bras. Cienc.* 74, 151–170. doi: 10.1590/S0001-37652002000100012

Khatiwora, E., Adsula, V. B., Kulkarni, M., Deshpande, N. R., and Kashalkar, R. V. (2013). Isolation and characterization of substituted dibutyl phthalate from Ipomoea carnea stem. *Der Pharma Chemica* 5, 5–10.

Kirilmis, C., Koca, M., Servi, S., and Gur, S. (2009). Synthesis and antimicrobial activity of dinaphtho[2,1-b]furan-2-yl-methanone and their oxime derivatives. *Turkish J. Chem.* 33, 375–384.

Kumar, V., Rao, D., Thomas, T., Kjelleberg, S., and Egan, S. (2011). Antidiatom and antibacterial activity of epiphytic bacteria isolated from *Ulva lactuca* in tropical waters. *World J. Microbiol. Biotechnol.* 27, 1543–1549. doi: 10.1007/s11274-010-0606-1

Lane, D. J. (1991). "16S/23S rRNA sequencing," in *Nucleic Acid Techniques in Bacterial Systematics*, eds E. Stackebrandt and M. Goodfellow (New York, NY: John Wiley & Sons Inc), 115–175.

Lee, Y. K., Jung, H. J., and Lee, H. K. (2006). Marine bacteria associated with the Korean brown alga, *Undaria pinnatifida*. *J. Microbiol.* 44, 694–698.

Lemos, M. L., Toranzo, A. E., and Barja, J. L. (1985). Antibiotic activity of epiphytic bacteria isolated from intertidal seaweeds. *Microbial. Ecol.* 11, 149–163. doi: 10.1007/BF02010487

Liu, C., and Shao, Z. (2005). *Alcanivorax dieselolei* sp. nov., a novel alkane-degrading bacterium isolated from sea water and deep-sea sediment. *Int. J. Syst Evol. Microbiol.* 55, 1181–1186. doi: 10.1099/ijs.0.63443-0

Martin, M., Portetelle, D., Michel, G., and Vandenbol, M. (2014). Microorganisms living on macroalgae: diversity, interactions, and biotechnological applications. *Appl Microbiol. Biotechnol.* 98, 2917–2935. doi: 10.1007/s00253-014-5557-2

Mohandass, C., Rajasabapathy, R., Ravindran, C., Colaco, A., and Meena, R. M. (2012). Bacterial diversity and their adaptations in the shallow water hydrothermal vent at D. Joao de Castro Seamount (DJCS), Azores, Portugal. *Cah. Biol. Mar.* 53, 65–76.

Murthy, K. N., Mohanraju, R., Karthick, P., and Ramesh, C. H. (2016). Phenotypic and molecular characterization of epiphytic Vibrios from the marine macro algae of Andaman Islands, India. *Indian J. Mar. Sci.* 45, 304–309.

Nagayama, K., Iwamura, Y., Shibata, T., Hirayama, I., and Nakamura, T. (2002). Bactericidal activity of phlorotannins from the brown alga *Ecklonia kurome*. *J. Antimicrob. Chemother.* 50, 889–893. doi: 10.1093/jac/dkf222

Padmavati, A. R., Abinaya, B., and Pandian, S. K. (2014). Phenol, 2,4-bis(1,1-dimethylethyl) of marine bacterial origin inhibits quorum sensing mediated biofilm formation in the uropathogen *Serratia marcescens*. *Biofouling* 30, 1111–1122. doi: 10.1080/08927014.2014.972386

Park, S. W., Back, J. H., Lee, S. W., Song, J. H., Shin, C. H., Kim, G. E., et al. (2013). Successful antibiotic treatment of *Pseudomonas stutzeri*-induced peritonitis without peritoneal dialysis catheter removal in continuous ambulatory peritoneal dialysis. *Kidney Res. Clin. Pract.* 32, 81–83. doi: 10.1016/j.krcp.2013.04.004

Pawar, R., Mohandass, C., Sivaperumal, E., Sabu, E., Rajasabapathy, R., and Jagtap, T. (2015). Epiphytic marine pigmented bacteria: a prospective source of antioxidants. *Braz. J. Microbiol.* 46, 29–39. doi: 10.1590/S1517-838246120130353

Penesyan, A., Marshall-Jones, Z., Holmstrom, C., Kjelleberg, S., and Egan, S. (2009). Antimicrobial activity observed among cultured marine epiphytic bacteria reflects their potential as a source of new drugs. *FEMS Microbiol. Ecol.* 69, 113–124. doi: 10.1111/j.1574-6941.2009.00688.x

Prieto, M., Sullivan, L. O., McLoughlin, P., Hughes, H., O'Connor, P. M., and Gardiner, G. E. (2012). Assessment of the bacteriocinogenic potential of marine bacteria reveals lichenicidin production by seaweed-derived *Bacillus* spp. *Mar. Drugs* 10, 2280–2299. doi: 10.3390/md10102280

Punnam Chander, M., Sachithanandam, V., and Vijayachari, P. (2014). Antimicrobial and hemolytic activity of seaweed *Padina gymnospora* from South Andaman, Andaman and Nicobar Islands of India. *Int. J. Curr. Microbiol. App. Sci.* 3, 364–369.

Ramasamy, M., and Balasubramanian, U. (2012). Identification of bioactive compounds and antimicrobial activity of marine clam *Anadara granosa* (LINN.). *Int. J. Sci. Nat.* 3, 263–266.

Rao, D., Webb, J. S., Holmstrom, C., Case, R., Low, A., Steinberg, P., et al. (2007). Low densities of epiphytic bacteria from the marine alga *Ulva australis* inhibit settlement of fouling organisms. *Appl. Environ. Microbiol.* 73, 7844–7852. doi: 10.1128/AEM.01543-07

Ravisankar, A., Gnanambal, M. E., and Sundaram, L. R. (2013). A newly isolated *Pseudomonas* sp., epibiotic on the seaweed, *Padina tetrastromatica*, off Southeastern Coast of India, reveals antibacterial action. *Appl. Biochem. Biotechnol.* 171, 1968–1985. doi: 10.1007/s12010-013-0473-y

Sasser, M. (1990). "Identification of bacteria through fatty acid analysis," in *Methods in Phytobacteriology*, eds Z. Klement, K. Rudolph, and D. C. Sands (Budapest: Akademiai Kiado).

Shatila, F., Yusef, H., and Beirut, H. H. (2013). Pigment production by *Exiguobacterium aurantiacum* FH, a novel Lebanese isolate. *Int. J. Curr. Microbiol. App. Sci.* 2, 176–191.

Singh, R. P., Baghel, R. S., Reddy, C. R. K., and Jha, B. (2015). Effect of quorum sensing signals produced by seaweed-associated bacteria on carpospore liberation from *Gracilaria dura*. *Front. Plant Sci.* 6:117. doi: 10.3389/fpls.2015.00117

Singh, R. P., Mantri, V. A., Reddy, C. R. K., and Jha, B. (2011). Isolation of seaweed-associated bacteria and their morphogenesis-inducing capability in axenic cultures of the green alga *Ulva fasciata*. *Aquat. Biol.* 12, 13–21. doi: 10.3354/ab00312

Susilowati, R., Sabdono, A., and Widowati, I. (2015). Isolation and characterization of bacteria associated with brown algae *Sargassum* spp. from Panjang Island and their antibacterial activities. *Procedia Environ. Sci.* 23, 240–246. doi: 10.1016/j.proenv.2015.01.036

Sutariya, S. D., Parmar, K. A., and Kharadi, G. J. (2012). Synthesis, spectral studies and antibacterial screening of some novel derivatives of 2-pyrrolidinones based on Schiff base. *Der Chem. Sin.* 3, 854–859.

Tamura, K., Dudley, J., Nei, M., and Kumar, S. (2007). MEGA4: molecular evolutionary genetics analysis (MEGA) software version 4.0. *Mol. Biol. Evol.* 24, 1596–1599. doi: 10.1093/molbev/msm092

Tamura, K., Nei, M., and Kumar, S. (2004). Prospects for inferring very large phylogenies by using the neighbor-joining method. *Proc. Natl. Acad. Sci. U.S.A.* 101, 11030–11035. doi: 10.1073/pnas.0404206101

Thakur, N. L., and Anil, A. C. (2000). Antibacterial activity of the sponge Ircinia ramosa: importance of its surface-associated bacteria. *J. Chem. Ecol.* 26, 57–71. doi: 10.1023/A:1005485310488

Thompson, J. D., Plewniak, F., Jeanmougin, F., and Higgins, D. G. (1997). The Clustal X windows interface: flexible strategies for multiple sequence alignment aided by quality analysis tools. *Nucleic Acids Res.* 24, 4876–4882. doi: 10.1093/nar/25.24.4876

Uzair, B., Ahmed, N., and Edwards, D. H. (2008). The isolation, purification and biological activity of a novel antibacterial compound produced by *Pseudomonas stutzeri*. *FEMS Microbiol. Lett.* 279, 243–250. doi: 10.1111/j.1574-6968.2007.01036.x

Vazquez, S., Nogales, B., Ruberto, L., Hernandez, E., Christie-Oleza, J., Lo Balbo, A., et al. (2009). Bacterial community dynamics during bioremediation of diesel oil-contaminated Antarctic soil. *Microb. Ecol.* 57, 598–610. doi: 10.1007/s00248-008-9420-9

Venkateshwarlu, T., Ravindernath, A., and Chennapragada, K. P. (2013). Synthesis and antimicrobial activity of novel benzo[b]furan derivatives. *Der Pharma Chemica* 5, 229–234.

Vijayalakshmi, S., Santhanaramasamy, M., Murugesh, S., and Murugan, A. (2008). Isolation and screening of marine associated bacteria from Tamil Nadu, Southeast coast of India for potential antibacterial activity. *Ann. Microbiol.* 58, 605–609. doi: 10.1007/BF03175564

Wahl, M. (2008). Ecological lever and interface ecology: epibiosis modulates the interactions between host and environment. *Biofouling* 24, 427–438. doi: 10.1080/08927010802339772

Wang, J., Zhang, H., Yang, X., Zhou, Y., Wang, H., and Bai, H. (2008). HS071, a new furan-type cytotoxic metabolite from *Streptomyces* sp. HS-HY-071. *J. Antibiot.* 61, 623–626. doi: 10.1038/ja.2008.82

Wiese, J., Thiel, V., Nagel, K., Staufenberger, T., and Imhoff, J. F. (2009). Diversity of antibiotic-active bacteria associated with the brown alga *Laminaria saccharina* from the Baltic Sea. *Mar. Biotechnol.* 11, 287–300. doi: 10.1007/s10126-008-9143-4

Wu, S., Liu, G., Jin, W., Xiu, P., and Sun, C. (2016). Antibiofilm and anti-Infection of a marine bacterial exopolysaccharide against *Pseudomonas aeruginosa*. *Front. Microbiol.* 7:102. doi: 10.3389/fmicb.2016.00102

Zheng, L., Han, X., Chen, H., Lin, W., and Yan, X. (2005). Marine bacteria associated with marine macroorganisms: the potential antimicrobial resources. *Ann. Microbiol.* 55, 119–124.

Conflict of Interest Statement: The authors declare that the research was conducted in the absence of any commercial or financial relationships that could be construed as a potential conflict of interest.

Copyright © 2018 Karthick and Mohanraju. This is an open-access article distributed under the terms of the Creative Commons Attribution License (CC BY). The use, distribution or reproduction in other forums is permitted, provided the original author(s) and the copyright owner are credited and that the original publication in this journal is cited, in accordance with accepted academic practice. No use, distribution or reproduction is permitted which does not comply with these terms.

frontiers in Microbiology

ORIGINAL RESEARCH
published: 12 April 2018
doi: 10.3389/fmicb.2018.00725

Prediction of Cell-Penetrating Potential of Modified Peptides Containing Natural and Chemically Modified Residues

Vinod Kumar[1,2†], *Piyush Agrawal*[1,2†], *Rajesh Kumar*[1,2†], *Sherry Bhalla*[1], *Salman Sadullah Usmani*[1,2], *Grish C. Varshney*[3] *and Gajendra P. S. Raghava*[1,2*]

[1] *Center for Computational Biology, Indraprastha Institute of Information Technology, Okhla, India,* [2] *Bioinformatics Centre, CSIR-Institute of Microbial Technology, Sector-39A, Chandigarh, India,* [3] *Cell Biology and Immunology, CSIR-Institute of Microbial Technology, Sector-39A, Chandigarh, India*

OPEN ACCESS

Edited by:
Noton Kumar Dutta, Johns Hopkins University, United States

Reviewed by:
Tikam Chand Dakal, Hospital Maisonneuve-Rosemont and University of Montreal, Canada
William Farias Porto, Universidade Católica Dom Bosco, Brazil

***Correspondence:**
Gajendra P. S. Raghava
raghava@iiitd.ac.in

[†] *These authors have contributed equally to this work.*

Specialty section:
This article was submitted to Antimicrobials, Resistance and Chemotherapy, a section of the journal Frontiers in Microbiology

Received: *08 January 2018*
Accepted: *28 March 2018*
Published: *12 April 2018*

Citation:
Kumar V, Agrawal P, Kumar R, Bhalla S, Usmani SS, Varshney GC and Raghava GPS (2018) Prediction of Cell-Penetrating Potential of Modified Peptides Containing Natural and Chemically Modified Residues. Front. Microbiol. 9:725. doi: 10.3389/fmicb.2018.00725

Designing drug delivery vehicles using cell-penetrating peptides is a hot area of research in the field of medicine. In the past, number of *in silico* methods have been developed for predicting cell-penetrating property of peptides containing natural residues. In this study, first time attempt has been made to predict cell-penetrating property of peptides containing natural and modified residues. The dataset used to develop prediction models, include structure and sequence of 732 chemically modified cell-penetrating peptides and an equal number of non-cell penetrating peptides. We analyzed the structure of both class of peptides and observed that positive charge groups, atoms, and residues are preferred in cell-penetrating peptides. In this study, models were developed to predict cell-penetrating peptides from its tertiary structure using a wide range of descriptors (2D, 3D descriptors, and fingerprints). Random Forest model developed by using PaDEL descriptors (combination of 2D, 3D, and fingerprints) achieved maximum accuracy of 95.10%, MCC of 0.90 and AUROC of 0.99 on the main dataset. The performance of model was also evaluated on validation/independent dataset which achieved AUROC of 0.98. In order to assist the scientific community, we have developed a web server "CellPPDMod" for predicting the cell-penetrating property of modified peptides (http://webs.iiitd.edu.in/raghava/cellppdmod/).

Keywords: modified cell-penetrating peptides, machine learning, Random Forest, SVM, *in silico* method, chemical descriptors, antimicrobial peptide

INTRODUCTION

Since the existence of human race, therapeutic molecules have been used to cure human illness and to extend lives (Tosato et al., 2007). In past, thousands of molecules have been studied to combat deadly diseases. The ideal molecule must attain the desired therapeutic effect without causing side effects. A large number of promising therapeutic molecules disparage before reaching to its target (Gupta and Jhawat, 2017). In order to overcome this, several delivery vehicles have been discovered in last three decades, such as nanoparticle (Wang et al., 2018) and lipid carrier conjugate (Xu et al., 2017). Cell-penetrating peptide (CPP) is one of the most emergent and widely accepted drug delivery vehicle, having ability to internalize even into eukaryotic cells in non-disruptive

way. These are short peptides of 3 to approximately 40 amino acids, mostly cationic followed by amphipathic in nature (Agrawal et al., 2016). CPPs can transport various biologically active molecules inside microbes as well as mammalian cells (Gao et al., 2014; Kurrikoff et al., 2016). CPPs such as TP10 and pVEC had been shown to significantly inhibit growth of few microbes as *Candida albicans*, *Staphylococcus aureus* as well as *Mycobacterium smegmatis* (Nekhotiaeva et al., 2004). CPPs and cationic antibacterial peptides have similar physicochemical properties, so many CPPs have shown antimicrobial activity (Splith and Neundorf, 2011; Bahnsen et al., 2013; Rodriguez Plaza et al., 2014). The poor membrane permeability of drug molecule always remains a concern in drug designing. In the era of drug resistance, where pathogen membrane provides a significant barrier, intracellular delivery of antibiotics/drugs by the virtue of CPP, proved to be a vital step in combating drug resistance to some extent (Sparr et al., 2013). CPP based conjugates (Ganguly et al., 2008; Jain et al., 2015) and combination therapy has been explored against several resistant pathogens (Randhawa et al., 2016). They have been proved effective against intracellular pathogens too (Gomarasca et al., 2017).

A universal mechanism of CPP internalization is always proved to be an exploring question, as the involved pathways are not fully clarified yet. The difficulty arises due to differing size, physicochemical properties, as well as concentration of diverse CPP and CPP-conjugates (Guidotti et al., 2017). Several mechanisms have been shown by various CPPs to translocate in to the cell, as micelle formation (Derossi et al., 1996), pore formation (Matsuzaki et al., 1996), membrane thinning (Pouny et al., 1992), endocytosis (Ferreira and Boucrot, 2018) and micropinocytosis (Jones, 2007). Majority of CPP internalization occurs via endocytosis, but several evidences suggest that at a threshold concentration direct penetration does occur (Palm-Apergi et al., 2012). CPPs can be used for intracellular delivery of small molecule-based drug (Lindgren et al., 2006), oligonucleotide (Margus et al., 2012), peptide and protein (Morris et al., 2001) and trans-epithelial delivery of peptides (Tan et al., 2014).

Despite, numerous properties and potential applications of CPPs, still there use in real life is limited. The primary limitation associated with CPP is endosomal compartment entrapment which reduces the bioavailability of the drug several times. In literature, it has been shown that bioavailability of CPPs can be increased several times by introducing a chemical modification in a CPP (Postlethwaite et al., 1996; Kim et al., 2006; Lundberg et al., 2007; Koppelhus et al., 2008; Aubry et al., 2009). N-terminal stearylation of Arg8 peptide improved the delivery of siRNA (Futaki et al., 2001), C-terminal cysteamidation of MPG peptide improved the delivery of siRNA (Simeoni et al., 2003), cysteine residue modification improved the stability of Tat peptide and thus enhances the plasmid delivery (Lo and Wang, 2008), Poly-L-ornithine modification in PepFect 14 peptide increases transfection efficiency of oligonucleotide in HeLa pLuc 705 (Ezzat et al., 2011). Thus, it is important to understand chemical modification of residues in a peptide and its impact on cell-penetrating property of peptides.

In the last few years, several computational methods have been developed for the prediction of CPPs. These methods have been developed on various features like amino acid composition (Sanders et al., 2011), dipeptide composition (Tang et al., 2016), binary profile, physiochemical properties and motifs (Gautam et al., 2013). They have also applied Z-scale based method (Sandberg et al., 1998), feature selection techniques (Tang et al., 2016), classifiers like Random Forest (RF) (Wei et al., 2017), Support Vector Machine (SVM) (Sanders et al., 2011). Beside this, few more methods have been developed in recent years for predicting CPPs with high accuracy (Chen et al., 2015; Tang et al., 2016; Wei et al., 2017). Best of authors knowledge, all methods developed so far for predicting CPPs are suitable for peptides containing natural residues only, but no method has been developed for predicting cell penetration property of peptides with non-natural and modified residues. In this study, a systematic attempt has been made to develop a machine learning method for predicting cell penetration ability of peptides containing non-natural and modified residues. Machine learning technique derive features/rules from the experimentally validated modified CPPs and Non-CPPs are used to predict cell penetration ability of a modified peptide. We hope this method will be useful for researchers working in the field of drug delivery.

MATERIALS AND METHODS

Creation of Dataset for CPPs and Non-CPPs

Cell-penetrating peptides were extracted from CPPsite2.0 database (Agrawal et al., 2016), which provides comprehensive information on wide-range of CPPs. It consists of 1,850 experimentally validated natural and modified CPPs. We remove CPPs that does not contain any modified residue; we also remove peptides whose tertiary structure is not available in the database. Finally, we got 732 chemically modified CPPs whose structure is available in CPPsite 2.0. We assign this set of 732 CPPs as positive set or set of CPPs. To develop any method, we also need equal number of negative examples. In this study, we extracted non-CPPs from SATPdb (Singh et al., 2016) database which maintains information of 19,192 peptides having several properties. We extracted structures of 732 peptides, which may exhibit any characteristic other than cell penetrating property. This set of peptides were assigned as negative set or set of non-CPPs. Finally, we built the dataset that contains 732 CPPs and 732 non-CPPs whose sequence and tertiary structure is available in CPPsites 2.0 or SATPdb.

Datasets for Internal and External Validation

The dataset was divided into two datasets namely training (main) and validation dataset (Bhalla et al., 2017). The training dataset consists of 80% of peptides, 582 CPPs, and 582 non-CPPs. The validation dataset consists of remaining 20% of peptides, 150 CPPs, and 150 non-CPPs. We used training dataset for developing models and for internal validation.

In internal validation, models were trained and tested using commonly used five-fold cross-validation technique (Nagpal et al., 2017). Performance of best model achieved on training dataset, was evaluated on validation dataset. The evaluation of the performance of model on validation or independent dataset is called external validation.

Model Development

Computation of Features From Peptide Structures

Composition Based Features

Atom composition is computed from CPPs and non-CPPs by converting peptide structures in SMILES format using openbabel (O'Boyle et al., 2011). These SMILES were further used to compute atom composition of following atoms C, H, O, N, S, Cl, Br, and F. The atomic composition provided the fixed length of 8 vectors.

$$Fraction\ of\ atom\ (a) = \frac{Total\ number\ of\ atom\ (a)}{Total\ number\ of\ all\ possible\ diatoms} \times 100 \quad (1)$$

Where atom (a) is one out of 8 atoms.

Diatom Composition

We computed diatom composition of amino acids just like the atomic composition for CPPs and non-CPPs. The diatomic composition provides the composition of the pair of atoms in each residue (e.g., C-C, C-O, etc.) of the peptide, and used to convert the variable length of modified peptides to fixed length feature vectors. The diatomic composition provided the fixed length of 64 (8×8) vectors.

$$Fraction\ of\ Diatom(a) = \frac{Total\ number\ of\ Diatom\ (a)}{Total\ number\ of\ all\ possible\ diatoms} \times 100 \quad (2)$$

Where diatom (a) is one out of 64 diatoms.

Chemical Descriptors

A biological property of any chemical molecule is determined by its chemical descriptors, which have been used in the past to develop QSAR based molecules (Kumar et al., 2015). PaDEL software, a freely available software was used for the calculation of chemical descriptors (Yap, 2011). We calculated 15,537 different types of descriptors, including 2D, 3D, and 10 different types of fingerprints. As all descriptors don't correlate with biological activity, we have done feature selection using "CsfSubsetEval" function present in WEKA software (Smith and Frank, 2016) to remove unnecessary descriptors hence reduced noise from dataset.

Computation of Features From Amino Acid Sequence of Peptide

Amino Acid Composition

We substitute the symbol of the modified residue with its original natural amino acid, for calculating amino acid composition for the positive and negative dataset. This left us with the sequence having 20 natural amino acids which generated the vector of 20.

$$AAC\ (a) = \frac{Ra}{N} x100 \quad (3)$$

Here, $AAC\ (a)$ is the percent composition of amino acid (a); R_a is the numbers of residues of type a, and N represents the total number of peptide's residues.

Dipeptide Composition

We also calculated dipeptide composition of the peptides since it provides global information of the peptide. The dipeptide composition was calculated using the formula 4, and it generated the vector of 400 (20×20).

$$Fraction\ of\ Dipeptide\ (a) = \frac{Total\ number\ of\ Dipeptide\ (a)}{Total\ number\ of\ all\ possible\ dipeptides} \times 100 \quad (4)$$

Where dipeptide (a) is one out of 400 dipeptides.

Terminus Composition-Based Model

We also calculated N and C terminus amino acid composition as well as dipeptide composition for developing prediction models. The composition of 5, 10, and 15 residues from N-terminus as well as C-terminus was taken into account. Also, we joined the terminal residues like N5C5, N10C10, and N15C15 and for developing models.

Residue Preference

In order to observe the residue preference at a particular position in the peptide, web-logos were prepared for first 15 N and 15 C-terminals along with their modifications using online WebLogo software (Crooks et al., 2004). These logos provide the position specific frequency of amino acids in a peptide. Each logo consists of stacks of symbols, one stack for each position in the sequence. The overall height of the stack indicates the sequence conservation at that position while the height of symbols within the stack indicates the relative frequency of each amino acid at that position.

Statistical Analysis

To check whether is there any significance difference between modified CPPs and non-CPPs, we performed Welch t-test on the selected features of 2D, 3D and Fingerprints descriptors using in house R-script. Adjusted p-values were calculated using Boneferroni adjustment.

Performance Measure

Different parameters were used to check the performance of various models developed in this study. These parameters are divided into two groups.

Threshold Dependent Parameters

This category includes Sensitivity (Sen), Specificity (Spc), Accuracy (Acc), and Matthews's correlation coefficient (MCC), where Sensitivity is true positive rate, Specificity is true negative rate, accuracy is ability to differentiate true positive and true negative and MCC is a correlation coefficient between observed and predicted. These can be calculated using the following

equations.

$$\text{Sensitivity} = \frac{TP}{PS} \times 100 \quad (5)$$

$$\text{Specificity} = \frac{TN}{NS} \times 100 \quad (6)$$

$$\text{Accuracy} = \frac{TP + TN}{PS + NS} \times 100 \quad (7)$$

$$\text{MCC} = \frac{1 - \left(\frac{FN}{PS} \times \frac{FP}{NS}\right)}{\sqrt{\left(1 + \frac{FP-FN}{PS}\right) \times \left(1 + \frac{FN-FP}{NS}\right)}} \quad (8)$$

Where *TP* represents correctly predicted positive, *TN* represents the correctly predicted negative examples, *PS* represents total sequences in positive set, *NS* represents total sequences in negative set, *FP* represents actual negative examples which have been wrongly predicted as positive and *FN* represents wrongly predicted positive examples. This is a well-established method of measuring performance and has been used earlier in many studies (Porto et al., 2017; Agrawal et al., 2018).

Threshold Independent Parameters

In this study, we also used threshold independent measure to evaluate the performance of models. In case of threshold independent measures, Receiver Operating Characteristics (ROC) curve is drawn between false positive and false negative rates. In order to measure performance, Area Under Curve ROC curve is computed called AUROC.

RESULTS

Analysis

We compute percent average composition of atoms in CPPs and non-CPPs to understand the preference of certain types of atoms present in the CPPs and non-CPPs. Overall, the profile is more or less same in both CPPs and non-CPPs.CPPs are slightly rich in H and N atoms whereas non-CPPs are slightly rich in C, O, and S (**Figure S1**). We analyzed the amino acid composition of both positive (CPPs) and negative (Non-CPPs) dataset. It has been observed that certain type of residues like R, K, and Q are more prominent in CPPs; in contrast residues are like C, L, V, P, and G are not preferred in CPPs (**Figure 1**). In the same manner, we also calculated the average amino acid composition of the first 15 N and 15 C- terminal amino acid residues (**Figure S2**). At the N terminal R, Q, I and M are more prominent in CPP as compared to Non-CPP (**Figure S2A**). Similarly at C terminal, R, K and Q are more prominent (**Figure S2B**).

In addition to compositional preference, we also computed preference of different types of residues in CPPs. It was revealed that some specific type of residues was preferred in the positive dataset contain CPPs as compared to the negative dataset contain non-CPPs. Residues like Rand K are highly preferred at various positions CPPs particularly at N terminal (**Figure 2**). Similarly, K and R are mostly preferred at C terminal also (**Figure 3**).

Machine Learning Based Prediction Model

We used various machine-learning approaches like SVM, Random Forest, Naive Bayes, J48 and SMO for developing the prediction model. These models utilize different features or descriptors to discriminate or classify CPPs and non-CPPs. The results are explained in details in the following sections.

Model Based on Peptide Structure

Tertiary structure of a peptide can present all type of modifications. Thus structure of peptide is used to predict cell penetration ability of modified peptide. In this study,

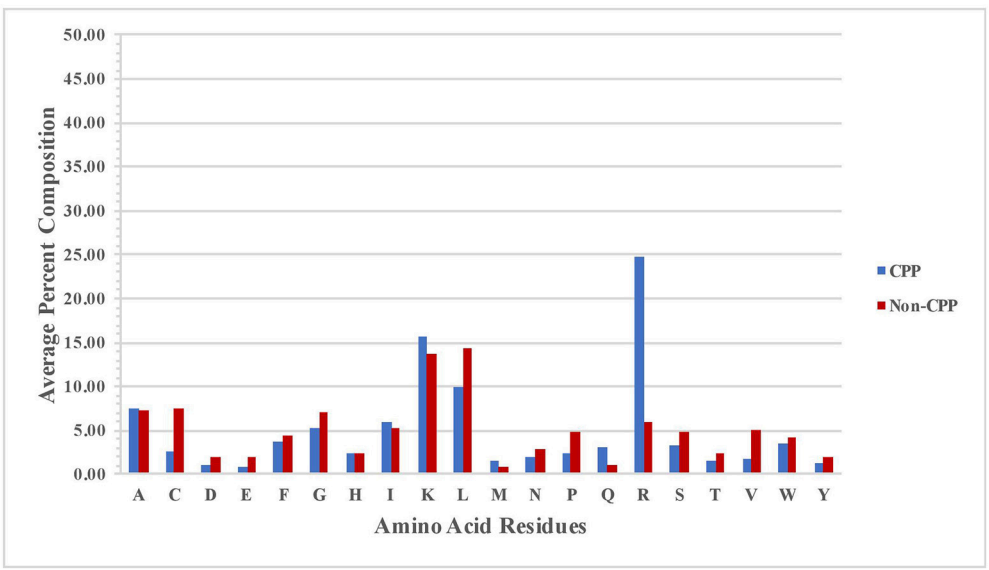

FIGURE 1 | Percentage amino acid composition of CPPs and non-CPPs.

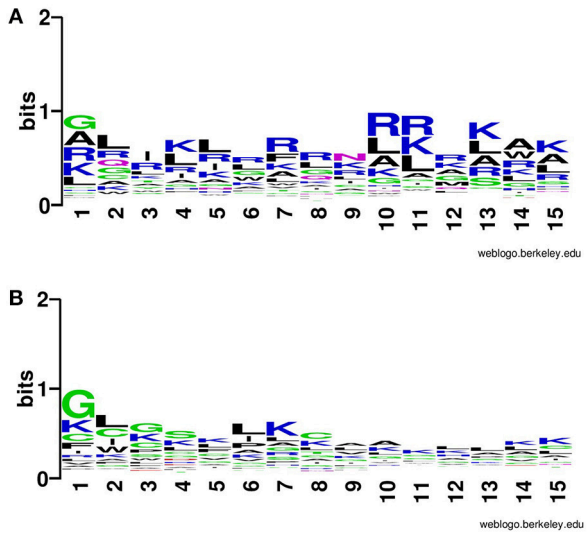

FIGURE 2 | Weblogo illustrating residue preference of first 15 N terminal residues of modified **(A)** CPPs and **(B)** non-CPPs.

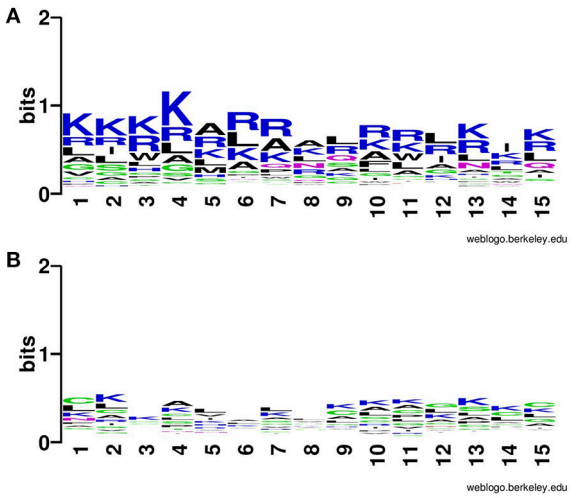

FIGURE 3 | Weblogo illustrating residue preference of first 15 C terminal residues of modified **(A)** CPPs and **(B)** non-CPPs.

we got structure of peptides from databases CPPsite 2.0 and SATPdb. The models were developed using various features of peptide structures. First, we developed model using atomic composition of peptides. In order to obtain atomic composition of peptides from its structure, we convert structure from sdf format to SMILES. The atomic composition of peptides was calculated from SMILES of peptide. Prediction models were developed using different classifiers like SVM, RF, Naive Bayes, SMO and J48 using atomic composition as an input feature. Random Forest based classification model provided the highest accuracy of 84.02%, MCC of 0.68 and AUROC of 0.91 on the training dataset. On validation dataset, we achieved maximum accuracy of 78.33%, MCC of 0.57 and AUROC of 0.88. Performance of different classifiers given in **Table 1.** We also developed model using diatom composition of peptides and obtained the highest accuracy of 88.40% with MCC of 0.77. On validation dataset, we achieved maximum accuracy of 91.00% with MCC 0.83. Here SVM based model performed best among all the classifiers used for prediction (**Table 2**).

We developed models individually for 2D descriptors, 3D descriptors, and Fingerprints as well as the single model by combining 2D, 3D descriptors, and Fingerprints. The descriptors were computed using PaDEL software from tertiary structure of peptides (sdf format). The models were developed on the features, selected after performing feature selection, by attribute evaluator named, "CfsSubsetEval" with search method of "BestFirst" at default parameters in the forward direction (amount of backtracking, $N = 5$ and lookup size $D = 1$). In case of 2D descriptors, total 144 descriptors were calculated initially and were reduced to 17 after feature selection. List of the selected features is provided in **Table S1**. We applied different machine learning techniques on these selected features and observed that Random Forest based model achieved the maximum accuracy of 92.34%, MCC of 0.85 and AUROC of 0.97 for the main dataset and 91.67% accuracy, 0.83 MCC and 0.97 AUROC for the validation dataset (**Table 3**).

In case of 3D descriptors, total 47 features were calculated and was reduced to 6 after applying feature selection (**Table S2**). On these features, Random Forest model performed better than other models and achieved maximum accuracy of 76.55%, MCC of 0.53 and AUROC value of 0.85 on the main dataset and 73.49% accuracy, 0.47 MCC and 0.83 AUROC on validation dataset (**Table 4**). The different types of fingerprints generated 14,532 features, which were reduced to 27 after feature selection (**Table S3**). Performance of different classifiers were evaluated on these features (**Table 5**) and once again Random Forest showed the best performance with maximum accuracy of 92.25%, MCC of 0.85 and AUROC of 0.98 on main dataset and accuracy of 92.33%, MCC of 0.85 and AUROC of 0.98 on validation dataset.

Finally, we calculated all the 2D, 3D descriptors and fingerprints at the same time, which generated 15,204 features. Feature selection reduced it down to 48 important features on which different machine learning classifiers were evaluated. Here we observe the maximum accuracy of 95.10%, MCC of 0.90 and AUROC of 0.99 on main dataset and 92.33% accuracy, 0.85 MCC and 0.98 AUROC on validation dataset by Random Forest model (**Table 6**). **Figure 4** shows the AUROC curve as well as AUROC values of different models.

Significance of features

We obtained significant difference between the positive and negative features based on adjusted *p*-values. *P*-values were found to be less than 0.05 for most of the features. Therefore, we can say that these features can be used to discriminate modified CPPs and non-CPPs. Mean value of positive and negative features along with their *p*-value for 2D, 3D, and fingerprint descriptors is provided in **Tables S1**–**S3**.

TABLE 1 | Performance of different machine learning methods on atom composition.

	Parameter	Main dataset					Validation dataset				
		Sen	Spc	Acc	MCC	AUROC	Sen	Spc	Acc	MCC	AUROC
SVM	$g = 1, c = 9$, j=4	81.10	80.58	80.84	0.62	0.84	79.33	75.33	77.33	0.55	0.81
Random Forest	Ntree = 30	83.33	84.71	84.02	0.68	0.91	79.33	77.33	78.33	0.57	0.88
SMO	$g = 1, c = 2$	77.66	83.51	80.58	0.61	0.80	75.33	82.67	79.00	0.58	0.79
J48	$c = 0.1, m = 1$	75.43	80.58	78.01	0.56	0.82	80.00	76.00	78.00	0.56	0.79
Naive Bayes	Default	74.57	65.46	70.02	0.40	0.80	80.00	69.33	74.67	0.50	0.82

TABLE 2 | Performance of different machine learning methods on diatom composition.

	Parameters	Main dataset					Validation dataset				
		Sen	Spc	Acc	MCC	AUROC	Sen	Spc	Acc	MCC	AUROC
SVM	$g = 0.01, c = 15$, j = 2	90.38	86.43	88.40	0.77	0.93	85.33	96.67	91.00	0.83	0.97
Random Forest	Ntree = 30	88.49	88.49	88.49	0.77	0.94	85.33	82.00	83.67	0.67	0.93
SMO	$g = 0.1, c = 4$	86.25	89.00	87.63	0.75	0.87	86.67	84.00	85.33	0.71	0.85
J48	$c = 0.3, m = 1$	82.47	81.10	81.79	0.64	0.81	85.33	81.33	83.33	0.67	0.82
Naive Bayes	Default	71.65	70.45	71.05	0.42	0.78	72.67	66.67	69.67	0.39	0.77

TABLE 3 | Performance of different machine learning methods on 2D descriptors.

	Parameters	Main dataset					Validation dataset				
		Sen	Spc	Acc	MCC	AUROC	Sen	Spc	Acc	MCC	AUROC
SVM	$g = 0.01, c = 6$, j = 2	89.00	84.48	86.75	0.74	0.92	86.00	82.67	84.33	0.69	0.92
Random Forest	Ntree = 60	92.78	91.90	92.34	0.85	0.97	94.67	88.67	91.67	0.83	0.97
SMO	$g = 0.001, c = 4$	83.16	86.38	84.77	0.70	0.84	81.33	87.33	84.33	0.69	0.84
J48	$c = 0.2, m = 2$	89.52	88.79	89.16	0.78	0.89	90.00	87.33	88.67	0.77	0.89
Naive Bayes	Default	75.09	78.79	76.94	0.54	0.85	74.67	77.33	76.00	0.52	0.84

TABLE 4 | Performance of different machine learning methods on 3D descriptors.

	Parameters	Main dataset					Validation dataset				
		Sen	Spc	Acc	MCC	AUROC	Sen	Spc	Acc	MCC	AUROC
SVM	$g =$ 1e-05, $c = 15, j = 1$	76.29	74.40	75.34	0.51	0.80	71.14	73.15	72.15	0.44	0.80
Random Forest	Ntree = 700	80.93	72.16	76.55	0.53	0.85	79.87	67.11	73.49	0.47	0.83
SMO	$g = 0.0005, c = 2$	69.42	72.85	71.13	0.42	0.71	63.09	76.51	69.80	040	0.69
J48	$c = 0.1, m = 3$	74.74	76.12	75.43	0.51	0.78	72.48	74.50	73.49	0.47	0.78
Naive Bayes	Default	69.24	74.40	71.82	0.44	0.78	69.80	75.84	72.82	0.46	0.79

TABLE 5 | Performance of different machine learning methods on fingerprints.

	Parameters	Main dataset					Validation dataset				
		Sen	Spc	Acc	MCC	AUROC	Sen	Spc	Acc	MCC	AUROC
SVM	$g = 0.005, c = 15, j = 1$	90.19	88.12	89.16	0.78	0.95	93.33	89.33	91.33	0.83	0.96
Random Forest	Ntree = 600	94.32	90.19	92.25	0.85	0.98	96.67	88.00	92.33	0.85	0.98
SMO	$g = 0.0005, c = 4$	85.54	85.03	85.28	0.71	0.85	88.67	85.33	87.00	0.74	0.87
J48	$c = 0.25, m = 1$	90.02	89.33	89.67	0.79	0.89	88.67	88.67	88.67	0.77	0.90
Naive Bayes	Default	86.40	84.34	85.37	0.71	0.90	82.67	85.33	84.00	0.68	0.90

TABLE 6 | Performance of different machine learning methods on 2D, 3D and fingerprints collectively.

	Parameters	Main dataset					Validation dataset				
		Sen	Spc	Acc	MCC	AUROC	Sen	Spc	Acc	MCC	AUROC
SVM	$g = 1e\text{-}05$, $c = 15$, $j = 1$	83.33	79.21	81.27	0.63	0.89	78.67	82.67	80.67	0.61	0.87
Random Forest	Ntree = 60	95.19	95.02	95.10	0.90	0.99	91.33	93.33	92.33	0.85	0.98
SMO	$g = 0.0001$, $c = 5$	76.80	76.98	76.89	0.54	0.76	75.33	83.33	79.33	0.59	0.79
J48	$c = 0.25$, $m = 5$	89.69	87.63	88.66	0.77	0.90	84.67	92.00	88.33	0.77	0.92
Naive Bayes	Default	95.19	88.14	91.67	0.84	0.95	92.00	89.33	90.67	0.81	0.96

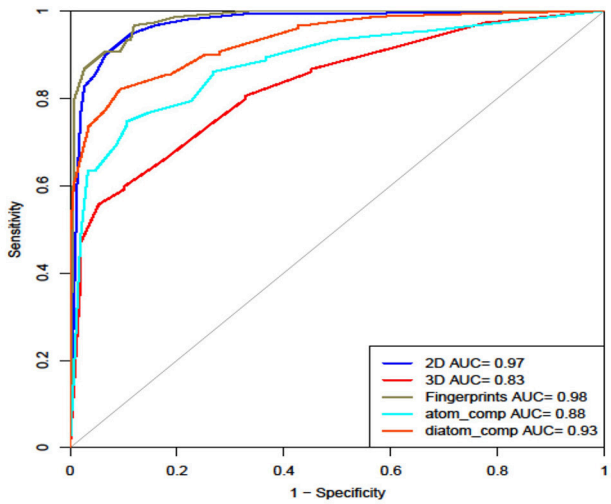

FIGURE 4 | ROC curve showing performance of models on various structural features.

Model Based on Peptide Sequence

It is nearly impossible to present a modified peptide by amino acid sequence. Thus, prediction of modified peptide from there sequence is not possible. Same time generating tertiary structure of a peptide is a tedious job for a biologist. We made an attempt to develop prediction model for cell penetration peptides of modified peptides from their amino acid sequence only by ignoring modifications in peptide. First, we developed simple composition-based models using various machine learning techniques. The SVM based model showed the best performance among all the classifiers used in the study. The accuracy of 91.67%, MCC of 0.83 and AUROC of 0.96 was achieved for the main dataset. On validation dataset, we obtained accuracy of 89.67%, MCC of 0.79 and AUROC of 0.96 (**Table S4**). We also developed SVM based model on first 5, 10, and 15 N and C-terminus residues. Results are given in **Table S5**.

Secondly, we developed models using dipeptide composition, SVM classifier showed the highest accuracy of 91.84%, MCC of 0.84 and AUROC of 0.96 for the main dataset. For independent dataset, the accuracy of 92.33%, MCC of 0.85 and AUROC of 0.97 was achieved (**Table S6**). Results of SVM based models on terminus residues for dipeptide composition is provided in **Table S7**. It is important for users to understand that sequence based model is not alternate to structure based models or alternate to past sequence based models developed for natural peptides. This sequence based is just approximate cell penetration potential of a modified peptide from its amino acid sequence.

Implementation of Webserver

To assist the scientific community, the best models are provided freely at http://webs.iiitd.edu.in/raghava/cellppdmod/. The "PREDICTION" module, consider tertiary structure (PDB format) of the modified peptide as an input and does the prediction. If a user has no structural information, he/she can generate PDB structure of their peptide up to 25 residues in length using server "PEPstrMOD" (Singh et al., 2015) (http://webs.iiitd.edu.in/raghava/pepstrmod/) developed by our group specifically for predicting the structure of the modified peptide. In case of natural peptide user can also use following servers PEP-FOLD (Thevenet et al., 2012) (http://bioserv.rpbs.univ-paris-diderot.fr/services/PEP-FOLD/) and QUARK (Xu and Zhang, 2012) (https://zhanglab.ccmb.med.umich.edu/QUARK/) for predicting structure of peptides. Multiple modification options are provided there, and the user can choose the desired modification. After generating the structure, user can do the prediction on "PREDICTION" module, whether the given modified PDB structure is CPP or non-CPP. Beside the main model, we have also implemented model based on peptide sequence (Subsidiary model). We have also provided a "DOWNLOAD" module from where the user can download the dataset used in this study.

DISCUSSION

CPPs has shown a promising impact in the field of therapeutics or for targeting a specific disease (Bechara and Sagan, 2013). However, the major limitations associated with some of these CPPs is their entrapment of CPP-cargo in endosomal compartments followed by endocytosis and therefore their bioavailability and half-life is severely reduced (Mäe et al., 2009). To overcome this limitation, people have tried to modify the CPP chemically. For example, to increase the delivery of nucleic acid more efficiently, people have introduced chemical modifications like N terminal stearylation (Futaki et al., 2001; Khalil et al., 2004), C-terminal cysteamidation (Simeoni et al., 2003; Morris et al., 2007), residue modifications (Lundberg et al., 2007).Tat

is one of the first CPP, discovered from protein of HIV and various studies showed that it enhances the uptake of various drug and protein (Brooks et al., 2005). But DNA delivery by Tat is limited, because of the instability of Tat-DNA complex (Lo and Wang, 2008). Lo and Wang (2008) showed that Cysteine makes the Tat-DNA complex more stable. Incorporation of two cysteine residues results into interpeptide disulphide bond, form by air oxidation once bind to DNA. This enhance the stability of Tat-DNA complex, as well as protect DNA in extracellular environment. Therefore, gene transfection efficiency is more in modified Tat than simple Tat.

Computational algorithms have been proved a wide success in designing therapeutic peptides (Dhanda et al., 2017), therefore a large number of sequence-based model to design CPP has been developed in past. But all of these models have one limitation in common that they can only handle peptides with natural residues. Due to the huge therapeutic importance of modified CPP, prediction and designing of modified CPPs is the need of hour. So, we have developed a computational method, which is based on structural features, can handle the natural as well as modified peptides both. Beside this we have also incorporated a subsidiary model based on the sequence of peptides which consider only natural residues, to handle large number of peptides simultaneously. Here, sequence-based model is not alternate to the methods developed in past to predict natural CPPs.

We have developed various models using machine learning techniques such as SVM, Random Forest, J48, naïve bayes, SMO; individually for atom composition, 2D descriptors, 3D descriptors, and Fingerprints as well as the single model by combining 2D, 3D descriptors, and Fingerprints. We obtain best performance by Random Forest for both combined (2D, 3D, and Fingerprint descriptors) as well as fingerprint with accuracy 92.33% and AUROC 0.98 on validation dataset. As fingerprint alone will be computationally more feasible as compared to the combined method, so we have implemented this model on webserver.

We believe this work will prove a great assist to the researchers aim to design cell penetrating peptide, as well as incorporate different modification and to check their effect on cell penetration ability. In future, we can improve this method, if better art of structure prediction will be developed, as right now PEPstrMOD could tackle only 7–25 amino acid length and other best model I-TASSER only deals with natural residues. So, in conclusion this field must grow simultaneously with the betterment of art-of-structure prediction.

AUTHOR CONTRIBUTIONS

VK and PA generated the dataset. VK, PA, RK, and SB performed the experiments. VK, PA, and RK performed data analysis and prepared the tables and figures. VK, PA, RK, SB, and SU developed the web interface. VK, RK, PA, SU, and GR write the manuscript. GR and GV conceived the idea and coordinated the project.

ACKNOWLEDGMENTS

Authors are thankful to funding agencies J. C. Bose National Fellowship (DST), Council of Scientific and Industrial Research (CSIR), Department of Science and Technology (DST-INSPIRE), Indian Council of Medical Research (ICMR), University Grant Commission (UGC) and Department of Biotechnology (DBT) for fellowships and financial support.

SUPPLEMENTARY MATERIAL

The Supplementary Material for this article can be found online at: https://www.frontiersin.org/articles/10.3389/fmicb.2018.00725/full#supplementary-material

Figure S1 | Percentage atomic composition of modified CPPs and non-CPPs.

Figure S2 | Percentage amino acid composition of CPPs and non-CPPs **(A)** 15 N-terminal residues and **(B)** 15 C-terminal residues.

Table S1 | List of 2D features with their positive mean value, negative mean value and *p*-value.

Table S2 | List of 3D features with their positive mean value, negative mean value and *p*-value.

Table S3 | List of fingerprints with their positive mean value, negative mean value and *p*-value.

Table S4 | Performance of different machine learning methods on amino acid composition.

Table S5 | Performance of SVM method on amino acid composition features of terminus residues.

Table S6 | Performance of different machine learning methods on dipeptide composition.

Table S7 | Performance of SVM method on dipeptide composition features of terminus residues.

REFERENCES

Agrawal, P., Bhalla, S., Chaudhary, K., Kumar, R., Sharma, M., and Raghava, G. P. S. (2018). *In silico* approach for prediction of antifungal peptides. *Front. Microbiol.* 9:323. doi: 10.3389/fmicb.2018.00323

Agrawal, P., Bhalla, S., Usmani, S. S., Singh, S., Chaudhary, K., Raghava, G. P. S., et al. (2016). CPPsite 2.0: a repository of experimentally validated cell-penetrating peptides. *Nucleic Acids Res.* 44, D1098–D1103. doi: 10.1093/nar/gkv1266

Aubry, S., Burlina, F., Dupont, E., Delaroche, D., Joliot, A., Lavielle, S., et al. (2009). Cell-surface thiols affect cell entry of disulfide-conjugated peptides. *FASEB J.* 23, 2956–2967. doi: 10.1096/fj.08-127563

Bahnsen, J. S., Franzyk, H., Sandberg-Schaal, A., and Nielsen, H. M. (2013). Antimicrobial and cell-penetrating properties of penetratin analogs: effect of sequence and secondary structure. *Biochim. Biophys. Acta* 1828, 223–232. doi: 10.1016/j.bbamem.2012.10.010

Bechara, C., and Sagan, S. (2013). Cell-penetrating peptides: 20 years later, where do we stand? *FEBS Lett.* 587, 1693–1702. doi: 10.1016/j.febslet.2013.04.031

Bhalla, S., Chaudhary, K., Kumar, R., Sehgal, M., Kaur, H., Sharma, S., et al. (2017). Gene expression-based biomarkers for discriminating early and late stage of clear cell renal cancer. *Sci. Rep.* 7:44997. doi: 10.1038/srep44997

Brooks, H., Lebleu, B., and Vivès, E. (2005). Tat peptide-mediated cellular delivery: back to basics. *Adv. Drug Deliv. Rev.* 57, 559–577. doi: 10.1016/j.addr.2004.12.001

Chen, L., Chu, C., Huang, T., Kong, X., and Cai, Y.-D. (2015). Prediction and analysis of cell-penetrating peptides using pseudo-amino acid composition and random forest models. *Amino Acids* 47, 1485–1493. doi: 10.1007/s00726-015-1974-5

Crooks, G. E., Hon, G., Chandonia, J.-M., and Brenner, S. E. (2004). WebLogo: a sequence logo generator. *Genome Res.* 14, 1188–1190. doi: 10.1101/gr.849004

Derossi, D., Calvet, S., Trembleau, A., Brunissen, A., Chassaing, G., and Prochiantz, A. (1996). Cell internalization of the third helix of the Antennapedia homeodomain is receptor-independent. *J. Biol. Chem.* 271, 18188–18193. doi: 10.1074/jbc.271.30.18188

Dhanda, S. K., Usmani, S. S., Agrawal, P., Nagpal, G., Gautam, A., and Raghava, G. P. S. (2017). Novel *in silico* tools for designing peptide-based subunit vaccines and immunotherapeutics. *Brief. Bioinform.* 18, 467–478. doi: 10.1093/bib/bbw025

Ezzat, K., Andaloussi, S. E. L., Zaghloul, E. M., Lehto, T., Lindberg, S., Moreno, P. M. D., et al. (2011). PepFect 14, a novel cell-penetrating peptide for oligonucleotide delivery in solution and as solid formulation. *Nucleic Acids Res.* 39, 5284–5298. doi: 10.1093/nar/gkr072

Ferreira, A. P. A., and Boucrot, E. (2018). Mechanisms of carrier formation during clathrin-independent endocytosis. *Trends Cell Biol.* 28, 188–200. doi: 10.1016/j.tcb.2017.11.004

Futaki, S., Ohashi, W., Suzuki, T., Niwa, M., Tanaka, S., Ueda, K., et al. (2001). Stearylated arginine-rich peptides: a new class of transfection systems. *Bioconjug. Chem.* 12, 1005–1011. doi: 10.1021/bc015508l

Ganguly, S., Chaubey, B., Tripathi, S., Upadhyay, A., Neti, P. V. S. V., Howell, R. W., et al. (2008). Pharmacokinetic analysis of polyamide nucleic-acid-cell penetrating peptide conjugates targeted against HIV-1 transactivation response element. *Oligonucleotides* 18, 277–286. doi: 10.1089/oli.2008.0140

Gao, H., Zhang, Q., Yu, Z., and He, Q. (2014). Cell-penetrating peptide-based intelligent liposomal systems for enhanced drug delivery. *Curr. Pharm. Biotechnol.* 15, 210–219. doi: 10.2174/1389201015666140617092552

Gautam, A., Chaudhary, K., Kumar, R., Sharma, A., Kapoor, P., Tyagi, A., et al. (2013). *In silico* approaches for designing highly effective cell penetrating peptides. *J. Transl. Med.* 11:74. doi: 10.1186/1479-5876-11-74

Gomarasca, M., F. C., Martins, T., Greune, L., Hardwidge, P. R., Schmidt, M. A., and Rüter, C. (2017). Bacterium-derived cell-penetrating peptides deliver gentamicin to kill intracellular pathogens. *Antimicrob. Agents Chemother.* 61:e02545-16. doi: 10.1128/AAC.02545-16

Guidotti, G., Brambilla, L., and Rossi, D. (2017). Cell-penetrating peptides: from basic research to clinics. *Trends Pharmacol. Sci.* 38, 406–424. doi: 10.1016/j.tips.2017.01.003

Gupta, S., and Jhawat, V. (2017). Quality by Design (QbD) approach of pharmacogenomics in drug designing and formulation development for optimization of drug delivery systems. *J. Control. Release* 245, 15–26. doi: 10.1016/j.jconrel.2016.11.018

Jain, A., Shah, S. G., and Chugh, A. (2015). Cell penetrating peptides as efficient nanocarriers for delivery of antifungal compound, natamycin for the treatment of fungal keratitis. *Pharm. Res.* 32, 1920–1930. doi: 10.1007/s11095-014-1586-x

Jones, A. T. (2007). Macropinocytosis: searching for an endocytic identity and role in the uptake of cell penetrating peptides. *J. Cell. Mol. Med.* 11, 670–684. doi: 10.1111/j.1582-4934.2007.00062.x

Khalil, I. A., Futaki, S., Niwa, M., Baba, Y., Kaji, N., Kamiya, H., et al. (2004). Mechanism of improved gene transfer by the N-terminal stearylation of octaarginine: enhanced cellular association by hydrophobic core formation. *Gene Ther.* 11, 636–644. doi: 10.1038/sj.gt.3302128

Kim, W. J., Christensen, L. V., Jo, S., Yockman, J. W., Jeong, J. H., Kim, Y.-H., et al. (2006). Cholesteryl oligoarginine delivering vascular endothelial growth factor siRNA effectively inhibits tumor growth in colon adenocarcinoma. *Mol. Ther.* 14, 343–350. doi: 10.1016/j.ymthe.2006.03.022

Koppelhus, U., Shiraishi, T., Zachar, V., Pankratova, S., and Nielsen, P. E. (2008). Improved cellular activity of antisense peptide nucleic acids by conjugation to a cationic peptide-lipid (CatLip) domain. *Bioconjug. Chem.* 19, 1526–1534. doi: 10.1021/bc800068h

Kumar, R., Chaudhary, K., Singh Chauhan, J., Nagpal, G., Kumar, R., Sharma, M., et al. (2015). An *in silico* platform for predicting, screening and designing of antihypertensive peptides. *Sci. Rep.* 5:12512. doi: 10.1038/srep12512

Kurrikoff, K., Gestin, M., and Langel, Ü. (2016). Recent *in vivo* advances in cell-penetrating peptide-assisted drug delivery. *Expert Opin. Drug Deliv.* 13, 373–387. doi: 10.1517/17425247.2016.1125879

Lindgren, M., Rosenthal-Aizman, K., Saar, K., Eiríksdóttir, E., Jiang, Y., Sassian, M., et al. (2006). Overcoming methotrexate resistance in breast cancer tumour cells by the use of a new cell-penetrating peptide. *Biochem. Pharmacol.* 71, 416–425. doi: 10.1016/j.bcp.2005.10.048

Lo, S. L., and Wang, S. (2008). An endosomolytic Tat peptide produced by incorporation of histidine and cysteine residues as a nonviral vector for DNA transfection. *Biomaterials* 29, 2408–2414. doi: 10.1016/j.biomaterials.2008.01.031

Lundberg, P., El-Andaloussi, S., Sütlü, T., Johansson, H., and Langel, U. (2007). Delivery of short interfering RNA using endosomolytic cell-penetrating peptides. *FASEB J.* 21, 2664–2671. doi: 10.1096/fj.06-6502com

Mäe, M. A., El-Andaloussi, S., Lehto, T., and Ulo, L. (2009). Chemically modified cell-penetrating peptides for the delivery of nucleic acids. *Expert Opin. Drug Deliv.* 6, 1195–1205. doi: 10.1517/17425240903213688

Margus, H., Padari, K., and Pooga, M. (2012). Cell-penetrating peptides as versatile vehicles for oligonucleotide delivery. *Mol. Ther.* 20, 525–533. doi: 10.1038/mt.2011.284

Matsuzaki, K., Yoneyama, S., Murase, O., and Miyajima, K. (1996). Transbilayer transport of ions and lipids coupled with mastoparan X translocation. *Biochemistry* 35, 8450–8456. doi: 10.1021/bi960342a

Morris, M. C., Depollier, J., Mery, J., Heitz, F., and Divita, G. (2001). A peptide carrier for the delivery of biologically active proteins into mammalian cells. *Nat. Biotechnol.* 19, 1173–1176. doi: 10.1038/nbt1201-1173

Morris, M. C., Gros, E., Aldrian-Herrada, G., Choob, M., Archdeacon, J., Heitz, F., et al. (2007). A non-covalent peptide-based carrier for *in vivo* delivery of DNA mimics. *Nucleic Acids Res.* 35:e49. doi: 10.1093/nar/gkm053

Nagpal, G., Usmani, S. S., Dhanda, S. K., Kaur, H., Singh, S., Sharma, M., et al. (2017). Computer-aided designing of immunosuppressive peptides based on IL-10 inducing potential. *Sci. Rep.* 7:42851. doi: 10.1038/srep42851

Nekhotiaeva, N., Elmquist, A., Rajarao, G. K., Hällbrink, M., Langel, U., and Good, L. (2004). Cell entry and antimicrobial properties of eukaryotic cell-penetrating peptides. *FASEB J.* 18, 394–396. doi: 10.1096/fj.03-0449fje

O'Boyle, N. M., Banck, M., James, C. A., Morley, C., Vandermeersch, T., and Hutchison, G. R. (2011). Open Babel: an open chemical toolbox. *J. Cheminform.* 3:33. doi: 10.1186/1758-2946-3-33

Palm-Apergi, C., Lönn, P., and Dowdy, S. F. (2012). Do cell-penetrating peptides actually "penetrate" cellular membranes? *Mol. Ther.* 20, 695–697. doi: 10.1038/mt.2012.40

Porto, W. F., Pires, Á. S., and Franco, O. L. (2017). Antimicrobial activity predictors benchmarking analysis using shuffled and designed synthetic peptides. *J. Theor. Biol.* 426, 96–103. doi: 10.1016/j.jtbi.2017.05.011

Postlethwaite, R. J., Garralda, M. E., Eminson, D. M., and Reynolds, J. (1996). Lessons from psychosocial studies of chronic renal failure. *Arch. Dis. Child.* 75, 455–459. doi: 10.1136/adc.75.5.455

Pouny, Y., Rapaport, D., Mor, A., Nicolas, P., and Shai, Y. (1992). Interaction of antimicrobial dermaseptin and its fluorescently labeled analogues with phospholipid membranes. *Biochemistry* 31, 12416–12423. doi: 10.1021/bi00164a017

Randhawa, H. K., Gautam, A., Sharma, M., Bhatia, R., Varshney, G. C., Raghava, G. P. S., et al. (2016). Cell-penetrating peptide and antibiotic combination therapy: a potential alternative to combat drug resistance in methicillin-resistant *Staphylococcus aureus*. *Appl. Microbiol. Biotechnol.* 100, 4073–4083. doi: 10.1007/s00253-016-7329-7

Rodriguez Plaza, J. G., Morales-Nava, R., Diener, C., Schreiber, G., Gonzalez, Z. D., Lara Ortiz, M. T., et al. (2014). Cell penetrating peptides and cationic antibacterial peptides: two sides of the same coin. *J. Biol. Chem.* 289, 14448–14457. doi: 10.1074/jbc.M113.515023

Sandberg, M., Eriksson, L., Jonsson, J., Sjöström, M., and Wold, S. (1998). New chemical descriptors relevant for the design of biologically active peptides. A multivariate characterization of 87 amino acids. *J. Med. Chem.* 41, 2481–2491. doi: 10.1021/jm9700575

Sanders, W. S., Johnston, C. I., Bridges, S. M., Burgess, S. C., and Willeford, K. O. (2011). Prediction of cell penetrating peptides by support vector machines. *PLoS Comput. Biol.* 7:e1002101. doi: 10.1371/journal.pcbi.1002101

Simeoni, F., Morris, M. C., Heitz, F., and Divita, G. (2003). Insight into the mechanism of the peptide-based gene delivery system MPG: implications for delivery of siRNA into mammalian cells. *Nucleic Acids Res.* 31, 2717–2724. doi: 10.1093/nar/gkg385

Singh, S., Chaudhary, K., Dhanda, S. K., Bhalla, S., Usmani, S. S., Gautam, A., et al. (2016). SATPdb: a database of structurally annotated therapeutic peptides. *Nucleic Acids Res.* 44, D1119–D1126. doi: 10.1093/nar/gkv1114

Singh, S., Singh, H., Tuknait, A., Chaudhary, K., Singh, B., Kumaran, S., et al. (2015). PEPstrMOD: structure prediction of peptides containing natural, non-natural and modified residues. *Biol. Direct* 10:73. doi: 10.1186/s13062-015-0103-4

Smith, T. C., and Frank, E. (2016). Introducing machine learning concepts with WEKA. *Methods Mol. Biol.* 1418, 353–378. doi: 10.1007/978-1-4939-3578-9_17

Sparr, C., Purkayastha, N., Kolesinska, B., Gengenbacher, M., Amulic, B., Matuschewski, K., et al. (2013). Improved efficacy of fosmidomycin against Plasmodium and Mycobacterium species by combination with the cell-penetrating peptide octaarginine. *Antimicrob. Agents Chemother.* 57, 4689–4698. doi: 10.1128/AAC.00427-13

Splith, K., and Neundorf, I. (2011). Antimicrobial peptides with cell-penetrating peptide properties and vice versa. *Eur. Biophys. J.* 40, 387–397. doi: 10.1007/s00249-011-0682-7

Tan, J., Cheong, H., Park, Y. S., Kim, H., Zhang, M., Moon, C., et al. (2014). Cell-penetrating peptide-mediated topical delivery of biomacromolecular drugs. *Curr. Pharm. Biotechnol.* 15, 231–239. doi: 10.2174/1389201015666140617094320

Tang, H., Su, Z.-D., Wei, H.-H., Chen, W., and Lin, H. (2016). Prediction of cell-penetrating peptides with feature selection techniques. *Biochem. Biophys. Res. Commun.* 477, 150–154. doi: 10.1016/j.bbrc.2016.06.035

Thevenet, P., Shen, Y., Maupetit, J., Guyon, F., Derreumaux, P., and Tuffery, P. (2012). PEP-FOLD: an updated de novo structure prediction server for both linear and disulfide bonded cyclic peptides. *Nucleic Acids Res.* 40, W288–W293. doi: 10.1093/nar/gks419

Tosato, M., Zamboni, V., Ferrini, A., and Cesari, M. (2007). The aging process and potential interventions to extend life expectancy. *Clin. Interv. Aging* 2, 401–412.

Wang, Y.-R., Chen, G.-X., Yang, S.-Y., and Wei, P. (2018). Barbaloin loaded polydopamine-polylactide-TPGS (PLA-TPGS) nanoparticles against gastric cancer as a targeted drug delivery system: studies *in vitro* and *in vivo*. *Biochem. Biophys. Res. Commun.* 499, 8–16. doi: 10.1016/j.bbrc.2018.03.069

Wei, L., Xing, P., Su, R., Shi, G., Ma, Z. S., and Zou, Q. (2017). CPPred-RF: a sequence-based predictor for identifying cell-penetrating peptides and their uptake efficiency. *J. Proteome Res.* 16, 2044–2053. doi: 10.1021/acs.jproteome.7b00019

Xu, D., and Zhang, Y. (2012). *Ab initio* protein structure assembly using continuous structure fragments and optimized knowledge-based force field. *Proteins* 80, 1715–1735. doi: 10.1002/prot.24065

Xu, J., Zhang, X., Chen, Y., Huang, Y., Wang, P., Wei, Y., et al. (2017). Improved micellar formulation for enhanced delivery for paclitaxel. *Mol. Pharm.* 14, 31–41. doi: 10.1021/acs.molpharmaceut.6b00581

Yap, C. W. (2011). PaDEL-descriptor: an open source software to calculate molecular descriptors and fingerprints. *J. Comput. Chem.* 32, 1466–1474. doi: 10.1002/jcc.21707

Conflict of Interest Statement: The authors declare that the research was conducted in the absence of any commercial or financial relationships that could be construed as a potential conflict of interest.

Copyright © 2018 Kumar, Agrawal, Kumar, Bhalla, Usmani, Varshney and Raghava. This is an open-access article distributed under the terms of the Creative Commons Attribution License (CC BY). The use, distribution or reproduction in other forums is permitted, provided the original author(s) and the copyright owner are credited and that the original publication in this journal is cited, in accordance with accepted academic practice. No use, distribution or reproduction is permitted which does not comply with these terms.

frontiers in Microbiology

ORIGINAL RESEARCH
published: 04 May 2018
doi: 10.3389/fmicb.2018.00823

Antibacterial Efficacy of Polysaccharide Capped Silver Nanoparticles Is Not Compromised by AcrAB-TolC Efflux Pump

*Mitali Mishra[1], Satish Kumar[2], Rakesh K. Majhi[1], Luna Goswami[2], Chandan Goswami[1] and Harapriya Mohapatra[1]**

[1] School of Biological Sciences, National Institute of Science Education and Research, Homi Bhabha National Institute, Bhubaneswar, India, [2] School of Biotechnology, Kalinga Institute of Industrial Technology, Bhubaneswar, India

Antibacterial therapy is of paramount importance in treatment of several acute and chronic infectious diseases caused by pathogens. Over the years extensive use and misuse of antimicrobial agents has led to emergence of multidrug resistant (MDR) and extensive drug resistant (XDR) pathogens. This drastic escalation in resistant phenotype has limited the efficacy of available therapeutic options. Thus, the need of the hour is to look for alternative therapeutic approaches to mitigate healthcare concerns caused due to MDR bacterial infections. Nanoparticles have gathered much attention as potential candidates for antibacterial therapy. Equipped with advantages of, wide spectrum bactericidal activity at very low dosage, inhibitor of biofilm formation and ease of permeability, nanoparticles have been considered as leading therapeutic candidates to curtail infections resulting from MDR bacteria. However, substrate non-specificity of efflux pumps, particularly those belonging to resistance nodulation division super family, have been reported to reduce efficacy of many potent antibacterial therapeutic drugs. Previously, we had reported antibacterial activity of polysaccharide-capped silver nanoparticles (AgNPs) toward MDR bacteria. We showed that AgNPs inhibits biofilm formation and alters expression of cytoskeletal proteins FtsZ and FtsA, with minimal cytotoxicity toward mammalian cells. In the present study, we report no reduction in antibacterial efficacy of silver nanoparticles in presence of AcrAB-TolC efflux pump proteins. Antibacterial tests were performed according to CLSI macrobroth dilution method, which revealed that both silver nanoparticles exhibited bactericidal activity at very low concentrations. Further, immunoblotting results indicated that both the nanoparticles modulate the transporter AcrB protein expression. However, expression of the membrane fusion protein AcrA did show a significant increase after exposure to AgNPs. Our results indicate that both silver nanoparticles are effective in eliminating MDR *Enterobacter cloacae* isolates and their action was not inhibited by AcrAB-TolC efflux protein expression. As such, the above nanoparticles have strong potential to be used as effective and alternate therapeutic candidates to combat MDR gram-negative Enterobacterial pathogens.

Keywords: nanoparticles, efflux pump, AcrAB-TolC, *Enterobacter cloacae*, antibiotic resistance

OPEN ACCESS

Edited by:
Rebecca Thombre,
Savitribai Phule Pune University, India

Reviewed by:
Amit Kumar Mandal,
Raiganj University, India
Rajashree Bhalchandra Patwardhan,
Savitribai Phule Pune University, India

***Correspondence:**
Harapriya Mohapatra
hm@niser.ac.in;
hmsbsniser@gmail.com

Specialty section:
This article was submitted to Antimicrobials, Resistance and Chemotherapy, a section of the journal Frontiers in Microbiology

Received: *26 November 2017*
Accepted: *11 April 2018*
Published: *04 May 2018*

Citation:
Mishra M, Kumar S, Majhi RK, Goswami L, Goswami C and Mohapatra H (2018) Antibacterial Efficacy of Polysaccharide Capped Silver Nanoparticles Is Not Compromised by AcrAB-TolC Efflux Pump. Front. Microbiol. 9:823. doi: 10.3389/fmicb.2018.00823

INTRODUCTION

The drastic escalation in the proportion of multiple antibiotic resistant bacteria is recognized as a serious health care concern globally (WHO, 2014). The evolution of drug resistant microbes has challenged the success of antimicrobial agents for combating infectious diseases. The group of opportunistic pathogens, belonging to genera *Enterococcus*, *Staphylococcus*, *Klebsiella*, *Acinetobacter*, *Pseudomonas,* and *Enterobacter* (acronymed as ESKAPE) are exhibiting resistance to virtually all available antimicrobial agents (Boucher et al., 2009). Indeed, the acronym 'ESKAPE' is perfect choice to reflect these 'bad bugs.' To complicate the scenario, many of the above-mentioned bacteria are increasingly becoming responsible for spread of multidrug resistant (MDR) community acquired infections (Pendleton et al., 2013).

The *Enterobacter* spp., particularly *E. aerogenes* and *E. cloacae* are often associated with nosocomial infections like urinary tract infection (specifically catheter related), abdominal cavity/intestinal infections, wound infections, pneumonia, and septicemia (Sanders and Sanders, 1997; Fraser and Arnett, 2010). These two clinically predominant species display one or more resistance mechanisms toward antimicrobials like β-lactams, cephalosporins, aminoglycosides. Ironically, *E. aerogenes* and *E. cloacae* are also exhibiting trends of increased resistance toward the last resort antimicrobial agents – carbapenems and colistin (Davin-Regli and Pagès, 2015). Well-equipped with armory of antibiotic resistance strategies such as, outer membrane permeability barrier, efflux pumps and antibiotic degrading enzymes, *Enterobacter* spp. form an interesting infectious model to explore (Grimont and Grimont, 2006; Mezzatesta et al., 2012; Davin-Regli and Pagès, 2015).

The rise in antimicrobial resistance coupled with diminishing available options has necessitated searching for alternative therapeutic options (Martins and McCusker, 2016). One such lucrative direction was use of combinatorial therapy for treatment of infections caused by gram-negative pathogens, such as *Pseudomonas aeruginosa*. Typically, the combinatorial therapies for gram-negative pathogens included a β-lactam with aminoglycoside or fluoroquinolone (Tamma et al., 2012). The strategy was to extract their synergistic potential and broader spectrum of activity. But, in many clinical trials, it developed adverse effects leading to nephrotoxicity and even greater multiple antibiotic resistance (Kerantzas and Jacobs, 2017). The limitations faced by combinatorial therapies led to further improvisation and antimicrobial peptides were the more sought after. These host-defense peptides were investigated due to their antimicrobial properties against both gram-positive and gram-negative pathogens and immunomodulatory roles. However, low metabolic stability and discrepancies between *in vivo* and *in vitro* antimicrobial effectiveness limited the scope of antimicrobial peptides (Mahlapuu et al., 2016). Other interesting alternatives were more conceptual driven, such as bacteriophage therapy (Yang et al., 2014) and/or repurposing the existing drugs for better antibacterial and anti-virulence features (Rangel-Vega et al., 2015). Although both of them appeared as promising candidates, but development of such therapy at large scale remains challenging and yet to be explored.

All of the above-developed strategies faced severe obstacles in getting translated for sustainable, practical and large-scale usage, as demanded by the present situation. Much of the aforementioned limitations were circumvented by development of nanoparticle as drugs (Salata, 2004; Singh and Lillard, 2009). Over the years, nanoparticle-based approaches have gathered much reputation due to their fast and effective antibacterial properties for various pathogens (Gelperina et al., 2005; Tran and Webster, 2011). Nanoparticles endowed with wide bactericidal spectrum, ability to inhibit biofilm, increased permeability and efficacy at low dose, form a powerful weapon to combat MDR bacteria (Kim et al., 2007; Pelgrift and Friedman, 2013; Chen et al., 2014; Sanyasi et al., 2016). Review of the literature reveals that presence of efflux pumps [particularly those belonging to resistance nodulation division (RND) super family, e.g., tripartite efflux pump AcrAB-TolC] in gram-negative bacteria compromises the antibacterial efficacy of the drugs by extruding them out of the cytoplasm (Zgurskaya, 2009). Efflux of drugs reduces their intracellular concentration, leading to increased resistance in pathogens toward the drug. Further, it has been reported that substrates to be effluxed (antibacterial drugs) induce overexpression of the efflux proteins (Rosenberg et al., 2003).

Previously we had reported antibacterial activity of polysaccharide-capped silver nanoparticles (AgNPs) toward several MDR bacteria *viz. E. coli*, *Klebsiella* spp., *Enterobacter* spp., and *S. aureus* (Sanyasi et al., 2016). We had demonstrated AgNPs to inhibit biofilm formation and alter expression of cytoskeletal proteins FtsZ and FtsA, with minimal cytotoxicity toward mammalian cells. In the present study, we have further investigated antibacterial effects of the aforementioned AgNPs and that of a newly developed silver-metal-carbohydrate nanoparticle (Ag-MCNP) particularly on MDR *E. cloacae* isolates. Further, with the objective to consolidate our findings, we also investigated the effect of these silver nanoparticles on expression of AcrAB-TolC efflux pump proteins in MDR *E. cloacae* isolates.

MATERIALS AND METHODS

Bacterial Strains and Media

A wild type *E. cloacae* (EspIMS6) urinary tract infection isolate from a tertiary care hospital at Bhubaneswar, India, and *E. cloacae* subsp. *cloacae* ATCC-13047 type strain were used in the present study. The bacterial isolates were identified by biochemical tests followed by 16S rRNA gene sequencing. As prescribed for Enterobacteriaceae (CLSI, 2016), *E. coli* strain ATCC 25922 was used as control during antibiotic susceptibility testing. Unless otherwise mentioned, bacterial cultures were grown on nutrient agar/broth (Hi-Media, India) and incubated at 37°C in a controlled environment shaker (New Brunswick, NJ, United States). Muller Hinton broth (MHB)/agar (MHA) medium (Hi-Media, India) was used for antibiotic susceptibility test. Following sub-culture, the strains were preserved at −80°C

in 20% glycerol for further use. All experiments were performed in triplicate and repeated at least three times.

Resistance Profiling

Antibiotic disks used in resistance profiling were obtained from Himedia, India. Each strain was tested for susceptibility to different antibiotics by disk diffusion method (Bauer et al., 1966). The diameter of the inhibition zones was interpreted following CLSI standard as proposed for Enterobacteriaceae (CLSI, 2016).

Characterization of Silver Nanoparticles Used

Physical Characterization of the Nanoparticles Used

Particle size and zeta potential (ζ) of the polysaccharide capped silver nanoparticles were measured by Zetasizer Nano ZS instrument (Malvern Instruments, United Kingdom) at a constant temperature of 25 ± 1°C. The samples (0.1 mg/ml) were suspended in Milli-Q water and sonicated for 1 min. The mean hydrodynamic diameter and zeta potential for each sample was measured in triplicate and the results were measured as mean size ± SD. The surface plasmon resonance (SPR) was recorded at different time points (10–150 min) for polysaccharide-capped silver nanoparticles (AgNP) against the only carboxyl methyl tamarind (CMT) polysaccharide solution as blank.

Determining Hemocompatibility of Silver Nanoparticle

Hemocompatibility of polysaccharide capped silver nanoparticle was determined in terms of percent hemolysis using sheep blood (Mangalaraj and Devi, 2017). The diluted suspension of extracted RBCs (0.2 ml) was mixed with varied concentrations (1, 3, 6, 9, and 12 μg/ml) of AgNPs in PBS (0.8 ml). Diluted suspension of RBCs mixed with 0.8 ml PBS and 0.8 ml double distilled water were used as negative and positive control, respectively. The mixture was gently vortexed and incubated at room temperature for 3 h. After centrifugation (1600 rpm, 5 min) of the incubated mixture, absorbance of the supernatant was recorded at 541 nm by UV-Vis spectrophotometer (Agilent Cary 100 UV-Vis, Germany). Finally, hemocompatibility was evaluated in terms of percent hemolysis using the formula: $(A_S - A_N)/(A_P - A_N) \times 100$; where "$A_S$" is the sample absorbance, "A_N" is the absorbance of negative control and "A_P" is the absorbance of positive control (Jana et al., 2016).

Determining Effect of CMT-Capped Ag-MCNP on Mammalian Cells

The cytotoxic effect of polysaccharide capped nanoparticles against Mouse macrophage (RAW 264.7) cells were evaluated by MTT [3-(4,5-Dimethylthiazol-2-Yl)-2,5-Diphenyltetrazolium Bromide] assay. Approximately, 1×10^4 cells were seeded in 96-well plates (Tarsons, India) and were incubated for 24 h at 37°C in a 5% CO_2 incubator with different concentration of Ag-MCNP's (1, 2, 3, 4, and 6 μg/ml, respectively). Raw cells seeded without nanoparticles were used as control. To determine the cell viability, MTT dye (100 μl from 0.1 mg/ml stock) was added to each well and incubated for 4 h at 37°C, 5% CO_2 in dark. In this assay, metabolically active cells reduce the MTT salt into water insoluble purple MTT formazan crystal by mitochondrial dehydrogenase. The formazan crystals formed as a result of cellular reduction of MTT were dissolved in buffer solution (4 g NP-40 detergent in 50 ml 0.02 M HCl and 50 ml isopropanol) and incubated for 1 h at 37°C and absorbance was measured at 570 nm in an ELISA reader (BioTek, Germany). The percentage of cell viability at different doses of Ag-MCNPs was obtained by the following formula: % cell viability = [OD sample – OD control] – 100/OD control.

Determination of Minimum Inhibitory Concentration (MIC) Breakpoints for Nanoparticles

Minimum inhibitory concentration (MIC) values were determined for both the nanoparticles *viz.* silver nanoparticle (AgNP) and silver-metal-carbohydrate nanoparticles (Ag-MCNP's) by macrobroth double dilution method based on the guidelines of Clinical Laboratory Standard Institute (CLSI) for Enterobacteriaceae (CLSI, 2016). Ten microliters of mid log bacterial cultures ($OD_{600\ nm}$: 0.6–0.8) were inoculated into MHB with different concentration (μg/ml) of nanoparticles. Inoculated tubes were incubated at 37°C, 220 rpm in bacteriological incubator shaker (New Brunswick, NJ, United States). MIC break point values (in μg/ml) were noted after overnight incubation at the above-mentioned conditions. Further, we checked survival of the bacteria by dilution plating onto MHA plates to enumerate viable colonies.

Determining Effect of Silver Nanoparticles on AcrAB-TolC Efflux Pump Protein Expression

The bacterial cells of ($OD_{600\ nm}$: 0.6–0.8), were treated with sub-MIC concentration of nanoparticles, i.e., AgNPs (6 μg/ml) and Ag-MCNPs (0.75 μg/ml), and incubated for specified time points (e.g., 0, 30, 60, 120, 180 min). Both the treated and control bacterial cells were pelleted down, washed once with 1X PBS (pH 7.4), dissolved in 1X PBS and kept on ice. The protein samples were preserved by adding proteinase-K, lysed by treating with 5X Lamelli buffer and heat denatured at 95°C for 5 min. Extracted protein samples were then loaded onto 12% polyacrylamide gels, transferred to polyvinylidene fluoride (PVDF) membrane (Millipore, United States) for 1 h at 17 V, blocked by 5% skimmed milk in Tris buffered Saline with 0.05% Tween-20 (1X TBST). Blots were incubated with custom synthesized anti-rabbit polyclonal anti-AcrA, anti-AcrB, and anti-TolC primary antibodies (GenScript, United States) at 1:1000 dilutions overnight at 4°C. After incubation, blots were washed thrice with 1X TBST. Further blots were incubated with goat anti-rabbit immunoglobulin secondary antibodies (1:10,000) conjugated to horseradish peroxidase. Specific bands were visualized by Chemiluminescence method using SuperSignal™ West Femto maximum sensitivity substrate kit (Thermo Scientific, United States). The images were acquired

using ChemiDoc and analyzed using Quantity-one software (Bio-Rad, United States).

RESULTS

Resistance Profile of *Enterobacter* Isolates

The wild type *E. cloacae* clinical isolate (EspIMS6) exhibited extreme drug resistant (XDR) phenotype with resistance to β-lactams, cephalosporins belonging to second and third-generation, imipenem, fluoroquinolones (**Table 1**). The type strain, *E. cloacae* ATCC 13047 displayed MDR phenotype. Both of these isolates harbor multidrug efflux system AcrAB-TolC belonging to RND superfamily (data not shown).

Characterization of Silver Nanoparticles Used

Physical Characterization of the Nanoparticles Used

The size of nanoparticles has direct relevance with the stability, surface charge, bio distribution, cellular uptake, and drug release of nanomedicine (Lamprecht et al., 2001). The average size measured from photon correlation spectroscopy was found to be 140 d.nm in terms of number percent distribution (**Figures 1A,B**). The poly-dispersity index (PDI) of 0.208 indicated the monodispersed pattern of nanoparticles (Chandni et al., 2013). The surface charge of nanoparticles is another vital physical characteristic affecting its stability. The surface characteristics of polysaccharide capped AgNPs was measured upon immediate synthesis and 6 months post-synthesis. The mean zeta potential of AgNP was measured to be -34.5 ± 2.2 mV (**Figures 1C,D**). Nanoparticles with zeta potential values outside the range of $+30$ to -30 mV are considered stable for a longer period in suspended state (Yue et al., 2008). To validate long-term stability of suspended AgNPs, hydrodynamic diameter, PDI and surface charge were measured 6 months post-synthesis by photon correlation spectroscopy and results compared with those obtained for initially synthesized AgNPs. Our data suggest that there is slight increase in hydrodynamic diameter (161 d.nm), with PDI (0.426) and surface charge (−28.6) (**Figures 1A,B**). However, PDI smaller than 0.5 suggested that there is no agglomeration of nanoparticles and thus these particles are stable at room temperature for longer period of time (Yue et al., 2008). Further CMT-capped AgNP was characterized by SPR observed from UV-Vis spectral analysis. The occurrence of single maximum peak at wavelength 420 nm corresponded to the SPR of AgNPs (**Figure 1E**), and reflected about the size of AgNPs to be around 30–40 nm (Oldenburg, 2012). Further characterization of this AgNP such as size, dispersion, crystallinity and presence of silver has been performed by TEM, FE-SEM, XRD and EDAX methods, which was reported in our previous article (Sanyasi et al., 2016).

TABLE 1 | Antibiotic susceptibility profile of clinical *Enterobacter cloacae* isolates.

Strains	Resistant (R)	Susceptible (S)	Intermediate (I)
EspIMS6	CZX, CX, LE, CTR, TCC, PIT, GAT, A/S, CTX, AMC, OF, CIP, AMP, CXM, IPM, CPM, COT, CAZ, CAC, AT	GEN, AK	MRP
ATCC 13047	AMC, CXM, AMP, CAZ, CX, CAC, A/S	COT, CPM, IPM, CIP, GEN, GAT, AT, OF, AK, MRP, PIT, CZX, LE	CTR, CTX

Antibiotic resistance profile of EspIMS6 and E. cloacae type strain ATCC 13047 control using DoDeca Enterobacteriaceae disks 1 and 2 (Himedia, India). Disk 1: Ampicillin-AMP (10 mcg), Gentamicin-GEN (10 mcg), Amikacin-AK (30 mcg), Ciprofloxacin-CIP (5 mcg), Ofloxacin-OF (5 mcg), Co-Trimoxazole-COT (25 mcg), Amoxyclav-AMC (30 mcg), Cefuroxime-CXM (30 mcg), Ceftazidime-CAZ (30 mcg), Ceftazidime/Clavulanic acid-CAC (30/10 mcg), Cefepime-CPM (30 mcg), Imipenem-IPM (10 mcg). Disk 2: Cefotaxime-CTX (30 mcg), Cetriaxone-CTR (30 mcg), Cefoxitin-CX (30 mcg), Meropenem-MRP (10 mcg), Piperacillin/Tazobactam-PIT (100/10 mcg), Aztreonam-AT (30 mcg), Gatifloxacin-GAT (5 mcg), Ampicillin/Sulbactam-A/S (10/10 mcg), Cefoperazone-CPZ (75 mcg), Levofloxacin-LE (5 mcg), Ceftizoxime-CZX (30 mcg), Ticarcillin/Clavulanic acid-TCC (75/10 mcg).

Hemocompatibility of Silver Nanoparticles

Extent of hemolysis of red blood cells was determined to check hemocompatibility of silver nanoparticles. It was observed that AgNPs at concentrations of 1, 3 and 6 μg/ml, exhibited only 0.063, 0.31, and 0.63% of hemolysis, respectively (**Figure 2**). At higher concentrations of AgNP (i.e., 9 and 12 μg/ml) hemolysis was approximately 2%. Nanoparticles exhibiting hemolysis below 5% are considered hemocompatible (Jana et al., 2016). Hence, our results indicated that AgNPs to be hemocompatible.

Effect of Ag-MCNPs on Cell Viability

We had previously shown that AgNP's were non-toxic to mammalian cells (Sanyasi et al., 2016). Here, we have assessed the cytotoxic effect of Ag-MCNPs on macrophage RAW 264.7 cell line using MTT assay. The MTT assay is rapid, sensitive, and inexpensive method to determine cell viability. The dose dependent viability of RAW 264.7 cells in different concentration of the Ag-MCNPs is shown in **Figure 3**. Cell viability result revealed that 99% cells were viable in presence of Ag-MCNPs at concentration of up to 3 μg/ml, while at 4 μg/ml concentration of Ag-MCNPs, 82% cells remained viable (**Figure 3**). However, at higher concentration (6 μg/ml) of Ag-MCNP, cell viability was reduced to 55% suggesting that Ag-MCNP was toxic to mammalian cells at this dosage. This indicated that Ag-MCNPs below concentrations of 6 μg/ml are non-toxic to mammalian cells. Notably, the concentration of Ag-MCNPs that was antibacterial in nature (i.e., 1.5 and 3 μg/ml), are non-toxic to mammalian cells and hence could be suitable for biomedical applications.

Antimicrobial Efficacy of AgNP and Ag-MCNP

We determined the MIC breakpoints for sliver nanoparticle (AgNP) and Ag-MCNP. We observed that both the nanoparticles tested significantly inhibited bacterial growth in a dose dependent manner (**Table 2** and Supplementary Figure S1). However, MIC

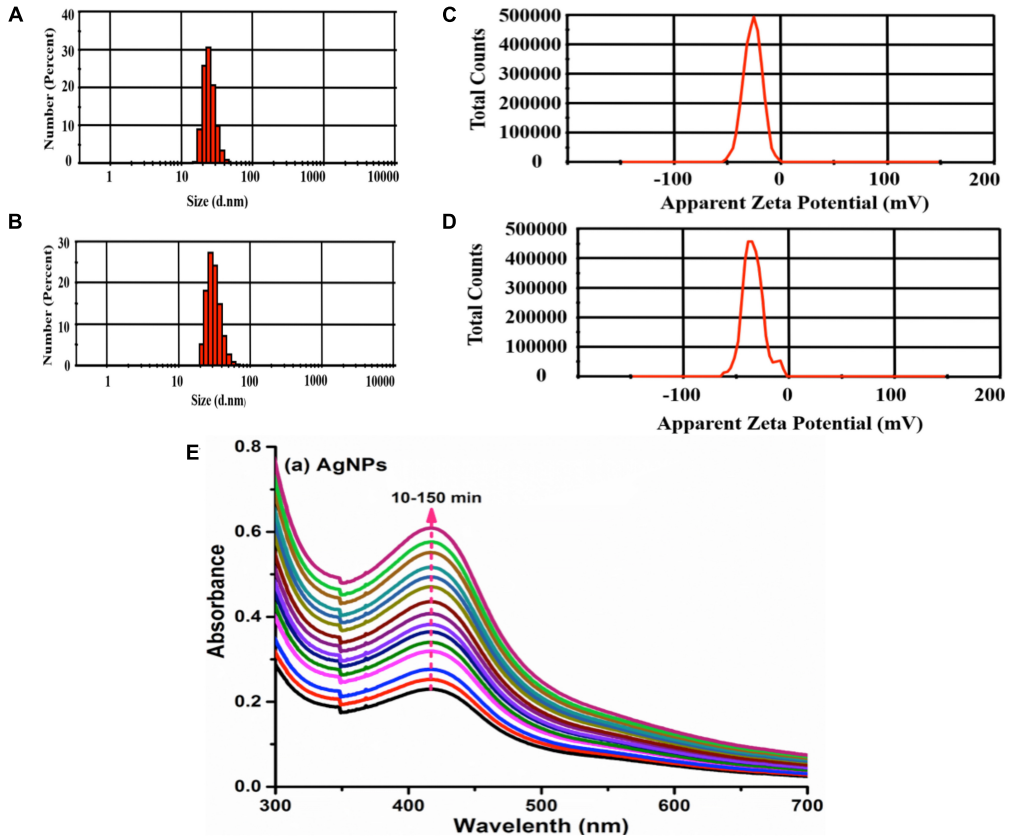

FIGURE 1 | Characterization of silver nanoparticles. Size of AgNps was determined by photon correlation spectroscopy immediately after synthesis **(A)** and 6 months post-synthesis **(B)**. Stability of AgNPs in terms of Zeta potential (–34 mV) was measured immediately after synthesis **(C)** and 6 months post-synthesis **(D)**. Determination of stability of AgNPs by SPR was conducted at λmax 420 over 10–150 min **(E)**.

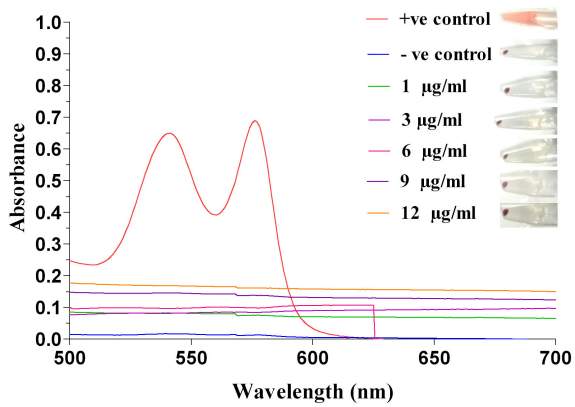

FIGURE 2 | Hemolysis activity of silver nanoparticle. Determination of hemolytic activity at different concentrations (1, 3, 6, 9, and 12 µg/ml) of Ag-NPs, along with positive and negative control, recorded at 541 nm by UV-Vis spectrophotometer.

breakpoint for AgNPs was 12 µg/ml for both EspIMS6 and *E. cloacae* ATCC 13047. Interestingly, Ag-MCNPs had a much lower MIC breakpoint of 1.5 and 3 µg/ml for isolates EspIMS6 and *E. cloacae* ATCC 13047, respectively. The results clearly indicated that Ag-MCNPs was more efficient in killing the MDR *E. cloacae* compared to AgNPs alone.

Effect of Silver Nanoparticles on AcrAB-TolC Efflux Pump Protein Expression

As reported from the literature, success of potential antibacterial agents rested upon their efficacy to be retained in the cell vis-à-vis being effluxed out. We investigated this by studying the effect of silver nanoparticles on expression of multidrug efflux pump proteins AcrAB-TolC.

Overall immunoblotting results revealed that presence of silver nanoparticles did not significantly affect AcrA and TolC efflux pump protein expression (**Figures 4A,C**). However, in the *E. cloacae* ATCC 13047, AcrB, and TolC protein expression showed slight albeit insignificant decrease in presence of Ag-MCNPs (**Figures 4B,C** and Supplementary Figure S2). Inhibition of AcrB monomeric protein expression was more prominent in clinical isolate EspIMS6, where only 38 kDa AcrB protein was consistently expressed at all the time points of exposure to AgNP (at 6 µg/ml) as well as Ag-MCNP (at 0.75 µg/ml) (**Figure 4B** and Supplementary Figure S2). Though, ∼112 kDa

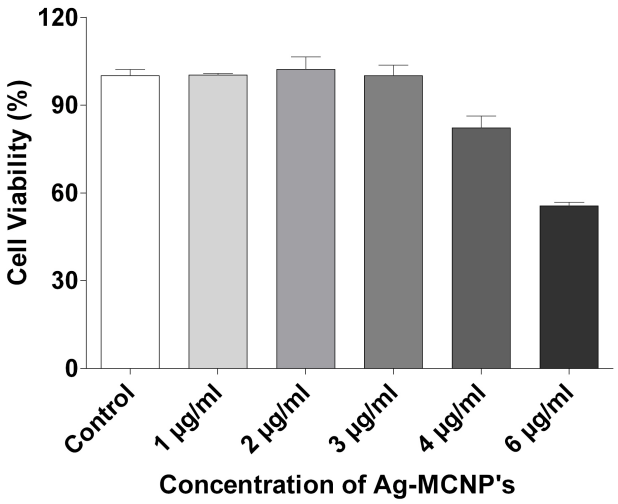

FIGURE 3 | Cytotoxicity assay of silver nanoparticle. Effect of Ag-MCNP on cell viability was determined by MTT assay with RAW 264.7 cells with increasing concentrations (1, 2, 3, 4, and 6 μg/ml) of the nanoparticle. Percentage of cell viability was calculated with respect to untreated cells.

TABLE 2 | Antibacterial activity of silver and silver-metal composite nanoparticles.

Isolates ID	MIC (in μg/ml)	
	AgNP	Ag-MCNP
EspIMS6	12	1.5
ATCC-13047	12	3

band was less expressed in *E. cloacae* ATCC 13047 in response to AgNP (at 6 μg/ml), a 38 kDa band of AcrB was observed post 30 min of treatment with Ag-MCNP at a concentration of 0.75 μg/ml in *E. cloacae* ATCC 13047 (**Figure 4B**, panels 3 and 4 and Supplementary Figure S2). It is pertinent to mention here that, AcrB is a transmembrane RND transporter protein of the tripartite efflux pump assembly. The functional membrane embedded protein is a homotrimer with molecular masses of ∼380 kDa, with each monomer of approximately 112 kDa (Tikhonova et al., 2011). However, in both isolates EspIMS6 and *E. cloacae* ATCC 13047 treated with the AgNP nanoparticles, it was shown to inhibit monomeric 112 kDa bands, and showed bands corresponding to ∼38 kDa (Supplementary Figure S2). This ∼38 kDa band perhaps represents the truncated by product of the AcrB protein complex. It is pertinent to mention that the antibodies used were beyond doubt.

Expression of outer membrane protein TolC decreased post 120 min in *E. cloacae* ATCC 13047, in presence both the silver nanoparticles tested *viz.* AgNPs and Ag-MCNPs (**Figure 4C**, panels 3 and 4). Here too we did not observe any significant changes in TolC expression for the wild type isolate EspIMS6 in presence of either of the nanoparticles (**Figure 4C**, panels 1 and 2).

DISCUSSION

The present study reports no decrease in antibacterial efficacy of silver nanoparticles *viz.* AgNP and Ag-MCNP, despite expression of AcrAB-TolC efflux protein in MDR bacteria. This finding is significant as it reports no noticeable effect of nanoparticles on AcrAB-TolC efflux pump protein expression that are implicated in MDR phenotype. Secondly, the results corroborate with our previous report and confirm sustainability of using the said silver nanoparticles as antibacterial agents.

During the past decade, silver nanoparticles owing to their low toxicity, antibacterial and wound healing properties, have emerged as promising therapeutic alternatives (Ambrožová et al., 2017). To ensure feasibility of large-scale use of nanoparticles for medicinal purposes, eco-friendly approaches have been widely adapted to generate silver nanoparticles. Such approaches circumvent the use of toxic chemicals and hazardous equipment. Eco-friendly green synthesis approach utilizes natural cost-effective reductants such as microorganisms and plant products (Rao and Tang, 2017). We had earlier reported utilization of green synthesis approach to generate polysaccharide-capped AgNPs (Sanyasi et al., 2016).

Few of the important physical parameters essential for development of nanoparticles include size and surface charge that affects their stability (Lamprecht et al., 2001). In the present study, photon correlation spectroscopy results revealed that the CMT-capped AgNPs were smaller in size and are monodispersed in nature (Chandni et al., 2013). The mean zeta potential of AgNPs used was measured to be -34.5 ± 2.2 mV, suggesting higher electrical charge on their surface and thus, approved their long-term stability (Yue et al., 2008). SPR characterization of AgNPs demonstrated their size to be around 30–40 nm, which corroborated well with previous report (Oldenburg, 2012). Biocompatibility is extremely important feature for nanoparticles to be used as therapeutic agents. For this, we performed hemolysis assay that described the AgNPs to be non-hemolytic. We had previously reported AgNPs to be less cytotoxic toward mammalian cells even at higher concentrations (Sanyasi et al., 2016). The newly developed Ag-MCNPs reported here, too displayed minimal cytotoxic activity toward mammalian cells. Both AgNPs and Ag-MCNPs revealed excellent antimicrobial activity against multiple drug resistant *E. cloacae* isolates at low dose. Our results corroborated well with previous reports suggesting antimicrobial properties of silver nanoparticles (Kim et al., 2007; Chen et al., 2014), that boosted their candidature as potential antimicrobial agents. Durán et al. (2016) proposed cell membrane disruption by the silver ions as a plausible mechanism of antibacterial activity by silver nanoparticles.

However, one of the less addressed aspect has been the effect of AgNPs on bacterial efflux systems. Kovács et al. (2016) reported AgNPs to inhibit activity of *p*-glycoproteins efflux pump (belonging to ABC transporter family) in MDR cancer cells, thereby enhancing effectiveness of chemotherapy. Christena et al. (2015) have established the efflux inhibitory properties of copper nanoparticles (CuNPs) in tackling MDR *Staphylococcus aureus* and *Pseudomonas aeruginosa* isolates. However, effect of AgNPs on expression of bacterial

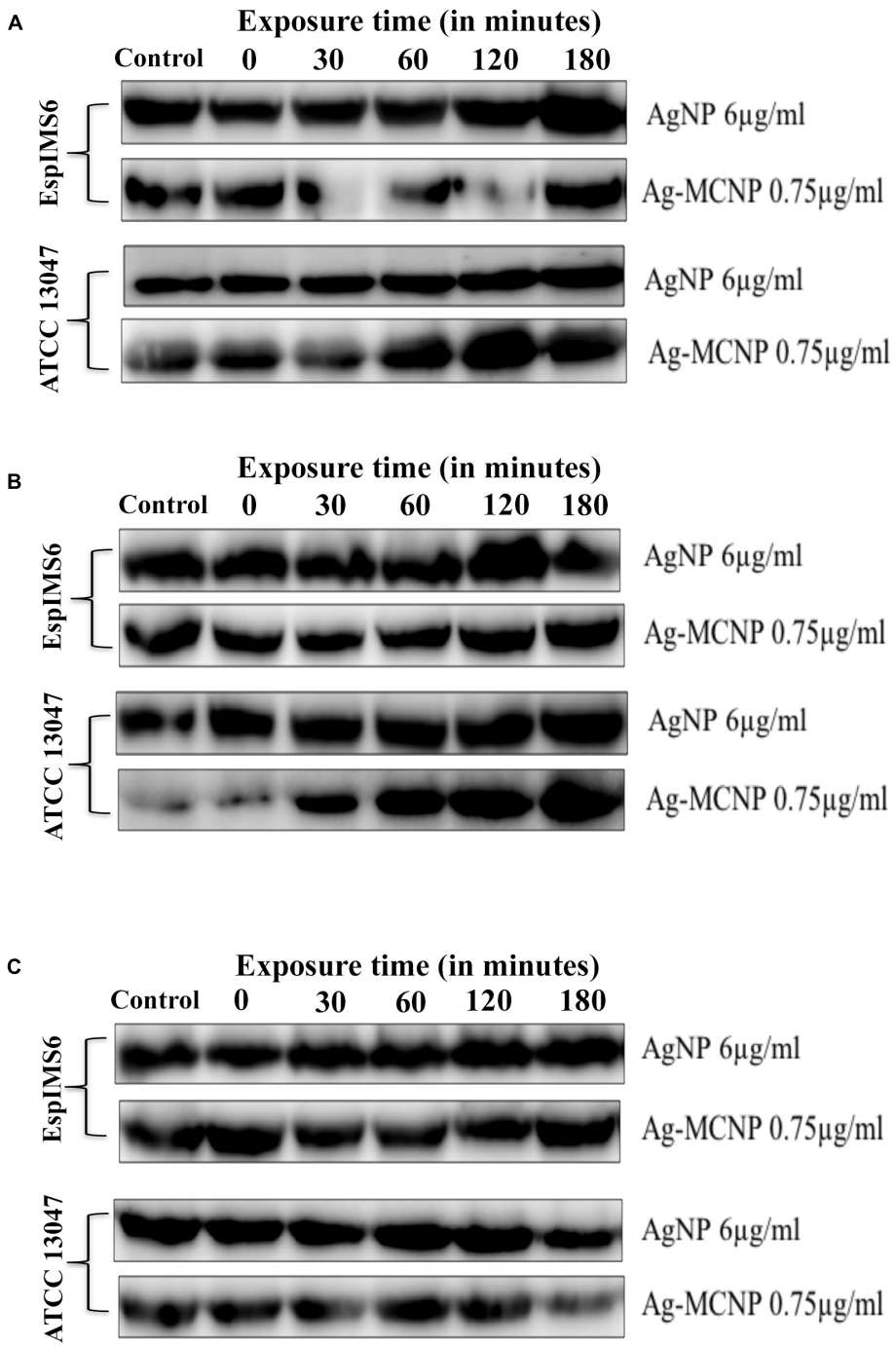

FIGURE 4 | Effect of silver and silver-metal composite nanoparticles on AcrAB-TolC expression. **(A)** AcrA (42 kDa) protein expression in EspIMS6 (top panel) and *Enterobacter cloacae* ATCC 13047 (bottom panel); **(B)** AcrB (∼38 kDa) protein expression in EspIMS6 (top panel) and *E. cloacae* ATCC 13047 (bottom panel); **(C)** TolC (55 kDa) protein expression in EspIMS6 (top panel) and *E. cloacae* ATCC 13047 (bottom panel).

MDR efflux pumps has not been elucidated. AcrAB-TolC efflux pumps have been found to mediate MDR phenotype in many clinically significant gram-negative pathogens including *E. cloacae* (Piddock, 2006; Pérez et al., 2012; Amaral et al., 2013). These efflux systems efficiently extrude out of the bacterial cell, structurally divergent classes of drugs, resulting in multiple antibiotic resistance phenotype (Poole, 2005; Sun et al., 2014). This prompted us to study the

effect of AgNPs and Ag-MCNPs on AcrAB-TolC efflux pump protein expression. Our results indicated that AgNPs affected the expression of AcrB transporter protein to a greater extent as compared to AcrA and TolC. Functional AcrB is a trimeric RND transporter protein with each monomer of ∼112 kDa (Du et al., 2015). Review of literature reveals antimicrobial drugs to induce over expression of AcrAB-TolC efflux pump protein, which in turn facilitates their rapid extrusion (Rosenberg et al., 2003). In the present study, expression of functional AcrB protein was reduced in *E. cloacae* isolates upon addition of silver nanoparticles (Supplementary Figure S2). It is pertinent to mention that AcrB protein is responsible for substrate recognition and binding of diverse structures (Sun et al., 2014). The results provide circumstantial evidence indicative of AgNPs functioning as efflux inhibitor. Efflux inhibitory role of metal nanoparticles have been hypothesized to be either by direct binding to active site of the efflux pumps or hindering efflux kinetics (Gupta et al., 2017). However, owing to the small size of nanoparticles and substrate non-specific nature of efflux pumps proteins these explicit mechanisms still remain elusive. Earlier studies have shown that expression of AcrB transporter is affected by cellular metabolites (Ruiz and Levy, 2014) and hence forms an ideal target for efflux and virulence inhibitor design (Blair et al., 2015). Also, AcrB is a proton motive force (PMF) dependent RND transporter. Interestingly, Dibrov et al. (2002) in a study on mechanism of action of nanoparticles, observed that metal nanoparticles such as AgNPs, dissipate PMF by interfering with bacterial respiration. Hence, energy required for this tripartite efflux system may be hindered by the addition of AgNPs. In the present study, in presence of AgNPs, though TolC and AcrA protein expression remained more or less unaffected, the absence of a functional monomeric AcrB perhaps renders the bacterial cells impaired for efflux activity. Change in efflux activity in *Enterobacter* spp. by AgNPs has been reported in context of EmmDR efflux pump [belonging to multiple antibiotic and toxic extrusion (MATE) superfamily] (Gui et al., 2013). However, to the best of our knowledge, this is the first report on effect of silver nanoparticles on AcrAB-TolC efflux protein expression. This study indicates potential efflux inhibitor property of the AgNPs.

To summarize, the reported silver nanoparticles generated by green synthesis method, are highly stable, small in size, non-hemolytic with minimal cytotoxic effect. Further, their antimicrobial activity is not affected by expression of AcrAB-TolC efflux proteins. Such versatile repertoire of qualities enables us to report the said silver nanoparticles as strong candidates as antibacterial agents. The results of the present study support further development of silver nanoparticle formulations as alternate therapeutic agents to combat infections caused by MDR gram-negative Enterobacterial pathogens.

AUTHOR CONTRIBUTIONS

The present study was conceived by HM and executed by MM. SK, LG, RM, and CG developed and characterized the nanoparticles.

FUNDING

MM received INSPIRE fellowship from the Department of Science and Technology, New Delhi (Grant No. IF110739).

ACKNOWLEDGMENTS

HM and MM thankfully acknowledge intramural financial support from NISER for the study.

SUPPLEMENTARY MATERIAL

The Supplementary Material for this article can be found online at: https://www.frontiersin.org/articles/10.3389/fmicb.2018.00823/full#supplementary-material

REFERENCES

Amaral, L., Martins, A., Spengler, G., and Molnar, J. (2013). Efflux pumps of Gram-negative bacteria: What they do, how they do it, with what and how to deal with them. *Front. Pharmacol.* 4:168. doi: 10.3389/fphar.2013.0900168

Ambrožová, N., Zálešák, B., Ulrichová, J., Čížková, K., and Galandáková, A. (2017). Low concentrations of silver nanoparticles have a beneficial effect on wound healing in vitro. *J. Nanoparticle Res.* 19:108. doi: 10.1007/s11051-017-3809-7

Bauer, A. W., Kirby, W. M., Sherris, J. C., Turck, A. M., and Von Graevenitz, A. (1966). 40 Microbiology:a centenary perspective 1966 antibiotic susceptibility testing by a standardized single disk method. *Am. J. Clin. Pathol.* 45, 493–496. doi: 10.1093/ajcp/45.4_ts.493

Blair, J. M., Smith, H. E., Ricci, V., Lawler, A. J., Thompson, L. J., and Piddock, L. J. V. (2015). Expression of homologous RND efflux pump genes is dependent upon AcrB expression: implications for efflux and virulence inhibitor design. *J. Antimicrob. Chemother.* 70, 424–431. doi: 10.1093/jac/dku380

Boucher, W. H., Talbot, G. H., Bradley, J. S., Edwards, J. E., Gilbert, D., Rice, L. B., et al. (2009). Bad bugs, no drugs: no ESKAPE! An update from the infectious diseases society of America. *Clin. Infect. Dis.* 48, 1–12. doi: 10.1086/595011

Chandni, Andhariya, N., Pandey, O., and Chudasama, B. (2013). A growth kinetic study of ultrafine monodispersed silver nanoparticles. *RSC Adv.* 3, 1127–1136. doi: 10.1039/C2RA21912C

Chen, C. W., Hsu, C. Y., Lai, S. M., Syu, W. J., Wang, T. Y., and Lai, P. S. (2014). Metal nanobullets for multidrug resistant bacteria and biofilms. *Adv. Drug Deliv. Rev.* 78, 88–104. doi: 10.1016/j.addr.2014.08.004

Christena, L. R., Mangalagowri, V., Pradheeba, P., Ahmed, K. B. A., Shalini, B. I. S., Vidyalakshmi, M., et al. (2015). Copper nanoparticles as an efflux pump inhibitor to tackle drug resistant bacteria. *RSC Adv.* 5, 12899–12909. doi: 10.1039/C4RA15382K

CLSI (2016). *M100S: Performance Standards for Antimicrobial Susceptibility Testing*. Wayne, PA: CLSI.

Davin-Regli, A., and Pagès, J. M. (2015). *Enterobacter* aerogenes and *Enterobacter cloacae*; Versatile bacterial pathogens confronting antibiotic treatment. *Front. Microbiol.* 6:392. doi: 10.3389/fmicb.2015.00392

Dibrov, P., Dzioba, J., Gosink, K. K., Häse, C. C., and Ha, C. C. (2002). Chemiosmotic mechanism of antimicrobial activity of Ag+ in *Vibrio*

cholerae. *Antimicrob. Agents Chemother.* 46, 2668–2670. doi: 10.1128/AAC.46.8.2668

Du, D., Wang, Z., James, N. R., Voss, J. E., Klimont, E., Ohene-, T., et al. (2015). Structure of the AcrAB-TolC multidrug efflux pump. *Nature* 509, 512–515. doi: 10.1038/nature13205

Durán, N., Durán, M., de Jesus, M. B., Seabra, A. B., Fávaro, W. J., and Nakazato, G. (2016). Silver nanoparticles: a new view on mechanistic aspects on antimicrobial activity. *Nanomedicine* 12, 789–799. doi: 10.1016/j.nano.2015.11.016

Fraser, S. L., and Arnett, M. (2010). *Enterobacter* infections. *J. WebM D* 7, 114–120.

Gelperina, S., Kisich, K., Iseman, M. D., and Heifets, L. (2005). The potential advantages of nanoparticle drug delivery systems in chemotherapy of tuberculosis. *Am. J. Respir. Crit. Care Med.* 172, 1487–1490. doi: 10.1164/rccm.200504-613PP

Grimont, F., and Grimont, P. (2006). The genus *Enterobacter*. *Prokaryotes* 6, 197–214. doi: 10.1007/0-387-30746-x_9

Gui, H., Wei, Z., Huizhong, C., Sam, S., Conner, T., Eugene, R., et al. (2013). Impacts of silver nanoparticles on bacterial multidrug efflux pump. *FASEB J.* 27. Available at: https://www.fasebj.org/doi/abs/10.1096/fasebj.27.1_supplement.575.12

Gupta, D., Singh, A., and Khan, A. U. (2017). Nanoparticles as efflux pump and biofilm inhibitor to rejuvenate bactericidal effect of conventional antibiotics. *Nanoscale Res. Lett.* 12:454. doi: 10.1186/s11671-017-2222-6

Jana, S. K., Mandal, A. K., Kumar, A., Puschmann, H., Hossain, M., and Dalai, S. (2016). Sensing of tryptophan by a non-toxic cobalt(II) complex. *RSC Adv.* 6, 95888–95896. doi: 10.1039/c6ra16086g

Kerantzas, C. A., and Jacobs, W. R. (2017). Origins of combination therapy for tuberculosis: lessons for future antimicrobial development and application. *mBio* 8:e01586-16. doi: 10.1128/mBio.01586-16

Kim, J. S., Kuk, E., Yu, K. N., Kim, J. H., Park, S. J., Lee, H. J., et al. (2007). Antimicrobial effects of silver nanoparticles. *Nanomedicine* 3, 95–101. doi: 10.1016/j.nano.2006.12.001

Kovács, D., Szoke, K., Igaz, N., Spengler, G., Molnár, J., Tóth, T., et al. (2016). Silver nanoparticles modulate ABC transporter activity and enhance chemotherapy in multidrug resistant cancer. *Nanomedicine* 12, 601–610. doi: 10.1016/j.nano.2015.10.015

Lamprecht, A., Schäfer, U., and Lehr, C. M. (2001). Size-dependent bioadhesion of micro- and nanoparticulate carriers to the inflamed colonic mucosa. *Pharm. Res.* 18, 788–793. doi: 10.1023/A:1011032328064

Mahlapuu, M., Håkansson, J., Ringstad, L., and Björn, C. (2016). Antimicrobial peptides: an emerging category of therapeutic agents. *Front. Cell. Infect. Microbiol.* 6:194. doi: 10.3389/fcimb.2016.00194

Mangalaraj, D., and Devi, D. N. (2017). "Ag/TiO2 (Metal/Metal Oxide) core shell nanoparticles for biological applications," in *Recent Trends in Materials Science and Applications*, ed. J. Ebenezar (Cham: Springer International Publishing), 9–17. doi: 10.1007/978-3-319-44890-9_2

Martins, M., and McCusker, M. P. (2016). Editorial: Alternative therapeutics against MDR bacteria - "Fighting the epidemic of antibiotic resistance." *Front. Microbiol.* 7:1559. doi: 10.3389/fmicb.2016.01559

Mezzatesta, M. L., Gona, F., and Stefani, S. (2012). *Enterobacter cloacae* complex: clinical impact and emerging antibiotic resistance. *Future Microbiol.* 7, 887–902. doi: 10.2217/fmb.12.61

Oldenburg, S. J. (2012). *Silver Nanoparticles: Properties and Applications. Sigma-Aldrich.* Available at: https://www.sigmaaldrich.com/technical-documents/articles/materials-science/nanomaterials/silver-nanoparticles.html

Pelgrift, R. Y., and Friedman, A. J. (2013). Nanotechnology as a therapeutic tool to combat microbial resistance. *Adv. Drug Deliv. Rev.* 65, 1803–1815. doi: 10.1016/j.addr.2013.07.011

Pendleton, J. N., Gorman, S. P., and Gilmore, B. F. (2013). Clinical relevance of the ESKAPE pathogens. *Expert Rev. Anti Infect. Ther.* 11, 297–308. doi: 10.1586/eri.13.12

Pérez, A., Poza, M., Fernández, A., Del Carmen Fernández, M., Mallo, S., Merino, M., et al. (2012). Involvement of the AcrAB-TolC efflux pump in the resistance, fitness, and virulence of *Enterobacter cloacae*. *Antimicrob. Agents Chemother.* 56, 2084–2090. doi: 10.1128/AAC.05509-11

Piddock, L. J. (2006). Clinically relevant chromosomally encoded multidrug resistance efflux pumps in bacteria. *Clin. Microbiol. Rev.* 19, 382–402. doi: 10.1128/CMR.19.2.382

Poole, K. (2005). Efflux-mediated antimicrobial resistance. *J Antimicrob Chemother.* 56, 20–51. doi: 10.1093/jac/dki171

Rangel-Vega, A., Bernstein, L. R., Mandujano-Tinoco, E. A., García-Contreras, S. J., and García-Contreras, R. (2015). Drug repurposing as an alternative for the treatment of recalcitrant bacterial infections. *Front. Microbiol.* 6:282. doi: 10.3389/fmicb.2015.00282

Rao, B., and Tang, R.-C. (2017). Green synthesis of silver nanoparticles with antibacterial activities using aqueous Eriobotrya japonica leaf extract. *Adv. Nat. Sci. Nanosci. Nanotechnol.* 80:015014. doi: 10.1088/2043-6254/aa5983

Rosenberg, E. Y., Bertenthal, D., Nilles, M. L., Bertrand, K. P., and Nikaido, H. (2003). Bile salts and fatty acids induce the expression of *Escherichia coli* AcrAB multidrug efflux pump through their interaction with Rob regulatory protein. *Mol. Microbiol.* 48, 1609–1619. doi: 10.1046/j.1365-2958.2003.03531.x

Ruiz, C., and Levy, S. B. (2014). Regulation of acrAB expression by cellular metabolites in *Escherichia coli*. *J. Antimicrob. Chemother.* 69, 390–399. doi: 10.1093/jac/dkt352

Salata, O. (2004). Applications of nanoparticles in biology and medicine. *J. Nanobiotechnol.* 2:3.

Sanders, W. E., and Sanders, C. C. (1997). *Enterobacter* spp.: Pathogens poised to flourish at the turn of the century. *Clin. Microbiol. Rev.* 10, 220–241.

Sanyasi, S., Majhi, R. K., Kumar, S., Mishra, M., Ghosh, A., Suar, M., et al. (2016). Polysaccharide-capped silver Nanoparticles inhibit biofilm formation and eliminate multi-drug-resistant bacteria by disrupting bacterial cytoskeleton with reduced cytotoxicity towards mammalian cells. *Sci. Rep.* 6:24929. doi: 10.1038/srep24929

Singh, R., and Lillard, J. W. (2009). Nanoparticle-based targeted drug delivery. *Exp. Mol. Pathol.* 86, 215–223. doi: 10.1016/j.yexmp.2008.12.004

Sun, J., Deng, Z., and Yan, A. (2014). Bacterial multidrug efflux pumps: Mechanisms, physiology and pharmacological exploitations. *Biochem. Biophys. Res. Commun.* doi: 10.1016/j.bbrc.2014.05.090

Tamma, P. D., Cosgrove, S. E., and Maragakis, L. L. (2012). Combination therapy for treatment of infections with gram-negative bacteria. *Clin. Microbiol. Rev.* 25, 450–470. doi: 10.1128/CMR.05041-11

Tikhonova, E. B., Yamada, Y., and Zgurskaya, H. I. (2011). Sequential mechanism of assembly of multidrug efflux pump AcrAB-TolC. *Chem. Biol.* 18, 454–463. doi: 10.1016/j.chembiol.2011.02.011

Tran, P. A., and Webster, T. J. (2011). Selenium nanoparticles inhibit *Staphylococcus aureus* growth. *Int. J. Nanomedicine* 6, 1553–1558. doi: 10.2147/IJN.S21729

WHO (2014). *ANTIMICROBIAL RESISTANCE Global Report on Surveillance 2014*. Geneva: WHO.

Yang, H., Yu, J., and Wei, H. (2014). Engineered bacteriophage lysins as novel anti-infectives. *Front. Microbiol.* 5:542. doi: 10.3389/fmicb.2014.00542

Yue, P. F., Yuan, H. L., Yang, M., You, R. H., Cong, L. B., Zhu, J., et al. (2008). Preparation, characterization, and pharmacokinetic evaluation of puerarin submicron emulsion. *PDA J. Pharm. Sci. Technol.* 62, 32–45.

Zgurskaya, H. I. (2009). Multicomponent drug efflux complexes: architecture and mechanism of assembly. *Future Microbiol.* 4, 919–932. doi: 10.2217/fmb.09.62. Multicomponent

Conflict of Interest Statement: The authors declare that the research was conducted in the absence of any commercial or financial relationships that could be construed as a potential conflict of interest.

The reviewer RP and handling Editor declared their shared affiliation.

Copyright © 2018 Mishra, Kumar, Majhi, Goswami, Goswami and Mohapatra. This is an open-access article distributed under the terms of the Creative Commons Attribution License (CC BY). The use, distribution or reproduction in other forums is permitted, provided the original author(s) and the copyright owner are credited and that the original publication in this journal is cited, in accordance with accepted academic practice. No use, distribution or reproduction is permitted which does not comply with these terms.

frontiers in Microbiology

ORIGINAL RESEARCH
published: 15 May 2018
doi: 10.3389/fmicb.2018.00912

Efficacy of Colistin and Its Combination With Rifampin *in Vitro* and in Experimental Models of Infection Caused by Carbapenemase-Producing Clinical Isolates of *Klebsiella pneumoniae*

María E. Pachón-Ibáñez[1], Gema Labrador-Herrera[1], Tania Cebrero-Cangueiro[1], Caridad Díaz[2], Younes Smani[1], José P. del Palacio[2], Jesús Rodríguez-Baño[3,4], Alvaro Pascual[3,5], Jerónimo Pachón[1,4] and M. Carmen Conejo[5]*

[1] Clinical Unit of Infectious Diseases, Microbiology, and Preventive Medicine, Institute of Biomedicine of Seville, University Hospital Virgen del Rocío/CSIC/University of Seville, Seville, Spain, [2] Fundacion Centro de Excelencia en Investigación de Medicamentos Innovadores en Andalucía, MEDINA Foundation, Granada, Spain, [3] Clinical Unit of Infectious Diseases, Microbiology, and Preventive Medicine, Institute of Biomedicine of Seville, University Hospital Virgen de Macarena/CSIC/University of Seville, Seville, Spain, [4] Department of Medicine, University of Seville, Seville, Spain, [5] Department of Microbiology, University of Seville, Seville, Spain

OPEN ACCESS

Edited by:
Noton Kumar Dutta, Johns Hopkins University, United States

Reviewed by:
Maria Bagattini, University of Naples Federico II, Italy
Remy A. Bonnin, Université Paris-Saclay, France

***Correspondence:**
María E. Pachón-Ibáñez
mpachon-ibis@us.es

Specialty section:
This article was submitted to Antimicrobials, Resistance and Chemotherapy, a section of the journal Frontiers in Microbiology

Received: *25 January 2018*
Accepted: *19 April 2018*
Published: *15 May 2018*

Citation:
Pachón-Ibáñez ME, Labrador-Herrera G, Cebrero-Cangueiro T, Díaz C, Smani Y, del Palacio JP, Rodríguez-Baño J, Pascual A, Pachón J and Conejo MC (2018) Efficacy of Colistin and Its Combination With Rifampin in Vitro and in Experimental Models of Infection Caused by Carbapenemase-Producing Clinical Isolates of Klebsiella pneumoniae. Front. Microbiol. 9:912. doi: 10.3389/fmicb.2018.00912

Despite the relevance of carbapenemase-producing *Klebsiella pneumoniae* (CP-Kp) infections there are a scarce number of studies to evaluate *in vivo* the efficacy of combinations therapies. The bactericidal activity of colistin, rifampin, and its combination was studied (time–kill curves) against four clonally unrelated clinical isolates of CP-Kp, producing VIM-1, VIM-1 plus DHA-1(acquired AmpC β-lactamase), OXA-48 plus CTX-M-15 (extended spectrum β-lactamase) and KPC-3, respectively, with colistin MICs of 0.5, 64, 0.5, and 32 mg/L, respectively. The efficacies of antimicrobials in monotherapy and in combination were tested in a murine peritoneal sepsis model, against all the CP-Kp. Their efficacies were tested in the pneumonia model against the OXA-48 plus CTX-M-15 producers. The development of colistin-resistance was analyzed for the colistin-susceptible strains *in vitro* and *in vivo*. *In vitro*, colistin plus rifampin was synergistic against all the strains at 24 h. *In vivo*, compared to the controls, rifampin alone reduced tissue bacterial concentrations against VIM-1 and OXA-48 plus CTX-M-15 strains; CMS plus rifampin reduced tissue bacterial concentrations of these two CP-Kp and of the KPC-3 strain. Rifampin and the combination increased the survival against the KPC-3 strain; in the pneumonia model, the combination also improved the survival. No resistant mutants appeared with the combination. In conclusion, CMS plus rifampin had a low and heterogeneous efficacy in the treatment of severe peritoneal sepsis model due to CP-Kp producing different carbapenemases, increasing survival only against the KPC-3 strain. The combination showed efficacy in the less severe pneumonia model. The combination prevented *in vitro* and *in vivo* the development of colistin resistant mutants.

Keywords: *Klebsiella pneumoniae*, animal models, carbapenemase producers, colistin, rifampin

INTRODUCTION

Carbapenem-resistant *Klebsiella pneumoniae* strains are spreading worldwide, representing an urgent threat to public health, as stressed by the Center for Disease Control and Prevention (CDC) of United States, the European Centre for Disease Prevention and Control (ECDC) and the World Health Organization (WHO). The rapid spread, mostly in hospital settings, is transforming many common health care-associated complications into infections that are sometimes untreatable with the currently available antimicrobials (Nordmann et al., 2012).

The carbapenem resistance *in K. pneumoniae* is mainly due to the production of acquired carbapenemases (Falagas et al., 2014). The most important carbapenemases found in this species may belong to the Ambler classes A (mainly KPC), B (the most frequent are VIM and IMP) and D (OXA-48-like enzymes). Invasive infections by isolates producing VIM and KPC are associated with high death rates (Tzouvelekis et al., 2012). The information about infections caused by OXA-48-producers is scarce, mostly because of its difficult identification (Nordmann et al., 2011; Canton et al., 2012; Tzouvelekis et al., 2012). Nevertheless, OXA-48 is the most frequent carbapenemase produced by Enterobacteriaceae isolated in many European countries (Canton et al., 2012; Palacios-Baena et al., 2016; De Laveleye et al., 2017).

Although the hydrolysis spectrum of these enzymes may vary, they hydrolyze most beta-lactams, including carbapenems. Moreover, carbapenemase producers often show co-resistance to other antimicrobial agents, leaving very few treatment options, such as tigecycline, colistin, and some aminoglycosides (de Oliveira et al., 2015). So, in an attempt to improve the poor clinical efficacy of the available drugs, combination therapy is often used as definitive therapy for infections caused by carbapenemase-producing *K. pneumoniae* (CP-Kp). To date, recommendations are based on few retrospective clinical studies and *in vitro* studies (Tzouvelekis et al., 2012). In addition, a scarce number of *in vivo* studies have assessed the efficacy of antimicrobial combinations against CP-Kp (Tzouvelekis et al., 2012). Clinical studies have reported favorable outcomes for patients treated with combinations of colistin and a carbapenem, tigecycline, fosfomycin, or an aminoglycoside (Michalopoulos et al., 2010; Lee and Burgess, 2012; Munoz-Price et al., 2013; Daikos et al., 2014). However, little data exists on which combination therapy is superior.

Several studies have reported synergistic activity of colistin and rifampin against colistin-resistant and colistin-susceptible KPC-producing *K. pneumoniae* clinical strains, using the checkerboard method. Similarly, studies based on time-kill experiments detected synergy with this combination against colistin-resistant KPC or NDM producers clinical strains, but no synergistic effect against VIM producers. To our knowledge, there is no data regarding the efficacy of this combination against *K. pneumoniae* producing OXA-48, nor *in vivo* studies to validate the *in vitro* results previously mentioned (Elemam et al., 2010; Tascini et al., 2013; Nastro et al., 2014; Tangden et al., 2014). Thus, the aim of this study was to evaluate the *in vitro* and *in vivo* efficacy of CMS plus rifampin against CP-Kp clinical strains producing different carbapenemases.

MATERIALS AND METHODS

Bacterial Strains, Beta-lactamase Characterization and Molecular Typing

Four genetically unrelated clinical isolates of CP-Kp were studied: Kp07, a VIM-1 ST 1603 clone producer (Miro et al., 2013); Kp21, which co-produced VIM-1 and the acquired AmpC type beta-lactamase DHA-1 ST 11 clone (Miro et al., 2013); Kp28, co-producing OXA-48 ST11 clone and the extended spectrum beta-lactamase (ESBL) CTX-M-15 (Oteo et al., 2015); and Kp29, co-producing KPC-3 ST512 clone with the broad spectrum beta-lactamases TEM-1 and SHV-11 (Lopez-Cerero et al., 2014), thereinafter VIM-1, VIM-1/DHA-1, OXA-48 plus CTX-M-15, and KPC-3 producers, respectively. Identification of these isolates was confirmed by a Microflex LT-MALDI Biotyper mass spectrometer (Bruker Daltonics GmbH, Bremen, Germany). The presence of carbapenemase genes, and genes coding for other beta-lactamases was confirmed by PCR and sequencing as described previously. The absence of genetic relation among the isolates was confirmed by PFGE analysis of chromosomal restriction fragments obtained after *Xba*I cleavage following the criteria of Tenover et al. (1995). Two of the strains, KPC-3 and VIM-1 (DHA-1) were multidrug-resistant while the other two were not. The antibiotic susceptibility profiles are included in the Supplementary Information.

Antimicrobials

For the *in vitro* assays, antimicrobials, colistin sulfate salt and rifampin, were used as standard laboratory powders (Sigma-Aldrich, Madrid, Spain). For *in vivo* experiments, clinical formulations were used: colistimethate sodium (CMS) (Genéricos Españoles S.A., Madrid, Spain) and rifampin (Sanofi-Aventis, Madrid, Spain).

In Vitro Studies

Antimicrobial Susceptibility Testing

MICs of antibiotics were determined by broth microdilution as recommended by the Clinical and Laboratory Standards Institute [CLSI] (2012), using Mueller Hinton broth II (MHB) (Becton Dickinson & Co., Sparks, MD, United States) and agar dilution method for fosfomycin. MIC results were interpreted according to the European Committee on Antimicrobial Susceptibility Testing [EUCAST] (2016)[1] breakpoints. Studies were performed in triplicate.

Time-Kill Curves

The concentrations of colistin used for susceptible strains corresponded to the MIC value obtained by microdilution,

[1]http://www.eucast.org/clinical_breakpoints/

whereas the concentration used for resistant strains was 2 mg/L, the susceptibility breakpoint recommended by European Committee on Antimicrobial Susceptibility Testing [EUCAST] (2016). Rifampin was used at a fixed concentration of 2 mg/L. Experiments were carried out with a starting inoculum of 1×10^6 cfu/mL and the antibiotics alone or in combination. Tubes were incubated at 37°C, with shaking, and samples were taken at 0, 1, 3, 6, and 24 h, serially diluted and plated using a spiral platter (Eddy Jet, IUL S.A., Barcelona, Spain). Bacterial colonies were counted using an automatic counter (Flash & Go, IUL S.A., Barcelona, Spain) (Pournaras et al., 2011; Souli et al., 2011). Experiments were performed three times on separate occasions. Synergy was defined as a decrease $\geq$ 2 $\log_{10}$ cfu/mL for the antimicrobial combination compared with the most active single agent. Bactericidal activities of single antibiotics or combination were defined as a decrease $\geq$ 3 $\log_{10}$ cfu/mL from the starting inoculum (Souli et al., 2009). Studies were performed in triplicate.

Animals

Immunocompetent C57BL/6 female mice weighing approximately 20 g (Production and Experimentation Animal Center, University of Seville, Seville, Spain) were used; they had a sanitary status of murine pathogen free and were assessed for genetic authenticity. Mice were housed in an individually ventilated cage system under specific pathogen-free conditions, and water and food supplied *ad libitum*. This study was carried out following the recommendations in the Guide for the Care and Use of Laboratory Animals (Souli et al., 2011). Experiments were approved by the Committee on the Ethics of Animal Experiments of the University Hospital Virgen Macarena, Seville, Spain (CI 1961). All procedures were performed under sodium thiopental (B. Braun Medical S.A., Spain) anesthesia, and all efforts were made to minimize suffering.

Pharmacokinetic/Pharmacodynamic Analysis

Serum antibiotic concentrations were determined in healthy mice after a single intraperitoneal (ip) administration of CMS (20 mg/kg) or rifampin (25 mg/kg). In sets of three anesthetized mice, blood samples from the periorbital plexus were obtained at different time points after the administration of CMS and rifampin. Blood samples were immediately centrifuged (4500 rpm, 15 min at 4°C), and serum samples stored at −80°C until the analysis. Both serum free and total antibiotic concentrations were measured using HPLC-tandem mass spectrometry (LC-MS/MS) (Waters et al., 2008; Gobin et al., 2010). Free fractions of the drugs were calculated as described previously (Waters et al., 2008; Gonzalez et al., 2013; Cheah et al., 2015).

Maximum concentration of drug in serum (C_{max}), elimination half-life ($t_{1/2}$), area under the concentration-time curve from 0 to 24 h (AUC_{0-24}), free AUC_{0-24} ($fAUC_{0-24}$), AUC_{0-24}/MIC and $fAUC_{0-24}$/MIC ratios were calculated using the PKSOLVER program (Zhang et al., 2010). The pharmacodynamic targets to assess the efficacy were $fAUC_{0-24}$/MIC and AUC_{0-24}/MIC for CMS and rifampin, respectively.

Experimental Models

Peritoneal Sepsis Model

A previously described murine peritoneal sepsis model was used (Parra Millan et al., 2016). Briefly, groups of un-anesthetized C57BL/6 mice were infected by ip injection of 0.5 mL of the Minimal Lethal Dose (MLD) of each strain, corresponding to ($\log_{10}$ cfu/mL): 8.97, 8.94 9.35, and 8.38 for VIM-1, VIM-1/DHA-1, OXA-48 plus CTX-M-15, and KPC-3 strains, respectively. Treatments were initiated 4 h post-inoculation. For each one of the strains, mice were randomly included into four different therapeutic groups: (1) controls (untreated), (2) CMS, 20 mg/kg/8 h/ip, (3) rifampin, 25 mg/kg/6 h/ip, and (4) CMS plus rifampin, using the same dosing schedule as in monotherapy. The sample size for the combination groups and CMS monotherapy for the colistin-susceptible strains (VIM-1 and OXA-48 plus CTX-M-15) was 15 mice; nevertheless, for the monotherapies in case of resistance to colistin (VIM-1/DHA-1 and KPC-3) and for rifampin, the sample size was 10 to accomplish the 3Rs (Replacement, Reduction and Refinement) rules for performing animal research. Afterward, mice were treated and monitored for 72 h. The antimicrobial dosages were based on the PK/PD data, and their proven efficacy, alone and in combination, in previous experimental murine models of infection (Pachon-Ibanez et al., 2010). Samples were extracted and processed immediately after the death of mice; the survivor mice were sacrificed (sodium thiopental) at the 72 h. Aseptic thoracotomies were carried out, and blood samples were obtained for qualitative blood cultures; results were expressed as positive ($\geq$1 cfu present in the plate) or negative. Spleens were aseptically extracted, weighed, and homogenized in sterile saline (Stomacher 80; Tekmar Co., Cincinnati, OH, United States) before quantitative cultures ($\log_{10}$ cfu/g) in Columbia agar with 5% sheep blood plates.

Pneumonia Model

A previously characterized murine pneumonia model was used (Pachon-Ibanez et al., 2010; Docobo-Perez et al., 2012; Parra Millan et al., 2016) with the OXA-48 plus CTX-M-15 strain, as OXA-48 is the most prevalent carbapenemase in Spain nowadays (Palacios-Baena et al., 2016). Anesthetized mice were infected intratracheally, using 50 μl of a final inoculum of 8.18 $\log_{10}$ cfu/mL. Therapies were initiated 4 h post-infection and treatment groups and dosages were the same as in the peritoneal sepsis model. Mice were treated and monitored over 72 h. After death or sacrifice of the mice at 72 h, blood and lungs samples were aseptically obtained and processed as detailed above.

In Vitro and *in Vivo* Selection of Colistin-Resistant and Rifampin-Resistant Mutants

Up to 10 colonies, of colistin-susceptible strains exposed during 24 h to colistin at the MIC, alone or in combination with rifampin, in time-kill curves, and from controls (non-exposed to

the antimicrobials), were sub-cultured twice in antimicrobial free medium and frozen at −80°C until MIC testing.

In the experimental murine pneumonia model, after processing the lungs as described above, the remaining homogenized tissue was vortexed and centrifuged, and the pellet was resuspended in 2 mL of sterile saline. All the volume was spread on agar and incubated for 48 h at 37°C. A maximum of ten colonies recovered from each lung were selected, sub cultured in antibiotic free medium twice and frozen at −80°C until MIC testing.

MICs determinations of colistin and rifampin were carried out in triplicate.

Statistical Analysis

Mortality and bacteremia rates are expressed as percentages and bacterial tissue concentrations ($\log_{10}$ cfu/g) as means ± *SD*. The two-tailed Fisher's test, analysis of variance (ANOVA), and the Dunnet and Tukey *post hoc* tests were used. A $P < 0.05$ was considered significant. The SPSS v22.0 statistical package was used (SPSS Inc).

RESULTS

In Vitro Results

Antimicrobial Susceptibility Testing

MICs of each antibiotic for the four clinical isolates are shown in **Table 1**. Two strains were resistant to colistin (VIM-1/DHA-1 and KPC-3 producers).

Time-Kill Curves

The results are shown in **Figure 1**. Colistin was bactericidal at 3 h against the VIM-1 producer, but an important regrowth at 24 h. In addition, colistin reduced bacterial concentration (2.5 $\log_{10}$ decrease in cfu/mL) of the OXA-48 plus CTX-M-15-producing isolate, again with an important regrowth at 24 h. Colistin did not display any bactericidal activity against the colistin-resistant isolates (VIM-1/DHA-1 and KPC-3 producers). Rifampin did not show bactericidal activity against any strain. The combination was synergistic against all the strains at 24 h, but achieving only a bacteriostatic effect against the VIM-1, VIM-1/DHA-1, and OXA-48 plus CTX-M-15 isolates; on the contrary, the combination was bactericidal against the KPC-3 isolate.

TABLE 1 | MICs of colistin and rifampin for the four carbapenemase-producing *K. pneumoniae* clinical strains.

Strains	MIC (mg/L) [SIR]	
	Colistin	Rifampin
VIM-1	0.5 [*]	32 [***]
VIM-1/DHA-1	64 [**]	>128 [***]
OXA-48/CTX-M-15	0.5 [*]	32 [***]
KPC-3	32 [**]	64 [***]

**Susceptible, MIC ≤ 2 mg/L. **Resistant, MIC > 2 mg/L. ***Breakpoints are not defined (intrinsically resistant).*

Pharmacokinetics and Pharmacodynamics

Pharmacokinetic parameters of each antimicrobial are shown in **Table 2**. Pharmacodynamics profiles are shown in **Tables 3**, **4**.

In Vivo Results: Peritoneal Sepsis Model

The efficacies of the antimicrobials are shown in **Table 3**. Mortality, bacterial clearance on spleen and bacteremia, are analyzed immediately after the death of mice or at the end of the experiment (72 h of treatment).

Mortality

Mortality in all control groups (non-treated) was 100% within the first 24 h post-infection. Rifampin and its combination with CMS reduced mortality in animals infected with the KPC-3 strain to a 66.67% and a 40%, respectively, but not CMS alone. There was no reduction of mortality with any treatment when the peritoneal sepsis was produced by the other strains.

Bacterial Clearance From Spleen

Rifampin alone improved significantly the clearance of bacteria from spleen (CFU/g of tissue) compared with the control and the CMS groups in mice infected with either of the two colistin-susceptible strains producing VIM-1 (7.14 ± 0.48 vs. 8.92 ± 0.46 and 7.14 ± 0.48 vs. 8.60 ± 0.30, respectively) or OXA-48 plus CTX-M-15 (8.24 ± 0.76 vs. 9.56 ± 0.47, and 8.24 ± 0.76 vs. 9.52 ± 0.55, respectively). CMS plus rifampin reduced the bacterial concentration compared with the controls for both colistin-susceptible strains, producing VIM-1 or OXA-48 plus CTX-M-15 and for the colistin-resistant strain producing KPC-3, (6.01 ± 1.77 vs. 8.92 ± 0.46, 7.06 ± 2.50 vs. 9.56 ± 0.47, and 6.76 ± 2.48 vs. 10.19 ± 0.29, respectively). The combination was also better than CMS alone for both colistin-susceptible strains (6.01 ± 1.77 vs. 8.60 ± 0.30, 7.06 ± 2.50 vs. 9.52 ± 0.55, respectively).

Bacteremia

CMS plus rifampin showed the best effect among all the treatment groups in sterilizing blood cultures of mice infected with any of the four strains. Nevertheless, this reduction was only significant in mice infected with the VIM-1 producer (53.33% vs. 100%).

Pneumonia Model Results

Table 4 summarizes the results for the pneumonia model.

Mortality

The severity of this model was lower, with a mortality of 40% at the end of the experiment (72 h) using the MLD in the control group. Only the combination therapy decreased significantly mortality compared with the control group (6.26% vs. 40%; $P < 0.05$).

Bacterial Clearance From Lungs

Rifampin alone and its combination with CMS decreased significantly bacterial lung concentration compared with the

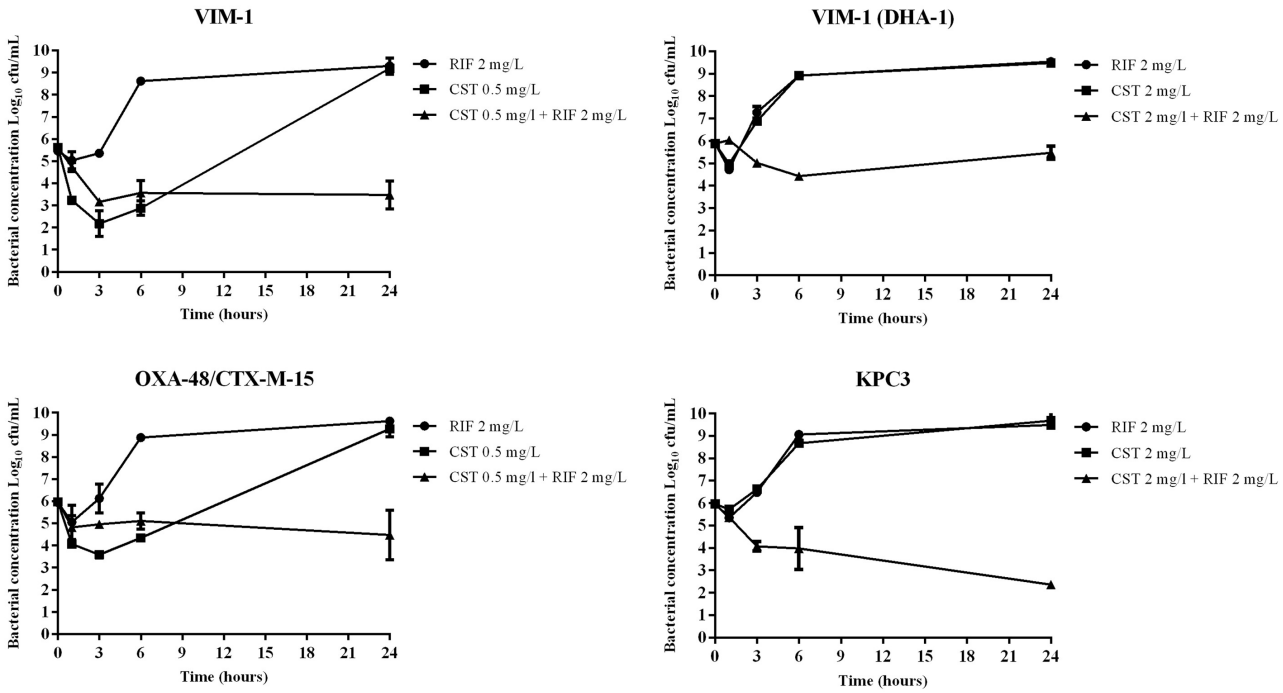

FIGURE 1 | Time-kill curves for colistin (CST) and rifampin (RIF) alone and in combination against four clinical strains of carbapenemase producing strains (VIM-1, VIM-1/DHA-1, OXA-48/CTX-M-15 and KPC3). The CST concentration used for colistin-susceptible strains corresponded to the value of their MICs (colistin 0.5 mg/L for VIM-1 and OXA-48/CTX-M-15); for colistin-resistant isolates the concentration of CST was that corresponding to the susceptibility breakpoint recommended by EUCAST (colistin 2 mg/L for VIM-1/DHA-1 and KPC-3). The RIF concentration used for all strains was 2 mg/L. RIF, filled circles; CST, filled squares; combination of both antimicrobials, filled triangles.

control (3.07 ± 1.63 vs. 8.05 ± 2.36, and 2.99 ± 1.36 vs. 8.05 ± 2.36, respectively).

Bacteremia

None of the antimicrobial treatments achieved a significant reduction of the bacteremia in comparison with the control group.

In Vitro and *in Vivo* Selection of Colistin-Resistant Mutants and Rifampin-Resistant Mutants

Colistin MICs of colonies recovered from susceptible strains (producing VIM-1 or OXA-48 plus CTX-M-15) after exposure at the MIC during 24 h in time-kill curves increased from 0.5 mg/L to > 8 mg/L. No mutants resistant to colistin were detected when these strains were exposed to the combination of colistin plus rifampin.

The MIC of rifampin for the colonies recovered from the lungs of mice challenged with OXA-48 plus CTX-M-15 producer and treated with rifampin alone increased from 16 to > 256 mg/L (16-folds) and the MIC of colistin from the colonies recovered from the lungs of mice treated with CMS as monotherapy increased from 1 to > 32 mg/L (32-folds). Nevertheless, the MICs of rifampin and colistin remained unchanged for those recovered from the control and the combination group.

DISCUSSION

The results of this study show that CMS alone has no significant efficacy in terms of bacterial clearance either from tissue and blood or in the survival rate in the peritoneal sepsis model, even in animals infected with strains susceptible to this antimicrobial. To investigate whether these disappointing results were due to a model effect, additional experiments were made in a less severe murine pneumonia model using the strain producing OXA-48 plus CTX-M-15. Once again, the bacterial lung and blood concentrations as well as mortality were no different from those

TABLE 2 | Pharmacokinetic profiles of CMS and rifampin in mice serum.

Antimicrobial (dose [mg/kg], route of administration)	Drug	C_{max} (mg/L)	$t_{1/2}$ (h)	AUC_{0-24} (mg·h/L)
CST (20, ip)	*t*CST	2.87	3.82	13.65
	*f*CST	0.24	3.82	1.15
RIF (25, ip)	*t*RIF	72.58	19.33	1103.58
	*f*RIF	2.90	19.33	44.14

CST, colistin; RIF, rifampin; ip, intraperitoneal; tCST, total colistin; fCST, free colistin; tRIF, total rifampin; fRIF, free rifampin; ip., intraperitoneal; C_{max}, maximum concentration of drug in serum; $t_{1/2}$, half-life; AUC_{0-24}, area under the concentration-time curve from 0 to 24 h; $fAUC_{0-24}$, the unbound fraction AUC_{0-24}.

TABLE 3 | *In vivo* efficacy and pharmacodynamics of CMS and rifampin, alone and in combination, for the experimental peritoneal sepsis model.

Strain	Treatment group	*n*	Log_{10} cfu/g spleen (mean ± *SD*)	Bacteremia (%)	Mice mortality (%)	AUC_{0-24}/MIC*	$fAUC_{0-24}$/MIC*
VIM-1	CTL	9	8.92 ± 0.46	100	100	NA	NA
	CST	15	8.60 ± 0.30	100	93.33	NA	2.30
	RIF	8	7.14 ± 0.48[a]	100	100	34.50	NA
	CST + RIF	15	6.01 ± 1.77[a]	53.33[b]	93.33	NA	NA
VIM-1/DHA-1	CTL	10	9.46 ± 0.32	100	100	NA	NA
	CST	6	9.54 ± 0.34	100	100	NA	0.04
	RIF	8	9.68 ± 0.09	100	100	8.60	NA
	CST+RIF	15	7.64 ± 3.02	73.33	73.33	NA	NA
OXA-48 plus CTX- M-15	CTL	10	9.56 ± 0.47	100	100	NA	NA
	CST	15	9.52 ± 0.55	100	100	NA	2.30
	RIF	10	8.24 ± 0.76[c]	100	100	34.50	NA
	CST+RIF	15	7.06 ± 2.50[c]	87.67	73.33	NA	NA
KPC-3	CTL	10	10.19 ± 0.29	100	100	NA	NA
	CST	8	9.19 ± 1.85	100	75	NA	0.02
	RIF	9	7.20 ± 2.96	88.88	66.67[d]	17.20	NA
	CST+RIF	15	6.76 ± 2.48[d]	77	40[d]	NA	NA

*CTL, control (no antimicrobial treatment); CST, colistin; RIF, rifampin; cfu, colony-forming unit; AUC_{0-24}, area under the concentration-time curve from 0 to 24 h; $fAUC_{0-24}$, the unbound fraction AUC_{0-24}. *PD parameters were determined in healthy mice after CMS or rifampin injection. [a]$P \leq 0.02$ compared to CTL and CST groups. [b]$P < 0.05$ compared to CTL, CST, and RIF groups. [c]$P < 0.05$ compared to CTL and CST groups. [d]$P < 0.05$ compared to CTL group.*

TABLE 4 | *In vivo* efficacy and pharmacodynamics of CMS and rifampin, alone and in combination, for the experimental pneumonia model.

Strain	Treatment group	*n*	Log_{10} cfu/g lung (mean ± *SD*)	Bacteremia (%)	Mice mortality (%)	AUC_{0-24}/MIC*	$fAUC_{0-24}$/MIC*
OXA-48 plus CTX- M-15	CTL	15	8.05 ± 2.36	53.30	40	NA	NA
	CST	15	5.14 ± 3.78	40	26.70	NA	2.30
	RIF	15	3.07 ± 1.63[a]	20	13.30	34.50	NA
	CST+RIF	16	2.99 ± 1.36[a]	31.25	6.26[a]	NA	NA

*CTL, control (no antimicrobial treatment); CST, colistin; RIF, rifampin; cfu, colony-forming unit, AUC_{0-24}, area under the concentration-time curve from 0 to 24 h; $fAUC_{0-24}$, the unbound fraction AUC_{0-24}. *PD parameters were determined in healthy mice after CMS or rifampin injection. [a]$P < 0.05$ compared to CTL group.*

of the control group. We believe that these results are related with the development of colistin resistance during the CMS monotherapy found in the pneumonia model.

The CMS dosage used in this study has been proven to be effective in several murine experimental studies using clinical multidrug-resistant (MDR) *Acinetobacter baumannii* strains susceptible to colistin (MIC = 0.5 mg/L) (Pachon-Ibanez et al., 2010; Docobo-Perez et al., 2012; Parra Millan et al., 2016). Nevertheless, when this CMS dosage was used in a murine pneumonia model by a NDM-1-producing *K. pneumoniae* clinical strain, CMS monotherapy was not effective as we found in the present study (Docobo-Perez et al., 2012). Similar results were reported by de Oliveira et al. (2015) in a retrospective clinical study, observing suboptimal efficacy of polymyxins in the treatment of KPC-producing Enterobacteriaceae infections, even in combination with imipenem or meropenem.

One possible explanation to the lack of efficacy found with CMS alone, could be that the PD parameter predictive of colistin efficacy, $fAUC_{0-24}$/MIC ratio (Cheah et al., 2015), has been described in infections caused by other Gram-negative bacilli, such as *Pseudomonas aeruginosa* and *A. baumannii*. So, the present results would suggest that the described $fAUC_{0-24}$/MIC values to achieve various magnitudes of bacterial killing in these Gram-negative bacilli are not the appropriate for the treatment of CP-Kp infections, even for isolates with the same MIC values. However, in these studies the end-point to define the $fAUC_{0-24}$/MIC values predicting colistin efficacy was to achieve a 2 log_{10} decrease in bacterial concentrations in lungs or thigh, but not to evaluate the mice survival rates.

Colistimethate sodium monotherapy did not reduce significantly the bacterial lung and blood results or the survival in the less severe pneumonia model by the strain producing OXA-48 plus CTX-M-15. However, it is noteworthy that CMS achieved a bacterial lung decrease of 2.91 log_{10} cfu/g, a value defined as optimal for *P. aeruginosa* and *A. baumannii* (Cheah et al., 2015), although the wide *SD* precluded the significance of these data.

In addition, the results in the pneumonia model demonstrate that the severity of the chosen animal model is important when studying the efficacy of antimicrobial treatments. Thus, new colistin $fAUC_{0-24}$/MIC values have to be defined for CP-Kp and, in our opinion, for the treatment of other Gram-negative bacilli infections.

The activity of rifampin in monotherapy in the peritoneal sepsis model was also limited, reducing only bacterial spleen concentration compared to control and CMS groups, infected with VIM-1 or OXA-48 plus CTX-M-15 strains, for which an $AUC_{0-24\ h}$/MIC = 34.5, predictor of efficacy was achieved. In the case of animals infected with the KPC-3 strain, rifampin did not decrease significantly the bacterial load in spleen or blood, but reduced the mortality. However, the survival mice conditions suggested that if the experiment were longer than 72 h, all animals included in this treatment group would have died shortly after. Moreover, a huge increase in MIC of rifampin was observed after rifampin *in vivo* monotherapy. In the less severe pneumonia model by OXA-48 plus CTX-M-15 strain, rifampin monotherapy increased significantly the bacterial clearing from lungs and blood, and also increased the mice survival. The efficacy of rifampin against other Gram-negative bacteria has been showed in experimental pneumonia models in mice (Wolff et al., 1999; Montero et al., 2004; Pachon-Ibanez et al., 2010, 2011). Nevertheless, rifampin alone cannot be an alternative due to the generation of rifampin-resistant mutants (Pachon-Ibanez et al., 2006).

Colistimethate sodium in combination with rifampin demonstrated *in vitro* a synergistic effect against the four strains, but the effect was bactericidal only against KPC-3 strain. These results are in accordance with other studies showing synergy of this combination against KPC-producing *K. pneumoniae* strains. Nastro et al. (2014) reported a synergistic effect at 24 h against 27 colistin-resistant KPC-2-producing *K. pneumoniae* clinical strains. Similarly, Elemam et al. (2010) found synergy with polymyxin B plus rifampin against 12 KPC-producing *K. pneumoniae* clinical strains. Tascini et al. (2013) also reported that CMS plus rifampin exhibited synergy against 13 colistin-resistant KPC-producing *K. pneumoniae* clinical strains, moreover being bactericidal against the 62%. On the contrary, in the case of *K. pneumoniae* producing VIM-1 the results of the present study differ from those by Tangden et al. (2014), where CMS plus rifampin did not exhibit synergy against two colistin-susceptible VIM-1-producing *K. pneumoniae* clinical strains.

With regard to the *in vivo* efficacy of CMS plus rifampin in the experimental murine peritoneal sepsis model by the colistin-susceptible VIM-1, the combination was better than the control and CMS groups taking into account the bacterial clearance from spleen and blood. When using the colistin-susceptible OXA-48 plus CTX-M-15 strain, the combination only reduced the bacterial spleen concentration. For these two colistin-susceptible strains, CMS and rifampin achieved the pharmacodynamic values described as optimal, $fAUC_{0-24}$/MIC and AUC_{0-24}/MIC, respectively (Jayaram et al., 2003; Gumbo et al., 2007; Landersdorfer et al., 2017). Nevertheless, is worth mentioning that the efficacy of the combination for both colistin-susceptible strains was not optimal, if we consider that mortality rates remained 93.3 and 73.3%, respectively.

Against the colistin-resistant KPC-3 strain, this combination reduced the bacterial spleen concentration and mortality, in accordance with the *in vitro* synergy studies. Nastro et al. (2014) reported a favorable outcome in five patients with colistin-resistant KPC-2-producing *K. pneumoniae* infections when treated with a combination of CMS plus rifampin. Against the other colistin-resistant strain, producing VIM-1/DHA-1, this combination was not efficacious, in contrast with the synergy observed in the time-kill studies.

In the pneumonia model caused by the OXA-48 plus CTX-M-15 strain, the activity of CMS plus rifampin was similar to that of rifampin in monotherapy, decreasing the bacterial lung concentration and increasing the mice survival compared with the control group. This combination has been successfully used against other Gram-negative bacilli (Pachon-Ibanez et al., 2010). In this pneumonia model, the strain of *K. pneumoniae* developed colistin resistance and a considerable increase in the MIC of rifampin when used as monotherapies, which was prevented with the combination. This prevention of colistin resistant mutant with this combination have been reported previously as in the *in vitro* study published by Rodriguez et al. (2010) in which they proved that the association of colistin plus rifampin was synergistic against heteroresistant *A. baumannii* isolates and prevented the development of colistin-resistant mutants (Rodriguez et al., 2010).

Limitations of the study have to be done, first that even though we wanted to evaluate the *in vitro* and *in vivo* effect of colistin plus rifampin combination against clonally unrelated clinical isolates of *K. pneumoniae* producing other carbapenemases, the number of the tested strains is low. Moreover, the less severe pneumonia model was only performed with one of the strains, and we believe it will be very interesting to do it with all of the strains.

In summary, the results obtained suggest that CMS plus rifampin has a low and heterogeneous efficacy in the treatment of severe infections, such as a peritoneal sepsis infection, caused by different CP-Kp strains, increasing only the mice survival in the infection caused by the KPC-3 strain. CMS plus rifampin combination prevents *in vivo* the development of mutants resistant to colistin. Because of the lack of available alternatives for these colistin-resistant KPC-3-producing strains, the combination of CMS and rifampin might be considered for further evaluation. Moreover, this combination showed efficacy in the less severe pneumonia model by the OXA-48 plus CTX-M-15 strain. Finally, an optimal PD index value for CMS efficacy needs to be defined for *K. pneumoniae*. Overall, the results of the present study suggest that the efficacy of CMS plus rifampin depends on the class of carbapenemase produced by *K. pneumoniae* and on the severity of the infection.

AUTHOR CONTRIBUTIONS

MP-I has planned and coordinated the experiments, analyzed the results, and written the manuscript. GL-H and TC-C had performed the *in vitro* and *in vivo* experiments. CD and JPP

had performed the antibiotic concentrations studies by HPLC-tandem mass spectrometry (LC-MS/MS). YS had reviewed the manuscript and the experiments. JR-B, AP, and JP had reviewed the manuscript and the experiments. MCC obtained the funds to perform the studies and wrote the project, contributed to the performance of the *in vitro* experiment, and reviewed the results and the manuscript.

FUNDING

This study was supported by the Consejería de Salud of the Junta de Andalucía (PI-0622-2012) and supported by Plan Nacional de I+D+i and Instituto de Salud Carlos III, Subdirección General de Redes y Centros de Investigación Cooperativa, Ministerio de Economía y Competitividad, Spanish Network for Research in Infectious Diseases (REIPI RD12/0015/0001) – co-financed by European Development Regional Fund "A way to achieve Europe" ERDF. The MEDINA authors disclosed the receipt of financial support from Fundación MEDINA, a public-private partnership of Merck Sharp & Dohme de España S.A./Universidad de Granada/Junta de Andalucía.

SUPPLEMENTARY MATERIAL

The Supplementary Material for this article can be found online at: https://www.frontiersin.org/articles/10.3389/fmicb.2018.00912/full#supplementary-material

REFERENCES

Canton, R., Akova, M., Carmeli, Y., Giske, C. G., Glupczynski, Y., Gniadkowski, M., et al. (2012). Rapid evolution and spread of carbapenemases among *Enterobacteriaceae* in Europe. *Clin. Microbiol. Infect.* 18, 413–431. doi: 10.1111/j.1469-0691.2012.03821.x

Cheah, S. E., Wang, J., Nguyen, V. T., Turnidge, J. D., Li, J., and Nation, R. L. (2015). New pharmacokinetic/pharmacodynamic studies of systemically administered colistin against *Pseudomonas aeruginosa* and *Acinetobacter baumannii* in mouse thigh and lung infection models: smaller response in lung infection. *J. Antimicrob. Chemother.* 70, 3291–3297. doi: 10.1093/jac/dkv267

Clinical and Laboratory Standards Institute [CLSI] (2012). *Methods for Dilution Antimicrobial Susceptibility Tests for Bacteria That Grow Aerobically; Approved Standard—Ninth Edition. CLSI Document M07-A9*. Wayne, PA: Clinical and Laboratory Standards Institute.

Daikos, G. L., Tsaousi, S., Tzouvelekis, L. S., Anyfantis, I., Psichogiou, M., Argyropoulou, A., et al. (2014). Carbapenemase-producing *Klebsiella pneumoniae* bloodstream infections: lowering mortality by antibiotic combination schemes and the role of carbapenems. *Antimicrob. Agents Chemother.* 58, 2322–2328. doi: 10.1128/AAC.02166-13

De Laveleye, M., Huang, T. D., Bogaerts, P., Berhin, C., Bauraing, C., Sacre, P., et al. (2017). Increasing incidence of carbapenemase-producing *Escherichia coli* and *Klebsiella pneumoniae* in Belgian hospitals. *Eur. J. Clin. Microbiol. Infect. Dis.* 36, 139–146. doi: 10.1007/s10096-016-2782-x

de Oliveira, M. S., De Assis, D. B., Freire, M. P., Boas Do Prado, G. V., Machado, A. S., Abdala, E., et al. (2015). Treatment of KPC-producing *Enterobacteriaceae*: suboptimal efficacy of polymyxins. *Clin. Microbiol. Infect.* 21, 179.e1–179.e7. doi: 10.1016/j.cmi.2014.07.010

Docobo-Perez, F., Nordmann, P., Dominguez-Herrera, J., Lopez-Rojas, R., Smani, Y., Poirel, L., et al. (2012). Efficacies of colistin and tigecycline in mice with experimental pneumonia due to NDM-1-producing strains of *Klebsiella pneumoniae* and *Escherichia coli*. *Int. J. Antimicrob. Agents* 39, 251–254. doi: 10.1016/j.ijantimicag.2011.10.012

Elemam, A., Rahimian, J., and Doymaz, M. (2010). In vitro evaluation of antibiotic synergy for polymyxin B-resistant carbapenemase-producing *Klebsiella pneumoniae*. *J. Clin. Microbiol.* 48, 3558–3562. doi: 10.1128/JCM.01106-10

European Committee on Antimicrobial Susceptibility Testing [EUCAST] (2016). *European Society of Clinical Microbiology and Infectious Diseases. Clinical Breakpoints*. Bochum: EUCAST.

Falagas, M. E., Tansarli, G. S., Karageorgopoulos, D. E., and Vardakas, K. Z. (2014). Deaths attributable to carbapenem-resistant *Enterobacteriaceae* infections. *Emerg. Infect. Dis.* 20, 1170–1175. doi: 10.3201/eid2007.121004

Gobin, P., Lemaitre, F., Marchand, S., Couet, W., and Olivier, J. C. (2010). Assay of colistin and colistin methanesulfonate in plasma and urine by liquid chromatography-tandem mass spectrometry. *Antimicrob. Agents Chemother.* 54, 1941–1948. doi: 10.1128/AAC.01367-09

Gonzalez, D., Schmidt, S., and Derendorf, H. (2013). Importance of relating efficacy measures to unbound drug concentrations for anti-infective agents. *Clin. Microbiol. Rev.* 26, 274–288. doi: 10.1128/CMR.00092-12

Gumbo, T., Louie, A., Deziel, M. R., Liu, W., Parsons, L. M., Salfinger, M., et al. (2007). Concentration-dependent *Mycobacterium tuberculosis* killing and prevention of resistance by rifampin. *Antimicrob. Agents Chemother.* 51, 3781–3788. doi: 10.1128/AAC.01533-06

Jayaram, R., Gaonkar, S., Kaur, P., Suresh, B. L., Mahesh, B. N., Jayashree, R., et al. (2003). Pharmacokinetics-pharmacodynamics of rifampin in an aerosol infection model of tuberculosis. *Antimicrob. Agents Chemother.* 47, 2118–2124. doi: 10.1128/AAC.47.7.2118-2124.2003

Landersdorfer, C. B., Nguyen, T. H., Lieu, L. T., Nguyen, G., Bischof, R. J., Meeusen, E. N., et al. (2017). Substantial targeting advantage achieved by pulmonary administration of colistin methanesulfonate in a large-animal model. *Antimicrob. Agents Chemother.* 61:e01934-16. doi: 10.1128/AAC.01934-16

Lee, G. C., and Burgess, D. S. (2012). Treatment of *Klebsiella pneumoniae* carbapenemase (KPC) infections: a review of published case series and case reports. *Ann. Clin. Microbiol. Antimicrob.* 11:32. doi: 10.1186/1476-0711-11-32

Lopez-Cerero, L., Egea, P., Gracia-Ahufinger, I., Gonzalez-Padilla, M., Rodriguez-Lopez, F., Rodriguez-Bano, J., et al. (2014). Characterisation of the first ongoing outbreak due to KPC-3-producing *Klebsiella pneumoniae* (ST512) in Spain. *Int. J. Antimicrob. Agents* 44, 538–540. doi: 10.1016/j.ijantimicag.2014.08.006

Michalopoulos, A., Virtzili, S., Rafailidis, P., Chalevelakis, G., Damala, M., and Falagas, M. E. (2010). Intravenous fosfomycin for the treatment of nosocomial infections caused by carbapenem-resistant *Klebsiella pneumoniae* in critically ill patients: a prospective evaluation. *Clin. Microbiol. Infect.* 16, 184–186. doi: 10.1111/j.1469-0691.2009.02921.x

Miro, E., Aguero, J., Larrosa, M. N., Fernandez, A., Conejo, M. C., Bou, G., et al. (2013). Prevalence and molecular epidemiology of acquired AmpC β-lactamases and carbapenemases in *Enterobacteriaceae* isolates from 35 hospitals in Spain. *Eur. J. Clin. Microbiol. Infect. Dis.* 32, 253–259. doi: 10.1007/s10096-012-1737-0

Montero, A., Ariza, J., Corbella, X., Domenech, A., Cabellos, C., Ayats, J., et al. (2004). Antibiotic combinations for serious infections caused by carbapenem-resistant *Acinetobacter baumannii* in a mouse pneumonia model. *J. Antimicrob. Chemother.* 54, 1085–1091. doi: 10.1093/jac/dkh485

Munoz-Price, L. S., Poirel, L., Bonomo, R. A., Schwaber, M. J., Daikos, G. L., Cormican, M., et al. (2013). Clinical epidemiology of the global expansion of *Klebsiella pneumoniae* carbapenemases. *Lancet Infect. Dis.* 13, 785–796. doi: 10.1016/S1473-3099(13)70190-7

Nastro, M., Rodriguez, C. H., Monge, R., Zintgraff, J., Neira, L., Rebollo, M., et al. (2014). Activity of the colistin-rifampicin combination against colistin-resistant, carbapenemase-producing Gram-negative bacteria. *J. Chemother.* 26, 211–216. doi: 10.1179/1973947813Y.0000000136

Nordmann, P., Dortet, L., and Poirel, L. (2012). Carbapenem resistance in *Enterobacteriaceae*: here is the storm! *Trends Mol. Med.* 18, 263–272. doi: 10.1016/j.molmed.2012.03.003

Nordmann, P., Naas, T., and Poirel, L. (2011). Global spread of Carbapenemase-producing *Enterobacteriaceae*. *Emerg. Infect. Dis.* 17, 1791–1798. doi: 10.3201/eid1710.110655

Oteo, J., Ortega, A., Bartolome, R., Bou, G., Conejo, C., Fernandez-Martinez, M., et al. (2015). Prospective multicenter study of carbapenemase-producing *Enterobacteriaceae* from 83 hospitals in Spain reveals high in vitro susceptibility to colistin and meropenem. *Antimicrob. Agents Chemother.* 59, 3406–3412. doi: 10.1128/AAC.00086-15

Pachon-Ibanez, M. E., Docobo-Perez, F., Jimenez-Mejias, M. E., Ibanez-Martinez, J., Garcia-Curiel, A., Pichardo, C., et al. (2011). Efficacy of rifampin, in monotherapy and in combinations, in an experimental murine pneumonia model caused by panresistant *Acinetobacter baumannii* strains. *Eur. J. Clin. Microbiol. Infect. Dis.* 30, 895–901. doi: 10.1007/s10096-011-1173-6

Pachon-Ibanez, M. E., Docobo-Perez, F., Lopez-Rojas, R., Dominguez-Herrera, J., Jimenez-Mejias, M. E., Garcia-Curiel, A., et al. (2010). Efficacy of rifampin and its combinations with imipenem, sulbactam, and colistin in experimental models of infection caused by imipenem-resistant *Acinetobacter baumannii*. *Antimicrob. Agents Chemother.* 54, 1165–1172. doi: 10.1128/AAC.00367-09

Pachon-Ibanez, M. E., Fernandez-Cuenca, F., Docobo-Perez, F., Pachon, J., and Pascual, A. (2006). Prevention of rifampicin resistance in *Acinetobacter baumannii* in an experimental pneumonia murine model, using rifampicin associated with imipenem or sulbactam. *J. Antimicrob. Chemother.* 58, 689–692. doi: 10.1093/jac/dkl303

Palacios-Baena, Z. R., Oteo, J., Conejo, C., Larrosa, M. N., Bou, G., Fernandez-Martinez, M., et al. (2016). Comprehensive clinical and epidemiological assessment of colonisation and infection due to carbapenemase-producing *Enterobacteriaceae* in Spain. *J. Infect.* 72, 152–160. doi: 10.1016/j.jinf.2015.10.008

Parra Millan, R., Jimenez Mejias, M. E., Sanchez Encinales, V., Ayerbe Algaba, R., Gutierrez Valencia, A., Pachon Ibanez, M. E., et al. (2016). Efficacy of lysophosphatidylcholine in combination with antimicrobial agents against *Acinetobacter baumannii* in experimental murine peritoneal sepsis and pneumonia models. *Antimicrob. Agents Chemother.* 60, 4464–4470. doi: 10.1128/AAC.02708-15

Pournaras, S., Vrioni, G., Neou, E., Dendrinos, J., Dimitroulia, E., Poulou, A., et al. (2011). Activity of tigecycline alone and in combination with colistin and meropenem against *Klebsiella pneumoniae* carbapenemase (KPC)-producing *Enterobacteriaceae* strains by time-kill assay. *Int. J. Antimicrob. Agents* 37, 244–247. doi: 10.1016/j.ijantimicag.2010.10.031

Rodriguez, C. H., De Ambrosio, A., Bajuk, M., Spinozzi, M., Nastro, M., Bombicino, K., et al. (2010). In vitro antimicrobials activity against endemic *Acinetobacter baumannii* multiresistant clones. *J. Infect. Dev. Ctries.* 4, 164–167. doi: 10.3855/jidc.604

Souli, M., Galani, I., Boukovalas, S., Gourgoulis, M. G., Chryssouli, Z., Kanellakopoulou, K., et al. (2011). In vitro interactions of antimicrobial combinations with fosfomycin against KPC-2-producing *Klebsiella pneumoniae* and protection of resistance development. *Antimicrob. Agents Chemother.* 55, 2395–2397. doi: 10.1128/AAC.01086-10

Souli, M., Rekatsina, P. D., Chryssouli, Z., Galani, I., Giamarellou, H., and Kanellakopoulou, K. (2009). Does the activity of the combination of imipenem and colistin in vitro exceed the problem of resistance in metallo-β-lactamase-producing *Klebsiella pneumoniae* isolates? *Antimicrob. Agents Chemother.* 53, 2133–2135. doi: 10.1128/AAC.01271-08

Tangden, T., Hickman, R. A., Forsberg, P., Lagerback, P., Giske, C. G., and Cars, O. (2014). Evaluation of double- and triple-antibiotic combinations for VIM- and NDM-producing *Klebsiella pneumoniae* by in vitro time-kill experiments. *Antimicrob. Agents Chemother.* 58, 1757–1762. doi: 10.1128/AAC.00741-13

Tascini, C., Tagliaferri, E., Giani, T., Leonildi, A., Flammini, S., Casini, B., et al. (2013). Synergistic activity of colistin plus rifampin against colistin-resistant KPC-producing *Klebsiella pneumoniae*. *Antimicrob. Agents Chemother.* 57, 3990–3993. doi: 10.1128/AAC.00179-13

Tenover, F. C., Arbeit, R. D., Goering, R. V., Mickelsen, P. A., Murray, B. E., Persing, D. H., et al. (1995). Interpreting chromosomal DNA restriction patterns produced by pulsed-field gel electrophoresis: criteria for bacterial strain typing. *J. Clin. Microbiol.* 33, 2233–2239.

Tzouvelekis, L. S., Markogiannakis, A., Psichogiou, M., Tassios, P. T., and Daikos, G. L. (2012). Carbapenemases in *Klebsiella pneumoniae* and other *Enterobacteriaceae*: an evolving crisis of global dimensions. *Clin. Microbiol. Rev.* 25, 682–707. doi: 10.1128/CMR.05035-11

Waters, N. J., Jones, R., Williams, G., and Sohal, B. (2008). Validation of a rapid equilibrium dialysis approach for the measurement of plasma protein binding. *J. Pharm. Sci.* 97, 4586–4595. doi: 10.1002/jps.21317

Wolff, M., Joly-Guillou, M. L., Farinotti, R., and Carbon, C. (1999). In vivo efficacies of combinations of beta-lactams, beta-lactamase inhibitors, and rifampin against *Acinetobacter baumannii* in a mouse pneumonia model. *Antimicrob. Agents Chemother.* 43, 1406–1411.

Zhang, Y., Huo, M., Zhou, J., and Xie, S. (2010). PKSolver: an add-in program for pharmacokinetic and pharmacodynamic data analysis in Microsoft Excel. *Comput. Methods Programs Biomed.* 99, 306–314. doi: 10.1016/j.cmpb.2010.01.007

Conflict of Interest Statement: The authors declare that the research was conducted in the absence of any commercial or financial relationships that could be construed as a potential conflict of interest.

Copyright © 2018 Pachón-Ibáñez, Labrador-Herrera, Cebrero-Cangueiro, Díaz, Smani, del Palacio, Rodríguez-Baño, Pascual, Pachón and Conejo. This is an open-access article distributed under the terms of the Creative Commons Attribution License (CC BY). The use, distribution or reproduction in other forums is permitted, provided the original author(s) and the copyright owner are credited and that the original publication in this journal is cited, in accordance with accepted academic practice. No use, distribution or reproduction is permitted which does not comply with these terms.

frontiers in Microbiology

ORIGINAL RESEARCH
published: 23 May 2018
doi: 10.3389/fmicb.2018.01011

Trans-Cinnamaldehyde and Eugenol Increase *Acinetobacter baumannii* Sensitivity to Beta-Lactam Antibiotics

*Deepti P. Karumathil[1], Meera Surendran Nair[1], James Gaffney[2], Anup Kollanoor-Johny[3] and Kumar Venkitanarayanan[1]**

[1] Department of Animal Science, University of Connecticut, Storrs, CT, United States, [2] College of Veterinary Medicine, Cornell University, Ithaca, NY, United States, [3] Department of Animal Science, University of Minnesota, Saint Paul, MN, United States

Multi-drug resistant (MDR) *Acinetobacter baumannii* is a major nosocomial pathogen causing a wide range of clinical conditions with significant mortality rates. *A. baumannii* strains are equipped with a multitude of antibiotic resistance mechanisms, rendering them resistant to most of the currently available antibiotics. Thus, there is a critical need to explore novel strategies for controlling antibiotic resistance in *A. baumannii*. This study investigated the efficacy of two food-grade, plant-derived antimicrobials (PDAs), namely *trans*-cinnamaldehyde (TC) and eugenol (EG) in decreasing *A. baumannii*'s resistance to seven β-lactam antibiotics, including ampicillin, methicillin, meropenem, penicillin, aztreonam, amoxicillin, and piperacillin. Two MDR *A. baumannii* isolates (ATCC 17978 and AB 251847) were separately cultured in tryptic soy broth (~6 log CFU/ml) containing the minimum inhibitory concentration (MIC) of TC or EG with or without the MIC of each antibiotic at 37°C for 18 h. *A. baumannii* strains not exposed to the PDAs or antibiotics served as controls. Following incubation, *A. baumannii* counts were determined by broth dilution assay. In addition, the effect of PDAs on the permeability of outer membrane and efflux pumps in *A. baumannii* was measured. Further, the effect of TC and EG on the expression of *A. baumannii* genes encoding resistance to β-lactam antibiotics (*blaP*), efflux pumps (*adeABC*), and multi-drug resistant protein (*mdrp*) was studied using real-time quantitative PCR (RT-qPCR). The experiment was replicated three times with duplicate samples of each treatment and control. The results from broth dilution assay indicated that both TC and EG in combination with antibiotics increased the sensitivity of *A. baumannii* to all the tested antibiotics ($P < 0.05$). The two PDAs inhibited the function of *A. baumannii* efflux pump, (AdeABC), but did not increase the permeability of its outer membrane. Moreover, RT-qPCR data revealed that TC and EG down-regulated the expression of majority of the genes associated with β-lactam antibiotic resistance, especially *blaP* and *adeABC* ($P < 0.05$). The results suggest that TC and EG could potentially be used along with β-lactam antibiotics for controlling MDR *A. baumannii* infections; however, their clinical significance needs to be determined using *in vivo* studies.

Keywords: *A. baumannii*, *trans*-cinnamaldehyde, eugenol, antibiotic resistance

OPEN ACCESS

Edited by:
Noton Kumar Dutta, Johns Hopkins University, United States

Reviewed by:
Vishvanath Tiwari, Central University of Rajasthan, India
Krassimira Hristova, Marquette University, United States
Nagendran Tharmalingam, Brown University, United States

***Correspondence:**
Kumar Venkitanarayanan
kumar.venkitanarayanan@uconn.edu

Specialty section:
This article was submitted to Antimicrobials, Resistance and Chemotherapy, a section of the journal Frontiers in Microbiology

Received: *22 August 2017*
Accepted: *30 April 2018*
Published: *23 May 2018*

Citation:
Karumathil DP, Nair MS, Gaffney J, Kollanoor-Johny A and Venkitanarayanan K (2018) Trans-Cinnamaldehyde and Eugenol Increase Acinetobacter baumannii Sensitivity to Beta-Lactam Antibiotics. Front. Microbiol. 9:1011. doi: 10.3389/fmicb.2018.01011

INTRODUCTION

Acinetobacter baumannii is a multi-drug resistant (MDR) Gram-negative, aerobic bacillus that has emerged as a major cause of nosocomial infections with mortality rates ranging from 34 to 61% (Karageorgopoulos and Falagas, 2008; Wieczorek et al., 2008; Esterly et al., 2011). In humans, MDR *A. baumannii* causes a wide-spectrum of clinical conditions, including pneumonia (Leung et al., 2005), blood-stream infections (Wisplinghoff et al., 2004; Centers for Disease Control and Prevention [CDC], 2004), meningitis (Metan et al., 2007), urinary tract infections (Sunenshine et al., 2007), and wound infections (Scott et al., 2007) In addition, reports of other manifestations such as endocarditis, peritonitis, and osteomyelitis associated with *A. baumannii* have been reported (Olut and Erkek, 2005; Menon et al., 2006) *A. baumannii* is ranked as one of the most common bacteria associated with intensive care units (Garnacho-Montero and Amaya-Villar, 2010; Ulu-Kilic et al., 2013), and is difficult to treat due to its resistance to most of the currently available antibiotics (Maragakis and Perl, 2008; Doi et al., 2009; Neonakis et al., 2011; Al Mobarak et al., 2014; Ellis et al., 2015) For example, carbapenems, which were once the antimicrobials of choice for treating *A. baumannii*, are no longer completely effective due to resistance development by the bacterium (Falagas et al., 2006; Bassetti et al., 2008; Abbott et al., 2013; Fonseca et al., 2013). Similarly, although polymyxins have been successfully used to treat *A. baumannii* infections, strains resistant to these drugs have appeared (Hernan et al., 2009; Lean et al., 2014; Pogue et al., 2015). In light of these reports, the Infectious Diseases Society of America ranked *A. baumannii* as one of the top priority, antibiotic-resistant pathogens to target due to its rapid propensity to develop drug resistance, and a limited choice of antibiotics available to treat infections caused by this bacterium (Talbot et al., 2006; Shlaes et al., 2013).

A. baumannii is considered to be multidrug resistant, if it exhibits resistance to more than three classes of antibiotics (Falagas et al., 2006). The resistance of *A. baumannii* to antibiotics has been attributed to multiple mechanisms, including reduced permeability of its outer membrane to antibiotics, constitutive expression of drug efflux pumps, and its ability to acquire and incorporate genetic elements such as plasmids, transposons, and integrons (Giamarellou et al., 2008; Cai et al., 2012). In addition, *A. baumannii* has a significant ability to produce biofilms on various surfaces (Espinal et al., 2012; Longo et al., 2014), which not only increases the potential of *A. baumannii* for nosocomial spread, but also contributes to its resistance to antibiotics and virulence (Lee et al., 2008; Rao et al., 2008). Thus, there is a critical need to explore novel strategies for treating *A. baumannii* infections.

Traditionally, plants have served as a source of novel drugs for treating a variety of diseases in humans (Cowan, 1999). A variety of plant-derived compounds possessing antimicrobial properties against a wide range of microorganisms have been documented (Kon and Rai, 2012; Upadhyay et al., 2014). The antimicrobial effects of four components of ginger against MDR strains of *A. baumannii* has been reported (Wang et al., 2010). Similarly, the essential oil from coriander was found to exert either synergistic or additive effects with antibiotics such as tetracycline, chloramphenicol, ciprofloxacin, gentamicin, piperacillin, and cefoperazone against *A. baumannii* (Duarte et al., 2012). Recently, aqueous extract of kiwi (*Actinidia deliciosa*) and clove (*Syzygium aromaticum*) were found to exert anti-biofilm activity against *A. baumannii* (Tiwari et al., 2017). Similarly, it was shown that plant extract from *Aegle marmelos* and imipenem had synergistic effect against carbapenem resistant strain of *Acinetobacter baumannii* (Tiwari et al., 2016). In another study, the essential oil from *Origanum vulgare* possessed potent antimicrobial activity against MDR *A. baumannii* (Saghi et al., 2015). In addition, previous research from our laboratory indicated that several plant-derived antimicrobials (PDAs), including *trans*-cinnamaldehyde (TC), an ingredient in cinnamon, eugenol (present in clove) and carvacrol and thymol obtained from oregano oil and oil of thyme, respectively, decreased antibiotic resistance in MDR *S.* Typhimurium DT 104 (Johny et al., 2010). These investigators observed that TC reduced DT 104's resistance to five antibiotics, where thymol and carvacrol decreased resistance to three antibiotics.

The β-lactam group of antibiotics are the most commonly prescribed antibiotics for the treatment of bacterial infections worldwide (Pitout et al., 1997; Thakuria and Lahon, 2013). *A. baumannii* is capable of producing β-lactamases that can hydrolyze the β-lactam ring of penicillins, cephalosporins, and carbapenems, thereby conferring resistance to these antibiotics. Therefore, this study investigated the efficacy of TC and eugenol (EG) in increasing the sensitivity of *A. baumannii* to seven β-lactam antibiotics. In addition, the effect of these PDAs on genes conferring resistance to β-lactam antibiotics in *A. baumannii* was determined.

MATERIALS AND METHODS

A. baumannii Cultures and Growth Conditions

Two clinical isolates of *A. baumannii*, namely 251847 (International Health Management Associates, IL), and 17978 (ATCC; fatal meningitis isolate) were used in the study. All bacteriological media used in the study, except Leeds MDR *Acinetobacter* agar, were purchased from Difco (Becton Dickinson, Sparks, MD, United States). Leeds MDR agar was procured from Hardy Diagnostics (Santa Maria, CA, United States). The bacterial isolates were cultured separately overnight in 10 ml tryptic soy broth (TSB), followed by streaking on Leeds MDR *Acinetobacter* agar plates and incubation at 37°C for 24 h. An individual colony from Leeds MDR *Acinetobacter* agar was sub-cultured twice in 10 ml of TSB at 37°C for 24 h with agitation to reach ∼8 $\log_{10}$ CFU/ml. The cultures were sedimented by centrifugation (3,700 × *g*, 15 min, 4°C), and the pellet was washed twice and re-suspended in sterile phosphate buffered saline (PBS; pH 7.2). The cultures were then diluted appropriately in PBS to obtain ∼5 to 6 $\log_{10}$ CFU/ml to be used as the inoculum. The bacterial population in the inoculum was confirmed by plating on tryptic soy agar (TSA) with incubation at 37°C for 24 h.

Plant-Derived Antimicrobials (PDAs) and Chemicals

Trans-cinnamaldehyde (≥98%; TC, *trans*-3-phenyl-2-propenal), eugenol (≥98%; EG,4-allyl-2-methoxyphenol), 1-*N*-phenylnaphthylamine (NPN), EDTA, ethidium bromide (EtBr), carbonyl cyanide m-chlorophenylhydrazone (CCP) and pyronin Y were purchased from Sigma-Aldrich (St. Louis, MO, United States).

Determination of Sub-inhibitory Concentration (SIC) and Minimum Inhibitory Concentration (MIC) of PDAs Against *A. baumannii*

The sub-inhibitory concentration (SIC) and minimum inhibitory concentration (MIC) of TC and EG against *A. baumannii* were determined as previously reported (Johny et al., 2010; Amalaradjou and Venkitanarayanan, 2011) TSB (10 ml) tubes containing 0.75–7.5 μM (TC) and 0.61–6.1 μM (EG) in increments of 0.375 μM (TC) and 0.305 μM (EG were inoculated separately with *A. baumannii* at ∼ 6 $\log_{10}$ CFU/ml, and incubated at 37°C for 24 h. Tubes without any added PDAs served as controls. After incubation, the samples were serially diluted (1:10) in PBS, plated on TSA, and incubated at 37°C for 24 h before counting the colonies. The highest concentration of TC or EG that did not inhibit *A. baumannii* growth after 24 h of incubation was selected as the SIC, while the lowest concentration of the antimicrobial that inhibited visible growth of the bacteria after 24 h incubation was taken as the MIC of that treatment. The experiment was done in duplicates and repeated three times.

Effect of PDAs on Antibiotic Resistance in *A. baumannii*

The β-lactam antibiotics tested in the current study included Ampicillin, Meropenem, Methicillin, Penicillin, Aztreonam, Amoxicillin, and Piperacillin (Sigma-Aldrich). Previously published MIC of each aforementioned antibiotic against *A. baumannii* was used in the study (Vashist et al., 2011; Morfin-Otero and Dowzicky, 2012; Malone and Kwon, 2013) (**Table 1**). To determine the effect of combination of PDAs and antibiotics on *A. baumannii*, the MIC of each antibiotic and that of TC/EG were added to 10 ml TSB containing *A. baumannii* (∼ 6 $\log_{10}$ CFU/ml), and incubated at 37°C for 24 h (Johny et al., 2010). The bacterial counts were determined after broth dilution assay and surface plating of appropriate dilutions on TSA. The treatments included only *A. baumannii* (positive control), *A. baumannii* + antibiotic, *A. baumannii* + PDA and *A. baumannii* + antibiotic + PDA. In addition, suitable controls, including *A. baumannii* + diluent (ethanol) and *A. baumannii* + ethanol + antibiotic were also included. Duplicate samples were included for each treatment, and the experiment was replicated three times.

TABLE 1 | MIC of antibiotics used in testing against *A. baumannii*.

Antibiotics	MIC (μg/ml)
Ampicillin	64
Meropenem	32
Methicillin	256
Penicillin	256
Aztreonam	256
Amoxicillin	64
Piperacillin	128

Efflux Pump Inhibition Assay

To study the effect of TC and EG on inhibiting the action of efflux pumps in *A. baumannii*, EtBr and pyronin Y efflux assays were performed according to a published protocol (Chusri et al., 2009). Overnight cultures of *A. baumannii* were washed twice and resuspended in PBS containing 0.4% glucose to an OD_{600} of ∼0.5. The bacterial suspension was added with the MIC of TC/EG or CCP (positive control, 100 μM), and incubated at 37°C for 5 h. *A. baumannii* suspension in PBS + 0.4% glucose served as control. After incubation, 200 μl of the treatments/control was separately transferred to a 96-well microtiter plate, followed by addition of EtBr (Sigma) to a final concentration of 4 mg/l, and the fluorescence was measured at excitation 530 nm and emission 645 nm. The assay was repeated with pyronin Y (Sigma) at a final concentration of 5 mg/l at 530 nm and emission 645 nm. The experiment was repeated three times with duplicates for *A. baumannii* 17978 and *A. baumannii* 251847.

Outer Membrane Permeabilization Assay

To study the effect of TC and EG on the outer membrane of *A. baumannii*, NPN uptake assay was performed using a published protocol (Chusri et al., 2009). Overnight *A. baumannii* 17978 and *A. baumannii* 251847 cultures were separately washed and resuspended in 5 mM HEPES buffer to an OD_{600} ∼ 0.5. Aliquots of 100 μl of *A. baumannii* suspension were transferred to a microtiter plate along with the MIC of TC/EG or EDTA 1 mM/HEPES buffer. This was followed by addition of 40 μM of NPN to make the total volume to 200 μl, the fluorescence was measured within 3 min at excitation 355 nm and emission 460 nm, and continuously recorded for 3 h every 10 min. The experiment was repeated three times with duplicates in each treatment.

Effect of PDAs on Antibiotic Resistance Gene Expression in *A. baumannii*

RNA Extraction and cDNA Synthesis

To study the effect of TC and EG on genes associated with resistance to β-lactam antibiotics in *A. baumannii*, bacterial cultures were grown separately with or without the SIC of TC/EG at 37°C in TSB to mid-log phase. *A. baumannii* grown with either antibiotic alone or PDA alone were also included as controls. After incubation, the cultures were subjected to centrifugation (12,000 × *g*, 15 min, 4°C) and the resultant pellet was added with 0.5 ml of RNAse free, sterile water and 1 ml of RNA protect reagent (Qiagen, Valencia, CA, United States). The total RNA from each sample was extracted using the RNeasy mini kit (Qiagen), and the manufacturer's instructions were followed

in estimating the total RNA using Nanodrop (Thermo Fisher Scientific, Waltham, MA, United States). Super-script II reverse transcriptase kit (Invitrogen, Carlsbad, CA, United States) was used for cDNA synthesis, and the resultant cDNA was used as a template for RT-qPCR. The amplified product was detected using SYBR Green reagents.

Real-Time Quantitative PCR (RT-qPCR)

The antibiotic resistance genes of *A. baumannii* assayed for expression analysis included efflux pump genes, namely *adeA, adeB, adeC*; β-lactam resistance gene, *blaP*; and the multidrug resistance protein gene, *mdrp*. Primer Express software® (Applied Biosystems, Foster city, CA, United States) was used for designing the primers specific for the genes and for the endogenous control (16S rRNA). The primers were designed from *A. baumannii* AB0057 genome (CP001182.1) published in the NCBI database (Adams et al., 2008) and their sequences are provided in **Table 2**. The custom synthesized primers were obtained from Integrated DNA Technologies (Foster City, CA, United States). RT-qPCR was performed with StepOnePlus™ Real Time PCR system (Applied Biosystems) using the SYBR green assay (Applied Biosystems) under custom thermal cycling conditions with the normalized RNA as the template (Bookout and Mangelsdorf, 2003). Duplicate samples were analyzed and standardized against 16S rRNA gene expression. The relative changes in mRNA expression levels were determined using comparative threshold cycle (CT) method ($2^{-\Delta\Delta C_T}$) between the control and the treatments.

Statistical Analysis

A completely randomized design with a factorial treatment structure was used. The factors included two *A. baumannii* strains, seven antibiotics, and two PDAs. The data were analyzed using the PROC GENMOD procedure of Statistical Analysis Software (SAS ver. 9.4; SAS Institute Inc., Cary, NC, United States). Least square means were considered significant at $P < 0.05$. The data comparisons for gene expression study were made using Students *t*-test. The difference was considered significant at $P < 0.05$.

TABLE 2 | List of primers used in detecting *A. baumannii* antibiotic resistance genes.

Gene	Sequence (5'→3')	Function
adeA (F)	TGACCGACCAATGCACCTT	Efflux pump
(R)	GCAACAGTTCGAGCGCCTAT	
adeB (F)	CCGATGACGTATCGAAGTTAGGA	Efflux pump
(R)	CCGATGACGTATCGAAGTTAGGA	
adeC (F)	ACGGCCCCAGAAGTCTAGTTC	Efflux pump
(R)	CGATTAACCCCAATAACCCAGTT	
blaP (F)	ACACTAGGAGAAGCCATGAAGCTT	Beta-lactam resistance Antibiotics
(R)	GCATGAGATCAAGACCGATAC G	
mdrp (F)	GTACGGCTTCTAGACCCACCATTTT	Multiple drug resistance protein
(R)	ACAAAGAGCCGTGCACAGTTT	
rRNA-16S (F)	TCGCTAGTAATCGCGGATCA CGCTGGCGGC	Endogenous control
(R)	GACGGGCGGTGTGTACAAG	

F, forward; R, reverse.

RESULTS

The SICs of TC and EG against *A. baumannii* were found to be 1.1 mM (0.015%) and 1.8 mM (0.03%), respectively, while the MIC was 4 mM (0.05% TC and 0.065% EG) for both PDAs. Although a previously reported MIC of each antibiotic against *A. baumannii* was used in the study, both *A. baumannii* isolates grew ∼ by 2.0 $\log_{10}$ CFU/ml after 24 h (antibiotic control), as observed in **Figures 1**, **2** and Supplementary Figures 1, 2. In the presence of the MIC of TC, the bacterial count after 24 h did not change significantly from the inoculation of level of 6.0 $\log_{10}$ CFU/ml (**Figure 1**) as expected. However, when *A. baumannii* was grown in the presence of each antibiotic and TC, its growth after 24 h was significantly decreased in comparison to that in the positive control, antibiotic control and TC control ($P < 0.05$). In both *A. baumannii* isolates, the greatest sensitivity was observed to methicillin and lowest sensitivity was seen against ampicillin and meropenem (**Figure 1** and Supplementary Figure 1). Similarly, the sensitivity of both *A. baumannii* isolates to all seven antibiotics was significantly increased in the presence of EG, as indicated by the reduced growth after 24 h ($P < 0.05$) (**Figure 2** and Supplementary Figure 2). In *A. baumannii* 17978, the greatest sensitivity was observed against ampicillin (**Figure 2**), whereas *A. baumannii* 251847 was maximally sensitive to amoxicillin (Supplementary Figure 2).

The results of the efflux pump inhibition assay using EtBr and pyronin Y in *A. baumannii* ATCC 17978 and *A. baumannii* 251847 are presented in **Figures 3**, **4** and Supplementary Figures 3, 4. EtBr and pyronin Y are known substrates for AdeABC and AdeIJK efflux pumps, respectively (Magnet et al., 2001; Xing et al., 2014). The MIC of TC and EG resulted in an increased accumulation of EtBr inside bacterial cells, as indicated by an increase in fluorescence compared to the PBS control ($P < 0.05$) (**Figures 5A–G**). CCP, an efflux pump inhibitor used as a positive control (Magnet et al., 2001) also resulted in an increase in fluorescence indicating suppression of efflux pump in *A. baumannii*. However, a similar increase in the fluorescence

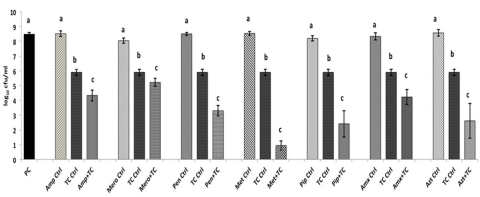

FIGURE 1 | Effect of TC in combination with β-lactam antibiotics in *A. baumannii* 17978. Bars with different superscripts differ from each other within a cluster ($P < 0.05$). *A. baumannii* 17978 was grown with each β-lactam antibiotic either alone or in combination with TC. Bacteria not exposed to any treatments (PC) and bacteria exposed to only TC (TC Ctrl) served as controls for the experiment.

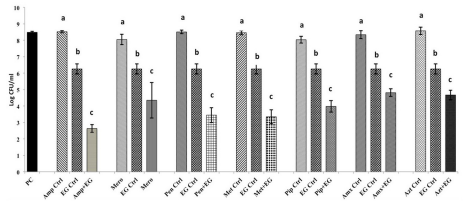

FIGURE 2 | Effect of EG in combination with β-lactam antibiotics in *A. baumannii* 17978. Bars with different superscripts differ from each other within a cluster ($P < 0.05$). *A. baumannii* 17978 was grown with each β-lactam antibiotic either alone or in combination with EG. Bacteria not exposed to any treatments (PC) and bacteria exposed to only EG (EG Ctrl) served as controls for the experiment.

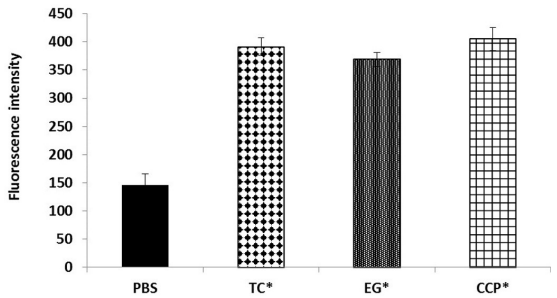

FIGURE 3 | Intracellular accumulation of ethidium bromide (EtBr) in *A. baumannii* ATCC 17978 after treatment with MIC of TC and EG, as measured by fluorescence intensity. *A. baumannii* ATCC 17978 was added with MIC of TC/EG or CCP (100 μM) and incubated for 5 h at 37°C. Fluorescence (excitation 530 nm and emission 645 nm) was measured after addition of EtBr (4 mg/l). Treatments with * are significantly different from PBS (control) ($P < 0.05$).

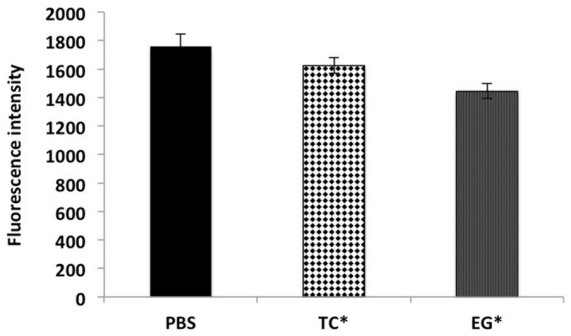

FIGURE 4 | Intracellular accumulation of pyronin Y in *A. baumannii* ATCC 17978 after treatment with MIC of TC and EG, as measured by fluorescence intensity. *A. baumannii* ATCC 17978 was added with MIC of TC/EG and incubated for 5 h at 37°C. Fluorescence (excitation 530 nm and emission 645 nm) was measured after addition of pyronin Y (5 mg/l). Treatments with * are significantly different from PBS (control) ($P < 0.05$).

was not observed for pyronin Y compared to the PBS control (**Figure 4** and Supplementary Figure 4). The results of NPN uptake assay in *A. baumannii* ATCC 17978 and *A. baumannii* 251847 are presented in Supplementary Figures 5, 6, respectively. Neither TC nor EG increased NPN uptake, while the EDTA control did show an increase in fluorescence. Further, the samples treated with TC or EG demonstrated a decrease in fluorescence over time (data not shown).

The effect of seven antibiotics and two PDAs and their combination on the expression of various antibiotic resistance genes in *A. baumannii* 17978 is depicted in **Figures 5A–G**. It was observed that compared to control, the expression of all tested genes was up-regulated ($P < 0.05$) following *A. baumannii* growth in the presence of the antibiotics. However, TC significantly down-regulated the expression of major genes conferring resistance to β-lactam antibiotics compared to control ($P < 0.05$). The genes encoding efflux pump *adeA* and *adeB* were down regulated by ∼6- and 9-fold, respectively. Moreover, the expression of genes encoding β-lactamase (*blaP*) and the multiple drug resistance protein (*mdrp*) was decreased by ∼3-fold ($P < 0.05$). Similar to the results observed with TC, all antibiotic resistance genes were down-regulated on exposure to EG compared to control ($P < 0.05$). The expression of genes encoding efflux pumps, *adeA* and *adeB* were down-expressed by 3- and 14-fold, respectively. Similarly, *blaP* and *mdrp* were also down-regulated in both strains ($P < 0.05$). The combination of TC or EG with the antibiotics also resulted in a down-regulation of majority of the tested genes ($P < 0.05$). Among the combinations of TC or EG with the seven antibiotics, the combination containing aztreonam resulted in a significant down-regulation of all the tested genes compared to control (**Figure 5D**). The combination of EG with piperacillin (**Figure 5C**) or penicillin (**Figure 5F**) also significantly reduced the expression of all the antibiotic resistance genes ($P < 0.05$).

DISCUSSION

Rapid emergence of antibiotic resistance in pathogenic microorganisms, especially to multiple antibiotics has ignited research efforts to discover novel antibiotics and develop effective derivatives of currently available antibiotics. However, no promising antibiotics are under development, and the rapidity and complexity of resistance development in pathogens have further exacerbated the situation. In light of this, a potential viable approach was explored to reduce bacterial antibiotic resistance in the development of inhibitors of resistance mechanisms in bacteria (Renau et al., 1999; Walsh and Fanning, 2008). This strategy involves the co-administration of an antibiotic with an "inhibitor," which counteracts bacterial resistance mechanism(s), thereby rendering the resistant pathogen sensitive to the drug. The advantage of this approach is that it makes it possible to continue the use of current antibiotics, for which in-depth pharmacological and toxicological data are already available. In this regard, PDAs represent a potential natural group of "inhibitors" of bacterial antibiotic resistance mechanisms.

Abundant literature exists on the antimicrobial properties of a variety of plant compounds against a wide range of microorganisms (Burt, 2004; Upadhyay et al., 2014). However, only a handful of studies have addressed their effect on bacterial

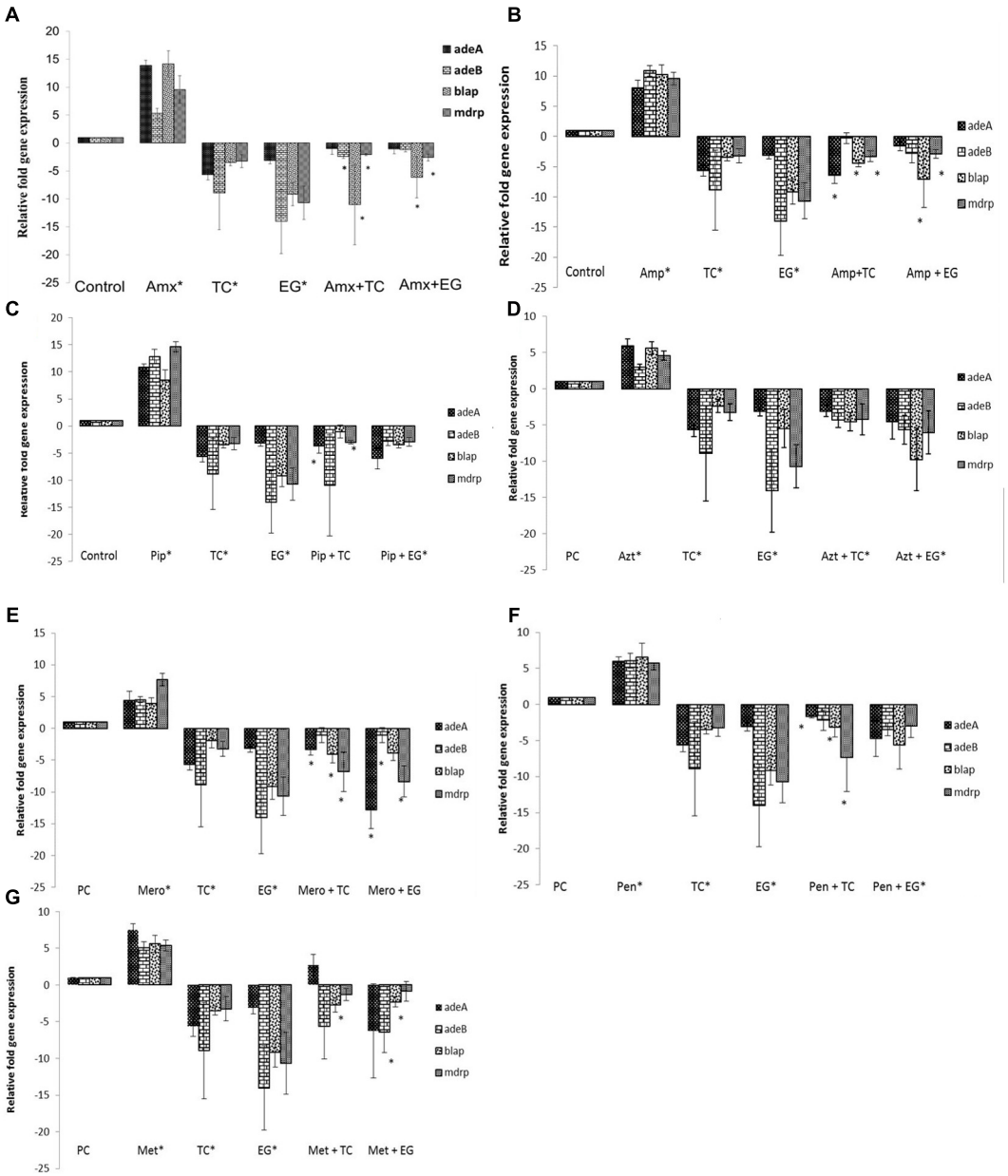

FIGURE 5 | Effect of TC and EG on antibiotic resistance genes in *A. baumannii* 17978. **(A)** *A. baumannii* 17978 was grown with the SIC of TC/EG either alone or in combination with amoxicillin, and RT-qPCR was done to test the effect of the treatments on major antibiotic genes in *A. baumannii.* Bacteria exposed to amoxicillin alone and bacteria not exposed to any treatments served as controls. Bars with * are significantly different from control ($P < 0.05$). **(B)** *A. baumannii* 17978 was treated with SICs of TC/EG either alone or in combination with ampicillin and RT-qPCR was done to test the effect of the treatments on major antibiotic genes in *A. baumannii.* Bacteria exposed to ampicillin alone and bacteria not exposed to any treatments served as controls. Bars with * are significantly different from control ($P < 0.05$). **(C)** *A. baumannii* 17978 was treated with SICs of TC/EG either alone or in combination with piperacillin and RT-qPCR was done to test the effect of the treatments on major antibiotic genes in *A. baumannii.* Bacteria exposed to piperacillin alone and bacteria not exposed to any treatments served as controls. Bars with * are significantly different from control ($P < 0.05$). **(D)** *A. baumannii* 17978 was treated with SICs of TC/EG either alone or in combination with aztreonam and RT-qPCR was done to test the effect of the treatments on major antibiotic genes in *A. baumannii.* Bacteria exposed to aztreonam alone and bacteria not exposed to any treatments served as controls. Bars with * are significantly different from control ($P < 0.05$). **(E)** *A. baumannii* 17978 was treated with SICs of TC/EG either alone or in combination with meropenem and RT-qPCR was done to test the effect of the treatments on major antibiotic genes in *A. baumannii.* Bacteria exposed to meropenem alone and bacteria not exposed to any treatments served as controls. Bars with * are significantly different from control ($P < 0.05$). **(F)** *A. baumannii* 17978 was treated with SICs of TC/EG either alone or in combination with penicillin and RT-qPCR was done to test the effect of the treatments on major antibiotic genes in *A. baumannii.* Bacteria exposed to penicillin alone and bacteria not exposed to any treatments served as controls. Bars with * are significantly different from control ($P < 0.05$). **(G)** *A. baumannii* 17978 was treated with SICs of TC/EG either alone or in combination with methicillin and RT-qPCR was done to test the effect of the treatments on major antibiotic genes in *A. baumannii.* Bacteria exposed to methicillin alone and bacteria not exposed to any treatments served as controls. Bars with * are significantly different from control ($P < 0.05$).

antibiotic resistance, especially in Gram negative bacteria (Gallucci et al., 2006; Chusri et al., 2009; Johny et al., 2010; Ilić et al., 2014). In the current study, both TC and EG enhanced the sensitivity of *A. baumannii* to all seven β-lactam antibiotics tested (**Figures 1**, **2** and Supplementary Figures 1, 2). This is evident from the significant reductions in bacterial counts observed in the samples containing PDA and antibiotics as compared to that in the treatments containing each PDA or antibiotic alone. A checkerboard assay testing a wide range of concentrations of two antimicrobials is commonly used for determining their combinatorial effects on a bacterium (Jayamani et al., 2017; Tharmalingam et al., 2018). However, since our preliminary studies revealed that concentrations of TC and EG below the MIC were not significantly effective in increasing *A. baumannii* sensitivity to antibiotics, we did not use a checkerboard assay, but instead tested the combinatorial effect of MIC of plant molecules and antibiotics on the pathogen.

A recent study also reported synergistic effect of *Eucalyptus camaldulensis* with polymyxin B against MDR *Acinetobacter baumannii* (Knezevic et al., 2016). In another study, Enrofloxacin and cinnamon were observed to possess synergistic effect against *Salmonella enterica* (Solarte et al., 2017). Further, extracts of medicinal plant *Holarrhena antidysenterica* with Conessine increased susceptibility of extensively drug resistant *A. baumannii* to novobiocin and rifampicin (Siriyong et al., 2016). Additionally, no cytotoxic effects on human epithelial cells at the tested concentrations were reported previously with TC and EG (Amalaradjou et al., 2010; Karumathil et al., 2016). Moreover our previous studies revealed that in-feed supplementation of TC and EG in broiler chicks (Kollanoor-Johny et al., 2012) and TC in mice (Narayanan et al., 2017) for 10 days did not result in any toxicity.

A. baumannii has been reported to exhibit resistance to β-lactam antibiotics through several mechanisms, including the production of β-lactamases, changes in penicillin-binding proteins (PBPs), altering the structure and number of porin proteins, decreased membrane permeability, and by use of efflux pumps that exit antibiotics out of the bacterial cell (Vila et al., 2007; Manchanda et al., 2010; Bonnin et al., 2013; Tang et al., 2014). Moreover, the presence of efflux pumps and MDR proteins in *A. baumannii* contribute significantly to both intrinsic and acquired resistance to antibiotics (Lomovskaya and Bostian, 2006). *A. baumannii* genome encodes a wide array of multidrug efflux systems, including AdeABC, a resistance-nodulation-division (RND) family-type pump (Damier-Piolle et al., 2008; Wieczorek et al., 2008; Yoon et al., 2013; Sun et al., 2014). The substrates for this pump include beta-lactams, aminoglycosides, erythromycin, chloramphenicol, tetracycline, fluoroquinolone, trimethoprim, and EtBr (Magnet et al., 2001; Higgins et al., 2004; Heritier et al., 2005; Peleg et al., 2007). The three component structures of AdeABC include the inner membrane fusion protein (AdeA), transmembrane component (AdeB) and an outer membrane protein (AdeC), with the inactivation of *adeB* resulting in the loss of pump function and multidrug resistance (Magnet et al., 2001).

In order to determine if TC or EG exerted an inhibitory effect on the aforementioned efflux pumps in *A. baumannii*, an efflux pump inhibition assay was performed with EtBr and pyronin Y along with CCP, a documented efflux pump inhibitor (Magnet et al., 2001; Chusri et al., 2009). EtBr and pyronin Y are known substrates for AdeABC and AdeIJK efflux pumps, respectively (Magnet et al., 2001; Damier-Piolle et al., 2008; Chusri et al., 2009; Xing et al., 2014). Both TC and EG resulted in the inhibition of AdeABC efflux pump in the two tested *A. baumannii* strains, as evident from the increase in fluorescence in the treated samples compared to PBS control (**Figure 3** and Supplementary Figure 3). However, the PDAs did not exert any inhibitory effect on the action of AdeIJK efflux pump in *A. baumannii*, as evident from the lack of difference in fluorescence units between PDA-treated and PBS control samples (**Figure 4** and Supplementary Figure 4). Similarly, the results from the NPN uptake assay revealed that TC and EG did not increase *A. baumannii*'s outer membrane permeability, as seen from Supplementary Figures 5, 6, where no increase in fluorescence was observed in PDA-treated *A. baumannii* as against the samples treated with EDTA, a known outer membrane permeabilizer in Gram-negative bacteria (Helander and Mattila-Sandholm, 2000; Alakomi et al., 2006). These results indicate that TC and EG increased the sensitivity of *A. baumannii* to the tested antibiotics at least in part by inhibiting the efflux pump, AdeABC.

For ascertaining if TC or EG exerted an inhibitory effect on any of the antibiotic resistance genes conferring resistance to β-lactam antibiotics in *A. baumannii*, we performed a RT-qPCR on mRNA extracted from *A. baumannii* following growth in the presence and absence of the PDAs. The results from the RT-qPCR revealed that TC and EG in combination with or without each antibiotic significantly down-regulated the expression of the majority of genes that confer resistance to β-lactam antibiotics (**Figures 5A–G**). Among the various genes screened, those encoding efflux pumps, *adeA* and *adeB* were maximally down-regulated by both PDAs. These results concur with the results from the EtBr efflux pump inhibition assay, and suggest that TC and EG enhanced the efficacy of the seven β-lactam antibiotics against *A. baumannii* by thwarting the various resistance mechanisms, especially those involving the efflux pumps.

CONCLUSION

The results of this study suggest the potential use of TC and EG in conjunction with the currently available β-lactam antibiotics for the treatment for MDR *A. baumannii* infections and could lead to development of new treatment options with reduced antibiotic dosage. However, efficacy studies in suitable animal models are warranted before recommending their clinical usage.

AUTHOR CONTRIBUTIONS

KV is the corresponding author and primary contact during manuscript submission, review, and publication process. The work was done under his supervision as the principal investigator. He significantly contributed to the design, drafting,

revisions, and interpretation of data. The manuscript is being submitted with his final approval for publication. MN is the submitting author. DK and AK-J designed the study. DK and JG conducted the experiments. DK and MN prepared the manuscript for submission.

SUPPLEMENTARY MATERIAL

The Supplementary Material for this article can be found online at: https://www.frontiersin.org/articles/10.3389/fmicb.2018.01011/full#supplementary-material

REFERENCES

Abbott, I., Cerqueira, G. M., Bhuiyan, S., and Peleg, A. Y. (2013). Carbapenem resistance in *Acinetobacter baumannii*: laboratory challenges, mechanistic insights and therapeutic strategies. *Expert Rev. Anti. Infect. Ther.* 11, 395–409. doi: 10.1586/eri.13.21

Adams, M. D., Goglin, K., Molyneaux, N., Hujer, K. M., Lavender, H., Jamison, J. J., et al. (2008). Comparative genome sequence analysis of multidrug-resistant *Acinetobacter baumannii*. *J. Bacteriol.* 190, 8053–8064. doi: 10.1128/JB.00834-08

Al Mobarak, M. F., Matbuli, R. M., Meir, H., Al Gehani, N., ElToukhy, A. A. M., Al Qureshey, K. F., et al. (2014). Antimicrobial resistance patterns among *Acinetobacter baumannii* isolated from King Abdulaziz Hospital, Jeddah, Saudi Arabia, Four-Year Surveillance Study (2010–2013). *Egypt. J. Med. Microbiol.* 23, 53–60. doi: 10.12816/0025920

Alakomi, H. L., Paananen, A., Suihko, M. L., Helander, I. M., and Saarela, M. (2006). Weakening effect of cell permeabilizers on gram-negative bacteria using biodeterioration. *Appl. Environ. Microbiol.* 72, 4695–4703. doi: 10.1128/AEM.00142-06

Amalaradjou, M. A. R., Narayanan, A., Baskaran, S. A., and Venkitanarayanan, K. (2010). Antibiofilm effect of trans-cinnamaldehyde on uropathogenic *Escherichia coli*. *J. Urol.* 184, 358–363. doi: 10.1016/j.juro.2010.03.006

Amalaradjou, M. A. R., and Venkitanarayanan, K. (2011). Effect of trans-cinnamaldehyde on reducing resistance to environmental stresses in Cronobacter sakazakii. *Foodborne Pathog. Dis.* 8, 403–409. doi: 10.1089/fpd.2010.0691

Bassetti, M., Righi, E., Esposito, S., Petrosillo, N., and Nicolini, L. (2008). Drug treatment for multidrug-resistant *Acinetobacter baumannii* infections. *Future Microbiol.* 3, 649–660. doi: 10.2217/17460913.3.6.649

Bonnin, R. A., Nordmann, P., and Poirel, L. (2013). Screening and deciphering antibiotic resistance in *Acinetobacter baumannii*: a state of the art. *Expert Rev. Anti. Infect. Ther.* 11, 571–583. doi: 10.1586/eri.13.38

Bookout, A. L., and Mangelsdorf, D. J. (2003). Quantitative real-time PCR protocol for analysis of nuclear receptor signaling pathways. *Nucl. Recept. Signal.* 1, 1–7. doi: 10.1621/nrs.01012

Burt, S. (2004). Essential oils: their antibacterial properties and potential applications in foods—a review. *Int. J. Food Microbiol.* 94, 223–253. doi: 10.1016/j.ijfoodmicro.2004.03.022

Cai, Y., Chai, D., Wang, R., Liang, B., and Bai, N. (2012). Colistin resistance of *Acinetobacter baumannii*: clinical reports, mechanisms and antimicrobial strategies. *J. Antimicrob. Chemother.* 67, 1607–1615. doi: 10.1093/jac/dks084

Centers for Disease Control and Prevention [CDC] (2004). Acinetobacter baumannii infections among patients at military medical facilities treating injured US service members, 2002-2004. *Morb. Mortal Wkly. Rep.* 53, 1063–1066.

Chusri, S., Villanueva, I., Voravuthikunchai, S. P., and Davies, J. (2009). Enhancing antibiotic activity: a strategy to control Acinetobacter infections. *J. Antimicrob. Chemother.* 64, 1203–1211. doi: 10.1093/jac/dkp381

Cowan, M. M. (1999). Plant products as antimicrobial agents. *Clin. Microbiol. Rev.* 12, 564–582.

Damier-Piolle, L., Magnet, S., Bremont, S., Lambert, T., and Courvalin, P. (2008). AdeIJK, a resistance-nodulation-cell division pump effluxing multiple antibiotics in *Acinetobacter baumannii*. *Antimicrob. Agents Chemother.* 52, 557–562. doi: 10.1128/AAC.00732-07

Doi, Y., Husain, S., Potoski, B. A., McCurry, K. R., and Paterson, D. L. (2009). Extensively drug-resistant *Acinetobacter baumannii*. *Emerg. Infect. Diseases* 15, 980–982. doi: 10.3201/eid1506.081006

Duarte, A., Ferreira, S., Silva, F., and Domingues, F. C. (2012). Synergistic activity of coriander oil and conventional antibiotics against *Acinetobacter baumannii*. *Phytomedicine* 19, 236–238. doi: 10.1016/j.phymed.2011.11.010

Ellis, D., Cohen, B., Liu, J., and Larson, E. (2015). Risk factors for hospital-acquired antimicrobial-resistant infection caused by *Acinetobacter baumannii*: antimicrob. *Resist. Infect. Control.* 4, 1–5. doi: 10.1186/s13756-015-0083-2

Espinal, P., Marti, S., and Vila, J. (2012). Effect of biofilm formation on the survival of *Acinetobacter baumannii* on dry surfaces. *J. Hosp. Infect.* 80, 56–60. doi: 10.1016/j.jhin.2011.08.013

Esterly, J. S., Griffith, M., Qi, C., Malczynski, M., Postelnick, M. J., and Scheetz, M. H. (2011). Impact of carbapenem resistance and receipt of active antimicrobial therapy on clinical outcomes of *Acinetobacter baumannii* bloodstream infections. *Antimicrob. Agents Chemother.* 55, 4844–4849. doi: 10.1128/AAC.01728-10

Falagas, M. E., Koletsi, P. K., and Bliziotis, I. A. (2006). The diversity of definitions of multidrug-resistant (MDR) and pandrug-resistant (PDR) *Acinetobacter baumannii* and *Pseudomonas aeruginosa*. *J. Med. Microbiol.* 55, 1619–1629. doi: 10.1099/jmm.0.46747-0

Fonseca, E. L., Scheidegger, E., Freitas, F. S., Cipriano, R., and Vicente, A. C. (2013). Carbapenem-resistant *Acinetobacter baumannii* from Brazil: role of carO alleles expression and blaOXA-23 gene. *BMC Microbiol.* 13:245. doi: 10.1186/1471-2180-13-245

Gallucci, N., Casero, C., Oliva, M., Zygadlo, J., and Demo, M. (2006). Interaction between terpenes and penicillin on bacterial strains resistant to beta-lactam antibiotics. *Mol. Med. Chem.* 10, 30–32.

Garnacho-Montero, J., and Amaya-Villar, R. (2010). Multiresistant *Acinetobacter baumannii* infections: epidemiology and management. *Curr Opin Infect Dis.* 23, 332–339. doi: 10.1097/QCO.0b013e32833ae38b

Giamarellou, H., Antoniadou, A., and Kanellakopoulou, K. (2008). *Acinetobacter baumannii*: a universal threat to public health? *Int. J. Antimicrob. Agents* 32, 106–119. doi: 10.1016/j.ijantimicag.2008.02.013

Helander, I. M., and Mattila-Sandholm, T. (2000). Fluorometric assessment of gram-negative bacterial permeabilization. *J. Appl. Microbiol.* 88, 213–219. doi: 10.1046/j.1365-2672.2000.00971.x

Heritier, C., Poirel, L., Lambert, T., and Nordmann, P. (2005). Contribution of acquired carbapenem-hydrolyzing oxacillinases to carbapenem resistance in *Acinetobacter baumannii*. *Antimicrob. Agents Chemother.* 49, 3198–3202. doi: 10.1128/AAC.49.8.3198-3202.2005

Hernan, R. C., Karina, B., Gabriela, G., Marcela, N., Carlos, V., and Angela, F. (2009). Selection of colistin-resistant *Acinetobacter baumannii* isolates in postneurosurgical meningitis in an intensive care unit with high presence of heteroresistance to colistin. *Diagn. Microbiol. Infect. Dis.* 65, 188–191. doi: 10.1016/j.diagmicrobio.2009.05.019

Higgins, P. G., Wisplinghoff, H., Stefanik, D., and Seifert, H. (2004). Selection of topoisomerase mutations and overexpression of adeB mRNA transcripts during an outbreak of *Acinetobacter baumannii*. *J. Antimicrob. Chemother.* 54, 821–823. doi: 10.1093/jac/dkh427

Ilić, B. S., Kocić, B. D., Ćirić, V. M., Cvetković, O. G., and Miladinović, D. L. (2014). An In Vitro synergistic interaction of combinations of *Thymus glabrescens* essential oil and its main constituents with chloramphenicol. *Sci.World J.* 2014:826219.. doi: 10.1155/2014/826219

Jayamani, E., Tharmalingam, N., Rajamuthiah, R., Coleman, J. J., Kim, W., Okoli, I., et al. (2017). Characterization of a *Francisella tularensis-Caenorhabditis elegans* pathosystem for the evaluation of therapeutic compounds. *Antimicrob. Agents Chemo.* 61, e310–e317. doi: 10.1128/AAC.00310-17

Johny, A. K., Hoagland, T., and Venkitanarayanan, K. (2010). Effect of subinhibitory concentrations of plant-derived molecules in increasing the sensitivity of multidrug-resistant *Salmonella enterica* serovar Typhimurium DT104 to antibiotics. *Foodborne Pathog. Dis.* 7, 1165–1170. doi: 10.1089/fpd.2009.0527

Karageorgopoulos, D. E., and Falagas, M. E. (2008). Current control and treatment of multidrug-resistant *Acinetobacter baumannii* infections. *Lancet Infect. Dis.* 8, 751–762. doi: 10.1016/S1473-3099(08)70279-2

Karumathil, D. P., Surendran-Nair, M., and Venkitanarayanan, K. (2016). Efficacy of trans-cinnamaldehyde and eugenol in reducing *Acinetobacter baumannii* adhesion to and invasion of human keratinocytes and controlling wound infection in vitro. *Phytother. Res.* 30, 2053–2059. doi: 10.1002/ptr.5713

Knezevic, P., Aleksic, V., Simin, N., Svircev, E., Petrovic, A., and Mimica-Dukic, N. (2016). Antimicrobial activity of *Eucalyptus camaldulensis* essential oils and their interactions with conventional antimicrobial agents against multi-drug resistant *Acinetobacter baumannii*. *J. Ethnopharmacol.* 178, 125–136. doi: 10.1016/j.jep.2015.12.008

Kollanoor-Johny, A., Mattson, T., Baskaran, S. A., Amalaradjou, M. A., Babapoor, S., March, B., et al. (2012). Reduction of *Salmonella enterica* serovar Enteritidis colonization in 20-day-old broiler chickens by the plant-derived compounds trans-cinnamaldehyde and eugenol. *Appl. Environ. Microbiol.* 78, 2981–2987. doi: 10.1128/AEM.07643-11

Kon, K. V., and Rai, M. K. (2012). Plant essential oils and their constituents in coping with multidrug-resistant bacteria. *Expert Rev. Anti. Infect. Ther.* 10, 775–790. doi: 10.1586/eri.12.57

Lean, S. S., Suhaili, Z., Ismail, S., Rahman, N. I. A., Othman, N., Abdullah, F. H., et al. (2014). Prevalence and genetic characterization of carbapenem-and polymyxin-resistant *Acinetobacter baumannii* Isolated from a tertiary hospital in Terengganu, Malaysia. *ISRN Microbiol.* 2014:953417. doi: 10.1155/2014/953417

Lee, H. W., Koh, Y. M., Kim, J., Lee, J. C., Lee, Y. C., Seol, S. Y., et al. (2008). Capacity of multidrug-resistant clinical isolates of *Acinetobacter baumannii* to form biofilm and adhere to epithelial cell surfaces. *Clin. Microbiol. Infect.* 14, 49–54. doi: 10.1111/j.1469-0691.2007.01842.x

Leung, W. S., Chu, C. M., Chan, V. L., Lam, J. Y., and Ho, P. L. (2005). Fulminant community acquired *Acinetobacter baumannii* pneumonia as a distinct clinical syndrome. *Chest* 128, 149S–149S. doi: 10.1378/chest.128.4_MeetingAbstracts.149S

Lomovskaya, O., and Bostian, K. A. (2006). Practical applications and feasibility of efflux pump inhibitors in the clinic–a vision for applied use. *Biochem. Pharmacol.* 71, 910–918. doi: 10.1016/j.bcp.2005.12.008

Longo, F., Vuotto, C., and Donelli, G. (2014). Biofilm formation in *Acinetobacter baumannii*. *New Microbiol.* 37, 119–127.

Magnet, S., Courvalin, P., and Lambert, T. (2001). Resistance-nodulation-cell division-type efflux pump involved in aminoglycoside resistance in *Acinetobacter baumannii* strain BM4454. *Antimicrob. Agents Chemother.* 45, 3375–3380. doi: 10.1128/AAC.45.12.3375-3380.2001

Malone, L., and Kwon, D. H. (2013). Carbapenem-associated multidrug-resistant *Acinetobacter baumannii* are sensitised by aztreonam in combination with polyamines. *Int. J. Antimicro. Agents* 41, 70–74. doi: 10.1016/j.ijantimicag.2012.08.009

Manchanda, V., Sanchaita, S., and Singh, N. (2010). Multidrug resistant Acinetobacter. *J. Glob. Infect. Dis.* 2, 291–304. doi: 10.4103/0974-777X.68538

Maragakis, L. L., and Perl, T. M. (2008). *Acinetobacter baumannii*: epidemiology, antimicrobial resistance, and treatment options. *Clin. Infect. Dis.* 46, 1254–1263. doi: 10.1086/529198

Menon, T., Shanmugasundaram, S., Nandhakumar, B., Nalina, K., and Balasubramaniam. (2006). Infective endocarditis due to *Acinetobacter baumannii* complex–a case report. *Indian J. Pathol. Microbiol.* 49, 576–578.

Metan, G., Alp, E., Aygen, B., and Sumerkan, B. (2007). *Acinetobacter baumannii* meningitis in post-neurosurgical patients: clinical outcome and impact of carbapenem resistance. *J. Antimicrob. Chemother.* 60, 197–199. doi: 10.1093/jac/dkm181

Morfin-Otero, R., and Dowzicky, M. J. (2012). Changes in MIC within a global collection of *Acinetobacter baumannii* collected as part of the Tigecycline Evaluation and Surveillance Trial, 2004 to 2009. *Clin. Ther.* 34, 101–112. doi: 10.1016/j.clinthera.2011.11.028

Narayanan, A., Muyyarikkandy, M. S., Mooyottu, S., Venkitanarayanan, K., and Amalaradjou, M. A. R. (2017). Oral supplementation of trans-cinnamaldehyde reduces uropathogenic *Escherichia coli* colonization in a mouse model. *Lett. Appl. Microbiol.* 64, 192–197. doi: 10.1111/lam.12713

Neonakis, I. K., Spandidos, D. A., and Petinaki, E. (2011). Confronting multidrug-resistant *Acinetobacter baumannii*: a review. *Int. J. Antimicro. Agents* 37, 102–109. doi: 10.1016/j.ijantimicag.2010.10.014

Olut, A. I., and Erkek, E. (2005). Early prosthetic valve endocarditis due to *Acinetobacter baumannii*: a case report and brief review of the literature. *Scand. J. Infect. Dis.* 37, 919–921. doi: 10.1080/00365540500262567

Peleg, A. Y., Adams, J., and Paterson, D. L. (2007). Tigecycline efflux as a mechanism for nonsusceptibility in *Acinetobacter baumannii*. *Antimicrob. Agents Chemother.* 51, 2065–2069. doi: 10.1128/AAC.01198-06

Pitout, J. D., Sanders, C. C., and Sanders, W. E. (1997). Antimicrobial resistance with focus on β-lactam resistance in gram-negative bacilli. *Am. J. Med.* 103, 51–59. doi: 10.1016/S0002-9343(97)00044-2

Pogue, J., Kaye, K., Cohen, D., and Marchaim, D. (2015). Appropriate antimicrobial therapy in the era of multidrug-resistant human pathogens. *Clin. Microbiol. Infect.* 21, 302–312. doi: 10.1016/j.cmi.2014.12.025

Rao, R. S., Karthika, R. U., Singh, S. P., Shashikala, P., Kanungo, R., Jayachandran, S., et al. (2008). Correlation between biofilm production and multiple drug resistance in imipenem resistant clinical isolates of *Acinetobacter baumannii*. *Indian J. Med. Microbiol.* 26, 333–337. doi: 10.4103/0255-0857.43566

Renau, T. E., Léger, R., Flamme, E. M., Sangalang, J., She, M. W., Yen, R., et al. (1999). Inhibitors of efflux pumps in *Pseudomonas aeruginosa* potentiate the activity of the fluoroquinolone antibacterial levofloxacin. *J. Med. Chem.* 42, 4928–4931. doi: 10.1021/jm9904598

Saghi, H., Bahador, A., Khaledi, A., Kachoei, R. A., Dastjerdi, F. A., and Esmaeili, D. (2015). Antibacterial effects of origanum vulgare essence against multidrug-resistant *Acinetobacter baumannii* isolated from selected hospitals of Tehran, Iran. *Avicenna J. Clin. Microb. Infect.* 2, 1–5. doi: 10.17795/ajcmi-22982

Scott, P., Deye, G., Srinivasan, A., Murray, C., Moran, K., Hulten, E., et al. (2007). An outbreak of multidrug-resistant *Acinetobacter baumannii*-calcoaceticus complex infection in the US military health care system associated with military operations in Iraq. *Clin. Infect. Dis.* 44, 1577–1584. doi: 10.1086/518170

Shlaes, D. M., Sahm, D., Opiela, C., and Spellberg, B. (2013). The FDA reboot of antibiotic development. *Antimicrob. Agents Chemother.* 57, 4605–4607. doi: 10.1128/AAC.01277-13

Siriyong, T., Chusri, S., Srimanote, P., Tipmanee, V., and Voravuthikunchai, S. P. (2016). Holarrhena antidysenterica extract and its steroidal alkaloid conessine as resistance modifying agents against extensively drug resistant *Acinetobacter baumannii*. *Microb. Drug Resist.* 22, 273–282. doi: 10.1089/mdr.2015.0194

Solarte, A. L., Astorga, R. J., Aguiar, F., Galan-Relano, A., Maldonado, A., and Huerta, B. (2017). Combination of antimicrobials and essential oils as an alternative for the control of *Salmonella enterica* multiresistant strains related to foodborne disesase. *Foodborne Pathog. Dis.*. 14, 558–563. doi: 10.1089/fpd.2017.2295

Sun, J., Deng, Z., and Yan, A. (2014). Bacterial multidrug efflux pumps: Mechanisms, physiology and pharmacological exploitations. *Biochem. Biophys. Res. Commun.* 453, 254–267. doi: 10.1016/j.bbrc.2014.05.090

Sunenshine, R. H., Wright, M. O., Maragakis, L. L., Harris, A. D., Song, X., Hebden, J., et al. (2007). Multidrug-resistant Acinetobacter infection mortality rate and length of hospitalization. *Emerg. Infect. Dis* 13, 97–103. doi: 10.3201/eid1301.060716

Talbot, G. H., Bradley, J., Edwards, J. E. Jr., Gilbert, D., Scheld, M., and Bartlett, J. G. (2006). Antimicrobial availability task force of the infectious diseases society of America, 2006. Bad bugs need drugs: an update on the development pipeline from the antimicrobial availability task force of the infectious diseases society of America. *Clin. Infect. Dis.* 42, 657–668. doi: 10.1086/499819

Tang, S. S., Apisarnthanarak, A., and Hsu, L. Y. (2014). Mechanisms of β-lactam antimicrobial resistance and epidemiology of major community- and healthcare-associated multidrug-resistant bacteria. *Adv. Drug Deliv. Rev.* 78, 3–13. doi: 10.1016/j.addr.2014.08.003

Thakuria, B., and Lahon, K. (2013). The beta lactam antibiotics as an empirical therapy in a developing country: an update on their current status and recommendations to counter the resistance against them. *J. Clin. Diagn. Res.* 7, 1207–1214. doi: 10.7860/JCDR/2013/5239.3052

Tharmalingam, N., Rajmuthiah, R., Kim, W., Fuchs, B. B., Jeyamani, E., Kelso, M. J., et al. (2018). Antibacterial properties of four novel hit compounds from a methicillin-resistant *Staphylococcus aureus–Caenorhabditis elegans* high-throughput screen. *Microb. Drug Resist.* doi: 10.1089/mdr.2017.0250 [Epub ahead of print].

Tiwari, M., Roy, R., and Tiwari, V. (2016). Screening of Herbal based bioactive extract against Carbapenem-resistant strain of *Acinetobacter baumannii*. *Microb. Drug Resist.* 22, 364–371. doi: 10.1089/mdr.2015.0270

Tiwari, V., Tiwari, D., Patel, V., and Tiwari, M. (2017). Effect of secondary metabolite of *Actinidia deliciosa* on the biofilm and extra-cellular matrix components of *Acinetobacter baumannii*. *Microb. Pathog.* 110, 345–351. doi: 10.1016/j.micpath.2017.07.013

Ulu-Kilic, A., Ahmed, S. S., Alp, E., and Doğanay, M. (2013). Challenge of intensive care unit-acquired infections and *Acinetobacter baumannii* in developing countries. *OA Crit. Care* 1:3. doi: 10.13172/2052-9309-1-1-382

Upadhyay, A., Upadhyaya, I., Kollanoor-Johny, A., and Venkitanarayanan, K. (2014). Combating pathogenic microorganisms using plant-derived antimicrobials: a mini review of the mechanistic basis. *Biomed. Res. Int.* 2014:761741. doi: 10.1155/2014/761741

Vashist, J., Tiwari, V., Das, R., Kapil, A., and Rajeswari, M. R. (2011). Analysis of penicillin-binding proteins (PBPs) in carbapenem resistant *Acinetobacter baumannii*. *Indian J. Med. Res.* 133, 332–338.

Vila, J., Martí, S., and Sánchez-Céspedes, J. (2007). Porins, efflux pumps and multidrug resistance in *Acinetobacter baumannii*. *J. Antimicrob. Chemother.* 59, 1210–1215. doi: 10.1093/jac/dkl509

Walsh, C., and Fanning, S. (2008). Antimicrobial resistance in food borne pathogens-A cause for concern? *Curr. Drug Targets.* 9, 808–815. doi: 10.2174/138945008785747761

Wang, H. M., Chen, C. Y., Chen, H. A., Huang, W. C., Lin, W. R., Chen, T. C., et al. (2010). *Zingiber officinale* (ginger) compounds have tetracycline-resistance modifying effects against clinical extensively drug resistant *Acinetobacter baumannii*. *Phytother. Res.* 24, 1825–1830. doi: 10.1002/ptr.3201

Wieczorek, P., Sacha, P., Hauschild, T., Zórawski, M., Krawczyk, M., and Tryniszewska, E. (2008). Multidrug resistant *Acinetobacter baumannii*–the role of AdeABC (RND family) efflux pump in resistance to antibiotics. *Folia Histochem. Cytobiol.* 46, 257–267. doi: 10.2478/v10042-008-0056-x

Wisplinghoff, H., Bischoff, T., Tallent, S. M., Seifert, H., Wenzel, R. P., and Edmond, M. B. (2004). Nosocomial bloodstream infections in US hospitals: analysis of 24,179 cases from a prospective nationwide surveillance study. *Clin. Infect. Dis.* 39, 309–317. doi: 10.1086/421946

Xing, L., Barnie, P., Su, Z., and Xu, H. (2014). Development of efflux pumps and inhibitors (EPIs) in *A. baumanii*. *Clin. Microbial.* 3:135.

Yoon, E. J., Courvalin, P., and Grillot-Courvalin, C. (2013). RND-type efflux pumps in multidrug-resistant clinical isolates of *Acinetobacter baumannii*: major role for AdeABC overexpression and AdeRS mutations. *Antimicrob. Agents Chemother.* 57, 2989–2995. doi: 10.1128/AAC.02556-12

Conflict of Interest Statement: The authors declare that the research was conducted in the absence of any commercial or financial relationships that could be construed as a potential conflict of interest.

Copyright © 2018 Karumathil, Nair, Gaffney, Kollanoor-Johny and Venkitanarayanan. This is an open-access article distributed under the terms of the Creative Commons Attribution License (CC BY). The use, distribution or reproduction in other forums is permitted, provided the original author(s) and the copyright owner are credited and that the original publication in this journal is cited, in accordance with accepted academic practice. No use, distribution or reproduction is permitted which does not comply with these terms.

frontiers in Microbiology

MINI REVIEW
published: 06 June 2018
doi: 10.3389/fmicb.2018.01184

Advance in Research on *Mycobacterium tuberculosis* FabG4 and Its Inhibitor

*Debajyoti Dutta**

Department of Biochemistry, Faculty of Medicine and Dentistry, University of Alberta, Edmonton, AB, Canada

Increasing evidence from recent reports of drug-resistant mycobacterial strains poses a challenge worldwide. Drug-resistant strains often undergo mutations, adopt alternative pathways, and express drug efflux pumps to reduce or eliminate drug doses. Besides these intrinsic resistance mechanisms, bacteria can evade drug doses by forming biofilms. Biofilms are the concerted growth of adherent microorganisms, which can also be formed at the air-water interface. The growth is supported by the extracellular polymer matrix which is self-produced by the microorganisms. Reduced metabolic activity in a nutrient-deficient environment in the biofilm may cause the microorganisms to take alternative pathways that can make the microorganisms recalcitrant to the drug doses. Recent works have shown that *Mycobacterium tuberculosis* expresses several proteins during its growth in biofilm, those when deleted, did not show any effect on mycobacterial growth in normal nutrient-sufficient conditions. Studying these unconventional proteins in mycobacterial biofilms is therefore of utmost importance. In this article, I will discuss one such mycobacterial biofilm-related protein FabG4 that is recently shown to be important for mycobacterial survival in the presence of antibiotic stressors and limited nutrient condition. In an attempt to find more effective FabG4 inhibitors and its importance in biofilm forming *M. tuberculosis*, present knowledge about FabG4 and its known inhibitors are discussed. Based on the existing data, a putative role of FabG4 is also suggested.

Keywords: FabG4, *Mycobacterium tuberculosis*, biofilm, β-oxo acyl-ACP reductase, inhibitor

OPEN ACCESS

Edited by:
Noton Kumar Dutta,
Johns Hopkins University,
United States

Reviewed by:
Luiz Augusto Basso,
Pontifícia Universidade Católica do Rio Grande do Sul, Brazil
Li Yuan,
Shihezi University, China

***Correspondence:**
Debajyoti Dutta
ddutta@ualberta.ca;
debajyoti.47@gmail.com

Specialty section:
This article was submitted to Antimicrobials, Resistance and Chemotherapy, a section of the journal Frontiers in Microbiology

Received: *26 March 2018*
Accepted: *16 May 2018*
Published: *06 June 2018*

Citation:
Dutta D (2018) Advance in Research on Mycobacterium tuberculosis FabG4 and Its Inhibitor. Front. Microbiol. 9:1184. doi: 10.3389/fmicb.2018.01184

INTRODUCTION

The ability of *Mycobacterium tuberculosis* to form biofilms was noted almost 120 years ago (Jones, 1896). However, the physiological and molecular basis of biofilm is only beginning to unravel until recently. The first protein that was found to be involved in *M. smegmatis* maturation of biofilm is the chaperone GroEL-1 (Ojha et al., 2005). GroEL-1 deficient mutant of *M. smegmatis* was suggested to lack GroEL-1 interaction with fatty acid synthesis type -II complex thereby reducing the mycolic acid content in biofilms. Mycolic acids are the predominant components of mycobacterial cell envelope that are produced by fatty acid synthesis type-II pathway in mycobacteria. The reason that mycobacterial cell envelope largely contributes to the biofilm attachment endorses mycolic acids may be involved in biofilm formation (Marrakchi et al., 2014). However the physiology of mycobacteria changes as it shifts from planktonic growth to biofilm

dependent growth and results in several modifications in the expression level of protein and molecules pertaining to the cell envelope (Ojha et al., 2008; Sambandan et al., 2013; Rastogi et al., 2017). Fatty acid synthesis and its associated pathways for mycobacterial cell envelope synthesis are one of the major areas for developing antitubercular drugs (Zumla et al., 2013). Because of this altered phenotypes and a waxy extra-cellular matrix of biofilm, Mycobacteria become resilient to drug doses (Islam et al., 2012). Therefore the conventional TB drugs may not be as effective for biofilm-forming mycobacteria.

Membrane and cell envelope-associated biofilm-related proteins are particularly of interest as these proteins are likely to be involved in the making of cellular attachment to the biofilms. For example, recent studies have shown that a lipid transporter MmpL11 is specifically required for biofilm formation (Pacheco et al., 2013). Other works have identified a number of proteins specific to mycobacterial growth in the biofilm at air-water interface (Kerns et al., 2014). One of the proteins that are conserved among mycobacterial species is FabG4. The protein was proposed to possess host antigenic property and has a potential to be a biofilm-specific marker (Kerns et al., 2014). In addition to that, FabG4 was recognized as one of the crucial protein for mycobacterial survival in a stressed condition. This article will discuss the known facts about FabG4, its inhibitors, and discuss its possibility to serve as a candidate to study and treat biofilm-related mycobacteria.

IMPORTANCE OF FABG4 IN MYCOBACTERIA

FabG commits the second step of fatty acid synthesis that is to convert β-oxo acyl-ACP to β-hydroxy acyl-ACP. *M. tuberculosis* genome contains multiple FabG homologs. Two of them are conserved among all mycobacterial species, FabG1 and FabG4. FabG1 remain at the focus of attention because it takes part in fatty acid synthesis type-II (Marrakchi et al., 2002). On the other hand, several studies have indicated that FabG4 is not an inactive gene in the *M. tuberculosis* genome. Its expression was first documented in the proteome by using 2-D gel electrophoresis accompanying MALDI-MS analysis (Jungblut et al., 1999) and later verified by others (Rosenkrands et al., 2000; Sinha et al., 2002). Gu et al. (2003), first provide the evidence that the protein is expressed in the mycobacterial membrane fraction. However, it's requirement in mycobacterial physiology was not shown until the comprehensive work done by McFadden and coworkers (Beste et al., 2009). The authors showed that the protein is uniquely required for mycobacterial growth in Roisin's minimal media, which contains limited carbon source (Beste et al., 2009). Proteomics studies have further identified that FabG4 is one of the major proteins which expression is induced by the antibiotic stressor (Sharma et al., 2010). The protein expression was also detected in the drug-resistant strains (Singh et al., 2016; Verma et al., 2017). Most interestingly, FabG4 can functionally complement eukaryotic β-oxoacyl-ACP reductase activity. FabG4, when expressed in the knockout of *ora1* yeast cells can restore the mitochondrial fatty acid synthesis type-II (Gurvitz et al., 2009). Because yeast ORA1 is a mitochondrial FabG1/FabG4 ortholog (Hiltunen et al., 2009), functional complementation of ORA1 with FabG4 is indicative of an active FabG4 protein that can utilize ACP/Coenzyme A tagged β-oxoacyl substrates and is utilized by mycobacteria during limiting resource or antibiotic stressed condition.

UNIQUE FEATURES OF FabG4

Characterization of recombinantly expressed FabG4 has shown that the protein is highly specific for NADH (Dutta et al., 2011). This is intriguingly different from its close relative (33% homology) FabG1 that utilizes NADPH. Crystal structure of the FabG4 complex with NADH reveals that the specificity comes from a single aspartate residue that reduces the volume of the phosphate binding groove of adenosine ribose phosphate moiety of NADPH (Dutta et al., 2013). Crystal structure further shows that FabG4 contains a "flavodoxin-type" structural domain in its N-terminal and a typical ketoreductase domain in its C-terminal (**Figure 1A**). The N-terminal structural domain is also found in modular polyketide synthase ketoreductase domain PlmKR1 (Bonnett et al., 2013). PlmKR1 exists as a monomer but FabG4 is different in the sense that the protein is a dimer, where the N-terminal domain of a protomer makes an extensive interaction with the C-terminal domain of the other protomer. Therefore, FabG4 was designated as "High Molecular weight FabG" (HMwFabG) (Dutta et al., 2011). Typical FabG does not contain this structural domain.

Many of the N-terminal residues (1–19) of FabG4 cannot be traced in crystal structure suggesting that the region has no rigid secondary structure. Most of the N-terminal residues were traced in FabG4 complex with NAD^+ structure (PDB 4FW8) showing a possibility of short helix containing seven residues (21–27) (**Figure 1A**). Long N-terminal sequences in FabGs are also found among eukaryotes, which were suggested to be the signal sequence (Wickramasinghe et al., 2006). Whether it is true for FabG4 is not known, but sequence alignment of HMwFabGs from actinobacteria and many proteobacteria reveals conserved residues Pro30, Leu33, and Arg35 in N-terminal sequence. Truncation of the N-terminal residues does not have any effect on catalytic activity. On the contrary, the C-terminal residues of FabG4 are apparently involved in catalytic activity since its truncation yields with a defective protein (Dutta et al., 2011). This is because the conserved C-terminal residues are engaged in electrostatic interaction with the active site proximal loops (Dutta et al., 2011).

INHIBITORS OF FabG4

Structure of FabG4 and its complex with a substrate mimic hexanoyl-CoA (PDB 3V1U) accelerated the work on structure-based inhibitor design against FabG4 (Dutta et al., 2013) (**Figure 1B**). The particular structure also provides a platform to design FabG specific inhibitors because the structure provided the first evidence of FabG-substrate complex (**Table 1**). The

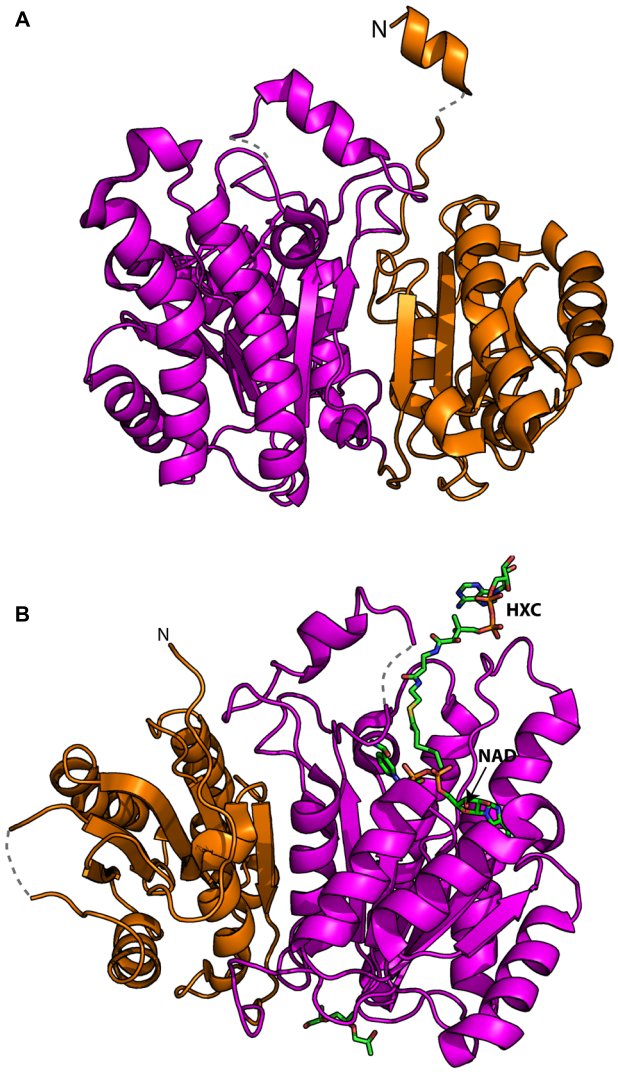

FIGURE 1 | Crystal structures of FabG4: **(A)** N-terminal "flavodoxin type" (orange) and C-terminal ketoreductase (magenta) domains. "N" indicated the N-terminal of the polypeptide chain. The regions those were not be traced in electron density are shown in dotted lines. **(B)** The substrate mimic hexanoyl coenzyme A (HXC) and NAD^+ bound structure shows the putative substrate binding modes.

first reported FabG4 inhibitors are based on the polyphenol compounds (Banerjee et al., 2014, 2015b). Synthesized compounds are also tested against *M. smegmatis* showing the MIC of 5 $\mu g\ mL^{-1}$. Docking studies had revealed that the compounds potentially occupy the NADH binding region with a few hydrogen-bonding interactions with the loop-residues responsible for CoA substrate binding. Another study to design and synthesize the inhibitors based on the common pharmacophores like β-lactam and Isoniazid was also successful inhibiting FabG4 with IC_{50} as low as 15.2 ± 0.5 μM (Banerjee et al., 2015a). Similar to the polyphenol based compounds β-lactam and Isoniazid-based compounds primarily dock on the NADH binding site. Isothermal titration calorimetry indicates two sequential binding sites showing positive cooperativity. Inhibitory effects of β-lactam and Isoniazid-based compounds have shown to be inhibitory toward mycobacterial biofilm formation. Recently, thiophene containing trisubstituted methane compound, *S*-S006-830 was found to have a substantial inhibitory effect on *M. tuberculosis* biofilm formation and possesses antitubercular activity (Singh et al., 2017). FabG4 is one of the three membrane-associated proteins identified to strongly interact with *S*-S006-830. Computational docking study predicts two possible binding sites. One comprises of the region overlapping NADH and CoA substrate binding and the other site is on the N-terminal domain. *S*-S006-830 is special because apart from the NADH-substrate binding site it also targets to the N-terminal structural domain. Two unique FabG inhibitors are worth mentioning in this regard. The first, Pyridomycin analog specifically targets NADH binding proteins and proposed to exhibit inhibitory effects on FabG4 by bridging both NADH and substrate-binding region (Hartkoorn et al., 2014). The second inhibitor was identified using library screening that uniquely binds to the helical dimeric interface of FabG (Cukier et al., 2013). The helical dimeric interface in FabG is responsible of NAD(P)H binding cooperativity (Dutta et al., 2012). All FabG4 and related inhibitors are summarized in **Table 1**.

POSSIBLE ROLE OF THE ENZYME

High Molecular weight FabG are exclusively found among bacteria. Homologous genes of FabG4 are found in actinobacteria and many proteobacteria (Dutta et al., 2011). Genomic analysis of HMwFabG containing bacteria shows another protein coexisting downstream to FabG4 ORF. In *M. tuberculosis* this protein is HtdX (Rv0241c). Both the proteins are conserved among mycobacterial species. Even in *M. leprae* genome where the genomic reduction had happened, retained both *fabG4* and its downstream *htdX* (Cole et al., 2001). However, deletion of *htdX* or *fabG4* does not show any apparent effect on bacterial survival *in vivo* (Sassetti and Rubin, 2003). Nonetheless, the protein is shown to be essential for survival in minimal media (Beste et al., 2009). Presumably, the conditional dependency of *M. tuberculosis* on FabG4 indicates an alternative pathway during limiting resource condition. Another clue is the FabG4 dependency on NADH. The NADH utilizing β-ketoacyl reductase activity of FabG4 is four times higher to the reverse reaction that utilizes NAD^+ for β-hydroxyacyl dehydrogenase activity (Dutta et al., 2013). Compared to NADPH, NADH is the low energy molecule and mostly associates to the catabolic pathways (Cantó et al., 2015). Shifting the coenzyme specificity toward low energy NADH possibly indicates that the bacteria are rewiring its metabolism toward the energy saving mode. Furthermore, FabG4 is isolated from the membrane fraction, which is indicative of its membrane-associated role (Gu et al., 2003; Singh et al., 2017). The role could be either fatty acid synthesis or modification. Notably, the other gene *htdX* was found to be responsive to the inhibitors of cell wall synthesis (Boshoff et al., 2004). Since both *fabG4* and *htdX* are situated in a conserved cluster it is tempting to predict that they are involved in the same

TABLE 1 | Inhibitors of FabG4.

Compound structure	Type of the compounds	General comments	Reference
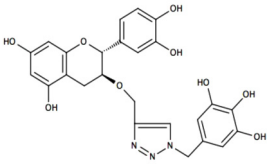	Triazole-polyphenol hybrid compounds	Possibly compete for NADH binding sites; Cooperative sequential binding with two binding sites IC_{50} = 34.9 μM K_i = 0.88 μM MIC = 5 μg ml^{-1}	Banerjee et al., 2014, 2015b
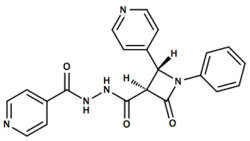	Beta-lactam isoniazid based compounds	Possibly compete for NADH binding sites; Cooperative sequential binding with two binding sites; acts as dual inhibitor of HtdX IC_{50} = 15.2 μM MIC = 15 μg ml^{-1}	Banerjee et al., 2015a
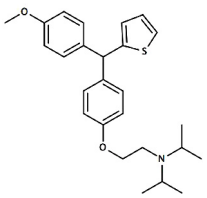	Thiophene containing trisubstituted methane	*S*-Enantiomer has more specificity toward FabG4; combination with rifampicin has a synergistic effect MIC = 3.125 μg ml^{-1}	Singh et al., 2017
Other inhibitors related to FabG4			
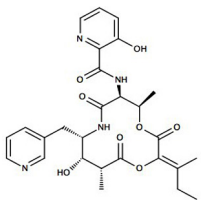	Pyridomycin analogs	An InhA inhibitor that can possibly inhibits FabG4 by binding to the both NADH and substrate binding region	Hartkoorn et al., 2014
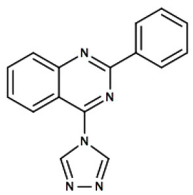	Triazol-quinazoline based compound	Inhibitor identified against *Pseudomonas aeruginosa* FabG from the screening small molecule library, Specifically binds to the helical dimer interface	Cukier et al., 2013

pathway. Both sequence analysis and preliminary enzymatic activities are corroborated that HtdX can commit a dehydratase reaction that is to convert β-hydroxyacyl-CoA to enoylacyl-CoA (Gurvitz, 2009; Sacco et al., 2010; Biswas et al., 2013; Banerjee et al., 2015a). The reaction is theoretically the successive step of FabG4 enzymatic reaction for fatty acid elongation cycle. Altogether the data suggests that during limiting resource condition FabG4 participates into some low-energy requiring pathway that is related to membrane biosynthesis, remodeling or recycling.

FUTURE SCOPE

FabG4 is a host antigenic protein reportedly expressed in mycobacterial biofilms. The protein expression was consistently found in membrane fraction and stressor-induced. As a conserved gene in all mycobacterial species, FabG4 can be a biomarker for biofilm. Although, FabG4 inhibitors are manifested antitubercular activity more experiments are needed to call it a drug target. Role of FabG4 and its connection with the membrane in mycobacteria also require further experimentations. To study FabG4 importance in biofilm forming *M. tuberculosis* it is, therefore, necessary to find out its targeting and interaction with other proteins. Identifying the role of FabG4 in mycobacteria might provide a hint of a new aspect of a survival strategy. The second aspect is the strategy to design more specific inhibitors of FabG4. While the C-terminal domain of FabG4 is common among FabGs, inhibitors against its N-terminal structural domain might be a way to target the protein more specifically. Designing the fluorophore inhibitors against its structural domain could be a way to find out its role *in vivo*.

AUTHOR CONTRIBUTIONS

DD is solely responsible for the conception or design, drafting, and revising the work.

ACKNOWLEDGMENTS

The author thanks Professor Amit Kumar Das, Department of Biotechnology, Indian Institute of Technology Kharagpur for his guidance during Ph.D. The author also thanks Professor Amit Basak, Department of Chemistry, Indian Institute of Technology Kharagpur and Dr. Deb Ranjan Banerjee and Rupam Biswas for their contribution to the FabG4 work from Indian Institute of Technology Kharagpur.

REFERENCES

Banerjee, D. R., Biswas, R., Das, A. K., and Basak, A. (2015a). Design, synthesis and characterization of dual inhibitors against new targets FabG4 and HtdX of *Mycobacterium tuberculosis*. *Eur. J. Med. Chem.* 100, 223–234. doi: 10.1016/j.ejmech.2015.06.007

Banerjee, D. R., Dutta, D., Saha, B., Bhattacharyya, S., Senapati, K., Das, A. K., et al. (2014). Design, synthesis and characterization of novel inhibitors against mycobacterial β-ketoacyl CoA reductase FabG4. *Org. Biomol. Chem.* 12, 73–85. doi: 10.1039/c3ob41676c

Banerjee, D. R., Senapati, K., Biswas, R., Das, A. K., and Basak, A. (2015b). Inhibition of *M. tuberculosis* β-ketoacyl CoA reductase FabG4 (Rv0242c) by triazole linked polyphenol-aminobenzene hybrids: comparison with the corresponding gallate counterparts. *Bioorg. Med. Chem. Lett.* 25, 1343–1347. doi: 10.1016/j.bmcl.2015.01.014

Beste, D. J., Espasa, M., Bonde, B., Kierzek, A. M., Stewart, G. R., and McFadden, J. (2009). The genetic requirements for fast and slow growth in mycobacteria. *PLoS One* 4:e5349. doi: 10.1371/journal.pone.0005349

Biswas, R., Dutta, D., and Das, A. K. (2013). Cloning, overexpression, purification, crystallization and preliminary X-ray diffraction analysis of Rv0241c (HtdX) from *Mycobacterium tuberculosis* H37Rv. *Acta Crystallogr. Sect. F Struct. Biol. Cryst. Commun.* 69, 1110–1113. doi: 10.1107/S1744309113023452

Bonnett, S. A., Whicher, J. R., Papireddy, K., Florova, G., Smith, J. L., and Reynolds, K. A. (2013). Structural and stereochemical analysis of a modular polyketide synthase ketoreductase domain required for the generation of a *cis*-alkene. *Chem. Biol.* 20, 772–783. doi: 10.1016/j.chembiol.2013.04.014

Boshoff, H. I., Myers, T. G., Copp, B. R., McNeil, M. R., Wilson, M. A., and Barry, C. E. III (2004). The transcriptional responses of *Mycobacterium tuberculosis* to inhibitors of metabolism: novel insights into drug mechanisms of action. *J. Biol. Chem.* 279, 40174–40184. doi: 10.1074/jbc.M406796200

Cantó, C., Menzies, K. J., and Auwerx, J. (2015). NAD^+ metabolism and the control of energy homeostasis: a balancing act between mitochondria and the nucleus. *Cell Metab.* 22, 31–53. doi: 10.1016/j.cmet.2015.05.023

Cole, S. T., Eiglmeier, K., Parkhill, J., James, K. D., Thomson, N. R., Wheeler, P. R., et al. (2001). Massive gene decay in the leprosy bacillus. *Nature* 409, 1007–1011. doi: 10.1038/35059006

Cukier, C. D., Hope, A. G., Elamin, A. A., Moynie, L., Schnell, R., Schach, S., et al. (2013). Discovery of an allosteric inhibitor binding site in 3-Oxo-acyl-ACP reductase from *Pseudomonas aeruginosa*. *ACS Chem. Biol.* 8, 2518–2527. doi: 10.1021/cb4005063

Dutta, D., Bhattacharyya, S., and Das, A. K. (2012). Crystal structure and fluorescence studies reveal the role of helical dimeric interface of staphylococcal FabG1 in positive cooperativity for NADPH. *Proteins* 80, 1250–1257. doi: 10.1002/prot.24024

Dutta, D., Bhattacharyya, S., Mukherjee, S., Saha, B., and Das, A. K. (2011). Crystal structure of FabG4 from *Mycobacterium tuberculosis* reveals the importance of C-terminal residues in ketoreductase activity. *J. Struct. Biol.* 174, 147–155. doi: 10.1016/j.jsb.2010.11.012

Dutta, D., Bhattacharyya, S., Roychowdhury, A., Biswas, R., and Das, A. K. (2013). Crystal structure of hexanoyl-CoA bound to β-ketoacyl reductase FabG4 of *Mycobacterium tuberculosis*. *Biochem. J.* 450, 127–139. doi: 10.1042/BJ20121107

Gu, S., Chen, J., Dobos, K. M., Bradbury, E. M., Belisle, J. T., and Chen, X. (2003). Comprehensive proteomic profiling of the membrane constituents of a *Mycobacterium tuberculosis* strain. *Mol. Cell. Proteomics* 2, 1284–1296. doi: 10.1074/mcp.M300060-MCP200

Gurvitz, A. (2009). The essential mycobacterial genes, fabG1 and fabG4, encode 3-oxoacyl-thioester reductases that are functional in yeast mitochondrial fatty acid synthase type 2. *Mol. Genet. Genomics* 282, 407–416. doi: 10.1007/s00438-009-0474-2

Gurvitz, A., Hiltunen, J. K., and Kastaniotis, A. J. (2009). Heterologous expression of mycobacterial proteins in *Saccharomyces cerevisiae* reveals two physiologically functional 3-hydroxyacyl-thioester dehydratases, HtdX and HtdY, in addition to HadABC and HtdZ. *J. Bacteriol.* 191, 2683–2690. doi: 10.1128/JB.01046-08

Hartkoorn, R. C., Pojer, F., Read, J. A., Gingell, H., Neres, J., Horlacher, O. P., et al. (2014). Pyridomycin bridges the NADH- and substrate-binding pockets of the enoyl reductase InhA. *Nat. Chem. Biol.* 10, 96–98. doi: 10.1038/nchembio.1405

Hiltunen, J. K., Schonauer, M. S., Autio, K. J., Mittelmeier, T. M., Kastaniotis, A. J., and Dieckmann, C. L. (2009). Mitochondrial fatty acid synthesis type II: more than just fatty acids. *J. Biol. Chem.* 284, 9011–9015. doi: 10.1074/jbc.R800068200

Islam, M. S., Richards, J. P., and Ojha, A. K. (2012). Targeting drug tolerance in mycobacteria: a perspective from mycobacterial biofilms. *Expert Rev. Anti Infect. Ther.* 10, 1055–1066. doi: 10.1586/eri.12.88

Jones, A. C. (1896). On the so-called tubercle bacilli. *Report of the 66th Meeting of the British Association for the Advancements of Science*. London: John Murray, 1015–1016.

Jungblut, P. R., Schaible, U. E., Mollenkopf, H. J., Zimny-Arndt, U., Raupach, B., Mattow, J., et al. (1999). Comparative proteome analysis of *Mycobacterium tuberculosis* and *Mycobacterium bovis* BCG strains: towards functional genomics of microbial pathogens. *Mol. Microbiol.* 33, 1103–1117. doi: 10.1046/j.1365-2958.1999.01549.x

Kerns, P. W., Ackhart, D. F., Basaraba, R. J., Leid, J. G., and Shirtliff, M. E. (2014). *Mycobacterium tuberculosis* pellicles express unique proteins recognized by the host humoral response. *Pathog. Dis.* 70, 347–358. doi: 10.1111/2049-632X.12142

Marrakchi, H., Ducasse, S., Labesse, G., Montrozier, H., Margeat, E., Emorine, L., et al. (2002). MabA (FabG1), a *Mycobacterium tuberculosis* protein involved in the long-chain fatty acid elongation system FAS-II. *Microbiology* 148, 951–960. doi: 10.1099/00221287-148-4-951

Marrakchi, H., Lanéelle, M. A., and Daffé, M. (2014). Mycolic acids: structures, biosynthesis, and beyond. *Chem. Biol.* 21, 67–85. doi: 10.1016/j.chembiol.2013.11.011

Ojha, A., Anand, M., Bhatt, A., Kremer, L., Jacobs, W. R. Jr., and Hatfull, G. F. (2005). GroEL1: a dedicated chaperone involved in mycolic acid biosynthesis during biofilm formation in mycobacteria. *Cell* 123, 861–873. doi: 10.1016/j.cell.2005.09.012

Ojha, A. K., Baughn, A. D., Sambandan, D., Hsu, T., Trivelli, X., Guerardel, Y., et al. (2008). Growth of *Mycobacterium tuberculosis* biofilms containing free mycolic acids and harbouring drug-tolerant bacteria. *Mol. Microbiol.* 69, 164–174. doi: 10.1111/j.1365-2958.2008.06274.x

Pacheco, S. A., Hsu, F. F., Powers, K. M., and Purdy, G. E. (2013). MmpL11 protein transports mycolic acid-containing lipids to the mycobacterial cell wall and contributes to biofilm formation in *Mycobacterium smegmatis*. *J. Biol. Chem.* 288, 24213–24222. doi: 10.1074/jbc.M113.473371

Rastogi, S., Singh, A. K., Pant, G., Mitra, K., Sashidhara, K. V., and Krishnan, M. Y. (2017). Down-regulation of PE11, a cell wall associated esterase, enhances the biofilm growth of *Mycobacterium tuberculosis* and reduces cell wall virulence lipid levels. *Microbiology* 163, 52–61. doi: 10.1099/mic.0.000417

Rosenkrands, I., King, A., Weldingh, K., Moniatte, M., Moertz, E., and Andersen, P. (2000). Towards the proteome of *Mycobacterium tuberculosis*. *Electrophoresis* 21, 3740–3756. doi: 10.1002/1522-2683(200011)21:17<3740::AID-ELPS3740>3.0.CO;2-3

Sacco, E., Slama, N., Bäckbro, K., Parish, T., Laval, F., Daffé, M., et al. (2010). Revisiting the assignment of Rv0241c to fatty acid synthase type II of *Mycobacterium tuberculosis*. *J. Bacteriol.* 192, 4037–4044. doi: 10.1128/JB.00386-10

Sambandan, D., Dao, D. N., Weinrick, B. C., Vilchèze, C., Gurcha, S. S., Ojha, A., et al. (2013). Keto-mycolic acid-dependent pellicle formation confers tolerance to drug-sensitive *Mycobacterium tuberculosis*. *mBio* 4:e00222-13. doi: 10.1128/mBio.00222-13

Sassetti, C. M., and Rubin, E. J. (2003). Genetic requirements for mycobacterial survival during infection. *Proc. Natl. Acad. Sci. U.S.A.* 100, 12989–12994. doi: 10.1073/pnas.2134250100

Sharma, P., Kumar, B., Singhal, N., Katoch, V. M., Venkatesan, K., Chauhan, D. S., et al. (2010). Streptomycin induced protein expression analysis in *Mycobacterium tuberculosis* by two-dimensional gel electrophoresis & mass spectrometry. *Indian J. Med. Res.* 132, 400–408.

Singh, A., Gupta, A. K., Gopinath, K., Sharma, D., Sharma, P., Bisht, D., et al. (2016). Comparative proteomic analysis of sequential isolates of *Mycobacterium tuberculosis* sensitive and resistant Beijing type from a patient with pulmonary tuberculosis. *Int. J. Mycobacteriol.* 5(Suppl. 1), S123–S124. doi: 10.1016/j.ijmyco.2016.10.028

Singh, P., Kumar, S. K., Maurya, V. K., Mehta, B. K., Ahmad, H., Dwivedi, A. K., et al. (2017). S-Enantiomer of the antitubercular compound S006-830 complements activity of frontline TB drugs and targets biogenesis of *Mycobacterium tuberculosis* cell envelope. *ACS Omega* 2, 8453–8465. doi: 10.1021/acsomega.7b01281

Sinha, S., Arora, S., Kosalai, K., Namane, A., Pym, A. S., and Cole, S. T. (2002). Proteome analysis of the plasma membrane of *Mycobacterium tuberculosis*. *Comp. Funct. Genomics.* 3, 470–483. doi: 10.1002/cfg.211

Verma, R., Pinto, S. M., Patil, A. H., Advani, J., Subba, P., Kumar, M., et al. (2017). Quantitative proteomic and phosphoproteomic analysis of H37Ra and H37Rv strains of *Mycobacterium tuberculosis*. *J. Proteome Res.* 16, 1632–1645. doi: 10.1021/acs.jproteome.6b00983

Wickramasinghe, S. R., Inglis, K. A., Urch, J. E., Müller, S., van Aalten, D. M., and Fairlamb, A. H. (2006). Kinetic, inhibition and structural studies on 3-oxoacyl-ACP reductase from *Plasmodium falciparum*, a key enzyme in fatty acid biosynthesis. *Biochem. J.* 393, 447–457. doi: 10.1042/BJ20050832

Zumla, A., Nahid, P., and Cole, S. T. (2013). Advances in the development of new tuberculosis drugs and treatment regimens. *Nat. Rev. Drug Discov.* 12, 388–404. doi: 10.1038/nrd4001

Conflict of Interest Statement: The author declares that the research was conducted in the absence of any commercial or financial relationships that could be construed as a potential conflict of interest.

Copyright © 2018 Dutta. This is an open-access article distributed under the terms of the Creative Commons Attribution License (CC BY). The use, distribution or reproduction in other forums is permitted, provided the original author(s) and the copyright owner are credited and that the original publication in this journal is cited, in accordance with accepted academic practice. No use, distribution or reproduction is permitted which does not comply with these terms.

frontiers in Microbiology

ORIGINAL RESEARCH
published: 15 June 2018
doi: 10.3389/fmicb.2018.01241

Herring Oil and Omega Fatty Acids Inhibit *Staphylococcus aureus* Biofilm Formation and Virulence

Yong-Guy Kim[1†], Jin-Hyung Lee[1†], Chaitany J. Raorane[1], Seong T. Oh[2], Jae G. Park[3] and Jintae Lee[1*]*

[1] School of Chemical Engineering, Yeungnam University, Gyeongsan, South Korea, [2] College of Pharmacy, Yeungnam University, Gyeongsan, South Korea, [3] Advanced Bio Convergence Center, Pohang Technopark Foundation, Pohang, South Korea

Staphylococcus aureus is notorious for its ability to become resistant to antibiotics and biofilms play a critical role in antibiotic tolerance. *S. aureus* is also capable of secreting several exotoxins associated with the pathogenesis of sepsis and pneumonia. Thus, the objectives of the study were to examine *S. aureus* biofilm formation *in vitro*, and the effects of herring oil and its main components, omega fatty acids [*cis*-4,7,10,13,16,19-docosahexaenoic acid (DHA) and *cis*-5,8,11,14,17-eicosapentaenoic acid (EPA)], on virulence factor production and transcriptional changes in *S. aureus*. Herring oil decreased biofilm formation by two *S. aureus* strains. GC-MS analysis revealed the presence of several polyunsaturated fatty acids in herring oil, and of these, two omega-3 fatty acids, DHA and EPA, significantly inhibited *S. aureus* biofilm formation. In addition, herring oil, DHA, and EPA at 20 μg/ml significantly decreased the hemolytic effect of *S. aureus* on human red blood cells, and when pre-treated to *S. aureus*, the bacterium was more easily killed by human whole blood. Transcriptional analysis showed that herring oil, DHA, and EPA repressed the expression of the α-hemolysin *hla* gene. Furthermore, in a *Caenorhabditis elegans* nematode model, all three prolonged nematode survival in the presence of *S. aureus*. These findings suggest that herring oil, DHA, and EPA are potentially useful for controlling persistent *S. aureus* infection.

Keywords: biofilm, hemolysis, herring oil, omega fatty acids, *Staphylococcus aureus*, virulence

OPEN ACCESS

Edited by:
Kamlesh Jangid, National Centre for Cell Science (NCCS), India

Reviewed by:
Nagendran Tharmalingam, Alpert Medical School, United States
Dane Parker, Columbia University, United States

***Correspondence:**
Jae G. Park
jaepark@pohangtp.org
Jintae Lee
jtlee@ynu.ac.kr

† These authors have contributed equally to this work.

Specialty section:
This article was submitted to Antimicrobials, Resistance and Chemotherapy, a section of the journal Frontiers in Microbiology

Received: *20 February 2018*
Accepted: *23 May 2018*
Published: *15 June 2018*

Citation:
Kim Y-G, Lee J-H, Raorane CJ, Oh ST, Park JG and Lee J (2018) Herring Oil and Omega Fatty Acids Inhibit Staphylococcus aureus Biofilm Formation and Virulence. Front. Microbiol. 9:1241. doi: 10.3389/fmicb.2018.01241

INTRODUCTION

The sticky conglomerations of bacteria that adhere to diverse medical devices or damaged body tissues can become causes of persistent infections. These bacteria encase themselves in a slime layer or biofilm, which poses serious problems to human health because of their abilities to tolerate conventional antibiotic chemotherapies, host immune systems, and external stresses (Potera, 1999; Hoffman et al., 2005).

Staphylococcus aureus is an important etiologic agent and a major cause of a diverse array of acute life-threatening bloodstream infections in man, and is often held responsible for worldwide outbreaks of nosocomial infections (Lowy, 1998). *S. aureus* biofilms play a critical role in antibiotic tolerance (Stewart and Costerton, 2001), and methicillin-resistant *S. aureus* (MRSA) and vancomycin-resistant *S. aureus* have become major nosocomial threats

(Speller et al., 1997). *S. aureus* secretes many exotoxins, including coagulase, enterotoxins, α-hemolysin, protein A, and TSST-1, which damage biological membranes and eventually cause cell death (Ohlsen et al., 1997; Otto, 2014). Also, *S. aureus* biofilms are found in medical devices and food surfaces, and are responsible for food-poisoning and toxic shock syndrome (Chambers and Deleo, 2009). In particular, α-hemolysin (Hla) is a major cytotoxic agent that has been associated with the pathogeneses of pneumonia, sepsis, and severe skin infections (Menzies and Kernodle, 1996; Wilke and Bubeck Wardenburg, 2010) and with biofilm formation (Caiazza and O'Toole, 2003). *S. aureus* biofilms also play a dominant role in the determination of disease severity and postoperative course (Singhal et al., 2011). Therefore, it is important to find means to inhibit biofilm formation and the virulent characteristics of *S. aureus*. For this purpose, novel and non-toxic compounds that prevent the development of drug tolerance are urgently required.

Semi-dried raw Pacific herring (*Clupea pallasi*), also known as Gwamegi (a Korean traditional food), is an important fishery product with a unique flavor, taste, and texture (Lee et al., 2002; Kang et al., 2011). Herring oil contains an abundance of two rare omega-3 polyunsaturated fatty acids (PUFAs), namely, docosahexaenoic acid (DHA; C22:6, ω-3) and eicosapentaenoic acid (EPA; C20:5, ω-3), which are commonly present at low concentrations in non-marine animals and are beneficial to the human body (Hirai et al., 1980; Schmidt and Dyerberg, 1994). Furthermore, it has been reported that two PUFAs act as bacteriocides on Gram-positive and Gram-negative bacteria, such as, *Helicobacter pylori* (Correia et al., 2012), *Burkholderia cenocepacia* (Mil-Homens et al., 2012), *S. aureus* (Desbois et al., 2009), *Fusobacterium nucleatum, Porphyromonas gingivalis*, and *Streptococcus mutans* (Huang and Ebersole, 2010; Sun et al., 2016, 2017). These two PUFAs have also been reported to possess significant anti-inflammatory, anti-tumorigenic (Bougnoux, 1999; Van Dyke, 2008), and antioxidant activities (Giordano and Visioli, 2014). Huang and Ebersole (2010), Sun et al. (2016, 2017) and Thibane et al. (2010) suggested that DHA and EPA could be considered as potential supplementary therapeutic agents due to their anti-biofilm activities on *Candida* species and periodontopathic bacteria. However, the abilities of DHA and EPA to inhibit biofilm formation and virulence production by *S. aureus* have not been assessed.

Therefore, the phenotypic effects of herring oil were studied and its active constituents were identified by gas chromatography-mass spectrometry (GC-MS). Two of its major constituents (DHA and EPA) were further investigated by confocal laser scanning microscopy (CSLM) and using a human blood assay to determine their effects on biofilm formation and toxin production by *S. aureus*. A *Caenorhabditis elegans* model was used to investigate the anti-virulent properties of herring oil, DHA, and EPA. qRT-PCR (quantitative real-time reverse transcription polymerase chain reaction) was used to investigate their effects on the transcriptional profiles of genes related to biofilm formation and virulence production *in vitro*.

MATERIALS AND METHODS

Ethics Statement

Human blood assays were authorized by the Ethical Committee of Yeungnam University (Gyeongsan, South Korea). The study was conducted according to the guidelines issued by the Ethical Committee of Yeungnam University. All blood donors provided written consent before blood collection.

Bacterial Strains, Materials, and Growth Assay

A methicillin-sensitive *S. aureus* strain (MSSA; ATCC 6538) and a methicillin-resistant *S. aureus* strain (MRSA; ATCC 33591) were used in the present study. All experiments were conducted at 37°C in Luria-Bertani (LB) broth for the MSSA strain and in LB broth containing 0.2% glucose for the MRSA strain. Herring (*Clupea pallasii*) oil was prepared from semi-dried fish bodies without organs (so called Gwamegi, Korean traditional food). Herring was dried at open air condition for 20 days in winter at Pohang, Korea. The semi-dried herring (764 g) was further dried in a freezing drier for 3 days to gain 586 g of dried herring. Then it was chopped, and the oil was extracted by soxhlet apparatus that was refluxed with n-hexane for a day at 70°C. After refluxing, the residual solution was collected and washed with 1% AcOH solution and brine to remove excess protein. Washed oil was dried over anhydrous $MgSO_4$ to gain clear yellow viscous oil (267 g, 45.6% yield). The omega fatty acids (*cis*-4,7,10,13,16,19-DHA, *cis*-5,8,11,14,17-EPA, *cis*-11-eicosenoic acid, and erucic acid), crystal violet, ethanol, ciprofloxacin, vancomycin and glucose were purchased from Sigma-Aldrich (St. Louis, MO, United States). For cell growth assays, optical densities were measured at 600 nm using a spectrophotometer (Optizen 2120UV, Mecasys, South Korea). To determine MIC (minimum inhibitory concentration), cells were inoculated into LB broth and cultured overnight at a dilution of 1:100 at 37°C, and then incubated for 24 h in the presence of a test substance. After sequential dilutions, cultures were spread on LB agar plates, incubated for 24 h at 37°C, and numbers of colonies were counted. Each experiment was performed using at least four independent cultures.

Gas Chromatograph/Mass Spectroscopy (GC-MS)

The chemical composition of air-dried herring oil was determined by GC using an Agilent 6890N GC and SP-2560 (Supelco, Sigma-Aldrich, St. Louis, MO, United States) fused silica capillary column (100 m × 0.25 mm i.d., film thickness 0.25 μm). Capillary column details, temperature conditions, and the derivatization (methylation) of fatty acids were as previously described (Lee et al., 2017). In brief, helium was used as the carrier at 0.75 ml/min and the GC injector was held at 225°C. The GC oven temperature was programmed as follows; 100°C for 4 min, increased to 240°C at 3°C/min, and followed by 15 min at 250°C. The split ratio was controlled at 200:1. Triundecanoin ($C_{11:00}$) was used as the internal standard and quantifications were performed by integrating areas and correcting for fatty acid

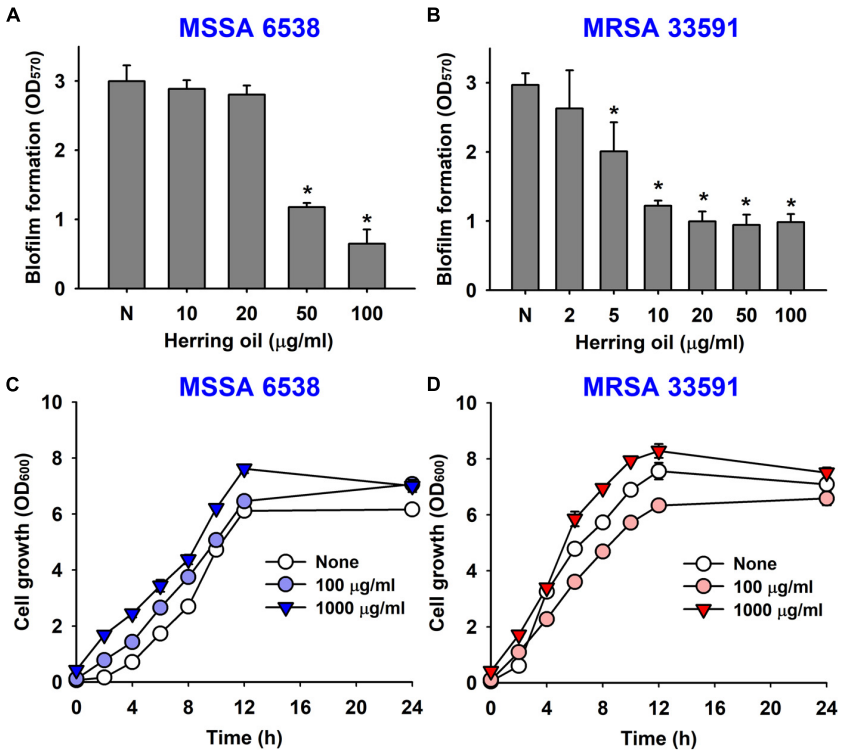

FIGURE 1 | Effects of herring oil on biofilm formation by *Staphylococcus aureus* strains and on their antimicrobial activities. *S. aureus* (MSSA 6538 or MRSA 33591) biofilm formations (OD_{570}) were quantified in the presence of herring oil for 24 h in 96-well polystyrene plates **(A,B)**. Planktonic cell growths (OD_{600}) of *S. aureus* cells (MSSA 6538 and MRSA 33591) were measured in the presence of herring oil in 250 ml flasks agitated at 250 rpm **(C,D)**. $*p < 0.05$ vs. non-treated controls.

methylation. Supelco 37 components FAME Mix (Supelco) were used as the reference standard.

Crystal-Violet Biofilm Assay

The two bacterial strains (MSSA 6538, MRSA 33591) were subjected to a static biofilm formation assay on 96-well polystyrene plates (SPL Life Sciences, South Korea), as previously described (Kim et al., 2015). Briefly, cells were inoculated into LB broth (300 μl) at an initial turbidity of 0.05 at 600 nm and herring oil, *cis*-11-eicosenoic acid, DHA, EPA, or erucic acid were added at different concentrations and incubated for 24 h without shaking at 37°C. To quantify biofilm formation, cell cultures were washed three times with water and then biofilms were stained with 0.1% crystal violet for 20 min. Biofilms were then dissolved in 300 μl of 95% ethanol and absorbances were measured at 570 nm (OD_{570}). For the biofilm dispersion assay, *S. aureus* was cultured in 96-well plates for 24 h without shaking at 37°C. Then, herring oil, DHA, or EPA was added to the cultures and incubated for another 10 h before the biofilm assay. Static biofilm formation results are the averages of four independent cultures of twelve replicate wells.

Confocal Laser Scanning Microscopy and COMSTAT Analysis

Static biofilm formation by *S. aureus* (MSSA 6538) in 96-well plates (without shaking) in the presence or absence of herring oil, DHA, or EPA were assessed by confocal laser scanning microscopy (Nikon Eclipse Ti, Tokyo, Japan). Cells were stained with carboxyfluorescein diacetate succinimidyl ester (Invitrogen, Molecular Probes Inc., Eugene, OR, United States), which stains viable cells in biofilms, as previously reported (Lee et al., 2016). Stained *S. aureus* ATCC 6538 biofilms were visualized by confocal laser scanning microscopy using an Ar laser (excitation wavelength 488 nm, and emission wavelength 500–550 nm) and a 20× objective. Color confocal images were constructed using NIS-Elements C version 3.2 (Nikon eclipse) under the same conditions. For each experiment, at least 10 random positions in two independent cultures were observed, and 20 planar images were analyzed per position. To quantify biofilm formation, COMSTAT biofilm software (Heydorn et al., 2000) was used to measure biovolumes (μm^3 per μm^2), mean thicknesses (μm), and substratum coverages (%). Thresholds were fixed for all image stacks, and at least 4 positions and 20 planar images were analyzed per position.

Hemolysis Assay

Human red blood cell hemolysis efficacies were assayed using whole cultures of *S. aureus*, as described previously (Lee et al., 2013; Tharmalingam et al., 2018). Briefly, *S. aureus* cells (MSSA 6538) were diluted 1:100 in LB broth (9×10^9 CFU/ml) with overnight culture and incubated with or without herring oil, DHA, or EPA for 20 h with shaking at 250 rpm. Separately,

human whole blood samples were centrifuged at 900g for 2 min and then washed three times with PBS and diluted in PBS (330 μl of red blood cells per 10 ml of PBS buffer). Bacterial culture (200 μl) was then added to 1 ml of diluted human red blood cells (3.3% in PBS). To determine hemolytic activities, mixtures of blood and *S. aureus* were incubated at 250 rpm for 2 h at 37°C. Supernatants were collected by centrifugation at 16,600 *g* for 10 min and optical densities were measured at 543 nm.

Whole Blood Bacterial Cell Killing Assay

The whole blood cell killing assay used was as previously described (Liu et al., 2008). Briefly, *S. aureus* (MSSA 6538) cells were inoculated (1:100 dilution, OD_{600} ~0.05) in LB broth with overnight culture and incubated at 37°C for 20 h with shaking at 250 rpm with herring oil, DHA, or EPA (1, 5, or 20 μg/ml) or DMSO (the negative control). Freshly drawn human whole blood (0.3 ml) was then mixed with the *S. aureus* cultures (0.1 ml), and mixtures were incubated at 37°C for 3 h with shaking at 250 rpm. *S. aureus* (MSSA 6538) survival was measured by counting CFUs on LB agar plates.

Caenorhabditis elegans Survival Assay

To investigate the effects of herring oil and unsaturated fatty acids on the virulence of *S. aureus* MSSA 6538, we used a nematode survival assay as previously described (Kim et al., 2016) with slight modification. In brief, *S. aureus* cells were incubated with or without herring oil, DHA, or EPA (2, 5, or 20 μg/ml) at 37°C for 24 h and synchronized adult *C. elegans fer-15;fem-1* nematodes were added into single wells of 96-well plate containing cultivated *S. aureus* cells. Approximately, 30 nematodes were allowed to feed on the cultured *S. aureus* MSSA 6538 at 25°C for 1 day.

For the cytotoxicity assay, 110 ± 10 nematodes were added into single well of 96-well plates containing M9 buffer and solutions of the compounds were added to final concentrations of 20 or 100 μg/ml at 25°C for 1 day. Then, nematodes were scored as alive or dead using an iRiS^{TM} Digital Cell Imaging System (Logos Bio Systems, South Korea). At least three independent experiments were conducted using quadruplicate wells.

RNA Isolation and qRT-PCR

Staphylococcus aureus MSSA 6538 cells were inoculated into 25 ml of LB broth at 37°C in 250 ml flasks at a starting OD_{600} of 0.05, and then incubated for 5 h with shaking at 250 rpm in the presence or absence of herring oil (100 μg/ml), DHA, or EPA (20 μg/ml). RNase inhibitor (RNAlater, Ambion, TX, United States) was then added and cells were immediately chilled for 30 s in dry ice bath having 95% ethanol to prevent RNA degradation. Cells were then harvested by centrifugation at 16,600 *g* for 1 min and total RNA was isolated using a Qiagen RNeasy mini Kit (Valencia, CA, United States).

Quantitative real-time reverse transcription polymerase chain reaction was used to investigate the transcriptional levels of 10 biofilm-related genes, that are, *agrA*, *arlR*, *arlS*, *aur*, *hla*, *icaA*, *nuc1*, *rbf*, *RNAIII*, *saeR*, *sarA*, *sarZ*, *seb*, *sigB*, and *spa* in *S. aureus* MSSA 6538 cells. Gene specific primers were used and 16s rRNA was used as the housekeeping control (Supplementary Table S1) to normalize the expressions of genes of interest. The qRT-PCR technique employed was an adaptation of a previously described method (Lee et al., 2016). qRT-PCR was performed using a SYBR Green master mix (Applied Biosystems, Foster City, CA, United States) and an ABI StepOne Real-Time PCR System (Applied Biosystems). Expression levels were determined using two independent cultures and six qRT-PCR reactions per gene.

Statistical Analysis

Values were expressed as means ± standard deviations, and data were analyzed by one-way ANOVA followed by Dunnett's test using SPSS version 23 (SPSS Inc., Chicago, IL, United States) to determine the significances of differences. Statistical significance was accepted for *p*-values of <0.05.

TABLE 1 | Herring oil – GC-MS analysis.

Lipid number	Fatty acid name	Composition (%)
C12:0	Lauric acid	0.13
C13:0	Tridecanoic acid	0.03
C14:0	**Myristic acid**	**5.78**
C14:1	Tetradecenoic	0.05
C15:0	Pentadecanoic acid	0.45
C16:0	**Palmitic acid**	**8.18**
C16:1	Palmitoleic acid	2.15
C17:0	Heptadecanoic acid	0.36
C17:1	*cis*-10-Heptadecenoic aid	0.05
C18:0	Stearic acid	1.35
C18:1n-9,trans	Elaidic acid	0.09
C18:1n-9,cis	Oleic acid	2.72
C18:2n-6,cis	Linoleic acid	1.11
C18:3n-6	γ-Linolenic acid	0.20
C20:1	***cis*-11-Eicosenoic acid**	**9.75**
C18:3n-3	α-Linolenic acid	1.23
C21:0	Heneicosanoic acid	0.22
C20:2n-6	Eicosadienoic acid	3.80
C22:0	Behenic acid	0.05
C20:3n-6	Dihomo-γ-Linolenic acid	0.07
C22:1n-9	**Erucic acid**	**17.49**
C20:3n-3	*cis*-11,14,17-Eicosatrienoic acid	0.1
C23:0	Tricosanoic acid	0.24
C22:2	Docosadienoic acid	0.91
C24:0	Lignoceric acid	0.02
C20:5n-3	***cis*-5,8,11,14,17-Eicosapentaenoic acid (EPA)**	**5.78**
C24:1	Nervonic acid	0.93
C22:6n-3	***cis*-4,7,10,13,16,19-Docosahexaenoic acid (DHA)**	**11.31**

Components present at levels >5% by weight are shown in blue/bold font.

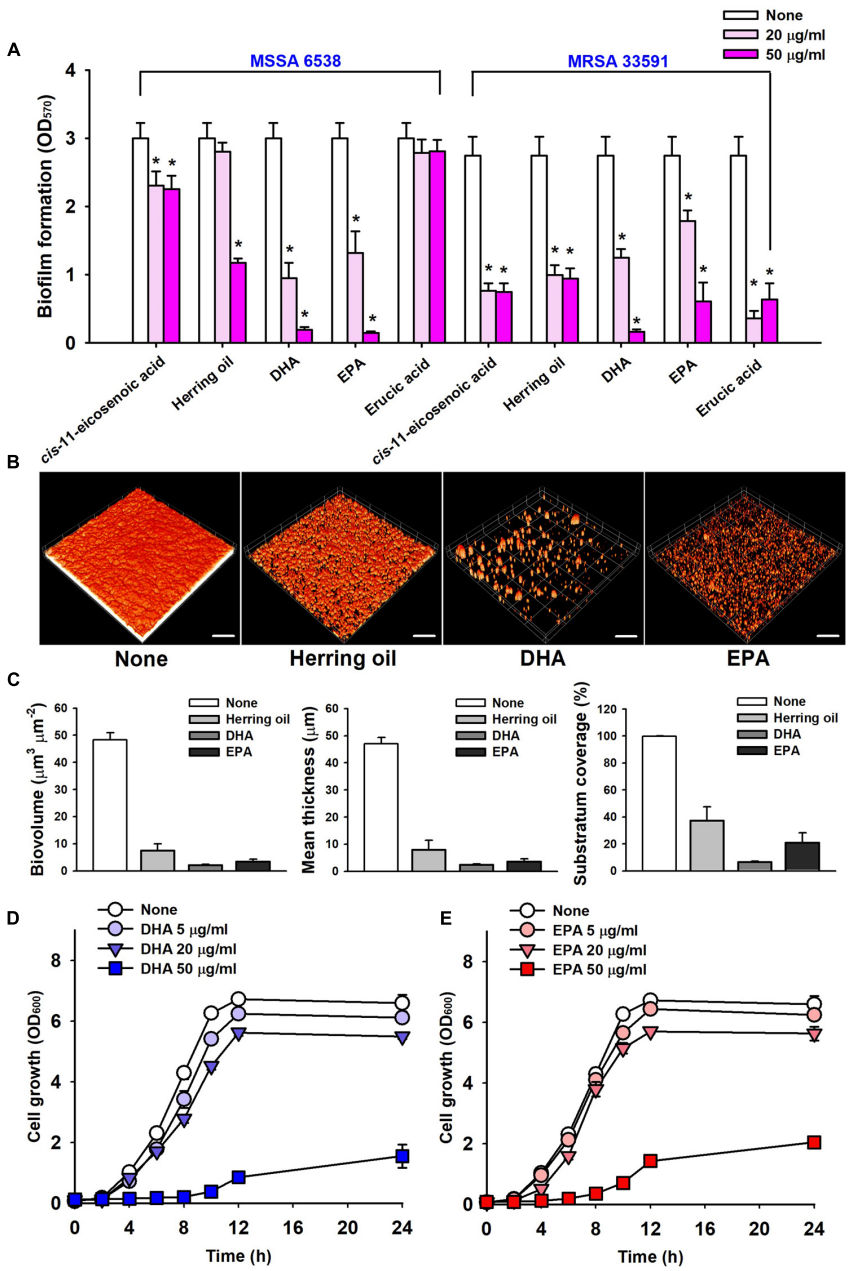

FIGURE 2 | Inhibitions of biofilm formation by herring oil, DHA, and EPA. Biofilm formations by the two *S. aureus* strains were quantified in the presence of *cis*-11-eicosenoic acid, herring oil, DHA, EPA, and erucic acid at 20 or 50 μg/ml after incubation for 24 h in 96-well polystyrene plates without agitation **(A)**. Biofilm formation of *S. aureus* MSSA 6538 was observed after 24 h in the presence of herring oil (50 μg/ml), DHA (20 μg/ml), or EPA (20 μg/ml) in 96-well plates by confocal laser scanning microscopy **(B)**. The scale bars represent 100 μm. Biofilm formation was analyzed using COMSTAT **(C)**. Cell growth of *S. aureus* MSSA 6538 was measured in the presence of DHA or EPA **(D,E)**. $^*p < 0.05$ vs. non-treated controls.

RESULTS AND DISCUSSION

Effect of Herring Oil on *S. aureus* Biofilm Formation

The anti-biofilm activity of herring oil was investigated against two *S. aureus* strains (MSSA 6538 and MRSA 33591) in 96-well polystyrene plates. The addition of herring oil at the beginning of bacterial culture dose-dependently inhibited *S. aureus* biofilm formation (**Figures 1A,B**). Specifically, herring oil at 100 μg/ml reduced biofilm formation by MSSA 6538 by >75%, whereas 20 μg/ml was required to inhibit biofilm formation by MRSA 33591 by >65%.

Herring oil did not decrease the growth of *S. aureus* strains (MSSA 6538 and MRSA 33591) at concentrations up

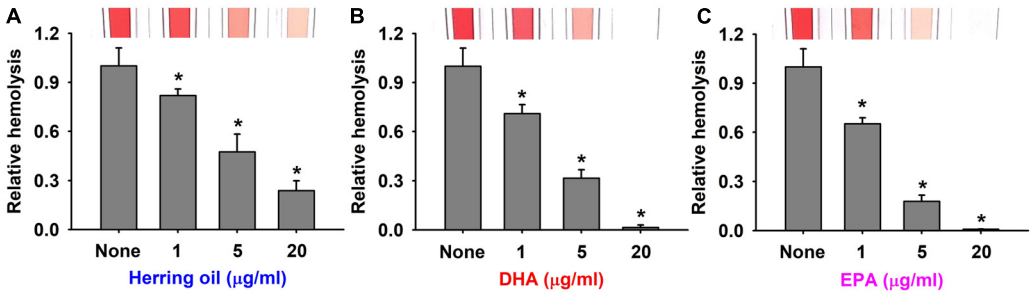

FIGURE 3 | Anti-hemolytic activities of herring oil, DHA, and EPA. Human red blood cell hemolysis by *S. aureus* was investigated in the presence of herring oil **(A)**, DHA **(B)**, or EPA **(C)** after culture for 20 h. The images show hemolysis activities in spectrophotometer cuvettes. *$p < 0.05$ vs. non-treated controls.

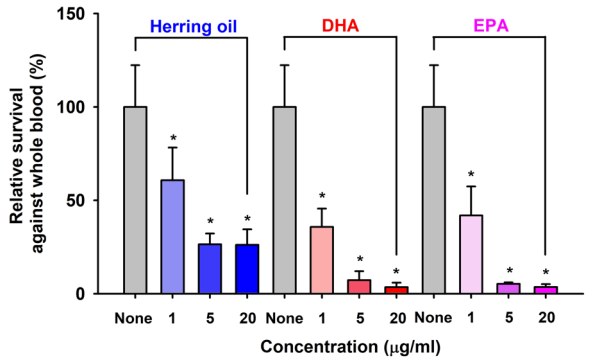

FIGURE 4 | Killing of *S. aureus* by whole blood cells in the presence of herring oil, DHA, or EPA. *S. aureus* cells were cultured in the presence of herring oil, DHA, or EPA at 1, 5, and 20 μg/ml for 20 h, then mixed with freshly drawn human whole blood and cultured for 3 h. Percent survival of *S. aureus* treated with or without the test compounds is represented. *$p < 0.05$ vs. non-treated controls.

to 1000 μg/ml (**Figures 1C,D**), and did not affect planktonic cell numbers of either *S. aureus* strain at concentrations up to 1000 μg/ml (data not shown). These findings show the anti-biofilm activity of herring oil was not due to any bactericidal effects.

Identification of Main Components in Herring Oil

Gas chromatography-mass spectrometry identified 28 fatty acids in herring oil (**Table 1**). Components that constituted more than 5% of herring oil were; erucic acid (17.49%), *cis*-4,7,10,13,16,19-DHA (11.31%), *cis*-11-eicosenoic acid (9.75%), palmitic acid (8.18%), myristic acid (5.78%), and *cis*-5,8,11,14,17-EPA (5.78%) (**Table 1**). The compositions of herring oil identified by GC-MS analysis concur with previous studies (Lambertsen and Braekkan, 1965). Previously, unsaturated fatty acids, such as, *cis*-11-eicosenoic acid and oleic acid showed strong anti-biofilm effect while saturated fatty acids (myristic acid and palmitic acid) did not have anti-biofilm activity against *S. aureus* (Lee et al., 2017). Therefore, this study was focused on the anti-biofilm activities of three unsaturated predominant omega fatty acids (DHA, EPA, and erucic acid).

Effect of DHA and EPA on Biofilm Formation by *S. aureus*

The anti-biofilm potencies of four major PUFAs (*cis*-11-eicosenoic acid, DHA, EPA, and erucic acid) were tested against the two *S. aureus* strains (MSSA 6538 and MRSA 33591) in 96-well plates. *cis*-11-Eicosenoic acid, DHA, and EPA at concentrations of 20 μg/ml significantly inhibited biofilm formation by both *S. aureus* strains (**Figure 2A**). DHA and EPA both inhibited biofilm formation by >90% at 50 μg/ml, which was greater than that previously reported for *cis*-11-eicosenoic acid (Lee et al., 2017). In this previous report, relationships between free fatty acids and bacterial biofilm formation were studied. In particular, oleic acid and *cis*-2-decenoic acid were found to suppress biofilm formation of *S. aureus* by blocking bacterial adhesion and dispersion from established biofilms, respectively (Stenz et al., 2008; Davies and Marques, 2009). In addition, it has been suggested that long chain unsaturated fatty acids like *cis*-11-eicosenoic acid (Lee et al., 2017) inhibit the biofilm forming ability of *S. aureus*. However, the present study is the first to report the anti-biofilm activities of DHA and EPA against *S. aureus*. The unsaturated fatty acid erucic acid, which was present in herring oil at high levels (**Table 1**), at 20 μg/ml inhibited biofilm formation by MRSA 33591 by >85%, but did not inhibit biofilm formation by MSSA 6538 (**Figure 2A**). However, higher concentrations of erucic acid at 500 and 1000 μg/ml significantly reduced biofilm formation of MSSA 6538 without affecting planktonic growth (data not shown). Hence, it appears that the effects of erucic acid are dose-dependent and strain dependent.

Confocal laser scanning microscopy was used to quantify biofilm formation by *S. aureus* in the presence of herring oil, DHA, or EPA. Fluorescent stacking 3D images indicated that herring oil (50 μg/ml), DHA (20 μg/ml), or EPA (20 μg/ml) markedly inhibited *S. aureus* biofilm formation (**Figure 2B**), and this, was confirmed by COMSTAT. More specifically, DHA, EPA, and herring oil reduced all three *S. aureus* MSSA 6538 parameters measured (biovolume, mean

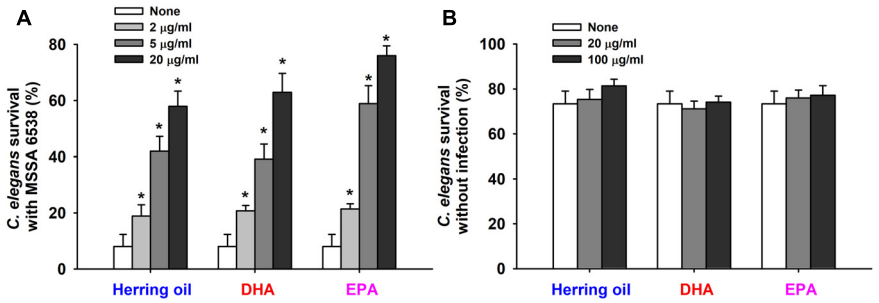

FIGURE 5 | Effects of herring oil, DHA, and EPA on nematode survival. *C. elegans fer-15;fem-1* strain survival after infection with *S. aureus* MSSA 6538 in the presence of DHA, EPA, or herring oil (2, 5, or 20 μg/ml) after exposure for 1 day at 25°C **(A)**. Herring oil, DHA, and EPA toxicities were assessed by determining survival rates versus non-infected nematodes **(B)**. Survival was assessed as dead or alive based on movement. $*p < 0.05$ versus non-treated controls.

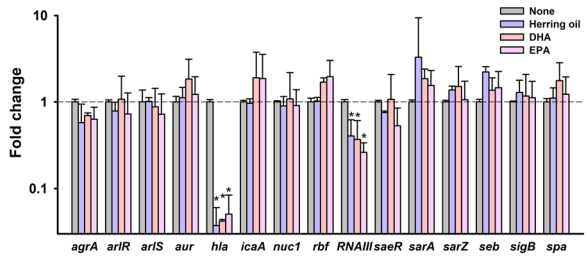

FIGURE 6 | Transcriptional profile changes in *S. aureus* after treatment with herring oil, DHA, or EPA. *S. aureus* MSSA 6538 was incubated in LB broth containing herring oil (100 μg/ml), DHA, or EPA (20 μg/ml) for 5 h with agitation at 250 rpm. Relative transcriptional profiles were determined by qRT-PCR with respect to 16s rRNA expression. qRT-PCR was performed in duplicate and fold-changes were calculated using treated versus untreated *S. aureus*. $*p < 0.05$ vs. non-treated controls.

thickness, and substratum coverage) (**Figure 2C**), actually, DHA and EPA reduced biomass and mean thickness by >90%, respectively. These results show herring oil, DHA, and EPA all effectively reduced biofilm formation on the bottom of 96-well plate.

Mature biofilm detachment by antibiotics, enzymes, and fatty acids is interest due to their resistance to antimicrobial agents (Flemming and Wingender, 2010; Gwisai et al., 2017; Lee et al., 2018). However, herring oil (1000 μg/ml), DHA (100 μg/ml), and EPA (100 μg/ml) could not disperse matured *S. aureus* ATCC 6538 biofilms (data not shown).

Anti-microbial Effects of DHA and EPA on *S. aureus*

The anti-microbial activities of DHA and EPA were evaluated by determining their minimum inhibitory concentrations (MICs) against *S. aureus* MSSA 6538 and MRSA 33591. Planktonic growth was completely inhibited by DHA and EPA at MICs (200 μg/ml), while MICs of ciprofloxacin and vancomycin are 0.5–1 μg/ml and 4 μg/ml, respectively, which concurs with previously reported values (Desbois and Lawlor, 2013; Gwisai et al., 2017). Notably, these MICs of DHA and EPA were 10 times higher than the concentration (20 μg/ml) required for anti-biofilm activities (**Figure 2A**).

Planktonic cell growths of *S. aureus* MSSA 6538 and MRSA 33591 in the presence of 5 μg/ml DHA or 20 μg/ml EPA were slightly inhibited (**Figures 2D,E**). However, the cell growths of both strains were more than 68% suppressed by DHA or EPA at 50 μg/ml, which indicates both DHA and EPA have anti-bacterial effects at relatively high concentrations (**Figures 2D,E**). These observations suggest DHA and EPA at low concentrations have anti-biofilm effects, but at higher levels these can also suppress the growth of planktonic cells.

Effects of Herring Oil, DHA, and EPA on Hemolysis by *S. aureus*

Staphylococcus aureus produces α-toxin, which is one of the most investigated *S. aureus* cytotoxins. α-Toxin integrates into the membranes of erythrocytes causing hemolysis (Bhakdi et al., 1984; Song et al., 1996), which contributes to biofilm formation (Caiazza and O'Toole, 2003). Thus, the effects of herring oil, DHA, and EPA on human red blood cell hemolysis by *S. aureus* were investigated. As a control, herring oil, DHA, and EPA without *S. aureus* cells did not show any hemolytic activity (data not shown). Interestingly, all three dose-dependently inhibited the hemolytic activity of *S. aureus* (**Figure 3**), and DHA and EPA at 20 μg/ml completely abolished its hemolytic activity, whereas herring oil at 20 μg/ml reduced its hemolytic activity by >75%. Also, herring oil, DHA, and EPA all significantly reduced the hemolytic activity by *S. aureus* even at 1 μg/ml, which is much lower than the concentrations required for anti-biofilm and antimicrobial activities.

These results support that the inhibitions of *S. aureus* biofilm formation by herring oil, DHA, and EPA are associated with the inhibition of hemolysis, and suggest that the genes related to biofilm formation and hemolysis might be responsible for these events. The present study is the first to report that herring oil, DHA, and EPA suppress the hemolysis of human red blood cells by *S. aureus*, which has important implications regarding the control of *S. aureus* virulence.

Effects of DHA, EPA, and Herring Oil on *S. aureus* Survival in the Presence of Human Whole Blood

Staphylococcus aureus characteristically exhibits resistance to phagocytes in humans and other animals, and thus, we used a survival test to investigate the effects of herring oil, DHA, and EPA on *S. aureus* survival in the presence of human whole blood. Herring oil, DHA, or EPA at 1, 5, or 20 μg/ml significantly reduced the survival of *S. aureus* exposed to fresh human whole blood (**Figure 4**), indicating that they weaken the ability of *S. aureus* to resist the human innate immune system.

Effects of DHA, EPA, and Herring Oil on *S. aureus* Virulence in the Nematode Model

Staphylococcus aureus colonizes and replicates in the digestive tract of *C. elegans* and has the ability to kill *C. elegans* by an infection-like process that exhibits remarkable overlap with that observed in mammals (Garsin et al., 2003). Hence, the effects of herring oil, DHA, and EPA on *S. aureus* virulence were investigated by analyzing *C. elegans* survival in the presence of *S. aureus*. Herring oil, DHA, and EPA were found to markedly prolong *C. elegans* survival in the presence of *S. aureus* (**Figure 5A**). For example, nematode survival was only ∼10% in the presence of untreated *S. aureus*, whereas in the presence of herring oil, DHA, or EPA at 20 μg/ml more than 55, 60, and 70%, respectively, of worms survived. In other words, the survival rate of *C. elegans* was increased more than seven and ninefold when worms were exposed to *S. aureus* in the presence of DHA or EPA at 20 μg/ml, respectively (**Figure 5A**). In addition, no toxic effects were observed when non-infected worms were exposed to herring oil, DHA, or EPA at concentrations up to 100 μg/ml (**Figure 5B**).

Transcriptional Changes Induced by DHA, EPA, and by Herring Oil in *S. aureus*

To investigate the molecular mechanisms underlying the inhibitory effects of herring oil, DHA, and EPA against *S. aureus*, expressions of selected biofilm- and virulence-related genes, and important regulatory genes were investigated in *S. aureus* cells by qRT-PCR. Herring oil, DHA, and EPA dramatically reduced the expression of α-hemolysin (*hla*) by 27-, 24-, and 20-fold, respectively (**Figure 6**). Also, herring oil, DHA, and EPA downregulated regulatory RNA molecule (*RNAIII*) that is present upstream of the *agr* operon while the expressions of other genes were not affected (**Figure 6**). It has been reported that RNAIII stimulate *hla* translation (Morfeldt et al., 1995). Hence, *hla* repression is partially due to the down-regulation of RNAIII by herring oil, DHA, and EPA.

α-Hemolysin is known to play a critical role in cell-to-cell interactions during biofilm formation (Caiazza and O'Toole, 2003; Anderson et al., 2012; Scherr et al., 2015). This reduction of α-hemolysin expression has been discovered in recently published articles showing that alizarin (Lee et al., 2016), azithromycin (Gui et al., 2014), flavonoids (Cho et al., 2015), norlichexanthone (Baldry et al., 2016), and stilbenoids (Lee et al., 2014) inhibit both biofilm formation and hemolysis by *S. aureus*. Our findings support that α-hemolysin has a positive relationship with biofilm formation in *S. aureus*. In addition, it has been shown *hla* is essential for *S. aureus* pathogenicity in a nematode model (Sifri et al., 2003, 2006). Notably, neither herring oil, DHA, or EPA significantly affected the expressions of the biofilm-related genes namely, *agrA*, *arlR*, *arlS*, *aur*, *icaA*, *nuc1*, *rbf*, *saeR*, *sarA*, *sarZ*, *seb*, *sigB*, or *spa*. Thus, the present study indicates that herring oil, DHA, and EPA attenuate *S. aureus* virulence, as evidenced by reductions in its anti-biofilm (**Figures 1**, **2**) and anti-hemolytic (**Figure 3**) activities, and partially by down-regulating the expression of the *hla* gene (**Figure 6**).

These results indicate that herring oil, DHA, and EPA could be used to treat *S. aureus* infections as lone drug or in combination with traditional antibiotics (**Figure 5**). Furthermore, because all three are considered intrinsically safe in animal, they could be used for medicinal purposes or for example, to surface treat in food processing facilities without undue restriction.

CONCLUSION

The DHA and EPA are long chain omega-3 fatty acids, which have major health benefits in man. More specifically, circulating levels of DHA and EPA are essential part of the body's defense system and play key roles in the inhibitions of inflammation and host immune responses (Calder, 2013). Herring oil was found to contain DHA and EPA at levels of 11.3 and 5.8% by weight, respectively, and inhibit biofilm formation and hemolysis by and the virulence of *S. aureus*. Interestingly, the ability of *S. aureus* to survive exposure to human whole blood was reduced in the presence of DHA or EPA, and exposure to DHA or EPA also increased infected nematode survival. These findings show for the first time that DHA and EPA suppress *S. aureus* biofilm formation and its virulence. Also, herring oil and its constituent omega-3 fatty acids (DHA and EPA) might be useful for the treatment and/or prevention of surface-associated biofilm formation by *S. aureus* (including MRSA strains) and for suppressing its virulence.

AUTHOR CONTRIBUTIONS

Y-GK, J-HL, CR, and SO performed the experiments and analyzed the data. Y-GK, J-HL, JP, and JL designed the study and wrote the paper. All authors read and approved the final manuscript.

FUNDING

This research was conducted under the industrial infrastructure program for fundamental technologies (N0000885) which is funded by the Ministry of Trade, Industry and Energy (MOTIE, South Korea). This research was also supported

by the Basic Science Research Program of a National Research Foundation of Korea (NRF) funded by the Korean Ministry of Education (2018R1D1A3B07040699 to J-HL) and (2017R1A6A3A01076089 to Y-GK), and a Priority Research Centers Program (#2014R1A6A1031189).

SUPPLEMENTARY MATERIAL

The Supplementary Material for this article can be found online at: https://www.frontiersin.org/articles/10.3389/fmicb.2018.01241/full#supplementary-material

REFERENCES

Anderson, M. J., Lin, Y. C., Gillman, A. N., Parks, P. J., Schlievert, P. M., and Peterson, M. L. (2012). Alpha-toxin promotes *Staphylococcus aureus* mucosal biofilm formation. *Front. Cell. Infect. Microbiol.* 2:64. doi: 10.3389/fcimb.2012.00064

Baldry, M., Nielsen, A., Bojer, M. S., Zhao, Y., Friberg, C., Ifrah, D., et al. (2016). Norlichexanthone reduces virulence gene expression and biofilm formation in *Staphylococcus aureus*. *PLoS One* 11:e0168305. doi: 10.1371/journal.pone.0168305

Bhakdi, S., Muhly, M., and Fussle, R. (1984). Correlation between toxin binding and hemolytic activity in membrane damage by staphylococcal alpha-toxin. *Infect. Immun.* 46, 318–323.

Bougnoux, P. (1999). n-3 polyunsaturated fatty acids and cancer. *Curr. Opin. Clin. Nutr. Metab. Care* 2, 121–126. doi: 10.1097/00075197-199903000-00005

Caiazza, N. C., and O'Toole, G. A. (2003). Alpha-toxin is required for biofilm formation by *Staphylococcus aureus*. *J. Bacteriol.* 185, 3214–3217. doi: 10.1128/JB.185.10.3214-3217.2003

Calder, P. C. (2013). Omega-3 polyunsaturated fatty acids and inflammatory processes: nutrition or pharmacology? *Br. J. Clin. Pharmacol.* 75, 645–662. doi: 10.1111/j.1365-2125.2012.04374.x

Chambers, H. F., and Deleo, F. R. (2009). Waves of resistance: *Staphylococcus aureus* in the antibiotic era. *Nat. Rev. Microbiol.* 7, 629–641. doi: 10.1038/nrmicro2200

Cho, H. S., Lee, J.-H., Cho, M. H., and Lee, J. (2015). Red wines and flavonoids diminish *Staphylococcus aureus* virulence with anti-biofilm and anti-hemolytic activities. *Biofouling* 31, 1–11. doi: 10.1080/08927014.2014.991319

Correia, M., Michel, V., Matos, A. A., Carvalho, P., Oliveira, M. J., Ferreira, R. M., et al. (2012). Docosahexaenoic acid inhibits *Helicobacter pylori* growth *in vitro* and mice gastric mucosa colonization. *PLoS One* 7:e35072. doi: 10.1371/journal.pone.0035072

Davies, D. G., and Marques, C. N. (2009). A fatty acid messenger is responsible for inducing dispersion in microbial biofilms. *J. Bacteriol.* 191, 1393–1403. doi: 10.1128/JB.01214-08

Desbois, A. P., and Lawlor, K. C. (2013). Antibacterial activity of long-chain polyunsaturated fatty acids against *Propionibacterium acnes* and *Staphylococcus aureus*. *Mar. Drugs.* 11, 4544–4557. doi: 10.3390/md11114544

Desbois, A. P., Mearns-Spragg, A., and Smith, V. J. (2009). A fatty acid from the diatom *Phaeodactylum tricornutum* is antibacterial against diverse bacteria including multi-resistant *Staphylococcus aureus* (MRSA). *Mar. Biotechnol.* 11, 45–52. doi: 10.1007/s10126-008-9118-5

Flemming, H. C., and Wingender, J. (2010). The biofilm matrix. *Nat. Rev. Microbiol.* 8, 623–633. doi: 10.1038/nrmicro2415

Garsin, D. A., Villanueva, J. M., Begun, J., Kim, D. H., Sifri, C. D., Calderwood, S. B., et al. (2003). Long-lived *C. elegans daf*-2 mutants are resistant to bacterial pathogens. *Science* 300, 1921–1921. doi: 10.1126/science.1080147

Giordano, E., and Visioli, F. (2014). Long-chain omega 3 fatty acids: molecular bases of potential antioxidant actions. *Prostaglandins Leukot. Essent. Fatty Acids* 90, 1–4. doi: 10.1016/j.plefa.2013.11.002

Gui, Z., Wang, H., Ding, T., Zhu, W., Zhuang, X., and Chu, W. (2014). Azithromycin reduces the production of alpha-hemolysin and biofilm formation in *Staphylococcus aureus*. *Indian J. Microbiol.* 54, 114–117. doi: 10.1007/s12088-013-0438-4

Gwisai, T., Hollingsworth, N. R., Cowles, S., Tharmalingam, N., Mylonakis, E., Fuchs, B. B., et al. (2017). Repurposing niclosamide as a versatile antimicrobial surface coating against device-associated, hospital-acquired bacterial infections. *Biomed. Mater.* 12:045010. doi: 10.1088/1748-605X/aa7105

Heydorn, A., Nielsen, A. T., Hentzer, M., Sternberg, C., Givskov, M., Ersboll, B. K., et al. (2000). Quantification of biofilm structures by the novel computer program COMSTAT. *Microbiology* 146, 2395–2407. doi: 10.1099/00221287-146-10-2395

Hirai, A., Hamazaki, T., Terano, T., Nishikawa, T., Tamura, Y., Kamugai, A., et al. (1980). Eicosapentaenoic acid and platelet function in Japanese. *Lancet* 2, 1132–1133. doi: 10.1016/S0140-6736(80)92558-1

Hoffman, L. R., D'Argenio, D. A., MacCoss, M. J., Zhang, Z., Jones, R. A., and Miller, S. I. (2005). Aminoglycoside antibiotics induce bacterial biofilm formation. *Nature* 436, 1171–1175. doi: 10.1038/nature03912

Huang, C. B., and Ebersole, J. L. (2010). A novel bioactivity of omega-3 polyunsaturated fatty acids and their ester derivatives. *Mol. Oral Microbiol.* 25, 75–80. doi: 10.1111/j.2041-1014.2009.00553.x

Kang, H.-S., Jeong, S.-W., Ko, J.-C., Jang, M., and Kim, J.-C. (2011). The quality characteristics of commercial gwamegi by product types. *J. Food Sci. Nutr.* 16, 253–260. doi: 10.3746/jfn.2011.16.3.253

Kim, Y.-G., Lee, J.-H., Gwon, G., Kim, S.-I., Park, J. G., and Lee, J. (2016). Essential oils and eugenols inhibit biofilm formation and the virulence of *Escherichia coli* O157:H7. *Sci. Rep.* 6:36377. doi: 10.1038/srep36377

Kim, Y.-G., Lee, J.-H., Kim, S.-I., Baek, K.-H., and Lee, J. (2015). Cinnamon bark oil and its components inhibit biofilm formation and toxin production. *Int. J. Food Microbiol.* 195, 30–39. doi: 10.1016/j.ijfoodmicro.2014.11.028

Lambertsen, G., and Braekkan, O. R. (1965). The fatty acid composition of herring oils. *Fiskeridirektoratets skrifter Ser. Teknol. Undersøkelser* 4, 13.

Lee, J.-H., Kim, Y.-G., and Lee, J. (2018). Thermostable xylanase inhibits and disassembles *Pseudomonas aeruginosa* biofilms. *Biofouling* 34, 346–356. doi: 10.1080/08927014.2018.1440551

Lee, J.-H., Kim, Y.-G., Park, J. G., and Lee, J. (2017). Supercritical fluid extracts of *Moringa oleifera* and their unsaturated fatty acid components inhibit biofilm formation by *Staphylococcus aureus*. *Food Control* 80, 74–82. doi: 10.1016/j.foodcont.2017.04.035

Lee, J.-H., Kim, Y.-G., Ryu, S. Y., and Lee, J. (2016). Calcium-chelating alizarin and other anthraquinones inhibit biofilm formation and the hemolytic activity of *Staphylococcus aureus*. *Sci. Rep.* 6:19267. doi: 10.1038/srep19267

Lee, J.-H., Park, J.-H., Cho, H. S., Joo, S. W., Cho, M. H., and Lee, J. (2013). Antibiofilm activities of quercetin and tannic acid against *Staphylococcus aureus*. *Biofouling* 29, 491–499. doi: 10.1080/08927014.2013.788692

Lee, K., Lee, J.-H., Ryu, S. Y., Cho, M. H., and Lee, J. (2014). Stilbenes reduce *Staphylococcus aureus* hemolysis, biofilm formation, and virulence. *Foodborne Pathog. Dis.* 11, 710–717. doi: 10.1089/fpd.2014.1758

Lee, J.-W., Cho, K.-H., Yook, H.-S., Jo, C., Kim, D.-H., and Byun, M.-W. (2002). The effect of gamma irradiation on the stability and hygienic quality of semi-dried pacific saury (*Cololabis seira*) flesh. *Radiat. Phys. Chem.* 64, 309–315. doi: 10.1016/S0969-806X(01)00675-2

Liu, C. I., Liu, G. Y., Song, Y., Yin, F., Hensler, M. E., Jeng, W. Y., et al. (2008). A cholesterol biosynthesis inhibitor blocks *Staphylococcus aureus* virulence. *Science* 319, 1391–1394. doi: 10.1126/science.1153018

Lowy, F. D. (1998). Staphylococcus aureus infections. *N. Engl. J. Med.* 339, 520–532. doi: 10.1056/NEJM199808203390806

Menzies, B. E., and Kernodle, D. S. (1996). Passive immunization with antiserum to a nontoxic alpha-toxin mutant from *Staphylococcus aureus* is protective in a murine model. *Infect. Immun.* 64, 1839–1841.

Mil-Homens, D., Bernardes, N., and Fialho, A. M. (2012). The antibacterial properties of docosahexaenoic omega-3 fatty acid against the cystic fibrosis multiresistant pathogen *Burkholderia cenocepacia*. *FEMS Microbiol. Lett.* 328, 61–69. doi: 10.1111/j.1574-6968.2011.02476.x

Morfeldt, E., Taylor, D., von Gabain, A., and Arvidson, S. (1995). Activation of alpha-toxin translation in *Staphylococcus aureus* by the trans-encoded antisense RNA. RNAIII. *EMBO J.* 14, 4569–4577.

Ohlsen, K., Koller, K. P., and Hacker, J. (1997). Analysis of expression of the alpha-toxin gene (hla) of *Staphylococcus aureus* by using a chromosomally encoded hla::lacZ gene fusion. *Infect. Immun.* 65, 3606–3614.

Otto, M. (2014). Staphylococcus aureus toxins. *Curr. Opin. Microbiol.* 17, 32–37. doi: 10.1016/j.mib.2013.11.004

Potera, C. (1999). Forging a link between biofilms and disease. *Science* 283, 1837–1839. doi: 10.1126/science.283.5409.1837

Scherr, T. D., Hanke, M. L., Huang, O., James, D. B., Horswill, A. R., Bayles, K. W., et al. (2015). Staphylococcus aureus biofilms induce macrophage dysfunction through leukocidin AB and alpha-toxin. *MBio* 6, e1021–e1015. doi: 10.1128/mBio.01021-15

Schmidt, E. B., and Dyerberg, J. (1994). Omega-3 fatty acids. Current status in cardiovascular medicine. *Drugs* 47, 405–424. doi: 10.2165/00003495-199447030-00003

Sifri, C. D., Baresch-Bernal, A., Calderwood, S. B., and von Eiff, C. (2006). Virulence of *Staphylococcus aureus* small colony variants in the *Caenorhabditis elegans* infection model. *Infect. Immun.* 74, 1091–1096. doi: 10.1128/IAI.74.2.1091-1096.2006

Sifri, C. D., Begun, J., Ausubel, F. M., and Calderwood, S. B. (2003). Caenorhabditis elegans as a model host for *Staphylococcus aureus* pathogenesis. *Infect. Immun.* 71, 2208–2217. doi: 10.1128/IAI.71.4.2208-2217.2003

Singhal, D., Foreman, A., Jervis-Bardy, J., and Wormald, P. J. (2011). *Staphylococcus aureus* biofilms: Nemesis of endoscopic sinus surgery. *Laryngoscope* 121, 1578–1583. doi: 10.1002/lary.21805

Song, L., Hobaugh, M. R., Shustak, C., Cheley, S., Bayley, H., and Gouaux, J. E. (1996). Structure of staphylococcal α-hemolysin, a heptameric transmembrane pore. *Science* 274, 1859–1866. doi: 10.1126/science.274.5294.1859

Speller, D. C., Johnson, A. P., James, D., Marples, R. R., Charlett, A., and George, R. C. (1997). Resistance to methicillin and other antibiotics in isolates of *Staphylococcus aureus* from blood and cerebrospinal fluid, England and Wales, 1989-95. *Lancet* 350, 323–325. doi: 10.1016/S0140-6736(97)12148-1

Stenz, L., Francois, P., Fischer, A., Huyghe, A., Tangomo, M., Hernandez, D., et al. (2008). Impact of oleic acid (cis-9-octadecenoic acid) on bacterial viability and biofilm production in *Staphylococcus aureus*. *FEMS Microbiol. Lett.* 287, 149–155. doi: 10.1111/j.1574-6968.2008.01316.x

Stewart, P. S., and Costerton, J. W. (2001). Antibiotic resistance of bacteria in biofilms. *Lancet* 358, 135–138. doi: 10.1016/S0140-6736(01)05321-1

Sun, M., Dong, J., Xia, Y., and Shu, R. (2017). Antibacterial activities of docosahexaenoic acid (DHA) and eicosapentaenoic acid (EPA) against planktonic and biofilm growing *Streptococcus mutans*. *Microb. Pathog.* 107, 212–218. doi: 10.1016/j.micpath.2017.03.040

Sun, M., Zhou, Z., Dong, J., Zhang, J., Xia, Y., and Shu, R. (2016). Antibacterial and antibiofilm activities of docosahexaenoic acid (DHA) and eicosapentaenoic acid (EPA) against periodontopathic bacteria. *Microb. Pathog.* 99, 196–203. doi: 10.1016/j.micpath.2016.08.025

Tharmalingam, N., Rajmuthiah, R., Kim, W., Fuchs, B. B., Jeyamani, E., Kelso, M. J., et al. (2018). Antibacterial properties of four novel hit compounds from a methicillin-resistant *Staphylococcus aureus-Caenorhabditis elegans* high-throughput screen. *Microb. Drug Resist.* doi: 10.1089/mdr.2017.0250 [Epub ahead of print].

Thibane, V. S., Kock, J. L., Ells, R., van Wyk, P. W., and Pohl, C. H. (2010). Effect of marine polyunsaturated fatty acids on biofilm formation of *Candida albicans* and *Candida dubliniensis*. *Mar. Drugs* 8, 2597–2604. doi: 10.3390/md8102597

Van Dyke, T. E. (2008). The management of inflammation in periodontal disease. *J. Periodontol.* 79, 1601–1608. doi: 10.1902/jop.2008.080173

Wilke, G. A., and Bubeck Wardenburg, J. (2010). Role of a disintegrin and metalloprotease 10 in *Staphylococcus aureus* α-hemolysin-mediated cellular injury. *Proc. Natl. Acad. Sci. U.S.A.* 107, 13473–13478. doi: 10.1073/pnas.1001815107

Conflict of Interest Statement: The authors declare that the research was conducted in the absence of any commercial or financial relationships that could be construed as a potential conflict of interest.

Copyright © 2018 Kim, Lee, Raorane, Oh, Park and Lee. This is an open-access article distributed under the terms of the Creative Commons Attribution License (CC BY). The use, distribution or reproduction in other forums is permitted, provided the original author(s) and the copyright owner are credited and that the original publication in this journal is cited, in accordance with accepted academic practice. No use, distribution or reproduction is permitted which does not comply with these terms.

frontiers in Microbiology

REVIEW
published: 02 July 2018
doi: 10.3389/fmicb.2018.01441

Nano-Strategies to Fight Multidrug Resistant Bacteria—"A Battle of the Titans"

Pedro V. Baptista[1], Matthew P. McCusker[2†], Andreia Carvalho[1], Daniela A. Ferreira[3], Niamh M. Mohan[3,4], Marta Martins[3]* and Alexandra R. Fernandes[1]**

[1] UCIBIO, Departamento de Ciências da Vida, Faculdade de Ciências e Tecnologia, Universidade Nova de Lisboa, Caparica, Portugal, [2] School of Food Science and Environmental Health, College of Sciences and Health, Dublin Institute of Technology, Dublin, Ireland, [3] Department of Microbiology, Moyne Institute of Preventive Medicine, Schools of Genetics and Microbiology, Trinity College Dublin, University of Dublin, Dublin, Ireland, [4] Nuritas Limited, Dublin, Ireland

OPEN ACCESS

Edited by:
Rebecca Thombre,
Pune University, India

Reviewed by:
Shahper Nazeer Khan,
Aligarh Muslim University, India
Rodolfo García-Contreras,
Universidad Nacional Autónoma de México, Mexico

***Correspondence:**
Pedro V. Baptista
pmvb@fct.unl.pt
Marta Martins
mmartins@tcd.ie
Alexandra R. Fernandes
ma.fernandes@fct.unl.pt

†Present Address:
Matthew P. McCusker,
Kerry Europe, Global Technology & Innovation Centre, Naas, Ireland

Specialty section:
This article was submitted to Antimicrobials, Resistance and Chemotherapy, a section of the journal Frontiers in Microbiology

Received: 31 March 2018
Accepted: 11 June 2018
Published: 02 July 2018

Citation:
Baptista PV, McCusker MP, Carvalho A, Ferreira DA, Mohan NM, Martins M and Fernandes AR (2018) Nano-Strategies to Fight Multidrug Resistant Bacteria—"A Battle of the Titans". Front. Microbiol. 9:1441. doi: 10.3389/fmicb.2018.01441

Infectious diseases remain one of the leading causes of morbidity and mortality worldwide. The WHO and CDC have expressed serious concern regarding the continued increase in the development of multidrug resistance among bacteria. Therefore, the antibiotic resistance crisis is one of the most pressing issues in global public health. Associated with the rise in antibiotic resistance is the lack of new antimicrobials. This has triggered initiatives worldwide to develop novel and more effective antimicrobial compounds as well as to develop novel delivery and targeting strategies. Bacteria have developed many ways by which they become resistant to antimicrobials. Among those are enzyme inactivation, decreased cell permeability, target protection, target overproduction, altered target site/enzyme, increased efflux due to over-expression of efflux pumps, among others. Other more complex phenotypes, such as biofilm formation and quorum sensing do not appear as a result of the exposure of bacteria to antibiotics although, it is known that biofilm formation can be induced by antibiotics. These phenotypes are related to tolerance to antibiotics in bacteria. Different strategies, such as the use of nanostructured materials, are being developed to overcome these and other types of resistance. Nanostructured materials can be used to convey antimicrobials, to assist in the delivery of novel drugs or ultimately, possess antimicrobial activity by themselves. Additionally, nanoparticles (e.g., metallic, organic, carbon nanotubes, etc.) may circumvent drug resistance mechanisms in bacteria and, associated with their antimicrobial potential, inhibit biofilm formation or other important processes. Other strategies, including the combined use of plant-based antimicrobials and nanoparticles to overcome toxicity issues, are also being investigated. Coupling nanoparticles and natural-based antimicrobials (or other repurposed compounds) to inhibit the activity of bacterial efflux pumps; formation of biofilms; interference of quorum sensing; and possibly plasmid curing, are just some of the strategies to combat multidrug resistant bacteria. However,

the use of nanoparticles still presents a challenge to therapy and much more research is needed in order to overcome this. In this review, we will summarize the current research on nanoparticles and other nanomaterials and how these are or can be applied in the future to fight multidrug resistant bacteria.

Keywords: antimicrobial resistance, multidrug resistance, nanomaterials, nanoparticles, plant-based compounds, novel antimicrobial agents, nanotheranostics

INTRODUCTION

Multidrug resistant (MDR) bacteria remain the greatest challenge in public health care. The numbers of infections produced by such resistant strains are increasing globally. This acquired resistance of pathogens presents a key challenge for many antimicrobial drugs. Recent advances in nanotechnology offer new prospects to develop novel formulations based on distinct types of nanoparticles (NPs) with different sizes and shapes and flexible antimicrobial properties.

NPs may offer a promising solution as they can not only combat bacteria themselves but can also act as carriers for antibiotics and natural antimicrobial compounds (Wang et al., 2017a). While various materials have been explored from liposomal to polymer based nano-drug carriers, metallic vectors, such as gold NPs, are attractive as core materials due to their essentially inert and nontoxic nature (Burygin et al., 2009). Arguably the most attractive aspect of NPs drug delivery systems is their ability to introduce a wide range of therapeutics, either bound to their large surface area or contained within the structure, to the site of infection effectively and safely by having a controlled rate of targeted delivery (Pissuwan et al., 2011; Gholipourmalekabadi et al., 2017). By improving the pharmacokinetic profile and therapeutic index of encapsulated drugs compared to free drug equivalents, the dose required to achieve clinical effects can be dramatically decreased (Gao et al., 2018). This in turn, can reduce the toxicity and the adverse side effects associated with high systemic drug concentrations and frequent dosing (Liu et al., 2009).

This review covers the latest approaches in the development of new nanobiotechnology approaches that may challenge the medical practice to fight bacteria and particularly MDR bacteria.

NANOMATERIALS AGAINST BACTERIA

Nanomaterials have at least one dimension in the nanometer scale range (1–100 nm) that convey particular physical and chemical properties considerably different from those of bulk materials (Wang et al., 2017a). Among the wide range of nanomaterials, particular interest has been directed toward NPs. NPs have a number of features, which make them favorable as vectors for drugs to combat disease-causing pathogens. These include their enhancement of drug solubility and stability (Huh and Kwon, 2011); their ease of synthesis (Gholipourmalekabadi et al., 2017); their biocompatibility with target agents; and their modulated release, which can be controlled by stimuli, such as light, pH and heat (Wang Z. et al., 2017). Their distinctive functionality in drug delivery is achieved by their ultra-small size and vast surface to volume ratios. This is a key competitive advantage over conventional therapies in the treatment of infections caused by intracellular pathogens and MDR strains. Their functionalization with different (bio)molecules is another important feature. These comprise NPs containing Ag, Au, Al, Cu, Ce, Cd, Mg, Ni, Se, Pd, Ti, Zn, and super-paramagnetic Fe (Hemeg, 2017; Slavin et al., 2017). AgNPs are considered the most effective nanomaterial against bacteria but other metallic NPs, such as CuONPs, TiONPs, AuNPs, and Fe_3O_2NPs, have also demonstrated bactericidal effects (Dakal et al., 2016; Hemeg, 2017; Slavin et al., 2017).

While poor membrane transport limits the potency of many antibiotics (Andrade et al., 2013), drug loaded NPs vehicles can enter host cells *via* endocytosis, facilitating their intracellular entry (Wang Z. et al., 2017). Membrane penetration can also be achieved through interactions with surface lipids, for example, using gold NPs in the co-administration of protein-based drugs (Huang et al., 2010). The therapeutic appeal of NPs is enhanced by their ability to confer physical protection against bacterial resistance mechanisms (Huh and Kwon, 2011). Furthermore, the potential to load multiple drug combinations into NPs presents a highly complex antimicrobial mechanism of action, to which, bacteria are unlikely to develop resistance (Huh and Kwon, 2011). Although, this is usually believed to be the case, there are some studies reporting development of bacterial resistance against silver NPs (Panáček et al., 2018). There is also evidence that exposure of bacteria to this type of NPs may increase its antibiotic tolerance (Kaweeteerawat et al., 2017).

NPs can exert their antibacterial activity *via* a multitude of mechanisms, such as: (1) direct interaction with the bacterial cell wall; (2) inhibition of biofilm formation; (3) triggering of innate as well as adaptive host immune responses; (4) generation of reactive oxygen species (ROS); and (5) induction of intracellular effects (*e.g.*, interactions with DNA and/or proteins). Because they do not present the same mechanisms of action of standard antibiotics (**Figure 1**), they can be of extreme use against MDR bacteria (Singh K. et al., 2014; Aderibigbe, 2017; AlMatar et al., 2017; Hemeg, 2017; Natan and Banin, 2017; Rai et al., 2017; Slavin et al., 2017; Zaidi et al., 2017; Bassegoda et al., 2018; Katva et al., 2018; Siddiqi et al., 2018).

Besides the broad-spectrum antibacterial properties that NPs have against Gram-positive and -negative bacteria, NPs have been used as vectors for the delivery of antimicrobial moieties that greatly improve their biocidal properties (Beyth et al., 2015; Rai A. et al., 2016; Singh J. et al., 2016; Esmaeillou et al.,

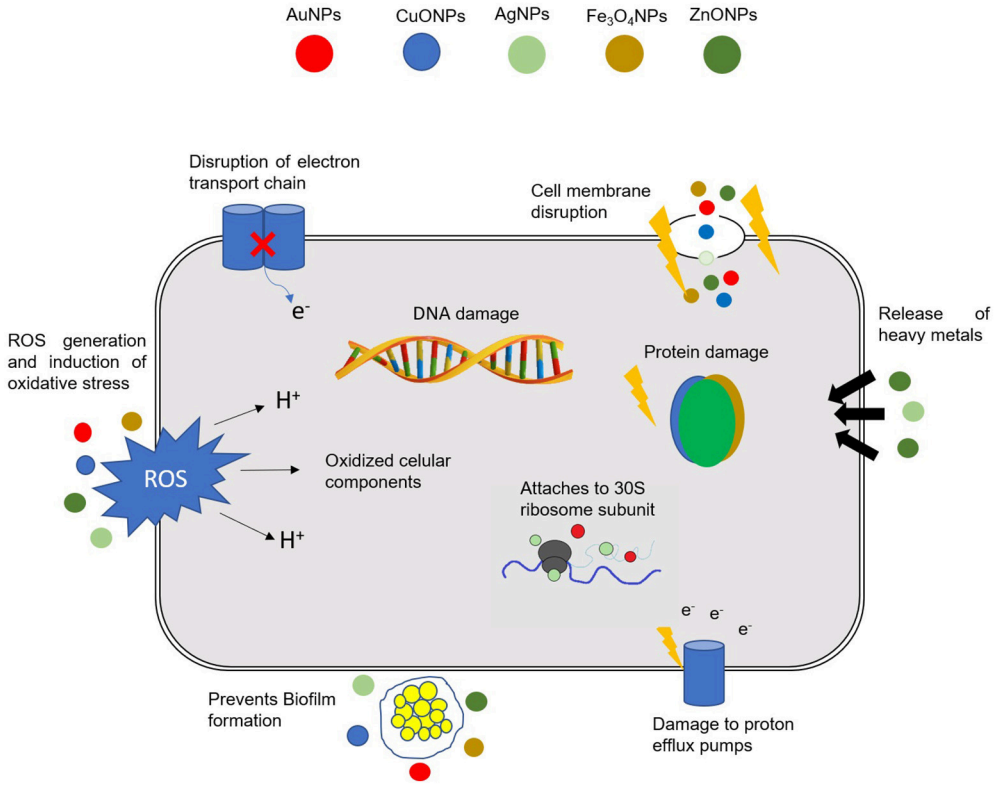

FIGURE 1 | Different mechanisms of action of NPs in bacterial cells. The combination in a single nanomaterial of a multitude of cellular effects may have a tremendous impact in fighting MDR bacteria. DNA, deoxyribonucleic acid; ROS, Reactive oxygen species; AuNPs, gold NPs; CuONPs, Copper oxide NPs; AgNPs, silver NPs; Fe_3O_4NPs, iron oxide NPs; ZnONPs, zinc oxide NPs.

2017; Wang et al., 2017a; Zaidi et al., 2017; Hadiya et al., 2018). Some of the advantages of using NPs as vectors are due to their small and controllable size; their protective action against enzymes that would otherwise destroy antimicrobial compounds; their ability to actively deliver antibiotics; and their capability to combine several therapeutic modalities onto a single nanomaterial (*e.g.*, several antibiotics/compounds onto the same NPs for combined action; combining silencing agents and drugs, etc.) (Turos et al., 2007; Huh and Kwon, 2011; Mohammed Fayaz et al., 2011; Liu et al., 2013; Qi et al., 2013; Li et al., 2014; Ranghar et al., 2014; Thomas et al., 2014; Wang et al., 2014; Payne et al., 2016; Rai A. et al., 2016; Singh J. et al., 2016; Yeom et al., 2016; Esmaeillou et al., 2017; Zaidi et al., 2017; Zong et al., 2017; Hadiya et al., 2018).

NPs carriers can tackle bacterial threats "passively," through prolonged drug retention at the specific infection site, or "actively," through surface conjugation with active molecules that bind a certain target (Wang Z. et al., 2017). The balance between the surface modification interaction strength, the compound release rate and the stability of the conjugate should be carefully considered for the design of an effective "active" delivery strategy (Burygin et al., 2009; Pissuwan et al., 2011). In an attempt to overcome their therapeutic limitations, various research groups have investigated the conjugation of antibiotics to NPs (Tiwari et al., 2011). For example, Saha et al. describe the direct conjugation of ampicillin, streptomycin and kanamycin to gold NPs (Saha et al., 2007). The resulting complexes were shown to have lower minimum inhibitory concentration (MIC) than the free drug counterparts against both Gram -negative and -positive bacteria. While the detailed mechanism of these effects are not explained by the authors in the above case, Fayaz et al. has attempted to uncover how their vancomycin functionalized gold NPs demonstrated activity against strains which are usually vancomycin resistant based either on mutations (vancomycin resistant *Staphylococcus aureus*), or membrane structure (*Escherichia coli*) (Mohammed Fayaz et al., 2011). They propose that only when the antibiotic was complexed with the NPs could this result in nonspecific, multivalent interactions and anchoring of the carrier to the cell wall synthesis proteins. Based on the presence of pits in the cells, which was observed using transmission electron microscopy, the authors concluded that the consequence of the non-specific binding was compromised membrane integrity, and subsequent cell death (Mohammed Fayaz et al., 2011; Gao et al., 2018).

ANTIBACTERIAL MECHANISM OF NPS

The antibacterial activity of NPs against MDR bacteria and biofilms depends on a number of factors, namely, their large

surface area in contact with bacteria through electrostatic attraction, van der walls forces or hydrophobic interactions; on the nanoparticle size and stability; together with the drug concentration (Chen et al., 2014; Gao et al., 2014; Li et al., 2015). The interaction of NPs with bacteria generally triggers oxidative stress mechanisms, enzymatic inhibition, protein deactivation and changes in gene expression. Still, the most common antibacterial mechanisms are related to oxidative stress, metal ion release, and non-oxidative mechanisms (Wang et al., 2017a; Zaidi et al., 2017 see **Figure 1**).

Oxidative stress induced by ROS is one of the most important mechanisms assisting the antibacterial activity of NPs (Dwivedi et al., 2014; Rudramurthy et al., 2016). ROS are natural byproducts of cellular oxidative metabolism and have significant important roles in the modulation of cell survival and death, differentiation and cell signaling. In bacteria, ROS are formed from aerobic respiration, and their production is balanced by the cell antioxidant machinery but upon an additional ROS insult, oxidation of biomolecules, and cell components result in severe cellular damage (Li et al., 2012b). The excessive production of ROS leads to a disturbed redox homeostasis resulting in oxidative stress, affecting membrane lipids and altering the structure of DNA and proteins (Dwivedi et al., 2014). It has been shown that while O_2^- and H_2O_2 can be neutralized by endogenous antioxidants, ·OH and singlet oxygen ($^1[O_2]$) lead to acute microbial death (Zaidi et al., 2017). Different NPs may generate distinctive ROS, such as superoxide (O_2^-) or hydroxyl radical (·OH), hydrogen peroxide (H_2O_2), and $^1[O_2]$) (Wang et al., 2017a). In this manner, the level of ROS generated by NPs is dependent on the chemical nature of the NPs themselves. Application of metallic NPs is currently being considered to overcome bacterial infections since they have shown antimicrobial efficacy due to their high surface-to-volume ratio. An increase ratio is usually accompanied by increased production of ROS, including free radicals. Zhang et al. (2013) demonstrated that ROS generation and metal ion release significantly enhanced the antibacterial activity through uncoated AuNPs in aqueous suspension under UV irradiation (365 nm). Umamaheswari (Umamaheswari et al., 2014) demonstrated that the antibacterial activity of AuNPs against *E. coli*, *Salmonella* Typhi, *Pseudomonas aeruginosa* and *Klebsiella pneumoniae* were due to oxidative stress caused by increased intracellular ROS. A recent study (Zhang et al., 2013) evaluated AuNPs and AuNPs -laser combined therapy against *C. pseudotuberculosis* and suggested that the mechanism of action is related with ROS production, that causes an increase of oxidative stress of microbial cells in the form of vacuole formation as an indication of potent activity. This effect was higher with AuNPs-laser, causing a rapid loss of bacterial cell membrane integrity due to the fact that laser light enhances at least one fold antimicrobial activity of AuNPs. Several other studies have addressed the role of metal NPs to induce MDR bacteria death *via* oxidative stress (**Table 1**) (Foster et al., 2011; Li et al., 2012b; Rai et al., 2012; Zhang et al., 2013; Reddy L. S. et al., 2014; Singh R. et al., 2014; Pan et al., 2016; Courtney et al., 2017; Ulloa-Ogaz et al., 2017; Zaidi et al., 2017). Indeed, titanium dioxide NPs were shown to adhere to the surface of the bacterial cell and trigger the production of ROS, which in turns lead to damage of the structure of cellular components and consequent cell death (Foster et al., 2011). In another important study using different metal NPs, AgNPs were shown to generate superoxide radicals and hydroxyl radicals, whereas Au, Ni, and Si NPs generated only singlet oxygen, which upon entering the cell produced an antibacterial effect (Zhang et al., 2013). More recently, Reddy and co-workers demonstrated that ZnONPs alone can also act as an effective antibacterial agent *via* the generation of ROS (Reddy L. S. et al., 2014). Exposure to UV irradiation may also potentiate the action of NPs. Li et al. (2012b) reported the augmented antibacterial effects of zinc oxide (ZnO) and titanium oxide (TiO) NPs triggered by UV irradiation as the results of the increased production of superoxide, hydroxyl and singlet oxygen radicals that potentiated bacteria mortality by severe oxidative stress. Graphene oxide–iron oxide NPs have also demonstrated maximum antibacterial activity due to the generation of hydroxyl radicals and diffusion into bacterial cells (Pan et al., 2016). More recently, Ulloa-Ogaz and collaborators demonstrated that copper oxide NPs interact with bacteria, generating an intracellular signaling cascade that trigger oxidative stress and, thus, an antibacterial effect (Ulloa-Ogaz et al., 2017).

Metal oxides slowly release metal ions that are up taken by the cell, reaching the intracellular compartment where they can interact with functional groups of proteins and nucleic acids, such as amino (–NH), mercapto (–SH), and carboxyl (–COOH) groups (Wang et al., 2017a). This interaction alters the cell structure, hampers enzymatic activity and interferes with the normal physiological processes in the bacterial cell. It has been shown that copper oxide (CuO) NPs cause a significant alteration of the expression of key proteins and may inhibit denitrification. Proteomic analysis showed that CuONPs cause an alteration of proteins involved in nitrogen metabolism, electron transfer and transport (Su et al., 2015). Also, the interaction of gold–superparamagnetic iron oxide NPs with bacterial proteins *via* disulfide bonds affects the metabolism and redox system of bacterial cells (Niemirowicz et al., 2014). NPs may also enter bacteria through absorption, releasing metal ions to the surrounding medium and/or binding to the negatively charged functional groups of the bacterial cell membrane. For example, silver ions (from silver NPs) are adsorbed on the cell membrane, leading to protein coagulation (Jung et al., 2008). Jankauskaitl and collaborators described the bactericidal effect of graphene oxide/Cu/Ag NPs against *E. coli*, *P. aeruginosa*, *K. pneumoniae*, *S. aureus,* and Methicillin-resistant *S. aureus* (MRSA) through a possible synergy between multiple toxic mechanisms (Jankauskaite et al., 2016).

Non-oxidative mechanisms involve interaction of the NPs with the cell wall. In bacteria, the cell wall and membrane behave as defensive barriers that protect against environmental insults. Cell membrane components provide different adsorption pathways for the NPs (Lesniak et al., 2013). The cell wall of Gram-negative bacteria is composed of lipoproteins, phospholipids and lipid polysaccharides (LPS), which form a barrier only allowing the entry of certain macromolecules (Zaidi et al., 2017). In Gram-positive bacteria, the cell wall is composed of a thin layer of

TABLE 1 | Nanoparticles against MDR pathogens and their mechanisms of action.

Type of nanoparticles	Targeted bacteria	Antibiotic resistance type	Mechanisms of antibacterial action	References
AgNPs	*Enterococcus faecalis, S. aureus*	Vancomycin-resistant	Combination with vancomycin. Bacterial cell death.	Saeb et al., 2014; Esmaeillou et al., 2017
	Enterococcus		On-going investigations.	Percival et al., 2007
	S. aureus	Methicillin-resistant	Combination with antibiotics.	Brown et al., 2012; Saeb et al., 2014; Esmaeillou et al., 2017
			Physical adhesion to the bacterial cell.	Su et al., 2011
			On-going investigations.	Percival et al., 2007
	E. coli, P. aeruginosa	Ampicillin- resistant	Combination with ampicillin leads to entry into the bacterial cell. Inhibition of cell wall synthesis, protein synthesis and nucleic acid synthesis.	Lara et al., 2010; Brown et al., 2012
	S. aureus, E. coli, P. aeruginosa, K. pneumoniae, E. faecalis, Salmonella Typhimurium, *Bacillus cereus*	Erythromycin-resistant	Cell surface damage and loss of the chain integrity.	Otari et al., 2013
	S. pneumoniae	Teicoplanin-resistant	ROS generation, cellular uptake of silver ions, cascade of intracellular reaction.	Thapa et al., 2017
	E. coli, S. aureus	Ampicillin- resistant		
	E. coli, S. aureus	Tetracycline-resistant	Combination with tetracycline.	Djafari et al., 2016
	P. aeruginosa	Ofloxacin-resistant	Evade multidrug efflux pumps.	Ding et al., 2018
	P. aeruginosa, MRSA, VRE, *Serratia marcescens*	Biofilm formation	Ongoing investigations.	Percival et al., 2007
	Enterobacter cloacae, S. mutans		ROS production and membrane disruption.	Kulshrestha et al., 2017
	S. epidermidis, S. aureus		Penetration in the bacterial biofilm using an external magnetic field.	Mahmoudi and Serpooshan, 2012
	E. coli	MDR	ROS generation.	Zhang et al., 2013; Siddiqi et al., 2018
	E. coli, P. aeruginosa			Ramalingam et al., 2016
	S. aureus, Enterococcus spp., *P. aeruginosa, A. baumannii, Enterobacteriaceae*		Interaction with components of the cells where chemical and physical properties are modified.	Cavassin et al., 2015
	E. coli			Lok et al., 2007
	S. aureus, E. coli, P. aeruginosa, K. pneumoniae, B. subtilis		Penetration in the bacterial cell wall.	Acharya et al., 2018
	P. aeruginosa		Combined therapy, using blue light.	El Din et al., 2016
	E. coli, Pseudomonas fluorescens, Pseudomonas putida, P. aeruginosa, B. subtilis, S. aureus		Disruption of the bacterial cell wall.	Bondarenko et al., 2013

(Continued)

TABLE 1 | Continued

Type of nanoparticles	Targeted bacteria	Antibiotic resistance type	Mechanisms of antibacterial action	References
	A. baumannii		Attach to the cell wall leading to structural changes in the permeability of the cell membrane.	Chang et al., 2017
	P. aeruginosa			Singh K. et al., 2014; Salomoni et al., 2017
	S. aureus, E. coli			Jung et al., 2008; Muniyan et al., 2017
	P. aeruginosa, E. coli		Combination with antibiotics.	Esmaeillou et al., 2017
	E. coli			Karimi et al., 2016
	E. faecalis			Katva et al., 2018
	Salmonella Typhimurium			McShan et al., 2015
	Enterobacteriaceae			Panáček et al., 2016b
	S. aureus, P. aeruginosa, E. coli			Panáček et al., 2016a
	S. aureus, E. coli		Upregulation of the expression of antioxidant genes and ATP pumps.	Nagy et al., 2011
	S. epidermidis	MDR/Biofilm formation	Conjugation with AMP.	Jaiswal et al., 2015
	Mycobacterium smegmatis			Mohanty et al., 2013
	Vibrio fluvialis, P. aeruginosa			Lambadi et al., 2015
	B. subtilis, E. coli			Liu et al., 2013
	E. coli			Pal et al., 2016
	E. coli, Acinetobacter calcoaceticus, Aeromonas bestiarum, B. Subtili, P. fluorescens, Kocuria rhizophila, Micrococcus luteus			Ruden et al., 2009
AuNPs	*S. aureus*	Vancomycin-resistant	Combination with vancomycin.	Mohammed Fayaz et al., 2011
	E. faecalis			Lai et al., 2015
	S. aureus	Methicillin-resistant	Photothermal therapy with ROS generation.	Kuo et al., 2009; Millenbaugh et al., 2015; Mocan et al., 2016; Hu et al., 2017; Ocsoy et al., 2017
			Combination with vancomycin.	Lai et al., 2015
	E. coli, K. pneumoniae	Cefotaxime-resistant	Disruption of the bacterial cell wall, DNA damage.	Shaikh et al., 2017
	S. aureus, E. coli, P. aeruginosa, Enterobacter aerogenes	Ampicillin-resistant	Combination with ampicillin. Lead to entry into the bacterial cell.	Brown et al., 2012
	Streptococcus bovis, S. epidermidis, E. Aerogenes	Kanamycin-resistant	Disruption of the bacterial cell wall.	Payne et al., 2016
	K. 45ellular45, Proteus mirabilis, A. baumannii	Carbapenems-resistant	Disturb of osmotic balance and disrupt the integrity of cell bacterial cell wall.	Shaker and Shaaban, 2017
	P. aeruginosa	Biofilm formation	Interaction with cell surface.	Yu et al., 2016
	S. aureus		Laser excitation of the near IR LSPR lead to an efficient photothermal response with efficient killing of bacteria biofilms.	Pallavicini et al., 2014

(Continued)

TABLE 1 | Continued

Type of nanoparticles	Targeted bacteria	Antibiotic resistance type	Mechanisms of antibacterial action	References
	E. coli, P. aeruginosa, S. aureus		Penetration through biofilm layers and interaction with cellular components.	Ramasamy et al., 2017a,b
	S. epidermidis, S. haemolyticus		Combination with antibiotics.	Roshmi et al., 2015
	Proteus species		Interaction between proteins and NPs.	Vinoj et al., 2015
	E. coli, P. aeruginosa, S. aureus, B. Subtilis		ROS generation.	Wang Z. et al., 2017
	Gram-negative bacteria	MDR	Automated microarray-based system that identifies Gram-negative pathogens from positive blood cultures and resistance mechanism.	Walker et al., 2016
	S. aureus		Photoacoustic detection and photothermal therapy	Galanzha et al., 2012
	E. coli		ROS generation	Zhang et al., 2013
	E. coli		Change of membrane potential and inhibition of ATP synthase; inhibition of the subunit of the ribosome for tRNA binding.	Cui et al., 2012
	E. coli, K. pneumoniae, S. aureus, B. subtilis			Shamaila et al., 2016
	E. coli, K. pneumoniae, E. cloacae		Photodynamic Therapy/ Photothermal therapy.	Khan et al., 2017
	S. aureus, E. coli, E. cloacae, P. aeruginosa			Mocan et al., 2017
	Salmonella Typhimurium			Lin and Hamme, 2015
	S. aureus			Gil-Tomás et al., 2007
	E. coli, S. aureus		Interaction with biomolecules.	Kim D. et al., 2017
	E. coli, K. pneumoniae		Not revealed.	Bresee et al., 2014
	S. aureus, E. coli, P. aeruginosa		Disruption of bacterial cell wall.	Li et al., 2014; Yang et al., 2017
	E. coli		Interaction between lysozyme microbubbles and cell wall.	Mahalingam et al., 2015
	E. coli, S. aureus, Salmonella Typhimurium		Depend of co-existing chemicals that were not removed from AuNPs.	Shareena Dasari et al., 2015; Zhang et al., 2015a
	E. coli, S. aureus, K. pneumoniae		Combination with antibiotics.	Pradeepa et al., 2016
	P. aeruginosa	MDR/Biofilm formation	Conjugation with AMP.	Casciaro et al., 2017
	Staphylococci, Enterococci and other bacterial strain			Kuo et al., 2016
	E. coli, S. aureus, K. pneumoniae, P. aeruginosa			Rai A. et al., 2016
	Salmonella Typhimurium			Yeom et al., 2016
ZnONPs	*K. pneumoniae*	Ampicillin-carbenicillin-resistant	ROS generation and disruption of bacterial cell wall.	Reddy L. S. et al., 2014

(Continued)

TABLE 1 | Continued

Type of nanoparticles	Targeted bacteria	Antibiotic resistance type	Mechanisms of antibacterial action	References
	S. aureus	Methicillin-resistant	Enzyme inhibition.	Cha et al., 2015
	E. coli	*MDR*	ROS generation and disruption of bacterial cell wall.	Li et al., 2012b; Tong et al., 2013; Chakraborti et al., 2014; Gelabert et al., 2016; Nagvenkar et al., 2016
	B. subtilis			Hsueh et al., 2015
	S. aureus			Lakshmi Prasanna and Vijayaraghavan, 2015; Nagvenkar et al., 2016
	Vibrio cholerae			Sarwar et al., 2016
	S. aureus, E. coli, Proteus, Acinetobacter, P. aeruginosa		Combination with antibiotics.	Ehsan and Sajjad, 2017
	S. aureus, E. coli, S. mutants		Depend on components and structure of the bacteria cell wall.	Yu et al., 2014
	S. aureus, P. aeruginosa	Biofilms formation	ROS generation.	Aswathanarayan and Vittal, 2017
	Streptococcus sobrinus			Aydin Sevinç and Hanley, 2010
CuONPs	*E. coli, S. aureus*	MDR	ROS generation.	Singh R. et al., 2014; Chakraborty et al., 2015
	S. aureus, P. aeruginosa			Ulloa-Ogaz et al., 2017
	Paracoccus denitrificans		Modulation of nitrogen metabolism.	Su et al., 2015
	S. aureus	Biofilm formation	Ongoing investigations.	Chen et al., 2014
CuNPs	*S. aureus*	Methicillin-resistant	Copper ions release and subsequently bind with DNA leading to disorder of helical structure.	Kruk et al., 2015
	P. aeruginosa	Biofilm formation	Penetrate the cell wall and damage the nucleic acid.	LewisOscar et al., 2015
	P. aeruginosa	MDR	Generation of Cu hydrosols.	Zhang et al., 2015b
Fe_3O_4NPs	*E. coli*	MDR	Radiofrequency (RF) coupled with magnetic core shell nanoparticles lead to RF-mediated physical perturbation of cell membranes and bacterial membrane dysfunction.	Chaurasia et al., 2016
	S. aureus, P. aeruginosa, E. coli		Penetrate the membrane and interference in the electron transfer.	El-Zowalaty et al., 2015
	Gram-positive and -negative bacteria		ROS generation.	Behera et al., 2012
	Gram-positive and -negative bacteria		Nanotechnology to capture Gram- positive and -negative bacteria.	Reddy P. M. et al., 2014
	S. aureus	Biofilm formation	ROS generation.	Leuba et al., 2013
Al_2O_3NPs	*S. aureus*	Methicillin-resistant	Disruption of bacterial cell wall and ROS generation.	Ansari et al., 2013
	E. coli	MDR	Penetration and accumulation inside bacterial cell wall.	Ansari et al., 2014

(Continued)

TABLE 1 | Continued

Type of nanoparticles	Targeted bacteria	Antibiotic resistance type	Mechanisms of antibacterial action	References
TiO_2NPs	*S. aureus*	Methicillin-resistant	Release ions and react with thiol group of proteins present on bacteria surface.	Roy et al., 2010
	E. coli	MDR	ROS generation and disruption of bacterial cell wall.	Li et al., 2012b
	E. coli and Gram-positive bacteria		Photocatalytic disinfection.	Foster et al., 2011
	E. coli		Peroxidation and decomposition of membrane fatty acids.	Joost et al., 2015
Cu/Zn bimetal NPs	*S. aureus*	Methicillin-resistant	Membrane disruption, DNA damage, inhibition of protein synthesis.	Ashfaq et al., 2016
Au/Ag bimetallic NPs	*Enterococcus*	Vancomycin-resistant	Theranostic system for SERS and aPDT.	Zhou et al., 2018
	E. coli, S. aureus, E. faecalis, P. aeruginosa	Biofilm formation	Disruption of bacterial cell wall and inactivate the proteins and enzymes for ATP production.	Ramasamy et al., 2016
	B. subtilis E. coli, K. pneumoniae, S. aureus	MDR	Combination with antibiotics.	Baker et al., 2017
	P. aeruginosa, E. coli, S. aureus, Micrococcus luteus			Fakhri et al., 2017
	E. coli, S. aureus			dos Santos et al., 2012
Au/Pt bimetallic NPS	*E. coli*	MDR	Damage of the inner membrane, increase intracellular ATP level.	Zhao et al., 2014
Au/ Fe_3O_4NPs	*P. aeruginosa*	MDR	Disruption of bacterial cell wall.	Niemirowicz et al., 2014
Cu/Ni bimetallic NPs	*S. aureus, E. coli*, *S. mutans*	MDR	Adsorption of ions to the bacteria cells.	Argueta-Figueroa et al., 2014
MgF_2NPs	*S. aureus*	Biofilm formation	Attach and penetrate cell surface leading to disruption in membrane potential, promotes the lipid peroxidation and DNA binding.	Lellouche et al., 2009; Chen et al., 2014
Graphene Oxide NPs	*S. aureus*	Methicillin-resistant	Combine antibiotics with exposure to NIR.	Pan et al., 2016
	E. coli, E. faecalis	MDR	UV irradiation lead to generation of ROS.	Govindaraju et al., 2016
	E. coli, P. aeruginosa, K. pneumoniae, *S. aureus*		Multiple toxic mechanisms.	Jankauskaite et al., 2016
	E. cloacae, S. mutans	Biofilm formation	ROS generation, release of ions.	Kulshrestha et al., 2017
SeNPs	*S. aureus, E. coli*	MDR	Theranostic nanoplatform for selective imaging and targeted therapy: Disruption of the bacteria cell wall.	Huang et al., 2017
SiNPs	*S. aureus*	Methicillin-resistant	Theranostics nanoprobe for near-infrared fluorescence imaging and photothermal therapy: Disruption of the bacteria cell wall.	Zhao et al., 2017

peptidoglycans and abundant pores that allow the penetration of foreign molecules, leading to covalent binding with proteins and cellular components, interrupting the proper functioning of the bacterial cell (Sarwar et al., 2015). In addition, Gram-positive bacteria have a highly negative charge on the surface of the cell wall. For example, LPS provides negatively charged regions on the cell wall of Gram-negative bacteria that attracts NPs; and, since teichoic acid is only expressed in Gram-positive bacteria, the NPs are distributed along the phosphate chain. As such, the antimicrobial effect is more foreshadowed in Gram-positive than -negative bacteria (Wang et al., 2017a). Indeed, Yu and colleagues synthesized a novel hydroxyapatite whisker (HAPw)/zinc oxide (ZnO) NPs and evaluated the antimicrobial effect against *S. aureus*, *E. coli,* and *Streptococcus mutans*. The authors demonstrate that the antibacterial effect depends on the components and structure of the bacterial cell wall. The antibacterial action of these NPs could be improved for Gram-positive bacteria and certain components could prevent the adhesion of ZnO NPs to the bacterial cell barrier (Yu et al., 2014). Ansari et al. reported that the accumulation on NPs in the bacterial cell wall causes irregularly shaped pit, perforation and disturbs metabolic processes (Ansari et al., 2014). In a study carried out by Joost and co-workers, it was demonstrated that a treatment with TiO_2 NPs increased the bacterial cell volume, resulting in membrane leakage (Joost et al., 2015).

BIOFILM FORMATION AND QUORUM-SENSING

Biofilm formation plays an important role in bacterial resistance protecting bacteria and allowing then to evade the action of antibiotics (Lebeaux et al., 2014; Khameneh et al., 2016). The most active fractions of bacteria are now recognized to occur as biofilms, where cells are adhered to each other on surfaces within a self-produced matrix of extracellular polymeric substance (EPS). EPS provide a barrier allowing to inhibit the penetration of antibiotics and further promote antibiotic resistance leading to a serious health threat worldwide since biofilms are resistant to antibiotics penetration and escape innate immune system by phagocytes (Hall-Stoodley et al., 2004; Bjarnsholt, 2013). Numerous experimental evidence show that NPs are capable of disrupting the bacterial membranes and can hinder biofilm formation thus reducing the survival of the microorganism (Peulen and Wilkinson, 2011; Leuba et al., 2013; Pelgrift and Friedman, 2013; Slomberg et al., 2013; Chen et al., 2014; Miao et al., 2016; Yu et al., 2016; Kulshrestha et al., 2017). This way, NPs provide an alternative strategy to target bacterial biofilms with potential to use both antibiotic-free and antibiotic-coated approaches (Gu et al., 2003; Li et al., 2012a; Sathyanarayanan et al., 2013). Earlier reports demonstrated that NPs are able to interfere with biofilm integrity by interacting with EPS and with the bacterial communication - quorum sensing (QS). The properties of NPs must be designed to be able to inhibit biofilm formation namely through size and surface chemistry. The size of NPs is important to it since they must be able to penetrate the EPS matrix and surface chemistry will command the amount of interactions with the EPS (Lundqvist et al., 2008). The majority of the strategies to achieve inhibition of biofilm formation are to target and interfere with QS molecules (Singh et al., 2017).

QS systems in bacterial populations act as major regulatory mechanisms of pathogenesis, namely in the formation of biofilm structures. These systems help bacteria to "communicate" with each other, through the production and detection of signal molecules (Rutherford and Bassler, 2012; Papenfort and Bassler, 2016). Using this cell-to-cell communication, bacterial populations are able to synchronize the expression of their genes, acquiring competitive advantage to respond to changes in the environment (Rutherford and Bassler, 2012). Therefore, QS systems are known to promote the formation of antibiotic tolerant biofilm communities. It is known that biofilm structures are a recalcitrant mode of bacterial growth that increases bacterial resistance to conventional antibiotics (Reen et al., 2018). This way, bacterial biofilms pose a significant challenge to the efficacy of conventional antibiotics being considered an essential platform for antibiotic resistance (Høiby et al., 2011). Taking this into account, it isn't surprising that the targeting and disruption of QS signaling systems and consequently, of the biofilm production, set the pillar for future next-generation anti-virulence therapies to be developed (LaSarre and Federle, 2013; Venkatesan et al., 2015; Jakobsen et al., 2017).

Surface-functionalized NPs with β-cyclodextrin (β-CD) or N-acylated homoserine lactonase proteins (AiiA) are able to interfere with signaling molecules preventing these molecules from reaching its cognate receptor, therefore inhibiting the signal/receptor interaction. This process will "turn off" QS and obstructing the bacterial communication (Kato et al., 2006; Ortíz-Castro et al., 2008). Several papers reported inhibition of biofilm formation namely by gold NPs (AuNPs). Acyl homoserine lactones (AHL) are signaling molecules with a role in bacterial QS and bind directly to transcription factors to regulate gene expression Recently, Gopalakrishnan and colleges synthesized (Vinoj et al., 2015) AuNPs coated AiiA purified from *Bacillus licheniformis*. These AiiA AuNPs inhibited EPs production and demonstrated potent antibiofilm activity against Proteus species at 2–8 μM concentrations without being harmful for the host cells at the 2μM concentration. Sathyanarayanan et al. (2013) demonstrated that using AuNPs there is a significant reduction of *S. aureus* and *P. aeruginosa* biofilms applied in high concentration (exceeding 50 mg/L). A recent study by Yu et al. (2016) demonstrated that AuNPs were able to strongly attenuate biofilm formation of *P. aeruginosa*. The inhibition observed in this study was related with interruption of adhesin- mediated interaction between the bacteria and the substrate surface due to electrostatic attractions between the AuNPs and cell wall surface of *P. aeruginosa*, instead of QS-related molecules. Positive charge AuNPs inhibited significantly *S. aureus* and *P. aeruginosa* biofilm formation (while minimizing mammalian cytotoxicity) (Ramasamy et al., 2016). The use of NPs demonstrates an exclusive approach to penetrate infectious biofilms and target bacterial communication, overcoming this major health issue related with biofilm infections.

Because most of these NPs-based platforms exert their action *via* distinct mechanisms/structures/pathways of those

used by traditional antibiotics, combined therapeutic regimens are promising strategies to tackle the surge of multidrug resistant (MDR) bacteria bypassing their defense mechanisms (Pelgrift and Friedman, 2013; Singh K. et al., 2014; Hemeg, 2017; Zaidi et al., 2017). Additionally, NPs have been shown to activate macrophages in a dose dependent manner (Patel and Janjic, 2015) which promotes the host defenses (Hemeg, 2017; Jagtap et al., 2017).

This multi-target action of NPs may overcome multidrug resistance by circumventing several obstacles encountered by traditional antibiotics (Pelgrift and Friedman, 2013; Chen et al., 2014; Singh K. et al., 2014; Hemeg, 2017; Jagtap et al., 2017; Rai et al., 2017; Zaidi et al., 2017). **Table 1** highlights several types of NPs that have shown effective bactericidal activity when administered isolated; combined with standard antibiotics; and/or radiation or as vectors for biocidal delivery allowing killing of MDR bacteria, and in some cases also inhibiting biofilm production.

We will now focus on the different types of metal NPs highlighting their most relevant mechanism/effects against MDR bacteria and/or biofilms structures.

SILVER NANOPARTICLES (AGNPS)

Since the ancient times, silver has been recognized as having antimicrobial effects (Rai et al., 2009; Reidy et al., 2013). Based on all the evidence to date, AgNPs are probably one of the most promising inorganic NPs that can be used for the treatment of bacterial infections (Natan and Banin, 2017). These NPs may be synthesized by traditional chemical reduction or *via* "green" chemistry approaches using plant and/or microbial extracts (Iravani et al., 2014; Ribeiro et al., 2018).

Several mechanisms have been proposed to understand how AgNPs mediate cell death, including cell wall disruption (Lok et al., 2007; Bondarenko et al., 2013), oxidation of cellular components, inactivation of the respiratory chain enzymes, production of ROS, and decomposition of the cellular components (Chen et al., 2014; Rizzello and Pompa, 2014; Dakal et al., 2016). The permeability of the membrane increases after incorporation of AgNPs into the cell membrane. The adsorption of the NPs leads to the depolarization of the cell wall, altering the negative charge of the cell wall to become more permeable. It was demonstrated disruption of the cell wall with subsequent penetration of the NPs. The entry of AgNPs induces ROS that will inhibit ATP production and DNA replication (Zhang et al., 2013; Dakal et al., 2016; Durán et al., 2016; Ramalingam et al., 2016). However, there is evidence that AgNPs can release Ag^{+}, known to exhibit antimicrobial activity, when interacting with thiol-containing proteins, which weaken their functions (Durán et al., 2010). The precise method of the antibacterial mechanism of AgNPs is still not completely understood (Franci et al., 2015; Durán et al., 2016). All the existing data indicates that AgNPs exert several bactericidal mechanisms in parallel, which may explain why bacterial resistance to silver is rare (Karimi et al., 2016). Concerns regarding the cytotoxicity and genotoxicity of AgNPs have been raised (Chopra, 2007) but various authors have conducted clinical trials based on AgNPs and no important clinical alterations have been detected (Munger et al., 2014a,b; Smock et al., 2014). Interestingly, AgNPs have been found to exhibit higher antimicrobial activity than antibiotics like gentamicin or vancomycin against *P. aeruginosa* and MRSA (Saeb et al., 2014). Lara *et al.* showed the potential bactericidal effect of AgNPs against MDR *P. aeruginosa*, ampicillin-resistant *E. coli* O157:H7 and erythromycin-resistant *Streptococcus pyogenes* (Lara et al., 2010). Nagy *et al.,* reported that AgNPs were capable of inhibiting the growth of *S. aureus* and *E. coli via* the up-regulation of the expression of several antioxidant genes and ATPase pumps (Nagy et al., 2011). Dolman *et al.* also showed that the Ag-containing Hydrofiber® dressing and nanocrystalline Ag-containing dressing are effective agents against antibiotic sensitive Gram-negative and -positive bacteria as well as antibiotic resistant bacteria, such as MRSA, Vancomycin-resistant *Enterococci* (VRE) and *Serratia marcescens*, avoiding the formation of biofilms on biomaterials (Percival et al., 2007). Su and collaborators showed that AgNPs immobilized on the surface of nanoscale silicate platelets (AgNP/NSPs) have strong antibacterial activity against MRSA and silver-resistant *E. coli via* generation of ROS (Su et al., 2011). Singh and collaborators showed that AgNPs from *P. amarus* extract exhibited excellent antibacterial potential against MDR strains of *P. aeruginosa* (Singh K. et al., 2014). Recently, two different shaped AgNPs (spheres and rods) were used against Gram-positive and -negative bacteria, both showing promising antibacterial activity against different strains (Acharya et al., 2018).

An emerging practice is to combine AgNPs with antibiotics to enhance antimicrobial potency. Recently, Katya and collaborators showed that the combination of gentamicin and chloramphenicol with AgNPs has a better antibacterial effect in MDR *E. faecalis* than both antibiotics alone (Katva et al., 2018). McShan *et al.* described that AgNPs combined with either one of two-different class of antibiotics (tetracycline and neomycin) can exhibit a synergistic effect, showing an enhanced antibacterial activity at concentrations below the MIC of either the NPs or the antibiotic (McShan et al., 2015). Other authors also reported similar results (Thomas et al., 2014; Panáček et al., 2016a,b; Salomoni et al., 2017). Djafari and collaborators described the synthesis of water-soluble AgNPs using the antibiotic tetracycline as co-reducing and stabilizing agent (AgNPs@TC) and demonstrated their effectiveness against tetracycline-resistant bacteria (Djafari et al., 2016).

Antimicrobial peptides (AMPs) represent one of the forms of defense strategy against infections in living organisms and are emerging as essential tools to kill pathogenic bacteria, since they exhibit broad-spectrum activity and low resistance development (Yeaman, 2003). Lytic peptides are AMPs produced by all organisms. In mammals, they are an innate host defense mechanism against pathogens (Bahar and Ren, 2013). The mechanism of action of AMPs relies on the ability to interact with bacterial membranes or the cell wall, thus inhibiting cellular biochemical pathways and ultimately killing the bacteria (Zhang and Gallo, 2016). Defensins and cathelicidin are two of the larger families of lytic peptides that kill bacteria by disrupting the

membrane. Unfortunately, AMPs have poor enzymatic stability, low permeability across biological barriers and may be rapidly degraded in the human body by proteases, which greatly limits their application (Wang, 2014). Immobilization of the peptides onto NPs can increase their stability, enhancing the antimicrobial properties of the NPs and therefore, has the potential to be used as a new tool to tackle antibiotic resistant bacteria (Brandelli, 2012; Rai A. et al., 2016). Indeed, the first author to demonstrate that functionalized AgNPs with peptides increased their antibacterial activity was Ruden and co-workers (Ruden et al., 2009). Based on this strategy several researchers functionalized AgNPs with AMPs (AgNP@AMP) with increases in the antimicrobial activity compared with free AMPs (Ruden et al., 2009; Liu et al., 2013; Mohanty et al., 2013). Polymyxin B is the most used AMP and exhibits antibacterial activity *via* interaction with the endotoxin LPS in the outer membrane of Gram-negative bacteria (Morrison and Jacobs, 1976; Lambadi et al., 2015). It was proved that AgNPs functionalized with polymyxin-B removed almost completely endotoxins from solutions and hindered the formation of biofilm onto surgical blades (Jaiswal et al., 2015; Lambadi et al., 2015). Liu *et al.,* demonstrated that the immobilization of peptides with AgNPs enhanced their antimicrobial activity compared to an unbound peptide and also minimized toxicity of AgNPs compared to using the AgNPs alone (Liu et al., 2013). A recent study by Pal *et al.* describes a system consisting of a cysteine containing AMP conjugated with AgNPs, which demonstrated that the Ag-S bonds increased stability and enhanced antimicrobial activity than conjugation using electrostatic interactions (Pal et al., 2016).

Other methods have been used to improve the antibacterial activity of AgNPs. One of these methods relies on the use of visible blue light, which was previously shown to exhibit strong antibacterial activity (Dai T. et al., 2013; Maclean et al., 2014). El Din and collaborators demonstrated that blue light combined with AgNPs exhibits therapeutic potential to treat MDR infections and can represent an alternative to conventional antibiotic therapy, since the antimicrobial activity of the combination was greater than the components alone. Moreover, this approach proved to be synergistic in the treatment of an unresponsive antibiotic-resistant bacteria responsible for a wound in a horse (El Din et al., 2016). Spherical shaped thioglycolic acid-stabilized AgNPs (TGA-AgNPs) conjugated with vancomycin were used as drug delivery systems and demonstrated to possess increased antimicrobial activity against MDR bacteria such as MRSA and VRE (Esmaeillou et al., 2017).

GOLD NANOPARTICLES (AuNPs)

Metallic gold is considered inert and non-toxic, which may vary when it shifts form metallic bulk to oxidation states (I and II) (Merchant, 1998). Gold NPs (AuNPs) may be synthesized by traditional chemical reduction of a gold salt or *via* "green" chemistry approaches using plant and/or microbial extracts (Shah et al., 2014). The most used and described method is the chemical synthesis based on the reduction of chloroauric acid by citrate (Lee and Meisel, 1982; Fernandes and Baptista, 2017). Some studies have addressed the potential of using AuNPs as antibacterial agents, but some controversy still exists (Cui et al., 2012; Bresee et al., 2014; Shah et al., 2014; Shareena Dasari et al., 2015; Zhang et al., 2015a; Shamaila et al., 2016).

According to Yu H and collaborators, AuNPs are usually not bactericidal at low concentrations and weakly bactericidal at high concentrations (Shareena Dasari et al., 2015; Zhang et al., 2015a). This is possibly due to the effect of co-existing chemicals, such as gold ions, surface coating agents, and chemicals involved in the synthesis that were not completely removed (Shareena Dasari et al., 2015; Zhang et al., 2015a). However, other authors describe that the antibacterial mechanism of AuNPs is associated to (i) the collapse in the membrane potential, hindering ATPase activity causing a deterioration of the cell metabolism; (ii) hindering of the binding subunit of the ribosome to tRNA (Cui et al., 2012); and (iii) Shamaila and co-workers showed that AuNPs may affect the bacterial respiratory chain by attacking nicotinamide (Shamaila et al., 2016). Since AuNPs are non-toxic to the host (Conde et al., 2014; Li et al., 2014; Rajchakit and Sarojini, 2017), the possibility of fine tuning their conjugation chemistry to act as carriers or delivery vehicles of antibiotics or other antibacterial moieties may enhance their bactericidal effect and potentiate the effect of antibiotics (Zhao and Jiang, 2013; Conde et al., 2014; Li et al., 2014; Uma Suganya et al., 2015; Zhang et al., 2015a; Fernandes et al., 2017).

Cationic and hydrophobic functionalized AuNPs were shown to be effective against both Gram-negative and -positive uropathogens, including MRSA. These AuNPs exhibited low toxicity to mammalian cells (biocompatibility) and the development of resistance to these NPs was very low (Li et al., 2014). Vinoj *et al.* demonstrated that coating AuNPs with N-acylated homoserine lactonase proteins (AiiA AuNPs) resulted in a nanocomposite with activity against MDR species compared with AiiA proteins alone (Vinoj et al., 2015). Other approaches were also studied, as adsorbing AuNPs to PVA-lysozyme micro bubbles potentiate the antibacterial activity due to the interaction of AuNPs with cells membranes causing bacterial lysis (Mahalingam et al., 2015). Galic acid capped AuNPs have also been found to be active against Gram-negative and -positive bacteria (Kim D. et al., 2017). Recently, Ramasamy and collaborators described the direct one-pot synthesis of cinnamaldehyde immobilized on gold nanoparticles (CGNPs) with effective biofilm inhibition of more than 80% against Gram-positive bacteria (methicillin-sensitive and -resistant strains of *S. aureus*, MSSA and MRSA, respectively) and Gram-negative (*E. coli* and *P. aeruginosa*) *in vitro* and *in vivo* (Ramasamy et al., 2017a,b). Also, the integration of AuNPs with ultrathin graphitic carbon nitride was described as having high bactericidal performance against both MDR Gram-negative and -positive bacteria, and a high effectiveness in eliminating existing MDR-biofilms and preventing the formation of new biofilms *in vitro* (Wang Z. et al., 2017). Also, conjugation of antibiotics to AuNPs, such as vancomycin, methicillin, etc., increases their intrinsic activity against MDR strains (Mohammed Fayaz et al., 2011; Lai et al., 2015; Roshmi et al., 2015; Payne et al., 2016). Recently Payne

and collaborators develop a single-step synthesis of kanamycin-capped AuNPs (Kan-AuNPs) with high antibacterial activity against both Gram-positive and -negative bacteria, including kanamycin resistant bacteria. The authors observed a significant reduction in the MIC against all the bacterial strains tested for Kan-AuNPs when compared to the free drug. This higher efficacy was due to the disruption of the bacterial envelope, resulting in leakage of the cytoplasmic content and consequent cell death (Payne et al., 2016). Pradeepa and collaborators synthesized AuNPs with bacterial exopolysaccharide (EPS) and functionalized them with antibiotics (levofloxacin, cefotaxime, ceftriaxone and ciprofloxacin). They observed that these AuNPs exhibited excellent bactericidal activity against MDR Gram-positive and -negative bacteria compared to free drugs. *E. coli* was the most susceptible MDR bacteria followed by *K. pneumoniae* and *S. aureus* (Pradeepa et al., 2016). Recently, Yang and collaborators described the effect of small molecule (6-aminopenicillanic acid, APA)-coated AuNPs to inhibit MDR bacteria (Yang et al., 2017). They doped AuNPs into electrospun fibers of poly(ε-caprolactone) (PCL)/gelatin to produce materials that avoid wound infection by MDR bacteria and demonstrated *in vitro* and *in vivo* that APA-AuNPs reduced MDR bacterial infections (Yang et al., 2017). Shaker and Shaaban evaluated the surface functionalization of AuNPs with carbapenems [imipenem (Ipm) and meropenem (Mem)] as a delivering strategy against carbapenem resistant Gram-negative bacteria isolated from an infected human. Both Ipm-AuNPs and Mem-AuNPs, with 35 nm diameter showed a significant increase in antibacterial activity against all the tested isolates (Shaker and Shaaban, 2017). Also, Shaikh and collaborators described recently the synthesis and characterization of cefotaxime conjugated AuNPs to target drug-resistant CTX-M-producing bacteria. The authors could invert resistance in cefotaxime resistant bacterial strains (i.e., *E. coli* and *K. pneumoniae*) by using cefotaxime-AuNPs. Their results reinforce the efficacy of conjugating an unresponsive antibiotic with AuNPs to restore its efficacy against otherwise resistant bacterial pathogens (Shaikh et al., 2017).

Combination of AuNPs with other approaches has also been demonstrated. Indeed, one of the most extraordinary properties of AuNPs is the capability to transform light into heat under laser irradiation (Mendes et al., 2017; Mocan et al., 2017). This property is extremely important because it can be exploited to develop photothermal nanovectors to destroy MDR bacteria at a molecular level (for a complete review see Mocan et al., 2017). For example, Khan and collaborators showed that the combination of Concanavalin-A (ConA) directed dextran capped AuNPs (GNPDEX-ConA) conjugated with methylene blue (MB) (MB@GNPDEX-ConA) and photodynamic therapy (PDT) enhanced the efficacy and selectivity of MB induced killing of MDR clinical isolates, including *E. coli*, *K. pneumoniae*, and *E. cloacae* (Khan et al., 2017). Gil-Tomas and collaborators described that the functionalization of AuNPs covalently with toluidine blue O–tiopronin forms an enhanced, exceptionally potent antimicrobial agent when activated by white light or 632 nm laser light (Gil-Tomás et al., 2007). Hu and collaborators prepared a mixed charged zwitterion-modified AuNPs consisting of a weak electrolytic 11-mercaptoundecanoic acid (HS-C10-COOH) and a strong electrolytic (10-mercaptodecyl)trimethylammonium bromide (HS-C10-N4) that exhibited *in vivo* and under near-infrared (NIR) light irradiation an enhanced photothermal ablation of MRSA biofilm with no damage to the healthy tissues around the biofilm (Hu et al., 2017). Also, the antibacterial activity of glucosamine-gold nanoparticle-graphene oxide (GlcN-AuNP-GO) and UV-irradiated GlcN-AuNP-GO was evaluated against *E. coli* and *E. faecalis*. Results show that UV irradiation of GlcN-AuNP-GO results in higher antibacterial activity than the standard drug kanamycin (Govindaraju et al., 2016). Ocsoy *et al*. reported the development of DNA aptamer-functionalized AuNPs (Apt@AuNPs) and gold nanorods (Apt@AuNRs) for inactivation of MRSA with targeted PTT (Ocsoy et al., 2017). The authors showed that although both NPs could specifically bind to MRSA cells, Apt@AuNPs and Apt@AuNRs increased resistant cell death for 5% and for more than 95%, respectively through PTT. This difference in induction of cell death was based on the relatively high longitudinal absorption of NIR radiation and strong photothermal conversion capability for the Apt@AuNRs compared to the Apt@AuNPs. However, with the new developments of using AuNPs for hyperthermia in the visible light (Mendes et al., 2017) might additionally potentiate the Apt@AuNPs results observed for these authors (Ocsoy et al., 2017). Recently, Mocan *et al*. also described the synthesis of AuNPs by wet chemistry, their functionalization with IgG molecules following laser irradiation. Their results indicate that administration of IgG-AuNPs following laser irradiation provided an extended and selective bacterial death in a dose dependent manner (Mocan et al., 2016).

In recent years, a new approach relying on the conjugation of AuNPs with AMPs has shown interesting results (Rajchakit and Sarojini, 2017). Indeed, Kuo and collaborators mixed synthetic-peptides containing arginine, tryptophan and cysteine termini [(DVFLG)2REEW4C and (DVFLG)2REEW2C], with aqueous tetrachloroauric acid to generate peptide-immobilized AuNPs [i.e., (DVFLG)2REEW4C-AuNPs and (DVFLG)2REEW2C-AuNPs] that were effective antibacterial agents against *Staphylococci*, *Enterococci,* and antibiotic-resistant bacterial strains (Kuo et al., 2016). Rai and co-workers demonstrated that the use of cecropin-melittin (CM-SH) a known peptide with antibacterial properties (Boman et al., 1989), functionalized in the surface of AuNPs through Au-S bond, showed higher antimicrobial activity and higher stability in media compared with an *in vitro* and *in vivo* infection animal model with the MIC of CM-SH AuNPs four times lower than free CM-SH (Rai A. et al., 2016). Conjugation of AMP with AuNPs usually involves the formation of the Au-S coordinate covalent bond, relying on the amine or thiol groups in peptides or conjugating specific linkers to AMPs with a terminal (N- or C-terminal) cysteine which helps conjugation with gold (Tielens and Santos, 2010; Xue et al., 2014). However, there is one example where covalent conjugation of an AMP to AuNPs has been achieved *via* Au-O bond (Lai et al., 2015). Other approaches use a linker for the conjugation to AuNPs, Poly(ethylene

glycol) carboxylic acid (PEGCOOH) covalently bound to AMP showed a significantly increase of the antibacterial and anti-biofilm activity for resistant Gram-negative bacteria (Casciaro et al., 2017). Yeom and co-workers demonstrated the most advanced *in vivo* clinical application for AuNPs@AMP using infected mice and resulting in the inhibition of *Salmonella* Typhimurium colonization in the organs of the animals (Yeom et al., 2016). The reason behind the increased antimicrobial activity of AuNPs@AMP over the free components is that AuNPs can get a higher concentration of the antibiotic at the site of action. These NPs can interact with LPS, proteins in the membrane of the bacteria and in some cases, penetrate the bacterial membrane through the porin channel. This way they can interact with the inner membrane making the AuNPs@AMP conjugate more efficient than the non-conjugated form (Katz and Willner, 2004; Wangoo et al., 2008; Chen J. et al., 2009).

BIMETALLIC NPS

Ag and Au may be used in a single NP to enhance the effects of a drug and reduce the required dose. Alternatively, they can be used alone since they possess antimicrobial properties that are enhanced when combined in the form of bimetallic NPs (Arvizo et al., 2010; Singh R. et al., 2016). The role of Ag against MDR pathogens has been previously described. However, AgNPs are difficult to functionalize with biomolecules and drugs. Such limitation may be circumvented by means of alloy/bimetallic NPs that excel their monometallic counterparts providing improved electronic, optical and catalytic properties (Cho et al., 2005; Shah et al., 2012). As reported above, AuNPs constitute good vectors to the delivery of pharmacologic compounds. Gold(Au)-silver(Ag) alloys are an optimal solution since they combine the antimicrobial effect of silver with the ease of functionalization and improved stability in complex biological media provided by gold (Doria et al., 2010; dos Santos et al., 2012). Fakhri and co-workers synthetized and functionalized AgAuNPs with a tetracycline and concluded that there exists a synergetic effect of the antibiotic with the bimetallic nanoparticle, with greater bactericidal activity of this form in detriment of its free forms. The mechanism of action was established as being the generation of ROS (Fakhri et al., 2017). Also recently, Baker and collaborators described the synthesis and antimicrobial activity of bimetallic AgAuNPs from the cell free supernatant of *Pseudomonas veronii* strain AS41G inhabiting *Annona squamosa L*. The authors showed their synergistic effect with standard antibiotics with 87.5, 18.5, 11.15, 10, 9.7, and 9.4% fold increased activity with bacitracin, kanamycin, gentamicin, streptomycin, erythromycin and chloramphenicol, respectively, against bacitracin resistant strains of *Bacillus subtilis*, *E. coli,* and *K. pneumoniae* (Baker et al., 2017). Zhao and collaborators have demonstrated the antibacterial activity of AuPtNPs bimetallic NPs against sensitive and drug-resistant bacteria *via* the dissipation of the bacterial membrane potential and the elevation of adenosine triphosphate (ATP) levels (Zhao et al., 2014).

Other types of bimetallic NPs have been studied and their antibacterial activity explored, but in most cases as coating agents and not as a delivery approach and antibacterial activity (Argueta-Figueroa et al., 2014).

METAL OXIDES

Metal oxides NPs are among one of the most explored and studied family of NPs and are known to effectively inhibit the growth of a wide range of sensitive and resistant Gram-positive and -negative bacteria, emerging as hopeful candidates to challenge antimicrobial resistance (Raghunath and Perumal, 2017; Reshma et al., 2017; Kadiyala et al., 2018). Iron oxide (Fe_3O_4), Zinc oxide (ZnO), and Copper oxide (CuO) possess antimicrobial properties and can be applied in clinical care (Sinha et al., 2011). Due to the intrinsic photocatalytic activity of the metal oxides they generate ROS and become powerful agents against bacteria (Tong et al., 2013; Singh R. et al., 2014). These will be described in more detail on the following sections.

IRON OXIDE (FE_3O_4)

The synthesis of iron oxide NPs may be achieved *via* different routes (Babes et al., 1999; Berry and Curtis, 2003). The antibacterial mechanism of these NPs is mainly attributed to dissolved metal ions and the generation of ROS (Wang et al., 2017a). It was shown that superparamagnetic iron oxide NPs interact with microbial cells by penetrating the membrane and interfering with the electron transfer (Behera et al., 2012; El-Zowalaty et al., 2015). Additionally, it has been described that iron oxide NPs can damage macromolecules, including DNA and proteins, through the formation of ROS (Leuba et al., 2013). Pan *et al.* developed a system of reduced graphene oxide (rGO)-iron oxide nanoparticles (rGO-IONP) by the chemical deposition of Fe^{2+}/Fe^{3+} ions on nanosheets of rGO in aqueous ammonia. The *in vivo* results showed maximum antibacterial activity due to the generation of hydroxyl radicals that can cause physical and chemical damage, which inactivated MRSA (Pan et al., 2016).

ZINC OXIDE (ZnO)

ZnO NPs are often used to restrict microorganism growth, being effective against planktonic bacteria, and also inhibiting the formation of biofilms (Hsueh et al., 2015; Sarwar et al., 2016) (Espitia et al., 2012). These NPs can be synthesized by various methods, from green chemistry to sonochemistry (Salem et al., 2015; Ali et al., 2016; Nagvenkar et al., 2016). The antibacterial mechanism of the NPs is partially attributed to two principal factors, the dissolution of metal ion and the generation of ROS (Gelabert et al., 2016; Nagvenkar et al., 2016; Sarwar et al., 2016). ZnO releases Zn^{2+} in liquid medium and is adsorbed on the surface of bacteria or may entry the cell, where it interacts with functional groups in proteins and nucleic acids, hindering enzyme activity and the normal physiological

processes (Yu et al., 2014). However, some authors demonstrated that Zn ions have little antimicrobial activity, implying that dissolution of Zn^{2+} might not be the main mechanism of action (Aydin Sevinç and Hanley, 2010). Sarwar and co-workers demonstrated that nanosized ZnO caused significant oxidative stress to *Vibrio cholera*, the damage inflicted was DNA degradation, protein leakage, membrane depolarization and fluidity (Sarwar et al., 2016). Ehsan and Sajjad, described that ZnO NPs impregnated with antibiotics showed good antibacterial activities against *S. aureus*, *Proteus*, *Acinetobacter*, *P. aeruginosa,* and *E. coli*, being that these were resistant to antibiotics but became sensitive in the presence of these NPs with antibiotics (Ehsan and Sajjad, 2017). It was also discovered that these NPs induce the production of ROS even in the dark, and this happens due to the surface defects on the NPs. The different shapes function as enzyme inhibitors, where nanopyramids are the most effective (Cha et al., 2015; Lakshmi Prasanna and Vijayaraghavan, 2015). Recently, Aswathanarayan and Vittal described the antimicrobial effect of ZnO NPs against MDR Gram-positive and -negative pathogens in comparison to gold and iron NPs and these could be used at concentrations less toxic to mammalian cells (Aswathanarayan and Vittal, 2017). ZnO NPs are also known for inhibiting biofilm formation and production of quorum-sensing-dependent virulence factors in *P. aeruginosa* (Lee et al., 2014; García-Lara et al., 2015).

COPPER OXIDE (CuO)

Copper containing NPs have been shown effective against animal and plant pathogens (LewisOscar et al., 2015), impeding formation of MDR biofilms, and showing the potential to serve as antimicrobial coating agents (LewisOscar et al., 2015). Kruk *et al.* and Zhang *et al.* showed that copper NPs are capable of inhibiting the growth of MDR bacteria, namely, *P. aeruginosa* and MRSA (Zhang et al., 2014, 2015b; Kruk et al., 2015). The antimicrobial activity of these NPs is comparable to that of AgNPs but at a lower cost (Kruk et al., 2015). Copper oxide NPs generate ROS that often leads to chromosomal DNA degradation, which seems to highlight a "particle-specific" action rather than resulting from the release of metallic ions (Chakraborty et al., 2015). Su and collaborators investigated the effects of CuONPs on bacterial denitrification and explored the effect on the expression of intracellular proteins. When CuONPs entry into bacteria metabolic functions are affected, such as active transport, electron transfer, and nitrogen metabolism (Su et al., 2015).

NPs can also be complexed with other metals, like gallium. Gallium NPs have been described to facilitate phagosome maturation of macrophages infected with virulent *M. tuberculosis* and therefore being able to inhibit growth of this pathogen (Choi et al., 2017).

THE POTENTIAL FOR NANOTHERANOSTICS

NPs applications in biodetection is huge and more insights on pathogen detection using NPs platforms can be seen in Veigas et al. (2013, 2014, 2015); Costa et al. (2014); Weng et al. (2015); Kim J. et al. (2017); Wang et al. (2017b); Galvan and Yu (2018), and Yang et al. (2018).

Theranostics is a combination of diagnosis and therapy onto a single platform, which allow for timely biodetection and/or real-time monitoring of therapy. By using NPs, this can be translated to the nanoscale—Nanotheranostics. NPs have been applied for multiplex high-throughput diagnostics to assist precision therapy. For example, Verigene® is an AuNPs test commercialized for diagnosis. It is an automated microarray-based system that identifies Gram-negative pathogens from positive blood cultures. Verigene® BC-GN also detects key resistance mechanisms (Walker et al., 2016; Claeys et al., 2018). Others have used, magnetic and functionalized magnetic iron oxide NPs as affinity probes to capture Gram-positive and -negative bacteria. The analyses of captured bacteria using matrix-assisted laser desorption/ionization mass spectrometry was <1 h (Reddy P. M. et al., 2014). One pioneer work on nanotheranostics against bacterial infection was the development of a method for *in vivo* photoacoustic detection and photothermal eradication of *S. aureus*. Two-color gold and multilayer magnetic nanoparticles were functionalized with an antibody cocktail for the targeting *of S. aureus*. These platform demonstrated ultrasensitive detections for circulating bacterial cells (CBCs), *in vivo* magnetic enrichment and PT eradication of CBCs (Galanzha et al., 2012). Recently, Zhou and collaborators developed a silicon 2,3-naphthalocyanine dihydroxide (Nc) and Vancomycin functionalized silica-encapsulated, silver-coated gold NPs (Au@AgNP@SiO2@Nc-Van) as a novel theranostic system for surface-enhanced Raman scattering (SERS) detection and antimicrobial photodynamic therapy (aPDT) of vancomycin (Van)-resistant enterococci (VRE) strains (Zhou et al., 2018). These authors observed a 4–5 logs reduction of bacteria upon *in vitro* aPDT of VRE treated with a nanomolar concentration of the Au@AgNP@SiO2@Nc-Van and an infection regression and even complete eradication of VRE *in vivo* using infected mice (Zhou et al., 2018).

A selenium nanoplatform (Se@PEP-Ru) was designed with excellent fluorescent properties for imaging bacteria and with high antimicrobial properties (Huang et al., 2017). Zhao and co-workers developed an activated theranostics nanoprobe for near-infrared fluorescence imaging and photothermal therapy of MRSA infections, based on SiO2/PAH-cypate nanosystems modified with PEG and Vancomycin-conjugated poly(acrylic acid) molecules (PAAPEG-Van). This probe is activated by bacteria-responsive polyelectrolyte dissociation from silica NPs. The authors believe that this concept can be used as an approach to design and for production of bacteria responsive multifunctional nanomaterials and constitute their ultimate functions in the treatment of drug-resistant bacterial infections (Zhao et al., 2017). Kuo and collaborators developed a nanotheranostics system using Au nanorods conjugated with a hydrophilic photosensitizer, toluidine blue O, that acted as dual-function agents in photodynamic inactivation and hyperthermia against MRSA (Kuo et al., 2009).

CLINICAL TRANSLATION

At present, there are a few metal NPs-based strategies against bacterial infections undergoing clinical trials. The costs associated to the use of nanotechnology platforms are very high, and therefore conventional treatments are preferred. However, these platforms might be preferable in specific situations, with direct impact on the quality of patients life (Caster et al., 2017).

Bio-kil® [3-(Trimethoxysilyl) propyloctadecyldimethyl ammonium chloride] (Cargico Group, Taiwan) is a patented technology that is based on affixing nano-sized antimicrobials onto a large surface area through covalent chemical bonding to form a durable polymer. Bio-kil® eliminates microorganism through a physical biocide process. This type of nanomaterial consists in inorganic metal components and organic quaternary ammonium components. Recently, Bio-Kil® has been shown to reduce the environmental bacterial burden and MDR organisms (Lee et al., 2017).

AgTive (NCT00337714) is a silver-impregnated central venous catheter and has been marketed with the claim to improved bactericidal activity. AgTive catheters are made of polyurethanes impregnated with silver NPs, and their interaction with body fluids and intravenous solutions results in the release of significantly larger amounts of silver ions from the catheter reducing bloodstream infection (Antonelli et al., 2012).

Acticoat is a nanocrystalline silver dressing that acts as an antimicrobial topical, releasing silver into the wound. This nanoformulation has been shown to inhibit *in vitro* biofilms formation in *P. aeruginosa* and *Acinetobacter baumannii* by more than 90% (Potgieter and Meidany, 2017). Madigan Army Medical Center is studying the efficacy of a silver NPs gel SilvaSorb (NCT00659204) and currently is in phase III of the clinical trials. The aim of this study is to compare the antimicrobial efficacy of a one-time application of SilverSorb (AcryMed, Inc., Portland) against the standard antibacterial hand gel Purell (GoJo Industries, Akron), in reducing transient bacterial counts isolated from the hands of 40 patients seeded with *S. marcescens*.

Nano Silver Fluoride is a new formulation that combines silver NPs, chitosan and fluoride and was developed with antimicrobial properties. This nanoformulation has excellent results as antibacterial agent *against S. mutan*s and *Lactobacilli*. Currently, is used to prevent dental caries in children (Dos Santos et al., 2014).

Despite this review do not concern liposomal formulations since it refers to clinical translation other formulations involving NPs, such as liposomal formulations, have been also identified as antimicrobial agents. Most of these formulations rely on the incorporation of traditional antibiotics into nanoliposomes to improve distribution and circulation times (Caster et al., 2017). **Table 2** summarizes antimicrobial liposomes, which are undergoing clinical trials. For example, Amikacin (NCT01315691) is a potent aminoglycoside antibiotic that is useful for the treatment of MDR Gram-negative bacteria. Arikace is an inhaled liposomal formulation that encapsulates amikacin composed of dipalmitoyl-phosphatidylcholine (DPPC) and cholesterol (Meers et al., 2008). These formulation have high drug loading and stability when administrated and in phase II trial, there was no notable difference in toxicity between liposomal drug treatment and placebo (Clancy et al., 2013). Another two-inhaled liposomal formulation are currently in clinical trials. Linhaliq (NCT02104245) is a combination of liposomal and aqueous phase ciprofloxacin, whereas Lipoquin (NCT00889967) is a liposomal ciprofloxacin that allows prolonged drug release. Both of these nanoformulation were developed for the treatment of non-cystic fibrosis bronchiectasis (NCFBE) patients with chronic lung infections with *P. aeruginosa.* Phase II in patients with both CF and non-CF bronchiectasis have been completed. After analysis of clinical data from the two different formulations, Linhaliq showed better performance. The Food and Drug Administration (FDA) has designated Linhaliq as a qualified infection disease product and made it eligible for Fast track designation. In 2016, Pulmanic completed two phases III clinical trials, but has not yet been approved by the FDA. The Hadassah Medical Organization (Jerusalem, Israel) has incorporated quaternary ammonium polyethyleneimine (QA-PEI) based polymers into dental composites. The bacterial membrane may be disturbed by the charged quaternary moiety, it also has potent activity against a series of Gram-positive and -negative pathogens (Ortega et al., 2015). In 2013, these nanoformulation completed phase II trials but no data on outcome have been released to date.

MAT2501 is designed to targeted delivery of the antibiotic amikacin while providing an improved safety and tolerability profile. Currently, Matinas Biopharma has reported positive data from the Phase I study in healthy volunteers for the treatment of MDR Gram-negative bacterial infections and is in preparation for a phase II in patients.

OTHER POTENTIAL APPLICATIONS OF NPS

In the case of non-antibiotic therapy, combinations of NPs with essential oils, peptides and other natural compounds have featured as promising antimicrobial strategies. The therapeutic applications of these substances are often limited by their toxicity and volatility (Chen F. et al., 2009; Allahverdiyev et al., 2011). A recent study has shown that chitosan NPs vectors, modified with eugenol and carvacrol essential oils on their surface, were active against *E. coli* and *S. aureus* at concentrations better or equal to unmodified NPs versions (Chen F. et al., 2009). Furthermore, the toxicity of the conjugates toward mouse fibroblasts was significantly less than the pure oils alone. With regards to peptides, the active sequences can be vulnerable to denaturation, aggregation or hydrolysis within end products or in the human body. Colloidal systems containing NPs are at the forefront of peptide research, as they can be designed to encapsulate and protect peptides during biological transit. Water in oil micelles have been successfully used to increase the potency of antimicrobial peptides against *E. coli* (Gontsarik et al., 2016). In another example, liposomes have been used to improve the stability of encapsulated nisin against pH and temperature extremes thereby increasing its potential in food processing (Taylor et al., 2007). Popular NPs vehicle materials

TABLE 2 | Antimicrobial liposomal nanoformulation in clinical development.

Name	Antimicrobial	Clinical trial phase	Target pathogens	ClinicalTrials.gov Identifier
Arikace	Amikacin	III	Gram-negative bacteria	NCT01315691
Lipoquin	Ciprofloxacin	II	Gram-negative bacteria	NCT00889967
Pulmaquin	Ciprofloxacin	III	Gram-negative bacteria	NCT02104245
Silvasorb	Silver	III	Gram-negative bacteria	NCT00659204
MAT2501	Amikacin	–	Gram-negative bacteria	–
QA-PEI	Ammonium Polyehtyleneimine	I-II	Gram-negative and -positive bacteria	NCT01167985

for peptides include phytoglycogen NPs (Bi et al., 2011), chitosan (Wu et al., 2017), pectin (Krivorotova et al., 2017), and alginate (Khaksar et al., 2014).

NPs have also been applied with tremendous success in biodetection systems, namely as sensors and diagnostics platforms with increased sensitivity and selectivity. Due to the decrease in size of the transduction mechanisms provided by NPs, most of these platforms have found applications at point-of-need and/or point-of-care (Costa et al., 2014; Veigas et al., 2014; Weng et al., 2015; Kim J. et al., 2017; Wang et al., 2017b; Galvan and Yu, 2018; Yang et al., 2018). In some cases, diagnostics/sensing and therapeutic properties have been combined onto single NPs, providing for innovative tools – Nanotheranostics. Recently, several nanotheranostics strategies against bacteria have been described (Kuo et al., 2009; DeGrasse, 2012; Dai X. et al., 2013; Khlebtsov et al., 2013; Kim et al., 2013; Gamella et al., 2014; Pei et al., 2014; Setyawati et al., 2014; Patel and Janjic, 2015; Thompson et al., 2015; Jagtap et al., 2017; Mocan et al., 2017; Zhao et al., 2017).

BOTTLENECKS AND FUTURE CHALLENGES OF NPS

Despite the foreseen potential of NPs for medical applications, there are still several bottlenecks related with their acute and long-term exposure in humans. Several routes of exposure must be considered when evaluating NPs exposure, such as oral and gastrointestinal tract, dermal, respiratory system, and endovenous administration directly to the bloodstream (De Matteis, 2017). It is well known also that the physicochemical properties of NPs (e.g., size, shape and surface chemistry) affect their interaction with biological systems, influencing cellular uptake, pharmacokinetics, biodistribution, all of them with direct impact on final biological effects (for recent reviews see Bakand and Hayes, 2016; Xia et al., 2016; De Matteis, 2017; Warheit, 2018). These aspects have been addressed over the past years *via* the evaluation of the *in vitro* and *in vivo* toxicity of metal and metal oxide NPs (Dobrovolskaia et al., 2007; Asharani et al., 2010; Li et al., 2010; Baek and An, 2011; Hackenberg et al., 2011; Conde et al., 2012, 2014; Bondarenko et al., 2013; Ivask et al., 2014; Larsen et al., 2016; Sukwong et al., 2016; Rai et al., 2017), whose conclusions concerning their nanosafety differ depending on the type of assessment. This poses a major concern to effectively draw critical conclusions on NPs safety due to the vast number of different types/shapes/surface modified nanoparticles, the different methods used to evaluate their safety and environmental effects, and also by the fact most of these *in vitro*/*in vivo* studies present acute studies rather than long-term exposure (Bakand and Hayes, 2016; Xia et al., 2016; De Matteis, 2017; Warheit, 2018). Nevertheless, these *in vivo* and *in vitro* studies have been providing clues to the specific mechanisms by which NPs trigger an adverse effect enabling future surface modification of NPs to make them safer and less toxic (De Matteis, 2017). These concerns relating to nanosafety have been addressed and implemented *via* European Commission FP7 and H2020-sponsored programs followed by some relevant conclusions issued by the US National Academy of Science Committee on Research Progress of Environmental Health and Safety Aspects of Engineered Nanomaterials (Warheit, 2018).

Due to the 3Rs (Replacement, Reduction and Refinement) policies of *in vivo* studies, the future challenge of Regulatory Agencies is the standardization of the *in vitro* methodologies to establish the toxicology profile of NPs based on good laboratory practice (GLP) and the construction of flexible and reliable databases in which NPs are classified according to the data derived from these toxicological investigations. Together, these efforts might provide information on the dosage at which a particular NP can be considered safe and thus appropriate for medical use.

CHALLENGES OF CURRENT RESEARCH

As mentioned above, nanomaterials have great potential to prevent and treat bacterial infection, but several challenges remain for the translation to the clinics. Some of these include assessing the interactions of nanoantibiotics with cells, tissues and organs, for dose recalibration and identification of appropriate routes of administration (Sandhiya et al., 2009). The biocompatibility of NPs is generally evaluated through *in vitro* assays, using cell culture. Because NPs, used as antimicrobial agents can enter through skin contact, ingestion, inhalation, oral and intravenous injection, *in vivo* models must also be applied to better understand their effects, including potential toxicity, clearance and metabolism (Beyth et al., 2015). Several studies have shown that intravenously injected NPs accumulate in the colon, lung, bone marrow, liver, spleen and lymphatics (Hagens et al., 2007). Inhalation has also been shown to cause cytotoxicity at the lung, and in the liver, heart and spleen through systemic circulation (Poma and Di Giorgio, 2008; Leucuta, 2013). This is of particular relevance for small NPs because of efficient cellular

uptake and transcytosis across epithelial and endothelial cells into the blood and lymphatic circulation. Several NPs systems have demonstrated toxicity in multiple organs, such as free radical-mediated oxidative stress generated by the interaction of antimicrobial NPs with cell components that can result in hepatotoxicity and nephrotoxicity (De Jong and Borm, 2008; Lei et al., 2008).

The effective translation to the clinics will require appropriate guidelines for production and scale-up of manufacturing these nanomaterials, for characterization of the physico-chemical properties and their impact on biocompatibility, for standardization of nanotoxicology assays and protocols to assist easy comparison of data originating from *in vitro* and *in vivo* studies, for the evaluation of their metabolism and mode of action (Duncan and Gaspar, 2011; Bertrand and Leroux, 2012; Beyth et al., 2015; Cordeiro et al., 2016; Rai M. et al., 2016; Zazo et al., 2016). Finally, the community still needs to address the economic impact of translation of these nanomaterials to the clinics.

CONCLUSIONS

Given their vast therapeutic potential, it is becoming increasingly important to understand the mechanisms by which NPs complexes can impact bacterial viability. While one of the beneficial aspects of NPs drug carriers involves "macro-targeting," *i.e.*, specific delivery to the site of infection, understanding the "micro-targeting" of bacterial mechanisms is imperative for the widespread future use of these vectors. Their impact of cell functions such as cell wall permeability, efflux activity, formation of reactive species, and inhibition of essential cellular metabolism and reproduction is of utmost importance.

AUTHOR CONTRIBUTIONS

PB supervision and correction of Nanoparticles part of the manuscript; MPM supervision and correction of MDR bacteria part of the manuscript; AC draft Nanoparticles part of the manuscript, figure draw, tables design; DF draft MDR bacteria part of the manuscript; NM draft MDR bacteria part of the manuscript; MM coordination of MDR bacteria part of the manuscript and final correction and integration; AF coordination of Nanoparticles part of the manuscript and final correction and integration.

ACKNOWLEDGMENTS

This work was supported by the Unidade de Ciências Biomoleculares Aplicadas-UCIBIO, which is financed by National Funds from FCT/MEC (PTDC_CVT-EPI_6685_2014; UID/Multi/04378/2013) and co-financed by the ERDF under the PT2020 Partnership Agreement (POCI-01-0145-FEDER-007728). DF is funded by the Trinity College Dublin Postgraduate Research (1252) Studentship. NM is funded by the Irish Research Council under the employment-based programme EBPPG/2015/233 in conjunction with Nuritas limited. We would like to acknowledge Ana Sofia Santos for preliminary revision of the manuscript.

REFERENCES

Acharya, D., Singha, K. M., Pandey, P., Mohanta, B., Rajkumari, J., and Singha, L. P. (2018). Shape dependent physical mutilation and lethal effects of silver nanoparticles on bacteria. *Sci. Rep.* 8:201. doi: 10.1038/s41598-017-18590-6

Aderibigbe, B. A. (2017). Metal-based nanoparticles for the treatment of infectious diseases. *Molecules* 22:E1370. doi: 10.3390/molecules22081370

Ali, K., Dwivedi, S., Azam, A., Saquib, Q., Al-Said, M. S., Alkhedhairy, A. A., et al. (2016). Aloe vera extract functionalized zinc oxide nanoparticles as nanoantibiotics against multi-drug resistant clinical bacterial isolates. *J. Colloid Interface Sci.* 472, 145–156. doi: 10.1016/j.jcis.2016.03.021

Allahverdiyev, A. M., Kon, K. V., Abamor, E. S., Bagirova, M., and Rafailovich, M. (2011). Coping with antibiotic resistance: combining nanoparticles with antibiotics and other antimicrobial agents. *Expert Rev. AntiInfect. Ther.* 9, 1035–1052. doi: 10.1586/eri.11.121

AlMatar, M., Makky, E. A., Var, I., and Koksal, F. (2017). The role of nanoparticles in the inhibition of multidrug-resistant bacteria and biofilms. *Curr. Drug Deliv.* 15, 470–484. doi: 10.2174/1567201815666171207163504

Andrade, F., Rafael, D., Videira, M., Ferreira, D., Sosnik, A., and Sarmento, B. (2013). Nanotechnology and pulmonary delivery to overcome resistance in infectious diseases. *Adv. Drug Deliv. Rev.* 65, 1816–1827. doi: 10.1016/j.addr.2013.07.020

Ansari, M. A., Khan, H. M., Khan, A. A., Cameotra, S. S., Saquib, Q., and Musarrat, J. (2014). Interaction of Al(2)O(3) nanoparticles with *Escherichia coli* and their cell envelope biomolecules. *J. Appl. Microbiol.* 116, 772–783. doi: 10.1111/jam.12423

Ansari, M. A., Khan, H. M., Khan, A. A., Pal, R., and Cameotra, S. S. (2013). Antibacterial potential of Al2O3 nanoparticles against multidrug resistance strains of *Staphylococcus aureus* isolated from skin exudates. *J. Nanoparticle Res.* 15:1970. doi: 10.1007/s11051-013-1970-1

Antonelli, M., De Pascale, G., Ranieri, V. M., Pelaia, P., Tufano, R., Piazza, O., et al. (2012). Comparison of triple-lumen central venous catheters impregnated with silver nanoparticles (AgTive®) vs conventional catheters in intensive care unit patients. *J. Hosp. Infect.* 82, 101–107. doi: 10.1016/j.jhin.2012.07.010

Argueta-Figueroa, L., Morales-Luckie, R. A., Scougall-Vilchis, R. J., and Olea-Mejía, O. F. (2014). Synthesis, characterization and antibacterial activity of copper, nickel and bimetallic Cu-Ni nanoparticles for potential use in dental materials. *Prog. Nat. Sci. Mater. Int.* 24, 321–328. doi: 10.1016/j.pnsc.2014.07.002

Arvizo, R., Bhattacharya, R., and Mukherjee, P. (2010). Gold nanoparticles: opportunities and challenges in nanomedicine. *Expert Opin. Drug Deliv.* 7, 753–763. doi: 10.1517/17425241003777010

Asharani, P. V., Xinyi, N., Hande, M. P., and Valiyaveettil, S. (2010). DNA damage and p53-mediated growth arrest in human cells treated with platinum nanoparticles. *Nanomedicine* 5, 51–64. doi: 10.2217/nnm.09.85

Ashfaq, M., Verma, N., and Khan, S. (2016). Copper/zinc bimetal nanoparticles-dispersed carbon nanofibers: a novel potential antibiotic material. *Mater. Sci. Eng. C* 59, 938–947. doi: 10.1016/j.msec.2015.10.079

Aswathanarayan, J. B., and Vittal, R. R. (2017). Antimicrobial, biofilm inhibitory and anti-infective activity of metallic nanoparticles against pathogens *MRSA* and *Pseudomonas aeruginosa* PA01. *Pharm. Nanotechnol.* 5, 148–153. doi: 10.2174/2211738505666170424121944

Aydin Sevinç, B., and Hanley, L. (2010). Antibacterial activity of dental composites containing zinc oxide nanoparticles. *J. Biomed. Mater. Res. B Appl. Biomater.* 94, 22–31. doi: 10.1002/jbm.b.31620

Babes, L., Denizot, B., Tanguy, G., Le Jeune, J. J., and Jallet, P. (1999). Synthesis of iron oxide nanoparticles used as MRI contrast agents: a parametric study. *J. Colloid Interface Sci.* 212, 474–482. doi: 10.1006/jcis.1998.6053

Baek, Y.-W., and An, Y.-J. (2011). Microbial toxicity of metal oxide nanoparticles (CuO, NiO, ZnO, and Sb2O3) to *Escherichia coli*, *Bacillus*

subtilis, and *Streptococcus aureus*. *Sci. Total Environ.* 409, 1603–1608. doi: 10.1016/j.scitotenv.2011.01.014

Bahar, A., and Ren, D. (2013). Antimicrobial peptides. *Pharmaceuticals* 6, 1543–1575. doi: 10.3390/ph6121543

Bakand, S., and Hayes, A. (2016). Toxicological considerations, toxicity assessment, and risk management of inhaled nanoparticles. *Int. J. Mol. Sci.* 17:E929. doi: 10.3390/ijms17060929

Baker, S., Pasha, A., and Satish, S. (2017). Biogenic nanoparticles bearing antibacterial activity and their synergistic effect with broad spectrum antibiotics:emerging strategy to combat drug resistant pathogens. *Saudi Pharm. J.* 25, 44–51. doi: 10.1016/j.jsps.2015.06.011

Bassegoda, A., Ivanova, K., Ramon, E., and Tzanov, T. (2018). Strategies to prevent the occurrence of resistance against antibiotics by using advanced materials. *Appl. Microbiol. Biotechnol.* 102, 2075–2089. doi: 10.1007/s00253-018-8776-0

Behera, S. S., Patra, J. K., Pramanik, K., Panda, N., and Thatoi, H. (2012). Characterization and evaluation of antibacterial activities of chemically synthesized iron oxide nanoparticles. *World J. Nano Sci. Eng.* 2, 196–200. doi: 10.4236/wjnse.2012.24026

Berry, C. C., and Curtis, A. S. G. (2003). Functionalisation of magnetic nanoparticles for applications in biomedicine. *J. Phys. D. Appl. Phys.* 36, R198–R206. doi: 10.1088/0022-3727/36/13/203

Bertrand, N., and Leroux, J. C. (2012). The journey of a drug-carrier in the body: an anatomo-physiological perspective. *J. Control. Release* 161, 152–163. doi: 10.1016/j.jconrel.2011.09.098

Beyth, N., Houri-Haddad, Y., Domb, A., Khan, W., and Hazan, R. (2015). Alternative antimicrobial approach: nano-antimicrobial materials. *Evid. Based Complement. Altern. Med.* 2015, 1–16. doi: 10.1155/2015/246012

Bi, L., Yang, L., Narsimhan, G., Bhunia, A., and Yao, Y. (2011). Designing carbohydrate nanoparticles for prolonged efficacy of antimicrobial peptide. *J. Control Release* 150, 150–156. doi: 10.1016/j.jconrel.2010.11.024

Bjarnsholt, T., (2013). The role of bacterial biofilms in chronic infections. *APMIS* 121, 1–58. doi: 10.1111/apm.12099

Boman, H. G., Wade, D., Boman, I. A., Wåhlin, B., and Merrifield, R. B. (1989). Antibacterial and antimalarial properties of peptides that are cecropin-melittin hybrids. *FEBS Lett.* 259, 103–106. doi: 10.1016/0014-5793(89)81505-4

Bondarenko, O., Ivask, A., Käkinen, A., Kurvet, I., and Kahru, A. (2013). Particle-cell contact enhances antibacterial activity of silver nanoparticles. *PLoS ONE* 8:e64060. doi: 10.1371/journal.pone.0064060

Brandelli, A. (2012). Nanostructures as promising tools for delivery of antimicrobial peptides. *Mini Rev. Med. Chem.* 12, 731–741. doi: 10.2174/138955712801264774

Bresee, J., Bond, C. M., Worthington, R. J., Smith, C. A., Gifford, J. C., Simpson, C. A., et al. (2014). Nanoscale structure–activity relationships, mode of action, and biocompatibility of gold nanoparticle antibiotics. *J. Am. Chem. Soc.* 136, 5295–5300. doi: 10.1021/ja408505n

Brown, A. N., Smith, K., Samuels, T. A., Lu, J., Obare, S. O., and Scott, M. E. (2012). Nanoparticles functionalized with ampicillin destroy multiple-antibiotic-resistant isolates of *Pseudomonas aeruginosa* and *Enterobacter aerogenes* and methicillin-resistant *Staphylococcus aureus*. *Appl. Environ. Microbiol.* 78, 2768–2774. doi: 10.1128/AEM.06513-11

Burygin, G., Khlebtsov, B., Shantrokha, A., Dykman, L., Bogatyrev, V., Khlebtsov, N., et al. (2009). On the enhanced antibacterial activity of antibiotics mixed with gold nanoparticles. *Nanoscale Res. Lett.* 4, 794–801. doi: 10.1007/s11671-009-9316-8

Casciaro, B., Moros, M., Rivera-Fernández, S., Bellelli, A., de la Fuente, J. M., and Mangoni, M. L. (2017). Gold-nanoparticles coated with the antimicrobial peptide esculentin-1a(1-21)NH2 as a reliable strategy for antipseudomonal drugs. *Acta Biomater.* 47, 170–181. doi: 10.1016/j.actbio.2016.09.041

Caster, J. M., Patel, A. N., Zhang, T., and Wang, A. (2017). Investigational nanomedicines in 2016: a review of nanotherapeutics currently undergoing clinical trials. *Wiley Interdiscip. Rev. Nanomed. Nanobiotechnol.* 9:e1416. doi: 10.1002/wnan.1416

Cavassin, E. D., de Figueiredo, L. F. P., Otoch, J. P., Seckler, M. M., de Oliveira, R. A., Franco, F. F., et al. (2015). Comparison of methods to detect the *in vitro* activity of silver nanoparticles (AgNP) against multidrug resistant bacteria. *J. Nanobiotechnol.* 13, 1–16. doi: 10.1186/s12951-015-0120-6

Cha, S. H., Hong, J., McGuffie, M., Yeom, B., Vanepps, J. S., and Kotov, N. A. (2015). Shape-dependent biomimetic inhibition of enzyme by nanoparticles and their antibacterial activity. *ACS Nano* 9, 9097–9105. doi: 10.1021/acsnano.5b03247

Chakraborti, S., Mandal, A. K., Sarwar, S., Singh, P., Chakraborty, R., and Chakrabarti, P. (2014). Bactericidal effect of polyethyleneimine capped ZnO nanoparticles on multiple antibiotic resistant bacteria harboring genes of high-pathogenicity island. *Colloids Surf. B. Biointerfaces* 121, 44–53. doi: 10.1016/j.colsurfb.2014.03.044

Chakraborty, R., Sarkar, R. K., Chatterjee, A. K., Manju, U., Chattopadhyay, A. P., and Basu, T. (2015). A simple, fast and cost-effective method of synthesis of cupric oxide nanoparticle with promising antibacterial potency: unraveling the biological and chemical modes of action. *Biochim. Biophys. Acta Gen. Subj.* 1850, 845–856. doi: 10.1016/j.bbagen.2015.01.015

Chang, T. Y., Chen, C. C., Cheng, K. M., Chin, C. Y., Chen, Y. H., Chen, X. A., et al. (2017). Trimethyl chitosan-capped silver nanoparticles with positive surface charge: their catalytic activity and antibacterial spectrum including multidrug-resistant strains of *Acinetobacter baumannii*. *Colloids Surf. B. Biointerfaces* 155, 61–70. doi: 10.1016/j.colsurfb.2017.03.054

Chaurasia, A. K., Thorat, N. D., Tandon, A., Kim, J. H., Park, S. H., and Kim, K. K. (2016). Coupling of radiofrequency with magnetic nanoparticles treatment as an alternative physical antibacterial strategy against multiple drug resistant bacteria. *Sci. Rep.* 6, 1–13. doi: 10.1038/srep33662

Chen, C. W., Hsu, C. Y., Lai, S. M., Syu, W. J., Wang, T. Y., and Lai, P. S. (2014). Metal nanobullets for multidrug resistant bacteria and biofilms. *Adv. Drug Deliv. Rev.* 78, 88–104. doi: 10.1016/j.addr.2014.08.004

Chen, F., Shi, Z., Neoh, K., and Kang, E. (2009). Antioxidant and antibacterial activities of eugenol and carvacrol-grafted chitosan nanoparticles. *Biotechnol Bioeng.* 104, 30–39. doi: 10.1002/bit.22363

Chen, J., Hessler, J. A., Putchakayala, K., Panama, B. K., Khan, D. P., Hong, S., et al. (2009). Cationic nanoparticles induce nanoscale disruption in living cell plasma membranes. *J. Phys. Chem. B* 113, 11179–11185. doi: 10.1021/jp9033936

Cho, K. H., Park, J. E., Osaka, T., and Park, S. G. (2005). The study of antimicrobial activity and preservative effects of nanosilver ingredient. *Electrochim. Acta* 51, 956–960. doi: 10.1016/j.electacta.2005.04.071

Choi, S. R., Britigan, B. E., Moran, D. M., and Narayanasamy, P. (2017). Gallium nanoparticles facilitate phagosome maturation and inhibit growth of virulent *Mycobacterium tuberculosis* in macrophages. *PLoS ONE* 12:e0177987. doi: 10.1371/journal.pone.0177987

Chopra, I. (2007). The increasing use of silver-based products as antimicrobial agents: a useful development or a cause for concern? *J. Antimicrob. Chemother.* 59, 587–590. doi: 10.1093/jac/dkm006

Claeys, K. C., Heil, E. L., Pogue, J. M., Lephart, P. R., and Johnson, J. K. (2018). The Verigene dilemma: gram-negative polymicrobial bloodstream infections and clinical decision making. *Diagn. Microbiol. Infect. Dis.* 91, 144–146. doi: 10.1016/j.diagmicrobio.2018.01.012

Clancy, J. P., Dupont, L., Konstan, M. W., Billings, J., Fustik, S., Goss, C. H., et al. (2013). Phase II studies of nebulised Arikace in CF patients with *Pseudomonas aeruginosa* infection. *Thorax* 68, 818–825. doi: 10.1136/thoraxjnl-2012-202230

Conde, J., Doria, G., and Baptista, P. V. (2012). Noble metal nanoparticles applications in cancer. *J. Drug Deliv.* 2012:751075. doi: 10.1155/2012/751075

Conde, J., Larguinho, M., Cordeiro, A., Raposo, L. R., Costa, M., Santos, S., et al. (2014). Gold-Nanobeacons for gene therapy : evaluation of genotoxicity, cell toxicity and proteome profiling analysis. *Nanotocicology* 8, 521–532. doi: 10.3109/17435390.2013.802821

Cordeiro, M., Ferreira Carlos, F., Pedrosa, P., Lopez, A., and Baptista, P. V. (2016). Gold nanoparticles for diagnostics: advances towards points of care. *Diagnostics* 6:43. doi: 10.3390/diagnostics6040043

Costa, M. N., Veigas, B., Jacob, J. M., Santos, D. S., Gomes, J., Baptista, P. V., et al. (2014). A low cost, safe, disposable, rapid and self-sustainable paper-based platform for diagnostic testing: lab-on-paper. *Nanotechnology* 25:94006. doi: 10.1088/0957-4484/25/9/094006

Courtney, C. M., Goodman, S. M., Nagy, T. A., Levy, M., Bhusal, P., Madinger, N. E., et al. (2017). Potentiating antibiotics in drug-resistant clinical isolates via stimuli-activated superoxide generation. *Sci. Adv.* 3:e1701776. doi: 10.1126/sciadv.1701776

Cui, Y., Zhao, Y., Tian, Y., Zhang, W., Lu, X., and Jiang, X. (2012). The molecular mechanism of action of bactericidal gold nanoparticles on *Escherichia coli*. *Biomaterials* 33, 2327–2333. doi: 10.1016/j.biomaterials.2011.11.057

Dai, T., Gupta, A., Murray, C. K., Vrahas, M. S., Tegos, G. P., and Hamblin, M. R. (2013). Blue Light for infectious diseases: *Propionibacterium acnes*, *Helicobacter pylori*, and beyond? *Drug Resist.* 15, 223–236. doi: 10.1016/j.drup.2012.07.001.Blue

Dai, X., Fan, Z., Lu, Y., and Ray, P. C. (2013). Multifunctional nanoplatforms for targeted multidrug-resistant-bacteria theranostic applications. *ACS Appl. Mater. Interfaces* 5, 11348–11354. doi: 10.1021/am403567k

Dakal, T. C., Kumar, A., Majumdar, R. S., and Yadav, V. (2016). Mechanistic basis of antimicrobial actions of silver nanoparticles. *Front. Microbiol.* 7:1831. doi: 10.3389/fmicb.2016.01831

De Jong, W. H., and Borm, P. J., a (2008). Drug delivery and nanoparticles:applications and hazards. *Int. J. Nanomedicine* 3, 133–149. doi: 10.2147/IJN.S596

De Matteis, V. (2017). Exposure to inorganic nanoparticles: routes of entry, immune response, biodistribution and *in vitro*/*in vivo* toxicity evaluation. *Toxics* 5:E29. doi: 10.3390/toxics5040029

DeGrasse, J. A. (2012). A single-stranded DNA aptamer that selectively binds to *Staphylococcus aureus* enterotoxin B. *PLoS ONE* 7:e33410. doi: 10.1371/journal.pone.0033410

Ding, F., Songkiatisak, P., Cherukuri, P. K., Huang, T., and Xu, X.-H. N. (2018). Size-dependent inhibitory effects of antibiotic drug nanocarriers against *Pseudomonas aeruginosa*. *ACS Omega* 3, 1231–1243. doi: 10.1021/acsomega.7b01956

Djafari, J., Marinho, C., Santos, T., Igrejas, G., Torres, C., Capelo, J. L., et al. (2016). New synthesis of gold- and silver-based nano-tetracycline composites. *ChemistryOpen* 5, 206–212. doi: 10.1002/open.201600016

Dobrovolskaia, M. A., McNeil, S. E., and Neil, S. E. M. (2007). Immunological properties of engineered nanomaterials. *Nat. Nanotechnol.* 2, 469–478. doi: 10.1038/nnano.2007.223

Doria, G., Larguinho, M., Dias, J. T., Pereira, E., Franco, R., and Baptista, P., V (2010). Gold–silver-alloy nanoprobes for one-pot multiplex DNA detection. *Nanotechnology* 21:255101. doi: 10.1088/0957-4484/21/25/255101

dos Santos, M. M., Queiroz, M. J., and Baptista, P. V. (2012). Enhancement of antibiotic effect via gold:silver-alloy nanoparticles. *J. Nanoparticle Res.* 14:859. doi: 10.1007/s11051-012-0859-8

Dos Santos, V. E., Filho, A. V., Ribeiro Targino, A. G., Pelagio Flores, M. A., Galembeck, A., Caldas, A. F., et al. (2014). A new "silver-Bullet" to treat caries in children - Nano Silver Fluoride: a randomised clinical trial. *J. Dent.* 42, 945–951. doi: 10.1016/j.jdent.2014.05.017

Duncan, R., and Gaspar, R. (2011). Nanomedicine(s) under the microscope. *Mol. Pharm.* 8, 2101–2141. doi: 10.1021/mp200394t

Durán, N., Durán, M., de Jesus, M. B., Seabra, A. B., Fávaro, W. J., and Nakazato, G. (2016). Silver nanoparticles: a new view on mechanistic aspects on antimicrobial activity. *Nanomed. Nanotechnol. Biol. Med.* 12, 789–799. doi: 10.1016/j.nano.2015.11.016

Durán, N., Marcato, P. D., De Conti, R., Alves, O. L., Costa, F. T. M., and Brocchi, M. (2010). Potential use of silver nanoparticles on pathogenic bacteria, their toxicity and possible mechanisms of action. *J. Braz. Chem. Soc.* 21, 949–959. doi: 10.1590/s0103-50532010000600002

Dwivedi, S., Wahab, R., Khan, F., Mishra, Y. K., Musarrat, J., and Al-Khedhairy, A. A. (2014). Reactive oxygen species mediated bacterial biofilm inhibition via zinc oxide nanoparticles and their statistical determination. *PLoS ONE* 9:e111289. doi: 10.1371/journal.pone.0111289

Ehsan, S., and Sajjad, M. (2017). Bioinspired synthesis of zinc oxide nanoparticle and its combined efficacy with different antibiotics against multidrug resistant bacteria. *J. Biomater. Nanobiotechnol.* 8, 159–175. doi: 10.4236/jbnb.2017.82011

El Din, S. N., El-Tayeb, T. A., Abou-Aisha, K., and El-Azizi, M. (2016). *In vitro* and *in vivo* antimicrobial activity of combined therapy of silver nanoparticles and visible blue light against *Pseudomonas aeruginosa*. *Int. J. Nanomedicine* 11, 1749–1758. doi: 10.2147/IJN.S102398

El-Zowalaty, M. E., Al-Ali, S. H. H., Husseiny, M. I., Geilich, B. M., Webster, T. J., and Hussein, M. Z. (2015). The ability of streptomycin-loaded chitosan-coated magnetic nanocomposites to possess antimicrobial and antituberculosis activities. *Int. J. Nanomed.* 10, 3269–3274. doi: 10.2147/IJN.S74469

Esmaeillou, M., Zarrini, G., Rezaee, M. A., Mojarrad, J. S., and Bahadori, A. (2017). Vancomycin capped with silver nanoparticles as an antibacterial agent against multi-drug resistance bacteria. *Adv. Pharm. Bull.* 7, 479–483. doi: 10.15171/apb.2017.058

Espitia, P. J. P., Soares, N., de, F. F., Coimbra, J. S. dos, R., de Andrade, N. J., Cruz, R. S., and Medeiros, E. A. A. (2012). Zinc oxide nanoparticles: synthesis, antimicrobial activity and food packaging applications. *Food Bioprocess Technol.* 5, 1447–1464. doi: 10.1007/s11947-012-0797-6

Fakhri, A., Tahami, S., and Naji, M. (2017). Synthesis and characterization of core-shell bimetallic nanoparticles for synergistic antimicrobial effect studies in combination with doxycycline on burn specific pathogens. *J. Photochem. Photobiol. B Biol.* 169, 21–26. doi: 10.1016/j.jphotobiol.2017.02.014

Fernandes, A. R., and Baptista, P. V. (2017). Gene silencing using multifunctionalized gold nanoparticles for cancer therapy. *Methods Mol. Biol.* 1530, 319–336. doi: 10.1007/978-1-4939-6646-2_19

Fernandes, A. R., Jesus, J., Martins, P., Figueiredo, S., Rosa, D., Martins, L. M., et al. (2017). Multifunctional gold-nanoparticles: a nanovectorization tool for the targeted delivery of novel chemotherapeutic agents. *J. Control. Release* 245, 52–61. doi: 10.1016/j.jconrel.2016.11.021

Foster, H. A., Ditta, I. B., Varghese, S., and Steele, A. (2011). Photocatalytic disinfection using titanium dioxide: spectrum and mechanism of antimicrobial activity. *Appl. Microbiol. Biotechnol.* 90, 1847–1868. doi: 10.1007/s00253-011-3213-7

Franci, G., Falanga, A., Galdiero, S., Palomba, L., Rai, M., Morelli, G., et al. (2015). Silver nanoparticles as potential antibacterial agents. *Molecules* 20, 8856–8874. doi: 10.3390/molecules20058856

Galanzha, E. I., Shashkov, E., Sarimollaoglu, M., Beenken, K. E., Basnakian, A. G., Shirtliff, M. E., et al. (2012). *In vivo* magnetic enrichment, photoacoustic diagnosis, and photothermal purging of infected blood using multifunctional gold and magnetic nanoparticles. *PLoS ONE* 7:e45557. doi: 10.1371/journal.pone.0045557

Galvan, D. D., and Yu, Q. (2018). Surface-enhanced raman scattering for rapid detection and characterization of antibiotic-resistant bacteria. *Adv. Healthc. Mater.* doi: 10.1002/adhm.201701335. [Epub ahead of print].

Gamella, M., Guz, N., Mailloux, S., Pingarrón, J. M., and Katz, E. (2014). Antibacterial drug release electrochemically stimulated by the presence of bacterial cells - theranostic approach. *Electroanalysis* 26, 2552–2557. doi: 10.1002/elan.201400473

Gao, W., Chen, Y., Chang, Y., Zhang, Y., Chang, Q., and Zhang, L. (2018). Nanoparticle-based local antimicrobial drug delivery. *Adv Drug Deliv Rev.* 127, 46–57. doi: 10.1016/j.addr.2017.09.015

Gao, W., Thamphiwatana, S., Angsantikul, P., and Zhang, L. (2014). Nanoparticle approaches against bacterial infections. *Wiley Interdiscip. Rev. Nanomed. Nanobiotechnol.* 6, 532–547. doi: 10.1002/wnan.1282

García-Lara, B., Saucedo-Mora, M. Á., Roldán-Sánchez, J. A., Pérez-Eretza, B., Ramasamy, M., Lee, J., et al. (2015). Inhibition of quorum-sensing-dependent virulence factors and biofilm formation of clinical and environmental *Pseudomonas aeruginosa* strains by ZnO nanoparticles. *Lett Appl Microbiol.* 61, 299–305. doi: 10.1111/lam.12456

Gelabert, A., Sivry, Y., Gobbi, P., Mansouri-Guilani, N., Menguy, N., Brayner, R., et al. (2016). Testing nanoeffect onto model bacteria: impact of speciation and genotypes. *Nanotoxicology* 10, 216–225. doi: 10.3109/17435390.2015.1048323

Gholipourmalekabadi, M., Mobaraki, M., Ghaffari, M., Zarebkohan, A., Omrani, V., Urbanska, A., et al. (2017). Targeted drug delivery based on gold nanoparticle derivatives. *Curr. Pharm. Des.* 23, 2918–2929. doi: 10.2174/1381612823666170419105413

Gil-Tomás, J., Tubby, S., Parkin, I. P., Narband, N., Dekker, L., Nair, S. P., et al. (2007). Lethal photosensitisation of *Staphylococcus aureus* using a toluidine blue O–tiopronin–gold nanoparticle conjugate. *J. Mater. Chem.* 17:3739. doi: 10.1039/b706615e

Gontsarik, M., Buhmann, M., Yaghmur, A., Ren, Q., Maniura-Weber, K., and Salentinig, S. (2016). Antimicrobial peptide - driven colloidal transformations in liquid crystalline nanocarriers. *J. Phys. Chem. Lett.* 7, 3482–3486. doi: 10.1021/acs.jpclett.6b01622

Govindaraju, S., Samal, M., and Yun, K. (2016). Superior antibacterial activity of GlcN-AuNP-GO by ultraviolet irradiation. *Mater. Sci. Eng. C* 69, 366–372. doi: 10.1016/j.msec.2016.06.052

Gu, H., Ho, P. L., Tong, E., Wang, L., and Xu, B. (2003). Presenting vancomycin on nanoparticles to enhance antimicrobial activities. *Nano Lett.* 3, 1261–1263. doi: 10.1021/nl034396z

Hackenberg, S., Scherzed, A., Kessler, M., Hummel, S., Technau, A., Froelich, K., et al. (2011). Silver nanoparticles: evaluation of DNA damage, toxicity and

functional impairment in human mesenchymal stem cells. *Toxicol. Lett.* 201, 27–33. doi: 10.1016/j.toxlet.2010.12.001

Hadiya, S., Liu, X., Abd El-Hammed, W., Elsabahy, M., and Aly, S. A. (2018). Levofloxacin-loaded nanoparticles decrease emergence of fluoroquinolone resistance in *Escherichia coli*. *Microb. Drug Resist.* doi: 10.1089/mdr.2017.0304. [Epub ahead of print].

Hagens, W. I., Oomen, A. G., de Jong, W. H., Cassee, F. R., and Sips, A. J. A. M. (2007). What do we (need to) know about the kinetic properties of nanoparticles in the body? *Regul. Toxicol. Pharmacol.* 49, 217–229. doi: 10.1016/j.yrtph.2007.07.006

Hall-Stoodley, L., Costerton, J. W., and Stoodley, P. (2004). Bacterial biofilms: from the Natural environment to infectious diseases. *Nat. Rev. Microbiol.* 2, 95–108. doi: 10.1038/nrmicro821

Hemeg, H. A. (2017). Nanomaterials for alternative antibacterial therapy. *Int. J. Nanomed.* 12, 8211–8225. doi: 10.2147/IJN.S132163

Høiby, N., Ciofu, O., Johansen, H. K., Song, Z.-J., Moser, C., Jensen, P. Ø., et al. (2011). The clinical impact of bacterial biofilms. *Int J Oral Sci.* 3, 55–65. doi: 10.4248/IJOS11026

Hsueh, Y. H., Ke, W. J., Hsieh, C., Te, L.in, K. S., Tzou, D. Y., and Chiang, C. L. (2015). ZnO nanoparticles affect bacillus subtilis cell growth and biofilm formation. *PLoS ONE* 10:e0128457. doi: 10.1371/journal.pone.0128457

Hu, D., Li, H., Wang, B., Ye, Z., Lei, W., Jia, F., et al. (2017). Surface-adaptive gold nanoparticles with effective adherence and enhanced photothermal ablation of methicillin-resistant *Staphylococcus aureus* biofilm. *ACS Nano* 11, 9330–9339. doi: 10.1021/acsnano.7b04731

Huang, N., Chen, X., Zhu, X., Xu, M., and Liu, J. (2017). Ruthenium complexes/polypeptide self-assembled nanoparticles for identification of bacterial infection and targeted antibacterial research. *Biomaterials* 141, 296–313. doi: 10.1016/j.biomaterials.2017.07.005

Huang, Y., Yu, F., Park, Y., Wang, J., Shin, M., Chung, H., et al. (2010). Co-administration of protein drugs with gold nanoparticles to enable percutaneous delivery. *Biomaterials* 31, 9086–9091. doi: 10.1016/j.biomaterials.2010.08.046

Huh, A. J., and Kwon, Y. J. (2011). "Nanoantibiotics": a new paradigm for treating infectious diseases using nanomaterials in the antibiotics resistant era. *J. Control. Release* 156, 128–145. doi: 10.1016/j.jconrel.2011.07.002

Iravani, S., Korbekandi, H., Mirmohammadi, S. V., and Zolfaghari, B. (2014). Synthesis of silver nanoparticles: chemical, physical and biological methods. *Res. Pharm. Sci.* 9, 385–406.

Ivask, A., Juganson, K., Bondarenko, O., Mortimer, M., Aruoja, V., Kasemets, K., et al. (2014). Mechanisms of toxic action of Ag, ZnO and CuO nanoparticles to selected ecotoxicological test organisms and mammalian cells *in vitro*: a comparative review. *Nanotoxicology* 8, 57–71. doi: 10.3109/17435390.2013.855831

Jagtap, P., Sritharan, V., and Gupta, S. (2017). Nanotheranostic approaches for management of bloodstream bacterial infections. *Nanomedicine* 13, 329–341. doi: 10.1016/j.nano.2016.09.005

Jaiswal, S., Bhattacharya, K., McHale, P., and Duffy, B. (2015). Dual effects of β-cyclodextrin-stabilised silver nanoparticles: enhanced biofilm inhibition and reduced cytotoxicity. *J. Mater. Sci. Mater. Med.* 26, 1–10. doi: 10.1007/s10856-014-5367-1

Jakobsen, T. H., Tolker-Nielsen, T., and Givskov, M. (2017). Bacterial biofilm control by perturbation of bacterial signaling processes. *Int. J. Mol. Sci.* 18:E1970. doi: 10.3390/ijms18091970

Jankauskaite, V., Vitkauskiene, A., Lazauskas, A., Baltrusaitis, J., Prosyčevas, I., and Andrulevičius, M. (2016). Bactericidal effect of graphene oxide/Cu/Ag nanoderivatives against *Escherichia coli*, *Pseudomonas aeruginosa*, *Klebsiella pneumoniae*, *Staphylococcus aureus* and Methicillin-resistant *Staphylococcus aureus*. *Int. J. Pharm.* 511, 90–97. doi: 10.1016/j.ijpharm.2016.06.121

Joost, U., Juganson, K., Visnapuu, M., Mortimer, M., Kahru, A., Nommiste, E., et al. (2015). Photocatalytic antibacterial activity of nano-TiO2 (anatase)-based thin films: effects on *Escherichia coli* cells and fatty acids. *J. Photochem. Photobiol. B* 142, 178–185. doi: 10.1016/j.jphotobiol.2014.12.010

Jung, W. K., Koo, H. C., Kim, K. W., Kim, S. H., Park, Y. H., Jung, W. K., et al. (2008). Antibacterial activity and mechanism of action of the silver ion in *Staphylococcus aureus* and *Escherichia coli*. *Appl. Environ. Microbiol.* 74, 2171–2178. doi: 10.1128/AEM.02001-07

Kadiyala, U., Kotov, N. A., and VanEpps, J. S. (2018). Antibacterial metal oxide nanoparticles: challenges in interpreting the literature. *Curr. Pharm. Des.* 24, 896–903. doi: 10.2174/1381612824666180219130659

Karimi, F., Dabbagh, S., Alizadeh, S., and Rostamnia, S. (2016). Evaluation of AgClNPs@SBA-15/IL nanoparticle-induced oxidative stress and DNA mutation in *Escherichia coli*. *Appl. Microbiol. Biotechnol.* 100, 7161–7170. doi: 10.1007/s00253-016-7593-6

Kato, N., Morohoshi, T., Nozawa, T., Matsumoto, H., and Ikeda, T. (2006). Control of gram- negative bacterial quorum sensing with cyclodextrin immobilized cellulose ether gel. *J. Incl. Phenom. Macrocycl. Chem.* 56, 55–59. doi: 10.1007/s10847-006-9060-y

Katva, S., Das, S., Moti, H. S., Jyoti, A., and Kaushik, S. (2018). Antibacterial synergy of silver nanoparticles with gentamicin and chloramphenicol against *Enterococcus faecalis*. *Pharmacogn. Mag.* 13, S828–S833. doi: 10.4103/pm.pm_120_17

Katz, E., and Willner, I. (2004). Integrated nanoparticle-biomolecule hybrid systems: synthesis, properties, and applications. *Angew. Chem. Int. Ed.* 43, 6042–6108. doi: 10.1002/anie.200400651

Kaweeteerawat, C., Na Ubol, P., Sangmuang, S., Aueviriyavit, S., and Maniratanachote, R. (2017). Mechanisms of antibiotic resistance in bacteria mediated by silver nanoparticles. *J. Toxicol. Environ. Health A*. 80, 1276–1289. doi: 10.1080/15287394.2017.1376727

Khaksar, R., Hosseini, S., Hosseini, H., Shijaee-Aliabadi, S., Mohammadifa, M., Mortazavian, A. M., et al. (2014). Nisin-loaded alginate-high methoxy pectin microparticles: preparation and physicochemical characterisation. *Int. J. Food Sci. Technol.* 49, 2076–2082. doi: 10.1111/ijfs.12516

Khameneh, B., Diab, R., Ghazvini, K., and Fazly Bazzaz, B. S. (2016). Breakthroughs in bacterial resistance mechanisms and the potential ways to combat them. *Microb. Pathog.* 95, 32–42. doi: 10.1016/j.micpath.2016.02.009

Khan, S., Khan, S. N., Meena, R., Dar, A. M., Pal, R., and Khan, A. U. (2017). Photoinactivation of multidrug resistant bacteria by monomeric methylene blue conjugated gold nanoparticles. *J. Photochem. Photobiol. B* 174, 150–161. doi: 10.1016/j.jphotobiol.2017.07.011

Khlebtsov, B. N., Tuchina, E. S., Khanadeev, V. A., Panfilova, E. V., Petrov, P. O., Tuchin, V. V., et al. (2013). Enhanced photoinactivation of *Staphylococcus aureus* with nanocomposites containing plasmonic particles and hematoporphyrin. *J. Biophotonics* 6, 338–351. doi: 10.1002/jbio.201200079

Kim, D., Kim, M., Shinde, S., Sung, J., and Ghodake, G. (2017). Cytotoxicity and antibacterial assessment of gallic acid capped gold nanoparticles synthesized at ambient temperature. *Coll. Surfaces B Biointerfaces* 149, 162–167. doi: 10.1016/j.colsurfb.2016.10.017

Kim, J., Kim, H., Park, J. H., and Jon, S. (2017). Gold nanorod-based photo-PCR system for one-step, rapid detection of bacteria. *Nanotheranostics* 1, 178–185. doi: 10.7150/ntno.18720

Kim, J.-W., Galanzha, E. I., Zaharoff, D. A., Griffin, R. J., and Zharov, V. P. (2013). Nanotheranostics of circulating tumor cells, infections and other pathological features *in vivo*. *Mol. Pharm.* 10, 813–830. doi: 10.1021/mp300577s

Krivorotova, T., Staneviciene, R., Luksa, J., Serviene, E., and Sereikaite, J. (2017). Impact of pectin esterification on the antimicrobial activity of nisin-loaded pectin particles. *Biotechnol. Prog.* 33, 245–251. doi: 10.1002/btpr.2391

Kruk, T., Szczepanowicz, K., Stefanska, J., Socha, R. P., and Warszynski, P. (2015). Synthesis and antimicrobial activity of monodisperse copper nanoparticles. *Coll. Surfaces B Biointerfaces* 128, 17–22. doi: 10.1016/j.colsurfb.2015.02.009

Kulshrestha, S., Qayyum, S., and Khan, A. U. (2017). Antibiofilm efficacy of green synthesized graphene oxide-silver nanocomposite using Lagerstroemia speciosa floral extract: a comparative study on inhibition of gram-positive and gram-negative biofilms. *Microb. Pathog.* 103, 167–177. doi: 10.1016/j.micpath.2016.12.022

Kuo, W.-S., Chang, C.-N., Chang, Y.-T., and Yeh, C.-S. (2009). Antimicrobial gold nanorods with dual-modality photodynamic inactivation and hyperthermia. *Chem. Commun.* 28, 4853–4855. doi: 10.1039/b907274h

Kuo, Y.-L., Wang, S.-G., Wu, C.-Y., Lee, K.-C., Jao, C.-J., Chou, S.-H., et al. (2016). Functional gold nanoparticle-based antibacterial agents for nosocomial and antibiotic-resistant bacteria. *Nanomedicine* 11, 2497–2510. doi: 10.2217/nnm-2016-0232

Lai, H. Z., Chen, W. Y., Wu, C. Y., and Chen, Y. C. (2015). Potent antibacterial nanoparticles for pathogenic bacteria. *ACS Appl. Mater. Interfaces* 7, 2046–2054. doi: 10.1021/am507919m

Lakshmi Prasanna, V., and Vijayaraghavan, R. (2015). Insight into the mechanism of antibacterial activity of ZnO: surface defects mediated reactive oxygen species even in the dark. *Langmuir* 31, 9155–9162. doi: 10.1021/acs.langmuir.5b02266

Lambadi, P. R., Sharma, T. K., Kumar, P., Vasnani, P., Thalluri, S. M., Bisht, N., et al. (2015). Facile biofunctionalization of silver nanoparticles for enhanced antibacterial properties, endotoxin removal, and biofilm control. *Int. J. Nanomed.* 10, 2155–2171. doi: 10.2147/IJN.S72923

Lara, H. H., Ayala-Núñez, N. V., Ixtepan Turrent, L., del, C., and Rodríguez Padilla, C. (2010). Bactericidal effect of silver nanoparticles against multidrug-resistant bacteria. *World J. Microbiol. Biotechnol.* 26, 615–621. doi: 10.1007/s11274-009-0211-3

Larsen, S. T., Jackson, P., Poulsen, S. S., Levin, M., Jensen, K. A., Wallin, H., et al. (2016). Airway irritation, inflammation, and toxicity in mice following inhalation of metal oxide nanoparticles. *Nanotoxicology* 10, 1254–1262. doi: 10.1080/17435390.2016.1202350

LaSarre, B., and Federle, M. J. (2013). Exploiting quorum sensing to confuse bacterial pathogens. *Microbiol. Mol. Biol. Rev.* 77, 73–111. doi: 10.1128/MMBR.00046-12

Lebeaux, D., Ghigo, J.-M., and Beloin, C. (2014). Biofilm-related infections: bridging the gap between clinical management and fundamental aspects of recalcitrance toward antibiotics. *Microbiol. Mol. Biol. Rev.* 78, 510–543. doi: 10.1128/MMBR.00013-14

Lee, J. H., Kim, Y. G., Cho, M. H., and Lee, J. (2014). ZnO nanoparticles inhibit *Pseudomonas aeruginosa* biofilm formation and virulence factor production. *Microbiol Res.* 169, 888–896. doi: 10.1016/j.micres.2014.05.005

Lee, P. C., and Meisel, D. (1982). Adsorption and surface-enhanced Raman of dyes on silver and gold sols. *J. Phys. Chem.* 86, 3391–3395. doi: 10.1021/j100214a025

Lee, W. S., Hsieh, T. C., Shiau, J. C., Ou, T. Y., Chen, F. L., Liu, Y. H., et al. (2017). Bio-Kil, a nano-based disinfectant, reduces environmental bacterial burden and multidrug-resistant organisms in intensive care units. *J. Microbiol. Immunol. Infect.* 50, 737–746. doi: 10.1016/j.jmii.2016.04.008

Lei, R., Wu, C., Yang, B., Ma, H., Shi, C., Wang, Q., et al. (2008). Integrated metabolomic analysis of the nano-sized copper particle-induced hepatotoxicity and nephrotoxicity in rats: a rapid *in vivo* screening method for nanotoxicity. *Toxicol. Appl. Pharmacol.* 232, 292–301. doi: 10.1016/j.taap.2008.06.026

Lellouche, J., Kahana, E., Elias, S., Gedanken, A., and Banin, E. (2009). Antibiofilm activity of nanosized magnesium fluoride. *Biomaterials* 30, 5969–5978. doi: 10.1016/j.biomaterials.2009.07.037

Lesniak, A., Salvati, A., Santos-Martinez, M. J., Radomski, M. W., Dawson, K. A., and Åberg, C. (2013). Nanoparticle adhesion to the cell membrane and its effect on nanoparticle uptake efficiency. *J. Am. Chem. Soc.* 135, 1438–1444. doi: 10.1021/ja309812z

Leuba, K. D., Durmus, N. G., Taylor, E. N., and Webster, T. J. (2013). Short communication: carboxylate functionalized superparamagnetic iron oxide nanoparticles (SPION) for the reduction of *S. aureus* growth post biofilm formation. *Int. J. Nanomedicine* 8, 731–736. doi: 10.2147/IJN.S38256

Leucuta, S. E. (2013). Systemic and biophase bioavailability and pharmacokinetics of nanoparticulate drug delivery systems. *Curr. Drug Deliv.* 10, 208–240. doi: 10.2174/1567201811310020007

LewisOscar, F., MubarakAli, D., Nithya, C., Priyanka, R., Gopinath, V., Alharbi, N. S., et al. (2015). One pot synthesis and anti-biofilm potential of copper nanoparticles (CuNPs) against clinical strains of *Pseudomonas aeruginosa*. *Biofouling* 31, 379–391. doi: 10.1080/08927014.2015.1048686

Li, H., Chen, Q., Zhao, J., and Urmila, K. (2015). Enhancing the antimicrobial activity of natural extraction using the synthetic ultrasmall metal nanoparticles. *Sci. Rep.* 5:11033. doi: 10.1038/srep11033

Li, J. J., Hartono, D., Ong, C. N., Bay, B. H., and Yung, L. Y. L. (2010). Autophagy and oxidative stress associated with gold nanoparticles. *Biomaterials* 31, 5996–6003. doi: 10.1016/j.biomaterials.2010.04.014

Li, X., Robinson, S. M., Gupta, A., Saha, K., Jiang, Z., Moyano, D. F., et al. (2014). Functional gold nanoparticles as potent antimicrobial agents against multi-drug-resistant bacteria. *ACS Nano* 8, 10682–10686. doi: 10.1021/nn5042625

Li, Y., Yu, S., Wu, Q., Tang, M., Pu, Y., and Wang, D. (2012a). Chronic Al2O3-nanoparticle exposure causes neurotoxic effects on locomotion behaviors by inducing severe ROS production and disruption of ROS defense mechanisms in nematode *Caenorhabditis elegans*. *J. Hazard Mater.* 219–220, 221–230. doi: 10.1016/j.jhazmat.2012.03.083

Li, Y., Zhang, W., Niu, J., and Chen, Y. (2012b). Mechanism of photogenerated reactive oxygen species and correlation with the antibacterial properties of engineered metal oxide nanoparticles. *ACS Nano* 6, 1–22. doi: 10.1021/nn300934k

Lin, Y., and Hamme, I. I., A. T. (2015). Gold nanoparticle labeling based ICP-MS detection/measurement of bacteria, and their quantitative photothermal destruction. *J. Mater. Chem. B* 3, 3573–3582. doi: 10.1039/C5TB00223K

Liu, L., Yang, J., Xie, J., Luo, Z., Jiang, J., Yang, Y. Y., et al. (2013). The potent antimicrobial properties of cell penetrating peptide-conjugated silver nanoparticles with excellent selectivity for Gram-positive bacteria over erythrocytes. *Nanoscale* 5:3834. doi: 10.1039/c3nr34254a

Liu, P. F., Lo, C. W., Chen, C. H., Hsieh, M. F., and Huang, C. M. (2009). Use of nanoparticles as therapy for methicillin-resistant *Staphylococcus aureus* infections. *Curr. Drug Metab.* 10, 875–884. doi: 10.2174/138920009790274522

Lok, C.-N., Ho, C.-M., Chen, R., He, Q.-Y., Yu, W.-Y., Sun, H., et al. (2007). Silver nanoparticles: partial oxidation and antibacterial activities. *J. Biol. Inorg. Chem.* 12, 527–534. doi: 10.1007/s00775-007-0208-z

Lundqvist, M., Stigler, J., Elia, G., Lynch, I., Cedervall, T., and Dawson, K. A. (2008). Nanoparticle size and surface properties determine the protein corona with possible implications for biological impacts. *Proc. Natl. Acad. Sci. U.S.A.* 105, 14265–14270. doi: 10.1073/pnas.0805135105

Maclean, M., McKenzie, K., Anderson, J. G., Gettinby, G., and MacGregor, S. J. (2014). 405 Nm light technology for the inactivation of pathogens and its potential role for environmental disinfection and infection control. *J. Hosp. Infect.* 88, 1–11. doi: 10.1016/j.jhin.2014.06.004

Mahalingam, S., Xu, Z., and Edirisinghe, M. (2015). Antibacterial activity and biosensing of PVA-lysozyme microbubbles formed by pressurized gyration. *Langmuir* 31, 9771–9780. doi: 10.1021/acs.langmuir.5b02005

Mahmoudi, M., and Serpooshan, V. (2012). Silver-coated engineered magnetic nanoparticles are promising for the success in the fight against antibacterial resistance threat. *ACS Nano* 6, 2656–2664. doi: 10.1021/nn300042m

McShan, D., Zhang, Y., Deng, H., Ray, P. C., and Yu, H. (2015). Synergistic antibacterial effect of silver nanoparticles combined with ineffective antibiotics on drug resistant *Salmonella typhimurium* DT104. *J. Environ. Sci. Heal. Part C* 33, 369–384. doi: 10.1080/10590501.2015.1055165

Meers, P., Neville, M., Malinin, V., Scotto, A. W., Sardaryan, G., Kurumunda, R., et al. (2008). Biofilm penetration, triggered release and *in vivo* activity of inhaled liposomal amikacin in chronic *Pseudomonas aeruginosa* lung infections. *J. Antimicrob. Chemother.* 61, 859–868. doi: 10.1093/jac/dkn059

Mendes, R., Pedrosa, P., Lima, J. C., Fernandes, A. R., and Baptista, P., V (2017). Photothermal enhancement of chemotherapy in breast cancer by visible irradiation of gold nanoparticles. *Sci. Rep.* 7, 1–9. doi: 10.1038/s41598-017-11491-8

Merchant, B. (1998). Gold, the noble metal and the paradoxes of its toxicology. *Biologicals* 26, 49–59. doi: 10.1006/biol.1997.0123

Miao, L., Wang, C., Hou, J., Wang, P., Ao, Y., Li, Y., et al. (2016). Aggregation and removal of copper oxide (CuO) nanoparticles in wastewater environment and their effects on the microbial activities of wastewater biofilms. *Bioresour. Technol.* 216, 537–544. doi: 10.1016/j.biortech.2016.05.082

Millenbaugh, N. J., Baskin, J. B., DeSilva, M. N., Elliott, W. R., and Glickman, R. D. (2015). Photothermal killing of *Staphylococcus aureus* using antibody-targeted gold nanoparticles. *Int. J. Nanomed.* 10, 1953–1960. doi: 10.2147/IJN.S76150

Mocan, L., Matea, C., Tabaran, F. A., Mosteanu, O., Pop, T., Puia, C., et al. (2016). Selective *in vitro* photothermal nano-therapy of MRSA infections mediated by IgG conjugated gold nanoparticles. *Sci. Rep.* 6:39466. doi: 10.1038/srep39466

Mocan, L., Tabaran, F. A., Mocan, T., Pop, T., Mosteanu, O., Agoston-Coldea, L., et al. (2017). Laser thermal ablation of multidrug-resistant bacteria using functionalized gold nanoparticles. *Int. J. Nanomed.* 12, 2255–2263. doi: 10.2147/IJN.S124778

Mohammed Fayaz, A., Girilal, M., Mahdy, S. A., Somsundar, S. S., Venkatesan, R., and Kalaichelvan, P. T. (2011). Vancomycin bound biogenic gold nanoparticles: a different perspective for development of anti VRSA agents. *Process Biochem.* 46, 636–641. doi: 10.1016/j.procbio.2010.11.001

Mohanty, S., Jena, P., Mehta, R., Pati, R., Banerjee, B., Patil, S., et al. (2013). Cationic antimicrobial peptides and biogenic silver nanoparticles kill mycobacteria without eliciting dna damage and cytotoxicity in mouse macrophages. *Antimicrob. Agents Chemother.* 57, 3688–3698. doi: 10.1128/AAC.02475-12

Morrison, D. C., and Jacobs, D. M. (1976). Binding of polymyxin B to the lipid A portion of bacterial lipopolysaccharides. *Immunochemistry* 13, 813–818. doi: 10.1016/0019-2791(76)90181-6

Munger, M. A., Hadlock, G., Stoddard, G., Slawson, M. H., Wilkins, D. G., Cox, N., et al. (2014a). Assessing orally bioavailable commercial silver nanoparticle product on human cytochrome P450 enzyme activity. *Nanotoxicology* 5390, 1–8. doi: 10.3109/17435390.2014.948092

Munger, M. A., Radwanski, P., Hadlock, G. C., Stoddard, G., Shaaban, A., Falconer, J., et al. (2014b). *In vivo* human time-exposure study of orally dosed commercial silver nanoparticles. *Nanomedicine Nanotechnology, Biol. Med.* 10, 1–9. doi: 10.1016/j.nano.2013.06.010

Muniyan, A., Ravi, K., Mohan, U., and Panchamoorthy, R. (2017). Characterization and *in vitro* antibacterial activity of saponin-conjugated silver nanoparticles against bacteria that cause burn wound infection. *World J. Microbiol. Biotechnol.* 33:147. doi: 10.1007/s11274-017-2309-3

Nagvenkar, A. P., Deokar, A., Perelshtein, I., and Gedanken, A. (2016). A one-step sonochemical synthesis of stable ZnO–PVA nanocolloid as a potential biocidal agent. *J. Mater. Chem. B* 4, 2124–2132. doi: 10.1039/C6TB00033A

Nagy, A., Harrison, A., and Dutta, P. K. (2011). Silver nanoparticles embedded in zeolite membranes : release of silver ions and mechanism of antibacterial action. *Int. J. Nanomed.* 6, 1833–1852. doi: 10.2147/IJN.S24019

Natan, M., and Banin, E. (2017). From nano to micro: using nanotechnology to combat microorganisms and their multidrug resistance. *FEMS Microbiol. Rev.* 41, 302–322. doi: 10.1093/femsre/fux003

Niemirowicz, K., Swiecicka, I., Wilczewska, A. Z., Misztalewska, I., Kalska-Szostko, B., Bienias, K., et al. (2014). Gold-functionalized magnetic nanoparticles restrict growth of *Pseudomonas aeruginosa*. *Int. J. Nanomed.* 9, 2217–2224. doi: 10.2147/IJN.S56588

Ocsoy, I., Yusufbeyoglu, S., Yilmaz, V., McLamore, E. S., Ildiz, N., and Ulgen, A. (2017). DNA aptamer functionalized gold nanostructures for molecular recognition and photothermal inactivation of methicillin-Resistant *Staphylococcus aureus*. *Coll. Surf. B. Biointerfaces* 159, 16–22. doi: 10.1016/j.colsurfb.2017.07.056

Ortega, A., Farah, S., Tranque, P., Ocana, A. V., Nam-Cha, S. H., Beyth, N., et al. (2015). Antimicrobial evaluation of quaternary ammonium polyethyleneimine nanoparticles against clinical isolates of pathogenic bacteria. *IET Nanobiotechnol.* 9, 342–348. doi: 10.1049/iet-nbt.2014.0078

Ortíz-Castro, R., Martínez-Trujillo, M., and López-Bucio, J. (2008). N -acyl-L-homoserine lactones: a class of bacterial quorum-sensing signals alter post-embryonic root development in *Arabidopsis thaliana*. *Plant Cell Environ.* 31, 1497–1509. doi: 10.1111/j.1365-3040.2008.01863.x

Otari, S. V., Patil, R. M., Waghmare, S. R., Ghosh, S. J., and Pawar, S. H. (2013). A novel microbial synthesis of catalytically active Ag–alginate biohydrogel and its antimicrobial activity. *Dalt. Trans.* 42, 9966–9975. doi: 10.1039/c3dt51093j

Pal, I., Brahmkhatri, V. P., Bera, S., Bhattacharyya, D., Quirishi, Y., Bhunia, A., et al. (2016). Enhanced stability and activity of an antimicrobial peptide in conjugation with silver nanoparticle. *J. Colloid Interface Sci.* 483, 385–393. doi: 10.1016/j.jcis.2016.08.043

Pallavicini, P., Don,à, A., Taglietti, A., Minzioni, P., Patrini, M., Dacarro, G., et al. (2014). Self-assembled monolayers of gold nanostars: a convenient tool for near-IR photothermal biofilm eradication. *Chem. Commun.* 50, 1969–1971. doi: 10.1039/C3CC48667B

Pan, W. Y., Huang, C. C., Lin, T. T., Hu, H. Y., Lin, W. C., Li, M. J., et al. (2016). Synergistic antibacterial effects of localized heat and oxidative stress caused by hydroxyl radicals mediated by graphene/iron oxide-based nanocomposites. *Nanomed. Nanotechnol. Biol. Med.* 12, 431–438. doi: 10.1016/j.nano.2015.11.014

Panáček, A., Kvítek, L., Smékalová, M., Večerová, R., Kolár, M., Röderová, M., et al. (2018). Bacterial resistance to silver nanoparticles and how to overcome it. *Nat Nanotechnol.* 13, 65–71. doi: 10.1038/s41565-017-0013-y

Panáček, A., Smékalová, M., Kilianová, M., Prucek, R., Bogdanová, K., Věcěrová, R., et al. (2016a). Strong and nonspecific synergistic antibacterial efficiency of antibiotics combined with silver nanoparticles at very low concentrations showing no cytotoxic effect. *Molecules* 21, 1–17. doi: 10.3390/molecules21010026

Panáček, A., Smékalová, M., Večerová, R., Bogdanová, K., Röderová, M., Kolár, M., et al. (2016b). Silver nanoparticles strongly enhance and restore bactericidal activity of inactive antibiotics against multiresistant *Enterobacteriaceae*. *Colloids Surfaces B Biointerfaces* 142, 392–399. doi: 10.1016/j.colsurfb.2016.03.007

Papenfort, K., and Bassler, B. (2016). Quorum-sensing signal-response systems in gram-negative bacteria. *Nat Rev Microbiol.* 14, 576–588. doi: 10.1038/nrmicro.2016.89

Patel, S. K., and Janjic, J. M. (2015). Macrophage targeted theranostics as personalized nanomedicine strategies for inflammatory diseases. *Theranostics* 5, 150–172. doi: 10.7150/thno.9476

Payne, J. N., Waghwani, H. K., Connor, M. G., Hamilton, W., Tockstein, S., Moolani, H., et al. (2016). Novel synthesis of kanamycin conjugated gold nanoparticles with potent antibacterial activity. *Front. Microbiol.* 7:607. doi: 10.3389/fmicb.2016.00607

Pei, H., Zuo, X., Zhu, D., Huang, Q., and Fan, C. (2014). Functional DNA nanostructures for theranostic applications. *Acc. Chem. Res.* 47, 550–559. doi: 10.1021/ar400195t

Pelgrift, R. Y., and Friedman, A. J. (2013). Nanotechnology as a therapeutic tool to combat microbial resistance. *Adv. Drug Deliv. Rev.* 65, 1803–1815. doi: 10.1016/j.addr.2013.07.011

Percival, S. L., Bowler, P. G., and Dolman, J. (2007). Antimicrobial activity of silver-containing dressings on wound microorganisms using an *in vitro* biofilm model. *Int. Wound J.* 4, 186–191. doi: 10.1111/j.1742-481X.2007.00296.x

Peulen, T.-O., and Wilkinson, K. J. (2011). Diffusion of nanoparticles in a biofilm. *Environ. Sci. Technol.* 45, 3367–3373. doi: 10.1021/es103450g

Pissuwan, D., Niidome, T., and Cortie, M. (2011). The forthcoming applications of gold nanoparticles in drug and gene delivery systems. *J. Control Release* 149, 65–71. doi: 10.1016/j.jconrel.2009.12.006

Poma, A., and Di Giorgio, M. (2008). Toxicogenomics to improve comprehension of the mechanisms underlying responses of *in vitro* and *in vivo* systems to nanomaterials: a review. *Curr. Genomics* 9, 571–585. doi: 10.2174/138920208786847962

Potgieter, M. D., and Meidany, P. (2017). Evaluation of the penetration of nanocrystalline silver through various wound dressing mediums: an *in vitro* study. *Burns* 44, 596–602. doi: 10.1016/j.burns.2017.10.011

Pradeepa, Vidya, S. M., Mutalik, S., Udaya Bhat, K., Huilgol, P., and Avadhani, K. (2016). Preparation of gold nanoparticles by novel bacterial exopolysaccharide for antibiotic delivery. *Life Sci.* 153, 171–179. doi: 10.1016/j.lfs.2016.04.022

Qi, G., Li, L., Yu, F., and Wang, H. (2013). Vancomycin-modified mesoporous silica nanoparticles for selective recognition and killing of pathogenic gram-positive bacteria over macrophage-like cells. *ACS Appl. Mater. Interfaces* 5, 10874–10881. doi: 10.1021/am403940d

Raghunath, A., and Perumal, E. (2017). Metal oxide nanoparticles as antimicrobial agents: a promise for the future. *Int. J. Antimicrob. Agents* 49, 137–152. doi: 10.1016/j.ijantimicag.2016.11.011

Rai, A., Pinto, S., Velho, T. R., Ferreira, A. F., Moita, C., Trivedi, U., et al. (2016). One-step synthesis of high-density peptide-conjugated gold nanoparticles with antimicrobial efficacy in a systemic infection model. *Biomaterials* 85, 99–110. doi: 10.1016/j.biomaterials.2016.01.051

Rai, M. K., Deshmukh, S. D., Ingle, A. P., and Gade, A. K. (2012). Silver nanoparticles: the powerful nanoweapon against multidrug-resistant bacteria. *J. Appl. Microbiol.* 112, 841–852. doi: 10.1111/j.1365-2672.2012.05253.x

Rai, M., Ingle, A. P., Gaikwad, S., Gupta, I., Gade, A., and Silvério da Silva, S. (2016). Nanotechnology based anti-infectives to fight microbial intrusions. *J. Appl. Microbiol.* 120, 527–542. doi: 10.1111/jam.13010

Rai, M., Ingle, A. P., Pandit, R., Paralikar, P., Gupta, I., Chaud, M. V., et al. (2017). Broadening the spectrum of small-molecule antibacterials by metallic nanoparticles to overcome microbial resistance. *Int. J. Pharm.* 532, 139–148. doi: 10.1016/j.ijpharm.2017.08.127

Rai, M., Yadav, A., and Gade, A. (2009). Silver nanoparticles as a new generation of antimicrobials. *Biotechnol. Adv.* 27, 76–83. doi: 10.1016/j.biotechadv.2008.09.002

Rajchakit, U., and Sarojini, V. (2017). Recent developments in antimicrobial-peptide-conjugated gold nanoparticles. *Bioconjug. Chem.* 28, 2673–2686. doi: 10.1021/acs.bioconjchem.7b00368

Ramalingam, B., Parandhaman, T., and Das, S. K. (2016). Antibacterial effects of biosynthesized silver nanoparticles on surface ultrastructure and nanomechanical properties of gram-negative bacteria viz. *Escherichia coli* and *Pseudomonas aeruginosa*. *ACS Appl. Mater. Interfaces* 8, 4963–4976. doi: 10.1021/acsami.6b00161

Ramasamy, M., Lee, J. H., and Lee, J. (2017a). Direct one-pot synthesis of cinnamaldehyde immobilized on gold nanoparticles and their antibiofilm properties. *Coll. Surfaces B Biointerfaces* 160, 639–648. doi: 10.1016/j.colsurfb.2017.10.018

Ramasamy, M., Lee, J.-H., and Lee, J. (2016). Potent antimicrobial and antibiofilm activities of bacteriogenically synthesized gold-silver nanoparticles against pathogenic bacteria and their physiochemical characterizations. *J. Biomater. Appl.* 31, 366–378. doi: 10.1177/0885328216646910

Ramasamy, M., Lee, J.-H., and Lee, J. (2017b). Development of gold nanoparticles coated with silica containing the antibiofilm drug cinnamaldehyde and their effects on pathogenic bacteria. *Int. J. Nanomed.* 12, 2813–2828. doi: 10.2147/IJN.S132784

Ranghar, S., Sirohi, P., Verma, P., and Agarwal, V. (2014). Nanoparticle-based drug delivery systems : promising approaches against infections. *Braz. Arch. Biol. Technol.* 57, 209–222. doi: 10.1590/S1516-89132013005000011

Reddy, L. S., Nisha, M. M., Joice, M., and Shilpa, P. N. (2014). Antimicrobial activity of zinc oxide (ZnO) nanoparticle against *Klebsiella pneumoniae*. *Pharm. Biol.* 52, 1388–1397. doi: 10.3109/13880209.2014.893001

Reddy, P. M., Chang, K.-C., Liu, Z.-J., Chen, C.-T., and Ho, Y.-P. (2014). Functionalized magnetic iron oxide (Fe3O4) nanoparticles for capturing gram-positive and gram-negative bacteria. *J. Biomed. Nanotechnol.* 10, 1429–1439. doi: 10.1166/jbn.2014.1848

Reen, F. J., Gutiérrez-Barranquero, J. A., Parages, M. L., and O'Gara, F. (2018). Coumarin: a novel player in microbial quorum sensing and biofilm formation inhibition. *Appl Microbiol Biotechnol.* 102, 2063–2073. doi: 10.1007/s00253-018-8787-x

Reidy, B., Haase, A., Luch, A., Dawson, K. A., and Lynch, I. (2013). Mechanisms of silver nanoparticle release, transformation and toxicity: a critical review of current knowledge and recommendations for future studies and applications. *Materials* 6, 2295–2350. doi: 10.3390/ma6062295

Reshma, V. G., Syama, S., Sruthi, S., Reshma, S. C., Remya, N. S., and Mohanan, P. V. (2017). Engineered nanoparticles with antimicrobial property. *Curr. Drug Metab.* 18, 1040–1054. doi: 10.2174/1389200218666170925122201

Ribeiro, A. P. C., Anbu, S., Alegria, E. C. B. A., Fernandes, A. R., Baptista, P. V., Mendes, R., et al. (2018). Evaluation of cell toxicity and DNA and protein binding of green synthesized silver nanoparticles. *Biomed. Pharmacother.* 101, 137–144. doi: 10.1016/j.biopha.2018.02.069

Rizzello, L., and Pompa, P. P. (2014). Nanosilver-based antibacterial drugs and devices: mechanisms, methodological drawbacks, and guidelines. *Chem. Soc. Rev.* 43, 1501–1518. doi: 10.1039/c3cs60218d

Roshmi, T., Soumya, K. R., Jyothis, M., and Radhakrishnan, E. K. (2015). Effect of biofabricated gold nanoparticle-based antibiotic conjugates on minimum inhibitory concentration of bacterial isolates of clinical origin. *Gold Bull.* 48, 63–71. doi: 10.1007/s13404-015-0162-4

Ruden, S., Hilpert, K., Berditsch, M., Wadhwani, P., and Ulrich, A. S. (2009). Synergistic interaction between silver nanoparticles and membrane-permeabilizing antimicrobial peptides. *Antimicrob. Agents Chemother.* 53, 3538–3540. doi: 10.1128/AAC.01106-08

Rudramurthy, G. R., Swamy, M. K., Sinniah, U. R., and Ghasemzadeh, A. (2016). Nanoparticles: alternatives against drug-resistant pathogenic microbes. *Molecules* 21:E836. doi: 10.3390/molecules21070836

Rutherford, S. T., and Bassler, B. L. (2012). Bacterial quorum sensing: its role in virulence and possibilities for its control. *Cold Spring Harb Perspect Med.* 2:a012427. doi: 10.1101/cshperspect.a012427

Roy, A., Parveen, A. R., Koppalkar, A., and Prasad, M. V. N. A. (2010). Effect of nano - titanium dioxide with different antibiotics against methicillin-resistant *Staphylococcus Aureus*. *J. Biomater. Nanobiotechnol.* 1, 37–41. doi: 10.4236/jbnb.2010.11005

Saeb, A. T. M., Alshammari, A. S., Al-brahim, H., and Al-rubeaan, K. A. (2014). Production of silver nanoparticles with strong and stable antimicrobial activity against highly pathogenic and multidrug resistant bacteria. *Sci. World J.* 2:704708. doi: 10.1155/2014/704708

Saha, B., Bhattacharya, J., Mukherjee, A., Ghosh, A., Santra, C., Anjan, K., et al. (2007). *In vitro* structural and functional evaluation of gold nanoparticles conjugated antibiotics. *Nanoscale Res. Lett.* 2, 614–622. doi: 10.1007/s11671-007-9104-2

Salem, W., Leitner, D. R., Zingl, F. G., Schratter, G., Prassl, R., Goessler, W., et al. (2015). Antibacterial activity of silver and zinc nanoparticles against *Vibrio cholerae* and enterotoxic *Escherichia coli*. *Int. J. Med. Microbiol.* 305, 85–95. doi: 10.1016/j.ijmm.2014.11.005

Salomoni, R., Léo, P., Montemor, A. F., Rinaldi, B. G., and Rodrigues, M. (2017). Antibacterial effect of silver nanoparticles in *Pseudomonas aeruginosa*. *Nanotechnol. Sci. Appl.* 10, 115–121. doi: 10.2147/NSA.S133415

Sandhiya, S., Dkhar, S. A., and Surendiran, A. (2009). Emerging trends of nanomedicine - an overview. *Fundam. Clin. Pharmacol.* 23, 263–269. doi: 10.1111/j.1472-8206.2009.00692.x

Sarwar, A., Katas, H., Samsudin, S. N., and Zin, N. M. (2015). Regioselective sequential modification of chitosan via azide-alkyne click reaction: synthesis, characterization, and antimicrobial activity of chitosan derivatives and nanoparticles. *PLoS ONE* 10:e0123084. doi: 10.1371/journal.pone.0123084

Sarwar, S., Chakraborti, S., Bera, S., Sheikh, I. A., Hoque, K. M., and Chakrabarti, P. (2016). The antimicrobial activity of ZnO nanoparticles against *Vibrio cholerae*: variation in response depends on biotype. *Nanomedicine Nanotechnology, Biol. Med.* 12, 1499–1509. doi: 10.1016/j.nano.2016.02.006

Sathyanarayanan, M. B., Balachandranath, R., Genji Srinivasulu, Y., Kannaiyan, S. K., and Subbiahdoss, G. (2013). The effect of gold and iron-oxide nanoparticles on biofilm-forming pathogens. *ISRN Microbiol.* 2013:272086. doi: 10.1155/2013/272086

Setyawati, M. I., Kutty, R. V., Tay, C. Y., Yuan, X., Xie, J., and Leong, D. T. (2014). Novel theranostic DNA nanoscaffolds for the simultaneous detection and killing of *Escherichia coli* and *Staphylococcus aureus*. *ACS Appl. Mater. Interfaces* 6, 21822–21831. doi: 10.1021/am502591c

Shah, A., Latif-Ur-Rahman, Qureshi, R., and Zia-Ur-Rehman (2012). Synthesis, characterization, and application of Au-Ag alloy nanoparticles for the sensing of an environmental toxin, pyrene. *Rev. Adv. Mater. Sci.* 30, 133–149. doi: 10.1007/s10800-015-0807-2

Shah, M., Badwaik, V., Kherde, Y., Waghwani, H. K., Modi, T., Aguilar, Z. P., et al. (2014). Gold nanoparticles: various methods of synthesis and antibacterial applications. *Front. Biosci.* 19, 1320–1344. doi: 10.2741/4284

Shaikh, S., Rizvi, S. M. D., Shakil, S., Hussain, T., Alshammari, T. M., Ahmad, W., et al. (2017). Synthesis and characterization of cefotaxime conjugated gold nanoparticles and their use to target drug-resistant CTX-M-producing bacterial pathogens. *J. Cell. Biochem.* 118, 2802–2808. doi: 10.1002/jcb.25929

Shaker, M. A., and Shaaban, M. I. (2017). Formulation of carbapenems loaded gold nanoparticles to combat multi-antibiotic bacterial resistance: *in vitro* antibacterial study. *Int. J. Pharm.* 525, 71–84. doi: 10.1016/j.ijpharm.2017.04.019

Shamaila, S., Zafar, N., Riaz, S., Sharif, R., Nazir, J., and Naseem, S. (2016). Gold nanoparticles: an efficient antimicrobial agent against enteric bacterial human pathogen. *Nanomaterials* 6:71. doi: 10.3390/nano6040071

Shareena Dasari, T. P., Zhang, Y., and Yu, H. (2015). Antibacterial activity and cytotoxicity of gold (I) and (III) ions and gold nanoparticles. *Biochem. Pharmacol.* 4:199. doi: 10.4172/2167-0501.1000199

Siddiqi, K. S., Husen, A., and Rao, R. A. K. (2018). A review on biosynthesis of silver nanoparticles and their biocidal properties. *J. Nanobiotechnology* 16:14. doi: 10.1186/s12951-018-0334-5

Singh, B. N., Prateeksha, Upreti D. K., Singh, B. R., Defoirdt, T., Gupta, V. K., De Souza, A. O., et al. (2017). Bactericidal, quorum quenching and anti-biofilm nanofactories: a new niche for nanotechnologists. *Crit. Rev. Biotechnol.* 37, 525–540. doi: 10.1080/07388551.2016.1199010

Singh, J., Garg, T., Rath, G., and Goyal, A. K. (2016). Advances in nanotechnology-based carrier systems for targeted delivery of bioactive drug molecules with special emphasis on immunotherapy in drug resistant tuberculosis - a critical review. *Drug Deliv.* 23, 1676–1698. doi: 10.3109/10717544.2015.1074765

Singh, K., Panghal, M., Kadyan, S., Chaudhary, U., and Yadav, J. P., arkas. (2014). Green silver nanoparticles of *Phyllanthus amarus*: as an antibacterial agent against multi drug resistant clinical isolates of *Pseudomonas aeruginosa*. *J. Nanobiotechnology* 12:40. doi: 10.1186/s12951-014-0040-x

Singh, R., Nawale, L., Arkile, M., Wadhwani, S., Shedbalkar, U., Chopade, S., et al. (2016). Phytogenic silver, gold, and bimetallic nanoparticles as novel antitubercular agents. *Int. J. Nanomed.* 11, 1889–1897. doi: 10.2147/IJN.S102488

Singh, R., Smitha, M. S., and Singh, S. P. (2014). The role of nanotechnology in combating multi-drug resistant bacteria. *J. Nanosci. Nanotechnol.* 14, 4745–4756. doi: 10.1166/jnn.2014.9527

Sinha, R., Karan, R., Sinha, A., and Khare, S. K. (2011). Interaction and nanotoxic effect of ZnO and Ag nanoparticles on mesophilic and halophilic bacterial cells. *Bioresour. Technol.* 102, 1516–1520. doi: 10.1016/j.biortech.2010.07.117

Slavin, Y. N., Asnis, J., Hafeli, U. O., and Bach, H. (2017). Metal nanoparticles: understanding the mechanisms behind antibacterial activity. *J. Nanobiotechnology* 15:65. doi: 10.1186/s12951-017-0308-z

Slomberg, D. L., Lu, Y., Broadnax, A. D., Hunter, R. A., Carpenter, A. W., and Schoenfisch, M. H. (2013). Role of size and shape on biofilm eradication for nitric oxide-releasing silica nanoparticles. *ACS Appl. Mater. Interfaces* 5, 9322–9329. doi: 10.1021/am402618w

Smock, K. J., Schmidt, R. L., Hadlock, G., Stoddard, G., Grainger, D. W., and Munger, M. A. (2014). Assessment of orally dosed commercial silver nanoparticles on human *ex vivo* platelet aggregation. *Nanotoxicology* 8, 328–333. doi: 10.3109/17435390.2013.788749

Su, H.-L., Lin, S.-H., Wei, J.-C., Pao, I.-C., Chiao, S.-H., Huang, C.-C., et al. (2011). Novel nanohybrids of silver particles on clay platelets for inhibiting silver-resistant bacteria. *PLoS ONE* 6:e21125. doi: 10.1371/journal.pone.0021125

Su, Y., Zheng, X., Chen, Y., Li, M., and Liu, K. (2015). Alteration of intracellular protein expressions as a key mechanism of the deterioration of bacterial denitrification caused by copper oxide nanoparticles. *Sci. Rep.* 5:15824. doi: 10.1038/srep15824

Sukwong, P., Pissuwan, D., Somkid, K., Kongseng, S., and Yoovathaworn, K. (2016). Respiratory tract toxicity of titanium dioxide nanoparticles and multi-walled carbon nanotubes on mice after intranasal exposure. *Micro Nano Lett.* 11, 183–187. doi: 10.1049/mnl.2015.0523

Taylor, T., Gaysinsky, S., Davidson, P., Bruce, B., and Weiss, J. (2007). Characterization of antimicrobial bearing liposomes by zeta potential, vesicle size, and encapsulation efficiency. *Food Biophys.* 2, 1–9. doi: 10.1007/s11483-007-9023-x

Thapa, R., Bhagat, C., Shrestha, P., Awal, S., and Dudhagara, P. (2017). Enzyme-mediated formulation of stable elliptical silver nanoparticles tested against clinical pathogens and MDR bacteria and development of antimicrobial surgical thread. *Ann. Clin. Microbiol. Antimicrob.* 16, 1–10. doi: 10.1186/s12941-017-0216-y

Thomas, R., Nair, A. P., Kr, S., Mathew, J., and Ek, R. (2014). Antibacterial activity and synergistic effect of biosynthesized AgNPs with antibiotics against multidrug-resistant biofilm-forming coagulase-negative *staphylococci* isolated from clinical samples. *Appl. Biochem. Biotechnol.* 173, 449–460. doi: 10.1007/s12010-014-0852-z

Thompson, M., Blaszykowski, C., Sheikh, S., and Romaschin, A. (2015). A true theranostic approach to medicine: towards tandem sensor detection and removal of endotoxin in blood. *Biosens. Bioelectron.* 67, 3–10. doi: 10.1016/j.bios.2014.07.008

Tielens, F., and Santos, E. (2010). AuS and SH bond formation/breaking during the formation of alkanethiol SAMs on Au(111): a theoretical study. *J. Phys. Chem. C* 114, 9444–9452. doi: 10.1021/jp102036r

Tiwari, P., Vig, K., Dennis, V., and Singh, S. (2011). Functionalised gold nanoparticles and their biomedical applications. *Nanomaterials* 1, 31–63. doi: 10.3390/nano1010031

Tong, G., Du, F., Wu, W., Wu, R., Liu, F., and Liang, Y. (2013). Enhanced reactive oxygen species (ROS) yields and antibacterial activity of spongy ZnO/ZnFe2O4 hybrid micro-hexahedra selectively synthesized through a versatile glucose-engineered co-precipitation/annealing process. *J. Mater. Chem. B* 1, 2647–2657. doi: 10.1039/c3tb20229a

Turos, E., Reddy, G. S. K., Greenhalgh, K., Ramaraju, P., Abeylath, S. C., Jang, S., et al. (2007). Penicillin-bound polyacrylate nanoparticles: restoring the activity of beta-lactam antibiotics against MRSA. *Bioorg. Med. Chem. Lett.* 17, 3468–3472. doi: 10.1016/j.bmcl.2007.03.077

Ulloa-Ogaz, A. L., Piñón-Castillo, H. A., Muñoz-Castellanos, L. N., Athie-García, M. S., Ballinas-Casarrubias, M. D. L., Murillo-Ramirez, J. G., et al. (2017). Oxidative damage to *Pseudomonas aeruginosa* ATCC 27833 and *Staphylococcus aureus* ATCC 24213 induced by CuO-NPs. *Environ. Sci. Pollut. Res.* 24, 22048–22060. doi: 10.1007/s11356-017-9718-6

Uma Suganya, K. S., Govindaraju, K., Ganesh Kumar, V., Stalin Dhas, T., Karthick, V., Singaravelu, G., et al. (2015). Blue green alga mediated synthesis of gold nanoparticles and its antibacterial efficacy against Gram positive organisms. *Mater. Sci. Eng. C* 47, 351–356. doi: 10.1016/j.msec.2014.11.043

Umamaheswari, K., Baskar, R., Chandru, K., Rajendiran, N., and Chandirasekar, S. (2014). Antibacterial activity of gold nanoparticles and their toxicity assessment. *BMC Infect. Dis.* 14:P64. doi: 10.1186/1471-2334-14-S3-P64

Veigas, B., Fernandes, A. R., and Baptista, P. V. (2014). AuNPs for identification of molecular signatures of resistance. *Front. Microbiol.* 5:455. doi: 10.3389/fmicb.2014.00455

Veigas, B., Pedrosa, P., Carlos, F. F., Mancio-Silva, L., Grosso, A. R., Fortunato, E., et al. (2015). One nanoprobe, two pathogens: gold nanoprobes multiplexing for point-of-care. *J. Nanobiotechnology* 13:48. doi: 10.1186/s12951-015-0109-1

Veigas, B., Pedrosa, P., Couto, I., Viveiros, M., and Baptista, P., V (2013). Isothermal DNA amplification coupled to Au-nanoprobes for detection of mutations associated to Rifampicin resistance in *Mycobacterium tuberculosis*. *J. Nanobiotechnology* 11:38. doi: 10.1186/1477-3155-11-38

Venkatesan, N., Perumal, G., and Doble, M. (2015). Bacterial resistance in biofilm-associated bacteria. *Future Microbiol.* 10, 1743–1750. doi: 10.2217/fmb.15.69

Vinoj, G., Pati, R., Sonawane, A., and Vaseeharan, B. (2015). *In vitro* cytotoxic effects of gold nanoparticles coated with functional acyl homoserine lactone lactonase protein from *Bacillus licheniformis* and their antibiofilm activity against proteus species. *Antimicrob. Agents Chemother.* 59, 763–771. doi: 10.1128/AAC.03047-14

Walker, T., Dumadag, S., Lee, C. J., Lee, S. H., Bender, J. M., Abbott, J. C., et al. (2016). Clinical impact of laboratory implementation of verigene BC-GN microarray-based assay for detection of gram-negative bacteria in positive blood cultures. *J. Clin. Microbiol.* 54, 1789–1796. doi: 10.1128/JCM.00376-16

Wang, G. (2014). Human antimicrobial peptides and proteins. *Pharmaceuticals* 7, 545–594. doi: 10.3390/ph7050545

Wang, L., Chen, Y. P., Miller, K. P., Cash, B. M., Jones, S., Glenn, S., et al. (2014). Functionalized nanoparticles complexed with antibiotic efficiently kill MRSA and other bacteria. *Chem. Commun.* 50, 12030–12033. doi: 10.1039/c4cc04936e

Wang, L., Hu, C., and Shao, L. (2017a). The antimicrobial activity of nanoparticles: present situation and prospects for the future. *Int. J. Nanomed.* 12, 1227–1249. doi: 10.2147/IJN.S121956

Wang, L., Huang, F., Cai, G., Yao, L., Zhang, H., and Lin, J. (2017b). An electrochemical aptasensor using coaxial capillary with magnetic nanoparticle, urease catalysis and PCB electrode for rapid and sensitive detection of *Escherichia coli* O157:H7. *Nanotheranostics* 1, 403–414. doi: 10.7150/ntno.22079

Wang, Z., Dong, K., Liu, Z., Zhang, Y., Chen, Z., Sun, H., et al. (2017). Activation of biologically relevant levels of reactive oxygen species by Au/g-C3N4 hybrid nanozyme for bacteria killing and wound disinfection. *Biomaterials* 113, 145–157. doi: 10.1016/j.biomaterials.2016.10.041

Wangoo, N., Suri, C. R., and Shekhawat, G. (2008). Interaction of gold nanoparticles with protein: a spectroscopic study to monitor protein conformational changes. *Appl. Phys. Lett.* 92, 1–4. doi: 10.1063/1.2902302

Warheit, D. B. (2018). Hazard and risk assessment strategies for nanoparticle exposures: how far have we come in the past 10 years? *F1000Res.* 7:376. doi: 10.12688/f1000research.12691.1

Weng, C.-I., Chang, H.-T., Lin, C.-H., Shen, Y.-W., Unnikrishnan, B., Li, Y.-J., et al. (2015). One-step synthesis of biofunctional carbon quantum dots for bacterial labeling. *Biosens. Bioelectron.* 68, 1–6. doi: 10.1016/J.BIOS.2014.12.028

Wu, T., Wu, C., Fang, Z., Ma, X., Chen, S., and Hu, Y. (2017). Effect of chitosan microcapsules loaded with nisin on the preservation of small yellow croaker. *Food Control* 72, 43–52. doi: 10.1016/j.foodcont.2017.04.016

Xia, Q., Li, H., and Xiao, K. (2016). Factors affecting the pharmacokinetics, biodistribution and toxicity of gold nanoparticles in drug delivery. *Curr. Drug Metab.* 17, 849–861. doi: 10.2174/1389200217666160629114941

Xue, Y., Li, X., Li, H., and Zhang, W. (2014). Quantifying thiol-gold interactions towards the efficient strength control. *Nat. Commun.* 5:4348. doi: 10.1038/ncomms5348

Yang, X., Dang, Y., Lou, J., Shao, H., and Jiang, X. (2018). D-alanyl-D-alanine-modified gold nanoparticles form a broad-spectrum sensor for bacteria. *Theranostics* 8, 1449–1457. doi: 10.7150/thno.22540

Yang, X., Yang, J., Wang, L., Ran, B., Jia, Y., Zhang, L., et al. (2017). Pharmaceutical intermediate-modified gold nanoparticles: against multidrug-resistant bacteria and wound-healing application via an electrospun scaffold. *ACS Nano* 11, 5737–5745. doi: 10.1021/acsnano.7b01240

Yeaman, M. R. (2003). Mechanisms of antimicrobial peptide action and resistance. *Pharmacol. Rev.* 55, 27–55. doi: 10.1124/pr.55.1.2

Yeom, J. H., Lee, B., Kim, D., Lee, J., kook, Kim, S., Bae, J., et al. (2016). Gold nanoparticle-DNA aptamer conjugate-assisted delivery of antimicrobial peptide effectively eliminates intracellular *Salmonella enterica serovar Typhimurium*. *Biomaterials* 104, 43–51. doi: 10.1016/j.biomaterials.2016.07.009

Yu, J., Zhang, W., Li, Y., Wang, G., Yang, L., Jin, J., et al. (2014). Synthesis, characterization, antimicrobial activity and mechanism of a novel hydroxyapatite whisker/nano zinc oxide biomaterial. *Biomed. Mater.* 10:015001. doi: 10.1088/1748-6041/10/1/015001

Yu, Q., Li, J., Zhang, Y., Wang, Y., Liu, L., and Li, M. (2016). Inhibition of gold nanoparticles (AuNPs) on pathogenic biofilm formation and invasion to host cells. *Sci. Rep.* 6:26667. doi: 10.1038/srep26667

Zaidi, S., Misba, L., and Khan, A. U. (2017). Nano-therapeutics : a revolution in infection control in post antibiotic era. *Nanomed. Nanotechnol. Biol. Med.* 13, 2281–2301. doi: 10.1016/j.nano.2017.06.015

Zazo, H., Colino, C. I., and Lanao, J. M. (2016). Current applications of nanoparticles in infectious diseases. *J. Control. Release* 224, 86–102. doi: 10.1016/j.jconrel.2016.01.008

Zhang, L., and Gallo, R. L. (2016). Antimicrobial peptides. *Curr. Biol.* 26, R14–R19. doi: 10.1016/j.cub.2015.11.017

Zhang, W., Li, Y., Niu, J., and Chen, Y. (2013). Photogeneration of reactive oxygen species on uncoated silver, gold, nickel, and silicon nanoparticles and their antibacterial effects. *Langmuir* 29, 4647–4651. doi: 10.1021/la400500t

Zhang, Y., Shareena Dasari, T. P., Deng, H., and Yu, H. (2015a). Antimicrobial activity of gold nanoparticles and ionic gold. *J. Environ. Sci. Health. C. Environ. Carcinog. Ecotoxicol. Rev.* 33, 286–327. doi: 10.1080/10590501.2015.1055161

Zhang, Y., Zhu, P., Li, G., Wang, W., Chen, L., Lu, D. D., et al. (2015b). Highly stable and re-dispersible nano Cu hydrosols with sensitively size-dependent catalytic and antibacterial activities. *Nanoscale* 7, 13775–13783. doi: 10.1039/C5NR03414K

Zhang, Y., Zhu, P., Li, G., Zhao, T., Fu, X., Sun, R., et al. (2014). Facile preparation of monodisperse, impurity-free, and antioxidation copper nanoparticles on a large scale for application in conductive ink. *ACS Appl. Mater. Interfaces* 6, 560–567. doi: 10.1021/am404620y

Zhao, Y., and Jiang, X. (2013). Multiple strategies to activate gold nanoparticles as antibiotics. *Nanoscale* 5:8340. doi: 10.1039/c3nr01990j

Zhao, Y., Ye, C., Liu, W., Chen, R., and Jiang, X. (2014). Tuning the composition of AuPt bimetallic nanoparticles for antibacterial application. *Angew Chem Int* 53, 8127–8131. doi: 10.1002/anie.201401035

Zhao, Z., Yan, R., Yi, X., Li, J., Rao, J., Guo, Z., et al. (2017). Bacteria-activated theranostic nanoprobes against methicillin-resistant *Staphylococcus aureus* infection. *ACS Nano* 11, 4428–4438. doi: 10.1021/acsnano.7b00041

Zhou, Z., Peng, S., Sui, M., Chen, S., Huang, L., Xu, H., et al. (2018). Multifunctional nanocomplex for surface-enhanced Raman scattering imaging and near-infrared photodynamic antimicrobial therapy of vancomycin-resistant bacteria. *Coll. Surfaces B Biointerfaces* 161, 394–402. doi: 10.1016/j.colsurfb.2017.11.005

Zong, J., Cobb, S. L., and Cameron, N. R. (2017). Peptide-functionalized gold nanoparticles: versatile biomaterials for diagnostic and therapeutic applications. *Biomater. Sci.* 5, 872–886. doi: 10.1039/C7BM00006E

Conflict of Interest Statement: NM was employed by the company Nuritas limited.

The remaining authors declare that the research was conducted in the absence of any commercial or financial relationships that could be construed as a potential conflict of interest.

Copyright © 2018 Baptista, McCusker, Carvalho, Ferreira, Mohan, Martins and Fernandes. This is an open-access article distributed under the terms of the Creative Commons Attribution License (CC BY). The use, distribution or reproduction in other forums is permitted, provided the original author(s) and the copyright owner(s) are credited and that the original publication in this journal is cited, in accordance with accepted academic practice. No use, distribution or reproduction is permitted which does not comply with these terms.

frontiers in Microbiology

ORIGINAL RESEARCH
published: 16 July 2018
doi: 10.3389/fmicb.2018.01555

In Vitro Antimicrobial Activity of Green Synthesized Silver Nanoparticles Against Selected Gram-negative Foodborne Pathogens

Yuet Ying Loo[1], Yaya Rukayadi[1], Mahmud-Ab-Rashid Nor-Khaizura[1], Chee Hao Kuan[2], Buong Woei Chieng[3,4], Mitsuaki Nishibuchi[5] and Son Radu[1,6]*

[1] Department of Food Science, Faculty of Food Science and Technology, Universiti Putra Malaysia, Selangor, Malaysia, [2] Department of Agricultural and Food Science, Faculty of Science, Universiti Tunku Abdul Rahman, Kampar, Malaysia, [3] Department of Chemistry, Faculty of Science, Universiti Putra Malaysia, Selangor, Malaysia, [4] Materials Processing and Technology Laboratory, Institute of Advanced Technology, Universiti Putra Malaysia, Selangor, Malaysia, [5] Center for Southeast Asian Studies, Kyoto University, Kyoto, Japan, [6] Laboratory of Food Safety and Food Integrity, Institute of Tropical Agriculture and Food Security (ITAFoS), Universiti Putra Malaysia, Selangor, Malaysia

OPEN ACCESS

Edited by:
Rebecca Thombre, Pune University, India

Reviewed by:
Leda Giannuzzi, National University of La Plata, Argentina
M. Oves, King Abdulaziz University, Saudi Arabia

****Correspondence:***
Yuet Ying Loo
yuetying88@gmail.com

Specialty section:
This article was submitted to Antimicrobials, Resistance and Chemotherapy, a section of the journal Frontiers in Microbiology

Received: *28 March 2018*
Accepted: *22 June 2018*
Published: *16 July 2018*

Citation:
Loo YY, Rukayadi Y, Nor-Khaizura M-A-R, Kuan CH, Chieng BW, Nishibuchi M and Radu S (2018) In Vitro Antimicrobial Activity of Green Synthesized Silver Nanoparticles Against Selected Gram-negative Foodborne Pathogens. Front. Microbiol. 9:1555. doi: 10.3389/fmicb.2018.01555

Silver nanoparticles (AgNPs) used in this study were synthesized using pu-erh tea leaves extract with particle size of 4.06 nm. The antibacterial activity of green synthesized AgNPs against a diverse range of Gram-negative foodborne pathogens was determined using disk diffusion method, resazurin microtitre-plate assay (minimum inhibitory concentration, MIC), and minimum bactericidal concentration test (MBC). The MIC and MBC of AgNPs against *Escherichia coli*, *Klebsiella pneumoniae*, *Salmonella* Typhimurium, and *Salmonella* Enteritidis were 7.8, 3.9, 3.9, 3.9 and 7.8, 3.9, 7.8, 3.9 μg/mL, respectively. Time-kill curves were used to evaluate the concentration between MIC and bactericidal activity of AgNPs at concentrations ranging from 0×MIC to 8×MIC. The killing activity of AgNPs was fast acting against all the Gram-negative bacteria tested; the reduction in the number of CFU mL^{-1} was >3 Log_{10} units (99.9%) in 1–2 h. This study indicates that AgNPs exhibit a strong antimicrobial activity and thus might be developed as a new type of antimicrobial agents for the treatment of bacterial infection including multidrug resistant bacterial infection.

Keywords: silver nanoparticles, tea leave extracts, antimicrobial activity, foodborne pathogens, Gram-negative, time-kill curves

INTRODUCTION

Recently, nanotechnology has emerged as a dynamically developing area of scientific interest in the world. Nanoparticles are defined as a nanoscale particle of size ranging from 1 to 100 nm. Among the metallic nanoparticles, silver nanoparticles (AgNPs) have gained increasingly attention due to its unique physical, biological and chemical properties. AgNPs are well-known to exhibit a strong antimicrobial activity against various microorganisms such as bacteria, viruses, and fungi due to its smaller in size and large surface area (Franci et al., 2015). AgNPs are also widely used as anti-fungal (Medda et al., 2015), anti-inflammatory (Hebeish et al., 2014), and anti-viral properties (Bekele et al., 2016).

Green synthesis of AgNPs employing either biological microorganisms or plant extracts has emerged as a simple and alternative to chemical synthesis. Green synthesis method provides advancements over chemical methods as it is environmental friendly and cost effective. Plant extracts-mediated synthesis of AgNPs can be advantageous compared with other biological processes as it does not require the process of maintaining the cell cultures and aseptic environments (Loo et al., 2012). Several studies on the green synthesis of AgNPs using plant extracts have been reported (Medda et al., 2015; Ahmed et al., 2016; Dhand et al., 2016; Selvam et al., 2017).

Foodborne illnesses have emerged as a major public health concern around the world. WHO (2014) reported that there is about 30% of the population in industrialized countries affected by foodborne diseases every year. The consumption of foods contaminated with foodborne pathogens such as bacteria, fungi, viruses, and toxins are often recognized as the main source of foodborne illness in humans. Food especially minimal-processed food can be contaminated during pre-harvesting, post-harvesting, processing, transport, handling, or preparation. The most common foodborne pathogens found in food are *Salmonella* spp. (Lee et al., 2015; D'Ostuni et al., 2016), *Listeria* spp. (Ferreira et al., 2014; Välimaa et al., 2015), *Escherichia coli* O157 (Heiman et al., 2015), *Campylobacter* spp. (Kaakoush et al., 2015), and *Clostridia* spp. (Chukwu et al., 2016).

The presence of multidrug resistance pathogens have increased the number of infectious disease and became the main cause of death in the world (WHO, 2000; Tanwar et al., 2014). Widely misuse and abuse of antibiotics are the leading cause of antibiotic resistance in the bacteria (O'Bryan et al., 2018). Multidrug resistant bacteria infection may lead to several impacts including increase of mortality and morbidity rates, prolong of hospitalization period, and economic loss (Patel et al., 2008). Woh et al. (2017) detected multi-drug resistant non-typhoidal *Salmonella* among migrant food handlers, which may cause cross-contamination to the food products. Thus, the development of a new and natural antimicrobial agent is needed as there is a growing concern in multidrug resistant foodborne pathogens.

The aim of this study is to determine the antibacterial activity of green synthesized AgNPs against a diverse range of Gram-negative foodborne pathogens by using disk diffusion method, resazurin microtitre-plate assay minimum inhibitory concentration (MIC), minimum bactericidal concentration test (MBC), and time-kill curve assay.

MATERIALS AND METHODS

Preparation of Silver Nanoparticles

The synthesis of AgNPs using pu-erh tea leaves extracts was done using the method as described previously (Loo et al., 2012). Ten gram of tea leaves was weighed in a beaker. The tea leaves was added with 100 mL of distilled water and maintained at 60°C for 10 min. After 10 min, the tea extract was filtered using 0.45 μm Millipore membrane filter and followed by 0.2 μm Millipore membrane filter. For synthesis of AgNPs, 12 mL of tea extracts was added into 100 mL of $AgNO_3$ (1 mM) in Erlenmeyer flask at room temperature. Color changes of the solution were observed. The synthesized AgNPs were characterized by UV-vis spectroscopy, X-ray diffraction (XRD), Fourier transform infrared (FTIR) spectroscopy, and transmission electron microscopy (TEM).

Bacteria Strains Preparation

Escherichia coli ATCC 25922 (*E. coli*), *Klebsiella pneumoniae* ATCC 13773 (*K. pneumoniae*), *Salmonella* Typhimurium ATCC 14028 (*S.* Typhimurium), and *Salmonella* Enteritidis ATCC 13076 (*S.* Enteritidis) were obtained from the American Type Culture Collection (Rockville, MD, United States). All the bacteria strains were cultured in Mueller Hinton broth (MHB) (Merck, Germany) at 37°C for 24 h with 200 rpm agitation.

Preparation of Resazurin Solution

The resazurin solution was prepared at 0.02% (wt/vol) according to Khalifa et al. (2013). A 0.002 g of resazurin salt powder was dissolved in 10 mL of distilled water and vortexed. The mixture was filtered by Millipore membrane filter (0.2 μm). The resazurin solution can be kept at 4°C for 2 weeks.

In Vitro Susceptibility Test

Disk Diffusion Method

The antibacterial activity of AgNPs against the selected Gram-negative foodborne pathogens was carried out using Kirby–Bauer Disk Diffusion Susceptibility Test method (Bauer et al., 1966). The bacteria strains were spread on the Mueller-Hinton agar (MHA) (Merck, Germany) using sterile cotton swab. Sterile blank antimicrobial susceptibility disk was used in the test. The disks were loaded with 10 μL of tea leaves extracts, silver nitrate solution (1 mM), and solution containing tea leaves mediated synthesized AgNPs separately. The disks were then placed on the agar plate and incubated at 37°C for 24 h. The zone of inhibition was observed after 24 h of incubation.

Minimum Inhibitory Concentration (MIC) and Minimum Bactericidal Concentration (MBC) Evaluation

The MIC and MBC of green synthesized AgNPs were done using the method described in the guideline of CLSI (2012). The MIC test was performed in 96-well round bottom microtiter plate using standard broth microdilution methods while the MBC test was performed on the MHA plates. The bacterial inoculums were adjusted to the concentration of 10^6 CFU/mL. For the MIC test, 100 μL of the synthesized AgNPs stock solution (500 μg/mL) was added and diluted twofold with the bacterial inoculums in 100 μL of MHB started from column 12 to column 3. Column 12 of the microtiter plate contained the highest concentration of AgNPs, while column 3 contained the lowest concentration. Column 1 served as negative control (only medium) and the column 2 served as positive control (medium and bacterial inoculums). Each well of the microtiter plate was added with 30 μL of the resazurin solution and incubated at 37°C for 24 h. Any color changes were observed. Blue/purple color indicated no bacterial growth while pink/colorless indicated bacterial growth.

The MIC value was taken at the lowest concentration of antibacterial agents that inhibits the growth of bacteria (color remained in blue).

The MBC was defined as the lowest concentration of the antibacterial agents that completely kill the bacteria. MBC test was performed by plating the suspension from each well of microtiter plates into MHA plate. The plates were incubated at 37°C for 24 h. The lowest concentration with no visible growths on the MHA plate was taken as MBC value.

Time-Kill Curve

Time-kill assay was done in MHB medium as described by Zainin et al. (2013) and Lau et al. (2014). The bacterial inoculums were adjusted to 10^6 CFU/mL. The AgNPs solution was diluted with MHB media containing bacterial inoculums to obtain the final concentration of 0× MIC, 0.5× MIC, 1× MIC, 2× MIC, 4× MIC, and 8× MIC for each type of bacteria in the total final volume of 1 mL. The cultures were then incubated at 37°C with 150 rpm agitation. The cultures (100 μL) were spread on MHA plates at time 0, 0.25, 0.5, 1, 2, and 4 h. The experiment was carried out in triplicate. The number of colonies on the MHA plates was quantified in CFU/mL after incubation at 37°C for 24 h. For statistical analysis, SPSS (v.19) statistical package was used to determine the significant ($P < 0.05$) difference among the tested foodborne pathogens.

RESULTS AND DISCUSSION

This study was aimed to determine the antibacterial effect of green synthesized AgNPs. The green synthesized AgNPs used in this study were characterized by UV-vis spectroscopy, XRD, FTIR spectroscopy, and TEM. The XRD patterns for synthesized AgNPs showed that five main characteristic diffraction peaks for Ag were observed at 2θ = 38.4, 44.5, 64.8, 77.7, and 81.7, which correspond to the (111), (200), (220), (311), and (222) crystallographic planes of face-centered cubic (fcc) Ag crystals. The UV-vis absorption spectrum of the synthesized AgNPs showed a broad peak at 436 nm which is a characteristic band for Ag. Three infrared bands were observed at 3,271, 1,637, and 386 cm^{-1} in FTIR measurement. The band at 3,271 and 1,637 cm^{-1} indicated that the presence of protein as capping agent for AgNPs which increases the stability of the nanoparticles, while the broad peak at 386 cm^{-1} corresponded to the Ag metal. TEM image revealed that the AgNPs is spherical with the particle size of 4.06 nm (Loo et al., 2012).

The antibacterial activity of AgNPs was determined against four species of Gram-negative foodborne pathogens: *E. coli* ATCC 25922, *K. pneumoniae* ATCC 13773, *S.* Typhimurium ATCC 14028, and *S.* Enteritidis ATCC 13076. The results for disk diffusion test, MIC and MBC of the AgNPs are summarized in **Table 1**. For the disk diffusion test, the presence of clear zone around the AgNPs disk suggesting that the AgNPs possessed antibacterial activity which is able to inhibit the growth of the Gram-negative foodborne pathogens. As previous study by Guzman et al. (2012), reported that AgNPs employed antibacterial activity on Gram-negative bacteria. The visible clear zone produced by AgNPs against four different species of Gram-negative bacteria is showed in **Figure 1**.

Disk diffusion test was described as the preliminary study in screening the antibacterial activity of an antimicrobial agent; therefore, a further evaluation in determining the antibacterial activity of AgNPs using MIC value was needed (Burt, 2004). MIC was defined as the lowest concentration of the antibacterial agent to inhibit the growth of bacteria by serial dilution. As showed in **Table 1**, the MIC values of AgNPs against the foodborne pathogens were ranged from 3.9 to 7.8 μg/mL. *K. pneumonia*, *S.* Typhimurium and *S.* Enteritidis showed the MIC value of 3.9 μg/mL while *E. coli* showed the MIC value of 7.8 μg/mL. MBC is the lowest concentration of antibacterial agent to kill the bacteria (showed no growth on the agar plate). In the study, MBC for *K. pneumoniae* and *S.* Enteritidis were 3.9 μg/mL while *S.* Typhimurium and *E. coli* showed the MBC value of 7.8 μg/mL. The MIC and MBC value of *E. coli* showed that *E. coli* was less susceptible to AgNPs. This may due to the positive charges of AgNPs trapped and blocked by lipopolysaccharide, thus make *E. coli* less susceptible to AgNPs (Lara et al., 2010b).

Resazurin dye was used in the study as an indicator in the determination of cell growth, especially in cytotoxicity assays (McNicholl et al., 2007). Oxidoreductases within viable cells reduced the resazurin salt to resorufin and changed the color from blue non-fluorescent to pink and fluorescent. According to McNicholl et al. (2007), resazurin dye has been applied for decades to check for the bacterial and yeast contamination in milk.

The time kill activity of four foodborne pathogens is shown in **Figure 2**. The bactericidal activity of AgNPs is effective against the selected Gram-negative pathogens; the reduction in the number of CFU/mL was ≥3 Log units (99%). The bactericidal endpoint of AgNPs for *E. coli* was reached after 2 h of incubation at 4× MIC (31.2 μg/mL) and 8× MIC (62.4 μg/mL); while for *K. pneumoniae*, the bacteria was killed after 2 h of incubation at 2× MIC (7.8 μg/mL), 4× MIC (15.6 μg/mL), and 8× MIC (31.2 μg/mL). *S.* Typhimurium was killed after 1 h of incubation at 4× MIC (15.6 μg/mL) and 8× MIC (31.2 μg/mL). The bactericidal endpoint of AgNP for *S.* Enteritidis was reached after 2 h of incubation at 2× MIC (7.8 μg/mL) and 4× MIC (15.6 μg/mL); however, the end point reached faster after 1 h of incubation at 8× MIC (31.2 μg/mL). No significant differences ($P > 0.05$) were found among the tested Gram-negative foodborne pathogens. This indicates that AgNPs are

TABLE 1 | The diameter of zone inhibition (mm), MIC value (μg/mL), and MBC value (μg/mL).

Bacteria	Diameter of inhibition zone (mm)	MIC (μg/mL)	MBC (μg/mL)
Escherichia coli	15	7.8	7.8
Klebsiella pneumoniae	10	3.9	3.9
Salmonella Typhimurium	20	3.9	7.8
Salmonella Enteritidis	20	3.9	3.9

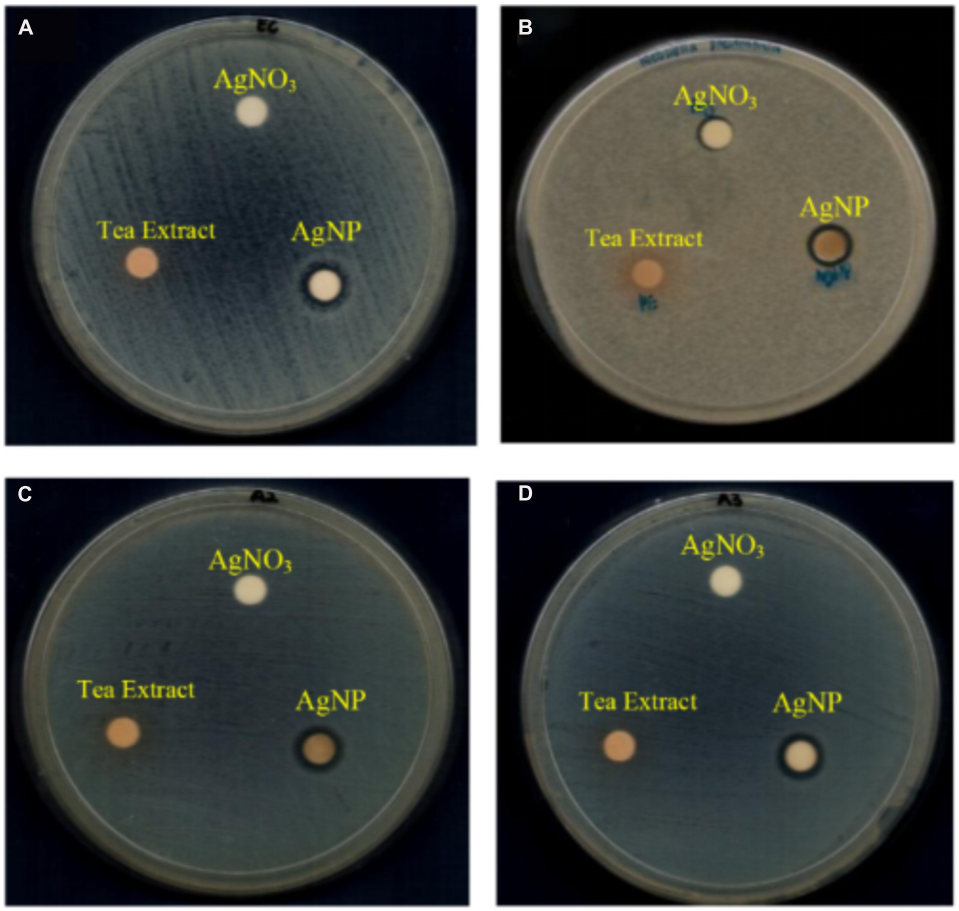

FIGURE 1 | Visible clear zone produced by tea leaves extract mediated AgNP against four species of foodborne pathogens: **(A)** *E. coli* ATCC 25922, **(B)** *K. pneumoniae* ATCC 13773, **(C)** *S.* Typhimurium ATCC 14028, and **(D)** *S.* Enteritidis ATCC 13076.

broad spectrum antimicrobial agents which exert the same effect to all Gram-negative bacteria strains.

Silver nanoparticles are well-known as the most universal antimicrobial substances due to their strong biocidal effect against microorganisms, which has been used for over the past decades to prevent and treat various diseases (Oei et al., 2012). AgNPs are also widely used as anti-fungal (Kim et al., 2009), anti-inflammatory (Nadworny et al., 2010), and anti-viral properties (Lara et al., 2010a). Recently, non-hazardous AgNPs can easily be synthesized using a cost-effective method and tested as a new type of antimicrobial agents.

In this study, the application of AgNPs as an antimicrobial agent was tested against selected Gram-negative bacteria on agar plate and liquid medium. The results showed that the tested bacteria could completely inhibit by AgNPs. The inhibition of bacteria growth was reported affected by the concentration of AgNPs and bacteria used in the experiments (Sondi and Salopek-Sondi, 2004). The green synthesized AgNPs in this study are able to inhibit the high concentration of bacteria (approximately 10^6 CFU/mL). This indicated that AgNPs showed an excellent antimicrobial effect as the high CFU concentration of bacteria used in this study are rarely appeared in real-life systems.

The antibacterial activity of AgNPs has been reported by many researchers. However, the MIC values from the previous studies showed the range through a large extent of variation. Therefore, the comparison of the results is difficult as there is no standard method for determination of antibacterial activity of AgNPs and different methods have been applied by the researchers (Zarei et al., 2014). In this study, AgNPs exhibit a good antibacterial activity against the tested foodborne pathogens. Based on the results, the tested bacteria were able to kill in a shorter time at low concentration of AgNPs. This may due to the cell wall structure of Gram-negative bacteria. The characteristic cell wall structure of Gram-negative bacteria is different from Gram-positive bacteria. Gram-negative bacteria have a cytoplasmic membrane, a thin peptidoglycan layer, and an outer membrane containing lipopolysaccharide. There is a space between the cytoplasmic membrane and the outer membrane called the periplasmic space or periplasm. The periplasmic space contains the loose network of peptidoglycan chains known as the peptidoglycan layer.

The rapid reproduction time of bacteria is one of the main causes of bacteria's infectivity (Lara et al., 2010b). However, the reproduction time of the bacteria could be an ideal way to prevent the viable infection as AgNPs were effective in inhibiting

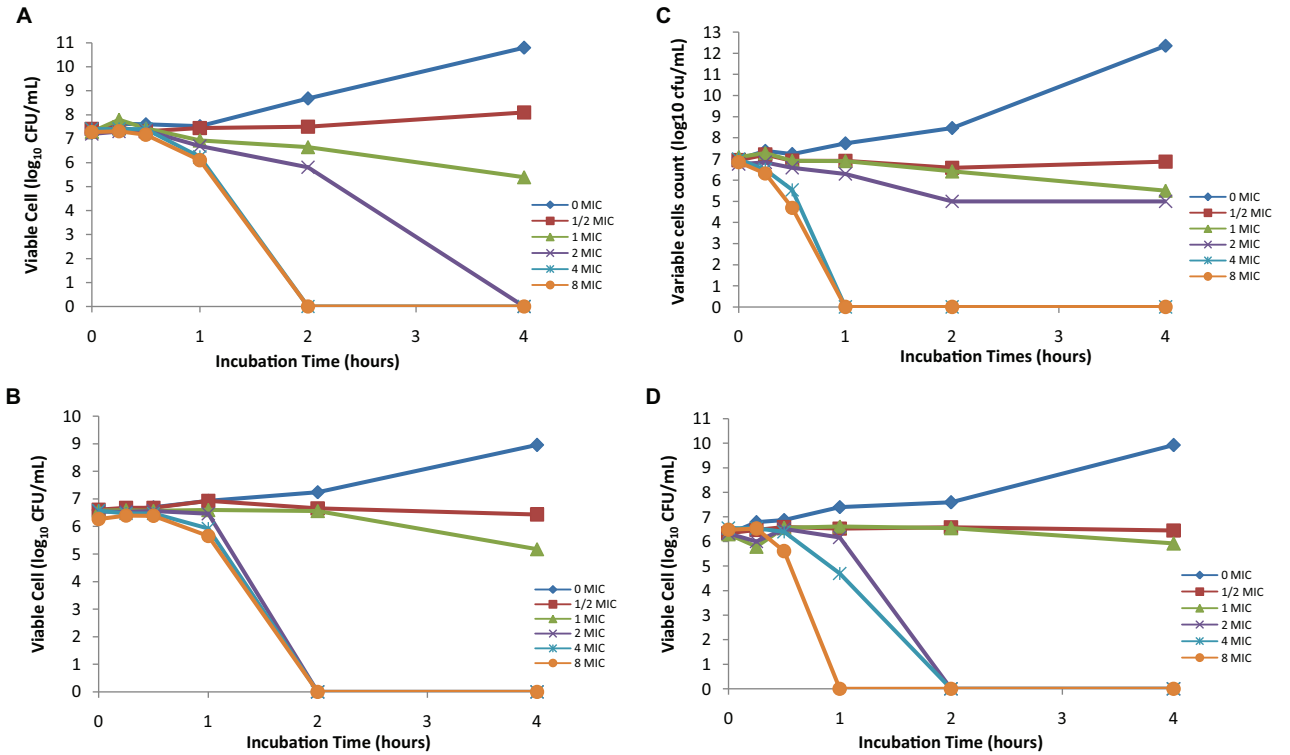

FIGURE 2 | Time-kill plots of AgNPs against **(A)** *E. coli* ATCC 25922, **(B)** *K. pneumoniae* ATCC 13773, **(C)** *S.* Typhimurium ATCC 14028, and **(D)** *S.* Enteritidis ATCC 13076 at different concentration and time-length.

and killing the bacteria in a dose and time dependent manner as shown in the time-kill assays. Zhang et al. (2016) reported that the smaller size of AgNPs could cause more toxicity to the bacteria and show better bactericidal effect compared to the larger particles as they have larger surface area. Previous study by Agnihotri et al. (2014) found that the antibacterial efficacy was increased for the AgNPs with less than 10 nm size. They also concluded that AgNPs with the size of 5 nm have the fastest antibacterial activity compared to others size of AgNPs.

Silver nanoparticles have emerged as antimicrobial agents against multidrug resistant bacteria due to their high surface-area-to-volume ration and unique chemical and physical properties. AgNPs have particle size ranging from 1 to 100 nm. The surface area-to-volume ratio of AgNPs increases as the particles size decreases. Morones et al. (2005) reported that AgNPs with the size of 10-100 nm showed strong antimicrobial effect against both Gram-positive and negative bacteria. The small particle size enables AgNPs to adhere to the cell wall and penetrate into the bacteria cell easily, which in turn improves their antimicrobial activity against bacteria. The antimicrobial effects of AgNPs against multidrug resistant bacteria have been studied by many researchers and it was proved that AgNPs are effective against multidrug resistant bacteria such as multidrug resistant *E. coli* (Paredes et al., 2014; Kar et al., 2016), multidrug resistant strain of *Pseudomonas aeruginosa* (Durairaj et al., 2012), methicillin-resistant *Staphylococcus aureus* (MRSA) (Paredes et al., 2014; Yuan et al., 2017), and extended-spectrum β-lactam (ESBL) producing bacteria (Doudi et al., 2013; Subashini et al., 2014).

On the other hands, AgNPs are advantageous compared to conventional chemical antimicrobial agents as the major problem caused by the conventional chemical antimicrobial agents is multidrug resistance. The effectiveness of the chemical antimicrobial agents depends on the specific binding of the microorganisms with the surface and metabolites of the antimicrobial agents. However, the chemical antimicrobial agents are limited to use especially in medical field as various microorganisms have developed multiple resistance traits over a period of generations. Thus, the development of AgNPs could be an alternative way to overcome the multidrug resistance microorganisms as bacteria are less likely to develop resistance to metal nanoparticles compared to the conventional antibiotics.

The exact mechanisms of AgNPs against bacteria still remain unknown. However, there are some researchers proposed that the action of AgNPs on bacteria may due to its ability to penetrate into the cell (Sondi and Salopek-Sondi, 2004), the formation of free radicals (Danilczuk et al., 2006; Kim et al., 2007), the inactivation of proteins in the cell by silver ions (Rai et al., 2012) and the production of reactive oxygen species (ROS) (Dakal et al., 2016). Besides that, there are also some factors in affecting the bactericidal mechanisms of AgNPs such as the concentration of AgNPs and bacteria class (Kim et al., 2007; Zhang et al., 2014), shape (Pal et al., 2007; Meire et al., 2012), size

(Martinez-Castanon et al., 2008), and the combination of various antibiotics (Fayaz et al., 2010; Singh et al., 2013).

CONCLUSION

Silver nanoparticles showed significant antibacterial activity against the selected Gram-negative foodborne pathogens. Thus, AgNPs might be a good alternative to develop as antibacterial agent against the multidrug-resistant strains of bacteria. The applications of AgNPs may lead to valuable findings in various fields such as medical devices and antimicrobial systems.

AUTHOR CONTRIBUTIONS

YL, BC, YR, and RS developed the study design. YL and CK carried out the confirmation for the selected foodborne pathogens. MN provided culture media and technical advice in the study. YL interpreted the data, drafted the manuscript, and revised the manuscript. YR, M-A-RN-K, CK, BC, and RS checked on the manuscript. All authors read and approved the final version of the manuscript.

FUNDING

This research was funded by a Research University Grant Scheme Initiative Six (RUGS 6) of Universiti Putra Malaysia (GP-IPS 9438703) and Fundamental Research Grant Scheme (FRGS) of Ministry of Higher Education (MOHE), Malaysia (02-01-14-1475FR) and, in part, by the Kakenhi Grant-in-Aid for Scientific Research (KAKENHI 24249038), Japan Society for the Promotion of Sciences and grant-in-aid of Ministry of Health, Labor and Welfare, Japan.

REFERENCES

Agnihotri, S., Mukherji, S., and Mukherji, S. (2014). Size-controlled silver nanoparticles synthesized over the range 5–100 nm using the same protocol and their antibacterial efficacy. *RSC Adv.* 4, 3974–3983. doi: 10.1039/C3RA44507K

Ahmed, S., Ahmad, M., Swami, B. L., and Ikram, S. (2016). A review on plants extract mediated synthesis of silver nanoparticles for antimicrobial applications: a green expertise. *J. Adv. Res.* 7, 17–28. doi: 10.1016/j.jare.2015.02.007

Bauer, A. W., Kirby, W. M., Sherris, J. C., and Turck, M. (1966). Antibiotic susceptibility testing by a standardized single disk method. *Am. J. Clin. Pathol.* 45, 493–496. doi: 10.1093/ajcp/45.4_ts.493

Bekele, A. Z., Gokulan, K., Williams, K. M., and Khare, S. (2016). Dose and size-dependent antiviral effects of silver nanoparticles on feline calicivirus, a human norovirus surrogate. *Foodborne Pathog. Dis.* 13, 239–244. doi: 10.1089/fpd.2015.2054

Burt, S. (2004). Essential oils: their antibacterial properties and potential applications in foods—a review. *Int. J. Food Microbiol.* 94, 223–253. doi: 10.1016/j.ijfoodmicro.2004.03.022

Chukwu, E. E., Nwaokorie, F. O., Coker, A. O., Avila-Campos, M. J., Solis, R. L., Llanco, L. A., et al. (2016). Detection of toxigenic *Clostridium perfringens* and *Clostridium botulinum* from food sold in Lagos, Nigeria. *Anaerobe* 42, 176–181. doi: 10.1016/j.anaerobe.2016.10.009

CLSI (2012). *Performance Standards for Antimicrobial Susceptibility Testing; Twenty-Second Informational Supplement*. Wayne, PA: The Clinical and Laboratory Standards Institute.

Dakal, T. C., Kumar, A., Majumdar, R. S., and Yadav, V. (2016). Mechanistic basis of antimicrobial actions of silver nanoparticles. *Front. Microbiol.* 7:1831. doi: 10.3389/fmicb.2016.01831

Danilczuk, M., Lund, A., Sadlo, J., Yamada, H., and Michalik, J. (2006). Conduction electron spin resonance of small silver particles. *Spectrochim. Acta A Mol. Biomol. Spectrosc.* 63, 189–191. doi: 10.1016/j.saa.2005.05.002

Dhand, V., Soumya, L., Bharadwaj, S., Chakra, S., Bhatt, D., and Sreedhar, B. (2016). Green synthesis of silver nanoparticles using *Coffea arabica* seed extract and its antibacterial activity. *Mater. Sci. Eng. C* 58, 36–43. doi: 10.1016/j.msec.2015.08.018

D'Ostuni, V., Tristezza, M., De Giorgi, M. G., Rampino, P., Grieco, F., and Perrotta, C. (2016). Occurrence of *Listeria monocytogenes* and *Salmonella* spp. in meat processed products from industrial plants in Southern Italy. *Food Control* 62, 104–109.

Doudi, M., Naghsh, N., and Setorki, M. (2013). Comparison of the effects of silver nanoparticles on pathogenic bacteria resistant to beta-lactam antibiotics (ESBLs) as a prokaryote model and Wistar rats as a eukaryote model. *Med. Sci. Monit. Basic Res.* 19, 103–110. doi: 10.12659/MSMBR.883835

Durairaj, R., Amirulhusni, A. N., Palanisamy, N. K., Mohd-Zain, Z., and Ping, L. J. (2012). Antibacterial effect of silver nanoparticles on multi drug resistant *Pseudomonas aeruginosa*. *World Acad. Sci. Eng. Technol.* 6, 210–213. doi: 10.12659/MSMBR.883835

Fayaz, A. M., Balaji, K., Girilal, M., Yadav, R., Kalaichelvan, P. T., and Venketesan, R. (2010). Biogenic synthesis of silver nanoparticles and their synergistic effect with antibiotics: a study against Gram-positive and Gram-negative bacteria. *Nanomedicine* 6, 103–109. doi: 10.1016/j.nano.2009.04.006

Ferreira, V., Wiedmann, M., Teixeira, P., and Stasiewicz, M. (2014). *Listeria monocytogenes* persistence in food-associated environments: epidemiology, strain characteristics, and implications for public health. *J. Food Prot.* 77, 150–170. doi: 10.4315/0362-028X.JFP-13-150

Franci, G., Falanga, A., Galdiero, S., Palomba, L., Rai, M., Morelli, G., et al. (2015). Silver nanoparticles as potential antibacterial agents. *Molecules* 20, 8856–8874. doi: 10.3390/molecules20058856

Guzman, M., Dille, J., and Godet, S. (2012). Synthesis and antibacterial activity of silver nanoparticles against gram-positive and gram-negative bacteria. *Nanomedicine* 8, 37–45. doi: 10.1016/j.nano.2011.05.007

Hebeish, A., El-Rafie, M., El-Sheikh, M., Seleem, A. A., and El-Naggar, M. E. (2014). Antimicrobial wound dressing and anti-inflammatory efficacy of silver nanoparticles. *Int. J. Biol. Macromol.* 65, 509–515. doi: 10.1016/j.ijbiomac.2014.01.071

Heiman, K. E., Mody, R. K., Johnson, S. D., Griffin, P. M., and Gould, L. H. (2015). *Escherichia coli* O157 outbreaks in the United States, 2003–2012. *Emerg. Infect. Dis.* 21, 1293–1301. doi: 10.3201/eid2108.141364

Kaakoush, N. O., Castaño-Rodríguez, N., Mitchell, H. M., and Man, S. M. (2015). Global epidemiology of *Campylobacter* infection. *Clin. Microbiol. Rev.* 28, 687–720. doi: 10.1128/CMR.00006-15

Kar, D., Bandyopadhyay, S., Dimri, U., Mondal, D. B., Nanda, P. K., Das, A. K., et al. (2016). Antibacterial effect of silver nanoparticles and capsaicin against MDR-ESBL producing *Escherichia coli*: an in vitro study. *Asian Pac. J. Trop. Dis.* 6, 807–810. doi: 10.1016/S2222-1808(16)61135-0

Khalifa, R. A., Nasser, M. S., Gomaa, A. A., Osman, N. M., and Salem, H. M. (2013). Resazurin Microtiter Assay Plate method for detection of susceptibility of multidrug resistant *Mycobacterium tuberculosis* to second-line anti-tuberculous drugs. *Egypt. J. Chest Dis. Tuberc.* 62, 241–247. doi: 10.1016/j.ejcdt.2013.05.008

Kim, J. S., Kuk, E., Yu, K. N., Kim, J.-H., Park, S. J., Lee, H. J., et al. (2007). Antimicrobial effects of silver nanoparticles. *Nanomedicine* 3, 95–101. doi: 10.1016/j.nano.2006.12.001

Kim, K.-J., Sung, W. S., Suh, B. K., Moon, S.-K., Choi, J.-S., Kim, J. G., et al. (2009). Antifungal activity and mode of action of silver nano-particles on *Candida albicans*. *Biometals* 22, 235–242. doi: 10.1007/s10534-008-9159-2

Lara, H. H., Ayala-Nuñez, N. V., Ixtepan-Turrent, L., and Rodriguez-Padilla, C. (2010a). Mode of antiviral action of silver nanoparticles against HIV-1. *J. Nanobiotechnol.* 8:1. doi: 10.1186/1477-3155-8-1

Lara, H. H., Ayala-Núnez, N. V., Turrent, L. D. C. I., and Padilla, C. R. (2010b). Bactericidal effect of silver nanoparticles against multidrug-resistant bacteria. *World J. Microbiol. Biotechnol.* 26, 615–621. doi: 10.1007/s11274-009-0211-3

Lau, K., Zainin, N., Abas, F., and Rukayadi, Y. (2014). Antibacterial and sporicidal activity of *Eugenia polyantha* Wight against *Bacillus cereus* and *Bacillus subtilis*. *Int. J. Curr. Microbiol. Appl. Sci.* 3, 499–510.

Lee, K.-M., Runyon, M., Herrman, T. J., Phillips, R., and Hsieh, J. (2015). Review of *Salmonella* detection and identification methods: aspects of rapid emergency response and food safety. *Food Control* 47, 264–276. doi: 10.1016/j.foodcont.2014.07.011

Loo, Y. Y., Chieng, B. W., Nishibuchi, M., and Radu, S. (2012). Synthesis of silver nanoparticles by using tea leaf extract from *Camellia sinensis*. *Int. J. Nanomed.* 7, 4263–4267. doi: 10.2147/IJN.S33344

Martinez-Castanon, G., Nino-Martinez, N., Martinez-Gutierrez, F., Martinez-Mendoza, J., and Ruiz, F. (2008). Synthesis and antibacterial activity of silver nanoparticles with different sizes. *J. Nanopart. Res.* 10, 1343–1348. doi: 10.1007/s11051-008-9428-6

McNicholl, B. P., McGrath, J. W., and Quinn, J. P. (2007). Development and application of a resazurin-based biomass activity test for activated sludge plant management. *Water Res.* 41, 127–133. doi: 10.1016/j.watres.2006.10.002

Medda, S., Hajra, A., Dey, U., Bose, P., and Mondal, N. K. (2015). Biosynthesis of silver nanoparticles from *Aloe vera* leaf extract and antifungal activity against *Rhizopus* sp. and *Aspergillus* sp. *Appl. Nanosci.* 5, 875–880. doi: 10.1007/s13204-014-0387-1

Meire, M., Coenye, T., Nelis, H., and De Moor, R. (2012). Evaluation of Nd: YAG and Er: YAG irradiation, antibacterial photodynamic therapy and sodium hypochlorite treatment on *Enterococcus faecalis* biofilms. *Int. Endod. J.* 45, 482–491. doi: 10.1111/j.1365-2591.2011.02000.x

Morones, J. R., Elechiguerra, J. L., Camacho, A., Holt, K., Kouri, J. B., Ramírez, J. T., et al. (2005). The bactericidal effect of silver nanoparticles. *Nanotechnology* 16, 2346–2353. doi: 10.1088/0957-4484/16/10/059

Nadworny, P. L., Wang, J., Tredget, E. E., and Burrell, R. E. (2010). Anti-inflammatory activity of nanocrystalline silver-derived solutions in porcine contact dermatitis. *Int. J. Inflamm.* 7:13. doi: 10.1186/1476-9255-7-13

O'Bryan, C. A., Crandall, P. G., and Ricke, S. C. (2018). *Antimicrobial Resistance in Foodborne Pathogens. Food and Feed Safety Systems and Analysis*. New York, NY: Elsevier.

Oei, J. D., Zhao, W. W., Chu, L., DeSilva, M. N., Ghimire, A., Rawls, H. R., et al. (2012). Antimicrobial acrylic materials with in situ generated silver nanoparticles. *J. Biomed. Mater. Res. B Appl. Biomater.* 100, 409–415. doi: 10.1002/jbm.b.31963

Pal, S., Tak, Y. K., and Song, J. M. (2007). Does the antibacterial activity of silver nanoparticles depend on the shape of the nanoparticle? A study of the Gram-negative bacterium *Escherichia coli*. *Appl. Environ. Microbiol.* 73, 1712–1720. doi: 10.1128/AEM.02218-06

Paredes, D., Ortiz, C., and Torres, R. (2014). Synthesis, characterization, and evaluation of antibacterial effect of Ag nanoparticles against *Escherichia coli* O157: H7 and methicillin-resistant *Staphylococcus aureus* (MRSA). *Int. J. Nanomed.* 9, 1717–1729. doi: 10.2147/IJN.S57156

Patel, G., Huprikar, S., Factor, S. H., Jenkins, S. G., and Calfee, D. P. (2008). Outcomes of carbapenem-resistant *Klebsiella pneumoniae* infection and the impact of antimicrobial and adjunctive therapies. *Infect. Control Hosp. Epidemiol.* 29, 1099–1106. doi: 10.1086/592412

Rai, M., Deshmukh, S., Ingle, A., and Gade, A. (2012). Silver nanoparticles: the powerful nanoweapon against multidrug-resistant bacteria. *J. Appl. Microbiol.* 112, 841–852. doi: 10.1111/j.1365-2672.2012.05253.x

Selvam, K., Sudhakar, C., Govarthanan, M., Thiyagarajan, P., Sengottaiyan, A., Senthilkumar, B., et al. (2017). Eco-friendly biosynthesis and characterization of silver nanoparticles using *Tinospora cordifolia* (Thunb.) Miers and evaluate its antibacterial, antioxidant potential. *J. Radiat. Res. Appl. Sci.* 10, 6–12. doi: 10.1016/j.jrras.2016.02.005

Singh, R., Wagh, P., Wadhwani, S., Gaidhani, S., Kumbhar, A., Bellare, J., et al. (2013). Synthesis, optimization, and characterization of silver nanoparticles from *Acinetobacter calcoaceticus* and their enhanced antibacterial activity when combined with antibiotics. *Int. J. Nanomed.* 8, 4277–4290. doi: 10.2147/IJN.S48913

Sondi, I., and Salopek-Sondi, B. (2004). Silver nanoparticles as antimicrobial agent: a case study on *E. coli* as a model for Gram-negative bacteria. *J. Colloid Interface Sci.* 275, 177–182. doi: 10.1016/j.jcis.2004.02.012

Subashini, J., Khanna, V. G., and Kannabiran, K. (2014). Anti-ESBL activity of silver nanoparticles biosynthesized using soil *Streptomyces* species. *Bioprocess Biosyst. Eng.* 37, 999–1006. doi: 10.1007/s00449-013-1070-8

Tanwar, J., Das, S., Fatima, Z., and Hameed, S. (2014). Multidrug resistance: an emerging crisis. *Interdiscip. Perspect. Infect. Dis.* 2014: 541340. doi: 10.1155/2014/541340

Välimaa, A.-L., Tilsala-Timisjärvi, A., and Virtanen, E. (2015). Rapid detection and identification methods for *Listeria monocytogenes* in the food chain–a review. *Food Control* 55, 103–114. doi: 10.1016/j.foodcont.2015.02.037

WHO (2000). *Overcoming Antimicrobial Resistance*. Geneva: World Health Organization.

WHO (2014). *Initiative to Estimate the Global Burden of Foodborne Diseases: Information and Publications*. Geneva: World Health Organization.

Woh, P. Y., Thong, K. L., Behnke, J. M., Lewis, J. W., and Zain, S. N. M. (2017). Characterization of nontyphoidal *Salmonella* isolates from asymptomatic migrant food handlers in Peninsular Malaysia. *J. Food Prot.* 80, 1378–1383. doi: 10.4315/0362-028X.JFP-16-342

Yuan, Y.-G., Peng, Q.-L., and Gurunathan, S. (2017). Effects of silver nanoparticles on multiple drug-resistant strains of *Staphylococcus aureus* and *Pseudomonas aeruginosa* from mastitis-infected goats: an alternative approach for antimicrobial therapy. *Int. J. Mol. Sci.* 18:E569. doi: 10.3390/ijms18030569

Zainin, N., Lau, K., Zakaria, M., Radu, S., Razis, A., Faizal, A., et al. (2013). Antibacterial activity of *Boesenbergia rotunda* (L.) Mansf. A. extract against *Escherichia coli*. *Int. Food Res. J.* 20, 3319–3323.

Zarei, M., Jamnejad, A., and Khajehali, E. (2014). Antibacterial effect of silver nanoparticles against four foodborne pathogens. *Jundishapur J. Microbiol.* 7, 8720–8723. doi: 10.5812/jjm.8720

Zhang, M., Zhang, K., De Gusseme, B., Verstraete, W., and Field, R. (2014). The antibacterial and anti-biofouling performance of biogenic silver nanoparticles by *Lactobacillus fermentum*. *Biofouling* 30, 347–357. doi: 10.1080/08927014.2013.873419

Zhang, X.-F., Liu, Z.-G., Shen, W., and Gurunathan, S. (2016). Silver nanoparticles: synthesis, characterization, properties, applications, and therapeutic approaches. *Int. J. Mol. Sci.* 17:E1534. doi: 10.3390/ijms17091534

Conflict of Interest Statement: The authors declare that the research was conducted in the absence of any commercial or financial relationships that could be construed as a potential conflict of interest.

Copyright © 2018 Loo, Rukayadi, Nor-Khaizura, Kuan, Chieng, Nishibuchi and Radu. This is an open-access article distributed under the terms of the Creative Commons Attribution License (CC BY). The use, distribution or reproduction in other forums is permitted, provided the original author(s) and the copyright owner(s) are credited and that the original publication in this journal is cited, in accordance with accepted academic practice. No use, distribution or reproduction is permitted which does not comply with these terms.

frontiers in Microbiology

ORIGINAL RESEARCH
published: 23 July 2018
doi: 10.3389/fmicb.2018.01553

Prevention of Dermal Abscess Formation Caused by *Staphylococcus aureus* Using Phage JD007 in Nude Mice

Bingyu Ding[1,2], Qingtian Li[2], Mingquan Guo[3], Ke Dong[3], Yan Zhang[3], Xiaokui Guo[3], Qingzhong Liu[1], Li Li[1] and Zelin Cui[1]**

[1] Department of Laboratory Medicine, Shanghai General Hospital, Shanghai Jiao Tong University School of Medicine, Shanghai, China, [2] Department of Laboratory Medicine, Ruijin Hospital, Shanghai Jiao Tong University School of Medicine, Shanghai, China, [3] Department of Immunology and Microbiology, Shanghai Jiao Tong University School of Medicine, Shanghai, China

OPEN ACCESS

Edited by:
Noton Kumar Dutta,
Johns Hopkins University,
United States

Reviewed by:
Ananda Shankar Bhattacharjee,
Bigelow Laboratory for Ocean Sciences, United States
Junji Xing,
Houston Methodist Research Institute, United States

***Correspondence:**
Li Li
annylish@126.com
Zelin Cui
czl_phage@126.com;
czl@sjtu.edu.cn

Specialty section:
This article was submitted to Antimicrobials, Resistance and Chemotherapy, a section of the journal Frontiers in Microbiology

Received: 11 October 2017
Accepted: 22 June 2018
Published: 23 July 2018

Citation:
Ding B, Li Q, Guo M, Dong K, Zhang Y, Guo X, Liu Q, Li L and Cui Z (2018) Prevention of Dermal Abscess Formation Caused by Staphylococcus aureus Using Phage JD007 in Nude Mice. Front. Microbiol. 9:1553. doi: 10.3389/fmicb.2018.01553

Aim: In this study, *Staphylococcus* phage JD007 bactericidal activity and induced immune responses during treatment were assessed in a dermal abscess model.

Materials and Methods: Dermal abscesses in nude mice were established by injecting a clinical isolate of *S. aureus* SA325 isolated from the back under-dermal abscess of an in-patient.

Results: Phage JD007 was able to inhibit the growth of *S. aureus* SA325 at MOI = 1 or 10, significantly preventing the formation of dermal abscesses. Moderate immune responses were observed in the prevention group through detection of cytokines.

Conclusion: Phage JD007 inhibits the formation of dermal abscesses caused by a clinical *S. aureus* strain in nude mice without robust immune responses.

Keywords: *Staphylococcus aureus*, dermal abscess, inhibition, nude mouse, phage JD007

INTRODUCTION

With the increasing prevalence antibiotic resistant infections, including MRSA (methicillin-resistant *Staphylococcus aureus*) and the emergence of VRSA (vancomycin-resistant *S. aureus*) (Xiao et al., 2013; Limbago et al., 2014), innovative treatments are urgently needed. Recently, there has been renewed interest in phage therapy (Thiel, 2004; Salmond and Fineran, 2015), which has been proposed as a potential antimicrobial therapy as far back as the 1920's (Salmond and Fineran, 2015). Advances in biotechnology have led to the identification of numerous classes of bacteriophages with different host specificities such as K, GH15, Twort, phiIPLA-RODI, and phiIPLA-C1C (O'Flaherty et al., 2004; Kwan et al., 2005; Gu et al., 2012b; Gutierrez et al., 2015). Furthermore, whole genome sequences of these phages enables us to understand their biology at a much deeper level (Cui et al., 2017b).

Phages have been used to treat infectious disease in various animal models. A single dose of phage MR10 exhibited efficacy similar to linezolid in resolving the course of hindpaw infection in diabetic animals, suggesting this approach could serve as an effective strategy in treating MRSA mediated foot infections in diabetic individuals (Chhibber et al., 2013). Phage LS2a has been shown to prevent abscess formation in rabbits when injected simultaneously with *S. aureus* into the subcutaneous site (Wills et al., 2005). Phage Kpn5 could potentially be used as stand-alone therapy for the *Klebsiella pneumoniae* induced burn wound infection, effective even against antibiotic-resistant strains (Kumari et al., 2009). Additionally, in clinical trials, phage products have showed efficacy according to some reports (Marza et al., 2006).

Phage host specificity narrows their use with lysing efficacies that can vary significantly depending on the phage strain. Reports have also documented failures of phage therapy *in vivo* (Sarker and Brussow, 2016), so, it is necessary to evaluate phages' bacteria killing efficacy both *in vitro* and in an animal model. *Staphylococcus* phage JD007, which belongs to family of *Myoviridae* was identified in 2012 and has been shown to have wide host range (Cui et al., 2012), capable of killing *S. aureus* of different MLST Types (Cui et al., 2017a). The aim of this study is to evaluate the treatment efficacy of JD007 in dermal abscesses caused by a clinical strain of MRSA and the immune responses elicited during therapy.

MATERIALS AND METHODS

Animals

BALB/c nude mice (WT, Shanghai Super B&K laboratory animal Corp. Ltd., [SCXK(HU)2005—0001], Shanghai, China) were used in this study. Dermal abscesses were stereo tactically induced as described previously (Capparelli et al., 2007). Uninfected mice served as controls. Mice were euthanized on days 1, 3 and 10 after infection. Ethics eligibility of this study was approved by the Shanghai General Hospital Ethics Committee (Shanghai Jiao Tong University School of Medicine). All experiments were performed in accordance with the national animal protection guidelines approved by the local animal ethics committee. Fifty mice were randomly divided into five groups, 10 mice in each group, including control group (no treatment), phage JD007 group (injected with purified phage JD007), infection group (infected by *S. aureus* SA325), prevention group (phage JD007 were injected 1 h before mice was infected by *S. aureus* SA325), and treatment group (phage JD007 was injected 1 h after mice were infected by *S. aureus* SA325).

Bacteriophage Purification

High-titre phage stocks were obtained through amplification in liquid LB (Luria-Bertani) medium supplemented with 10 μM $MgCl_2$ and 5 μM $CaCl_2$. In culture, *S. aureus* SA325 was infected phage JD007 at a MOI of 0.1 and incubated at 37°C overnight. The visible bacterial lysate in liquid culture were obtained, and then incubated with chloroform (final concentration was 2%) for 30 min with gentle shaking to kill residual bacteria. Remaining bacterial products were removed by centrifugation at 6,500 rpm (Beckman, JA18.0, United States) for 15 min. Phage contained in the supernatant was enriched at 4°C overnight using polyethylene glycol (PEG) 8000 (final concentration 10% w/v), and precipitated at 8,500 rpm for 20 min (Beckman, JA18.0, United States). Afterwards, the pellet was dissolved in TM buffer [(Tris-Mg^{2+} Buffer) 10 mM Tris–HCl (pH 7.2–7.5), 100 mM NaCl, 10 mM $MgCl_2$.5 mM $CaCl_2$] and vortexed. PEG 8000 was removed by adding the same volume of chloroform after vortexing. The solution was centrifuged at 4,000 *g*/min for 10 min, and the supernatant containing the phage was

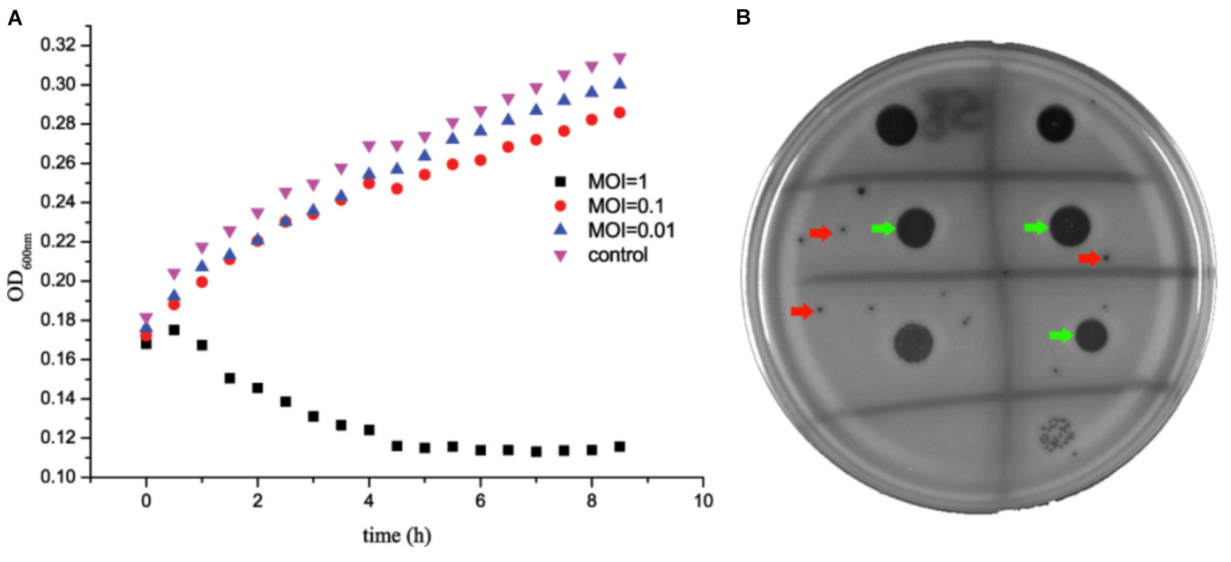

FIGURE 1 | *Staphylococcus aureus* SA325 growth was inhibited by phage JD007 *in vitro*. **(A)** Phage JD007 could inhibit the growth of SA325 at MOI = 1. **(B)** Inhibition zones and plaques were formed by phage JD007 in two-layer agar plate of SA325 and were marked using green and red arrows, respectively.

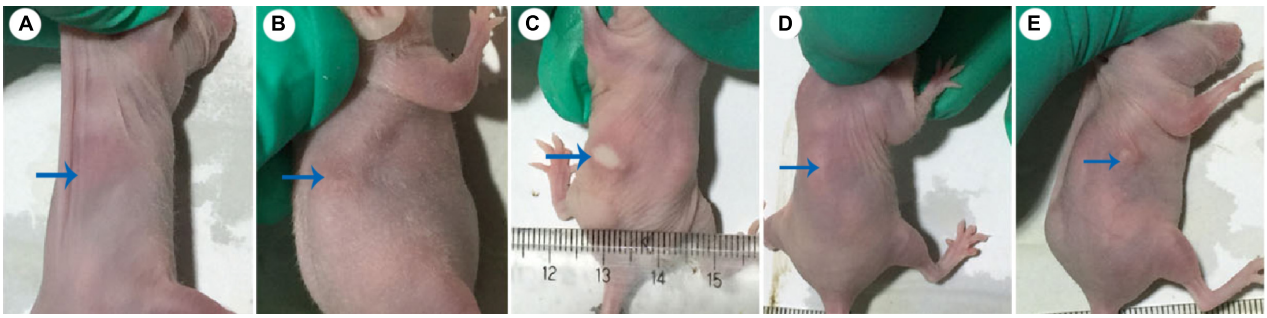

FIGURE 2 | Photos of dermal abscesses in nude BALB/c mice using phage JD007. **(A–E)** Represented the dermal abscesses of mice individually in control group, phage group, infection group, prevention group, and treatment group. The blue arrows showed the skin sites injected with *S. aureus* SA325.

isolated. CsCl was added at a concentration of 0.5 g per 1 mL, and the phages were purified by discontinuous centrifugation in a CsCl gradient (1.33, 1.45, 1.50, and 1.70g/cm^3) in TM buffer in Ultra-Clear tubes (Beckman Coulter, Inc., Fullerton, CA, United States) by centrifuging at 35000 rpm/min for 4 h. Finally, the layer with enriched phage was obtained with a syringe, dialyzed against TM buffer and stored at 4°C (Boulanger, 2009).

S. aureus Strain and Culture Condition

Staphylococcus aureus strain SA325 (MRSA, confirmed by antibiotic resistant profile) was isolated from an in-patient with a re-occurring back under-dermal abscess due to long-term bed rest. SA325 concentration was calculated by serial dilutions when grown to $OD_{600\,nm}$ = 0.4, and plated uniformly using the glass spreading rod, and cultured overnight at 37°C, the value of SA325 per $OD_{600\,nm}$ was 9.5 × 10^9 CPU/mL.

S. aureus Growth Inhibition Assay

Drop tests were conducted using two-layer agar plates. *S. aureus* SA325 was cultured to $OD_{600\,nm}$ = 0.4 in TSB (Tryptic soy broth) supplemented with 10 μM $MgCl_2$ and 5 μM $CaCl_2$. Bacteria grown to logarithmic phase were mixed with 0.7% agar LB and then poured on the plate of LB agar (1.5%) uniformly, incubating at room temperature for 30 min. Finally, 3 μL of serial dilutions of phage JD007 was dropped on the plate. The inhibition zones were observed after an overnight culture.

The inhibition growth curves for phage JD007 infected *S. aureus* SA325 were determined using MOIs of 0, 0.01, 0.1, and 1 inoculated in 96 well plates separately and incubated at 37°C. $OD_{600\,nm}$ of these cultures was measured every 30 min extending for 8 h. Assay was performed three times (n = 3) with three biological replicates.

Mice Dermal Abscess Infection Model

Staphylococcus aureus was prepared by culturing at 37°C in TSB to exponential phase at which time the bacteria was collected and washed twice with PBS with immediate centrifugation. SA325 was re-suspended at final concentration of 1 × 10^9 CFUs/100μL, and kept on ice before injecting nude mice intradermally.

All animal experiments were approved by the Shanghai General Hospital Ethics Committee (Shanghai Jiao Tong University, China), and conducted according to the Chinese Law for Animal Protection. To investigate the antimicrobial efficacy of phage JD007 for subcutaneous abscesses, BALB/c nude mice (6–8 weeks old) were anesthetized by intraperitoneal injection of a saline solution containing fentanyl (0.05 mg/kg), midazolam (5 mg/kg), and medetomidine (0.5 mg/kg). The backs of the animals were disinfected with 70% ethanol, and 50 μL suspension containing 5 × 10^8 CFU *S. aureus* SA325 in PBS were inoculated subcutaneously; 50 μL of phage JD007 was injected into the infected region. Mice were weighed before inoculation. Weight and abscess formation were measured daily extending for 10 days. The length (L) and width (W) of abscesses were determined using a caliper. The size of the abscesses was then calculated with the standard formula for area: V = [π/2] × L × W (Weinandy et al., 2014).

Immune Response During Treatment Using *Staphylococcus* Phage JD007

Three mice in each described above were randomly enrolled and euthanized on the third day of the experimental protocol. Serum from each mouse was obtained, and immune cytokines

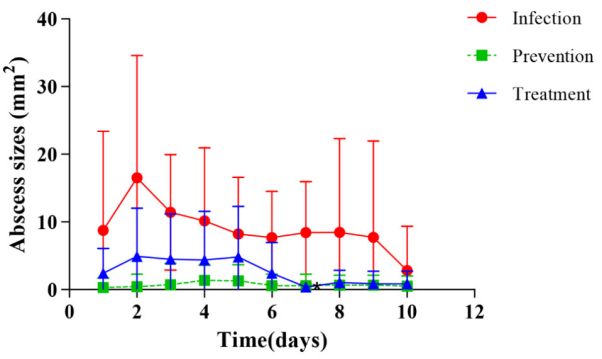

FIGURE 3 | Changes of dermal abscesses sizes formed in nude BALB/c mice during phage therapy. There are no abscesses formed in control and phage groups during the whole procession of observation periods.

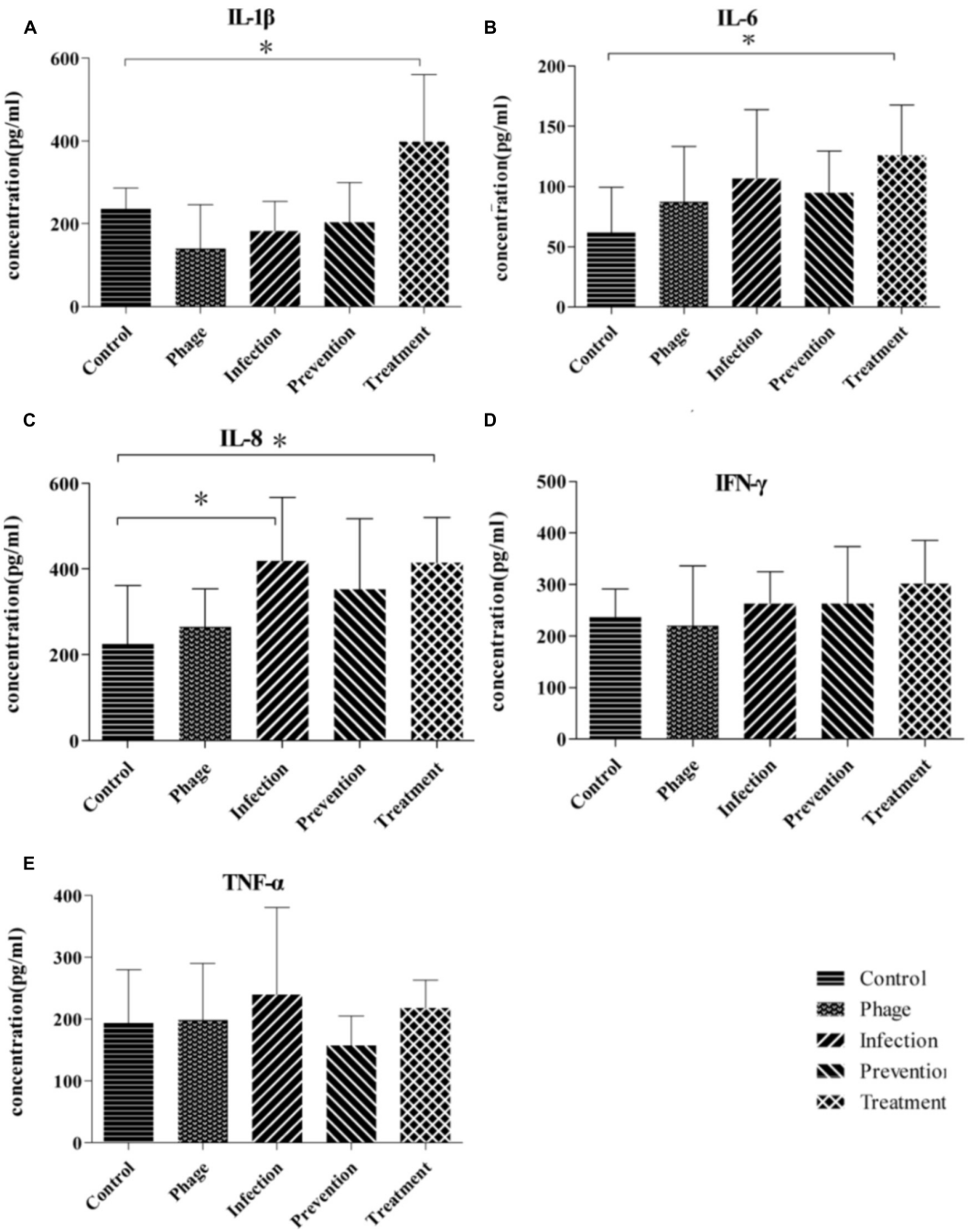

FIGURE 4 | Inflammatory cytokines responses in nude BALB/c mice during phage therapy. **(A–E)** Are separately represents the sera level of IL-1β, IL-6, IL-8, IFN-γ, and TNF-α of mice from different groups, $*p < 0.05$.

(IL-1β, IL-6, IL-8, IFN-γ, and TNF-α) were measured using ELISA (Beijing 4A Biotech Co., Ltd.).

Statistical Analysis

A two-tailed unpaired Student's *t*-test was used for statistical analysis with GraphPad Prism Software. *P*-values of less than 0.05 were considered significant unless specifically indicated otherwise.

RESULTS

S. aureus SA325 Growth Is Inhibited by Phage JD007 *in Vitro*

Staphylococcus aureus SA325 was co-cultured with phage JD007 at 37°C with co-culture $OD_{600\,nm}$ measurements made at 30 min intervals for 8 h. Results showed that phage JD007 inhibited the

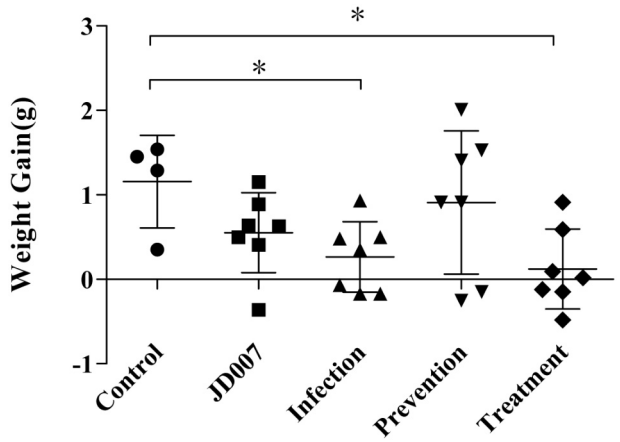

FIGURE 5 | Weights gains in nude BALB/c mice during phage therapy. Body weights gain were calculated by subtracting original body weight from weights on the 10th day. Body weights gains in groups of infection and treatment were significantly lower than that in control group, $*p < 0.05$.

growth of *S. aureus* SA325 as early as 1 h after co-incubation at MOI = 1 (**Figure 1**). Whereas, *S. aureus* SA325 grew normally when infected by phage JD007 at lowers MOIs = 0.1 and 0.01. The drop test results showed that phage JD007 formed clear inhibition zones in two-layer agar plates.

Phage JD007 Prevents *S. aureus* SA325-Mediated Dermal Abscess Formation in Nude BALB/c Mice *in Vivo*

Dermal abscess formation was established in the back of nude mice and observed daily for 10 days. Results showed that the maximum sizes of dermal abscesses were achieved on the second day following infection. On the seventh day, all of the abscesses were scarred. As shown in **Figures 2**, **3**, we could see no visible dermal abscesses formed in control group, phage group, and prevention group during the entire observation period. On the third day, the abscess sizes tended to decrease in size, and mice's dermal abscess size in the treatment group were significantly smaller than those in the infection group ($p < 0.05$).

Inflammatory Cytokines Responses of Nude BALB/c Mice During Phage Therapy

Cytokines of IL-1β, IL-6, IL-8, IFN-γ, and TNF-α in the sera were measured using ELISA on the third day. As shown in **Figure 4**, there were no significant differences between IFN-γ and TNF-α among those groups. IL-1β, IL-6, and IL-8 in treatment groups were higher than those in control group, whereas there were no significant differences between the negative control and prevention groups.

Weight of Nude BALB/c Mice During Phage Therapy

Weights of mice in each group were measured daily, encompassing the entire observation period. Body weights gain were calculated by subtracting original body weight from weights on the tenth day. As shown in **Figure 5**, weight gains in infection group and phage treatment were much lower than that compared with control group. The weight gain in the prevention and phage JD007 groups had no significant difference compared with the PBS control group during treatment.

DISCUSSION

Staphylococcus aureus SA325 was isolated from a re-occurring back under-dermal abscess of an in-patient with long-term bed rest. *In vitro* bactericidal activity tests showed that phage JD007 could form a clear inhibition zones using a two-layer soft agar plate assay, and could inhibit growth of SA325 at MOI = 1 or 10.

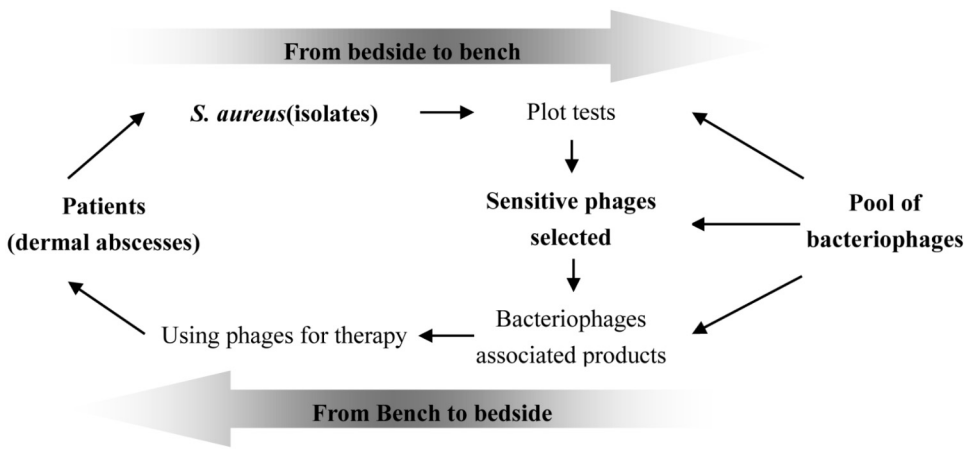

FIGURE 6 | Proposed scheme of selecting phages for therapy. The success of phage therapy needs the pool of phages and their susceptibility to the definite infectious bacterial pathogen at infection sites should be tested previously; the products containing of different phages were produced firstly and the sensitive phages would be chosen for therapy.

In order to evaluate the ability of phage JD007 to prevent or treat of abscesses caused by *S. aureus*, a dermal abscess model was established in nude mice model using clinical isolate SA325, as reported previously (Malachowa et al., 2013). In this study, we successfully established the dermal abscess infection in nude BALB/c mice using *S. aureus* SA325. Furthermore, the efficacies of treatment of the abscesses using phage JD007 were evaluated. There were no observed abscess formation in the prevention group. The average abscess sizes of phage treatment group were smaller than those of the infection group. The results indicate that phage JD007 prevents formation of abscess. Also, it supports earlier observations on phage M^{Sa} inhibition *S. aureus* dermal abscess formation (Capparelli et al., 2007).

To evaluate the response of mice during prevention and treatment after phage JD007 inoculation, the weight changes were observed during the whole process. As bacteriophages are viruses containing nucleic acid and proteins, they may bring some risk to humans when used for the treatment of bacteremia, as the complex composition of the phage may induce unpredictable immune responses when administered to the blood. The average weights gains in the infection and treatment groups were significantly lower than those in the control, PBS, phage JD007, and prevention groups. Furthermore, immune responses of the mice during treatment were evaluated, mice sera was taken on the third day, and the inflammatory cytokines of IL-1β, IL-6, IL-8, IFN-γ, and TNF-α in serum were measured using ELISA. The cytokines IL-1β and IL-6 both belong to endogenous pyrogens, and they can be applied to the hypothalamus regulating center to cause fever. IL-1β and IL-6 levels were significantly higher in the treatment group, while there were no significant differences among prevention, infection, or control groups, indicating that phage JD007 treatment may destroy the cells of *S. aureus* robustly, leading to increase of IL-1β and IL-6 that may cause fever. It's reported that TRIM29 could negatively regulate the proinflammatory cytokine IL-6 and TNF-α production in response to LPS and bacteria *Haemophilus influenzae* (Xing et al., 2016). Whether *S. aureus* infection suppresses the TRIM 29 expression and leads to increased expression of IL-6 should be further examined. IL-8 was significantly elevated in infection and treatment groups. IL-8 can signal chemotactic neutrophil leukocytes and activate T cells in the infection sites, clearing the pathogen. IFN-γ and TNF-α can activate mononuclear macrophages, which can enhance the phagocytosis and killing functions; TNF-α can directly kill the cell infected by virus. There were no significant changes in any of these groups.

The specificity of bacteriophages is one of important reason hindering clinical use of phage for therapy, though cocktails may overcome this fault (Gu et al., 2012a; Mendes et al., 2014). There are numerous public reports describing the success of phage therapy inhibiting infectious diseases caused by dermal associated infections (Vieira et al., 2012; Trigo et al., 2013). We postulate that phage therapy could become an important choice for the treatment of wound infections. As shown in **Figure 6**, the pool of different phages should be established before using them for therapy; at the same time, the bacteria causing infection should be isolated and its sensitivity to the phages in the pool confirmed. The formula of sensitive phages must be prepared at first; once the bacteria causing the infection is confirmed to be sensitive to phages in the pool, the formula containing the sensitive phage should be chosen for treatment of the infections. The success of phage therapy depends upon the pool of different kinds of bacteriophages.

In summary, phage JD007 could inhibit the growth of *S. aureus* both *in vitro* and *in vivo*. Phage JD007 can prevent abscess formation caused by *S. aureus* isolated from an in-patient's abscess samples through under-dermal injection, and can also significantly reduce the severity of dermal abscess caused by *S. aureus*. In conclusion, phage JD007 is a promising candidate phage for use in preventing dermal abscess.

AUTHOR CONTRIBUTIONS

ZC, QTL, and BD carried out the experiments and drafted the manuscript. QTL, KD, BD, QZL, YZ, and MG participated in the mice model experiments. ZC, QTL, XG, and LL participated in the design of the study and performed the statistical analysis. ZC, QTL, and LL conceived the study, participated in its design, and coordinated to help draft the manuscript.

FUNDING

This work was sponsored in part by the National Natural Science Foundation of China (No. 31500154), the fund of Shanghai Health and Family Planning Committee (No. 201440289), and the outstanding medical youth program A of Shanghai General Hospital (No. 06N1702002).

ACKNOWLEDGMENTS

Thanks Luis J. Cocka for suggestions of modification manuscript.

REFERENCES

Boulanger, P. (2009). Purification of bacteriophages and SDS-PAGE analysis of phage structural proteins from ghost particles. *Methods Mol. Biol.* 502, 227–238. doi: 10.1007/978-1-60327-565-1_13

Capparelli, R., Parlato, M., Borriello, G., Salvatore, P., and Iannelli, D. (2007). Experimental phage therapy against *Staphylococcus aureus* in mice. *Antimicrob. Agents Chemother.* 51, 2765–2773. doi: 10.1128/AAC.01513-06

Chhibber, S., Kaur, T., and Sandeep, K. (2013). Co-therapy using lytic bacteriophage and linezolid: effective treatment in eliminating methicillin resistant *Staphylococcus aureus* (MRSA) from diabetic foot infections. *PLoS One* 8:e56022. doi: 10.1371/journal.pone.0056022

Cui, Z., Feng, T., Gu, F., Li, Q., Dong, K., Zhang, Y., et al. (2017a). Characterization and complete genome of the virulent *Myoviridae* phage JD007 active against a variety of *Staphylococcus aureus* isolates from different hospitals in Shanghai, China. *Virol. J.* 14:26. doi: 10.1186/s12985-017-0701-0

Cui, Z., Guo, X., Dong, K., Zhang, Y., Li, Q., Zhu, Y., et al. (2017b). Safety assessment of *Staphylococcus* phages of the family *Myoviridae* based on complete genome sequences. *Sci. Rep.* 7:41259. doi: 10.1038/srep41259

Cui, Z., Song, Z., Wang, Y., Zeng, L., Shen, W., Wang, Z., et al. (2012). Complete genome sequence of wide-host-range *Staphylococcus aureus* phage JD007. *J. Virol.* 86, 13880–13881. doi: 10.1128/JVI.02728-12

Gu, J., Liu, X., Li, Y., Han, W., Lei, L., Yang, Y., et al. (2012a). A method for generation phage cocktail with great therapeutic potential. *PLoS One* 7:e31698. doi: 10.1371/journal.pone.0031698

Gu, J., Liu, X., Lu, R., Li, Y., Song, J., Lei, L., et al. (2012b). Complete genome sequence of *Staphylococcus aureus* bacteriophage GH15. *J. Virol.* 86, 8914–8915. doi: 10.1128/JVI.01313-12

Gutierrez, D., Vandenheuvel, D., Martinez, B., Rodriguez, A., Lavigne, R., and Garcia, P. (2015). Two phages, phiIPLA-RODI and phiIPLA-C1C, lyse mono- and dual-staphylococcal biofilms. *Appl. Environ. Microbiol.* 81, 3336–3348. doi: 10.1128/AEM.03560-14

Kumari, S., Harjai, K., and Chhibber, S. (2009). Efficacy of bacteriophage treatment in murine burn wound infection induced by *Klebsiella pneumoniae*. *J. Microbiol. Biotechnol.* 19, 622–628.

Kwan, T., Liu, J., DuBow, M., Gros, P., and Pelletier, J. (2005). The complete genomes and proteomes of 27 *Staphylococcus aureus* bacteriophages. *Proc. Natl. Acad. Sci. U.S.A.* 102, 5174–5179. doi: 10.1073/pnas.0501140102

Limbago, B. M., Kallen, A. J., Zhu, W., Eggers, P., McDougal, L. K., and Albrecht, V. S. (2014). Report of the 13th vancomycin-resistant *Staphylococcus aureus* isolate from the United States. *J. Clin. Microbiol.* 52, 998–1002. doi: 10.1128/JCM.02187-13

Malachowa, N., Kobayashi, S. D., Braughton, K. R., and DeLeo, F. R. (2013). Mouse model of *Staphylococcus aureus* skin infection. *Methods Mol. Biol.* 1031, 109–116. doi: 10.1007/978-1-62703-481-4_14

Marza, J. A., Soothill, J. S., Boydell, P., and Collyns, T. A. (2006). Multiplication of therapeutically administered bacteriophages in *Pseudomonas aeruginosa* infected patients. *Burns* 32, 644–646. doi: 10.1016/j.burns.2006.02.012

Mendes, J. J., Leandro, C., Mottola, C., Barbosa, R., Silva, F. A., Oliveira, M., et al. (2014). In vitro design of a novel lytic bacteriophage cocktail with therapeutic potential against organisms causing diabetic foot infections. *J. Med. Microbiol.* 63, 1055–1065. doi: 10.1099/jmm.0.071753-0

O'Flaherty, S., Coffey, A., Edwards, R., Meaney, W., Fitzgerald, G. F., and Ross, R. P. (2004). Genome of staphylococcal phage K: a new lineage of *Myoviridae* infecting gram-positive bacteria with a low G+C content. *J. Bacteriol.* 186, 2862–2871. doi: 10.1128/JB.186.9.2862-2871.2004

Salmond, G. P., and Fineran, P. C. (2015). A century of the phage: past, present and future. *Nat. Rev. Microbiol.* 13, 777–786. doi: 10.1038/nrmicro3564

Sarker, S. A., and Brussow, H. (2016). From bench to bed and back again: phage therapy of childhood *Escherichia coli* diarrhea. *Ann. N. Y. Acad. Sci.* 1372, 42–52. doi: 10.1111/nyas.13087

Thiel, K. (2004). Old dogma, new tricks–21st Century phage therapy. *Nat. Biotechnol.* 22, 31–36. doi: 10.1038/nbt0104-31

Trigo, G., Martins, T. G., Fraga, A. G., Longatto-Filho, A., Castro, A. G., Azeredo, J., et al. (2013). Phage therapy is effective against infection by *Mycobacterium ulcerans* in a murine footpad model. *PLoS Negl. Trop. Dis.* 7:e2183. doi: 10.1371/journal.pntd.0002183

Vieira, A., Silva, Y. J., Cunha, A., Gomes, N. C., Ackermann, H. W., and Almeida, A. (2012). Phage therapy to control multidrug-resistant *Pseudomonas aeruginosa* skin infections: in vitro and ex vivo experiments. *Eur. J. Clin. Microbiol. Infect. Dis.* 31, 3241–3249. doi: 10.1007/s10096-012-1691-x

Weinandy, F., Lorenz-Baath, K., Korotkov, V. S., Bottcher, T., Sethi, S., Chakraborty, T., et al. (2014). A beta-lactone-based antivirulence drug ameliorates *Staphylococcus aureus* skin infections in mice. *ChemMedChem* 9, 710–713. doi: 10.1002/cmdc.201300325

Wills, Q. F., Kerrigan, C., and Soothill, J. S. (2005). Experimental bacteriophage protection against *Staphylococcus aureus* abscesses in a rabbit model. *Antimicrob. Agents Chemother.* 49, 1220–1221. doi: 10.1128/AAC.49.3.1220-1221.2005

Xiao, M., Wang, H., Zhao, Y., Mao, L. L., Brown, M., Yu, Y. S., et al. (2013). National surveillance of methicillin-resistant *Staphylococcus aureus* in China highlights a still-evolving epidemiology with 15 novel emerging multilocus sequence types. *J. Clin. Microbiol.* 51, 3638–3644. doi: 10.1128/JCM.01375-13

Xing, J., Weng, L., Yuan, B., Wang, Z., Jia, L., Jin, R., et al. (2016). Identification of a role for TRIM29 in the control of innate immunity in the respiratory tract. *Nat. Immunol.* 17, 1373–1380. doi: 10.1038/ni.3580

Conflict of Interest Statement: The authors declare that the research was conducted in the absence of any commercial or financial relationships that could be construed as a potential conflict of interest.

Copyright © 2018 Ding, Li, Guo, Dong, Zhang, Guo, Liu, Li and Cui. This is an open-access article distributed under the terms of the Creative Commons Attribution License (CC BY). The use, distribution or reproduction in other forums is permitted, provided the original author(s) and the copyright owner(s) are credited and that the original publication in this journal is cited, in accordance with accepted academic practice. No use, distribution or reproduction is permitted which does not comply with these terms.

frontiers in Microbiology

REVIEW
published: 26 July 2018
doi: 10.3389/fmicb.2018.01700

Non-toxigenic *Clostridioides* (Formerly Clostridium) *difficile* for Prevention of *C. difficile* Infection: From Bench to Bedside Back to Bench and Back to Bedside

Dale N. Gerding[1]*, *Susan P. Sambol*[1,2] and *Stuart Johnson*[1,2]

[1] Research Service, Edward Hines Jr. VA Hospital, Hines, IL, United States, [2] Department of Medicine, Loyola University Chicago Medical Center, Maywood, IL, United States

The beneficial effect of colonization of the gastrointestinal tract by non-toxigenic *Clostridioides difficile* (NTCD) strains as a preventive of toxigenic *C. difficile* infection (CDI) has been known since the early 1980s. Investigators in both the USA and United Kingdom demonstrated that prior colonization by randomly selected NTCD strains provided prevention against infection by toxigenic *C. difficile* in hamsters, albeit with limited durability. In the 1980s two patients with multiply recurrent CDI in the UK were treated with vancomycin followed by NTCD to prevent further recurrences, with one success and one failure. Epidemiologic studies of hospitalized patients using weekly rectal swab cultures demonstrated that asymptomatic colonization of patients by toxigenic *C. difficile* was much more common than CDI, but also that the rate of asymptomatic NTCD colonization of patients was unexpectedly high. Development of molecular strain typing of *C. difficile* was instrumental in characterizing different strains of both toxigenic *C. difficile* and NTCD leading to identification of NTCD strains that were effective human colonizers. These strains were reintroduced in hamsters in the 1990s and shown to prevent CDI efficiently and durably when challenged with epidemic toxigenic *C. difficile* strains. One strain of NTCD, NTCD-M3, was manufactured under cGMP standards and was demonstrated to be safe in a phase 1 volunteer trial. NTCD-M3 was then tested in a phase 2 double-blind placebo controlled trial for the prevention of recurrent CDI in patients experiencing their first CDI episode or first CDI recurrence. NTCD-M3 was given at doses of 10^4 or 10^7 spores per day orally for 7 or 14 days following successful treatment of CDI with vancomycin and/or metronidazole. CDI recurred in 30% of placebo patients and 11% of all NTCD-M3 patients ($p = 0.006$); recurrence rate for the best dose, 10^7 spores/d × 7 days, was 5% ($p = 0.01$ vs. placebo). Detection of colonization predicted prevention success; among the 86 patients who were colonized with NTCD-M3 the recurrence rate was 2% vs. 31% in patients who received NTCD-M3 but were not colonized ($p < 0.001$). Additional trials of NTCD-M3 for primary prevention of CDI and prevention of CDI recurrence seem warranted by these promising results.

Keywords: non-toxigenic, *Clostridium difficile*, NTCD-M3, prevention, NTCD, colonization, spores, *Clostridioides difficile*

OPEN ACCESS

Edited by:
Noton Kumar Dutta, Johns Hopkins University, United States

Reviewed by:
Sarah J. Kuhl, VA Northern California Health Care System, United States
Xingmin Sun, University of South Florida, United States

***Correspondence:**
Dale N. Gerding
dale.gerding2@va.gov

Specialty section:
This article was submitted to Antimicrobials, Resistance and Chemotherapy, a section of the journal Frontiers in Microbiology

Received: *02 March 2018*
Accepted: *09 July 2018*
Published: *26 July 2018*

Citation:
Gerding DN, Sambol SP and Johnson S (2018) Non-toxigenic Clostridioides (Formerly Clostridium) difficile for Prevention of C. difficile Infection: From Bench to Bedside Back to Bench and Back to Bedside. Front. Microbiol. 9:1700. doi: 10.3389/fmicb.2018.01700

INTRODUCTION

The purpose of this review is to summarize the experimental, pre-clinical, and clinical data for the use of non-toxigenic *Clostridioides difficile* (NTCD) for prevention of *C. difficile* infection (CDI) caused by toxigenic strains of *C. difficile*. NTCD strains in which the pathogenicity locus (PaLoc) for the main *C. difficile* virulence factors, toxin A and B is replaced by a 115 bp sequence occur naturally. Multiple investigators have published convincing results of experiments over the last 35 years that demonstrate the efficacy of NTCD as a colonizing bacterial agent that prevents infection with toxigenic strains of *C. difficile* in animals and humans. Although a definitive mechanism for this protection remains to be determined, the effectiveness of this approach in multiple animal models and human clinical observations and trials suggests that it is a safe and effective biotherapeutic strategy that could be used for both primary prevention of CDI and prevention of CDI recurrence.

Background Bench Discoveries in the 1980s

The concept of NTCD inhibiting or interfering with the infectivity of a toxigenic strain of *C. difficile* was first reported by Wilson and Sheagren (1983) in the hamster model in 1983. They demonstrated that following cefoxitin administration, colonization with NTCD prior to challenge with toxigenic *C. difficile* increased hamster survival from 21% to 93%, however, durability of prevention was not determined. Simultaneous administration of the NTCD strain and a toxigenic *C. difficile* strain did not increase survival. Borriello and Barclay (1985) extended these observations by colonization of hamsters with three different strains of NTCD, M-1, D-1 and S-1 administered at doses ranging from 3×10^6 to 3×10^9 organisms followed by challenge 5 days later with a toxigenic strain B-1 at a dose of 3×10^7 organisms. Results of these experiments showed at 25 days post toxigenic challenge survival of 13 of 18 (72%) vs. 0/21 (0%) hamsters not given an NTCD strain. Additional experiments showed (1) that protection was dependent upon live NTCD organisms; heat-killed NTCD did not protect hamsters, (2) that protection was dependent upon NTCD colonization; decolonization with vancomycin resulted in no protection against toxigenic challenge, and (3) that protection was specific to *C. difficile*; attempts to colonize with *C. perfringens, C. bifermentans,* and *C. beijerincki*, failed, and *C. sporogenes* colonized but failed to protect against toxigenic *C. difficile* challenge.

Borriello and Barclay (1985) also attempted to identify the mechanism by which NTCD protected against toxigenic *C. difficile*. They showed that NTCD did not degrade or alter the potency of *C. difficile* toxin. They investigated the mucosal association of NTCD by harvesting cecum samples from three NTCD-colonized hamsters at day 51 of colonization, washing them eight times with brain heart infusion (BHI) broth and saline, then homogenizing the tissue and doing quantitative culture of the homogenate. They found association of NTCD with the cecal mucosa ranging from 6×10^3 to 3×10^5 cfu/g tissue, suggesting there may be association of NTCD with the cecal mucosa or alternatively, they suggested competition for essential nutrients. However, in the discussion they report that after day 25 death occurred in most animals and that toxigenic *C. difficile* and cytotoxin could be detected in the cecum of these animals. Sequential analysis of the fecal pellets in these animals detected a change over time from only NTCD recovery to recovery of toxigenic *C. difficile* or both. This was of concern and the authors speculated that the presence of toxin enabled toxigenic strains of *C. difficile* to have a colonization advantage over NTCD. In a subsequent publication, Borriello et al. (1988) showed that a virulent toxigenic strain B-1 of *C. difficile* was more adherent to mucosa of small and large bowel in the hamster than NTCD strain M-1. They also showed that injection of toxin into the cecum of hamsters enhanced colonization of M-1 in the colon, but not in the small bowel or cecum when compared to toxigenic strain B-1.

Similar observations of protection against toxigenic *C. difficile* by NTCD were shown in gnotobiotic mice by Corthier and Muller (1988). NTCD protected against toxigenic challenge from 18h to 10 days following NTCD in 100% of gnotobiotic mice. If there was no delay in administration of the toxigenic strain following NTCD, 60% of mice survived. Survival of mice beyond 10 days was not recorded.

These early bench and animal studies were not further pursued beyond the 1980s, most likely because the protective effect in hamsters did not appear to be durable. However, these observations provide a valuable early insight into the potential utility of NTCD as a preventive strategy for CDI.

Bedside Clinical Observations

The first published report of the use of NTCD in patients was by Seal et al. (1987). Two patients with multiple recurrences of CDI were treated orally with a BHI culture of NTCD strain M-1 previously shown by Borriello and Barclay (1985) to prevent CDI in hamsters transiently. One ml of the 24h culture was diluted in 50 ml of milk (final concentration $\sim 1 \times 10^7$ cfu/ml) which was administered once daily for 3 days. **Patient A**, age 88 years, was treated for her first CDI episode with metronidazole and for episodes two and three with oral vancomycin. Although successfully treated with resolution of symptoms, she had persistent *C. difficile* in her stool for at least 3 days following the last vancomycin treatment but was negative on stool culture just prior to receiving NTCD. Following NTCD her stool cultures were positive for NTCD for 14 days with no toxigenic *C. difficile* detected, and she had no further CDI recurrences for at least 4 months. **Patient B**, age 76, was also treated for her first CDI episode with metronidazole and for episodes two and three with vancomycin. She was treated successfully for her diarrhea symptoms with vancomycin, but had high counts of toxigenic *C. difficile* in her stool for the first 3 days of NTCD administration (5.9–7.5 $\log_{10}$/gm stool) with no NTCD detected. NTCD did not appear in the stool until day 6 at which time there were $\sim 10^7$ cfu/gm stool of both NTCD and toxigenic *C. difficile*, but on days 9 and 10 only toxigenic *C. difficile* was found at a concentration of $\sim 10^5$ cfu/gm stool. Starting on day 17 she had 2 days of self-limited diarrhea with both toxigenic *C. difficile* and NTCD at $\sim 10^3$ cfu/gm stool and stool toxin detected. On day

28 counts of both toxigenic *C. difficile* and NTCD had declined to $\sim 10^2$ cfu/gm and on day 45 neither were detected in stool. The patient died 1 month later of an unrelated cause but had no further diarrhea. In view of the mild recurrence of diarrhea with stool toxin detected at day 17 it is likely that this patient failed preventive treatment with NTCD, whereas patient A was a success. No further patient treatments with NTCD were reported until well into the 21st century, however, considerable clinical information on detection of NTCD in patients was obtained in the interim.

In the 1980s it became apparent that CDI was a healthcare associated infection (Gerding et al., 1986; McFarland et al., 1989), and typing systems for identification of specific *C. difficile* strains were developed (Kuijper et al., 1987; McFarland et al., 1989; Clabots et al., 1993) based not only on isolates from patients with CDI, but also from specimens collected from asymptomatic patients using rectal swabs (McFarland et al., 1989; Johnson et al., 1990; Clabots et al., 1992). McFarland et al. (1989) were the first to detect the presence of large numbers of patients in hospital that were asymptomatically colonized with *C. difficile*. They demonstrated that transmission of *C. difficile* was frequent in the hospital setting using immunoblot organism typing and space/time relations. They found that nearly 2/3 of patients that acquired *C. difficile* remained asymptomatic whereas just over 1/3 had symptomatic CDI (McFarland et al., 1989).

The use of restriction endonuclease analysis (REA) typing of *C. difficile* markedly enhanced the epidemiologic investigation of CDI in hospitals (Kuijper et al., 1987; Clabots et al., 1993). Early in the development of REA there were 75 distinct groups identified by letters of the alphabet, 43 cytotoxin positive groups, 28 NTCD groups, and 4 groups that included both cytotoxin positive and negative isolates. Isolates for typing were obtained from CDI patients, rectal swabs of asymptomatic patients and multiple environmental sites. In comparison with other typing systems then in use REA demonstrated greater sensitivity than immunoblot typing, bacteriophage-bacteriocin typing and ribotyping (Clabots et al., 1993). Remarkably, the most frequently isolated REA group was the NTCD group M which was found more commonly than any toxigenic groups and may be a reflection of the inclusion of large numbers of isolates collected from asymptomatic patients using rectal swabs.

Using a similar weekly rectal swab methodology used by McFarland et al. (1989) to detect *C. difficile* asymptomatic colonization coupled with REA typing of *C. difficile* (Kuijper et al., 1987; Clabots et al., 1993), Johnson et al. (1990) showed that 21% of patients hospitalized on three wards were culture-positive for *C. difficile*, the majority 51 of 60 (85%) were asymptomatic. All of the 9 cases of CDI were caused by two closely related toxigenic REA types, B and B2, and none occurred among the 51 asymptomatic colonized patients, 9 of whom were colonized with the B or B2 strain types but remained asymptomatic. Fifteen of the 17 patients with the B or B2 isolates were located on the same surgical ward suggesting transmission on that ward. Among the 18 different REA type *C. difficile* isolates found on the 3 study wards, 10 were toxigenic and 8 (44%) were non-toxigenic including 7 distinct REA groups of NTCD, groups A, C, M, P, S, T, and U. This was the first indication that NTCD strains were carried frequently by hospital patients. In addition, it was found that asymptomatic *C. difficile* colonization occurred in approximately the same frequency on all 3 hospital wards, ranging from 12.2 to 19.3% of patients, all of whom had relatively long hospital stays. All the patients with toxigenic *C. difficile* or NTCD in their stool remained asymptomatic.

A larger similar study using rectal swab cultures was conducted on a single surgical ward with a historically high rate of CDI by Clabots et al. (1992). The study was conducted over 9 months and enrolled 634 (94%) of 678 admissions to this ward, obtaining rectal swab cultures on admission and weekly thereafter. Of the 634 ward admissions, 65 (10.3%) were either asymptomatically culture-positive for *C. difficile* (61 patients) or had CDI (4 patients). Twelve additional asymptomatic admissions were positive for *C difficile* when first sampled, but were not sampled within 48 h of admission and were indeterminate as to whether they acquired *C. difficile* on the ward or were already colonized when admitted. The majority of admissions (355, 56%) were admitted from home and had not been hospitalized within the previous 30 days. Twenty-two (7%) of these home admissions were culture-positive for *C. difficile* indicating the high potential for introduction of *C. difficile* strains to the hospital from the community. Of the 557 admissions to the ward that were not culture-positive for *C. difficile*, 54 (9.7%) acquired *C difficile* while on the ward, but only 3 had CDI. REA typing identified 58 different distinct types during the study. Of the top seven most frequently isolated REA types, three were NTCD types and constituted 23/68 (34%) of these isolates. The most commonly isolated NTCD strain type was M3 which subsequently, together with types M23 and T7, was selected for laboratory trials in hamsters for prevention of CDI.

Low rates of CDI among patients previously asymptomatically colonized with *C. difficile* were observed in several trials utilizing weekly rectal swab cultures and suggested that colonization might be protective against CDI if symptoms did not develop relatively quickly following toxigenic *C. difficile* exposure, or if patients were colonized by NTCD. Data from four such prospective studies were combined in a random effects model by Shim et al. (1998). All four studies employed similar weekly rectal swab cultures for *C. difficile* in asymptomatic hospitalized patients and utilized stool cultures for *C. difficile* if CDI symptoms developed. Patients recovering from prior CDI were excluded as they have a high colonization rate with toxigenic *C. difficile* post treatment and are prone to recurrences of CDI. Asymptomatic patients were included if they had at least two consecutive weekly *C. difficile* rectal swab cultures and were classified as either colonized or not colonized. Colonized patients were further categorized as colonized with a toxigenic *C. difficile* strain or NTCD. All isolates underwent REA typing as well as toxin testing. Among the 618 non-colonized patients, 22 (3.6%) developed CDI whereas only 2 (1%) of 192 colonized patients developed CDI (pooled risk difference −2.3%, $p = 0.021$, **Figure 1**). When the analysis was confined only to patients who had received antibiotics within 14–21 days of the start of the sampling or during sampling, the pooled risk difference was −3.2%, $p = 0.024$. Greater exposure to antibiotics in non-colonized patients could explain the increased rate of CDI, but

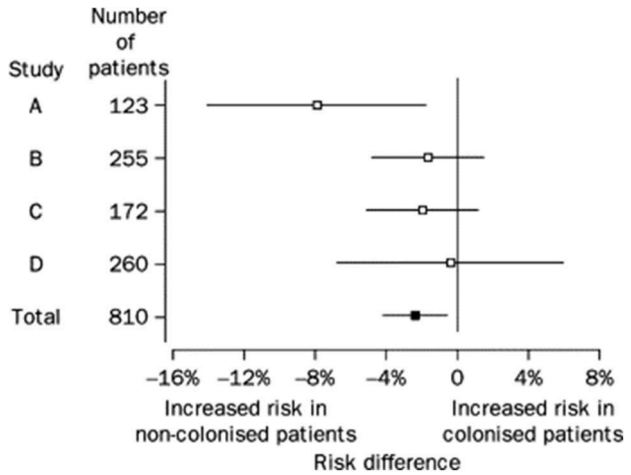

FIGURE 1 | Risk difference (95% CI) for CDI among patients initially colonized and non-colonized with *C difficile* in four studies. Risk difference pooled across studies with a random effects model is shown in bottom row (Total). From Shim et al. (1998).

antibiotic exposure was lower (79%) in non-colonized patients compared to colonized patients (92%). The mechanism by which colonization prevents CDI is unknown, and toxigenic strains of *C. difficile* as typed by REA that caused CDI were also found to be carried asymptomatically suggesting that strain type did not explain prevention. In these 4 studies there was a very high proportion (44%) of patients that were colonized by NTCD. There were 15 different REA groups of NTCD found among the 76 NTCD isolates, but the majority of NTCD were in two REA groups, M (49%) and T (19%). No CDI occurred among NTCD colonized patients and may account at least partially for the reduced CDI rates in colonized patients.

Taken together these clinical observations documented the relatively high rate of colonization of hospitalized patients by non-toxigenic strains of *C. difficile* and documented a very low rate of CDI among all colonized patients. Furthermore, REA typing demonstrated the ability to group and type NTCD strains in a manner similar to toxigenic *C. difficile* and identified two dominant groups of NTCD, the M and T groups by REA typing.

Back to Bench Investigation: Pre-clinical NTCD Development

Bedside clinical and epidemiologic observations coupled with the evolution of molecular typing of *C. difficile* prompted further laboratory testing of *C. difficile*, particularly in animal models. Of specific interest was whether strains of *C. difficile* responsible for hospital outbreaks were more virulent than other strains that were found to asymptomatically colonize patients more often than they caused CDI. Sambol et al. (2001) tested three toxigenic epidemic *C. difficile* strains, REA types B1, J9, and K14 in the hamster model and compared them to toxigenic REA type Y2 which was found to commonly colonize patients but caused little CDI. A fifth strain, toxin variant REA type CF2, which is toxin A-negative, toxin B-positive and associated with CDI outbreaks was also included. The hamster protocol was similar to that of Borriello and Barclay (Borriello and Barclay, 1985), but differed in that only spores of *C. difficile* were administered by gavage 5 days following a single oral clindamycin dose of 30 mg/kg. A minimum infective dose for each *C. difficile* strain was predetermined to be 100 spores to mimic a postulated low inoculum exposure. The epidemic strains B1, J9, and K14 infected hamsters within 24–48 h of administration and caused 100% mortality by 48 h. REA type Y2 infected 9 of 10 hamsters over a range of 1–4 days, somewhat more slowly than the epidemic strains, but eventually all 9 infected hamsters died. Toxin variant strain CF2 infected only 6 of 10 hamsters over a range of 1 to 10 days and only 3 of the 6 died; the remaining 3 hamsters were colonized through study termination at day 79 and appeared to have no symptoms. The study documented differences in virulence of *C. difficile* strains in the hamster model and served as a basis on which to test preventive strategies with NTCD in the hamster model.

NTCD Prevention

To test the effectiveness of NTCD as a preventive of infection with toxigenic *C. difficile*, the above described hamster model was used (Sambol et al., 2002). Three NTCD strains were selected from among isolates collected with rectal swabs from asymptomatic hospitalized patients; M3, M23, and T7, all of which were isolated at high frequency from patients (**Figure 2**). The NTCD inoculum was 10^6 spores by oral gavage on day 2 following clindamycin 30 mg/kg orally. Toxigenic *C. difficile* challenge with strains B1, J9, or K14 with 100 spores by oral gavage occurred on day 5 following clindamycin (3 days after the NTCD inoculum). Prevention of CDI mortality ranged from 87 to 97% (**Figure 3**) and correlated closely with detection of NTCD colonization of the stool prior to challenge with toxigenic *C. difficile* strains. Colonization with NTCD persisted in these surviving hamsters until end of study which varied from 55 to 106 days and there was no late mortality from toxigenic *C. difficile*.

NTCD Prevention Durability

Durability of protection against late challenge with toxigenic *C. difficile* was performed with M3 and M23 NTCD. In the first of these studies M3 colonized 5 of 5 hamsters on day 4 following inoculation on day 2 following clindamycin. All 5 hamsters lost colonization between days 23 and 44. The uncolonized hamsters were challenged with 100 spores of toxigenic B1 *C. difficile* on day 62 and survived until day 153 end of study. In a second M3 experiment 3 of 4 hamsters were colonized on day 3 following inoculation on day 2 post clindamycin and were challenged on day 63 with 100 spores of toxigenic J9 and all survived with 3 of 4 remaining colonized with M3 until end of study day 125. In a third experiment, 12 hamsters were given clindamycin on day 0; 10 received NTCD strain M23 on day 2 and became colonized by day 5. All 12 hamsters were challenged with toxigenic strain B1 on day 41 and all survived (10 colonized with M23 and 2 uncolonized). All 10 remained colonized until day 49 when the study ended. These studies suggest that hamsters apparently recover colonization resistance following clindamycin by days

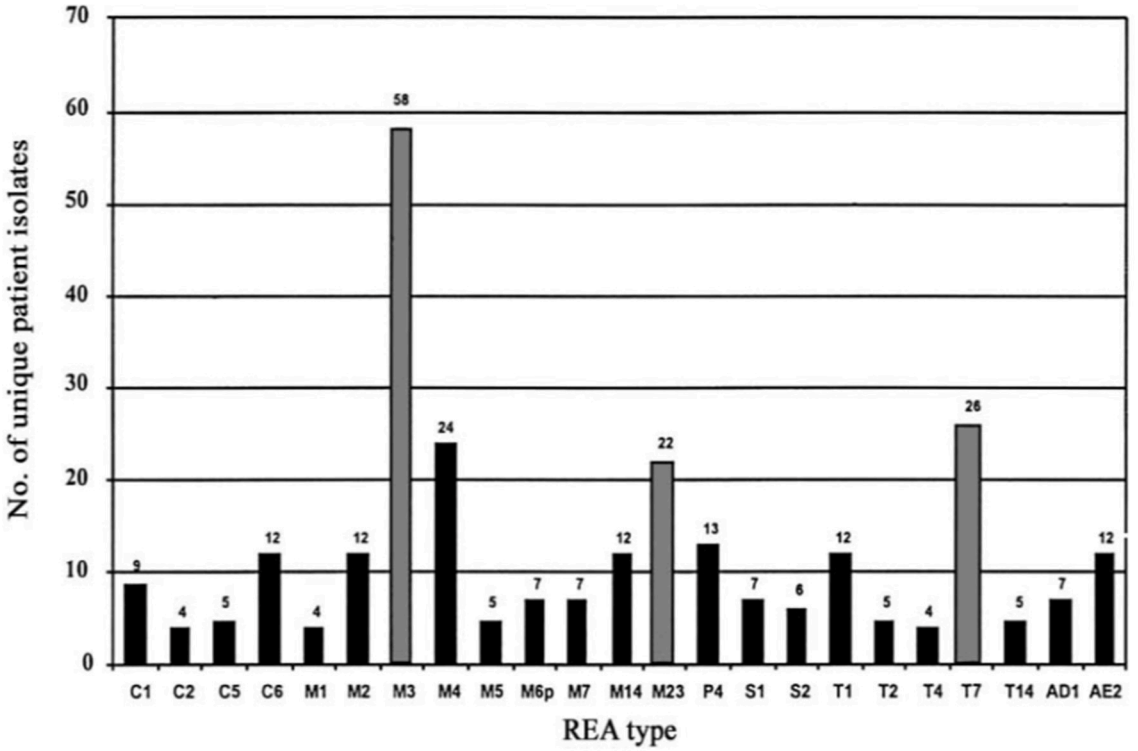

FIGURE 2 | Frequency of isolation of *Clostridium difficile* nontoxigenic restriction endonuclease analysis (REA) types from individual patients during 1982–1993. Gray bars indicate frequency of REA types used in hamster prevention trials. From Sambol et al. (2002) with permission.

41–62 and are protected from late challenge with toxigenic *C. difficile* whether colonized with NTCD or not.

Patients are occasionally treated with a single antibiotic dose, as for example when undergoing surgical prophylaxis, and would be representative of the experiments with hamsters following a single dose of antibiotic. However, most infection treatment is carried out using multiple doses, often on the same day and for multiple days at a time. This raises the question of how NTCD might be employed to prevent CDI since many of the antibiotics used systemically will be active against NTCD and presumably prevent it from colonizing the patient. NTCD REA types M3, M23, and T7 are susceptible to most antibiotics including ampicillin, clindamycin, erythromycin, tetracycline, trimethoprim-sulfamethoxazole and metronidazole, but resistant to ciprofloxacin and ceftriaxone (Sambol et al., 2002), patterns that are typical of most *C. difficile* isolates. Resistance to clindamycin, tetracyclines, carbapenems and erythromycins as well as very high-level resistance to fluoroquinolones is known to occur in *C. difficile* and may be transferrable. Whereas use of a highly antibiotic resistant strain of NTCD would favor more frequent colonization, it would also increase the risk of antibiotic resistance transfer to other bacteria in the gastrointestinal tract.

Effect of Daily Clindamycin and Resistance in NTCD

To assess the effect of antibiotic resistance of NTCD on colonization and prevention of infection by toxigenic *C. difficile*, Merrigan et al. (2003) conducted experiments in hamsters treated with daily oral doses (30 mg/kg) of clindamycin for 5 consecutive days. Two strains of NTCD, REA type M3 (clindamycin susceptible at 0.5 mcg/ml), REA type M13 (clindamycin resistant at >256 mcg/ml) and a toxigenic strain of *C. difficile*, REA type B1 (clindamycin resistant at >256 mcg/ml) were used. Clindamycin resistance in type M13 and B1 was determined to be due to presence of the *erm*(B) gene. M3 was negative for *erm*(B). Colonization experiments with M3 and M13 were conducted in groups of 5 hamsters by administering (1) a single dose of 1×10^6 spores on day 3 of clindamycin, (2) a daily dose of 1×10^6 spores on days 3–5 of clindamycin or (3) a daily dose of 1×10^6 spores on days 3–7. Colonization occurred with all doses of resistant strain M13 within 1.25 days of the first dose. No colonization occurred following the single dose of susceptible strain M3, but following the 3-day and 5-day administrations all 10 hamsters eventually became colonized but after a mean lag time of 6.4 to 6.6 days following the first dose. When the experiment was repeated with challenge with toxigenic strain B1, 100 spores orogastrically, on day 5, day 7, or day 9, all hamsters were protected by all doses of clindamycin resistant M13. Clindamycin susceptible M3 gave no protection against challenge with B1 on day 5, but protected 1 of 5 hamsters challenged on day 7, and 5 of 5 challenged on day 9. The results of the experiment clearly show the advantage of an antibiotic resistant NTCD strain in preventing CDI, but also suggest that an antibiotic susceptible strain can be effective if administered daily past the end of antibiotic administration,

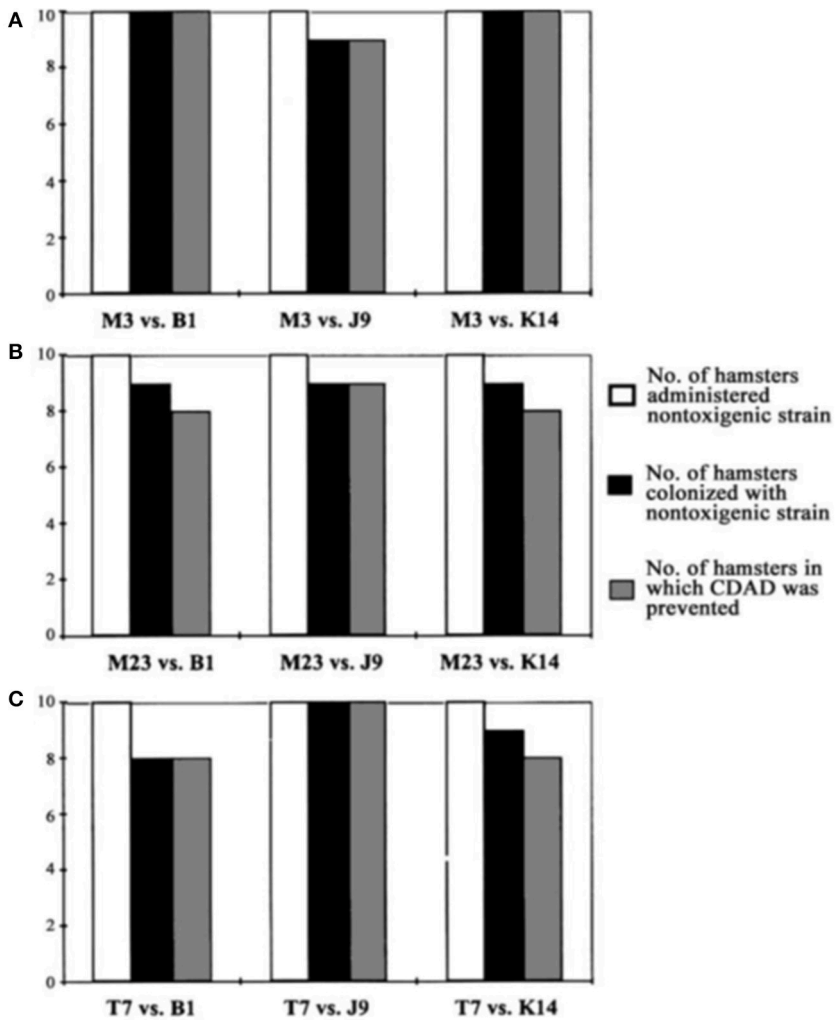

FIGURE 3 | Colonization by nontoxigenic restriction endonuclease analysis (REA) types and prevention of *Clostridium difficile*-associated disease (CDAD) in hamsters. Bars indicate number of animals colonized by nontoxigenic *C. difficile* REA type M3 **(A)**, type M23 **(B)**, and type T7 **(C)** and challenged with 3 different toxigenic *C. difficile* REA types (B1, J9, and K14). From Sambol et al. (2002) with permission.

albeit without as many days of prevention due to the longer time required to establish colonization in the presence of an antibiotic to which it is susceptible. Obviously, a toxigenic *C. difficile* strain resistant to the antibiotic being given has an advantage over susceptible NTCD while the antibiotic is being given, an advantage that is lost within a few days of stopping the antibiotic.

NTCD Prevention After Daily Exposure to Antibiotics Other Than Clindamycin

Similar experiments were conducted to determine NTCD protection during continuous daily administration of ampicillin or ceftriaxone (Merrigan et al., 2009) with the exception that the dose of the toxigenic challenge strain was raised to 1×10^6 spores to further test NTCD prevention. Most strains of *C. difficile* are resistant to cephalosporins including ceftriaxone, and are susceptible to penicillins such as ampicillin. In the ceftriaxone experiments the antibiotic was given intraperitoneally (60 mg/kg) daily for 5 days and NTCD strains M3, M23, or T7 were given to groups of 5 hamsters orogastrically at a dose of 1×10^6 spores 3 h following the first ceftriaxone dose. The toxigenic challenge strain (REA type J9, 1×10^6 spores orogastrically) was responsible for multiple outbreaks of CDI in U.S. hospitals in the 1990s (Johnson et al., 1999). All the strains used were resistant to ceftriaxone; M3 and M23 MIC = 128 mg/mL; T7 MIC = 96 mg/mL; and J9 MIC = >256 mg/mL. Results are shown in **Figure 4** and demonstrate colonization within 48h for all NTCD strains and protection from J9 challenge on day 3 in all hamsters. A single control animal died within 48h as expected with J9 challenge.

Protection against daily administration of an antibiotic such as ampicillin to which NTCD and toxigenic *C. difficile* are both susceptible poses a different challenge (Merrigan et al., 2009). In these experiments NTCD REA type M3 (ampicillin MIC=2.0 mcg/ml) was utilized for prevention (1×10^6 spores daily) and challenged at intervals of 2 days with 1×10^6 spores of toxigenic

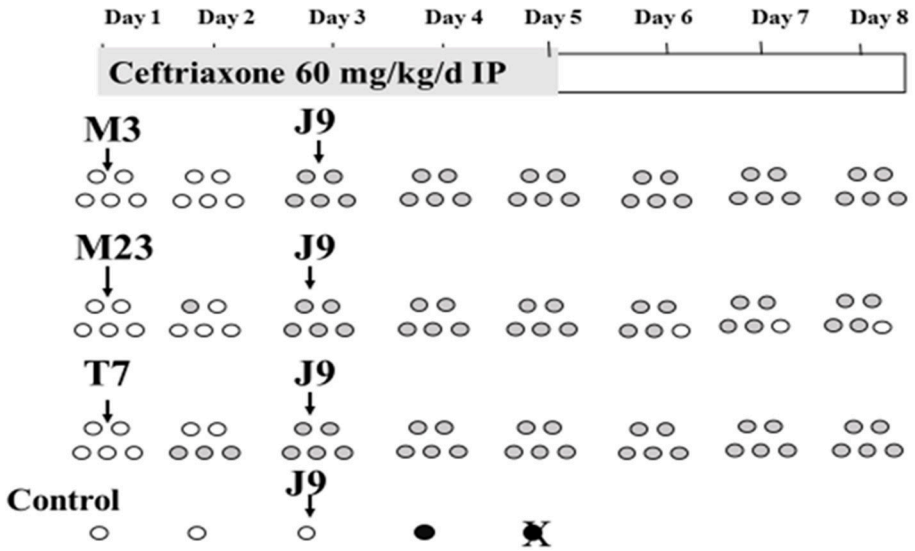

FIGURE 4 | Colonization of non-toxigenic *Clostridium difficile* strains M3, M23, or T7 and subsequent challenge with toxigenic strain J9 during daily ceftriaxone administration. Animals are indicated by ovals: open ovals indicate no detection of *C. difficile* in stool; gray-shaded ovals indicate detection of non-toxigenic *C. difficile* in stool; black ovals indicate detection of toxigenic strain J9 in stool. An X superimposed over an oval indicates the day of death. IP, intraperitoneally. From Merrigan et al. (2009).

strain J9 (ampicillin MIC = 0.75 mcg/ml). Ampicillin was given orogastrically (60 mg/kg daily) to groups of 4 hamsters for 5 days. As expected based on pilot studies, neither M3 or J7 colonized during ampicillin administration, but were able to establish colonization by day 8 if given near the end of the ampicillin course, indicating that following fecal excretion of the inhibitory antibiotic colonization could be established. Experiments were then designed to determine if NTCD M3 administered daily for 5 days to 3 groups of 4 hamsters beginning on day 1, day 3, and day 5 could protect against toxigenic J9 challenges on the middle day of each 5-day M3 course, days 3, 5, and 7, with both strains administered orogastrically at 1×10^6 spores. The study was designed to simulate periodic exposure to toxigenic *C. difficile* while being given NTCD daily. The experiment is shown schematically in **Figure 5** and demonstrates absence of J9 infection despite no colonization by either strain during the 5 days of ampicillin, followed by progressive colonization by M3 on days 7 and 8 in all hamsters. Results of these experiments suggest that in the presence of daily administration of an antibiotic to which NTCD is susceptible, that NTCD should be given daily and for several days after cessation of the antibiotic to attain successful colonization. Toxigenic *C. difficile* is not likely to infect during antibiotic administration and daily NTCD prophylaxis unless the toxigenic strain is resistant to the antibiotic and NTCD is susceptible.

NTCD Prevention Against the Highly Virulent BI Strain of C. difficile

Early in the twenty first century it became apparent that CDI rates, morbidity and mortality were increasing in North America and were attributed at least in part to the presence of an epidemic strain characterized as BI group by REA, NAP1 by pulsed field gel electrophoresis, and 027 by PCR ribotyping and referred to as NAP1/BI/027 (Loo et al., 2005; McDonald et al., 2005). This strain spread throughout the United States and Canada as well as the United Kingdom and much of Europe as CDI rates rose precipitously in these countries. NAP1/BI/027 carries a third toxin, binary toxin and when compared to historic isolates of the same type it was apparent that high-level fluoroquinolone resistance had been acquired (McDonald et al., 2005). This prompted study of these strains in the hamster model by Razaq et al. (2007) who compared epidemic BI strains BI6 and BI17 to historic non-epidemic BI strain BI1 and 2 standard toxigenic strains, K14 and 630 (REA type R23). In these studies groups of 10 hamsters were given 100 spores of each strain of *C. difficile* orogastrically 5 days following a single clindamycin dose (30 mg/kg orally). Although group BI strains were not more rapidly fatal than standard toxinotype 0 strain K14, they were more rapidly fatal than strain 630 and epidemic strain BI6 was the most rapidly fatal of all the strains tested.

The widespread clinical presence of epidemic strain NAP1/BI/027 raised the question of whether NTCD strains would be effective in preventing disease due to BI strains in the hamster model. Nagaro et al. (2013) gave groups of 12 hamsters oral clindamycin (30 mg/kg orally) followed 2 days later by 1×10^6 spores of NTCD strains M3 or T7 in 10 hamsters, and on day 5 challenged all 12 with 100 spores of historic strain BI1 or epidemic strain BI6. All hamsters colonized with M3 or T7 and were protected against challenge with historic strain BI1. NTCD strain M3 colonized 9 of 10 hamsters and protected against BI6 challenge in the 9 colonized hamsters, but not the uncolonized animal. However, epidemic strain BI6 proved more difficult for protection by NTCD strain T7. For the first time in these hamster experiments we found NTCD colonization

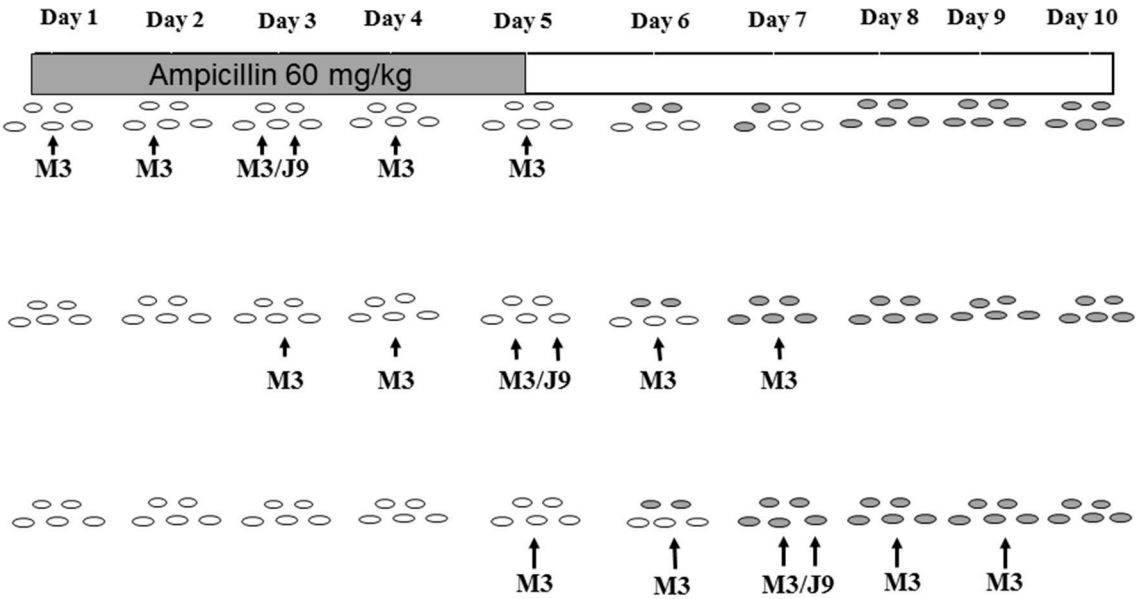

FIGURE 5 | Colonization with non-toxigenic *Clostridium difficile* M3 and challenge with toxigenic strain J9 during daily oral ampicillin administration for 5 days. Both J9 and M3 are susceptible to ampicillin. Animals are indicated by ovals: open ovals indicate no detection of *C. difficile* in stool; gray-shaded ovals indicate detection of non-toxigenic M3 in stool. PO, orally. From Merrigan et al. (2009).

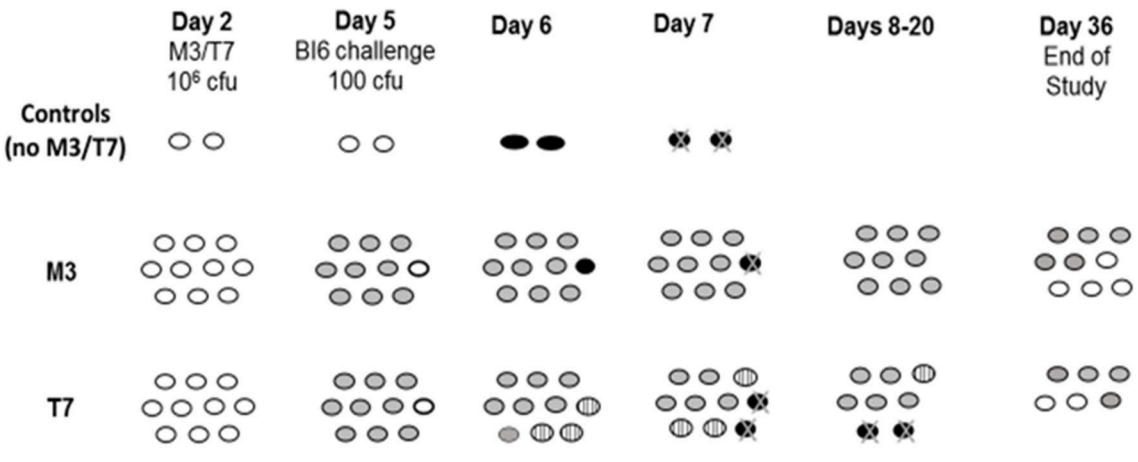

FIGURE 6 | Hamsters ($n = 10$/group) challenged with epidemic toxigenic BI6 *Clostridium difficile*. Day 2 = 2 days post-clindamycin treatment. *White ovals*; uncolonized hamsters. *Gray ovals*; non-toxigenic colonized hamsters. *Striped ovals*; hamsters co-colonized with non-toxigenic and toxigenic *C. difficile*. *Black ovals with "X"*; hamster death from toxigenic BI6. From Nagaro et al. (2013).

displaced by the toxigenic strain (**Figure 6**). Five of 10 hamsters were co-colonized with T7 and BI6 on day 7 and 4 of the 5 died. The remaining co-colonized hamster lost BI6 colonization on day 21 and survived. These results suggest that toxigenic and NTCD strains of *C. difficile* compete for colonization and that certain strains such as BI6 (but not its historic predecessor BI1) despite their lower inoculum and later administration are able to compete more effectively than other toxigenic strains against NTCD strain T7, but not against strain M3. Thus, differences in colonization efficiency are evident for both toxigenic strains of *C. difficile* as well as NTCD strains.

Possible Mechanism of NTCD Prevention

The mechanism by which *C. difficile* strains establish colonization is not established. One possibility is that strains differ in their ability to adhere to colonic mucosal cells or mucus. Merrigan et al. (2013) utilized a derivative of the Caco-2-derived human intestinal epithelial cell-line to assess adherence of 33 strains of toxigenic *C. difficile* (with an emphasis on epidemic NAP1/BI/027 and ribotype 078 strains) and 3 NTCD strains (REA types M3, M23, and T7) in this assay with a focus on differences in surface layer protein A (SlpA) in the strains. The average adherence range of vegetative cells was approximately 8–11% for

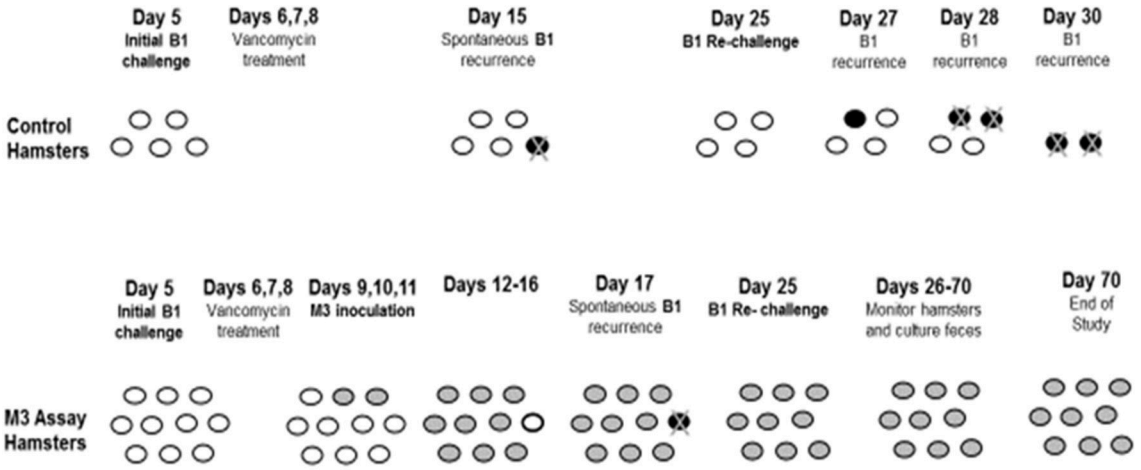

FIGURE 7 | Prevention of recurrence with NTCD-M3 following vancomycin treatment of toxigenic B1 *C. difficile* infection in hamsters. Day 5 = 5 days post-clindamycin treatment. *White ovals*: uncolonized hamsters. *Black ovals*: toxigenic infected hamsters. *Gray ovals*: non-toxigenic colonized hamsters. *Black ovals with "X"*: hamster death from toxigenic B1. From Sambol et al. (2004).

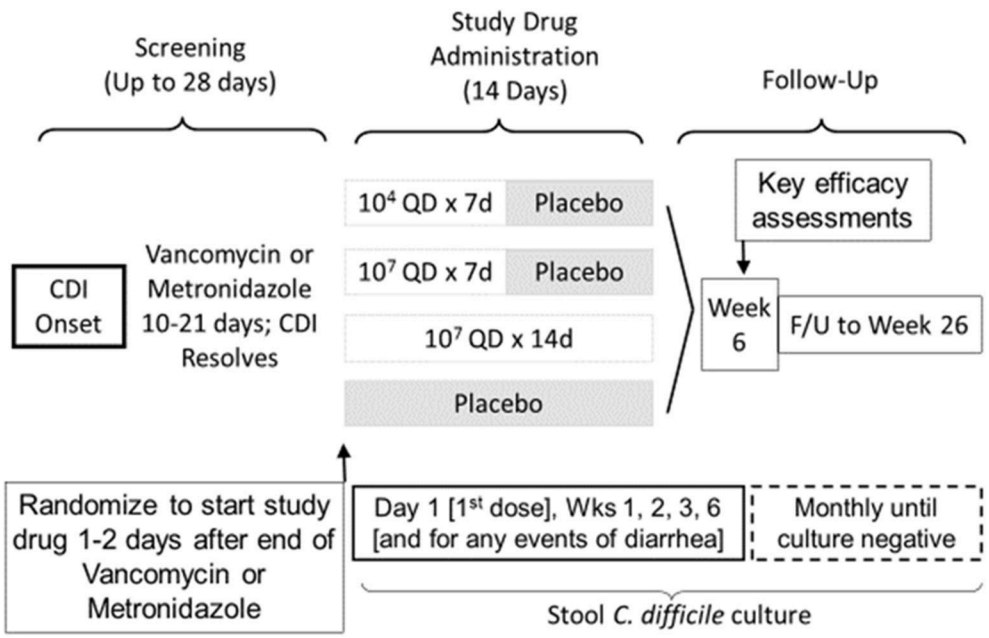

FIGURE 8 | Trial Design for Phase 2 clinical trial of study drug NTCD-M3, spores of non-toxigenic *C. difficile* strain M3 (Gerding et al., 2015).

strain 630, 2–4% for strain K14, 5–9% for strain BI17, 8–14% for NTCD strain M3, and 9–12% for NTCD strain T7. As a group, BI/NAP1/027 strains exhibited a mean adherence value of 4.6%. Further experiments showed that pretreatment of cell layers with surface layer protein (SLP) preparations inhibited *C. difficile* adherence up to 80% with the maximum SLP dose. SLP inhibition was not strain specific; NTCD M3 SLP inhibited M3 and BI17 adherence equally, and BI17 SLP inhibited BI17 and M3 adherence equally. Sequence analysis of the SlpA proteins for both the high molecular weight and low molecular weight subunits was compared among strains. One might postulate that there would be a high degree of conservation of amino acid sequences among highly competitive strains, yet NTCD strain M3 displayed the least sequence conservation, especially in the low molecular weight subunit, compared not only to epidemic toxigenic strains, but also when compared to NTCD strain T7.

NTCD Prevention of Recurrent CDI

Patients who have CDI incur about a 20–30% risk of having a recurrence of their symptoms following successful treatment. If

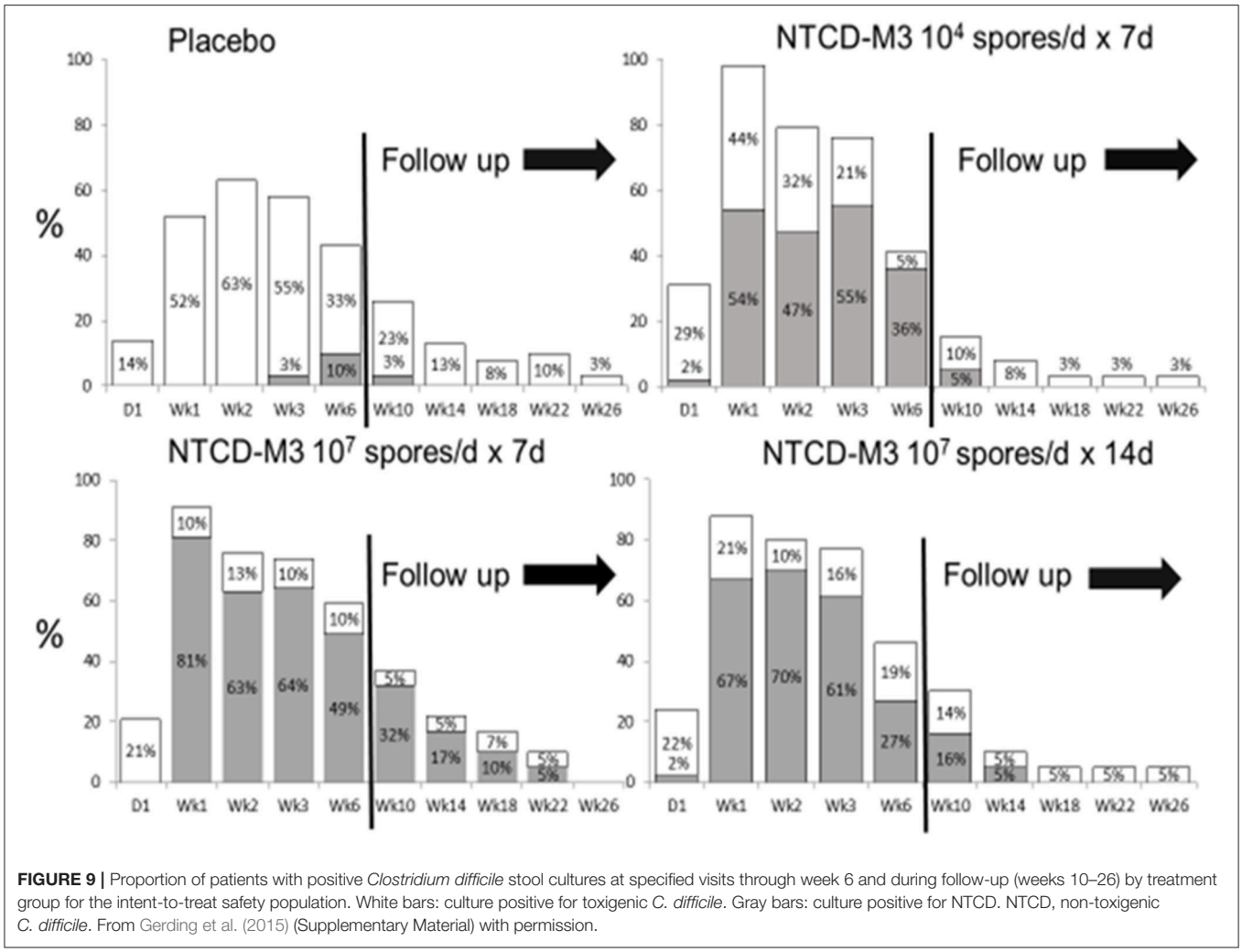

FIGURE 9 | Proportion of patients with positive *Clostridium difficile* stool cultures at specified visits through week 6 and during follow-up (weeks 10–26) by treatment group for the intent-to-treat safety population. White bars: culture positive for toxigenic *C. difficile*. Gray bars: culture positive for NTCD. NTCD, non-toxigenic *C. difficile*. From Gerding et al. (2015) (Supplementary Material) with permission.

such patients could be colonized with NTCD following antibiotic treatment of CDI, it could prevent subsequent recurrence. To test this possibility, the CDI treatment model in hamsters that demonstrated late recurrence of CDI mortality following treatment with vancomycin was modified to administer NTCD M3 following vancomycin treatment (Swanson et al., 1991; Sambol et al., 2004). Sambol et al. (2004) gave a group of 15 hamsters oral clindamycin (30 mg/kg) followed 5 days later by 1×10^4 spores of epidemic strain B1. Vancomycin was administered orogastrically in doses of 100 mg/kg daily for 3 consecutive days on Days 6, 7, and 8 with the first dose administered within 14 h of the initial B1 challenge. On Days 9, 10, and 11, NTCD strain M3 was orally administered to 10 of the 15 hamsters at 1×10^6 spores/day per hamster (5 control hamsters did not receive NTCD). On Day 25, all surviving hamsters were given a re-challenge dose of 1×10^4 toxigenic B1 spores to simulate re-exposure to the toxigenic strain (**Figure 7**). Of the control hamsters, one out of 5 was infected with B1 three days after vancomycin treatment, and died on Day 15, a spontaneous B1 recurrence. After the B1 re-challenge on Day 25, 4 of 4 surviving control hamsters became infected with B1 between Days 27 and 30, and died by Day 30.

Of the hamsters given NTCD, 9 of 10 colonized with M3 between Days 10–16; one hamster remained uncolonized until Day 17, when it became infected with epidemic strain B1 and died, a spontaneous CDI recurrence. After the B1 re-challenge on Day 25, all 9 surviving hamsters remained colonized with M3 until study end on Day 70 with no evidence of B1 infection. These results demonstrate that NTCD colonization following vancomycin treatment is successful and will prevent recurrent *C. difficile* infection.

Potential for NTCD Acquisition of Toxin Genes

Concern has been raised that in clinical use NTCD strains may acquire the toxin A and B pathogenicity locus (PaLoc) and become pathogenic. Brouwer et al. (2013) have shown *in vitro* that toxigenic strain 630Δerm can transfer the PaLoc to NTCD strain CD37, which is REA type T18. PaLoc-containing transconjugants were obtained at a frequency of 7.5×10^{-9} transconjugants per donor in filter matings. DNA fragments containing the PaLoc ranged in size from 66,034 to 272,977 bp.

TABLE 1 | *C. difficile* recurrence and any diarrhea event by treatment arm in a phase 2 clinical trial of NTCD-M3 administered at two different doses of 10^4 and 10^7 spores for 7 or 14 days vs. placebo for 14 days (Gerding et al., 2015).

		Placebo	10^4 × 7d	10^7 × 7d	10^7 × 14d	All NTCD
Number of patients, n		43	41	43	41	125
CDI recurrence, n (%)		13 (30)	6 (15)	2 (5)	6 (15)	14 (11)
	p-value*		0.11	0.01	0.10	0.006
CDI recurrence defined by antibacterial use for CDI treatment, n (%)		14 (33)	6 (15)	4 (9)	7 (17)	17 (14)
	p-value*		0.07	0.02	0.14	0.009
Any event of diarrhea (of any severity) or CDI, n (%)		33 (77)	23 (56)	25 (58)	23 (56)	71 (57)
	p-value*		0.05	0.09	0.02	0.020

**p-values adjusted for pre-specified parameters: use of metronidazole vs. vancomycin, and primary episode vs. first recurrence.*

Transfers from 630Δerm to two other NTCD isolates, PCR ribotypes 138 and 140, were also successful demonstrating that PaLoc transfer is not restricted to a specific donor-recipient pair. Supernatants of recipient strain CD37 following PaLoc transfer were found to cause cell rounding in the cell cytotoxicity assay that was neutralized by toxin B antibodies indicating that the PaLoc transfer resulted in functional toxin production. The mechanism by which PaLoc transfer takes place has not been precisely defined, but transfer via a cell-to-cell conjugation-like transfer mechanism has been proposed (Brouwer et al., 2016). The likelihood of such transfers occurring *in vitro* is unknown, but would presumably require high concentrations of a toxigenic *C. difficile* strain and NTCD in close proximity in the gastrointestinal tract of a host. In the hamster model, we have demonstrated that vancomycin administered daily for 3 days will eliminate NTCD detection in stool, and would presumably be effective in managing CDI if PaLoc transfers were to occur in patients.

Back Again to Bedside: Clinical Trials

The above pre-clinical data were used to file investigational new drug applications with agencies in the US, Canada and Europe. Manufacturing of spores of NTCD-M3 under cGMP was undertaken successfully by ViroPharma, Inc. and the spores prepared in liquid suspension for safety testing in healthy volunteers at doses of 10^4, 10^6, and 10^8 spores/dose or placebo (Villano et al., 2012). NTCD-M3 was found to be safe in younger volunteers age 18–45 years at all three single doses given in the absence of any antibiotic pre-treatment. To better simulate the likely age of patients with CDI, volunteers age >60 years (age range 60–73 years) were given single doses of 10^4, 10^6, and 10^8 spores or placebo safely. Volunteers >60 years were then given the highest dose, 10^8 spores twice daily for 5 days and tolerated this safely. This was the only group in which NTCD could be detected in the stools of the volunteers in the absence of prior antibiotic administration. Stool cultures first became positive on days 2–4 and were positive in 6 of 8 volunteers at day 7 but in none at day 14 and 21 suggesting the possibility that this may have been pass-through of NTCD spores and not colonization.

Finally, groups of 12 >60 year old volunteers were pre-treated with 5 days of oral vancomycin 125 mg 4 × daily to simulate patients being treated for CDI to determine if colonization with NTCD would occur post vancomycin treatment. Each group of 9 NTCD and 3 placebo subjects was given 10^4 or 10^6 or 10^8 spores of NTCD-M3 or placebo daily for 14 days beginning the day following the last vancomycin dose. In each group the 9 volunteers given NTCD-M3 had NTCD detected in their stools during the 14-day administration and in 4 to 5 volunteers on days 21 and 28 following NTCD. In the 3 volunteers receiving placebo in the 10^4 and 10^6 NTCD-M3 spore cohorts one volunteer in each cohort became colonized with a toxigenic strain of *C. difficile* but remained asymptomatic. In the cohort receiving 10^8 spores of NTCD-M3 the 3 placebo patients all became colonized with NTCD-M3, indicating that at this highest dose of NTCD-M3 there was transmission of NTCD-M3 from the active recipient group or the environment to the placebo group who were housed on the same clinical trial facility. No safety issues were identified in the volunteers receiving NTCD-M3.

For the first time since Seal et al. (1987) reported the treatment of 2 CDI patients with NTCD in 1987, NTCD was again administered in a Phase 2 double blind, randomized, dose-ranging, placebo controlled trial of NTCD for prevention of recurrent CDI in patients who have had their first episode or first recurrence of CDI. The primary outcome of the study was safety, with fecal colonization rate, CDI recurrence rate, and optimal dosing of NTCD-M3 as exploratory secondary outcomes. The study design shown in **Figure 8** compared 2 doses, 10^4 and 10^7 spores given orally in liquid once daily for 2 durations, 7 days (10^7 spores) and 14 days (10^4 and 10^7 spores) compared to placebo for 14 days. NTCD-M3 was begun 1–2 days following completion of successful treatment of CDI with vancomycin or metronidazole (Gerding et al., 2015). A total of 168 patients were randomized and treated and 157 completed treatment. The four arms of the study were well balanced in terms of patient age (range 18–94 years) with 39% >65 years old. Most patients were having their primary CDI episode (83%), were outpatients (76%), and were treated with metronidazole (60%). Vancomycin was used for treatment in 20% of subjects and 20% were treated with both vancomycin and metronidazole.

Safety results indicated that participants who received NTCD-M3 had fewer treatment emergent adverse events and fewer serious adverse events than placebo patients with the exception of headache which occurred in 10% of NTCD-M3 recipients and 2% of placebo (Gerding et al., 2015). No serious adverse events were considered treatment related. Colonization by NTCD-M3 was defined as detection of NTCD-M3 in stool at any time following completion of treatment. **Figure 9** demonstrates that colonization with toxigenic *C. difficile* following antibiotic treatment of CDI is common (63% of placebo subjects at week 2) whereas with administration of NTCD-M3, much of the toxigenic *C. difficile* colonization was replaced by NTCD-M3; 71% of participants who received 10^7 spores and 63% who received 10^4 spores. Colonization with NTCD-M3 was maximal in weeks 1–3 and slowly declined thereafter until last detected in week 22. A small number of participants still harbored toxigenic *C. difficile* at 26 weeks, the last time stools were sampled.

Prevention of recurrence of CDI is summarized in **Table 1**. Using the protocol definition of recurrence of CDI at 6 weeks, recurrence rate was 13 (30%) of 43 placebo subjects and 14 (11%) of 125 NTCD-M3 subjects (odds ratio [OR], 0.28; 95%CI, 0.11–0.69; $P = 0.006$); the lowest recurrence was in 2 of 43 (5%) patients receiving 10^7 spores/day for 7 days (OR, 0.1; 95%CI, 0.0–0.6; $P = 0.01$ vs. placebo). Using an alternate definition of recurrent CDI defined as use of antibacterial treatment for CDI, the recurrence rate was 14 of 43 (33%) placebo subjects and 17 of 125 (14%) NTCD-M3 subjects ($p = 0.009$). NTCD-M3 also reduced all-cause diarrhea from 77% in placebo subjects to 57% of NTCD-M3 subjects ($p = 0.020$). There was good correlation of CDI prevention with colonization by NTCD-M3; among subjects who received NTCD-M3 and became colonized, the CDI recurrence rate was 2 of 86 (2%) vs. 12 of 39 (31%) subjects who received NTCD-M3 and were not colonized ($p < 0.001$). Dose-ranging indicated that 10^7 spores were more effective than 10^4 spores, and there was no advantage to extending treatment to 14 days vs. 7 days for the 10^7 dose. In summary, NTCD-M3 was safe and effective in preventing CDI in patients who were experiencing their first CDI episode or first recurrence of CDI.

SUMMARY

NTCD has a long history of basic laboratory and clinical experience that suggests it is a safe and very effective preventive for recurrent CDI (hamster and human data) and as a preventive for first episode CDI if used in subjects receiving antibiotics (hamster data only). Further development is required with phase 3 clinical trials for recurrent CDI prevention and for phase 2 and 3 primary CDI prevention clinical trials.

AUTHOR CONTRIBUTIONS

DG wrote the first manuscript draft and designed the experiments described from his laboratory and provided funding. SJ and SS edited the manuscript, contributed text and figures, and were instrumental in designing and carrying out the described experiments in the DG laboratory.

FUNDING

This work has been supported by multiple Merit Review grants from the Department of Veterans Affairs Research Service.

REFERENCES

Borriello, S. P., and Barclay, F. E. (1985). Protection of hamsters against *Clostridium difficile* ileocaecitis by prior colonization with non-pathogenic strains. *J. Med. Microbiol.* 19, 339–350. doi: 10.1099/00222615-19-3-339

Borriello, S. P., Welch, A. R., Barclay, F. E., and Davies, H. A. (1988). Mucosal association by *Clostridium difficile* in the hamster gastrointestinal tract. *J. Med. Microbiol.* 25, 191–196. doi: 10.1099/00222615-25-3-191

Brouwer, M. S., Mullany, P., Allan, E., and Roberts, A. P. (2016). Investigating transfer of large chromosomal regions containing the pathogenicity locus between clostridium difficile strains. *Methods Mol. Biol.* 1476, 215–222. doi: 10.1007/978-1-4939-6361-4_16

Brouwer, M. S., Roberts, A. P., Hussain, H., Williams, R. J., Allan, E., Mullany, P., et al. (2013). Horizontal gene transfer converts non-toxigenic Clostridium difficile strains into toxin producers. *Nat. Commun.*4:2601. doi: 10.1038/ncomms3601

Clabots, C. R., Johnson, S., Bettin, K. M., Mathie, P. A., Mulligan, M. E., Schaberg, D. S., et al. (1993). Development of a rapid and efficient endonuclease analysis typing system for *Clostridium difficile* and correlation with other typing systems. *J. Clin. Microbiol.* 31, 1870–1895.

Clabots, C. R., Johnson, S., Olson, M. M., Peterson, L. R., and Gerding, D. N. (1992). Acquisition of *Clostridium difficile* by hospitalized patients: evidence for colonized new admissions as a source of infection. *J. Infect. Dis.* 166, 561–567.

Corthier, G., and Muller, M. C. (1988). Emergence in gnotobiotic mice of nontoxinogenic clones of *Clostridium difficile* from a toxinogenic one. *Infect. Immunity* 56, 1500–1504.

Gerding, D. N., Meyer, T., Lee, C., Cohen, S. H., Murthy, U. K., Poirier, A., et al. (2015). Administration of spores of nontoxigenic *Clostridium difficile* strain M3 for prevention of recurrent *C. difficile* infection: a randomized clinical trial. *J. Am. Med. Assoc.* 313, 1719–1727. doi: 10.1001/jama.2015.3725

Gerding, D. N., Olson, M. M., Peterson, L. R., Teasley, D. G., Gebhard, R. L., Schwartz, M. L., et al. (1986). *Clostridium difficile* associateddiarrhea and colitis in adults. *Arch. Intern. Med.* 146, 95–100.

Johnson, S., Clabots, C. R., Linn, F. V., Olson, M. M., Peterson, L. R., and Gerding, D. N. (1990). Nosocomial *Clostridium difficile* colonization and disease. *Lancet* 336, 97-100.

Johnson, S., Samore, M. H., Farrow, K. A., Killgore, G. E., Tenover, F. C., Lyras, D.,et al. (1999). Epidemics of diarrhea caused by a clindamycin-resistant strain of *Clostridium difficile* in four hospitals. *N. Engl. J. Med.* 341, 1645–1651. doi: 10.1056/NEJM199911253412203

Kuijper, E. J., Oudbier, J. H., Stuifbergen, W. N. H. M., Jansz, A., and Zanen, H. C. (1987). Application of whole-cell DNA restriction endonuclease profiles to the epidemiology of *Clostridium difficile*-induced diarrhea. *J. Clin. Microbiol.* 25, 751–753.

Loo, V. G., Poirier, L., Miller, M. A., Oughton, M., Libman, M. D., Michaud, S., et al. (2005). A predominantly clonal multi-institutional outbreak of *Clostridium difficile*-associated diarrhea with high morbidity and mortality. *N. Engl. J. Med.* 353, 2442–2449. doi: 10.1056/NEJMoa051639

McDonald, L. C., Killgore, G. E., Thompson, A., Owens, R. C. Jr, Kazakova, S. V., Sambol, S. P., et al. (2005). Emergence of an epidemic, toxin gene variant strain of *Clostridium difficile* responsible for outbreaks in the United States between 2000 and 2004. *N. Engl. J. Med.* 353, 2433–2441. doi: 10.1056/NEJMoa051590

McFarland, L. V., Mulligan, M. E., Kwok, R. Y. Y., and Stamm, W. E. (1989). Nosocomial acquisition of *Clostridium difficile* infection. *N. Engl. J. Med.* 320, 204–210. doi: 10.1056/NEJM198901263200402

Merrigan, M. M., Sambol, S. P., Johnson, S., and Gerding, D. N. (2003). Prevention of fatal *Clostridium-difficile*-associated disease during continuous administration of clindamycin in hamsters. *J. Infect. Dis*. 188, 1922–1927. doi: 10.1086/379836

Merrigan, M. M., Sambol, S. P., Johnson, S., and Gerding, D. N. (2009). New approach to the management of *Clostridium difficile* Infection: colonization with Non-toxigenic *C. difficile* during daily ampicillin or ceftriaxone administration. *Int. J. Antimicrob. Agents* 33, S46–S50. doi: 10.1016/S0924-8579(09)70017-2

Merrigan, M. M., Venugopal, A. A., Roxas, J. L., Anwar, F., Mallozzi, M. J., Gerding, D. N., et al. (2013). Surface-layer protein A (SlpA) is a major contributor to host-cell adherence of the diarrheagenic pathogen *Clostridium difficile*. *PLoS ONE* 8:e78404. doi: 10.1371/journal.pone.0078404

Nagaro, K. J., Phillips, S. T., Cheknis, A. K., Sambol, S. P., Zukowski, W. E., Johnson, S., et al. (2013). Non-toxigenic *Clostridium difficile* protects hamsters against challenge with historic and epidemic toxigenic BI/NAP1/027 *C. difficile*. *Antimicrob. Agents Chemother*. 57, 5266–5270. doi: 10.1128/AAC.00580-13

Razaq, N., Sambol, S., Nagaro, K., Zukowski, W., Cheknis, A., Johnson, S., et al. (2007). Infection of hamsters with historic and epidemic "BI" Types of *Clostridium difficile*. *J. Infect. Dis.* 196, 1813–1819. doi: 10.1086/523106

Sambol, S. P., Merrigan, M. M., Johnson, S. J., and Gerding, D. N. (2004). "Susceptibility of hamsters to colonization by toxigenic or non-toxigenic *Clostridium difficile* (CD) following treatment with vancomycin or metronidazole," in *Anaerobe 2004 Meeting of the Anaerobe Society of the Americas* (Annapolis, MD).

Sambol, S. P., Merrigan, M. M., Tang, J. K., Johnson, S., and Gerding, D. N. (2002). Colonization for the prevention of *Clostridium difficile* disease in hamsters. *J. Infect. Dis.* 186, 1781–1789 doi: 10.1086/345676

Sambol, S. P., Tang, J. K., Merrigan, M. M., Johnson, S., and Gerding, D. N. (2001). Infection of hamsters with epidemiologically important strains of *Clostridium difficile*. *J. Infect. Dis.* 183, 1760–1766. doi: 10.1086/320736

Seal, D., Borriello, S. P., Barclay, F., Welch, A., Piper, M., and Bonnycastle, M. (1987). Treatment of relapsing *Clostridium difficile* diarrhoea by administration of a non-toxigenic strain. *Eur. J. Clin. Microbiol.* 6, 51–53. doi: 10.1007/BF02097191

Shim, J. K., Johnson, S., Samore, M. H., Bliss, D. Z., and Gerding, D. N. (1998). Primary symptomless colonization by *Clostridium difficile* and decreased risk of subsequent diarrhoea. *Lancet* 351, 633–636. doi: 10.1016/S0140-6736(97)08062-8

Swanson, R. N., Hardy, D. J., Shipkowitz, N. L., Hanson, C. W., Ramer, N. C., Fernandes, P. B., et al. (1991). *In vitro* and *in vivo* evaluation of tiacumicins B and C against *Clostridium difficile*. *Antimicrob. Agents Chemother*. 35, 1108–1111. doi: 10.1128/AAC.35.6.1108

Villano, S. A., Seiberling, M., Tatarowicz, W., Monnot-Chase, E., and Gerding, D. N. (2012). Evaluation of an oral suspension of VP20621, spores of nontoxigenic *Clostridium difficile* strain M3, in healthy subjects. *Antimicrob. Agents Chemother.* 56, 5224–5229. doi: 10.1128/AAC.00913-12

Wilson, K. H., and Sheagren, J. N. (1983). Antagonism of toxigenic *Clostridium difficile* by nontoxigenic *C.* difficile. *J. Infect. Dis.* 147, 733–736. doi: 10.1093/infdis/147.4.733

Conflict of Interest Statement: DG holds patents (unlicensed, no royalties) and technology for the use of NTCD for prevention of CDI and is Scientific Advisory Board Member for Rebiotix, Actelion, Merck, Summit and DaVolterra, is a consultant for Pfizer, MGB Pharma, and Sanofi Pasteur, and holds a research grant from Seres Therapeutics. SJ is Scientific Advisory Board Member for Bio-K+, Synthetic Biologics, Summit and CutisPharma.

The remaining author declares that the research was conducted in the absence of any commercial or financial relationships that could be construed as a potential conflict of interest.

Copyright © 2018 Gerding, Sambol and Johnson. This is an open-access article distributed under the terms of the Creative Commons Attribution License (CC BY). The use, distribution or reproduction in other forums is permitted, provided the original author(s) and the copyright owner(s) are credited and that the original publication in this journal is cited, in accordance with accepted academic practice. No use, distribution or reproduction is permitted which does not comply with these terms.

frontiers in Microbiology

ORIGINAL RESEARCH
published: 20 September 2018
doi: 10.3389/fmicb.2018.02207

Efficiency of Biosynthesized Silver and Zinc Nanoparticles Against Multi-Drug Resistant Pathogens

Kapil Punjabi[1], Sourabh Mehta[2], Rujuta Chavan[3], Vidushi Chitalia[1], Dhanashree Deogharkar[1] and Sunita Deshpande[1]*

[1] Department of Clinical Pathology, Haffkine Institute for Training, Research and Testing, Mumbai, India, [2] National Centre for Nanoscience and Nanotechnology, University of Mumbai, Mumbai, India, [3] Department of Microbiology, Guru Nanak Khalsa College, Mumbai, India

Biosynthesis of metallic nanoparticles has acquired particular attention due to its economic feasibility, low toxicity, and simplicity of the process. In this study, extracellular synthesis of silver and zinc nanoparticle was carried out by *Pseudomonas hibiscicola* isolated from the effluent of an electroplating industry in Mumbai. Characterization studies revealed synthesis of 40 and 60 nm nanoparticles of silver (AgNP) and zinc (ZnNP), respectively, with distinct morphology as observed in TEM and its crystalline nature confirmed by XRD. DLS, zeta potential, NTA, and FTIR studies further characterized nanoparticles giving data about its size, stability, and functional groups. Considering the toxicity of nanoparticles the evaluation of antimicrobial activity was studied in the range of non-toxic concentration for normal cell lines. Silver nanoparticles were found to be the most effective antimicrobial against all tested strains and drug-resistant clinical isolates of MRSA, VRE, ESBL, MDR, *Pseudomonas aeruginosa* with MIC in the range of 1.25–5 mg/ml. Zinc nanoparticles were found to be specifically active against Gram-positive bacteria like *Staphylococcus aureus* including its drug-resistant variant MRSA. Both AgNP and ZnNP were found to be effective against *Mycobacterium tuberculosis* and its MDR strain with MIC of 1.25 mg/ml. The synergistic action of nanoparticles assessed in combination with a common antibiotic gentamicin (590 μg/mg) used for the treatment of various bacterial infections by Checker board assay. Silver nanoparticles profoundly exhibited synergistic antimicrobial activity against drug-resistant strains of MRSA, ESBL, VRE, and MDR *P. aeruginosa* while ZnNP were found to give synergism with gentamicin only against MRSA. The MRSA, ESBL, and *P. aeruginosa* strains exhibited MIC of 2.5 mg/ml except VRE which was 10 mg/ml for both AgNPs and ZnNPs. These results prove the great antimicrobial potential of AgNP and ZnNP against drug-resistant strains of community and hospital-acquired infections and opens a new arena of antimicrobials for treatment, supplementary prophylaxis, and prevention therapy.

Keywords: silver nanoparticles, zinc nanoparticles, *Pseudomonas hibiscicola*, MRSA, VRE, MDR-TB

OPEN ACCESS

Edited by:
Rebecca Thombre, Modern College, India

Reviewed by:
M. Oves, King Abdulaziz University, Saudi Arabia
Rajashree Bhalchandra Patwardhan, Savitribai Phule Pune University, India

****Correspondence:***
Kapil Punjabi
kapil9372@gmail.com

Specialty section:
This article was submitted to Antimicrobials, Resistance and Chemotherapy, a section of the journal Frontiers in Microbiology

Received: *19 March 2018*
Accepted: *29 August 2018*
Published: *20 September 2018*

Citation:
Punjabi K, Mehta S, Chavan R, Chitalia V, Deogharkar D and Deshpande S (2018) Efficiency of Biosynthesized Silver and Zinc Nanoparticles Against Multi-Drug Resistant Pathogens. Front. Microbiol. 9:2207. doi: 10.3389/fmicb.2018.02207

INTRODUCTION

New-age researchers are dedicated to upgrading the current world to a better and easier habitation. To achieve this, nanotechnology will play an important role in newer and improved materials that are robust, economic, and sources of renewable energy and pollution-free environment. The future doctors will use devices made up of such enhanced materials to not only ease the process of diagnostics but also considerably reduce the time and help treatment at early stages. Simpler and faster diagnosis coupled with efficient and reliable treatments will help to cure cancer, diabetes, and various infections. This may seem easy but a difficult road-map lies in front of these researchers, but certainly leads with help of nanotechnology makes it look possible and a revolution seems to be around the corner (Bhattacharyya et al., 2009).

With many arms of nanotechnology being shaped, one major domain is the biomedical application. The biomedical applications of nanotechnology comprise of many sub areas predominantly therapeutic and diagnostic areas have received considerable attention. Different nanoparticles and nanomaterials owing to their small size can easily interact with biomolecules at cellular as well as sub cellular levels. This greatly enhances the signaling of markers in case of diagnostics and improved specificity for targeted therapeutics (Conde et al., 2012).

Multiple applications of nanotechnology across fields like medical, chemical, environmental, agricultural, industrial, energy sciences, and information technology. This attracts major attention from various organizations in both developed and developing nations throughout the world (Roco, 2007).

Many approaches for the synthesis of nanoparticles have been proposed principally categorized into three classes namely – physical, chemical, and biological. Both physical and chemical methods are the major source of nanoparticles in the current period. While these methods ensure continuous supply they also have price to pay in terms of high energy requirements, toxic by-products. This highlights the requirement of sustainable and eco-friendly mode of synthesis. This brings into picture the biological methods with microorganisms playing a significant role. Thus, microbiologists around the world try to identify microorganisms for this capability and develop a simple and cost-effective method to synthesize nanoparticles of constant size, shape, and mono-dispersity (Babu et al., 2011; Horikoshi and Serpone, 2013).

Biosynthesized nanoparticles are ideal candidates for medical applications as they are biocompatible and naturally stable. One of the important property of such nanoparticles is antimicrobial activity. Many green silver nanoparticles have been reported for antibacterial and antibiofilm activity through mechanisms like ROS generation (Qayyum et al., 2017). Also supportive studies on plant derived silver nanoparticles conclude that biogenic nanomaterials are biocompatible and an effective therapeutic agent against bacterial, fungal infections, and cancer treatment (Oves et al., 2018).

Although nanoparticles are considered as future to many areas of science and technology, its probable environmental toxicity is a matter of concern. Thus, in this study, we synthesized nanoparticle, using bacteria isolated from a challenged environment like soil and effluent of electroplating industry and characterized to check potential therapeutic applications if rendered usable by evaluation of its *in vitro* toxicity.

MATERIALS AND METHODS

Synthesis and Characterization of Nanoparticles

The synthesis and characterization of AgNP was followed by our previously reported work using the bacterial culture of *Pseudomonas hibiscicola* isolated from effluent of an electroplating industry. The culture inoculated in sterile nutrient broth and incubated at 37°C for 24 h in an orbital shaker. After incubation, it was centrifuged till clear supernatant was achieved. The supernatant was subjected to 1 mM concentration of silver nitrate AgNO3 (Sigma-Aldrich, United States) and incubated on a shaker with similar conditions. The bio-reduction of silver ions was monitored by visual observation and measuring absorption spectrum of samples using UV–vis Spectrophotometer Thermo scientific Nanodrop – 1000 v3.7 scanning range from 200 to 800 nm (Punjabi et al., 2017). For synthesis of ZnNP, similar procedure was followed; briefly the culture supernatant of *P. hibiscicola* was challenged with 10 mM zinc acetate [$Zn(O_2CCH_3)_2$] (Himedia labs Pvt. Ltd., India) in 1:2 v/v ratio and incubated in similar conditions. After 24 h of incubation, precipitate formation and turbidity indicated presence of ZnNP in the reaction mixture. Reduction of metal ion to nanoparticle was confirmed by observing plasmon peak in the range of 320–380 nm in UV–Vis spectra (Waghmare et al., 2011).

To determine the size, morphology, and other characters of synthesized ZnNPs, characterization studies were undertaken. Suspension of zinc nanoparticles was subjected to UV–Vis spectroscopy, nanoparticle tracking, and analysis (NTA), DLS – particle size analyzer, and zeta potential analysis of the liquid suspension was done using NanoPlus DLS (Micromeritics Instrument Corporation). While powdered material was used for X-ray diffraction (XRD) patterns that were recorded on normal focus diffractometer (Regaku Miniflex, Japan) at voltage of 30 kV and current 15 mA with scan rate of 3°/min. The data were recorded in the range of 20°–50° and analyzed using Jade 6.0 software. Fourier transform infrared (FTIR) spectra obtained on a JASCO spectrometer (6100 type-A) instrument in the range of 400–4000 cm^{-1} were identified spectroscopy and TEM analysis on a Philips CEM 200 Microscope (Pattanayak, 2013).

Toxicity of Nanoparticles

Toxicity of nanoparticles was assessed on Vero cell line (Monkey kidney cell line). The cell line, Vero passage number 27 was obtained from National Centre for Cell Sciences, Pune, India, in Dulbecco's Modified Essential Medium (DMEM) supplemented with 10% fetal bovine serum (FBS) (complete medium).

To evaluate the effect of AgNP and ZnNP on cell toxicity colorimetric MTT (3-(4, 5-dimethylthiazol-2)-2, 5 diphenyl tetrazolium bromide) assay was performed. The MTT assay is a

colorimetric technique wherein amount of absorbance is directly proportional to number of living cells. The MTT tetrazolium compound is reduced by viable cells into an intensely colored formazan precipitate that subsequently is solubilized into a uniformly colored solution with a second procedural step before absorbance is measured using a plate reading spectrophotometer (Freshney, 2010).

Known number (1×10^4 cells) of cells was seeded into tissue culture grade 96-well plates (Riss et al., 2011). Cells were treated with various concentrations (10.0–0.6 mg/ml) of nanoparticles for 24 h and treated with 0. 5% MTT (HiMedia Laboratories Pvt. Ltd., India).

After 4 h, all the contents of wells were removed and 100 μl of dimethyl sulfoxide (DMSO) was added. The absorbance of colored solution was measured on the Multimode reader (Synergy HTX Multimode reader, BIOTEK, India) using a test wavelength of 490 nm (Freshney, 2010; Satyavani et al., 2011). Percentage toxicity was estimated for each concentration, and the IC_{50} value was calculated for both nanoparticles (Freshney, 2005).

Antimicrobial Activity of Nanoparticles

Bacterial Strains

Gram-negative bacteria

Proteus mirabilis ATCC 21100, *Escherichia coli* ATCC 25922, *Klebsiella pneumoniae* ATCC 10031, *K. pneumoniae* ATCC 700603 (extended spectrum β lactamases producer, ESBL), *Pseudomonas aeruginosa* ATCC 27853, *Enterobacter aerogenes* ATCC 13048, *Salmonella typhimurium* ATCC 14028, *Salmonella abony* ATCC 6017, and *Shigella boydii* ATCC 8700.

Gram-positive bacteria

Staphylococcus aureus ATCC 25923, *Bacillus subtillis* ATCC 6633, *S. aureus* ATCC 43300 (methicillin-resistant *S. aureus*, MRSA), *S. aureus* ATCC 6538 *Enterococcus faecalis* ATCC 51299 (vancomycin-resistant *Enterococci*, VRE), *Staphylococcus epidermidis* ATCC 12228, and *Bacillus cereus* ATCC 11778.

Mycobacteria

Mycobacterium tuberculosis H37Rv.

Clinical strains

MDR *P. aeruginosa* and MDR *M. tuberculosis.*

ATCC strains were procured from Clinical Pathology department, Haffkine Institute, microbial culture collection (MCC) Pune, India, and Himedia laboratories Pvt. Ltd., Mumbai, India. The MDR strains of clinical isolates were procured from tertiary care hospital in Mumbai. The drug resistance of the isolates was confirmed before use in the study as per standard protocols of Clinical and Laboratory Standards Institute [CLSI] (2012).

Minimum Inhibitory Concentration

Antimicrobial activity of the nanoparticles synthesized was determined by broth dilution method and confirmation by growth on solid media (Wiegand et al., 2008; Ataee et al., 2011). For determining the minimum concentration of nanoparticles required for the inhibition of bacterial growth, broth dilution method was used according to standard broth microdilution method M07 A9 of Clinical and Laboratory Standards Institute [CLSI] (2012). This method facilitates the testing of inhibitory activity at various nanoparticle concentrations (Clinical and Laboratory Standards Institute [CLSI], 2012).

Anti-mycobacterial Activity – Broth Dilution Method

The minimum inhibitory concentrations (MICs) of silver and zinc nanoparticles were assessed by broth dilution method against *M. tuberculosis* H37Rv and MDR strain. Tenfold serial dilutions of the inoculum suspension were made in M7H9 broth supplemented with Middlebrook OADC enrichment. The stock concentrations of nanoparticles were serially diluted to obtain concentrations in the range 1.25–10 mg/ml. The prepared bacilli suspension (500 μl) was added to all tubes except the control tubes, all the tubes were incubated at 37°C for 7 days, which is physiological temperature favorable for growth of pathogenic strains. To determine the MIC, 10 μl of each tube was transferred to Lowenstein Jensen Medium (LJ medium) and incubated at 37°C for 3 weeks. After incubation, growth on LJ media was analyzed for each concentration of both nanoparticles. The observations were recorded and MIC values were determined (Andrews, 2001; Jadaun et al., 2007).

Synergistic Activity of Gentamicin and Nanoparticles

Disk Diffusion Test for Gentamicin

Antibiotic susceptibility test (AST) against gentamicin (10 μg) and high-level gentamicin (120 μg) (HiMedia labs Pvt. Ltd.) was performed by the Kirby–Bauer disk diffusion test to study the drug-resistant pattern of the aforementioned organisms (Bauer et al., 1966; Clinical and Laboratory Standards Institute [CLSI], 2012).

E-Test

To determine the MIC of gentamicin for these isolates EzyMIC™ Strip (GEN) (0.016–256 mcg/ml) and EzyMIC™ Strip (HLG) (0.064–1024 mcg/ml) (HiMedia labs Pvt. Ltd.) were used. The test was performed on Mueller Hinton agar (HiMedia labs Pvt. Ltd.) swabbing a sterile cotton-swab soaked in inoculum prepared by comparing the turbidity of direct colony suspension to standard 0.5 McFarland. The EzyMIC™ Strip were placed at the center of the agar plate and incubated at 37°C for 24 h. After incubation, the plates were read at the point of complete inhibition of all growth, including hazes, micro-colonies, and isolated colonies as indicated (Nachnani et al., 1992).

MIC of Gentamicin

To determine the MIC of gentamicin, broth dilution method was used according to standard broth microdilution method M07 A9 of Clinical and Laboratory Standards Institute [CLSI] (2012).

Checkerboard Assay

The stock solutions of gentamicin used ranged 2.5 to 160 μg/ml. The stock solutions of silver and zinc nanoparticles used ranged from 0.3 to 20 mg/ml. Double dilutions of both the antibiotic as well as the nanoparticles was used for the assay according to the recommendations of CLSI. A total of 50 μl of sterile nutrient



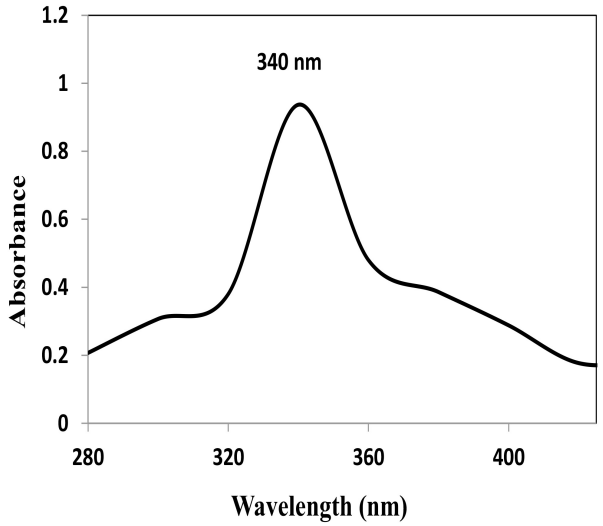

FIGURE 1 | Typical precipitate formation and UV–Vis spectra of the synthesized zinc nanoparticles.

broth was distributed aseptically in all the sterile microtiter plate (96-well plate). The antibiotic gentamicin was serially diluted along the abscissa, while the nanoparticle was diluted along the ordinate. An inoculum equal to 0.5 McFarland turbidity standards was prepared for each culture in sterile saline. Each well was inoculated with 10 μl of the culture. The microtiter plate was incubated at 37°C for 24 h. After incubation, the growth was observed by streaking a loopful from each well in sterile nutrient agar plates. The plates were incubated at 37°C for 24 h. The plates were observed for growth of the test organism. The combination of the drugs in which the growth is completely inhibited was considered as effective MIC for the combination (Breitinger, 2010).

The ΣFICs (fractional inhibitory concentrations) were calculated as follows:

$$\Sigma \text{FIC} = \text{FIC A} + \text{FIC B}$$

where FIC A is the MIC of drug A (gentamicin) in the combination/MIC of drug A (gentamicin) alone, and FIC B is the MIC of drug B (nanoparticle) in the combination/MIC of drug B (nanoparticle) alone. The combination is considered synergistic when the ΣFIC is $\leq$0.5, indifferent when the ΣFIC is $>$0.5 to $<$2, and antagonistic when the ΣFIC is $\geq$2 (Rabadia et al., 2013). The overall study period was 12 months from material synthesis to performing all *in vitro* activities.

RESULTS

Synthesis and Characterization of Nanoparticles

Synthesis of AgNP and ZnNP was achieved extracellularly using *P. hibiscicola* isolated from effluent of electroplating industry. Polydispersed silver nanoparticles of average 40 nm in size were obtained as mentioned in the previous work. In case of ZnNP, typical white precipitate formation as seen in **Figure 1** indicated the synthesis of zinc nanoparticles. The UV–Vis spectra (**Figure 1**) confirm the synthesis of zinc nanoparticles in the reaction mixture.

Further characterization studies gave details about the nanoparticle size, morphology, surface charge, and crystalline nature. The dynamic light scattering (DLS) and zeta potential of the zinc nanoparticles (**Figure 2**) indicated synthesis of stable nanoparticles of size 110 nm and polydispersity index of −0.2. The zeta potential of the zinc nanoparticles was found to be 24.64 mV.

Fourier transform infrared **Figure 3** shows absorption bands at 3513, 2931, and 1020 cm^{-1} indicating the presence of capping agent with the nanoparticles. The spectra correspond to secondary alcohol, alkane, and amine regions. These functional groups have a role in stability/capping of nanoparticles. XRD pattern **Figure 4** shows 2θ values at 31.96°, 34.58°, 36.38°, 47.5°, 56.6°, 62.8°, and 67.9°. All evident peaks could be indexed as the zinc oxide wurtzite structure (JCPDS Data Card No: 36-1451), which confirms the synthesized nanoparticles were free of impurities as it does not contain any characteristics XRD peaks other than zinc oxide peaks.

Nanoparticle tracking and analysis of AgNP and ZnNP (**Figure 5**) shows the particle size distribution which was in the range of 10–70 nm for silver nanoparticles while the mean size was found to be 39 nm with concentration of 3.79×10^8 particles/ml; whereas for ZnNP, the particle size distribution was in the range of 5–90 nm, and mean size was 62 nm with concentration of 4.72×10^8 particles/ml.

The size and morphology of silver nanoparticles synthesized were observed in TEM with average size of 40 nm and most of the population consisting of single crystalline nanoparticles. Spherical zinc nanoparticles of varying size were observed with average size of 60 nm (**Figure 6**).

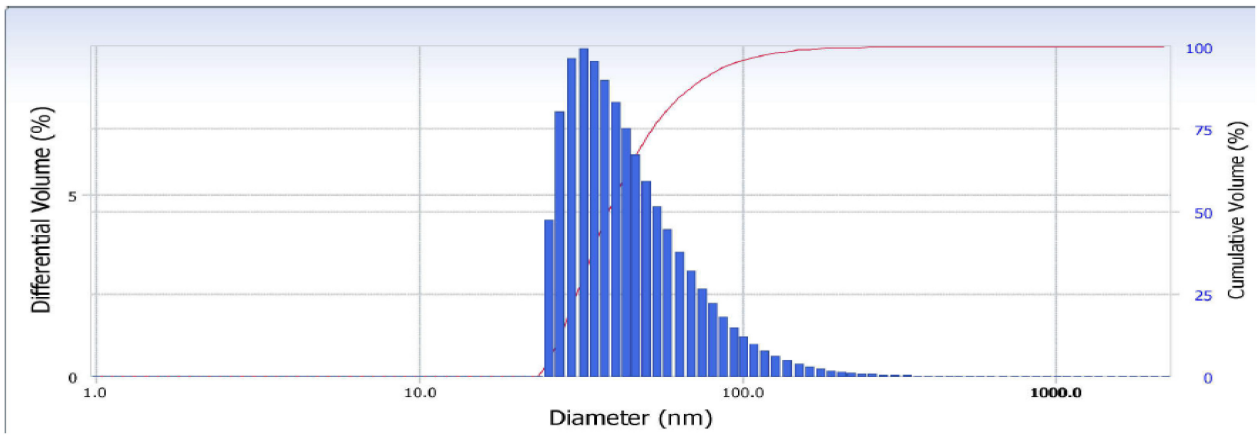

FIGURE 2 | DLS of synthesized zinc nanoparticles.

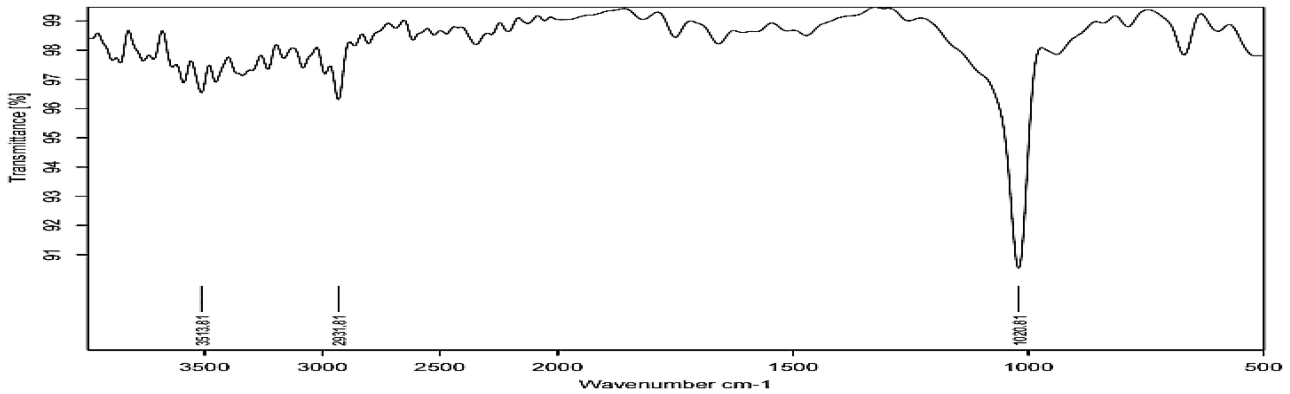

FIGURE 3 | FTIR spectra of zinc nanoparticles.

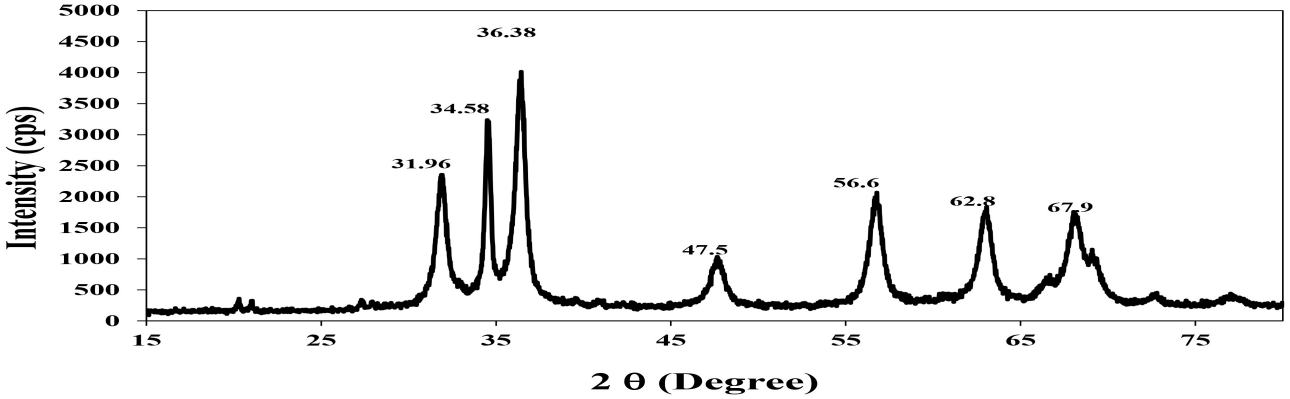

FIGURE 4 | XRD pattern of zinc nanoparticles.

Toxicity of Nanoparticles

Cytotoxicity was evaluated in the range of 0.3 to 10 mg/ml concentration of nanoparticles. Toxicity of a compound is calculated by determining the IC_{50} value, which is that concentration at which growth of cells is inhibited by 50%. The percentage cytotoxicity is plotted against the concentration of nanoparticle as seen in **Figure 7**.

Based on toxicity of nanoparticles to Vero cell line, the IC_{50} values for silver and zinc nanoparticles were found to be 5.54 and 6.24 mg/ml, respectively.

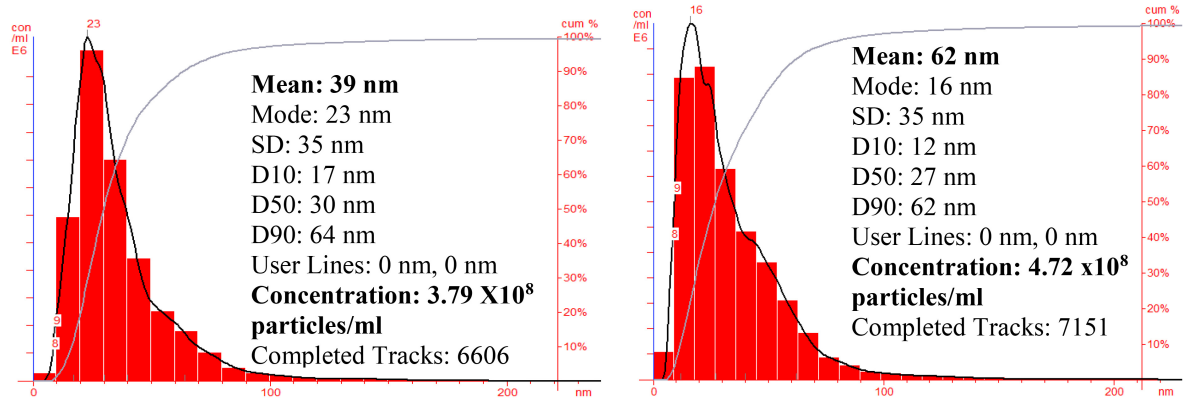

FIGURE 5 | NTA of silver and zinc nanoparticles.

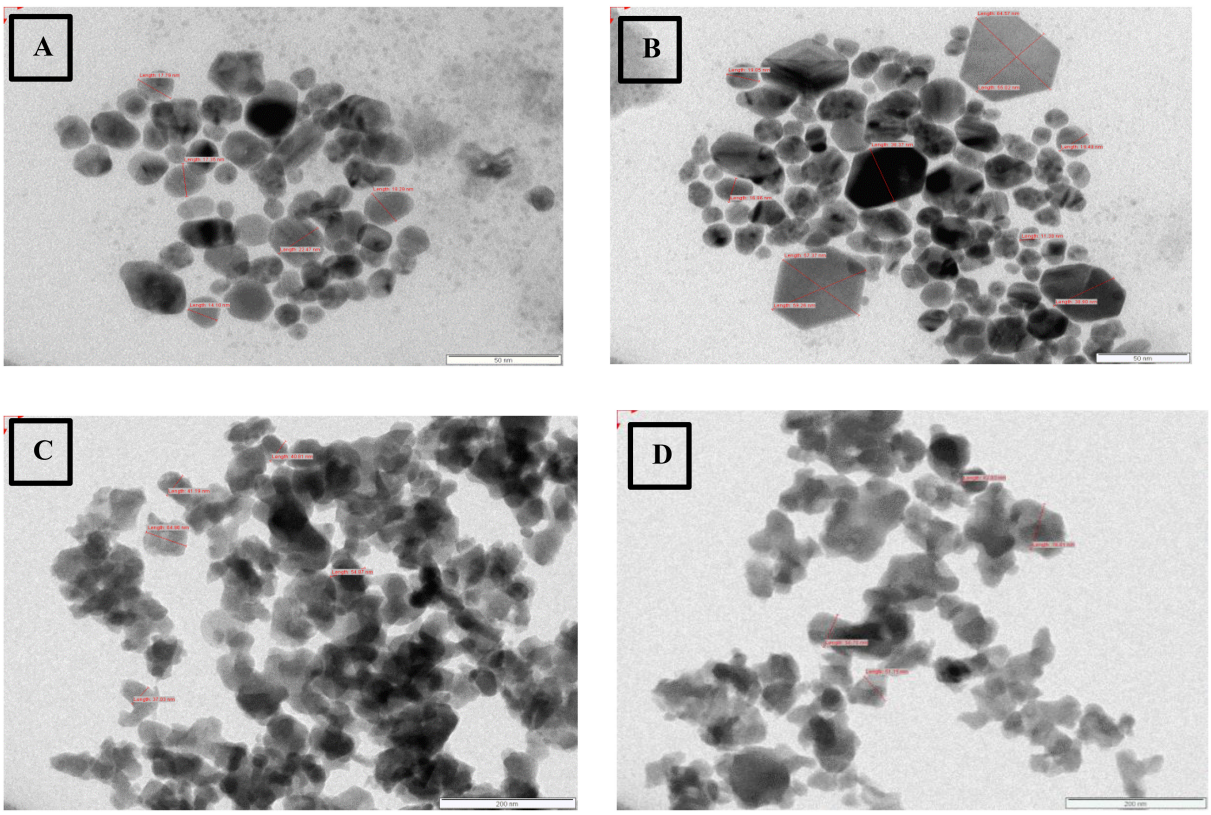

FIGURE 6 | TEM of silver nanoparticles **(A,B)** and zinc nanoparticles **(C,D)**.

Antimicrobial Activity of Nanoparticles

Minimum Inhibitory Concentration

Antimicrobial activity was assessed up to 10 mg/ml concentration of nanoparticle, which is almost double the concentration of cell toxicity to normal cells. For therapeutic consideration as an antimicrobial for synthesized nanoparticles only activity obtained at 5 mg/ml or below was considered. The MIC of both nanoparticles against range pathogenic bacterial strains is as mentioned in **Table 1**.

Anti-mycobacterial Activity – Broth Dilution Method

Table 2 shows the MICs obtained for standard strain and MDR strain of *M. tuberculosis* against both nanoparticles.

Synergistic Activity of Gentamicin and Nanoparticles

Nanoparticles were estimated for its synergistic action with gentamicin against MDR strains. For which susceptibility and MIC of gentamicin were checked, and results of that were

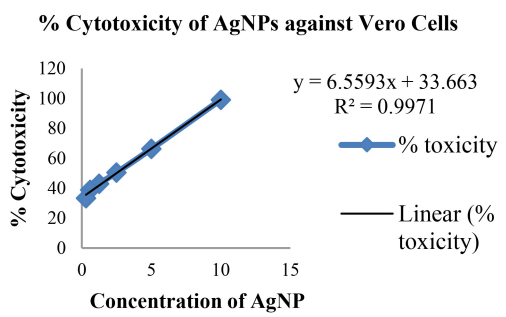

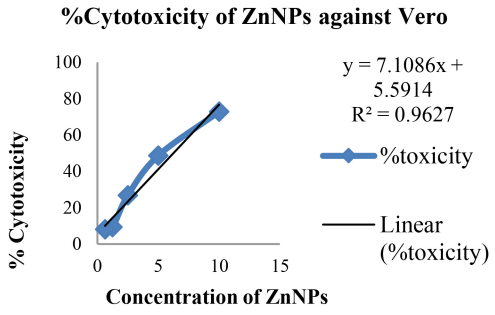

FIGURE 7 | Plot of cytotoxicity vs concentration of nanoparticles.

TABLE 1 | MIC of nanoparticles against range of pathogenic bacteria.

Sr. No.	Organism	ATCC No.	MIC mg/ml	
			AgNPs	ZnNPs
Gram-Negative Bacteria				
1.	*E. coli*	25922	2.5	10
2.	*E. aerogenes*	13048	0.6	>10
3.	*K. pneumoniae* (ESBL)	700603	2.5	>10
4.	*K. pneumoniae*	10031	5	10
5.	*S. typhimurium*	14028	2.5	5
6.	*S. abony*	6017	2.5	>10
7.	*S. boydii*	8700	2.5	>10
8.	*P. mirabilis*	21100	10	1.25
9.	*P. aeruginosa*	27853	2.5	>10
Gram-Positive Bacteria				
10.	*S. aureus*	25923	5	2.5
11.	*S. aureus*	6538	5	5
12.	*S. aureus* (MRSA)	43300	2.5	2.5
13.	*S. epidermidis*	12228	5	5
14.	*E. faecalis* (VRE)	51299	10	>10
15.	*B. subtilis*	6633	>10	>10
16.	*B. cereus*	11778	5	10

TABLE 2 | MIC of nanoparticles against standard and MDR strain of *Mycobacterium tuberculosis.*

Sr. No.	Organism	MIC (mg/ml)	
		AgNPs	ZnNPs
1.	*M. tuberculosis* (H37RV)	1.25	1.25
2.	*M. tuberculosis* (MDR – Clinical isolate)	1.25	1.25

as summarized in **Tables 3**, **4**. Representative images in the **Supplementary Material**.

MIC of Gentamicin

The MIC of gentamicin by microbroth dilution method was evaluated up to 320 μg/ml, considering the limit and toxicity of gentamicin. **Table 5** shows the MICs obtained for each test strain.

TABLE 3 | Susceptibility for gentamicin.

Sr. No.	Organism	Diameter of Zone of Inhibition (mm)	
		Gentamicin (10 μg)	High-Level Gentamicin (120 μg)
1.	*S. aureus* ATCC 43300 (MRSA)	6 (R)	12 (R)
2.	*K. pneumoniae* ATCC 700603 (ESBL)	18 (S)	24 (S)
3.	*P. aeruginosa* ATCC 27853	25 (R)	32 (R)
4.	*E. faecalis* ATCC 51299 (VRE)	6 (R)	6 (R)
5.	*P. aeruginosa* (MDR) Clinical isolate	6 (R)	6 (R)

R, resistant; S, susceptible (Clinical and Laboratory Standards Institute [CLSI], 2014).

TABLE 4 | *E*-test MIC for gentamicin.

Sr. No.	Organism	EZY-MIC	
		Gentamicin (0.016–256 mg)	High-Level Gentamicin (0.064–1024 mg)
1.	*S. aureus* ATCC 43300 (MRSA)	256 (R)	1024 (R)
2.	*K. pneumoniae* ATCC 700603 (ESBL)	3 (S)	4 (S)
3.	*P. aeruginosa* ATCC 27853	1 (S)	1.5 (S)
4.	*E. faecalis* ATCC 51299 (VRE)	256 (R)	1024 (R)
5.	*P. aeruginosa* (MDR) clinical isolate	256 (R)	1024 (R)

R, resistant; S, susceptible (Clinical and Laboratory Standards Institute [CLSI], 2014).

Checkerboard Assay

For determination of synergistic activity of synthesized nanoparticles with gentamicin against test strains checkerboard

TABLE 5 | MIC for gentamicin – microbroth dilution method.

Sr. No.	Organism	MIC of Gentamicin (μg/ml)
1.	*S. aureus* ATCC 43300 (MRSA)	20
2.	*K. pneumoniae* ATCC 700603 (ESBL)	2.5
3.	*P. aeruginosa* ATCC 27853	<0.6
4.	*E. faecalis* ATCC 51299 (VRE)	>320
5.	*P. aeruginosa* (MDR) clinical isolate	>320

TABLE 6 | Synergistic activity of nanoparticles and gentamicin.

Sr. No.	Organism	ΣFIC Value	Result
1.	*S. aureus* ATCC 43300 (MRSA)	0.5	Synergistic (with AgNPs)
2.	*K. pneumoniae* ATCC 700603 (ESBL)	0.3	Synergistic (with AgNPs)
3.	*P. aeruginosa* (MDR) clinical isolate	0.2–0.5	Synergistic (with AgNPs)
4.	*S. aureus* ATCC 43300 (MRSA)	0.5	Synergistic (with ZnNPs)

AgNPS, silver nanoparticles; ZnNPs, zinc nanoparticles.

assay was performed. The FIC values and interpretation of synergism are as shown in **Table 6**.

DISCUSSION

Bacterial synthesis of silver nanoparticles by *P. hibiscicola* was first reported in our previous work (Punjabi et al., 2017). Silver nanoparticles synthesized were characterized by various spectral and microscopic techniques to specifically confirm the synthesis and determine the details of synthesized nanoparticles.

In this study, the NTA revealed the average size of AgNP ranged 10 to 70 nm, but the mean size of synthesized silver nanoparticles was found to be 39 nm. This is in accordance to similar studies with biosynthesis of nanoparticles and its measurement by NTA. Birla et al. (2013) report the size distribution of nanoparticles obtained on a particle-by-particle basis in case of NTA which enables particle population, size, intensity of nanoparticle in suspension, and simultaneously determining their Brownian motion. The NTA calculates the particles size by distance traveled by them, and calculation is based on Stokes–Einstein equation. The average size distribution of silver nanoparticles synthesized by *Fusarium oxysporum* in their study was 41 nm (Birla et al., 2013). TEM revealed an average size of 40.0 nm, which is in accordance with results obtained by NTA. The TEM analysis indicated that the particles were crystalline in nature.

The extracellular biosynthesis of silver and zinc oxide nanoparticles was investigated using *Pichia fermentans* JA2 by Chauhan et al. (2015). The biosynthesized silver nanoparticles were found to inhibit most Gram-negative clinical pathogens used in the study, while zinc oxide nanoparticles only inhibited *P. aeruginosa*. The silver and zinc oxide nanoparticles synthesized using *Pichia fermentans* JA2 had potent antibacterial effect that leads to notable contribution to pharmaceutical associations.

The above report boosts the idea of synthesizing zinc nanoparticles by *P. hibiscicola*. Thus, studies were undertaken to synthesize, optimize, and characterize zinc nanoparticles, which were found to be of variable shapes and the average size of 60 nm. Although DLS reports 110 nm, NTA shows 62 nm final size of nanoparticles was only considered as obtained in TEM micrographs, which were 60 nm. In most case, synthesis of zinc oxide nanoparticles often takes place which could highly be possible in this case as well. This could be alleged on basis of the spectra in UV–Vis spectrophotometer and XRD pattern, which does indicate the presence of oxide specific peaks. Different functional groups identified as secondary alcohols, amines, and alkanes by FTIR analysis, which could mainly be due to biological synthesis.

Jayaseelan et al. (2012) present a work for biosynthesis of zinc oxide nanoparticles (ZnONPs) using bacteria, *Aeromonas hydrophila*. The ZnO NPs were characterized, and a peak at 374 nm in the UV–vis spectrum was observed. Further, XRD confirmed the crystalline nature of the nanoparticles and AFM exhibited the morphology of the nanoparticle to be spherical, oval with an average size of 57.72 nm. The FTIR peaks summarized as alkynes, alkanes, alkenes, primary amines, alcohols, acetate, ethers, and carboxyl compounds. The results of zinc nanoparticles synthesized by *P. hibiscicola* are highly compatible with this study. It could well be said so that synthesis of zinc oxide nanoparticles formation takes place by *P. hibiscicola* also.

The most vital parameter to determine the therapeutic feasibility is toxicity of the material. Therefore, *in vitro* cytotoxicity of both nanoparticles synthesized were assessed on animal tissue. The technique employed to do so was MTT assay, which is a colorimetric estimation of living cells determined by absorbance values upon treatment with the drug for a stipulated amount of time. The cell line used to evaluate the toxicity of nanoparticles was Vero a non-cancerous epithelial cell line commonly used for the said purpose.

In one of the reports, use of AgNP as a therapeutic agent is limited due to its cytotoxicity against mammalian cells. Wherein cytotoxicity of *P. putida* synthesized silver nanoparticles against HEp-2 cells was determined by MTT assay. No significant cytotoxic effect at 25 μg/ml concentration was found, which was lethal for the bacteria tested for antibacterial efficacy (Gopinath et al., 2017). This study highlights and supports the results obtained for nanoparticles synthesized by *P. hibiscicola* although the range of concentration varies mainly due to the presence of protein in the nanomaterial. The purification of nanoparticles was not carried out and freeze-dried powders of as-synthesized nanoparticle were used for cytotoxicity and other activities, leading to the larger amount of material.

One of the most important ailments affecting thousands around the world is microbial infections and more to concern is its drug resistance happening at a rapid pace. Special emphasis needs to be given to drug-resistant infections of bacteria in the community and hospital-acquired infections like ESBL, MRSA, VRE, MDR, *P. aeruginosa* infections, and MDR *M. tuberculosis* infections. The resistance development

has been concerning, and world organizations have been raising alarms at regular intervals. This has also lead to screening a vast number of agents from both biological as well as the chemical cluster for antimicrobial potential. Nanoparticles have potentially all the requisites for qualification as an antimicrobial agent. Not only can nanoparticles have efficiency against this infection causing etiological agents but can also prevent the current therapeutic agents from being rendered useless due to resistance, by alternative or supplementary therapies with nanoparticles along with regular antibiotics. Thus, an interesting aspect was to evaluate nanoparticles synthesized by *P. hibiscicola* for its antimicrobial activity.

Only activity obtained at or below 5 mg/ml was considered suitable for antimicrobial potential against the test strain considering the toxicity of nanoparticles at higher concentrations. Zinc nanoparticle gave activity only against two Gram-negative and four Gram-positive strains, importantly against MRSA at 2.5 mg/ml. Silver nanoparticles were the most potent antimicrobial with activity against most bacteria. In case of the drug-resistant variants for both ESBL and MRSA, activity was observed at 2.5 mg/ml. Both AgNP and ZnNP had anti-TB activity at 1.25 mg/ml for both strains. These results definitely imply that nanoparticles synthesized by *P. hibiscicola* have great antimicrobial potential. This is encouraging to do further evaluations and assess its practical application with more specific *in vivo* studies.

Abd-Elnaby et al. (2016) reported an excellent antibacterial activity against Gram-negative and Gram-positive bacterial pathogens by microbiologically synthesized AgNPs. Mostafa et al. (2015) report activity of chemically synthesized silver nanoparticles against *P. aeruginosa*, *S. aureus*, *Streptococcus pyogenes*, and *S. typhi*. A report stating anti-tuberculosis activity of biosynthesized silver nanoparticles-mentioned spherical-shaped silver nanoparticles with the average particle size of 5 nm, had anti-mycobacterial activity against *M. tuberculosis* and clinical isolates of multi-drug resistant *M. tuberculosis* (MDR-TB) (Banu and Rathod, 2013).

Arrays of pathogens causing different infections were inhibited with the synthesized nanoparticles suggesting its efficiency in controlling infections. This also recommends for assessment of these nanoparticles for synergistic activity with common antibiotics. Thus, synergistic activity against drug-resistant strains was evaluated with antibiotic gentamicin. Gentamicin is an aminoglycoside and commonly used antibiotic against both Gram-positive and Gram-negative bacteria. Currently, gentamicin is susceptible to some and resistant to some bacterial isolates, but it could fast be completely resistant if measures to control resistance are not in place soon. Thus, hypothetically nanoparticles could rescue this situation with its potential synergistic efficiency if found.

Antibacterial susceptibility against gentamicin was assessed by disk diffusion method followed by MIC of gentamicin by *E* – test and micro broth dilution method. The results of disk diffusion and *E*-test identify all the isolates as resistant to gentamicin as per CLSI guidelines of 2014. The MIC of gentamicin by micro broth dilution method was evaluated with a maximum concentration of 320 μg/ml, which is reportedly a toxic concentration. Synergistic activity of nanoparticles and gentamicin was evaluated by Checkerboard method, considering the MICs and toxicity of both gentamicin and nanoparticles.

Promising results were obtained for synergistic activity, zinc nanoparticles exhibited synergism with gentamicin in case of MRSA, so did silver nanoparticles for MRSA, ESBL, and MDR *P. aeruginosa*. A study on the fugal-mediated synthesis of silver nanoparticles reports synergistic activity of silver nanoparticles with amikacin, kanamycin, and streptomycin against *E. coli*, *S. aureus*, and *P. aeruginosa.* The report concluded synergistic action of antimicrobial agent can significantly curtail side effects by reducing dosages. Thus, use of nanoparticles combined with antibiotics can improve their efficacy against various pathogenic microbes (Barapatre et al., 2016). The results of synergistic activity of nanoparticles synthesized by *P. hibiscicola* are in accordance with this report and rightly suggested nanoparticles can indeed be one of the most effective agents in combating serious infections that are rendered untreatable with available antibiotics. There are limited studies with this extent of antimicrobial activity, with qualitative as well as quantitative data against wide range of ATCC and clinical strains. Further to this, determining the mode of action will be an important aspect. But it is well known that most metallic nanoparticles cause oxidative damage to microbes due to excessive generation of reactive oxygen species (ROS), this can be extended to the nanoparticles synthesized.

The extensive potential of silver and zinc nanoparticles against drug-resistant strains of community and hospital-acquired infections opens a new arena of antimicrobials for treatment, supplementary prophylaxis, and prevention therapy. Biologically synthesized nanoparticles can become future anti-infectives and prove to be one of the most potential therapeutic agents.

CONCLUSION

This study covers certain major areas of nanoscience like biological synthesis, characterization, and biomedical application. It provides an extremely potential isolate capable of synthesizing silver and zinc nanoparticles. Characterization studies revealed synthesis of stable nanoparticles of average size 50 nm for silver and 60 nm for zinc nanoparticles. The cytotoxicity studies of nanoparticles against normal cells (non – cancerous) revealed the toxic concentrations for both. Toxicity is the most important factor for therapeutic application. Efficiency of these nanoparticles against drug-resistant pathogen makes it a viable candidate for therapeutics. Thus, biologically synthesized nanoparticles can become future

anti-infective agents and can be formulated for drugs or topical agents.

AUTHOR CONTRIBUTIONS

KP conceptualized and executed the entire experiment as well as the writing of this work. SM helped with the characterization studies, mainly the XRD analysis. RC, VC, and DD helped with the experimental work, including microbial assays and toxicity analysis. VC also helped write and format the manuscript. SD managed the successful completion of the entire project and played an instrumental role in the manuscript.

SUPPLEMENTARY MATERIAL

The Supplementary Material for this article can be found online at: https://www.frontiersin.org/articles/10.3389/fmicb.2018.02207/full#supplementary-material

REFERENCES

Abd-Elnaby, H. M., Abo-Elala, G. M., Abdel-Raouf, U. M., and Hamed, M. M. (2016). Antibacterial and anticancer activity of extracellular synthesized silver nanoparticles from marine *Streptomyces rochei* MHM13. *Egypt. J. Aquat. Res.* 42, 301–312. doi: 10.1016/j.ejar.2016.05.004

Andrews, J. M. (2001). Determination of minimum inhibitory concentrations. *J. Antimicrob. Chemother.* 48(Suppl. 1), 5–16. doi: 10.1093/jac/48.suppl_1.5

Ataee, R., Derakhshanpour, J., Mehrabi Tavana, A., and Eydi, A. (2011). Antibacterial effect of calcium carbonate nanoparticles on *Agrobacterium tumefaciens*. *J. Mil. Med.* 13, 65–70.

Babu, M. M., Sridhar, J., and Gunasekaran, P. (2011). Global transcriptome analysis of *Bacillus cereus* ATCC 14579 in response to silver nitrate stress. *J. Nanobiotechnol.* 9:49. doi: 10.1186/1477-3155-9-49

Banu, A., and Rathod, V. (2013). Biosynthesis of monodispersed silver nanoparticles and their activity against *Mycobacterium tuberculosis*. *Int. J. Biomed. Nanosci. Nanotechnol.* 3, 211–220. doi: 10.1504/IJBNN.2013.054507

Barapatre, A., Aadil, K. R., and Jha, H. (2016). Synergistic antibacterial and antibiofilm activity of silver nanoparticles biosynthesized by lignin-degrading fungus. *Bioresour. Bioprocess.* 3:8. doi: 10.1186/s40643-016-0083-y

Bauer, A., Kirby, W., Sherris, J. C., and Turck, M. (1966). Antibiotic susceptibility testing by a standardized single disk method. *Am. J. Clin. Pathol.* 45, 493–496. doi: 10.1093/ajcp/45.4_ts.493

Bhattacharyya, D., Singh, S., Satnalika, N., Khandelwal, A., and Jeon, S. H. (2009). Nanotechnology, big things from a tiny world: a review. *Nanotechnology* 2, 29–38.

Birla, S. S., Gaikwad, S. C., Gade, A. K., and Rai, M. K. (2013). Rapid synthesis of silver nanoparticles from *Fusarium oxysporum* by optimizing physicocultural conditions. *Sci. World J.* 2013:796018. doi: 10.1155/2013/796018

Breitinger, H. (2010). "Drug synergy–mechanisms and methods of analysis," in *Toxicity and Drug Testing*, ed. B. Acree (London: InTech), 143–166.

Chauhan, R., Reddy, A., and Abraham, J. (2015). Biosynthesis of silver and zinc oxide nanoparticles using *Pichia* fermentans JA2 and their antimicrobial property. *Appl. Nanosci.* 5, 63–71. doi: 10.1007/s13204-014-0292-7

Clinical and Laboratory Standards Institute [CLSI] (2012). *Performance Standards for Antimicrobial Susceptibility Testing; Twenty-Second Informational Supplement. CLSI Document M100-S22*. Wayne, PA: Clinical and Laboratory Standards Institute.

Clinical and Laboratory Standards Institute [CLSI] (2014). *Performance Standards for Antimicrobial Susceptibility Testing: Twenty-Fourth Informational Supplement, M100-S24*, Vol. 34. Wayne, PA: Clinical and Laboratory Standards Institute.

Conde, J., Doria, G., and Baptista, P. (2012). Noble metal nanoparticles applications in cancer. *J. Drug Deliv.* 2012:751075. doi: 10.1155/2012/751075

Freshney, R. I. (2005). *Culture of Animal Cells: A Manual of Basic Technique*. New York, NY: John Wiley and Sons, Inc. doi: 10.1002/9780471747598

Freshney, R. I. (2010). *Culture of Animal Cells*. New York, NY: John Wiley and Sons. doi: 10.1002/9780470649367

Gopinath, V., Priyadarshini, S., Loke, M. F., Arunkumar, J., Marsili, E., MubarakAli, D., et al. (2017). Biogenic synthesis, characterization of antibacterial silver nanoparticles and its cell cytotoxicity. *Arab. J. Chem.* 10, 1107–1117. doi: 10.1016/j.arabjc.2015.11.011

Horikoshi, S., and Serpone, N. (2013). *Introduction to Nanoparticles*. Weinheim: Wiley-VCH Verlag GmbH and Co. KGaA.

Jadaun, G. P., Agarwal, C., Sharma, H., Ahmed, Z., Upadhyay, P., Faujdar, J., et al. (2007). Determination of ethambutol MICs for *Mycobacterium tuberculosis* and *Mycobacterium avium* isolates by resazurin microtitre assay. *J. Antimicrob. Chemother.* 60, 152–155. doi: 10.1093/jac/dkm117

Jayaseelan, C., Rahuman, A. A., Kirthi, A. V., Marimuthu, S., Santhoshkumar, T., Bagavan, A., et al. (2012). Novel microbial route to synthesize ZnO nanoparticles using *Aeromonas hydrophila* and their activity against pathogenic bacteria and fungi. *Spectrochim. Acta A Mol. Biomol. Spectrosc.* 90, 78–84. doi: 10.1016/j.saa.2012.01.006

Mostafa, A. A., Sayed, S. R., Solkamy, E. N., Khan, M., Shaik, M. R., Al-Warthan, A., et al. (2015). Evaluation of biological activities of chemically synthesized silver nanoparticles. *J. Nanomater.* 16:443. doi: 10.1155/2015/789178

Nachnani, S., Scuteri, A., Newman, M. G., Avanessian, A. B., and Lomeli, S. L. (1992). E-test: a new technique for antimicrobial susceptibility testing for periodontal microorganisms. *J. Periodontol.* 63, 576–583. doi: 10.1902/jop.1992.63.7.576

Oves, M., Aslam, M., Rauf, M. A., Qayyum, S., Qari, H. A., Khan, M. S., et al. (2018). Antimicrobial and anticancer activities of silver nanoparticles synthesized from the root hair extract of *Phoenix dactylifera*. *Mater. Sci. Eng. C* 89, 429–443. doi: 10.1016/j.msec.2018.03.035

Pattanayak, U. (2013). *Green Synthesis of Zinc Nano Particle By Microbes*. Doctoral thesis, National Institute of technology, Rourkela.

Punjabi, K., Yedurkar, S., Shah, S., Deshapnde, S., and Vaidya, S. (2017). Biosynthesis of silver nanoparticles by *Pseudomonas* spp isolated from effluent of an electroplating industry. *IET Nanobiotechnol.* 11, 584–590. doi: 10.1049/iet-nbt.2016.0172

Qayyum, S., Oves, M., and Khan, A. U. (2017). Obliteration of bacterial growth and biofilm through ROS generation by facilely synthesized green silver nanoparticles. *PLoS One* 12:e0181363. doi: 10.1371/journal.pone.0181363

Rabadia, A., Kamat, S., and Kamat, D. (2013). Study of synergistic action of cefotaxime and *Terminalia chebula* on *Acinetobacter baumannii* using checkerboard assay. *Int. J. Pharm. Pharm. Sci.* 5, 830–832.

Riss, T. L., Moravec, R. A., and Niles, A. L. (2011). Cytotoxicity testing: measuring viable cells, dead cells, and detecting mechanism of cell death. *Methods Mol. Biol.* 740, 103–114. doi: 10.1007/978-1-61779-108-6_12

Roco, M. C. (2007). "National nanotechnology initiative-past, present, future," in *Handbook on Nanoscience, Engineering and Technology,* eds W. A. Goddard, D. Brenner, S. E. Lyshevski, and G. J. Iafrate (Boca Raton, FL: CRC Press).

Satyavani, K., Gurudeeban, S., Ramanathan, T., and Balasubramanian, T. (2011). Biomedical potential of silver nanoparticles synthesized from calli cells of *Citrullus colocynthis* (L.) schrad. *J. Nanobiotechnol.* 9:43. doi: 10.1186/1477-3155-9-43

Waghmare, S., Deshmukh, A., Kulkarni, S., and Oswaldo, L. (2011). Biosynthesis and characterization of manganese and zinc nanoparticles. *Univ. J. Environ. Res. Technol.* 1, 64–69.

Wiegand, I., Hilpert, K., and Hancock, R. E. (2008). Agar and broth dilution methods to determine the minimal inhibitory concentration (MIC) of antimicrobial substances. *Nat. Protoc.* 3, 163–175. doi: 10.1038/nprot.2007.521

Conflict of Interest Statement: The authors declare that the research was conducted in the absence of any commercial or financial relationships that could be construed as a potential conflict of interest.

Copyright © 2018 Punjabi, Mehta, Chavan, Chitalia, Deogharkar and Deshpande. This is an open-access article distributed under the terms of the Creative Commons Attribution License (CC BY). The use, distribution or reproduction in other forums is permitted, provided the original author(s) and the copyright owner(s) are credited and that the original publication in this journal is cited, in accordance with accepted academic practice. No use, distribution or reproduction is permitted which does not comply with these terms.

frontiers in Microbiology

ORIGINAL RESEARCH
published: 27 September 2018
doi: 10.3389/fmicb.2018.02300

Efficient Production of Recombinant Protegrin-1 From *Pichia pastoris*, and Its Antimicrobial and *in vitro* Cell Migration Activity

*Evanna Huynh[1], Nadeem Akhtar[1] and Julang Li[1,2]**

[1] Department of Animal Biosciences, University of Guelph, Guelph, ON, Canada, [2] College of Life Science and Engineering, Foshan University, Foshan, China

Protegrin (PG) belongs to the antimicrobial peptide cathelicidin family. To date, five protegrin sequences have been identified in pigs, PG-1 to PG-5. Of these, PG-1 exhibits potent antimicrobial activity against a broad range of antibiotic-resistant microorganisms as well as viruses. However, the other potential role(s) of PG beyond antimicrobial has largely been unexplored. The aim of this study was to use nonpathogenic yeast *Pichia pastoris* to express antimicrobially active recombinant protegrin (rPG-1). Additionally, the effect of PG-1 on cell migration and proliferation was also examined *in vitro* using pig intestinal epithelial cells as a model. Highest level of rPG-1 (104 ± 11 μg/mL) was detected at 24 h in fermentation culture medium. Similar to rPG-1, 0.8 ± 0.10 g/L of proform PG-1 (rProPG-1) and 0.2 ± 0.02 g/L of the PG-1 cathelin domain (rCath) was detected in fermentation culture medium. Resulting recombinant PG-1 and cleaved rProPG-1 exerted antimicrobial activity against *Escherichia coli* DH5α at the same level as chemically synthesized PG-1. Enhanced cell migration was observed ($p < 0.05$) in groups treated with rProPG-1, rCath, and rPG-1 compared to the control. Furthermore, rPG-1 was stable at temperatures ranging from 25°C to 80°C. In summary, biologically active recombinant protegrin in its pro-, cathelin-, and mature- forms were successfully expressed in *P. pastoris* suggesting potential feasibility for future therapeutic applications.

Keywords: antimicrobial peptide, cell migration, fermentation, *Pichia pastoris*, protegrin

OPEN ACCESS

Edited by:
Kamlesh Jangid, National Centre for Cell Science (NCCS), India

Reviewed by:
César de la Fuente, Massachusetts Institute of Technology, United States
Pedro Ismael Da Silva Junior, Instituto Butantan, Brazil

***Correspondence:**
Julang Li
jli@uoguelph.ca

Specialty section:
This article was submitted to Antimicrobials, Resistance and Chemotherapy, a section of the journal Frontiers in Microbiology

Received: *12 November 2017*
Accepted: *10 September 2018*
Published: *27 September 2018*

Citation:
Huynh E, Akhtar N and Li J (2018) Efficient Production of Recombinant Protegrin-1 From Pichia pastoris, and Its Antimicrobial and in vitro Cell Migration Activity. Front. Microbiol. 9:2300. doi: 10.3389/fmicb.2018.02300

INTRODUCTION

Tissue repair, including those happened after gastrointestinal infection, is an orchestrated process with inflammation and tissue re-epithelialization as critical approaches for successful healing. In addition to growth and repair factors (e.g., epidermal growth factor, trefoil factors), antimicrobial peptides (AMPs) are also expressed and secreted upon mucosal injury (Frohm et al., 1997; Hase et al., 2003; Kovach et al., 2012). AMPs, as well as the recently identified unusual amino acid L-cyclopropylalanine with anti-fungal and -bacterial activity (Ma et al., 2017) represent the first line of defense, or innate immunity, against foreign pathogens. These low-molecular weight molecules can exert antimicrobial activity at a nanomolar to micromolar range against a broad spectrum of microorganisms including bacteria, fungi, enveloped viruses, and parasites

(Hancock and Sahl, 2006; Sang and Blecha, 2008; Dias et al., 2017). In recent years, AMPs appear to be functionally multifaceted, fulfilling a variety of functions beyond microbial killing, including immunomodulation, tissue regeneration and vascularization in inflammation, tissue repair and even tumor surveillance (Hirano et al., 2000; Ishihara and Hirano, 2002; Proudfoot, 2002; Choi et al., 2012; de la Fuente-Núñez et al., 2014). A cationic AMP P17 from ant venom induces an alternative phenotype of human monocyte-derived macrophages (h-MDMs) promoting its anti-fungal activities (Benmoussa et al., 2017).

Cathelicidin is an evolutionary distinct group of AMPs in mammals. This peptide group has a highly conserved N-terminal (cathelin) domain in the pro-peptide followed by a variable AMP domain on the C-terminus (Kovach et al., 2012). Protegrin (PG) belongs to the cathelicidin family, and to date, five protegrin sequences have been identified in pigs, PG-1, PG-2, PG-3, PG-4, and PG-5. Of these, PG-1 exhibits potent antimicrobial activity against a broad range of antibiotic-resistant microorganisms as well as viruses, including HIV (Hancock and Sahl, 2006; Liu and Stappenbeck, 2016). Increasing evidence of alterations of mucosal AMP levels has leaded to the suggestion on their influential role on the gut immune protection (Schauber et al., 2006; Termén et al., 2008; Inaba et al., 2010), although the immuno- and tissue repair-modulating roles of PGs have not been investigated.

PG-1 possesses potential therapeutic utility. However, chemical synthesis of peptides is associated with high production costs and increased peptide length often limits success of the synthesis, and thusly, potentially limiting therapeutic application. *Pichia pastoris* is a highly appealing expression system which has advantages including rapid growth rate, high levels of protein production and eukaryotic post-translational modifications. The commercial applications of recombinant protein of phospholipase C (Ciofalo et al., 2006) and biopharmaceutical product (Thompson, 2010) produced by *P. pastoris* have the FDA generally recognized as safe (GRAS) status in the United States. Furthermore, administration of *P. pastoris* cells as a vehicle for recombinant vaccine delivery via intramuscular injection and oral delivery have been shown to be safe and effective in chickens (Taghavian et al., 2013). Previous work on the PG-3 cathelin domain revealed that the pro-piece cathelin domain has a role in activating cathepsin L (Zhu et al., 2008), and the pro-piece of human hCAP-18 has been suggested to have a role in preventing cysteine-proteinase-mediated tissue damage during inflammation (Zaiou et al., 2003). However, the role of PG-1 and its cathelin domain in regulating other cellular activity is unclear. We hypothesized that the proform, pro-piece and mature form of PG-1 can be efficiently produced in yeast, and that they may process tissue repair function, in addition to the well known antimicrobial role of PG-1.

The first objectives of this investigation was to examine the feasibility of expressing recombinant PG-1 in its pro-, cathelin- and mature- form in *P. pastoris* and characterize its antimicrobial activity *in vitro*. Considering the wound healing role, besides antimicrobial activity, of PG-1 has not been investigated to date, we will also examine the effect of PG on cell migration and proliferation *in vitro* using pig intestinal epithelial cells as a model.

MATERIALS AND METHODS

Construction of *P. pastoris* DNA Expression Vector

Expression vector designed to express pro-form PG-1 (pJ912-proPG-1) was codon-optimized (**Supplementary Material 1**) for optimal expression in *P. pastoris* and synthesized by DNA2.0 (Menlo Park, CA, United States). Native PG-1 sequence was used as a starting sequence (NCBI accession number: CAA56251). Enterokinase (EK) cleavage site (DDDDK) replaced the native neutrophil elastase site between the cathelin domain and the mature PG-1 domain (**Figure 1A**). Resultant plasmids were transformed into *Escherichia coli* DH5α (*E. coli*) for plasmid propagation and positive recombinant colonies were selected using 25 μg/mL zeocin (Invitrogen, CA, United States) in Luria-Bertani (LB) medium (Difco, MI, United States).

Electroporation of *P. pastoris* X-33 and Screening for Recombinant Strains

Plasmid DNA was linearized with *Swa*I (New England Biolabs, Ipswich, MA, United States) and purified by phenol-chloroform extraction and ethanol precipitation. Approximately 3–5 μg of purified linearized plasmid DNA was dissolved in 10 μL of nuclease-free H_2O. Electrocompetent *P. pastoris* X33 (Invitrogen, Carlsbad, CA, United States) was prepared according to the manufacturer's instruction. Competent cells (100 μL) were mixed with the dissolved purified DNA in a 0.4 cm electroporation cuvette (BTX, CA, United States). Electroporation was carried out in Electro Cell Manipulator 600 (BTX, CA, United States) at 1.5 kV. Immediately after electroporation, 1.0 mL of 1 M ice-cold sorbitol (Fisher Scientific, Pittsburgh, PA, United States) was added to the cuvette. Cells were transferred to a sterile 1.5 mL tube and incubated at 30°C without shaking for 2 h. Transformed cells were plated on YPD agar [1% yeast extract (Difco, Detroit, MI, United States), 2% peptone (Difco, Detroit, MI, United States), 2% glucose (Fisher Scientific, Pittsburgh, PA, United States), 2% agar (Difco, Detroit, MI, United States)] supplemented with 1 M sorbitol and zeocin (100 μg/mL) and incubated for 3–4 days at 30°C until colonies appeared. Colonies were purified by streaking onto YPD agar with zeocin (100 μg/mL).

Genomic DNA Analysis to Determine *P. pastoris* Mut-Genotype

To confirm recombinant gene integration and *P. pastoris* transformant Mut phenotype, genomic DNA was isolated from *P. pastoris* transformants using the freeze-and-thaw method previously described in (Jafari et al., 2011). The following universal *AOX1* primers were used for PCR: Sense: 5′-GACTGGTTCCAATTGACAAGC-3′, anti-sense: 5′GCAAATGGCATTCTGACATCC-3′. Amplification was

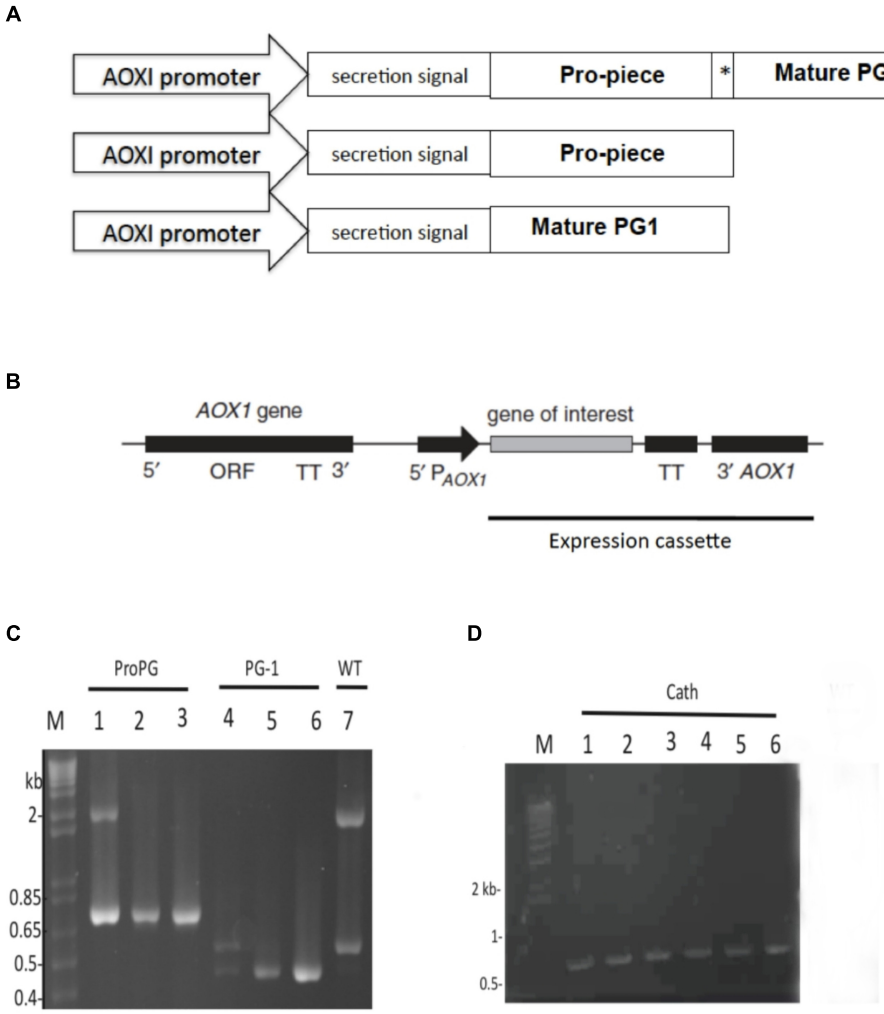

FIGURE 1 | Schematic construct of open reading frames (OFRs), expression cassette, and PCR amplicons. **(A)** ORF construct for proform PG-1, cathelin, and mature PG-1 expression. MeOH-inducible *AOX1* promoter and α-mating factor secretion signal sequence was used in all expression constructs. Asterisk (*) indicate enterokinase (EK) cleavage site. **(B)** Schematic representation of the integration of the expression cassette into *Pichia pastoris* genome. **(C)** PCR products amplified from gDNA to confirm integration of constructs for the expression of rProPG-1 (lane 1, 2 from two representative positive clones, respectively, at 760 bp) and rPG-1 (lane 4, 5 from two representative positive clones, respectively, at 458 bp). Expression plasmids for rProPG-1 and rPG-1 were used as an assay control (lane 3 and 6, respectively). **(D)** PCR products amplified from gDNA to confirm integration of constructs for the expression of rCath (lane 1–5). Expression plasmids for rCath were used as an assay control (lane 6). Wild-type AOXI gene yields a 2.2 kb product (Lane 7). Scales are not proportional to the sizes of the elements in **(A)** and **(B)**.

carried out at 94°C for 30 s, 55°C for 30 s, and 72°C for 1 min for 35 cycles. PCR was performed using *Taq* DNA polymerase (Invitrogen, Carlsbad, CA, United States).

Expression Cassette Copy Number Determination in *P. pastoris*

The number of copies of pJ912-ProPG expression cassettes integrated into the *P. pastoris* genome was determined by quantitative real-time PCR as described by (Abad et al., 2010) and copy number of each clone was determined using the $2^{-\Delta\Delta Ct}$ method (Livak and Schmittgen, 2001; Schmittgen and Livak, 2008). Blank *P. pastoris* X33, *AOX1* promoter, and endogenous *ARG4* gene were used as calibrator, target gene, and reference gene, respectively.

Inducing Expression of Pro-form PG-1 in *P. pastoris*

Positive transformant colonies were inoculated into a 500 mL flask containing 50 mL BMGY medium [1% yeast extract, 2% peptone, 100 mM potassium phosphate (pH 6.0), 1.4% yeast nitrogen base (Difco, Detroit, MI, United States), 0.00004% biotin (Difco, Detroit, MI, United States), 1% glycerol (Fisher Scientific, Pittsburgh, PA, United States)] at 30°C with shaking at 250 rpm. After 16–24 h, cultures reached an optical density at 600 nm (OD600) = 2.0–6.0 and were harvested by centrifugation and resuspended in BMMY medium (BMGY medium containing 0.5% v/v methanol instead of glycerol) to induce expression. Cells were grown for 72 h at 30°C with shaking (250 rpm) and 100% methanol was added every 24 h to a final concentration

of 0.5% (v/v). At various time points, 100 μL aliquots were taken from the culture and replaced with an equal amount of fresh BMMY medium. Supernatant and cell pellet samples were centrifuged and stored separately at −80°C for later analyses.

Recombinant Protegrin Production in a Bioreactor

Pichia pastoris expressing recombinant ProPG-1, Cath, and PG-1were grown independently in a 3-L BioFlo 115 Benchtop Bioreactor (New Brunswick Scientific, CA, United States). Fermentation was carried out in a total volume of 1 L basal salt medium (BSM) (Stratton et al., 1998) with modifications. *Pichia* trace minerals 1 (PTM1) solution was prepared with (g/L) $CuSO_4 \cdot 5H_2O$ (6.0), NaI (0.08), $MnSO_4 \cdot H_2O$ (3.0), $Na_2MoO_4 \cdot 2H_2O$ (0.2), H_3BO_3 (0.02), $CoCl_2$ (0.5), $ZnCl_2$ (7.0), $FeSO_4 \cdot 7H_2O$ (65.0), biotin (0.2), and 5 mL of concentrated H_2SO_4. A 100 mL recombinant *P. pastoris* inoculum prepared in YPD (OD at 600 = 15 ± 1.3) was transferred to the sterilized bioreactor containing 1 L of BSM. Antifoam A (Sigma, St. Louis, MO, United States) was added manually to control foaming in the bioreactor, if needed. Temperature was maintained at 30°C and pH at 5.6 using 12.5% (v/v) NH_4OH. Aeration rate of 5 L min^{-1} was constant throughout the fermentation. The stirrer speed was controlled between 250 and 700 rpm aiming at dissolved oxygen (DO) concentration of 20% air saturation. After ∼24 h of fermentation, consumption of glycerol was indicated by an increase in DO concentration at an OD of 30 ± 2.1, a glycerol feed [50% (v/v) glycerol containing PTM1 (12 mL/L glycerol)] was then maintained for another12 h at 15 mL/L/h. After completion of the glycerol feeding OD reaches to 170 ± 14.6. This was followed by a methanol feed [100% methanol containing PTM1 (12 mL/L methanol)] and maintained at a constant rate of 3 mL/L/h. The OD of the culture medium after 24 of methanol induction was 288 ± 19.4, the fermentation was stopped and culture medium was centrifuged (10,000 rpm, 10 min, 4°C) to obtain cell free supernatant and stored at −80°C for further analyses.

Protein Sample Preparation

Standard lyophilized PG-1 was synthesized at approximately 95% purity (EZbiolabs, Carmel, IN, United States) and was dissolved in and diluted to 200 μg/mL with filter-sterilized acidified water (0.01% acetic acid) supplemented with 0.1% bovine serum albumin (BSA) (Sigma, St. Louis, MO, United States) to reduce non-specific adsorption of PG-1 to plastic ware. Standard PG-1 was stored at −80°C. Pro-form PG-1 expressed by *P. pastoris* in the supernatant was dialyzed against 25 mMTris-Cl (pH 7.0) and concentrated 60-foldby ultracentrifugation with a 10 kDa cut-off (Millipore Inc., Burlington, MA, United States). Ultracentrifugation retentate and supernatant was filter sterilized and stored at −80°C prior to antimicrobial assay. EK at 0.8 U and 2.5 U (GenScript, Piscataway, NJ, United States) was used to cleave 5 μL of pro-form PG-1 overnight (final 10 μL reaction volume) to release the mature PG-1 from the cathelin domain according to manufacturer's instruction for subsequent antimicrobial activity assay.

Two-Stage Radial Diffusion Assay

The antimicrobial activity of recombinant pro-form PG-1 and cleaved pro-form PG-1 were tested by a two-stage radial diffusion assay as previously described by (Steinberg and Lehrer, 1997) against *E. coli* and methicillin-resistant *Staphylococcus aureus* (MRSA). Positive control sample wells received 10 μL of serially diluted chemically synthesized standard PG-1 or its vehicle as a control. Sample wells received 10 μL of pro-form PG-1 containing 0.01% acetic acid and 0.1% BSA after EK digestion. Minimum inhibition concentration (MIC) was defined at a concentration of PG-1 that resulted in a clear inhibition zone around the well. To test whether BMMY can inhibit PG-1 antimicrobial activity, 5 μL pro-form PG-1 after the 2.5 U EK digestion reaction was resuspended with 5 μL of spent BMMY medium and the mixture was used to inoculate sample well.

Antimicrobial Activity Assay Using Colony-Count Method

The MIC of rPG-1 against *E. coli* was tested according to the antimicrobial assay previously described (Pizzo et al., 2015) with slight modification. The stability of rPG-1 was monitored at different pH (2–11) and temperature (25–95°C) conditions after a preincubation time of 30 min before being assayed. Briefly, overnight grown *E. coli* in LB medium was diluted to an OD 600 of 1 and further diluted 1:100. *E. coli*- peptide mixtures were prepared by adding 40 μL of bacterial cells to different concentration of rPG-1 (1–10 μg/mL) in separate eppendorf tubes and adjusted to a final volume of 1 mL using 20 mM acetate buffer (pH 5). Cells without rPG-1 and with 0.05 mg/mL ampicillin were taken as negative and positive controls, respectively. Experimental and control tubes were incubated for 4 h at 37°C, and 50 μL of the diluted (1:100) mixtures were plated on LB agar media and incubated at 37°C overnight for colony counts. The survived cells in each plate were compared with controls. All concentrations of rPG-1 at different pH and temperature were tested in triplicate experiments and <5% standard deviation were observed for each experiment.

Western Blot

Culture supernatants were subjected to 12% SDS-PAGE and electrophorectically transferred to 0.45 μm pore size PVDF membrane (Millipore Inc., Burlington, CA, United States). The membrane was blocked in 5% (w/v) skim milk in TBST buffer (0.3% Tris, 0.8% NaCl, 0.02% KCl, 0.1% Tween 20) for 1 h and then incubated with affinity purified polyclonal rabbit anti-PG-1 antibody at 1:500 dilution, synthesized from Biomatik (Cambridge, ON, Canada) overnight at 4°C. After washing the membrane three times at 5 min each in TBST, the membrane was incubated with anti-rabbit IgG secondary antibody (1:1000 dilution) conjugated to horseradish peroxidase (Cell Signaling, Danvers, MA, United States) for 1 h at room temperature. Bands were visualized using an ECL Plus Western blotting system according to manufacturer's instruction (Amersham Biosciences, Piscataway, NJ, United States).

In vitro Cell Proliferation Assay

IPEC-J2 cells were grown in six-well plates (Corning, Corning, NY, United States) until 50% confluent in medium consisting of DMEM F-12 containing 5% fetal bovine serum at 37°C in 5% CO_2 and were then serum starved for 24 h. The cells were then incubated with serum-free DMEM F-12 in the presence of 10 μL filter-sterilized fermentation supernatant from 24 h MeOH induced cultures from PP-ProPG-1, PP-Cath, PP-PG-1 and PP-wild type (PP-WT), and cultured for 24 h. Cells were then trypsinized and enumerated using a hemocytometer.

Transwell Assay

To analyze migration of IPEC-J2 cells, 8-micron pore sized Millicell Cell culture transwell inserts (Millipore Inc., Burlington, CA, United States) were used. A total of 1×10^5 cells were plated in the upper inserts and the lower chamber contained serum-free DMEM F-12 in the presence of 10 μL filter-sterilized fermentation supernatant from 24 h MeOH induced cultures from PP-ProPG-1, PP-Cath, PP-PG-1, and PP-WT. After incubation for 16 h, the cells were fixed with 4% (w/v) paraformaldehyde. Cells that did not migrate into the membrane were gently scraped off the upper surface of the transwell with a cotton swab. Migration was quantified by cell enumeration through Hoechst 33342 staining of cell nuclei (Life Technologies, Grand Island, NY, United States).

Statistical Analysis

Results are expressed as mean ± SEM (standard error mean) from at least three independent experiments. The data were analyzed by two-factor analysis of variance (ANOVA) using a GraphPad Prism software version 5.0. Data sets were analyzed by Tukey's test for multiple comparisons to determine statistical differences between groups. The results were considered significant at a P value of <0.05.

RESULTS

Generation of *P. pastoris* Expressing Recombinant ProPG-1, Cath and PG-1

To generate *P. pastoris* that could express recombinant ProPG-1 (rProPG-1), Cath (rCath), and PG-1 (rPG-1), the cDNA sequence of codon-optimized porcine protegrin ProPG-1, Cath, and PG-1 were ligated into the respective pJexpress *P. pastoris* expression vector, respectively. The α-mating factor secretion signal sequence was placed at the N-terminal (**Figure 1A**) to facilitate secretion of the expressed recombinant proteins into the culture fermentation medium, also referred to as supernatant. In our study, we replaced the native elastase cleavage site of preform-protegrin with an EK site. The addition of the EK cleavage site can permit the potential application of recombinant PG-1 in animal feed, as EK is a serine protease and is naturally produced and secreted in the intestinal duodenum (Baratti et al., 1973; Fonseca and Light, 1983).

The DNA sequence-verified recombinant plasmids were linearized with *Swa*I and transformed into electrocompetent *P. pastoris* X-33. Transformants harboring the pJexpress-ProPG-1, pJexpress-Cath and pJexpress-PG-1 constructs are here on referred to as PP-ProPG-1, PP-Cath, and PP-PG-1, respectively. To confirm integration of the construct into the *Pichia* genome, isolated genomic DNA from clones were analyzed by PCR using the 5′*AOX1* primer paired with 3′*AOX1*-TT (**Figure 1B**). PCR results showed chromosomal integration of the expression cassette resulting in a 760 bp, 458 bp, and 700 bp PCR product for positive PP-ProPG-1, PP-PG-1, and PP-Cath transformants, respectively. Mut^+ strains had a 2.2 kb PCR product corresponding to the intact *AOX1* gene. Mut^s strains do not have a 2.2 kb PCR product and only a PCR product corresponding to the *AOX1* and insert part of the expression construct (**Figures 1C,D**).

Effect of Copy Number on Recombinant Protegrin Expression

To employ the expression potential of the *P. pastoris* system, we examined the influence of gene copy number on the expression of rProPG-1, rCath, and rPG-1 from PP-ProPG-1, PP-Cath, and PP-PG-1, respectively. Clones with putative multiple copies of the rProPG, rCath, and rPG1 expression cassette from varying concentrations of G418 antibiotic selection were selected for copy number determination by qPCR. The purpose was to examine the effects of copy number on rProPG-1, rCath, and rPG-1 expression. Clones containing 1–14 copies of the rProPG-1 expression cassette were analyzed for the expression rProPG-1 under shake-flask conditions. As shown in **Table 1**, rProPG-1 expression level increased progressively as the copy number increased from 1 to 7, with seven copies resulting in earlier and highest expression of rProPG-1 at 24 h post-induction. As the number of copies increased from 7 to 11, the expression level did not further increase. However, 14 copies of the cassette yielded higher expression level than 11 copies, but 14 copies of the cassette yielded lower rProPG-1 than in the clone with seven copies at 24 h methanol induction. This indicates a potential maximal limit number of copies that can have a direct influence on rProPG-1 expression level. Similarly, rCath expressed by PP-Cath increased progressively from one copy to six, and decreased at eight copies (**Table 2**). PP-Cath transformant with six copies yielded the highest rCath (**Figure 2A**). Furthermore, gene copy number from 2 to 11 were evaluated in PP-PG-1 clones and clones with six and eight copies yielded highest

TABLE 1 | Expression cassette copy number and rProPG-1 expression level.

PP-ProPG-1 clone	rProPG-1 (24 h)	rProPG-1 (72 h)	Copy #
Pro4	–	+	11
Pro22	+	+++	14
Pro44	++	+++	7
Pro50	–	–	1

Supernatant samples at 24 and 72 h methanol induction from small-scale fermentations of different PP-ProPG-1 clones were assessed for rProPG-1 expression. (–) indicates no rProPG-1 was detected and (+), (++), (+++) indicate low, medium and high levels of rProPG-1 detected using dot blot analysis, respectively.

TABLE 2 | Expression cassette copy number and rCath expression level.

PP-Cath clone	rCath expression level	Copy #
C1	++	2
C2	++	4
C3	+	1
C4	++	3
C5	+++	6
C6	++	8

Supernatant samples at 24 and 72 h methanol induction from small-scale fermentations of different PP-Cath clones were assessed for rCath expression. (+), (++), (+++) indicate low, medium and high levels of rCath detected using dot blot analysis, respectively.

rPG-1 activity (**Figure 2B**, **Table 3**). Progressive increase in rPG-1 was observed as copy number increased up to eight and appeared to decrease at eleven copies. Interestingly, two clones both with six copies of rPG-1 construct expressed at different levels (**Table 3**), suggesting other factors, in addition to gene copy number, can influence recombinant protein expression level in *P. pastoris*.

Pichia pastoris Recombinant Protegrin Expression in a Bioreactor

To potentially obtain increased yield of recombinant protegrin, high-density fermentation was performed in a 3-L bioreactor. Initially, the transition from shake-flask culturing to a bioreactor unexpectedly yielded much lower recombinant protein concentrations using the standard media composition (Invitrogen manual, Carlsbad, CA, United States). By reducing BSM concentration by 50% during culture media optimization, expression level increased. For rPG-1 expression, rPG-1 was not detected until yeast extract and peptone were added to the BSM. These improvements suggest that the media formulation could be optimized to improve the yield.

Expression with all the three recombinant *P. pastoris* strains was performed using three-step procedures, including glycerol-batch phase, glycerol fed-batch and methanol induction phase. The DO spike was found to be an effective indicator to initiate a new feeding profile and to monitor the overall health of the culture for successful recombinant protegrin expression. Aliquots of the fermentation supernatant were examined by Western blot and ELISA. Highest level of rPG-1 (104 ± 11 μg/mL) was

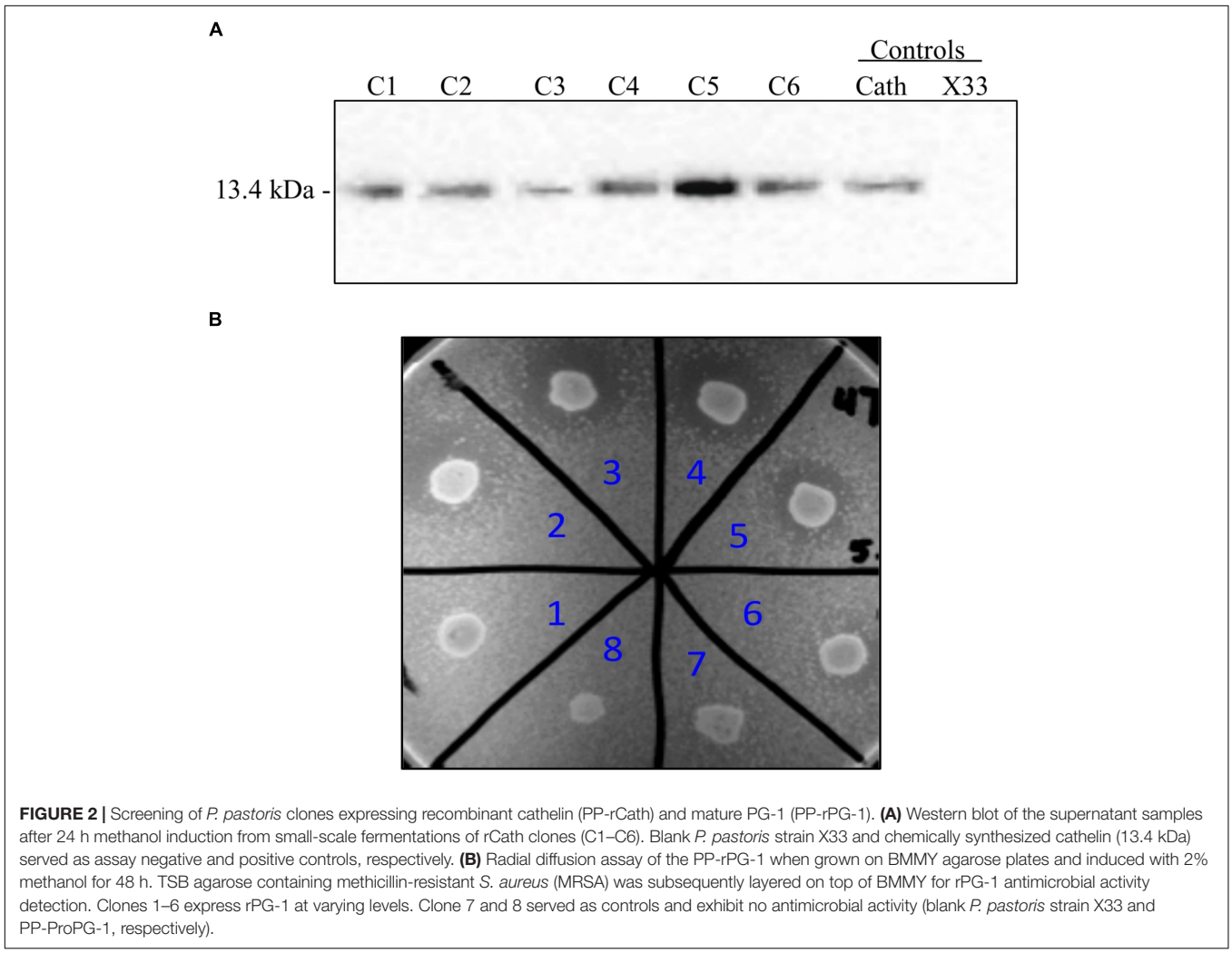

FIGURE 2 | Screening of *P. pastoris* clones expressing recombinant cathelin (PP-rCath) and mature PG-1 (PP-rPG-1). **(A)** Western blot of the supernatant samples after 24 h methanol induction from small-scale fermentations of rCath clones (C1–C6). Blank *P. pastoris* strain X33 and chemically synthesized cathelin (13.4 kDa) served as assay negative and positive controls, respectively. **(B)** Radial diffusion assay of the PP-rPG-1 when grown on BMMY agarose plates and induced with 2% methanol for 48 h. TSB agarose containing methicillin-resistant *S. aureus* (MRSA) was subsequently layered on top of BMMY for rPG-1 antimicrobial activity detection. Clones 1–6 express rPG-1 at varying levels. Clone 7 and 8 served as controls and exhibit no antimicrobial activity (blank *P. pastoris* strain X33 and PP-ProPG-1, respectively).

TABLE 3 | Expression cassette copy number and rPG-1 activity level.

PP-PG-1 clone	rPG-1 antimicrobial activity	Copy #
1	–	2
2	+	6
3	+++	6
4	+++	8
5	++	11
6	+	4

rPG-1 antimicrobial activity level correlates with amount of rPG1 produced. PP-PG-1 clones were assessed for antimicrobial activity against MRSA. (–) indicates no rPG-1 activity was detected and in the others, the activities of rPG-1 are indicated as + (clear zone 0.5–1.5 mm), ++ (clear zone 1.5–2.5 mm), and +++ (clear zone > 2.5 mm).

detected at 24 h of methanol induction in the fermentation culture medium. Post 24 h, rPG-1concentration decreased (**Figure 3A**). Similar to rPG-1, 0.8 ± 0.10 g/L rProPG-1, and 0.2 ± 0.02 rCath g/L was detected in fermentation culture medium at 24 h of methanol induction (**Figures 3B–D**).

Enterokinase Cleavage of rProPG-1 and Antimicrobial Activity

To determine whether the rProPG-1 could yield antimicrobial activity upon removal of the N-terminus pro- domain, EK was used to cleave the introduced amino acid DDDDK site on rProPG-1 (**Table 4**). Cleavage of rProPG-1 was detected by Western blot using antibodies specific to mature PG-1 in the C-terminal domain. EK successfully cleaved rProPG-1 as the detection of mature PG-1 decreased from 13.4 kDa to 2.1 kDa, indicating the removal of the 11 kDa pro- domain (**Figure 4A**). The resulting cleaved rProPG-1 also conferred antimicrobial activity against *E. coli* DH5αat the same level as chemically synthesized PG-1 (**Figure 4B** and **Table 5**). The uncleaved rProPG-1 and rCath did not exhibit antimicrobial activity as expected.

Protegrin Peptide Properties and Boman Index

Peptide properties such as molecular weight, pI value, net charge and Boman Index can be used to predict a peptide's antimicrobial potential under various conditions (Boman, 2003). rProPG, rCath, and rPG-1 were calculated using both Innovagen's Peptide Property Calculator and a predictive tool available at AMP Database v2.34, respectively. The rPG-1 showed highly basic pI value (>10), positive net charge (+6), and high Boman index (>2.5; **Table 4**). The peptides containing the cathelin domain, rProPG-1, and rCath, have pI values of 6.49 and 4.6, respectively. ProPG is neutral at pH 7.0 (net charge −0.3) and Cath has a negative net charge (−6.2). Both of these peptides share similar

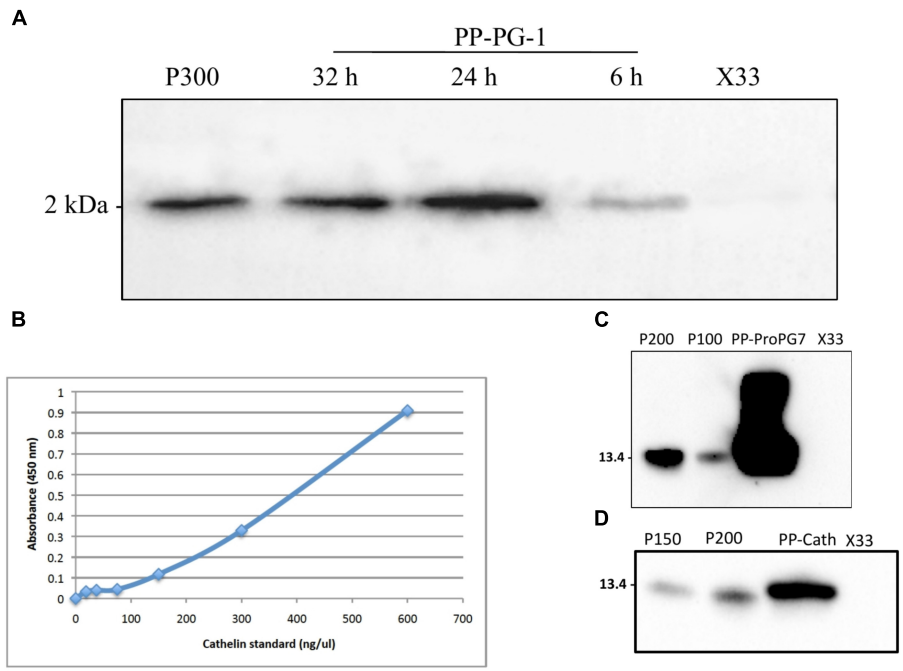

FIGURE 3 | Quantification of rPro-PG-1, rCath, and rPG-1 produced by *P. pastoris* in separate bioreactor. **(A)** rPG-1 (from PP-PG-1) was detected with antibody against pig PG-1 in Western blot. Blank *P. pastoris* strain X33 and 300 ng of chemically synthesized rPG-1 served as assay negative and positive controls, respectively. **(B)** Indirect-HRP ELISA standard curve. Antibody detecting the cathelin domain of ProPG-1 and cathelin was used as the primary antibody. Cathelin peptide was used to generate the standard curve. **(C)** Recombinant ProPG-1 (from PP-ProPG-7) was detected with antibody against pig PG-1 in Western blot. 200 ng and 100 ng of chemically synthesized ProPG-1 served as positive controls (P200 and P100, respectively). **(D)** Recombinant cathelin (from PP-Cath) was detected with antibody against pig cathelin in Western blot. 200 ng and 150 ng of chemically synthesized cathelin served as positive controls (P200 and P150, respectively). Empty *P. pastoris* X33 strain served as a negative control.

TABLE 4 | Summary of protegrin peptide properties.

Peptide	Amino acid sequence	Size (kDa)	pI value	Net charge (at pH 7.0)	Boman Index (kcal/mol)
Proform PG-1 (rProPG-1)	Q ALSYREAVLR AVDRLNEQSS EANLYRLLEL DQPPKADEDP GTPKPVSFTV KETVCPRPTR QPPELCDFKE NGRVKQCVGT VTLDQIKDPL DITCN **DDDDK*** RGGRLCYCRR RFCVCVGR	13.4	6.49	−0.3	2.9
Cathelin PG-1 (rCath)	Q ALSYREAVLR AVDRLNEQSS EANLYRLLEL DQPPKADEDP GTPKPVSFTV KETVCPRPTR QPPELCDFKE NGRVKQCVGT VTLDQIKDPL DITCN **DDDDK***	11.3	4.6	−6.2	2.8
PG-1 (rPG-1)	RGGRLCYCRR RFCVCVGR	2.1	10.7	+6	3.65

Size, pI value, net charges were calculated by Innovagen's Peptide Property Calculator. Boman index was calculated by the predictive tool available at Antimicrobial Peptide Database v2.34. Native elastase site was replaced by enterokinase cleavage site (DDDDK).*

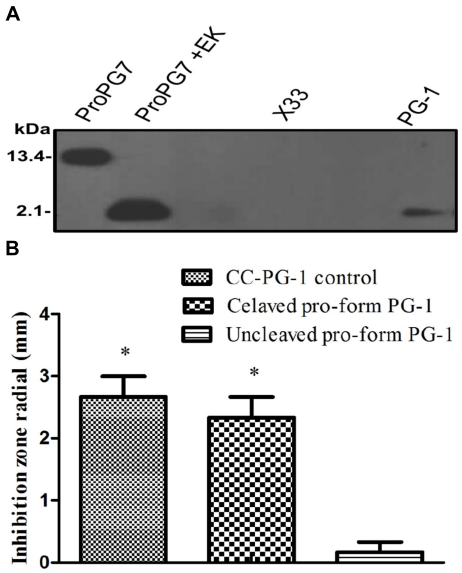

FIGURE 4 | Detection and activity of rProPG after enterokinase (EK) cleavage. **(A)** Recombinant ProPG (ProPG7) and EK cleaved ProPG (ProPG7 + EK), yielding mature peptide (PG-1), was detected with antibody against pig PG-1 in Western blot. Blank *P. pastoris* strain X33 and chemically synthesized PG-1 (CC-PG-1) served as negative and positive controls, respectively. **(B)** Upon EK digestion, rProPG-1 exhibit antimicrobial activity against *E. coli* in radial diffusion antimicrobial activity assay. Data shown is the mean ± SEM of three repeats for inhibitory zones of CC-PG-1 control (I), cleaved pro-form PG-1 (II) and uncleaved pro-form PG-1 (III). Asterisk (*$p < 0.05$) denotes significant difference from uncleaved pro-form PG-1.

Boman Index (2.8–2.9). A high Boman Index in rProPG-1, rCath, and rPG-1 can indicate the potential of these peptides to interact with other proteins *in vivo*.

Enhanced Cell Migration by PG-1 in Its Pro-, Cathelin-, and Mature- Form

We next sought to examine the effect of protegrin on modulating cell proliferation and migration *in vitro* using transwell cell migration assays with IPEC-J2 cells, a cell line derived from porcine intestine epithelium. As shown in **Figure 5A**, cell migration in groups treated with recombinant proform PG-1 (rProPG-1), pro-piece cathelin domain (rCath), and mature PG-1 (rPG-1) was enhanced. Migrated cell count analysis revealed that there was a two-fold (rPro-PG-1), 2.3-fold (rCath), and 2.5-fold (rPG-1) increase in cell migration when compared to the untreated negative control ($p < 0.05$, **Figure 5B**). To study if these peptides (rProPG-1, rCath, and rPG-1) can increase cell proliferation, cell counting proliferation assay was performed. In comparison to the untreated control, groups treated with the peptides resulted in no significant change in cell proliferation (data not shown).

TABLE 5 | Minimum inhibitory concentration (MIC) values of the resulting mature PG-1 cleaved from rProPG-1 after enterokinase (EK) digestion, and rPG-1 expresses by PP-PG-1.

Microorganism	MIC (μg/mL)		
	Control[a]	PG-1[b]	rPG-1[c]
E. coli	2	2	2
MRSA	5	10	8

[a] Chemically synthesized mature PG-1 (CC-PG-1); [b]PG-1 cleaved from rProPG-1 after EK digestion; [c]rPG-1 expressed by PP-PG-1.
MRSA: Methylene-resistant Staphylococcus aureus.

Antimicrobial Activity of rPG-1 and Its Stability at Various pH and Temperature

The minimum inhibitory concentration (MIC) values of the resulting mature peptide (rPG-1) expressed by PP-PG-1 was determined by a two-stage radial diffusion assay. The lowest concentration of the rPG-1 that inhibited the visible growth of *E. coli* and MRSA after overnight incubation is the MIC (**Table 6**). rPG-1 conferred similar antimicrobial activity against *E. coli* at the same level as chemically synthesized PG-1 (CS-PG-1). The MIC value for rPG-1 expressed by PP-rPG-1 against MRSA is 37.5% lower than the CS-PG-1 at 8 μg/mL versus 5 μg/mL, respectively (**Table 5**). Differences in MIC may be attributed to differences in quantification methods of the chemically synthesized and recombinant peptides (e.g., empirical weighing

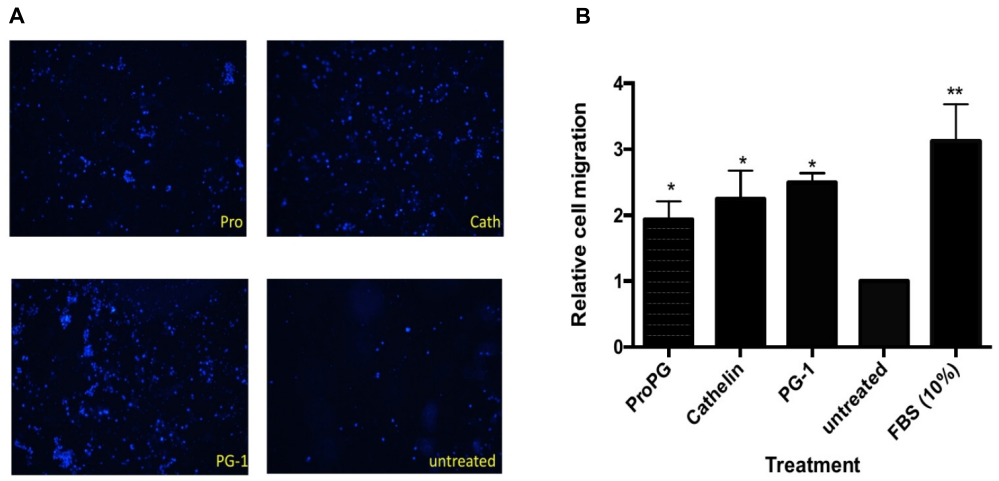

FIGURE 5 | Effect of proform PG-1, cathelin domain and mature PG-1 on cell migration. **(A)** Representative images of transwell migrated IPEC-J2 cells stained with Hoechst 33342. **(B)** Quantification of cell migration from transwell migration assay. Bars represent the mean ± SEM of three experiments. Asterisk * ($p < 0.05$) and ** ($p < 0.01$) denote significant difference from untreated control group.

TABLE 6 | Stability of the rPG-1 at different pH and temperature in terms of MIC against *E. coli* after a pre-incubation time of 30 min, antimicrobial activity assay using colony count method was performed to determine the antimicrobial activity.

Parameters	pH/temperature	MIC (μg/mL)
pH	2	2.5
	4	2.5
	6	2
	11	2.5
Temperature (°C)	25	2
	50	2
	80	2
	95	2.5

versus western blot densitometry). Various pH and temperature conditions were used to investigate the stability of rPG-1 after an incubation time of 30 min. As shown in **Table 6**, rPG1 retained potent activity in both acidic and alkaline (pH 2.0, 4.0, 6.0, and 11.0), and temperature conditions (25–80°C). Antimicrobial activity was quite stable over a pH range of 2.0–11.0, although the MIC at a higher temperature (90°C) increased by 25% compared to the MIC observed at 25°C.

DISCUSSION

The use of *P. pastoris* as an expression system has numerous advantages such as rapid and high-density growth in defined and relatively inexpensive media, high recombinant protein yield, and post-translational modification abilities similar to that of mammalian cells. *P. pastoris* also secrete a low number of endogenous proteins, making downstream protein recovery and purification more feasible. AMPs that have been expressed by *P. pastoris* such as hPAB-β, Ch-penaeidin, MP1102 (Li et al., 2005; Chen et al., 2011; Zhang et al., 2015) are driven by the *AOX* promoter system. These studies indicate methylotrophic yeast-inducible system is suitable for high-level expression of active AMPs. Pro-healing and immune-modulating aspect of cathelicidin AMPs are primarily based on the human and mouse cathelicidin AMP. In our work, we investigated the feasibility of expressing recombinant PG-1 in its pro-, cathelin-, and mature-form in *P. pastoris* and characterized their antimicrobial activity *in vitro*. We then examined the effect of recombinant PG-1 in its various forms on cell migration and proliferation *in vitro*. To our knowledge, our finding is the first report on the role of PG-1 on cell migration and thus tissue repair potential. Interestingly, a recent report showed an increased expression of porcine β-Defensin2 (PBD2), pBD3, pBD114, pBD129, and protegrins (PG) 1-5 in IPEC-J2 cells when exposed to a host defense peptide (HDP)- synthesizing *Lactobacillus reuteri* I5007 (Liu et al., 2017). Similarly, butyrate and its analogs showed induction of porcine HDP gene expression with approximately 20-, 45-, 60-, and 80-fold induction was observed for pBD2, PG1-5, pEP2C, and pBD3, respectively, using IPEC-J2 intestinal epithelial cells (Zeng et al., 2013). These findings together with our findings on the PG-1 tissue damage healing potential suggest that PG-1 may be one of the components of innate defense during infection.

To investigate the feasibility of producing rProPG-1, rCath, and rPG-1 for downstream studies and application, we constructed plasmids for the expression and secretion of these three peptides in *P. pastoris*. Stable clones were generated via integration of the constructs into the *P. pastoris* genome. This will also eliminate the need for constant selective pressure during fermentation. With integration, it is possible to generate strains harboring more than one copy of the introduced expression cassette via repeated single crossover DNA recombinant events (Clare et al., 1991a; Nordén et al., 2011). Insertion of multiple recombinant gene copies is often desired to enhance recombinant protein yield, as low transcript levels can be a limiting factor in protein production (Nordén et al., 2011). To increase the

number of integrated expression cassettes, we initially attempted to construct a known number of concatemers of the expression cassette prior to transformation into *P. pastoris*, similar to Mansur et al. (2005). We found the stable generation of long concatemers of the expression construct difficult to achieve. Instead, we then enriched for strains with an increased number of vector copies by plating transformants on medium containing increasing levels of the selection drug (e.g., G418), where higher drug resistant clones can correlate with higher gene dosage (Nordén et al., 2011). Clones with putative multiple copies of the rProPG-1, rCath, and rPG-1 expression cassette from varying concentrations of G418 antibiotic selection were then selected to evaluate recombinant protein expression levels. Although it was evident that there is a positive correlation between gene dosage level and level of expression (**Tables 1–3**), an upper limit of gene dosage was observed. This bell-shaped correlation curve between gene copy number and protein yield has been reported in *P. pastoris*, where production and secretion level gradually decline with increased gene dosage (Zhu et al., 2009). This upper limit of gene dosage has been suggested to be related to endoplasmic reticulum (ER) stress with the accumulation of recombinant protein within the ERs, also further indicating there may be other bottleneck factors limiting recombinant protein production in addition to gene dosage.

To potentially obtain increased yield of recombinant protegrin (rProPG-1, rCath, and rPG-1), high-density fermentation was also performed. Recombinant protein was detected upon modification of the bioreactor BSM by reducing salt concentrations by 50% (BSM50). It has been reported that high salt concentration can increase cell death, possibly caused by high osmotic pressure in the medium (Brady et al., 2001; Jahic et al., 2006). Upon cell lysis, the secreted recombinant protein can undergo proteolysis as cellular proteases are released into the culture medium. The addition of casamino acids, yeast extract and peptone can help address the issue of protein degradation during the cultivation process (Jahic et al., 2003). During rPG-1 expression by PP-PG-1, rPG-1 was not detected until yeast extract and peptone was added to the BSM50 culture medium, suggesting modification of media formulation can improve yield. The yeast extract, peptone and casamino acids may serve as preferential substrates for proteolytic enzymes, thereby decreasing degradation of the expressed recombinant protein of interest (Clare et al., 1991b; Jafari et al., 2011). Interestingly, the addition of these substrates to the medium was more critical in PP-PG-1 fermentation than PP-ProPG-1 and PP-Cath. This could be due to the peptide properties of rPG-1 toxicity against the *P. pastoris* host cells. These substrates can potentially bind or interact with rPG-1 to limit its toxicity against *P. pastoris*. Components of microbial growth medium have been shown to exhibit binding activity to metal ions (Ramamoorthy and Kushner, 1975) and may also affect recombinant protein folding by modulating the expression of chaperone proteins (Rosano and Ceccarelli, 2014). Furthermore, fermentation medium composition can influence the physio-chemical surface properties of microbes. Microbial cell wall protein composition can differ when cultured in medium with and without peptone and yeast extract (Schär-Zammaretti et al., 2005). The expression level of rPG-1 (104 $\pm$ 11 mg/L) is comparable to other AMPs expressed using the similar *P. pastoris* expression system ranging from 108 mg/L to 292 mg/L (Li et al., 2005; Chen et al., 2011; Zhang et al., 2015). Of the three protegrin peptides expressed, rPG-1 had the lowest yield compared to rProPG-1 and rCath (0.8 $\pm$ 0.10 g/L and 0.2 $\pm$ 0.02 rCath g/L, respectively). The isoelectric point (pI) of a recombinant protein can affect expression level, where high pI is associated with no detectable protein expression (Boettner et al., 2007). This is in line with the high pI value of rPG-1 (10.7; **Table 4**) and the lower expression level obtained. This further suggests pI can be a potential parameter influencing protein expression. Addition of fusion protein tags to aid purification can potentially affect recombinant protein expression level. To increase protein yield in future experiments, the theoretical pI of rPG-1 can be reduced from 10.6 to 8.3 upon the fusion of glutathione S-transferase (GST) tag.

To reduce the likelihood of AMPs exerting their toxicity effect against host cells, fusing AMPs to a foreign or native partner protein can aid in enhancing protein production and reduce proteolytic degradation. In our work, we replaced the native elastase cleavage site of proform protegrin with an EK cleavage site. Antimicrobial activity was not exhibited until cleavage occurred in the presence of EK, releasing the mature and active PG-1 (**Figure 4B**). EK is a serine protease and is naturally produced and secreted in the intestinal duodenum to convert trypsinogen into its active trypsin form for subsequent activation of pancreatic digestive enzymes in pigs (Baratti et al., 1973). The addition of the EK cleavage site can permit rProPG-1 to be cleaved by the endogenous intestinal EK to release the mature antimicrobial PG-1. This allows the potential application of rProPG-1 in animal feed to replace the use of conventional antibiotics that are contributing to the rapid emergence of antibiotic resistant bacteria. Interestingly, while the MIC for both rPG-1 and the EK cleaved rProPG-1 for *E. coli* is the same as that of the chemically synthesized PG-1 control, their MICs (10, and 8 μg/mL for the mature PG-1 cleaved from rProPG-1 and the mature rPG-1, respectively) for MSRA are higher than that of the control (5 μg/mL). Similar MIC results were found using protegrin-1 against *E. coli* (4 μg/mL), and MRSA (4 μg/mL) (Yan and Hancock, 2001). In another report, the MICs of PG-1 against Gram-positive and Gram-negative bacteria range from 0.12 to 2 μg/mL (Steinberg et al., 1997).

A high Boman index value (e.g., 2.50–3.00) can indicate an AMP to be multifunctional within the cell due to its ability to interact with a wide range of proteins (Boman, 2003; Nam et al., 2014). A lower index value ($\leq$1) can suggest that the AMP has low side effects (e.g., low hemolytic activity). Since protegrin, in its pro-, cathelin-, and mature-form, is predicted to interact with other proteins, we sought to examine if these peptides have other functions besides antimicrobial activity. We found pro-, cathelin-, and mature-form PG-1 enhanced cell migration but not cell proliferation (**Figure 5**), suggesting these peptides may interact with cell-surface receptors. It was reported that cathelicidin LL-37 and mCRAMP trans-activated epidermal growth factor receptor (EGFR) (Tokumaru et al., 2005; Yang et al., 2006). Whether PG-1, and its proform and the cathelin domain

have their migration function via activating membrane receptor warrant further investigation.

For therapeutic applications, the stability of the recombinant AMPs produced is important. The stability test results indicated that the rPG-1 retain antimicrobial activity in a wide range of pH conditions ranging from pH 2.0 to 11.0. The pH in wounds ranges from 5.0 to 8.5, which is suitable for rPG-1 use. Oral application of rPG-1 may also be feasible in the digestive tract (pH 3.0 and 4.4 in mouse and pig, respectively). The activity of rPG-1 remained stable over a broad temperature range from 25°C to 95°C. This stability may be due to the high cysteine content (disulfide bonds) in rPG-1 (Lai and Gallo, 2009). In conclusion, recombinant protegrin in its pro-, cathelin-, and mature- forms were successfully expressed in *P. pastoris* using the *AOX* expression system. These peptides exhibit antimicrobial activity as well as cell migration activity. Further *in vivo* studies on the role of PG in modulating intestinal health would be of interest for intestinal inflammation application (Harwig et al., 1996).

AUTHOR CONTRIBUTIONS

EH performed the major experiments and wrote the manuscript. NA performed parts of experiments and helped in writing. JL helped in designing the research, data interpretation and editing.

FUNDING

This project has been funded by Ontario Pork (grant # 051379), Natural Sciences and Engineering Research Council of Canada (NSERC, grant # 400876), and Foshan University (grant # 053385).

SUPPLEMENTARY MATERIAL

The Supplementary Material for this article can be found online at: https://www.frontiersin.org/articles/10.3389/fmicb.2018.02300/full#supplementary-material

REFERENCES

Abad, S., Kitz, K., Hörmann, A., Schreiner, U., Hartner, F. S., and Glieder, A. (2010). Real-time PCR-based determination of gene copy numbers in *Pichia pastoris*. *Biotechnol. J.* 5, 413–420. doi: 10.1002/biot.200900233

Baratti, J., Maroux, S., Louvard, D., and Desnuelle, P. (1973). On porcine enterokinase. Further purification and some molecular properties. *Biochim. Biophys. Acta* 315, 147–161. doi: 10.1016/0005-2744(73)90138-1

Benmoussa, K., Authier, H., Prat, M., AlaEddine, M., Lefèvre, L., Rahabi, M. C., et al. (2017). P17, an original host defense peptide from ant venom. *Front. Immunol.* 8:1650. doi: 10.3389/fimmu.2017.01650

Boettner, M., Steffens, C., von Mering, C., Bork, P., Stahl, U., and Lang, C. (2007). Sequence-based factors influencing the expression of heterologous genes in the yeast *Pichia pastoris*—A comparative view on 79 human genes. *J. Biotechnol.* 130, 1–10. doi: 10.1016/j.jbiotec.2007.02.019

Boman, H. G. (2003). Antibacterial peptides: basic facts and emerging concepts. *J. Intern. Med.* 254, 197–215. doi: 10.1046/j.1365-2796.2003.01228.x

Brady, C. P., Shimp, R. L., Miles, A. P., Whitmore, M., and Stowers, A. W. (2001). High-level production and purification of P30P2MSP119, an important vaccine antigen for Malaria, expressed in the methylotropic yeast *Pichia pastoris*. *Protein Expr. Purif.* 23, 468–475. doi: 10.1006/prep.2001.1526

Chen, Z., Wang, D., Cong, Y., Wang, J., Zhu, J., Yang, J., et al. (2011). Recombinant antimicrobial peptide hPAB-β expressed in *Pichia pastoris*, a potential agent active against methicillin-resistant *Staphylococcus aureus*. *Appl. Microbiol. Biotechnol.* 89, 281–291. doi: 10.1007/s00253-010-2864-0

Choi, K.-Y., Chow, L. N. Y., and Mookherjee, N. (2012). Cationic host defence peptides: multifaceted role in immune modulation and inflammation. *J. Innate Immun.* 4, 361–370. doi: 10.1159/000336630

Ciofalo, V., Barton, N., Kreps, J., Coats, I., and Shanahan, D. (2006). Safety evaluation of a lipase enzyme preparation, expressed in *Pichia pastoris*, intended for use in the degumming of edible vegetable oil. *Regul. Toxicol. Pharmacol.* 45, 1–8. doi: 10.1016/j.yrtph.2006.02.001

Clare, J. J., Rayment, F. B., Ballantine, S. P., Sreekrishna, K., and Romanos, M. A. (1991a). High-level expression of tetanus toxin fragment C in *Pichia pastoris* strains containing multiple tandem integrations of the gene. *Biotechnology* 9, 455–460.

Clare, J. J., Romanes, M. A., Rayment, F. B., Rowedder, J. E., Smith, M. A., Payne, M. M., et al. (1991b). Production of mouse epidermal growth factor in yeast: high-level secretion using *Pichia pastoris* strains containing multiple gene copies. *Gene* 105, 205–212.

de la Fuente-Núñez, C., Mansour, S. C., Wang, Z., Jiang, L., Breidenstein, E. B. M., Elliott, M., et al. (2014). Anti-biofilm and immunomodulatory activities of peptides that inhibit biofilms formed by pathogens isolated from cystic fibrosis patients. *Antibiotics* 3, 509–526. doi: 10.3390/antibiotics3040509

Dias, S. A., Freire, J. M., Pérez-Peinado, C., Domingues, M. M., Gaspar, D., Vale, N., et al. (2017). New potent membrane-targeting antibacterial peptides from viral capsid proteins. *Front. Microbiol.* 8:775. doi: 10.3389/fmicb.2017.00775

Fonseca, P., and Light, A. (1983). The purification and characterization of bovine enterokinase from membrane fragments in the duodenal mucosal fluid. *J. Biol. Chem.* 258, 14516–14520.

Frohm, M., Agerberth, B., Ahangari, G., Ståhle-Bäckdahl, M., Lidén, S., Wigzell, H., et al. (1997). The expression of the gene coding for the antibacterial peptide LL-37 is induced in human keratinocytes during inflammatory disorders. *J. Biol. Chem.* 272, 15258–15263. doi: 10.1074/jbc.272.24.15258

Hancock, R. E. W., and Sahl, H.-G. (2006). Antimicrobial and host-defense peptides as new anti-infective therapeutic strategies. *Nat. Biotechnol.* 24, 1551–1557. doi: 10.1038/nbt1267

Harwig, S. S., Waring, A., Yang, H. J., Cho, Y., Tan, L., and Lehrer, R. I. (1996). Intramolecular disulfide bonds enhance the antimicrobial and lytic activities of protegrins at physiological sodium chloride concentrations. *Eur. J. Biochem.* 240, 352–357. doi: 10.1111/j.1432-1033.1996.0352h.x

Hase, K., Murakami, M., Iimura, M., Cole, S. P., Horibe, Y., Ohtake, T., et al. (2003). Expression of LL-37 by human gastric epithelial cells as a potential host defense mechanism against *Helicobacter pylori*. *Gastroenterology* 125, 1613–1625. doi: 10.1053/j.gastro.2003.08.028

Hirano, T., Ishihara, K., and Hibi, M. (2000). Roles of STAT3 in mediating the cell growth, differentiation and survival signals relayed through the IL-6 family of cytokine receptors. *Oncogene* 19, 2548–2556. doi: 10.1038/sj.onc.1203551

Inaba, Y., Ashida, T., Ito, T., Ishikawa, C., Tanabe, H., Maemoto, A., et al. (2010). Expression of the antimicrobial peptide alpha-defensin/cryptdins in intestinal crypts decreases at the initial phase of intestinal inflammation in a model of inflammatory bowel disease, IL-10-deficient mice. *Inflamm. Bowel Dis.* 16, 1488–1495. doi: 10.1002/ibd.21253

Ishihara, K., and Hirano, T. (2002). IL-6 in autoimmune disease and chronic inflammatory proliferative disease. *Cytokine Growth Factor Rev.* 13, 357–368. doi: 10.1016/S1359-6101(02)00027-8

Jafari, R., Sundström, B. E., and Holm, P. (2011). Optimization of production of the anti-keratin 8 single-chain Fv TS1-218 in *Pichia pastoris* using design of experiments. *Microb. Cell Fact.* 10:34. doi: 10.1186/1475-2859-10-34

Jahic, M., Gustavsson, M., Jansen, A.-K., Martinelle, M., and Enfors, S.-O. (2003). Analysis and control of proteolysis of a fusion protein in *Pichia pastoris* fed-batch processes. *J. Biotechnol.* 102, 45–53. doi: 10.1016/S0168-1656(03)00003-8

Jahic, M., Knoblechner, J., Charoenrat, T., Enfors, S.-O., and Veide, A. (2006). Interfacing *Pichia pastoris* cultivation with expanded bed adsorption. *Biotechnol. Bioeng.* 93, 1040–1049. doi: 10.1002/bit.20811

Kovach, M. A., Ballinger, M. N., Newstead, M. W., Zeng, X., Bhan, U., Yu, F.-S., et al. (2012). Cathelicidin-related antimicrobial peptide is required for effective lung mucosal immunity in Gram-negative bacterial pneumonia. *J. Immunol.* 189, 304–311. doi: 10.4049/jimmunol.1103196

Lai, Y., and Gallo, R. L. (2009). AMPed up immunity: how antimicrobial peptides have multiple roles in immune defense. *Trends Immunol.* 30, 131–141. doi: 10.1016/j.it.2008.12.003

Li, L., Wang, J.-X., Zhao, X.-F., Kang, C.-J., Liu, N., Xiang, J.-H., et al. (2005). High level expression, purification, and characterization of the shrimp antimicrobial peptide. Ch-penaeidin, in *Pichia pastoris*. *Protein Expr. Purif.* 39, 144–151. doi: 10.1016/j.pep.2004.09.006

Liu, H., Hou, C., Wang, G., Jia, H., Yu, H., Zeng, X., et al. (2017). *Lactobacillus reuteri* I5007 modulates intestinal host defense peptide expression in the model of IPEC-J2 cells and neonatal piglets. *Nutrients* 9:E559. doi: 10.3390/nu9060559

Liu, T.-C., and Stappenbeck, T. S. (2016). Genetics and pathogenesis of inflammatory bowel disease. *Annu. Rev. Pathol.* 11, 127–148. doi: 10.1146/annurev-pathol-012615-044152

Livak, K. J., and Schmittgen, T. D. (2001). Analysis of relative gene expression data using real-time quantitative PCR and the 2(-Delta Delta C(T)) Method. *Methods* 25, 402–408. doi: 10.1006/meth.2001.1262

Ma, B., Shen, J., Yindeeyoungyeon, W., and Ruan, Y. (2017). A novel antibiotic mechanism of l-Cyclopropylalanine blocking the biosynthetic pathway of essential amino acid l-leucine. *Molecules* 22:E2224. doi: 10.3390/molecules22122224

Mansur, M., Cabello, C., Hernández, L., País, J., Varas, L., Valdés, J., et al. (2005). Multiple gene copy number enhances insulin precursor secretion in the yeast *Pichia pastoris*. *Biotechnol. Lett.* 27, 339–345. doi: 10.1007/s10529-005-1007-7

Nam, B.-H., Moon, J.-Y., Park, E.-H., Kim, Y.-O., Kim, D.-G., Kong, H. J., et al. (2014). Antimicrobial activity of peptides derived from olive flounder lipopolysaccharide binding protein/bactericidal permeability-increasing protein (LBP/BPI). *Mar. Drugs* 12, 5240–5257. doi: 10.3390/md12105240

Nordén, K., Agemark, M., Danielson, J. ÅH., Alexandersson, E., Kjellbom, P., and Johanson, U. (2011). Increasing gene dosage greatly enhances recombinant expression of aquaporins in *Pichia pastoris*. *BMC Biotechnol.* 11:47. doi: 10.1186/1472-6750-11-47

Pizzo, E., Zanfardino, A., Di Giuseppe, A. M. A., Bosso, A., Landi, N., Ragucci, S., et al. (2015). A new active antimicrobial peptide from PD-L4, a type 1 ribosome inactivating protein ofPhytolacca dioica L.: a new function of RIPs for plant defence?. *FEBS Lett.* 589, 2812–2818. doi: 10.1016/j.febslet.2015.08.018

Proudfoot, A. E. I. (2002). Chemokine receptors: multifaceted therapeutic targets. *Nat. Rev. Immunol.* 2, 106–115. doi: 10.1038/nri722

Ramamoorthy, S., and Kushner, D. J. (1975). Binding of mercuric and other heavy metal ions by microbial growth media. *Microb. Ecol.* 2, 162–176. doi: 10.1007/BF02010436

Rosano, G. L., and Ceccarelli, E. A. (2014). Recombinant protein expression in *Escherichia coli*: advances and challenges. *Front. Microbiol.* 5:172. doi: 10.3389/fmicb.2014.00172

Sang, Y., and Blecha, F. (2008). Antimicrobial peptides and bacteriocins: alternatives to traditional antibiotics. *Anim. Health Res. Rev.* 9, 227–235. doi: 10.1017/S1466252308001497

Schär-Zammaretti, P., Dillmann, M.-L., D'Amico, N., Affolter, M., and Ubbink, J. (2005). Influence of fermentation medium composition on physicochemical surface properties of *Lactobacillus acidophilus*. *Appl. Environ. Microbiol.* 71, 8165–8173. doi: 10.1128/AEM.71.12.8165-8173.2005

Schauber, J., Rieger, D., Weiler, F., Wehkamp, J., Eck, M., Fellermann, K., et al. (2006). Heterogeneous expression of human cathelicidin hCAP18/LL-37 in inflammatory bowel diseases. *Eur. J. Gastroenterol. Hepatol.* 18, 615–621. doi: 10.1097/00042737-200606000-00007

Schmittgen, T. D., and Livak, K. J. (2008). Analyzing real-time PCR data by the comparative CT method. *Nat. Protoc.* 3, 1101–1108. doi: 10.1038/nprot.2008.73

Steinberg, D. A., Hurst, M. A., Fujii, C. A., Kung, A. H., Ho, J. F., Cheng, F. C., et al. (1997). Protegrin-1: a broad-spectrum, rapidly microbicidal peptide with in vivo activity. *Antimicrob. Agents Chemother.* 41, 1738–1742.

Steinberg, D. A., and Lehrer, R. I. (1997). "Designer assays for antimicrobial peptides," in *Antibacterial Peptide Protocols*, ed. W. M. Shafer (Totowa, NJ: Humana Press), 169–186.

Stratton, J., Chiruvolu, V., and Meagher, M. (1998). "High cell-density fermentation," in *Pichia Protocols*, ed. J. M. Cregg (Totowa, NJ: Humana Press), 107–120.

Taghavian, O., Spiegel, H., Hauck, R., Hafez, H. M., Fischer, R., and Schillberg, S. (2013). Protective oral vaccination against infectious bursal disease virus using the major viral antigenic protein VP2 produced in *Pichia pastoris*. *PLoS One* 8:e83210. doi: 10.1371/journal.pone.0083210

Termén, S., Tollin, M., Rodriguez, E., Sveinsdóttir, S. H., Jóhannesson, B., Cederlund, A., et al. (2008). PU.1 and bacterial metabolites regulate the human gene CAMP encoding antimicrobial peptide LL-37 in colon epithelial cells. *Mol. Immunol.* 45, 3947–3955. doi: 10.1016/j.molimm.2008.06.020

Thompson, C. A. (2010). FDA approves kallikrein inhibitor to treat hereditary angioedema. *Am. J. Health Syst. Pharm.* 67:93. doi: 10.2146/news100005

Tokumaru, S., Sayama, K., Shirakata, Y., Komatsuzawa, H., Ouhara, K., Hanakawa, Y., et al. (2005). Induction of keratinocyte migration via transactivation of the epidermal growth factor receptor by the antimicrobial peptide LL-37. *J. Immunol.* 175, 4662–4668. doi: 10.4049/jimmunol.175.7.4662

Yan, H., and Hancock, R. E. (2001). Synergistic interactions between mammalian antimicrobial defense peptides. *Antimicrob. Agents Chemother.* 45, 1558–1560. doi: 10.1128/AAC.45.5.1558-1560.2001

Yang, Y. H., Wu, W. K. K., Tai, E. K. K., Wong, H. P. S., Lam, E. K. Y., So, W. H. L., et al. (2006). The cationic host defense peptide rCRAMP promotes gastric ulcer healing in rats. *J. Pharmacol. Exp. Ther.* 318, 547–554. doi: 10.1124/jpet.106.102467

Zaiou, M., Nizet, V., and Gallo, R. L. (2003). Antimicrobial and protease inhibitory functions of the human cathelicidin (hCAP18/LL-37) prosequence. *J. Invest. Dermatol.* 120, 810–816. doi: 10.1046/j.1523-1747.2003.12132.x

Zeng, X., Sunkara, L. T., Jiang, W., Bible, M., Carter, S., Ma, X., et al. (2013). Induction of porcine host defense peptide gene expression by short-chain fatty acids and their analogs. *PLoS One* 8:e72922. doi: 10.1371/journal.pone.0072922

Zhang, Y., Teng, D., Wang, X., Mao, R., Cao, X., Hu, X., et al. (2015). In vitro and in vivo characterization of a new recombinant antimicrobial peptide, MP1102, against methicillin-resistant *Staphylococcus aureus*. *Appl. Microbiol. Biotechnol.* 99, 6255–6266. doi: 10.1007/s00253-015-6394-7

Zhu, S., Wei, L., Yamasaki, K., and Gallo, R. L. (2008). Activation of cathepsin L by the cathelin-like domain of protegrin-3. *Mol. Immunol.* 45, 2531–2536. doi: 10.1016/j.molimm.2008.01.007

Zhu, T., Guo, M., Tang, Z., Zhang, M., Zhuang, Y., Chu, J., et al. (2009). Efficient generation of multi-copy strains for optimizing secretory expression of porcine insulin precursor in yeast *Pichia pastoris*. *J. Appl. Microbiol.* 107, 954–963. doi: 10.1111/j.1365-2672.2009.04279.x

Conflict of Interest Statement: The authors declare that the research was conducted in the absence of any commercial or financial relationships that could be construed as a potential conflict of interest.

Copyright © 2018 Huynh, Akhtar and Li. This is an open-access article distributed under the terms of the Creative Commons Attribution License (CC BY). The use, distribution or reproduction in other forums is permitted, provided the original author(s) and the copyright owner(s) are credited and that the original publication in this journal is cited, in accordance with accepted academic practice. No use, distribution or reproduction is permitted which does not comply with these terms.

frontiers in Microbiology

ORIGINAL RESEARCH
published: 05 October 2018
doi: 10.3389/fmicb.2018.02329

Bactericidal Property of Oregano Oil Against Multidrug-Resistant Clinical Isolates

Min Lu[1], Tianhong Dai[1], Clinton K. Murray[2] and Mei X. Wu[1]**

[1] Wellman Center for Photomedicine, Massachusetts General Hospital, Harvard Medical School, Boston, MA, United States, [2] First Area Medical Laboratory, JBSA-Fort Sam Houston, Houston, TX, United States

Development of non-antibiotic alternatives to treat infections caused by multidrug-resistant (MDR) microbes represents one of the top priorities in healthcare and community settings, especially in the care of combat trauma-associated wound infections. Here, we investigate efficacy of oregano oil against pathogenic bacteria including MDR isolates from the combat casualties *in vitro* and in a mouse burn model. Oregano oil showed a significant anti-bacterial activity against 11 MDR clinical isolates including four *Acinetobacter baumannii*, three *Pseudomonas aeruginosa*, and four methicillin-resistant *Staphylococcus aureus* (MRSA) obtained from combat casualties and two luminescent strains of PA01 and MRSA USA300, with a MIC ranging from 0.08 mg/ml to 0.64 mg/ml. Oregano oil also effectively eradicated biofilms formed by each of the 13 pathogens above at similar MICs. Transmission electron microscopy (TEM) and scanning electron microscopy (SEM) revealed that oregano oil damaged bacterial cells and altered the morphology of their biofilms. While efficiently inactivating bacteria, there was no evidence of resistance development after up to 20 consecutive passages of representative bacterial strains in the presence of sublethal doses of oregano oil. *In vivo* study using the third-degree burn wounds infected with PA01 or USA300 demonstrated that oregano oil, topically applied 24 h after bacterial inoculation, sufficiently reduced the bacterial load in the wounds by 3 $\log_{10}$ in 1 h, as measured by drastic reduction of bacterial bioluminescence. This bactericidal activity of oregano oil concurred with no significant side effect on the skin histologically or genotoxicity after three topical applications of oregano oil at 10 mg/ml for three consecutive days. The investigation suggests potentials of oregano oil as an alternative to antibiotics for the treatment of wound-associated infections regardless of antibiotic susceptibility.

Keywords: oregano oil, *Pseudomonas aeruginosa*, *Acinetobacter baumannii*, MRSA, biofilms, burn wound, mouse model, bioluminescence imaging

OPEN ACCESS

Edited by:
Noton Kumar Dutta, Johns Hopkins University, United States

Reviewed by:
Nagendran Tharmalingam, Brown University, United States
Sougata Ghosh, RK University, India

***Correspondence:**
Tianhong Dai
TDAI@mgh.harvard.edu
Mei X. Wu
MWU5@mgh.harvard.edu

Specialty section:
This article was submitted to Antimicrobials, Resistance and Chemotherapy, a section of the journal Frontiers in Microbiology

Received: *30 March 2018*
Accepted: *11 September 2018*
Published: *05 October 2018*

Citation:
Lu M, Dai T, Murray CK and Wu MX (2018) Bactericidal Property of Oregano Oil Against Multidrug-Resistant Clinical Isolates. Front. Microbiol. 9:2329. doi: 10.3389/fmicb.2018.02329

INTRODUCTION

Skin wound infection is a widespread problem in both civilian and military healthcare settings. Skin wounds are particularly prone to bacterial infections because the wounds provide an ideal medium for bacterial proliferation and a portal of entry into the bloodstream and are direct exposure to the "dirty" environment. The infections can be readily treated with a variety of antibiotics if the bacteria involved are susceptible. However, there are only extremely limited or no treatment options when

antibiotic resistant strains are involved in the wound infections, which occurs at a worrying speed. If the wound infection cannot be eliminated in a timely fashion, the infection would alter cellular metabolisms and induce persistent inflammation systemically that can predispose the patients to various complications and life-threatening sepsis (Fitzwater et al., 2003; Wang et al., 2018). For instance, burn wound infection outbreaks caused by multidrug-resistant (MDR) organisms emerged as a serious problem early in the course of Iraq military operations despite that the United States military has provided rapid and highly effective care for wounded soldiers (Scott et al., 2007; Vento et al., 2013). As a matter of fact, skin infections caused by MDR bacteria are the most common cause of morbidity and mortality in patients infected with MDR microbes and represent almost 61% of deaths of this infected population (Gomez et al., 2009).

Extensive uses of broad spectrum antibiotics are the single most important factor in evolution of bacterial resistance (Hampton, 2013). A number of studies have shown that the most frequently identified MDR strains of bacteria in nosocomial infections and on the battlefield are Gram-negative bacteria *Acinetobacter baumannii* and *Pseudomonas aeruginosa*, and Gram-positive bacterium methicillin-resistant *Staphylococcus aureus* (MRSA) (Scott et al., 2007; Calhoun et al., 2008; Li et al., 2014; Levin-Reisman et al., 2017). In addition, bacterial biofilms formed by MDR bacteria are the major obstacles in treatment of burn wounds (Bloemsma et al., 2008; Jiang et al., 2017). Bacteria within biofilms can be as much as 1,000 times more resistant to antibiotics and are responsible for recurrent antibiotic-resistant infections elsewhere in the body upon dissemination from the site of the biofilm (Ceri et al., 1999; Caraher et al., 2007). Currently, the only effective treatments available to fight these infections are older drugs like colistin, which are highly toxic and detrimental to the overall health of the patients (Crane et al., 2009). There is a pressing need for the development of non-antibiotic approaches to combat MDR microbes.

Essential oils (EOs) are a mixture of volatile constituents produced by aromatic plant/herbs. There are about 3,000 well-recognized EOs, of which 300 are generally recognized as safe (GRAS) to humans by the United States Food and Drug Administration (U.S. FDA) and have broad applications in food preservation, additives, and favors, perfume, cosmetic industries, antiseptic oral solutions, toothpastes, cleaner, and air fresheners for centuries (Pandey et al., 2017; Sakkas and Papadopoulou, 2017). These natural products are of particular interest as "green" antimicrobial agents because of their low-cost, biocompatibility, potential antibiofilm properties, and friendly to eukaryote cells and environment (Burt, 2004; Nostro et al., 2007; Kavanaugh and Ribbeck, 2012). Among these safe EOs, oregano oil has been shown to have a variety of activities such as antioxidant (Yan et al., 2016), anti-inflammatory (Ocana-Fuentes et al., 2010; Shen et al., 2010), anti-fungal (Akgul and Kivanc, 1988; Soylu et al., 2007), and anti-allergic (Benito et al., 1996). Its antimicrobial effect has been demonstrated *in vitro* cell culture, food systems studies (Lopez-Reyes et al., 2010; Soylu et al., 2010; Munhuweyi et al., 2017), and *in vivo* systemic infections (Manohar et al., 2001; Preuss et al., 2005). In the present study, we investigate effectiveness of oregano oil in inactivation of MDR bacteria isolated from combat casualties *in vitro* and bioluminescent strains of *P. aeruginosa* (PA01) and MRSA (USA300) in mouse burn wounds. Our study showed that oregano oil effectively inactivated various pathogenic bacteria and their biofilms irrespective of their antibiotic susceptibility. The study is the first *in vivo* attempt on the use of oregano oil for the treatment of burn wounds infected with clinically important MDR bacteria.

MATERIALS AND METHODS

Chemical Constituents of Oregano Oil

Oregano oil was purchased from Bulk Apothecary (Aurora, OH, United States) and used throughout the study. To define the constituents of oregano oil, gas chromatography/mass spectrometry (GC-MS) analyses were carried out using an Agilent 6980 GC coupled to an Agilent 5973N MS and a fused-silica capillary column (HP-5MS: 30 m × 0.25 mm i.d., film thickness 0.25 μm). The initial column temperature was set at 60°C for 10 min and then increased at 3°C/min till 220°C. The temperature was held at 220°C for 10 min and raised to 240°C by increments of 1°C/min; the injector port temperature was 250°C with the carrier gas of helium at a flow rate of 0.8 ml/min. Ionization voltage of MS in the EI-mode was 70 eV and ionization source temperature at 250°C with a mass range of 35–465 amu. The volatile components were identified by comparison of their retention indices relative to *n*-alkanes (C6-C28) and mass spectra with those of authentic compounds by means of NIST and Wiley databases and with the Adams library spectra.

Bacterial Strains

The antibacterial activity of oregano oil was tested against a panel of MDR bacteria isolated from combat casualties, including seven Gram-negative strains *A. baumannii* (AF0004, AF0005, IQ0012, and IQ0013) and *P. aeruginosa* (AF0001, IQ0042, and IQ0046), and four Gram-positive MRSA (AF0003, IQ0064, IQ0103, and IQ0211). All the bacterial isolates were obtained from San Antonio Military Medical Center under a Materials Transfer Agreement and demonstrated MDR according to the microbiology tests performed at the United States Army Institute of Surgical Research (**Table 2**). Amongst the *A. baumannii* and *P. aeruginosa* tested, only strains of IQ0012, IQ0013, and IQ0042 were susceptible to imipenem; the rest of strains were resistant to all antibiotics tested. The five MRSA strains were resistant to amikacin, ampicillin, cefazolin, cefoxitin, and erythromycin, but susceptible to gentamicin, levofloxacin, nitrofurantoin, and tetracycline. In addition, luminescent strains of *P. aeruginosa* (PA01) and MRSA USA300 were used in the *in vivo* study, allowing real-time monitoring of infection in the mouse burn wounds *in vivo* via bioluminescence imaging (Dai et al., 2013; Zhang et al., 2014; Wang et al., 2016).

Determinations of Minimum Inhibitory Concentration (MIC)

In order to determine a MIC, a broth microdilution assay was employed as previously described (Joshi et al., 2010; Gao et al., 2011). Stock solution of oregano oil was prepared at 40 mg/ml in DMSO and twofold dilutions (0.04–1.28 mg/ml) of the stock EO in brain heart infusion (BHI) medium were added into 96-well plates for bactericidal tests. In each well, 20 μL of the suspensions containing 10^8 CFU/ml of bacteria was added to 180 μL of the above medium containing oregano oil at varying concentrations. Medium supplemented with a similar amount of DMSO only severed as controls. The microplates were incubated at 37°C for 24 h and examined for bacterial growth. The first well without turbidity was determined as a MIC value. All assays were performed in triplicate.

Antibiofilm Activity

Bacteria were incubated in trypticase soy broth (TSB) with 0.1% glucose at 37°C for 18 h, after which the cultures were harvested by centrifugation and washed twice with PBS. Bacterial suspensions with an optical density of OD_{600} equal to 0.1 in TSB were added to 96-well plates at 100 μL/well, followed by incubation at 37°C under static condition for 24 h to form biofilms. Oregano oil was added at indicated concentrations and incubated with the biofilms for 1 h, after which biofilms were washed twice with PBS and bacterial viability was determined using an Alamar Blue assay. TSB without bacteria was used as a negative control. All experiments were performed in triplicate.

Assessment of Possible Resistance Development to Oregano Oil

To study any potential development of resistance to oregano oil, three representative strains (*A. baumannii* AF0005, *P. aeruginosa* IQ0042, and MRSA IQ0064) were propagated for 20 generations in the presence of sublethal doses of oregano oil as previously described (Li et al., 2014). Briefly, 200-μL aliquots of the bacterial suspensions (10^7 CFU/ml) were inoculated into 96-well plates and exposed to the sub-MIC (2/3 MIC) of oregano oil at 37°C for 1 h, and the resultant bacteria were labeled as the first generation and tested for a MIC as above. The second generation was obtained by exposing the first generation to its sub-MIC for 1 h and determined for its MIC again. The procedure was repeated for up to 20 times. Oregano-resistance was determined by any significant increases in the MIC of successive generations.

Transmission Electron Microscopy (TEM)

To determine bactericidal mechanism of oregano oil, *A. baumannii* AF0005 and *P. aeruginosa* IQ0042 were investigated as the representative strains for oregano-induced ultrastructural damages using transmission electron microscopy (TEM). Bacterial suspensions were fixed in 2.5% glutaraldehyde plus 2% paraformaldehyde overnight at 4°C. Fixed cells were collected by centrifugation at 4,000 × *g* for 5 min and rinsed with 0.1 M sodium cacodylate buffer (pH 7.2) for three times. After the final wash, hot agar was added to each pellet and the cell pellets were post-fixed in 2% osmium tetroxide for 1 h, dehydrated with a graded ethanol series, embedded in fresh Epon, and then polymerized at 60°C for 48 h. Ultra-thin sections were cut on ultramicrotome and collected onto 200 mesh bare copper grids. Samples were stained for 30 min with uranyl acetate and lead citrate and examined with a CM-10 TEM (Philips, Eindhoven, Netherlands).

Scanning Electron Microscopy (SEM)

To investigate the ultrastructural changes of bacterial biofilms caused by oregano oil, scanning electron microscopy (SEM) was performed using the representative strains of *P. aeruginosa* IQ0042 and MRSA IQ0064. Briefly, biofilms of IQ0042 and IQ0064 were grown for 24 h on sterilized squares of ACLAR 33C (Electron Microscopy Sciences, Hatfield, PA, United States), and treated for 1 h with oregano oil at 0.75 mg/ml or 0.3 mg/ml, respectively. Untreated and oregano-treated biofilms were fixed at 4°C for 24 h in 0.1 M sodium cacodylate buffer containing 2.5% glutaraldehyde, 0.15% alcian blue, and 0.15% safranin O. The fixed biofilms were washed with 0.1 M sodium cacodylate buffer, infiltrated with 2% osmium tetroxide for 2 h, and dehydrated to 100% ethanol. The biofilms were dried using a critical-point dryer (Tousimis Research Corporation, Rockville, MD, United States), mounted on specimen stubs, sputter-coated with 10 nm Cressington 208 platinum (Cressington Scientific Instruments, Watford, United Kingdom), and examined on a S4800 SEM (Hitachi Ltd., Tokyo, Japan). Micrographs were acquired under high vacuum using an accelerating voltage of 3.0 kV.

Animal

Female BALB/c mice at 8 weeks of age and 17–19 g were purchased from Charles River Laboratories (Wilmington, MA, United States). All animal procedures were approved by the Institutional Animal Care and Used Committees (IACUC) of Massachusetts General Hospital (Protocol 2014N000009) and were in accordance with guidelines of the National Institutes of Health.

Treatment of Burn Infection in Mice by Oregano Oil

Mice were anesthetized with an intraperitoneal injection of ketamine-xylazine cocktail and shaved on the lower dorsal skin. The burn was introduced by a brass block (1 cm^2) heated to thermal equilibration with boiling water prior to application of its extremity onto the shaved skin for 5 s, which generated a third-degree burn wound. Sterile saline was intraperitoneally administered at 0.5 ml/mouse to support fluid balance during recovery. Aliquots of 50 μL bacterial suspensions containing 5×10^6 CFU in PBS were inoculated onto the burn 30 min after the injury and remained in place while the mice recovered from anesthesia. Luminescent strains of *P. aeruginosa* PA01 and MRSA USA300 were used as the causative pathogens in the study. At 24 h after bacterial inoculation when the biofilms were formed in the wounds, oregano oil was diluted with grape seed oil, which is commonly used for EO dilution in aromatherapy, at a final

concentration of 5 or 10 mg/ml, and topically applied to the infected wounds.

Bioluminescence emission of the bacteria in the wounds was recorded in real time by a Lumina *in vivo* image system (IVIS) (PerkinElmer, Waltham, MA, United States). Bioluminescence images were acquired (60 s exposure, medium binning) at different time points after infection. During imaging, mice were anesthetized in chambers containing 2.0% isoflurane inhalant mixed with oxygen via an IVIS manifold placed within the imaging chamber. Bioluminescence was quantified with the Living Image software (Xenogen).

For measurement of bacterial burden, the infected burn wounds were collected after sacrifice of the mice on day 7 of bacterial inoculation. The collected tissues were homogenized in 2 ml sterile PBS. The resultant homogenate was serially diluted and spotted onto BHI agar plate containing Skirrow's supplement (10 μg/ml vancomycin, 5 μg/ml trimethoprim lactate, and 2500 IU/L polymyxin B). The plates were then incubated at 37°C for 24 h and bacterial colonies were enumerated in a treatment-blind fashion.

Gram Stain

Gram stain was carried out as previously described, with some modifications, to corroborate formation of PA01 biofilms in the infected wounds (Christensen et al., 2013; Wang et al., 2016). Briefly, at 24 h after bacterial inoculation, the infected wounds were excised, fixed in 10% phosphate-buffered formalin for 2 days, and then embedded in paraffin. Tissue sections were cut at 5 μm, de-paraffined, and rehydrated, followed by staining with 0.8% crystal violet in 1% sodium bicarbonate for 1 min and then in gram's iodine for 2 min. After decolorization with acetone/alcohol = 1:1 (v/v), the tissue sections were counterstained with 0.1% safranin O for 2 min, washed, air dried, and mounted with permount (Fisher Scientific, Waltham, MA, United States). Sections were visualized by Hamamatsu NanoZoomer 2.0 HT and the images were processed using NDP viewer software.

Toxicity of Oregano Oil to Mouse Skin *in vivo*

To evaluate any possible toxicity of oregano oil to the skin *in vivo*, mice were shaved on the low dorsal skin 24 h prior to application of oregano oil. Oregano oil *at* 10 mg/ml was applied topically on the shaved area once a day for three consecutive days. Mice treated with PBS served as negative controls. The mice were sacrificed 24 h after the final oregano oil application, and the skin was cross-sectioned using 8 mm biopsy punch for standard histological examination. The tissue sections stained with hematoxylin and eosin (HE) were visualized by Hamamatsu Nanozommer 2.0 HT and the images were processed using NDP viewer software.

DNA damage in oregano oil-treated skin was assessed using the DeadEnd Fluorometric TUNEL system (Promega, Madison, WI, United States), in which damage DNA undergoes end labeling with fluorophore as per the manufacturer's instruction. Briefly, after deparaffinization and rehydration, the tissue sections were incubated with Proteinase K for 10 min to permeabilize the cells, washed, and stained with the TUNEL reaction mixture for 1 h at 37°C in a humidifies chamber. The sections were counterstained with DAPI to mark cell nuclei. Fluorescence images were captured using a FluoView FV1000-MPE confocal microscopy (Olympus Corporation, Tokyo, Japan). For the positive control, tissue sections were pre-treated with 10 unit/ml of RQ1 RNase-free DNase I for 10 min to induce DNA fragmentation before the sections were assayed by the TUNEL staining kit.

Statistical Analyses

Data are presented as means ± standard deviations (SDs). Statistical significance was assessed with two-tailed Student's *t*-test between two groups or one-way ANOVA for multiple group comparison. *P*-values of < 0.05 were considered statistically significant. All statistical analyses were performed using GraphPad Prism 7.0 (GraphPad Software).

RESULTS

GC/MS Analysis of Constituents in Oregano Oil

Chemical ingredients of commercial oregano oil were identified by GC/MS analysis (**Table 1**). The twenty constituents accounted for 97.45% of the total amount of ingredients in

TABLE 1 | Chemical composition (%) of the oregano EO determined by GC-MS analyses.

No.	Constituents	RI[a]	RI[b]	Peak area (%)[c]
1	α-Thujene	926	924	0.21
2	α-Pinene	939	932	1.21
3	Camphene	953	946	0.13
4	1-Octen-3-ol	982	974	0.23
5	Myrcene	991	988	2.12
6	α-Phellandrene	1002	1002	0.62
7	α-Terpinene	1018	1014	0.10
8	*p*-Cymene	1026	1020	5.21
9	Limonene	1031	1024	0.56
10	γ-Terpinene	1060	1054	4.12
11	Terpinolene	1092	1086	0.10
12	Linalool	1100	1095	1.21
13	Borneol	1165	1165	0.35
14	Terpinen-4-ol	1178	1174	0.56
15	Thymol	1295	1289	6.62
16	Carvacrol	1315	1298	72.25
17	Caryophyllene	1426	1417	0.66
18	α-Humulene	1456	1452	0.12
19	β-Bisabolene	1509	1505	0.35
20	Isocaryophyllene oxide	1585	1582	0.72
	Total			97.45

[a]Retention index relative to C6-C28 n-alkanes on the HP-5MS capillary column. [b]Retention index identification by using the Kovats index. [c]Expressed as percentage of the total peak area of the chromatograms without correction.

TABLE 2 | MIC (mg/ml) of the oregano EO and results of antibiotic susceptibility testing for the pathogens.

Species	Strain no.	Oregano	AMK	AMP	ATM	CFZ	FOX	CRO	CXM	CIP	ERY	GEN	IPM	LVX	MEM	NIT	TET
		MIC	R/S	R/S	R/S	R/S	R/S	R/S	R/S	R/S	R/S	R/S	R/S	R/S	R/S	R/S	R/S
A. baumannii	AF0004	0.16	R	R	R	R	R	R	R	R		R	R	R	R	R	R
	IQ0012	0.08	R	R	R	R	R	R	R	R		R	S	R	R	R	R
	AF0005	0.16	R	R	R	R	R	R	R	R		R	R	R	R	R	R
	IQ0013	0.16	R	R	R	R	R	R	R	R		R	S	R	R	R	R
P. aeruginosa	AF0001	0.64	R	R	R	R	R	R	R	R		R	R	R	R	R	R
	IQ0042	0.56	R	R	R	R	R	R	R	R		R	S	R	R	R	R
	IQ0046	0.64	R	R	R	R	R	R	R	R		R	R	R	R	R	R
	PA01	0.56	R	R	R	R	R	R	R	R		R	R	R	R	R	R
Methicillin-resistant *S. aureus*	AF0003	0.16	R	R		R	R	R			R	S		S		S	S
	IQ0064	0.32	R	R		R	R	R			R	S		S		S	S
	IQ0103	0.32	R	R		R	R	R			R	S		S		S	S
	IQ0211	0.16	R	R		R	R	R			R	S		S		S	S
	USA300	0.32	R	R		R	R	R			R	S		S		S	S

AMK, amikacin; AMP, ampicillin; ATM, aztreonam; CFZ, cefazolin; FOX, cefoxitin; CRO, ceftriaxone; CXM, cefuroxime; CIP, ciprofloxacin; ERY, erythromycin; GEN, gentamicin; IPM, imipenem; LVX, levofloxacin; MEM, meropenem; NIT, nitrofurantoin; TET, tetracycline; R, resistant; S, susceptible.

oregano oil. The phenols carvacrol (72.25%) and thymol (6.62%), as well as the monoterpene hydrocarbons *p*-cymene (5.21%), γ-terpinene (4.12%), and α-pinene (1.21%) were the predominant components of oregano oil.

Oregano Oil Effectively Inactivated Bacteria *in vitro* Irrespective of Antibiotic Sensitivity

The MIC values of oregano oil against the 13 bacterial strains are shown in **Table 2**. Oregano oil showed a significant antibacterial activity over PBS controls against *A. baumannii* strains of AF0004, AF0005, IQ0012, and IQ0013 and MRSA strains of AF0003 and IQ0211, with the MICs ranging from 0.08 to 0.16 mg/ml. The MICs were significantly lower than those MICs ranging from 0.32 to 0.64 mg/ml against strains of *P. aeruginosa* and MRSA strains IQ0064, IQ0103, and USA300 (**Table 1**). Oregano oil also exhibited similar antibacterial activities against established biofilms (24-h-old) formed by the 13 bacterial strains within 1 h, with complete inactivation of the biofilms of *A. baumannii*, *P. aeruginosa*, and MRSA at the concentrations of 0.3, 1.0, and 0.4 mg/ml, respectively, in good agreement with the MIC values for planktonic bacterial cells (**Table 1** and **Figure 1**). The results clearly suggest that oregano oil can overcome the obstacles of biofilms and kill bacteria within as sufficiently as planktonic bacteria, in contrast to antibiotics that kills bacterial biofilms poorly.

TEM and SEM Illustrated Ultrastructural Damages of Bacteria

Transmission electron microscopy showed ultrastructural damages of *A. baumannii* AF0005 (**Figure 2B**) and *P. aeruginosa* IQ0042 cells (**Figure 2D**) after exposure to oregano oil for 1 h at 0.16 mg/ml and 0.56 mg/ml, respectively. The cell wall and membrane damages were apparent in *A. baumannii* AF0005 and *P. aeruginosa* IQ0042 cells with a severe leakage of intracellular substances resulting in cell membrane shrinking and separating from cell wall (**Figures 2B,D**, arrows). Moreover, cytoplasmic vacuoles in *A. baumannii* AF0005 (**Figure 2B**, asterisk) and many stainless-vesicles in *P. aeruginosa* IQ0042 (**Figure 2D**, asterisk) were observed. Intracellular structural discontinuation such as dissociation between cell wall and membrane was also seen in *A. baumannii* AF0005 (**Figure 2B**, oval). In comparison, untreated *A. baumannii* AF0005 (**Figure 2A**) and *P. aeruginosa* IQ0042 cells (**Figure 2C**) had intact, clear cell wall and membrane and dense and homogeneous cytoplasm. However, we did not find any significant differences in the ultrastructure between the control and oregano oil-treated MRSA USA300 by TEM (data not shown), which probably hints at different responses of MRSA from *A. baumannii* or *P. aeruginosa*. As with biofilms, dense and thick bacterial biofilm was observed on the dentin surface, comprised of numerous layers of densely concentrated cocci in 24-h-old *P. aeruginosa* IQ0042 (**Figure 2E**) and MRSA IQ0064 (**Figure 2G**) biofilms. The biofilms of *P. aeruginosa* IQ0042 (**Figure 2E**) and MRSA IQ0064 (**Figure 2G**) were treated with oregano oil at 1 mg/ml and 0.4 mg/ml for 1 h, respectively. The cells decohered in the extracellular polymeric matrix, dead

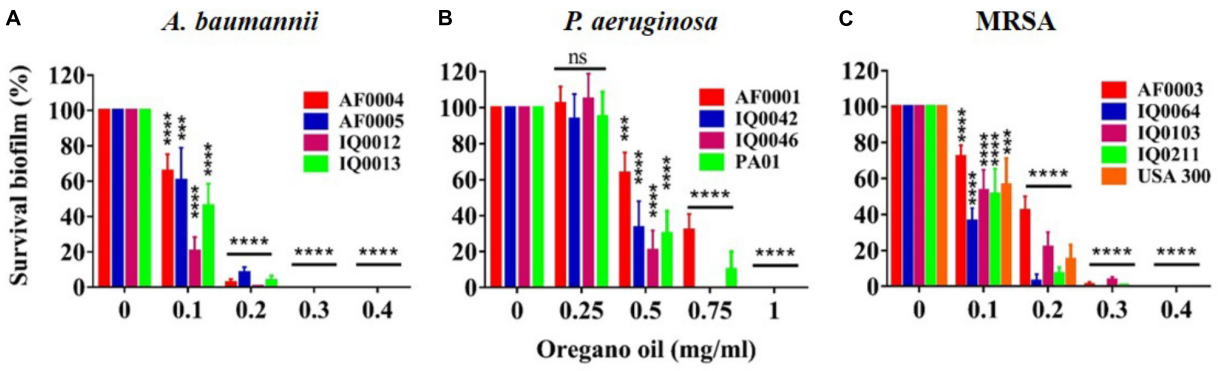

FIGURE 1 | Bacterial viability of 24 h-old-biofilms formed by MDR strains of *A. baumannii* **(A)**, *P. aeruginosa* **(B)**, and MRSA **(C)** after 1 h treatment with oregano oil at indicated concentrations. The viability of bacterial biofilms was determined using an Alamar Blue assay. Data represent means ± SDs. ***$p < 0.001$ and ****$p < 0.0001$ in the presence vs. absence of oregano oil. ns, no significance.

bacteria were readily seen all over, and biofilms were destroyed completely in oregano oil-treated samples (**Figures 2F,H**, arrows). There were only a few bacteria scantly growing on the dentin surface owing to intensive cell death (**Figures 2F,H**).

No Evidence of Resistant Development to Oregano Oil

Risk of resistant development was evaluated with three representative strains: *A. baumannii* AF0005, *P. aeruginosa* IQ0042, and MRSA IQ0064. The bacteria were cultured up to 20 successive passages in the presence of sub-lethal doses of oregano oil for bacterial inactivation. As shown in **Figure 3A**, *A. baumannii* AF0005, *P. aeruginosa* IQ0042, and MRSA IQ0064 retained susceptibility to the original MIC values of 0.16, 0.32, or 0.56 mg/ml, respectively, after 20 cycles of treatment. Moreover, there were no statistically significant differences in the survival rates of all the bacterial strains among the cycles 0, 1, and 20 in the three tested strains, after exposure to oregano oil at the MICs for 24 h (**Figures 3B–D**). The results indicate that resistance to oregano oil of the bacterial strains did not take place under this condition.

Oregano Oil Significantly Reduced Bacterial Burden in Burn Wounds Infected With PA01

Gram stain of histological longitudinal section (**Figure 4A**) and crossing section (**Figure 4B**) of a representative skin specimen demonstrated the presence of PA01 biofilms at 24 h after bacterial inoculation, as evidenced by abundant bacteria densely clustered together (red) in a highly hydrated extracellular matrix on the surface of skin and in the epidermis (**Figure 4A**, outline in red). In addition, highly resilient microbial assemblies were readily found in the dermis suggesting that the PA01 could infect not only the epidermis but also the dermis within 24 h (**Figure 4B**). In successive bacterial luminescence images of representative wounds infected with 5×10^6 CFU of PA01, oregano oil treatment at 10 mg/ml almost completely eradicated bacterial luminescence in 60 min, while luminescence remained unchanged during the same period in untreated mice (**Figures 4C,D**). Moreover, there was no recurrence of infection in the following days in oregano oil-treated mice, whereas the mice remained significantly infected in untreated mice in the same experimental period (**Figures 4C,D**). An average reduction in bacterial luminescence of 2.9 $\log_{10}$ and 3.5 $\log_{10}$ were achieved in 60 min at a concentration of 5 or 10 mg/ml of oregano oil, respectively (**Figure 4E**). On the contrary, bacterial luminescence of the wounds in the absence of oregano oil treatment was almost unaltered with only 0.08 $\log_{10}$ reduction during the equivalent period (**Figure 4E**, $P < 0.0001$). A time course study of the mean bacterial luminescence from days 2 to 7 after bacterial inoculation corroborated that the treatment consistently and significantly lowered the luminescence compared to untreated mice during the whole period of the experiment regardless of whether oregano oil was used at 5 or 10 mg/ml (**Figure 4F**). The mean areas under the curve (AUC) of the bioluminescence time course were 6.9×10^9 and 2.4×10^9 for oregano oil-treated groups at 5 and 10 mg/ml, respectively, but it was 5.9×10^{10} for untreated mice ($P < 0.0001$; **Figure 4G**), representing an 8.6-fold or a 24.6-fold reduction of the AUC in infected burns by oregano oil. We next excised the infected wounds on day 7 to determine bacterial CFU remaining in the wounds. There were 6.7×10^6 and 2.4×10^6 CFU in the wounds treated with oregano oil at a concentration of 5 or 10 mg/ml, respectively, which was significantly lower than the bacterial burden of 6.6×10^7 CFU/wound in untreated mice (**Figure 4H**).

Oregano Oil Significantly Reduced Bacterial Burden in Burn Wounds Infected With USA300

As shown in **Figure 5A**, an average reduction in bacterial luminescence of 2.9 $\log_{10}$ was attained when the infected wounds were treated with oregano oil at 5 mg/ml for 40 min, which was highly significant compared to only 0.4 $\log_{10}$ decline of the bioluminescence in the absence of oregano oil during the same period ($P < 0.0001$; **Figure 5A**). The diminished bacterial luminescence was persistent for 7 days after a single oregano

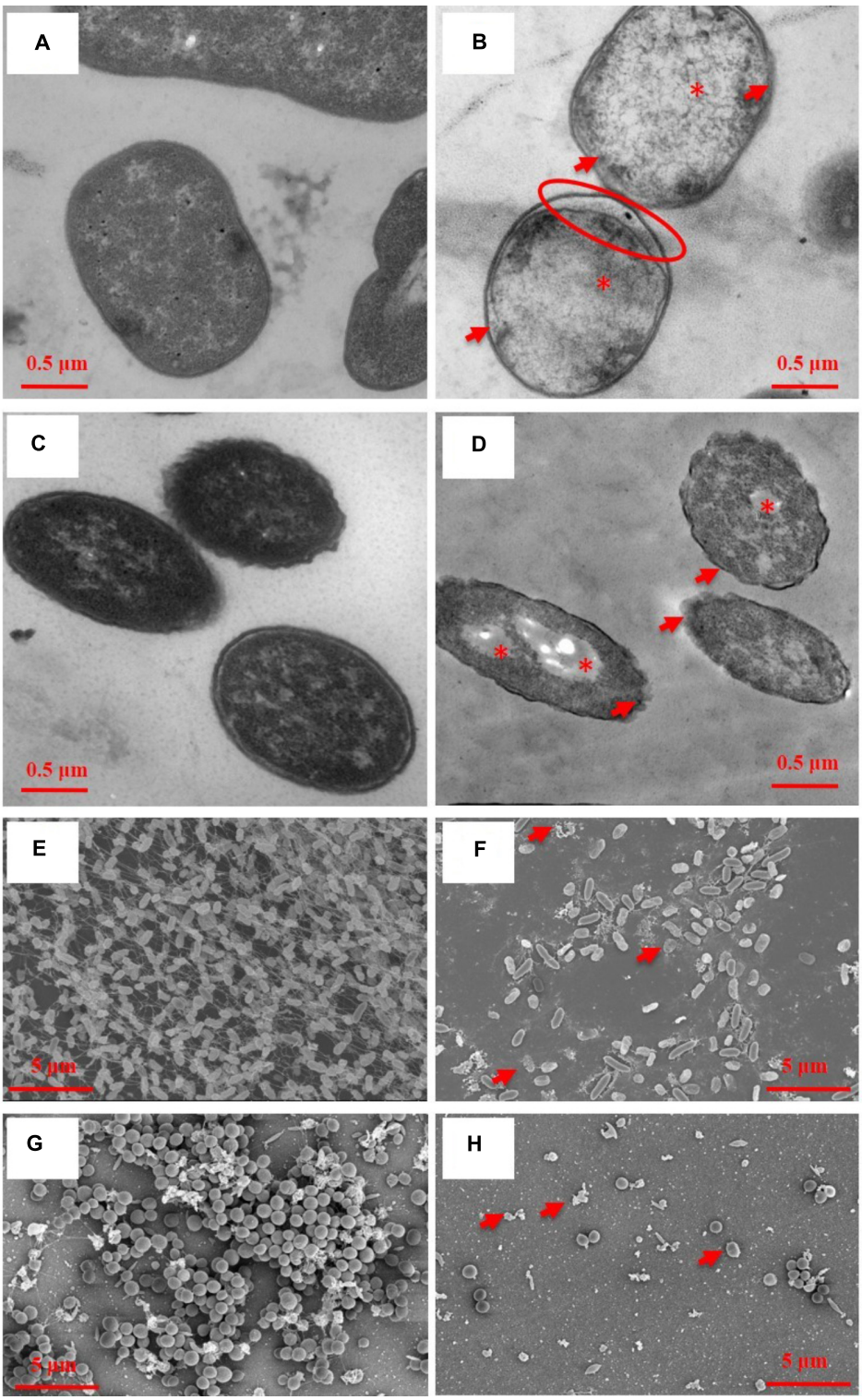

FIGURE 2 | Representative TEM images of planktonic cells **(A–D)** and SEM images of bacterial biofilms **(E–H)** with **(B,D,E,F)** or without **(A,C,E,G)** oregano oil treatment for 1 h. Oregano oil was used at 0.16 mg/ml for *A. baumannii* AF0005 cells, 0.56 mg/ml for *P. aeruginosa* IQ0042 cells, 1.0 mg/ml for *P. aeruginosa* IQ0042 biofilms, and 0.4 mg/ml for MRSA IQ0064 biofilm. **(A,B)** *A. baumannii* AF0005 cells; **(C,D)** *P. aeruginosa* IQ0042 cells; **(E,F)** *P. aeruginosa* IQ0042 biofilms; and **(G,H)** MRSA IQ0064 biofilms. Shown are cell wall and membrane damages **(B,D; arrows)**; dissociation between cell wall and membrane **(B; oval)**, cytoplasmic vacuoles and bubbles **(B,D; asterisk)**, and cell collapse **(F,H, arrows)**. The number of bacteria was drastically reduced after oregano oil treatment in **(F,H)** as compared to untreated controls **(E,G)**.

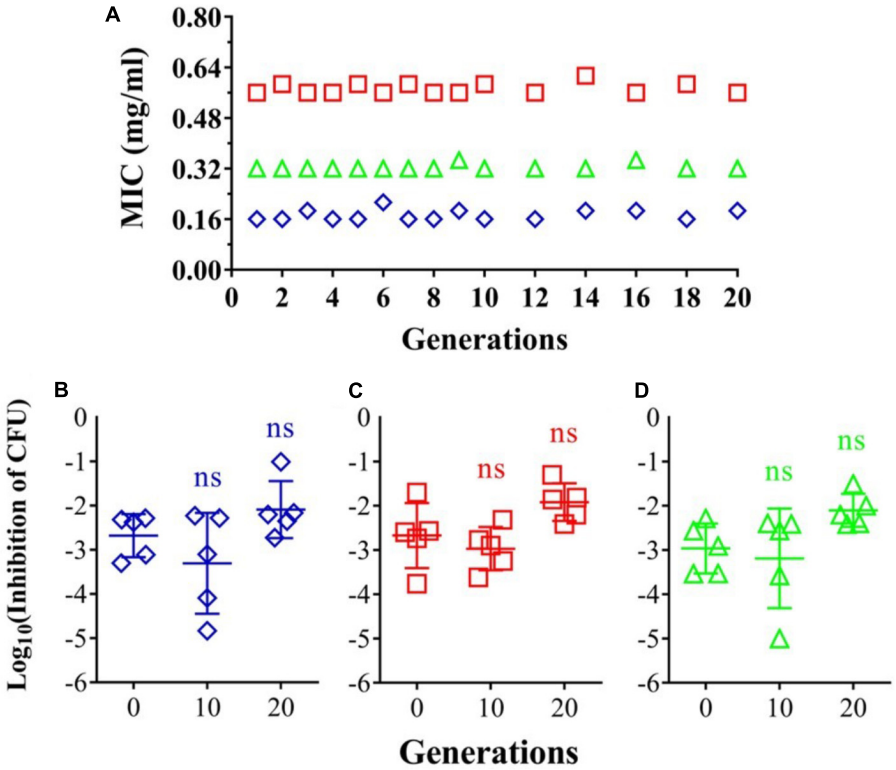

FIGURE 3 | Possible development of bacterial resistance to oregano oil. **(A)** *A. baumannii* AF0005, *P. aeruginosa* IQ0042, and MRSA IQ0064 were passaged for 20 generations each in the presence of indicated MIC doses of oregano oil. The inhibition rate of *A. baumannii* AF0005 **(B)**, *P. aeruginosa* IQ0042 **(C)**, or MRSA IQ0064 **(D)** was unaltered when the bacteria of indicated generations were exposed to oregano oil at an initial MIC concentration. ns, no significance.

oil treatment at 5 mg/ml (**Figure 5B**). The mean AUC of the bioluminescence were 3.7×10^7 in oregano oil-treated group, but it was 1.8×10^9 for untreated mice ($P < 0.0001$; **Figure 5C**), a 48.6-fold reduction of the AUC by oregano oil treatment. In accordance with this, a single dose of oregano oil treatment diminished bacterial load to 2.7×10^7 CFU/mouse that was 18-fold lower than 4.8×10^8 CFU/mouse in the untreated group ($P < 0.0001$; **Figure 5D**).

No Side Effects in Mouse Skin Caused by Oregano Oil

There was no noticeable skin reaction, as visualized with the naked eye, after three consecutive days of oregano oil treatment at 10 mg/ml (**Figure 6B**) when compared to untreated skin (**Figure 6A**). On the histological levels, the skin maintained an undisturbed structure with a clear layer of healthy epidermal cells on the top of the dermis, indistinguishable to mock-treated skins (**Figures 6C,D**). Genotoxicity was next evaluated by a TUNEL assay to examine any DNA damage induced by oregano oil. In comparison with mock-treated controls, there was no any apparent increase of DNA staining in oregano oil-treated skin (**Figures 6E,F**), while the staining was readily seen in the positive control in which skin section was treated with DNase I (**Figure 6G**). The absence of any oregano oil-induced skin reaction and DNA damage after a 3-day treatment suggests that topical application of oregano oil is neither cytotoxic nor genotoxic to the host.

DISCUSSION

In seeking non-antibiotic microbicides, we have screened dozens of EOs from Chinese indigenous aromatic plants/spices because EOs have been long recognized as one of the most promising natural products for safe microbicides in folk medicines (Lu et al., 2013a,b,c). The selection was initially based on their antiseptic applications in the food industry and in agricultures after an extensive database search. Among the dozen EOs tested, about one third showed significant antibacterial activities against clinically and agricultural important microbes (Lu et al., 2013a,b,c). Oregano oil stood out as one of the best ones in terms of safety and efficacy. We thus detailed the bactericidal activity of oregano oil against 11 MDR clinical isolates of *P. aeruginosa, A. baumannii* and MRSA as well as two bioluminescent strains of *P. aeruginosa* PA01 and MRSA USA300 in the current study. Oregano oil effectively killed all the bacterial strains tested, with the MICs ranging from 0.08 to 0.64 mg/ml and at an order of sensitivity of *A. baumannii* > MRSA > *P. aeruginosa* (**Table 1**). The finding is in agreement with previous studies demonstrating that oregano oil and its main component carvacrol had a higher MIC against *P. aeruginosa*

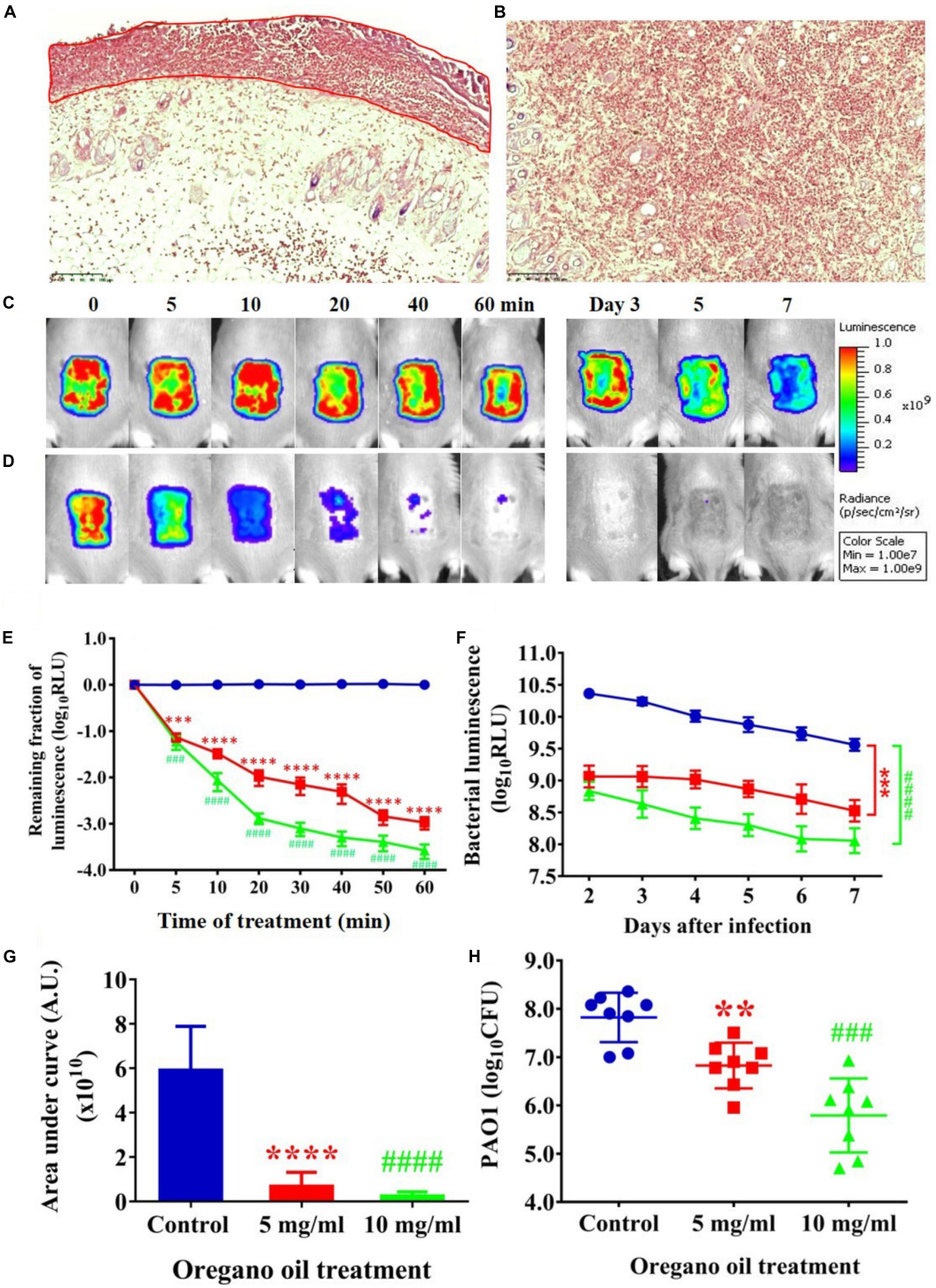

FIGURE 4 | Oregano oil treatment of PA01 infections in the burn wounds. **(A,B)** Gram-stained longitudinal section **(A)** and crossing section **(B)** of a representative wound showing the presence of PA01 biofilms outlined in red. The skin sample was harvested 24 h after bacterial inoculation. **(C,D)** Successive bacterial luminescence images of representative wounds infected with 5×10^6 CFU of luminescent PA01 with **(D)** and without **(C)** oregano oil at 10 mg/ml. The oregano oil was topically applied onto the wounds at 24 h after bacterial inoculation. **(E)** A dose response of mean bacterial luminescence of the wounds infected with 5×10^6 CFU of PA01 in the presence or absence of oregano oil treatment at 5 or 10 mg/ml. **(F)** Time courses of mean bacterial luminescence of the infected wounds in the presence or absence of oregano oil treatment at 5 or 10 mg/ml from days 2 to 7. **(G)** Mean areas under the bacterial luminescence curves **(F)**, representing the overall bacterial burden of infected wounds. **(H)**. The wounds were treated with grape seed oil (control) or oregano oil 24 h after infection and bacterial CFU were quantified on day 7 after bacterial inoculation. RLU, relative luminescence units; A.U., arbitrary units. The data represent means ± SDs ($n = 8$). $^{**}p < 0.01$, $^{\#\#\#}$ or $^{***}p < 0.001$ and $^{\#\#\#\#}$ or $^{****}p < 0.0001$ in the presence vs. absence of oregano oil. ns, no significance.

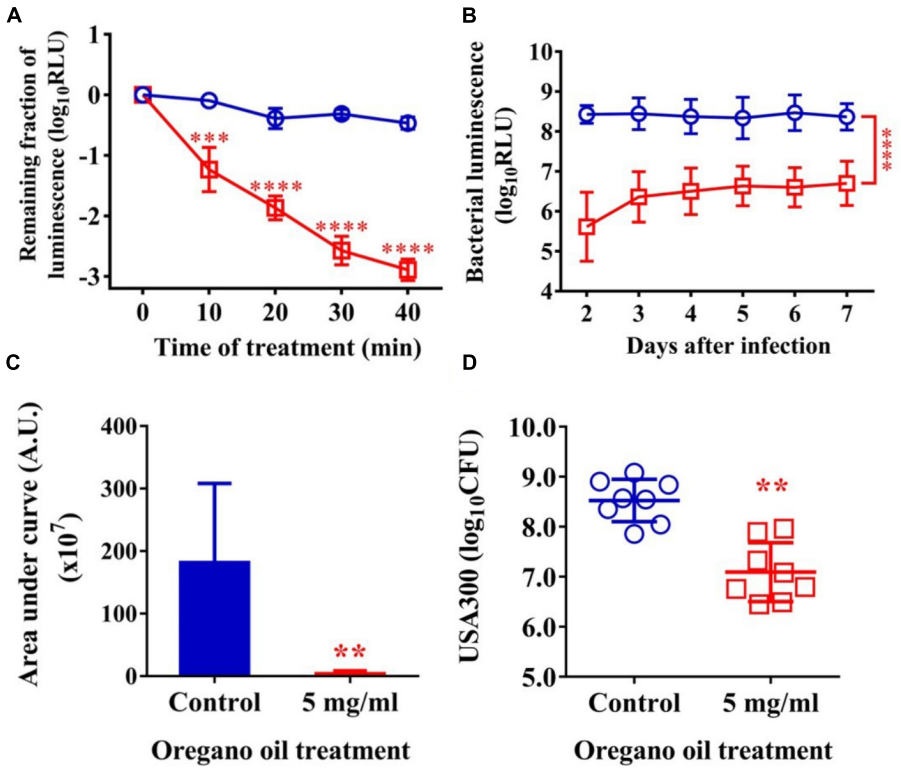

FIGURE 5 | Oregano oil treatment of MRSA USA300 in infected wounds. **(A)** The change in mean bacterial luminescence of the wounds infected with 5×10^6 CFU of USA300 with or without 5 mg/ml oregano oil treatment. **(B)** Time courses of mean bacterial luminescence of the infected wounds with and without oregano oil treatment. **(C)** Mean areas under the bacterial luminescence curves in **(B)**. **(D)** The wounds were treated with grape seed oil (control) or oregano oil once 24 h after infection and bacterial CFU were quantified on day 7 after bacterial inoculation. The data represent means ± SDs ($n = 8$). $^{**}p < 0.01$, $^{***}p < 0.001$, and $^{****}p < 0.0001$ in the presence vs. absence of 5 mg/ml of oregano oil.

compared to other species, such as *S.* spp. (Nostro et al., 2007), *Chromobacterium violaceum*, *Salmonella typhimurium*, and *S. aureus* (Burt et al., 2014). Similar to the clinical isolates, oregano oil also inactivated standard strains of *A. baumannii* ATCC 19606 (Rosato et al., 2010), *P. aeruginosa* ATCC 27853 and *S. aureus* ATCC 29213 (Bouhdid et al., 2009), with the MICs 0.15 mg/mL, 1 mg/mL, and 0.33 mg/mL, respectively, which are comparable to our investigation. Previous studies suggested that Gram-negative bacteria appeared to be more resistant than Gram-positive bacteria in response to EO (Tepe et al., 2005; Longaray Delamare et al., 2007; Gilles et al., 2010). This relative resistance of Gram-negative over Gram-positive bacteria may be ascribed to their cell wall structure and outer membrane arrangement. The outer membrane of Gram-negative bacteria is rich in lipopolysaccharide molecules, relatively impermeable to lipophilic compounds, thereby presenting a barrier to penetration of EO antimicrobial substances (Gao et al., 2011). It may be also associated with the enzymes in the periplasmic space, which are capable of breaking down the antimicrobial substances upon their entrance of the cells (Nikaido, 1996). However, our studies disagreed with these observations and found Gram-negative *A. baumannii* was more sensitive to oregano oil than Gram-positive MRSA. This different outcome suggests that antibacterial activity of oregano oil may not depend on the type of Gram reaction in contrast to other EOs, a possibility that is supported by the studies of Gao et al. (2011). In their studies, Gram-negative bacteria *Klebsiella pneumoniae* was the most sensitive bacteria whereas the Gram-positive bacteria *Listeria monocytogenes* was the most resistant strain to the *Sphallerocarpus gracilis* seed EO (Gao et al., 2011).

The possibility that the cell wall and membrane were primary targets of oregano oil was supported by TEM imaging of the ultrastructure of the bacteria. We found damages of the cell wall and membranes, occurrent with cytoplasmic vacuoles, stainless-vesicles, and disruption and discontinuation of the intracellular structures in a large number of bacterial cells after oregano oil treatment (**Figures 2B,E**). This finding is consistent with an association of the antibacterial activity of oregano oil/carvacrol with disturbance of membrane embedded proteins and disruption of lipids, RNA synthesis, ATPase activity, and efflux pump previously demonstrated (Simoes et al., 2009; Tapia-Rodriguez et al., 2017). Moreover, oregano oil may cause an imbalance in intracellular osmotic pressure owing to a leakage of cytoplasmic contents following cell wall and membrane damages, and formation of cytoplasmic vacuoles, eventually inducing cell necrosis, although more investigations are required to conclude the mechanism in detail.

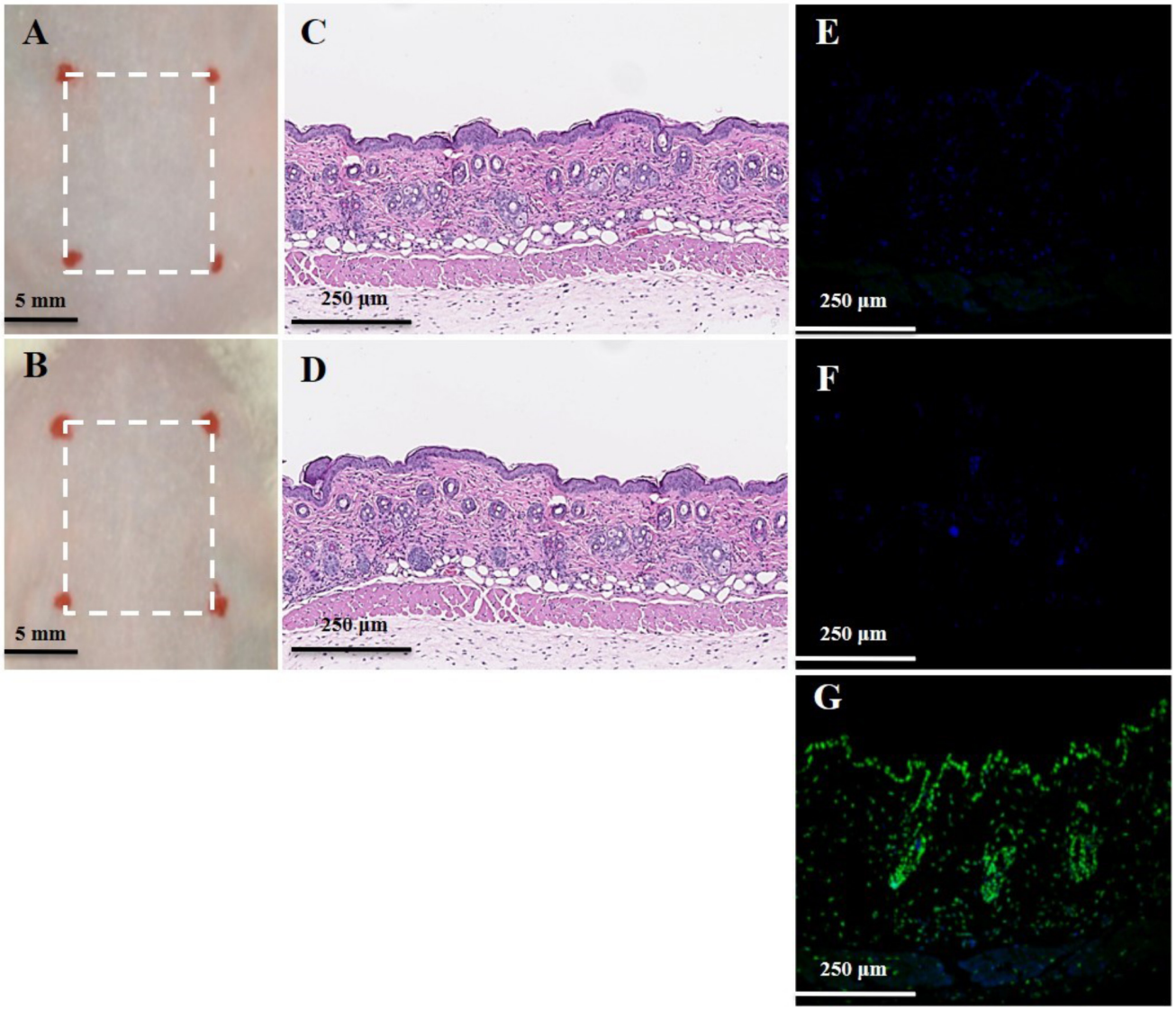

FIGURE 6 | Toxicity evaluation of oregano oil to normal mouse skins. The dorsal skin of mice was topically treated with **(A,C,E)** or without 10 mg/ml oregano oil **(B,D,F)** once a day for three consecutive days. On day 4, the skins were photographed **(A,B)**, followed by histological examination **(C,D)**. The skin sections were also TUNEL stained **(E,F)**. DNase I treated skin samples **(G)** were TUNEL stained in parallel as positive-staining controls.

Biofilms are sessile organizations of bacterial cells with a strong adherence to surfaces. Biofilm-associated microbial cells are well protected by an extracellular matrix that comprises exopolysaccharides, proteins and DNA and is poorly permeable (Donlan, 2002; Husain et al., 2015). Systemic antibiotics administered to treat bacterial infections frequently fails at least in part due to the poor permeability of biofilms. Interestingly, oregano oil was capable of biofilm-killing at least at an early stage (24-h-old biofilms) as efficiently as planktonic cells. Biofilms of *A. baumannii*, *P. aeruginosa*, and MRSA were eliminated by oregano oil at a concentration of 0.3, 1.0, or 0.4 mg/ml, respectively, similar to the corresponding MICs attained in planktonic cells. The similarity can be extended to the order of sensitivity with *P. aeruginosa* biofilms more resistant than MRSA biofilms than *A. baumannii* biofilms (**Figure 1** and **Table 1**). This may be attributed to the superior permeability and lipid solubility of oregano oil to bacterial cell membrane and wall (Magi et al., 2015; Khan et al., 2017). Likewise, the effectiveness of oregano oil to inactivate *S. aureus*, *S. epidermidis*, and *P. aeruginosa* biofilms was also found at similar MICs as those against planktonic cells (Nostro et al., 2007; dos Santos Rodrigues et al., 2017; Tapia-Rodriguez et al., 2017). SEM observations confirmed the physical damage and considerable morphological alteration in the *P. aeruginosa* IQ0042 (**Figures 2E,F**) and MRSA IQ0064 (**Figures 2G,H**) biofilms following oregano oil treatment. These observations raise an intriguing possibility that EO may have advantages over water soluble antibiotics in treatment of biofilms because bacteria living in the biofilms are well known to be more

resistant to antibiotics (up to 1,000 times) than their planktonic counterparts, in part owing to poor permeability of biofilms to the antibiotics (Ceri et al., 1999; Caraher et al., 2007).

One concern of using oregano oil as an alternative for the treatment of infections in clinics will be whether MDR bacteria can develop resistance to oregano oil. Although this remains largely unaddressed to date, our results suggest that resistance may not be readily developed because 20 passages in the presence of sublethal concentrations of oregano oil did not alter their susceptibility to the oil (**Figure 3A**). Moreover, oregano oil has been used in food prevention and other antiseptic application for centuries and no resistance has been reported so far. It is commonly believed that EOs act at multiple sites within bacterial cells (cell membrane, cell wall, structural proteins, enzymes, nucleic acids, unsaturated lipids, etc.) and would be less likely to induce the development of resistance (Burt, 2004; Simoes et al., 2009; Tapia-Rodriguez et al., 2017). On the contrary, the MIC of conventional antibiotics could gradually increase with a treatment length due to their single action to inactivate the bacteria (Baym et al., 2016; Levin-Reisman et al., 2017).

The bactericidal activity of oregano oil was corroborated in mouse burn models using model bioluminescent strains of Gram-negative *P. aeruginosa* PA01 and Gram-positive MRSA USA300. When applied at 24 h after bacterial inoculation forming early stage biofilms, oregano oil effectively reduced the bacterial burden by 25-folds for PA01 and 49-folds for USA300, respectively, in comparison to untreated wounds. While efficiently inactivating bacteria, oregano oil exhibited no cytotoxicity or genotoxicity to the skin, in good agreement with its long record of safety. Moreover, oregano oil did not adversely affect human keratinocytes (Babili et al., 2011) and was safe when administered orally in mice (Manohar et al., 2001; Preuss et al., 2005; Feng et al., 2017).

In summary, we reported here the effectiveness of oregano oil against a panel of MDR bacteria isolated from combating casualties and demonstrated for the first time efficacy of oregano oil for the treatment of burn infections in mice. The study serves as an initial effort in the pursuit of a novel therapeutic option for wound infections, especially those caused by MDR bacteria.

AUTHOR CONTRIBUTIONS

ML designed and performed all the experiments, analyzed the data, and wrote the manuscript. TD supervised and designed the experiments, analyzed the data, and wrote the paper. CM isolated and characterized all the clinical bacteria and wrote the paper. and MW designed and supervised the study, analyzed the data, and wrote the manuscript.

FUNDING

This study was supported in part by FA9550-16-1-00173, Department of Defense/Air Force Office of Scientific Research Military Photomedicine Program and Department funds to MW and TD.

ACKNOWLEDGMENTS

We thank Drs. Michael R. Hamblin and Ji Wang for stimulating comments and discussions from Massachusetts General Hospital and the staff at the photopathology core at Wellman Center for Photomedicine for assisting transmission electron microscopy and histopathology.

REFERENCES

Akgul, A., and Kivanc, M. (1988). Inhibitory effects of selected Turkish spices and oregano components on some foodborne fungi. *Int. J. Food Microbiol.* 6, 263–268. doi: 10.1016/0168-1605(88)90019-0

Babili, F. E., Bouajila, J., Souchard, J. P., Bertrand, C., Bellvert, F., Fouraste, I., et al. (2011). Oregano: chemical analysis and evaluation of its antimalarial, antioxidant, and cytotoxic activities. *Food Sci.* 3, 512–518. doi: 10.1111/j.1750-3841.2011.02109.x

Baym, M., Lieberman, T. D., Kelsic, E. D., Chait, R., Gross, R., Yelin, I., et al. (2016). Spatiotemporal microbial evolution on antibiotic landscapes. *Science* 353, 1147–1151. doi: 10.1126/science.aag0822

Benito, M., Jorro, G., Morales, C., Pelaez, A., and Fernandez, A. (1996). Labiatae allergy: systemic reactions due to ingestion of oregano and thyme. *Ann. Allergy Asthma Immunol.* 76, 416–418. doi: 10.1016/S1081-1206(10)63456-4

Bloemsma, G. C., Dokter, J., Boxma, H., and Oen, I. M. (2008). Mortality and causes of death nin a burn centre. *Burns* 34, 1103–1107. doi: 10.1016/j.burns.2008.02.010

Bouhdid, S., Abrini, J., Zhiri, A., Espuny, M. J., and Manresa, A. (2009). Investigation of functional and morphological changes in *Pseudomonas aeruginosa* and *Staphylococcus aureus* cells induced by *Origanum compactum* essential oil. *J. Appl. Microbiol.* 106, 1558–1568. doi: 10.1111/j.1365-2672.2008.04124.x

Burt, S. (2004). Essential oils: their antibacterial properties and potential applications in foods – A review. *Int. J. Food Microbiol.* 94, 223–253. doi: 10.1016/j.ijfoodmicro.2004.03.022

Burt, S. A., Ojo-Fakunle, V. T. A., Woertman, J., and Veldhuizen, E. J. A. (2014). The natural antimicrobial carvacrol inhibits quorum sensing in chromobacterium violaceum and reduces bacterial biofilm formation at sub-lethal concentrations. *PLoS One* 9:e93414. doi: 10.1371/journal.pone.0093414

Calhoun, J. H., Murray, C. K., and Manring, M. M. (2008). Multidrug-resistant organisms in military wounds from iraq and afghanistan. *Clin. Orthop.* 466, 1356–1362. doi: 10.1007/s11999-008-0212-9

Caraher, E., Reynolds, G., Murphy, P., McClean, S., and Callaghan, M. (2007). Comparison of antibiotic susceptibility of *Burkholderia cepacia* complex organisms when grown planktonically or as biofilm in vitro. *Eur. J. Clin. Microbiol. Infect. Dis.* 26, 213–216. doi: 10.1007/s10096-007-0256-x

Ceri, H., Olson, M., Stremick, C., Read, R., Morck, D., and Buret, A. (1999). The calgary biofilm device: new technology for rapid determination of antibiotic susceptibilities of bacterial biofilms. *J. Clin. Microbiol.* 37, 1771–1776.

Christensen, L., Breiting, V., Bjarnsholt, T., Eickhardt, S., Hogdall, E., Janssen, M., et al. (2013). Bacterial infection as a likely cause of adverse reactions to polyacrylamide hydrogel fillers in cosmetic surgery. *Clin. Infect. Dis.* 56, 1438–1444. doi: 10.1093/cid/cit067

Crane, D. P., Gromov, K., Li, D., Soballe, K., Wahnes, C., Buechner, H., et al. (2009). Efficacy of colistin-impregnated beads to prevent multidrug-resistant *A. baumannii* implant-associated osteomyelitis. *J. Orthop. Res.* 27, 1008–1015. doi: 10.1002/jor.20847

Dai, T., Gupta, A., Huang, Y., Yin, R., Murray, C. K., Vrahas, M. S., et al. (2013). Blue light rescues mice from potentially fatal *Pseudomonas aeruginosa* burn infection: efficacy, safety, and mechanism of action. *Antimicrob. Agents Chemother.* 57, 1238–1245. doi: 10.1128/AAC.01652-12

Donlan, R. (2002). Biofilms: microbial life on surfaces. *Emerg. Infect. Dis.* 8, 881–890. doi: 10.3201/eid0809.020063

dos Santos Rodrigues, J. B., de Carvalho, R. J., de Souza, N. T., Oliveira, K. d. S., Franco, O. L., Schaffner, D., et al. (2017). Effects of oregano essential oil and carvacrol on biofilms of *Staphylococcus aureus* from food-contact surfaces. *Food Control* 73, 1237–1246. doi: 10.1016/j.foodcont.2016.10.043

Feng, J., Zhang, S., Shi, W., Zubcevik, N., Miklossy, J., and Zhang, Y. (2017). Selective essential oils from spice or culinary herbs have high activity against stationary phase and biofilm borrelia burgdorferi. *Front. Med.* 4:169. doi: 10.3389/fmed.2017.00169

Fitzwater, J., Purdue, G., Hunt, J., and O'Keefe, G. (2003). The risk factors and time course of sepsis and organ dysfunction after burn trauma. *J. Trauma-Injury Infect. Crit. Care* 54, 959–966. doi: 10.1097/01.TA.0000029382.26295.AB

Gao, C., Tian, C., Lu, Y., Xu, J., Luo, J., and Guo, X. (2011). Essential oil composition and antimicrobial activity of *Sphallerocarpus gracilis* seeds against selected food-related bacteria. *Food Control* 22, 517–522. doi: 10.1016/j.foodcont.2010.09.038

Gilles, M., Zhao, J., An, M., and Agboola, S. (2010). Chemical composition and antimicrobial properties of essential oils of three Australian Eucalyptus species. *Food Chem.* 119, 731–737. doi: 10.1016/j.foodchem.2009.07.021

Gomez, R., Murray, C. K., Hospenthal, D. R., Cancio, L. C., Renz, E. M., Holcomb, J. B., et al. (2009). Causes of mortality by autopsy findings of combat casualties and civilian patients admitted to a burn unit. *J. Am. Coll. Surg.* 208, 348–354. doi: 10.1016/j.jamcollsurg.2008.11.012

Hampton, T. (2013). Report reveals scope of US antibiotic resistance threat. *JAMA* 310, 1661–1663. doi: 10.1001/jama.2013.280695

Husain, F. M., Ahmad, I., Khan, M. S., Ahmad, E., Tahseen, Q., Khan, M. S., et al. (2015). Sub-MICs of *Mentha piperita* essential oil and menthol inhibits AHL mediated quorum sensing and biofilm of ram-negative bacteria. *Front. Microbiol.* 6:420. doi: 10.3389/fmicb.2015.00420

Jiang, B., Yin, S., You, B., Huang, G., Yang, Z., Zhang, Y., et al. (2017). A 5-year survey reveals increased susceptibility to glycopeptides for methicillin-resistant *Staphylococcus aureus* isolates from *Staphylococcus aureus* bacteremia patients in a Chinese burn center. *Front. Microbiol.* 8:2531. doi: 10.3389/fmicb.2017.02531

Joshi, S. C., Verma, A. R., and Mathela, C. S. (2010). Antioxidant and antibacterial activities of the leaf essential oils of Himalayan *Lauraceae* species. *Food Chem. Toxicol.* 48, 37–40. doi: 10.1016/j.fct.2009.09.011

Kavanaugh, N. L., and Ribbeck, K. (2012). Selected antimicrobial essential oils eradicate *Pseudomonas* spp. and *Staphylococcus aureus* biofilms. *Appl. Environ. Microbiol.* 78, 4057–4061. doi: 10.1128/AEM.07499-11

Khan, I., Bahuguna, A., Kumar, P., Bajpai, V. K., and Kang, S. C. (2017). Antimicrobial potential of carvacrol against uropathogenic *Escherichia coli* via membrane disruption, depolarization, and reactive oxygen species generation. *Front. Microbiol.* 8:2421. doi: 10.3389/fmicb.2017.02421

Levin-Reisman, I., Ronin, I., Gefen, O., Braniss, I., Shoresh, N., and Balaban, N. Q. (2017). Antibiotic tolerance facilitates the evolution of resistance. *Science* 355, 826–830. doi: 10.1126/science.aaj2191

Li, X., Robinson, S. M., Gupta, A., Saha, K., Jiang, Z., and Moyano, D. F. (2014). Functional gold nanoparticles as potent antimicrobial agents against multi-drug-resistant bacteria. *ACS Nano* 8, 10682–10686. doi: 10.1021/nn5042625

Longaray Delamare, A. P., Moschen-Pistorello, I. T., Artico, L., Atti-Serafini, L., and Echeverrigaray, S. (2007). Antibacterial activity of the essential oils of *Salvia officinalis* L. and *Salvia triloba* L. cultivated in South Brazil. *Food Chem.* 100, 603–608. doi: 10.1016/j.foodchem.2005.09.078

Lopez-Reyes, J. G., Spadaro, D., Gullino, M. L., and Garibaldi, A. (2010). Efficacy of plant essential oils on postharvest control of rot caused by fungi on four cultivars of apples in vivo. *Flavour Fragrance J.* 25, 171–177. doi: 10.1002/ffj.1989

Lu, M., Han, Z., Xu, Y., and Yao, L. (2013a). In vitro and in vivo anti-tobacco mosaic virus activities of essential oils and individual compounds. *J. Microbiol. Biotechnol.* 23, 771–778. doi: 10.4014/jmb.1210.10078

Lu, M., Han, Z., and Yao, L. (2013b). In vitro and in vivo antimicrobial efficacy of essential oils and individual compounds against *Phytophthora parasitica* var. nicotianae. *J. Appl. Microbiol.* 115, 187–198. doi: 10.1111/jam.12208

Lu, M., Han, Z., Xu, Y., and Yao, L. (2013c). Effects of essential oils from Chinese indigenous aromatic plants on mycelial growth and morphogenesis of three phytopathogens. *Flavour Fragrance J.* 28, 84–92. doi: 10.1002/ffj.3132

Magi, G., Marini, E., and Facinelli, B. (2015). Antimicrobial activity of essential oils and carvacrol, and synergy of carvacrol and erythromycin, against clinical, erythromycin-resistant Group A *Streptococci*. *Front. Microbiol.* 6:165. doi: 10.3389/fmicb.2015.00165

Manohar, V., Ingram, C., Gray, J., Talpur, N., Echard, B., Bagchi, D., et al. (2001). Antifungal activities of origanum oil against *Candida albicans*. *Mol. Cell Biochem.* 228, 111–117. doi: 10.1023/A:1013311632207

Munhuweyi, K., Caleb, O. J., Lennox, C. L., van Reenen, A. J., and Opara, U. L. (2017). In vitro and in vivo antifungal activity of chitosan-essential oils against pomegranate fruit pathogens. *Postharvest. Biol. Technol.* 129, 9–22. doi: 10.1016/j.postharvbio.2017.03.002

Nikaido, H. (1996). Multidrug efflux pumps of gram-negative bacteria. *J. Bacteriol.* 178, 5853–5859. doi: 10.1128/jb.178.20.5853-5859.1996

Nostro, A., Roccaro, A. S., Bisignano, G., Marino, A., Cannatelli, M. A., Pizzimenti, F. C., et al. (2007). Effects of oregano, carvacrol and thymol on *Staphylococcus aureus* and *Staphylococcus epidermidis* biofilms. *J. Med. Microbiol.* 56, 519–523. doi: 10.1099/jmm.0.46804-0

Ocana-Fuentes, A., Arranz-Gutierrez, E., Senorans, F. J., and Reglero, G. (2010). Supercritical fluid extraction of oregano (*Origanum vulgare*) essentials oils: anti-inflammatory properties based on cytokine response on THP-1 macrophages. *Food Chem. Toxicol.* 48, 1568–1575. doi: 10.1016/j.fct.2010.03.026

Pandey, A. K., Kumar, P., Singh, P., Tripathi, N. N., and Bajpai, V. K. (2017). Essential oils: sources of antimicrobials and food preservatives. *Front. Microbiol.* 7:2161. doi: 10.3389/fmicb.2016.02161

Preuss, H., Echard, B., Dadgar, A., Talpur, N., Manohar, V., Enig, M., et al. (2005). Effects of essential oils and monolaurin on *Staphylococcus aureus*: in vitro and in vivo studies. *Toxicol. Mech. Methods* 15, 279–285. doi: 10.1080/15376520590968833

Rosato, A., Piarulli, M., Corbo, F., Muraglia, M., Carone, A., Vitali, M. E., et al. (2010). In vitro synergistic action of certain combinations of gentamicin and essential oils. *Curr. Med. Chem.* 17, 3289–3295. doi: 10.2174/092986710792231996

Sakkas, H., and Papadopoulou, C. (2017). Antimicrobial activity of basil, oregano, and thyme essential oils. *J. Microbiol. Biotechnol.* 28, 429–438. doi: 10.4014/jmb.1608.08024

Scott, P., Deye, G., Srinivasan, A., Murray, C., Moran, K., Hulten, E., et al. (2007). An outbreak of multidrug-resistant *Acinetobacter baumannii*-calcoaceticus complex infection in the US military health care system associated with military operations in Iraq. *Clin. Infect. Dis.* 44, 1577–1584. doi: 10.1086/518170

Shen, D., Pan, M., Wu, Q., Park, C., Juliani, H. R., Ho, C., et al. (2010). LC-MS method for the simultaneous quantitation of the anti-inflammatory constituents in oregano (*Origanum* Species). *J. Agric. Food Chem.* 58, 7119–7125. doi: 10.1021/jf100636h

Simoes, M., Bennett, R. N., and Rosa, E. A. S. (2009). Understanding antimicrobial activities of phytochemicals against multidrug resistant bacteria and biofilms. *Nat. Prod. Rep.* 26, 746–757. doi: 10.1039/b821648g

Soylu, E. M., Kurt, S., and Soylu, S. (2010). In vitro and in vivo antifungal activities of the essential oils of various plants against tomato grey mould disease agent *Botrytis cinerea*. *Int. J. Food Microbiol.* 143, 183–189. doi: 10.1016/j.ijfoodmicro.2010.08.015

Soylu, S., Yigitbas, H., Soylu, E. M., and Kurt, S. (2007). Antifungal effects of essential oils from oregano and fennel on *Sclerotinia sclerotiorum*. *J. Appl. Microbiol.* 103, 1021–1030. doi: 10.1111/j.1365-2672.2007.03310.x

Tapia-Rodriguez, M. R., Hernandez-Mendoza, A., Gonzalez-Aguilar, G. A., Martinez-Tellez, M. A., Martins, C. M., and Ayala-Zavala, J. F. (2017). Carvacrol as potential quorum sensing inhibitor of *Pseudomonas aeruginosa* and biofilm production on stainless steel surfaces. *Food Control* 75, 255–261. doi: 10.1016/j.foodcont.2016.12.014

Tepe, B., Daferera, D., Sokmen, A., Sokmen, M., and Polissiou, M. (2005). Antimicrobial and antioxidant activities of the essential oil and various extracts of *Salvia tomentosa* Miller (Lamiaceae). *Food Chem.* 90, 333–340. doi: 10.1016/j.foodchem.2003.09.013

Vento, T. J., Cole, D. W., Mende, K., Calvano, T. P., Rini, E. A., Tully, C. C., et al. (2013). Multidrug-resistant gram-negative bacteria colonization of healthy US military personnel in the US and Afghanistan. *BMC Infect. Dis.* 13:68. doi: 10.1186/1471-2334-13-68

Wang, Y., Beekman, J., Hew, J., Jackson, S., Issler-Fisher, A. C., Parungao, R., et al. (2018). Burn injury: challenges and advances in burn wound healing, infection, pain and scarring. *Adv. Drug Deliv. Rev.* 123, 3–17. doi: 10.1016/j.addr.2017.09.018

Wang, Y., Wu, X., Chen, J., Amin, R., Lu, M., Bhayana, B., et al. (2016). Antimicrobial blue light inactivation of ram-negative pathogens in biofilms: in vitro and in vivo studies. *J. Infect. Dis.* 213, 1380–1387. doi: 10.1093/infdis/jiw070

Yan, F., Azizi, A., Janke, S., Schwarz, M., Zeller, S., and Honermeier, B. (2016). Antioxidant capacity variation in the oregano (*Origanum vulgare* L.) collection of the German National Genebank. *Ind. Crops Prod.* 92, 19–25. doi: 10.1016/j.indcrop.2016.07.038

Zhang, Y., Zhu, Y., Gupta, A., Huang, Y., Murray, C. K., Vrahas, M. S., et al. (2014). Antimicrobial blue light therapy for multidrug-resistant *Acinetobacter baumannii* infection in a mouse burn model: implications for prophylaxis and treatment of combat-related wound infections. *J. Infect. Dis.* 209, 1963–1971. doi: 10.1093/infdis/jit842

Conflict of Interest Statement: The authors declare that the research was conducted in the absence of any commercial or financial relationships that could be construed as a potential conflict of interest.

Copyright © 2018 Lu, Dai, Murray and Wu. This is an open-access article distributed under the terms of the Creative Commons Attribution License (CC BY). The use, distribution or reproduction in other forums is permitted, provided the original author(s) and the copyright owner(s) are credited and that the original publication in this journal is cited, in accordance with accepted academic practice. No use, distribution or reproduction is permitted which does not comply with these terms.

frontiers in Microbiology

ORIGINAL RESEARCH
published: 06 November 2018
doi: 10.3389/fmicb.2018.02638

Effects of Monolaurin on Oral Microbe–Host Transcriptome and Metabolome

Viviam de Oliveira Silva[1,2†], Luciano José Pereira[3], Silvana Pasetto[2], Maike Paulino da Silva[2], Jered Cope Meyers[4] and Ramiro Mendonça Murata[4,5]*

[1] Department of Veterinary Medicine, Federal University of Lavras, Lavras, Brazil, [2] Division of Periodontology, Diagnostic Sciences, Dental Hygiene and Biomedical Science, Herman Ostrow School of Dentistry, University of Southern California, Los Angeles, CA, United States, [3] Department of Health Sciences, Federal University of Lavras, Lavras, Brazil, [4] Department Foundational Sciences, School of Dental Medicine, East Carolina University, Greenville, NC, United States, [5] Department of Microbiology and Immunology, Brody School of Medicine, East Carolina University, Greenville, NC, United States

The aim of this *in vitro* study was to evaluate the effects of monolaurin against *Aggregatibacter actinomycetemcomitans* (Aa) and determine their effects on the host transcriptome and metabolome, using an oral cell/bacteria co-culture dual-chamber model to mimic the human periodontium. For this, the Aa, was applied to cross the monolayer of epithelial keratinocytes (OBA-9) to reach the fibroblasts layer (HGF-1) in the basal chamber. The Monolaurin treatments (25 or 50 μM) were added immediately after the inoculation of the dual-chamber with Aa. After 24 h, the transcriptional factors and metabolites produced were quantified in the remaining cell layers (insert and basal chamber) and in supernatant released from the cells. The genes IL-1α, IL-6, IL-18, and TNF analyzed in HGF-1 concentrations showed a decreased expression when treated with both concentration of Monolaurin. In keratinocytes, the genes IL-6, IL-18, and TNF presented a higher expression and the expression of IL-1α decreased when treated with the two cited concentrations. The production of glycerol and pyruvic acid increased, and the 2-deoxytetronic acid NIST, 4-aminobutyric acid, pinitol and glyceric acid, presented lower concentrations because of the treatment with 25 and/or 50 μM of Monolaurin. Use of monolaurin modulated the immune response and metabolite production when administered for 24 h in a dual-chamber model inoculated with *A. actinomycetemcomitans*. In summary, this study indicates that monolaurin had antimicrobial activity and modulated the host immune response and metabolite production when administered for 24 h in a dual-chamber model inoculated with *A. actinomycetemcomitans*.

Keywords: ***Aggregatibacter actinomycetemcomitans*, periodontal disease, immune system, fibroblast, keratinocyte, monolaurin**

OPEN ACCESS

Edited by:
Rebecca Thombre, Pune University-Shivajinagar, India

Reviewed by:
Piyush Baindara, National Centre for Biological Sciences, India
Karishma R. Pardesi, Savitribai Phule Pune University, India

****Correspondence:***
Ramiro Mendonça Murata
murartar16@ecu.edu

†Present address:
Viviam de Oliveira Silva, Department of Research and Scientific Initiation, Centro Universitário Atenas, Paracatu, Brazil

Specialty section:
This article was submitted to Antimicrobials, Resistance and Chemotherapy, a section of the journal Frontiers in Microbiology

Received: *28 May 2018*
Accepted: *16 October 2018*
Published: *06 November 2018*

Citation:
Silva VO, Pereira LJ, Pasetto S, Silva MP, Meyers JC and Murata RM (2018) Effects of Monolaurin on Oral Microbe–Host Transcriptome and Metabolome. Front. Microbiol. 9:2638. doi: 10.3389/fmicb.2018.02638

INTRODUCTION

Periodontal disease is characterized by bacterial infection associated with the presence of biofilm, resulting in chronic inflammation of the tooth supporting tissues leading to a progressive destruction of periodontal tissue and alveolar bone. Signs and symptoms of periodontitis can include gingival swelling, bleeding during brushing, periodontal pockets, increased spacing

between the teeth and tooth loss (Irfan et al., 2001; Michaud et al., 2007; Savage et al., 2009; Gurav, 2014).

The most common form of periodontal disease, denominated periodontitis, affects approximately 50% of the adult population with its severe forms affecting 10–15% of these individuals (Chapple and Genco, 2013).

The oral biofilm is composed of at least 800 different species of bacteria (Paster et al., 2006; Filoche et al., 2010). Numerous periodontopathogenic bacteria (*Porphyromonas gingivalis*, *Fusobacterium nucleatum*, *Streptococcus intermedius*, and others) are responsible for the initiation and maintenance of periodontal inflammation (Coussens and Werb, 2002; Oringer, 2002; Loos, 2005; Moutsopoulos and Madianos, 2006; de Almeida et al., 2007). The *Aggregatibacter actinomycetemcomitans* is a fermentative, gram-negative and capnophilic coccobacillus. It is not only considered the most important agent of localized aggressive periodontitis lesions, but is associated with chronic periodontitis as well (Slots et al., 1980; Zambon et al., 1983; Haraszthy et al., 2000; Gafan et al., 2004; Yang et al., 2004; Cortelli et al., 2009; Rakić et al., 2010; da Silva-Boghossian et al., 2011). The progression of periodontal disease is associated with the virulence factors of the microorganism, together with the vulnerability of the host. Aa produces leukotoxin, adhesins, bacteriocins, and lipopolysaccharide, which are responsible for interacting with the host cells triggering an inflammatory response in the periodontium (Cortelli et al., 2009). In addition, another critical factor for soft tissue inflammation and bone resorption is the immune-inflammatory host response to the bacterial biofilm (Salvi and Lang, 2005).

According to Aimetti (2014), non-surgical periodontal treatments possess limitations, such as the long-term maintainability of deep periodontal pockets, risk of disease recurrence, and skill of the operator. The development of new therapeutic agents that have the ability to inhibit the biofilm formation and modulate the inflammatory response can have a major impact in the prevention and treatment of periodontal disease. Monolaurin, also known as glycerol monolaurate or lauroyl, is a natural surfactant compound commonly used in cosmetics and the food industry. It is recognized by the Food and Drug Administration (FDA) as a GRAS (Generally Recognized as Safe) food additive since 1977. This natural compound is found in coconut oil and human breast milk (Fu et al., 2006; Peterson and Schlievert, 2006).

Monolaurin presents antibacterial and antiviral activity *in vitro* (Projan et al., 1994; Isaacs, 2001; Preuss et al., 2005; Peterson and Schlievert, 2006; Carpo et al., 2007), which may be of great interest in the treatment and/or prevention of various infections. However, the effect of monolaurin on periodontopathogenic bacteria has yet to be determined.

Therefore, the aims of this *in vitro* study were to evaluate the cytotoxicity, the antimicrobial effect of monolaurin against *A. actinomycetemcomitans* and to determine its effect on the host transcriptome and metabolome using a gum cell – bacteria co-culture model.

MATERIALS AND METHODS

Monolaurin

For carrying out the experiments, the monolaurin utilized was 1-lauroyl-rac-glycerol (Sigma-Aldrich, St. Louis, MO, United States). For dilution, sterilized deionized water was used as the vehicle.

Cells and Bacterial Strain

Human gingival fibroblast – HGF-1 (ATCC® CRL-2014) were cultured in Dulbecco's Modified Eagle's Medium (DMEM) (Lonza, Walkersville, MD, United States) with 10% Fetal Bovine Serum (FBS) (Lonza, Walkersville, MD, United States). Human gingival epithelial cells (keratinocyte OBA-9) were cultured in specific medium for keratinocytes, Defined Keratinocyte-SFM (Life Technologies, Carlsbad, CA, United States) (Oda and Watson, 1990; Kusumoto et al., 2004).

Aggregatibacter actinomycetemcomitans (strain D7S-1) was cultivated from a subgingival plaque from an African-American female patient diagnosed with generalized aggressive periodontitis (Chen et al., 2010). The bacteria were grown in Trypticase Soy Broth (TSB) (Becton Dickinson, Franklin Lakes, NJ, United States).

Antimicrobial Activity

Monolaurin antimicrobial activity was evaluated in *A. actinomycetemcomitans* after 24 h of treatment. Microorganisms were inoculated [1×10^6 colony-forming unit per milliliter (CFU/mL) in a 96-well microtiter plate with TSB (Becton Dickinson, Franklin Lakes, NJ, United States)] and monolaurin was immediately added in various concentrations (0.5–1,000 μM) to determine the minimum inhibitory concentration (MIC) (Branco-de-Almeida et al., 2011). Microplates were maintained in a humidified incubator at 37°C and 5% CO_2. After incubation, bacterial growth was assayed by measurement of absorbance at 660 nm. MIC was defined as the lowest concentration of monolaurin that had restricted growth to a level, 0.05 at 660 nm (no visible growth).

Cytotoxicity Assay

In vitro cytotoxicity effect was measured by the fluorometric resazurin method (O'Brien et al., 2000). OBA-9 or HGF-1 cells were seeded (1×10^5 cells/mL) in 96-well microtiter plates and maintained in a humidified incubator at 37°C and 5% CO_2. After 24 h, cell morphology was observed under an inverted microscope (EVOS FL Life Technologies, Carlsbad, CA, United States) to confirm that they had adhered to the bottom of each well and were presenting proper morphology. The monolaurin (0.5–1,000 μM) was added to the cell cultures and incubated at 37°C and 5% CO_2. After 24 h, the medium was discarded, cells were washed with room temperature phosphate buffered saline (PBS) (Lonza, Walkersville, MD, United States), and fresh, room temperature medium was added with resazurin (Cell Titer Blue Viability Assay – Promega Corp., Madison, WI, United States). Subsequently, the plate was incubated at 37°C and 5% CO_2. After 4 h, the contents

of the wells were transferred to a new microplate and the fluorescence was read in a microplate reader (SpectraMax M5, Molecular Devices, Sunnyvale, CA, United States) with excitation 550 nm, emission 585 nm, and cut off 570 nm (Pasetto et al., 2014). To calculate the results and obtain the LD_{50} (Lethal Dose), we performed a non-linear regression the program MasterPlex ReaderFit (Hitachi Solutions America).

Dual-Chamber Model

A dual-chamber, oral cell/bacteria co-culture was used to investigate the immunological effects of monolaurin (Silva et al., 2017). HGF-1 cells (1×10^5) were seed in the basal chamber of a 24-well plate. Transwell inserts (8 μm pore × 0.3 cm^2 of culture surface – Greiner Bio-One, Monroe, NC, United States) were positioned in each well and OBA-9 cells (1×10^5) were seeded into the inserts. DMEM (Lonza, Walkersville, MD, United States) with 10% FBS (Lonza, Walkersville, MD, United States) was used for the medium. The plates were incubated at 37°C in humid air containing 5% CO_2 for 24 h (Silva et al., 2017). Trans Epithelial Electric Resistance (TEER) of each cell layer was measured with a Millicell-ERS Volt-Ohm Meter (Millipore, Bedford, MA, United States). Cell layer confluence in the Transwell insert was measured daily until reaching optimal TEER (>150 Ohm/cm^2) after 48 h. Once reaching optimal TEER, the media of the basal chamber and the insert were replaced with new media containing *A. actinomycetemcomitans* (1×10^6 CFU/mL). Medium containing the microorganism was added to the insert, passing through the upper layer of cells (OBA-9) and reaching the bottom cell layer (HGF-1). Immediately after the inoculation of oral cell/bacteria co-culture with *A. actinomycetemcomitans* the monolaurin treatments (25 and 50 μM) were added and the plate was incubated at 37°C in humid air containing 5% CO_2. The time of exposure of the microorganism to monolaurin was 24 h. Each experiment was repeated three times with two replicates per group ($n = 6$). The experiment was divided in three groups: (1) Control – oral cell/bacteria co-culture with Aa inoculated and no treatment; (2) Mono 25 – oral cell/bacteria co-culture with Aa inoculated and treated with 25 μM of monolaurin; (3) Mono 50 – oral cell/bacteria co-culture with Aa inoculated and treated with 50 μM of monolaurin.

Collecting Samples for Analysis

After the treatment period, liquid contents from each well was collected and centrifuged at 1,200 rpm for 10 min. Following centrifugation, supernatant was divided into two aliquots for enzyme-linked immunosorbent assay (ELISA) and metabolome analysis. RNA was isolated from the remaining cell layers of HGF-1 and OBA-9 (surface of the wells and inserts) for gene analysis in quantitative real-time PCR.

ELISA Assay

Inflammatory cytokines were determined using a commercial ELISA (Multi-Analyte ELISArray – Qiagen, Valencia, CA, United States). The cytokines were measured by standard ELISA protocol using a panel of 12 inflammatory cytokines: interleukin-1 alpha (IL-1α), interleukin-1 beta (IL-1β), interleukin-2 (IL-2), interleukin-4 (IL-4), interleukin-6 (IL-6), interleukin-8 (IL-8), interleukin-10 (IL-10), interleukin-12 (IL-12), interleukin-17 alpha (IL-17α), interferon gamma (IFNγ), tumor necrosis factor alpha (TNFα), Granulocyte-Macrophage Colony Stimulating Factor (GM-CSF). Cytokines that presented the greatest change in concentration were selected for detailed analysis. These cytokines were analyzed using a standard ELISA protocol (Single Analyte ELISA Kit – Qiagen, Valencia, CA, United States).

Gene Expression – Quantitative Real-Time PCR

Total RNA was extracted through a commercial RNA purification kit (Mini Kit Qiagen RNeasy Protocol – Qiagen, Valencia, CA, United States) and the purity and quantity were measured in a NanoPhotometer P360 (Implen, Westlake Village, CA, United States). Total RNA was converted into single-stranded cDNA using a high-capacity reverse transcription kit (QuantiTec Reverse Transcription Kit – Qiagen, Valencia, CA, United States). An array for evaluation of gene expression of the inflammatory response was completed by quantitative real-time PCR (Prime PCR Pathway Plate/Acute Inflammation Response – Bio-Rad, Hercules, CA, United States) from the cDNA obtained. Based on these results, six genes/primers were selected for detailed study: interleukin 1 alpha (IL-1α), interleukin 6 (IL-6), interleukin 18 (IL-18), caspase 3 (CASP3), matrix metallopeptidase 1 (MMP-1), and tumor necrosis factor (TNF) (QuantiTect Primer Assay – Qiagen, Valencia, CA, United States). QuantiTect SYBR Green PCR Kits (Qiagen, Valencia, CA, United States) were used to determine the gene expression of the selected primers. The reaction product was quantified by relative quantification using Glyceraldehyde 3-phosphate dehydrogenase (GAPDH) as the reference gene. Data were analyzed as fold-change compared to control. The cycle threshold was calculated and interpreted using CFX Connect (Bio-Rad, Hercules, CA, United States) (Pfaffl, 2001).

Metabolome Analysis

Samples for metabolome analysis were treated as described by Silva et al. (2017) and analyzed at the West Coast Metabolomics Center (UC Davis Genome Center, Davis, CA, United States) by means of gas chromatography/mass spectrometry (Agilent 6890, Santa Clara, CA/Leco Pegasus IV, St. Joseph, MI, United States). Then, the metabolites were compared with the standard library for proper identification (Fiehn and Kind, 2007).

Statistical Analysis

Data were expressed as mean ± standard deviation. The comparison between the groups was made through analysis of variance (ANOVA) and when a difference was determined, the Bonferroni test was applied. Data were analyzed using GraphPad Prism (version 5.01, GraphPad Software, San Diego, United States). The level of significance was set at $p < 0.05$.

RESULTS

Antimicrobial Activity and Cytotoxicity Assay

In order to determine antimicrobial activity of monolaurin, a range of 0.5–1,000 μM was tested. Antibacterial activity was detected at 25–50 μM. The minimum inhibitory concentration (MIC) was established between 25 and 50 μM. The cytotoxicity assays were conducted in HGF-1 and OBA-9 cells and the results are shown in **Figure 1**. For HGF-1 the LD_{50} was 146 μM of monolaurin and for OBA-9 the LD_{50} was 69 μM of monolaurin.

ELISA

Enzyme-linked immunosorbent assay (ELISA) results are presented in **Figure 2**. Both treatments (25 and 50 μM) of monolaurin increased the concentrations of GM-CSF and IL-1α. The concentrations of IL-6 and IL-10 increased only with the 50 μM treatment. On the other hand, IL-1β decreased as a function of monolaurin.

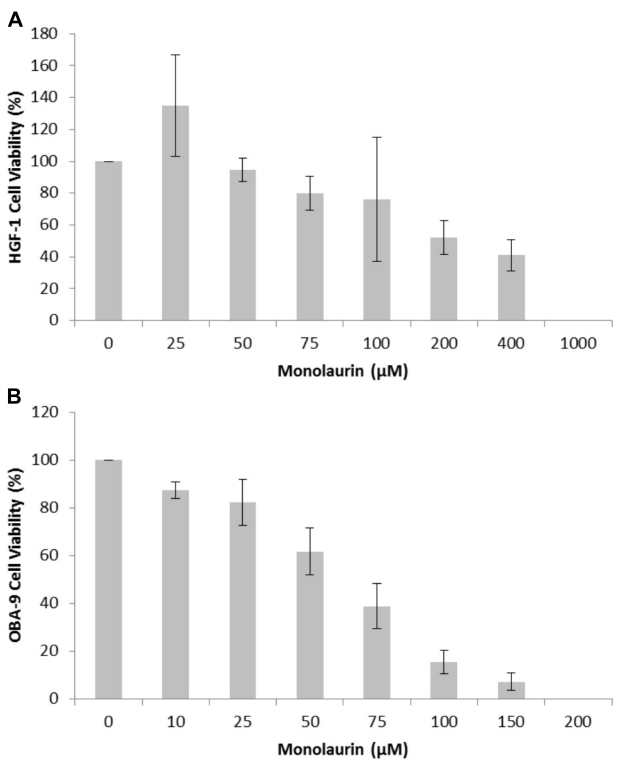

FIGURE 1 | Cytotoxicity assay of cells treated with different doses of monolaurin in an oral cell/bacteria co-culture inoculated with *A. actinomycetemcomitans*: **(A)** HGF-1 cell (fibroblasts); **(B)** OBA-9 cell (keratinocytes). Cell viability was presented in percentage (%) ± standard deviation. Control group = 100% viability, $n = 6$. Non-treated cells were considered as 100% viability; DMSO was used as positive control to demonstrate an appropriate system-cell response (100% cytotoxicity – data not shown).

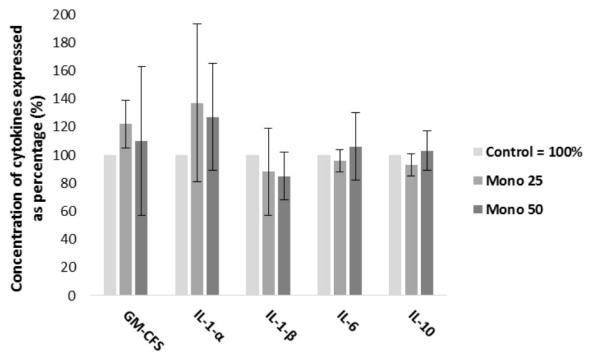

FIGURE 2 | Percent concentrations of GM-CSF, IL-1α, IL-1-β, IL-6, and IL-10 by ELISA, obtained from cell culture supernatant. Oral cell co-culture inoculated with *A. actinomycetemcomitans* and treated with 25 μM of monolaurin (Mono 25) or 50 μM of monolaurin (Mono 50) compared with the control group. Control group is oral cell co-culture inoculated with *A. actinomycetemcomitans* and no treatment. The control group mean is expressed as 100% and treated groups have their mean relative to the control group. Mean ± standard deviation; $n = 4$.

Gene Expression – Quantitative Real-Time PCR

Quantitative real-time PCR results are presented in **Figures 3**, **4**. The genes IL-1α, IL-6, IL-18, and TNF analyzed in HGF-1 showed a decreased expression ($p < 0.05$) when treated with 25 or 50 μM of monolaurin compared with group Control (**Figures 3A–C,F**). CASP3 and MMP-1 genes showed no difference (**Figures 3D,E**).

Keratinocytes presented a higher IL-6, IL-18, and TNF gene expression ($p < 0.05$) when treated with 25 or 50 μM of monolaurin compared with the control group (**Figures 4B,C,F**). IL-1α gene decreased expression ($p < 0.05$) in the group treated with both concentrations (**Figure 4A**). CASP-3 and MMP-1 genes showed no difference (**Figures 4D,E**).

Metabolome

The metabolome study returned a total of 283 metabolites. Of these, 120 were identified and only 6 presented a statistical difference as a function of monolaurin treatment. Some metabolites presented significantly altered concentrations (**Figure 5**). It was observed that both treatments of monolaurin increased the production of glycerol (**Figure 5D**) and pyruvic acid (**Figure 5F**) when compared to control. On the other hand, the 2-deoxytetronic acid NIST (**Figure 5A**) showed the opposite result, lower concentrations of this metabolite, in function of the treatment with 25 and 50 μM of monolaurin. The 50 μM monolaurin treatment group presented lower concentrations of 4-aminobutyric acid (**Figure 5B**), glyceric acid (**Figure 5C**), and pinitol (**Figure 5E**), against the control group.

DISCUSSION

Periodontal disease is known to be a widespread oral health problem across the world. Several methods for prevention and treatment of oral diseases have been used over time and new

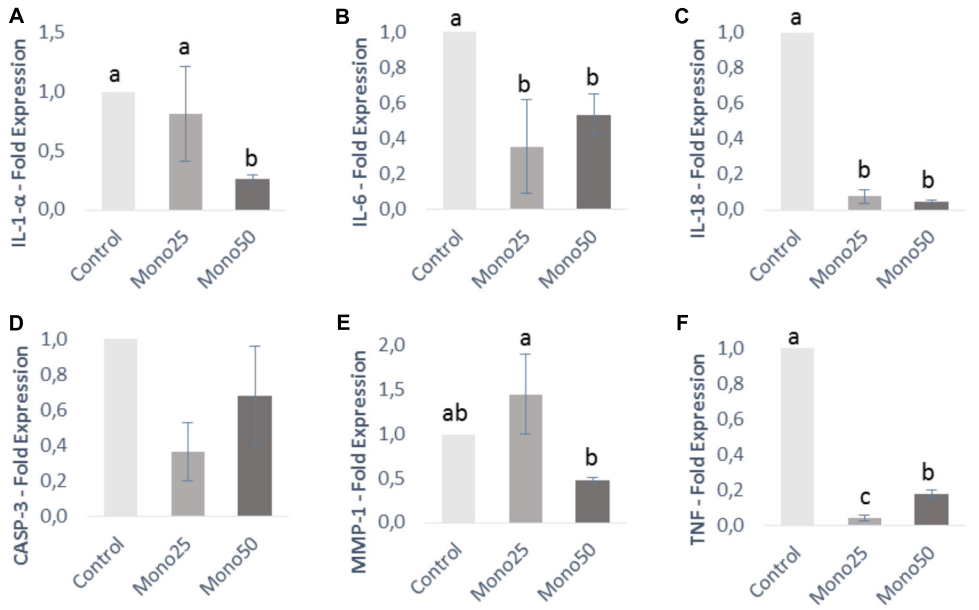

FIGURE 3 | Relative expression of genes from HGF-1 cells (fibroblasts) by quantitative PCR: **(A)** IL-1α; **(B)** IL-6; **(C)** IL-18; **(D)** CASP3; **(E)** MMP-1; **(F)** TNF. Oral cell/bacteria co-culture inoculated with *A. actinomycetemcomitans* and treated with different doses of monolaurin (25 μM – Mono 25 or 50 μM – Mono 50). Control group is oral cell co-culture inoculated with *A. actinomycetemcomitans* and no treatment. The control group has their mean expressed equal to 1 and treated groups have their mean relative to the control group. Different letters (a, b, and c) indicate statistical difference between groups. The results were expressed by mean ± standard deviation; $n = 6$ and $p < 0.05$.

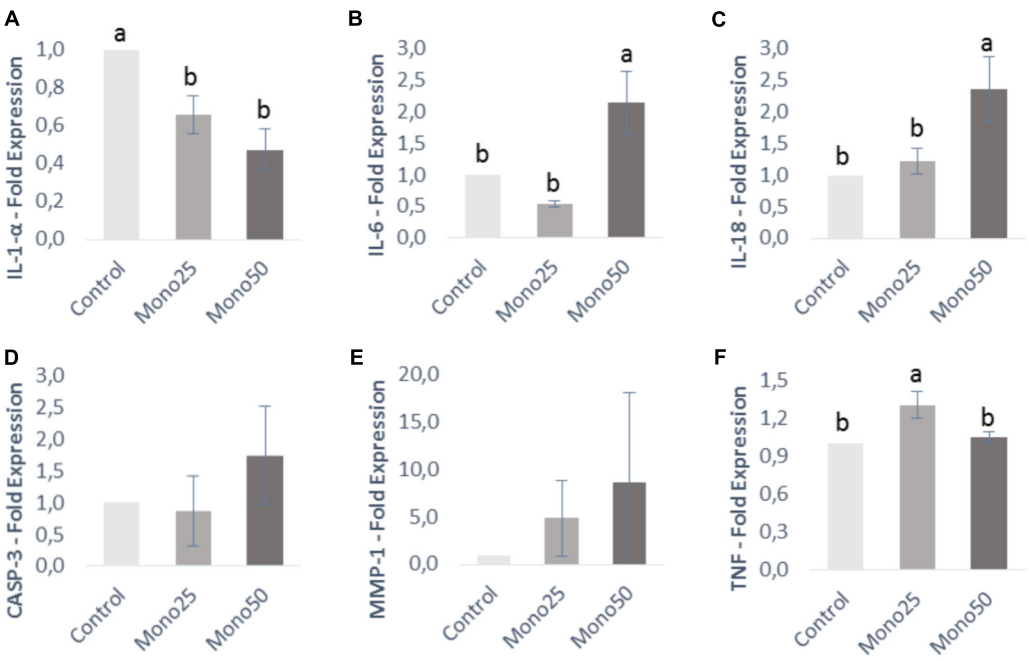

FIGURE 4 | Relative expression of genes from OBA-9 cells (keratinocytes) by quantitative PCR: **(A)** IL-1α; **(B)** IL-6; **(C)** IL-18; **(D)** CASP3; **(E)** MMP-1; **(F)** TNF. Oral cell/bacteria co-culture inoculated with *A. actinomycetemcomitans* and treated with different doses of monolaurin (25 μM – Mono 25 or 50 μM – Mono 50). Control group is oral cell co-culture inoculated with *A. actinomycetemcomitans* and no treatment. The control group has their mean expressed equal to 1 and treated groups have their mean relative to the control group. Different letters (a, b, and c) indicate statistical difference between groups. The results were expressed by mean ± standard deviation; $n = 6$ and $p < 0.05$.

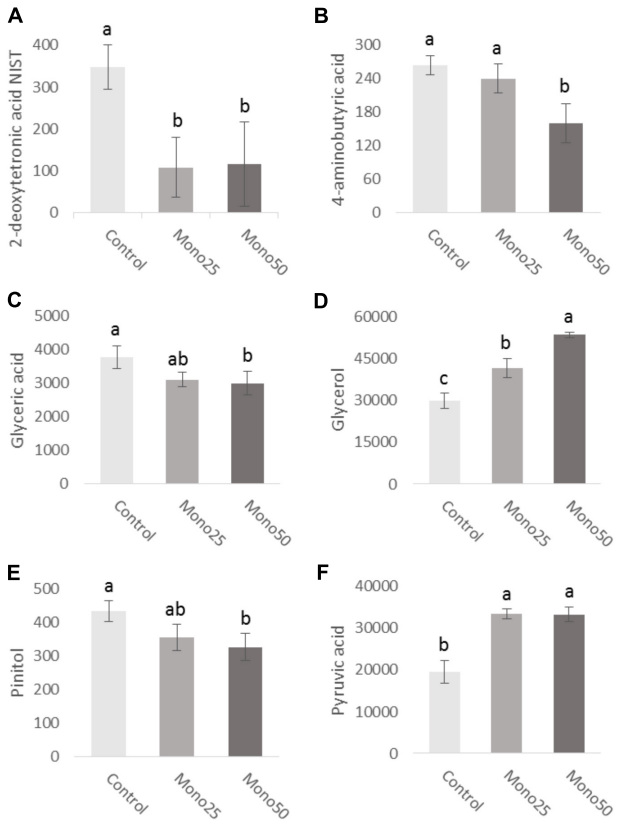

FIGURE 5 | Metabolites obtained from cell culture supernatant (HGF-1 and OBA-9 co-culture cells): **(A)** 2-deoxytetronic acid NIST; **(B)** 4-aminobutyric acid; **(C)** glyceric acid; **(D)** glycerol; **(E)** pinitol; **(F)** pyruvic acid. Oral cell/bacteria co-culture model inoculated with *A. actinomycetemcomitans* and treated with different doses of monolaurin (25 μM – Mono 25 or 50 μM – Mono 50). Control group is oral cell co-culture inoculated with *A. actinomycetemcomitans* and no treatment. Different letters (a, b, and c) indicate statistical difference between groups. The data is expressed in relative peak heights (mAU) from HPLCMS analysis, which are unitless (mean ± standard deviation); $n = 4$ and $p < 0.05$.

technologies are being developed. However, little attention has been given to the understanding of how periodontal structures are affected and how these structures react to different types of treatments (Balloni et al., 2016). Currently, some mouthwashes and toothpastes have been used as topical antimicrobial agents (Barnett, 2003). However, monolaurin is not listed as an active ingredient in commercially available mouthwashes. Monolaurin has been shown to possess diverse biological activities, such as antibacterial and antiviral properties (Preuss et al., 2005; Li et al., 2009; Tangwatcharin and Khopaibool, 2012; Seleem et al., 2016). In our *in vitro* study, susceptibility assays of monolaurin showed inhibition of microorganism grow at 25–50 μM with minimal cytotoxicity. The putative pathways by which monolaurin affects Aa may involve: (i) increased membrane permeability and cell lysis, (ii) disruption of electron transport chain and uncoupling oxidative phosphorylation, and (iii) inhibition of membrane enzymatic activities and nutrient uptake (Yoon et al., 2018). In addition, co-culture supernatant were assessed for expression of host pro-inflammatory cytokines, gene expression of inflammatory cytokines and metabolomic profile in human cells infected with *A. actinomycetemcomitans*.

The gingival tissue comprises the oral epithelium and superficial underlying connective tissue. These tissues are sites of initiation for inflammatory processes and the first to be affected by biofilm (Balloni et al., 2016). Gingival epithelial cells represent a physical barrier against bacteria and are involved in processes of innate immunity (Jang et al., 2015). Keratinocytes and fibroblasts represent the major cell types present in gingival epithelial tissues. They interact directly with pathogenic microorganisms and are able to express a variety of cytokines and chemokines such as IL-1α, IL-6, IL-8, TNF, among others (Bodet et al., 2007; Groeger and Meyle, 2015). In the present study, there was a decrease in the gene expression of IL-1α, IL-6, and IL-18 and TNF in HGF-1 and an increase in the expression of IL-6, IL-18, and TNF in OBA-9 cells treated with monolaurin indicating a positive modulation in the inflammatory response of these cells.

Interleukin-1 alpha is a polypeptide that plays several roles in tissue homeostasis, immunity and has a proinflammatory nature. It is produced mainly by macrophages and monocytes, but also epithelial cells and fibroblasts (Champagne et al., 2003; Balloni et al., 2016). IL-1α plays a critical role in protecting the body against invaders, such as bacteria and viruses, and is involved in extracellular matrix and bone metabolism (bone resorption, disintegration, and removal of bone tissue that is no longer needed). Therefore, IL-1α is considered a marker of periodontal disease (Govindarajan et al., 2015; Groeger and Meyle, 2015).

Here, we observed a decrease in the expression of IL-1α by HGF-1 and OBA-9 cells in the monolaurin-treated groups which may be related to a beneficial inflammatory response since, elevated levels of IL-1α and IL-1β in the gingival crevicular fluid are commonly found in patients with periodontal disease. This increased production of IL-1 is associated with a higher inflammatory response to the bacterial stimulus, resulting in more severe disease as well as an unfavorable response to treatments (Kornman et al., 1997; Engebretson et al., 1999; McGuire and Nunn, 1999; Shirodaria et al., 2000).

Interleukin-6 is associated with acute phase reactions and is usually secreted concomitantly with other proinflammatory cytokines. Some authors relate this cytokine to the destruction of periodontal tissue by favoring the accumulation of inflammatory cells and by activating and releasing inflammatory mediators that in turn accentuate the response to periodontal disease (de Lima Oliveira et al., 2012; Zhang et al., 2016).

The kinetics of production of IL-18 against the action of bacteria is rapid, according to its proinflammatory nature. It plays a central role in systemic and local inflammation (Biet et al., 2002). One study evaluated IL-18 levels in crevicular gingival fluid in four groups of patients: healthy periodontium, gingivitis, chronic periodontitis, and aggressive periodontitis. The results demonstrated that IL-18 concentration in the crevicular gingival fluid was low in the group with healthy periodontium and progressively increased in groups from gingivitis, to aggressive periodontitis, and finally chronic periodontitis. As the inflammation increased, there was a concomitant increase in IL-18 level (Nair et al., 2016). In the current study, treatment with

monolaurin decreased the IL-18 gene expression in fibroblasts, however, an opposite result was observed in keratinocytes, where IL-18 expression was increased in the group treated with 50 μM monolaurin.

Tumor necrosis factor plays a central role in periodontitis, being associated with the disease because of its ability to induce destruction of connective tissue and its effects on bone resorption through the activation of osteoclasts. Thus, TNF is one of the first proinflammatory cytokines produced in response to infection by pathogenic bacteria (Stashenko et al., 1987; de Lima Oliveira et al., 2012; Zhang et al., 2016). Here, the authors observed a reduction in the gene expression of TNF in monolaurin treated fibroblasts. On the other hand, in keratinocytes, TNF expression was higher in cells treated with 25 μM of this compound. Animal models challenged with *P. gingivalis* were treated with antimicrobial drugs (chlorhexidine, minocycline, and doxycycline) in order to evaluate its effect on the inflammatory response. Minocycline induced higher levels of TNF while chlorhexidine reduced TNF levels, this result led the authors to believe that these agents modified the inflammatory response to *P. gingivalis* regardless of its antimicrobial effect, each in its own way (Houri-Haddad et al., 2008). Overall, monolaurin modulate the expression of inflammatory cytokines, suggesting it may have a modulatory role on the host pro-inflammatory response to help eradicate the bacterial infection. Similarly, previous studies suggested that monolaurin play a significant role on T cell functions and signaling by altering TCR-induced LAT, PLC-γ, and AKT cluster formation PI3K-AKT signaling axis, and calcium influx which ultimately decrease the cytokine production (Zhang et al., 2016).

The knowledge of the metabolic profile can contribute to understanding of the periodontal disease course as well as identify possible metabolites as biomarkers. This study evaluated the effects caused by monolaurin on the cellular metabolome and found significant variations. Relative quantification revealed lower levels of 2-deoxytetronic acid NIST, 4-aminobutyric acid, glyceric acid and pinitol, and higher levels of glycerol and pyruvic acid in cells treated with 25 or 50 μM monolaurin. Analysis of fibroblast metabolome (HGF) treated with IL-1β in combination with titanium dioxide nanoparticles (TiO_2 NPs), demonstrated that IL-1β induction reduced concentrations of primary metabolites, especially those of urea cycle, polyamine, S-adenosylmethionine and glutathione synthetic pathways. The addition of TiO_2 NPs further increased these metabolic changes induced by IL-1β. These findings may be useful for the future establishment of new metabolic markers and therapeutic strategy for gingival inflammations (Garcia-Contreras et al., 2015). One study compared the salivary metabolic profile of healthy patients and patients with periodontal disease. Changes in several classes of metabolites have been observed in individuals with periodontal disease. According to the authors, such changes reflected an increase in host–bacterial interactions in the diseased state (Barnes et al., 2011).

CONCLUSION

In summary, this study indicates that monolaurin possesses antimicrobial activity and modulates the host immune response and modulates production when administered for 24 h in a dual-chamber model inoculated with *A. actinomycetemcomitans*. These findings demonstrate that monolaurin could be considered a potential candidate for *in vivo* studies, which may translate into its potential clinical use to treat pathogenic microbe–host interactions.

AUTHOR CONTRIBUTIONS

VS conceived and designed the experiments, performed the experiments, analyzed the data, performed the statistical analysis, and wrote the paper. LP conceived and designed the experiments, contributed to reagents, materials, and analysis tools, analyzed and critically reviewed the data. MS and SP performed the experiments and analyzed the data. JM analyzed the data, and critically reviewed and interpreted the data. RM conceived and designed the experiments, contributed to reagents, materials, and analysis tools, performed the experiments, analyzed and critically reviewed the data. All authors contributed to manuscript revision, read, and approved the submitted version.

ACKNOWLEDGMENTS

The authors thank to CAPES (Coordination of Improvement of Higher Education Personnel), FAPEMIG (Research Sponsoring Agency of the State of Minas Gerais), and CNPq (National Counsel of Technological and Scientific Development) for support. Research reported in this publication was also supported by the NIH/NCCIH under award number AT006507. The content is solely the responsibility of the authors and does not represent the official views of the National Institutes of Health.

SUPPLEMENTARY MATERIAL

The Supplementary Material for this article can be found online at: https://www.frontiersin.org/articles/10.3389/fmicb.2018.02638/full#supplementary-material

REFERENCES

Aimetti, M. (2014). Nonsurgical periodontal treatment. *Int. J. Esthet. Dent.* 9, 251–267.

Balloni, S., Locci, P., Lumare, A., and Marinucci, L. (2016). Cytotoxicity of three commercial mouthrinses on extracellular matrix metabolism and human gingival cell behaviour. *Toxicol. Vitr.* 34, 88–96. doi: 10.1016/j.tiv.2016.03.015

Barnes, V. M., Ciancio, S. G., Shibly, O., Xu, T., Devizio, W., Trivedi, H. M., et al. (2011). Metabolomics reveals elevated macromolecular degradation in periodontal disease. *J. Dent. Res.* 90, 1293–1297. doi: 10.1177/0022034511416240

Barnett, M. L. (2003). The role of therapeutic antimicrobial mouthrinses in clinical practice: control of supragingival plaque and gingivitis. *J. Am. Dent. Assoc.* 134, 699–704. doi: 10.14219/jada.archive.2003.0255

Biet, F., Locht, C., and Kremer, L. (2002). Immunoregulatory functions of interleukin 18 and its role in defense against bacterial pathogens. *J. Mol. Med.* 80, 147–162. doi: 10.1007/s00109-001-0307-1

Bodet, C., Andrian, E., Tanabe, S.-I., and Grenier, D. (2007). *Actinobacillus actinomycetemcomitans* lipopolysaccharide regulates matrix metalloproteinase, tissue inhibitors of matrix metalloproteinase, and plasminogen activator production by human gingival fibroblasts: a potential role in connective tissue destructio. *J. Cell. Physiol.* 212, 189–194. doi: 10.1002/jcp.21018

Branco-de-Almeida, L. S., Murata, R. M., Franco, E. M., dos Santos, M. H., de Alencar, S. M., Koo, H., et al. (2011). Effects of 7-epiclusianone on *Streptococcus mutans* and caries development in rats. *Planta Med.* 77, 40–45. doi: 10.1055/s-0030-1250121

Carpo, B. G., Verallo-Rowell, V. M., and Kabara, J. (2007). Novel antibacterial activity of monolaurin compared with conventional antibiotics against organisms from skin infections: an in vitro study. *J. Drugs Dermatol.* 6, 991–998.

Champagne, C. M. E., Buchanan, W., Reddy, M. S., Preisser, J. S., Beck, J. D., and Offenbacher, S. (2003). Potential for gingival crevice fluid measures as predictors of risk for periodontal diseases. *Periodontol. 2000* 31, 167–180. doi: 10.1034/j.1600-0757.2003.03110.x

Chapple, I. L. C., and Genco, R. (2013). Diabetes and periodontal diseases: consensus report of the Joint EFP/AAP Workshop on Periodontitis and Systemic Diseases. *J. Clin. Periodontol.* 40(Suppl. 1), S106–S112. doi: 10.1111/jcpe.12077

Chen, C., Kittichotirat, W., Chen, W., Downey, J. S., Si, Y., and Bumgarner, R. (2010). Genome sequence of naturally competent *Aggregatibacter actinomycetemcomitans* serotype a strain D7S-1. *J. Bacteriol.* 192, 2643–2644. doi: 10.1128/JB.00157-10

Cortelli, S. C., Costa, F. O., Kawai, T., Aquino, D. R., Franco, G. C. N., Ohara, K., et al. (2009). Diminished treatment response of periodontally diseased patients infected with the JP2 clone of Aggregatibacter (Actinobacillus) actinomycetemcomitans. *J. Clin. Microbiol.* 47, 2018–2025. doi: 10.1128/JCM.00338-09

Coussens, L. M., and Werb, Z. (2002). Inflammation and cancer. *Nature* 420, 860–867. doi: 10.1038/nature01322

da Silva-Boghossian, C. M., do Souto, R. M., Luiz, R. R., and Colombo, A. P. V. (2011). Association of red complex, *A. actinomycetemcomitans* and non-oral bacteria with periodontal diseases. *Arch. Oral Biol.* 56, 899–906. doi: 10.1016/j.archoralbio.2011.02.009

de Almeida, J. M., Theodoro, L. H., Bosco, A. F., Nagata, M. J. H., Oshiiwa, M., and Garcia, V. G. (2007). Influence of photodynamic therapy on the development of ligature-induced periodontitis in rats. *J. Periodontol.* 78, 566–575. doi: 10.1902/jop.2007.060214

de Lima Oliveira, A. P., de Faveri, M., Gursky, L. C., Mestnik, M. J., Feres, M., Haffajee, A. D., et al. (2012). Effects of periodontal therapy on GCF cytokines in generalized aggressive periodontitis subjects. *J. Clin. Periodontol.* 39, 295–302. doi: 10.1111/j.1600-051X.2011.01817.x

Engebretson, S. P., Lamster, I. B., Herrera-Abreu, M., Celenti, R. S., Timms, J. M., Chaudhary, A. G., et al. (1999). The influence of interleukin gene polymorphism on expression of interleukin-1beta and tumor necrosis factor-alpha in periodontal tissue and gingival crevicular fluid. *J. Periodontol.* 70, 567–573. doi: 10.1902/jop.1999.70.6.567

Fiehn, O., and Kind, T. (2007). Metabolite profiling in blood plasma. *Methods Mol. Biol.* 358, 3–17. doi: 10.1007/978-1-59745-244-1_1

Filoche, S., Wong, L., and Sissons, C. H. (2010). Oral biofilms: emerging concepts in microbial ecology. *J. Dent. Res.* 89, 8–18. doi: 10.1177/0022034509351812

Fu, X., Feng, F., and Huang, B. (2006). Physicochemical characterization and evaluation of a microemulsion system for antimicrobial activity of glycerol monolaurate. *Int. J. Pharm.* 321, 171–175. doi: 10.1016/j.ijpharm.2006.05.019

Gafan, G. P., Lucas, V. S., Roberts, G. J., Petrie, A., Wilson, M., and Spratt, D. A. (2004). Prevalence of periodontal pathogens in dental plaque of children. *J. Clin. Microbiol.* 42, 4141–4146. doi: 10.1128/JCM.42.9.4141-4146.2004

Garcia-Contreras, R., Sugimoto, M., Umemura, N., Kaneko, M., Hatakeyama, Y., Soga, T., et al. (2015). Alteration of metabolomic profiles by titanium dioxide nanoparticles in human gingivitis model. *Biomaterials* 57, 33–40. doi: 10.1016/j.biomaterials.2015.03.059

Govindarajan, K., Muthukumar, S., and Rangarao, S. (2015). Relationship between interleukin 1α levels in the gingival crevicular fluid in health and in inflammatory periodontal disease and periodontal inflamed surface area: a correlative study. *J. Indian Soc. Periodontol.* 19, 618–623. doi: 10.4103/0972-124X.162197

Groeger, S. E., and Meyle, J. (2015). Epithelial barrier and oral bacterial infection. *Periodontol. 2000* 69, 46–67. doi: 10.1111/prd.12094

Gurav, A. N. (2014). The association of periodontitis and metabolic syndrome. *Dent. Res. J.* 11, 1–10.

Haraszthy, V. I., Hariharan, G., Tinoco, E. M., Cortelli, J. R., Lally, E. T., Davis, E., et al. (2000). Evidence for the role of highly leukotoxic Actinobacillus actinomycetemcomitans in the pathogenesis of localized juvenile and other forms of early-onset periodontitis. *J. Periodontol.* 71, 912–922. doi: 10.1902/jop.2000.71.6.912

Houri-Haddad, Y., Halabi, A., and Soskolne, W. A. (2008). Inflammatory response to chlorhexidine, minocycline HCl and doxycycline HCl in an in vivo mouse model. *J. Clin. Periodontol.* 35, 783–788. doi: 10.1111/j.1600-051X.2008.01290.x

Irfan, U. M., Dawson, D. V., and Bissada, N. F. (2001). Epidemiology of periodontal disease: a review and clinical perspectives. *J. Int. Acad. Periodontol.* 3, 14–21.

Isaacs, C. E. (2001). The antimicrobial function of milk lipids. *Adv. Nutr. Res.* 10, 271–285.

Jang, D. H., Bhawal, U. K., Min, H.-K., Kang, H. K., Abiko, Y., and Min, B.-M. (2015). A transcriptional roadmap to the senescence and differentiation of human oral keratinocytes. *J. Gerontol. A Biol. Sci. Med. Sci.* 70, 20–32. doi: 10.1093/gerona/glt212

Kornman, K. S., Crane, A., Wang, H. Y., di Giovine, F. S., Newman, M. G., Pirk, F. W., et al. (1997). The interleukin-1 genotype as a severity factor in adult periodontal disease. *J. Clin. Periodontol.* 24, 72–77. doi: 10.1111/j.1600-051X.1997.tb01187.x

Kusumoto, Y., Hirano, H., Saitoh, K., Yamada, S., Takedachi, M., Nozaki, T., et al. (2004). Human gingival epithelial cells produce chemotactic factors interleukin-8 and monocyte chemoattractant protein-1 after stimulation with *Porphyromonas gingivalis* via toll-like receptor 2. *J. Periodontol.* 75, 370–379. doi: 10.1902/jop.2004.75.3.370

Li, Q., Estes, J. D., Schlievert, P. M., Duan, L., Brosnahan, A. J., and Southern, P. J. (2009). Glycerol monolaurate prevents mucosal SIV transmission. *Nature* 458, 1034–1038. doi: 10.1038/nature07831

Loos, B. G. (2005). Systemic markers of inflammation in periodontitis. *J. Periodontol.* 76, 2106–2115. doi: 10.1902/jop.2005.76.11-S.2106

McGuire, M. K., and Nunn, M. E. (1999). Prognosis versus actual outcome. IV. The effectiveness of clinical parameters and IL-1 genotype in accurately predicting prognoses and tooth survival. *J. Periodontol.* 70, 49–56. doi: 10.1902/jop.1999.70.1.49

Michaud, D. S., Joshipura, K., Giovannucci, E., and Fuchs, C. S. (2007). A prospective study of periodontal disease and pancreatic cancer in US male health professionals. *J. Natl. Cancer Inst.* 99, 171–175. doi: 10.1093/jnci/djk021

Moutsopoulos, N. M., and Madianos, P. N. (2006). Low-grade inflammation in chronic infectious diseases: paradigm of periodontal infections. *Ann. N. Y. Acad. Sci.* 1088, 251–264. doi: 10.1196/annals.1366.032

Nair, V., Bandyopadhyay, P., Kundu, D., and Das, S. (2016). Estimation of interleukin-18 in the gingival crevicular fluid and serum of Bengali population with periodontal health and disease. *J. Indian Soc. Periodontol.* 20, 260–264. doi: 10.4103/0972-124X.183098

O'Brien, J., Wilson, I., Orton, T., and Pognan, F. (2000). Investigation of the Alamar Blue (resazurin) fluorescent dye for the assessment of mammalian cell cytotoxicity. *Eur. J. Biochem.* 267, 5421–5426. doi: 10.1046/j.1432-1327.2000.01606.x

Oda, D., and Watson, E. (1990). Human oral epithelial cell culture I. Improved conditions for reproducible culture in serum-free medium. In vitro cell. *Dev. Biol.* 26, 589–595. doi: 10.1007/BF02624208

Oringer, R. J. (2002). Modulation of the host response in periodontal therapy. *J. Periodontol.* 73, 460–470. doi: 10.1902/jop.2002.73.4.460

Pasetto, S., Pardi, V., and Murata, R. M. (2014). Anti-HIV-1 activity of flavonoid myricetin on HIV-1 infection in a dual-chamber in vitro model. *PLoS One* 9:e115323. doi: 10.1371/journal.pone.0115323

Paster, B. J., Olsen, I., Aas, J. A., and Dewhirst, F. E. (2006). The breadth of bacterial diversity in the human periodontal pocket and other oral sites. *Periodontol. 2000* 2006, 80–87. doi: 10.1111/j.1600-0757.2006.00174.x

Peterson, M. L., and Schlievert, P. M. (2006). Glycerol monolaurate inhibits the effects of Gram-positive select agents on eukaryotic cells. *Biochemistry* 45, 2387–2397. doi: 10.1021/bi051992u

Pfaffl, M. W. (2001). A new mathematical model for relative quantification in real-time RT-PCR. *Nucleic Acids Res.* 29:e45. doi: 10.1093/nar/29.9.e45

Preuss, H. G., Echard, B., Enig, M., Brook, I., and Elliott, T. B. (2005). Minimum inhibitory concentrations of herbal essential oils and monolaurin for gram-positive and gram-negative bacteria. *Mol. Cell. Biochem.* 272, 29–34. doi: 10.1007/s11010-005-6604-1

Projan, S. J., Brown-Skrobot, S., Schlievert, P. M., Vandenesch, F., and Novick, R. P. (1994). Glycerol monolaurate inhibits the production of beta-lactamase, toxic shock toxin-1, and other staphylococcal exoproteins by interfering with signal transduction. *J. Bacteriol.* 176, 4204–4209. doi: 10.1128/jb.176.14.4204-4209.1994

Rakić, M., Zelić, K., Pavlica, D., Hadzimihajlović, M., Milasin, J., Milicić, B., et al. (2010). [Association between clinical parameters and the presence of *Aggregatibacter actinomycetemcomitans* and *Porphyromonas gingivalis* in patients with progressive periodontal lesions]. *Vojnosanit. Pregl.* 67, 898–902. doi: 10.2298/VSP1011898R

Salvi, G. E., and Lang, N. P. (2005). Host response modulation in the management of periodontal diseases. *J. Clin. Periodontol.* 32(Suppl. 6), 108–129. doi: 10.1111/j.1600-051X.2005.00785.x

Savage, A., Eaton, K. A., Moles, D. R., and Needleman, I. (2009). A systematic review of definitions of periodontitis and methods that have been used to identify this disease. *J. Clin. Periodontol.* 36, 458–467. doi: 10.1111/j.1600-051X.2009.01408.x

Seleem, D., Chen, E., Benso, B., Pardi, V., and Murata, R. M. (2016). In vitro evaluation of antifungal activity of monolaurin against *Candida albicans* biofilms. *PeerJ* 4:e2148. doi: 10.7717/peerj.2148

Shirodaria, S., Smith, J., McKay, I. J., Kennett, C. N., and Hughes, F. J. (2000). Polymorphisms in the IL-1A gene are correlated with levels of interleukin-1alpha protein in gingival crevicular fluid of teeth with severe periodontal disease. *J. Dent. Res.* 79, 1864–1869. doi: 10.1177/00220345000790110801

Silva, V., de, O., Pereira, L. J., and Murata, R. M. (2017). Oral microbe-host interactions: influence of β-glucans on gene expression of inflammatory cytokines and metabolome profile. *BMC Microbiol.* 17:53. doi: 10.1186/s12866-017-0946-1

Slots, J., Reynolds, H. S., and Genco, R. J. (1980). *Actinobacillus actinomycetemcomitans* in human periodontal disease: a cross-sectional microbiological investigation. *Infect. Immun.* 29, 1013–1020.

Stashenko, P., Dewhirst, F. E., Peros, W. J., Kent, R. L., and Ago, J. M. (1987). Synergistic interactions between interleukin 1, tumor necrosis factor, and lymphotoxin in bone resorption. *J. Immunol.* 138, 1464–1468.

Tangwatcharin, P., and Khopaibool, P. (2012). Activity of virgin coconut oil, lauric acid or monolaurin in combination with lactic acid against *Staphylococcus aureus*. *Southeast Asian J. Trop. Med. Public Health* 43, 969–985.

Yang, H. W., Asikainen, S., Doğan, B., Suda, R., and Lai, C. H. (2004). Relationship of *Actinobacillus actinomycetemcomitans* serotype b to aggressive periodontitis: frequency in pure cultured isolates. *J. Periodontol.* 75, 592–599. doi: 10.1902/jop.2004.75.4.592

Yoon, B. K., Jackman, J. A., Valle-González, E. R., and Cho, N. J. (2018). Antibacterial free fatty acids and monoglycerides: biological activities, experimental testing, and therapeutic applications. *Int. J. Mol. Sci.* 8:E1114. doi: 10.3390/ijms19041114

Zambon, J. J., Christersson, L. A., and Slots, J. (1983). *Actinobacillus actinomycetemcomitans* in human periodontal disease. Prevalence in patient groups and distribution of biotypes and serotypes within families. *J. Periodontol.* 54, 707–711. doi: 10.1902/jop.1983.54.12.707

Zhang, M. S., Sandouk, A., and Houtman, J. C. (2016). Glycerol Monolaurate (GML) inhibits human T cell signaling and function by disrupting lipid dynamics. *Sci. Rep.* 26:30225. doi: 10.1038/srep30225

Zhang, Q., Chen, B., Zhu, D., and Yan, F. (2016). Biomarker levels in gingival crevicular fluid of subjects with different periodontal conditions: a cross-sectional study. *Arch. Oral Biol.* 72, 92–98. doi: 10.1016/j.archoralbio.2016.08.020

Conflict of Interest Statement: The authors declare that the research was conducted in the absence of any commercial or financial relationships that could be construed as a potential conflict of interest.

Copyright © 2018 Silva, Pereira, Pasetto, da Silva, Meyers and Murata. This is an open-access article distributed under the terms of the Creative Commons Attribution License (CC BY). The use, distribution or reproduction in other forums is permitted, provided the original author(s) and the copyright owner(s) are credited and that the original publication in this journal is cited, in accordance with accepted academic practice. No use, distribution or reproduction is permitted which does not comply with these terms.

frontiers in Microbiology

ORIGINAL RESEARCH
published: 08 November 2018
doi: 10.3389/fmicb.2018.02618

Purification and Characterization of an Active Principle, Lawsone, Responsible for the Plasmid Curing Activity of *Plumbago zeylanica* Root Extracts

Rajashree Bhalchandra Patwardhan[1], Prashant Kamalakar Dhakephalkar[2]*, Balu Ananda Chopade[3], Dilip D. Dhavale[4] and Ramesh R. Bhonde[5]*

[1] Department of Microbiology, Haribhai V. Desai College of Arts, Science and Commerce, Pune University, Pune, India, [2] Bioenergy Group, Agharkar Research Institute, Pune, India, [3] Department of Microbiology, Savitribai Phule Pune University, Aurangabad, India, [4] Department of Chemistry, Savitribai Phule Pune University, Pune, India, [5] School of Regenerative Medicine – Manipal Academy of Higher Education, Bengaluru, India

OPEN ACCESS

Edited by:
Rebecca Thombre, Pune University-Shivajinagar, India

Reviewed by:
Sunil D. Saroj, Symbiosis International University, India
Kapil Punjabi, Indian Institute of Technology Bombay, India

***Correspondence:**
Rajashree Bhalchandra Patwardhan
dr.rbpatwardhan@gmail.com
Prashant Kamalakar Dhakephalkar
pkdhakephalkar@aripune.org

Specialty section:
This article was submitted to Antimicrobials, Resistance and Chemotherapy, a section of the journal Frontiers in Microbiology

Received: *31 March 2018*
Accepted: *12 October 2018*
Published: *08 November 2018*

Citation:
Patwardhan RB, Dhakephalkar PK, Chopade BA, Dhavale DD and Bhonde RR (2018) Purification and Characterization of an Active Principle, Lawsone, Responsible for the Plasmid Curing Activity of Plumbago zeylanica Root Extracts. Front. Microbiol. 9:2618. doi: 10.3389/fmicb.2018.02618

Plasmid curing is the process of obviating the plasmid encoded functions such as antibiotic resistance, virulence, degradation of aromatic compounds, etc. in bacteria. Several plasmid curing agents have been reported in literature, however, no plasmid curing agent can eliminate all plasmids from different hosts. Hence, there is always a need for novel plasmid curing agents that can be effectively used for reversal of plasmid encoded functions such as virulence, antibiotic resistance, etc. In the present study, an active principle responsible for the plasmid curing activity was purified from roots of *Plumbago zeylanica* by bioassay guided fractionation and identified as 2-hydroxy-1,4-naphthoquinone (lawsone), on the basis of spectral and analytical data such as NMR, GCMS, FTIR. Plasmid curing activity of lawsone was observed against reference as well as wild plasmids (pBR322, pRK2013, R136, pUPI281, and pUPI282) residing in a range of hosts. Curing of plasmid was confirmed by agarose gel electrophoresis. MICs of antibiotics against *A. baumannii* A24 (pUPI281) and *E. coli* (pRK2013) decreased significantly in presence of lawsone suggesting synergy between lawsone and antibiotics. Lawsone also inhibited transfer of plasmid pRK2013 to *E. coli* either by transformation or conjugation. Viability assays (MTT) revealed that lawsone was not toxic to mammalian cells. Thus, the present investigation has revealed lawsone as an effective plasmid curing agent capable of suppressing development and spread of antibiotic resistance. Further, lawsone has important application in basic research to identify phenotypes encoded by the plasmids in plasmid curing experiments. To the best of our knowledge this is the first report of plasmid curing activity of lawsone isolated from roots of *P. zeylanica.*

Keywords: lawsone(2-hydroxy-1, 4 naphthoquinone), *Plumbago zeylanica*, extraction, purification, plasmid curing, antibiotic resistance

INTRODUCTION

Plasmids are independent, circular, self-replicating extra-chromosomal DNA elements with characteristic copy numbers within the host. Various properties encoded by plasmid include resistance to antibiotics and heavy metals, degradation of hydrocarbons, synthesis of bacteriocins and antibiotics, etc. Plasmid mediated antibiotic resistance can be transferred easily from one bacterium to another by transformation, conjugation or mobilization (Opal et al., 2000). Plasmid encoded resistance to multiple antibiotics has been increasingly recognized as a major challenge in the treatment of infections. In addition to the antibiotic resistance, some bacterial plasmids confer pathogenicity as well, to the host cell (Saunders, 1981).

Plasmid curing agents are the chemicals or physical agents that inhibit the replication of plasmid resulting in subsequent elimination of such plasmids from the host population after several replication cycles. Obtaining plasmid cured derivatives is desired in the investigation of bacterial harboring plasmids. Comparison of plasmid harboring strain and its cured derivative allows assigning phenotypic characters to genes located on plasmids. Simultaneous loss of a particular character by curing, gives a strong indication of its plasmid borne genetic character (Trevors, 1986). Further, plasmid curing converts the antibiotic resistant bacterial cells into sensitive ones (Molnar, 1988). Thus, elimination of R-plasmids makes the antibiotic therapy effective. Novel strategies to struggle antimicrobial multidrug resistance are required, and plasmid curing, and anti-plasmid strategies could reduce antimicrobial resistance genes frequency and sensitize bacteria to antibiotics (Michelle et al., 2018).

Plasmid curing agents reported in the scientific literature include sodium lauryl sulfate, ethidium bromide, acridine orange, etc. (Bouanchaud et al., 1969; Chopade et al., 1994). However, it is known from earlier studies that acridine dyes and ethidium bromide cannot be used *in vivo* because of their mutagenicity, carcinogenicity, teratogenicity while SDS, because of its detergent action (Shriram et al., 2010). Hence, these curing agents are not useful in controlling the spread of antibiotic resistance in hospital environment. The curing agents have been effectively used to study plasmid encoded phenotypes in various laboratory studies. Till date no curing agent is known that can universally cure all plasmids from bacterial population. So non-toxic and highly effective plasmid eliminating agents are required to be developed constantly.

Plants are known to produce diverse bioactive substances of chemotherapeutic value (Chopra et al., 1992; Samy and Ignacimuthu, 2000). Ahmad et al. (2000) reported ability of aqueous extracts of *Plumbago zeylanica* to eliminate plasmid encoded antibiotic resistance in *Escherichia coli*. However, active principle responsible was not purified and identified.

In the view of this background, root extracts of *P. zeylanica* were explored for the presence of novel plasmid curing agent that was effective against antibiotic resistant plasmids in *Escherichia coli, Salmonella* Typhi as well as *Acinetobacter baumannii*. In the present investigation, lawsone was purified from the roots of *P. zeylanica* and identified as a plasmid curing agent capable of reversing multiple antibiotic resistance in broad range of clinical isolates as well as reference strains.

MATERIALS AND METHODS

Plant Material

P. zeylanica plants were collected from Western Ghat region of India. The roots were harvested, dried in shade, powdered and used for further extraction procedures. The plant material was authenticated by Botanical Survey of India, Ministry of Environments and forests, Government of India. A voucher specimen (RBPUP1) is deposited at the Herbarium of Botanical Survey of India, Office of Joint Director, Pune, India.

Extraction and Purification of Plasmid Curing Agent From *P. zeylanica* Roots

Active principle responsible for the plasmid curing activity was purified by the bioassay guided fractionation procedure as described previously (Shriram et al., 2008). Air-dried and powdered roots (2.5 kg) of *Plumbago zeylanica* were successively extracted in Soxhlet apparatus with petroleum ether, cyclohexane, benzene, diethyl ether, chloroform, acetone, ethanol, and methanol (according to eluotropic series based on polarity) at boiling temperature for respective solvents (Shriram et al., 2008). Each extract was filtered and concentrated to dryness under vacuum on a rotary evaporator (Heidolph-Germany) and dissolved in 10 ml of dimethyl sulfoxide (DMSO). Isolation and purification of active compounds from *P. zeylanica* roots was performed by column chromatography with silica gel (100–200 mesh) (Sadasivam and Manickam, 1992). Ethanol extract showing antimicrobial and plasmid curing activity was then coarsely fractionated over silica gel using a stepwise gradient solvent system consisting of hexane: ethyl acetate (9:1, 8:2, 7:3, 6:4, 5:5, 4:5, 3:6) to separate the respective fractions (25–40 μm, 3′ 50 cm, eluent hexane-ethyl acetate, flow rate 3 ml/min). TLC analysis was carried out on 0.25 mm precoated silica gel sheets (polygram sil Gluv 254). Chromatographic fractions as well as pure compounds were monitored by TLC, detected by UV light at 250 nm (UV GL-25 Mineralight lamp) and color reaction by spraying with a solution of 2% 2,4-dinitro phenyl hydrazine in methanolic sulphuric acid followed by 5 min heating at 100°C. A total of 83 sub-fractions (10 ml) were collected and monitored by TLC. Sub-fractions 17–23 yielded (64 mg), a single pure compound detected by TLC (hexane-ethyl acetate 7:3, R_f = 0.617). This compound was further purified by preparative TLC (Macherey-Nagel-Germany Precoated TLC plates SIL G-200 UV_{254} 2 mm thickness) using hexane-ethyl acetate solvent system.

Characterization of Purified Plasmid Curing Agent

Melting point was determined in degree Celsius (°C) with Thomas Hoover Capillary Melting point apparatus (New Jersey,

United States). IR spectra were recorded with Perkin Elmer 1600 FTIR and Shimadzu FTIR spectrophotometer as a thin film or in nujol mull or using KBr pellets and were expressed in cm^{-1}. Spectral data on GCMS was acquired with the direct insertion probe on a Shimadzu spectrometer at 70 eV. Isolated compound was analyzed for structure elucidation by techniques such as ^{1}H nuclear magnetic resonance (NMR) and ^{13}C NMR (Choudhary and Atta-ur-Rahman, 1997). The ^{1}H NMR spectra (300 MHz) were recorded in $CDCl_3$ as a solvent on a Varian (mercury) instrument. ^{1}H NMR chemical shifts were expressed in δ (ppm) units, downfield to internal standard TMS (Daniel, 1991). Assignment of signals was confirmed by decoupling experiments.

Microbial Strains and Culture Conditions Used

Bacterial isolates and standard plasmids used in this study are enlisted in **Tables 1**, **2**. Clinical isolates of *Acinetobacter* were identified based on their morphological, cultural and biochemical characteristics according to the Bergey's Manual of Systematic Bacteriology (Kloos and Schleifer, 1986) and using API20NE system (Biomeraux, France) as per manufacturer's instructions. All strains were preserved as glycerol stocks at −20°C or as agar slants at 4–8°C. All bacterial cultures were grown on Luria agar at 37°C (Hi Media, Mumbai, India).

Determination of Resistance to Antibiotics

Antibiotic resistance profile was determined by the disk diffusion method (Bauer et al., 1966). Multi-disks containing antibiotics (Don Whitley Scientific Equipments, Mumbai, India) were placed on Muller Hinton agar plates (Hi Media, India) spread with ca. 10^5 cells of actively growing test culture and incubated at 37°C. The inhibition zones measured after 24 h incubation and were interpreted according to the manufacturer's interpretation table. MICs of antibiotics were determined by agar dilution method as described previously (Dhakephalkar and Chopade, 1994). Concentrations of each antibiotic used ranged from 1 μg/ml to 1,024 μg/ml. MIC was interpreted as the lowest concentration of the antibiotic inhibiting bacterial growth.

TABLE 1 | Antibacterial activity of lawsone from *P. zeylanica* ethanol root extract.

Sr. No.	Bacterial strains	Strain designation	MIC (μg/disk)
1	*P. aeruginosa*	PUPU103	800
2	*S. aureus*	PUPU107	400
3	*S.* Typhi	PUST112	200
4	*B. cereus*	PUBL123	200
5	*E. coli*	PUUR119	800
6	*S. dysenteriae*	PUST115	400
7	*B. subtilis*	PUBL126	200
8	*S. marcescens*	PUUR120	>1600
9	*P. mirabilis*	PUUR121	>1600
10	*K. pneumoniae*	PUSP134	800
11	*Enterobacter*	PUST114	800
12	*A. baumannii*	PUBL130	800

MIC (minimum inhibitory concentration) was detected by disk diffusion assay using 10^5 cells as inoculum on NA for bacteria. DMSO without lawsone, used as a solvent control, did not inhibit growth of any of the bacterial cultures tested. All the strains were isolated from clinical specimens like pus, stool, blood, urine, and sputum.

Plasmid Isolation

Plasmid isolation was carried out by alkali lysis method as well as boiling method described by Sambrook et al. (1989). DNA was detected by horizontal agarose gel (0.7%) electrophoresis using Tris-acetate-EDTA buffer (pH 8.0).

Curing of Antibiotic Resistance

The plasmid curing was performed as described earlier by Deshpande et al. (2001). In brief, microbial culture was exposed to different concentrations of curing agent during cultivation in Luria broth at 37°C for 24 h. Subsequently, the culture was serially diluted and plated on Luria agar to obtain isolated colonies. A total of 100 colonies was replica plated on Luria agar with and without antibiotic. Cured derivatives were scored by their failure to grow in presence of antibiotics. Efficiency of curing was calculated as number of colonies showing reversal of antibiotic resistance per 100 colonies tested. Agarose gel electrophoresis was performed to confirm the removal of plasmid DNA from the plasmid cured strain. Effect of pH (range 5.5–8.0), lawsone concentrations (range 64–512 μg/ml) and inoculum densities (range 10^4–10^7 cells/ml) on curing efficiency of lawsone was studied in *E. coli* (pRK2013) and *A. baumannii* (pUPI281). All the experiments were performed at least in duplicate.

Effect of Purified Active Principle (Lawsone) on Transformation of Plasmid

E. coli HB101was used as host for the transformation experiments. Calcium chloride method (Sambrook et al., 1989) was used for the preparation of competent cells. Transformation experiments were performed by "heat shock method" as described previously (Sambrook et al., 1989) using plasmid pRK2013 and competent cells of *E. coli* HB101 as recipient. Transformation efficiency was expressed as number of transformants obtained per μg of plasmid DNA. Purified active principle, at specified concentrations, was added to competent cells along with transforming DNA to evaluate its effect on plasmid transformation.

Effect of Purified Active Principle (Lawsone) on Plasmid Transfer by Conjugation

Conjugation experiments were performed by membrane filter mating method as described by Towner and Chopade (1987). Effect of lawsone on plasmid transfer was studied by incubating both donor *E. coli* (pRK2013) and recipient *E. coli* HB101 (adsorbed on membrane filter) on nutrient agar containing varying concentrations of curing agent. Difference in the percentage efficiency of conjugation in the presence or absence

TABLE 2 | Plasmid curing with purified lawsone.

Strain and plasmid	Size of plasmid	Antibiotic resistance[@]	MIC (μg/ml)	SIC (μg/ml)	Curing efficiency (%)
E. coli K12 (RP4) MTCC 391	56.4 kb	Ap^r, Km^r, Tc^r	512	256	ND
E. coli (pBR 322) MTCC 78	4.3 kb	Ap^r, Tc^r	800	512	11 ± 1.4
E. coli (pRK 2013) MTCC 398	48.0 kb	Ap^r, Km^r	800	512	20 ± 1.4
P. aeruginosa (RIP64) MTCC 1262	95 Mdal	Gm^r, Cm^r	512	256	ND
S. Typhi (R136) MTCC 1264	59 kb	Tc^r	800	512	4.2 ± 0.3
B. subtilis (pUB110) MTCC 1558	4.5 kb	Km^r, Nm^r	800	512	ND
A. baumannii A23 (pUPI280) (present study)	—	Ap^r, Gm^r, Km^r, Cm^r, Am^r	1024	800	ND
A. baumannii A24 (pUPI281) (present study)	—	St^r, Ap^r, Gm^r, Ak^r	800	512	13.5 ± 1.4
A. baumannii A26 (pUPI282) (present study)	—	St^r, Ap^r, Gm^r, Ak^r, Lf^r	512	256	8.5 ± 0.7

MIC, minimum inhibitory concentration; SIC, sub inhibitory concentration. ND, none of the 300 colonies tested showed curing of plasmid. [@]Am, amoxicillin; Ak, amikacin; Ap, ampicillin; Cm, chloramphenicol; Gm, gentamicin; Km, kanamycin; Lf, lomefloxacin; Nm, neomycin; St, streptomycin; Tc, tetracycline; ***MTCC (Reference cultures),*** *Microbial Type Culture Collection, Chandigarh, India.*

of curing agent was calculated to evaluate effect of lawsone on transfer of plasmid by conjugation.

Synergistic Action of Lawsone With the Antibiotic: Combination Studies

Synergism between lawsone and antibiotics such as streptomycin and kanamycin was tested against *A. baumannii* (pUPI281) and *E. coli* (pRK2013), respectively. Concentration of lawsone as well as the antibiotic tested was in the range 0–1,000 μg/ml. Actively growing culture was inoculated (10^4 cells/ml) in Luria broth supplemented with varying concentrations of lawsone and streptomycin or kanamycin and incubated at 37°C for 18 h. Culture growth was monitored on spectrophotometer at 600 nm. Interactions of curing agents with antibiotics were assessed by a modified Chequerboard agar dilution method (Charles et al., 1997). Synergistic or otherwise effect of curing agent and antibiotic in combination was evaluated by determining the fractional inhibitory concentration index (minimum FIC index). The FIC was calculated for each combination using the following formula: **FIC A + FIC B = FICI** Where, FICA = MIC of drug A in combination/MIC of drug A alone, and FICB = MIC of drug B in combination/MIC of drug B alone. The FICI was interpreted as follows: synergy = FICI < 0.5; no interaction = FICI > 0.5–4; antagonism = FICI > 4 (Dorsthorst et al., 2002).

Toxicity Testing of Lawsone

Actively growing BHK 21 (baby hamster kidney fibroblast cell line) and AV3 (human amniotic epithelial cell line) cells were obtained from the NCCS repository (Pune, India). These cells were subcultured using TPVG solution (2% trypsin, 0.1% EDTA, and 0.1% glucose in PBS) and seeded on to a 6-well tissue culture plate (Falcon, BD Biosciences, United States) at the concentration of 3×10^5 cells per well with Eagle's minimal essential medium (EMEM) supplemented with 10% fetal calf serum (FCS). Plates were incubated for 24 h for the monolayer formation. The monolayers of both, BHK 21 and AV3 were then exposed to different concentrations of lawsone. Plates were observed under inverted microscope (Olympus IX70) for the cell morphology and floating cell population after 24 h of incubation at 37°C in 5% CO_2 environment. Control cells were grown in absence of lawsone.

MTT Assay for Examination of the Viability of Cells

BHK21 and AV3 cells were seeded in a 96-well tissue culture plate (Falcon, BD Biosciences, United States) and incubated overnight. The cells were then exposed to varying concentrations of lawsone for 24 h. Control cells were not exposed to the lawsone treatment. MTT assay was performed to determine the toxicity of the plasmid curing agent to the cells upon exposure (Bahuguna et al., 2017) In this assay yellow colored 3-(4,5-dimethylazol-2-yl)-2,5-diphenyl-tetrazolium bromide (MTT) is enzymatically converted into purple formazan in the exposed cells. The intensity of purple formazan was measured at 570 nm. using Spectra Max 250 UV-vis microplate reader (Molecular Devices, Sunnyvale, CA, United States). Experiment was performed in duplicate and the average for all wells was shown as cell-viability percentage related to unexposed control cells.

RESULTS

Purification and Identification of Plasmid Curing Agent From *P. zeylanica* Roots

Crude ethanol extract of roots of *P. zeylanica* demonstrated significant antimicrobial as well as plasmid curing activity (Patwardhan, 2007). An active principle responsible for the plasmid curing activity of the ethanol extract of *P. zeylanica* was purified by bioassay guided fractionation. Molecular formula of the purified compound, isolated as yellow crystals, (melting point, 192°C) was established as $C_{10}H_6O_3$ (**Figure 1**) based on GCMS spectral data (molecular ion peak at m/z = 174). Further structural characterization was made by UV, FTIR, ^{1}H NMR and ^{13}C NMR spectroscopic methods. UV λ_{max} at 273 nm for the same compound clearly indicated conjugation in the compound. In the IR spectra, the peak observed at 1,587 cm^{-1} suggested the presence of C=C. The peak at 1,641 cm^{-1} indicated the presence of α, β-unsaturated carbonyl group. The broad band at 3,056–3,350 cm^{-1} was suggestive of hydroxyl group.

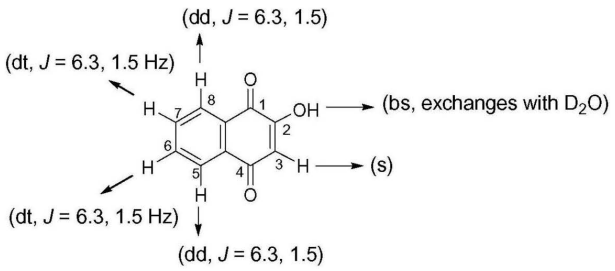

FIGURE 1 | Chemical structure of lawsone demonstrating antimicrobial and plasmid curing activity.

In the ^{1}H-NMR spectrum, the singlet at 6.36 δ was assigned to H-3. The broad singlet 7.33 was due to hydroxyl group which was found to be exchangeable with D_2O. The signal at δ 7.71 appeared as doublet of triplet with J = 6.3 and 1.5 Hz was assigned to either H6 or H7. Similarly, appearance of doublet of triplet at δ 7.79 with J = 6.3 and 1.5 Hz was assigned to either H6 or H7. The signal at δ 8.11, corresponding to two protons, appeared as doublet of doublet with J = 6.3 and 1.5 Hz was assigned to H5 and H8. The compound was identified as lawsone based on spectral data (**Figure 1** and **Table 3**). This data was found to be in good agreement with the spectral and analytical data of lawsone (Sigma, United States) thus confirming our assignment. To the best of our knowledge, this is the first report of lawsone extracted from roots of *Plumbago zeylanica*.

Curing of Antibiotic Resistance by Lawsone

Lawsone inhibited the growth of *A. baumannii, P. aeruginosa*, *S.* Typhi and *E. coli,* in disk diffusion assay (200–800 μg/disk) (**Table 1**). Plasmid curing activity of lawsone against R-plasmids harbored in reference as well as clinical isolates is illustrated in **Table 2** and **Supplementary Figures S1**, **S2**. Lawsone cured plasmids pBR322 and pRK2013 at 11% and 20% efficiencies, respectively. Lawsone also cured plasmid R136 in *S.* Typhi at 4.2% curing efficiency. However, it was not able to cure plasmid RP4 in *E. coli*. Lawsone eliminated plasmids pUPI281 and pUPI282 in *A. baumannii* with 8.5% and 13.5% efficiency, respectively. Curing efficiencies of lawsone observed against plasmids in reference strains as well as clinical isolates of *A. baumannii* were comparable to those observed for conventional curing agents such as DNA-intercalating dyes, acridine orange and ethidium bromide (**Table 4**). Plasmid curing efficiency of lawsone was determined against plasmid pBR322, pRK2013, and pUPI281 at different cell densities of host harboring these plasmids. It was observed that curing efficiencies were higher at lower cell densities (10^4 cells/ml) than at higher cell densities (10^5 cells/ml or 10^6 cells/ml) (**Table 5**). Similarly, increasing concentrations of lawsone (64–512 μg/ml) resulted in higher curing efficiencies when initial inoculum density was maintained constant (**Table 6**). Lawsone could not cure either pUPI281 or pRK2013 at 64 μg/ml or lower concentrations. Plasmid curing activity of lawsone was studied at different pH ranging from 6.0 to 8.0 with plasmids pRK2013 and pUPI281. It was observed that lawsone cured pRK2013 and pUPI281 with curing efficiency of 27% and 17%, respectively at pH 6.0 and 8.0. There exists a possibility of reversal of antibiotic resistance if and when a bacterial culture is grown in absence of antibiotics. Hence, in the present study bacterial culture was grown in absence of antibiotics as well as plasmid curing agent (solvent control). Such culture was plated to obtain isolated colonies in absence of antibiotics. The isolated colonies were replicated on agar media with or without antibiotic to determine the frequency of spontaneous loss of plasmid or reversal of antibiotic resistance. None of the 100 colonies tested were spontaneously cured derivative of plasmid bearing host. However, in this technique only 100 colonies were tested by replica plating. Hence, in another modification, cultures were grown in absence of antibiotics or plasmid curing agents for several generations and then plated on agar media with and without antibiotics. The frequency of spontaneous reversal of antibiotic resistance was found to be less than one in $10^{8.}$ This observation was consistent with earlier observation (Inoue, 1997). In comparison, curing efficiencies reported in this study were extremely high ($>10^4$ times). Both these observations (reversal of antibiotic resistance or plasmid curing observed only upon exposure to plasmid curing agents and not spontaneously) clearly indicated that reversal of antibiotic resistance as a consequence of plasmid curing was not a spontaneous phenomenon but was caused by the exposure of plasmid harboring strains to plasmid curing agent, i.e., lawsone in the present study. In the present investigation, loss of plasmid in the cured derivatives was confirmed by agarose gel electrophoresis analysis (**Figure 2**). Loss of plasmid and not mutation was thus, confirmed as a cause of reversal of antibiotic resistance in the cured derivative. It may be noted here that even mutation could have caused reversal of antibiotic resistance. However, mutagenic activity of the plasmid curing agents is undesired for potential clinical application. Lawsone was able to cure plasmid and inhibit the transfer of plasmid by conjugation as well as by transformation which is significant in containing the spread of antibiotic resistance. Controls did not show loss of plasmids at various pH values, indicating that pH alone did not have any effect on the plasmid curing.

TABLE 3 | ^{1}H NMR and ^{13} C NMR data of lawsone.

Position	^{1}H NMR (δ)	Position	^{13} C NMR (δ)
H-3	6.19 (S)	C-1	184.9
H-5	8.19 (dd, J = 6.3 and 1.4 Hz)	C-2	156.3
H-6	7.72 (dt, J = 6.3 and 1.4 Hz)	C-3	110.7
H-7	7.81 (dt, J = 6.3 and 1.4 Hz)	C-4	181.9
H-8	8.19 (dd, J = 6.3 and 1.4 Hz)	C-4a	132.9
		C-5	133.13
		C-6	126.7
		C-7	126.4
		C-8	135.3
		C-8a	129.4

TABLE 4 | Curing of R plasmids with conventional curing agents.

Plasmid	Antibiotic resistance markers	Purified lawsone		Ethidium bromide		Acridine orange	
		Conc. (μg/ml)	Curing efficiency	Conc. (μg/ml)	Curing efficiency	Conc. (μg/ml)	Curing efficiency
			(%)		(%)		(%)
RP4	Ap^r, Km^r, Tc^r	256	_	128	13 ± 1.4	64	ND
pBR 322	Ap^r, Tc^r	512	11 ± 1.4	128	21.5 ± 2.1	128	12.5 ± 2.1
pRK 2013	Ap^r, Km^r	512	20 ± 1.4	256	59.5 ± 3.5	128	ND
RIP64	Gm^r, Cm^r	256	_	128	16	256	ND
R136	Tc^r	512	4.2 ± 0.3	256	13.5 ± 0.7	256	ND
pUP110	Km^r, Nm^r	512	_	256	_	128	ND
pUPI 280	Ap^r, Gm^r, Km^r, Cm^r, Am^r	800	_	512	18 ± 2.8	512	6.5 ± 0.7
pUPI 281	St^r, Ap^r, Gm^r, Ak^r	512	13.5 ± 1.4	256	15 ± 1.4	256	17.25 ± 1.06
pUPI 282	St^r, Ap^r, Gm^r, Ak^r, Lf^r	256	8.5 ± 0.7	256	10.25 ± 1.0	256	_

Three hundred clones were tested for each plasmid in the curing experiments. ND, none of the 300 colonies tested showed curing of plasmid.

TABLE 5 | Effect of cell density on plasmid curing efficiency of lawsone.

Plasmid	Curing efficiency (%) at			
	10^4 (cells/ml)	10^5 (cells/ml)	10^6 (cells/ml)	10^7 (cells/ml)
E. coli (pBR 322)	31.3 ± 1.8	16.5 ± 2.1	2 ± 0	ND
E. coli (pRK 2013)	20 ± 1.4	9.3 ± 2.5	4.5 ± 0.7	9 ± 0
A. baumannii (pUPI 281)	12.5 ± 2.1	15.5 ± 2.1	15 ± 0	5.8 ± 1.0

Above desired number of cells were incubated in Luria broth in the presence of 512 μg of lawsone/ml at 37°C for 24 h. Number of clones tested – 300. ND, none of the 300 colonies tested showed curing of plasmid.

Effect of Lawsone on Plasmid Transfer by Conjugation and Transformation

Effect of lawsone on plasmid transfer by conjugation or transformation was investigated with plasmid pRK2013. More than 90% decrease in the frequency of plasmid transfer was observed when conjugation was performed in the presence of lawsone (12.5 μg/ml) by membrane mating method. Plasmid pRK2013 was transferred from *A. baumannii* to *E. coli* with conjugation frequencies of 2.1×10^{-5} and 2×10^{-4} in the presence and absence of lawsone, respectively (**Table 7**). The similar inhibition was observed when the conjugation was performed by broth mating (8.8×10^{-6} and below detection limit). Similarly, lawsone inhibited transfer of plasmid by transformation. Frequency of transformation of *E. coli* HB101 with pRK2013 was observed to be 1.1×10^4 transformants/μg plasmid DNA. However, 63% decrease in the transformation efficiency was observed in the presence of lawsone.

TABLE 6 | Effect of concentration of lawsone on curing efficiency.

Plasmid	Curing efficiency (%) at			
	64 (μg/ml)	128 (μg/ml)	256 (μg/ml)	512 (μg/ml)
E. coli (pBR 322)	ND	ND	13 ± 1.4	31.74 ± 1.06
E. coli (pRK 2013)	ND	ND	20 ± 1.4	22 ± 1.4
A. baumannii (pUPI 281)	ND	7.5 ± 2.1	18 ± 1.4	14.3 ± 0.4

Number of clones tested – 300. 10^4 cells/ml were incubated in the presence of above described concentrations of lawsone at 37°C for 24 h. ND, none of the 300 colonies tested showed curing of plasmid.

TABLE 7 | Effect of lawsone on R plasmid transfer from ampicillin resistant *E. coli* to streptomycin resistant *E. coli* by conjugation.

Conjugation	Frequency of conjugation	
	In absence of curing agent	In presence of curing agent
With membrane filter	2×10^{-4}	2.1×10^{-5}
Without membrane filter	8.8×10^{-6}	Below the detection limit

10^8 cells of donor E. coli (pRK2013) and recipient E. coli (HB101) were mixed and incubated in absence or presence of 12.5 μg of lawsone/ml at 37°C for 24 h. The growth was serially diluted and plated out to score number of transconjugants formed. The data represents average values of two parallel experiments.

Synergistic Action of Lawsone With the Antibiotic: Combination Studies

Synergy between lawsone and antibiotics was investigated against *A. baumannii* (pUPI281) and *E. coli* (pRK2013). The MICs were determined for the curing agent alone and in combination with the different antibiotics by checkerboard assay method. *A. baumannii* (pUPI281) and *E. coli* (pRK2013) were resistant to streptomycin and kanamycin, respectively

(MIC > 1,000 μg/ml). Growth of *A. baumannii* (pUPI281) was inhibited when lawsone and streptomycin were added together at 250 μg/ml concentrations each. Similarly, growth of *E. coli* (pRK2013) was inhibited when lawsone and kanamycin were added together at 100 μg/ml and 250 μg/ml concentrations, respectively. The Fractional Inhibition Concentration (FIC) indices were calculated (**Table 8**). These results clearly indicated that FICI was synergistic (<0.5) for lawsone in combination with antibiotic when used against *A. baumannii.* Additive action of lawsone with antibiotic was observed against *E. coli*. These results suggested that the plasmid curing activity of naphthoquinone directly or indirectly rendered the clinical isolates susceptible to the inhibitory action of antibiotics at significantly lower concentration, and hence, were considered encouraging.

Toxicity Testing and Viability Assay (MTT) of Lawsone

Toxicity testing of lawsone revealed that BHK 21 cells which are fibroblastic in nature are more affected with lawsone than AV3 cells which are epithelial indicating its selective toxicity to fibroblast only. In MTT assay BHK 21 cells showed more drop in % viability with increased concentration of lawsone compared to AV3 Cells (**Table 9** and **Figure 3**).

DISCUSSION

The bioassay guided fractionation of the organic extracts of *P. zeylanica* roots resulted in identification of lawsone as an active principle exhibiting the plasmid curing activity. Lawsone has been reported to be a major constituent of *Lawsonia inermis.* However, to the best of our knowledge, this is the first report of lawsone extracted from roots of *Plumbago zeylanica*. Antimicrobial properties of lawsone have been documented in the literature (Ahmed and Beg, 2001).

Treatment of chronic infections caused by multidrug resistant bacteria is a serious challenge for the physicians. In most of the cases the resistance to multiple antibiotics is mediated by the plasmids. Curing of plasmid-mediated antibiotic resistance in pathogenic strains of bacteria is of great practical importance both in treatment of bacterial infection and in microbial genetics. In the present investigation, curing of plasmids effected by lawsone was confirmed on the basis of reversal of antibiotic resistance phenotype evident from the significant reduction in the MIC of antibiotics; as well as elimination of plasmids in the cured derivatives. Agarose gel electrophoresis revealed presence of plasmid DNA in wild host. However, gel electrophoresis of DNA from cured derivatives revealed loss of the corresponding plasmid band confirming plasmid curing. Plasmid curing was not observed in host exposed to DMSO, a solvent control used for lawsone. Spontaneous loss of plasmid DNA has been reported at low frequency of less than 1 in 10^9 cells· (Inoue, 1997). In comparison curing efficiencies observed in the present study were significantly higher ($>10^4$ times), thus attributing reversal of antibiotic resistance to the exposure of cells to the curing agent (lawsone). Cured strains were tested for the loss of plasmids by agarose gel electrophoresis to confirm that reversal of antibiotic resistance was due to elimination of plasmid carrying genes encoding resistance to antibiotics and not due to mutations. Physical loss of plasmid as evidenced by agarose gel electrophoresis of plasmid DNA preparation of cured strains (**Figure 2**) indicated that genes encoding antibiotic resistance

TABLE 8 | FIC index of individual curing agents and in combination with antibiotics.

Test organism	FIC_c*	FIC_a@	FIC_i#	Interpretation
A. baumannii	0.25	0.133	0.383	Synergistic
E. coli	0.4	0.25	0.65	Additive

**Fractional Inhibition Concentration of curing agent (lawsone).* @*Fractional Inhibition Concentration of antibiotics.* #*Fractional Inhibition Concentration index.*

TABLE 9 | Toxicity testing with MTT assay.

Conc. (μg/ml)	Cell line used			
	BHK 21		AV3	
	Average absorbance	% Viable cells	Average absorbance	% Viable cells
100	0.7715	84.8268	1.1035	98.55
200	0.6625	72.8422	1.1395	97.27
300	0.6650	73.1170	1.064	90.82
400	0.5995	65.9153	0.99	84.50
500	0.6275	68.9939	0.897	76.57
Control blank	0.9095	100	1.1715	100

BHK 21, baby hamster kidney fibroblast cells; AV3, human amnionic epithelial cells. Formula used: % viable cells = (average of test OD/average of control OD) × 100.

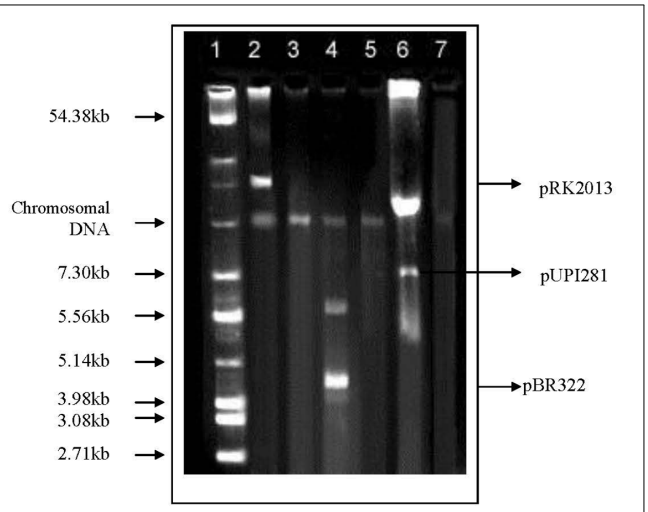

FIGURE 2 | Agarose gel electrophoresis of plasmid DNA in standard strains as well as clinical isolates harboring R-plasmids and their cured derivatives. Lane 1, Reference plasmids from *E. coli* MTCC 131; Lane 2, *E. coli* MTCC398 (pRK2013); Lane 3, Cured derivative of *E. coli* MTCC398; Lane 4, *E. coli* K12 (pBR322); Lane 5, Cured derivative of *E. coli* K12; Lane 6, *Ac. baumannii* A24 (pUPI281); Lane 7, Cured derivative of *Ac. baumannii* A24.

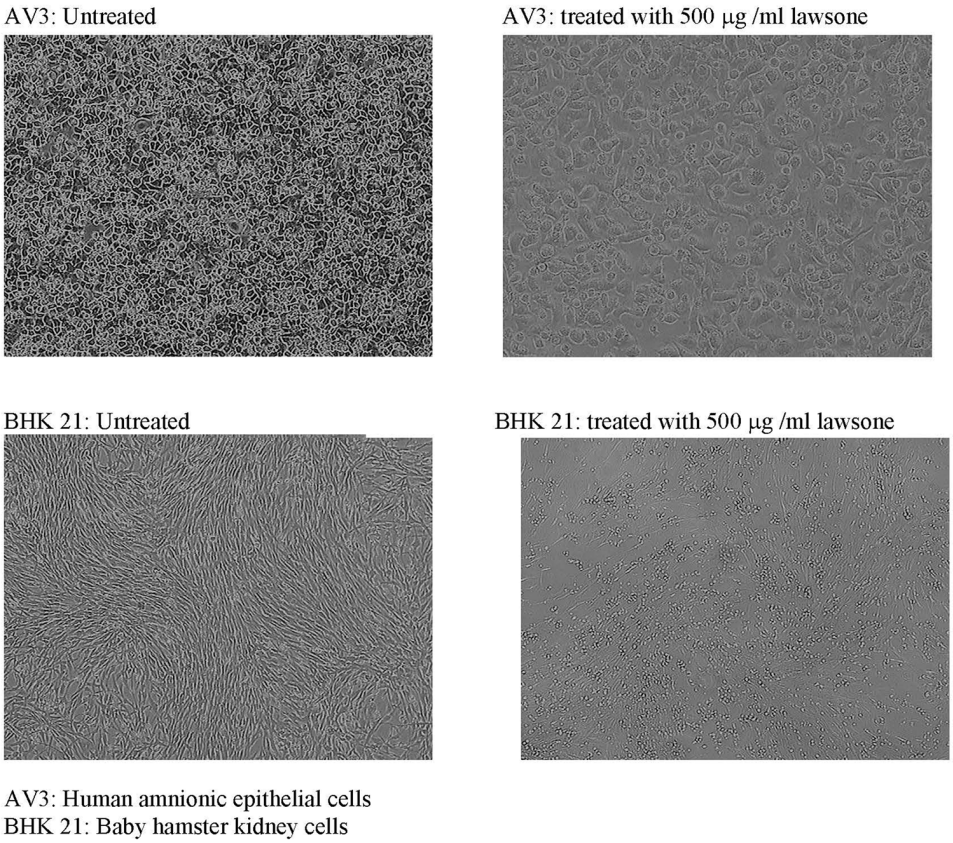

FIGURE 3 | Toxicity testing of lawsone on AV3 and BHK 21 cell lines. AV3, human amnionic epithelial cells; BHK 21, baby hamster kidney cells.

were located on plasmid and that plasmid loss resulted in subsequent loss of antibiotic resistance.

Ability of lawsone to cure plasmid encoded antibiotic resistance in *Acinetobacter* strains is particularly significant since *Acinetobacter* strains are known to act as a reservoir of natural or acquired antibiotic resistance genes in the nosocomial environment facilitating in the spread of antibiotic resistance genes to more pathogenic bacteria (Towner, 1997; Deshpande et al., 2001; Cisneros and Rodriguez-Bano, 2005). Bacteria have tendency to develop resistance against any antimicrobial agent used against them. Concentrations of curing agents used in the plasmid curing experiments were significantly lower than inhibitory concentrations. Hence, it is proposed that chances of bacteria developing any mechanism to inactivate plasmid curing agents or their activity are extremely low. It must be remembered here that plasmids are after all dispensable elements in a bacterial cell.

Plasmids are the extrachromosomal elements that are responsible for development and spread of antibiotic resistance in bacteria. Their role assumes even more significance in the nosocomial environment as plasmid encoded resistance to multiple antibiotics can be transferred from one host to another by inter species transfer modes such as conjugation and/or transformation. Such acquired resistance can make otherwise sensitive pathogens resistant to multiple antibiotics. Thus, making the treatment of infections more difficult and in some cases almost impossible. Ability of lawsone to interfere with interspecies plasmid transfer by conjugation and transformation and thus contain the spread of multi-resistance to antibiotics was investigated in the present study. It was observed that Lawsone not only cured plasmids but also inhibited the transfer of plasmid by both conjugation as well as by transformation. Membrane filter mating technique and broth mating are the two different techniques used to investigate plasmid transfer by conjugation in bacteria. Lawsone was able to inhibit the plasmid transfer by conjugation in both techniques. *Acinetobacter* has been reported as a reservoir of antibiotic resistance genes in nosocomial environment and is frequently reported to be involved in the transfer of multi-resistance to antibiotics. *E. coli* has been the most extensively investigated organism for the inter species gene transfer. Hence, in the present study both organisms were included to investigate the effect of lawsone on inter species plasmid transfer. Ability of lawsone to inhibit plasmid transfer among these organisms may thus assume special significance in nosocomial environment. Ability of lawsone to inhibit plasmid transfer by transformation or conjugation was reported for the first time in the present investigation.

FIC clearly indicated that combination of curing agent and antibiotic was synergistic against *A. baumannii* and additive against *E. coli*. This observation was considered encouraging as

it suggested that the plasmid curing activity of naphthoquinone rendered the clinical isolates susceptible to the inhibitory action of antibiotics at significantly lower concentration. Efficacy of extended antibiotic therapy in several microbial infections may be improved with the combination of plasmid curing agent lawsone, as a synergistic drug. Such synergistic combination of antibiotic and lawsone, may serve as a prospective device in selection of appropriate drug therapy that is likely to contribute to the ongoing crusade against microbial drug-resistance.

Plant derived compounds have been previously reported as plasmid curing agents. Such compounds included 8-epidiosbulbin E acetate isolated from the bulbs of *Dioscorea bulbifera* (Shriram et al., 2008); 1'-acetoxychavicol acetate from *Alpinia galanga* (L.) Swartz, (Latha et al., 2009); Plumbagin (5-hydroxy-2-methyl-1,4- naphthoquinone) derived from the root of the tropical/subtropical Plumbago species (Patwardhan et al., 2015), etc. These plasmids curing agents have been proven to be effective at curing plasmids *in vitro*. Unsaturated fatty acids have been shown to be effective conjugation inhibitors in laboratory studies on a variety of plasmids (Lopatkin et al., 2017). Furthermore, they are associated with reduced toxicity on tissue culture cells. Lawsone, a plant derived compound reported in the present investigation has shown dual ability to cure plasmid and also inhibit interspecies plasmid transfer. However, more research is needed to confirm *in vivo* efficacy and to determine potential toxicity of these compounds if administered *in vivo*.

Sauriasari et al. (2007) reported that lawsone was not mutagenic to bacterial strains. However dose dependent cytotoxicity of lawsone was reported in the same study. Cytotoxicity of lawsone was reported to be significantly lower than that of other naphthoquinone derivatives including cisplatin, a widely used anticancer drug (Oliveira et al., 2017). Cytotoxicity of naphthoquinones such as lawsone could be attributed to generation of reactive oxygen species, disruption of mitochondrial functions, inhibition of thymidine incorporation into DNA and DNA intercalation (Aithal et al., 2009; Bonifazi et al., 2010; Klaus et al., 2010; Babula et al., 2012). A series of tests in the published literature have identified lawsone as non-genotoxic agent. Such tests included Ames test, V79 hprt test, Syrian hamster embryo cell transformation assay, bone marrow micronucleus tests in CD1 mice, and bone marrow chromosome aberration test in mice and hamsters (Kirkland and Marzin, 2003). An additional genetic toxicity program performed to clarify *in vivo* genotoxic potential of lawsone revealed that lawsone was devoid of clastogenic potential *in vivo* (Marzin and Kirkland, 2004). Thus, the review of literature illustrating evaluation of genotoxicity of lawsone in a series of *in vivo* and *in vitro* tests has revealed that lawsone is not genotoxic when administered orally up to a dose of 300 mg/kg body weight. Ability of lawsone to intercalate with double stranded DNA has been reported in the published literature (Kirkland and Marzin, 2003). Also, the ability of lawsone to alter the cell membrane by generating free radicle stress has been reported earlier (Sauriasari et al., 2007). However, the plasmid curing activity reported in the present study was observed at concentration significantly lower than the inhibitory concentrations. Elucidation of exact mechanism by which lawsone effected plasmid curing in bacterial scale is not known at present and requires further extensive investigation.

Thus, in conclusion, this investigation has revealed a compound with an ability to eliminate antibiotic resistance and cure plasmids from pathogenic strains that are resistant to multiple antibiotics without any ill effect on mammalian cells at lower concentrations. The results obtained provide endorsement for investigating the potential value of lawsone in combating clinical drug resistance. The synergistic effect of lawsone with the antibiotic exhibits its tremendous potential in modern day therapeutics. The non-toxic, non-mutagenic, plasmid curing and plasmid transfer inhibiting role of lawsone demands further investigation to make it a potential drug of choice in the treatment of antibiotic resistant bacterial strains; thus, demonstrating a new dimension in antibiotic therapy.

AUTHOR CONTRIBUTIONS

RP, PD, and BC designed and executed the experiments. RP performed the experiments. RP, PD, BC, DD, and RB interpreted the results and analyzed the data. RP, PD, DD, and RB contributed to the writing of the manuscript. RP and PD revised the manuscript.

ACKNOWLEDGMENTS

RP is grateful to University Grants Commission (Teacher Fellowship for the period of two years under FIP according to Xth Plan by UGC; letter No. 34-8/2003 (WRO) dated 25th February, 2004) as well as Principal, Haribhai V. Desai College for teacher fellowship.

SUPPLEMENTARY MATERIAL

The Supplementary Material for this article can be found online at: https://www.frontiersin.org/articles/10.3389/fmicb.2018.02618/full#supplementary-material

REFERENCES

Ahmad, I., Mehmood, Z., Mohammad, F., and Ahmad, S. (2000). Antimicrobial potency and synergistic activity of five traditionally used indian medicinal plants. *J. Med. Arom. Plant Sci.* 2223, 173–176.

Ahmed, I., and Beg, A. Z. (2001). Antimicrobial and phytochemical studies on 45 indian medicinal plants against multidrug resistant human pathogens. *J. Ethnopharmacol.* 74, 113–123. doi: 10.1016/S0378-8741(00)00335-4

Aithal, B. K., Kumar, M. R. S., Rao, B. N., Udupa, N., and Rao, B. S. S. (2009). Juglone, a naphthoquinone from walnut, exerts cytotoxic and genotoxic effects

against cultured melanoma tumor cells. *Cell Biol. Int.* 33, 1039–1049. doi: 10.1016/j.cellbi.2009.06.018

Babula, P., Vanco, J., Krejcova, L., Hynek, D., Sochor, J., Adam, V., et al. (2012). Voltammetric characterization of lawsone-copper (II) ternary complexes and their interactions with dsDNA. *Int. J. Electrochem. Sci.* 7, 7349–7366.

Bahuguna, A., Khan, I., Bajpai, V. K., and Kang, S. C. (2017). MTT assay to evaluate the cytotoxic potential of a drug. *Bangladesh J. Pharmacol.* 12, 115–118. doi: 10.3329/bjp.v12i2.30892

Bauer, A. W., Kirby, M. M., Sherris, J. C., and Turck, M. (1966). Antibiotic susceptibility testing by a standardized single disk method. *Am. J. Clin. Pathol.* 36, 493–496. doi: 10.1093/ajcp/45.4_ts.493

Bonifazi, E. L., Rios-Luci, C., Leon, L. G., Burton, G., Padron, J. M., and Misico, R. I. (2010). Antiproliferative activity of synthetic naphthoquinones related to lapachol. First synthesis of 5-hydroxylapachol. *Bioorg. Med. Chem.* 18, 2621–2630. doi: 10.1016/j.bmc.2010.02.032

Bouanchaud, D. D., Scavizzi, M. R., and Chabbert, Y. A. (1969). Elimination by ethidium bromide of antibiotic resistance in enterobacteria and staphylococci. *J. Gen. Microbiol.* 54, 417–425. doi: 10.1099/00221287-54-3-417

Charles, E., Smith, B. E., Foleno, J. F., and Barrett- Frosco, M. B. (1997). Assessment of the synergistic interactions of levofloxacin and ampicillin against *Enterococcus faecium* by the checkerboard agar dilution and time-kill methods. *Diagn. Microbiol. Infect. Dis.* 27, 85–92. doi: 10.1016/S0732-8893(96)00222-2

Chopade, B. A., Patwardhan, R. B., Vaidya, V. C., Khairnar, S., Dhakephalkar, P. K., and Padhye, S. B. (1994). "Curing of antibiotic and metal resistance plasmids in *Acinetobacter baumannii*," in *Tropical Diseases: Molecular Biology and Control Strategies*, eds A. K. Sushil Kumar, G. P. Sen, and R. N. Sharma (New Delhi: CSIR Publications & Information Directorate), 695–703.

Chopra, R. N., Nayer, S. L., and Chopra, I. C. (1992). *In Glossary of Indian Medicinal Plants*, 3rd Edn. New Delhi: Council of Scientific and Industrial Research, 237–246.

Choudhary, M. I., and Atta-ur-Rahman. (1997). "Bioactivity guided isolation of phytochemicals from medicinal plants," in *Photochemical Diversity. A Source of New Industrial Products*, eds S. Wrigley, M. Hayes, R. Thomas, and E. Chrystal (Cambridge: Royal Soc. Chem), 41–52.

Cisneros, J. M., and Rodriguez-Bano, J. (2005). Risk-factors for the acquisition of imipenem-resistant *Acinetobacter baumannii* in spain: a nationwide study. *Clin. Microbiol. Infect.* 11, 874–879. doi: 10.1111/j.1469-0691.2005.01256.x

Daniel, M. (1991). *Methods in Plant Chemistry and Economic Botany*. New Delhi: Kalyani Publishers, 1–4.

Deshpande, N. M., Dhakephalkar, P. K., and Kanekar, P. P. (2001). Plasmid mediated dimethoate degradation in *Pseudomonas aeruginosa* MCMB-427. *Lett. Appl. Microbiol.* 33, 275–279. doi: 10.1046/j.1472-765X.2001.00995.x

Dhakephalkar, P. K., and Chopade, B. A. (1994). High levels of multiple metal resistance and its correlation to antibiotic resistance in environmental isolates of acinetobacter. *Biometals* 7, 67–74. doi: 10.1007/BF00205197

Dorsthorst, T. E., Verweij, D. T., Meis, P. E., Punt, J. F., and Mouton, J. W. (2002). Comparison of fractional inhibitory concentration index with response surface modeling for characterization of in vitro interaction of antifungals against itraconazole-susceptible and resistant *Aspergillus fumigatus* isolates. *Antimicrob. Agents Chemother.* 46, 702–707. doi: 10.1128/AAC.46.3.702-707.2002

Inoue, Y. (1997). Spontaneous loss of antibiotic-resistant plasmids transferred to *Escherichia coli* in experimental chronic bladder infection. *Int. J. Urol.* 4, 285–288. doi: 10.1111/j.1442-2042.1997.tb00191.x

Kirkland, D., and Marzin, D. (2003). An assessment of the genotoxicity of 2-hydroxy-1,4-naphthoquinone, the natural dye ingredient of henna. *Mutat. Res.* 537, 183–199. doi: 10.1016/S1383-5718(03)00077-9

Klaus, V., Hartmann, T., Gambini, J., Graf, P., Stahl, W., Hartwig, A., et al. (2010). 1,4-naphthoquinones as inducers of oxidative damage and stress signaling in HaCaT human keratinocytes. *Arch. Biochem. Biophys.* 496, 93–100. doi: 10.1016/j.abb.2010.02.002

Kloos, W. E., and Schleifer, K. H. (1986). "Genus IV *Staphylococcus*," in *Bergey's Manual of Systematic Bacteriology*, eds P. H. A. Sneath, N. S. Mair, M. E. Sharpe, and J. G. Holt (Baltimore, MD: Williams and Wilkins, Rosenbach), 1013–1035.

Latha, C., Shriram, V. D., Jahagirdar, S. S., Dhakephalkar, P. K., and Rojatkar, S. R. (2009). Antiplasmid activity of 1'-acetoxychavicol acetate from *Alpinia galanga* against multi-drug resistant bacteria. *J. Ethnopharmacol.* 123, 522–525. doi: 10.1016/j.jep.2009.03.028

Lopatkin, A. J., Meredith, H. R., Srimani, J. K., Pfeiffer, C., Durrett, R., and You, L. (2017). Persistence and reversal of plasmid-mediated antibiotic resistance. *Nat. Commun.* 8:1689. doi: 10.1038/s41467-017-01532-1

Marzin, D., and Kirkland, D. (2004). 2-hydroxy-1,4-naphthoquinone, the natural dye of henna, is non-genotoxic in the mouse bone marrow micronucleus test and does not produce oxidative DNA damage in chinese hamster varies cells. *Mutat. Res.* 560, 41–47. doi: 10.1016/j.mrgentox.2004.02.004

Michelle, M. C. B., Maria, L. C., and Laura, J. V. P. (2018). Strategies to combat antimicrobial resistance: anti-plasmid and plasmid curing. *FEMS Microbiol. Rev.* doi: 10.1093/femsre/fuy031 [Epub ahead of print]. doi: 10.1093/femsre/fuy031

Molnar, J. (1988). Antiplasmid activity of tricyclic compounds. Methods and findings. *Exp. Clin. Pharmacol.* 10, 467–474.

Oliveira, K. M., Liany, L. D., Corrêa, R. S., Deflon, V. M., Cominetti, M. R., and Batista, A. A. (2017). Selective Ru (II)/lawsone complexes inhibiting tumor cell growth by apoptosis. *J. Inorg. Biochem.* 176, 66–76. doi: 10.1016/j.jinorgbio.2017.08.019

Opal, S. M., Mayer, K. H., and Medecros, A. A. (2000). "Mechanisms of bacterial resistance," in *Principles and Practice of Infectious Diseases*, 5th Edn, Vol. 2, ed. R. Dolin (New York, NY, Churchill Livingstone), 236–253.

Patwardhan, R. B. (2007). *Herbal Naphthoquinones as Antimicrobial and Plasmid Curing Agents*. Ph.D. thesis, University of Pune, Pune.

Patwardhan, R. B., Shinde, P. S., Chavan, K. R., and Devale, A. (2015). Reversal of plasmid encoded antibiotic resistance from nosocomial pathogens by using plumbago auriculata root extracts. *Int. J. Curr. Microbiol. App. Sci.* 187–198.

Sadasivam, S., and Manickam, A. (1992). *Biochemical Methods for Agricultural Science*. New Delhi: Wiley Eastern Ltd.

Sambrook, J., Fritsch, E. F., and Maniatis, T. (1989). *Plasmid Vectors. In Molecular Cloning: A Laboratory Manual*, 2nd Edn. Cold Spring Harbour, NY: CSH Press.

Samy, R. P., and Ignacimuthu, S. (2000). Antibacterial activity of some folklore medicinal plants used by tribals in Western Ghats of India. *J. Ethnopharmacol.* 69, 63–71. doi: 10.1016/S0378-8741(98)00156-1

Saunders, J. R. (1981). Plasmids and bacterial pathogens. *Nature* 290:362. doi: 10.1038/290362a0

Sauriasari, R., Wang, D. H., Takemura, Y., Tsutsui, K., Masuoka, N., Sano, K., et al. (2007). Cytotoxicity of lawsone and cytoprotective activity of antioxidants in catalase mutant *Escherichia coli*. *Toxicology* 235, 103–111. doi: 10.1016/j.tox.2007.03.019

Shriram, V., Jahagirdar, S., Latha, C., Kumar, V., Puranik, V., Rojatkar, S., et al. (2008). A potential plasmid curing agent, 8- pidiosbulbin E acetate, from *Dioscorea bulbifera* L. against multidrug-resistant bacteria. *Int. J. Antimicrob. Agents* 32, 405–410. doi: 10.1016/j.ijantimicag.2008.05.013

Shriram, V., Jahagirdar, S. C., Latha, C. V., Dhakephalkar, P. K., Rojatkar, S., and Shitole, M. G. (2010). Antibacterial & antiplasmid activities of *Helicteres isora* L. *Indian J. Med. Res.* 132, 94–99.

Towner, K. J. (1997). Clinical importance and antibiotic resistance of *Acinetobacter* spp. Proceedings of a symposium held on 4-5 November 1996 at Eilat, Israel. *J. Med. Microbiol.* 46, 721–746. doi: 10.1099/00222615-46-9-721

Towner, K. J., and Chopade, B. A. (1987). Biotyping of *Acinetobacter calcoaceticus* using the API 2ONE system. *J. Hosp. Infect.* 10, 145–151. doi: 10.1016/0195-6701(87)90140-X

Trevors, J. T. (1986). Plasmid curing in bacteria. *FEMS Microbiol. Rev.* 32, 149–157. doi: 10.1111/j.1574-6968.1986.tb01189.x

Conflict of Interest Statement: The authors declare that the research was conducted in the absence of any commercial or financial relationships that could be construed as a potential conflict of interest.

Copyright © 2018 Patwardhan, Dhakephalkar, Chopade, Dhavale and Bhonde. This is an open-access article distributed under the terms of the Creative Commons Attribution License (CC BY). The use, distribution or reproduction in other forums is permitted, provided the original author(s) and the copyright owner(s) are credited and that the original publication in this journal is cited, in accordance with accepted academic practice. No use, distribution or reproduction is permitted which does not comply with these terms.

frontiers in Microbiology

REVIEW
published: 10 December 2018
doi: 10.3389/fmicb.2018.02990

Inhibiting Bacterial Drug Efflux Pumps via Phyto-Therapeutics to Combat Threatening Antimicrobial Resistance

Varsha Shriram[1], *Tushar Khare*[2], *Rohit Bhagwat*[3], *Ravi Shukla*[4] *and Vinay Kumar*[2,3]*

[1] Department of Botany, Prof. Ramkrishna More College, Savitribai Phule Pune University, Pune, India, [2] Department of Biotechnology, Modern College of Arts, Science and Commerce (Savitribai Phule Pune University), Pune, India, [3] Department of Environmental Science, Savitribai Phule Pune University, Pune, India, [4] Centre for Advanced Materials and Industrial Chemistry, School of Science, RMIT University, Melbourne, VIC, Australia

Antibiotics, once considered the lifeline for treating bacterial infections, are under threat due to the emergence of threatening antimicrobial resistance (AMR). These drug-resistant microbes (or superbugs) are non-responsive to most of the commonly used antibiotics leaving us with few treatment options and escalating mortality-rates and treatment costs. The problem is further aggravated by the drying-pipeline of new and potent antibiotics effective particularly against the drug-resistant strains. Multidrug efflux pumps (EPs) are established as principal determinants of AMR, extruding multiple antibiotics out of the cell, mostly in non-specific manner and have therefore emerged as potent drug-targets for combating AMR. Plants being the reservoir of bioactive compounds can serve as a source of potent EP inhibitors (EPIs). The phyto-therapeutics with noteworthy drug-resistance-reversal or re-sensitizing activities may prove significant for reviving the otherwise fading antibiotics arsenal and making this combination-therapy effective. Contemporary attempts to potentiate the antibiotics with plant extracts and pure phytomolecules have gained momentum though with relatively less success against Gram-negative bacteria. Plant-based EPIs hold promise as potent drug-leads to combat the EPI-mediated AMR. This review presents an account of major bacterial multidrug EPs, their roles in imparting AMR, effective strategies for inhibiting drug EPs with phytomolecules, and current account of research on developing novel and potent plant-based EPIs for reversing their AMR characteristics. Recent developments including emergence of *in silico* tools, major success stories, challenges and future prospects are also discussed.

Keywords: antimicrobial resistance, efflux pumps, efflux pump inhibitors, phyto-therapeutics, drug resistance reversal

OPEN ACCESS

Edited by:
Henrietta Venter,
University of South Australia, Australia

Reviewed by:
Daniel Pletzer,
University of British Columbia, Canada
Manuel Varela,
Eastern New Mexico University, United States

***Correspondence:**
Vinay Kumar
vinaymalik123@gmail.com

Specialty section:
This article was submitted to Antimicrobials, Resistance and Chemotherapy, a section of the journal Frontiers in Microbiology

Received: *22 May 2018*
Accepted: *19 November 2018*
Published: *10 December 2018*

Citation:
Shriram V, Khare T, Bhagwat R, Shukla R and Kumar V (2018) Inhibiting Bacterial Drug Efflux Pumps via Phyto-Therapeutics to Combat Threatening Antimicrobial Resistance. Front. Microbiol. 9:2990. doi: 10.3389/fmicb.2018.02990

INTRODUCTION

Antimicrobial resistance (AMR) or ineffectiveness of commonly used drugs/antibiotics against specific bacteria has emerged as one of the most threatening human health concerns and a major challenge for global drug discovery programs. AMR (also known as drug resistance) has been reported at three increasing levels, multidrug resistance (MDR), extensive drug resistance (XDR)

and pan-drug resistance (PDR). By definition, MDR stands for acquisition of non-susceptibility to at least one agent in three or more antimicrobial classes, while XDR shows the non-susceptibility to at least one agent in all, except two or fewer antimicrobial classes, while PDR implies non-susceptibility to all antimicrobial agents from all available classes (Exner et al., 2017; Spengler et al., 2017). AMR is threatening millions of lives worldwide, and is rightly declared as a *global risk* by the World Economic Forum (World Economic Forum, 2013). Since the very first report on AMR in *Enterobacteria* in 1950s (Watanabe, 1963; Levy, 2001), many drug-resistant strains have been reported and their number as well as the resistance level is on the rise. Though several classes of antibiotics were discovered in the antibiotic era (**Table 1**), we are heading to a post-antibiotic era, where an increasing number of previously curable infections are turning into non-curable and life-threatening (Spengler et al., 2017). Though development of AMR or antibiotic resistance is a natural phenomenon, irrational use of antibiotics speed-ups the emergence of drug-resistant strains (World Health Organization, 2014). Once the AMR is gained by the bacteria, it is successively transmitted to the next progeny via vertical gene transfer or other bacteria through horizontal gene transfer process, making their treatment more difficult (Chandra et al., 2017).

The drug resistance characteristics may be attributed to the abilities of such strains in fast altering their genetic make-up or inducing epigenetic changes (Davies and Davies, 2010; Motta et al., 2015; Rahman et al., 2017). Necessary adaptations are achieved by bacteria to-respond-to and to counteract the antibiotics either via procurement of foreign genetic material encoding resistance via horizontal gene transfer or mutations in drug-targets / antibiotics-degrading enzymes and alterations in permeability of the outer bacterial membrane. There is an unprecedented upsurge in bacterial strains with elevated AMR in both Gram-negative and Gram-positive phenotypes. The ESKAPE (*Enterococcus faecium*, *Staphylococcus aureus*, *Klebsiella pneumoniae*, *Acinetobacter baumannii*, *Pseudomonas aeruginosa*, and *Enterobacter* species) pathogens have emerged with high degree of AMR and are major cause of life-threatening nosocomial infections (Santajit and Indrawattana, 2016). Even other strains like *Escherichia coli*, *Shigella* species, *Neisseria gonorrhoeae*, and *Proteus mirabilis* have shown significant levels of AMR (Fair and Tor, 2014; Prasch and Bucar, 2015; Cerceo et al., 2016). Development of resistance against the carbapenem, a class of highly effective antibiotics and regarded as the last line of defense against pathogenic Gram-negative bacteria hints at the alarming situation (Kumarasamy et al., 2010; Dwivedi et al., 2015).

Intrinsically, AMR is more prevalent and severe in Gram-negative bacteria than their Gram-positive counterparts due mainly to the outer membranes serving as permeability barrier for drug-influx into the Gram-negative bacteria (Silhavy et al., 2010; Exner et al., 2017). To attain low sensitivity against biocidal compounds, Gram-negative bacteria reduce their outer membrane permeability by reducing the number of porins and inducing drug efflux pumps (EPs) for outward transport of drug molecules, often in a non-specific manner making the bacterial cells resistant to multiple antibiotics (Masi et al., 2017). However, despite these morphological differences, Gram-positive bacteria cannot be ignored or underestimated and noteworthy examples include methicillin resistant *S. aureus* (MRSA) and vancomycin resistant *S. aureus* (VRSA), coagulase negative *Staphylococci* members including *S. epidermidis* and *S. haemolyticus*, *Streptococcus pneumonia*, *E. faecalis*, *E. faecium*, and *Clostridium difficile* (Schindler and Kaatz, 2016). **Figure 1** shows a gradual upsurge in the number of research articles focused on most-prevalent MDR strains.

In recent years, EPs have emerged as key drivers for AMR in Gram-negative and Gram-positive bacteria, and therefore, are looked upon as potent and universal targets for containing the drug-resistant phenotypes. EPs are vital in other physiological processes also including stress-adaptations, virulence, pathogenicity and transportation of essential nutrients (Piddock, 2006; Fernandez and Hancock, 2012; Costa et al., 2013; Kourtesi et al., 2013; Sun et al., 2014). Identifying novel and potent EP inhibitors (EPIs) to revert the AMR is therefore gaining momentum. EPIs are the compounds with capability to reduce resistance or a complete reversal of AMR against otherwise ineffective antibiotics via inhibiting the EPs (Sun et al., 2014; Gill et al., 2015; Wright, 2016; Spengler et al., 2017). The first EPI against RND-type EPs was reported by Lomovskaya et al. (2001) a phenylalanine-arginine β-naphthylamide (PAβN) effective against Mex pumps in *P. aeruginosa* and AcrAB-TolC pump in *E. coli*. Since then, various synthetic and natural compounds have been screened for their EPI capabilities (reviewed by Prasch and Bucar, 2015; Spengler et al., 2017; Shin et al., 2018; Yang et al., 2018). **Figure 2** illustrates the inhibition of microbial drug efflux via synthetic and natural EPIs.

Medicinal plants with antimicrobial properties have the potential to serve as the reservoir of novel and effective EPIs (Newman and Cragg, 2012). Though there are several reports on assessing medicinal plants for their antimicrobial properties (crude extracts and occasionally pure molecules), few investigations were aimed against MDR/XDR strains and fewer on deciphering the underlying resistance mechanisms targeted by the plant products (Kumar et al., 2013). But newer studies are coming up for identifying novel phytomolecules capable of reversing EP-mediated AMR. Some striking phytochemicals which have recently been identified for their EPI potentials include catechol, pinene, gingerol, capsaicin, resveratrol and the number is increasing (Prasch and Bucar, 2015).

In this review, we are presenting an account of major EPs, their roles in imparting bacterial AMR, strategies for identifying plant-based EPIs emphasizing on the potent phyto-EPIs active at relatively lower concentrations, reported during the last 8 years. High throughput screening and *in silico* approaches for predicting the EPIs and their binding targets/sites are also discussed.

PHYSIOLOGICAL ROLES PLAYED BY BACTERIAL EFFLUX PUMPS

Bacterial genome comprises of EP genes, expressed under tight regulation of global/local transcription factors (e.g., BmrR:

TABLE 1 | Classes of commonly used antibiotics along with their examples and corresponding modes of action.

Class of antibiotics				Examples	Mode of action
Beta Lactams	Beta lactamase inhibitors			Sulbactam, Tazobactam, Clavulanic acid, Avibactam	Cell wall synthesis inhibitors
	Penicillins	Penicillinase sensible	Aminopenicillins	Ampicillin, Amoxicillin	
			Natural penicillins	Penicillin G, Penicillin VK	
		Penicillinase resistant		Nafcillin, Dicloxacillin, Oxacillin	
		Anti-pseudomonal	Carboxypenicillins	Ticarcillin, Carbenicillin	
			Ureidopenicillins	Piperacillin, Mezlocillin, Azlocillin	
	Cephalo-sporins	1st generation		Cephalexine, Cefadroxil, Cefazolin, Cephradrine	
		2nd generation		Cefuroxime, Cefoxitin, Cefaclor, Loracarbef, Cefprozil	
		3rd generation		Cefoperazone, Cefpodoxime, Ceftriaxone, Cefotaxime, Ceftazidime	
		4th generation		Cefepime, Cefpirome	
		5th generation		Ceftaroline, Ceftolozane	
	Carbapenems			Meropenem, Doripenem, Ertapenem, Imipenem	
	Monobactams			Aztreonam	
No lactams	Glycopeptides			Vancomycin, Dalbavancin, Telavancin, Oritavancin	
	Other			Colistin, Daptomycin, Polymixin B, Isoniazid	
	Amino-glycosides			Amikacin, Streptomycin, Neomycin, Gentamicin, Tobramycin	Protein synthesis inhibitors
	Tetracyclins			Doxycyclin, Tetracyclin, Democlocyclin, Minocyclin, Tigecyclin	
	Oxazolidonones			Linezolid, Tidezolid	
	Streptogramins			Quinupristin	
				Chloramphenicol	
	Macrolides			Erythromycin, Clarithromycin, Azithromycin	
	Lincosamides			Clindamycin, Lincomycin	
	Fluorquinolones			Ciprofloxacin, Sparfloxacin, Levofloxacin, , Norfloxacin	DNA topoisomerases inhibitors
	Quinolones			Nalidixic acid	
	Sulfonamides			Sulfamethoxazole, Sulfasalazine, Ag sulfadiazine, Sulfisoxazole	Folic acid synthesis inhibitor
	DHFR inhibitors			Trimethoprim, Pyrimethamine	
	Nitroimidazoles			Metronidazole, Tinidazole	DNA Damage
				Rifampin	mRNA synthesis

transcriptional regulator of efflux pump Bmr in *B. subtilis*; QacR: transcriptional repressor of QacA transporter in *S. aureus;* AcrR: transcription repressor of acrB efflux pump in *E. coli*) proposing the important physiological roles the EPs play during cell development, stress adaptations and bacterial pathogenesis (Sun et al., 2014). The knowledge about these regulatory mechanisms may advance the understandings of physiologically originated AMR, frequently observed in nature (Sun et al., 2014). As discussed above, bacterial EPs have a tremendous capacity to extrude the variety of toxic compounds, needed for the cell survival in a given physiological niche and are vital for maintaining pathogenicity. This is further supported by the studies showing reduced pathogenicity in the bacterial strains lacking EPs. Buckley et al. (2006) showed that *S. typhimurium acrB* or *tolC* deficient mutant poorly colonized in the avian gut, highlighting the requirement of complete AcrAB-TolC system for virulence. The *S. typhimurium* strain lacking all the drug efflux assemblies became avirulent, when tested in a mouse model (Nishino et al., 2006). To confirm the role of EPs in bacterial pathogenesis, Hirakata et al. (2002) assessed the ability of EP (MexAB-OprM, MexCD-OprJ, MexEF-OprM, and MexXY-OprM) mutants of *P. aeruginosa* to invade Madin-Darby canine kidney cells. The findings revealed that except mexCD-OprJ, all other systems evidenced decreased bacterial invasion abilities.

EPs are also known to effect the bacterial cell communication during the stress-responses, especially in the quorum-sensing (González and Keshavan, 2006). As transportation of auto-inducers (chemical signals generated during quorum sensing) is a key-event during cell-cell interactions via quorum-sensing, drug EPs assist their transport across the membrane (Liang et al., 2016). Moore et al. (2014) confirmed a vital role played by MexAB-OprM efflux system in the secretion of a major auto-inducer N-acylated L-homoserine lactone by *P. aeruginosa* cells. The study also postulated this auto-inducer as a substrate for MexAB-OprM system (Moore et al., 2014).

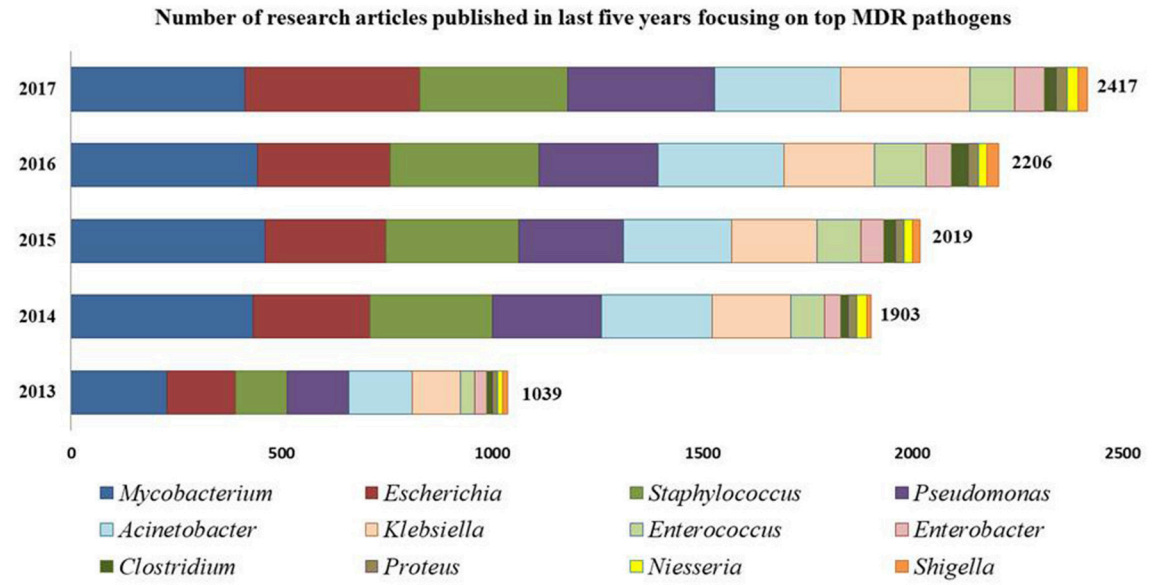

FIGURE 1 | Number of research articles reported from 2013 to 2017 focusing on MDR bacterial strains. [Source: PubMed; Key words used: Multidrug resistant "*Genus name*"].

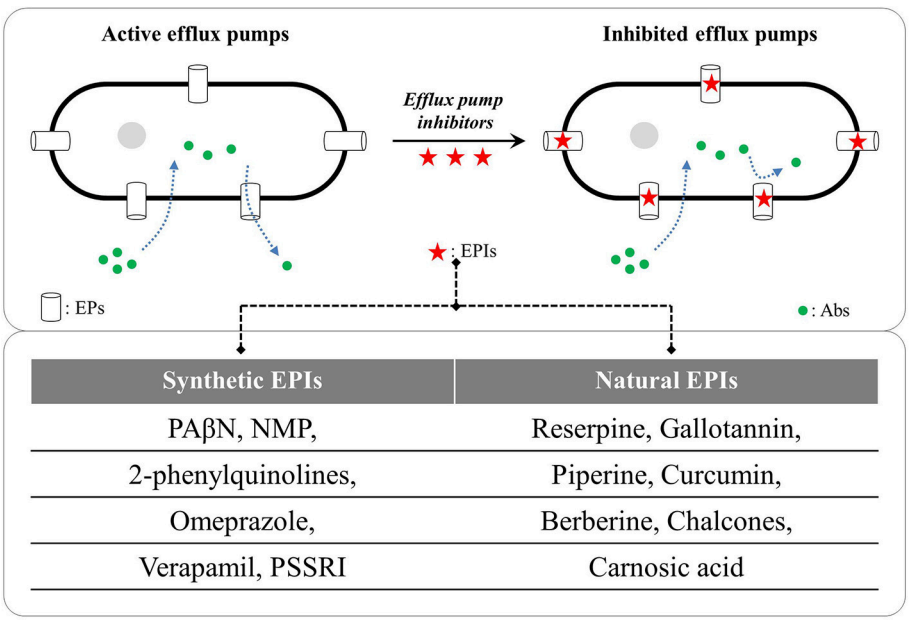

Synthetic EPIs	Natural EPIs
PAβN, NMP,	Reserpine, Gallotannin,
2-phenylquinolines,	Piperine, Curcumin,
Omeprazole,	Berberine, Chalcones,
Verapamil, PSSRI	Carnosic acid

FIGURE 2 | Examples of synthetic and natural efflux pump inhibitors (EPIs); PAβN: phenyl-arginine-β-naphthylamide, NMP: 1-(1- naphthylmethyl)-piperazine, PSSRIs: phenylpiperidine selective serotonin re-uptake inhibitors (German et al., 2008; Hannula and Hänninen, 2008; Li et al., 2015; Ni et al., 2016; Willers et al., 2016; Sabatini et al., 2017). Abs, antibiotics; EPs, efflux pumps.

Further, Martinez et al. (2009) advocated the EP-mediated ceasing of quorum-sensing via augmented efflux of auto-inducers, facilitating quick bacterial response to stress signals. One more physiological role attributed to EPs is in the biofilm formation. Recent studies confirm the involvement of many well-characterized efflux systems, AcrAB-TolC of *E. coli*, AcrD of *S. enterica*, AdeFGH of *A. baumannii* and MexAB-OpeM of *P. aeruginosa* in biofilm formation (Alav et al., 2018). Kvist et al. (2008) reported an up-regulation of 20 genes encoding EP-transporters in *E. coli* during the growth of biofilm. Similarly,

the EP-mediated export of colanic acid for capsule-matrix formation was observed along with up-regulated TetA(C) in *E. coli*, facilitating the biofilm formation (May et al., 2009). Collectively, the physiological roles of EPs are vital for pathogenic stability and virulence maintenance in bacteria.

The synthetic EPIs namely carbonylcyanide m-chlorophenylhydrazone (CCCP), chlorpromazine and PAβN were reported to prevent biofilm formation in *E. coli*, *P. aeruginosa* and *S. aureus* (Baugh et al., 2014). However, investigations on evaluating phytochemicals for their anti-biofilm potencies via inhibiting EPs are few. Fiamegos et al. (2011) isolated 4,5-O-dicaffeoylquinic acid from *Artemisia absinthium* which was proved to be a potent inhibitor of MFS pumps in *E. coli* and *E. faecalis* and as an anti-biofilm agent (Fiamegos et al., 2011). Recent reports advocate that nanomaterials in combination with phyto-EPIs can also be an effective therapy for containing drug-resistant infections (Gupta et al., 2017).

BACTERIAL EFFLUX PUMPS: THE WARHEADS IN AMR STRAINS

Though bacterial AMR has several origins and many adaptive mechanisms are employed by drug-resistant strains against the antibiotics, the intrinsic EPs hold the key. Recent clinical and laboratory data establish that bacterial EPs are not only critical for drug-extrusion but also contribute to their virulence and adaptive responses (Du et al., 2018). Often, antimicrobial drug exposure induces intricate bacterial reactions including altered expressions of several genes encoding the transporters, as revealed by the phenotypic profiling of *E. coli* (Nichols et al., 2011).

Bacterial EPs are acknowledged either as primary active transporters using ATPs as an energy source, or as secondary active transporters acquired due to electrochemical potential difference created by pumping out Na^+ and H^+ outside the membrane (Dwivedi et al., 2017a).

This may be considered for classifying EPs into two broad super-families namely; ATP-binding cassette (ABC) multidrug transporters and secondary transporters using proton motive force (PMF) as an energy source (Putman et al., 2000). The second super-family can again be categorized in four subclasses, the major facilitator superfamily (MFS), resistance-nodulation-cell division (RND), multidrug and toxic compound extrusion (MATE) and small-MDR (SMR) family (Fernandez and Hancock, 2012; Sun et al., 2014). RND and MFS pumps are the most common in bacteria. With relatively narrow spectrum of specificity, MFS pumps are found in both Gram-negative and Gram-positive bacteria; while poly-selective RND pumps are exclusive to Gram-negative bacteria (Ward et al., 2001; Molnár et al., 2010). The SMR transporters show specificity for broad-spectrum polyaromatic cations convening resistance for compounds sharing similar chemical description. The MATE transporters are similar in size to MFS transporters but they do not share any sequence similarity with them (Jack et al., 2001). Apart from the classified super-families and sub-families, the MATE, SMR, and RND classes are distributed uniquely to prokaryotes whereas MFS and ABC transporters are dispersed in both prokaryotes and eukaryotes.

The large MFS is one of the most functionally diverse transporter families comprising multiple transportation types for drugs as well as sugars. These transporters comprise ∼400 amino acids arranged as membrane-spanning helices (Saier et al., 1998). Based on the helical structure, MFS transporters can be classified as either 12-[e.g., TatA(B): class B tetracyclin transporter from *E. coli*] or 14-helix transporters [e.g., TatA(K): class K tetracyclin transporter from *S. aureus*], and TetA(B) is one of the most extensively studied members of the family (Lynch, 2006).

The SMR pumps represent smallest multidrug transporters, possessing only four trans-membrane helices without any extra membrane domain. But single minimal functional SMR unit represents eight helices as these are functionally active in dimeric form (Higgins, 2007). Well-illustrated example from this family is the electromagnetic antiporter EmrE from *E. coli*, responsible for resistance to a range of cationic-hydrophobic entities including antibiotics.

The latest structurally characterized class of EPs is MATE, involved in various vital biological functions (He et al., 2010). These transporters are equivalent to MFS transporters with a typical composition of ∼450 amino acids putatively arranged in 12 helices; but with no sequence similarity with MFS counterparts (Jack et al., 2001). Some characterized MATE members include NorM from *N. gonorrhoeae* and *N. meningitides* and YdhE from *E. coli.* However, limited structural and functional knowledge is available about this family (Dwivedi et al., 2017a).

Though EPs from other families contribute to the AMR against certain antibiotics, RND pumps are the most potent drug efflux systems conferring resistance against clinically important antibiotics and biocides. Members of this family are known for their roles against a wide range of molecules with dissimilar structures including antibiotics, biocides, organic solvents, antimicrobial peptides, detergents, dyes, and bile salts (Poole, 2004). The tripartite complex of pumps from this family comprises inner membrane protein (IMP), outer membrane protein (OMP) along with a periplasmic membrane fusion protein (MFP) as a connector (Venter et al., 2015). The best understood tripartite complexes include AcrA-AcrB-TolC from *E. coli* and MexA-MexB-OprM from *P. aeruginosa* (Du et al., 2013, 2014). Greater structural and functional similarities between IMPs of these two systems are described by Welch et al. (2010). Exploration on biochemical and structural aspects of AcrB has revealed that these IMPs contain proximal and distal binding pockets, divided by G-loop (with 614–621 residues). Conformational flexibility of G-loop is crucial for movement of substrate along the binding site (Eicher et al., 2012; Cha et al., 2014). **Table 2** lists various EPs belonging to the major families from prevalent pathogenic bacteria.

Collectively, the complex EP assemblies are critical for bacterial pathogenesis, virulence, biofilm formation, and adaptive-responses ultimately conferring and defining bacterial AMR (Piddock, 2006; Martinez et al., 2009; Baugh et al., 2012, 2014; Du et al., 2018). EPs are critical for bacterial AMR as they exclude most of the unwanted entities

TABLE 2 | Examples of various efflux pumps belonging to major efflux pump families from prevalent pathogenic bacterial strains.

Pathogen	EP Family	Example	Substrate	References
Acinetobacter baumannii	ABC	*MacAB-TolC*	ML	Okada et al., 2017
	MATE	*AbeM*	ACR, AG, DAU, DOR, FQ	Su et al., 2005
	MFS	*CraA*	CHL	Roca et al., 2009
	RND	*AdeABC, AdeFGH, AdeIJK*	AG, BL, FQ, ML, TET, BIO	Coyne et al., 2010, Rajamohan et al., 2010
Campylobacter jejuni	RND	*CmeABC, CmeDEF*	AG, BL, CHL, FQ, ML, RIF, TET, EB	Lin et al., 2002; Akiba et al., 2006
Enterococcus faecalis	ABC	*EfrAB*	ACR, CIP, DAU, DOR, DOX, NOR, TPP	Lee et al., 2003
Escherichia coli	ABC	*MacAB-TolC*	ML	Kobayashi et al., 2001
	MFS	*MdfA*	CHL, DOR, NOR, TET	Nishino et al., 2006
		QepA/QepA2	FQ	Cattoir et al., 2008
	RND	*AcrAB-TolC*	BL, CHL, FQ, ML, NOV, RIF, TET, TGC, R6G	Swick et al., 2011, Lennen et al., 2013
		OqxAB	CHL, FQ	Hansen et al., 2004
	SMR	*EmrE*	ACR, EB, QAC	Schuldiner, 2009, Beketskaia et al., 2014
Klebsiella pneumoniae	MATE	*KetM*	DAPI	Ogawa et al., 2015
	MFS	*KpnGH*	CAZ, CEF, STR, TET	Srinivasan et al., 2014
	RND	*OqxAB*	CHL, FQ	Hansen et al., 2004
	SMR	*KnpEF*	BAC, CEF, CHX, ERY, STR, TET, TRI	Srinivasan and Rajamohan, 2013
Mycobacterium tuberculosis	ABC	*Rv1218c*	BAP, BPD, PRI, PYR	Balganesh et al., 2010, Balganesh et al., 2012
	MFS	*Tap*	PAS, SPE, TET	Ramón-García et al., 2012
	SMR	*Mmr*	CAB, CLA, TPP	Balganesh et al., 2012, Rodrigues et al., 2013
Pseudomonas aeruginosa	RND	*MexAB-OprM, MexXY-OprM/A, MexCD-OprJ, MexEF-OprN*	AG, BL, CHL, FQ, ML, SUL, TET, TGC, TMP, BIO, EB	Poole et al., 1996, Köhler et al., 1997
Staphylococcus aureus	ABC	*Isa(E)*	LIN, PLE, STA	Wendlandt et al., 2015
		Msr(A)	ML, TEL	Vimberg et al., 2015
	MATE	*MepA*	BIO, EB, FQ, TIG	Kaatz et al., 2005
	MFS	*NorA*	FQ	Yoshida et al., 1990
		QacA	ACR, CHX, EB, QAC	Littlejohn et al., 1992
Streptococcus pneumoniae	ABC	*PatAB*	FQ	Marrer et al., 2006
	MFS	*MefE*	ML	Tait-Kamradt et al., 1997
Vibrio spp.	ABC	*VcaM*	CIP, DAU, DOR, NOR, TET	Huda et al., 2003
	MATE	*NorM*	AG, EB, FQ	Morita et al., 1998
	MFS	*EmrD-3*	EB, LNZ, ERY, CHL	Bruns et al., 2017

ACR, acriflavine; AG, aminoglycosides; BAC, benzalkonium chloride; BAP, biaryl-piperazines; BL, β-lactams; BIO, biocides; BPD, bisanilino-pyridines; CAB, cetyl-trimethyl-ammoniumbromide; CAP, cationic antibacterial peptides; CAZ, ceftazidime; CEF:cefepime; CHL, chloramphenicol; CHX, chlorhexidine; CIP, ciprofloxacin; CLA, clofazimine; DAU, daunomycin; DAPI, 4',6-diamidino-2-phenyl indole; DOR, doxorubicin; DOX, doxycycline; EB, ethidium bromide; ERY, erythromycin; FQ, fluoroquinolones; FUA, fusidic acid; LIN:lincosamide; LNZ, linezolid; ML, macrolides; NOR, norfloxacin; NOV, novobiocin; PAS, p-aminosalicylate; PLE, pleuromutilin; PRI, pridones; PYR, pyrroles; QAC, quaternary ammonium compounds; SPE, spectinomycin; STA, streptogramin A; STR, streptomycin; SUL, sulfonamides; TEL, telithromycin; TET, tetracycline; TGC, tigecycline; TMP, trimethoprim; TPP, tetraphenylphosphonium,TRI, triclosan.

until the cell gets required time for acquiring resistance (Piddock, 2014; Venter et al., 2015).

BACTERIAL EFFLUX PUMPS: THE URGENT THREATS REQUIRING IMMEDIATE REMEDY

It is well-established that EPs comprise one of the most vital systems in bacteria responsible for both innate and acquired AMR (Blair et al., 2015). There are reports of EPs from different superfamilies and the occurrence of various types of EPs from the same superfamily in a single bacterial species (Piddock, 2006). For instance, whole genome sequencing of the colistin resistant *Enterobacter cloacae* showed presence of multiple EPs (Norgan et al., 2016). Differential substrate profiles of EPs are also a characteristic feature which may diverge between or within the superfamily (Poole, 2005, 2007). Although the core motive of EPs related studies is focused on AMR, several reports however confirmed other but significant functions of bacterial

EPs including quorum-sensing, biofilm formation, virulence, pathogenicity and bacterial behavior (Piddock, 2006; Yang et al., 2006; Fahmy et al., 2016).

Up-regulation of gene expression levels are one of the main drivers for chromosomally acquired AMR. This can be triggered due to the gene induction, activated transcription, or due to regulatory mutations (Grkovic et al., 2002). The coding region for an EP is usually found contiguous to the regulatory proteins controlling the expression levels of pump gene in response to substrates. For example, AdeL, an LTTR (LysR-type transcriptional regulator) family protein exists opposite to the adeFGH operon that regulates the expression of genes encoding RND efflux system in *A. baumannii* (Liu et al., 2018). The expression levels of EP-associated proteins along with porins is mutually controlled by several global regulatory elements, modifying the transcription patterns of EP-family transcripts either directly or through a cascade of regulatory events (Warner and Levy, 2010; Sun et al., 2014). Further, the expression of MexAB-OprM efflux system is governed by repressor protein mexR, encoded by a gene located upstream of the mexAB-oprM operon in *P. aeruginosa* (Suresh et al., 2018). Similarly, the acrAB operon system is regulated by regulator acrR in *E. coli*, located 140 bp up-stream of the acrAB operon (Ma et al., 1996).

Another striking bacterial character adding to the AMR nature is heteroresistance, the occurrence of differential responses to antibiotics by the bacterial cells from the same population, a phenomenon first reported in *S. aureus* (Kayser et al., 1970). Interestingly, drug resistant and sensitive bacterial cells may co-exist in a single culture (Morand and Mühlemann, 2007). The mechanism underlying heteroresistance acquirements are yet to be fully understood, however, the active EPs are strongly linked to heteroresistance (Chen et al., 2017). Designing a treatment course against such strains is difficult as there are high chances of increase in the frequency of resistant-bacterial-population and stimulation of cross-resistance to antimicrobial lysozymes of the host system (Napier et al., 2014; Telke et al., 2017). Up-regulation of OpxAB gene in *Salmonella typhimurium* (Chen et al., 2017) and AdeABC gene in *A. calcoaceticus-A. baumannii* (Ruzin et al., 2007) are attributed for mediating the tigecyclin heteroresistance. Similarly, colistin associated heteroresistance is also reported in *E. asburiae* LH74 and *E. cloacae* NH52 (Telke et al., 2017), showing its association with overexpression of *acrAB-tolC* EPs under the regulation of soxRS genes.

AMR phenotypes may result from concurrent acquisition of several AMR mechanisms simultaneously. It may include a combination of phenomena like chromosomally acquired resistance, multiple chromosomal changes with time, and/or a single mutational event activating the AMR mechanisms including the EPs (Lister et al., 2009). The over-expressions of EPs and their corresponding genes have been reported to contribute to MDR in *P. aeruginosa* (Shigemura et al., 2015). Recent studies have confirmed the role of EPs in fluoroquinolone resistant *E. coli* (Amabile-Cuevas et al., 2010; Swick et al., 2011; Yasufuku et al., 2011). Similarly, two fluoroquinolone resistant clinical isolates of *Shigella* showed overexpression of the TolC channels, part of AcrAB-TolC tripartite responsive to ciprofloxacin (Kim et al., 2008). These findings confirm that the up-regulation of EP genes contribute significantly to diminish intracellular antibiotics level, with a selectivity of the efflux transporter.

Overall, the poly-specificity of EPs, their overexpression in response to drugs along with the phenomenon of heteroresistance seem key factors responsible for drug-resistance in a wide-range of bacterial species, especially in Gram-negative bacteria making them difficult to treat with conventional drug arsenal. The drug-efflux mediated bacterial AMR is a mounting threat to global healthcare, therefore EPs are gaining unprecedented attention not only from the perspectives of basic understandings that how they work and impart drug-resistance but also as emerging targets for development of novel and potent adjunct-therapies for combating AMR in community and nosocomial infections. As a result, inhibition of drug efflux from bacterial cells via inhibiting or disrupting the EPs is an emerging approach for combating the threatening AMR. Various approaches have been developed in recent past and a schematic for these strategies for inhibition or disruption of bacterial drug efflux is illustrated in **Figure 3**.

PHYTOTHERAPEUTICS–THE POTENT EFFLUX PUMP INHIBITORS

Phytochemicals are critical for human health-care since ancient times. Medicinal plants are hailed as a reservoir for phytochemicals capable of providing new and potent drug leads to contain the AMR via targeting the principal determinants of drug-resistance including EPs (Newman and Cragg, 2012; Prasch and Bucar, 2015). This review focuses mainly on EPIs of plant origin (phyto-EPIs) reported in the running decade. We are discussing some important and successful case studies on phyto-EPIs effective against AMR phenotypes. **Table 3** summarizes the list of phytochemicals, their source and effective concentrations used for inhibiting the efflux pumps of AMR bacterial strains.

One of the potent EPIs, the anti-hypersensitive alkaloid reserpine was isolated from *Rauwolfia vomitoria* (Stavri et al., 2007). Similarly, EP inhibitory activity of gallotannin (1,2,6-tri-O-galloyl-b-D-glucopyranose) isolated from hydro-alcoholic extracts of *Terminalia chebula* fruits was demonstrated by Bag and Chattopadhyay (2014) against MDR uropathogenic *E. coli.* Gallotannin induced a 2- to 4-fold reduction in minimal inhibitory concentration (MIC) of test antibiotics via inhibiting the ethidium bromide (EtBr) pump (**Table 3**). As EtBr is a known EP-substrate, inhibition of EtBr efflux backs the postulated EP-inhibitory activity of gallotannin (Bag and Chattopadhyay, 2014). Methanolic sap extracts of *Acer saccharum* was evaluated for its drug efflux inhibitory potentials against *P. aeruginosa* (ATCC 15692 and UCBPPPA14), *E. coli* (ATCC 700928) and *P. mirabilis* (HI4320) confirmed via monitoring the EtBr efflux (Maisuria et al., 2015).

A clavine alkaloid lysergol from *Ipomoea muricata* was evaluated against AMR *E. coli* strains (MTCC1652 and KG4) to test its EP inhibitory potentials, and strong activities (higher than the standard reserpine) were exhibited by lysergol and its derivative, 17-O-3″,4″,5″-trimethoxybenzoyllysergol (Maurya

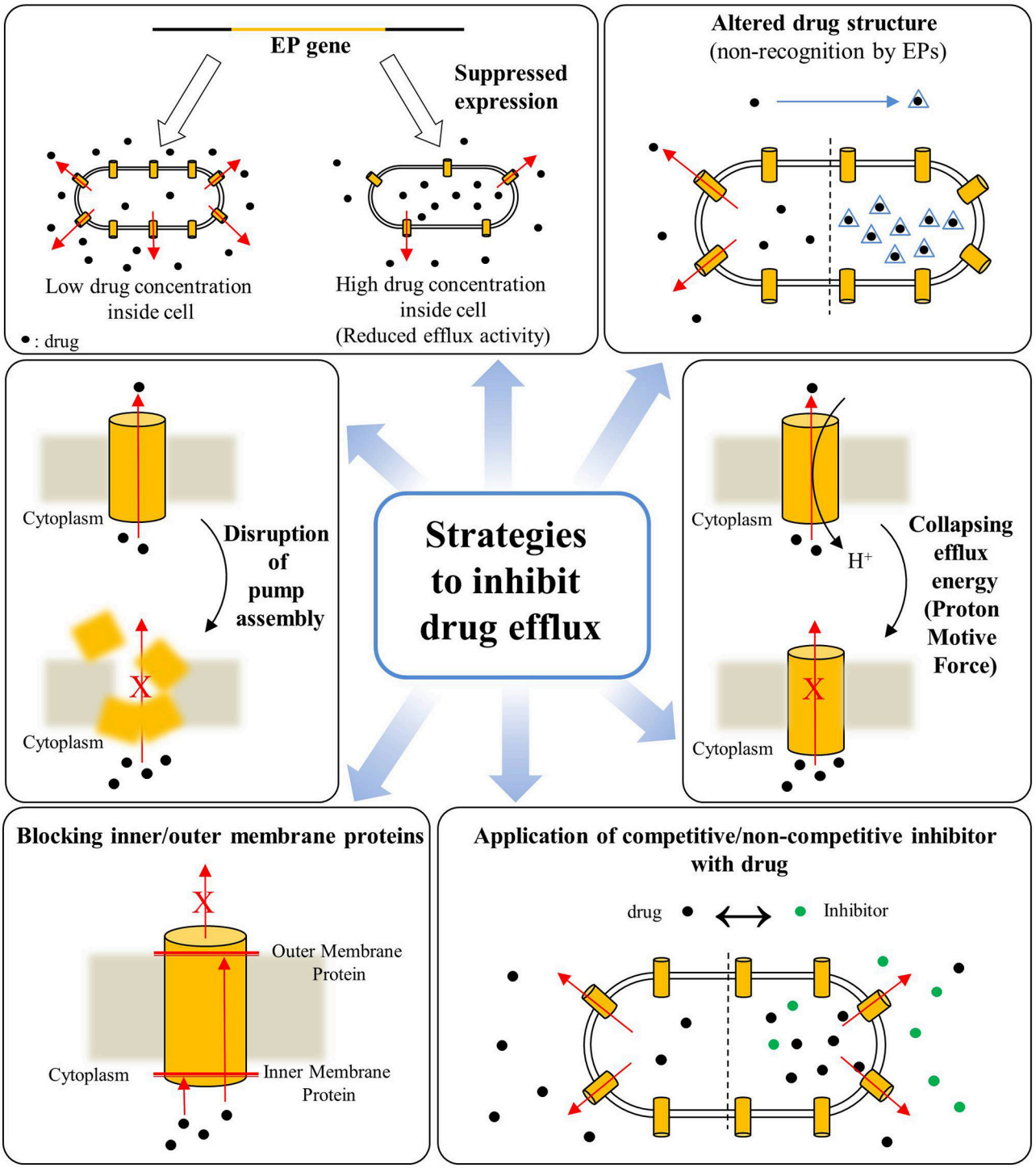

FIGURE 3 | Various strategies for inhibition of drug efflux from bacterial cells for combating antimicrobial resistance (Based on reviews by Pagès and Amaral, 2009; Venter et al., 2015).

et al., 2013). Authors also reported the inhibitory activities of this compound against ABC pump YojI in *E. coli* (Maurya et al., 2013). Similarly, falcarindiol, isolated from *Levisticum officinale* exhibited EPI activities against the Gram-negative strains (Garvey et al., 2011).

On the similar lines, Dwivedi et al. (2017b) reported the antibiotic-potentiating activities of catharanthine against superbug *P. aeruginosa*. The investigation involved *in silico* docking followed by the *in vitro* evaluation revealed that catharanthine potentiates the activity of tetracyclin and

TABLE 3 | A summarized list of phytochemicals, their source and effective concentrations for inhibiting efflux pumps from antimicrobial resistant bacteria.

Active Compound	Verified effective concentration/s	Plant	Antimicrobial resistant microbes	Targeted efflux pumps	References
1′-S-1′-acetoxyeugenol acetate	3.12–25 mg L^{-1}	*Alpinia galanga*	*Mycobacterium smegmatis* mc^2 155	EtBr EP	Roy et al., 2012
4-hydroxy-α-tetralone	125 μg mL^{-1}	*Ammannia* spp.	MDR *E. coli*	YojI	Dwivedi et al., 2014b
Baicalein	16 μg mL^{-1}	*Scutellaria baicalensis*	*S. aureus* SA-1199B	NorA	Chan et al., 2011
Berberine and Palmatine	250–1,000 μg mL^{-1} 500–100 μg mL^{-1}	*Berberis vulgaris*	MDR *P. aeruginosa* (clinical isolates)	MexAB-OprM	Aghayan et al., 2017
Capsaicin	25 μg mL^{-1}	*Capsicum* spp.	*S. aureus* SA-1199B	NorA	Kalia et al., 2012
Catechol	5 and 10 mg mL^{-1}	*Acer saccharum*	*P. aerugenosa* ATCC 15692 and UCBPPPA14, *E. coli* ATCC 700928, *P. mirabilis* HI4320	EtBr EP	Maisuria et al., 2015
Catharanthine	25 mg L^{-1}	*Catharanthus roseus*	*P. aeruginosa*	EtBr EP	Dwivedi et al., 2017b
Conessine	20 mg L^{-1}	*Holarrhena antidysenterica*	*P. aeruginosa*	MexAB-OprM	Siriyong et al., 2017
Cumin-methanol extract	5 mg mL^{-1}	*Cuminum cyminum*	*S. aureus* MRSA OM505	LmrS	Kakarla et al., 2016
Essential oil	5 μl mL^{-1}	*Salvia fruticosa*	*S. epidermidis* (clinical isolates)	Tet(K) EP	Chovanova et al., 2015
Essential oil	170.6 μl mL^{-1}	*Chenopodium Ambrosioides*	*Staphylococcus aureus IS-58*	Tet(K) EP	Limaverde et al., 2017
Gallotannin	12.1–97.5 μg mL^{-1}	*Terminalia chebula*	MDR uropathogenic *E. coli*	EtBr EP	Bag and Chattopadhyay, 2014
Indirubin	1.25 and 2.5 mg L^{-1}	*Wrightia tinctoria*	*S. aureus* SA-1199B	NorA	Ponnusamy et al., 2010
Kaempferolrhamnoside	1.56 mg L^{-1}	*Persea lingue*	*S. aureus* SA-1199B	NorA	Holler et al., 2012
Lysergol	10 μg mL^{-1}	*Ipomoea muricata*	*E. coli* MTCC1652 and KG4	YojI	Maurya et al., 2013
Olympicin A	50 μM	*Hypericum olympicum*	*S. aureus* 1199B	NorA	Shiu et al., 2013
Sarothrin	100 μM	*Alkanna orientalis*	*Staphylococcus aureus* NCTC 8325-4	NorA	Bame et al., 2013
Ursolic acid and derivatives	25 and 50 μg mL^{-1}	*Eucalyptus tereticornis*	MDR *E. coli* (KG4)	AcrA/B, MacB, TolC and YojI	Dwivedi et al., 2014a

streptomycin, as confirmed by a reduced MIC, and acts as a potent EPI (Dwivedi et al., 2017b). A pentacyclic triterpenoid ursolic acid from leaves of *Eucalyptus tereticornis* described as a precursor of putative EPI was evaluated against MDR *E. coli* (KG4), two promising semi-synthetic, esterified derivatives of ursolic acid, 3-O-acetyl-urs-12-en-28-isopropyl ester and 3-O-acetyl-urs-12-en-28-n-butyl ester and the parent compound exhibited better EP inhibitory potencies than the standard reserpine (Dwivedi et al., 2014a). The molecular docking confirmed the targets of these compounds as AcrA/B, MacB, TolC, and YojI (Dwivedi et al., 2014a). Similarly, two alkaloids isolated from roots and rhizomes of *Berberis vulgaris*, the barberine and palmatine showed potent EP inhibitory efficacies against *P. aeruginosa* isolated from burn infections (Aghayan et al., 2017).

Phenylpropanoids from the *n*-hexane and chloroform fractions of *Alpinia galanga* exhibited EP inhibitory activities against *Mycobacterium smegmatis* mc^2 155ATCC 700084 (Roy et al., 2012). A dose-dependent EP inhibition was observed with 1′-S-1′-acetoxyeugenol acetate (Roy et al., 2012). Mukanganyama et al. (2012) examined another mycobacterial member *Mycobacterium aurum* A+ against a naphthoquinone diospyrine isolated from *Diospyros montana* along with its derivatives. Two derivatives proved highly potent EPI and allowed bacterial cells to accumulate high concentrations of ciprofloxacin (Mukanganyama et al., 2012).

The acylphloroglucinol isolated from *n*-hexane fractions from *Hypericum olympicum*, olympicin-A showed promising activities against *S. aureus* (Shiu et al., 2013). The radiometric accumulation assay of the strain overexpressing NorA pump indicated the enhanced accumulation of (14)C-enoxacin, thus confirming efflux inhibition (Shiu et al., 2013). Two coumarins [5,7-dihydroxy-6-(2-methylbutanoyl)-8-(3-methylbut-2-enyl)-4-phenyl-2H-chromen-2-one and 5,7-dihydroxy-8-(2-methylbutanoyl)-6-(3-methylbut-2-enyl)-4-phenyl-2H-chromen-2-one] obtained from floral buds of *Mesua ferrea* were assessed against NorA-overexpressing *S. aureus* 1199B and the clinical isolate MRSA 831 (Roy et al., 2013). Linoleic acid isolated from ethanolic extracts of *Portulaca oleracea* showed efflux inhibitory potential at 64 mg L^{-1} concentration, equivalent to reserpine when quantified against MRSA (RN4220/pUL5054: erythromycin resistant, over-expressing MsrA ABC EP, Chan et al., 2015). In search of the drug-resistance reversal agents, dos Santos et al. (2018) assessed caffeic acid and gallic acid against four strains of *S. aureus*; 1199 as a wild type strain, 1199B as NorA harboring fluroquinolone

resistant, IS-58 possessing TetK pump and RN4220 possessing MrsA pump. The study confirmed caffeic acid as a potent AMR-reversal agent, as it effectively inhibited MrsA and NorA EPs from *S. aureus* strains RN4220 and 1190B, respectively (dos Santos et al., 2018). In another interesting study, Kakarla et al. (2016) reported LmrS inhibitory activities of *Cuminum cyminum*. The study revealed that the cumin inhibits the LmrS mediated transport of drugs resulting in growth inhibition of MRSA clinical isolate in a dose-dependent manner (Kakarla et al., 2016).

Traditionally, most of the investigations were aimed at identifying EPIs for Gram-positive strains for reversing their AMR characters with very few reports against Gram-negative members. This can be because Gram-negative bacteria are more difficult targets then their positive counterparts due mainly to the presence of powerful EPs and other effective membrane barriers (lipophilic layer) averting them from external impacts (Stavri et al., 2007; Prasch and Bucar, 2015). Though, some approaches have emerged in recent years for improving antibiotic-penetration across the permeability membranes of Gram-negative bacteria such as the inhibition of new accessible target, identification of uptake pathways and the "Trojan Horse" approach (achieving fast or facilitated antibiotics uptake), establishing the rules of permeation (for predicting whether elevated uptake or reduced efflux would be the most efficient way for increasing the potency of specific antimicrobial class) and identifying potent EPIs, last one being probably the most potent (Zgurskaya et al., 2015).

Recently, Bruns et al. (2017) successfully inhibited EmrD-3 pump-mediated drug efflux from a Gram-negative bacterium *Vibrio cholerae* by garlic extract and its bioactive compound, allyl sulfide. At relatively low concentrations, the extract seems to target the EmrD-3 pump, but at higher garlic extract concentrations, the respiratory chain was affected. This example confirms targeting the energization of the efflux system by plant compounds as a potential strategy for drug efflux inhibition (Bruns et al., 2017).

Further, the MFS conserved sequence motifs, present across the entire superfamily, provide vital information regarding alignments of MFS transporter sequences (at least motif containing region), which may help in understanding the structural templates and actual binding events achieved via these transporters. Molecular dynamic simulation (MDS) studies of VMAT2 multidrug transporter (MFS family) revealed the presence of two domains of six trans-membrane helices (Yaffe et al., 2013). The trans-membrane residues at anchoring sites are identified as hinge points, at which straightening and flexing movement of helices occur, required for transport. These anchor point residues are highly conserved throughout the MFS family (Yaffe et al., 2013) and are emerging targets for drug efflux inhibition. Recent advances in scientific and technological arena have added significant in-depth understandings of the structural and biochemical basis of drug efflux, substrate profiles, molecular regulation and inhibition of major EPs.

Active EPs play a critical role in intrinsic and elevated drug resistance acquired via overproduction or over-activation of pumps in Gram-negative bacteria, and the development of clinically useful EPIs or new antibiotics to bypass pump-effects continues to be a challenge in combating Gram-negative bacterial infections (Li et al., 2015). As practically all the antibiotics are susceptible to active drug efflux, the potent EPIs can target these pumps antagonistically and can make old antibiotics effective again (the phenomenon known as re-sensitization). Besides, considering the fact that several antimicrobial agents like lipophilic penicilines, many glycopeptides, oxazolidinones, macrolides and lipopeptide daptomycin are effective in treating only Gram-positive bacterial infections and their poor potencies against Gram-negative pathogens is at least partially due to their active drug efflux, novel and potent EPIs are needed to significantly broaden the range of these antimicrobial agents. All this clearly indicates that EPIs have tremendous potential in adjunctive therapies along with the known but otherwise ineffective antibiotics ultimately reducing the emergence of AMR and virulence (Opperman and Nguyen, 2015). But developing novel and potent EPI is difficult and needs to overcome several hurdles such as choice of antibiotics for potentiation and matching the pharmacological properties of EPI-antibiotics pair (Opperman and Nguyen, 2015; Zgurskaya et al., 2015).

Considering the serious threats posed by the Gram-negative bacteria and their drug-resistance nature, more investigations aiming to target them with the novel, alternative and effective approaches including exploration of natural products are coming up. Though there are limited success stories, but they may lay the foundation for developing potent EPIs to avert the AMR phenotypes with the help of natural sources.

IN SILICO MOLECULAR DYNAMICS SIMULATIONS (MDS) TO SCREEN AND DEVELOP EPIS

The MDS is a commanding approach for computational validation and to support the hypothesized mechanisms of EPs and EPIs (Nikaido and Takatsuka, 2009). It has made possible to simulate the membrane protein complex structures with micro-second time-scales. The MDS approach along with molecular docking and other *in silico* tools are successfully utilized for screening and prediction of molecular interactions between potential EPs and their corresponding inhibitors (Jamshidi et al., 2016). This has led to the unraveling of the mechanism how drug efflux systems recognize and transfer specific molecules; thus helping researchers in challenging the efflux-mediated resistance and finding appropriate EPIs for improvement in antibiotics efficacy during AMR (MDR/XDR) infections (Collu et al., 2012; Nakashima et al., 2013). There are several recent reports describing the successful applications of these *in silico* approaches for screening and identifying potent EPIs of plant origin (Bhaskar et al., 2016; Jamshidi et al., 2016; Mangiaterra et al., 2017; Verma et al., 2017).

A general scheme for MDS-based approaches is depicted in **Figure 4**. Briefly, it starts with the identification of three-dimensional structures of potential EP-binding sites (pockets). The next step is the prediction of trans-membrane segments

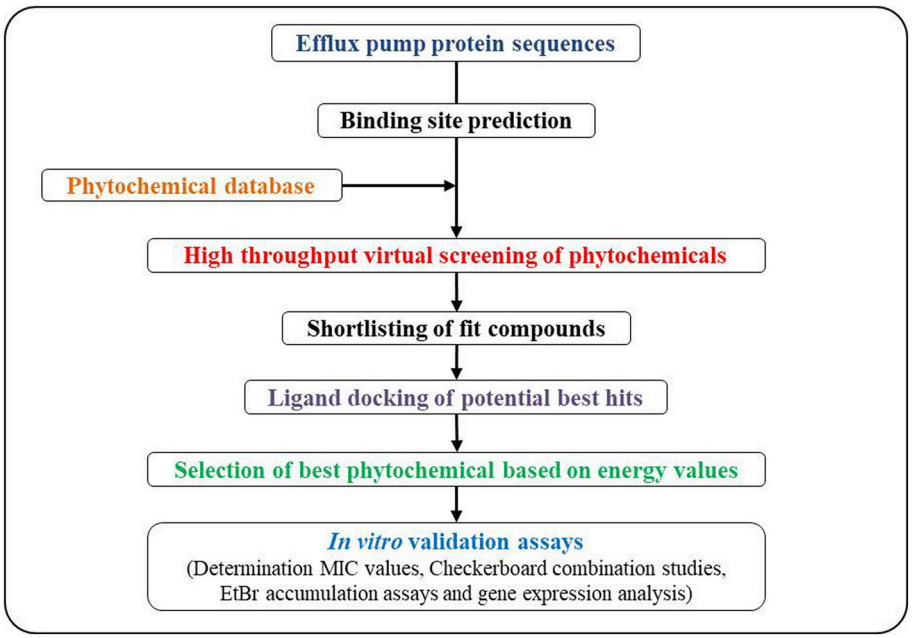

FIGURE 4 | A general scheme for *in silico* molecular dynamics simulations approach for screening and developing plant based efflux pump inhibitors.

from protein sequences. The predicted structure can then be checked for its stereochemical properties by analyzing the overall and residue-by-residue geometry. The modeled protein structure is then reduced with the solvent implied by chimera programs (http://www.cgl.ucsf.edu/chimera/, Pettersen et al., 2004) and the projected protein structure can be used for its interaction with potential EPI molecules. The three-dimensional structure of the EPI is then explored to attain perfect and stable EPI-EP complex. Potent tools for docking studies include AutoDock (http://autodock.scripps.edu/, Morris et al., 2009), and SwissDock (http://www.swissdock.ch/, Grosdidier et al., 2011). Such automated docking tools can predict the exact binding position of the candidate drug-molecule to the receptors, and provides vital information about exact amino residues taking part in bond-formation with potential drug(s), their bond lengths and type and other interactions adding to the stability of the docking complexes.

Recently, Kesherwani et al. (2017) used high throughput virtual screening of natural compounds against NorM, a MATE transporter from *N. gonorrhea* followed by flexible docking. Authors performed molecular simulation in a membrane environment for investigating the stability and binding energy of top lead compounds, and identified a phytomolecule from *Terminalia chebula* with higher binding free energy than the substrates (rhodamine 6 g, ethidium). The compound successfully blocked the disruption of Na^+-coordination along with an equilibrium state bias toward occlude state of NorM transporter, ultimately blocking the extrusion of antimicrobial drugs via inhibiting the NorM transporter in drug-resistant *N. gonorrhea*.

Similarly, Suriyanarayanan and Sarojini (2015) analyzed EPI potentials of plant-derived flavonoid quercetin in bringing down the drug efflux via inhibiting the EmrE, a transporter belonging to SMR family from *E. coli*. Authors used *in silico* approaches and molecule docking approaches. The docking analysis of quercetin with EP-protein showed the importance of residues for function and stability, and notably quercetin showed best interactions as compared to the compounds like verapamil, reserpine, chlorpromazine, and carbonyl cyanide m-chloro phenylhydrazone. MDS confirmed the stability of quercetin-Mmr complex, which insights the potential of quercetin as a non-antibiotics adjuvant for treatment of bacterial infection via reducing the drug efflux from bacteria.

Mangiaterra et al. (2017) identified two phyto-EPIs using *in silico* high-throughput virtual screening. Molecular docking revealed these two compounds morelloflavone and pregnan-20-one derivative as inhibitors of MexAB-OprM EPs of *P. aeruginosa* and supportive *in vitro* assays confirmed their synergism with ciprofloxacin (Mangiaterra et al., 2017).

Molecular docking plays a crucial role and help in defining drug-protein interactions which determines whether compounds act as substrates for EP proteins. Therefore, inhibitors or modulators of EPs are well-recognized along with their comparative binding efficiencies via detailed docking analyses (Collu et al., 2012). Putative EPI activities of quercetin, plumbagin, nordihydroguaretic acid, shikonion and mangiferin were confirmed (Ohene-Agyei et al., 2014). Similarly, docking of reserpine, salvin, totarol, ferruginol along with known antibiotics to NorA revealed that all the tested compounds showed binding at large hydrophobic cleft, suggesting the substantial interactions with key-residues (Bhaskar et al., 2016). Notably, all these investigations were backed by the bioassays confirming the validity of information generated via *in silico* screening.

Owing to the importance of an instantaneous requirement of curing the XDR/MDR strains with utmost specificity, a greater understanding of exact drug-identification and its transport by MDR-EPs is important. The *in silico* MDS approach along with virtual docking and wet laboratory validation therefore can be considered as an imperative path in identifying potent phyto-EPIs.

MOLECULAR INTERACTIONS UNDERLYING INHIBITION OF EFFLUX PUMPS BY PHYTO-THERAPEUTICS

The inhibition of active drug efflux by EPIs results into the elevated intracellular antimicrobial concentrations, and lowered or complete reversal of efflux-mediated bacterial drug resistance, prevention of microbial invasiveness by inhibiting the export of virulence-factors and shortened adaptation-time required for bacteria, prohibiting the emergence of mutant strains with high AMR (Bhardwaj and Mohanty, 2012; Sun et al., 2014). Major strategies developed for drug efflux inactivation are, first, alterations in regulatory mechanisms for activation/repression of EP gene expressions (Purssell and Poole, 2013), second, deprivation of motive forces required for working of pumps by diminishing the proton gradient (Viveiros et al., 2005; Martins et al., 2008), third structural modifications in existing antimicrobials to bypass the chemophore recognition by the EPs (Chollet et al., 2004; Rice et al., 2005), fourth disrupting the pump-functionality by averting assembly of pumps by targeting protein interfaces (Tikhonova et al., 2011); interaction between protein motifs (Hobbs et al., 2012); obstructing the exit duct (Zeng et al., 2010), and fifth, the trapping of EPs in the inactivated form by competitive binding of EPIs and cytoplasmic membrane proteins (Nakashima et al., 2013; Opperman et al., 2014; Nguyen et al., 2015; Opperman and Nguyen, 2015; **Figure 3**). In addition, targeting the molecular hinge structures by the conserved sequence motifs is also an emerging strategy for EP inhibition (Abdali et al., 2017). The conserved sequence motifs (7–13 residues) are characteristics of MFS family and these motifs on c-terminal end of trans-membrane helix are rich in glycine and proline, vital for promotion of hinge formation. These conserved residues are considered as major contributors in binding and transportation of respective substrates (Luo and Parsons, 2010), and therefore targeting them holds significance for drug efflux inhibition.

To identify the phyto-EPIs, some authors tried to decipher the physiological and molecular interactions involved in EP dysfunction. Sharma et al. (2010) described piperine as an inhibitor of Rv1258c, an efflux protein transporter present on cytoplasmic membrane [encoding for tetracyclin/aminoglycoside resistance (TAP-2)-like EP] in *M. tuberculosis* H37Rv. After structural prediction of the protein, further investigation revealed the binding pocket of Rv1258c. Authors showed H-bond interaction (2.06 Å) with Arg141 residue and piperine provided stable protein-ligand interaction. The findings confirmed the role of piperine in augmenting rifampicin sensitivity in *M. tuberculosis* (Sharma et al., 2010). Capsaicin also proved a potent EPI, inhibiting NorA pump of *S. aureus* (Kalia et al., 2012). The study showed the involvement of Arg98 and Ile23 residues from active binding site in the key binding interactions. The stable interaction between capsaicin and active site at the proposed orientation allows an aliphatic chain of capsaicin, extending in a hydrophobic cleft (containing residues Pro24, Phe140, Ile244, and Phe303) permitting strong hydrophobic interactions due to a lesser distance between ligand and molecule (1.7–3.2 Å). A weak H-bond formation between OH-group (from aryl moiety of capsaicin) and Arg98 was attributed for providing extra-stability to capsaicin/NorA complex (Kalia et al., 2012). Another study by Zhang et al. (2014) described the interactions between ginsenoside 20(S)-Rh2 and NorA from *S. aureus*. The stable H-bond formation between ginsenoside 20(S)-Rh2 and Gln51/Asn340/Ser226 residues at active binding site in the central cavity of protein was attributed for the inhibition of NorA pump, thus promoting accumulation of ciprofloxacin inside the bacterial cell (Zhang et al., 2014). In the similar vein, Ohene-Agyei et al. (2014) assessed five phytochemicals (plumbagin, shikonin, quercetin, mangiferin and nordihydroguaretic acid) for their EPI potentials against AcrB protein from AcrAB-TolC drug transporter. The stable H-bond formation between T monomer of AcrB with minocycline attached to binding pocket and phytochemicals was responsible for efflux inhibition by the phytochemicals (Ohene-Agyei et al., 2014). Further, the authors also postulated that the considered natural compound act as a substrate and compete with the antibiotics for drug-resistance reversal (similar to PAβN). Therefore, these natural products act as high-affinity substrate inhibitors rather than substances for trapping the EPs in an inactive state.

CONCLUDING REMARKS

Increasing AMR in community and nosocomial settings is a big threat to human healthcare and accounts for a large number of mortalities and morbidities globally. Bacterial EPs make up a major warhead of the drug-resistant pathogens and increase and maintain the AMR via extruding or reducing the intracellular concentrations of applied antibiotics, often in a non-specific manner. The drug EPs are also emerging as chemical tools to understand molecular mechanisms underlying drug extrusion from the bacterial cells. EPs play several important physiological and molecular roles in bacterial cell survival and stress-responses. The necessity to overcome AMR has encouraged investigators to characterize resistance-inhibiting or modulating EPIs to block the drug extrusion, restoring antibacterial susceptibility and returning existing antibiotics into the clinic. The severity of the AMR is higher in Gram-negative bacteria, owing to their superior capabilities in maintaining high drug efflux levels coupled with lower intracellular levels of toxic drugs including antibiotics. MDR/XDR strains maintain their intrinsic and acquired resistance via overproduction of pumps. The development of clinically useful EPIs to bypass pump effects continues to be a challenge. Though there are some noteworthy developments in recent past aimed at reversing the AMR phenotypes including facilitation of better drug-penetration across the outer

membranes of Gram-negative bacteria, and establishing new rules of permeation, identifying new and powerful EPIs seems best approach that can be explored as drug leads or in adjunctive therapies.

Several recent developments in *in-silico* MDS approaches have enabled the researchers to computationally validate and support the hypothesized mechanisms of EPs and EPIs (Suriyanarayanan and Sarojini, 2015; Ramaswamy et al., 2017; Vargiu et al., 2018). It is now possible to simulate membrane protein complex structures with micro-second time-scales. The MDS approach along with molecular docking and other *in silico* tools are successfully utilized for screening and prediction of the molecular interactions between potential EPs and their corresponding EPIs, ultimately helping in identification of the potent EPIs particularly from plant origin. However, this field is yet to be explored fully.

Considering the fact that practically all the antibiotics are susceptible to active drug-efflux, use of the potent EPIs to target and block these pumps can help in potentiating the old antibiotics effective again against a range of drug-resistant bacteria. EPIs are being looked as promising adjunctive therapies with the known antibiotics to improve their antibacterial potency at low concentrations, reduce the emergence of AMR and virulence. But developing novel and potent EPI is not easy and needs to overcome several hurdles such as choice of antibiotics for potentiation and matching the pharmacological properties of EPI-antibiotic(s) pair. More comprehensive and deeper investigations are therefore needed that involve the exploring the high-throughput screening assisted by *in silico* tools for identifying the potent EPI phytomolecules and their corresponding targets. Newer studies are being undertaken for identifying phytomolecules effective in inhibiting bacterial efflux pumps via potentiation of antibiotics against pathogenic bacteria including Gram-negative pathogens. This may pave the way for identification of phyto-EPIs that can head toward clinical phases and ultimately clinical practices with an aim to contain the AMR.

AUTHOR CONTRIBUTIONS

VK conceived the idea. VS, TK, RB, RS, and VK wrote the manuscript. All the authors made substantial contribution to the work and approved it for publication.

ACKNOWLEDGMENTS

The support under Star College Scheme of Department of Biotechnology, Government of India implemented at Modern College, Ganeshkhind, Pune is gratefully acknowledged. The use of facilities created under FIST program of Department of Science and Technology (DST), Government of India, implemented at Prof. Ramkrishna More College, Akurdi, Pune and Modern College, Ganeshkhind, Pune are gratefully acknowledged.

REFERENCES

Abdali, N., Parks, J. M., Haynes, K. M., Chaney, J. L., Green, A. T., Wolloscheck, D., et al. (2017). Reviving antibiotics: efflux pump inhibitors that interact with acra, a membrane fusion protein of the AcrAB-TolC multidrug efflux pump. *ACS Infect Dis.* 3, 89–98. doi: 10.1021/acsinfecdis.6b00167

Aghayan, S. S., Mogadam, H. K., Fazli, M., Darban-Sarokhalil, D., Khoramrooz, S. S., Jabalameli, F., et al. (2017). The effects of berberine and palmatine on efflux pumps inhibition with different gene patterns in *Pseudomonas aeruginosa* isolated from burn infections. *Avicenna J. Med. Biotechnol.* 9:2.

Akiba, M., Lin, J., Barton, Y. W., and Zhang, Q. (2006). Interaction of CmeABC and CmeDEF in conferring antimicrobial resistance and maintaining cell viability in *Campylobacter jejuni*. *J. Antimicrob. Chemother.* 57, 52–60. doi: 10.1093/jac/dki419

Alav, I., Sutton, J. M., and Rahman, K. M. (2018). Role of bacterial efflux pumps in biofilm formation. *J. Antimicrob. Chemother*. 73, 2003–2020. doi: 10.1093/jac/dky042

Amabile-Cuevas, C. F., Arredondo-Garcia, J. L., Cruz, A., and Rosas, I. (2010). Fluoroquinolone resistance in clinical and environmental isolates of *Escherichia coli* in Mexico City. *J. Appl. Microbiol.* 108, 158–162. doi: 10.1111/j.1365-2672.2009.04401.x

Bag, A., and Chattopadhyay, R. R. (2014). Efflux-pump inhibitory activity of a gallotannin from *Terminalia chebula* fruit against multidrug-resistant uropathogenic *Escherichia coli*. *Nat. Prod. Res.* 28, 1280–1283. doi: 10.1080/14786419.2014.895729

Balganesh, M., Dinesh, N., Sharma, S., Kuruppath, S., Nair, A. V., and Sharma, U. (2012). Efflux pumps of *Mycobacterium tuberculosis* play a significant role in antituberculosis activity of potential drug candidates. *Antimicrob. Agents Chemother.* 56, 2643–2651. doi: 10.1128/AAC.06003-11

Balganesh, M., Kuruppath, S., Marcel, N., Sharma, S., Nair, A, and Sharma, U. (2010). Rv1218c, an ABC transporter of *Mycobacterium tuberculosis* with implications in drug discovery. *Antimicrob. Agents Chemother.* 54, 5167–5172. doi: 10.1128/AAC.00610-10

Bame, J. R., Graf, T., Junio, H., Bussey, R., Jarmusch, S., El-Elimat, T., et al. (2013). Sarothrin from *Alkanna orientalis* is an antimicrobial agent and efflux pump inhibitor. *Planta Med.* 79, 327–329. doi: 10.1055/s-0032-1328259

Baugh, S., Ekanayaka, A. S., Piddock, L. J., and Webber, M. A. (2012). Loss of or inhibition of all multidrug resistance efflux pumps of *Salmonella enterica* serovar *Typhimurium* results in impaired ability to form a biofilm. *J. Antimicrob. Chemother.* 67, 2409–2417. doi: 10.1093/jac/dks228

Baugh, S., Phillips, C. R., Ekanayaka, A. S., Piddock, L. J., and Webber, M. A. (2014). Inhibition of multidrug efflux as a strategy to prevent biofilm formation. *J. Antimicrob.Chemother.* 69, 673–681. doi: 10.1093/jac/dkt420

Beketskaia, M. S., Bay, D. C., and Turner, R. J. (2014). Outer membrane protein OmpW participates with small multidrug resistance protein member EmrE in quaternary cationic compound efflux. *J. Bacteriol.* 196, 1483–1414. doi: 10.1128/JB.01483-14

Bhardwaj, A. K., and Mohanty, P. (2012). Bacterial efflux pumps involved in multidrug resistance and their inhibitors: rejuvenating the antimicrobial chemotherapy. *Recent Pat. Antiinfect. Drug Discov.* 7, 73–89. doi: 10.2174/157489112799829710

Bhaskar, B. V., Babu, T. M. C., Reddy, N. V., and Rajendra, W. (2016). Homology modeling, molecular dynamics, and virtual screening of NorA efflux pump inhibitors of *Staphylococcus aureus*. *Drug Des. Devel. Ther.* 10, 3237. doi: 10.2147/DDDT.S113556

Blair, J. M., Webber, M. A., Baylay, A. J., Ogbolu, D. O., and Piddock, L. J. (2015). Molecular mechanisms of antibiotic resistance. *Nat. Rev. Microbiol.* 13, 42–51. doi: 10.1038/nrmicro3380

Bruns, M. M., Kakarla, P., Floyd, J. T., Mukherjee, M. M., Ponce, R. C., Garcia, J. A., et al. (2017). Modulation of the multidrug efflux pump EmrD-3 from *Vibrio cholerae* by *Allium sativum* extract and the bioactive agent allyl sulfide plus synergistic enhancement of antimicrobial susceptibility by *A. sativum* extract. *Arch. Microbiol.* 199, 1103–1112. doi: 10.1007/s00203-017-1378-x

Buckley, A. M., Webber, M. A., Cooles, S., Randall, L. P., La Ragione, R. M., Woodward, M. J., et al. (2006). The AcrAB–TolC efflux system of *Salmonella enterica* serovar *Typhimurium* plays a role in pathogenesis. *Cell. Microbiol.* 8, 847–856. doi: 10.1111/j.1462-5822.2005.00671.x

Cattoir, V., Poirel, L., and Nordmann, P. (2008). Plasmid-mediated quinolone resistance pump QepA2 in an *Escherichia coli* isolate from France. *Antimicrob. Agents Chemother.* 52, 3801–3804. doi: 10.1128/AAC.00638-08

Cerceo, E., Deitelzweig, S. B., Sherman, B. M., and Amin, A. N. (2016). Multidrug-resistant gram-negative bacterial infections in the hospital setting: overview, implications for clinical practice, and emerging treatment options. *Microb. Drug Resist.* 22, 412–431. doi: 10.1089/mdr.2015.0220

Cha, H. J., Muller, R. T., and Pos, K. M. (2014). Switch-loop flexibility affects transport of large drugs by the promiscuous AcrB multidrug efflux transporter. *Antimicrob. Agents Chemother.* 58, 4767–4772. doi: 10.1128/AAC.02733-13

Chan, B. C., Han, X., Lui, S., Wong, C., Wang, T., Cheung, D., et al. (2015). Combating against methicillin-resistant *Staphylococcus aureus*—two fatty acids from purslane (*Portulaca oleracea* L.) exhibit synergistic effects with erythromycin. *J. Pharm. Pharmacol.* 67, 107–116. doi: 10.1111/jphp.12315

Chan, B. C., Ip, M., Lau, C. B., Lui, S. L., Jolivalt, C., Ganem-Elbaz, C., et al. (2011). Synergistic effects of baicalein with ciprofloxacin against NorA over-expressed methicillin-resistant *Staphylococcus aureus* (MRSA) and inhibition of MRSA pyruvate kinase. *J. Ethnopharmacol.* 137, 767–773. doi: 10.1016/j.jep.2011.06.039

Chandra, H., Bishnoi, P., Yadav, A., Patni, B., Mishra, A. P., and Nautiyal, A. R. (2017). Antimicrobial resistance and the alternative resources with special emphasis on plant-based antimicrobials—a review. *Plants* 6:16. doi: 10.3390/plants6020016

Chen, Y., Hu, D., Zhang, Q., Liao, X-P., Liu, Y-H., and Sun, J. (2017). Efflux Pump Overexpression contributes to tigecycline heteroresistance in *Salmonella enterica* serovar Typhimurium. *Front. Cell. Infect. Microbiol.* 7:37. doi: 10.3389/fcimb.2017.00037

Chollet, R., Chevalier, J., Bryskier, A., and Pagès, J. M. (2004). The AcrAB-TolC pump is involved in macrolide resistance but not in telithromycin efflux in *Enterobacter aerogenes* and *Escherichia coli*. *Antimicrob. Agents Chemother.* 48, 3621–3624. doi: 10.1128/AAC.48.9.3621-3624.2004

Chovanova, R., Mezovska, J., Vaverkova, S., and Mikulasova, M. (2015). The inhibition the Tet(K) efflux pump of tetracycline resistant *Staphylococcus epidermidis* by essential oils from three *Salvia* species. *Lett. Appl. Microbiol.* 61, 58–62. doi: 10.1111/lam.12424

Collu, F., Vargiu, A. V., Dreier, J., Cascella, M., and Ruggerone, P. (2012). Recognition of imipenem and meropenem by the RND transporter MexB studied by computer simulations. *J. Am. Chem. Soc.* 134, 19146–19158. doi: 10.1021/ja307803m

Costa, S. S., Viveiros, M., Amaral, L., and Couto, I. (2013). Multidrug efflux pumps in *Staphylococcus aureus*: an update. *Open Microbiol. J.* 7, 59–71. doi: 10.2174/1874285801307010059

Coyne, S., Rosenfeld, N., Lambert, T., Courvalin, P., and Perichon, B. (2010). Overexpression of resistance- nodulation-cell division pump AdeFGH confers multidrug resistance in *Acinetobacter baumannii*. *Antimicrob. Agents Chemother.* 54, 4389–4393. doi: 10.1128/AAC.00155-10

Davies, J., and Davies, D. (2010). Origins and evolution of antibiotic resistance. *Microbiol. Mol. Biol. Rev.* 74, 417–433. doi: 10.1128/MMBR.00016-10

dos Santos, J. F., Tintino, S. R., de Freitas, T. S., Campina, F. F., Irwin, R. D. A., Siqueira-Júnior, J. P., et al. (2018). *In vitro* e *in silico* evaluation of the inhibition of *Staphylococcus aureus* efflux pumps by caffeic and gallic acid. *Comp. Immunol. Microbiol. Infect. Dis.* 57, 22–28. doi: 10.1016/j.cimid.2018.03.001

Du, D., Venter, H., Pos, K. M., and Luisi, B. F. (2013). "The machinery and mechanism of multidrug efflux in Gram-negative bacteria," in *Microbial Efflux Pumps: Current Research*, eds E. W. Yu, Q. Zhang, and M. H. Brown (Ames, IA: Caister Academic Press), 35–48.

Du, D., Wang, Z., James, N. R., Voss, J. E., Klimont, E., Ohene-Agyei, T., et al. (2014). Structure of the AcrAB-TolC multidrug efflux pump. *Nature* 509, 512–515. doi: 10.1038/nature13205

Du, D., Wang-Kan, X., Neuberger, A., van Veen, H. W., Pos, K. M., Piddock, L. J., et al. (2018). Multidrug efflux pumps: structure, function and regulation. *Nat. Rev. Microbiol.* 16, 523–539. doi: 10.1038/s41579-018-0048-6

Dwivedi, G., Maurya, A., Yadav, D., Khan, F., Darokar, M., and Srivastava, S. (2014a). Drug resistance reversal potential of ursolic acid derivatives against nalidixic acid- and multidrug-resistant *Escherichia coli*. *Chem. Biol. Drug Des.* 86, 272–283. doi: 10.1111/cbdd.12491

Dwivedi, G. R., Gupta, S., Maurya, A., Tripathi, S., Sharma, A., Srivastava, S. K., et al. (2015). Synergy potential of indole alkaloids and its derivative against drug resistant *Escherichia coli*. *Chem. Biol. Drug Des.* 86, 1471–1481. doi: 10.1111/cbdd.12613

Dwivedi, G. R., Singh, D. P., Sharma, S. A., and Darokar, M. P. (2017a). "Efflux Pumps: Warheads of Gram-Negative Bacteria and Efflux Pump Inhibitors" in *New Approaches in Biological Research*, eds R. P. Sinha and Richa (New York, NY: Nova Science Publishers), 35–72.

Dwivedi, G. R., Tyagi, R., Sanchita, Tripathi, S., Pati, S., Srivastava, S. K., et al. (2017b). Antibiotics potentiating potential of catharanthine against superbug *Pseudomonas aeruginosa*. *J. Biomol. Struct. Dyn.* 1–15. doi: 10.1080/07391102.2017.1413424. [Epub ahead of print].

Dwivedi, G. R., Upadhyay, H. C., Yadav, D. K., Singh, V., Srivastava, S. K., Khan, F., et al. (2014b). 4-hydroxy-α-tetralone and its derivative as Drug resistance reversal agents in multidrug resistant *Escherichia coli*. *Chem. Biol. Drug Des.* 83, 482–492. doi: 10.1111/cbdd.12263

Eicher, T., Cha, H. J., Seeger, M. A., Brandstatter, L., El-Delik, J., Bohnert, J. A., et al. (2012). Transport of drugs by the multidrug transporter AcrB involves an access and a deep binding pocket that are separated by a switch-loop. *Proc. Natl. Acad. Sci. U.S.A.* 109, 5687–5692. doi: 10.1073/pnas.1114944109

Exner, M., Bhattacharya, S., Christiansen, B., Gebel, J., Goroncy-Bermes, P., Hartemann, P., et al. (2017). Antibiotic resistance: what is so special about multidrug-resistant Gram-negative bacteria? *GMS Hyg. Infect. Control.* 12:Doc05. doi: 10.3205/dgkh000290

Fahmy, A., Srinivasan, A., and Webber, M. A. (2016). "The relationship between bacterial multidrug efflux pumps and biofilm formation," in *Efflux-Mediated Antimicrobial Resistance in Bacteria*, edd X. Z. Li, C. A. Elkins, and H. I. Zgurskaya (Adis; Cham: Springer International Publishing), 651–663.

Fair, R. J., and Tor, Y. (2014). Antibiotics and bacterial resistance in the 21st century. *Perspect. Medicin. Chem.* 6, 25–64. doi: 10.4137/PMC.S14459

Fernandez, L., and Hancock, R. (2012). Adaptive and mutational resistance: role of porins and efflux pumps in drug resistance. *Clin. Microbiol. Rev.* 25, 661–681. doi: 10.1128/CMR.00043-12

Fiamegos, Y. C., Kastritis, P. L., Exarchou, V., Han, H., Bonvin, A. M., Vervoort, J., et al. (2011). Antimicrobial and efflux pump inhibitory activity of caffeoylquinic acids from *Artemisia absinthium* against gram-positive pathogenic bacteria. *PLoS ONE* 6:e18127. doi: 10.1371/journal.pone.0018127

Garvey, M., Rahman, M., Gibbons, S., and Piddock, L. (2011). Medicinal plant extracts with efflux inhibitory activity against Gram negative bacteria. *Int. J. Antimicrob. Agents* 37, 145–151. doi: 10.1016/j.ijantimicag.2010.10.027

German, N., Kaatz, G. W., and Kerns, R. J. (2008). Synthesis and evaluation of PSSRI-based inhibitors of *Staphylococcus aureus* multidrug efflux pumps. *Bioorg. Med. Chem. Lett.* 18, 1368–1373. doi: 10.1016/j.bmcl.2008.01.014

Gill, E. E., Franco, O. L., and Hancock, R. E. W. (2015). Antibiotic adjuvants: diverse strategies for controlling drug-resistant pathogens. *Chem. Biol. Drug Des.* 85, 56–78. doi: 10.1111/cbdd.12478

González, J. E., and Keshavan, N. D. (2006). Messing with bacterial quorum sensing. *Microbiol. Mol. Biol. Rev.* 70, 859–875. doi: 10.1128/MMBR.00002-06

Grkovic, S., Brown, M. H., and Skurray, R. A. (2002). Regulation of bacterial drug export systems. *Microbiol. Mol. Biol. Rev.* 66, 671–701. doi: 10.1128/MMBR.66.4.671-701.2002

Grosdidier, A., Zoete, V., and Michielin, O. (2011). SwissDock, a protein-small molecule docking web service based on EADock DSS. *Nucleic Acids Res.* 39, W270–W277. doi: 10.1093/nar/gkr366

Gupta, D., Singh, A., and Khan, A. U. (2017). Nanoparticles as efflux pump and biofilm inhibitor to rejuvenate bactericidal effect of conventional antibiotics. *Nanoscale Res. Lett.* 12, 454. doi: 10.1186/s11671-017-2222-6

Hannula, M., and Hänninen, M. L. (2008). Effect of putative efflux pump inhibitors and inducers on the antimicrobial susceptibility of *Campylobacter jejuni* and *Campylobacter coli*. *J. Med. Microbiol.* 57, 851–855. doi: 10.1099/jmm.0.47823-0

Hansen, L. H., Johannesen, E., Burmolle, M., Sørensen, A. H., and Sørensen, S. J. (2004). Plasmid-encoded multidrug efflux pump conferring resistance to olaquindox in *Escherichia coli*. *Antimicrob. Agents Chemother.* 48, 3332–3337. doi: 10.1128/AAC.48.9.3332-3337.2004

He, X., Szewczyk, P., Karyakin, A., Evin, M., and Hong, W. X. (2010). Structure of a cation-bound multidrug and toxic compound extrusion transporter. *Nature* 467, 991–994. doi: 10.1038/nature09408

Higgins, C. F. (2007). Multiple molecular mechanisms for multidrug resistance transporters. *Nature* 446, 749–757. doi: 10.1038/nature05630

Hirakata, Y., Srikumar, R., Poole, K., Gotoh, N., Suematsu, T., Kohno, S., et al. (2002). Multidrug efflux systems play an important role in the invasiveness of *Pseudomonas aeruginosa*. *J. Exp. Med.* 196, 109–118. doi: 10.1084/jem.20020005

Hobbs, E. C., Yin, X., Paul, B. J., Astarita, J. L., and Storz, G. (2012). Conserved small protein associates with the multidrug efflux pump AcrB and differentially affects antibiotic resistance. *Proc. Natl. Acad. Sci. U.S.A.* 109, 16696–16701. doi: 10.1073/pnas.1210093109

Holler, J. G., Christensen, S. B., Slotved, H. C., Rasmussen, H. B., Gúzman, A., Olsen, C. E., et al. (2012). Novel inhibitory activity of the *Staphylococcus aureus* NorA efflux pump by a kaempferol rhamnoside isolated from *Persea lingue* Nees. *J. Antimicrob. Chemother.* 67, 1138–1144. doi: 10.1093/jac/dks005

Huda, N., Lee, E. W., Chen, J., Morita, Y., Kuroda, T., Mizushima, T., et al. (2003). Molecular cloning and characterization of an ABC multidrug efflux pump, VcaM, in non-O1 *Vibrio cholerae*. *Antimicrob. Agents Chemother.* 47, 2413–2417. doi: 10.1128/AAC.47.8.2413-2417.2003

Jack, D. L., Yang, N. M., and Saier, M. H. (2001). The drug/metabolite transporter superfamily. *Eur. J. Biochem.* 68, 3620–3639. doi: 10.1046/j.1432-1327.2001.02265.x

Jamshidi, S., Sutton, J. M., and Rahman, K. M. (2016). An overview of bacterial efflux pumps and computational approaches to study efflux pump inhibitors. *Future Med. Chem.* 8, 195–210. doi: 10.4155/fmc.15.173

Kaatz, G. W., McAleese, F., and Seo, S. M. (2005). Multidrug resistance in *Staphylococcus aureu* s due to overexpression of a novel multidrug and toxin extrusion (MATE) transport protein. *Antimicrob. Agents Chemother.* 49, 1857–1864. doi: 10.1128/AAC.49.5.1857-1864.2005

Kakarla, P., Floyd, J., Mukherjee, M., Devireddy, A. R., Inupakutika, M. A., Ranweera, I., et al. (2016). Inhibition of the multidrug efflux pump LmrS from *Staphylococcus aureus* by cumin spice *Cuminum cyminum*. *Arch. Microbiol.* 199, 465–474. doi: 10.1007/s00203-016-1314-5

Kalia, N. P., Mahajan, P., Mehra, R., Nargotra, A., Sharma, J. P., Koul, S., et al. (2012). Capsaicin, a novel inhibitor of the NorA efflux pump, reduces the intracellular invasion of *Staphylococcus aureus*. *J. Antimicrob. Chemother.* 67, 2401–2408. doi: 10.1093/jac/dks232

Kayser, F. H., Benner, E. J., and Hoeprich, P. D. (1970). Acquired and native resistance of *Staphylococcus aureus* to cephalexin and other beta-lactam antibiotics. *Appl. Microbiol.* 20, 1–5.

Kesherwani, M., Michael Gromiha, M., Fukui, K., and Velmurugan, D. (2017). Identification of novel natural inhibitor for NorM–a multidrug and toxic compound extrusion transporter–an *insilico* molecular modeling and simulation studies. *J. Biomol. Struct. Dyn.* 35, 58–77. doi: 10.1080/07391102.2015.1132391

Kim, J. Y., Kim, S. H., Jeon, S. M., Park, M. S., Rhie, H. G., and Lee, B. K. (2008). Resistance to fluoroquinolones by the combination of target site mutations and enhanced expression of genes for efflux pumps in *Shigella flexneri* and *Shigella sonnei* strains isolated in Korea. *Clin. Microbiol. Infec.* 14, 760–765. doi: 10.1111/j.1469-0691.2008.02033.x

Kobayashi, N., Nishino, K., and Yamaguchi, A. (2001). Novel macrolide-specific ABC-type efflux transporter in *Escherichia coli*. *J. Bacteriol.* 183, 5639–5644. doi: 10.1128/JB.183.19.5639-5644.2001

Köhler, T., Michea-Hamzehpour, M., Henze, U., Gotoh, N., Curty, L. K., and Pechere, J. C. (1997). Characterization of MexE-MexF-OprN, a positively regulated multidrug efflux system of *Pseudomonas aeruginosa*. *Mol. Microbiol.* 23, 345–354. doi: 10.1046/j.1365-2958.1997.2281594.x

Kourtesi, C., Ball, A., Huang, Y., Jachak, S., Vera, D., Khondkar, P., et al. (2013). Microbial efflux systems and inhibitors: approaches to drug discovery and the challenge of clinical implementation. *Open Microbiol. J.* 7, 34–52. doi: 10.2174/1874285801307010034

Kumar, V., Shriram, V., and Mulla, J. (2013). Antibiotic resistance reversal of multiple drug resistant bacteria using *Piper longum* fruit extract. *J. Appl. Pharm. Sci.* 3, 112–116. doi: 10.7324/JAPS.2013.30322

Kumarasamy, K. K., Toleman, M. A., Walsh, T. R., Bagaria, J., Butt, F., Balakrishnan, R., et al. (2010). Emergence of a new antibiotic resistance mechanism in India, Pakistan, and the UK: a molecular, biological, and epidemiological study. *Lancet Infect. Dis.* 10, 597–602. doi: 10.1016/S1473-3099(10)70143-2

Kvist, M., Hancock, V., and Klemm, P. (2008). Inactivation of efflux pumps abolishes bacterial biofilm formation. *Appl. Environ. Microbiol.* 74, 7376–7382. doi: 10.1128/AEM.01310-08

Lee, E. W., Huda, M. N., Kuroda, T., Mizushima, T., and Tsuchiya, T. (2003). EfrAB, an ABC multidrug efflux pump in *Enterococcus faecalis*. *Antimicrob. Agents Chemother.* 47, 3733–3738. doi: 10.1128/AAC.47.12.3733-3738.2003

Lennen, R. M., Politz, M. G., Kruziki, M. A., and Pfleger, B. F. (2013). Identification of transport proteins involved in free fatty acid efflux in *Escherichia coli*. *J. Bacteriol.* 195, 135–144. doi: 10.1128/JB.01477-12

Levy, S. B. (2001). Antibiotic resistance: consequences of inaction. *Clin. Infect. Dis.* 33, S124–S129. doi: 10.1086/321837

Li, X-Z., Plésiat, P., and Nikaido, H. (2015). The challenge of efflux-mediated antibiotic resistance in Gram-negative bacteria. *Clin. Microbiol. Rev.* 28, 337–418. doi: 10.1128/CMR.00117-14

Liang, Z., Chen, Y. M., Chen, Y., Cheng, Y. Y., and and Zhang, L. H. (2016). RND efflux pump and its interrelationship with quorum sensing system. *Hereditas (Beijing)*, 38, 894–901. doi: 10.16288/j.yczz.16-139

Limaverde, P. W., Campina, F. F., da Cunha, F. A., Crispim, F. D., Figueredo, F. G., Lima, L. F., et al. (2017). Inhibition of the TetK efflux-pump by the essential oil of *Chenopodium ambrosioides* L. and α-terpinene against *Staphylococcus aureus* IS-58. *Food Chem. Toxicol.* 109, 957–961. doi: 10.1016/j.fct.2017.02.031

Lin, J., Michel, L. O., and Zhang, Q. (2002). CmeABC functions as a multidrug effl ux system in *Campylobacter jejuni*. *Antimicrob. Agents Chemother.* 46, 2124–2131. doi: 10.1128/AAC.46.7.2124-2131.2002

Lister, P. D., Wolter, D. J., and Hanson, N. D. (2009). Antibacterial-resistant *Pseudomonas aeruginosa*: clinical impact and complex regulation of chromosomally encoded resistance mechanisms. *Clin. Microbiol. Rev.* 22, 582–610. doi: 10.1128/CMR.00040-09

Littlejohn, T. G., Paulsen, I. T., Gillespie, M. T., Tennent, J. M., Midgley, M., Jones, I. G., et al. (1992). Substrate specifi city and energetics of antiseptic and disinfectant resistance in *Staphylococcus aureus*. *FEMS Microbiol. Lett.* 95, 259–265. doi: 10.1111/j.1574-6968.1992.tb05376.x

Liu, Q., Hassan, K. A., Ashwood, H. E., Gamage, H. K. A. H., Li, L., Mabbutt, B. C., et al. (2018). Regulation of the *aceI* multidrug efflux pump gene in *Acinetobacter baumannii*. *J. Antimicrob. Chemother.* 73, 1492–1500. doi: 10.1093/jac/dky034

Lomovskaya, O., Warren, M. S., Lee, A., Galazzo, J., Fronko, R., Lee, M., et al. (2001). Identification and characterization of inhibitors of multidrug resistance efflux pumps in *Pseudomonas aeruginosa*: novel agents for combination therapy. *Antimicrob. Agents Chemother.* 45, 105–116. doi: 10.1128/AAC.45.1.105-116.2001

Luo, J., and Parsons, S. M. (2010). Conformational propensities of peptides mimicking transmembrane helix 5 and motif C in wild-type and mutant vesicular acetylcholine transporters. *ACS Chem. Neurosci.* 1, 381–390. doi: 10.1021/cn900033s

Lynch, A. S. (2006). Efflux systems in bacterial pathogens: an opportunity for therapeutic intervention? An industry view. *Biochem. Pharmacol.* 71, 949–956. doi: 10.1016/j.bcp.2005.10.021

Ma, D., Alberti, M., Lynch, C., Nikaido, H., and Hearst, J. E. (1996). The local repressor AcrR plays a modulating role in the regulation of acrAB genes of *Escherichia coli* by global stress signals. *Mol. Microbiol.* 19, 101–112.

Maisuria, V., Hosseinidoust, Z., and Tufenkji, N. (2015). Polyphenolic extract from maple syrup potentiates antibiotic susceptibility and reduces biofilm formation of pathogenic bacteria. *Appl. Environ. Microbiol.* 81, 3782–3792. doi: 10.1128/AEM.00239-15

Mangiaterra, G., Laudadio, E., Cometti, M., Mobbili, G., Minnelli, C., Massaccesi, L., et al. (2017). Inhibitors of multidrug efflux pumps of *Pseudomonas aeruginosa* from natural sources: an *in silico* high-throughput virtual screening and *in vitro* validation. *Med. Chem. Res.* 26, 414–430. doi: 10.1007/s00044-016-1761-1

Marrer, E., Schad, K., Satoh, A. T., Page, M. G., Johnson, M. M., and Piddock, L. J. (2006). Involvement of the putative ATP-dependent effl ux proteins PatA and PatB in fluoroquinolone resistance of a multidrug- resistant mutant

of *Streptococcus pneumoniae*. *Antimicrob. Agents Chemother.* 50, 685–693. doi: 10.1128/AAC.50.2.685-693.2006

Martinez, J. L., Sánchez, M. B., Martínez-Solano, L., Hernandez, A., Garmendia, L., Fajardo, A., et al. (2009). Functional role of bacterial multidrug efflux pumps in microbial natural ecosystems. *FEMS Microbial. Rev.* 33, 430–449. doi: 10.1111/j.1574-6976.2008.00157.x

Martins, M., Dastidar, S. G., Fanning, S., Kristiansen, J. E., Molnar, J., Pagès, J. M., et al. (2008). Potential role of non-antibiotics (helper compounds) in the treatment of multidrug- resistant Gram-negative infections: mechanisms for their direct and indirect activities. *Int. J. Antimicrob. Agents* 31, 198–208. doi: 10.1016/j.ijantimicag.2007.10.025

Masi, M., Refregiers, M., Pos, K. M., and Pages, J. M. (2017). Mechanisms of envelope permeability and antibiotic influx and efflux in Gram-negative bacteria. *Nat. Microbiol.* 2:17001. doi: 10.1038/nmicrobiol.2017.1

Maurya, A., Dwivedi, G., Darokar, M., and Srivastava, S. (2013). Antibacterial and synergy of clavine alkaloid lysergol and its derivatives against nalidixic acid-resistant *Escherichia coli*. *Chem. Biol. Drug Des.* 81, 484–490. doi: 10.1111/cbdd.12103

May, T., Ito, A., and Okabe, S. (2009). Induction of multidrug resistance mechanism in *Escherichia coli* biofilms by interplay between tetracycline and ampicillin resistance genes. *Antimicrob. Agents Chemother.* 53, 4628–4639. doi: 10.1128/AAC.00454-09

Molnár, J., Engi, H., Hohmann, J., Molnár, P., and Deli, J. (2010). Reversal of multidrug resistance by natural substances from plants. *Curr. Topics Medi. Chem.* 10, 1757–1768. doi: 10.2174/156802610792928103

Moore, J. D., Gerdt, J. P., Eibergen, N. R., and Blackwell, H. E. (2014). Active efflux influences the potency of quorum sensing inhibitors in *Pseudomonas aeruginosa*. *Chembiochem* 15, 435–442. doi: 10.1002/cbic.201300701

Morand, B., and Mühlemann, K. (2007). Heteroresistance to penicillin in *Streptococcus pneumoniae*. *Proc. Natl. Acad. Sci. U.S.A.* 104, 14098–14103. doi: 10.1073/pnas.0702377104

Morita, Y., Kodama, K., Shiota, S., Mine, T., Kataoka, A., Mizushima, T., et al. (1998). NorM, a putative multidrug efflux protein, of *Vibrio parahaemolyticus* and its homolog in *Escherichia coli*. *Antimicrob. Agents Chemother.* 42, 1778–1782. doi: 10.1128/AAC.42.7.1778

Morris, G. M., Huey, R., Lindstrom, W., Sanner, M. F., Belew, R. K., Goodsell, D. S., et al. (2009). Autodock4 and AutoDockTools4: automated docking with selective receptor flexiblity. *J. Comput. Chem.* 16, 2785–2791. doi: 10.1002/jcc.21256

Motta, S. S., Cluzel, P., and Aldana, M. (2015). Adaptive resistance in bacteria requires epigenetic inheritance, genetic noise, and cost of efflux pumps. *PLoS ONE* 10:e0118464. doi: 10.1371/journal.pone.0118464

Mukanganyama, S., Chirisa, E., and Hazra, B. (2012). Antimycobacterial activity of diospyrin and its derivatives against *Mycobacterium aurum*. *Res. Pharm.* 2, 1–13.

Nakashima, R., Sakurai, K., Yamasaki, S., Hayashi, K., Nagata, C., Hoshino, K., Onodera, Y., Nishino, K., et al. (2013). Structural basis for the inhibition of bacterial multidrug exporters. *Nature* 500, 102–106. doi: 10.1038/nature12300

Napier, B. A., Band, V., Burd, E. M., and Weiss, D. S. (2014). Colistin heteroresistance in *Enterobacter cloacae* is associated with cross-resistance to the host antimicrobial lysozyme. *Antimicrob. Agents Chemother.* 58, 5594–5597. doi: 10.1128/AAC.02432-14

Newman, D., and Cragg, G. (2012). Natural products as sources of new drugs over the 30 years from 1981 to 2010. *J. Nat. Prod.* 75, 311–335. doi: 10.1021/np200906s

Nguyen, S. T., Kwasny, S. M., Ding, X., Cardinale, S. C., McCarthy, C. T., Kim, H-S., et al. (2015). Structure–activity relationships of a novel pyranopyridine series of Gram negative bacterial efflux pump inhibitors. *Bioorg. Med. Chem.* 23, 2024–2034. doi: 10.1016/j.bmc.2015.03.016

Ni, W., Li, Y., Guan, J., Zhao, J., Cui, J., Wang, R., et al. (2016). Effects of efflux pump inhibitors on colistin resistance in multidrug resistant Gram-negative bacteria. *Antimicrob. Agents Chemother.* 60, 3215–3218. doi: 10.1128/AAC.00248-16

Nichols, R. J., Sen, S., Choo, Y. J., Beltrao, P., Zietek, M., Chaba, R., et al. (2011). Phenotypic landscape of a bacterial cell. *Cell* 144, 143–156. doi: 10.1016/j.cell.2010.11.052

Nikaido, H., and Takatsuka, Y. (2009). Mechanisms of RND multidrug efflux pumps. *Biochem. Biophys. Acta* 1794, 769–781. doi: 10.1016/j.bbapap.2008.10.004

Nishino, K., Latifi, T., and Groisman, E. A. (2006). Virulence and drug resistance roles of multidrug efflux systems of *Salmonella enterica* serovar *Typhimurium*. *Mol. Microbiol.* 59, 126–141. doi: 10.1111/j.1365-2958.2005.04940.x

Norgan, A. P., Freese, J. M., Tuin, P. M., Cunningham, S. A., Jeraldo, P. R., and Patel, R. (2016). Carbapenem- and colistin-resistant *Enterobacter cloacae* from Delta, Colorado, in 2015. *Antimicrob. Agents Chemother.* 60, 3141–3144. doi: 10.1128/AAC.03055-15

Ogawa, W., Minato, Y., Dodan, H., Onishi, M., Tsuchiya, T., and Kuroda, T. (2015). Characterization of MATE-type multidrug efflux pumps from *Klebsiella pneumoniae* MGH78578. *PLoS ONE* 10:e0121619. doi: 10.1371/journal.pone.0121619

Ohene-Agyei, T., Mowla, R., Rahman, T., and Venter, H. (2014). Phytochemicals increase the antibacterial activity of antibiotics by acting on a drug efflux pump. *Microbiologyopen* 3, 885–896. doi: 10.1002/mbo3.212

Okada, U., Yamashita, E., Neuberger, A., Morimoto, M., van Veen, H. W., and Murakami, S. (2017). Crystal structure of tripartite-type ABC transporter MacB from *Acinetobacter baumannii*. *Nat. Commun*, 8, 1336. doi: 10.1038/s41467-017-01399-2

Opperman, T. J., Kwasny, S. M., Kim, H. S., Nguyen, S. T., Houseweart, C., D'Souza, S., et al. (2014). Characterization of a novel pyranopyridine inhibitor of the AcrAB efflux pump of *Escherichia coli*. *Antimicrob. Agents Chemother.* 58, 722–733. doi: 10.1128/AAC.01866-13

Opperman, T. J., and Nguyen, S. T. (2015). Recent advances toward a molecular mechanism of efflux pump inhibition. *Front. Microbiol.* 6:421. doi: 10.3389/fmicb.2015.00421

Pagès, J. M., and Amaral, L. (2009). Mechanisms of drug efflux and strategies to combat them: challenging the efflux pump of Gram-negative bacteria. *Biochim. Biophys. Acta, Proteins Proteomics* 1794, 826–833. doi: 10.1016/j.bbapap.2008.12.011

Pettersen, E. F., Goddard, T. D., Huang, C. C., Couch, G. S., Greenblatt, D. M., Meng, E. C., et al. (2004). UCSF Chimera—a visualization system for exploratory research and analysis. *J. Comput. Chem.* 25, 1605–1612. doi: 10.1002/jcc.20084

Piddock, L. J. (2006). Multidrug-resistance efflux pumps-Not just for resistance. *Nat. Rev. Microbiol.* 4, 629–636. doi: 10.1038/nrmicro1464

Piddock, L. J. (2014). Understanding the basis of antibiotic resistance: a platform for drug discovery. *Microbiology* 160, 2366–2373. doi: 10.1099/mic.0.082412-0

Ponnusamy, K., Ramasamy, M., Savarimuthu, I., and Paulraj, M. G. (2010). Indirubin potentiates ciprofloxacin activity in the NorA efflux pump of *Staphylococcus aureus*. *Scand. J. Infect. Dis.* 42, 500–505. doi: 10.3109/00365541003713630

Poole, K. (2004). Efflux-mediated multiresistance in Gram-negative bacteria. *Clin. Microbiol. Infect.* 10, 12–26. doi: 10.1111/j.1469-0691.2004.00763.x

Poole, K. (2005). Efflux-mediated antimicrobial resistance. *J. Antimicrob. Chemother.* 56, 20–51. doi: 10.1093/jac/dki171

Poole, K. (2007). Efflux pumps as antimicrobial resistance mechanisms. *Ann. Med.* 39, 162–176. doi: 10.1080/07853890701195262

Poole, K., Gotoh, N., Tsujimoto, H., Zhao, Q., Wada, A., Yamasaki, T., et al. (1996). Overexpression of the *mexC - mexD - oprJ* effl ux operon in *nfxB* -type multi drug resistant strains of *Pseudomonas aeruginosa*. *Mol. Microbiol.* 21, 713–724. doi: 10.1046/j.1365-2958.1996.281397.x

Prasch, S., and Bucar, F. (2015). Plant derived inhibitors of bacterial efflux pumps: an update. *Phytochem. Rev.* 14:961. doi: 10.1007/s11101-015-9436-y

Purssell, A., and Poole, K. (2013). Functional characterization of the NfxB repressor of the mexCD -oprJ multidrug efflux operon of *Pseudomonas aeruginosa*. *Microbiology* 159, 2058–2073. doi: 10.1099/mic.0.069286-0

Putman, M., van Veen, H., and Konings, W. (2000). Molecular properties of bacterial multidrug transporters. *Microbiol. Mol. Biol. Rev.* 64, 672–693. doi: 10.1128/MMBR.64.4.672-693.2000

Rahman, T., Yarnall, B., and Doyle, D. A. (2017). Efflux drug transporters at the forefront of antimicrobial resistance. *Eur. Biophys. J.* 46, 647–653. doi: 10.1007/s00249-017-1238-2

Rajamohan, G., Srinivasan, V. B., and Gebreyes, W. A. (2010). Novel role of *Acinetobacter baumannii* RND efflux transporters in mediating

decreased susceptibility to biocides. *J. Antimicrob. Chemother.* 65, 228–232. doi: 10.1093/jac/dkp427

Ramaswamy, V. K., Cacciotto, P., Malloci, G., Vargiu, A. V., and Ruggerone, P. (2017). Computational modelling of efflux pumps and their inhibitors. *Essays Biochem.* 61, 141–156. doi: 10.1042/EBC20160065

Ramón-García, S., Mick, V., Dainese, E., Martin, C., Thompson, C. J., De Rossi, E., et al. (2012). Functional and genetic characterization of the Tap efflux pump in *Mycobacterium bovis* BCG. *Antimicrob. Agents Chemother.* 56, 2074–2083. doi: 10.1128/AAC.05946-11

Rice, A., Liu, Y., Michaelis, M. L., Himes, R. H., Georg, G. I., and Audus, K. L. (2005). Chemical modification of paclitaxel (Taxol) reduces P-glycoprotein interactions and increases permeation across the blood-brain barrier *in vitro* and *in situ*. *J. Med. Chem.* 48, 832–838. doi: 10.1021/jm040114b

Roca, I., Marti, S., Espinal, P., Martinez, P., Gibert, I., and Vila, J. (2009). CraA: an MFS efflux pump associated with chloramphenicol resistance in *Acinetobacter baumannii*. *Antimicrob. Agents Chemother.* 53, 4013–4014. doi: 10.1128/AAC.00584-09

Rodrigues, L., Villellas, C., Bailo, R., Viveiros, M., and Ainsa, J. A. (2013). Role of the Mmr efflux pump in drug resistance in *Mycobacterium tuberculosis*. *Antimicrob. Agents Chemother.* 57, 751– 757. doi: 10.1128/AAC.01482-12

Roy, S., Pahwa, S., Nandanwar, H., and Jachak, S. (2012). Phenylpropanoids of *Alpinia galanga* as efflux pump inhibitors in *Mycobacterium smegmatis* mc2 155. *Fitoterapia* 83, 1248–1255. doi: 10.1016/j.fitote.2012.06.008

Roy, S. K., Kumari, N., Pahwa, S., Agrahari, U. C., Bhutani, K. K., Jachak, S. M., et al. (2013). NorA efflux pump inhibitory activity of coumarins from *Mesua ferrea*. *Fitoterapia* 90, 140–150. doi: 10.1016/j.fitote.2013.07.015

Ruzin, A., Keeney, D., and Bradford, P. A. (2007). AdeABC multidrug efflux pump is associated with decreased susceptibility to tigecycline in *Acinetobacter calcoaceticus-Acinetobacter baumannii* complex. *J. Antimicrob. Chemother.* 59, 1001–1004. doi: 10.1093/jac/dkm058

Sabatini, S., Piccioni, M., Felicetti, T., De Marco, S., Manfroni, G., Pagiotti, R., et al. (2017). Investigation on the effect of known potent *S. aureus* NorA efflux pump inhibitors on the staphylococcal biofilm formation. *RSC Adv.* 7, 37007–37014. doi: 10.1039/C7RA03859C

Saier, M. H., Paulsen, I. T., Sliwinski, M. K., Pao, S. S., and Skurray, R. A. (1998). Evolutionary origins of multidrug and drug-specific efflux pumps in bacteria. *FASEB J.* 12, 265–274. doi: 10.1096/fasebj.12.3.265

Santajit, S., and Indrawattana, N. (2016). Mechanisms of antimicrobial resistance in ESKAPE pathogens. *Biomed Res. Int.* 2016:2475067. doi: 10.1155/2016/2475067

Schindler, B. D., and Kaatz, G. W. (2016). Multidrug efflux pumps of Gram-positive bacteria. *Drug Resist. Updat.* 27, 1–13. doi: 10.1016/j.drup.2016.04.003

Schuldiner, S. (2009). EmrE, a model for studying evolution and mechanism of ion-coupled transporters. *Biochim. Biophys. Acta* 1794,748–762. doi: 10.1016/j.bbapap.2008.12.018

Sharma, S., Kumar, M., Sharma, S., Nargotra, A., Koul, S., and Khan, I. A. (2010). Piperine as an inhibitor of Rv1258c, a putative multidrug efflux pump of *Mycobacterium tuberculosis*. *J. Antimicrob. Chemother.* 65, 1694–1701. doi: 10.1093/jac/dkq186

Shigemura, K., Osawa, K., Kato, A., Tokimatsu, I., Arakawa, S., Shirakawa, T., et al. (2015). Association of overexpression of efflux pump genes with antibiotic resistance in *Pseudomonas aeruginosa* strains clinically isolated from urinary tract infection patients. *J. Antibiot.* 68, 568. doi: 10.1038/ja.2015.34

Shin, J., Prabhakaran, V. S., and Kim, K. S. (2018). The multi-faceted potential of plant-derived metabolites as antimicrobial agents against multidrug-resistant pathogens. *Microb. Pathog.* 116, 209–214. doi: 10.1016/j.micpath.2018.01.043

Shiu, W., Malkinson, J., Rahman, M., Curry, J., Stapleton, P., Gunaratnam, M., et al. (2013). A new plant-derived antibacterial is an inhibitor of efflux pumps in *Staphylococcus aureus*. *Int. J. Antimicrob. Agents* 42, 513–518. doi: 10.1016/j.ijantimicag.2013.08.007

Silhavy, T. J., Kahne, D., and Walker, S. (2010). The bacterial cell envelope. *Cold Spring Harb. Perspect. Biol.* 2:a000414. doi: 10.1101/cshperspect.a000414

Siriyong, T., Srimanote, P., Chusri, S., Yingyongnarongkul, B. E., Suaisom, C., Tipmanee, V., et al. (2017). Conessine as a novel inhibitor of multidrug efflux pump systems in *Pseudomonas aeruginosa*. *BMC Complement. Altern. Med.* 17:405. doi: 10.1186/s12906-017-1913-y

Spengler, G., Kincses, A., Gajdacs, M., and Amaral, L. (2017). New roads leading to old destinations: efflux pumps as targets to reverse multidrug resistance in bacteria. *Molecules* 22:468. doi: 10.3390/molecules22030468

Srinivasan, V. B., and Rajamohan, G. (2013). KpnEF, a new member of the *Klebsiella pneumonia* cell envelope stress response regulon, is an SMR-type efflux pump involved in broadspectrum antimicrobial resistance. *Antimicrob. Agents Chemother.* 57, 4449–4462. doi: 10.1128/AAC.02284-12

Srinivasan, V. B., Singh, B. B., Priyadarshi, N., Chauhan, N. K., and Rajamohan, G. (2014). Role of novel multidrug efflux pump involved in drug resistance in *Klebsiella pneumoniae*. *PLoS ONE* 9:e96288. doi: 10.1371/journal.pone.0096288

Stavri, M., Piddock, L., and Gibbons, S. (2007). Bacterial efflux pump inhibitors from natural sources. *J. Antimicrob. Chemother.* 59, 1247–1260. doi: 10.1093/jac/dkl460

Su, X. Z., Chen, J., Mizushima, T., Kuroda, T., and Tsuchiya, T. (2005). AbeM, an H^+-coupled *Acinetobacter baumannii* multidrug efflux pump belonging to the MATE family of transporters. *Antimicrob. Agents Chemother.* 49, 4362–4364. doi: 10.1128/AAC.49.10.4362-4364.2005

Sun, J., Deng, Z., and Yan, A. (2014). Bacterial multidrug efflux pumps: Mechanisms, physiology and pharmacological exploitations. *Biochem. Biophys. Res. Commun.* 453, 254–267. doi: 10.1016/j.bbrc.2014.05.090

Suresh, M., Nithya, N., Jayasree, P. R., Vimal, K. P., and Kumar, P. M. (2018). Mutational analyses of regulatory genes, *mexR, nalC, nalD* and *mexZ* of *mexAB-oprM*and *mexXY* operons, in efflux pump hyperexpressing multidrug-resistant clinical isolates of *Pseudomonas aeruginosa*. *World J. Microbiol. Biotechnol.* 34, 83. doi: 10.1007/s11274-018-2465-0

Suriyanarayanan, B., and Sarojini, S. R. (2015). Docking analysis insights quercetin can be a non-antibiotic adjuvant by inhibiting Mmr drug efflux pump in Mycobacterium sp. and its homologue EmrE in *Escherichia coli*. *J. Biomol. Struct. Dyn.* 33, 1819–1834. doi: 10.1080/07391102.2014.974211

Swick, M. C., Morgan-Linnell, S. K., Carlson, K. M., and Zechiedrich, L. (2011). Expression of multidrug efflux pump genes *acrAB-tolC, mdfA,* and *norE* in *Escherichia coli* clinical isolates as a function of fluoroquinolone and multidrug resistance. *Antimicrob. Agents Chemother.* 55, 921–924. doi: 10.1128/AAC.00996-10

Tait-Kamradt, A., Clancy, J., Cronan, M., Dib-Hajj, F., Wondrack, L., Yuan, W., et al. (1997). *mefE* is necessary for the erythromycin-resistant M phenotype in *Streptococcus pneumoniae*. *Antimicrob. Agents Chemother.* 41, 2251–2255. doi: 10.1128/AAC.41.10.2251

Telke, A. A., Olaitan, A. O., Morand, S., and Rolain, J-M. (2017). *soxRS* indices colistin hetero-resistance in *Enterobacter asburiae* and *Enterobacter cloacae* by regulating the acrAB-tolC efflux pump. *J. Antimicrob. Chemother.* 72, 2715–2721. doi: 10.1093/jac/dkx215

Tikhonova, E. B., Yamada, Y., and Zgurskaya, H. I. (2011). Sequential mechanism of assembly of multidrug efflux pump AcrAB-TolC. *Chem. Biol.* 18, 454–463. doi: 10.1016/j.chembiol.2011.02.011

Vargiu, A. V., Ramaswamy, V. K., Malvacio, I., Malloci, G., Kleinekathöfer, U., and Ruggerone, P. (2018). Water-mediated interactions enable smooth substrate transport in a bacterial efflux pump. *Biochim. Biophys. Acta Gen. Sub.* 1862, 836–845. doi: 10.1016/j.bbagen.2018.01.010

Venter, H., Mowla, R., Ohene-Agyei, T., and Ma, S. (2015). RND-type drug efflux pumps from Gram-negative bacteria: molecular mechanism and inhibition. *Front. Microbiol.* 6:377. doi: 10.3389/fmicb.2015.00377

Verma, P., Tiwari, M., and Tiwari, V. (2017). *In silico* high-throughput virtual screening and molecular dynamics simulation study to identify inhibitor for AdeABC efflux pump of *Acinetobacter baumannii*. *J. Biomol. Struct. Dyn.* 36, 1182–1194. doi: 10.1080/07391102.2017.1317025

Vimberg, V., Lenart, J., Janata, J., and Balikova Novotna, G. (2015). ClpP-independent function of ClpX interferes with telithromycin resistance conferred by Msr(A) in *Staphylococcus aureus*. *Antimicrob. Agents Chemother.* 59, 3611–3614. doi: 10.1128/AAC.04367-14

Viveiros, M., Jesus, A., Brito, M., Leandro, C., Martins, M., Ordway, D., et al. (2005). Inducement and reversal of tetracycline resistance in *Escherichia coli* K-12 and expression of proton gradient-dependent multidrug efflux pump genes. *Antimicrob. Agents Chemother.* 49, 3578–3582. doi: 10.1128/AAC.49.8.3578-3582.2005

Ward, A., Hoyle, C., Palmer, S., O'Reilly, J., and Griffith, J. (2001). Prokaryote multidrug efflux proteins of the major facilitator superfamily: amplified

expression, purification and characterisation. *J. Mol. Microbiol. Biotechnol.* 3, 193–200.

Warner, D. M., and Levy, S. B. (2010). Different effects of transcriptional regulators MarA, SoxS and Rob on susceptibility of *Escherichia coli* to cationic antimicrobial peptides (CAMPs): rob-dependent CAMP induction of the *marRAB* operon. *Microbiol.* 156, 570–578. doi: 10.1099/mic.0.033415-0

Watanabe, T. (1963). Infective heredity of multiple drug resistance in bacteria. *Bacteriol. Rev.* 27, 87–115.

Welch, A., Awah, C. U., Jing, S., van Veen, H. W., and Venter, H. (2010). Promiscuous partnering and independent activity of MexB, the multidrug transporter protein from *Pseudomonas aeruginosa*. *Biochem. J.* 430, 355–364. doi: 10.1042/BJ20091860

Wendlandt, S., Kadlec, K., Fessler, A. T., and Schwarz, S. (2015). Identification of ABC transporter genes conferring combined pleuromutilin-lincosamide-streptogramin A resistance in bovine methicillin- resistant *Staphylococcus aureus* and coagulase-negative staphylococci. *Vet. Microbiol.* 177, 353–358. doi: 10.1016/j.vetmic.2015.03.027

Willers, C., Wentzel, J. F., du Plessis, L. H., Gouws, C., and Hamman, J. H. (2016). Efflux as a mechanism of antimicrobial drug resistance in clinical relevant microorganisms: the role of efflux inhibitors. *Expert Opin. Ther. Targets* 21, 23–36. doi: 10.1080/14728222.2017.1265105

World Economic Forum (2013). *Global Risks, Eighth Edition Ed. 2013*. 28–33. Available online at: http://www3.weforum.org/docs/WEF_GlobalRisks_Report_2013.pdf (Accessed March 15, 2018).

World Health Organization (2014). *Antimicrobial Resistance*. Available online at: http://www.searo.who.int/thailand/factsheets/fs0023/en/ (Accessed October 22, 2018).

Wright, G. D. (2016). Antibiotic adjuvants: Rescuing antibiotics from resistance. *Trends Microbiol.* 24, 862–871. doi: 10.1016/j.tim.2016.06.009

Yaffe, D., Radestock, S., Shuster, Y., Forrest, L. R., and Schuldiner, S. (2013). Identification of molecular hinge points mediating alternating access in the vesicular monoamine transporter VMAT2. *Proc. Natl. Acad. Sci. U.S.A.* 110, E1332–1341. doi: 10.1073/pnas.1220497110

Yang, S., Lopez, C. R., and Zechiedrich, E. L. (2006). Quorum sensing and multidrug transporters in *Escherichia coli*. *Proc. Natl. Acad. Sci. U.S.A.*103, 2386–2391. doi: 10.1073/pnas.0502890102

Yang, S. K., Low, L. Y., Yap, P. S. X., Yusoff, K., Mai, C. W., Lai, K. S., et al. (2018). Plant-Derived Antimicrobials: Insights into Mitigation of Antimicrobial Resistance. *Rec. Nat. Prod.* 12, 295–316. doi: 10.25135/rnp.41.17.09.058

Yasufuku, T., Shigemura, K., Shirakawa, T., Matsumoto, M., Nakano, Y., Tanaka, K., et al. (2011). Correlation of overexpression of efflux pump genes with antibiotic resistance in *Escherichia coli* strains clinically isolated from urinary tract infection patients. *J. Clin. Microbiol.* 49, 189–194. doi: 10.1128/JCM.00827-10

Yoshida, H., Bogaki, M., Nakamura, S., Ubukata, K., and Konno, M. (1990). Nucleotide sequence and characterization of the *Staphylococcus aureus norA* gene, which confers resistance to quinolones. *J. Bacteriol.* 172, 6942–6949. doi: 10.1128/jb.172.12.6942-6949.1990

Zeng, B., Wang, H., Zou, L., Zhang, A., Yang, X., and Guan, Z. (2010). Evaluation and target validation of indole derivatives as inhibitors of the AcrAB-TolC efflux pump. *Biosci. Biotechnol. Biochem.* 74, 2237–2241. doi: 10.1271/bbb.100433

Zgurskaya, H. I., Lopez, C. A., and Gnanakaran, S. (2015). Permeability barrier of Gram-negative cell envelopes and approaches to bypass it. *ACS Infect. Dis.* 1, 512–522. doi: 10.1021/acsinfecdis.5b00097

Zhang, J., Sun, Y., Wang, Y., Lu, M., He, J., Liu, J., et al. (2014). Non-antibiotic agent ginsenoside 20(S)-Rh2 enhanced the antibacterial effects of ciprofloxacin *in vitro* and *in vivo* as a potential NorA inhibitor. *Eur. J. Pharmacol.* 740, 277–284. doi: 10.1016/j.ejphar.2014.07.020

Conflict of Interest Statement: The authors declare that the research was conducted in the absence of any commercial or financial relationships that could be construed as a potential conflict of interest.

Copyright © 2018 Shriram, Khare, Bhagwat, Shukla and Kumar. This is an open-access article distributed under the terms of the Creative Commons Attribution License (CC BY). The use, distribution or reproduction in other forums is permitted, provided the original author(s) and the copyright owner(s) are credited and that the original publication in this journal is cited, in accordance with accepted academic practice. No use, distribution or reproduction is permitted which does not comply with these terms.

frontiers in Microbiology

REVIEW
published: 01 April 2019
doi: 10.3389/fmicb.2019.00539

Emerging Strategies to Combat ESKAPE Pathogens in the Era of Antimicrobial Resistance: A Review

*Mansura S. Mulani, Ekta E. Kamble, Shital N. Kumkar, Madhumita S. Tawre and Karishma R. Pardesi**

Department of Microbiology, Savitribai Phule Pune University, Pune, India

The acronym ESKAPE includes six nosocomial pathogens that exhibit multidrug resistance and virulence: *Enterococcus faecium, Staphylococcus aureus, Klebsiella pneumoniae, Acinetobacter baumannii, Pseudomonas aeruginosa*, and *Enterobacter* spp. Persistent use of antibiotics has provoked the emergence of multidrug resistant (MDR) and extensively drug resistant (XDR) bacteria, which render even the most effective drugs ineffective. Extended spectrum β-lactamase (ESBL) and carbapenemase producing Gram negative bacteria have emerged as an important therapeutic challenge. Development of novel therapeutics to treat drug resistant infections, especially those caused by ESKAPE pathogens is the need of the hour. Alternative therapies such as use of antibiotics in combination or with adjuvants, bacteriophages, antimicrobial peptides, nanoparticles, and photodynamic light therapy are widely reported. Many reviews published till date describe these therapies with respect to the various agents used, their dosage details and mechanism of action against MDR pathogens but very few have focused specifically on ESKAPE. The objective of this review is to describe the alternative therapies reported to treat ESKAPE infections, their advantages and limitations, potential application *in vivo,* and status in clinical trials. The review further highlights the importance of a combinatorial approach, wherein two or more therapies are used in combination in order to overcome their individual limitations, additional studies on which are warranted, before translating them into clinical practice. These advances could possibly give an alternate solution or extend the lifetime of current antimicrobials.

Keywords: ESKAPE, multidrug resistance, alternative therapy, combination therapy, phage therapy, antimicrobial peptides, silver nanoparticles, photodynamic light therapy

OPEN ACCESS

Edited by:
Rebecca Thombre, Modern College of Arts, Science and Commerce, Pune University, India

Reviewed by:
Vishvanath Tiwari, Central University of Rajasthan, India
Rajashree Bhalchandra Patwardhan, Savitribai Phule Pune University, India

****Correspondence:***
Karishma R. Pardesi
karishma@unipune.ac.in

Specialty section:
This article was submitted to Antimicrobials, Resistance and Chemotherapy, a section of the journal Frontiers in Microbiology

Received: *31 May 2018*
Accepted: *01 March 2019*
Published: *01 April 2019*

Citation:
Mulani MS, Kamble EE, Kumkar SN, Tawre MS and Pardesi KR (2019) Emerging Strategies to Combat ESKAPE Pathogens in the Era of Antimicrobial Resistance: A Review. Front. Microbiol. 10:539. doi: 10.3389/fmicb.2019.00539

INTRODUCTION

Wonder drug penicillin started the era of antibiotics in 1928 and since then it has tremendously developed modern medicine. Persistent use of antibiotics, self-medication, and exposure to infections in hospitals has provoked the emergence of multidrug resistant (MDR) bacteria responsible for 15.5% Hospital Acquired Infection (HAIs) in the world (Rice, 2008; Allegranzi et al., 2011; Ibrahim et al., 2012; Pendleton et al., 2013). The term "ESKAPE" encompasses six such pathogens with growing multidrug resistance and virulence: *Enterococcus faecium, Staphylococcus aureus, Klebsiella pneumoniae, Acinetobacter baumannii, Pseudomonas aeruginosa,* and *Enterobacter* spp. (Rice, 2008). ESKAPE pathogens are responsible for majority of nosocomial infections and are capable of "escaping" the biocidal action of antimicrobial agents (Rice, 2008; Navidinia, 2016).

A systematic review of clinical and economic impact of antibiotic resistance reveals that, ESKAPE pathogens are associated with the highest risk of mortality thereby resulting in increased health care costs (Founou et al., 2017). World Health Organization (WHO) has also recently listed ESKAPE pathogens in the list of 12 bacteria against which new antibiotics are urgently needed (Tacconelli et al., 2018). They describe three categories of pathogens namely critical, high and medium priority, according to the urgency of need for new antibiotics. Carbapenem resistant *A. baumannii* and *P. aeruginosa* along with extended spectrum β-lactamase (ESBL) or carbapenem resistant *K. pneumoniae* and *Enterobacter* spp. are listed in the critical priority list of pathogens; whereas, vancomycin resistant *E. faecium (VRE)* and methicillin and vancomycin resistant *S. aureus* (MRSA and VRSA) are in the list of high priority group. The mechanisms of multidrug resistance exhibited by ESKAPE are broadly grouped into three categories namely, drug inactivation commonly by an irreversible cleavage catalyzed by an enzyme, modification of the target site where the antibiotic may bind, reduced accumulation of drug either due to reduced permeability or by increased efflux of the drug (Santajit and Indrawattana, 2016). They are also able to form biofilms that physically prevent the immune response cells of host as well as antibiotics to inhibit the pathogen. Moreover, biofilms protect specialized dormant cells called persister cells that are tolerant to antibiotics which cause difficult-to-treat recalcitrant infections (Lewis, 2007).

The general antimicrobial therapy to effectively treat infections involves the use of antibiotics either singly or in combination. With every passing year, the overall number of antibiotics effective against ESKAPE is declining, which is predisposing us toward a future with antibiotics that are ineffective. Analysis of the antibiotic lists recommended in the Clinical & Laboratory Standards Institute (CLSI) guidelines revealed that many antibiotics suggested against ESKAPE since 2010 have been deleted with addition of relatively few antibiotics/antibiotic combinations. Furthermore, there are incidences of resistance reported against some of these newly added antibiotics (**Table 1**). It is, therefore, imperative to find alternative ways to treat infections especially those caused by ESKAPE pathogens.

Alternative therapies that are currently in practice or under trial include the use of antibiotics in combination or with adjuvants, bacteriophage therapy, use of antimicrobial peptides, photodynamic therapy, antibacterial antibodies, phytochemicals and nanoparticles as antibacterial agents (Mandal et al., 2014; Kaur, 2016). There are several reviews published which describe alternative/novel therapies against MDR pathogens, however, not many have specifically focused on the ESKAPE group as a whole. These reviews describe the various therapeutic agents used with respect to their dosage, mode of action, pharmacokinetics and pharmacodynamics, stability, and toxicity. Although many alternative therapies reported have shown promising results *in vitro*, their efficacy when applied *in vivo* may not be the same due to one or several limitations. It therefore, becomes necessary to understand the action of these therapeutic agents *in vivo*. This review highlights therapies used to treat ESKAPE infections namely, antibiotics in combination or with adjuvants, bacteriophage therapy, antimicrobial peptides, photodynamic light therapy, and nanoparticles which have received significant attention in the last 5 years. Hereby, we have also tried to include studies especially focusing on *in vivo* efficacy of above mentioned therapy/therapeutic agents, their advantages and limitations. **Figure 1** summarizes the major limitations of each alternative therapy which has been elaborately discussed in the following sections. To improve the efficiency and/or minimize the limitations of any therapy/therapeutic agents, combinatorial approaches are suggested. It involves use of two or more monotherapies together (co-administered, functionalized, or conjugated) which is also further described. Altogether, combinatorial approach could be a prospect for exploring novel alternate solutions against ESKAPE.

ANTIBIOTICS IN COMBINATION

Antibiotics in combination have been tested as a treatment method by a number of researchers because the possibility of a pathogen to develop resistance against a combination of two drugs is much less than that against a single drug. Similarly, the synergistic effect of combined antibiotics is more than that of the individual antibiotic. A combination of drugs also increases the spectrum of coverage (Vazquez-grande and Kumar, 2015) and has been found to be beneficial in severe infections caused by multiple pathogens (Ahmed et al., 2014). Some of these combinations tested against the ESKAPE are listed in **Table 2**. The problem of antibiotic resistance is so severe that it has become necessary to try combinations of the most recently synthesized antibiotics and/or last resort antibiotics to study their potential in antimicrobial therapy. The Gram positive members of the ESKAPE, *E. faecium* and *S. aureus*, have been tested against a combination of fosfomycin and daptomycin which has shown to successfully clear infection (Hall Snyder et al., 2016; Coronado-Álvarez et al., 2018). The former is a broad spectrum antibiotic that has shown promising results against Gram negative bacteria while the latter is a last resort antibiotic used to treat infections caused by *E. faecium* and *S. aureus*. Despite being a resistant pathogen there is a lack of substantial research in antibiotic combination therapy against *E. faecium* over the last 5 years. Most combinations tested against *S. aureus in vitro* include daptomycin or vancomycin with other antibiotics including ceftaroline, a newly added antibiotic to the CLSI guidelines. The effect of these and other such combinations have also been tested in various mouse models which cleared away the *S. aureus* infection with minimal to no toxicity. Colistin (polymyxin E) is the last resort antibiotic prescribed against Gram negative bacilli. In recent years, research has been conducted to treat infections caused by *K. pneumoniae* and *A. baumannii* using a combination of colistin or tigecycline with other antibiotics and has shown promising results *in vitro* and in cohort studies.

Some molecules when combined with antibiotics make an ineffective drug effective. These molecules, named "adjuvants" or "resistance breakers," have little to no antimicrobial activity of their own (González-Bello, 2017) but inhibit the mechanism

TABLE 1 | Antibiotics added/revised and eliminated against ESKAPE from CLSI document M100 since 2010.

Antibiotics added/with revised breakpoint	Tested against pathogen					
	Ef	S	K	A	P	E
Amikacin, Amoxicillin-clavulanate, Ampicillin-sulbactam, Cefaclor, Cefamandole, Cefdinir, Cefmetazole, Cefonicid, Cefotetan, Cefpodoxime, Cefprozil, Cefuroxime, Kanamycin, Loracarbef, Netilmicin, Oxacillin, Tobramycin		0				
Aztreonam			1			1
Cefazolin, Cefepime, Ceftazidime		0	1			1
Cefoperazone, Moxalactam		0			0	
Cefotaxime, Ceftizoxime, Ceftriaxone		0	1		0	1
Ceftaroline		1	1			1
Ceftazidime-avibactam, Ceftolozane-tazobactam			1			1
Cephalothin		0	0			0
Colistin, Piperacillin					1	
Dalbavancin, Telavancin, Oritavancin, Tedizolid	1	1				
Doripenem, Imipenem, Meropenem		0	1	1	1	1
Ertapenem		0	1	1		1
Mezlocillin				0		
Nalidixic acid			0			0
Piperacillin-tazobactam, Ticarcillin-clavulanate		0			1	
Ticarcillin			0	0	0	0

Please note that the table includes ONLY those antibiotics which are deleted or newly added since 2010.

0 = Antibiotics deleted from CLSI guidelines between 2010 and 2018; 1, New antibiotics added in the CLSI guidelines since 2010; 1 = No resistance reported till date; 1 = Resistance reported; Ef, E. faecium; S, S. aureus; K, K. pneumoniae; A, A. baumannii; P, P. aeruginosa; E= Enterobacter spp.

S = (Long et al., 2014; Chan et al., 2015; Nigo et al., 2017); K = (Zowawi et al., 2015; Vuotto et al., 2017; Stanley et al., 2018); A = (Göttig et al., 2014; Goic-Barisic et al., 2017; Nowak et al., 2017; Caio et al., 2018; Chuang and Ratnayake, 2018); P = (Prakash et al., 2014; Gill et al., 2016; Alipour et al., 2017; Mohapatra et al., 2018; Palavutitotai et al., 2018); E = (Lee et al., 2015; Babouee Flury et al., 2016; Zeng et al., 2016; Kulengowski et al., 2018).

of resistance by increasing the uptake of the antibiotic through the bacterial membrane, blocking of efflux pumps, and changing the physiology of resistant cells (i.e., dispersal of biofilms to planktonic cells) (Kalan and Wright, 2011; Bernal et al., 2013). Essential oils and phenothiazines enhance the antimicrobial activity of drugs and also inhibit the transmission of resistance to other populations (Bueno, 2016).

The most popularly known adjuvants are β-lactamase inhibitors while the most recent adjuvant tested to restore meropenem activity is vaborbactam which inhibits *K. pneumoniae* carbapenemase activity (Jorgensen and Rybak, 2018). It has also undergone a clinical trial; registered on ClinicalTrials.gov under identifier NCT02020434; which proved the combination to be safe after testing 41 subjects (Rubino et al., 2018). However, it has a limited inhibition activity as it has been unable to do so with class B and class D β-lactamases. Other β-lactamase inhibitors include avibactam, nacubactam, and tazobactam (Monogue et al., 2018a,b). Metal chelators like EDTA, deferasirox, and deferoxamine also inhibit β-lactamases as these enzymes require metal ions for their activity (Aoki et al., 2010; Santos et al., 2012; Yoshizumi et al., 2013). These chelators have been tested in combination with antibiotics like imipenem, tobramycin, and vancomycin against *S. aureus*, *P. aeruginosa,* and *E. coli* in murine models with successful decrease in bacterial load. Quorum quenchers, molecules that inhibit quorum sensing thereby inhibiting biofilm formation, have also shown potential to cure infection in combination with certain antibiotics (Balamurugan et al., 2015; Chatterjee et al., 2016). 1-[(2,4-Dichlorophenethyl)amino]-3-Phenoxypropan-2-ol is so far the most promising antimicrobial agent as it has been reported to kill not only persister cells of *P. aeruginosa* but also non-persister cells of all the other ESKAPE members. It has also been shown to enhance killing of antibiotic resistant strains in both planktonic and biofilm forms. Its combination with a variety of antibiotics is shown to kill all of the ESKAPE making it an ideal candidate as an adjuvant (Defraine et al., 2017).

Even though there is increased activity of antibiotics when used in combination against pathogens *in vitro*, there are limited studies demonstrating the same *in vivo* and some among those have proven disadvantageous. If monotherapy selects for a narrow spectrum of resistance, a combination of two or more antibiotics selects for a broad spectrum of resistance defeating the purpose of combination therapy entirely (Vestergaard et al., 2016). Certain combinations that are meant to treat infections tend to have the opposite effect resulting in far worse damage. One antibiotic can lead to the induction of a resistance mechanism against a second antibiotic administered in combination leading to antagonistic effect (Fallah, 2018). A clinical trial conducted in Italy in which infections caused by XDR *A. baumannii* were treated with a combination of colistin and rifampin showed no improvement in survival rates. In fact, this combination led

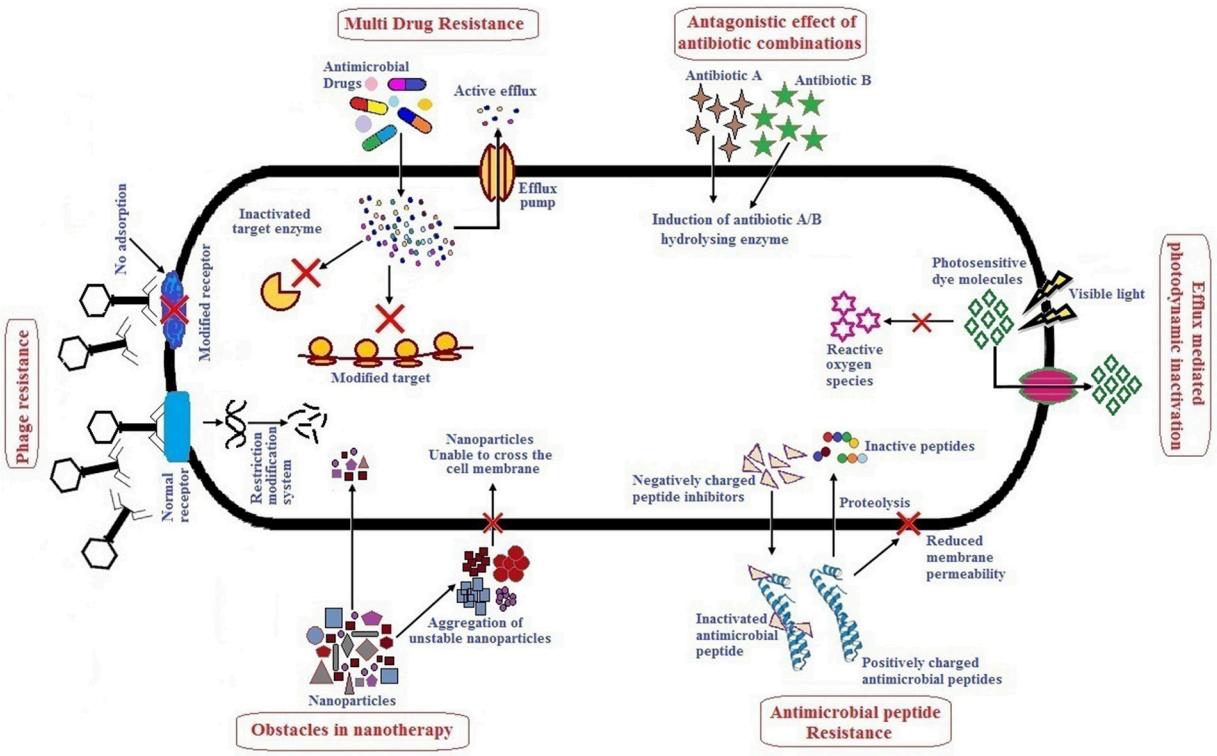

FIGURE 1 | Major challenges of antibacterial monotherapies.

to increased hepatic toxicity (Durante-Mangoni et al., 2013). A similar study using a combination of colistin, tigecycline and carbapenems against *A. baumannii* showed futile results (López-Cortés et al., 2014). Metal chelators have shown to sequester ions not only from bacterial cells but also from host tissue cells (Yoshizumi et al., 2013).

The most recent alternative to antibiotics or their combination that shows a promising future is antibiotic hybrids which have been defined by Domalaon et al. (2018) as synthetic constructs of two or more pharmacophores belonging to an established agent known to elicit a desired antimicrobial effect. This method provides the advantage of combination therapy through the mono therapy approach, where chances of resistance are curbed, while overcoming the problem of non-complementary pharmacodynamic profiles of the individual antibiotics.

The ESKAPE tend to become resistant to either or both antibiotics used in combination with every passing year due not only to natural selection of resistant strains but also horizontal gene transfer from them to sensitive strains. This warrants testing of still new combinations. The result is a never-ending cycle from which there is no escape. It can therefore be concluded that antibiotics in combination may not always be effective and that there is a need for extensive research of alternative strategies.

BACTERIOPHAGE THERAPY

Phages are century old therapeutic agents that were used for the treatment of bacterial infections. The discovery of antibiotics was an influential factor in side-lining this ambition (Mann, 2005). The focus on phage therapy has sharpened ever since antimicrobial resistance has been on a dramatic rise. Lytic phages against ESKAPE pathogens have been isolated from hospital wastewater, making them easily available therapeutic agents (Latz et al., 2016). Bacteriophages used for therapy present many advantages such as high host specificity (prevent damage to normal flora, do not infect the eukaryotic cells), low dosages for treatment, rapid proliferation inside the host bacteria, etc. that make them ideal candidates to treat bacterial infections (Domingo-Calap and Delgado-Martínez, 2018). Unlike antibiotics, the advantage of using phages is that, they develop new infectivity and regain an upper hand over bacteria as they mutate alongside their host (Pirnay et al., 2018).

Several studies carried out *in vitro* have proven phages to be effective as antibacterial agents against biofilm and planktonic cells of ESKAPE (Pallavali et al., 2017; Dvořáčková et al., 2018; Jamal et al., 2019). **Table 2** gives information of phage therapy studied in various animal models as well as recent case studies and case reports of patients infected with ESKAPE pathogens. Phage therapy carried out in animal wound infection models have shown reduced mortality and enhanced wound healing. Additional studies carried out *in vivo* have also demonstrated efficacy and safety (non-toxic with reduced inflammatory responses) of phages used in treatment of bacterial infections.

Phage therapy, though promising, comes with some limitations. It can, however, be overcome by appropriate modifications (Wittebole et al., 2014; El-Shibiny and El-Sahhar,

TABLE 2 | Alternative strategies against ESKAPE pathogens.

Target ESKAPE	Model used	Agent used and dosage details	Route of administration	*In vivo* efficacy: log reduction of pathogen; % survival of host	Other advantages	References
ANTIBIOTICS IN COMBINATION						
Ef	*Galleria mellonella* larvae infection model	Rifampin (0.5–2) μg/ml+Tigecycline (0.03 μg/ml)/Vancomycin (64, 128 μg/ml)/Linezolid (2 μg/ml)	Injection into hemocoel	20–73% survival	–	Skinner et al., 2017
S	Retrospective study 2011–2017	Fosfomycin+Daptomycin/ Oxacillin/Vancomycin	–	Successful treatment in 81% patients	–	Coronado-Álvarez et al., 2018
S	Wistar mouse	Rifampin (20 mg/kg) + Flucloxacillin (200 mg/kg)/ Moxifloxacin (10 mg/mg)	Intraperitoneal (IP)	4 log decrease with both combinations	Antibiofilm	Greimel et al., 2017
S	Wistar rats	Gentamicin (8, 50 mg/kg) + 4-(Benzylamino) cyclohexyl 2-hydroxycinnamate (16, 64 mg/kg)	–	4 log reduction; 100% survival	Antibiofilm	Balamurugan et al., 2015
K	Murine complicated urinary tract infection model	Meropenem (400 mg/kg) + Nacubactam (150 mg/kg)	–	>3 log reduction in isolates resistant to meropenem-nacubactam	–	Monogue et al., 2018a
A	Murine Thigh and Lung Infection Models	Colistin + Tazobactam/Avibactam	IP	No effect	–	Monogue et al., 2018b
P	Murine thigh infection model	Imipenem (4 or 5 g/day with a 1-g loading dose)+ Tobramycin (7 mg/kg)	–	≥2.5 or ≥1.50 log reduction	–	Yadav et al., 2017
P	Murine infection model	Colistin (2.5–5 mg/kg) + Rifampicin (10 mg/kg)	Subcutaneous	∼5 log reduction	–	Cai et al., 2018
E	*G.mellonella* infection model	Colistin (2.5 mg/kg) + Imipenem (15 mg/kg)	Injection into hemocoel	80–90% survival	–	Yang et al., 2018a
PHAGE THERAPY						
Ef	Murine bacteraemia model	Phage ENB6 and C3 (A2 morphotype group), of 3×10^8 PFU	IP	Single dose: 50% survival; Multiple doses: 100% survival	Immunocompatible	Biswas et al., 2002
S	65-year-old woman with Corneal abscess	SATA-8505 (ATCC PTA-9476)	Topical (eye drops and nasal spray) and intravenous (IV)	Eradication of pathogen and stabilization of ocular signs	-	Fadlallah et al., 2015
S	Case series (six human subjects suffering from diabetic foot ulcer)	Commercial staphylococcal phage Sb-1; (0.05–0.4 ml of 10^7-10^8 PFU/ml)	Topical	–	Wound healing within 7 weeks	Fish et al., 2016
S	Rabbit osteomyelitis model	Cocktail of phages (SA-BHU1, 2, 8, 15, 21, 37 and 47); 15 μl of 5×10^{12} PFU/ml of each	Intramuscular (IM)	100% survival	Viruses with stable genomic structure	Kishor et al., 2016
S	Murine bacteraemia model	Phage SLPW Podoviridae; 0.2 mL of 1×10^9 PFU	IP	∼100% decrease in bacterial count; up to 80% survival	Stable up to 45°C, pH 6-10; Immunocompatible	Wang et al., 2016
S	Murine wound infection model	MR 5 and MR 10, Myoviridae; free phage 10^9 PFU/50 μl and its liposomal formulation	Topical	Up to 3 log reduction on day 10	Wound healing within 7 days	Chhibber et al., 2018

(Continued)

TABLE 2 | Continued

Target ESKAPE	Model used	Agent used and dosage details	Route of administration	*In vivo* efficacy: log reduction of pathogen; % survival of host	Other advantages	References
K	Murine burn wound infection model	Five phages KØ1 to 5 (10^7 PFU/ml) in equal proportion as a cocktail or loaded in liposomes	IP	>4 log reduction; 100% survival	Enhanced wound healing	Chadha et al., 2017
A	Case study 77-year-old man with post-operative infection	Five phages active against 104 *A. baumannii* from the NMRC's phage-Biolog system 2.14 × 10^7 PFU/mL	Intravenous (IV)	No effect	–	LaVergne et al., 2018
A	Murine wound infection model	Cocktail of AB-Army 1 and AB-Navy 1 to 4 (~4 × 10^9 PFU)	Topical, IP or loaded on TegadermTM bandage	3 log tested *in vitro*; ND	Antibiofilm; Reduction in wound bio-burden and size (loss of capsule production in phage infected *Acinetobacter*)	Regeimbal et al., 2016
A	Murine wound infection model	Acinetobacter phage- Siphoviridae; (400 μl of 3 × 10^9 PFU/ml)	Topical	100% clearance of infection in 8 days	Reduction in wound bio-burden but no difference in time required for wound healing	Shivaswamy et al., 2015
A	*G.mellonella* infection model	Phage WCHABP1 and WCHABP12 Myoviridae; 10^4 PFU/larva	Injection into hemocoel	75% survival	No integrase and repressor genes were identified in both bacteriophages	Zhou et al., 2018
A	Case study (68 year old patient with infected diabetic patient)	Cocktails of AB Phage ΦPC (AB-Navy1, 4, 71, 97, and AbTP3Φ1); ~10^9 PFU/dose	Percutaneous catheter, IV	Clearance of infection	–	Schooley et al., 2017
P	Murine infected model	Phage PEV20, Podoviridae; Inhalable powder 2 × 10^7 PFU/mg	Intranasal and intratracheal	5 log reduction	Non-toxic	Chang et al., 2018
P	Case study (2-year-old boy with a history of DiGeorge syndrome)	Cocktail from US Navy library of bacteriophages 3.5 × 10^5 every 6 h. six doses total and resumed after 11 days	IV	Blood cultures negative After phage treatment	-	Duplessis et al., 2018
P	Case study (61 year old male patient with acute septicaemia and large necrotic pressure sores)	Phage BFC1 50 μl IV infusion every 6 h for 10 days; Wounds irrigation-50 ml BFC1 every 8 h for 10 days	IV infusion and Topical	Clearance of septicaemia immediately after therapy; pressure sores remained infected with several bacterial species, including *P. aeruginosa*	No adverse effects	Jennes et al., 2017
P	*G.mellonella* infection model	Phage KTN4; MOI100	Injection into hemocoel	4–7 log reduction; 100% survival	Antibiofilm; Stable up to 40–70°C	Danis-Wlodarczyk et al., 2016
E & P	Case series (9 UTI patients)	Pyophage	Pyophage instillation by suprapubic catheter	bacterial titers decreased after bacteriophage treatment in six out of nine patients (67%).	No bacteriophage-associated adverse events detected	Ujmajuridze et al., 2018
S, A, & P	Murine sepsis model	Phage against *A. baumanni*, *P. aeruginosa,* and *S. aureus*	IP	100% reduction in A and P; 100% survival	–	Soothill, 1992; Lin et al., 2017

(Continued)

TABLE 2 | Continued

Target ESKAPE	Model used	Agent used and dosage details	Route of administration	*In vivo* efficacy: log reduction of pathogen; % survival of host	Other advantages	References
K & E	*G. mellonella* infection model	Cocktail of Escherichia phage ECP311, Klebsiella phage KPP235, and Enterobacter phage ELP140	–	100% reduction after 5 doses; 90% survival	–	Manohar et al., 2018
SILVER NANOPARTICLES						
S	Infected *Daniorerio*-Zebrafish model	Sunlight mediated AgNP synthesized using plantextract (HWP AgNP) (10–40 nm)	–	>1 log reduction	Antibiofilm; Non-toxic	Lotha et al., 2018
S	Murine wound infection model	Chitosan-coated AgNPs (10–30 nm) (50 μg/g·bw)	Topical	–	Wound healing within 14 days; Non-toxic	Peng et al., 2017
S	Rabbit flexor tendon rupture model	Core-shell nanofibrous membranes with embedded AgNPs in PEG/poly (caprolactone) shell and hyaluronic acid/ibuprofen in the core	AgNP Coated implant	–	Antibacterial activity; Prevention of peritendinous adhesion after tendon surgery; Non-toxic	Shalumon et al., 2018
S	Murine model	Wound dressing containing nanosilver nanohydrogels (nSnH) along with *Aloe vera*	Topical	–	Antibacterial; Wound healing within 16 days; Non-toxic	Anjum et al., 2016
S	Murine wound infection model	Sodium carboxymethylcellulose hydrogel loaded with PEG-coated-AgNPs (19.2 ± 3.6 nm) (500 μg AgNPs/g of hydrogel)	Topical	97.30% reduction; 100% survival	Wound healing within 10 days	Mekkawy et al., 2017
S	Murine model	Mesoporous silica nanoparticles coated with AgNPs (Ag-MSNs)	Topical	–	Antibacterial; Wound healing within 5 weeks; Anti-inflammatory	Dong et al., 2016
S	Rabbit flexor tendon model	AgNPs embedded in electrospun hyaluronic acid (HA)/polycaprolactone (PCL) nanofibrous membranes (NFMs)	AgNP Coated implant	–	Antibacterial; Prevention of peritendinous adhesion after tendon surgery	Chen et al., 2015
S & P	Murine wound infection model	AgNPs (20 nm)/chitosan composite dressing (0.5 mM)	Topical	–	Wound healing within 8 days; Non-toxic	Liang et al., 2016
S & P	*G. mellonella* model	Electrochemically synthesized AgNPs (8–10 nm) (6.8 and 3.4 mg/mL)	Injected into hemocoel	–	Antibiofilm; Non-toxic	Pompilio et al., 2018
S & P	Murine model	Bilayer composite of Chitosan-AgNPs (5–50 nm) (CS-AgG) on CSGB (*Bletilla striata* polysaccharide) both linked with genipin	Topical	–	Antibacterial; Wound healing; Non toxic	Ding et al., 2017
S & P	Murine model	NanoAg (<50 nm) wound dressings; 100 μL of 1 mg/mL	Topical	–	Antibacterial; Antibiofilm; Biocompatible	Radulescu et al., 2016
S & P	Murine model	Collagen nanofiber mats containing AgNPs (25–55 nm)	Topical	–	Antibacterial; Wound healing within 14 weeks; No hypersensitive; Anti-inflammatory	Rath et al., 2016

(Continued)

TABLE 2 | Continued

Target ESKAPE	Model used	Agent used and dosage details	Route of administration	*In vivo* efficacy: log reduction of pathogen; % survival of host	Other advantages	References
S & P	Gottingen minipigs femur model	Nanocomposite coating formed by polysaccharide 1-deoxylactit-1-yl chitosan (Chitlac) and AgNPs on methacrylate thermosets	AgNP Coated implant	–	Antibiofilm; Anti-inflammatory; Non-toxic	Marsich et al., 2013
ANTIMICROBIAL PEPTIDE (AMP)						
A	Murine infection model	Chex1-Arg20 amide; 2 and 5 mg/kg	IM	>2 log reduction; >50% survival	Anti-inflammatory	Ostorhazi et al., 2018
A	Murine wound infection model	K11, a hybrid peptide of melittin, cecropin A1, and magainin 2	Topical	∼100% pathogen clearance; 100% survival	Wound healing (21 days)	Rishi et al., 2018
P	Murine infection model	Feleucin-K3 analogs; 5 mg/kg	IP	∼ 1 log reduction	Stable; Low toxicity; Antibiofilm	Xie et al., 2018
S	*G. mellonella* infection model	PT-13, Plant derived crude extract; 64 μM	Injection into hemocoel	60% survival	–	Al Akeel et al., 2018
P	*G. mellonella* infection model	SP-E, a proline-rich pig saliva derived peptide; 6.1 μmol/kg	Injection into hemocoel	∼50% survival	Non-toxic	Ciociola et al., 2018
S & A	*S. aureus* murine sepsis model, *A. baumannii* infected murine lung model	D-150–177C, peptide modified by attaching C-terminal Cysteine; 5 and 10 mg/kg	IP	70% survival	Non-toxic	Chen et al., 2018
S & A	Murine skin infection model	SAAP-148, a LL-37 human cathelicidin inspired peptide used to prepare ointment; 0.125 to 0.5% (w/w)	Topical	87% and complete clearance of *S. aureus* and *A. baumannii,* respectively After a single treatment with 2% (w/w) SAAP-148 ointment	Antibiofilm; Kills persister cells; Reducing bioburden and wound healing; Non-toxic	de Breij et al., 2018
P	Murine lung infection model	Esc (1–21)-1c, frog skin derived AMP; 0.1 mg/kg	Intra-tracheal injection	2 log reduction	Anti-inflammatory	Chen et al., 2017
ANTIMICROBIAL LIGHT THERAPY						
S	Murine burn infection model	Laser light-50 J/cm^2; PS-PS-sinoporphyrin sodium (DVDMS)- 2, 5, and 10 μM, 75 min	Topical	4 log reduction at 5 μM of DVDMS with 50 J/cm^2 light	DVDMS promoted wound healing after burn infections	Mai et al., 2017
S	Murine ulcer infection model	Laser light-LED 410 nm, 50 J/cm^2; PS-5-ALA; 200 mg/kg	Topical	2 log reduction	–	Morimoto et al., 2014
S	Murine infection model	Light: 660 nm- 45 J/cm^2- 10 min exposure; household light- 7.5 J/cm^2- 10 min exposure; PS pentalysine-β-carbonylphthalocyanine Zinc (ZnPc(Lys)5)- 5 μl at 1 mM	Topical	44.3% clearance of infection at 7.5 J/cm^2	Improved wound healing	Ullah et al., 2018
A	Murine burn infection model	Light- LED 415 nm 72–360 J/cm^2	Topical	3 log reduction	Antibiofilm	Wang et al., 2017
P	Murine skin abrasion model	Light- 415 nm, 48 J/cm^2	Topical	5 log reduction	–	Amin et al., 2016

Ef, Enterococcus faecium; S, Staphylococcus aureus; K, Klebsiella pneumonia; A, Acinetobacter baumannii; P, Pseudomonas aeruginosa; and E, Enterobacter spp.

2017; Domingo-Calap and Delgado-Martínez, 2018). High specificity of the phages can be considered as both advantageous and a limiting factor. Monophage therapy involves the need to check the efficacy of the phage by testing it *in vitro* against the disease-causing bacteria before applying it to a patient which can be a difficult process. The use of phage cocktails, comprising of a combination of phages acting against different bacterial species or strains, can avoid these problems (Chan et al., 2013). International experts believe that an ideal phage cocktail should be prepared using phages belonging to different families or groups such as having broad host range, high adsorption ability to the highly conserved cell wall structures in bacteria. Using such phage cocktails may reduce the emergence of phage resistant bacterial population. However, others advocate strategies wherein individual active phages are applied sequentially to the patient. In clinical practice, however, it appears to be difficult (Rohde et al., 2018).

Genomic characterization of phages is very important so as to predict their "safety" in therapeutic applications as demonstrated by several experts in this field. Phages can be vectors for horizontal gene transfer in bacteria, sometimes being involved in exchange of virulence or antibiotic resistance genes making a microbe more pathogenic or resistant to an antibiotic (Chen and Novick, 2009). Phages reported for therapeutic applications should not harbor virulence or antibiotic resistance genes as well as integrases, site-specific recombinases, and repressors of the lytic cycle that may accelerate the transfer/integration of these genes in the host bacterial genome. Algorithms that can be used for predicting lifestyle of a phage, and its virulent traits are available but their database needs to be updated with more genome sequences of phages (Mcnair et al., 2012). Two recent reviews excellently describe the work flow to select ideal phage candidates for therapeutic purposes (Casey et al., 2018; Philipson et al., 2018). Recent studies demonstrating *in vivo* efficacy of phages against ESKAPE infections have used fully characterized phages that show no virulence or antibiotic resistance genes, are considered safe as they do not exhibit any allergic or immune response, and are also reported to remain stable at varied pH and temperature which make them ideal candidates for therapy (Fish et al., 2016; Kishor et al., 2016; Wang et al., 2016; Zhou et al., 2018).

Similarly, it has also been reported that the bacterial strains used for phage production should ideally be free of functional prophages. These prophages may get induced and contaminate the phage preparation. However, a recent report discusses the risk benefit evaluation that needs to be done in highly experimental treatments of patients infected with MDR pathogens such as ESKAPE (Rohde et al., 2018).

Another limitation reported is the stability of phages and their proper administration in order to reach the site of action. Phage formulations are ingested orally, administered nasally or applied topically (Malik et al., 2017; Cooper et al., 2018). Studies have shown improved efficacy of phage when entrapped with liposomes (Singla et al., 2016; Chadha et al., 2017; Malik et al., 2017; Chhibber et al., 2018). Phages can be targeted at the infection site in the form of powdered formulations (Chang et al., 2018). Phage derived product like phage encoded lytic enzymes showing function similar to lysozyme can also be used as an antibacterial agent or can be combined with other antimicrobials like antibiotics to improve efficacy of treatment (Lin et al., 2017). A phage derived protein, "endolysin" is reported for its antibacterial and antibiofilm activity against ESKAPE (Viertel et al., 2014; Gong et al., 2016; Rios et al., 2016; Lin et al., 2017; Zhang et al., 2018). V12CBD a recombinant protein derived from bacteriophage lysine, PlyV12, was able to attenuate virulence of *S. aureus,* and enhance its phagocytosis in mice (Yang et al., 2018b).

Several commercial phage preparations which can be used against ESKAPE are available some of which include, "Stafal," "Sextaphage," "PhagoBioDerm," and "Pyophage". Stafal (Bohemia Pharmaceuticals, Slovakia) is an antistaphylococcal phage preparation, Sextaphage (Microgen, ImBio Nizhny Novgorod, Russia) is a cocktail against *P. aeruginosa and E. coli* while, Pyophage (Georgian Eliava Institute of Bacteriophage, Microbiology, and Virology) contains bacteriophages specifically eliminating causative agents of pyoinflammatory and enteric diseases. PhagoBioDerm, a polymeric bandage impregnated with cocktail of phages, ciprofloxacin, and other active ingredients ensured for sustained release of phages to treat ulcers or wound infections caused by *S. aureus* and *P. aeruginosa* (Markoishvili et al., 2002). Clinical potential of these preparations has been investigated further to determine their broad spectrum activity against other strains *in vitro*, *in vivo* efficacy in animal models as well as through several case studies or clinical trials described below.

Recent human case studies involving treatment of ESKAPE associated infections with different phages are described in **Tables 2**, **3**. Readers may refer to previous reviews published on phage therapy which have described in numerous studies (Abedon et al., 2011; Chan et al., 2013; Górski et al., 2017; Lin et al., 2017; Sybesma et al., 2018). Most of the case studies report phage therapy given to patients on a compassionate care basis where antibiotic treatment fails.

Several case studies have demonstrated the efficacy of phage therapy in treating patients suffering from eye infections (Fadlallah et al., 2015), pancreatitis (Schooley et al., 2017), diabetic foot ulcer (Fish et al., 2016), and urinary tract infection (Ujmajuridze et al., 2018). Fadlallah et al. (2015), reported a case study of a 65 year old woman suffering from a secondary eye infection by VRSA, treated with a well-characterized commercially available lytic phage, SATA-8505 (ATCC PTA-9476) against MRSA. After 6 months of treatment, the patient was diagnosed as negative for cultures of VRSA. This case study suggests that bacteriophage eye-drops can be used as an alternative treatment of infectious keratitis by MDR pathogens. Fish et al. (2016), reported a case involving nine patients suffering from diabetic foot ulcer, who were treated with a preparation of anti-staphylococcal phages (Sb-1) on a compassionate care basis. The average healing time reported was ∼7 weeks. However, one ulcer, with poor vascularity required 18 weeks of treatment. Similarly, Ujmajuridze et al. (2018), reported a preclinical pilot study for a double blind RCT registered at ClinicalTrials: NCT03140085 (Leitner et al., 2017). Pyophage were used in this study to treat nine patients suffering from UTI infections. The first phase

TABLE 3 | Alternative strategies used in combination against ESKAPE pathogens.

Target ESKAPE member	Study model	Agent used and dosage details	Efficacy: log reduction of pathogen using combination; % survival of host, additional advantage	References
PHAGE + ANTIBIOTIC				
P	Case study (76 year old male with postoperative infection after arch replacement surgery)	Phage OMKO1 titer of 10^7 PFU/ml + Ceftazidime (0.2 gm/ml)−10 ml of this combination was injected into the mediastinal fistula which was in continuity with the perigraft collection	Eradication of *the P. aeruginosa* infection	Chan et al., 2018
K	*in vitro*–antibiofilm assay, *in vivo*—murine model (for raising antibodies)	KPO1K2, Podoviridae; free and liposome encapsulated (1.2×10^{13} in 200 μl, MOI = 1) + amikacin (40 μg/ml)	*in vitro*: 94.6% reduction in intracellular pathogen load; Antibiofilm activity (liposome entrapped phage −7 ± 0.1 logs reduction in bacterial count upto day 4 of biofilm formation)	Singla et al., 2016
P	*in vitro*–antibiofilm assay	NP1 and NP3 phages + ceftazidime, ciprofloxacin, colistin, gentamicin or tobramycin	Synergy between phage and ciprofloxacin/ tobramycin reduced bioburden within the biofilm	Chaudhry et al., 2017
P	*in vitro*	Phage PEV20 (10^{10} PFU/mL; MOI 0.1 and 100) + ciprofloxacin, amikacin, aztreonam, colistin or tobramycin	No obvious growth of pathogen throughout 24 h of incubation for ciprofloxacin or amikacin in combination with phage PEV20	Lin Q. et al., 2018
SILVER NANOPARTICLES + ANTIBIOTICS				
A	*in vivo* (murine peritonitis model)	Citrate capped AgNPs (5–12 nm, 2 mg/kg) + Polymyxin B (10 μg/kg)	60% survival; Non-toxic; Anti-inflammatory	Wan et al., 2016
S	*in vitro*	AgNPs (synthesized using two actinobacteria, 5–50 and 5–20 nm) + ampicillin, kanamycin /tetracycline	Antibiofilm; Non toxic	Wypij et al., 2018
A	*in vitro*	AgNPs (synthesized using *A. calcoaceticus*, 8–12 nm) + tetracycline, erythromycin or doxycycline	MBEC of combination with AgNPs was 0.5 mg/ml for doxycycline and 4 mg/mL for erythromycin	Singh et al., 2018
S & P	*in vitro*	AgNPs (synthesized using *Garcinia indica* fruit extract, 5 and 30 nm) + tetracycline	Increase in zone of inhibition in S and P with combination	Sangaonkar and Pawar, 2018
P	*in vitro*	Citrate-capped silver nanoparticles (10 nm and 20 nm) + tobramycin	Antibiofilm activity observed using combination	Habash et al., 2017
S, K, & P	*in vitro*	AgNPs (synthesized using Actinomycetes, 59 and 28 nm) + kanamycin,ampicillin or tetracycline	Increase in zone of inhibition using combination	Golińska et al., 2016
ANTIMICROBIAL PEPTIDES (AMP) + NPS;				
Ef	*in vitro*	Synthetic peptide-immobilized gold nanoparticles; 250 μg/ml	Reduced bacterial load (by 0.4 OD units)	Kuo et al., 2016
S	*in vitro*	AMP TP359 covalently linked to silver coated single walled carbon nanotubes	100% reduction	Chaudhari et al., 2016

(Continued)

TABLE 3 | Continued

Target ESKAPE member	Study model	Agent used and dosage details	Efficacy: log reduction of pathogen using combination; % survival of host, additional advantage	References
S & P	*in vitro*	Paenipeptin analog (synthetic linear lipopeptide analogs) + rifampicin, clarithromycin, or erythromycin	Reduction in cell count of biofilms- *S. aureus*−5 logs and *P. aeruginosa*−3 logs	Moon et al., 2017
K	*in vitro*	SPR741, a cationic peptide derived from Polymyxin B + antibiotics	128-fold reduction in MIC with rifampin and clarithromycin –	Corbett et al., 2017
ANTIMICROBIAL PHOTODYNAMIC LIGHT THERAPY (aPDT) + ANTIBIOTIC				
Ef	*in vivo* (G. mellonella infection model)	Light- 660 ± 15 nm, 0.9 J/cm^2 PS: Methylene blue (MB); Time 30 s + vancomycin-50 mg/kg	100% reduction; ∼60% survival	Chibebe Junior et al., 2013
S	*in vitro*	UVC light−254 nm, 6.4 mW + vancomycin (16 μg/mL) or quinupristin/ dalfopristin (32 μg/mL) or linezolid (64 μg/mL)	40% reduction in bacterial load with vancomycin or quinupristin/ dalfopristin and 20% in with linezolid; Synergy reduced viability of cells within the biofilm considerably	El-Azizi and Khardori, 2016
S	*in vitro*	LED light 650 nm, 2.8–22.4 J/cm^2. PS-MB 6.25–400 μg/mL, ciprofloxacin (0.5 μg/mL)	5 log reduction in bacterial load; 4 log reduction in bacterial cell count in biofilm	Ronqui et al., 2016
aPDT + EFFLUX PUMP INHIBITOR				
S	*in vitro*	Light- 22 J/cm^2; PS- MB-200 μg/mL + EPI- verapamil 312 μg/mL	3.38 log reduction in biofilm	de Aguiar Coletti et al., 2017
S	*in vitro and in vivo* (Murine wound infection model)	aPDT using NorA EPI-MB hybrid, INF55-(Ac)en-MB	*in vitro*: 6 log reduction; *in vivo*: 100% reduction within 4 days; enhanced wound healing	Rineh et al., 2017
A	*in vitro* and *in vivo* (Murine wound infection model)	*in vitro*: aPDT using NorA EPI-MB hybrid, INF55-(Ac)en-MB	*in vitro*: 5 log reduction; *in vivo*: 100% reduction within 6 days; enhanced wound healing	Rineh et al., 2018
ANTIBACTERIAL BLUE LIGHT (aBL) + AgNP				
S & P	*in vitro*, *in vivo* (murine burn wound infection model) and Case study (chronic wound infection of horse)	AgNP- chemically synthesized (15–20 nm) + Light-aBL- 460 nm, 2 h exposure after AgNP application	*in vitro*: 10 log reduction in bacterial count in biofilms; *in vivo*: 100% reduction in 2 h in mice; Reduction in wound bioburden; Case study: Wound healed completely within 4 weeks in the horse	Nour El Din et al., 2016
P	*in vitro*	Light- 650 nm, PS: Sodium salt of tetrasulfonated hydroxyaluminum phthalocyanine [Al(OH)Pc(SO3Na)4] + A. pullulans synthesized Au-AgNPs- 14 nm (20 ppm)	3 log reduction	Maliszewska et al., 2018

(Continued)

TABLE 3 | Continued

Target ESKAPE member	Study model	Agent used and dosage details	Efficacy: log reduction of pathogen using combination; % survival of host, additional advantage	References
BL + AgNP + ANTIBIOTICS				
S	*in vitro*	Light-aBL-460 nm, 250 mW, 1 h, various antibiotics + AgNP- chemically synthesized (15–20 nm). Double combination- AgNP at sub MIC + antibiotics/ aBL; Triple combination- AgNP+ antibiotic+ aBL	100% reduction in 8 h, synergistic activities of AgNP when used in double or triple combinations.	Akram et al., 2016
aPDT + AMP				
S, A, Ef	*in vitro*	MB, MB-PDT at 45 J/cm² or Chlorin 6, Ce6-PDT at 30 J/cm² + AMP- aurein 1.2, AU at 16 μM	*S. aureus*- 6 log reduction, *A. baumannii*- 5 log reduction, *E. faecium*-2.5 log reduction	de Freitas et al., 2018
P	*in vitro*	Rose Bengal (RB)-antimicrobial peptide conjugate to enhance the sonodynamic therapy	7 log reduction, increase in diffusion of RB 2.6 fold through the biofilm	Costley et al., 2017
P	*in vitro*	AMP (CAMEL or pexiganan) aPDT RB at 15–60 J/cm^2. aPDT with RB and PEX at 5μM each OR RB and CAM at 10μM each	5 log reduction	Nakonieczna et al., 2018
aPDT + ADJUVANT				
P	*in vitro* and *in vivo* (murine wound infection model)	*in vitro*: green light 0, 10, and 20 J/cm^2; PS- RB- 100 nM; KI- 0–100 mM; *in vivo*: green light-20 J/cm^2; PS - 500 μM RB alone or mixed with 1M KI	*in vitro*: 7 log reduction; *in vivo*-100% reduction; Inhibition of wound bioburden	Wen et al., 2017
P	*in vitro* and *in vivo* (murine cutaneous ulcer infection model)	*in vitro*: LED 410 nm, 6 and 9 J/cm^2; PS- 5-Aminolevulinic acid (ALA)-0.05–0.5%, EDTA-2Na 0.001–0.005%; *in vivo*: LED 410 nm, 6 and 9 J/cm^2; KY jelly with 5-ALA-0.1 and 0.5%, EDTA-2Na 0.001 and 0.005%.	*in vitro*: Combination was less efficient than EDTA-2Na in biofilm inhibition; *in vivo:* 6 log reduction in wound bioburden with 60% healing within 13 days	Katayama et al., 2018
S & A	*in vitro* and *in vivo* (murine skin abrasion model)	*in vitro*: UVA Light 360 ± 20 nm- 0–20 J/cm^2-exposure; white light- 400–700 nm, 0–120 J/cm^2; PS- C60-fullerene (LC16)- 20 μM with or without KI (1 M−30 μl); *in vivo*: UVA Light 360 ± 20 nm- 20 J/cm^2-exposure; white light- 400–700 nm 120 J/cm^2; PS- C60-fullerene (LC16)- 200 μM with or without KI (10 mM)	*in vitro*: 1–2 log reduction; *in vivo*: 1–2 log reduction in *A. baumannii* only	Zhang et al., 2015

Ef, Enterococcus faecium; S, Staphylococcus aureus; K, Klebsiella pneumonia; A, Acinetobacter baumannii; P, Pseudomonas aeruginosa; and E, Enterobacter spp.

of this study involved adaptation cycles of the commercial Pyophage preparation to increase its sensitivity toward the uropathogens. In the second phase, six of the nine patients responded to the adapted bacteriophage showing up to five log reduction in CFU of the infecting bacteria. Another study by Schooley et al. (2017) described the case of a 68 year old male diabetic patient having necrotizing pancreatitis which was complicated by an MDR *A. baumannii*. The patient responded to a phage therapy which consisted of a cocktail of nine phages against *A. baumannii*.

Few cases showing partial success of phage therapy in treating the infection are also reported (Jennes et al., 2017; Duplessis et al., 2018). Jennes et al. (2017) reported a case study of 61-year-old man diagnosed with septicaemia caused by a colistin-only-sensitive *P. aeruginosa.* Blood cultures turned negative immediately after BFC1 phage therapy but sores remained infected. No adverse side effects were observed during this therapy. In another study, a 2-year-old boy with a history of DiGeorge syndrome and complex congenital heart disease developed post-operative recalcitrant *P. aeruginosa* bacteraemia. A cocktail of two phages were used to target the infecting pathogen turning the blood cultures negative. However, the bacteraemia re-occurred after the discontinuation of phage therapy (Duplessis et al., 2018). It is however felt that commonly approved guidelines for application of phages is warranted in order to compare the efficacies of various phage treatments.

Several clinical trials have demonstrated the safety of phages and phage lytic enzymes which are in agreement with the studies carried out in animal models or as reported in numerous case studies. Although, many phase I and/or phase II clinical trials to demonstrate the efficacy of phages against ESKAPE infections have been registered in the past few years, the number of well-documented and completed trials are too low to draw meaningful conclusions (Sybesma et al., 2018). Moreover, the number of patients enrolled for the trials have severely limited the conclusions. A notable example of this is "PhagoBurn," a multicentric randomized single blind and controlled clinical study on phage therapy to treat burn wound infections caused by *P. aeruginosa* and *E. coli* (ClinicalTrials.gov registry, NCT02116010). Twenty seven patients were enrolled for the trial which resulted in being too low from the pre-calculated 220 patients expected to give statistically significant results. Restrictive patient inclusion criteria, shorter duration of patient enrolment, and low incidence of burn wound infection during the period of study were described as possible reasons for the very few eligible patients (Servick, 2016). The 27 patients were randomly assigned to the phage treatment group and safety control group for further investigation. A cocktail of 12 phages (PP1131) with lytic activity against *P. aeruginosa* were added to an alginate template that was applied directly to the wound of the treated group. A diluted phage cocktail was used due to its high endotoxin content. The control group received a topical application of the standard care treatment (1% sulfadiazine silver). Few adverse events were reported both in phage treated and safety control group. The trial, however, was terminated prematurely due to insufficient efficacy of PP1131. A supporting study showed that the bacteria isolated from patients with the failed treatment were resistant to low phage doses used for this study. This, however, was the first Randomised Clinical Trial (RCT) performed following both good manufacturing practices as well as good clinical practices and was approved by three national health regulators (Belgium, France, and Switzerland). Further studies with increased phage concentration and higher number of participants are needed (Jault et al., 2019). In case of phage lytic enzymes, the first-in-human phase I clinical trial study for phage endolysin-based candidate drug SAL200, after a single intravenous administration among healthy volunteers showed no clinically significant detrimental effect (Youn Jun et al., 2017).

The other recent ongoing trial includes a randomized placebo controlled double blind clinical trial (ClinicalTrials.gov registry, NCT03140085) to study the efficacy and safety of commercially available Pyophages for treating UTI infections in patients planned for transurethral resection of prostate. Eighty-one patients were expected to enroll for this interventional study design planned between Nov 2015–Dec 2018 that may provide necessary insights into this potentially transforming alternative treatment option (Leitner et al., 2017). Similarly, another multicentric, randomized, two-parallel group, double blind controlled trial expected to enroll 60 patients was registered (ClinicalTrials.gov registry, NCT02664740) to compare efficacy of anti-staphylococcal phages verses standard treatment and placebo for diabetic foot ulcers infected by *S. aureus*. This study has not yet begun recruiting patients.

To further overcome limitations of phage therapy, phages can be combined with antibiotics which may show synergistic action by making either a phage or antibiotic or both to act more effectively (**Table 3**). Reduction in the formation of bacterial biofilms has also been reported when antibiotic treatment is used in combination with phages (Jo et al., 2016; Chaudhry et al., 2017). Endolysin produced by bacteriophages, proves to be more beneficial than lysing cell wall and facilitating entry of the antibiotic inside the bacteria (Rios et al., 2016). Phage PEV20 and ciprofloxacin exhibited a synergistic effect *in vitro* against *P. aeruginosa* (Lin Y. et al., 2018). Another interesting study reported that *P. aeruginosa,* while developing phage resistance when under attack by OMKO1 phage, changed the efflux pump mechanism which ultimately increased the sensitivity of *P. aeruginosa* to antibiotics. Such an approach creates a win-win situation causing the killing of the bacteria either through phage or by antibiotic action (Chan et al., 2016). Similarly, it has been reviewed that such changes in the surface receptors of any bacterium may also reduce its virulence (Rios et al., 2016). A case study reported OMKO1 phage in combination with ceftazidime could successfully treat a complicated postoperative *P. aeruginosa* infection in a patient who underwent an aortic arch replacement surgery (Chan et al., 2018). The success or failure of phage antibiotic combination therapy is still in a state of immaturity as the mechanisms involved in synergy have not been fully understood and the data of *in vivo* models and case reports is scarce. Further investigations are warranted in order to make any conclusive remarks.

ANTIMICROBIAL PEPTIDES (AMPs) IN THERAPY

Antimicrobial peptides (AMPs) are short, positively charged, diverse host defense oligopeptides produced by all living forms including protozoa, bacteria, archaea, fungi, plants, and animals (Wang et al., 2010). They show a broad spectrum of activity against a wide range of pathogens. The capacity of AMPs to interact with bacterial cell membrane and thereby cause cell lysis makes them a potential alternative to combat MDR pathogens (Berglund et al., 2015). Furthermore, in contrast to conventional antibiotics, AMPs physically damage the bacterial cell through electrostatic interactions thereby making it difficult for bacteria to develop resistance against AMPs (Pfalzgraff et al., 2018).

Considering the critical status of ESKAPE pathogens, several attempts have been made to find out AMP based effective therapeutics. To date, there are numerous natural as well as bioengineered AMPs reported to show *in vitro* (Björn et al., 2016; Cappiello et al., 2016; Liu et al., 2017; Gandt et al., 2018; Irani et al., 2018; Téllez et al., 2018) as well as *in vivo* (Björn et al., 2016; Liu et al., 2017) antimicrobial, antibiofilm, anti-inflammatory, and wound healing abilities with minimum cytotoxicity. Histatin 5, a natural histidine rich cationic human salivary peptide, is an example. This peptide shows a strong *in vitro* anti-biofilm as well as potent bactericidal activity (≥70%) against ESKAPE (Du et al., 2017). Similarly, a *de novo*-engineered cationic peptide, WLBU-2, and a natural AMP LL-37 at 1/3X MIC has demonstrated 90% biofilm inhibition as compared to that shown by antibiotics such as tobramycin, ciprofloxacin, ceftazidime, and vancomycin at 1X MIC (Lin Q. et al., 2018). In 2017, Gaglione et al. examined human ApoB derived recombinant peptides namely r(P)ApoB$_L$ and r(P)ApoB$_S$. Both peptides showed effective *in vitro* wound healing, anti-inflammatory, antimicrobial, and antibiofilm properties against MDR strains of *S. aureus* and *P. aeruginosa*.

Similar to their remarkable *in vitro* properties, AMPs also exhibit promising *in vivo* activity against ESKAPE. For example, peptide HLR1r, a structural derivative of human milk protein, lactoferrin, at very low concentration (5 mg/kg) was found to show anti-infectivity against MRSA infected wound excision model in rat along with *in vitro* anti-inflammatory and non-cytotoxic effects suggesting use of HLR1r in topical formulation to treat skin infections (Björn et al., 2016). PT-13 a peptide derived from seeds and leaves of *Populus trichocarpa* crude extract also demonstrated effective *in vivo* antibacterial activity in *S. aureus* infected *G. mellonella* model (Al Akeel et al., 2018). In another instance, a synthetic analog of Feleucin-K3 has shown to clear *P. aeruginosa* induced bacteremia in mice model with good stability and very low cytotoxicity (Xie et al., 2018). Also, a hydrogelformulation containing K-11, a hybrid peptide of melittin, cecropin A1 and magainin-2 has shown to possess wound healing ability against *A. baumannii* infected murine excision model proposing its possible use as a topical anti-infective therapeutic agent (Rishi et al., 2018).

Over the past decades, intense efforts taken by the scientific community and pharmaceutical industries together has made it possible to introduce certain peptides such as vancomycin, telavancin, telaprevir, teicoplanin, enfuvirtide, daptomycin, dalbavancin, bacitracin etc. for clinical use (Gomes et al., 2018). A clinical trial conducted on rabbits and humans using the peptide melamine proved it to be a stable and safe antibacterial coating for eye lenses (Dutta et al., 2014). Similarly, Pexiganan (analog of magainin), LL-37 (analog of human cathelicidin peptide), hLF1-11, and PXL-01 (derivatives of human milk protein), Novexatin (derivative of human defense peptide), Iseganan (derivative of porcine leukocytes), PAC-113 (derivative of human saliva histatin-3 peptide) etc. are few examples of AMPs which also are under clinical trials (Mahlapuu et al., 2016).

Unfortunately, such a low number of AMPs seeking clinical approval is quite discouraging. Despite their successful *in vitro* and/or *in vivo* broad-spectrum activities, numerous AMPs have not yet crossed the hurdle of clinical trial. Amongst the few challenges that hamper the *in vivo* efficacy of AMPs are their cytotoxicity to mammalian cells, liability to degradation by tissue proteases, loss of activity at low salt concentrations or in presence of plasma proteins and higher production cost (Mahlapuu et al., 2016; Rios et al., 2016). The issue of peptide degradation can be solved by structural modification of AMPs such as addition of non-natural amino acids or their D-isomers, peptide cyclisation, acetylation, and amidation of N-terminus. Introduction of peptide mimetics or the use of suitable delivery system like liposome encapsulation can be done to improve their stability and reduce toxicity (Seo et al., 2012; Reinhardt and Neundorf, 2016). Additionally, efficiency of AMPs can be enhanced by combining AMPs with antibiotics (Gaglione et al., 2017; Zheng et al., 2017; Pletzer et al., 2018) or nanoparticles (Chaudhari et al., 2016; Kuo et al., 2016). Otvos et al. (2018), reported a synergestic effect of A3-APO, a proline-rich AMP, and colistin when studied in a *K. pneumoniae* infected bacteremia mice model. The basis for *in vitro* decrease in MIC of A3-APO when combined with colistin can be explained by considering the fact that colistin kills bacteria by interfering with bacterial membrane assembly and, therefore, slight reductions in bacterial membrane integrity potentiate A3-APO antibacterial action. Surprisingly, the same combination also showed a 100% survival in mice. This observation can be a direct consequence of A3-APO ability to induce immune augmentation or the deactivation of bacterial toxins. Enhanced *in vitro* bactericidal activity against *S. aureus* was also found in the case where LL-37, a human cathelicidin peptide, combined with gold nanoparticles as compared to vancomycin alone (Wang et al., 2018). In this case, gold nanoparticles increased the local density of positive charges and peptide mass and thereby enhanced the bactericidal properties of LL-37.

To summarize, owing to their *in vitro* and *in vivo* broad-spectrum antibacterial activities AMPs offer a hopeful alternative to conventional therapeutics. However, to overcome challenges in developing a safe, stable and efficient commercial product, a thorough understanding of their structure and interaction with bacterial as well as host cells is still needed. It will also be helpful to find better AMP formulation strategies to obtain maximum therapeutic actions. Overall, considering the extensive research being carried out on different AMPs against various infectious

agents, the future of peptide based commercial drug formulations looks hopeful.

PHOTODYNAMIC LIGHT THERAPY

Antimicrobial light therapy, either alone or combined with a photosensitizer (PS), results in a photooxidative stress response that leads to microbial death. Excitation of PS with light of an appropriate wavelength leads to formation of an excited triplet state. An excited PS can transfer electrons or energy to biomolecules or molecular oxygen, resulting in the formation of reactive oxygen species (ROS) or singlet oxygen radicals, which are toxic to cellular targets such as nucleic acids, proteins and lipids (Mai et al., 2017; Yang M.-Y. et al., 2018). Some of the most frequently used PSs include phenothiazinium derivatives (methylene blue, toluidine blue), xanthine derivatives (rose bengal), porphyrin, chlorin, or fullerene derivatives amongst many others (Abrahamse and Hamblin, 2016; Cieplik et al., 2018). Antimicrobial photodynamic therapy is widely used for treating dental, skin, and soft tissue infections. For a more detailed description of the current state and future prospects of light therapy with respect to the various photosensitisers, light sources, and methods used, mechanism of antimicrobial action or antibiofilm potential, the reader may be referred to the excellent reviews published recently (Cieplik et al., 2018; Hu et al., 2018; Tomb et al., 2018; Wozniak and Grinholc, 2018). However, none of these reviews have especially focused on *in vivo* studies of aPDT against ESKAPE pathogens.

There has been extensive research on designing the PSs so as to improve their pharmaceutical potential. An ideal PS used for antimicrobial therapy should have greater permeability to cross the microbial cell wall/cell membrane, selective toxicity toward the microbial cell with minimal or no damage to the host tissue and an absorption coefficient appropriate for effective penetration at the site of action. The PS chosen should not have a long half-life which causes prolonged photosensitization in the host cells even after the infection is cured. It should also not be effluxed out by the microbial efflux systems (Cieplik et al., 2018; Hu et al., 2018; Tomb et al., 2018; Wozniak and Grinholc, 2018). Efficacy of aPDT also depends on the light fluence, PS concentration and treatment time (Tomb et al., 2017; Sueoka et al., 2018; Ullah et al., 2018).

PSs chosen preferably have a large absorption coefficient in the visible spectrum, especially in the long wavelength (red near infrared) region, to allow effective penetration of light in the infected tissue (**Table 2**). Many researchers have attempted to improve the availability of PS by potentiating or functionalizing it with other molecules including galactose, amino acids, efflux pump inhibitors, potassium iodide, EDTA etc. A variety of PSs functionalized with addends are used to target ESKAPE pathogens. A boron-dipyrrolemethene (BODIPY)-based polygalactose, named pGEMA-I (7.3 kDa) with increased water solubility was used to demonstrate antibacterial and antibiofilm activity against *P. aeruginosa*, without much affecting the viability of normal cells. It was demonstrated that the selective recognition of the pathogen was due its carbohydrate binding lectin protein (LecA) which interacted with the galactose moiety of the PS (Zhao et al., 2018). C60-fullerene (LC16) bearing deca-quaternary chain and deca-tertiary-amino groups facilitates electron-transfer reactions via the photoexcited fullerene for antimicrobial effect studied in *A. baumannii* and *S. aureus* (Huang et al., 2014; Zhang et al., 2015). Another drawback of aPDT is that the ROS generation may cease after the light irradiation is turned off thus allowing un-killed bacteria to re-grow. Potentiating aPDT with potassium iodide allows the formation of iodine/tri-iodide that may remain active in the wound for a longer duration sufficient enough to prevent bacterial re-growth (Zhang et al., 2015; Wen et al., 2017).

In vitro studies have shown that blue light (aBL) has a broad spectrum antibacterial and antibiofilm activity against all six ESKAPE members (Halstead et al., 2016). *In vivo* data also corroborated this finding and further confirmed that using a low penetrating blue light of 415 ± 10 nm should be a preferred choice of treatment in case of topical wound infections as it causes minimal damage to the uninfected tissue cells below (Amin et al., 2016; Wang et al., 2017; Katayama et al., 2018). Some studies additionally report that an exogenous PS may not be required (Amin et al., 2016; Wang et al., 2017). Their finding was supported by experimental data showing that the endogenous porphyrins present in the bacterial cell membrane play a role in triggering the photoxidative response (Amin et al., 2016). aBL using 5-aminolevulinic acid with disodium EDTA (ALA-EDTA/2Na) had antibacterial and antibiofilm potential thus showing significant wound healing of *P. aeruginosa* infected cutaneous ulcers in mice model (Katayama et al., 2018). However, the role of EDTA in increasing the antibacterial action of aBL needs further investigation. The physiological mechanism behind wound healing was studied in a *S. aureus* infected burn model in mice revealing that the enhanced levels of factors promoting angiogenesis and epithelial regeneration (bFGF, TGFβ1, and VEGF) led to the inhibition of inflammatory factors (TNFα and IL6) in the aPDT treated group as compared to the control (Mai et al., 2017).

Sueoka et al. (2018) studied the time dependant effect of aPDT-TON 504 on *P. aeruginosa* and showed that a repeated exposure to light emitting diode (LED) enhanced the inhibitory effect on bacterial growth. This enhanced effect was possibly because the bacteria that survived the initial aPDT were injured by singlet oxygen generated due to excitation of remaining photosensitizer. On the contrary there are also a few reports investigating the development of resistance/tolerance to aBL. It was observed that initial exposure to low doses of aBL increased the tolerance of methicillin susceptible *S. aureus* (MSSA) to subsequent doses of high intensity aBL-405 nm. It is likely that increased tolerance to high intensity light may be due to up-regulation of bacterial stress responses which needs detailed investigations. However, a second set of experiment showed that repeated sub-lethal exposures of 405 nm light indicate no evidence of tolerance in *S. aureus* (Tomb et al., 2017).

A considerable amount of literature has been published on combined efficacy of aPDT and antibiotics demonstrated *in vitro* (El-Azizi and Khardori, 2016; Ronqui et al., 2016). Synergistic effects of aPDT-antibiotic combination resulted in inactivation

of several virulence factors in *P. aeruginosa* isolates (Fila et al., 2017). aPDT when used in combination with vancomycin prolonged the survival of *Galleria mellonella* infected with a vancomycin resistant strain of *E. faecium* as compared to either of the two therapies used alone (Chibebe Junior et al., 2013). Wozniak and Grinholc (2018) in their comprehensive review analysis have, however, pointed out that most of the aPDT carried out in combination with antibiotics lack a standard methodology followed to evaluate the synergistic effect.

One of the strategies for improved PS delivery involves the use of nanoparticles which are co-administered to allow the PS entry across the membrane or for a synergistic ROS response resulting in an antimicrobial action. A combination of tetrasulfonated hydroxyl aluminum phthalocyanine ($AlPcS_4$) and bimetallic gold/silver nanoparticles (Au/Ag-NPs) synthesized using a cell-free filtrate of *Aureobasidium pullulans* showed significantly higher killing as compared to the agents used individually (Maliszewska et al., 2018). Au/Ag-NPs possibly disrupted the cell membrane allowing enhanced uptake of the PS, $AlPcS_4$. *In vitro* and *in vivo* studies demonstrated that AgNPs used in combination with blue light showed synergistic antimicrobial and antibiofilm activities against *P. aeruginosa* infection. Interestingly, this combination was also effective for the treatment of a chronic wound caused by mixed infection in a horse (Nour El Din et al., 2016). More recently, an *in vitro* study carried out using *A. baumannii* isolates, demonstrated that the antibacterial action of ZnO-NPs with blue light irradiation was due to their ability to damage the cytomembrane but not DNA (Yang M.-Y. et al., 2018).

Over expressing multidrug efflux pumps, commonly found in resistant pathogens, are reported to affect the intracellular concentration of PS used in aPDT, thus limiting its action (Tegos and Hamblin, 2006). Tegos et al. (2008) carried out *in vitro* experiments by co-incubating various combinations of PS with efflux pump inhibitors to select the best combination showing antibacterial activity. Photodynamic killing mediated by toluidine blue (TBO), when used in combination with PaβN, or INF271 (as EPIs) was most effective against *P. aeruginosa* and *S. aureus* isolates, respectively. Similarly, an *in vitro* study demonstrated that verapamil, an efflux pump inhibitor, when combined with aPDT, required a lower light dose for effective antibacterial, and antibiofilm action against *S. aureus* (de Aguiar Coletti et al., 2017). In further development of such an approach, it was recently demonstrated that INF55-(Ac)en–MB, synthetic antimicrobial hybrids designed by covalently linking a PS (methylene blue) to efflux pump inhibitors (INF55 and INF271) were more effective in treating wound infections caused by *S. aureus* or *A. baumannii* studied in mice models (Rineh et al., 2017, 2018).

It is also worth noting that synergistic effect of aPDT when used in combination with antimicrobial peptide was also demonstrated recently (de Freitas et al., 2018; Nakonieczna et al., 2018). Aurein 1.2 augmented the aPDT activity mediated by methylene blue or chlorin-e6 against strains of *S. aureus, A. baumannii* and more importantly against vancomycin resistant *E. faecium*, whereas the AMP aPDT combination with curcumin (as PS) had no effect thus revealing a PS-dependent mechanism (de Freitas et al., 2018). Later, Nakonieczna et al. (2018) carried out a similar study showing synergistic effect of rose bengal-aPDT with two synthetic AMPs, CAMEL, and pexiganan against 35 isolates of *P. aeruginosa*. Notably, it was also shown that this combination was non-toxic to human keratinocytes. Conjugates such as $ZnPc(Lys)_5$ (a zinc phthalocyanine derivative coupled with pentalysine) also showed a synergistic antibacterial action which was sufficient to heal *S. aureus* wound infection in mice models (Ullah et al., 2018).

Overall, photodynamic therapy appears to be a promising option for treatment of infections caused due to ESKAPE pathogens, particularly effective in topical applications. aPDT co administered or conjugated with antibiotics, antimicrobial peptides, nanoparticles, or efflux pump inhibitors show a synergistic effect. However, it is difficult to compare efficacy between different combinatorial approaches due to lack of uniform methodologies. More studies on investigation of toxicity and biocompatibility of various combinations should be investigated using *in vivo* models for translating them into clinical practice.

SILVER NANOPARTICLES IN THERAPY

Nanomedicine is one of the emerging branches for treating drug resistant pathogens. Metal nanoparticles have wide biomedical applications as antimicrobial agents due to their unique physical and chemical properties (Beyth et al., 2015; Hemeg, 2017). Amongst metal nanoparticles, silver nanoparticles (AgNPs) synthesized using physical, chemical or biological methods have shown promising antibacterial activity due to their multi-targeted approach which reduces the probability of resistance (Möhler et al., 2018; Siddiqi et al., 2018). AgNPs act by releasing Ag^+ ions which results in disruption of electron transport or signal transduction pathway or leads to generation of ROS, ultimately damaging important biomolecules such as cell wall, cell membrane, cellular DNA, and/or proteins (Dakal et al., 2016; Qayyum et al., 2017).

AgNPs act by inhibiting or disrupting planktonic cells as well as biofilms of MDR pathogens. Even though earlier reports have suggested the cytotoxic effects of AgNPs (Mohanty et al., 2012), recently *in vitro* and *in vivo* studies have demonstrated the safe usage of AgNPs (Möhler et al., 2018). AgNPs synthesized using aqueous leaf extract of *Corchorus capsularis* exhibited antibacterial activity against *S. aureus* and *P. aeruginosa* and were found to be non-toxic to mouse fibroblast cells (Kasithevar et al., 2017). Electrochemically synthesized AgNPs showing antimicrobial activity against planktonic and biofilm forming *P. aeruginosa* strain were non-toxic to *G. mellonella* larvae model (Pompilio et al., 2018). Recently, sunlight mediated AgNPs synthesized using *Capsicum annuum* was tested in *S. aureus* infected zebra fish model which proved to be effective in inhibiting biofilm formation. Histological studies revealed that they are non-toxic and hence can be tested for efficacy in higher mammalian *in vivo* models (Lotha et al., 2018). A single-blind clinical trial (Clinical Trial Registration: NCT01243320 and NCT01405794) carried out in 60 healthy human volunteers,

showed that commercial AgNPs when administered orally at dose of 10 and 32 ppm and monitored over 14 days were found to be non-toxic. The study revealed no significant changes in metabolic, hematologic and pro-inflammatory responses as well as no morphological changes in vital organs (Munger et al., 2014).

One of the widely explored applications of AgNPs is their use in the form of composite dressings or hydrogels for treatment of topical wound infections. AgNPs incorporated in chitosan composite dressings offer sustained release of Ag^+ ions at low dosage which are non-toxic to fibroblast cells. Studies in mice models suggested that AgNPs/chitosan composite dressings and low molecular weight chitosan-coated silver nanoparticles were effective in reducing bacterial load, were non-toxic and biocompatible, had low absorption in body and promoted better wound healing against *S. aureus* and *P. aeruginosa* (Liang et al., 2016; Peng et al., 2017). Similarly, studies using three other polymer dressings made of chitosan, nylon, and collagen incorporated with AgNPs exhibited *in vitro* antibacterial activities against ESKAPE pathogens (Radulescu et al., 2016; Rath et al., 2016; Ding et al., 2017). These dressings did not exhibit inflammatory responses, showed re-epithelization of cells and better wound contraction leading to accelerated wound healing in mice models. Sodium carboxymethyl cellulose hydrogel loaded with polyethylene glycol coated AgNPs showed antibacterial activity, re-epithelization, and wound healing in MRSA infected mice model (Mekkawy et al., 2017). Similarly, topical application of nanosilvernanohydrogels in combination with *Aloe vera* accelerated wound contraction and enhanced wound healing due to the moist environment provided by *Aloe vera* (Anjum et al., 2016). In yet another formulation, AgNPs coated on to MCM-41 type mesoporous silica nanoparticles prevented their aggregation and allowed sustained release of Ag^+ ions displaying a long-term antibacterial activity against *S. aureus*. These antibacterial nanofibrous membranes could reduce inflammatory response and accelerate wound healing in wistar rats (Dong et al., 2016). A randomized clinical trial was carried out to test the antibacterial effect of two silver dressings and their healing time in burn patients. It was demonstrated that the hydrofiber silver dressing (Aquacel^R) was preferred over the nanocrystalline silver dressing (Acticoat^{TM}) due to reduction of bioburden, quick wound healing, ease of using, comfort to the patients, and low cost (Verbelen et al., 2014). On the other hand Acticoat^{TM} showed complete wound healing within 12 weeks in 64% of the patients with leg ulcers as compared to those who were treated with Iodosorb dressings (cadexomer iodine) (Miller et al., 2010).

Polymer-based nanomaterials and metal NPs are used in antimicrobial coatings on surface of medical devices, such as catheters and implants for prevention of infections. AgNPs when embedded in electrospun hyaluronic acid/polycaprolactonenanofibrous membranes coated on flexor tendon animal models prevented bacterial infection during the early postsurgical period (Chen et al., 2015; Shalumon et al., 2018). Likewise, implants coated with nanocomposite layer of polysaccharide 1-deoxylactit-1-yl chitosan and AgNPs in a mini-pig animal model showed good biocompatibility with the bone tissue (Marsich et al., 2013). All these studies demonstrated that the entrapped AgNPs allowed controlled release of Ag^+ ions displaying prolonged antibacterial and antibiofilm action as well as reduced inflammatory responses. A randomized clinical trial demonstrated the efficacy of triple-lumen central venous catheters impregnated with AgNPs (AgTive) which showed reduced bacterial colonization as compared to conventional catheters in intensive care unit patients (Antonelli et al., 2012).

Repeated exposure of AgNPs at sub inhibitory concentrations may lead to resistance in bacterial pathogens. To overcome this limitation, a combination of AgNPs with antibiotics has been suggested in order to increase the therapeutic efficacy of either, resulting in reduction of dose and hence toxicity. *In vitro* studies demonstrating AgNPs co-incubated with different antibiotics showed synergistic antibacterial activities against ESKAPE (Ghosh et al., 2012; Panáček et al., 2015; Golińska et al., 2016; Habash et al., 2017; Singh et al., 2018; Wypij et al., 2018). Synergistic antibacterial activity of AgNPs in combination with polymyxin B was demonstrated in *A. baumannii* infected mouse model with 60% survival rate as compared to the controls treated with antibiotic or AgNPs alone (Wan et al., 2016).

Despite the use of AgNPs as a potential therapeutic agent, literature survey indicates a paucity of data obtained from *in vivo* studies carried out to test the toxicity, efficacy, pharmacokinetic, and immuno-modulatory response of the AgNPs. Further investigations through well-defined studies and clinical trials will lead to applications of AgNPs in wound dressings or medical devices.

CONCLUDING REMARKS

There is an urgent need to restock our armamentarium of antimicrobials in order to stay ahead of the ever rising drug resistant ESKAPE pathogens. There is an insufficiency of effective antibiotic combinations in addition to the dry pipeline of new drugs. Huge efforts have been taken to use antibiotics in combination with adjuvants targeting important metabolic mechanisms/pathways contributing to drug resistance (permeablisers, lactamase inhibitors, efflux pump inhibitors, quorum sensing inhibitors, toxin inhibitors etc.) The modest success received to date with such antibiotic-adjuvant combinations has paved way to explore other alternative strategies to combat drug resistance. There is a significant rise in the interest shown by the scientific community to use novel therapeutic agents such as phages, antimicrobial peptides, metal nanoparticles, and photodynamic light which, although, have some limitations as discussed above. Some of the commonly described limitations of these therapies include stability and toxicity of the therapeutic agent, its targeted delivery at the site of infection, or immune response developed by the host against the therapeutic agent. Ongoing research has therefore led to further develop or modify these novel therapeutic agents or therapies so as to surmount the limitations as well as to overcome the barriers of bacterial resistance.

This review summarizes studies that demonstrate potential alternative therapies using *in vivo* models some of which have extended further to the level of clinical trials. The interest in phage therapy to treat bacterial infections is fast

growing leading to development of commercial preparations such as "Stafal," "Sextaphage," "PhagoBioDerm," and "Pyophage" against MDR pathogens. Similarly, use of silver nanoparticles as antibiofilm coatings in surgical implants, antimicrobial agents in topical applications or as formulations in wound dressings has shown promising activities in animal models. Clinical trials using commercially available nanosilver coated dressings (Acticoat^{TM}, Aquacel^{R}) or catheters (AgTive) is another noteworthy advancement. AMPs have received great attention due to their broad spectrum activity; however, they have shown limited pharmaceutical potential due to their toxicity, stability, and production costs. Photodynamic light therapy which is widely used for cancer therapy has also been demonstrated to be an effective strategy for clearing wound infections. However, additional studies demonstrating the efficacy and safety of these therapeutic agents against ESKAPE infections are desired. Similarly, randomized clinical trials would enable these therapeutic agents to cross the regulatory hurdles and find application in clinical practice.

It was observed that, majority of these studies have used animal models infected by *S. aureus, A. baumannii,* and *P. aeruginosa* to test the efficacy of the therapeutic agent. The probable reason for this could be that these pathogens mostly cause topical infections (wound, burn and abscess) and because majority of the limitations (targeted delivery, stability, immune response, toxicity etc.) described for each therapy can be minimized though not avoided in such models. It would be important to study the effect of these therapeutic agents against systemic infections caused by ESKAPE members. It was also observed that, the methods used for estimating efficacy of any therapeutic agent were not uniform. **Table 2** reveals that, the *in vivo* efficacy of various therapies is given either in terms of log or percent reduction of microbial load or as percent survival of the infected host (animal model). The methods followed to estimate the reduced pathogen loads as well as dosages used for treatment also vary. It is therefore not appropriate to compare these studies to identify the best therapeutic agent/therapy against any ESKAPE member.

In addition to the growing concern in searching and evaluating the clinical potential of the above discussed alternative therapies, research on combinatorial approach, based on the synergistic action of two or more therapies is also gaining attention. Most commonly studied combinations involve use of a therapeutic agent/ therapy (phage, aPDT, AMP, or AgNP) in combination with antibiotic/s or in some cases with an efflux pump inhibitor or quorum sensing inhibitor. Another interesting option used was the combination of the therapeutic agents in a conjugate or hybrid (antibiotic-antibiotic, antibiotic-EPI, PS-AMP, PS-EPI etc.) for an increased efficacy against the pathogen. Most of these studies demonstrated that the combinatorial approach helped overcome the limitation caused by individual therapeutic agent. For example, an antibiotic combined with an efflux pump inhibitor or a photosensitizer conjugated with an AMP improved their entry and retention into the target pathogen for enhanced antimicrobial action. Similarly, combinations of antibiotics with nanoparticles or AMPS reduced the toxicity caused by these agents which were required at high dosages when used alone. The synergistic action allows for an increased bioavailability of the drug or therapeutic agent, broad antimicrobial spectrum, reduced toxicity, and decreased chances of development of resistance. However, **Table 3** shows that most of the studies demonstrating potential of combinatorial approach are currently based on *in vitro* evaluation only. Data supporting the potential of a combinatorial therapy with respect to the mechanism of synergy, its *in vivo* efficacy, toxicity, and immune response is scarce and needs further investigation.

Finally, cost effectiveness of the above described therapeutic agents/therapy over the conventional antimicrobial agents also play a crucial role in their clinical application. Production cost for any therapeutic agent will strongly depend on the various regulatory hurdles they pass to come into clinical practice. An agent or therapy which is too expensive may not be a preferred choice for treatment in under developed countries or weaker economies thus leading to over-use of conventional antimicrobials thus contributing to the growing drug resistance.

To conclude, a uniform research methodology used to test the efficacy of these therapeutic agents in accordance with well-defined standards will make it possible to reliably compare the data presented by various research groups. Well-performed clinical trials of these therapeutic agents used as monotherapy or as a combinatorial approach will allow us to derive the real potential of these therapeutic combinations for being translated into clinical practice.

AUTHOR CONTRIBUTIONS

KP conceived the concept and edited. MM, EK, SK, and MT wrote and edited the manuscript and agreed for submission.

FUNDING

MT is a Project Assistant under UPE-Phase II (UGC-262-A-2); EK is a recipient of CSIR-SRF; SK is a Project Assistant DST-PURSE (GOI-A-670).

REFERENCES

Abedon, S. T., Kuhl, S. J., Blasdel, B. G., and Kutter, E. M. (2011). Phage treatment of human infections. *Bacteriophage* 1, 66–85. doi: 10.4161/bact.1.2.15845

Abrahamse, H., and Hamblin, M. R. (2016). New photosensitizers for photodynamic therapy. *Biochem. J.* 473, 347–364. doi: 10.1042/BJ20150942

Ahmed, A., Azim, A., Gurjar, M., and Baronia, A. K. (2014). Current concepts in combination antibiotic therapy for critically ill patients. *Indian J. Crit. Care Med.* 18, 310–314. doi: 10.4103/0972-5229.132495

Akram, F. E., El-Tayeb, T., Abou-Aisha, K., and El-Azizi, M. (2016). A combination of silver nanoparticles and visible blue light enhances the antibacterial efficacy of ineffective antibiotics against methicillin-resistant *Staphylococcus aureus* (MRSA). *Ann. Clin. Microbiol. Antimicrob.* 15, 48. doi: 10.1186/s12941-016-0164-y

Al Akeel, R., Mateen, A., Syed, R., Alqahtani, M. S., and Alqahtani, A. S. (2018). Alanine rich peptide from *Populus trichocarpa* inhibit growth of *Staphylococcus aureus* via targetting its extracellular domain of Sensor Histidine Kinase YycGex protein. *Microb. Pathog.* 121, 115–122. doi: 10.1016/j.micpath.2018.05.010

Alipour, N., Karagoz, A., Taner, A., Gaeini, N., Alipour, N., Zeytin, H., et al. (2017). Outbreak of hospital infection from biofilm-embedded pan drug-resistant *Pseudomonas aeroginosa*, due to a contaminated bronchoscope. *J. Prev. Med.* 2:1. doi: 10.21767/2572-5483.100014

Allegranzi, B., Nejad, S. B., Combescure, C., Graafmans, W., Attar, H., Donaldson, L., et al. (2011). Burden of endemic health-care-associated infection in developing countries: systematic review and meta-analysis. *Lancet* 377, 228–241. doi: 10.1016/S0140-6736(10)61458-4

Amin, R. M., Bhayana, B., Hamblin, M. R., and Dai, T. (2016). Antimicrobial blue light inactivation of *Pseudomonas aeruginosa* by photo-excitation of endogenous porphyrins: *in vitro* and *in vivo* studies. *Lasers Surg. Med.* 48, 562–568. doi: 10.1002/lsm.22474

Anjum, S., Gupta, A., Sharma, D., Gautam, D., Bhan, S., Sharma, A., et al. (2016). Development of novel wound care systems based on nanosilver nanohydrogels of polymethacrylic acid with *Aloe vera* and curcumin. *Mater. Sci. Eng. C. Mater. Biol. Appl.* 64, 157–166. doi: 10.1016/j.msec.2016.03.069

Antonelli, M., De Pascale, G., Ranieri, V. M., Pelaia, P., Tufano, R., Piazza, O., et al. (2012). Comparison of triple-lumen central venous catheters impregnated with silver nanoparticles (AgTive®) vs. conventional catheters in intensive care unit patients. *J. Hosp. Infect.* 82, 101–107. doi: 10.1016/j.jhin.2012.07.010

Aoki, N., Ishii, Y., Tateda, K., Saga, T., Kimura, S., Kikuchi, Y., et al. (2010). Efficacy of calcium-EDTA as an inhibitor for metallo-β-lactamase in a mouse model of *Pseudomonas aeruginosa* pneumonia. *Antimicrob. Agents Chemother.* 54, 4582–4588. doi: 10.1128/AAC.00511-10

Babouee Flury, B., Ellington, M. J., Hopkins, K. L., Turton, J. F., Doumith, M., Loy, R., et al. (2016). Association of novel nonsynonymous single nucleotide polymorphisms in ampD with cephalosporin resistance and phylogenetic variations in ampC, ampR, ompF, and ompC in *Enterobacter cloacae* isolates that are highly resistant to carbapenems. *Antimicrob. Agents Chemother.* 60, 2383–2390. doi: 10.1128/AAC.02835-15

Balamurugan, P., Hema, M., Kaur, G., Sridharan, V., Prabu, P. C., Sumana, M. N., et al. (2015). Development of a biofilm inhibitor molecule against multidrug resistant *Staphylococcus aureus* associated with gestational urinary tract infections. *Front. Microbiol.* 6:832. doi: 10.3389/fmicb.2015.00832

Berglund, N. A., Piggot, T. J., Jefferies, D., Sessions, R. B., Bond, P. J., and Khalid, S. (2015). Interaction of the antimicrobial peptide polymyxin B1 with both membranes of *E. coli*: a molecular dynamics study. *PLoS Comput. Biol.* 11:e1004180. doi: 10.1371/journal.pcbi.1004180

Bernal, P., Molina-Santiago, C., Daddaoua, A., and Llamas, M. A. (2013). Highlight Antibiotic adjuvants: identification and clinical use. *Microb. Biotechnol.* 6, 445–449. doi: 10.1111/1751-7915.12044

Beyth, N., Houri-Haddad, Y., Domb, A., Khan, W., and Hazan, R. (2015). Alternative antimicrobial approach: nano-antimicrobial materials. *Evid. Based Complement. Altern. Med.* 2015:246012. doi: 10.1155/2015/246012

Biswas, B., Adhya, S., Washart, P., Paul, B., Trostel, A. N., Powell, B., et al. (2002). Bacteriophage therapy rescues mice bacteremic from a clinical isolate of vancomycin-resistant *Enterococcus faecium*. *Infect. Immun.* 70, 204–210. doi: 10.1128/IAI.70.1.204-210.2002

Björn, C., Mahlapuu, M., Mattsby-Baltzer, I., and Håkansson, J. (2016). Anti-infective efficacy of the lactoferrin-derived antimicrobial peptide HLR1r. *Peptides* 81, 21–28. doi: 10.1016/j.peptides.2016.04.005

Bueno, J. (2016). Antimicrobial adjuvants drug discovery, the challenge of avoid the resistance and recover the susceptibility of multidrug-resistant strains. *J. Microb. Biochem. Technol.* 8, 169–176. doi: 10.4172/1948-5948.1000281

Cai, Y., Yang, D., Wang, J., and Wang, R. (2018). Activity of colistin alone or in combination with rifampicin or meropenem in a carbapenem-resistant bioluminescent *Pseudomonas aeruginosa* intraperitoneal murine infection model. *J. Antimicrob. Chemother.* 73, 456–461. doi: 10.1093/jac/dkx399

Caio, C., Maugeri, G., Zingali, T., Gona, F., Stefani, S., and Mezzatesta, M. L. (2018). Extensively drug-resistant ArmA-producing *Acinetobacter baumannii* in an Italian intensive care unit. *N. Microbiol.* 41, 159–161.

Cappiello, F., Di Grazia, A., Segev-Zarko, L.-A., Scali, S., Ferrera, L., Galietta, L., et al. (2016). Esculentin-1a-derived peptides promote clearance of *Pseudomonas aeruginosa* internalized in bronchial cells of cystic fibrosis patients and lung cell migration: biochemical properties and a plausible mode of action. *Antimicrob. Agents Chemother.* 60, 7252–7262. doi: 10.1128/AAC.00904-16

Casey, E., van Sinderen, D., and Mahony, J. (2018). *In vitro* characteristics of phages to guide 'real life' phage therapy suitability. *Viruses* 10:E163. doi: 10.3390/v10040163

Chadha, P., Katare, O. P., and Chhibber, S. (2017). Liposome loaded phage cocktail: enhanced therapeutic potential in resolving *Klebsiella pneumoniae* mediated burn wound infections. *Burns* 43, 1532–1543. doi: 10.1016/j.burns.2017.03.029

Chan, B. K., Abedon, S. T., and Loc-Carrillo, C. (2013). Phage cocktails and the future of phage therapy. *Future Microbiol.* 8, 769–783. doi: 10.2217/fmb.13.47

Chan, B. K., Sistrom, M., Wertz, J. E., Kortright, K. E., Narayan, D., and Turner, P. E. (2016). Phage selection restores antibiotic sensitivity in MDR *Pseudomonas aeruginosa*. *Sci. Rep.* 6:26717. doi: 10.1038/srep26717

Chan, B. K., Turner, P. E., Kim, S., Mojibian, H. R., Elefteriades, J. A., and Narayan, D. (2018). Phage treatment of an aortic graft infected with *Pseudomonas aeruginosa*. *Evol. Med. Public Heal.* 2018, 60–66. doi: 10.1093/emph/eoy005

Chan, L. C., Basuino, L., Diep, B., Hamilton, S., Chatterjee, S. S., and Chambers, H. F. (2015). Ceftobiprole- and ceftaroline-resistant methicillin-resistant *Staphylococcus aureus*. *Antimicrob. Agents Chemother.* 59, 2960–2963. doi: 10.1128/AAC.05004-14

Chang, R. Y. K., Chen, K., Wang, J., Wallin, M., Britton, W., Morales, S., et al. (2018). Proof-of-principle study in a murine lung infection model of antipseudomonal activity of phage PEV20 in a dry-powder formulation. *Antimicrob. Agents Chemother.* 62:e01714-17. doi: 10.1128/AAC.01714-17

Chatterjee, M., Anju, C. P., Biswas, L., Anil Kumar, V., Gopi Mohan, C., and Biswas, R. (2016). Antibiotic resistance in *Pseudomonas aeruginosa* and alternative therapeutic options. *Int. J. Med. Microbiol.* 306, 48–58. doi: 10.1016/j.ijmm.2015.11.004

Chaudhari, A. A., Ashmore, D., Nath, S., deb, Kate, K., Dennis, V., Singh, S. R., et al. (2016). A novel covalent approach to bio-conjugate silver coated single walled carbon nanotubes with antimicrobial peptide. *J. Nanobiotechnol.* 14:58. doi: 10.1186/s12951-016-0211-z

Chaudhry, W. N., Concepcion-Acevedo, J., Park, T., Andleeb, S., Bull, J. J., and Levin, B. R. (2017). Synergy and order effects of antibiotics and phages in killing *Pseudomonas aeruginosa* biofilms. *PLoS ONE* 12:e0168615. doi: 10.1371/journal.pone.0168615

Chen, C., Mangoni, M. L., and Di, Y. P. (2017). *In vivo* therapeutic efficacy of frog skin-derived peptides against *Pseudomonas aeruginosa*-induced pulmonary infection. *Sci. Rep.* 7:8548. doi: 10.1038/s41598-017-08361-8

Chen, C. H., Chen, S. H., Shalumon, K. T., and Chen, J. P. (2015). Dual functional core–sheath electrospun hyaluronic acid/polycaprolactone nanofibrous membranes embedded with silver nanoparticles for prevention of peritendinous adhesion. *Acta Biomater.* 26, 225–235. doi: 10.1016/j.actbio.2015.07.041

Chen, H. L., Su, P. Y., Kuo, S. C., Lauderdale, T. L. Y., and Shih, C. (2018). Adding a C-terminal cysteine (CTC) can enhance the bactericidal activity of three different antimicrobial peptides. *Front. Microbiol.* 9:1440. doi: 10.3389/fmicb.2018.01440

Chen, J., and Novick, R. P. (2009). Phage-mediated intergeneric transfer of toxin genes. *Science* 323, 139–141. doi: 10.1126/science.1164783

Chhibber, S., Kaur, J., and Kaur, S. (2018). Liposome entrapment of bacteriophages improves wound healing in a diabetic mouse MRSA infection. *Front. Microbiol.* 9:561. doi: 10.3389/fmicb.2018.00561

Chibebe Junior, J., Fuchs, B. B., Sabino, C. P., Junqueira, J. C., Jorge, A. O. C., Ribeiro, M. S., et al. (2013). Photodynamic and antibiotic therapy impair the pathogenesis of *Enterococcus faecium* in a whole animal insect model. *PLoS ONE* 8:e55926. doi: 10.1371/journal.pone.0055926

Chuang, L., and Ratnayake, L. (2018). Overcoming challenges of treating extensively drug-resistant *Acinetobacter baumannii* bacteraemic urinary tract infection. *Int. J. Antimicrob. Agents.* 52, 521–522. doi: 10.1016/j.ijantimicag.2018.07.016

Cieplik, F., Deng, D., Crielaard, W., Buchalla, W., Hellwig, E., Al-Ahmad, A., et al. (2018). Antimicrobial photodynamic therapy – what we know and what we don't. *Crit. Rev. Microbiol.* 44, 571–589. doi: 10.1080/1040841X.2018.1467876

Ciociola, T., Giovati, L., Giovannelli, A., Conti, S., Castagnola, M., and Vitali, A. (2018). The activity of a mammalian proline-rich peptide

against Gram-negative bacteria, including drug-resistant strains, relies on a nonmembranolytic mode of action. *Infect. Drug Resist.* 11, 969–979. doi: 10.2147/IDR.S165179

Cooper, C. J., Koonjan, S., and Nilsson, A. S. (2018). Enhancing whole phage therapy and their derived antimicrobial enzymes through complex formulation. *Pharmaceuticals* 11:E34. doi: 10.3390/ph11020034

Corbett, D., Wise, A., Langley, T., Skinner, K., Trimby, E., Birchall, S., et al. (2017). Potentiation of antibiotic activity by a novel cationic peptide: potency and spectrum of activity of SPR741. *Antimicrob. Agents Chemother.* 61, e00200–e00217. doi: 10.1128/AAC.00200-17

Coronado-Álvarez, N. M., Parra, D., and Parra-Ruiz, J. (2018). Clinical efficacy of fosfomycin combinations against a variety of gram-positive cocci. *Enferm. Infecc. Microbiol. Clin.* 37, 4–10. doi: 10.1016/j.eimc.2018.05.009

Costley, D., Nesbitt, H., Ternan, N., Dooley, J., Huang, Y. Y., Hamblin, M. R., et al. (2017). Sonodynamic inactivation of gram-positive and gram-negative bacteria using a rose bengal-antimicrobial peptide conjugate. *Int. J. Antimicrob. Agents* 49, 31–36. doi: 10.1016/j.ijantimicag.2016.09.034

Dakal, T. C., Kumar, A., Majumdar, R. S., and Yadav, V. (2016). Mechanistic basis of antimicrobial actions of silver nanoparticles. *Front. Microbiol.* 7:1831. doi: 10.3389/fmicb.2016.01831

Danis-Wlodarczyk, K., Vandenheuvel, D., Jang, H. B., Briers, Y., Olszak, T., Arabski, M., et al. (2016). A proposed integrated approach for the preclinical evaluation of phage therapy in Pseudomonas infections. *Sci. Rep.* 6:28115. doi: 10.1038/srep28115

de Aguiar Coletti, T. M. S. F., de Freitas, L. M., Almeida, A. M. F., and Fontana, C. R. (2017). Optimization of antimicrobial photodynamic therapy in biofilms by inhibiting efflux pump. *Photomed. Laser Surg.* 35, 378–385. doi: 10.1089/pho.2016.4246

de Breij, A., Riool, M., Cordfunke, R. A., Malanovic, N., de Boer, L., Koning, R. I., et al. (2018). The antimicrobial peptide SAAP-148 combats drug-resistant bacteria and biofilms. *Sci. Transl. Med.* 10:eaan4044. doi: 10.1126/scitranslmed.aan4044

de Freitas, L. M., Lorenzón, E. N., Santos-Filho, N. A., Zago, L. H. P., Uliana, M. P., de Oliveira, K. T., et al. (2018). Antimicrobial photodynamic therapy enhanced by the peptide aurein 1.2. *Sci. Rep.* 8:4212. doi: 10.1038/s41598-018-22687-x

Defraine, V., Verstraete, L., Van Bambeke, F., Anantharajah, A., Townsend, E. M., Ramage, G., et al. (2017). Antibacterial activity of 1-[(2,4-Dichlorophenethyl)amino]-3-Phenoxypropan-2-ol against antibiotic-resistant strains of diverse bacterial pathogens, biofilms and in pre-clinical infection models. *Front. Microbiol.* 8:2585. doi: 10.3389/fmicb.2017.02585

Ding, L., Shan, X., Zhao, X., Zha, H., Chen, X., Wang, J., et al. (2017). Spongy bilayer dressing composed of chitosan-Ag nanoparticles and chitosan-*Bletilla striata* polysaccharide for wound healing applications. *Carbohydr. Polym.* 157, 1538–1547. doi: 10.1016/j.carbpol.2016.11.040

Domalaon, R., Idowu, T., Zhanel, G. G., and Schweizer, F. (2018). Antibiotic hybrids: the next generation of agents and adjuvants against gram-negative pathogens? *Clin. Microbiol. Rev.* 31, e00077–e00017. doi: 10.1128/CMR.00077-17

Domingo-Calap, P., and Delgado-Martínez, J. (2018). Bacteriophages: protagonists of a post-antibiotic era. *Antibiotics* 7:66. doi: 10.3390/antibiotics7030066

Dong, R. H., Jia, Y. X., Qin, C. C., Zhan, L., Yan, X., Cui, L., et al. (2016). *In situ* deposition of a personalized nanofibrous dressing via a handy electrospinning device for skin wound care. *Nanoscale* 8, 3482–3488. doi: 10.1039/C5NR08367B

Du, H., Puri, S., McCall, A., Norris, H. L., Russo, T., and Edgerton, M. (2017). Human salivary protein histatin 5 has potent bactericidal activity against ESKAPE pathogens. *Front. Cell. Infect. Microbiol.* 7:41. doi: 10.3389/fcimb.2017.00041

Duplessis, C., Biswas, B., Hanisch, B., Perkins, M., Henry, M., Quinones, J., et al. (2018). Refractory *Pseudomonas* bacteremia in a 2-year-old sterilized by bacteriophage therapy. *J. Pediatric Infect. Dis. Soc.* 7, 253–256. doi: 10.1093/jpids/pix056

Durante-Mangoni, E., Signoriello, G., Andini, R., Mattei, A., De Cristoforo, M., Murino, P., et al. (2013). Colistin and rifampicin compared with colistin alone for the treatment of serious infections due to extensively drug-resistant *Acinetobacter baumannii*: a multicenter, randomized clinical trial. *Clin. Infect. Dis.* 57, 349–358. doi: 10.1093/cid/cit253

Dutta, D., Ozkan, J., and Willcox, M. D. P. (2014). Biocompatibility of antimicrobial melimine lenses. *Optom. Vis. Sci.* 91, 570–581. doi: 10.1097/OPX.0000000000000232

Dvořáčková, M., Růžička, F., Benešík, M., Pantůček, R., and Dvořáková-Heroldová, M. (2018). Antimicrobial effect of commercial phage preparation Stafal® on biofilm and planktonic forms of methicillin-resistant *Staphylococcus aureus*. *Folia Microbiol.* 64, 121–126. doi: 10.1007/s12223-018-0622-3

El-Azizi, M., and Khardori, N. (2016). Efficacy of ultraviolet C light at sublethal dose in combination with antistaphylococcal antibiotics to disinfect catheter biofilms of methicillin-susceptible and methicillin-resistant *Staphylococcus aureus* and *Staphylococcus epidermidis in vitro*. *Infect. Drug Resist. Volume* 9, 181–189. doi: 10.2147/IDR.S109343

El-Shibiny, A., and El-Sahhar, S. (2017). Bacteriophages: the possible solution to treat infections caused by pathogenic bacteria. *Can. J. Microbiol.* 63, 865–879. doi: 10.1139/cjm-2017-0030

Fadlallah, A., Chelala, E., and Legeais, J. M. (2015). Corneal infection therapy with topical bacteriophage administration. *Open Ophthalmol. J.* 9, 167–168. doi: 10.2174/1874364101509010167

Fallah, K. N. (2018). *The Effects of Combination Antibiotic Therapy on Methicillin-Resistant Staphylococcus aureus*. Doctoral dissertation.

Fila, G., Kawiak, A., and Grinholc, M. S. (2017). Blue light treatment of *Pseudomonas aeruginosa*: strong bactericidal activity, synergism with antibiotics and inactivation of virulence factors. *Virulence* 8, 938–958. doi: 10.1080/21505594.2016.1250995

Fish, R., Kutter, E., Wheat, G., Blasdel, B., Kutateladze, M., and Kuhl, S. (2016). Bacteriophage treatment of intransigent diabetic toe ulcers: a case series. *J. Wound Care* 25, S27–S33. doi: 10.12968/jowc.2016.25.Sup7.S27

Founou, R. C., Founou, L. L., and Essack, S. Y. (2017). Clinical and economic impact of antibiotic resistance in developing countries: a systematic review and meta-analysis. *PLoS ONE* 12:e0189621. doi: 10.1371/journal.pone.0189621

Gaglione, R., Dell'Olmo, E., Bosso, A., Chino, M., Pane, K., Ascione, F., et al. (2017). Novel human bioactive peptides identified in Apolipoprotein B: evaluation of their therapeutic potential. *Biochem. Pharmacol.* 130, 34–50. doi: 10.1016/j.bcp.2017.01.009

Gandt, A., Griffith, E. C., Lister, I. M., Billings, L. L., Han, A., Tangallapally, R., et al. (2018). *In vivo* and *in vitro* effects of a ClpP-activating antibiotic against vancomycin-resistant *Enterococci*. *Antimicrob. Agents Chemother.* 62, e00424–e00418. doi: 10.1128/AAC.00424-18

Ghosh, S., Patil, S., Ahire, M., Kitture, R., Kale, S., Pardesi, K., et al. (2012). Synthesis of silver nanoparticles using *Dioscorea bulbifera* tuber extract and evaluation of its synergistic potential in combination with antimicrobial agents. *Int. J. Nanomed.* 7, 483–96. doi: 10.2147/IJN.S24793

Gill, J. S., Arora, S., Khanna, S. P., and Kumar, K. H. (2016). Prevalence of multidrug-resistant, extensively drug-resistant, and pandrug-resistant *Pseudomonas aeruginosa* from a tertiary level intensive care unit. *J. Glob. Infect. Dis.* 8, 155–159. doi: 10.4103/0974-777X.192962

Goic-Barisic, I., Seruga Music, M., Kovacic, A., Tonkic, M., and Hrenovic, J. (2017). Pan drug-resistant environmental isolate of *Acinetobacter baumannii* from croatia. *Microb. Drug Resist.* 23, 494–496. doi: 10.1089/mdr.2016.0229

Golińska, P., Wypij, M., Rathod, D., Tikar, S., Dahm, H., and Rai, M. (2016). Synthesis of silver nanoparticles from two acidophilic strains of *Pilimelia columellifera* subsp. pallida and their antibacterial activities. *J. Basic Microbiol.* 56, 541–556. doi: 10.1002/jobm.201500516

Gomes, B., Augusto, M. T., Felício, M. R., Hollmann, A., Franco, O. L., Gonçalves, S., et al. (2018). Designing improved active peptides for therapeutic approaches against infectious diseases. *Biotechnol. Adv.* 36, 415–429. doi: 10.1016/j.biotechadv.2018.01.004

Gong, P., Cheng, M., Li, X., Jiang, H., Yu, C., Kahaer, N., et al. (2016). Characterization of *Enterococcus faecium* bacteriophage IME-EFm5 and its endolysin LysEFm5. *Virology* 492, 11–20. doi: 10.1016/j.virol.2016.02.006

González-Bello, C. (2017). Antibiotic adjuvants – a strategy to unlock bacterial resistance to antibiotics. *Bioorg. Med. Chem. Lett.* 27, 4221–4228. doi: 10.1016/j.bmcl.2017.08.027

Górski, A., Jończyk-Matysiak, E., Łusiak-Szelachowska, M., Międzybrodzki, R., Weber-Dąbrowska, B., and Borysowski, J. (2017). The potential of phage therapy in sepsis. *Front. Immunol.* 8:1783. doi: 10.3389/fimmu.2017.01783

Göttig, S., Gruber, T. M., Higgins, P. G., Wachsmuth, M., Seifert, H., and Kempf, V. A. J. (2014). Detection of pan drug-resistant *Acinetobacter baumannii* in Germany. *J. Antimicrob. Chemother.* 69, 2578–2579. doi: 10.1093/jac/dku170

Greimel, F., Scheuerer, C., Gessner, A., Simon, M., Kalteis, T., Grifka, J., et al. (2017). Efficacy of antibiotic treatment of implant-associated *Staphylococcus aureus* infections with moxifloxacin, flucloxacillin, rifampin, and combination therapy: an animal study. *Drug Des. Devel. Ther.* 11, 1729–1736. doi: 10.2147/DDDT.S138888

Habash, M. B., Goodyear, M. C., Park, A. J., Surette, M. D., Vis, E. C., Harris, R. J., et al. (2017). Potentiation of tobramycin by silver nanoparticles against *Pseudomonas aeruginosa* Biofilms. *Antimicrob. Agents Chemother.* 61: e00415-17. doi: 10.1128/AAC.00415-17

Hall Snyder, A. D., Werth, B. J., Nonejuie, P., McRoberts, J. P., Pogliano, J., Sakoulas, G., et al. (2016). Fosfomycin enhances the activity of daptomycin against vancomycin-resistant *Enterococci* in an *in vitro* pharmacokinetic-pharmacodynamic model. *Antimicrob. Agents Chemother.* 60, 5716–5723. doi: 10.1128/AAC.00687-16

Halstead, F. D., Thwaite, J. E., Burt, R., Laws, T. R., Raguse, M., Moeller, R., et al. (2016). Antibacterial activity of blue light against nosocomial wound pathogens growing planktonically and as mature biofilms. *Appl. Environ. Microbiol.* 82, 4006–4016. doi: 10.1128/AEM.00756-16

Hemeg, H. (2017). Nanomaterials for alternative antibacterial therapy. *Int. J. Nanomed. Vol.* 12, 8211–8225. doi: 10.2147/IJN.S132163

Hu, X., Huang, Y. Y., Wang, Y., Wang, X., and Hamblin, M. R. (2018). Antimicrobial photodynamic therapy to control clinically relevant biofilm infections. *Front. Microbiol.* 9, 1–24. doi: 10.3389/fmicb.2018.01299

Huang, L., Wang, M., Dai, T., Sperandio, F. F., Huang, Y. Y., Xuan, Y., et al. (2014). Antimicrobial photodynamic therapy with decacationic monoadducts and bisadducts of [70]fullerene: *in vitro* and *in vivo* studies. *Nanomedicine* 9, 253–266. doi: 10.2217/nnm.13.22

Ibrahim, M. E., Bilal, N. E., and Hamid, M. E. (2012). Increased multi-drug resistant *Escherichia coli* from hospitals in Khartoum state, Sudan. *Afr. Health Sci.* 12, 368–375. doi: 10.4314/ahs.v12i3.19

Irani, N., Basardeh, E., Samiee, F., Fateh, A., Shooraj, F., Rahimi, A., et al. (2018). The inhibitory effect of the combination of two new peptides on biofilm formation by *Acinetobacter baumannii*. *Microb. Pathog.* 121, 310–317. doi: 10.1016/j.micpath.2018.05.051

Jamal, M., Andleeb, S., Jalil, F., Imran, M., Nawaz, M. A., Hussain, T., et al. (2019). Isolation, characterization and efficacy of phage MJ2 against biofilm forming multi-drug resistant *Enterobacter cloacae*. *Folia Microbiol.* 64, 101–111. doi: 10.1007/s12223-018-0636-x

Jault, P., Leclerc, T., Jennes, S., Pirnay, J. P., Que, Y. A., Resch, G., et al. (2019). Efficacy and tolerability of a cocktail of bacteriophages to treat burn wounds infected by *Pseudomonas aeruginosa* (PhagoBurn): a randomised, controlled, double-blind phase 1/2 trial. *Lancet Infect. Dis.* 19, 35–45. doi: 10.1016/S1473-3099(18)30482-1

Jennes, S., Merabishvili, M., Soentjens, P., Pang, K. W., Rose, T., Keersebilck, E., et al. (2017). Use of bacteriophages in the treatment of colistin-only-sensitive *Pseudomonas aeruginosa* septicaemia in a patient with acute kidney injury-a case report. *Crit. Care* 21:129. doi: 10.1186/s13054-017-1709-y

Jo, A., Ding, T., and Ahn, J. (2016). Synergistic antimicrobial activity of bacteriophages and antibiotics against *Staphylococcus aureus*. *Food Sci. Biotechnol.* 25, 935–940. doi: 10.1007/s10068-016-0153-0

Jorgensen, S. C. J., and Rybak, M. J. (2018). Meropenem and vaborbactam: stepping up the battle against carbapenem-resistant Enterobacteriaceae. *Pharmacotherapy* 38, 444–461. doi: 10.1002/phar.2092

Kalan, L., and Wright, G. D. (2011). Antibiotic adjuvants: multicomponent anti-infective strategies. *Expert Rev. Mol. Med.* 13:e5. doi: 10.1017/S1462399410001766

Kasithevar, M., Periakaruppan, P., Muthupandian, S., and Mohan, M. (2017). Antibacterial efficacy of silver nanoparticles against multi-drug resistant clinical isolates from post-surgical wound infections. *Microb. Pathog.* 107, 327–334. doi: 10.1016/j.micpath.2017.04.013

Katayama, B., Ozawa, T., Morimoto, K., Awazu, K., Ito, N., Honda, N., et al. (2018). Enhanced sterilization and healing of cutaneous pseudomonas infection using 5-aminolevulinic acid as a photosensitizer with 410-nm LED light. *J. Dermatol. Sci.* 90, 323–331. doi: 10.1016/j.jdermsci.2018.03.001

Kaur, I. (2016). Novel strategies to combat antimicrobial resistance. *J. Infect. Dis. Ther.* 4:292. doi: 10.4172/2332-0877.100029

Kishor, C., Mishra, R. R., Saraf, S. K., Kumar, M., Srivastav, A. K., and Nath, G. (2016). Phage therapy of staphylococcal chronic osteomyelitis in experimental animal model. *Indian J. Med. Res.* 143, 87–94. doi: 10.4103/0971-5916.178615

Kulengowski, B., Rutter, W. C., Campion, J. J., Lee, G. C., Feola, D. J., and Burgess, D. S. (2018). Effect of increasing meropenem MIC on the killing activity of meropenem in combination with amikacin or polymyxin B against MBL- and KPC-producing *Enterobacter cloacae*. *Diagn. Microbiol. Infect. Dis.* 92, 262–266. doi: 10.1016/j.diagmicrobio.2018.06.013

Kuo, Y. L., Wang, S. G., Wu, C. Y., Lee, K. C., Jao, C. J., Chou, S. H., et al. (2016). Functional gold nanoparticle-based antibacterial agents for nosocomial and antibiotic-resistant bacteria. *Nanomedicine* 11, 2497–2510. doi: 10.2217/nnm-2016-0232

Latz, S., Wahida, A., Arif, A., Häfner, H., Hoß, M., Ritter, K., et al. (2016). Preliminary survey of local bacteriophages with lytic activity against multi-drug resistant bacteria. *J. Basic Microbiol.* 56, 1117–1123. doi: 10.1002/jobm.201600108

LaVergne, S., Hamilton, T., Biswas, B., Kumaraswamy, M., Schooley, R. T., and Wooten, D. (2018). Phage therapy for a multidrug-resistant *Acinetobacter baumannii* craniectomy site infection. *Open Forum Infect. Dis.* 5:ofy064. doi: 10.1093/ofid/ofy064

Lee, N. Y., Lee, C. C., Li, C. W., Li, M. C., Chen, P. L., Chang, C. M., et al. (2015). Cefepime therapy for monomicrobial *Enterobacter cloacae* bacteremia: unfavorable outcomes in patients infected by cefepime-susceptible dose-dependent isolates. *Antimicrob. Agents Chemother.* 59, 7558–7563. doi: 10.1128/AAC.01477-15

Leitner, L., Sybesma, W., Chanishvili, N., Goderdzishvili, M., Chkhotua, A., Ujmajuridze, A., et al. (2017). Bacteriophages for treating urinary tract infections in patients undergoing transurethral resection of the prostate: a randomized, placebo-controlled, double-blind clinical trial. *BMC Urol.* 17:90. doi: 10.1186/s12894-017-0283-6

Lewis, K. (2007). Persister cells, dormancy and infectious disease. 5, 48–56. doi: 10.1038/nrmicro1557

Liang, D., Lu, Z., Yang, H., Gao, J., and Chen, R. (2016). Novel asymmetric wettable AgNPs/Chitosan wound dressing: *in vitro* and *in vivo* evaluation. *ACS Appl. Mater. Interfaces* 8, 3958–3968. doi: 10.1021/acsami.5b11160

Lin, D., Koskella, B., and Lin, H. C. (2017). Phage therapy: An alternative to antibiotics in the age of multi-drug resistance. *World J. Gastrointest. Pharmacol. Ther.* 8, 162–173. doi: 10.4292/wjgpt.v8.i3.162

Lin, Q., Deslouches, B., Montelaro, R. C., and Di, Y. P. (2018). Prevention of ESKAPE pathogen biofilm formation by antimicrobial peptides WLBU2 and LL37. *Int. J. Antimicrob. Agents.* 52, 667–672. doi: 10.1016/j.ijantimicag.2018.04.019

Lin, Y., Chang, R. Y. K., Britton, W. J., Morales, S., Kutter, E., and Chan, H.-K. (2018). Synergy of nebulized phage PEV20 and ciprofloxacin combination against *Pseudomonas aeruginosa*. *Int. J. Pharm.* 551, 158–165. doi: 10.1016/j.ijpharm.2018.09.024

Liu, S., Long, Q., Xu, Y., Wang, J., Xu, Z., Wang, L., et al. (2017). Assessment of antimicrobial and wound healing effects of Brevinin-2Ta against the bacterium *Klebsiella pneumoniae* in dermally-wounded rats. *Oncotarget* 8, 111369–111385. doi: 10.18632/oncotarget.22797

Long, S. W., Olsen, R. J., Mehta, S. C., Palzkill, T., Cernoch, P. L., Perez, K. K., et al. (2014). PBP2a mutations causing high-level Ceftaroline resistance in clinical methicillin-resistant *Staphylococcus aureus* isolates. *Antimicrob. Agents Chemother.* 58, 6668–6674. doi: 10.1128/AAC.03622-14

López-Cortés, L. E., Cisneros, J. M., Fernández-Cuenca, F., Bou, G., Tomás, M., Garnacho-Montero, J., et al. (2014). Monotherapy versus combination therapy for sepsis due to multidrug-resistant *Acinetobacter baumannii*: analysis of a multicentre prospective cohort. *J. Antimicrob. Chemother.* 69, 3119–3126. doi: 10.1093/jac/dku233

Lotha, R., Shamprasad, B. R., Sundaramoorthy, N. S., Ganapathy, R., Nagarajan, S., and Sivasubramanian, A. (2018). Zero valent silver nanoparticles capped with capsaicinoids containing *Capsicum annuum* extract, exert potent anti-biofilm effect on food borne pathogen *Staphylococcus aureus* and curtail

planktonic growth on a zebrafish infection model. *Microb. Pathog.* 124, 291–300. doi: 10.1016/j.micpath.2018.08.053

Mahlapuu, M., Håkansson, J., Ringstad, L., and Björn, C. (2016). Antimicrobial peptides: an emerging category of therapeutic agents. *Front. Cell. Infect. Microbiol.* 6:194. doi: 10.3389/fcimb.2016.00194

Mai, B., Gao, Y., Li, M., Wang, X., Zhang, K., Liu, Q., et al. (2017). Photodynamic antimicrobial chemotherapy for *Staphylococcus aureus* and multidrug-resistant bacterial burn infection *in vitro* and *in vivo*. *Int. J. Nanomed.* 12, 5915–5931. doi: 10.2147/IJN.S138185

Malik, D. J., Sokolov, I. J., Vinner, G. K., Mancuso, F., Cinquerrui, S., Vladisavljevic, G. T., et al. (2017). Formulation, stabilisation and encapsulation of bacteriophage for phage therapy. *Adv. Colloid Interface Sci.* 249, 100–133. doi: 10.1016/j.cis.2017.05.014

Maliszewska, I., Kałas, W., Wysokiéska, E., Tylus, W., Pietrzyk, N., Popko, K., et al. (2018). Enhancement of photo-bactericidal effect of tetrasulfonated hydroxyaluminum phthalocyanine on *Pseudomonas aeruginosa*. *Lasers Med. Sci.* 33, 79–88. doi: 10.1007/s10103-017-2337-0

Mandal, S. M., Roy, A., Ghosh, A. K., Hazra, T. K., Basak, A., and Franco, O. L. (2014). Challenges and future prospects of antibiotic therapy: from peptides to phages utilization. *Front. Pharmacol.* 5:105. doi: 10.3389/fphar.2014.00105

Mann, N. H. (2005). The third age of phage. *PLoS Biol.* 3:182. doi: 10.1371/journal.pbio.0030182

Manohar, P., Nachimuthu, R., and Lopes, B. S. (2018). The therapeutic potential of bacteriophages targeting gram-negative bacteria using *Galleria mellonella* infection model. *BMC Microbiol.* 18:97. doi: 10.1186/s12866-018-1234-4

Markoishvili, K., Tsitlanadze, G., Katsarava, R., Morris, J. G., and Sulakvelidze, A. (2002). A novel sustained-release matrix based on biodegradable poly(ester amide)s and impregnated with bacteriophages and an antibiotic shows promise in management of infected venous stasis ulcers and other poorly healing wounds. *Int. J. Dermatol.* 41, 453–458. doi: 10.1046/j.1365-4362.2002.01451.x

Marsich, E., Travan, A., Donati, I., Turco, G., Kulkova, J., Moritz, N., et al. (2013). Biological responses of silver-coated thermosets: an *in vitro* and *in vivo* study. *Acta Biomater.* 9, 5088–5099. doi: 10.1016/j.actbio.2012.10.002

Mcnair, K., Bailey, B. A., and Edwards, R. A. (2012). PHACTS, a computational approach to classifying the lifestyle of phages. *Bioinformatics* 28, 614–618. doi: 10.1093/bioinformatics/bts014

Mekkawy, A. I., El-Mokhtar, M. A., Nafady, N. A., Yousef, N., Hamad, M. A., El-Shanawany, S. M., et al. (2017). *In vitro* and *in vivo* evaluation of biologically synthesized silver nanoparticles for topical applications: effect of surface coating and loading into hydrogels. *Int. J. Nanomedicine* 12, 759–777. doi: 10.2147/IJN.S124294

Miller, C. N., Newall, N., Kapp, S. E., Lewin, G., Karimi, L., Carville, K., et al. (2010). A randomized-controlled trial comparing cadexomer iodine and nanocrystalline silver on the healing of leg ulcers. *Wound Repair Regen.* 18, 359–367. doi: 10.1111/j.1524-475X.2010.00603.x

Mohanty, S., Mishra, S., Jena, P., Jacob, B., Sarkar, B., and Sonawane, A. (2012). An investigation on the antibacterial, cytotoxic, and antibiofilm efficacy of starch-stabilized silver nanoparticles. *Nanomedicine* 8, 916–924. doi: 10.1016/j.nano.2011.11.007

Mohapatra, D. P., Debata, N. K., and Singh, S. K. (2018). Extensively drug-resistant and pan-drug resistant Gram-negative bacteria in a tertiary-care hospital in Eastern India: A 4 year retrospective study. *J. Glob. Antimicrob. Resist.* 15, 246–249. doi: 10.1016/j.jgar.2018.08.010

Möhler, J. S., Sim, W., Blaskovich, M. A. T., Cooper, M. A., and Ziora, Z. M. (2018). Silver bullets: a new lustre on an old antimicrobial agent. *Biotechnol. Adv.* 36, 1391–1411. doi: 10.1016/j.biotechadv.2018.05.004

Monogue, M. L., Giovagnoli, S., Bissantz, C., Zampaloni, C., and Nicolau, D. P. (2018a). *In vivo* efficacy of meropenem, with a novel non-β-lactam β-lactamase inhibitor, nacubactam, against gram-negative organisms exhibiting various resistance mechanisms in a murine complicated urinary tract infection model. *Antimicrob. Agents Chemother.* 62:e02596-17. doi: 10.1128/AAC.02596-17

Monogue, M. L., Sakoulas, G., Nizet, V., and Nicolau, D. P. (2018b). Humanized exposures of a β-lactam-β-lactamase inhibitor, tazobactam, versus non-β-lactam-β-lactamase inhibitor, avibactam, with or without colistin, against *Acinetobacter baumannii* in murine thigh and lung infection models. *Pharmacology* 101, 255–261. doi: 10.1159/000486445

Moon, S. H., Zhang, X., Zheng, G., Meeker, D. G., Smeltzer, M. S., and Huang, E. (2017). Novel linear lipopeptide paenipeptins with potential for eradicating biofilms and sensitizing gram-negative bacteria to rifampicin and clarithromycin. *J. Med. Chem.* 60, 9630–9640. doi: 10.1021/acs.jmedchem.7b01064

Morimoto, K., Ozawa, T., Awazu, K., Ito, N., Honda, N., Matsumoto, S., et al. (2014). Photodynamic therapy using systemic administration of 5-aminolevulinic acid and a 410-nm wavelength light-emitting diode for methicillin-resistant *Staphylococcus aureus*-infected ulcers in mice. *PLoS ONE* 9:e105173. doi: 10.1371/journal.pone.0105173

Munger, M. A., Radwanski, P., Hadlock, G. C., Stoddard, G., Shaaban, A., Falconer, J., et al. (2014). *In vivo* human time-exposure study of orally dosed commercial silver nanoparticles. *Nanomed. Nanotechnol. Biol. Med.* 10, 1–9. doi: 10.1016/j.nano.2013.06.010

Nakonieczna, J., Wolnikowska, K., Ogonowska, P., Neubauer, D., Bernat, A., and Kamysz, W. (2018). Rose bengal-mediated photoinactivation of multidrug resistant *Pseudomonas aeruginosa* is enhanced in the presence of antimicrobial peptides. *Front. Microbiol.* 9:1949. doi: 10.3389/fmicb.2018.01949

Navidinia, M. (2016). The clinical importance of emerging ESKAPE pathogens in nosocomial infections. *J. Paramed. Sci.* 7, 2008–4978. doi: 10.22037/jps.v7i3.12584

Nigo, M., Diaz, L., Carvajal, L. P., Tran, T. T., Rios, R., Panesso, D., et al. (2017). Ceftaroline-resistant, daptomycin-tolerant, and heterogeneous vancomycin-intermediate methicillin-resistant *Staphylococcus aureus* causing infective endocarditis. *Antimicrob. Agents Chemother.* 61:e01235-16. doi: 10.1128/AAC.01235-16

Nour El Din, S., El-Tayeb, T. A., Abou-Aisha, K., and El-Azizi, M. (2016). *In vitro* and *in vivo* antimicrobial activity of combined therapy of silver nanoparticles and visible blue light against *Pseudomonas aeruginosa*. *Int. J. Nanomed.* 11, 1749–1758. doi: 10.2147/IJN.S102398

Nowak, J., Zander, E., Stefanik, D., Higgins, P. G., Roca, I., Vila, J., et al. (2017). High incidence of pandrug-resistant *Acinetobacter baumannii* isolates collected from patients with ventilator-associated pneumonia in Greece, Italy and Spain as part of the magicbullet clinical trial. *J. Antimicrob. Chemother.* 72, 3277–3282. doi: 10.1093/jac/dkx322

Ostorhazi, E., Hoffmann, R., Herth, N., Wade, J. D., Kraus, C. N., and Otvos, L. (2018). Advantage of a narrow spectrum host defense (Antimicrobial) peptide over a broad spectrum analog in preclinical drug development. *Front. Chem.* 6:359. doi: 10.3389/fchem.2018.00359

Otvos, L., Ostorhazi, E., Szabo, D., Zumbrun, S. D., Miller, L. L., Halasohoris, S. A., et al. (2018). Synergy between proline-rich antimicrobial peptides and small molecule antibiotics against selected gram-negative pathogens *in vitro* and *in vivo*. *Front. Chem.* 6:309. doi: 10.3389/fchem.2018.00309

Palavutitotai, N., Jitmuang, A., Tongsai, S., Kiratisin, P., and Angkasekwinai, N. (2018). Epidemiology and risk factors of extensively drug-resistant *Pseudomonas aeruginosa* infections. *PLoS ONE* 13:e0193431. doi: 10.1371/journal.pone.0193431

Pallavali, R. R., Degati, V. L., Lomada, D., Reddy, M. C., and Durbaka, V. R. P. (2017). Isolation and *in vitro* evaluation of bacteriophages against MDR-bacterial isolates from septic wound infections. *PLoS ONE* 12:e0179245. doi: 10.1371/journal.pone.0179245

Panáček, A., Smékalová, M., Kilianová, M., Prucek, R., Bogdanová, K., Večeřová, R., et al. (2015). Strong and nonspecific synergistic antibacterial efficiency of antibiotics combined with silver nanoparticles at very low concentrations showing no cytotoxic effect. *Molecules* 21:26. doi: 10.3390/molecules21010026

Pendleton, J. N., Gorman, S. P., and Gilmore, B. F. (2013). Clinical relevance of the ESKAPE pathogens. *Expert Rev. Anti. Infect. Ther.* 11, 297–308. doi: 10.1586/eri.13.12

Peng, Y., Song, C., Yang, C., Guo, Q., and Yao, M. (2017). Low molecular weight chitosan-coated silver nanoparticles are effective for the treatment of MRSA-infected wounds. *Int. J. Nanomed.* 12, 295–304. doi: 10.2147/IJN.S122357

Pfalzgraff, A., Brandenburg, K., and Weindl, G. (2018). Antimicrobial peptides and their therapeutic potential for bacterial skin infections and wounds. *Front. Pharmacol.* 9:281. doi: 10.3389/fphar.2018.00281

Philipson, C., Voegtly, L., Lueder, M., Long, K., Rice, G., Frey, K., et al. (2018). Characterizing phage genomes for therapeutic applications. *Viruses* 10:188. doi: 10.3390/v10040188

Pirnay, J. P., Verbeken, G., Ceyssens, P. J., Huys, I., De Vos, D., Ameloot, C., et al. (2018). The magistral phage. *Viruses* 10:64. doi: 10.3390/v10020064

Pletzer, D., Mansour, S. C., and Hancock, R. E. W. (2018). Synergy between conventional antibiotics and anti-biofilm peptides in a murine, sub-cutaneous abscess model caused by recalcitrant ESKAPE pathogens. *PLoS Pathog.* 14:e1007084. doi: 10.1371/journal.ppat.1007084

Pompilio, A., Geminiani, C., Bosco, D., Rana, R., Aceto, A., Bucciarelli, T., et al. (2018). Electrochemically synthesized silver nanoparticles are active against planktonic and biofilm cells of *Pseudomonas aeruginosa* and other cystic fibrosis-associated bacterial pathogens. *Front. Microbiol.* 9:1349. doi: 10.3389/fmicb.2018.01349

Prakash, V., Mishra, P., Premi, H., Walia, A., Dhawan, S., and Kumar, A. (2014). Increasing incidence of multidrug resistant *Pseudomonas aeruginosa* in inpatients of a tertiary care hospital. *Int. J. Res. Med. Sci.* 2:1302. doi: 10.5455/2320-6012.ijrms20141111

Qayyum, S., Oves, M., and Khan, A. U. (2017). Obliteration of bacterial growth and biofilm through ROS generation by facilely synthesized green silver nanoparticles. *PLoS ONE* 12:0181363. doi: 10.1371/journal.pone.0181363

Radulescu, M., Andronescu, E., Dolete, G., Popescu, R. C., Fufă, O., Chifiriuc, M. C., et al. (2016). Silver nanocoatings for reducing the exogenous microbial colonization of wound dressings. *Materials* 9:345. doi: 10.3390/ma9050345

Rath, G., Hussain, T., Chauhan, G., Garg, T., and Goyal, A. K. (2016). Collagen nanofiber containing silver nanoparticles for improved wound-healing applications. *J. Drug Target.* 24, 520–529. doi: 10.3109/1061186X.2015.1095922

Regeimbal, J. M., Jacobs, A. C., Corey, B. W., Henry, M. S., Thompson, M. G., Pavlicek, R. L., et al. (2016). Personalized therapeutic cocktail of wild environmental phages rescues mice from *Acinetobacter baumannii* wound infections. *Antimicrob. Agents Chemother.* 60, 5806–5816. doi: 10.1128/AAC.02877-15

Reinhardt, A., and Neundorf, I. (2016). Design and application of antimicrobial peptide conjugates. *Int. J. Mol. Sci.* 17:E701. doi: 10.3390/ijms17050701

Rice, L. B. (2008). Federal funding for the study of antimicrobial resistance in nosocomial pathogens: no ESKAPE. *J. Infect. Dis.* 197, 1079–1081. doi: 10.1086/533452

Rineh, A., Bremner, J. B., Hamblin, M. R., Ball, A. R., Tegos, G. P., and Kelso, M. J. (2018). Attaching NorA efflux pump inhibitors to methylene blue enhances antimicrobial photodynamic inactivation of *Escherichia coli* and *Acinetobacter baumannii in vitro* and *in vivo*. *Bioorg. Med. Chem. Lett.* 28, 2736–2740. doi: 10.1016/j.bmcl.2018.02.041

Rineh, A., Dolla, N. K., Ball, A. R., Magana, M., Bremner, J. B., Hamblin, M. R., et al. (2017). Attaching the NorA efflux pump inhibitor INF55 to methylene blue enhances antimicrobial photodynamic inactivation of methicillin-resistant *Staphylococcus aureus in vitro* and *in vivo*. *ACS Infect. Dis.* 3, 756–766. doi: 10.1021/acsinfecdis.7b00095

Rios, A. C., Moutinho, C. G., Pinto, F. C., Del Fiol, F. S., Jozala, A., Chaud, M. V., et al. (2016). Alternatives to overcoming bacterial resistances: state-of-the-art. *Microbiol. Res.* 191, 51–80. doi: 10.1016/j.micres.2016.04.008

Rishi, N. P., Vashist, T., Sharma, A., Kaur, A., Kaur, A., Kaur, N., et al. (2018). Efficacy of designer K11 antimicrobial peptide (a hybrid of melittin, cecropin A1 and magainin 2) against *Acinetobacter baumannii* infected wounds. *Pathog. Dis.* 76:fty072. doi: 10.1093/femspd/fty072

Rohde, C., Resch, G., Pirnay, J. P., Blasdel, B., Debarbieux, L., Gelman, D., et al. (2018). Expert opinion on three phage therapy related topics: bacterial phage resistance, phage training and prophages in bacterial production strains. *Viruses* 10:178. doi: 10.3390/v10040178

Ronqui, M. R., de Aguiar Coletti, T. M. S. F., de Freitas, L. M., Miranda, E. T., and Fontana, C. R. (2016). Synergistic antimicrobial effect of photodynamic therapy and ciprofloxacin. *J. Photochem. Photobiol. B Biol.* 158, 122–129. doi: 10.1016/j.jphotobiol.2016.02.036

Rubino, C. M., Bhavnani, S. M., Loutit, J. S., Lohse, B., Dudley, M. N., and Griffith, D. C. (2018). Single-dose pharmacokinetics and safety of meropenem-vaborbactam in subjects with chronic renal impairment. *Antimicrob. Agents Chemother.* 62:e02103-17. doi: 10.1128/AAC.02103-17

Sangaonkar, G. M., and Pawar, K. D. (2018). Garcinia indica mediated biogenic synthesis of silver nanoparticles with antibacterial and antioxidant activities. *Colloids Surf. B. Biointerfaces* 164, 210–217. doi: 10.1016/j.colsurfb.2018.01.044

Santajit, S., and Indrawattana, N. (2016). Mechanisms of antimicrobial resistance in ESKAPE pathogens. *Biomed Res. Int.* 2016:2475067. doi: 10.1155/2016/2475067

Santos, A., L., Sodre, C. L., Valle, R. S., Silva, B. A., Souza-Goncalves, A. L., Sangenito, L. S., et al. (2012). Antimicrobial action of chelating agents: repercussions on the microorganism development, virulence and pathogenesis. *Curr. Med. Chem.* 19, 2715–2737. doi: 10.2174/092986712800609788

Schooley, R. T., Biswas, B., Gill, J. J., Hernandez-Morales, A., Lancaster, J., Lessor, L., et al. (2017). Development and use of personalized bacteriophage-based therapeutic cocktails to treat a patient with a disseminated resistant *Acinetobacter baumannii* Infection. *Antimicrob. Agents Chemother.* 61:e00954-17. doi: 10.1128/AAC.00954-17

Seo, M. D., Won, H. S., Kim, J. H., Mishig-Ochir, T., Lee, B. J., Seo, M. D., et al. (2012). Antimicrobial peptides for therapeutic applications: a review. *Molecules* 17, 12276–12286. doi: 10.3390/molecules171012276

Servick, K. (2016). Beleaguered phage therapy trial presses on. *Science* 352, 1506–1506. doi: 10.1126/science.352.6293.1506

Shalumon, K. T., Sheu, C., Chen, C. H., Chen, S. H., Jose, G., Kuo, C. Y., et al. (2018). Multi-functional electrospun antibacterial core-shell nanofibrous membranes for prolonged prevention of post-surgical tendon adhesion and inflammation. *Acta Biomater.* 72, 121–136. doi: 10.1016/j.actbio.2018.03.044

Shivaswamy, V. C., Kalasuramath, S. B., Sadanand, C. K., Basavaraju, A. K., Ginnavaram, V., Bille, S., et al. (2015). Ability of bacteriophage in resolving wound infection caused by multidrug-resistant *Acinetobacter baumannii* in uncontrolled diabetic rats. *Microb. Drug Resist.* 21, 171–177. doi: 10.1089/mdr.2014.0120

Siddiqi, K. S., Husen, A., and Rao, R. A. K. (2018). A review on biosynthesis of silver nanoparticles and their biocidal properties. *J. Nanobiotechnol.* 16:14. doi: 10.1186/s12951-018-0334-5

Singh, R., Vora, J., Nadhe, S. B., Wadhwani, S. A., Shedbalkar, U. U., and Chopade, B. A. (2018). Antibacterial activities of bacteriagenic silver nanoparticles against nosocomial *Acinetobacter baumannii*. *J. Nanosci. Nanotechnol.* 18, 3806–3815. doi: 10.1166/jnn.2018.15013

Singla, S., Harjai, K., Katare, O. P., and Chhibber, S. (2016). Encapsulation of bacteriophage in liposome accentuates its entry in to macrophage and shields it from neutralizing antibodies. *PLoS ONE* 11:e0153777. doi: 10.1371/journal.pone.0153777

Skinner, K., Sandoe, J. A. T., Rajendran, R., Ramage, G., and Lang, S. (2017). Efficacy of rifampicin combination therapy for the treatment of enterococcal infections assessed *in vivo* using a *Galleria mellonella* infection model. *Int. J. Antimicrob. Agents* 49, 507–511. doi: 10.1016/j.ijantimicag.2016.12.006

Soothill, J. S. (1992). Treatment of experimental infections of mice with bacteriophages. *J. Med. Microbiol.* 37, 258–261. doi: 10.1099/00222615-37-4-258

Stanley, I. J., Kajumbula, H., Bazira, J., Kansiime, C., Rwego, I. B., and Asiimwe, B. B. (2018). Multidrug resistance among *Escherichia coli* and *Klebsiella pneumoniae* carried in the gut of out-patients from pastoralist communities of Kasese district, Uganda. *PLoS ONE* 13:e0200093. doi: 10.1371/journal.pone.0200093

Sueoka, K., Chikama, T., Latief, M. A., Ko, J. A., Kiuchi, Y., Sakaguchi, T., et al. (2018). Time-dependent antimicrobial effect of photodynamic therapy with TONS 504 on *Pseudomonas aeruginosa*. *Lasers Med. Sci.* 33, 1455–1460. doi: 10.1007/s10103-018-2490-0

Sybesma, W., Rohde, C., Bardy, P., Pirnay, J. P., Cooper, I., Caplin, J., et al. (2018). Silk route to the acceptance and re-implementation of bacteriophage therapy—part II. *Antibiotics* 7:35. doi: 10.3390/antibiotics7020035

Tacconelli, E., Carrara, E., Savoldi, A., Harbarth, S., Mendelson, M., Monnet, D. L., et al. (2018). Discovery, research, and development of new antibiotics: the WHO priority list of antibiotic-resistant bacteria and tuberculosis. *Lancet Infect. Dis.* 18, 318–327. doi: 10.1016/S1473-3099(17)30753-3

Tegos, G. P., and Hamblin, M. R. (2006). Phenothiazinium antimicrobial photosensitizers are substrates of bacterial multidrug resistance pumps. *Antimicrob. Agents Chemother.* 50, 196–203. doi: 10.1128/AAC.50.1.196-203.2006

Tegos, G. P., Masago, K., Aziz, F., Higginbotham, A., Stermitz, F. R., and Hamblin, M. R. (2008). Inhibitors of bacterial multidrug efflux pumps potentiate antimicrobial photoinactivation. *Antimicrob. Agents Chemother.* 52, 3202–3209. doi: 10.1128/AAC.00006-08

Téllez, G. A., Zapata, J. A., Toro, L. J., Henao, D. C., Bedoya, J. P., Rivera, J. D., et al. (2018). Identification, characterization, immunolocalization, and biological activity of lucilin peptide. *Acta Trop.* 185, 318–326. doi: 10.1016/j.actatropica.2018.06.003

Tomb, R. M., Maclean, M., Coia, J. E., MacGregor, S. J., and Anderson, J. G. (2017). Assessment of the potential for resistance to antimicrobial violet-blue light in *Staphylococcus aureus*. *Antimicrob. Resist. Infect. Control* 6:100. doi: 10.1186/s13756-017-0261-5

Tomb, R. M., White, T. A., Coia, J. E., Anderson, J. G., MacGregor, S. J., and Maclean, M. (2018). Review of the comparative susceptibility of microbial species to photoinactivation using 380–480 nm violet-blue light. *Photochem. Photobiol.* 94, 445–458. doi: 10.1111/php.12883

Ujmajuridze, A., Chanishvili, N., Goderdzishvili, M., Leitner, L., Mehnert, U., Chkhotua, A., et al. (2018). Adapted bacteriophages for treating urinary tract infections. *Front. Microbiol.* 9:1832. doi: 10.3389/fmicb.2018.01832

Ullah, A., Zhang, Y., Iqbal, Z., Zhang, Y., Wang, D., Chen, J., et al. (2018). Household light source for potent photo-dynamic antimicrobial effect and wound healing in an infective animal model. *Biomed. Opt. Express* 9, 1006–1019. doi: 10.1364/BOE.9.001006

Vazquez-grande, G., and Kumar, A. (2015). Optimizing antimicrobial therapy of sepsis and septic shock : focus on antibiotic combination therapy. *Semin Respir Crit Care Med.* 1, 154–166. doi: 10.1055/s-0034-1398742

Verbelen, J., Hoeksema, H., Heyneman, A., Pirayesh, A., and Monstrey, S. (2014). Aquacel® Ag dressing versus Acticoat™ dressing in partial thickness burns: a prospective, randomized, controlled study in 100 patients. Part 1: burn wound healing. *Burns* 40, 416–427. doi: 10.1016/j.burns.2013.07.008

Vestergaard, M., Paulander, W., Marvig, R. L., Clasen, J., Jochumsen, N., Molin, S., et al. (2016). Antibiotic combination therapy can select for broad-spectrum multidrug resistance in *Pseudomonas aeruginosa*. *Int. J. Antimicrob. Agents* 47, 48–55. doi: 10.1016/j.ijantimicag.2015.09.014

Viertel, T. M., Ritter, K., and Horz, H. P. (2014). Viruses versus bacteria-novel approaches to phage therapy as a tool against multidrug-resistant pathogens. *J. Antimicrob. Chemother.* 69, 2326–2336. doi: 10.1093/jac/dku173

Vuotto, C., Longo, F., Pascolini, C., Donelli, G., Balice, M. P., Libori, M. F., et al. (2017). Biofilm formation and antibiotic resistance in *Klebsiella* pneumoniae urinary strains. *J. Appl. Microbiol.* 123, 1003–1018. doi: 10.1111/jam.13533

Wan, G., Ruan, L., Yin, Y., Yang, T., Ge, M., and Cheng, X. (2016). Effects of silver nanoparticles in combination with antibiotics on the resistant bacteria *Acinetobacter baumannii*. *Int. J. Nanomed. Vol.* 11, 3789–3800. doi: 10.2147/IJN.S104166

Wang, G., Li, X., and Zasloff, M. (2010). "A database view of naturally occurring antimicrobial peptides: nomenclature, classification and amino acid sequence analysis," in *Antimicrobial Peptides: Discovery, Design and Novel Therapeutic Strategies* (Oxfordshire: CABI), 1–21. doi: 10.1079/9781845936570.0001

Wang, S., Yan, C., Zhang, X., Shi, D., Chi, L., Luo, G., et al. (2018). Antimicrobial peptide modification enhances the gene delivery and bactericidal efficiency of gold nanoparticles for accelerating diabetic wound healing. *Biomater. Sci.* 6, 2757–2772. doi: 10.1039/C8BM00807H

Wang, Y., Harrington, O. D., Wang, Y., Murray, C. K., Hamblin, M. R., and Dai, T. (2017). *In vivo* investigation of antimicrobial blue light therapy for multidrug-resistant *Acinetobacter baumannii* burn infections using bioluminescence imaging. *J. Vis. Exp.* 122:e54997. doi: 10.3791/54997

Wang, Z., Zheng, P., Ji, W., Fu, Q., Wang, H., Yan, Y., et al. (2016). SLPW: a virulent bacteriophage targeting methicillin-resistant *Staphylococcus aureus* in vitro and *in vivo*. *Front. Microbiol.* 7:934. doi: 10.3389/fmicb.2016.00934

Wen, X., Zhang, X., Szewczyk, G., El-Hussein, A., Huang, Y.-Y., Sarna, T., et al. (2017). Potassium iodide potentiates antimicrobial photodynamic inactivation mediated by rose bengal in *in vitro* and *in vivo* studies. *Antimicrob. Agents Chemother.* 61:e00467-17. doi: 10.1128/AAC.00467-17

Wittebole, X., De Roock, S., and Opal, S. M. (2014). A historical overview of bacteriophage therapy as an alternative to antibiotics for the treatment of bacterial pathogens. *Virulence* 5, 226–235. doi: 10.4161/viru.25991

Wozniak, A., and Grinholc, M. (2018). Combined antimicrobial activity of photodynamic inactivation and antimicrobials-state of the art. *Front. Microbiol.* 9:930. doi: 10.3389/fmicb.2018.00930

Wypij, M., Świecimska, M., Czarnecka, J., Dahm, H., Rai, M., and Golinska, P. (2018). Antimicrobial and cytotoxic activity of silver nanoparticles synthesized from two haloalkaliphilic actinobacterial strains alone and in combination with antibiotics. *J. Appl. Microbiol.* 124, 1411–1424. doi: 10.1111/jam.13723

Xie, J., Li, Y., Li, J., Yan, Z., Wang, D., Guo, X., et al. (2018). Potent effects of amino acid scanned antimicrobial peptide Feleucin-K3 analogs against both multidrug-resistant strains and biofilms of *Pseudomonas aeruginosa*. *Amino Acids* 50, 1471–1483. doi: 10.1007/s00726-018-2625-4

Yadav, R., Bulitta, J. B., Wang, J., Nation, R. L., and Landersdorfer, C. B. (2017). Evaluation of pharmacokinetic/ pharmacodynamic model-based optimized combination regimens against multidrug-resistant *Pseudomonas aeruginosa* in a murine thigh infection model by using humanized dosing schemes. *Antimicrob. Agents Chemother.* 61:e01268-17. doi: 10.1128/AAC.01268-17

Yang, H., Chen, G., Hu, L., Liu, Y., Cheng, J., Ye, Y., et al. (2018a). Enhanced efficacy of imipenem-colistin combination therapy against multiple-drug-resistant *Enterobacter cloacae*: *in vitro* activity and a *Galleria mellonella* model. *J. Microbiol. Immunol. Infect.* 51, 70–75. doi: 10.1016/j.jmii.2016.01.003

Yang, H., Xu, J., Li, W., Wang, S., Li, J., Yu, J., et al. (2018b). *Staphylococcus aureus* virulence attenuation and immune clearance mediated by a phage lysin-derived protein. *EMBO J.* 37:e98045. doi: 10.15252/embj.201798045

Yang, M. Y., Chang, K. C., Chen, L. Y., Wang, P. C., Chou, C. C., Wu, Z. B., et al. (2018). Blue light irradiation triggers the antimicrobial potential of ZnO nanoparticles on drug-resistant *Acinetobacter baumannii*. *J. Photochem. Photobiol. B.* 180, 235–242. doi: 10.1016/j.jphotobiol.2018.02.003

Yoshizumi, A., Ishii, Y., Livermore, D. M., Woodford, N., Kimura, S., Saga, T., et al. (2013). Efficacies of calcium-EDTA in combination with imipenem in a murine model of sepsis caused by *Escherichia coli* with NDM-1 β-lactamase. *J. Infect. Chemother.* 19, 992–995. doi: 10.1007/s10156-012-0528-y

Youn Jun, S., Jin Jang, I., Yoon, S., Jang, K., Yu, K. S., Youn Cho, J., et al. (2017). Pharmacokinetics and tolerance of the phage endolysin-based candidate drug SAL200 after a single intravenous administration among healthy volunteers. *Antimicrob. Agents Chemother.* 61:e02629-16. doi: 10.1128/AAC.02629-16

Zeng, K. J., Doi, Y., Patil, S., Huang, X., and Tian, G. B. (2016). Emergence of the plasmid-mediated mcr-1 gene in colistin-resistant *Enterobacter aerogenes* and *Enterobacter cloacae*. *Antimicrob. Agents Chemother.* 60, 3862–3863. doi: 10.1128/AAC.00345-16

Zhang, J., Xu, L. L., Gan, D., and Zhang, X. (2018). *In vitro* study of bacteriophage AB3 endolysin LysAB3 activity against *Acinetobacter baumannii* biofilm and biofilm-bound *A. baumannii*. *Clin. Lab.* 64, 1021–1030. doi: 10.7754/Clin.Lab.2018.180342

Zhang, Y., Dai, T., Wang, M., Vecchio, D., Chiang, L. Y., and Hamblin, M. R. (2015). Potentiation of antimicrobial photodynamic inactivation mediated by a cationic fullerene by added iodide: *in vitro* and *in vivo* studies. *Nanomedicine* 10, 603–614. doi: 10.2217/nnm.14.131

Zhao, Y., Lu, Z., Dai, X., Wei, X., Yu, Y., Chen, X., et al. (2018). Glycomimetic-conjugated photosensitizer for specific *Pseudomonas aeruginosa* recognition and targeted photodynamic therapy. *Bioconjug. Chem.* 29, 3222–3230. doi: 10.1021/acs.bioconjchem.8b00600

Zheng, Z., Tharmalingam, N., Liu, Q., Jayamani, E., Kim, W., Fuchs, B. B., et al. (2017). Synergistic efficacy of *Aedes aegypti* antimicrobial peptide cecropin A2 and tetracycline against *Pseudomonas aeruginosa*. *Antimicrob. Agents Chemother.* 61:e00686-17. doi: 10.1128/AAC.00686-17

Zhou, W., Feng, Y., and Zong, Z. (2018). Two new lytic bacteriophages of the myoviridae family against carbapenem-resistant *Acinetobacter baumannii*. *Front. Microbiol.* 9:850. doi: 10.3389/fmicb.2018.00850

Zowawi, H. M., Forde, B. M., Alfaresi, M., Alzarouni, A., Farahat, Y., Chong, T. M., et al. (2015). Stepwise evolution of pandrug-resistance in *Klebsiella pneumoniae*. *Sci. Rep.* 5:15082. doi: 10.1038/srep15082

Conflict of Interest Statement: The authors declare that the research was conducted in the absence of any commercial or financial relationships that could be construed as a potential conflict of interest.

The reviewer RP declared a shared affiliation, with no collaboration, with the authors to the handling editor at the time of the review.

Copyright © 2019 Mulani, Kamble, Kumkar, Tawre and Pardesi. This is an open-access article distributed under the terms of the Creative Commons Attribution License (CC BY). The use, distribution or reproduction in other forums is permitted, provided the original author(s) and the copyright owner(s) are credited and that the original publication in this journal is cited, in accordance with accepted academic practice. No use, distribution or reproduction is permitted which does not comply with these terms.

Advantages of publishing in Frontiers

OPEN ACCESS
Articles are free to read for greatest visibility and readership

FAST PUBLICATION
Around 90 days from submission to decision

HIGH QUALITY PEER-REVIEW
Rigorous, collaborative, and constructive peer-review

TRANSPARENT PEER-REVIEW
Editors and reviewers acknowledged by name on published articles

Frontiers
Avenue du Tribunal-Fédéral 34
1005 Lausanne | Switzerland

Visit us: www.frontiersin.org
Contact us: info@frontiersin.org | +41 21 510 17 00

REPRODUCIBILITY OF RESEARCH
Support open data and methods to enhance research reproducibility

DIGITAL PUBLISHING
Articles designed for optimal readership across devices

FOLLOW US
@frontiersin

IMPACT METRICS
Advanced article metrics track visibility across digital media

EXTENSIVE PROMOTION
Marketing and promotion of impactful research

LOOP RESEARCH NETWORK
Our network increases your article's readership